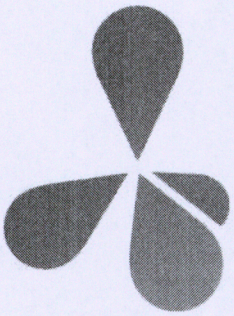

Instytut Chemii Organicznej
Polskiej Akademii Nauk

Zastosowanie diazoalkanów i oksadiazolin w fotochemicznych reakcjach tworzenia wiązań C–C

mgr inż. Katarzyna Orłowska

Monotematyczny cykl publikacji wraz z komentarzem przedstawiony Radzie Naukowej Instytutu Chemii Organicznej Polskiej Akademii Nauk w celu uzyskania stopnia doktora

Promotor: prof. dr hab. Dorota Gryko

WARSZAWA, 2023

Pragnę podziękować wszystkim osobom, które pośrednio lub bezpośrednio przyczyniły się do powstania niniejszej rozprawy doktorskiej, a w szczególności:

Prof. Dorocie Gryko, za możliwość rozwoju w Zespole XV IChO PAN oraz wsparcie na każdym etapie przygotowywania niniejszej rozprawy doktorskiej.

KRJ (najwspanialszej chemicznej mamie), **Dżoanie** (najwspanialszej współlokatorce labu 118), **Łukaszkowi** (najwspanialszemu 4P), za wsparcie i przyjaźń.

Oli P., **Oli W.**, **Agniesi** i **Lolo** za *„sporadyczne”* spotkania.

Piotrusiowi i **JV**, za świetną współpracę przy projektach i wspólnie spędzony czas.

Tomeczkowi, **Pięknemu Michałowi**, **Maksowi**, **Joe**, **Misiowi**, **Maćkowi**, **Krzysiowi**, **Klaudii**, **Dominiczce**, oraz wszystkim pozostałym byłym i obecnym członkom Zespołu XV za wspaniałą atmosferę pracy.

Hubertowi, Natalii, Marcie, Mamie, za ogromne wsparcie i wiarę we mnie w czasie tej trudnej drogi.

Praca doktorska wykonana w ramach projektów:

„Fotoautokatalityczne, bezpośrednie arylowanie porfiryn w pozycjach β- i mezo-”

realizowanego w ramach grantu **DIAMENTOWY GRANT**

Ministerstwa Nauki i Szkolnictwa Wyższego

Numer grantu: DI2016 013246

„Diazoalkany donorowo-akceptorowe w reakcjach indukowanych światłem widzialnym”

realizowanego w ramach programu **ETIUDA**

Narodowego Centrum Nauki

Numer grantu: UMO-2020/36/T/ST4/00208

Spis treści

1. Spis publikacji wchodzących w skład rozprawy doktorskiej

Publikacje przeglądowe:

[R1] K. Goliszewska, **K. Orłowska**, D. Gryko

Photoorganocatalysis in Organic Synthesis, Chapter 4: Sulfur Heterocycles.

World Scientific Publishing Company, 2019. (rozdział w monografii naukowej)

Publikacje oryginalne:

[P1] K. Orłowska, K. Rybicka-Jasińska, P. Krajewski, D. Gryko

Org. Lett. **2020**, *22*, 1018-1021.

Photochemical Doyle–Kirmse Reaction: A Route to Allenes

[P2] K. Orłowska, J. V. Santiago, P. Krajewski, K. Kisiel, I. Deperasińska, K. Zawada, W. Chaładaj, D. Gryko

ACS Catal. **2023**, *13*, 1964-1973.

UV Light Is No Longer Required for the Photoactivation of 1,3,4-Oxadiazolines

Praca wyróżniona okładką.

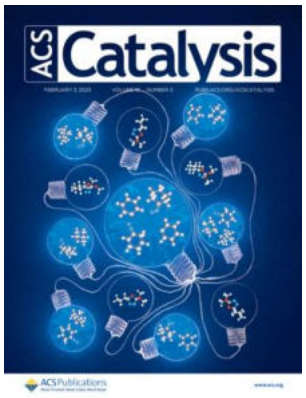

[P3] K. Orłowska, K. Łuczak, P. Krajewski, J. V. Santiago, K. Rybicka-Jasińska, D. Gryko*Chem. Commun.* **2023**, DOI: 10.1039/D3CC05174A

Unlocking the Reactivity of Diazo Compounds on Red Light with the Use of Photochemical Tools

2. Spis wystąpień konferencyjnych

Wyniki przedstawione w niniejszej pracy zostały zaprezentowane na konferencjach:

1. *COST CHAOS 2nd Training School*, Ateny, Grecja, 2019:
   Prezentacja posterowa: *Visible Light Induced Allenes Formation Through [2,3] Sigmathropic Rearrangement*

2. *The Third International Symposium on Carbene and Nitrene Chemistry*, San Antonio, Stany Zjednoczone (Teksas), 2020:
   Prezentacja posterowa: *Visible Light Induced Allene Formation Via Doyle Kirmse Reaction*

3. *DIAZO 2021: VI International Symposium – The Chemistry of Diazo Compounds and Related Systems*, Sankt Petersburg, Rosja, 2021:
   Prezentacja ustna: *Visible light-induced activation of 1,3,4-oxadiazolines*
   Prezentacja wyróżniona II nagrodą

4. *22nd Tetrahedron Symposium*, Lizbona, Portugalia, 2022:
   Prezentacja posterowa: *Visible light-induced activation of 1,3,4-oxadiazolines via Triplet Energy Transfer*

3. Spis publikacji niewchodzących w skład rozprawy doktorskiej

Publikacje oryginalne:

1. M. Hapka, K. Orłowska, M. Dranka, G. Chałasiński, M. M. Szczęśniak, J. Zachara
   Dalton Trans. **2015**, *44*, 13641-13650.
   Noncovalent interactions determine the conformation of aurophilic complexes with 2-mercapto-4-methyl-5-thiazoleacetic acid ligands

2. K. Rybicka-Jasińska, **K. Orłowska**, M. Karczewski, K. Zawada, D. Gryko
   Eur. J. Org. Chem. **2018**, *2018*, 6634-6642.
   Why Cyclopropanation is not involved in Photoinduced α-Alkylation of Ketones with Diazo Compounds?

3. J. V. Santiago, **K. Orłowska**, M. Ociepa, D. Gryko
   Org. Lett. **2023**, *25*, 6267-6271.
   Aryl versus Alkyl Redox-Active Diazoacetates ─ Light-Induced C–H Insertion or 1,2-Rearrangement

4. Wykaz stosowanych skrótów

1,3-DC	1,3-dipolarna cykloaddycja
Boc	grupa *tert*-butyloksykarbonylowa
CFL	kompaktowa lampa fluorescencyjna
DBU	1,8-diazabicyklo[5.4.0]undek-7-en
DCE	dichloroetan
DCM	dichlorometan
DFT	teoria funkcjonałów gęstości
DIPEA	*N*,*N*-diizopropyloetyloamina
DMF	*N*,*N*-dimetyloformamid
DMSO	dimetylosulfotlenek
EDA	diazooctan etylu
EDG	grupa elektronodonorowa
EnT	transfer energii
EPR	elektronowy rezonans paramagnetyczny
EWG	grupa elektronoakceptorowa
HAT	transfer atomu wodoru
HE	1,4-dihydro-2,6-dimetylo-3,5-pirydynokarboksylan dietylu, ester Hantzscha
ISC	przejście międzysystemowe
LED	dioda elektroluminescencyjna
MNP	2-metylo-2-nitrozopropan
NFSI	*N*-fluorobenzenosulfonamid
NHC	*N*-heterocykliczny karben
NHPI	*N*-hydroksyftalimid
Nphtl	ftalimid
PC	fotokatalizator
PCET	transfer elektronu sprzężony z przeniesieniem protonu
PET	fotoindukowany transfer elektronu
Piv	grupa piwaloilowa
PMP	grupa *p*-metoksyfenylowa
PPT	fotowzbudzony transfer protonu
PS	fotouczulacz
RB	róż bengalski
RED	reduktor

TEMPO	2,2,6,6-tetrametylopiperydyno-1-oksyl
TFE	2,2,2-trifluoroetanol
TMS	grupa trimetylosililowa
Ts	grupa 4-toluenosulfonowa
UTL	utleniacz
UV	promieniowanie ultrafioletowe

5. Przewodnik po rozprawie doktorskiej

5.1. Cel i zakres pracy

Wdrażanie nowych, ekologicznych rozwiązań w syntezie organicznej jest aktualnie kluczowym wyzwaniem dla współczesnego przemysłu chemicznego. Istotny nacisk kładzie się na pozyskiwanie energii z odnawialnych źródeł i zmniejszanie negatywnego wpływu procesów produkcyjnych na środowisko naturalne. Wraz ze swoimi licznymi zaletami, fotochemia bazująca na wykorzystaniu światła widzialnego wpisuje się w zasady zielonej chemii. Podejście to umożliwia aktywację reagentów w łagodnych warunkach reakcji poprzez unikalne ścieżki reakcyjne, często nieosiągalne innymi metodami.[1–7] Jedną z pierwszych transformacji fotokatalitycznych w syntezie organicznej, zachodzących pod wpływem światła widzialnego jest opracowana przez grupę MacMillana metoda α-alkilowania aldehydów z użyciem elektrofilowych bromków.[8] Od tego czasu, przekształcanie energii fotonów w energię chemiczną cieszy się coraz większym zainteresowaniem chemików organików.

Związki diazoorganiczne stanowią interesującą grupę reagentów, która znalazła szerokie zastosowanie w syntezie prostych i złożonych struktur, w tym produktów farmaceutycznych.[9–12] Łatwo ulegają one reakcjom C–H, X–H insercji, cykloaddycji, przegrupowaniom.[13–18] Przekształcenia te, na ogół, cechują się dobrą ekonomią atomową. *Bogactwo strukturalne tego typu reagentów zachęca do projektowania metod umożliwiających generowanie reaktywnych indywiduów o różnym charakterze chemicznym.* Początkowo badane reakcje diazo związków w warunkach termicznych lub pod wpływem światła UV cechowały się niskimi selektywnościami.[15] Natomiast najlepiej poznanym rodzajem ich reaktywności są transformacje przebiegające przez stadium metalokarbenu, katalizowane kompleksami metali tj. rod, miedź, srebro, żelazo.[11,14,16,17] Biorąc pod uwagę, iż obecność nawet śladowych ilości tych metali w produktach farmaceutycznych jest niepożądana, proponowanie alternatywnych metod aktywacji diazo związków jest szczególnie istotne.

Inspirując się odkryciem MacMillana, Zespół XV IChO PAN opracował pierwszą fotokatalityczną reakcję z zastosowaniem α-diazoestrów w obecności światła widzialnego. Zaproponowana metoda zakładała użycie ich jako reagentów alkilujących aldehydy i wymagała zastosowania kompleksu rutenu jako katalizatora fotoredoks.[19]

W alternatywnym podejściu, również zaprojektowanym przez zespół Gryko, katalizator ten zastąpiono porfiryną – inspirowanym naturą, tanim i łatwo dostępnym barwnikiem organicznym.[20] W kolejnych latach badaną transformację rozszerzyliśmy o α-funkcjonalizację ketonów.[21] Od tego czasu, nastąpił intensywny wzrost zainteresowania związkami diazoorganicznymi jako reagentami w reakcjach indukowanych światłem widzialnym. Późniejsze odkrycie przez Daviesa fotolizy α-arylo-α-diazoestrów na świetle niebieskim, zainicjowało opracowanie szeregu ich transformacji fotochemicznych w obecności różnorodnych reagentów. [22–25]

Mimo, iż potencjał zastosowania diazo związków jako reagentów w reakcjach indukowanych światłem widzialnym został zauważony, wciąż nie jest on w pełni poznany. Większość dostępnych metod bazuje na udziale stabilizowanych pochodnych. Niestety, reaktywność prekursorów niestabilnych diazoalkanów, np. 1,3,4-oksadiazolin pod wpływem światła widzialnego pozostaje niezbadana. Wciąż niewiele wiadomo także na temat fotokatalitycznego generowania rodników z diazo związków. Dlatego też, **celem mojej pracy doktorskiej było wykorzystanie fotochemicznych przemian diazoalkanów i 1,3,4-oksadiazolin do opracowania nowych metod tworzenia wiązań C−C w obecności światła widzialnego.**

Korzystając z zalet wynikających z zastosowania światła widzialnego do tworzenia nowych wiązań chemicznych oraz bogatej reaktywności diazoalkanów w ramach niniejszej pracy doktorskiej:

1. Zbadałam reaktywność α-arylo-α-diazoestrów w reakcji z udziałem sulfidów propargilowych w obecności światła niebieskiego, prowadzącej do otrzymywania allenów (Schemat 1).

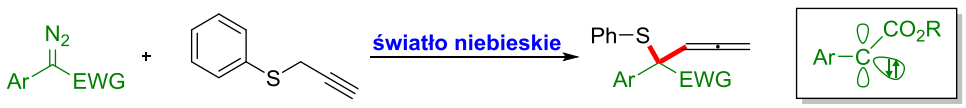

Schemat 1. Fotochemiczna reakcja syntezy allenów z udziałem α-arylo-α-diazoestrów

2. Opracowałam indukowaną światłem widzialnym fotokatalityczną metodę aktywacji 1,3,4-oksadiazolin, której użyteczność przedstawiłam na przykładzie syntezy spirocyklopropanów (Schemat 2).

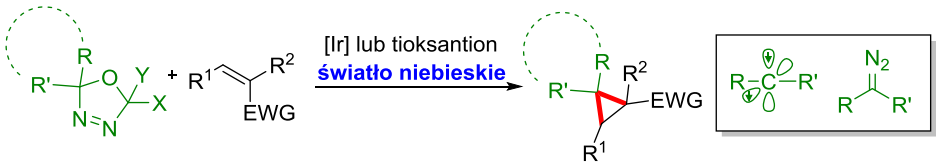

Schemat 2. Fotokatalityczna reakcja syntezy spirocyklopropanów z udziałem 1,3,4-oksadiazolin

3. Wykazałam, że niskoenergetyczne światło czerwone może być stosowane w fotokatalitycznych reakcjach związków diazoorganicznych, na przykładzie reakcji syntezy oksymów i fenantrydyn, w których diazo związki są prekursorami rodników (Schemat 3A) oraz reakcji otrzymywania hydrazonów z użyciem diazo związków jako akceptorów reaktywnych indywiduów (Schemat 3B).

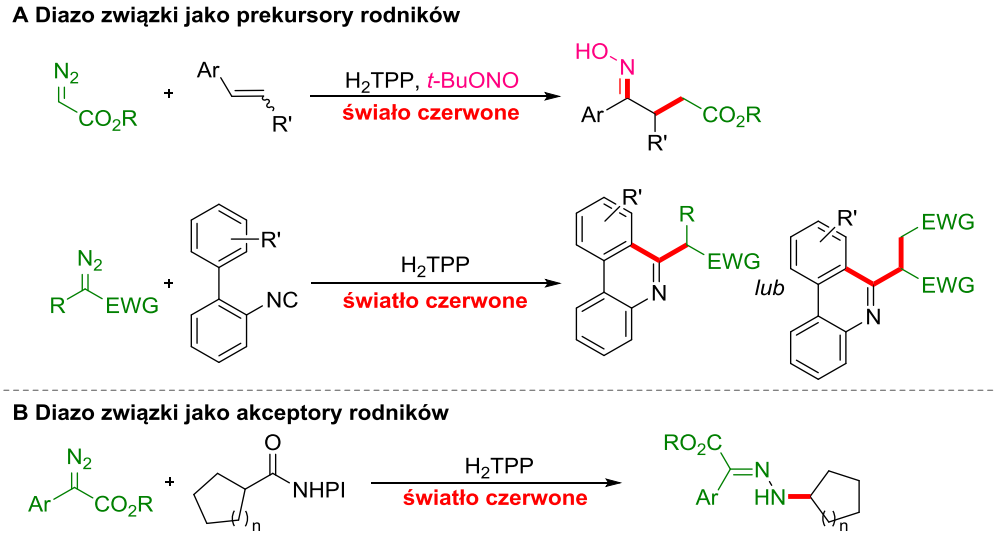

Schemat 3. Fotokatalityczne reakcje diazo związków w obecności światła czerwonego

5.2. Wstęp literaturowy

5.2.1. Fotochemia i mechanizmy reakcji fotochemicznych

Zjawiska obserwowane w Naturze od zawsze stanowiły źródło inspiracji dla naukowców. Światło słoneczne, regulujące m.in. jeden z kluczowych procesów biochemicznych flory – fotosyntezę, a także procesy wpływające na funkcjonowanie organizmu człowieka np. syntezę melaniny, czy prowitaminy D_3, zostało rozpoznane jako łatwo dostępne i odnawialne źródło energii. Potencjał wykorzystania promieniowania słonecznego jako siły napędowej reakcji chemicznych dostrzegł już na początku XX wieku włoski chemik Giacomo Ciamician, a jego odkrycia przyczyniły się do narodzin *fotochemii, nauki o procesach chemicznych indukowanych światłem*.[26]

Obecnie, fotochemia jest jednym z najprężniej rozwijających się narzędzi współczesnej syntezy organicznej.[1–7] Stanowi ona nie tylko alternatywę dla znanych transformacji, ale modyfikując profil energetyczny reakcji daje dostęp do nieoczywistych reaktywności i przemian nieosiągalnych na drodze klasycznych metod syntetycznych. Reakcje indukowane światłem przebiegają w łagodnych warunkach, bez konieczności stosowania stechiometrycznych ilości silnych utleniaczy/reduktorów lub kwasów/ zasad, co zwiększa zakres tolerancji grup funkcyjnych w strukturze substratów. Z uwagi na generowanie mniejszej ilości odpadów, podejście to cechuje się niską uciążliwością dla środowiska i niewątpliwie wpisuje się w zasady zielonej chemii. Mimo, iż dotychczas energię fotonów wykorzystano w nielicznych procesach przemysłowych (np. fotoutlenianie cytronelolu czy synteza artemizyny),[27–29] najnowsze doniesienia naukowe obfitują w badania podstawowe dotyczące fotoindukowanych transformacji prowadzących do zarówno prostych jak i złożonych struktur, farmaceutyków i produktów naturalnych.[7,30–33]

Wyróżniamy trzy główne mechanizmy reakcji indukowanych światłem (Schemat 4). Substraty, które absorbują światło z zakresu naświetlania ulegają *bezpośredniemu wzbudzeniu*, prowadzącemu do wytworzenia reaktywnych indywiduów, dalej uczestniczących w przemianach wewnątrz-, bądź międzycząsteczkowych. W celu aktywacji związku organicznego, który nie absorbuje fotonów o danej energii koniecznie jest zastosowanie katalizatora, który je pochłania – fotouczulacza (**PS**), bądź katalizatora fotoredoks (**PC**). Fotosensybilizator ze wzbudzonego stanu singletowego ^{1}**[PS]*** może

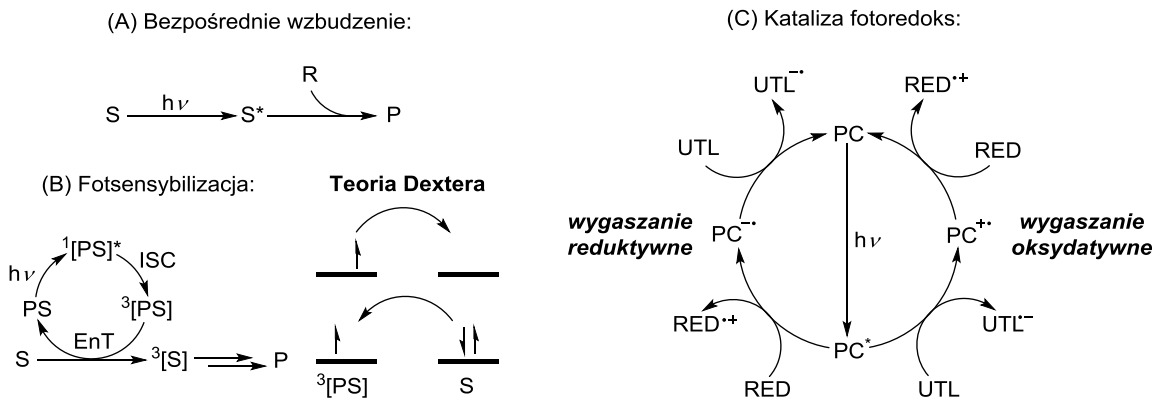

Schemat 4. Mechanizmy reakcji fotochemicznych

przejść na skutek wzbronionego spinowo przejścia międzysystemowego (**ISC**) do niższego energetycznie stanu trypletowego **^{3}[PS]*** o dłuższym czasie życia. Taka reaktywna forma, jeśli charakteryzuje się wartością energii zbliżoną do poziomu trypletowego substratu **^{3}[S]***, może pośrednio wzbudzić go na drodze fotoindukowanego transferu energii (**EnT**). Mechanizm ten nazywamy *fotosensybilizacją*, a proces przeniesienia energii od fotouczulacza do substratu zachodzi, według teorii Dextera, na drodze jednoczesnej wymiany elektronów ze stanu wzbudzonego donora (**PS**) i stanu podstawowego akceptora (**S**).[34,35] Szerzej przebadanym w chemii organicznej podejściem katalitycznym jest kataliza fotoredoks bazująca na właściwościach redukująco-utleniających fotokatalizatora w stanie wzbudzonym.[1–5] Między wzbudzonymi cząsteczkami katalizatora a cząsteczkami reagenta dochodzi do fotoindukowanego transferu elektronu (**PET**), w skutek tego cząsteczki fotokatalizatora redukują się do anionorodników **PC$^{\bullet-}$** utleniając reagent (*wygaszanie reduktywne*), bądź redukując go ulegają utlenieniu do kationorodników **PC$^{\bullet+}$** (*wygaszanie oksydatywne*). Regeneracja katalizatora do stanu podstawowego zachodzi na drodze, odpowiednio, utlenienia **PC$^{\bullet-}$** bądź redukcji **PC$^{\bullet+}$**. W niektórych przypadkach do zamknięcia cyklu katalitycznego konieczne jest zastosowanie zewnętrznych utleniaczy/reduktorów (ang. *sacrificial oxidant/reductant*). Jeżeli jednak w cyklu katalitycznym uczestniczą wyłącznie cząsteczki substratów i następcze reaktywne indywidua z nich wytworzone, cykl taki nazywamy *redoks-neutralnym* i jest on najbardziej korzystnym wariantem katalizy fotoredoks pod względem ekonomii atomowej reakcji. Innym rodzajem mechanizmów fotokatalitycznych są cykle bazujące na transferze atomu (np. wodoru – HAT, lub fluorowca – XAT),[36,37] w przypadku których do aktywacji substratu dochodzi na skutek oderwania nie elektronu a atomu (wodoru lub fluorowca) od jego cząsteczki przez

wzbudzony fotokatalizator. Choć najczęściej stosowanymi fotokatalizatorami są kompleksy irydu oraz rutenu,[32] opracowano wiele alternatywnych metod wykorzystujących tanie i łatwo dostępne barwniki organiczne np. Eozyna Y, róż bengalski, błękit metylenowy, czy inspirowane naturą porfiryny.[1,6,31]

Opisane powyżej procesy fotochemiczne, w niektórych przypadkach, mogą współistnieć tworząc bardziej złożone mechanizmy reakcyjne. Ponadto, wraz z intensywnym rozwojem współczesnej fotokatalizy opracowano także strategie tzw. katalizy podwójnej (ang. *dual catalysis*) opierającej się na współistnieniu cykli fotokatalitycznego i cyklu np. organokatalizatora lub katalizatora metalu przejściowego na przykład kompleksu kobaltu, niklu, czy palladu.[38,39] Jednym z najnowszych podejść jest fotoelektrochemia, w myśl której procesy na elektrodach zachodzą przy jednoczesnej obecności fotokatalizatorów i światła.[40]

Fotochemia jest potężnym narzędziem do tworzenia wiązań chemicznych. Jednak wiele z opracowanych metod wymaga zastosowania wysokoenergetycznego, fototoksycznego światła ultrafioletowego. Reakcje indukowane światłem UV, z uwagi na różnorodność chromoforów występujących w obrębie złożonych substratów i produktów reakcji, zwykle cechują się niską selektywnością. Dlatego też do wyzwań współczesnej fotochemii należy opracowanie nowych i alternatywnych metod tworzenia wiązań chemicznych z udziałem: a) światła widzialnego, którego zastosowanie wraz z fotokatalizatorem może prowadzić do reaktywności nieznanych na świetle UV; b) tanich i nietoksycznych barwników organicznych w miejsce kompleksów metali; c) substratów o dotąd niezbadanej reaktywności fotochemicznej będących potencjalnymi prekursorami form reaktywnych, do takich bez wątpienia należą związki diazoorganiczne.

5.2.2. Związki diazoorganiczne

Diazo związki są reagentami powszechnie stosowanymi w syntezie związków organicznych, także tych o znaczeniu biologicznym. [9–12] Ich użyteczność wynika nie tylko z zazwyczaj prostych metod otrzymywania, ale także różnorodnych reaktywności zapewniających dostęp do różnych reaktywnych indywiduów takich jak metalokarbeny, karbeny, ylidy, czy rodniki. Związki te łatwo ulegają reakcjom cykloaddycji, insercji

i przegrupowania, a transformacje te cechują się dobrą ekonomią atomową, przebiegając często z wydzieleniem cząsteczek azotu. [13–18]

Historycznie pierwsze reakcje związków diazoorganicznych polegały na rozkładzie termicznym, jednakże z uwagi na niską selektywność i silne właściwości wybuchowe diazoalkanów, podejście to zostało uznane za niepraktycznie i niebezpieczne.[15] Zastąpiono je strategią używaną do dziś - katalizą kompleksami metali, głównie rodu, srebra i miedzi, umożliwiającą generowanie wysoce reaktywnych metalokarbenów. Reakcje przebiegające z ich udziałem charakteryzują się bardzo dobrymi wydajnościami i regioselektywnościami, a użycie odpowiednich katalizatorów pozwala na wydajną syntezę asymetryczną.[11,16,17] Mimo to, zastosowanie toksycznych i często drogich kompleksów metali jest rozwiązaniem nieatrakcyjnym dla przemysłu farmaceutycznego. Dobrze zbadaną reaktywnością diazo związków jest także fotoliza indukowana światłem UV, zachodząca bez dodatku katalizatora, lecz często nieselektywnie.[15] Obecnie, konkurencyjnym podejściem są transformacje przebiegające pod wpływem światła widzialnego.[22–25] Zostaną one szczegółowo omówione w punktach 5.2.2.2. oraz 5.2.2.3 niniejszego przewodnika.

5.2.2.1. Struktura i klasyfikacja

Związki diazoorganiczne są reagentami o bogatej różnorodności strukturalnej, a charakter podstawników w pozycjach α- do atomu węgla związanego z grupą $–N_2$, ma bezpośredni wpływ na ich stabilność i reaktywność.[15] Wśród znanych literaturowo diazo związków znajdują się zarówno diazoalkany stabilizowane, jak i semi-stabilizowane oraz niestabilizowane (Rysunek 1). Stabilizacja zdelokalizowanego ładunku ujemnego, przynajmniej jednym podstawnikiem o charakterze elektronoakceptorowym (EWG), przyczynia się do relatywnie wysokiej trwałości tego typu związków. Dlatego też, stabilizowane pochodne stanowią najbardziej przebadaną grupę diazoalkanów.

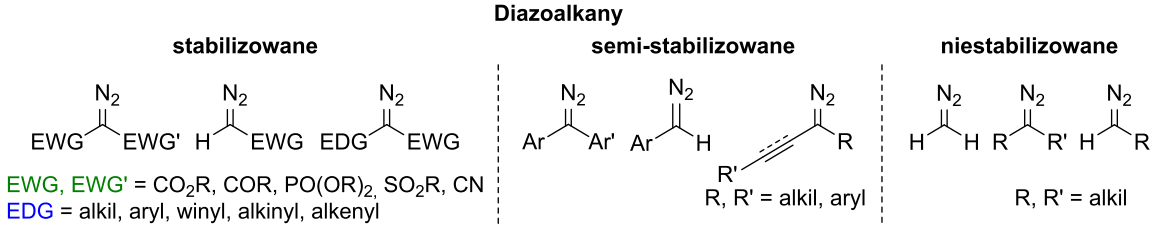

Rysunek 1. Klasyfikacja związków organicznych ze względu na stabilność

Wśród nich wyróżnić możemy diazoalkany akceptorowo-akceptorowe (podstawione dwoma grupami EWG), akceptorowe (podstawione jedną grupą EWG) oraz donorowo-akceptorowe (podstawione jedną grupą EWG i drugą o charakterze elektronodonorowym, EDG). Trudniejsze do otrzymania są semi-stabilizowane diazoalkany, zawierające wiązania typu π (pierścienie aromatyczne bądź ugrupowania alkenylowe/alkinylowe) w bliskim sąsiedztwie węgla diazowego. Z kolei brak podstawników stabilizujących powoduje drastyczny spadek trwałości i sprawia, że są one silnie wybuchowe.[15] Z tego względu są one najmniej przebadanymi z diazo związków na świetle, a do prowadzenia transformacji z ich udziałem konieczna jest synteza *in situ* ze stabilnych prekursorów, takich jak hydrazony,[41] diazyryny,[42,43] czy 1,3,4-oksadiazoliny.[44,45] Korzyści wynikające z zastosowania 1,3,4-oksadiazolin jako bezpiecznych prekursorów diazoalkanów i karbenów zostały opisane w sekcji 5.2.3..

Struktura diazo związku wpływa nie tylko na jego stabilność, ale także na właściwości fotofizyczne. Zarówno diazoalkany akceptorowo-akceptorowe, jak i akceptorowe pochłaniają światło z zakresu UV (Wykres 1). Z pomiarów absorpcji wynika, iż im bardziej stabilizowany jest diazo związek, tym wyższym wartościom energii odpowiadają jego pasma absorpcji (λ_{max}= 346 nm dla **1** w porównaniu z λ_{max} = 380 nm dla **2**). W 2018 roku Davies i Jurberg odkryli, że zastąpienie atomu wodoru/jednej z grup EWG w strukturze diazoalkanu pierścieniem aromatycznym powoduje batochromowe przesunięcie lokalnego maksimum absorpcji w stronę światła niebieskiego.[46] Z kolei najnowsze doniesienia grupy Koenigsa dotyczące fotochemii diarylodiazoalkanów dowodzą, że zwiększenie donorowego charakteru pierścieni aromatycznych skutkuje jeszcze silniejszym efektem batochromowym i ma znaczący wpływ na stan elektronowy generowanych karbenów.[47] Co więcej, badania zrealizowane

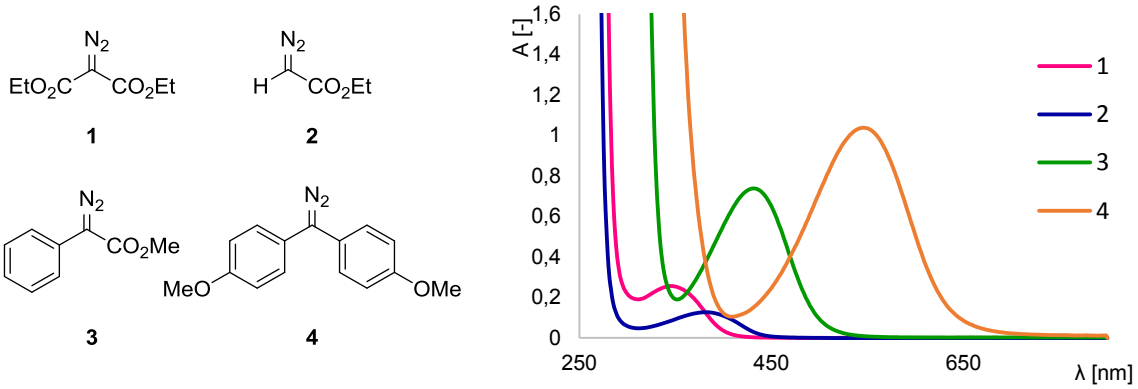

Wykres 1. Widmo UV-Vis wybranych związków diazoorganicznych, c = 0.01 M w DCM

w Zespole XV IChO PAN wykazują, że fotoliza di(*p*-metoksy- fenylo)diazometanu **4** jest możliwa nawet pod wpływem światła czerwonego.[48]

5.2.2.2. Reaktywność diazo związków w obecności światła widzialnego

Użyteczność syntetyczna związków diazoorganicznych oraz korzyści wynikające z zastosowania światła jako źródła energii do tworzenia nowych wiązań powoduje, że fotochemiczne metody ich aktywacji są tematem intensywnych badań. [22–25] Najnowsze doniesienia naukowe wykazują, że zastąpienie światła UV promieniowaniem z zakresu widzialnego pozytywnie wpływa na wydajność i selektywność fotochemicznych transformacji z udziałem diazo związków.

Właściwości fotofizyczne danego diazoalkanu determinują dostępne metody jego fotoaktywacji pod wpływem światła widzialnego. W przypadku pochodnych absorbujących światło z tego zakresu (ʎ > 380 nm), takich jak diazoalkany donorowo-akceptorowe, możliwe jest przeprowadzenie fotolizy na drodze wzbudzenia bezpośredniego (Schemat 5). Na skutek tego procesu, generowane są karbeny singletowe, reaktywne indywidua posiadające niewiążącą parę elektronową, która bierze udział w tworzeniu nowych wiązań chemicznych.[46] Jeśli jednak dany diazo związek nie absorbuje światła z zakresu naświetlania, do generowania form reaktywnych koniecznie jest zastosowanie fotokatalizatora (fotouczulacza lub katalizatora fotoredoks), który je pochłania. Gdy poziom energii trypletowej katalizatora jest zbliżony do wartości energii diazoalkanu w stanie trypletowym, dochodzi do fotoindukowanego transferu energii (EnT) z wytworzeniem karbenów trypletowych, o charakterze dwurodników. Natomiast jeśli fotokatalizator charakteryzuje się odpowiednimi właściwościami redoks, możliwa jest redukcja diazoalkanu do rodników w wyniku fotoindukowanego transferu elektronu (PET) od wzbudzonych cząsteczek fotokatalizatora.

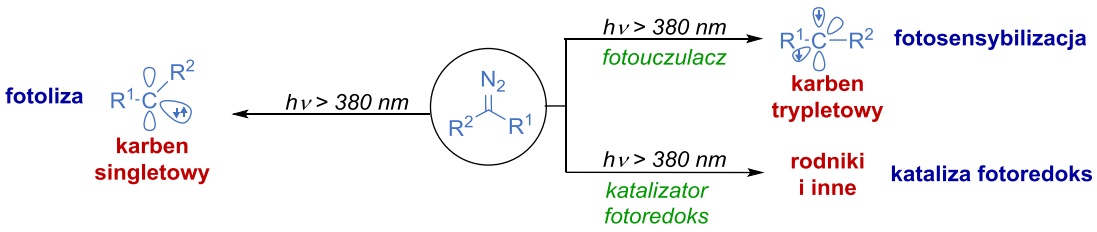

Schemat 5. Indukowane światłem widzialnym metody aktywacji diazo związków

Fotochemiczne metody aktywacji diazoalkanów dają dostęp do różnorodnych indywiduów chemicznych.[22–25] Warto jednak zaznaczyć, że aby diazo związek uczestniczył w reakcji fotochemicznej, nie musi on ulegać wzbudzeniu, ani oddziaływać z fotokatalizatorem. W literaturze bowiem, występują również liczne przykłady zastosowania diazoalkanów, w których są one akceptorami rodników wytworzonych w cyklach fotokatalitycznych. Poniższy przegląd transformacji diazoalkanów w obecności światła widzialnego w sposób zwięzły przedstawia tylko najistotniejsze doniesienia literaturowe dotyczące każdego z wymienionych rodzajów reaktywności.

5.2.2.2.1. Bezpośrednia fotoliza związków diazoorganicznych

Przełomowe odkrycie właściwości fotofizycznych α-arylo-α-diazoestrów zapoczątkowało gwałtowny wzrost zainteresowania fotolizą diazo związków do karbenów w obecności światła widzialnego.[46] Wśród dotychczas opracowanych transformacji bazujących na tym podejściu dominują reakcje C–H/X–H insercji, cykloaddycji oraz przegrupowania z udziałem ylidów.[22–25]

Fotochemiczne reakcji C–H/X–H insercji

Insercja karbenów w wiązania C–H/X–H (X = N, Si, S, O) jest prostą i efektywną strategią umożliwiającą szybką syntezę małych cząsteczek oraz złożonych struktur chemicznych.[13,49,50] Pierwsze tego typu reakcje zachodzące z udziałem związków diazoorganicznych w obecności światła widzialnego zostały zaobserwowane przez Daviesa i Jurberga podczas badania wpływu rozpuszczalnika na fotoreaktywność α-arylo-α-diazoestrów.[46] Zauważyli oni, że za wyjątkiem dichlorometanu, większość rozpuszczalników organicznych reaguje z generowanymi *in situ* karbenami, prowadząc do produktów cykloaddycji, C–H insercji, czy O–H insercji. Badania te sugerowały również singletową naturę generowanych karbenów.

Do tej pory zaprojektowano wiele indukowanych światłem widzialnym metod, które umożliwiają insercję karbenów typu **A** w struktury rozmaitych substratów (Schemat 6). W obecności węglowodorów cyklicznych otrzymywane są produkty C–H insercji, jednak z uwagi na ich niską reaktywność reakcje te wymagają stosowania wysokich nadmiarów stechiometrycznych (nawet 100 ekwiwalentów). W przypadku cykloalkenów, czynnikiem obniżającym wydajność reakcji jest konkurencyjna cykloaddycja karbenu do

wiązania podwójnego. Analogicznie, uboczna reakcja cyklopropanowania obserwowana jest dla bogatych w elektrony arenów i heteroarenów, stosowanych w znacznie mniejszych ilościach (5 ekwiw.). Ponadto, α-arylo-α-diazo-estry o odpowiedniej budowie ulegają reakcji wewnątrzcząsteczkowej, prowadzącej do laktonów (**8**, Schemat 6A).[46] W obecności reagentów wychwytujących (0.33-5.0 ekwiw.) takich jak aminy, w tym cykliczne i aromatyczne, karbazole, pirazole, 1,2,3-triazole, indole, amidy i sulfonamidy otrzymywane są produkty N–H insercji (np. związki **11-17**, Schemat 6B).[46,51–53] Reakcja diazo związków z silanami prowadzi natomiast do tworzenia nowych wiązań C–Si (Schemat 6C).[54] Nieco odmienny mechanizm postulowany jest w przypadku syntezy tioeterów, zachodzącej z udziałem tiolu alifatycznego bądź tiofenolu.[55] Zakłada on, że kluczowym etapem jest reakcja karbenu **A** nie z samym substratem a wygenerowanym z niego fotochemicznie rodnikiem **B** (Schemat 6D).

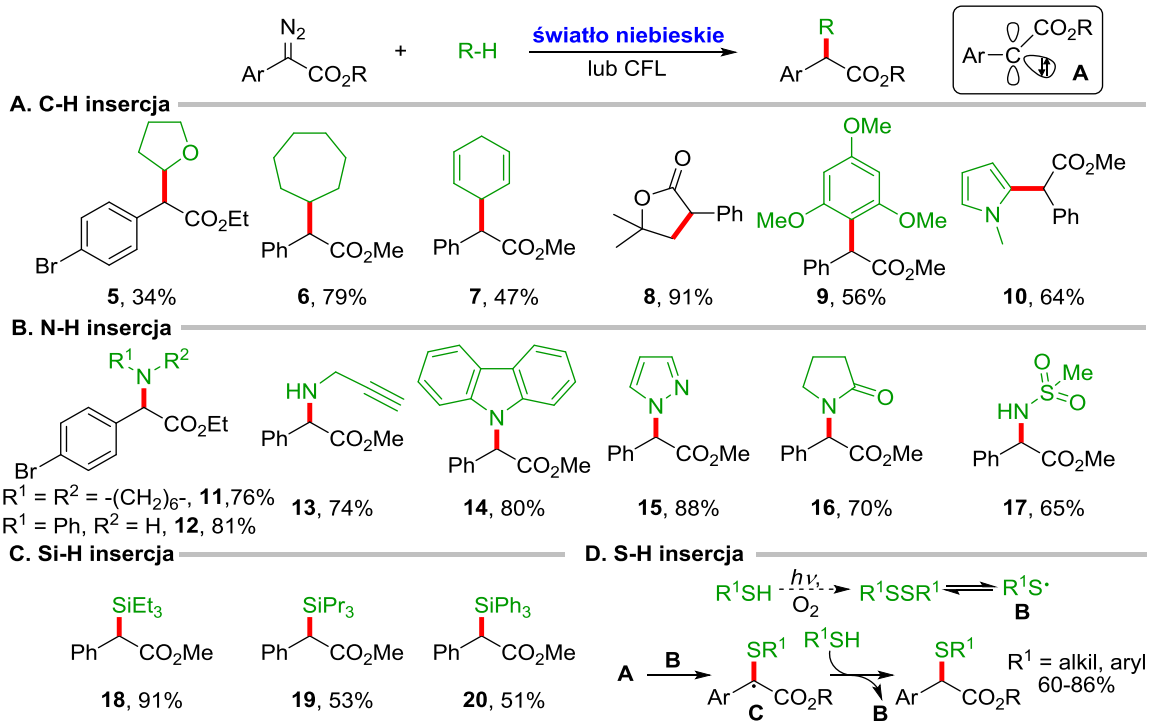

Schemat 6. Wybrane przykłady reakcji C-H/X-H insercji na drodze fotolizy α-arylo-α-diazoestrów na świetle widzianym

Insercja karbenów zachodzi wydajnie w wiązania O–H kwasów zarówno alifatycznych, jak i aromatycznych. Dla kwasów mocniejszych np. but-2-ynowego, estry powstają bez naświetlania mieszaniny reakcyjnej, w wyniku protonowania diazoalkanu oraz następczej substytucji grupy diazowej (ester **23**, Schemat 7A).[46] *O*-Alkilowanie 2-pirydonów, dotąd problematyczne, przeprowadzono selektywnie z udziałem α-arylo-

α-diazoestrów.[56] Rozważane ścieżki reakcyjne sugerują możliwy udział rodników **D**-**F**, generowanych na skutek reakcji karbenów **A** z substratem **C** (Schemat 7A), selektywność reakcji tłumaczona jest zaś niższą energią dysocjacji wiązania O–H w porównaniu z wiązaniem N–H. Dodatkowo, grupa Koenigsa opracowała strategię bazującą na foto-wzbudzonym transferze protonu (PPT, ang. Photoexcited Proton Transfer), która umożliwia formalną O–H insercję diazo związków do alkoholi o słabych właściwościach kwasowych oraz fenoli.[57,58] Podejście to wykorzystuje wytworzenie międzycząsteczkowego wiązania wodorowego między grupą estrową diazoestru a hydroksylową alkoholu/fenolu. Powstały w ten sposób kompleks **G** w obecności światła ulega wzbudzeniu i rozpada się na parę jonową **H** lub **I**, a następcza substytucja nukleofilowa prowadzi do otrzymania żądanego eteru **B** (Schemat 7B). Ta fotochemiczna metoda okazała się skuteczna nie tylko dla α-arylo-α-diazo-estrów, ale również cyklicznych α-diazoamidów, podczas gdy stosując związki miedzi/rodu w ciemności nie wyizolowano analogicznych produktów.[59]

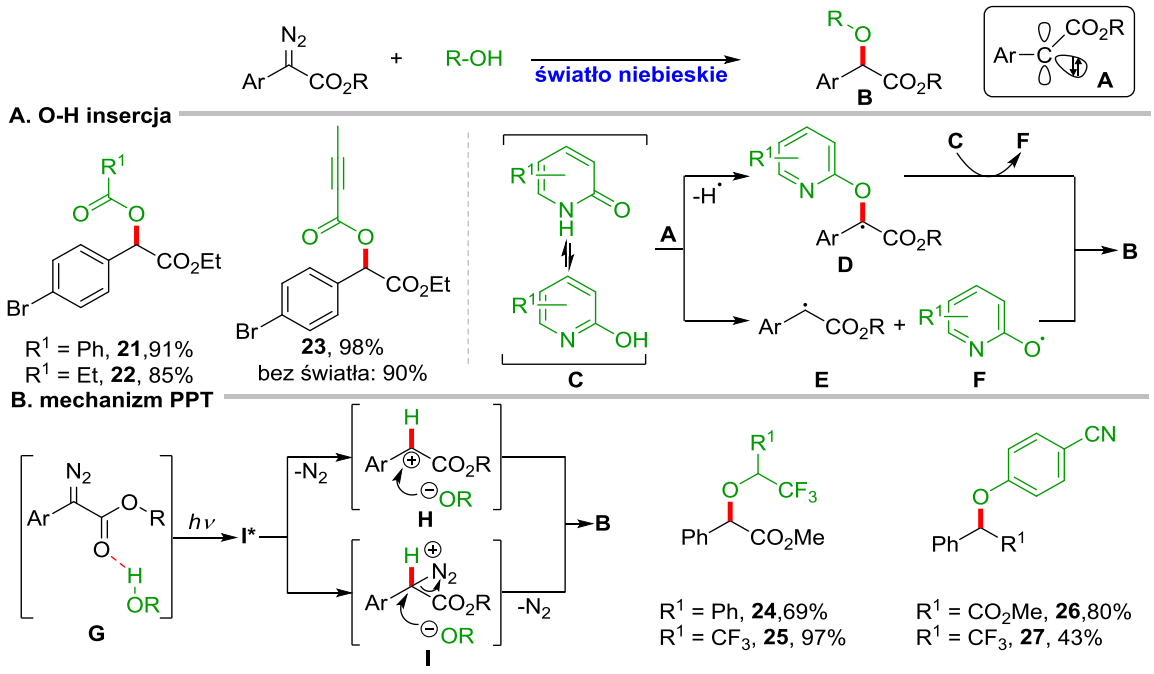

Schemat 7. Wybrane przykłady reakcji O-H insercji oraz formalnej O-H z udziałem α-arylo-α-diazoestrów na świetle widzianym

Obok α-arylo-α-diazoestrów, światło widzialne pochłaniają także diarylodiazo-alkany. W zależności od rodzaju podstawników pierścienia aromatycznego, pochodne diarylodiazometanu charakteryzują się odmiennymi widmami absorpcji i reaktywnością.[47] Pod wpływem światła niebieskiego, diazoalkany posiadające

w strukturze bogate w elektrony pierścienie aromatyczne ulegają fotolizie do karbenów o charakterze nukleofilowym. Z uwagi na niewielkie różnice w poziomach energetycznych karbenu trypletowego i singletowego postuluje się współistnienie obydwu stanów elektronowych w roztworze. W obecności alkinów ulegają one formalnej insercji, w wiązania C_{sp}–H dla arylowych pochodnych lub C_{sp3}–H dla alkinów alifatycznych (Schemat 8A). Co ciekawe, analogiczna reakcja w obecności związków rodu/miedzi prowadzi jedynie do nieselektywnego rozkładu diazoalkanu.[47] Korzystając z faktu, iż związek **4** (λ_{max} = 543 nm) w niewielkim stopniu absorbuje także światło czerwone, w zespole XV IChO PAN wykazano, że absorpcja ta jest wystarczająca do przeprowadzenia fotolizy. Użyteczność opracowanej strategii zilustrowano na przykładzie reakcji O–H, N–H i S–H insercji w struktury różnorodnych substratów, w tym cząsteczek o znaczeniu biologicznym (Schemat 8B).[48]

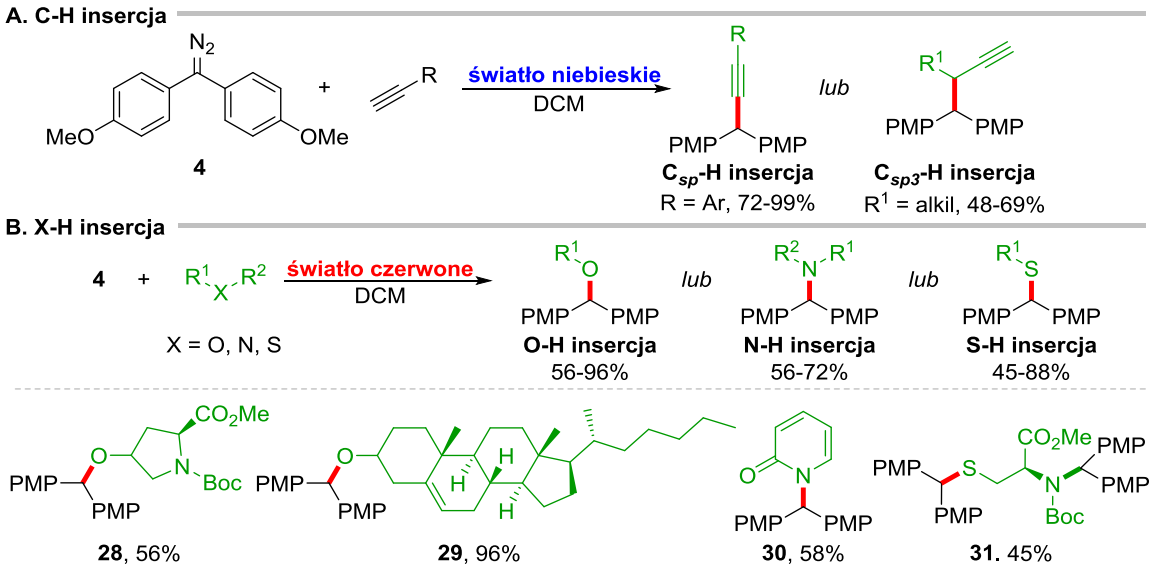

Schemat 8. Indukowane światłem widzialnym reakcje C-H/X-H insercji z udziałem di(*p*-metoksy-fenylo)diazometanu (**4**)

Fotochemiczne reakcje z udziałem ylidów

Przegrupowania sigmatropowe są transformacjami pozwalającymi na szybką reorganizację struktur cząsteczek. Przykładowo, ylidy generowane w reakcjach karbenów/metalokarbenów z reagentami zawierającymi wolną parą elektronową na heteroatomie (X = O, N, S) mogą ulegać przegrupowaniom [2,3]- i [1,2] sigmatropowym.[60–62]

Zakres stosowalności fotochemicznych metod, bazujących na przegrupowaniach [2,3]-sigmatropowych ogranicza się do α-arylo-α-diazoestrów jako prekursorów karbenów **A** oraz różnorodnych sulfidów lub amin propargilowych, **B**. Powstałe ylidy **C** ulegają przegrupowaniu [2,3]-σ z zerwaniem wiązania C–X i wytworzeniem nowego wiązania C–C, a otrzymany produkt **D** posiada czwartorzędowy atom węgla (Schemat 9). W zależności od budowy sulfidu, ylidy mogą przegrupować się na różne sposoby, prowadząc do odmiennych produktów (Schemat 9A). W 2019 roku, grupa Koenigsa opracowała metodę fotolizy α-arylo-α-diazoestrów w obecności sulfidów allilowych.[63] W podobnym czasie, Xiao zaproponował transformację wykorzystującą *gem*-difluorowane pochodne.[64] W obydwu przypadkach, otrzymano sulfidy homoallilowe, analogicznie do reakcji Doyla-Kirmsego, katalizowanej związkami np. miedzi,[65] srebra,[66] czy żelaza.[67] Natomiast ylidy typu **E** generowane z 2-merkaptooctu i karbenów **A** ulegają tauotomeryzacji do formy **F**, która w wyniku tzw. przegrupowania Sommeleta-Hausera prowadzi do produktów formalnej *orto*-C–H funkcjonalizacji pierścienia aromatycznego diazo związku (Schemat 9A).[68]

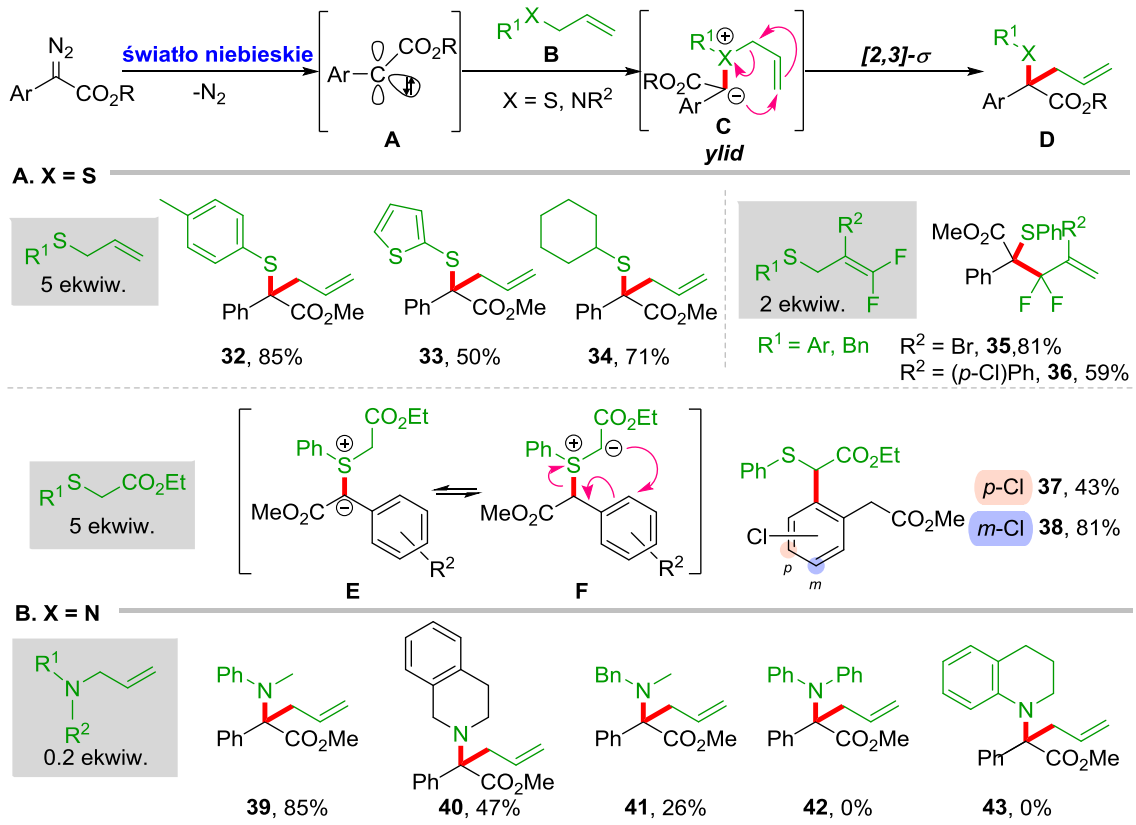

Schemat 9. Indukowane światłem widzialnym przegrupowania [2,3]-sigmatropowe z udziałem α-arylo-α-diazoestrów

Ylidy pochodzące od trzeciorzędowych amin allilowych, jak w przypadku reakcji z udziałem sulfidów allilowych, ulegają przegrupowaniu [2,3]-σ (Schemat 9B).[69] Reakcja przebiega z wysokimi wydajnościami dla *N*-allilo-*N*-alkiloanilin (np. produkt **39**), ograniczeniami metody są jednak 1,2,3,4-tetrahydrochinolina i aminy *N*,*N*-diarylowe (**42**-**43**).

Karbeny **A** generowane pod wpływem światła niebieskiego ulegają także reakcjom formalnej insercji w wiązania S–N, C–S oraz C–O w obecności ftalimidów *N*-sulfenylowych, sulfidów benzylowych lub tietanów oraz oksetanów (Schemat 10).[68,70] Transformacje te zachodzą na drodze przegrupowania [1,2]-sigmatropowego ylidów **C**. Obliczenia DFT dla reakcji diazo związków z oksetanami/tietanami sugerują, że przegrupowanie powstałego ylidu prowadzące do ekspansji pierścienia ma charakter rodnikowy.

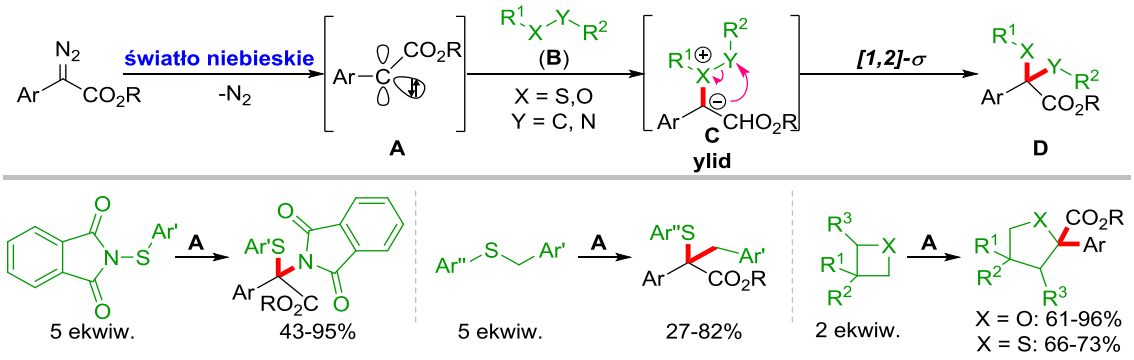

Schemat 10. Indukowane światłem widzialnym przegrupowania [1,2]-sigmatropowe z udziałem α-arylo-α-diazoestrów

Charakter pierścienia aromatycznego diazoestru ma znaczący wpływ na przebieg indukowanej światłem niebieskim reakcji z udziałem *N*-fluorobenzenosulfonimidu (NFSI) w cyklicznym eterze jako rozpuszczalniku.[71] Podczas gdy neutralne i ubogie w elektrony α-arylo-α-diazoestry tworzą z rozpuszczalnikiem ylidy, karbeny generowane z bogatych w elektrony analogów reagują bezpośrednio z reagentem fluorującym a rozpuszczalnik nie ulega inkorporacji w strukturę otrzymanych produktów.

Fotochemiczne reakcje cykloaddycji

Reakcje cykloaddycji są transformacjami użytecznymi do syntezy głównie trój-sześcioczłonowych pierścieni cyklicznych, obficie występujących w strukturach związków naturalnych i cząsteczkach biologicznie czynnych.[72] W literaturze znane są

przykłady indukowanych światłem widzialnym reakcji cykloaddycji [2+1], przebiegających z udziałem diazo związków i reagentów nienasyconych, prowadzących przez karbeny **A** do pochodnych cyklopropanu lub cyklopropenu. (Schemat 11). Pierwsza tego typu transformacja została przetestowana przez Daviesa i Jurberga z użyciem styrenu (5 ekwiw.) dla α-arylo-α-diazoestrów w ramach kompleksowych badań nad ich reaktywnością fotochemiczną.[46] Produkty otrzymano z dobrymi i bardzo dobrymi wydajnościami (do 99%) i wysokimi diastereoselektywnościami (d.r. do >20:1) (Schemat 11A). Dodatkowo, reakcje cyklopropanowania przeprowadzono także dla pochodnej indolu i benzenu, a w ich wyniku otrzymano produkty bicykliczne.[46] Badania te w kolejnych latach kontynuowano, a zakres stosowalności [2+1] cykloaddycji z udziałem α-arylo-α-diazoestrów został poszerzony o różnorodne areny,[73] indole,[74] cyklooktatetraen i polinienasycone węglowodory (Schemat 11A).[75]

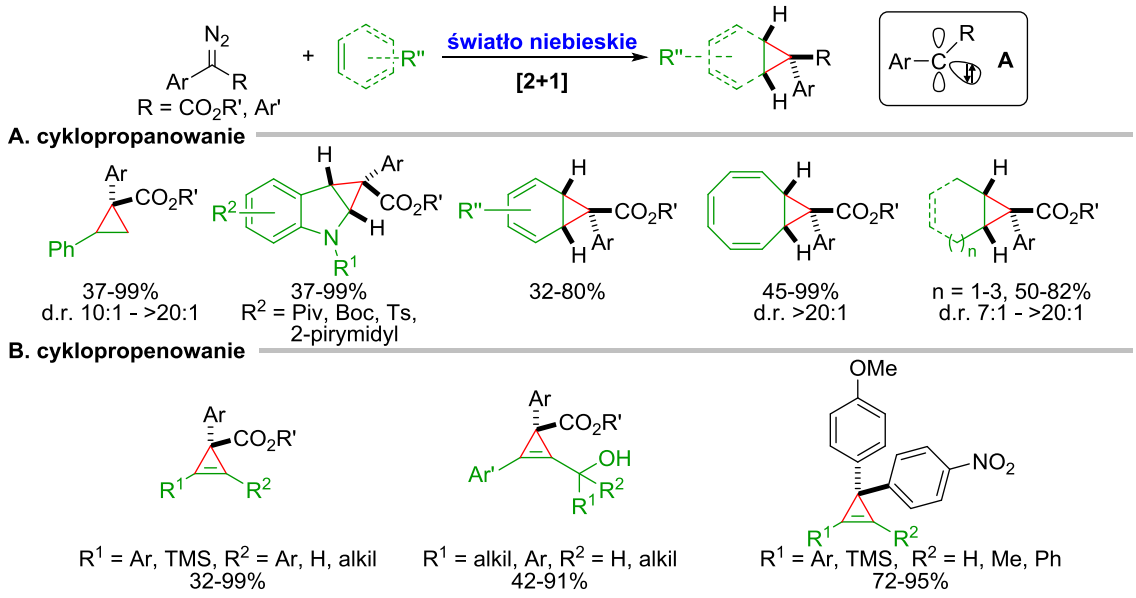

Schemat 11. Indukowane światłem widzialnym reakcje [2+1] cykloaddycji z udziałem diazo związków

Analogicznie do reakcji cyklopropanowania, grupa Koenigsa zaproponowała metodę syntezy cyklopropenów z udziałem alkinów i α-arylo-α-diazoestrów (Schemat 11B).[63] Transformację tę przetestowano także dla alkoholi propargilowych.[76] Mimo, iż stosowane substraty posiadały w strukturze niezabezpieczoną grupę hydroksylową, reakcja cyklopropenowania zachodziła selektywnie dla alkoholi drugo- i trzecio-rzędowych. W opracowanych warunkach pierwszorzędowe alkohole propargilowe ulegały natomiast O–H insercji. Co istotne, reakcja przeprowadzana z użyciem standardowych niefotochemicznych metod katalitycznych, w obecności związków rodu

lub złota prowadzi przez stadium ylidu odpowiednio na drodze przegrupowania sigmatropowego do allenu,[77] lub do 2,5-dihydrofuranu na skutek insercji migracyjnej.[78] Wspominane odmienne ścieżki reakcyjne podkreślają korzyści płynące z zastosowania podejścia fotochemicznego, stanowiącego komplementarność dostępnych już metod.

Charakter podstawników aromatycznych diarylodiazometanu ma drastyczny wpływ na stan elektronowy generowanych karbenów, a w konsekwencji na ich reaktywność. Podczas gdy bogaty w elektrony diazoalkan **4** w obecności alkinu arylowego ulega indukowanej światłem C_{sp}–H insercji (Schemat 8A), (*p*-nitrofenylo)-(*p*-metoksyfenylo)diazometan w warunkach naświetlania z tym samym reagentem prowadzi do cyklopropenu (Schemat 11B). Jeśli jednak zastosowano alkin alifatyczny, dla obydwu diazo związków powstaje produktu formalnej C_{sp3}–H insercji (Schemat 8A). [47]

Inne typy reakcji

Szeroko przebadanym typem indukowanych światłem transformacji związków diazokarbonylowych jest przegrupowanie Wollfa, w wyniku którego powstają reaktywne keteny **A**.[79] Większość doniesień naukowych w tym zakresie dotyczy reaktywności pod wpływem światła ultrafioletowego, jednak najnowsze metody opisują fotolizę także w zakresie światła widzialnego (Schemat 12). Wśród opisanych w literaturze procedur znajdują się reakcje ketenów z alkoholami lub fenolami jako reagentami nukleofilowymi[80,81] oraz katalizowane kompleksami palladu lub katalizatorami NHC reakcje cykloaddycji [n+2], umożliwiające syntezę rozbudowanych produktów heterocyklicznych.[82–85]

Ciekawym przykładem indukowanej światłem widzialnym transformacji związków diazoorganicznych jest reakcja sprzęgania dwóch diazoalkanów, spośród których tylko jeden – α-arylo-α-diazoester – absorbuje fotony z zakresu naświetlania (Schemat 13).[86] Generowane na drodze jego fotolizy karbeny typu **A** reagują z α-diazoestrami, tworząc betainy **B**. Następcza eliminacja cząsteczki azotu prowadzi do trójpodstawionych (*E*)-olefin z dobrymi i bardzo dobrymi wydajnościami i wysoką selektywnością.

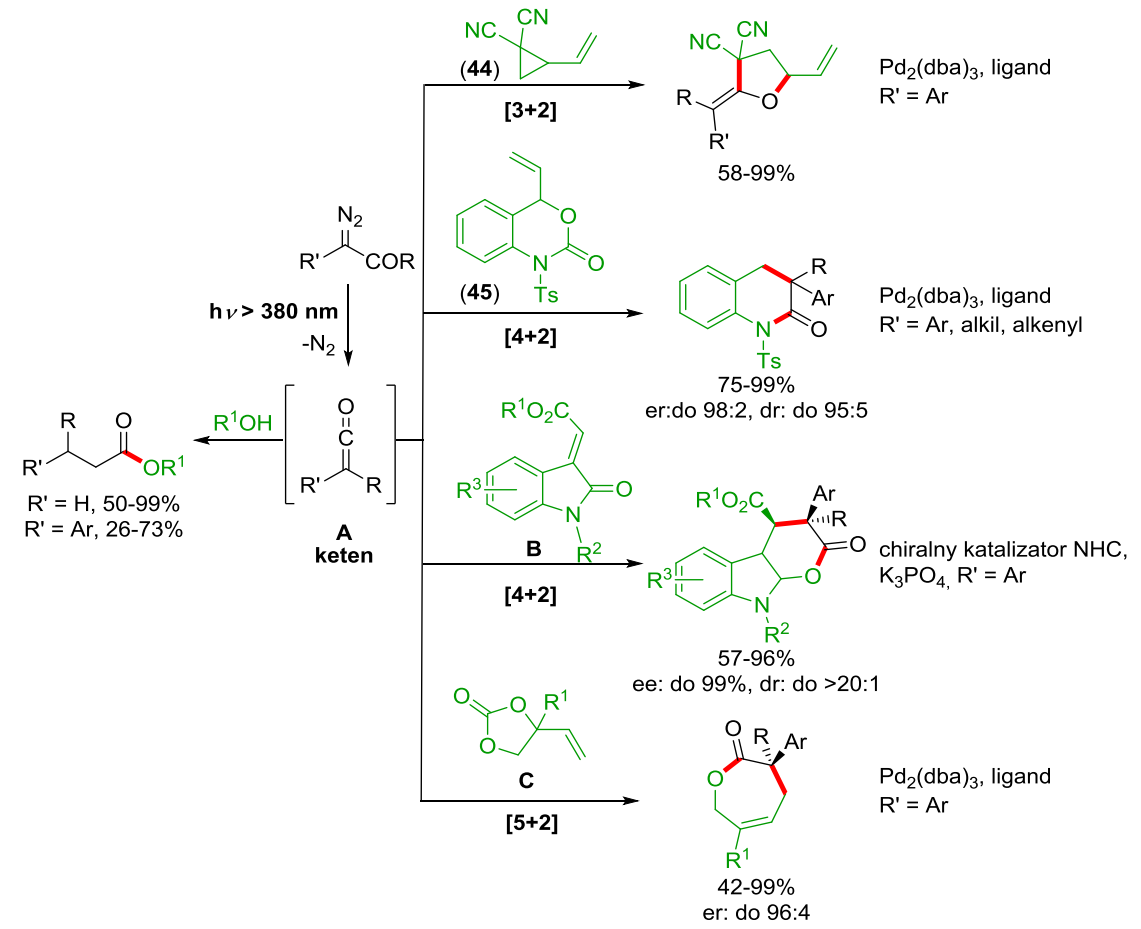

Schemat 12. Reakcje z udziałem ketenów generowanych z diazo związków pod wpływem światła widzialnego

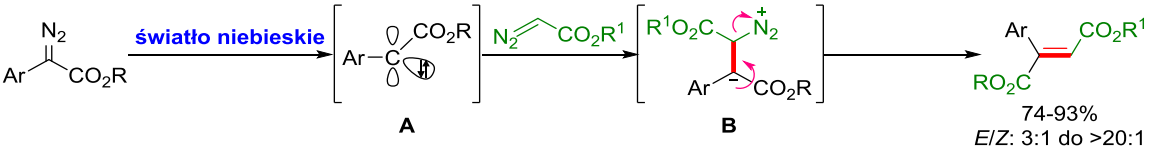

Schemat 13. Fotoindukowana reakcja sprzęgania α-arylo-α-diazoestrów z α-diazoestrami

Difenylodiazometan (**46**) w obecności światła niebieskiego i alkinu ulega reakcji kaskadowej prowadzącej do pochodnych indenu (Schemat 14).[47] Obserwowana reaktywność kontrastuje z fotochemią ubogich i bogatych w elektrony diarylodiazo-alkanów, które w takich samych warunkach ulegają odpowiednio: cykloaddycji (Schemat 11B) oraz formalnej C–H insercji (Schemat 8A). Eksperymenty mechanistyczne sugerują

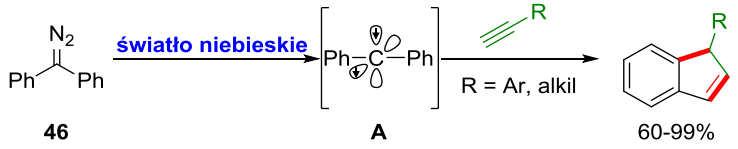

Schemat 14. Fotoindukowana reakcja sprzęgania α-arylo-α-diazoestrów z α-diazoestrami

udział karbenów trypletowych.

5.2.2.2.2. Fotokatalityczne transformacje związków diazoorganicznych

Z uwagi na prostotę metodologii oraz wysoką reaktywność α-arylo-α-diazoestrów w obecności światła niebieskiego, większość indukowanych światłem widzialnym transformacji diazo związków bazuje na bezpośredniej fotolizie. Podejście to jest jednak dostępne tylko dla diazoalkanów absorbujących fotony z zakresu naświetlania. Do przeprowadzenia reakcji z udziałem pozostałych pochodnych konieczne jest zastosowanie fotokatalizatorów, które na drodze fotoindukowanego transferu elektronu/energii generują reaktywne indywidua z diazo związków lub reagujących z nimi substratów. Biorąc pod uwagę fakt, że wiele katalizatorów fotoredoks może jednocześnie pełnić funkcję fotouczulacza, niejednokrotnie fotosensybilizacja związków diazoorganicznych może współistnieć równolegle z procesami fotoindukowanego transferu elektronu. Poniżej opisane zostały najważniejsze metody fotochemiczne, w których diazo związki są prekursorami, lub akceptorami rodników generowanych fotokatalitycznie.

Diazo związki jako prekursory rodników

Zastosowanie fotokatalizatorów o odpowiednich właściwościach redoks pozwala na redukcję diazo związków do rodników alkilowych. Tego typu sposób aktywacji został zasugerowany w 2016 roku przez grupę Meggersa w reakcji enancjoselektywnego alkilowania 2-acyloimidazoli za pomocą α-diazoestrów w obecności fotokatalizatora rutenowego i chiralnego kompleksu rodu.[87] Wówczas założono, że rodniki te generowane są na skutek redukcji α-diazoestrów, prowadzącej do wydzielenia cząsteczek azotu oraz następczego protonowania. Mechanizm ten został dokładniej zbadany przez grupę Gryko na przykładzie fotokatalitycznej metody alkilowania indoli oraz piroli (Schemat 15).[88] Analiza pomiarów prowadzonych techniką woltamperometrii cyklicznej wykazała, że potencjał α-diazooctanu etylu (**2**) jest zbyt niski, aby ulegał on redukcji na drodze transferu elektronu od wzbudzonych cząsteczek fotokatalizatora. Natomiast w wyniku protonowania diazoestru **2** powstaje forma **A**, która posiada wystarczająco wysoki potencjał redukcji, aby uczestniczyć w procesie PET z fotoreduktorem. Generowane, w konsekwencji, elektrofilowe rodniki **B** reagują z pochodną indolu prowadząc do produktów alkilowania w pozycji C-2. W przypadku diazoalkanów absorbujących w zakresie naświetlania, obserwowane są produkty funkcjonalizacji w pozycji C-3

(np. produkt **50**), co tłumaczone jest możliwym udziałem karbenów w mechanizmie reakcji. Analogiczna strategia została wykorzystana w reakcji alkilowania pochodnych imidazoli z zastosowaniem α-diazooctanu etylu (**2**, EDA).

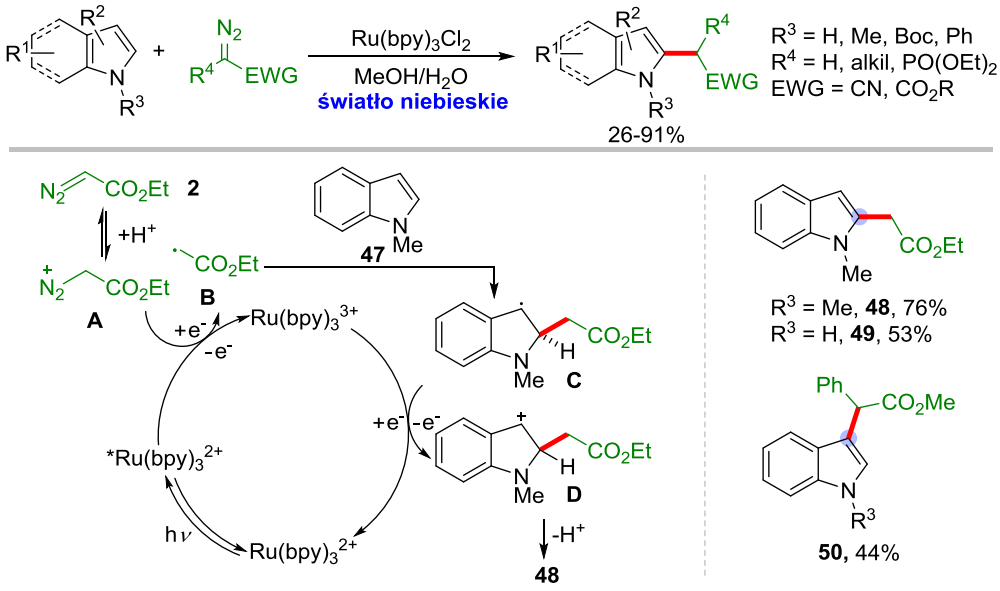

Schemat 15. Fotokatalityczna reakcja alkilowania indoli i piroli z udziałem diazo związków

α-Diazoestry mogą ulegać redukcji nie tylko na etapie wygaszania oksydatywnego fotokatalizatora, ale również na etapie regeneracji katalizatora w cyklu wygaszania reduktywnego. Wówczas, do zainicjowania reakcji katalitycznej koniecznie jest użycie zewnętrznego reduktora (np. związki **55-57**), który redukuje wzbudzony fotokatalizator do anionorodników $PC^{\bullet-}$ (Schemat 16). Podejście to zostało opracowane w 2020 roku przez grupę Doyla, a redukcję diazo związku do rodnika alkilowego typu **A** uznano za zachodzącą na drodze PCET (ang. *Proton-Coupled Electron Transfer*).[89] Generowane w obecności olefin rodniki typu **B** na skutek addycji wodoru w procesie HAT (ang. Hydrogen Atom Transfer) prowadziły do produktów hydroalkilowania z wysokimi wydajnościami (np. produkt **52**, 97%).

Metodologia ta okazała się użyteczna w wieloskładnikowych reakcjach z udziałem wodoronadtlenku lub azotynu *tert*-butylu umożliwiających syntezę, odpowiednio: δ-ketoestrów (np. **53**)[90] oraz oksymów (np. **54**).[91] Analogicznie, redukcja różnorodnych strukturalnie diazo związków poprzez PCET w obecności izocyjanianów prowadzi do syntezy fenantrydyn.[92] Opisywany mechanizm zakłada jednak PCET na etapie wygaszania oksydatywnego barwnika organicznego - Eozyny Y.

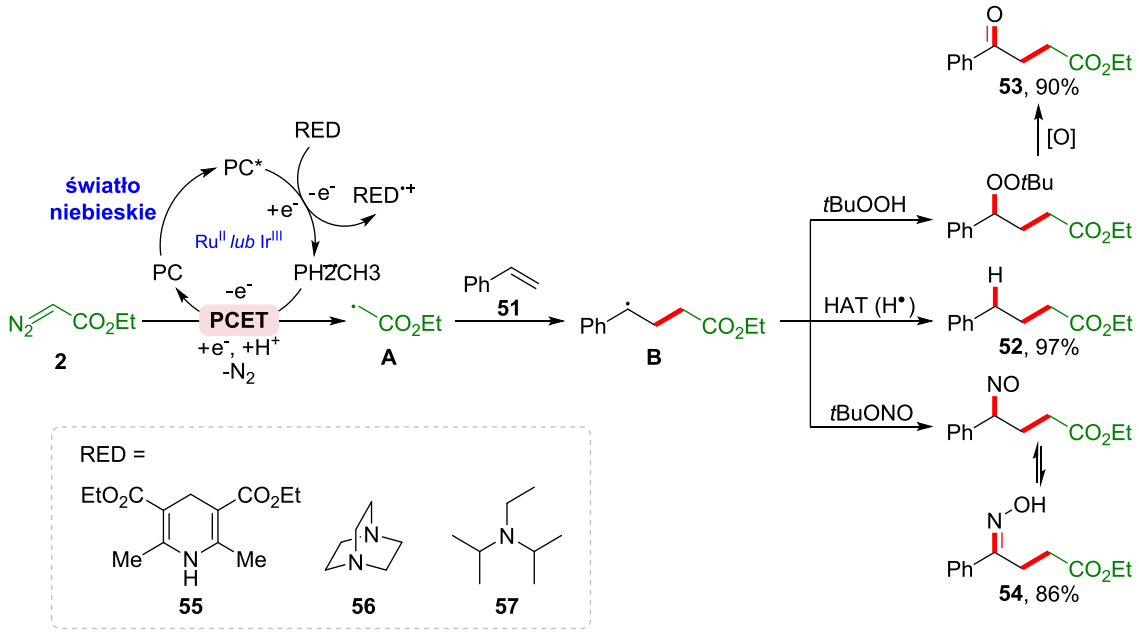

Schemat 16. Fotokatalityczna reakcje 1,2-difunkcjonalizacji olefin z użyciem diazo związków

W odpowiednich warunkach reakcji α-diazoestry **A** ulegają rozkładowi do rodników winylowych **D** (Schemat 17). Rodniki te generowane są w wyniku redukcji soli diazoniowych **C**, powstających z diazo związków typu **A** w obecności czwartorzędowych soli amoniowych. Taki sposób aktywacji α-diazoestrów **A** zastosowano w indukowanej światłem niebieskim fotokatalitycznej benzannulacji do podstawionych 1-natfoli **B**.[93] Mechanizm przemiany zakłada reakcję rodników **D** z alkinem, z wytworzeniem formy reaktywnej **E**, której cyklizacja i utlenienie zamyka cykl katalityczny reakcji. Ostatnim etapem jest wymiana kationów prowadząca do produktu końcowego **B**. Alternatywna procedura, bazująca na zbliżonym mechanizmie, wykorzystuje ester Hantzscha w roli fotokatalizatora a jej szeroki zakres stosowalności obejmuje różnorodne strukturalnie alkiny – także alkilowe i ubogie w elektrony pochodne.[94]

Fotokatalityczna redukcja związków diazoorganicznych o odpowiednio zaprojektowanej strukturze umożliwia generowanie rodników diazometylowych typu **C**, które rozpatrywane są jako tzw. ekwiwalenty karbinowe. Ta innowacyjna strategia została zaprezentowana przez Suero w 2018 roku dla hiperwalencyjnych związków jodu **A** zawierających ugrupowanie diazowe (Schemat 18A).[95] Reagenty te, stabilne w obecności światła białego, nie rozpadają się do karbenów, lecz w cyklu fotokatalitycznym ulegają redukcji do reaktywnych indywiduów **C** z zachowaniem grupy $–N_2$ w strukturze. W wyniku ich reakcji ze związkami aromatycznymi otrzymywane są α-arylo-α-diazoalkany o charakterze donorowo-akceptorowym **B**.

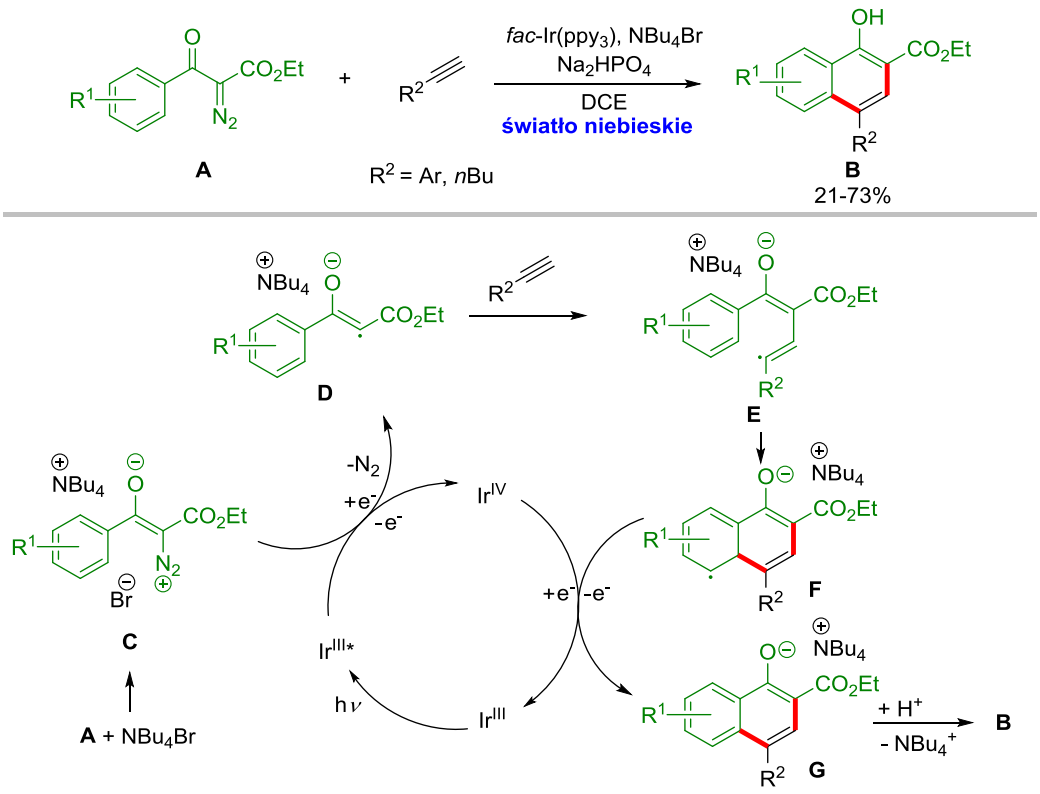

Schemat 17. Fotokatalityczna reakcja benzannulacji α-diazoketonów i alkinów

Opracowana metoda cechuje się wysoką tolerancją grup funkcyjnych, zapewniając dostęp do diazo związków także o złożonej strukturze, często problematycznych do otrzymania

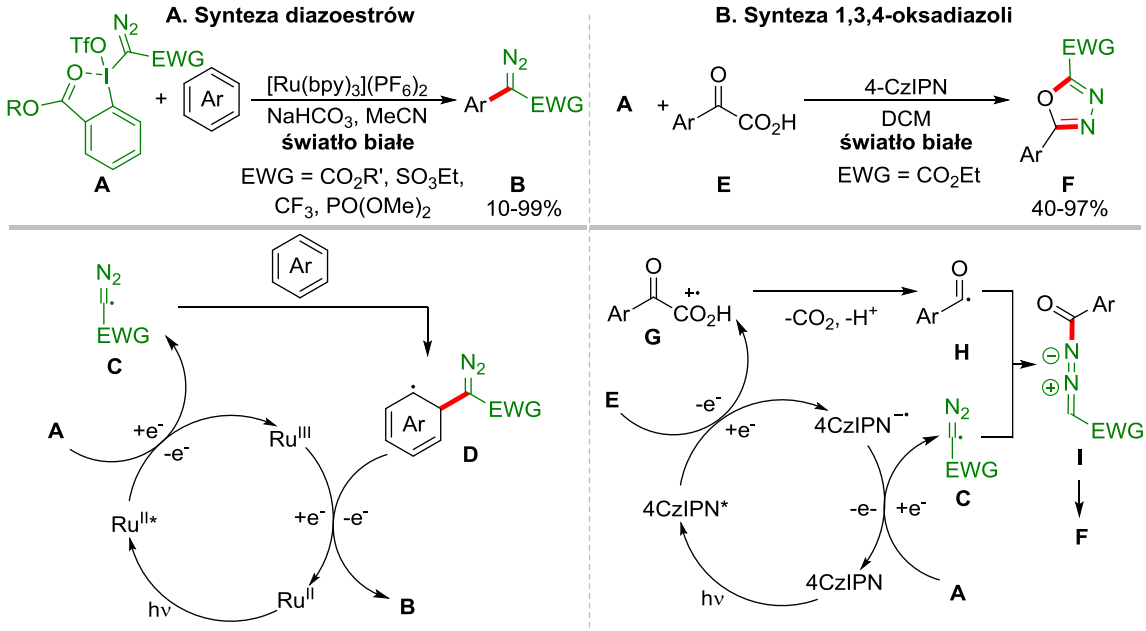

Schemat 18. Hiperwalencyjne związki jodu jako prekursory rodników diazometylowych

za pomocą standardowych metod. Zsyntezowane pochodne mogą następnie ulegać dalszym transformacjom na drodze indukowanej światłem niebieskim fotolizy do

karbenów w obecności różnorodnych reagentów. Niewątpliwie największą zaletą tego podejścia jest zatem możliwość selektywnej difunkcjonalizacji atomu węgla pierwotnie związanego z grupą N_2. Reagent **A** okazał się również skutecznym substratem do syntezy 2,5-dipodstawionych 1,3,4-oksadiazoli **F** (Schemat 18B).[96] Według proponowanego mechanizmu, heterocykle **F** powstają w wyniku reakcji rodników **H** z acylowymi rodnikami **F**, generowanymi z kwasów α-oksokarboksylowych **E**.

Innymi prekursorami rodników diazometylowych **D** są triflany typu **A**, o dodatnim ładunku zlokalizowanym na atomie siarki. W przypadku także tych reagentów, reaktywne indywidua **D** generowane są na drodze redukcji. Prekursory te wykorzystano w fotokatalitycznej reakcji syntezy diazo związków **B**, ulegających tauotomeryzacji do 1-amino-1,2,3-triazoli **C** (Schemat 19).[97] Analogiczną procedurę opracowano z zastosowaniem hiperwalencyjnych α-diazo-związków jodu.[98]

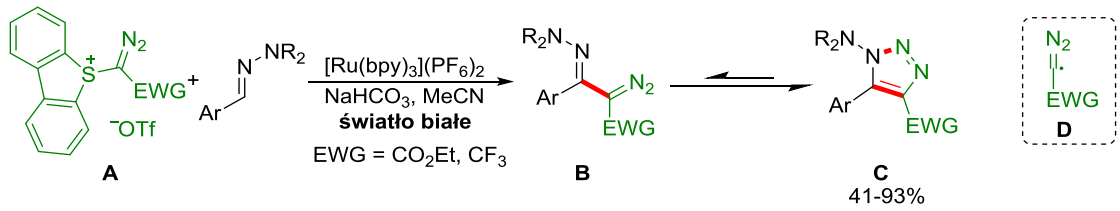

Schemat 19. Triflany jako prekursory rodników diazometylowych

W porównaniu z popularnością transformacji diazo związków przebiegających w obecności katalizatorów fotoredoks, ich aktywacja poprzez EnT jest niezwykle rzadka. W 2022 roku Koenigs zaproponował metodę syntezy furanów w wyniku fotosensybilizacji diazoalkanów akceptorowo-akceptorowych w obecności alkinów.[99] Natomiast jedna z najnowszych fotokatalitycznych metod aktywacji α-arylo-α-diazoestrów polega na ich pośrednim wzbudzeniu przez cząsteczki tetrafenyloporfiryny (H_2TPP, **58**) (Schemat 20).[48] Zastosowanie tego barwnika organicznego w roli fotouczulacza pozwala na generowanie karbenów trypletowych **A** w obecności niskoenergetycznego światła czerwonego. Transformacje z udziałem reaktywnych indywiduów **A** otrzymanych w wyniku fotoindukowanego transferu energii (EnT), w zależności od warunków reakcji, prowadzą do α-ketoestrów **B**, estrów **C**, czy cyklopropanów **D**.

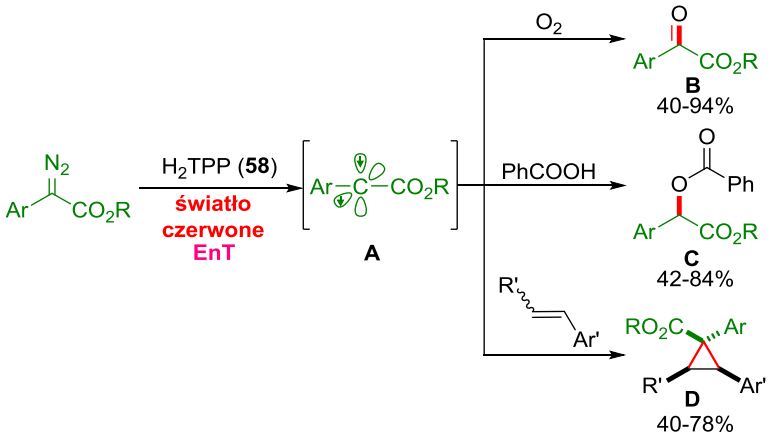

Schemat 20. Fotosensybilizacja α-arylo-α-diazoestrów

Diazo związki jako akceptory rodników

Związki diazoorganiczne są dobrymi akceptorami reaktywnych indywiduów generowanych w cyklach fotokatalitycznych. Udowodnił to zespół Gryko już w 2016 roku, prezentując metodę α-funkcjonalizacji aldehydów z zastosowaniem α-diazoestrów jako reagentów alkilujących.[19,20] Strategia ta jest przykładem katalizy podwójnej – obok katalizatora fotoredoks, dla przebiegu reakcji konieczny jest dodatek organokatalizatora – aminy, tworzącej ze związkiem karbonylowym enaminę **E** (Schemat 21).

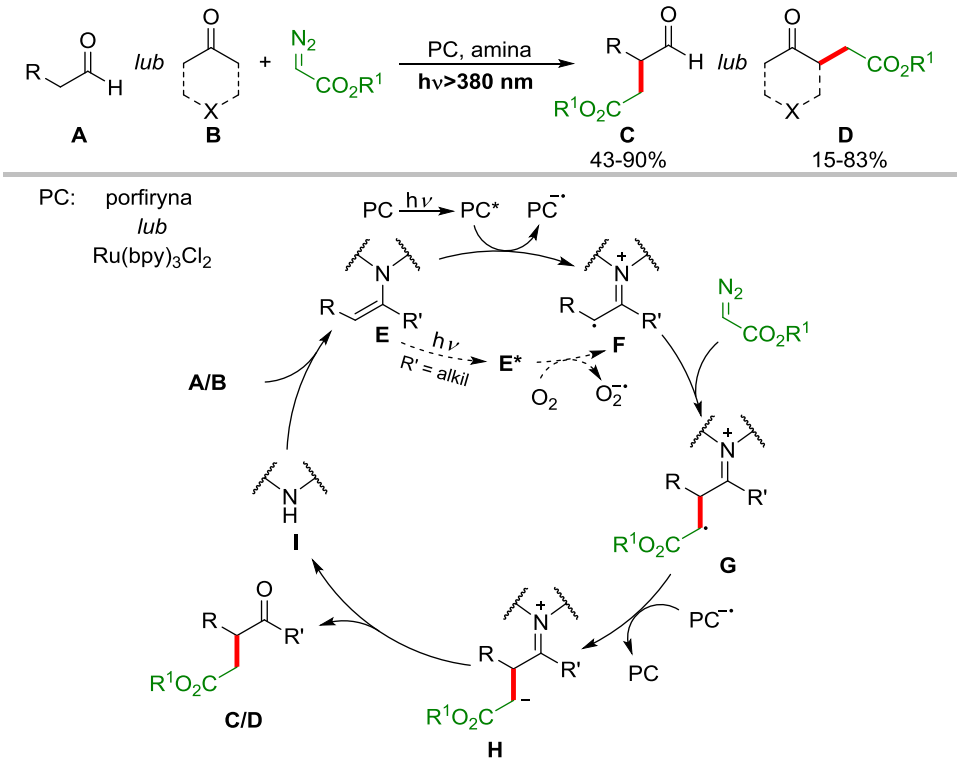

Schemat 21. Fotokatalityczne α-alkilowane aldehydów i ketonów

W wyniku fotoindukowanego transferu elektronu ulega ona utlenieniu do kationorodnika **F**, który następnie reaguje z α-diazoestrem. Powstały w ten sposób kationorodnik **G** ulega redukcji odtwarzając fotokatalizator, a hydroliza następczej betainy **H** prowadzi do produktu końcowego.

Według analogicznego mechanizmu przebiega reakcja alkilowania ketonów cyklicznych, jednak w tym przypadku niektóre produkty **D** otrzymano, choć ze znacząco niższymi wydajnościami, również w warunkach bez dodatku fotokatalizatora.[21] Eksperymenty wykazały, że niektóre enaminy **E** mogą ulegać bezpośredniemu wzbudzeniu w warunkach reakcji, a następnie utlenieniu do kationorodników **F** w obecności tlenu. Analogicznie, w badaniach nad zastosowaniem porfiryn jako katalizatorów fotoredoks w obecności światła czerwonego zespól XV IChO PAN udowodnił, że reakcja α-alkilowania 3-fenylopropanalu z udziałem EDA zachodzi wydajnie także w obecności niskoenergetycznych fotonów z zakresu promieniowania czerwonego.[100]

Diazo związki reagują również z kationorodnikami **C/H** powstałymi w wyniku fotokatalitycznego utlenienia olefin, a ich struktura ma znaczący wpływ na przebieg reakcji (Schemat 22).

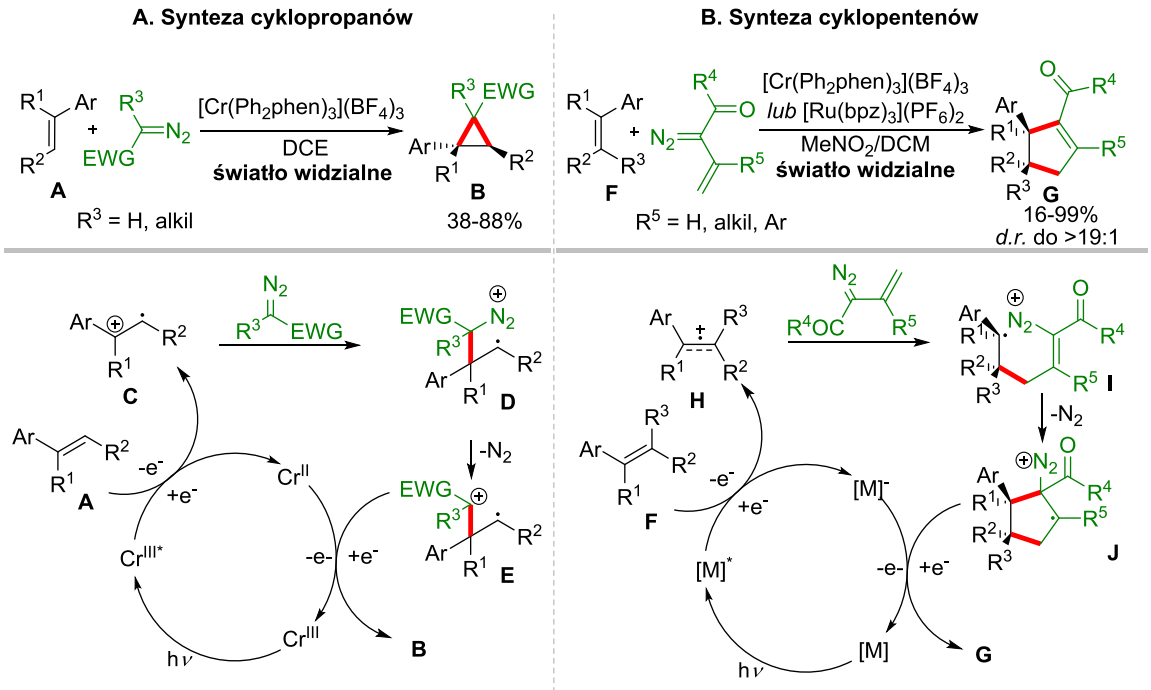

Schemat 22. Diazoalkany jako akceptory fotokatalitycznie generowanych kationorodników olefin

W przypadku α-diazo estrów oraz α-alkilo-α-diazo estrów cyklizacja form reaktywnych prowadzi do cyklopropanów **B**.[101] Natomiast dla winylowych pochodnych otrzymywane są cyklopenteny **G**.[102] Opisywane procedury wymagają zastosowania kompleksów chromu bądź rutenu w roli katalizatora fotoredoks a zakres ich stosowalności ograniczony jest do olefin o połówkowych potencjałach utlenienia mieszczących się w zasięgu właściwości utleniających stosowanego fotokatalizatora.

Innym przykładem reaktywnych indywiduów chemicznych, uczestniczących w reakcjach z α-diazoestrami są kationorodniki **C** generowane na drodze utleniania arenów (Schemat 23).[103] Opracowana procedura zakłada użycie stechiometrycznych ilości obydwu reagentów a w przypadku obecności kilku podstawników w pierścieniu aromatycznym substratu, zwykle obserwuje się mieszaninę regioizomerów alkilowania. Postulowany mechanizm sugeruje udział związku bicyklicznego **D**, ulegającego utlenieniu z otworzeniem pierścienia. Następcza redukcja prowadzi do produktu alkilowania **A**.

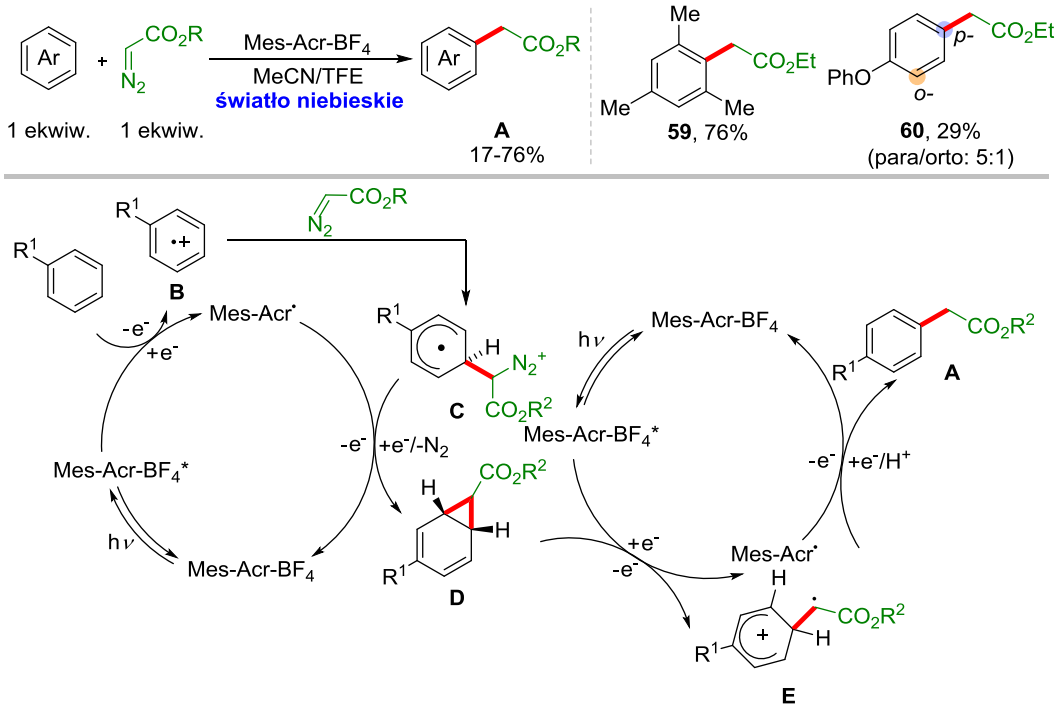

Schemat 23. Fotokatalityczne alkilowanie arenów

Obok fotochemicznych reakcji z kationorodnikami, diazo związki mogą reagować z rodnikami o obojętnym ładunku eklektycznym. Wśród tego typu reaktywności wyróżniamy reakcje z indywiduami o niesparowanym elektronie na atomie węgla oraz tlenu (Schemat 24). Estry *N*-hydroksyftalimidu **A** są dobrze zbadanymi prekursorami

rodników węglowych o różnej rzędowości. Rodniki te, wytworzone w cyklach fotokatalitycznych, reagują z różnorodnymi strukturalnie związkami diazoorganicznymi z otrzymaniem hydrazonów **B** (Schemat 24A)[104]. Z kolei bromki **E** są źródłem rodników acylowych, które w obecności tlenu ulegają konwersji do rodników zlokalizowanych na atomie tlenu **H**. W wyniku ich reakcji z α-diazoestrami otrzymywane są estry kwasu szczawiowego **F** (Schemat 24B).[105]

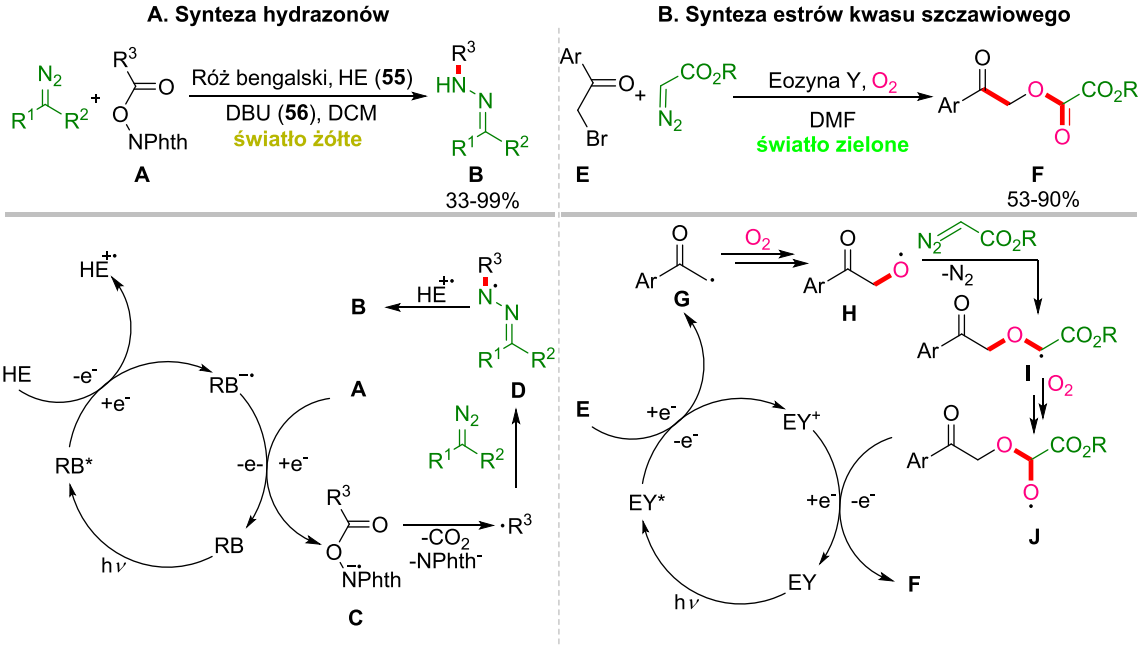

Schemat 24. Związki α-diazokarbonylowe jako akceptory rodników

Diazo związki reagują nie tylko z wytworzonymi w cyklach fotokatalitycznych rodnikami, ale również z formami będącymi wynikiem ich przemian. Przykładem takiej transformacji jest indukowana światłem zielonym reakcja związków α-diazo-karbonylowych z aminami trzeciorzędowymi **A** (Schemat 25).[106] Kationorodniki **C**, generowane z amin na drodze wygaszania reduktywnego fotokatalizatora, ulegają eliminacji wodoru w obecności jonów $O_2^{\bullet-}$. W konsekwencji, tworzą się kationy **D** i to z tymi indywiduami reagują diazo związki prowadząc do otrzymania β-amino-α-diazoalkanów **B**. Według analogicznego mechanizmu zachodzi również fotochemiczna reakcja Mannicha z udziałem amin trzeciorzędowych i enolowych związków diazoorganicznych[107] oraz fotochemiczna reakcja *N*-arylowych pochodnych glicyny z α-diazoestrami prowadząca do *N*-arylowych azyrydyn.[108]

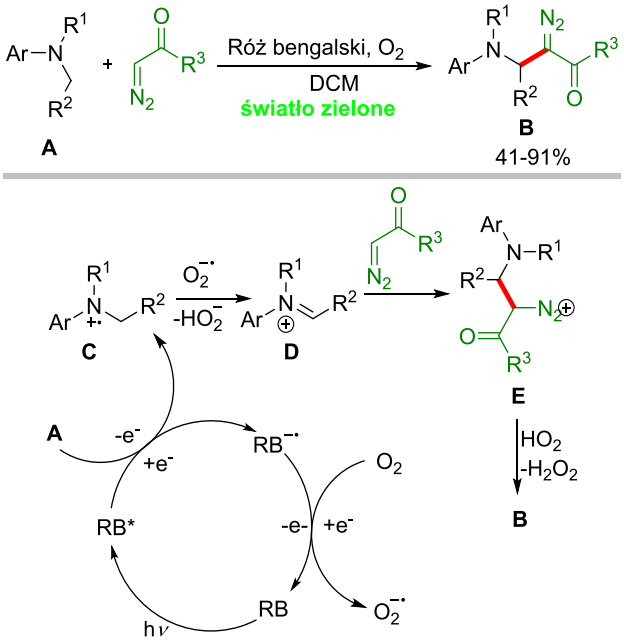

Schemat 25. Związki α-diazokarbonylowe jako akceptory kationów iminiowych

5.2.3. 1,3,4-Oksadiazoliny jako prekursory niestabilnych diazoalkanów i karbenów

1,3,4-Oksadiazoliny reprezentują różnorodną strukturalnie grupę prekursorów związków diazoorganicznych oraz karbenów. Wśród ich zalet wymienić należy przede wszystkim prostotę syntezy, zwykle możliwej do przeprowadzenia z handlowo dostępnych substratów oraz wysoką stabilność większości pochodnych. Ponadto, w zależności od warunków reakcji, związki te stanowią źródło odmiennych indywiduów chemicznych, tj. karbeny, ylidy, diazoalkany, a nawet rodniki (Schemat 26).[44,45,109] W wyniku termolizy 1,3,4-oksadiazoliny ulegają 1,3-dipolarnej cyklorewersji z wydzieleniem azotu i generowaniem ylidu karbonylowego **B**.[109] Ylidy te uczestniczą w dalszych przekształceniach, bądź rozpadają się do nukleofilowych karbenów podstawionych heteroatomami **C**. Podejście to znalazło szerokie zastosowanie do syntezy różnych związków heterocyklicznych z udziałem 2,2-dimetoksylowych pochodnych jako prekursorów karbenu dimetoksylowego.[110]

Ponadto, badania reaktywności oksadiazolin pod wpływem impulsów laserowych wykazały ich rozpad do wysoce reaktywnych, niestabilizowanych karbenów **D** (Schemat 26).[111,112] Mechanizm tego rodzaju aktywności pozostaje jednak nieznany, a indywidua te w obecności reagentów wychwytujących np. pirydyny identyfikowane są jako ylidy.

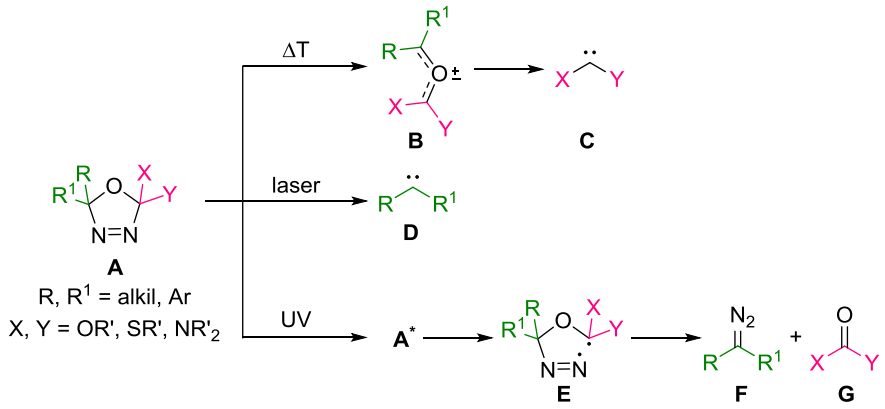

Schemat 26. 1,3,4-Oksadiazoliny jako prekursory reaktywnych indywiduów

1,3,4-Oksadiazoliny wykazują absorpcję w zakresie światła ultrafioletowego, o lokalnych maksimach dla dialkoksylowych pochodnych zlokalizowanych w zakresie: 218-230 mm oraz 318-326 nm i odpowiadających przejściom π→π* oraz n→π*.[113] Pod wpływem światła UV dochodzi zatem do bezpośredniego wzbudzenia reagenta **A**, a w konsekwencji do zerwania wiązania C–N z wytworzeniem rodnika diazenylowego **E** (Schemat 26). Rodnik ten ulega rozpadowi na diazoalkan **F** oraz związek karbonylowy **G**.

Mimo, iż pierwsza fotoliza 1,3,4-oksadiazoliny została przeprowadzona już w 1968 roku,[114] dopiero pół wieku później grupa Ley zaprezentowała syntetyczne zastosowanie 2-metoksy-2-metylo pochodnych jako prekursorów niestabilizowanych diazoalkanów. Analiza widm spektroskopowych IR naświetlanego roztworu prekursora **61** wykazała obecność pasm charakterystycznych dla drgań grupy diazowej oraz grupy karbonylowej estru **62**, potwierdzając generowanie diazoalkanu **63** w warunkach reakcji (Schemat 27A).[115] Fotoliza w wyniku bezpośredniego wzbudzenia jest procesem szybkim, dlatego aby uniknąć niebezpiecznej akumulacji wysoce reaktywnych diazo związków transformacje 2-metoksy-2-metylooksadiazolin realizowano w reaktorze przepływowym. Opisane podejście zastosowano do przeprowadzenia reakcji, bazujących na addycji nukleofilowej diazoalkanów z następczym wydzieleniem cząsteczek azotu (Schemat 27B). Otrzymane na skutek sprzęgania z kwasami boronowymi pochodne **B** przekształcono w alkany **C** oraz alkohole trzeciorzędowe **D**.[115] Z kolei transformacje z udziałem aldehydów, przebiegające według mechanizmu jonowego z 1,2-H migracją, pozwoliły na otrzymanie ketonów arylowo-alkilowych oraz alkilowo-alkilowych lub homologów formaldehydu **F**.[116,117] Opracowano również wieloskładnikową reakcję syntezy alkoholi homoallilowych **H** z zastosowaniem oksadiazolin jako prekursorów diazo związków, winylowych kwasów boronowych oraz aldehydów.[118]

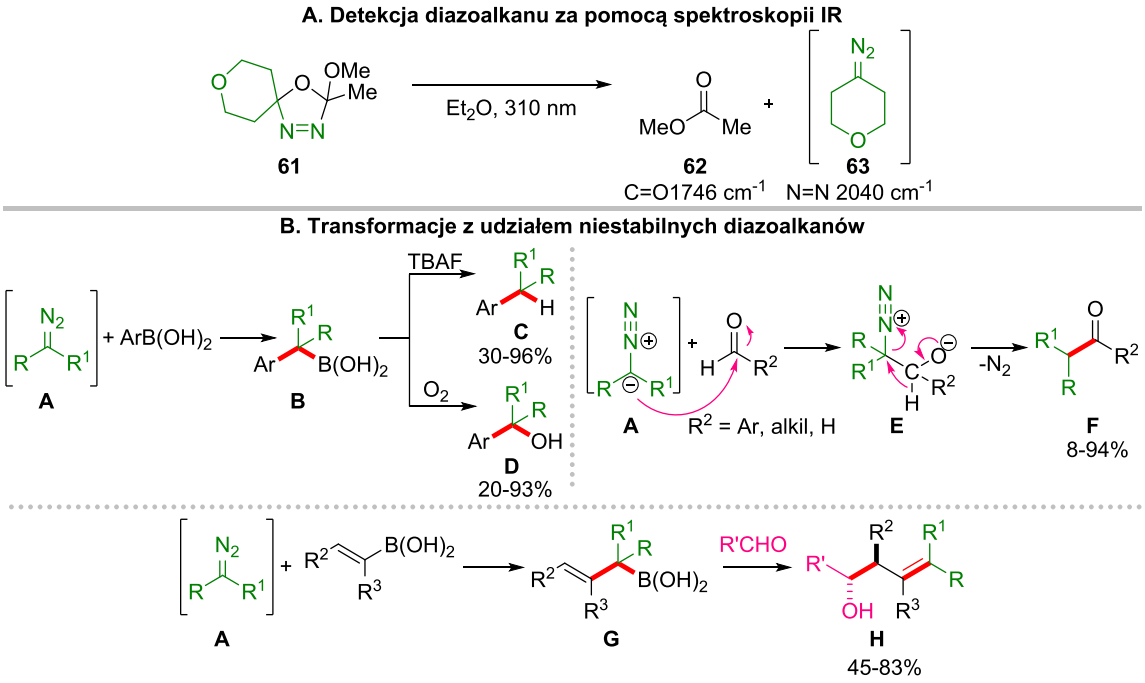

Schemat 27. Indukowane światłem UV transformacje chemiczne z udziałem 1,3,4-oksadiazolin

5.2.4. Podsumowanie

Związki diazoorganiczne są reagentami, które znalazły szerokie zastosowanie w transformacjach organicznych. Ich znaczenie syntetyczne wynika przede wszystkim z prostoty syntezy, także *in situ* oraz bogatej różnorodności strukturalnej i wysokich reaktywności. Klasyczne metody ich aktywacji opierają się jednak na katalizie drogimi i toksycznymi obecnością wprowadzonych grup kierujących w cząsteczkach substratów. Z kolei naświetlanie wysokoenergetycznym światłem ultrafioletowym prowadzi często do licznych produktów ubocznych na skutek nieselektywnego wzbudzania wielu chromoforów.

Przełomowe odkrycie Davisa i Jurberga z 2018 roku stało się punktem zwrotnym w chemii karbenów generowanych fotochemicznie. Od tego momentu nastąpił gwałtowny wzrost zainteresowania fotolizą związków diazoorganicznych pod wpływem światła widzialnego. Sukcesywnie przeprowadzono reakcje wydajnie prowadzące do produktów insercji, cykloaddycji i przegrupowania. Dotychczas opracowane metodologie skupiają się głównie na zastosowaniu α-arylo-α-diazoestrów, które absorbują światło z zakresu 400-500 nm, odpowiadającego barwie niebieskiej. Nieliczne procedury syntetyczne obejmują również α-arylo-α-diazoketony i α-trifluorometylo-α-arylo-diazometan, jednak reakcje z ich udziałem zwykle cechują się niskimi selektywnościami.

Ostatnio, grupa Koenigsa wykazała, że diarylodiazoalkany pochłaniają promieniowanie w zakresie 500-600 nm. Choć na ten moment jest to grupa diazo związków w niewielkim stopniu przebadana pod kątem reaktywności fotochemicznej, z pewnością tematyka ta będzie zgłębiana w najbliższych latach. Wśród wyzwań bezpośredniej fotolizy pod wpływem światła widzialnego znajdują się dalsze projektowanie nowych transformacji oraz opracowanie warunków dla innych diazoalkanów donorowo-akceptorowych, wykazujących absorpcję w zakresie >380 nm.

Dla indukcji reaktywności pozostałych diazo związków, które nie pochłaniają światła widzialnego, atrakcyjnym rozwiązaniem jest zastosowanie metod fotokatalitycznych. Choć na ten moment opracowano jeszcze niewiele takich transformacji, oferują one dostęp do zarówno karbenów trypletowych, jak i rodników, bądź pozwalają na zastosowanie diazoalkanów jako biernych akceptorów form reaktywnych. Obecnie, istnieje potrzeba znaczącego wzbogacenia portfolio reakcji fotokatalitycznych z udziałem związków diazoorganicznych. Pożądane jest również opracowanie większej ilości metod alternatywnych, które umożliwią zastąpienie kompleksów metali barwnikami organicznymi w roli fotokatalizatora. Ponadto, większość znanych transformacji bazuje na naświetlaniu światłem fioletowym/ niebieskim. Korzystnym z punktu widzenia potencjalnych aplikacji biologicznych, będzie zastąpienie go światłem niskoenergetycznym np. czerwonym.

Niestety, z uwagi na niską trwałość i silne właściwości wybuchowe, dostęp do diazoalkanów niestabilizowanych jest wciąż utrudniony. W literaturze znane są różnorodne prekursory homologów diazometanu, wśród których wysoką stabilnością i unikalną reaktywnością wyróżniają się 1,3,4-oksadiazoliny. Mimo, iż wykazano, że pod wpływem światła UV rozkładają się one do diazoalkanów, ich reaktywność w obecności światła widzialnego pozostaje nieznana.

Powyższy przegląd literaturowy potwierdza, że metody indukowane światłem widzialnym stanowią dobrą alternatywę dla wcześniej opracowanych strategii aktywacji diazo związków. Podejście to charakteryzuje się łagodnymi warunkami reakcji, które zwykle nie wymagają stosowania dużych rozcieńczeń, bezwodnych rozpuszczalników czy eliminacji tlenu. Reakcje te dają dostęp nie tylko do karbenów i ylidów, ale również reaktywnych rodników. W konsekwencji, dostępne są innowacyjne ścieżki reakcyjne, czyniąc fotochemię w obecności światła widzialnego strategią komplementarną

i konkurencyjną w stosunku do tradycyjnych metod. Podejście to wciąż jednak nie zostało jeszcze dostatecznie zbadane i wymaga wprowadzenia nowych rozwiązań, niezbędnych do eliminacji jego ograniczeń. Tematyka ta stanowi zatem interesujący przedmiot do dalszych badań naukowych, a osiągnięcia z nich wynikające stanowić będą istotny wkład w nowoczesną syntezę organiczną.

5.3. Badania własne

Mimo, iż początki fotochemii sięgają XX wieku, dopiero od niedawna reakcje indukowane światłem widzialnym stały się przedmiotem intensywnych badań. Wykorzystanie promieniowania widzialnego jako źródła energii do tworzenia nowych wiązań chemicznych jest szeroko docenianym podejściem, lecz jego potencjał nie został jeszcze w pełni poznany. Wciąż istnieje potrzeba odkrywania nowych reaktywności znanych reagentów i projektowania indukowanych światłem metodologii, pozwalających na otrzymywanie struktur będących wyzwaniem współczesnej chemii organicznej. **Celem mojej pracy doktorskiej było wykorzystanie fotochemicznych przemian diazoalkanów i 1,3,4-oksadiazolin do opracowania nowych metod tworzenia wiązań C−C w obecności światła widzialnego.** W poniższym rozdziale opisałam zaprojektowane przeze mnie indukowane światłem widzialnym metody, wykorzystujące jako substraty różnorodne strukturalnie diazo związki, a także 1,3,4-oksadiazoliny – ich znane prekursory. W kolejnych podrozdziałach przedstawiam strategie bazujące na wszystkich możliwych sposobach aktywacji fotochemicznej: bezpośrednim wzbudzeniu, fotosensybilizacji oraz katalizie fotoredoks. Część z opracowanych metod wymaga zastosowania kompleksu metalu, bądź barwnika organicznego w roli fotouczulacza, bądź katalizatora fotoredoks.

Najbardziej popularną grupę fotokatalizatorów stanowią kompleksy irydu i rutenu, jednakże z uwagi na ich wysoką cenę i toksyczność, chętnie zastępowane są one barwnikami organicznymi. Rozdział *Sulfur Heterocycles* w monografii *Photoorganocatalysis in Organic Synthesis* przygotowany we współpracy z dr Katarzyną Goliszewską obejmuje zestawienie powszechnie stosowanych organicznych fotokatalizatorów siarkowych tj. błękit metylenowy, fenotiazyny i sole tiapyryliowe, ze szczególnym podkreśleniem właściwości fotofizycznych oraz mechanizmów typowych dla reakcji katalizowanych przez dane grupy barwników.

[R1] K. Goliszewska, **K. Orłowska**, D. Gryko
Photoorganocatalysis in Organic Synthesis, Chapter 4: Sulfur Heterocycles.
World Scientific Publishing Company, 2019. (rozdział w monografii naukowej)

5.3.1. Indukowana światłem widzialnym reakcja Doyla-Kirmsego

Struktury o skumulowanych układach wiązań podwójnych, tj. alleny, są występującymi w naturze związkami o unikalnych właściwościach biologicznych, jednakże ich efektywna synteza wciąż stanowi wyzwanie. Wykazano, że związki te są reaktywnymi substratami, uczestniczącymi w reakcjach cykloizomeryzacji, cykloaddycji oraz sprzęgania, a ich struktura ma znaczący wpływ na selektywność reakcji.[119–122] Wśród wydajnych metod syntezy 1,2-dienów wyróżniamy, na przykład przegrupowanie [2,3]-sigmatropowe ylidów siarkowych lub tlenowych, generowanych z sulfidów/alkoholi propargilowych i diazo związków w obecności soli np. żelaza, srebra, rodu.[67,123,124] Taka strategia, początkowo opracowana dla sulfidów allilowych przez Kirmsego, została dalej rozwijana przez Doyla, m.in. dla pochodnych propargilowych. Niestety opracowane metodologie wymagają użycia toksycznych związków metali, co znacząco podwyższa koszty syntez i czyni je nieprzyjaznymi dla środowiska oraz przemysłu farmaceutycznego. **Odkrycie zjawiska absorpcji światła widzialnego przez α-arylo-α-diazoestry oraz interesujące właściwości allenów zainspirowały mnie i dr Katarzynę Rybicką-Jasińską do opracowania fotochemicznej reakcji Doyla-Kirmsego z udziałem α-arylo-α-diazo-estrów i sulfidów propargilowych.**

Optymalizacja warunków reakcji modelowej diazoalkanu **64** z sulfidem **65** pozwoliła na otrzymanie produktu **66** z wysoką wydajnością w obecności światła niebieskiego, bez dodatku katalizatora oraz konieczności stosowania bezwodnego rozpuszczalnika i atmosfery gazu obojętnego (Schemat 28). Eksperymenty kontrolne potwierdziły, że światło niebieskie jest czynnikiem niezbędnym dla wydajnego przebiegu reakcji. Mimo, iż diazoalkan **64** wykazuje nieznaczną absorpcję w zakresie światła zielonego, jest ona niewystarczająca do produktywnej fotolizy, natomiast w wyniku naświetlania UV powstaje złożona mieszanina produktów na skutek nieselektywnego wzbudzenia reagentów.

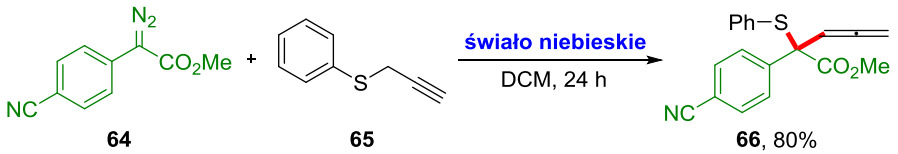

64 **65** **66**, 80%

Warunki reakcji: diazoester **64** (0.15 mmol, dodawany w dwóch porcjach: pierwsza w t = 0 h, druga w t = 3 h), sulfid **65** (1.35 mmol, 9.0 ekwiw.), $DCM_{cz.d.a.}$ (0.3 M), niebieska dioda LED (455÷475 nm, 3 W), RT, 24 h.

Schemat 28. Fotochemiczny wariant reakcji Doyla-Kirmsego – reakcja modelowa

Opracowane optymalne warunki reakcji wykorzystałam następnie do zbadania zakresu i ograniczeń stosowalności metody w odniesieniu do diazo związków (Schemat 29). Proponowana strategia pozwala na otrzymanie allenów **66-85** z dobrymi i bardzo dobrymi wydajnościami nie tylko z α-arylo-α-diazoestrów, ale także dla α-arylo-α-diazoeketonu (produkt **82**, 43%). Dobrze tolerowane są pochodne o pierścieniach aromatycznych, podstawionych różnorodnymi grupami funkcyjnymi z niewielkim spadkiem wydajności dla pochodnej *p*-nitrowej **69** i *p*-metoksylowej **70**. Rodzaj grupy estrowej oraz pozycja podstawnika w pierścieniu nieznacznie wpływa na wydajność reakcji (związki **74-76** i **79-81**, **85**). Metoda pozwala również na otrzymanie allenów zawierających w swojej strukturze pierścienie naftalenu lub tiofenu. Indukowana światłem synteza jest bardzo dobrze skalowalna, z zachowaniem wysokich wydajności (produkt **67**), a jej jedynym istotnym ograniczeniem jest konieczność stosowania diazo związku, który absorbuje światło niebieskie. Równolegle do opisywanych badań, grupy Koenigsa i Xiao opublikowały komplementarne strategie z wykorzystaniem sulfidów allilowych do syntezy pochodnych homoallilowych.[63,64] Co ciekawe, analogiczna reakcja opracowana z zastosowaniem alkoholi propargilowych prowadzi do pochodnych cyklopropenu (Sekcja 5.2.2.2.1., Schemat 11B).[76]

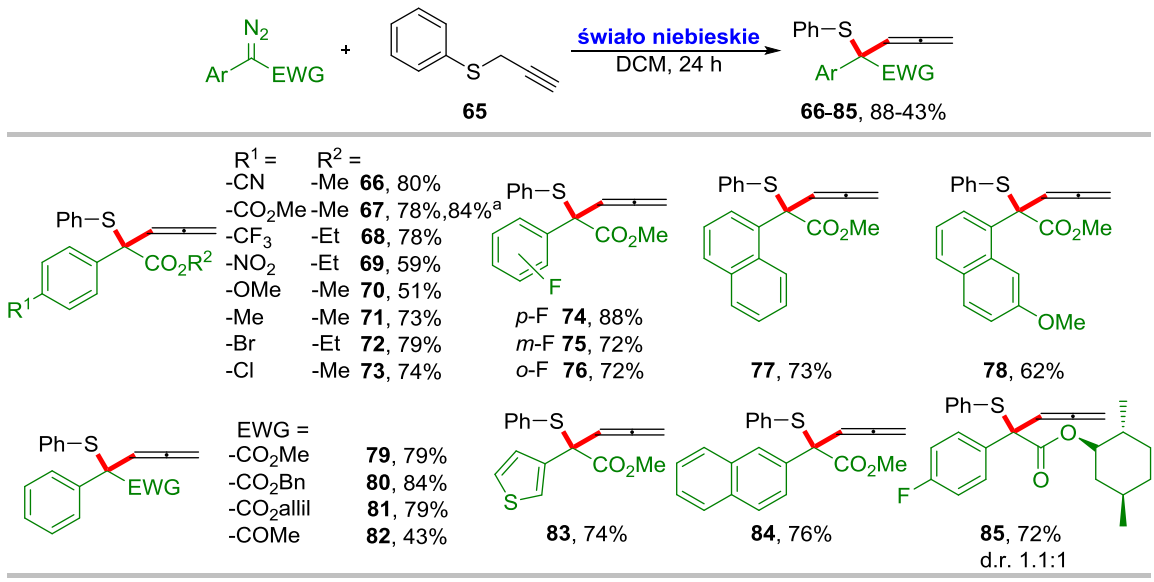

Warunki reakcji: diazoester (0.15 mmol, dodawany w 2 porcjach: pierwsza w t = 0 h, druga w t = 3 h), sulfid **65** (1.35 mmol, 9.0 ekwiw.), $DCM_{cz.d.a.}$ (0.3 M), niebieska dioda LED (455÷475 nm, 3 W), RT, 24 h. [a]skala: 1 mmol.

Schemat 29. Zakres stosowalności opracowanej metody w odniesieniu do związków α-arylo-α-diazokarbonylowych

W oparciu o doniesienia literaturowe zaproponowałam mechanizm reakcji, inicjowany przez bezpośrednie wzbudzenie związku α-arylo-α-diazo karbonylowego

(Schemat 30). W wyniku następczej fotolizy, z wydzieleniem cząsteczek azotu, generowane są karbeny singletowe **A**, które w wyniku przejścia międzysystemowego (ISC) mogą przekształcać się w karbeny trypletowe **B**. Niezależnie od multipletowości, indywidua te reagują z sulfidem tworząc ylidy **C**, ulegające przegrupowaniu [2,3]-sigmatropowemu do żądanego allenu.

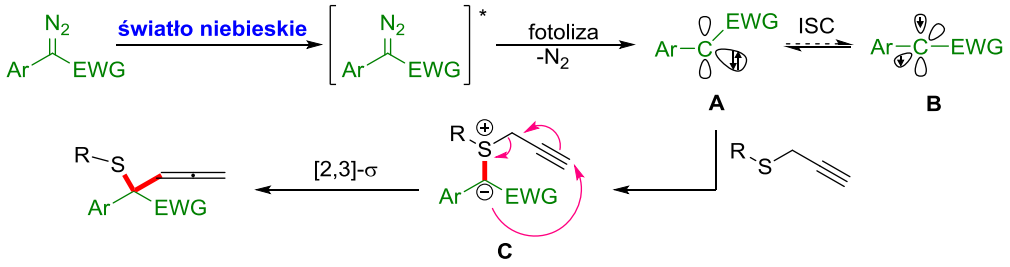

Schemat 30. Proponowany mechanizm reakcji

Przeprowadzone przeze mnie eksperymenty mechanistyczne wskazują na przeważający udział karbenów singletowych w mechanizmie reakcji. W wyniku fotosensybilizacji diazo związków generowane są karbeny trypletowe. Zatem spadek wydajności reakcji w obecności tetrafenyloporfiryny (**58**) jako fotouczulacza stanów trypletowych dowodzi, że indywidua te nie odgrywają istotnej roli w mechanizmie reakcji (Schemat 31A). Dodatkowo, indukowane światłem widzialnym cyklopropanowanie z udziałem *cis*-stilbenu (**87**) zachodzi w sposób stereospecyficzny z przewagą izomeru *cis*, co dodatkowo wyklucza zaangażowanie karbenów trypletowych (Schemat 31B).

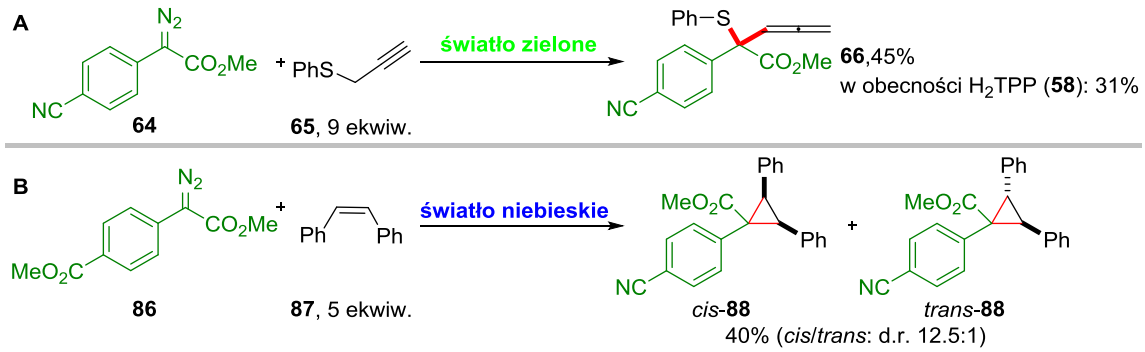

Schemat 31. Determinacja multipletowości karbenu – eksperymenty. **A.** Wpływ dodatku fotouczulacza **B.** Diastereoselektywne fotochemiczne cyklopropanowanie

Powyższe wyniki zostały opublikowane w artykule naukowym:

[P1] **K. Orłowska**, K. Rybicka-Jasińska, P. Krajewski, D. Gryko Photochemical Doyle–Kirmse Reaction: A Route to Allenes, *Org. Lett.* **2020**, *22*, 1018-1021.

5.3.2. Indukowana światłem widzialnym fotokatalityczna synteza spirocyklopropanów z udziałem 1,3,4-oksadiazolin

Wysoka reaktywność, a w konsekwencji silne właściwości wybuchowe niestabilizowanych diazo związków przyczyniają się do ich ograniczonego zastosowania syntetycznego. Dla zachowania bezpieczeństwa tego typu pochodne otrzymuje się *in situ* z bardziej stabilnych prekursorów, jednak problematyczna synteza i konieczność kontrolowania warunków reakcji powoduje, że znanych transformacji z udziałem prostych diazoalkanów jest znacznie mniej niż tych, w których biorą udział stabilizowane analogi. Wysoką trwałością oraz łatwym dostępem do różnorodnie sfunkcjonalizowanych pochodnych charakteryzują się 1,3,4-oksadiazoliny. Podczas, gdy w warunkach termicznych rozkładają się do karbenów podstawionych heteroatomami, ich fotoliza pod wpływem światła ultrafioletowego generuje niestabilizowane diazo związki.[44] **Niestety, wysokoenergetyczne światło UV negatywnie wpływa na selektywność reakcji fotochemicznych i ogranicza zakres ich stosowalności. Dlatego też postanowiłam opracować strategię umożliwiającą aktywację 1,3,4-oksadiazolin w łagodniejszych warunkach - w obecności światła widzialnego.**

1,3,4-Oksadiazoliny nie absorbują światła z zakresu >380 nm, zatem do ich aktywacji pod wpływem światła widzialnego koniecznie było zastosowanie fotokatalizatora o odpowiednich właściwościach. Jednak wartości potencjałów utlenienia i redukcji tych prekursorów znacząco odbiegają od możliwości utleniających/ redukujących dostępnych katalizatorów fotoredoks, co wyklucza skuteczność tego podejścia. Zdecydowałam się więc na opracowanie rozwiązania bazującego na fotoindukowanym transferze energii (EnT), które powinno umożliwić generowanie diazoalkanów lub karbenów trypletowych z 1,3,4-oksadiazolin. W celu oszacowania poziomów trypletowych różnorodnych pochodnych oksadiazolin, prof. Irena Deperasińska wykonała obliczenia kwantowo-mechaniczne przybliżające wartości dla pochodnych **89-93** (Schemat 32A). Otrzymane dane teoretyczne sugerują, że użycie w roli fotouczulacza popularnego kompleksu irydu **91** (E_T = 258 kJ/mol), o energii trypletowej zbliżonej do wartości wyliczonych dla oksadiazolin, umożliwiłoby wydajny proces fotosensybilizacji. Przeprowadzone przeze mnie eksperymenty wstępne potwierdzają tę hipotezę, bowiem w obecności światła niebieskiego oksadiazolina **90** ulega konwersji przy zastosowaniu katalizatora **91**, podczas gdy w warunkach bez jego dodatku konwersja ta jest znikoma (Schemat 32B). Dodatkowo, fotokatalityczny rozkład

prowadzi do m.in. cykloheksenu (**94**) jako produktu 1,2-migracji wodoru, co wskazuje na możliwy udział karbenów trypletowych.

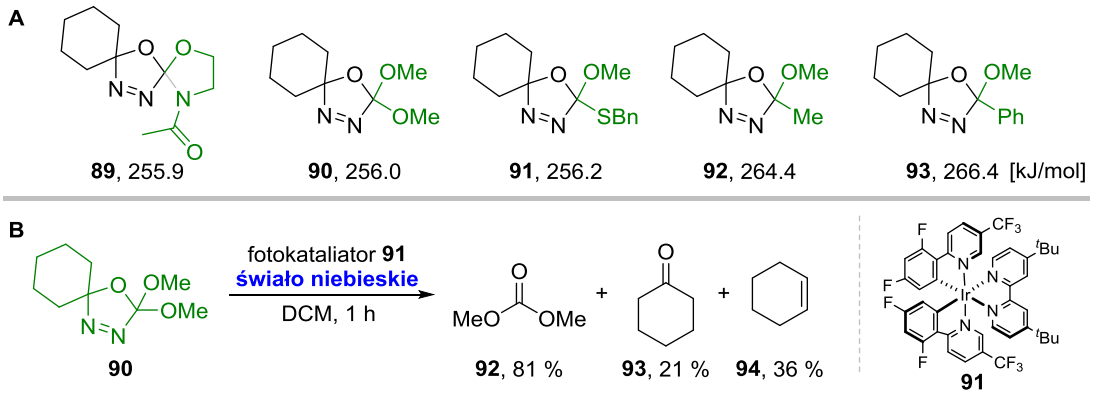

Warunki reakcji: Ir[dF(CF$_3$)ppy)$_2$(dtbpy)]PF$_6$ (**91**, 0.5 mol%), oksadiazolina **90** (0.1 mmol), DCM$_{bezw.}$ (0.05 M), niebieskie diody LED (450 nm, 25 W), 25 ^{o}C, [Ar], 17 h.

Schemat 32. Fotosensybilizacja 1,3,4-oksadiazolin – eksperymenty wstępne **A.** Zależność energii trypletowej od struktury **B.** Fotokatalityczny rozkład oksadiazoliny **90**

Użyteczność syntetyczną zaprojektowanego podejścia wykazałam na przykładzie transformacji z udziałem ubogich w elektrony olefin, prowadzącej do syntezy zwykle trudno dostępnych spirocyklopropanów. Przeprowadzone przeze mnie badania mające na celu optymalizację warunków reakcji pozwoliły na otrzymanie produktu **96** z bardzo dobrą wydajnością (81%, Schemat 33). Na tym etapie badań potwierdziłam, że właściwości fotofizyczne fotokatalizatora mają kluczowy wpływ na przebieg reakcji cyklopropanowania. Zastosowanie fotouczulacza o zbyt niskiej wartości E_T, spodziewanie, skutkowało brakiem bądź śladową konwersją prekursora **90**. Zweryfikowałam również wpływ podstawienia C-2 w strukturze 1,3,4-oksadiazoliny na wydajność transformacji, przeprowadzając je z udziałem pochodnych **89**-**93**. Badania te wykazały, że na wydajność cyklopropanowania wpływa nie tylko poziom E_T prekursora, ale również jego stabilność elektrochemiczna i reaktywność generowanych w wyniku jego rozpadu indywiduów chemicznych.

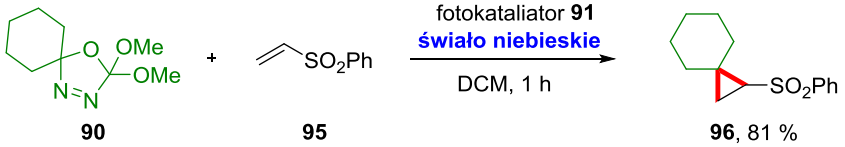

Warunki reakcji: Ir[dF(CF$_3$)ppy)$_2$(dtbpy)]PF$_6$ (**91**, 0.25 mol%), oksadiazolina **90** (0.2 mmol, 2.0 ekwiw.), olefina **95** (0.1 mmol), DCM$_{cz.d.a.}$ (0.05 M), niebieskie diody LED (450 nm, 25 W), 25 ^{o}C, 1 h.

Schemat 33. Fotokatalityczna synteza spirocyklopropanów – reakcja modelowa

Ponadto, skutecznym fotokatalizatorem dla omawianego przekształcenia okazał się tioksanton – handlowo dostępny barwnik organiczny o długim czasie życia w stanie wzbudzonym, pochłaniający światło z zakresu fioletowego. Dla zapewnienia dobrej wydajności cyklopropanowania konieczne było jego użycie w ilości aż 2.5 mol%. W reakcji tej obok cyklopropanu wyizolowałam niewielką ilość pirazolu **97**, powstającego w wyniku 1,3-dipolarnej cykloaddycji diazoalkanu **99** z olefiną **95** (Schemat 34). Eksperymenty kontrolne bez dodatku fotouczulacza na świetle fioletowym (z użyciem diod emitujących promieniowanie z zakresu 405 nm +/- 50 nm, a więc w nieznacznym stopniu także światło UV) wykazały obecność pirazolu **97** w mieszaninie poreakcyjnej jako głównego produktu reakcji. Bezpośrednia fotoliza oksadiazoliny **90** jest jednak w tych warunkach powolnym procesem i wymaga naświetlania przez co najmniej 17 h, podczas gdy pełna konwersja substratu **90** w warunkach fotokatalitycznych osiągana jest w czasie <30 min.

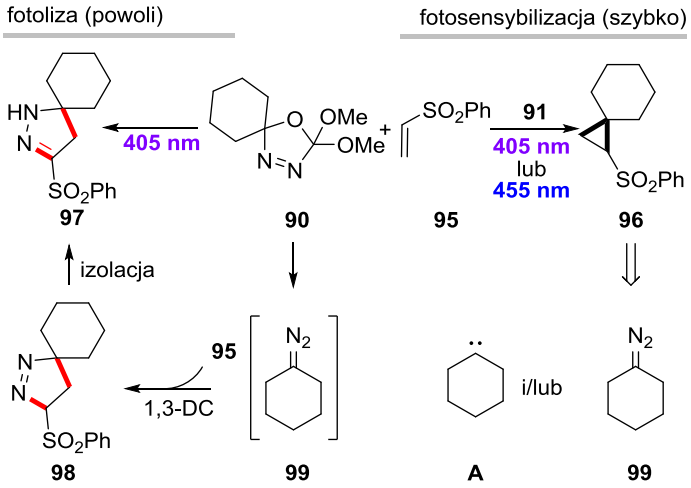

Schemat 34. Porównanie ścieżki bezpośredniego wzbudzenia i fotokatalitycznej

Otrzymane wyniki wskazują, że wzbudzenie bezpośrednie 1,3,4-oksadiazoliny oraz na drodze fotoindukowanego transferu energii prowadzą do różnych produktów reakcji, a zatem w ich wyniku generowane są różne indywidua chemiczne. W przypadku wariantu fotokatalitycznego nie można jednak wykluczyć wytwarzania zarówno karbenu **A**, jak i diazoalkanu **99**, ponieważ szczegółowe eksperymenty mechanistyczne wykazały, że otrzymywana *in situ* 1-pirazolina **98** ulega fotokatalitycznemu rozkładowi w obecności kompleksu irydu **91** do cyklopropanu **96**. Karbeny to wysoce reaktywne, a w konsekwencji trudno wykrywalne indywidua, jednak ich obecność w mieszaninie reakcyjnej popierają wyniki eksperymentów EPR, gdzie zidentyfikowano je jako addukty

z MNP (2-metylo-2-nitrozopropan), popularnym reagentem wychwytującym karbeny trypletowe. Ponadto, rodnikowy charakter reakcji został potwierdzony za pomocą eksperymentów z pułapką TEMPO, której zastosowanie prowadziło do całkowitego zatrzymania reakcji. Natomiast wygaszanie fluorescencji kompleksu irydu **91** przez 1,3,4-oksadiazoliny dowodzi interakcji cząsteczek prekursorów z fotokatalizatorem w stanie wzbudzonym.

Na podstawie przeprowadzonych eksperymentów zaproponowałam mechanizm reakcji, która inicjowana jest poprzez fotoindukowany transfer energii od cząsteczek fotokatalizatora **91** w stanie trypletowym (Schemat 35). W wyniku rozerwania wiązania w strukturze wzbudzonej oksadiazoliny powstaje rodnik diazenylowy **B**, który może ulegać dalszemu rozkładowi do karbenu trypletowego **A** oraz niestabilnego diazoalkanu **99**. Diazoalkan ten, na drodze fotosensybilizacji, generuje karben **A**, bądź reaguje z olefiną **95**. W wyniku 1,3-dipolarnej cykloaddycji powstaje 1-pirazolina **98**, która na skutek kolejnego fotoindukowanego transferu energii od cząsteczek fotokatalizatora generuje dirodnik **C**, powstający również w reakcji karbenu **A** z olefiną **95**. W końcowym etapie reakcji, ta reaktywna forma cyklizuje do pierścienia cyklopropanu generując produkt spirocykliczny **96**. Wspomniane ścieżki reakcyjne są popierane przez szczegółowe obliczenia DFT wykonane przez dr hab. Wojciecha Chaładaja.

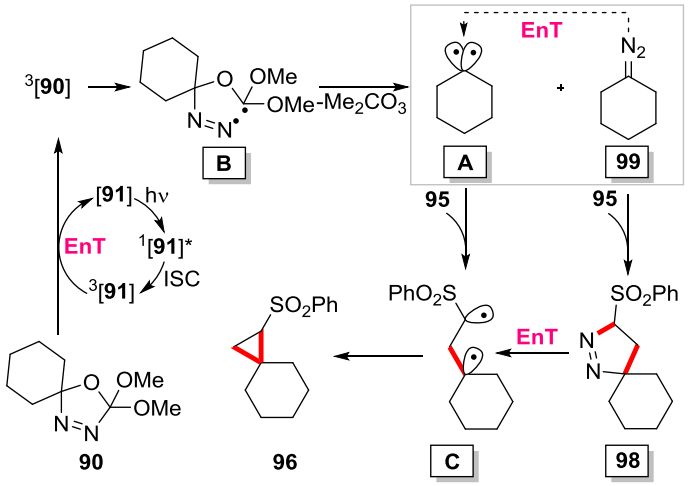

Schemat 35. Proponowany mechanizm reakcji

W oparciu o badania optymalizacyjne przeprowadziłam ocenę zakresu stosowalności i ograniczeń proponowanej metody. Fotokatalityczna reakcja cyklopropanowania zachodzi wydajnie dla różnorodnych 1,3,4-oksadiazolin (Schemat 36). Wśród przetestowanych pochodnych znajdują się zarówno pochodne podstawione

w pozycji C-5 grupami cyklicznymi i heterocyklicznymi, jak i podstawnikami alifatycznymi, zawierającymi w strukturze różnorodne grupy funkcyjne. Z dobrą wydajnością otrzymane zostały pochodne nortropinonu (**113**, 63%), *(-)*-tujonu (**117**, 51%) oraz steroidu (**118**, 55%), podkreślając możliwość adaptacji metody do funkcjonalizacji związków o znaczeniu biologicznym. Wydajna synteza związku **96** na skalę 1.0 mmol potwierdza bardzo dobrą skalowalność opracowanej metody.

Zakres stosowalności metody w odniesieniu do olefin jest także szeroki (Schemat 37). Wśród wydajnych reagentów znajdują się ubogie w elektrony olefiny tj. sulfony, estry, ketony, amidy, nitryl a nawet redoks-aktywna pochodna *N*-hydroksyftalimidu (produkt **125**), czy aldehyd (produkt **127**).

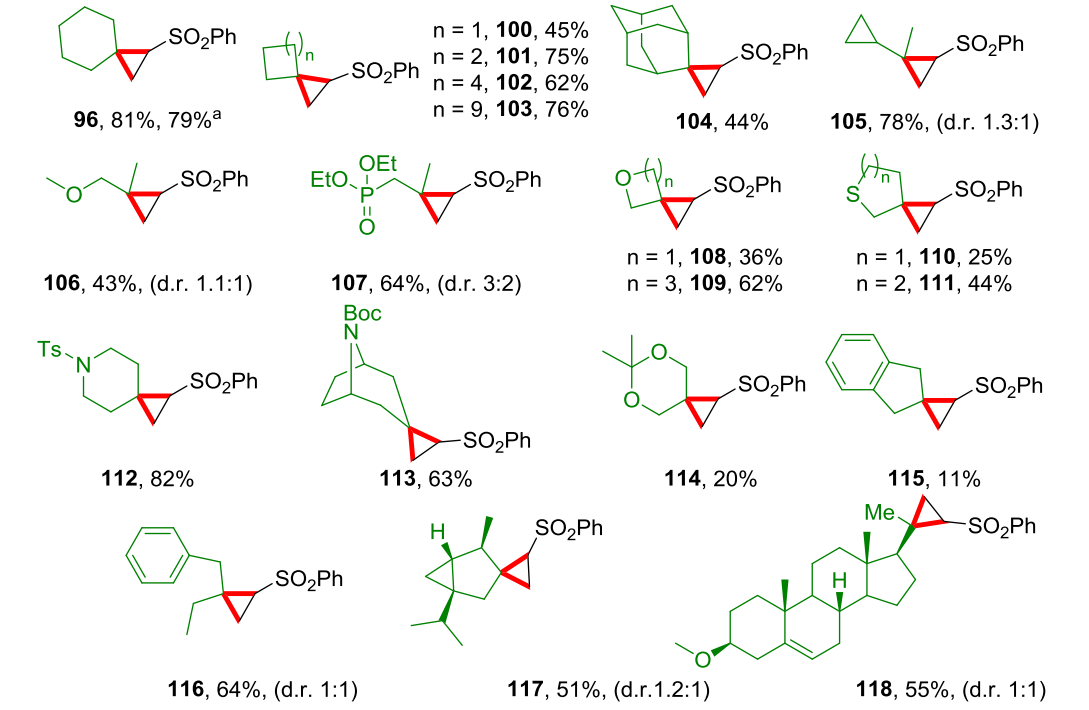

Warunki reakcji: $Ir[dF(CF_3)ppy)_2(dtbpy)]PF_6$ (**91**, 0.25 mol%), oksadiazolina (0.2 mmol, 2.0 ekwiw.), olefina **95** (0.1 mmol), $DCM_{cz.d.a.}$ (0.05 M), niebieskie diody LED (450 nm, 25 W), 25 °C, 1 h. [a]skala 1.0 mmol

Schemat 36. Zakres stosowalności metody w odniesieniu do 1,3,4-oksadiazolin

Dobrze tolerowane są akrylany zawierające w strukturze wiązania nienasycone – fotokatalityczna reakcja syntezy spirocyklopropanów **119** oraz **120** zachodzi z wysoką selektywnością a uboczne produkty cykloaddycji karbenów do nieaktywowanych wiązań typu π nie zostały wykryte. Metoda działa wydajnie także dla dipodstawionych olefin, jednak dla alkenów wicynalnych otrzymywane są jedynie umiarkowane wydajności (np. związki **140**, **141**).

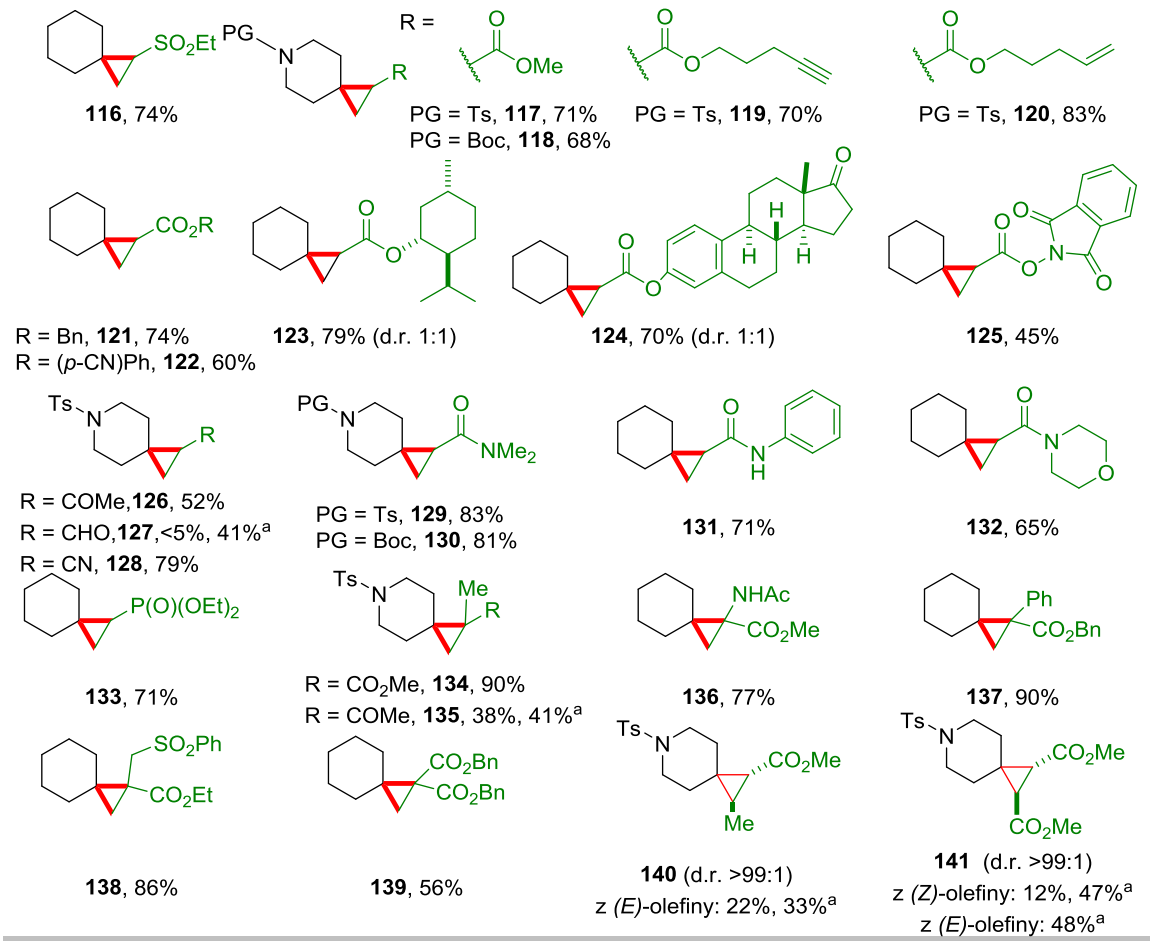

Warunki reakcji: $Ir[dF(CF_3)ppy)_2(dtbpy)]PF_6$ (**91**, 0.25 mol%), oksadiazolina (0.4 mmol, 2.0 ekwiw.), olefina (0.2 mmol), $DCM_{cz.d.a.}$ (0.05 M), niebieskie diody LED (450 nm, 25 W), 25 °C, 1 h. [a]5.0 ekwiw.olefiny

Schemat 37. Zakres stosowalności metody w odniesieniu do olefin

Co istotne, zastosowanie jako reagenta zarówno fumaranu, jak i maleinianu dimetylu prowadzi do otrzymania tego samego diastereoizomeru – bardziej korzystnego termodynamicznie *trans*-cyklopropanu **141**. Taki wynik reakcji potwierdza zaangażowanie dirodnik **C** w mechanizm reakcji. W przypadku niektórych reakcji dla uzyskania umiarkowanej/dobrej wydajności reakcji konieczna była modyfikacja warunków i odwrócenie stosunku stechiometrycznego (przy zwiększeniu nadmiaru olefiny do 5 ekwiw). Istotnym ograniczeniem metody są zaś olefiny bogate w elektrony – dla styrenów produktów cyklopropanowania nie zaobserwowano.

Powyższe wyniki zostały opublikowane w artykule naukowym:

[P2] **K. Orłowska**, J. V. Santiago, P. Krajewski, K. Kisiel, I. Deperasińska, K. Zawada, W. Chaładaj, D. Gryko UV Light Is No Longer Required for the Photoactivation of 1,3,4-Oxadiazolines, *ACS Catal.* **2023**, *13*, 1964-1973.

5.3.3. Wykorzystanie światła czerwonego w transformacjach diazo związków z wytworzeniem wiązań C–C i C–N

Szkodliwe działanie wysokoenergetycznego światła ultrafioletowego i niska selektywność reakcji zachodzących pod jego wpływem powoduje, że fotochemiczne transformacje indukowane promieniowaniem UV są często uznawane za niekorzystne do zastosowania w systemach biologicznych. Rozwiązaniem tego problemu jest opracowanie alternatywnych strategii bazujących na aplikacji niskoenergetycznych fotonów z zakresu światła czerwonego i podczerwonego, które wydajnie penetrują różnorodne media w tym tkanki, nie naruszając przy tym ich delikatnej struktury. Znane są już nieliczne przykłady biooortogonalnych transformacji w obecności światła czerwonego.[125]

Diazo związki jako grupa reagentów o zróżnicowanej strukturze i reaktywności zostały już wielokrotnie wykorzystane do wydajnej syntezy farmaceutyków i substancji znaczeniu biologicznym. Do tej pory jednak, opracowane przez nasz Zespół α-alkilowanie 3-fenylopropanalu z udziałem α-diazooctanu etylu stanowiło jedyny przykład transformacji diazo związku przebiegającej w obecności światła czerwonego.[100]

W odpowiedzi na lukę w fotochemii związków diazoorganicznych, w Zespole XV postanowiliśmy zbadać ich reaktywność w obecności niskoenergetycznego światła czerwonego i udowodnić, że w odpowiednich warunkach reakcji, możliwa jest aktywacja różnorodnych strukturalnie diazo związków. W naszych badaniach wykazaliśmy, że indukowane światłem czerwonym transformacje tych reagentów mogą zachodzić na drodze różnych strategii fotochemicznych: fotolizy, fotosensybilizacji i katalizy fotoredoks. Poniżej opisałam zrealizowane przeze mnie badania, dotyczące strategii katalizy fotoredoks z udziałem diazoalkanów w obecności światła czerwonego. Badania te są integralną część projektu, prezentującego także indukowane promieniowaniem czerwonym: fotolizę diarylodiazoalkanów oraz fotosensybilizację α-arylo-α-diazoestrów, opracowane przez mgr inż. Piotra Krajewskiego oraz mgr inż. Klaudię Łuczak (Schemat 8B i Schemat 20, sekcje 5.2.2.2.1 i 5.2.2.2.2.).

W ramach swoich badań opracowałam warunki reakcji umożliwiające przeprowadzenie transformacji z udziałem związków diazoorganicznych, będących akceptorami lub prekursorami rodników wytworzonych w cyklach katalitycznych,

w obecności światła czerwonego. Zastosowanym przeze mnie do badanych przekształceń katalizatorem fotoredoks jest tetrafenyloporfiryna (H_2TPP, **58**) – tani i łatwo dostępny barwnik organiczny, który pochłania światło z zakresu czerwonego, a w reakcjach fotochemicznych może pełnić funkcję zarówno fotoreduktora, jak i fotoutleniacza.

W wyniku redukcji α-diazoestrów na drodze PCET powstają rodniki o charakterze elektrofilowym – podejście to zastosowano już w reakcjach indukowanych światłem niebieskim, katalizowanych np. kompleksem $Ru(bpy)_3(PF_6)_2$ lub Eozyną Y. Bazując na znanej strategii redukcji diazo związków poprzez PCET, dokonałam re-optymalizacji warunków dla opracowanej przez zespół Li syntezy oksymów (Schemat 38)[91] oraz zaproponowanej przez zespół Xuana syntezy fenantrydyn (Schemat 39),[92] używając niskoenergetycznego światła czerwonego w miejsce niebieskiego oraz porfiryny w roli katalizatora.

Optymalizacja warunków multikomponentowej reakcji syntezy oksymów z udziałem styrenów, α-diazoestrów oraz azotynu *t*-butylu pozwoliła na skrócenie czasu reakcji z zaproponowanych przez Li 60 h do 37 h, w tym: 17 h naświetlania światłem czerwonym w obecności H_2TPP (**58**), a następnie ogrzewanie do 60 °C przez kolejne 20 h (Schemat 38). Zastosowanie warunków termicznych umożliwiło przyspieszenie izomeryzacji nitrozo związku do oksymu.

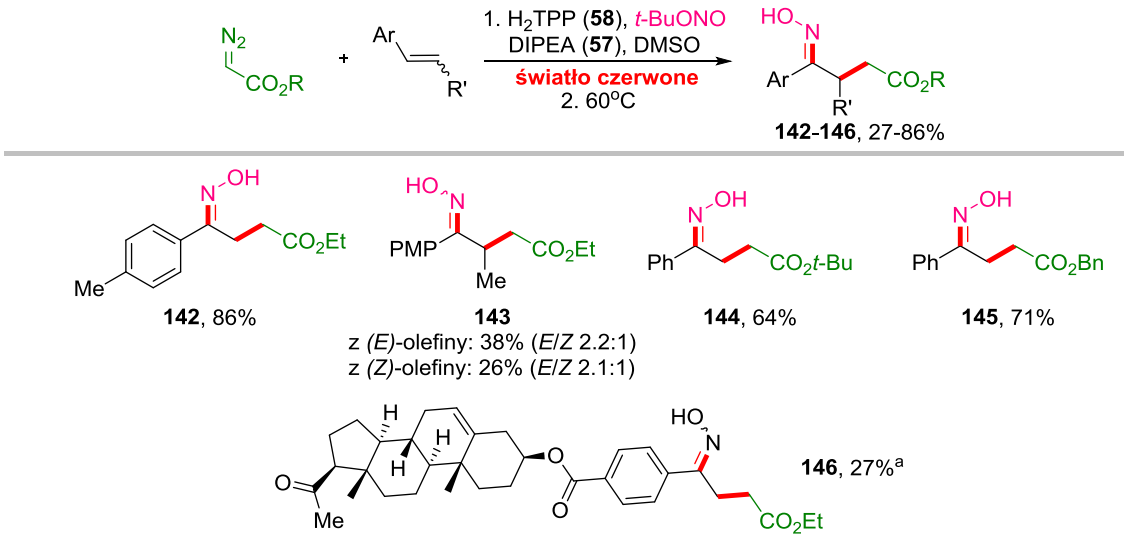

Warunki reakcji: H_2TPP (**58**, 5 mol%), DIPEA (**57**, 0.6 mmol, 1.5 ekwiw.), alken (0.2 mmol), diazoester (0.4 mmol, 2.0 ekwiw.), *t*-BuONO (0.4 mmol, 2.0 ekwiw.), $DMSO_{cz.d.a.}$ (0.05 M), czerwone diody LED (655 nm, 25 W), [Ar], 17 h, następnie 60 °C przez 20 h. [a]naświetlanie 66 h, potem 60 °C przez 20 h, DMSO/MeCN = 1:1 (v/v), (0.03 M).

Schemat 38. Indukowana światłem czerwonym fotokatalityczna synteza γ-oksoiminoestrów

Zaproponowane podejście pozwala na otrzymanie produktów **142**, **144** i **145** z wydajnościami porównywalnymi do warunków Li,[91] jednak w znacznie krótszym czasie i w obecności światła niskoenergetycznego oraz barwnika organicznego. Niewielki spadek wydajności w porównaniu z metodą indukowaną światłem niebieskim zaobserwowałam w przypadku *trans*-anetolu, przy zachowaniu podobnego stosunku *E*/*Z* produktu **143**. Niestety w związku z ograniczoną rozpuszczalnością pochodnej steroidowej, produkt **146** otrzymałam z niską wydajnością, nawet przy wydłużonym czasie naświetlania.

Zastosowanie H_2TPP pozwala na wydajną syntezę fenantrydyn **147-151** w obecności światła czerwonego (Schemat 39), z wydajnościami lepszymi bądź porównywalnymi z wcześniej opracowaną na świetle niebieskim metodologią Xuana.[92] Wstępnie określony przeze mnie zakres stosowalności indukowanej promieniowaniem czerwonym metody jest szeroki – reakcji ulegają zarówno diazoalkany akceptorowe, diazomalonian, jak i α-alkilo-α-diazoester. W przypadku α-arylo-α-diazoestrów zaobserwowałam jednak brak selektywności reakcji, co najprawdopodobniej spowodowane jest konkurencyjnym procesem fotosensybilizacji diazo związku i ubocznymi reakcjami następczych karbenów trypletowych. W Zespole XV wykazaliśmy bowiem, że poziom energii trypletowej H_2TPP ($E_T \approx 138$ kJ/mol) jest wystarczający do fotoindukowanego transferu energii do cząsteczek tego typu diazo związków ($E_T \approx 133$ kJ/mol, wartość obliczona przez dr Wojciecha Chaładaja dla α-fenylo-α-diazooctanu metylu).

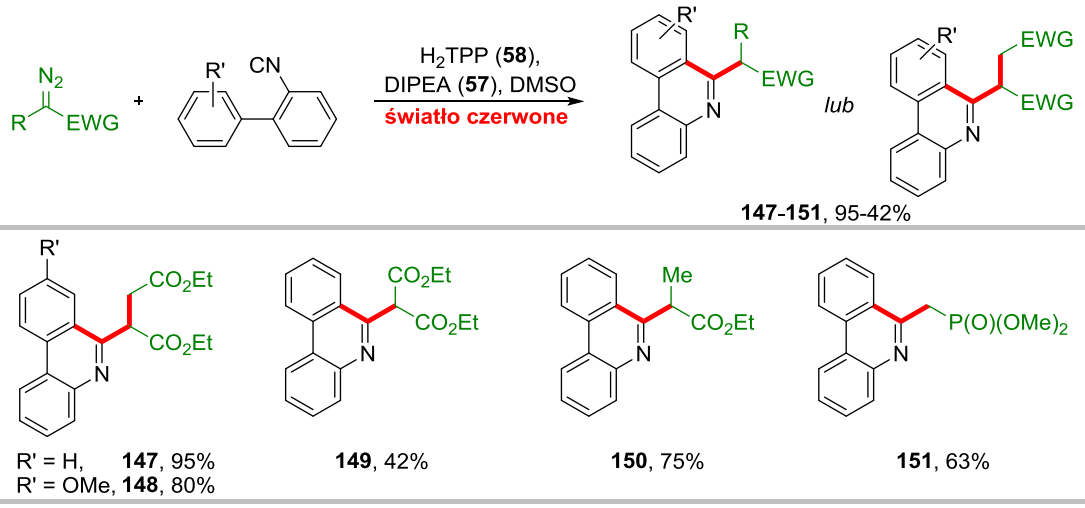

Warunki reakcji: H_2TTP (**58**, 5 mol%), DIPEA (**57**, 0.2 mmol, 1.0 ekwiw.), diazo związek (1.0 mmol, 5.0 ekwiw.), izocyjanian (0.2 mmol), $DMSO_{bezw.}$ (0.2 M), czerwone diody LED (655 nm, 25 W), [Ar], RT, 18 h.

Schemat 39. Indukowana światłem czerwonym fotokatalityczna synteza fenantrydyn

Diazo związki mogą być również akceptorami rodników generowanych w cyklu fotokatalitycznym porfiryny inicjowanym absorpcją światła czerwonego. Tezę tę udowodniłam na przykładzie reakcji z udziałem redoks aktywnych estrów ftalimidowych jako prekursorów rodników węglowych oraz α-arylo-α-diazoestrów, prowadzącej do syntezy hydrazonów **147**-**151** (Schemat 40), uprzednio opracowanej w obecności światła żółtego i różu bengalskiego.[104] Przeprowadzone przeze mnie badania optymalizacyjne wykazały, że dla utrzymania dobrych wydajności reakcji, konieczne jest praktycznie całkowite wyeliminowanie tlenu ze środowiska reakcyjnego. Podobnie, jak w przypadku syntezy fenantrydyn, na wydajność reakcji wpływa konkurencyjny proces fotosensybilizacji.

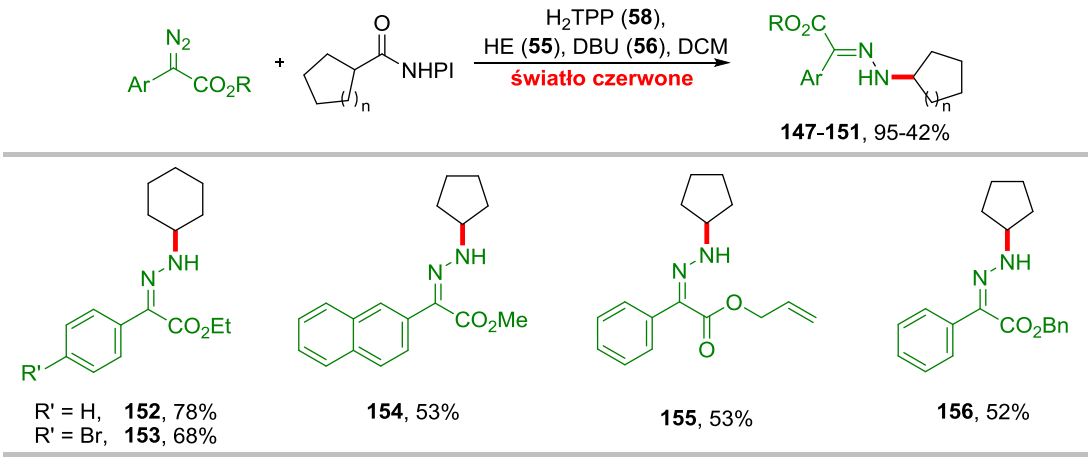

Warunki reakcji: H_2TTP (**58**, 5 mol%), HE (**55**, 0.24 mmol, 1.2 ekwiw.), DBU (**56**, 0.4 mmol, 2.3 ekwiw.), diazo związek (0.2 mmol), ester-NHPI (0.3 mmol, 1.5 ekwiw.), $DCM_{bezw.}$ (0.2 M), czerwone diody LED (655 nm, 25 W), [Ar], RT, 18 h.

Schemat 40. Indukowana światłem czerwonym fotokatalityczna synteza hydrazonów

Powyższe wyniki zostały opublikowane w artykule naukowym:

[P3] K. Orłowska, K. Łuczak, P. Krajewski, J. V. Santiago, K. Rybicka-Jasińska, D. Gryko

Chem. Commun. **2023**, DOI: 10.1039/D3CC05174A

Unlocking the Reactivity of Diazo Compounds on Red Light with the Use of Photochemical Tools

5.3.4. Podsumowanie

Celem mojej pracy doktorskiej było wykorzystanie fotochemicznych przemian diazoalkanów i oksadiazolin do opracowania nowych metod tworzenia wiązań C−C w obecności światła widzialnego. W ramach wykonanych przeze mnie badań:

I. **Opracowałam fotochemiczną metodę syntezy allenów z α-arylo-α-diazo-estrów i sulfidów propargilowych.**
Proponowana procedura pozwala na wydajne otrzymywanie wysoce sfunkcjonalizowanych produktów w łagodnych warunkach reakcji bez dodatku katalizatora. Mechanizm transformacji bazuje na ***bezpośrednim wzbudzeniu diazo związku*** absorbującego światło niebieskie. Generowane w wyniku tego procesu ***karbeny singletowe*** reagują z sulfidem tworząc ylidy, które ulegają [2,3]-sigmatropowemu przegrupowaniu do allenów.

II. **Zbadałam dotychczas nieznaną reaktywność 1,3,4-oksadiazolin w obecności światła widzialnego oraz opracowałam metodę syntezy spirocyklopropanów z ich udziałem.**
Zaprojektowana strategia wykorzystuje 1,3,4-oksadiazoliny jako prekursory ***niestabilizowanych diazo związków*** i ***karbenów trypletowych***. Zaproponowane podejście polega na aktywacji tych prekursorów na drodze ***fotoindukowanego transferu energii*** od fotouczulacza o odpowiednim poziomie energii trypletowej. Generowane na skutek ***fotosensybilizacji 1,3,4-oksadiazolin*** indywidua reagują z elektrofilowymi olefinami prowadząc do spirocyklicznych produktów.

III. **Wykazałam, że zastosowanie porfiryny jako katalizatora umożliwia przeprowadzanie transformacji fotoredoks z udziałem diazoalkanów pod wpływem światła czerwonego.**
Zrealizowane przeze mnie badania dowodzą, że możliwe jest zastosowanie ***niskoenergetycznego światła czerwonego*** w przekształceniach, w których ***różnorodne strukturalnie diazo związki*** pełnią funkcję ***prekursorów bądź akceptorów rodników***. Do tego celu, koniecznie jest jednak zastosowanie porfiryny - inspirowanego naturą barwnika organicznego, który pochłaniają światło czerwone, a w reakcjach fotokatalitycznych może pełnić funkcję zarówno fotoreduktora, jak i fotoutleniacza. Skuteczność opracowanej strategii

potwierdziłam na przykładzie transformacji prowadzących do tworzenia nowych wiązań C–C i C–N.

Podsumowując, zrealizowane w ramach niniejsze pracy doktorskiej badania znacząco poszerzają stan wiedzy z zakresu fotochemii związków diazoorganicznych oraz 1,3,4-oksadiazolin. Potwierdzają one, że diazo związki oraz 1,3,4-oksadiazoliny są reagentami o interesujących reaktywnościach fotochemicznych, w zależności od mechanizmu reakcji, umożliwiających dostęp do wielu indywiduów chemicznych, tj. karbeny, ylidy i rodniki. Indywidua te, jak i same diazo związki jako akceptory rodników, mogą wydajnie uczestniczyć w procesach indukowanych światłem widzialnym, w tym niskoenergetycznym światłem czerwonym. Użyteczność opracowanych przeze mnie strategii wykazałam na przykładzie szeregu przekształceń fotochemicznych, prowadzących do wytworzenia nowych wiązań C–C i C–N z otrzymaniem różnorodnych strukturalnie produktów, także pochodnych substancji biologicznie czynnych. Omówione przeze mnie wyniki eksperymentalne stanowią nie tylko istotny wkład w dostępną wiedzę, ale z pewnością zainspirują naukowców do zgłębiania fotochemii tych reagentów.

5.4. Bibliografia

1. Romero, N. A.; Nicewicz, D. A. *Chem. Rev*. **2016**, *116*, 10075-10166.
2. McAtee, R. C.; McClain, E. J.; Stephenson, C. R. J. *Trends Chem*. **2019**, *1*, 111-125.
3. Xuan, J.; Xiao, W. J. *Angew. Chem. Int. Ed*. **2012**, *51*, 6828-6838.
4. Shaw, M. H.; Twilton, J.; MacMillan, D. W. C. *J. Org. Chem*. **2016**, *81*, 6898-6926.
5. Crisenza, G. E. M.; Melchiorre, P. *Nat. Commun*. **2020**, *11*, 1-8.
6. Lee, Y.; Kwon, M. S. *Eur. J. Org. Chem*. **2020**, *2020*, 6028-6043.
7. Narayanam, J. M. R.; Stephenson, C. R. J. *Chem. Soc. Rev*. **2011**, *40*, 102-113.
8. Nicewicz, D. A.; MacMillan, D. W. C. *Science* **2008**, *322*, 77-80.
9. Davies, H. M. L.; Denton, J. R. *Chem. Soc. Rev*. **2009**, *38*, 3061-3071.
10. Yang S. *et al. RSC Adv*. **2018**, *8*, 29428-29454.
11. Harada, S. *Chem. Pharm. Bull.* **2021**, *69*, 1170-1178.
12. Mix, K. A.; Aronoff, M.R.; Raines, R.T. *ACS Chem. Biol*. **2016** *11*, 3233-3244.
13. Davies, H. M. L.; Beckwith, R. E. J. *Chem. Rev*. **2003** *103*, 2861-2903.
14. Ye, T.; McKervey, M. A. *Chem. Rev*. **1994**, *94*, 1091-1160.
15. Regitz, M., Maas, G. Diazo Compounds: Properties and Synthesis, Academic Press, Orlando, 1986.
16. Ford, A.; Miel, H.; Ring, A.; Slattery, C. N.; Maguire, A. R.; McKervey, M. A. *Chem. Rev*. **2015**, *115*, 9981-10080.
17. Zhang, Z.; Wang, J. *Tetrahedron* **2008**, *64*, 6577-6605.
18. Maas, G. *Chem. Soc. Rev*. **2004**, *33*, 183-190.
19. Rybicka-Jasińska, K.; Ciszewski, Ł. W.; Gryko, D. *Adv. Synth. Catal*. **2016**, *358*, 1671-1678.
20. Rybicka-Jasińska, K.; Shan, W.; Zawada, K.; Kadish, K. M.; Gryko, D. *J. Am. Chem. Soc*. **2016**, *138*, 15451-15458.
21. Rybicka-Jasińska, K.; Orłowska, K.; Karczewski, M.; Zawada, K.; Gryko, D. *Eur. J. Org. Chem*. **2018**, *2018*, 6634-6642.
22. Ciszewski, Ł. W.; Rybicka-Jasińska, K.; Gryko, D. *Org. Biomol. Chem*. **2019**, *17*, 432-448.
23. Durka, J.; Turkowska, J.; Gryko, D. *ACS Sustainable Chem. Eng*. **2021**, *9*, 8895-8918.
24. Candeias, N.; Afonso, C. A. M. *Curr. Org. Chem*. **2009**, *13*, 763-787.
25. Yang, Z.; Stivanin, M. L.; Jurberg, I. D.; Koenigs, R. M. *Chem. Soc. Rev*. **2020**, *49*, 6833-6847.
26. Ciamician, G. *Science* **1912**, *36*, 385-394.
27. Alsters, P. L.; Jary, W.; Nardello-Rataj, V.; Aubry, J. -M. *Org. Process Res. Dev*. **2010**, *14*, 259-262.
28. Monnerie, N.; Ortner, J. *J. Sol. Energy Eng*. **2001**, *123*, 171-174.

29. Rossen, K.; Poliakoff, M.; George, M. W. *et al. Nat. Chem*. **2015**, *7*, 489-495.
30. Bogdos, M. K.; Pinard, E.; Murphy, J. A. *Beilstein J. Org. Chem.* **2018**, *14*, 2035-2064.
31. Nicewicz, D. A.; Nguyen, T. M. *ACS Catal*. **2014**, *4*, 355-360.
32. Prier, C. K.; Rankic, D. A.; MacMillan, D. W. C. *Chem. Rev*. **2013**, *113*, 5322-5363.
33. Pitre, S. P.; Overman, L. E. *Chem. Rev*. **2022**, *122*, 1717-1751.
34. Strieth-Kalthoff, F.; James, M. J.; Teders, M.; Pitzer, L; Glorius, F. *Chem. Soc. Rev*. **2018**, *47*, 7190-7202.
35. Strieth-Kalthoff, F.; Glorius, F. *Chem*. **2020**, *6*, 1888-1903.
36. Constantin, T.; Zanini, M.; Regni, A.; Sheikh, N. S.; Juliá, F.; Leonori, D. *Science* **2020**, *367*, 1021-1026.
37. Bonciolini, S.; Noël, T.; Capaldo, L. *Eur. J. Org. Chem*. **2022**, *2022,* e202200417.
38. Hopkinson, M. N.; Sahoo, B.; Li, J. -L.; Glorius, F. *Chem. Eur. J*. **2014**, *20*, 3874-3886.
39. Skubi, K. L.; Blum, T. R.; Yoon, T. P. *Chem. Rev*. **2016**, *116*, 10035-10074.
40. Qian, L.; Shi, M. *Chem. Commun.* **2023**, *59*, 3487-3506.
41. Shao, Z.; Zhang, H. *Chem. Soc. Rev*. **2012**, *41*, 560-572.
42. Moss, R. A. *Acc. Chem. Res*. **2006**, *39*, 267-272.
43. Platz, M. S.; Huang, H.; Ford, F.; Toscano, J. *Pur. App. Chem.* **1997**, *69*, 803-807.
44. Warkentin, J. *J. Chem. Soc. Perkin 1*. **2000**, 2161-2169.
45. Majchrzak. M. W.; Bekhazi, M.; Tse-Sheepy, I.; Warkentin, J. *J. Org. Chem.* **1989**, *54*, 1842-1845.
46. Jurberg, I. D.; Davies, H. M. L. *Chem. Sci*. **2018**, *9*, 5112-5118.
47. Sripati, J.; Chao, P.; Empel, C.; Koenigs, R. M. *Angew. Chem. Int. Ed.* **2021**, *60*, 13271-1379.
48. Orłowska, K.; Łuczak, K.; Krajewski, P.; Santiago, J. V.; Rybicka-Jasińska, K.; Gryko, D. *Chem. Commun.* **2023**, 10.1039/D3CC05174A.
49. Gillingham, D.; Fei, N. *Chem. Soc. Rev*. **2013**, *42*, 4918-4931.
50. Doyle, M. P.; Duffy, R.; Ratnikov. M.; Zhou, L. *Chem. Rev*. **2010**, *110*, 704-724.
51. Empel, C.; Patureau, F. W.; Koenigs, R. M. *J. Org. Chem*. **2019**, *84*, 11316-11322.
52. Stivanin, M. L.; Fernandes, A. A. G.; da Silva, A. F.; Okada, C. Y.; Jurberg, I. D. *Adv. Synth. Catal*. **2020**, *362*, 1106-1111.
53. Okada, C. Y.; dos Santos, C. Y.; Jurberg, I. D. *Tetrahedron* **2020**, *76*, 131316.
54. He, F.; Li, F.; Koenigs, R. M. *J. Org. Chem*. **2020**, *85*, 1240-1246.
55. Huo. C. *et al. Org. Biomol. Chem*. **2020,** *18*, 9494-9498.
56. Huo. C. *et al. Org. Biomol. Chem*. **2021**, *19*, 394-398.
57. Jana, S.; Yang, Z.; Li, F.; Empel, C.; Ho, J.; Koenigs, R. M. *Angew. Chem. Int. Ed.* **2020**, 59, 5562-5566.
58. Empel, C.; Jana, S.; Pei, C.; Nguyen, T. V.; Koenigs, R. M. *Org. Lett*. **2020**, *22*, 7225-7229.

59. Empel, C.; Verspeek, D.; Jana, S.; Koenigs, R. M. *Adv. Synth. Catal*. **2020**, *362*, 4716-4722.

60. Zhang, Y.; Wang, J. *Coord, Chem. Rev*. **2010**, *254*, 941-953.

61. Oost, R.; Neuhaus, J.D.; Merad, J.; Maulide, N. Sulfur Ylides in Organic Synthesis and Transition Metal Catalysis. In: Gessner VH, ed. *Modern Ylide Chemistry: Applications in Ligand Design, Organic and Catalytic Transformations*, Springer International Publishing, 2018, 73-115.

62. Padwa, A.; Hornbuckle, S. F. *Chem. Rev.* **1991***, 91*, 263-309.

63. Hommelsheim, R.; Guo, Y.; Yang, Z.; Empel, C.; Koenigs, R. M. *Angew. Chem. Int. Ed.* **2019**, *58*, 1203-1207.

64. Yang, J.; Wang, J.; Huang, H.; Qin, G.; Jiang, Y.; Xiao, T. *Org. Lett*. **2019**, *21*, 2654-2657.

65. Li, W. -S.; Zhang, J.; Lu, S.; Cheng, G.; Wan, W. -J.; Wang, L. -X. *Tetrahedron Lett*. **2023**, *122*, 154506.

66. Davies, P. W.; Albrecht, S. J. -C.; Assanelli, G. *Org. Biomol. Chem*. **2009**, *7*, 1276-1279.

67. Holzwarth, M. S.; Alt, I.; Plietker, B. *Angew. Chem. Int. Ed.* **2012**, *51*, 5351-5354.

68. Yang, Z.; Guo, Y.; Koenigs, R. M. *Chem. Eur. J.* **2019**, *25*, 6703-6706.

69. Li, F.; He, F.; Koenigs, R. M. *Synthesis* **2019**, *51*, 4348-4358.

70. Jana, S.; Yang, Z.; Pei, C.; Xu, X.; Koenigs, R. M. *Chem. Sci*. **2019**, *10*, 10129-10134.

71. He, F,; Pei, C.; Koenigs, R. M. *Chem. Comm.* **2020**, *56*, 599-602.

72. Kobayashi, S.; Jørgensen, K. Cycloaddition Reactions in Organic Synthesis, Wiley-VCH, 2002.

73. Guo, Y.; Nguyen, T. V.; Koenigs, R. M. *Org. Lett.* **2019**, *21*, 8814-8818.

74. Niu, J. -L; Song, M.-P. *et al. Synthesis* **2019**, *51*, 889-898.

75. Guo, Y.; Empel, C.; Pei, C.; Atodiresei, I.; Fallon, T.; Koenigs, R. M. *Org Lett*. **2020**, *22*, 5126-5130.

76. He, F.; Koenigs, R. M. *Chem. Commun*. **2019**, *55*, 4881-4884.

77. Li, Z.; Boyarskikh, V.; Hansen, J. H.; Autschbach, J.; Musaev, D. G.; Davies, H. M. L. *J. Am. Chem. Soc*. **2012**, *134*, 15497-15504.

78. Zhang, Z. *et al. Org. Lett*. **2015**, *17*, 5124-5127.

79. Kirmse, W. *Eur. J. Org. Chem.* **2002**, *2002*, 2193-2256.

80. Bernardim, B.; Hardman-Baldwin, A. M.; Burtoloso, A. C. B. *RSC Adv*. **2015**, *5*, 13311-13314.

81. Meng, J.; Ding. W. -W.; Han, Z. -Y. *Org Lett*. **2019**, *21*, 9801-9805.

82. Liu. J.; Li, M. -M.; Qu, B. -L.; Lu. L. -Q.; Xiao. W. -J. *Chem. Commun*. **2019**, *55*, 2031-2034.

83. Wang, C.; Wang, Z.; Yang, J.; Shi, S. -H.; Hui, X. -P. *Org. Lett*. **2020**, *22*, 4440-4443.

84. Li, M. -M.; Wei, Y.; Liu, J.; Chen, H. -W.; Lu, L. -Q.; Xiao, W. -J. *J. Am. Chem. Soc*. **2017**, *139*, 14707-14713.

85. Lu, L. -Q.; Xiao, W. -J. *et al. J. Am. Chem. Soc*. **2019**, *141*, 133-137.

86. Xiao, T.; Mei, M.; He, Y.; Zhou, L. *Chem. Commun.* **2018**, *54*, 8865-8868.

87. Huang, X.; Webster, R. D.; Harms, K.; Meggers, E. *J. Am. Chem. Soc*. **2016**, *138*, 12636-12642.

88. Ciszewski, Ł. W.; Durka, J.; Gryko, D. *Org. Lett*. **2019**, *21*, 7028-7032.

89. Su, Y. -L.; Liu, G. -X.; Liu, J. -W.; Tram, L.; Qiu, H.; Doyle, M. P. *J. Am. Chem. Soc*. **2020**, *142*, 13846-13855.

90. Li, F.; Zhu, S.; Koenigs, R. M. *Chem. Commun.* **2022**, *58,* 7526-7529.

91. Liu, Y.; Zhu, K.; Zhao, J.; Li, P. *Org. Lett*. **2022**, *24*. 6834-6838.

92. Ye, H. -B.; Zhou, X. -Y.; Li, L.; He, X. -K.; Xuan, J. *Org. Lett*. **2022**, *24*, 6018-6023.

93. Zhou, L. et al. *J. Photochem. Photobiol. A Chem*. **2018**, *355*, 220-225.

94. Nagode, S. B.; Kant, R.; Rastogi, N. *Org. Lett*. **2019**, *21*, 6249-6254.

95. Wang, Z.; Herraiz, A. G.; Del Hoyo, A. M.; Suero, M. G. *Nature* **2018**, *554*, 86-91.

96. Li, J.; Lu, X. -C.; Xu, Y.; Wen, J. -X.; Hou, G. -Q.; Liu, L. *Org. Lett*. **2020**, *22*, 9621-9626.

97. Li, X.; Golz, C.; Alcarazo, M. *Angew. Chem. Int. Ed.* **2021**, *60*, 6943-6948.

98. Dong, J. -Y.; Wang, H.; Mao, S.; Wang, X.; Zhou, M. -D.; Li, L. *Adv. Synth. Catal*. **2021**, *363*, 2133-2139.

99. Zhu, S.; Li, F.; Empel, C.; Jana, S.; Pei, C.; Koenigs, R. M. *Adv. Synth. Catal*. **2022**, 364, 3149-3154.

100. Rybicka-Jasińska, K.; Wdowik, T.; Łuczak, K.; Wierzba, A. J.; Drapała, O.; Gryko, D. *ACS Org. Inorg. Au*. **2022**, *2*, 422-426.

101. Sarabia, F. J,; Ferreira, E. M. *Org. Lett*. **2017**, *19*, 2865-2868.

102. Sarabia, F. J.; Li, Q.; Ferreira, E. M. *Angew. Chem. Int. Ed*. **2018**, 57, 11015-11019.

103. Holmberg-Douglas, N.; Onuska, N. P. R.; Nicewicz, D. A. *Angew. Chem. Int. Ed*. **2020**, *59*, 7425-7429.

104. Chan, C. -M.; Xing, Q.; Chow, Y. -C.; Hung, S. -F.; Yu, W. -Y. *Org. Lett*. **2019**, *21*, 8037-8043.

105. Ma, M.; Hao, W.; Ma, L.; Zheng, Y.; Lian, P.; Wan, X. *Org. Lett*. **2018**, 5799-5802.

106. Xiao, T.; Li, L.; Lin, G.; Mao, Z. -W.; Zhou, L. *Org. Lett*. **2014**, *16*, 4232-4235.

107. Pramanik, M. M. D.; Nagode, S. B.; Kant, R.; Rastogi, N. *Org. Biomol. Chem*. **2017**, *15*, 7369-7373.

108. Liu, Y.; Dong, X.; Deng, G.; Zhou, L. *Sci. China Chem*. **2016**, *59,* 199-202.

109. El-Saidi, M.; Kassam, K.; Pole, D. L.; Tadey, T.; Warkentin J. *J. Am. Chem. Soc*. **1992**, *114*, 8751-8752.

110. Aasmul, M.; Heimgartner, H.; Mloston, G. 2,2-Dimetoxy-5,5-Dimethyl-Δ^3-1,3,4-Oxadiazoline. Electronic Encyclopedia of Reagents for Organic Synthesis, Paquette, L. A., Ed.; Wiley, 2012.

111. Warkentin, J. *et al. J. Am. Chem. Soc.* **1997**, *18*, 3191-3192.

112. Platz, M. S. *et. al. J. Org. Chem.* **1999**, *64*, 4456-4464.

113. Majchrzak, M. W.; Bekhazi, M.; Tse-Sheepy, I.; Warkentin, J. *J. Org. Chem.* **1989**, *54*, 1842-1845.

114. Hoffmann, R. W.; Luthardt, H. J. *Chem. Ber*. **1968**, *101*, 3861-3871.

115. Ley, S. V. *et al. Angew. Chem. Int. Ed.* **2017**, *56*, 16602-16605.

116. Ley, S. V. *et al. J. Org. Chem*. **2018**, *83*, 15558-15568.

117. Ley, S. V. *et al. Chem. Commun.* **2018**, 54, 11685-11688.

118. Chen, Y.; Blakemore, D. C.; Pasau, P.; Ley, S. V. *Org. Lett*. **2018**, *20*, 6569-6572.

119. Zimmer, R.; Dinesh, C. U.; Nandanan, E.; Khan, F. A. *Chem. Rev*. **2000**, *100,* 3067-3126.

120. Hashmi, A. S. K. Modern Allene Chemistry, WILEY- VCH, 2008.

121. Yang, W.; Hashmi, A. S. K. *Chem. Soc. Rev*. **2014**, *43*, 2941-2955.

122. Ma, S. *Chem. Rev*. **2005**, *105*, 2829-2871.

123. Davies, P. W.; Albrecht, S. J. -C.; Assanelli, G. *Org. Biomol. Chem*. **2009**, 7, 1276-1279.

124. Doyle, M. P.; Bagheri, V.; Claxton, E. E. *J. Chem. Soc., Chem. Commun.* **1990**, 46-48.

125. Jia, S.; Sletten, E. M. *ACS Chem. Biol*. **2022**, *17*, 3255-3269.

6. Streszczenie w języku polskim

Związki diazoorganiczne są powszechnie stosowane w syntezie prostych i złożonych struktur, w tym produktów farmaceutycznych. W zależności od sposobu aktywacji, mogą być one źródłem karbenów, metalokarbenów, ylidów lub rodników. Z uwagi na niską stabilność prostych diazoalkanów, do reakcji z ich udziałem konieczne jest użycie prekursorów, np. 1,3,4-oksadiazolin. Niestety, fotoliza pod wpływem światła UV bądź termoliza diazo związków w obecności różnych substratów zachodzi często w sposób nieselektywny. Z kolei obecność metali w reakcjach przebiegających przez stadium metalokarbenu, powoduje, ze są one niekorzystne do zastosowania w przemyśle farmaceutycznym. Obecnie dużym zainteresowaniem cieszą się transformacje diazo związków zachodzące w obecności światła widzialnego, lecz dostępne metody są wciąż nieliczne i ograniczają się do zastosowania jedynie stabilizowanych pochodnych.

Celem mojej pracy doktorskiej było wykorzystanie fotochemicznych przemian diazoalkanów i oksadiazolin do opracowania nowych metod tworzenia wiązań C−C w obecności światła widzialnego. W pierwszej części moich badań opracowałam fotochemiczną metodę syntezy allenów z α-arylo-α-diazo-estrów i sulfidów propargilowych. Eksperymenty mechanistyczne potwierdzają, że powstałe w wyniku bezpośredniego wzbudzenia diazo związków karbeny singletowe odgrywają istotną rolę w mechanizmie reakcji. Następnie, zbadałam dotychczas nieznaną reaktywność 1,3,4-oksadiazolin w obecności światła widzialnego oraz opracowałam metodę syntezy spirocyklopropanów z ich udziałem. Zaproponowana strategia zakłada, że na skutek fotoindukowanego transferu energii do cząsteczek 1,3,4-oksadiazolin, generowane są zarówno diazoalkany, jak i karbeny trypletowe. W ostatniej części moich badań wykazałam, że zastosowanie porfiryny jako katalizatora fotoredoks umożliwia przeprowadzanie indukowanych światłem czerwonym transformacji z udziałem diazoalkanów, w których pełnią one rolę prekursorów bądź akceptorów rodników. Użyteczność zaprojektowanego podejścia przedstawiłam na przykładzie syntezy oksymów, fenantrydyn oraz hydrazonów.

Zrealizowane przeze mnie badania dowodzą, że diazo związki oraz 1,3,4-oksadiazoliny są reagentami o interesujących reaktywnościach fotochemicznych, które w zależności od mechanizmu reakcji, umożliwiają dostęp do wielu indywiduów chemicznych, tj. karbeny, ylidy i rodniki.

7. Streszczenie w języku angielskim/ Abstract in English

Diazo compounds are versatile reagents commonly applied in the synthesis of small molecules and complex structures, and even pharmaceuticals. Depending on the activation mode, they serve as precursors of various reactive intermediates such us carbenes, metal carbenes, ylides and radicals. Due to low stability, simple diazoalkanes should, however, be generated *in situ* from stable precursors, e.g. 1,3,4-oxadiazolines. Although thermolysis and UV light-mediated photolysis of diazo compounds in the presence of diverse substrates are well known approaches, these reactions generally occur with low selectivity. On the other hand, presence of even traces of metals in products obtained via metal-catalyzed methods limits their application in pharmaceutical industry. Taking into consideration the benefits arising from light-induced strategies, such transformations of diazo compounds bring the attention of organic chemists. Nevertheless, already established methods are limited and mostly targeted at stabilized diazoalkanes.

The aim of this thesis is the design of visible light-induced transformations of diazo compounds and 1,3,4-oxadiazolines leading to new C–C bonds formation. In the first part of my work, I proposed a photochemical allene synthesis from α-aryl-α-diazoesters and propargyl sulfides. Mechanistic experiments confirm that singlet carbenes generated via direct photolysis of diazo compounds are the key intermediates. Next, I have explored yet unknown reactivity of 1,3,4-oxadiazolines upon visible light irradiation. The developed activation mode relies on photoinduced energy transfer from photocatalyst to 1,3,4-oxadiazoline, upon which both triplet carbenes and diazoalkanes are generated. Within this part of my work, I illustrated the utility of proposed activation method with spirocyclopropane synthesis in the presence of electrophilic olefins. Finally, I demonstrated that with the use of porphyrins as photoredox catalysts diazo compounds undergo photochemical transformations under red light irradiation, within which they can serve as precursors or acceptors of reactive intermediates. This was evidenced with the photocatalytic synthesis of oximes, phenantridines and hydrazones.

In summary, I have shown that diazo compounds and 1,3,4-oxadiazolines are reagents of distinct photochemical reactivities, which depending on activation mode give access to various reactive species e.g. carbenes, ylides or radicals.

8. Publikacje przeglądowe i oryginalne

CATALYTIC SCIENCE SERIES — VOL. 18
Series Editor: Graham J. Hutchings

Photoorganocatalysis in Organic Synthesis

edited by
Maurizio Fagnoni
Stefano Protti
Davide Ravelli

World Scientific

Photoorganocatalysis in Organic Synthesis

CATALYTIC SCIENCE SERIES

ISSN 1793-1398 (Print)
ISSN 2399-4495 (Online)

Series Editor: Graham J. Hutchings *(Cardiff University)*

Catalysis is at the forefront of the chemical industry and is essential to many fields in the chemical sciences. This series explores all aspects of catalysis in authored and edited volumes drawing on expertise from around the globe in a focussed manner. Volumes are accessible by postgraduate students and professionals in academia and industry.

Published

Vol. 18 *Photoorganocatalysis in Organic Synthesis*
edited by Maurizio Fagnoni, Stefano Protti and Davide Ravelli

Vol. 17 *Hydroprocessing Catalysts and Processes: The Challenges for Biofuels Production*
edited by Bo Zhang and Duncan Seddon

Vol. 16 *Electro-Catalysis at Chemically Modified Solid Surfaces*
by Jacques Simonet

Vol. 15 *Noble Metal Noble Value: Ru-, Rh-, Pd-catalyzed Heterocycle Synthesis*
edited by Xiao-Feng Wu

Vol. 14 *Enantioselective Titanium Catalysed Transformations*
by Hélène Pellissier

Vol. 13 *Gold Catalysis: An Homogeneous Approach*
edited by F. Dean Toste and Véronique Michelet

Vol. 12 *Catalysis by Ceria and Related Materials (Second Edition)*
edited by A. Trovarelli and P. Fornasiero

Vol. 11 *Supported Metals in Catalysis (Second Edition)*
by J. A. Anderson

Vol. 10 *Concepts in Syngas Manufacture*
by J. Rostrup-Nielsen and L. J. Christiansen

Vol. 9 *Deactivation and Regeneration of Zeolite Catalysts*
edited by M. Guisnet and F. R. Ribeiro

More information on this series can be found at http://www.worldscientific.com/series/css

(Continued at end of book)

CATALYTIC SCIENCE SERIES — VOL. 18

Series Editor: Graham J. Hutchings

Photoorganocatalysis in Organic Synthesis

edited by

Maurizio Fagnoni
Stefano Protti
Davide Ravelli

University of Pavia, Italy

World Scientific

NEW JERSEY • LONDON • SINGAPORE • BEIJING • SHANGHAI • HONG KONG • TAIPEI • CHENNAI • TOKYO

OL | Organic Letters

Letter

Cite This: Org. Lett. 2020, 22, 1018−1021

pubs.acs.org/OrgLett

Photochemical Doyle−Kirmse Reaction: A Route to Allenes

Katarzyna Orłowska,[†,§] Katarzyna Rybicka-Jasińska,[†,§] Piotr Krajewski,[†,‡] and Dorota Gryko*[,†]

[†]Institute of Organic Chemistry, Polish Academy of Sciences, Kasprzaka 44/52, 01-224 Warsaw, Poland

[‡]Department of Chemistry, Warsaw University of Technology, Noakowskiego 3, 00-664 Warsaw, Poland

Supporting Information

ABSTRACT: This Letter describes the metal-free, blue-light-induced [2,3]-sigmatropic rearrangement of sulfonium ylides generated from donor/acceptor diazoalkanes and propargyl sulfides. The reaction furnishes highly functionalized allenes from a broad range of starting materials in decent yield. Mechanistic experiments supported by the literature data suggest singlet carbenes as intermediates in this reaction.

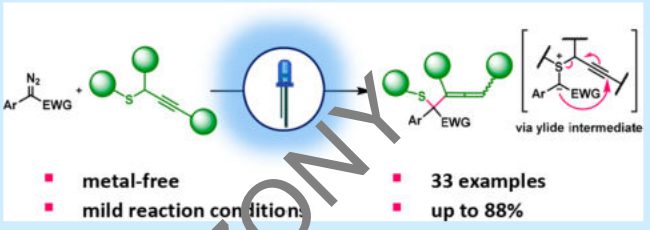

DOI: 10.1021/acs.orglett.9b04560
Org. Lett. 2020, 22, 1018−1021

DOI: 10.1021/acs.orglett.9b04560
Org. Lett. 2020, 22, 1018−1021

DOI: 10.1021/acs.orglett.9b04560
Org. Lett. 2020, 22, 1018 1021

DOI: 10.1021/acs.orglett.9b04560
Org. Lett. 2020, 22, 1018−1021

Supporting Information

Photochemical Doyle-Kirmse reaction – a route to allenes

Katarzyna Orłowska,[a] Katarzyna Rybicka-Jasińska,[a] Piotr Krajewski[a,b] and Dorota Gryko[a,*]

[a]*Institute of Organic Chemistry, Polish Academy of Sciences, Kasprzaka 44/52, 01-224 Warsaw, Poland*

[b]*Department of Chemistry, Warsaw University of Technology, Noakowskiego 3, 00-664 Warsaw, Poland*

correspondence: dorota.gryko@icho.edu.pl

Table of Contents

1. General Information

All solvents and commercially available reagents were purchased as reagent grade and were used without further purification, unless otherwise stated. Reactions were monitored by thin layer chromatography (TLC), using 0.20 mm Merck silica plates (60F-254) and visualized using UV-light, anisaldehyde or cerium molybdate stain, with heat as a developing agent. Colum chromatography was performed on Merck silica gel 60 (230-400 mesh). Yields refer to spectroscopically (^{1}H NMR) homogeneous materials. Preparative HPLC separations were performed using Knauer HPLC chromatograph with PDA detector and preparative column chromatography Knauer EII 100-10 Si column (250 x 20 mm).

NMR spectra were recorded on a Bruker 400 MHz and calibrated using a residual undeuterated solvent ($CHCl_3$ – 7.26 ppm ^{1}H NMR, 77.16 ppm ^{13}C NMR) or TMS as an internal reference. Low-resolution mass spectra (LRMS) were recorded on an Applied Biosystems API 365 mass spectrometer using electrospray ionization (ESI) technique. High-resolution mass spectra (HRMS) were recorded on a Waters AutoSpec Premier instrument using electron ionization (EI) or a Waters SYNAPT G2-S HDMS instrument using electrospray ionization (ESI) with time of flight detector (TOF). Elemental analysis (C, H, N) were performed using a PERKIN-ELMER 240 Elemental Analyzer.

2. Photoreactor Setup

Photoredox reactions were carried out in bottom plane irradiated vials in a specially constructed photoreactor composed of cooling block and LED plate connected to constant current (0.7 A) power supply (Figure S1). This particular setup was obtained by courtesy of Dr. Burkhard König. LED plates are commercially available radiators (Fischer Elektronik part no. SK 105 100 SA) with 6 epoxy-glued star-cased 3W LEDs (ProLight Opto Technology Corporation part no. PM2B-3LBS-SD) connected in series.

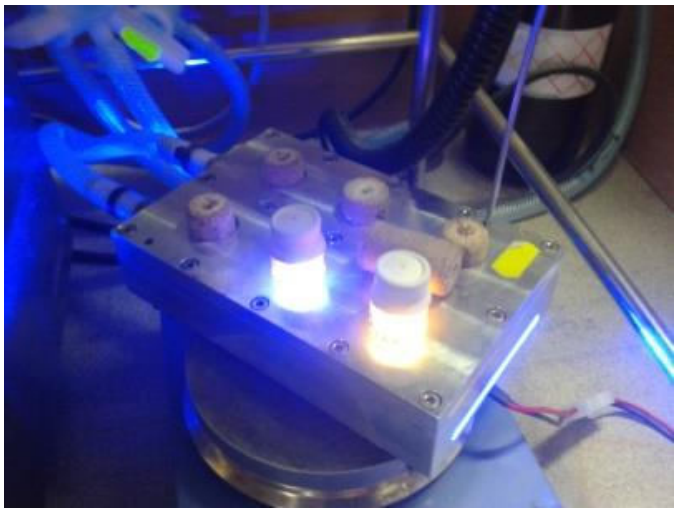

Figure S1. Photoreactor setup with aluminum cooling block

3. Optimization studies

3.1. Background reactions

Table S1. Background reactions

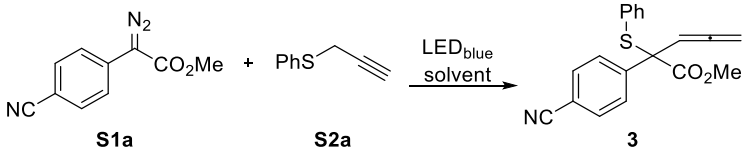

S1a S2a 3

entry	solvent	light	yield[a] [%]
1	DCM_{dry}	-	0
2	DCM_{dry}	+	62
3[b]	DCM_{dry}	+	61
4	DCM	+	61
5[c]	DCM	+	65

Reaction conditions: propargyl sulfide (**S2a**, 1.5 mmol), (4-cyano)phenyl methyl diazoacetate (**S1a**, 0.15 mmol) in DCM (2.0 mL), irradiation at 455 nm, 17 h. [a]Isolated yield, [b]Reaction mixture was not degassed, [c]DCM (1.5 mL).

3.2. Screening of solvents

Table S2. Optimization - screening of solvents

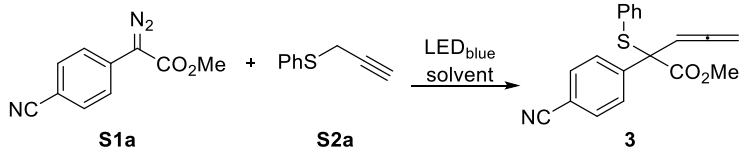

S1a S2a 3

entry	solvent	yield[a] [%]
1	DCM	65
2	$CHCl_3$	51
3	DCE	64
4	toluene	57

Reaction conditions: propargyl sulfide (**S2a**, 1.5 mmol), (4-cyano)phenyl methyl diazoacetate (**S1a**, 0.15 mmol) in solvent (1.5 mL), irradiation at 455 nm, 17 h. [a]Isolated yield.

3.3. Concentration effects

Table S3. Optimization – concentration effects

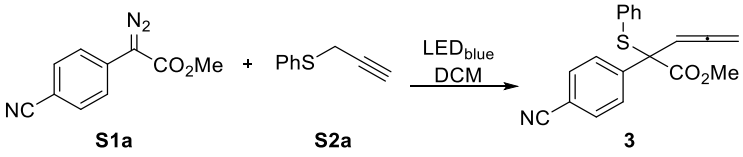

S1a S2a 3

entry	solvent [mL]	yield[a] [%]
1	2	60
2	1.5	65
3	1	65
4	0.5	68
5	0.25	68

Reaction conditions: propargyl sulfide (**S2a**, 1.5 mmol), (4-cyano)phenyl methyl diazoacetate (**S1a**, 0.15 mmol) in DCM (xx mL), irradiation at 455 nm, 17 h. [a]Isolated yield.

3.4. Substrate ratio

Table S4. Optimization - substrate ratio

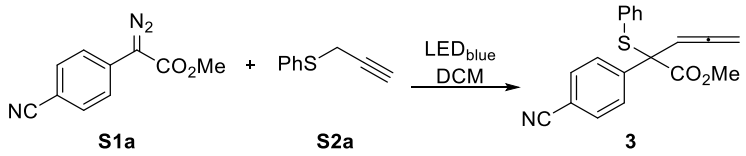

S1a S2a 3

entry	**S1a** [equiv.]	**S2a** [equiv.]	yield[a] [%]
1	1	10	68
2	1	9	68
3	1	8	58
4	1	7	62

Reaction conditions: propargyl sulfide (**S2a**, xx mmol), (4-cyano)phenyl methyl diazoacetate (**S1a**, 0.15 mmol) in DCM (0.5 mL), irradiation at 455 nm, 17 h. [a]Isolated yield.

3.5. Time

Table S5. Optimization - time

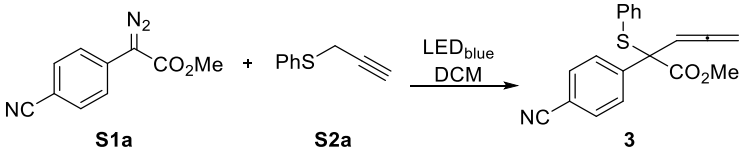

S1a S2a 3

entry	time [h]	yield[a] [%]
1	24	76
2[b]	**24**	**80**
3	20	73
4	17	68
5	10	58
6	5	54

Reaction conditions: propargyl sulfide (**S2a**, 1.35 mmol), (4-cyano)phenyl methyl diazoacetate (**S1a**, 0.15 mmol) in DCM (0.5 mL), irradiation at 455 nm. [a]Isolated yield. [b]Diazo reagent added in two portions.

4. Mechanistic studies

4.1. Addition of photosensitizers

Table S6. Mechanistic experiments – addition of photosensitizers

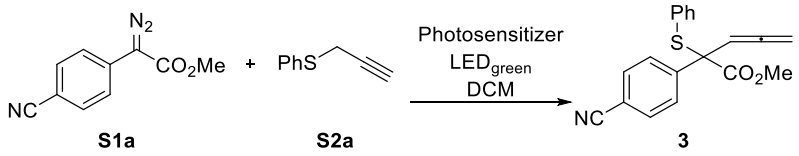

S1a S2a 3

entry	photosensitizer	yield[a] [%]
1	-	45
2	Eosin Y	65
3	$Ru(bpy)_3Cl_2 \cdot 6H_2O$	67
4	TPP	31

Reaction conditions: propargyl sulfide (**S2a**, 1.35 mmol), (4-cyano)phenyl methyl diazoacetate (**S1a**, 0.15 mmol), photosensitizer (1 mol%) in DCM (0.5 mL), irradiation at 525 nm, 24 h.
[a]Isolated yield.

4.2. Addition of TEMPO

Table S7. Mechanistic experiments – addition of a trapping agent

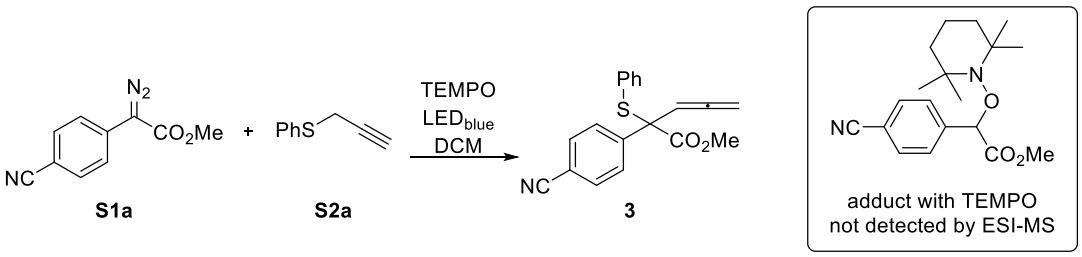

S1a S2a 3

entry	addition of TEMPO	yield[a] [%]
1	no TEMPO	76
2[b]	2 eq.	71
3	2 eq.	65

Reaction conditions: propargyl sulfide (**S2a**, 1.35 mmol), (4-cyano)phenyl methyl diazoacetate (**S1a**, 0.15 mmol), TEMPO (0.3 mmol) in DCM (0.5 mL), irradiation at 455 nm, 24 h. [a]Isolated yield, [b]TEMPO was added after 2 hours in half of the solvent volume and the reaction was run for additional 22 h.

5. General synthetic procedures

5.1. Preparation of diazo compounds

Diazo compounds **S1a-u** were prepared via diazo transfer with tosyl azide according to the literature procedure.[1]

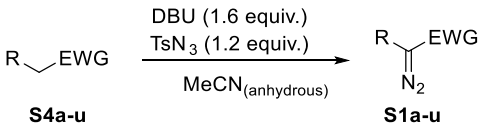

Scheme S1. Synthesis of diazo compounds **S1a-u**.

A solution of a carbanion precursor (2 mmol) in anhydrous MeCN (1 M) was stirred under argon atmosphere at 0 °C. Tosyl azide (1.2 equiv.) and DBU (1.6 equiv.) were added, then cooling bath was removed. The mixture was stirred until full conversion of the starting material was observed by the TLC. The reaction was quenched with sat. NH_4Cl and extracted with DCM (3 times), combined organic layers were washed with brine and dried over magnesium sulfate. The mixture was then filtered and evaporated *in vacuo*, crude product was purified by column chromatography (hexane:AcOEt as eluent).

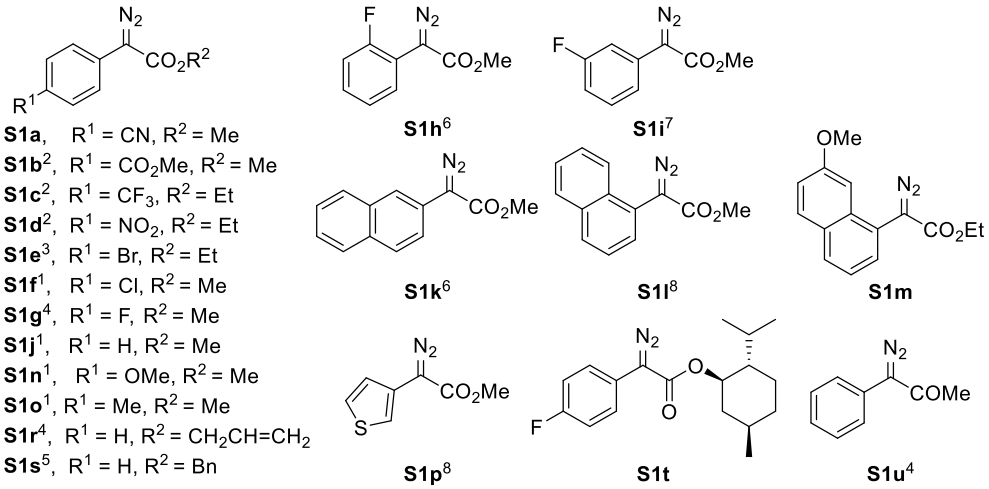

Figure S2. Diazo compounds **S1a-u**

Diazo compounds: **S1a-u** were prepared according to literature procedures. The observed characterization data (^{1}H and ^{13}C NMR) are consistent with those previously reported.[1-8]

Methyl 2-(4-cyanophenyl)-2-diazoacetate (S1a)

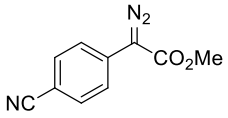

Synthesized according to the general procedure. Product purified by column chromatography (eluent: AcOEt/hexane), isolated as 362 mg (1.80 mmol, 90% yield) of yellow solid.

^{1}H NMR (400 MHz, $CDCl_3$) δ 7.68-7.55 (m, 4H), 3.89 (s, 3H) ppm.

^{13}C NMR (100 MHz, $CDCl_3$) δ 164.3, 132.6, 131.6, 123.4, 118.7, 108.7, 52.3 ppm.

HRMS (EI) *m/z*: [$M^{\bullet+}$] Calcd for $C_{10}H_7N_3O_2$ 201.0538; Found 201.0540.

Ethyl 2-[7-metoxy(1-naftyl)]-2-diazoacetate (S1m)

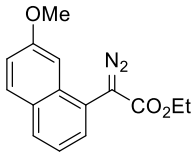

Synthesized according to the general procedure. Product purified by column chromatography (eluent: AcOEt/hexane), isolated as 465 mg (1.72 mmol, 90% yield) of orange oil.

^{1}H NMR (400 MHz, $CDCl_3$) δ 7.83-7.77 (m, 2H), 7.60 (dd, *J* = 7.2, 1.2 Hz, 1H), 7.39 (dd, *J* = 8.1, 7.3 Hz, 1H), 7.19 (dd, *J* = 9.0, 2.5 Hz, 1H), 7.05 (d, *J* = 2.5 Hz, 1H), 4.33 (q, *J* = 7.1 Hz, 2H), 3.93 (s, 3H), 1.32 (t, *J* = 7.1 Hz, 3H).

^{13}C NMR (100 MHz, $CDCl_3$) δ 158.5, 132.8, 130.4, 130.3, 129.5, 129.3, 123.3, 120.6, 119.0, 102.7, 77.2, 61.2, 55.4, 14.6.

HRMS (EI) *m/z*: [$M^{\bullet+}$] Calcd for $C_{15}H_{14}N_2O_3$ 270.1004; Found 270.0995.

(1S,2R,5S)-2-Isopropyl-5-methylcyclohexyl 2-(4-fluorophenyl)acetate (S4t)

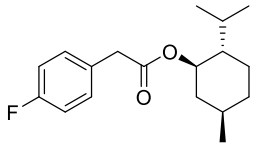

Synthesized according to the literature procedure.[9] Product isolated as 623 mg (2.13 mmol, 71% yield) of colorless oil from column chromatography (eluent: AcOEt/hexane).

^{1}H NMR (400 MHz, $CDCl_3$) δ 7.26-7.20 (m, 2H), 7.04-6.95 (m, 2H), 4.66 (td, *J* = 10.9, 4.4 Hz, 1H), 3.56 (s, 2H), 2.00-1.91 (m, 1H), 1.76-1.60 (m, 3H), 1.48-1.43 (m, 1H), 1.40-1.30 (m, 1H), 1.12-0.92 (m, 2H), 0.92-0.78 (m, 7H), 0.68 (d, *J* = 7.0 Hz, 3H) ppm.

^{13}C NMR (100 MHz, $CDCl_3$) δ 171.0 (d, J_{C-F} = 1.3 Hz), 162.0 (d, J_{C-F} = 245.1 Hz), 130.7 (d, J_{C-F} = 8.0 Hz), 130.1 (d, J_{C-F} = 3.3 Hz), 115.3 (d, J_{C-F} = 21.4 Hz), 74.8, 47.0, 41.0, 40.8, 34.2, 31.4, 26.2, 23.4, 22.0, 20.7, 16.2 ppm.

Elemental analysis (%) calculated for $C_{18}H_{25}O_2F$: C 73.94, H 8.62, found: C 74.12, H 8.56.

HRMS (EI) *m/z*: [$M^{\bullet+}$] Calcd for $C_{18}H_{25}O_2F$ 292.1839; Found 292.1849.

(1S,2R,5S)-2-Isopropyl-5-methylcyclohexyl 2-diazo-2-(4-fluorophenyl)acetate (S1t)

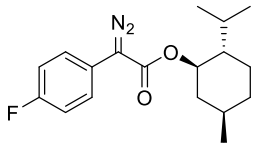

Synthesized according to the general procedure. Product isolated as 478 mg (1.38 mmol, 83% yield) of orange oil from column chromatography (eluent: AcOEt/hexane).

^{1}H NMR (400 MHz, $CDCl_3$) δ 7.49-7.41 (m, 2H), 7.11-7.04 (m, 2H), 4.86 (td, *J* = 10.9, 4.4 Hz, 1H), 2.14-2.07 (m, 1H), 1.96-1.83 (m, 1H), 1.74-1.66 (m, 2H), 1.58-1.48 (m, 1H), 1.47-1.39 (m, 1H), 1.14-1.00 (m, 2H), 0.96-0.86 (m, 7H), 0.81 (d, *J* = 7.0 Hz, 3H) ppm.

^{13}C NMR (100 MHz, $CDCl_3$) δ 164.8, 161.0 (d, J_{C-F} = 246.1 Hz), 125.8 (d, J_{C-F} = 7.9 Hz), 121.6 (d, J_{C-F} = 3.2 Hz), 115.9 (d, J_{C-F} = 22.0 Hz), 75.2, 47.2, 41.3, 34.2, 31.5, 26.6, 23.7, 22.0, 20.7, 16.6 ppm.

HRMS (EI) *m/z*: [$M^{\bullet+}$] Calcd for [$M^{\bullet+}$] $C_{18}H_{23}N_2FO_2$ 318.1744; Found 318.1751.

5.2. Preparation of (prop-2-yn-1-yl)sulfanes

Thioether alkynes, i.e., (prop-2-yn-1-yl)sulfanes (**S2a-n**), were prepared via the reaction of thiols with propargyl bromides in the presence of potassium carbonate in DMF according to the literature procedure.[11] The mixtures were stirred until full conversion of a starting material was observed by the TLC.

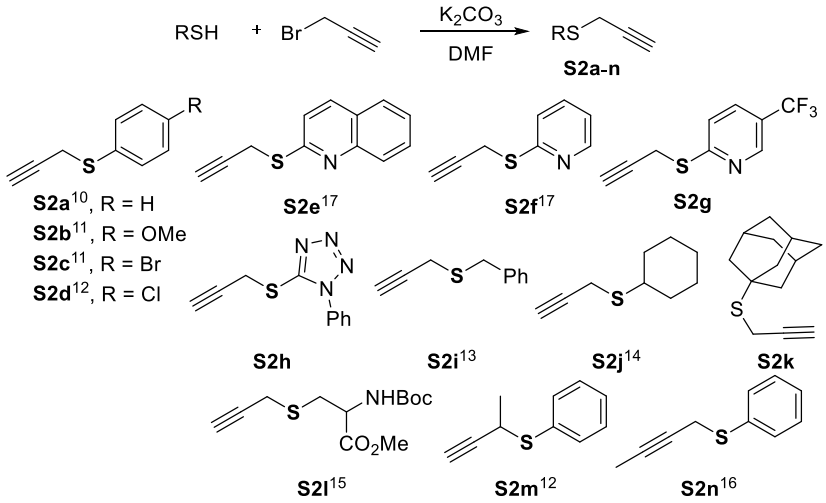

Scheme S2. Synthesis of (prop-2-yn-1-yl)sulfanes **S2a-n**.

The observed characterization data (^{1}H and ^{13}C NMR) are consistent with those previously reported.[11-17]

2-(Prop-2-yn-1-ylthio)-5-(trifluoromethyl)pyridine (S2g)

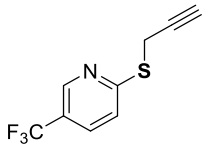

Synthesized according to the general procedure. Product isolated as 1031 mg (4.75 mmol, 80% yield) of pale yellow oil from column chromatography (eluent: hexane).

^{1}H NMR (400 MHz, $CDCl_3$) δ 8.80-8.63 (m, 1H), 7.80-7.62 (m, 1H), 7.34-7.28 (m, 1H), 4.00 (d, J = 2.6 Hz, 2H), 2.20 (t, J = 2.6 Hz, 1H) ppm.

^{13}C NMR (100 MHz, $CDCl_3$) δ 162.1 (m), 146.4 (q, J_{C-F} = 4.3 Hz), 132.8 (q, J_{C-F} = 3.4 Hz), 125.0, 122.8 (q, J_{C-F} = 33.0 Hz), 121.4, 79.3, 70.8, 18.3 ppm.

Elemental analysis (%) compound is too volatile.

HRMS (ESI) *m/z*: $[M+H]^+$ Calcd for C_9H_7NSF 218.0251; Found 218.0247.

1-Phenyl-5-(prop-2-yn-1-ylthio)-1H-tetrazole (S2h)

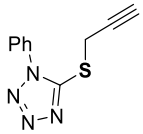

Synthesized according to the general procedure. Product isolated as 972 mg (4.75 mmol, 90% yield) of white solid from column chromatography (eluent: hexane).

m.p. 96-98 °C

^{1}H NMR (400 MHz, $CDCl_3$) δ 7.62-7.53 (m, 5H), 4.17 (d, J = 2.7 Hz, 2H), 2.31 (t, J = 2.7 Hz, 1H) ppm.

^{13}C NMR (100 MHz, $CDCl_3$) δ 152.8, 133.5, 130.3, 129.9, 123.8, 77.1, 73.1, 21.9 ppm.

Elemental analysis (%) calculated for $C_{10}H_8N_4S$: C 55.54, H 3.73, found: C 55.41, H 3.63.
HRMS (ESI) *m/z*: $[M+Na]^+$ Calcd for $C_{10}H_8N_4SNa$ 239.0367; Found 239.0360.

(3S,5S,7S)-Adamantan-1-yl(prop-2-yn-1-yl)sulfane (S2k)

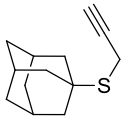

Synthesized according to the general procedure. Product isolated as 979 mg (4.75 mmol, 95% yield) of pale yellow oil from column chromatography (eluent: hexane).
^{1}H NMR (400 MHz, $CDCl_3$) δ 3.25 (d, *J* = 2.7 Hz, 2H), 2.18 (t, *J* = 2.6 Hz, 1H), 2.10-2.03 (m, 3H), 1.94-1.85 (m, 6H), 1.72-1.68 (m, 6H) ppm.
^{13}C NMR (100 MHz, $CDCl_3$) δ 82.1, 70.3, 45.5, 43.3, 36.2, 29.7, 14.0 ppm.
Elemental analysis (%) compound is too volatile.
HRMS (EI) *m/z*: $[M^{\bullet+}]$ Calcd for $C_{13}H_{18}S$ 206.1129; Found 206.1131.

5.3. General procedure for the photoinduced Doyle-Kirmse reaction

A glass vial equipped with a stirring bar and sealed with a septum was charged with (prop-2-yn-1-yl)sulfide (1.35 mmol, 9 equiv.), a diazo carbonyl compound (0.075 mmol) and DCM (0.25 mL). The reaction mixture was placed in a photoreactor and irradiated with blue LED (3W) for 3 hours. Then, the second portion of the diazo carbonyl compound (0.075 mmol) in DCM (0.25 mL) was added and the reaction mixture was stirred for another 21 hours. The crude reaction mixture was purified by column chromatography using hexanes:EtOAc as eluent to afford the final product.

Methyl 2-(4-cyanophenyl)-2-(phenylthio)penta-3,4-dienoate (3)

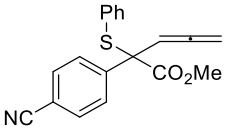

Synthesized according to the general procedure. Product isolated as 39 mg (0.12 mmol, 80% yield) of yellowish oil from column chromatography (eluent: AcOEt/hexane).
^{1}H NMR (400 MHz, $CDCl_3$) δ 7.58-7.57 (m, 4H), 7.35-7.28 (m, 3H), 7.24-7.20 (m, 2H), 5.74 (t, *J* = 6.6 Hz, 1H), 4.76 (d, *J* = 6.6 Hz, 2H), 3.69 (s, 3H) ppm.
^{13}C NMR (100 MHz, $CDCl_3$) δ 208.4, 170.2, 144.2, 136.8, 131.7, 130.6, 129.7, 129.2, 128.7, 118.5, 111.6, 93.4, 79.5, 64.0, 53.1 ppm.
Elemental analysis (%) calculated for $C_{19}H_{15}NO_2S$: C 71.00, H 4.70, N 4.36, found: C 71.00, H 4.62, N 4.13.
HRMS (ESI) *m/z*: $[M+Na]^+$ Calcd for $C_{19}H_{15}NO_2SNa$ 344.0715; Found 344.0721.

Methyl 4-(1-ethoxy-1-oxo-2-(phenylthio)penta-3,4-dien-2-yl)benzoate (4)

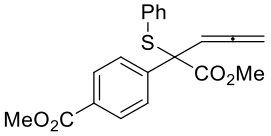

Synthesized according to the general procedure. Product isolated as 41 mg (0.12 mmol, 78% yield) of yellowish oil from column chromatography (eluent: AcOEt/hexane).
^{1}H NMR (400 MHz, $CDCl_3$) δ 7.93-7.86 (m, 2H), 7.48-7.43 (m, 2H), 7.27-7.22 (m, 3H), 7.17-7.12 (m, 2H), 5.69 (t, *J* = 6.6 Hz, 1H), 4.67 (dd, *J* = 6.6 Hz, *J* = 1.0 Hz, 2H), 3.85 (s, 3H), 3.62 (s, 3H) ppm.

^{13}C NMR (100 MHz, $CDCl_3$) δ 208.3, 170.7, 166.7, 143.9, 136.7, 131.0, 129.5, 129.4, 129.2, 128.5, 128.3, 93.7, 79.2, 64.2, 53.0, 52.1 ppm.
Elemental analysis (%) calculated for $C_{20}H_{18}O_4S$: C 67.78, H 5.12, found: C 67.85, H 4.95.
HRMS (ESI) *m/z*: $[M+Na]^+$ Calcd for $C_{20}H_{18}O_4SNa$ 377.0823; Found 377.0823.

Methyl 2-(phenylthio)-2-(4-(trifluoromethyl)phenyl)penta-3,4-dienoate (5)

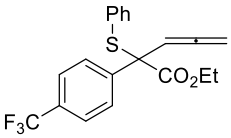

Synthesized according to the general procedure. Product isolated as 44 mg (0.12 mmol, 78% yield) of yellowish oil from column chromatography (eluent: AcOEt/hexane).
^{1}H NMR (400 MHz, $CDCl_3$) δ 7.54-7.47 (m, 4H), 7.26-7.22 (m, 3H), 7.17-7.11 (m, 2H), 5.70 (t, J = 6.6 Hz, 1H), 4.67 (d, J = 6.7 Hz, 2H), 4.15-4.04 (m, 2H), 1.10 (t, J = 7.1 Hz, 3H) ppm.
^{13}C NMR (100 MHz, $CDCl_3$) δ 208.4, 170.1, 143.1, 136.6, 131.1, 129.8 (q, J_{C-F} = 32.4 Hz), 129.4-129.3 (m), 128.7, 128.5, 124.9 (q, J_{C-F} = 3.7 Hz), 124.0 (m), 93.7, 79.2, 63.8, 62.3, 13.9 ppm.
Elemental analysis (%) calculated for $C_{20}H_{17}F_3O_2S$: C 63.48, H 4.53, found: C 63.31, H 4.61.
HRMS (ESI) *m/z*: $[M+Na]^+$ Calcd for $C_{20}H_{17}F_3O_2SNa$ 401.0799; Found 401.0801.

Methyl 2-(4-nitrophenyl)-2-(phenylthio)penta-3,4-dienoate (6)

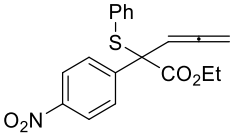

Synthesized according to the general procedure. Product isolated as 32 mg (0.09 mmol, 59% yield) of yellowish oil from column chromatography (eluent: AcOEt/hexane).
^{1}H NMR (400 MHz, $CDCl_3$) δ 8.13-8.04 (m, 2H), 7.62-7.55 (m, 2H), 7.29-7.23 (m, 3H), 7.19-7.13 (m, 2H), 5.71 (t, J = 6.6 Hz, 1H), 4.71 (d, J = 6.6 Hz, 2H), 4.18-4.04 (m, 2H), 1.11 (t, J = 7.1 Hz, 3H) ppm.
^{13}C NMR (100 MHz, $CDCl_3$) δ 208.4, 169.6, 147.1, 146.3, 136.7, 130.7, 129.6, 129.5, 128.7, 123.0, 93.5, 79.5, 63.7, 62.5, 13.9 ppm.
Elemental analysis (%) calculated for $C_{19}H_{17}NO_4S$: C 64.21, H 4.82, found: C 64.11, H 5.03.
HRMS (ESI) *m/z*: $[M+Na]^+$ Calcd for $C_{19}H_{17}NO_4SNa$ 378.0776; Found 378.0770.

Ethyl 2-(4-bromophenyl)-2-(phenylthio)penta-3,4-dienoate (7)

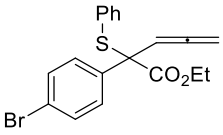

Synthesized according to the general procedure. Product isolated as 46 mg (0.12 mmol, 79% yield) of yellowish oil from column chromatography (eluent: AcOEt/hexane).
^{1}H NMR (400 MHz, $CDCl_3$) δ 7.44-7.41 (m, 2H), 7.38-7.29 (m, 5H), 7.24-7.20 (m, 2H), 5.73 (t, J = 6.6 Hz, 1H), 4.73 (d, J = 6.7 Hz, 2H), 4.19-4.10 (m, 2H), 1.16 (t, J = 7.1 Hz, 3H) ppm.
^{13}C NMR (100 MHz, $CDCl_3$) δ 208.4, 170.2, 138.2, 136.5, 131.4, 131.0, 130.1, 129.2, 128.5, 121.8, 93.8, 79.1, 63.7, 62.2, 13.9 ppm.
Elemental analysis (%) calculated for $C_{19}H_{17}BrO_2S$: C 58.62, H 4.40, found: C 58.78, H 4.41.
HRMS (ESI) *m/z*: $[M+Na]^+$ Calcd for $C_{19}H_{17}BrO_2SNa$ 411.0030; Found 411.0030.

Methyl 2-(4-chlorophenyl)-2-(phenylthio)penta-3,4-dienoate (8)

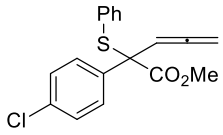

Synthesized according to the general procedure. Product isolated as 37 mg (0.11 mmol, 74% yield) of yellowish oil from column chromatography (eluent: AcOEt/hexane).
^{1}H NMR (400 MHz, $CDCl_3$) δ 7.36-7.32 (m, 2H), 7.27-7.14 (m, 7H), 5.66 (t, J = 6.6 Hz, 1H), 4.67 (d, J = 6.8 Hz, 2H), 3.60 (s, 3H) ppm.
^{13}C NMR (100 MHz, $CDCl_3$) δ 208.4, 170.8, 137.4, 136.7, 133.7, 131.2, 129.7, 129.3, 128.5, 128.1, 93.8, 79.1, 63.8, 53.0 ppm.
Elemental analysis (%) calculated for $C_{18}H_{15}ClO_2S$: C 65.35, H 4.57, found: C 65.33, H 4.61.
HRMS (ESI) *m/z*: $[M+Na]^+$ Calcd for $C_{18}H_{15}ClO_2SNa$ 353.0379; Found 353.0378.

Ethyl 2-(4-fluorophenyl)-2-(phenylthio)penta-3,4-dienoate (9)

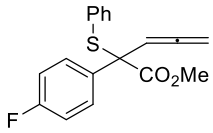

Synthesized according to the general procedure. Product isolated as 41 mg (0.13 mmol, 88% yield) of yellowish oil, by column chromatography (eluent: AcOEt/hexane).
^{1}H NMR (400 MHz, $CDCl_3$) δ 7.41-7.34 (m, 2H), 7.29-7.21 (m, 3H), 7.18-7.13 (m, 2H), 6.94-6.88 (m, 2H), 5.67 (t, J = 6.6 Hz, 1H), 4.66 (dd, J = 6.6 Hz, 2H), 3.61(s, 3H) ppm.
^{13}C NMR (100 MHz, $CDCl_3$) δ 208.3, 171.0, 162.14 (d, J_{C-F} = 247.6 Hz), 136.6, 134.65 (d, J_{C-F} = 3.3 Hz), 131.4, 130.03 (d, J_{C-F} = 8.2 Hz), 129.3, 128.5, 114.88 (d, J_{C-F} = 21.6 Hz), 94.0, 79.0, 63.8, 52.9 ppm.
Elemental analysis (%) calculated for $C_{18}H_{15}FO_2S$: C 68.77, H 4.81, found: C 68.62, H 4.88.
HRMS (ESI) *m/z*: $[M+Na]^+$ Calcd for $C_{18}H_{15}FO_2SNa$ 337.0674; Found 337.0672.

Methyl 2-(2-fluorophenyl)-2-(phenylthio)penta-3,4-dienoate (10)

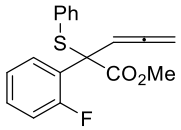

Synthesized according to the general procedure. Product isolated as 34 mg (0.11 mmol, 72% yield) of yellowish oil from column chromatography (eluent: AcOEt/hexane).
^{1}H NMR (400 MHz, $CDCl_3$) δ 7.65-7.59 (m, 1H), 7.33-7.14 (m, 6H), 7.06-7.02 (m, 1H), 6.96-6.90 (m, 1H), 5.85-5.67 (m, 1H), 4.70-4.61 (m, 2H), 3.52 (s, 3H) ppm.
^{13}C NMR (100 MHz, $CDCl_3$) δ 207.8, 170.3, 160.1 (d, J_{C-F} = 248.2 Hz), 137.1, 130.7, 129.7 (d, J_{C-F} = 8.8 Hz), 129.6, 129.4 (d, J_{C-F} = 3.0 Hz), 128.5, 127.2 (d, J_{C-F} = 12.3 Hz), 123.5 (d, J_{C-F} = 3.4 Hz), 115.50 (d, J_{C-F} = 22.3 Hz), 93.7, 79.1, 60.5, 52.7 ppm.
^{19}F NMR (376 MHz, $CDCl_3$) δ -110.63 (s) ppm.
Elemental analysis (%) calculated for $C_{18}H_{15}FO_2S$: C 68.77, H 4.81, found: C 68.83, H 5.09.
HRMS (ESI) *m/z*: $[M+Na]^+$ Calcd for $C_{18}H_{15}FO_2SNa$ 337.0661; Found 337.0674.

Methyl 2-(2-fluorophenyl)-2-(phenylthio)penta-3,4-dienoate (11)

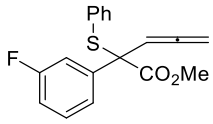

Synthesized according to the general procedure. Product isolated as 34 mg (0.11 mmol, 72% yield) of yellowish oil from column chromatography (eluent: AcOEt/hexane).
^{1}H NMR (400 MHz, $CDCl_3$) δ 7.36-7.21 (m, 8H), 7.03-6.93 (m, 1H), 5.73 (t, J = 6.6 Hz, 1H), 4.75 (dd, J = 6.6 Hz, J = 1.3 Hz, 2H), 3.69 (s, 3H) ppm.
^{13}C NMR (100 MHz, $CDCl_3$) δ 208.4, 170.7, 169.2, 162.40 (d, $J_{C\text{-}F}$ = 245.6 Hz), 141.40 (d, $J_{C\text{-}F}$ = 7.3 Hz), 136.7, 130.3 (d, $J_{C\text{-}F}$ = 169.8 Hz), 129.4 (d, $J_{C\text{-}F}$ = 1.2 Hz), 128.5, 123.9 (d, $J_{C\text{-}F}$ = 2.9 Hz), 115.6 (d, $J_{C\text{-}F}$ = 23.6 Hz), 114.7 (d, $J_{C\text{-}F}$ = 21.1 Hz), 93.7, 79.0, 63.9, 53.0 ppm.
Elemental analysis (%) calculated for $C_{18}H_{15}FO_2S$: C 68.77, H 4.81, found: C 68.80, H 4.69.
HRMS (ESI) *m/z*: $[M+Na]^+$ Calcd for $C_{18}H_{15}FO_2SNa$ 337.0674; Found 337.0665.

Methyl 2-phenyl-2-(phenylthio)penta-3,4-dienoate (12)

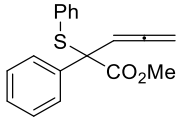

Synthesized according to the general procedure. Product isolated as 35 mg (0.12 mmol, 79% yield) of yellowish oil via column chromatography (eluent: AcOEt/hexane).
^{1}H NMR (400 MHz, $CDCl_3$) δ 7.41-7.36 (m, 2H), 7.28-7.13 (m, 8H), 5.69 (t, J = 6.6 Hz, 1H), 4.70-4.61 (m, 2H), 3.61 (s, 3H) ppm.
^{13}C NMR (100 MHz, $CDCl_3$) δ 208.4, 171.2, 138.9, 136.6, 131.6, 129.1, 128.4, 128.1, 128.0, 127.8, 94.0, 78.8, 64.4, 52.9 ppm.
Elemental analysis (%) calculated for $C_{18}H_{16}O_2S$: C 72.94, H 5.44, found: C 72.80, H 5.37.
HRMS (ESI) *m/z*: $[M+Na]^+$ Calcd for $C_{18}H_{16}O_2SNa$ 319.0769; Found 319.0763.

Methyl 2-(naphthalen-2-yl)-2-(phenylthio)penta-3,4-dienoate (13)

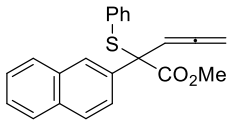

Synthesized according to the general procedure. Product isolated as 40 mg (0.11 mmol, 76% yield) of yellowish oil from column chromatography (eluent: AcOEt/hexane).
^{1}H NMR (400 MHz, $CDCl_3$) 7.92 (d, J = 1.7 Hz, 1H), 7.86-7.76 (m, 3H), 7.60 (dd, J = 8.7, 2.0 Hz, 1H), 7.52-7.45 (m, 2H), 7.38-7.33 (m, 2H), 7.31-7.26 (m, 1H), 7.22-7.15 (m, 2H), 5.86 (t, J = 6.6 Hz, 1H), 4.79-4.70 (m, 2H), 3.70 (s, 3H).
^{13}C NMR (100 MHz, $CDCl_3$) δ 208.4, 171.2, 136.7, 136.2, 132.8, 132.7, 131.5, 129.2, 128.4, 128.4, 127.8, 127.5, 127.1, 126.4, 126.2, 93.9, 78.9, 64.7, 53.0.
Elemental analysis (%) calculated for $C_{22}H_{18}O_2S$: C 76.27, H 5.24, found: C 76.06, H 5.25.
HRMS (ESI) *m/z*: $[M+Na]^+$ Calcd for $C_{22}H_{18}O_2SNa$ 369.0925; Found 369.0918.

Methyl 2-(naphthalen-1-yl)-2-(phenylthio)penta-3,4-dienoate (14)

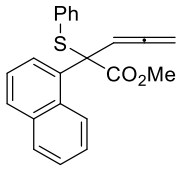

Synthesized according to the general procedure. Product isolated as 38 mg (0.11 mmol, 73% yield) of yellowish oil from column chromatography (eluent: AcOEt/hexane).
^{1}H NMR (400 MHz, $CDCl_3$) δ 7.92-7.84 (m, 2H), 7.80-7.75 (m, 1H), 7.75-7.69 (m, 1H), 7.41-7.30 (m, 3H), 7.25-7.19 (m, 3H), 7.15-7.08 (m, 2H), 5.95 (t, *J* = 6.6 Hz, 1H), 4.58 (dd, *J* = 11.4, 6.6 Hz, 1H), 4.40 (dd, *J* = 11.4, 6.6 Hz, 1H), 3.41 (s, 3H) ppm.
^{13}C NMR (100 MHz, $CDCl_3$) δ 208.1, 171.9, 137.1, 134.6, 134.2, 131.2, 129.4, 129.2, 129.0, 128.4, 126.7, 125.9, 125.3, 124.9, 124.6, 94.7, 78.7, 64.2, 52.7 ppm.
Elemental analysis (%) calculated for $C_{22}H_{18}O_2S$: C 76.27, H 5.24, found: C 76.19, H 5.19.
HRMS (ESI) *m/z*: $[M+Na]^+$ Calcd for $C_{22}H_{18}O_2SNa$ 369.0925; Found 369.0916.

Methyl 2-[7-metoxy(naphthalen-2-yl)]-2-(phenylthio)penta-3,4-dienoate (15)

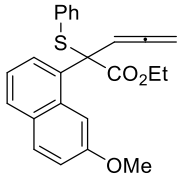

Synthesized according to the general procedure. Product isolated as 36 mg (0.09 mmol, 62% yield) of yellowish oil from column chromatography (eluent: AcOEt/hexane).
^{1}H NMR (400 MHz, $CDCl_3$) δ 7.83 (d, *J* = 7.3 Hz, 1H), 7.77-7.69 (m, 2H), 7.39 (d, *J* = 2.1 Hz, 1H), 7.31-7.23 (m, 4H), 7.21-7.15 (m, 2H), 7.12 (dd, *J* = 8.9, 2.4 Hz, 1H), 5.99 (t, *J* = 6.6 Hz, 1H), 4.70 (dd, *J* = 11.4, 6.6 Hz, 1H), 4.56 (dd, *J* = 11.4, 6.6 Hz, 1H), 4.12-3.96 (m, 2H), 3.86 (s, 3H), 0.96 (t, *J* = 7.1 Hz, 3H).
^{13}C NMR (100 MHz, $CDCl_3$) δ 208.1, 171.5, 157.4, 137.1, 133.5, 132.3, 131.4, 130.3, 129.5, 129.3, 128.7, 128.3, 127.1, 122.3, 118.0, 104.1, 94.4, 78.7, 64.1, 62.0, 55.3, 13.8.
Elemental analysis (%) calculated for $C_{24}H_{22}O_3S$: C 73.82, H 5.68, found: C 73.58, H 5.61.
HRMS (ESI) *m/z*: $[M+Na]^+$ Calcd for $C_{24}H_{22}O_3SNa$ 413.1187; Found 413.1183.

Methyl 2-(4-methoxyphenyl)-2-(phenylthio)penta-3,4-dienoate (16)

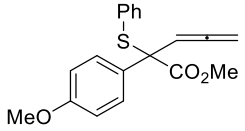

Synthesized according to the general procedure. Product isolated as 25 mg (0.08 mmol, 51% yield) of yellowish oil from column chromatography (eluent: AcOEt/hexane).
^{1}H NMR (400 MHz, $CDCl_3$) δ 7.42-7.37 (m, 2H), 7.36-7.33 (m, 2H), 7.32-7.27 (m, 1H), 7.24-7.20 (m, 2H), 6.86-6.82 (m, 2H), 5.74 (t, *J* = 6.6 Hz, 1H), 4.77-4.67 (m, 2H), 3.80 (s, 3H), 3.68 (s, 3H) ppm.
^{13}C NMR (100 MHz, $CDCl_3$) δ 208.4, 171.4, 159.1, 136.5, 131.8, 130.9, 129.3, 129.0, 128.4, 113.4, 94.1, 78.7, 64.0, 55.3, 52.8 ppm.
Elemental analysis (%) calculated for $C_{19}H_{18}O_3S$: C 69.91, H 5.56, found: C 69.87, H 5.51.
HRMS (ESI) *m/z*: $[M+Na]^+$ Calcd for $C_{19}H_{18}O_3SNa$ 349.0874; Found 349.0871.

Methyl 2-(phenylthio)-2-(p-tolyl)penta-3,4-dienoate (17)

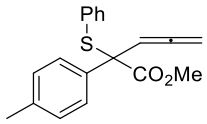

Synthesized according to the general procedure. Product isolated as 34 mg (0.11 mmol, 73% yield) of yellowish oil from column chromatography (eluent: AcOEt/hexane).

^{1}H NMR (400 MHz, $CDCl_3$) δ 7.38-7.27 (m, 5H), 7.25-7.19 (m, 2), 7.14-7.11 (m, 2H), 5.67 (t, *J* = 6.6 Hz, 1H), 4.69-4.59 (m, 2H), 3.60 (s, 3H), 2.26 (s, 3H) ppm.
^{13}C NMR (100 MHz, $CDCl_3$) δ 208.4, 171.4, 137.6, 136.5, 135.9, 131.8, 129.0, 128.8, 128.4, 127.9, 94.0, 78.7, 64.2, 52.8, 21.0 ppm.
Elemental analysis (%) calculated for $C_{19}H_{18}O_2S$: C 73.52, H 5.85, found: C 73.76, H 5.66.
HRMS (ESI) *m/z*: $[M+Na]^+$ Calcd for $C_{19}H_{18}O_2SNa$ 333.0925; Found 333.0921.

Methyl 2-(phenylthio)-2-(thiophen-3-yl)penta-3,4-dienoate (18)

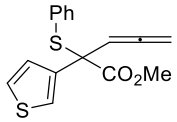

Synthesized according to the general procedure. Product isolated as 34 mg (0.11 mmol, 74% yield) of yellowish oil from column chromatography (eluent: AcOEt/hexane).
^{1}H NMR (400 MHz, $CDCl_3$) δ 7.28-7.22 (m, 3H), 7.20-7.14 (m, 4H), 7.10 (dd, *J* = 4.6 Hz, *J* = 1.9 Hz, 1H), 5.67 (t, *J* = 6.7 Hz, 1H), 4.71 (d, *J* = 6.7 Hz, 2H), 3.64 (s, 3H) ppm.
^{13}C NMR (100 MHz, $CDCl_3$) δ 208.2, 170.7, 139.3, 136.6, 131.5, 129.3, 128.4, 128.1, 125.2, 124.1, 93.8, 79.0, 60.5, 52.9 ppm.
Elemental analysis (%) calculated for $C_{16}H_{14}O_2S_2$: C 63.55, H 4.67, S 21.20 found: C 63.54, H 4.55, S 21.26.
HRMS (ESI) *m/z*: $[M+Na]^+$ Calcd for $C_{16}H_{14}O_2S_2Na$ 325.0333; Found 325.0327.

Allyl 2-phenyl-2-(phenylthio)penta-3,4-dienoate (19)

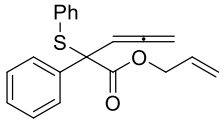

Synthesized according to the general procedure. Product isolated as 38 mg (0.12 mmol, 79% yield) of yellowish oil from column chromatography (eluent: AcOEt/hexane).
^{1}H NMR (400 MHz, $CDCl_3$) δ 7.43-7.39 (m, 2H), 7.29-7.13 (m, 8H), 5.78-5.67 (m, 2H), 5.18-5.06 (m, 2H), 4.72-4.58 (m, 2H), 4.54-4.50 (m, 2H) ppm.
^{13}C NMR (100 MHz, $CDCl_3$) δ 208.5, 170.4, 138.9, 136.6, 131.7, 131.5, 129.0, 128.4, 128.1, 128.0, 127.8, 118.6, 94.0, 78.9, 66.4, 64.3 ppm.
Elemental analysis (%) calculated for $C_{20}H_{18}O_2S$: 74.50, H 5.63, found: C 74.29, H 5.48.
HRMS (ESI) *m/z*: $[M+Na]^+$ Calcd for $C_{20}H_{18}O_2SNa$ 345.0925; Found 345.0921.

Benzyl 2-phenyl-2-(phenylthio)penta-3,4-dienoate (20)

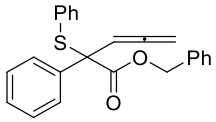

Synthesized according to the general procedure. Product isolated as 47 mg (0.13 mmol, 84% yield) of yellowish oil from column chromatography (eluent: AcOEt/hexane).
^{1}H NMR (400 MHz, $CDCl_3$) δ 7.49-7.43 (m, 2H), 7.31-7.24 (m, 9H), 7.22-7.13 (m, 4H), 5.76 (t, *J* = 6.6 Hz, 1H), 5.13 (d, *J* = 4.2 Hz, 2H), 4.66 (dd, *J* = 6.6, 2.8 Hz, 2H) ppm.
^{13}C NMR (100 MHz, $CDCl_3$) δ 208.4, 170.5, 138.8, 136.6, 135.3, 131.6, 129.0, 128.4, 128.4, 128.2, 128.2, 128.1, 128.0, 127.8, 93.9, 78.8, 67.5, 64.2 ppm.
Elemental analysis (%) calculated for $C_{24}H_{20}O_2S$: 77.39, H 5.41, found: C 77.33, H 5.32.
HRMS (ESI) *m/z*: $[M+Na]^+$ Calcd for $C_{24}H_{20}O_2SNa$ 395.1082; Found 395.1074.

(1S,2S,5S)-2-Isopropyl-5-methylcyclohexyl 2-(4-fluorophenyl)-2-(phenylthio)penta-3,4-dienoate (21)

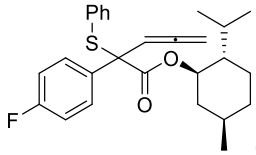

(two diastereoisomers)

Synthesized according to the general procedure. Product isolated as a mixture of diastereoisomers (1.1:1) 48 mg (0.11 mmol, 72% yield) of yellowish oil from column chromatography (eluent: AcOEt/hexane).

^{1}H NMR (400 MHz, $CDCl_3$) δ 7.52-7.44 (m, 2H), 7.34-7.26 (m, 3H), 7.23-7.16 (m, 2H), 7.02-6.93 (m, 2H), 5.71 (2xt, J = 6.6 Hz, 1H), 4.75-5.60 (m, 3H), 1.99-1.88 (m, 1 H), 1.70-1.38 (m, 5H), 1.34-1.26 (m, 1H), 1.04-0.82 (m, 5H), 0.75 (dd, J = 10.3, 7.0 Hz, 3H), 0.63 (dd, J = 6.9, 3.6 Hz, 3H) ppm.

^{13}C NMR (100 MHz, $CDCl_3$) δ 208.7, 208.4, 170.1, 170.0, 162.1 (d, J_{C-F} = 247.3 Hz),, 136.3, 136.2, 135.2 (d, J_{C-F} = 3.3 Hz), 135.0 (d, J_{C-F} = 3.3 Hz), 131.9, 130.2 (d, J_{C-F} = 8.1 Hz), 130.0 (d, J_{C-F} = 8.2 Hz), 128.8, 128.8, 128.3, 128.3,114.8 (d, J_{C-F} = 5.5 Hz), 114.6 (d, J_{C-F} = 5.5 Hz), 94.1, 93.5, 79.0, 79.0, 63.8, 63.7, 46.9, 46.8, 40.4, 40.2, 34.1, 34.1, 31.4, 25.6, 25.5, 23.0, 22.9, 22.0, 20.7, 20.7, 15.8, 15.8.

^{19}F NMR (376 MHz, $CDCl_3$) δ -114.7 (s), -114.8 (s) ppm.

Elemental analysis (%) calculated for $C_{27}H_{31}FO_2S$: C 73.94, H 7.12, found: C 74.00, H 7.34.

HRMS (ESI) *m/z*: $[M+Na]^+$ Calcd for $C_{27}H_{31}FO_2SNa$ 461.1926; Found 461.1923.

3-Phenyl-3-(phenylthio)hexa-4,5-dien-2-one (22)

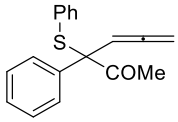

Synthesized according to the general procedure. Product isolated as 18 mg (0.07 mmol, 43% yield) of yellowish oil from column chromatography (eluent: AcOEt/hexane).

^{1}H NMR (400 MHz, $CDCl_3$) δ 7.44-7.39 (m, 2H), 7.38-7.30 (m, 6H), 7.26-7.23 (m, 2H), 5.67 (t, J = 6.7 Hz, 1H), 4.69 (dd, J = 11.5, 6.7 Hz, 1H), 4.61 (dd, J = 11.5, 6.7 Hz, 1H), 2.16 (s, 3H) ppm.

^{13}C NMR (100 MHz, $CDCl_3$) δ 208.5, 201.7, 138.2, 136.7, 130.8, 129.2, 128.6, 128.5, 128.1, 128.0, 93.0, 78.2, 69.8, 26.7 ppm.

Elemental analysis (%) calculated for $C_{18}H_{16}OS$: C 77.11, H 5.75, found: C 76.85, H 6.02.

HRMS (ESI) *m/z*: $[M+Na]^+$ Calcd for $C_{18}H_{16}OSNa$ 303.0820; Found 303.0812.

Methyl 2-(4-cyanophenyl)-2-((4-methoxyphenyl)thio)penta-3,4-dienoate (23)

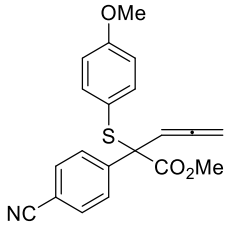

Synthesized according to the general procedure. Product isolated as 35 mg (0.10 mmol, 67% yield) of yellowish oil from column chromatography (eluent: AcOEt/hexane).

^{1}H NMR (400 MHz, $CDCl_3$) δ 7.60-7.54 (m, 4H), 7.25-7.21 (m, 2H), 6.78-6.74 (m, 2H), 5.73 (t, J = 6.7 Hz, 1H), 4.76 (dd, J = 6.6, 0.7 Hz, 2H), 3.78 (s, 3H), 3.70 (s, 3H) ppm.

^{13}C NMR (100 MHz, $CDCl_3$) δ 208.2, 170.3, 161.1, 144.3, 138.8, 131.6, 129.2, 121.0, 118.6, 114.2, 111.5, 93.4, 79.3, 64.0, 55.3, 53.1 ppm.

Elemental analysis (%) calculated for $C_{20}H_{17}NO_3S$: C 68.36, H 4.88, N 3.99, found: C 68.37, H 5.10, N 3.89.
HRMS (ESI) *m/z*: $[M+Na]^+$ Calcd for $C_{20}H_{17}NO_3SNa$ 374.0826; Found 374.0827.

Methyl 2-((4-bromophenyl)thio)-2-(4-cyanophenyl)penta-3,4-dienoate (24)

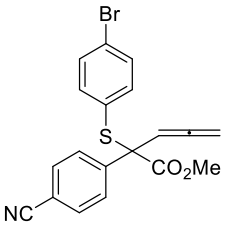

Synthesized according to the general procedure. Product isolated as 45 mg (0.11 mmol, 74% yield) of yellowish oil from column chromatography (eluent: AcOEt/hexane).
^{1}H NMR (400 MHz, $CDCl_3$) δ 7.63-7.54 (m, 4H), 7.39-7.35 (m, 2H), 7.17-7.13 (m, 2H), 5.72 (t, *J* = 6.6 Hz, 1H), 4.80 (dd, *J* = 6.6, 0.6 Hz, 2H), 3.71 (s, 3H) ppm.
^{13}C NMR (100 MHz, $CDCl_3$) δ 208.4, 170.0, 143.9, 138.1, 131.9, 131.8, 129.7, 129.1, 124.6, 118.4, 111.8, 93.1, 79.7, 64.1, 53.2 ppm.
Elemental analysis (%) calculated for $C_{19}H_{14}BrNO_2S$: C 57.01, H 3.53, N 3.50, found: C 57.19, H 3.69, N 3.33.
HRMS (ESI) *m/z*: $[M+Na]^+$ Calcd for $C_{19}H_{14}BrNO_2SNa$ 421.9826; Found 421.9814.

Methyl 2-((4-chlorophenyl)thio)-2-(4-cyanophenyl)penta-3,4-dienoate (25)

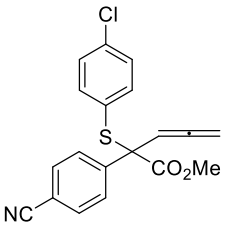

Synthesized according to the general procedure. Product isolated as 45 mg (0.13 mmol, 84% yield) of yellowish oil from column chromatography (eluent: AcOEt/hexane).
^{1}H NMR (400 MHz, $CDCl_3$) δ 7.61-7.59 (m, 2H), 7.56-7.54 (m, 2H), 7.22-7.21 (m, 4H), 5.72 (t, *J* = 6.6 Hz, 1H), 4.80 (dd, *J* = 6.6, 0.8 Hz, 2H), 3.70 (s, 3H) ppm.
^{13}C NMR (100 MHz, $CDCl_3$) δ 208.4, 170.1, 143.9, 137.9, 136.3, 131.8, 129.1, 129.1, 128.9, 118.4, 111.8, 93.1, 79.7, 64.1, 53.2 ppm.
Elemental analysis (%) calculated for $C_{19}H_{14}ClNO_2S$: C 64.13, H 3.97, N 3.94, found: C 64.19, H 3.90, N 3.79.
HRMS (ESI) *m/z*: $[M+Na]^+$ Calcd for $C_{19}H_{14}ClNO_2SNa$ 378.0331; Found 378.0320.

Methyl 2-(4-cyanophenyl)-2-(quinolin-2-ylthio)penta-3,4-dienoate (26)

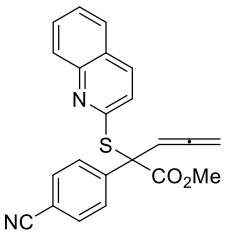

Synthesized according to the general procedure. Product isolated as 25 mg (0.07 mmol, 45% yield) of yellowish oil from column chromatography (eluent: AcOEt/hexane).

^{1}H NMR (400 MHz, $CDCl_3$) δ 7.94-7.91 (m, 1H), 7.84-7.76 (m, 3H), 7.74-7.72 (m, 1H), 7.67-7.61 (m, 3H), 7.47-7.7.43 (m, 1H),7.20 (d, *J* = 8.6 Hz, 1H), 6.42 (t, *J* = 6.7 Hz, 1H), 4.79 (dd, *J* = 11.5, 6.7 Hz, 1H), 4.72 (dd, *J* = 11.5, 6.7 Hz, 1H), 3.77 (s, 3H) ppm.
^{13}C NMR (125 MHz, $CDCl_3$) δ 208.3, 170.7, 156.4, 147.9, 143.2, 135.9, 131.9, 129.9, 129.0, 127.6, 125.9, 125.9, 120.1, 118.5, 112.0, 94.6, 79.5, 62.1, 53.5 ppm.
Elemental analysis (%) decomposition
HRMS (ESI) *m/z*: $[M+H]^+$ Calcd for $C_{22}H_{17}N_2O_2S$ 373.1011; Found 373.1010.

Methyl 2-(4-cyanophenyl)-2-(pyridin-2-ylthio)penta-3,4-dienoate (27)

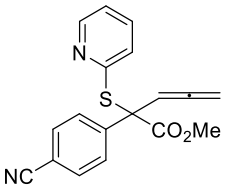

compound unstable

Synthesized according to the general procedure. Product isolated as 28 mg (0.09 mmol, 60% yield) of yellowish oil, by column chromatography (eluent: AcOEt/hexane).
^{1}H NMR (400 MHz, $CDCl_3$) δ 8.34-8.30 (m, 1H), 7.73-7.68 (m, 2H), 7.61-7.59 (m, 2H), 7.48 (td, *J* = 1.9 Hz, *J* = 7.9 Hz, 1H), 7.18-7.14 (m, 1H), 7.03-6.99 (m, 1H), 6.21 (t, *J* = 6.6 Hz, 1H), 4.78 (dd, *J* = 6.6 Hz, *J* = 11.5 Hz, 1H), 4.70 (dd, *J* = 6.6 Hz, *J* = 11.5 Hz, 1H), 3.74 (s, 3H) ppm.
^{13}C NMR (125 MHz, $CDCl_3$) δ 208.2, 170.6, 156.3, 149.1, 143.3, 136.2, 131.9, 129.1, 123.3, 120.6, 118.5, 111.9, 94.5, 79.5, 62.0, 53.4 ppm.
Elemental analysis (%) decomposition
HRMS (ESI) *m/z*: $[M+H]^+$ Calcd for $C_{18}H_{15}N_2O_2S$ 323.0854; Found 323.0854.

Methyl 2-(4-cyanophenyl)-2-((5-(trifluoromethyl)pyridin-2-yl)thio)penta-3,4-dienoate (28)

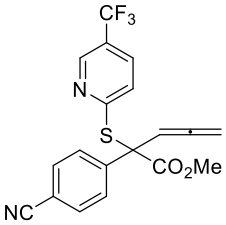

Synthesized according to the general procedure. Product isolated as 38 mg (0.10 mmol, 66% yield) of yellowish oil from column chromatography (eluent: AcOEt/hexane).
^{1}H NMR (400 MHz, $CDCl_3$) δ 8.60-8.56 (m, 1H), 7.75-7.68 (m, 3H), 7.65-7.62 (m, 2H), 7.30-7.26(m, 1H), 6.25 (t, *J* = 6.6 Hz, 1H), 4.84 (dd, *J* = 6.7 Hz, *J* = 11.6 Hz, 1H), 4.74 (dd, *J* = 6.6 Hz, *J* = 11.6 Hz, 1H), 3.78 (s, 3H) ppm.
^{13}C NMR (100 MHz, $CDCl_3$) δ 208.3, 170.1, 161.6 (q, J_{C-F} = 1.4 Hz), 145.8 (q, J_{C-F} = 4.1 Hz), 142.6, 133.0 (q, J_{C-F} = 3.3 Hz), 132.0, 128.9, 123.5 (q, J_{C-F} = 271.9 Hz), 123.1 (q, J_{C-F} = 33.4 Hz), 121.7, 118.3, 112.3, 94.0, 79.7, 62.1, 53.6 ppm.
Elemental analysis (%) calculated for $C_{19}H_{13}F_3N_2O_2S$: C 58.46, H 3.36, N 7.18, found: C 58.31, H 3.50, N 6.92.
HRMS (ESI) *m/z*: $[M+Na]^+$ Calcd for $C_{19}H_{13}F_3N_2O_2SNa$ 413.0544; Found 413.0548.

Methyl 2-(4-cyanophenyl)-2-((1-phenyl-1H-tetrazol-5-yl)thio)penta-3,4-dienoate (29)

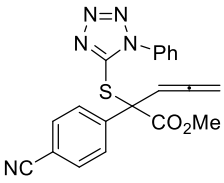

unstable compound

Synthesized according to the general procedure. Product isolated as 36 mg (0.09 mmol, 62% yield) of yellowish oil, by column chromatography (eluent: AcOEt/hexane).

^{1}H NMR (400 MHz, $CDCl_3$) δ 7.64-7.60 (m, 2H), 7.58-7.53 (m, 5H), 7.46-7.42 (m, 2H), 6.29 (t, *J* = 6.6 Hz, 1H), 4.95 (dd, *J* = 11.9, 6.6 Hz, 1H), 4.88 (dd, *J* = 11.9, 6.6 Hz, 1H), 3.79 (s, 3H) ppm.

^{13}C NMR (125 MHz, $CDCl_3$) δ 208.4, 168.9, 150.7, 142.1, 133.3, 132.2, 130.4, 129.8, 128.7, 124.4, 118.0, 112.7, 92.4, 80.2, 66.2, 54.1 ppm.

Elemental analysis (%) decomposition

HRMS (ESI) *m/z*: $[M+Na]^+$ Calcd for $C_{20}H_{15}N_5O_2SNa$ 412.0844; Found 412.0850.

Methyl 2-(benzylthio)-2-(4-cyanophenyl)penta-3,4-dienoate (30)

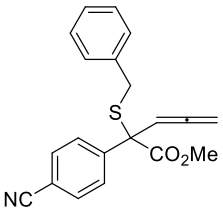

Synthesized according to the general procedure. Product isolated as 31 mg (0.09 mmol, 61% yield) of yellowish oil, by column chromatography (eluent: AcOEt/hexane).

^{1}H NMR (400 MHz, $CDCl_3$) δ 7.66-7.60 (m, 4H), 7.27-7.21 (m, 5H), 5.84 (t, *J* = 6.6 Hz, 1H), 4.88 (dd, *J* = 6.6, 3.3 Hz, 2H), 3.75 (s+s, 5H) ppm.

^{13}C NMR (100 MHz, $CDCl_3$) δ 208.5, 170.5, 143.8, 136.1, 131.9, 129.2, 129.0, 128.6, 127.4, 118.5, 111.7, 93.6, 79.7, 60.7, 53.2, 36.2 ppm.

Elemental analysis (%) calculated for $C_{20}H_{17}NO_2S$: C 71.62, H 5.11, N 4.18, found: C 71.40, H 4.93, N 4.01.

HRMS (ESI) *m/z*: $[M+Na]^+$ Calcd for $C_{20}H_{17}NO_2SNa$ 358.0878; Found 358.0877.

Methyl 2-(4-cyanophenyl)-2-(cyclohexylthio)penta-3,4-dienoate (31)

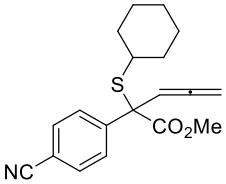

Synthesized according to the general procedure. Product isolated as 33 mg (0.10 mmol, 67% yield) of yellowish oil from column chromatography (eluent: AcOEt/hexane).

^{1}H NMR (400 MHz, $CDCl_3$) δ 7.69-7.59 (m, 4H), 5.85 (t, *J* = 6.6 Hz, 1H), 4.80 (dd, *J* = 6.6, 2.9 Hz, 2H), 3.77 (s, 3H), 2.73-2.70 (m, 1H), 1.86-1.74 (m, 2H), 1.69-1.63 (m, 2H), 1.55-1.46 (m, 1H), 1.40-1.32 (m, 2H), 1.27-1.19 (m, 3H) ppm.

^{13}C NMR (100 MHz, $CDCl_3$) δ 208.4, 171.0, 144.7, 131.7, 129.2, 118.6, 111.5, 94.3, 79.4, 60.4, 53.1, 44.3, 34.8, 34.5, 26.2, 26.1, 25.4 ppm.

Elemental analysis (%) calculated for $C_{19}H_{21}NO_2S$: C 69.69, H 6.46, N 4.28, found: C 69.54, H 6.67, N 4.07.

HRMS (ESI) *m/z*: $[M+Na]^+$ Calcd for $C_{19}H_{21}NO_2SNa$ 350.1191; Found 350.1187.

Methyl 2-((3S,5S,7S)-adamantan-1-ylthio)-2-(4-cyanophenyl)penta-3,4-dienoate (32)

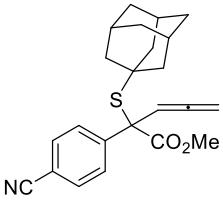

Synthesized according to the general procedure. Product isolated as 29 mg (0.08 mmol, 51% yield) of yellowish oil, by column chromatography (eluent: AcOEt/hexane).
^{1}H NMR (400 MHz, $CDCl_3$) δ 7.78-7.74 (m, 2H), 7.62-7.58 (m, 2H), 6.02 (t, *J* = 6.7 Hz, 1H), 4.72 (qd, *J* = 11.6 Hz, 6.7 Hz, 2H), 3.79 (s, 3H), 2.00-1.96 (m, 3H), 1.91-1.87 (m, 6H), 1.66-1.62 (m, 6H) ppm.
^{13}C NMR (100 MHz, $CDCl_3$) δ 208.5, 171.6, 145.4, 131.4, 129.3, 118.7, 111.3, 96.1, 79.4, 59.6, 53.0, 51.7, 43.9, 36.1, 30.0 ppm.
Elemental analysis (%) calculated for $C_{23}H_{25}NO_2S$: C 72.79, H 6.64, N 3.69, found: C 73.00, H 6.78, N 3.52.
HRMS (ESI) *m/z*: $[M+Na]^+$ Calcd for $C_{23}H_{25}NO_2SNa$ 402.1504; Found 402.1492.

Methyl 2-((2-((tert-butoxycarbonyl)amino)-3-methoxy-3-oxopropyl)thio)-2-(4-cyanophenyl)penta-3,4-dienoate (33)

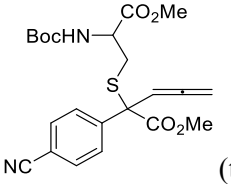

(two diastereoisomers)
Synthesized according to the general procedure. Product isolated as a mixture of diastereoisomers (1:1) 39 mg (0.09 mmol, 58% yield) of yellowish oil from column chromatography (eluent: AcOEt/hexane).
^{1}H NMR (400 MHz, $CDCl_3$) δ 7.67-7.60 (m, 4H), 5.80-5.74 (m, 1H), 5.30-5.18 (m, 1H), 4.95-4.90 (m, 2H), 4.51 (brs, 1H), 3.78 (2 x s, 3H), 3.75 (2 x s, 3H), 3.05-2.95 (m, 2H), 1.45 (2 x s, 9H) ppm.
^{13}C NMR (100 MHz, $CDCl_3$) δ 208.6, 208.6, 171.0, 171.0, 170.5, 170.4, 155.0, 143.6, 132.0, 128.9, 118.3, 111.9, 93.2, 93.2, 80.3, 79.9, 79.9, 60.6, 60.5, 53.4, 53.3, 52.7, 52.6, 52.6, 33.8, 33.6, 28.3 ppm.
Elemental analysis (%) calculated for $C_{22}H_{26}N_2O_6S$: C 59.18, H 5.87, N 6.27, found: C 59.36, H 5.72, N 6.09.
HRMS (ESI) *m/z*: $[M+Na]^+$ Calcd for $C_{22}H_{26}N_2O_6SNa$ 469.1409; Found 469.1403.

Methyl 2-(4-cyanophenyl)-2-(phenylthio)hexa-3,4-dienoate (34)

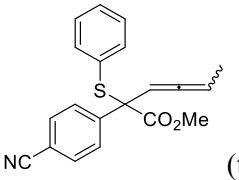

(two diastereoisomers)
Synthesized according to the general procedure. Product isolated as a mixture of diastereoisomers (1:1) 29 mg (0.09 mmol, 58% yield) of yellowish oil, by column chromatography (eluent: AcOEt/hexane).
^{1}H NMR (500 MHz, $CDCl_3$) δ 7.53-7.45 (m, 4H), 7.26-7.22 (m, 3H), 7.19-7.15 (m, 2H), 5.62-5.57 (m, 1H), 5.13-5.02 (m, 1H), 2.62 (2 x s, 3H), 1.48-1.39 (m, 3H) ppm.
^{13}C NMR (125 MHz, $CDCl_3$) δ 205.4, 205.2, 170.5, 144.6, 144.5, 136.7, 136.6, 131.6, 131.6, 130.9, 129.5, 129.5, 129.3, 129.1, 128.6, 128.6, 118.6, 111.4, 93.6, 93.4, 90.7, 90.7, 77.2, 64.6, 64.6, 53.0, 13.5, 13.3 ppm.

Elemental analysis (%) calculated for$C_{20}H_{17}NO_2S$: C 71.62, H 5.11, N 4.18, found: C 71.42, H 5.39, N 3.96.
HRMS (ESI) *m/z*: $[M+Na]^+$ Calcd for $C_{20}H_{17}NO_2SNa$ 358.0878; Found 358.0867.

Methyl 2-(4-cyanophenyl)-3-methyl-2-(phenylthio)penta-3,4-dienoate (35)

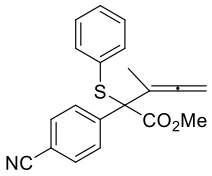

compound unstable

Synthesized according to the general procedure. Product isolated as 22 mg (0.07 mmol, 44% yield) of yellowish oil, by column chromatography (eluent: AcOEt/hexane).
^{1}H NMR (500 MHz, $CDCl_3$) δ 7.68-7.64 (m, 2H), 7.56-7.53 (m, 2H), 7.31-7.27 (m, 1H), 7.20-7.14 (m, 4H), 4.83-4.71 (m, 2H), 3.73 (s, 3H). 1.71 (t, *J* = 2.9 Hz, 3H) ppm.
^{13}C NMR (125 MHz, $CDCl_3$) δ 208.1, 169.8, 143.5, 136.0, 131.4, 130.1, 129.3, 128.5, 118.6, 111.3, 99.2, 78.7, 77.2, 67.2, 53.0, 17.2 ppm.
Elemental analysis (%) decomposition
HRMS (ESI) *m/z*: $[M+Na]^+$ Calcd for $C_{20}H_{17}NO_2SNa$ 358.0878; Found 358.0870.

5.4. The photochemical Doyle-Kirmse reaction on 1 mmol scale – procedure of synthesis of compound 4

A glass vial equipped with a stirring bar and sealed with a septum was charged with (prop-2-yn-1-yl)sulfide (1240 µmL, 9.00 mmol, 9 equiv.), a diazo carbonyl compound **S1b** (117.1 mg, 0.5 mmol) and DCM (1.65 mL). The reaction mixture was placed in a photoreactor and irradiated with blue LED (3W) for 3 hours. Then, the second portion of the diazo carbonyl compound **S1b** (117.1 mg, 0.5 mmol) in DCM (1.65 mL) was added and the reaction mixture was stirred for another 21 hours. The crude reaction mixture was purified by column chromatography using hexanes : EtOAc as eluent to afford 298 mg of the final product **4** (84%, 0.84 mmol) as a yellowish oil.

6. Cyclopropanation experiments

6.1. Synthesis of cyclopropanes *S3a* and *S3b*

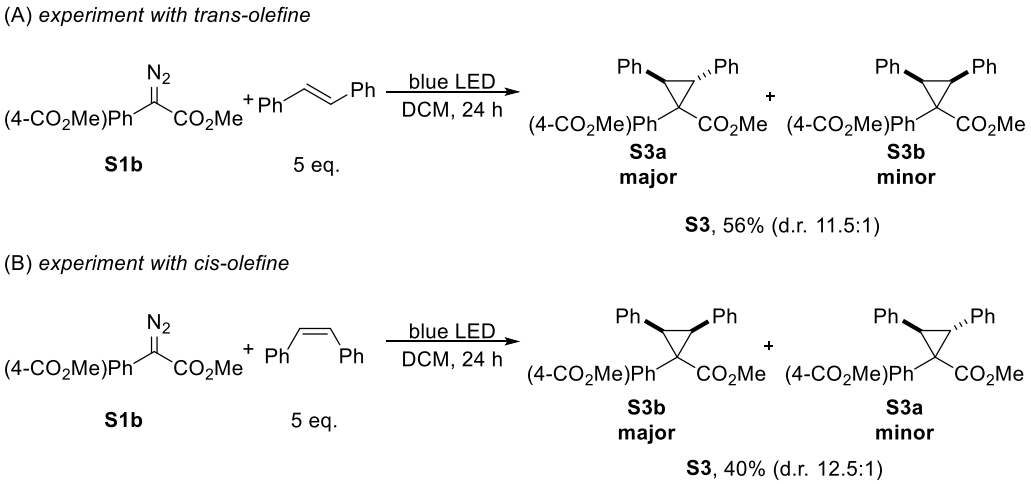

Scheme S3. Diastereoselective cyclopropanation of (A) *trans*-stilbene or (B) *cis*-stilbene.

A glass vial equipped with a stirring bar and sealed with a septum was charged with either *trans*-stilbene or *cis*-stilbene (0.75 mmol, 5 equiv.), diazo carbonyl compound **S1b** (0.15 mmol) and DCM (1.5 mL). The reaction mixture was placed in a photoreactor and irradiated with blue LED (3W) for 24 hours. The crude reaction mixture was purified by column chromatography using hexanes : EtOAc as an eluent to afford the final products as predominantly diastereoisomer **S3a** from *trans*-stilbene or **S3b** from *cis*-stilbene. The diastereoisomeric ratio was determined by NMR technique (from ^{1}H NMR spectra of crude reaction mixtures). (*Note: In the cyclopropanation reactions, carbene dimerization product is formed as a byproduct. It has similar polarity to photoadducts **S3a** and **S3b**, therefore preparative HPLC was used for the purification of cyclopropanes. We recommend to increase the excess of olefins and addition of diazo portionwise to eliminate/reduce dimerization side reaction.*)

Table S8. HPLC method for separation of the compound **S3b** (Flow rate = 15 mL/min). Detection at 254 nm and 220 nm, t_r = 12.3 min.

Time	hexane [%]	AcOEt [%]
Initial	90.0	10.0
15.00	60.0	40.0
20.00	50.0	50.0
30.00	30.0	70.0
40.00	30.0	70.0

Methyl 4-(1-(methoxycarbonyl)-2,3-diphenylcyclopropyl)benzoate-trans isomer (S3a)

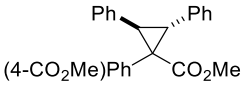

Product isolated as a single diastereoisomer 28 mg (0.11 mmol, 48% yield) of white solid from column chromatography (eluent: AcOEt/hexane).

m.p. 111-112 °C

^{1}H NMR (400 MHz, $CDCl_3$) δ 7.90-7.85 (m, 2H), 7.49-7.43 (m, 2H), 7.39-7.33 (m, 2H), 7.31-7.23 (m, 3H), 7.16-7.06 (m, 3H), 6.98-6.92 (m, 2H), 3.89 (d, *J* = 7.9 Hz, 1H), 3.86 (s, 3H), 3.57 (d, *J* = 7.9 Hz, 1H), 3.36 (s, 3H) ppm.

^{13}C NMR (100 MHz, $CDCl_3$) δ 170.1, 166.8, 141.1, 135.9, 135.6, 131.3, 129.3, 129.0, 129.0, 128.3, 128.1, 128.1, 127.2, 126.7, 52.4, 52.1, 45.6, 36.5, 35.1.

Elemental analysis (%) calculated for $C_{25}H_{22}O_4$: C 77.70, H 5.47, found: C 77.62, H 5.89.

HRMS (ESI) *m/z*: $[M+Na]^+$ Calcd for $C_{25}H_{22}O_4Na$ 409.1416; Found 409.1409.

Methyl 4-(1-(methoxycarbonyl)-2,3-diphenylcyclopropyl)benzoate-cis isomer (S3b)

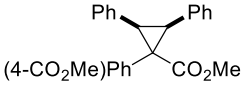

Product isolated as single diastereoisomer 22 mg (0.06 mmol, 38% yield) of white solid from column chromatography (eluent: AcOEt/hexane).

m.p. 186-188 °C

^{1}H NMR (400 MHz, $CDCl_3$) δ 7.78-7.76 (m, 2H), 7.20-7.16 (m, 2H), 7.15-7.05 (m, 6H), 6.90-6.84 (m, 4H), 3.84 (s, 3H), 3.67 (s, 3H), 3.58 (s, 2H).

^{13}C NMR (100 MHz, $CDCl_3$) δ 174.5, 166.9, 137.8, 133.8, 133.5, 131.6, 128.9, 128.6, 127.3, 126.6, 53.1, 52.0, 40.2, 36.7.

HRMS (ESI) *m/z*: $[M+Na]^+$ Calcd for $C_{25}H_{22}O_4Na$ 409.1416; Found 409.1411.

6.2. Photoisomerization of reagents

6.2.1. Photoisomerization of *cis*- and *trans*-stilbene

A glass vial equipped with a stirring bar and sealed with a septum was charged with *trans*-stilbene or *cis*-stilbene (0.75 mmol) and DCM (1.5 mL). The solution was placed in a photoreactor and irradiated with blue LED (3W) for 24 hours. A crude reaction mixture was evaporated, diluted with $CDCl_3$ and NMR spectra were recorded to check if photoisomerization occurs. Olefins were purchased from TCI and their purity was determined by ^{1}H NMR spectra. While *trans*-stilbene was completely pure, *cis*-stilbene was contaminated with 2% of *trans* isomer, this was taken into consideration while determining level of isomerization.

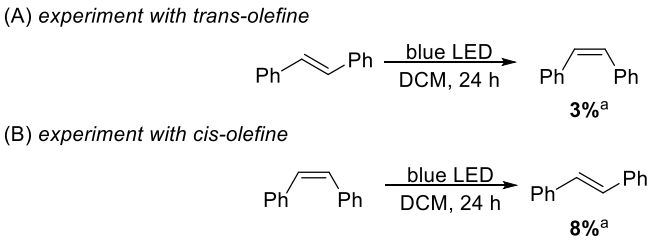

Scheme S4. Photoizomerization of (A) *trans*-stilbene and (B) *cis*-stilbene. [a]photoisomerization level determined by NMR analysis of stilbene solution after irradiation.

experiment A – 3% of photoizomerization of *trans*-stilbene to *cis*-stilbene (24 h upon blue light irradiation)

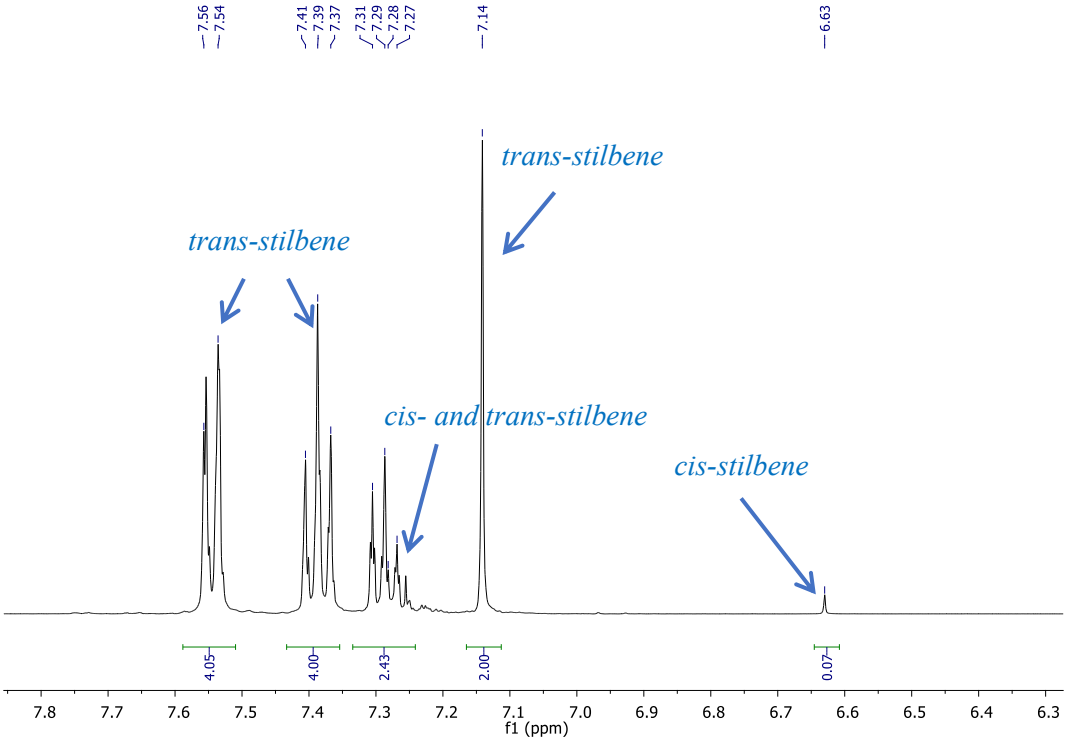

experiment B – 8% of photoizomerization of *cis*-stilbene to *trans*-stilbene (24 h upon blue light irradiation)

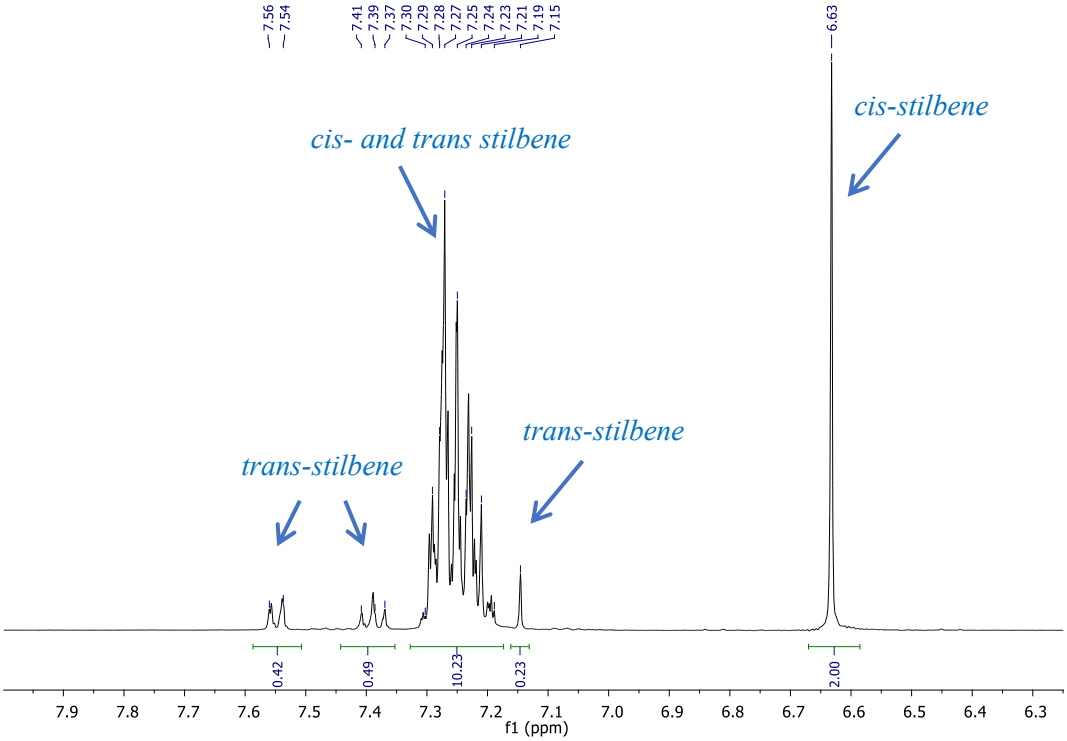

6.2.2. Photoizomerization of photoadducts

Isolated cyclopropanes **S3a** and **S3b** were dissolved with $CDCl_3$ and exposed to blue LEDs (3 W) for 3 hours. After the irradiation NMR spectra were recorded. No signs of photoizomerization of **S3a** to **S3b** and **S3b** to **S3a** were observed and pure cyclopropanes were recovered.

6.3. Determination of cyclopropanation diastereoselectivity

Determination of diastereoselectivity in cyclopropanation of *trans*-stilbene

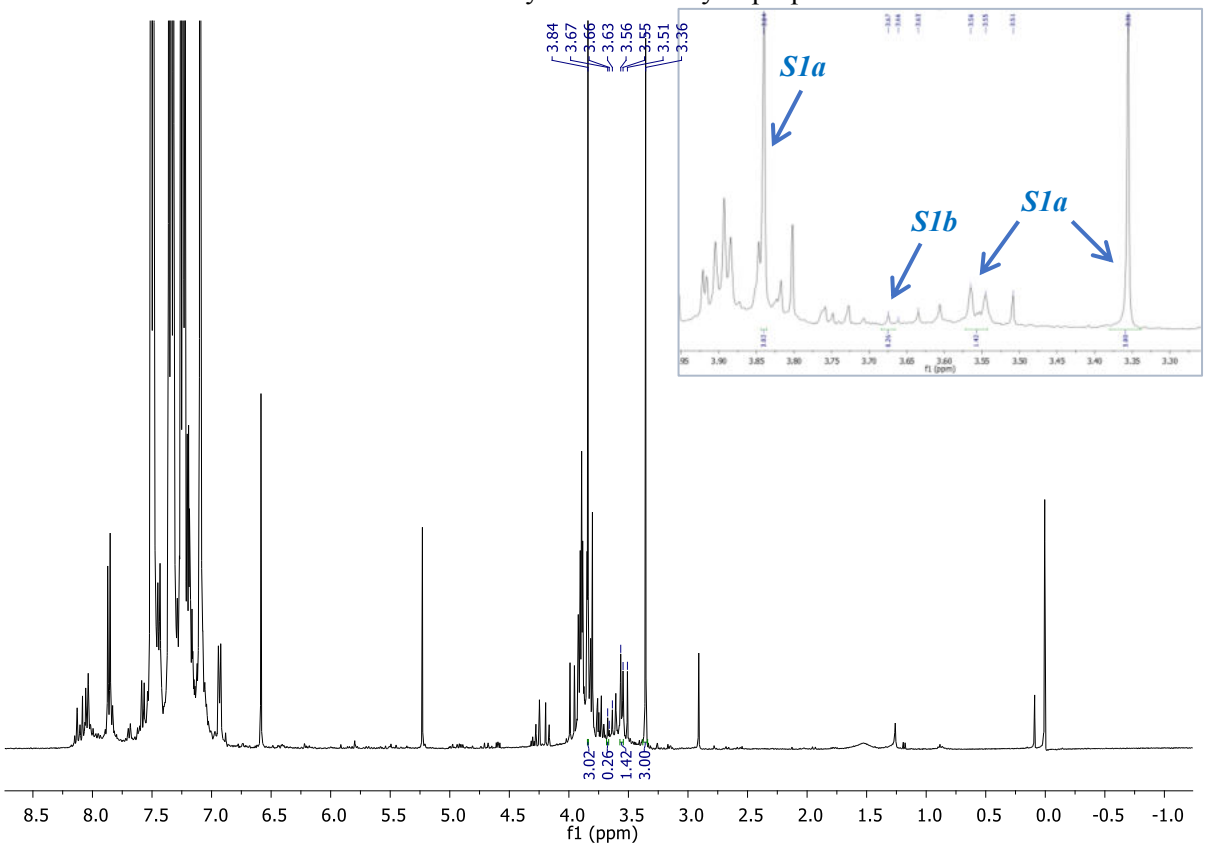

(Note: the diastereoisomeric ratio is determined by comparison of the relative areas under signals corresponding to ester methyl groups attached to the cyclopropane ring: 3.00 at 3.36 ppm for **S1a** and 0.26 for 3.67 ppm of **S1b**; the rest of characteristic signals of cyclopropane **S1b** overlap with other signals on the spectra)

Determination of diastereoselectivity in cyclopropanation of *cis*-stilbene

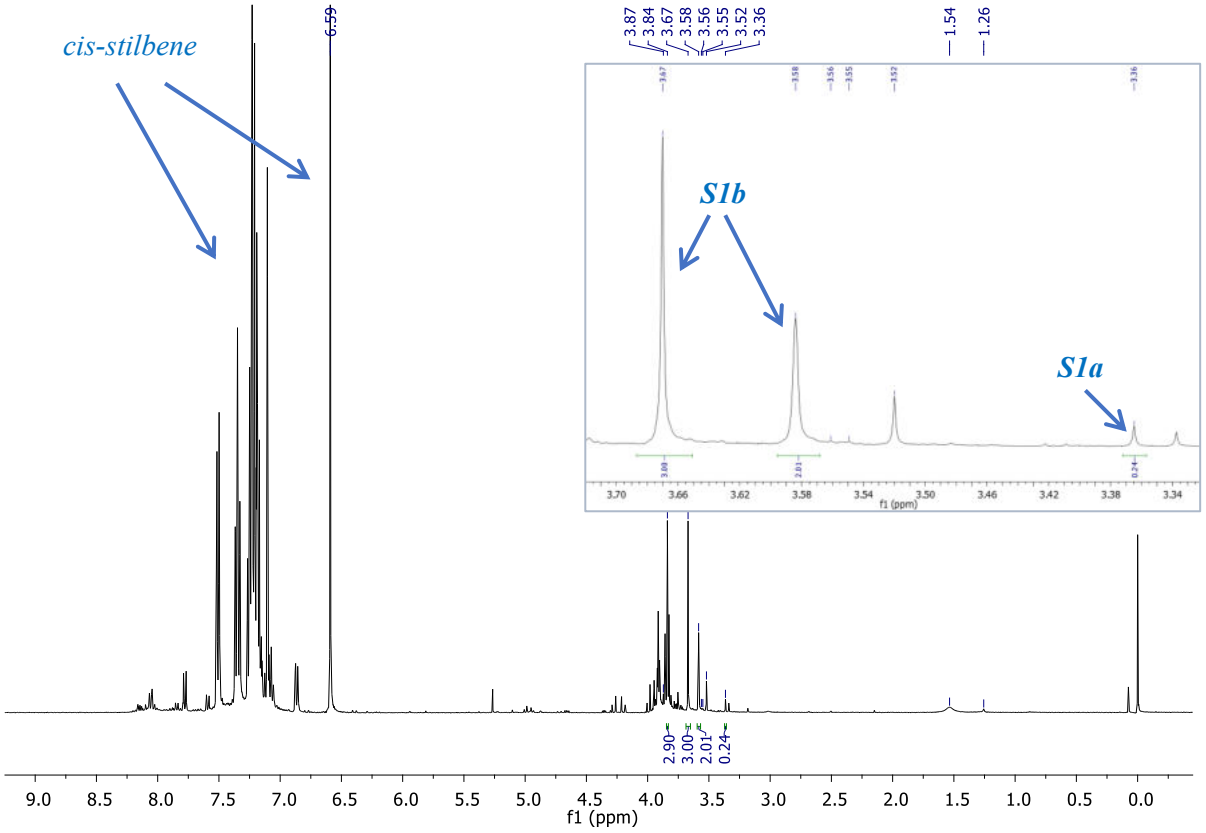

(Note: the diastereoisomeric ratio is determined by comparison of the integrals of ester methyl groups attached to the cyclopropane ring: 3.00 at 3.67 ppm for **S1b** and 0.24 for 3.36 ppm of **S1a**; the rest of characteristic signals of cyclopropane **S1a** overlap with other signals on the spectra)

7. UV-Vis absorption spectra of diazocompounds

7.1. Influence of EWG group type

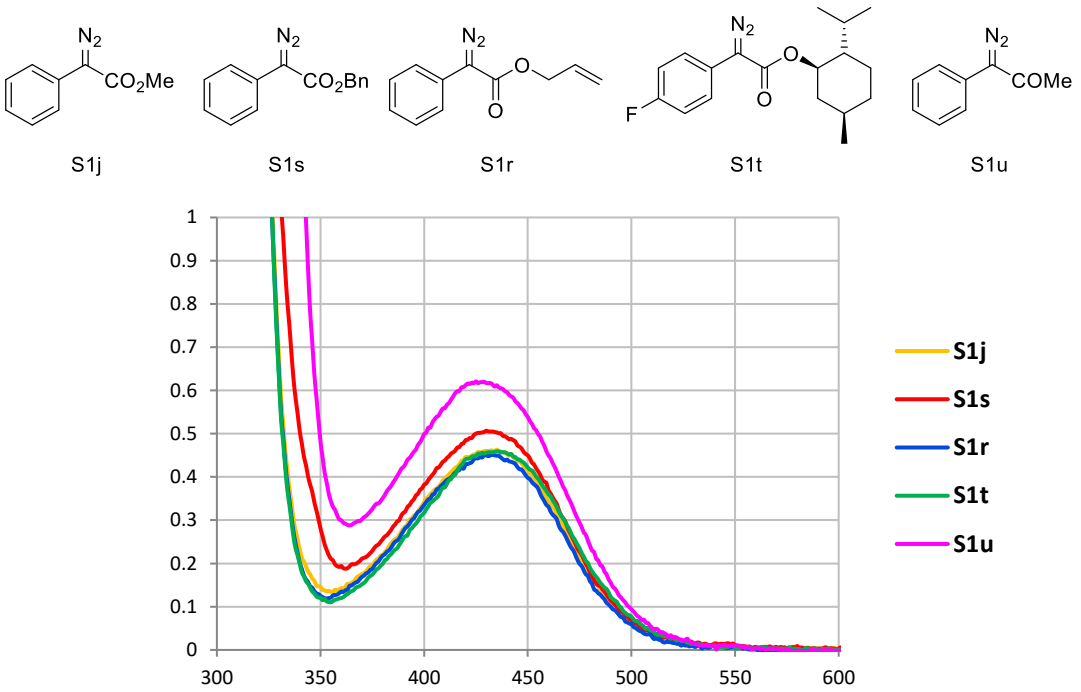

Figure S3. Influence of EWG group type on absorption spectra. Concentration: 6 µmol/mL in DCM

7.2. Influence of substituent on 4- position of aryl ring

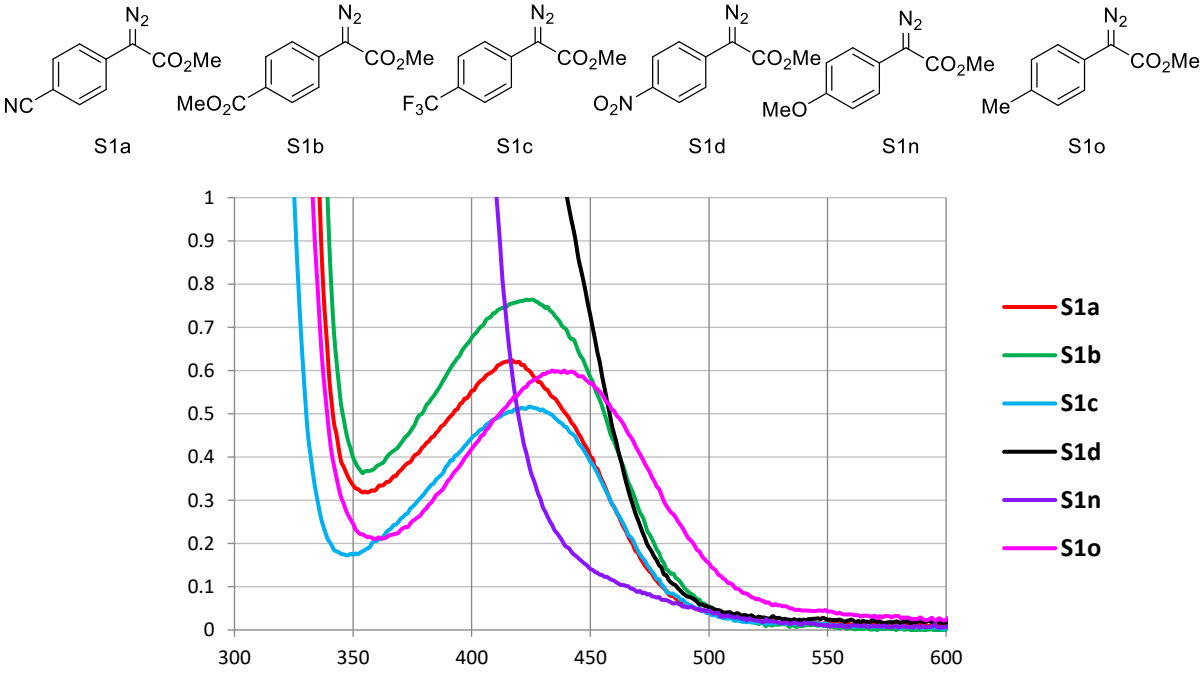

Figure S4. Influence of 4- position of aryl ring on absorption spectra. Concentration: 6 µmol/mL in DCM

7.3. Influence of the position of the substituent on the aryl ring

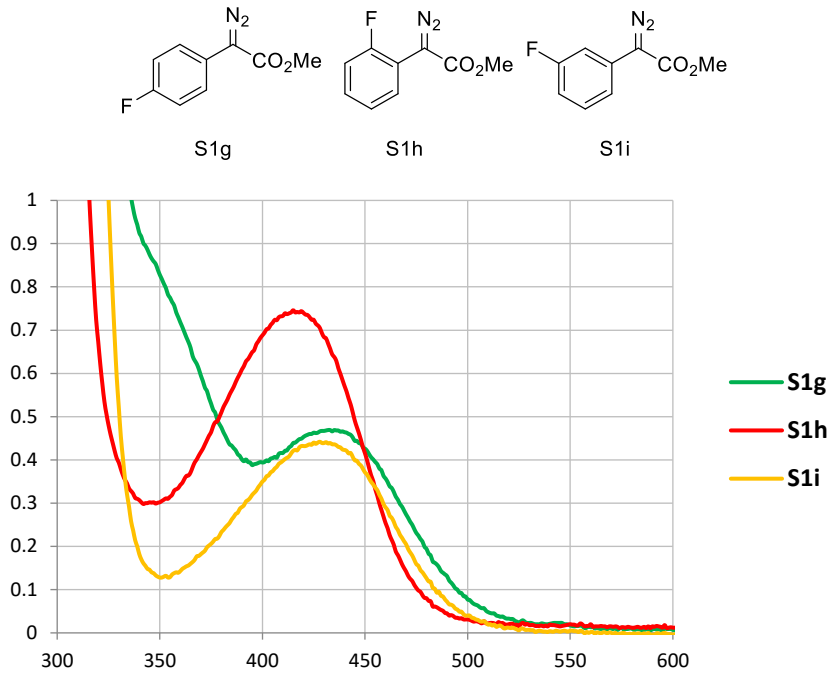

Figure S5. Influence of the position of the substituent on the aryl ring on absorption spectra. Concentration: 6 µmol/mL in DCM

7.4. Influence of halogen atom at the 4- position of aryl ring

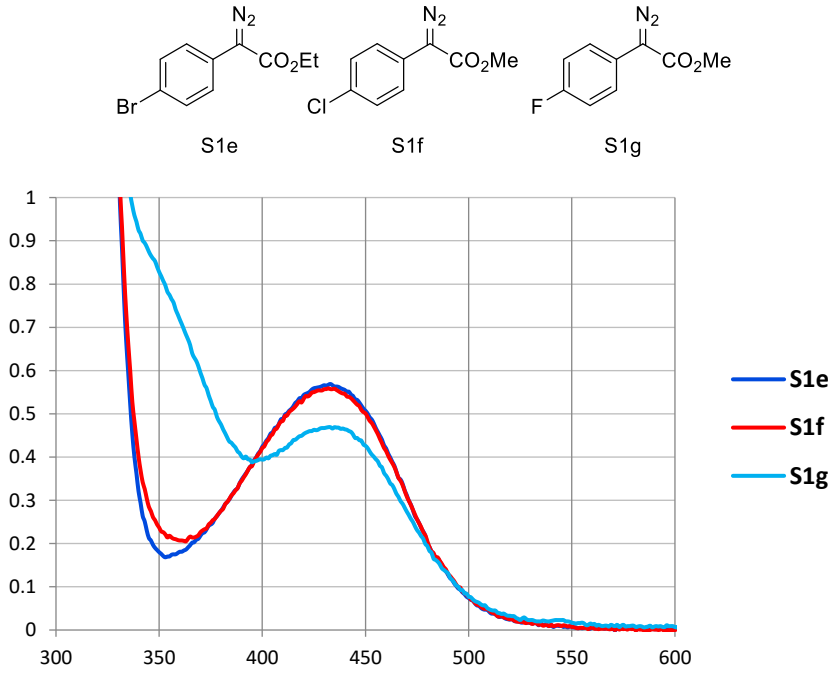

Figure S6. Influence of halogen atom at the 4-position of aryl ring on absorption spectra. Concentration: 6 µmol/mL in DCM

7.5. Influence of aromatic ring type

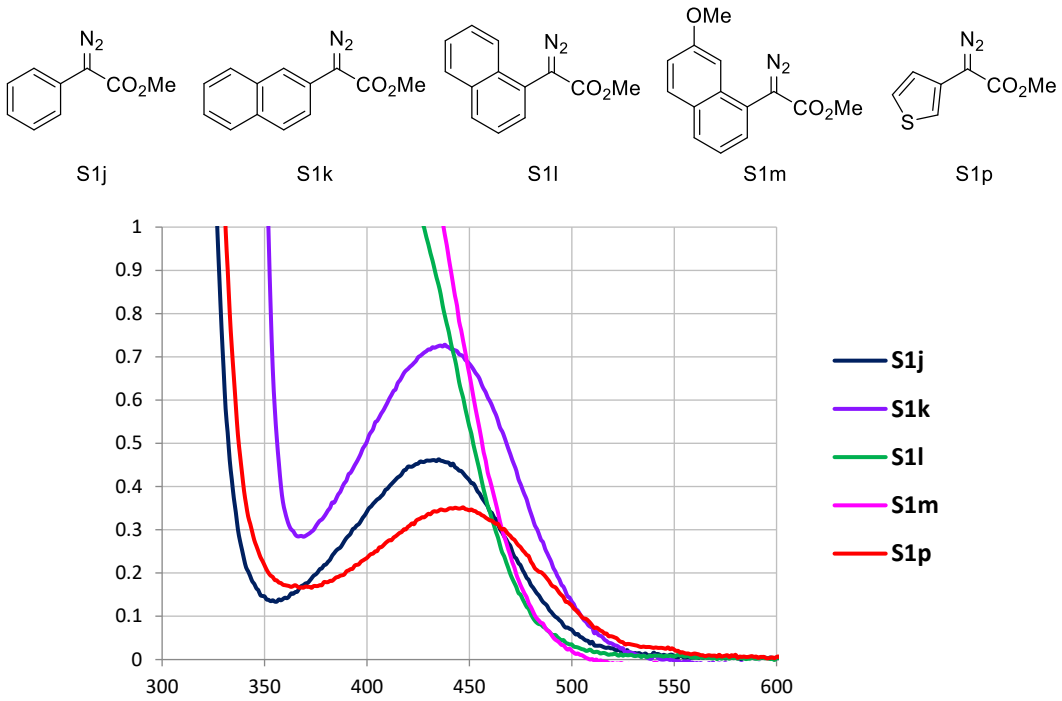

Figure S7. Influence of aromatic ring type on absorption spectra. Concentration: 6 µmol/mL in DCM

8. References

(1) Tayama, E.; Saito, S. *Synlett* **2015**, *26*, 1880.
(2) Ye, F.; Wang, C.; Zhang, U.; Wang, J. *Angew. Chem. Int. Ed.* **2014**, *53*, 11625.
(3) Ye, F.; Qu, S.; Zhou, L.; Peng, C.; Wang, C.; Cheng, J.; Hossain, M. L.; Liu, Y.; Zhang, Y.; Wang, Z.-X.; Wang, J. *J. Am. Chem. Soc.* **2015**, *137*, 4435.
(4) Kidonakis, M.; Stratakis, M. *Org. Lett.* **2018**, *20*, 4086.
(5) Gallo, R. D. C.; Burtoloso, A. C. B. *Green. Chem.* **2018**, *20*, 4547.
(6) Hao, J.; Xu, Y.; Hu, Z.; Zhang, Z.; Yang, W. *Org. Lett.* **2018**, *20*, 7888.
(7)Keipour, H.; Jalba, A.; Delage-Laurin, L.; Ollevier, T. *J. Org. Chem.* **2017**, *82*, 3000.
(8) Chan, W.-W.; Yeung, S.-H.; Zhou, Z.; Chan, A. S.C.; Yu, W.-Y. *Org. Lett.* **2010**, *12*, 604.
(9) Park, E. J.; Lee, S.; Chang, S. *J. Org. Chem.* **2010**, *75*, 2760.
(10) Nocentini, A.; Carta, F.; Ceruso, M.; Bartolucci, G.; Supuran, C. T. *Bioorg. Med. Chem.* **2015**, *23*, 6955.
(11) Kaushik, C. P.; Pahwa, A.; Thakur, R.; Kaur, P. *Synth. Commun.* **2017**, *47*, 368.
(12) Wagh, S. B.; Singh, R. R.; Sahani, R. L.; Liu, R.-S. *Org. Lett.* **2019**, *21*, 2755.
(13) Castro, J.; Moyano, A.; Pericas, M. A.; Riera, A. *Synthesis* **1997**, 518.
(14) Reddy, T. I.; Varma, R. S. *Chem. Commun.* **1997**, 621.
(15) Struthers, H.; Spingler, B.; Mindt, T. L.; Schibili, R. *Chem. Eur. J.* **2008**, *14*, 6173.
(16) Colas, K.; Martin-Montero, R., Mendoza, A. *Angew. Chem. Int. Ed.* **2017**, *56*, 16042.
(17) Abele, R.; Abele, E.; Rubina, K.; Dzenitis, O.; Arsenyan, P.; Shestakova, I.; Nesterova, A.; Domracheva, I.; Popelis, J.; Grinberga, S.; Lukevis, E. *Chem. Heterocycl. Compd.* **2002**, *38*, 867.

9. NMR spectra

Methyl 2-(4-cyanophenyl)-2-diazoacetate (S1a)

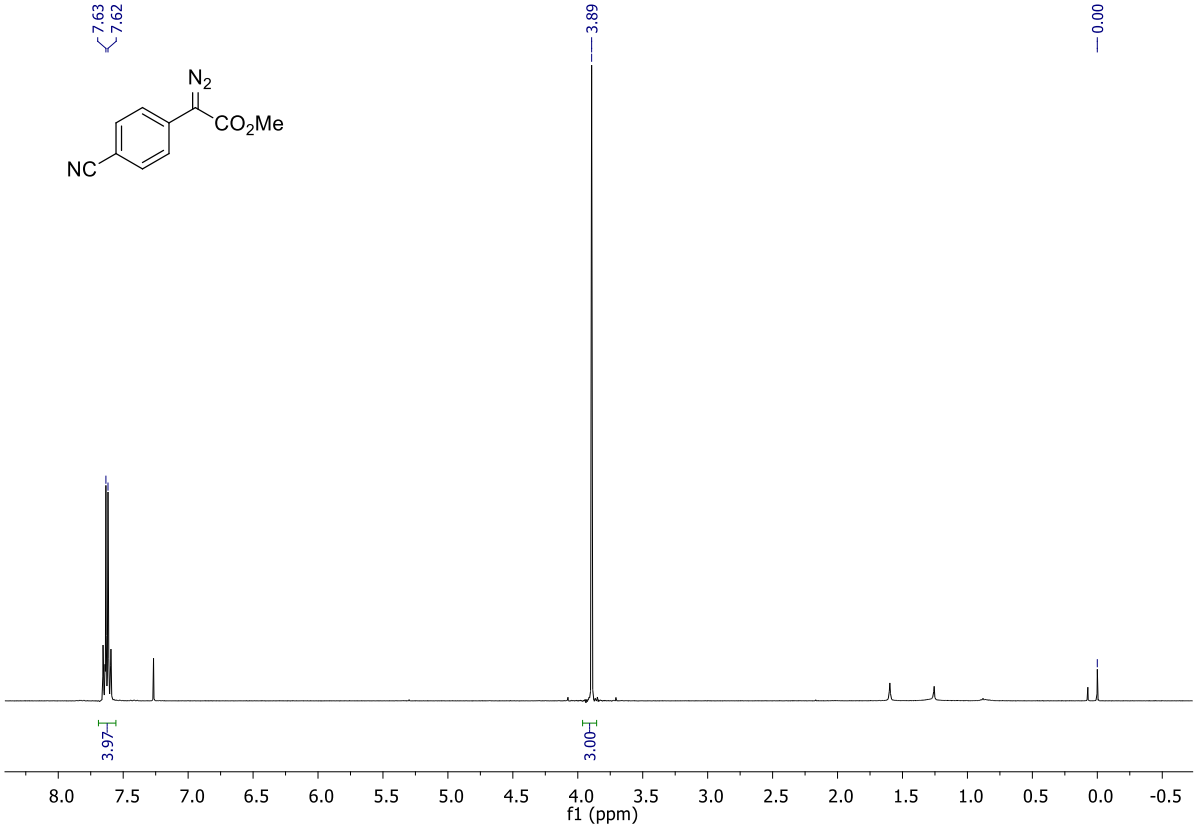

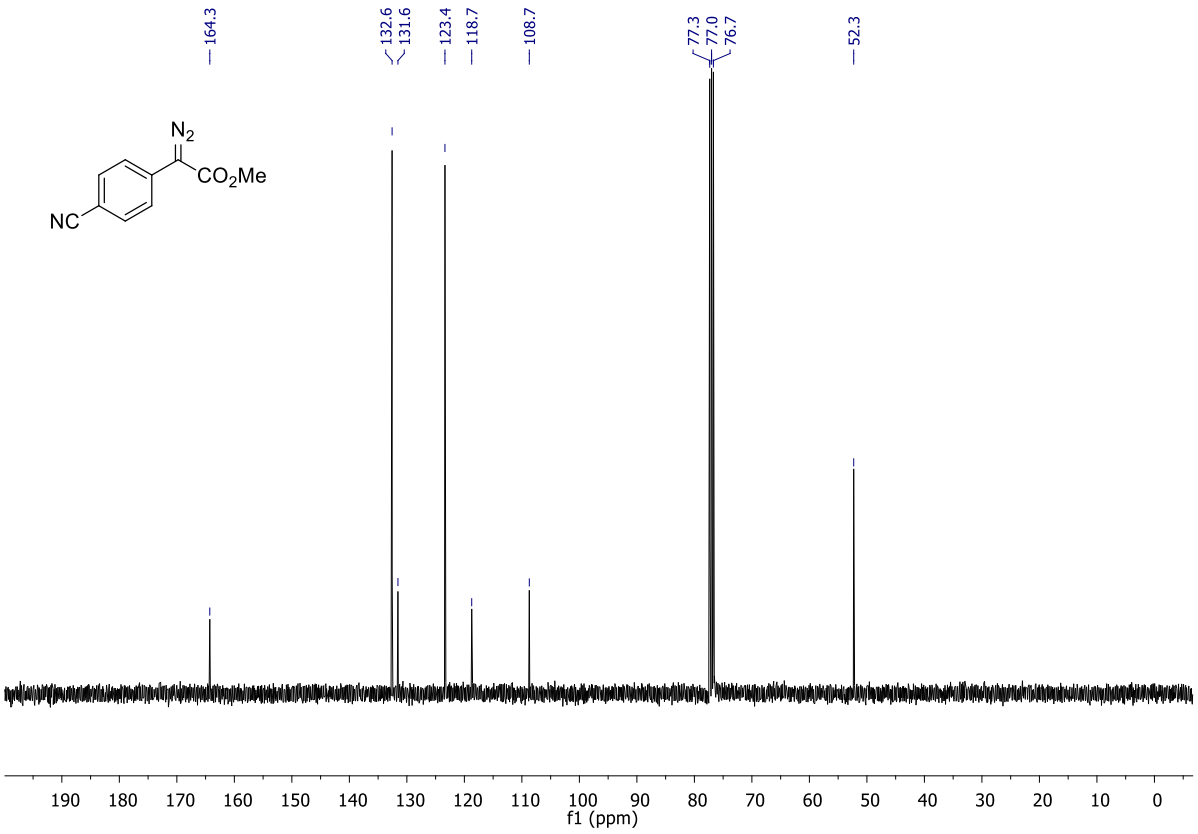

Ethyl 2-[7-metoxy(1-naftyl)]-2-diazoacetate (S1m)

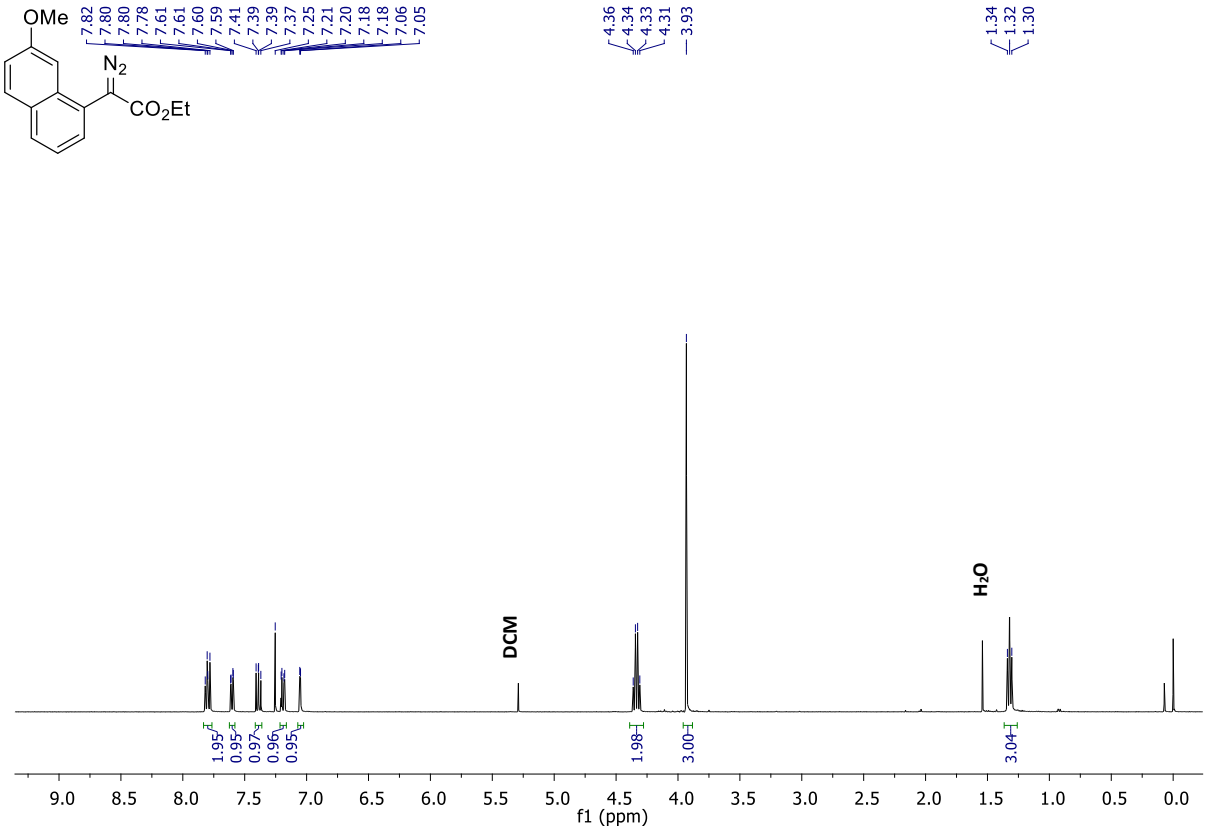

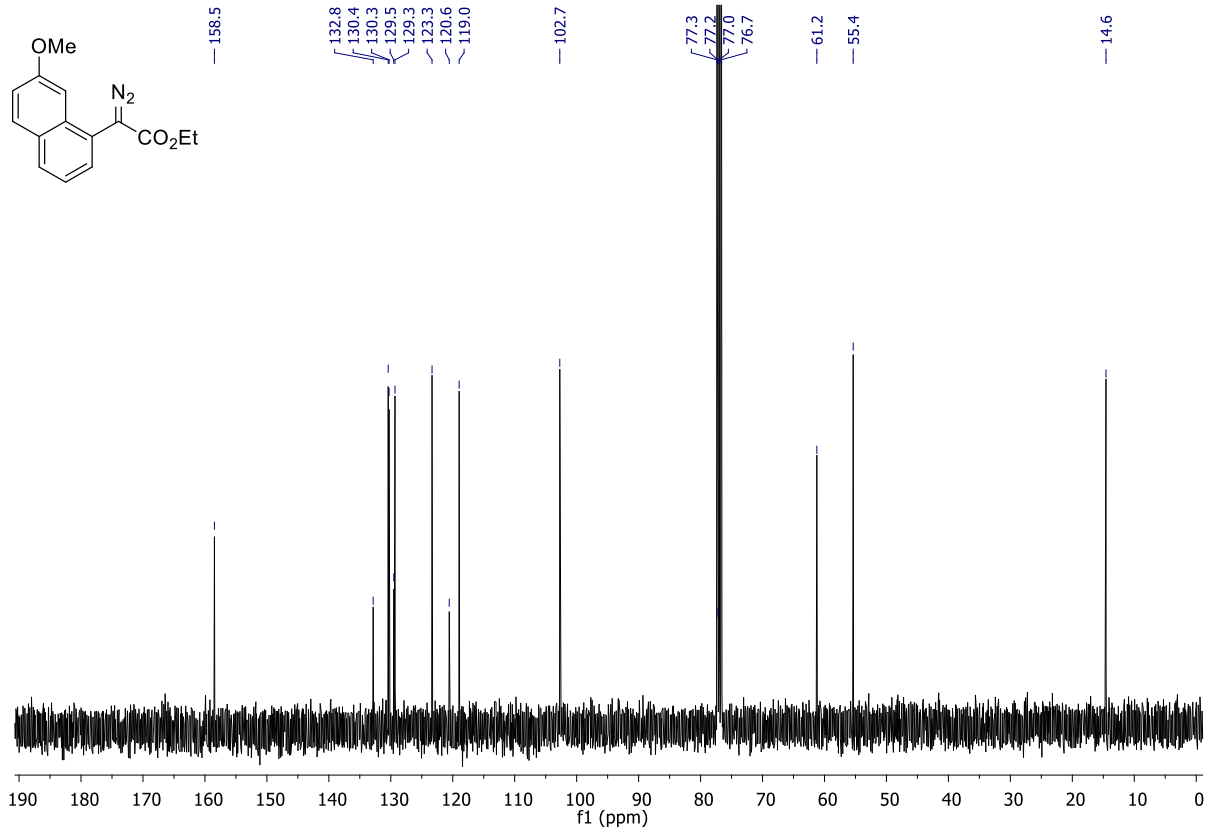

(1S,2R,5S)-2-isopropyl-5-methylcyclohexyl 2-(4-fluorophenyl)acetate (S4t)

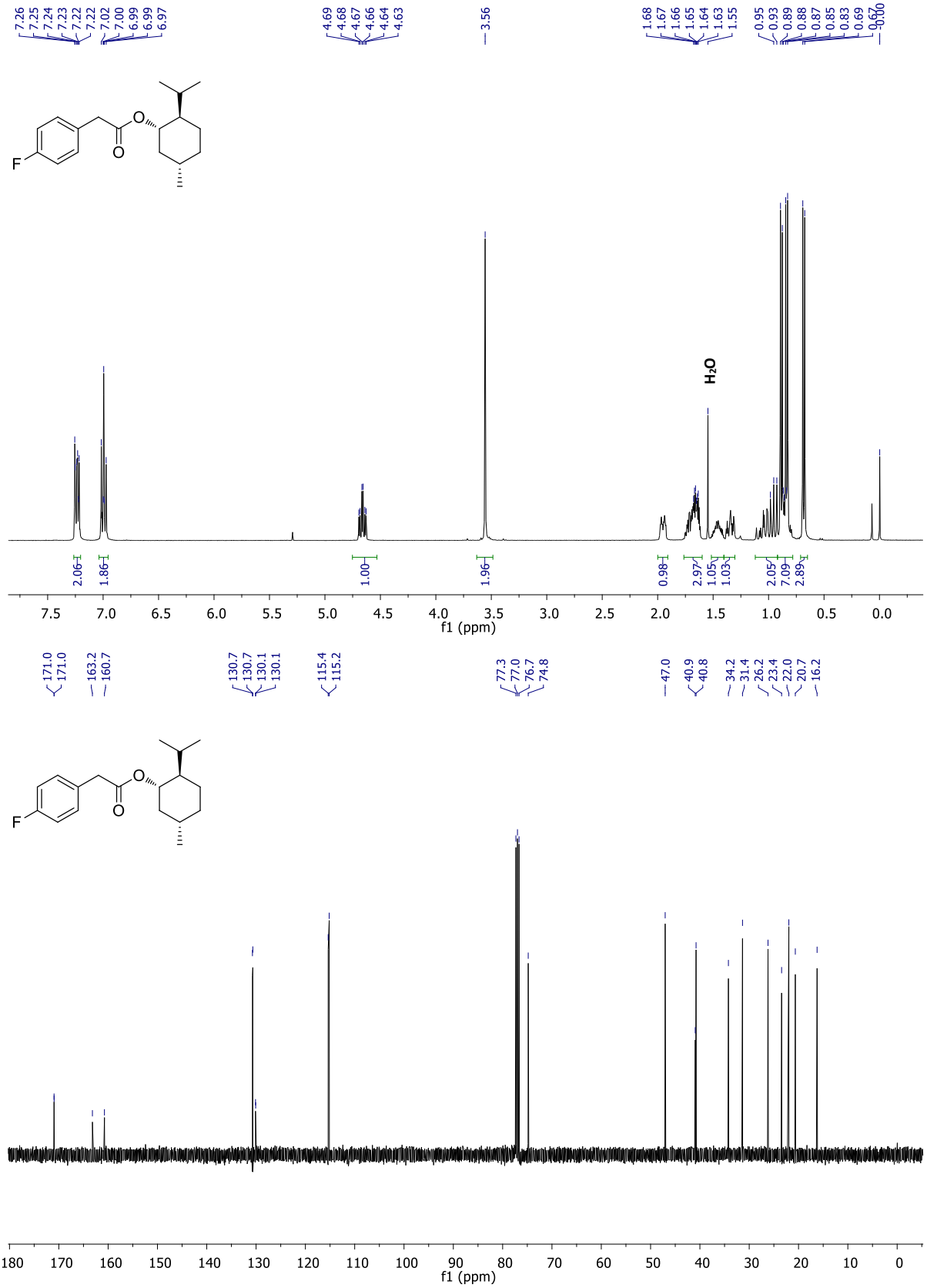

(1S,2R,5S)-2-Isopropyl-5-methylcyclohexyl 2-diazo-2-(4-fluorophenyl)acetate (S1t)

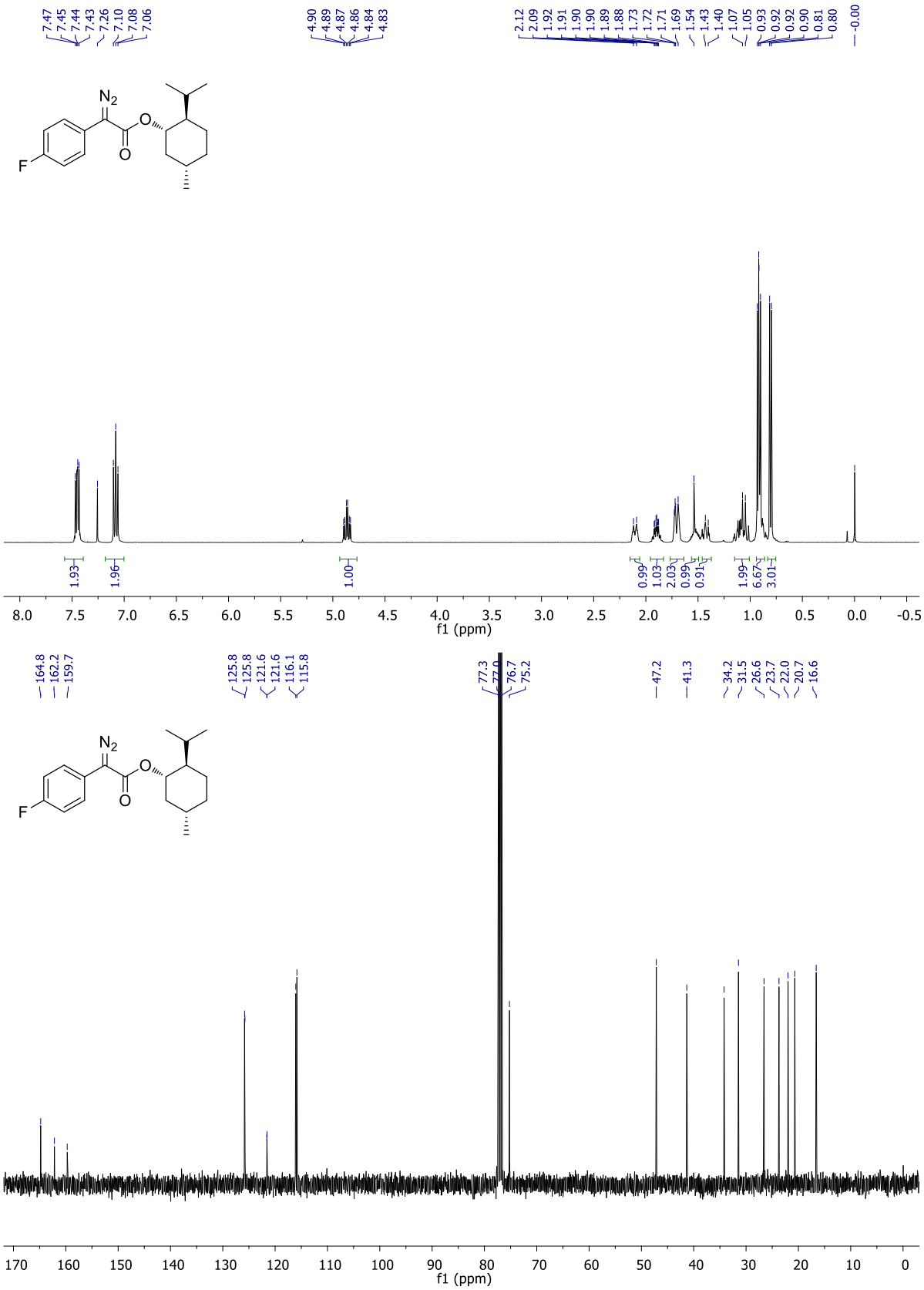

2-(Prop-2-yn-1-ylthio)-5-(trifluoromethyl)pyridine (S2g)

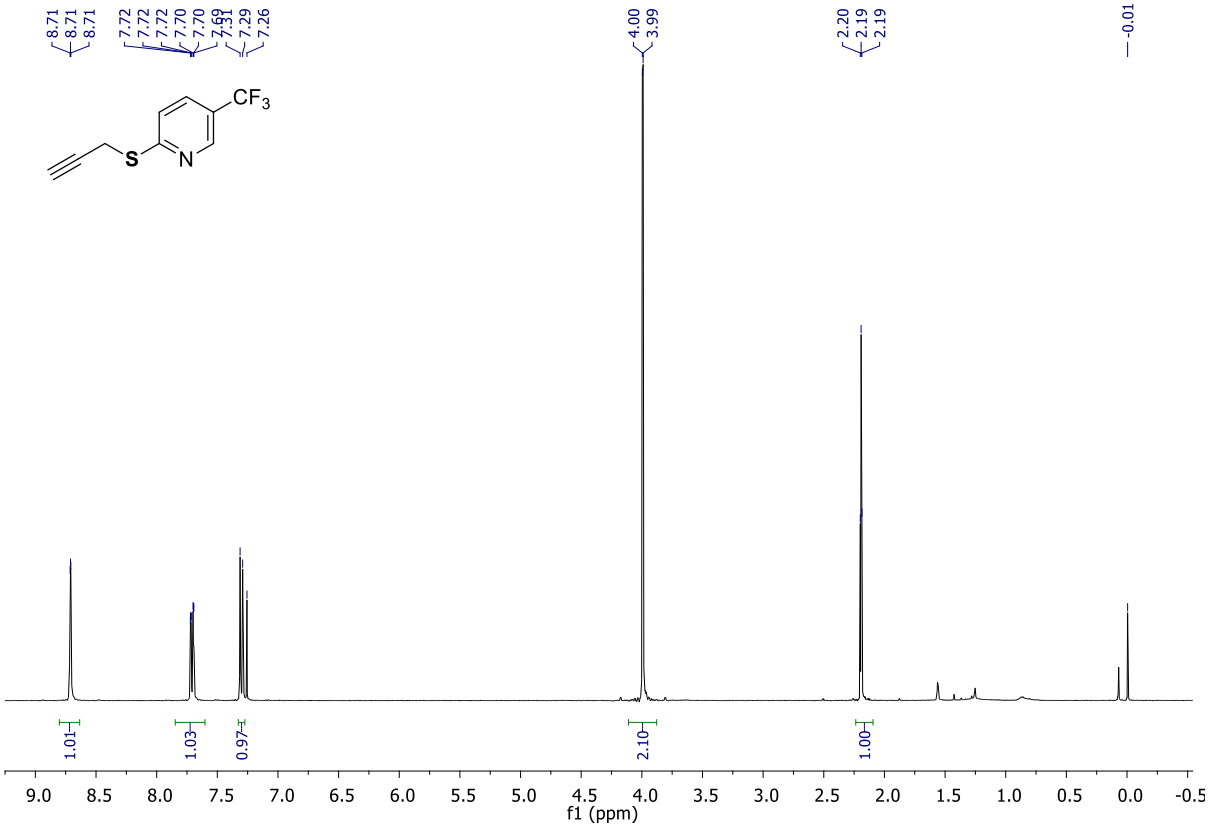

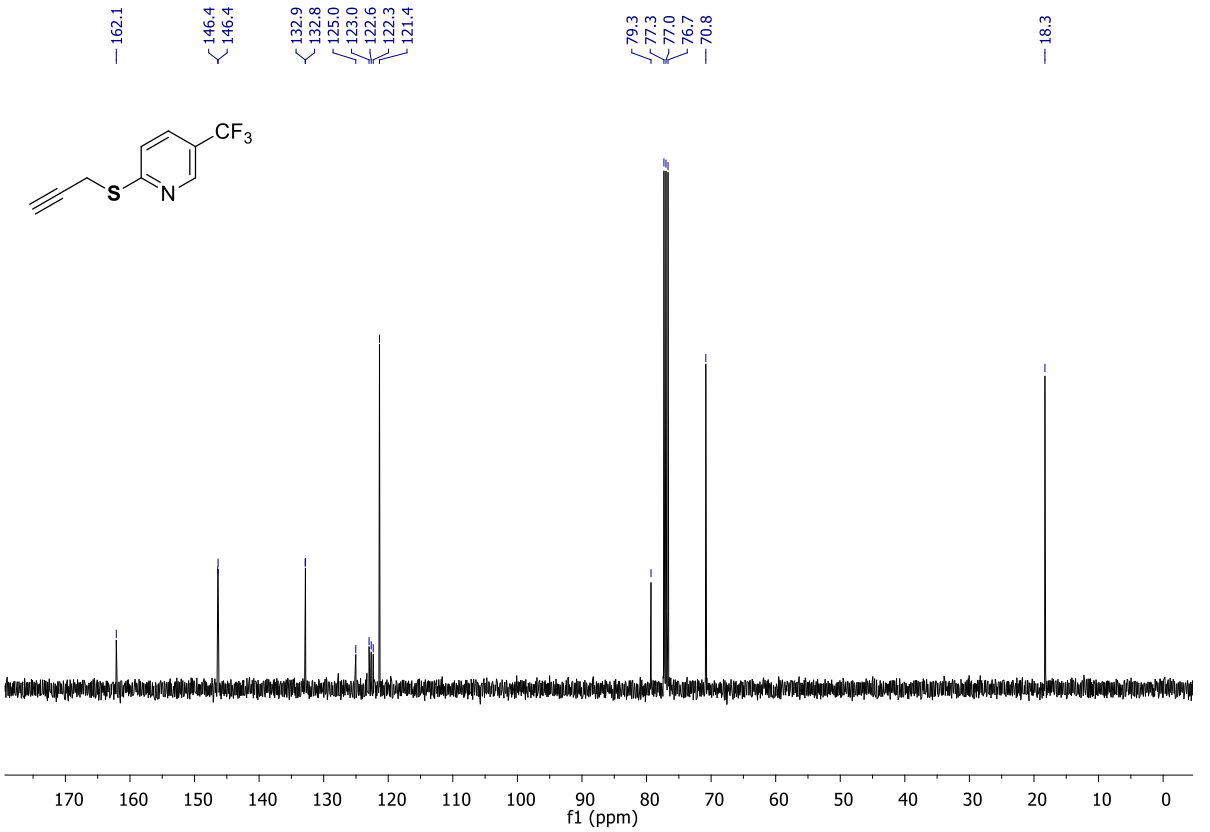

1-Phenyl-5-(prop-2-yn-1-ylthio)-1H-tetrazole (S2h)

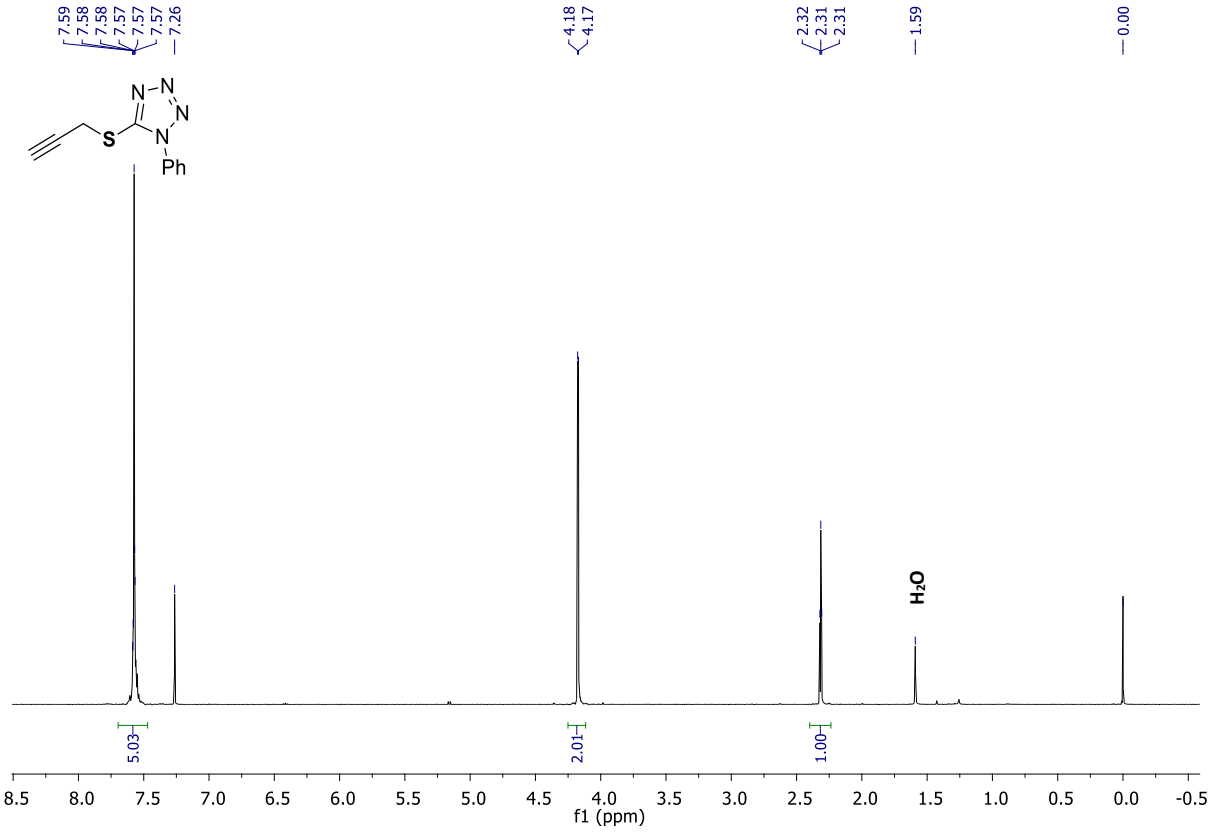

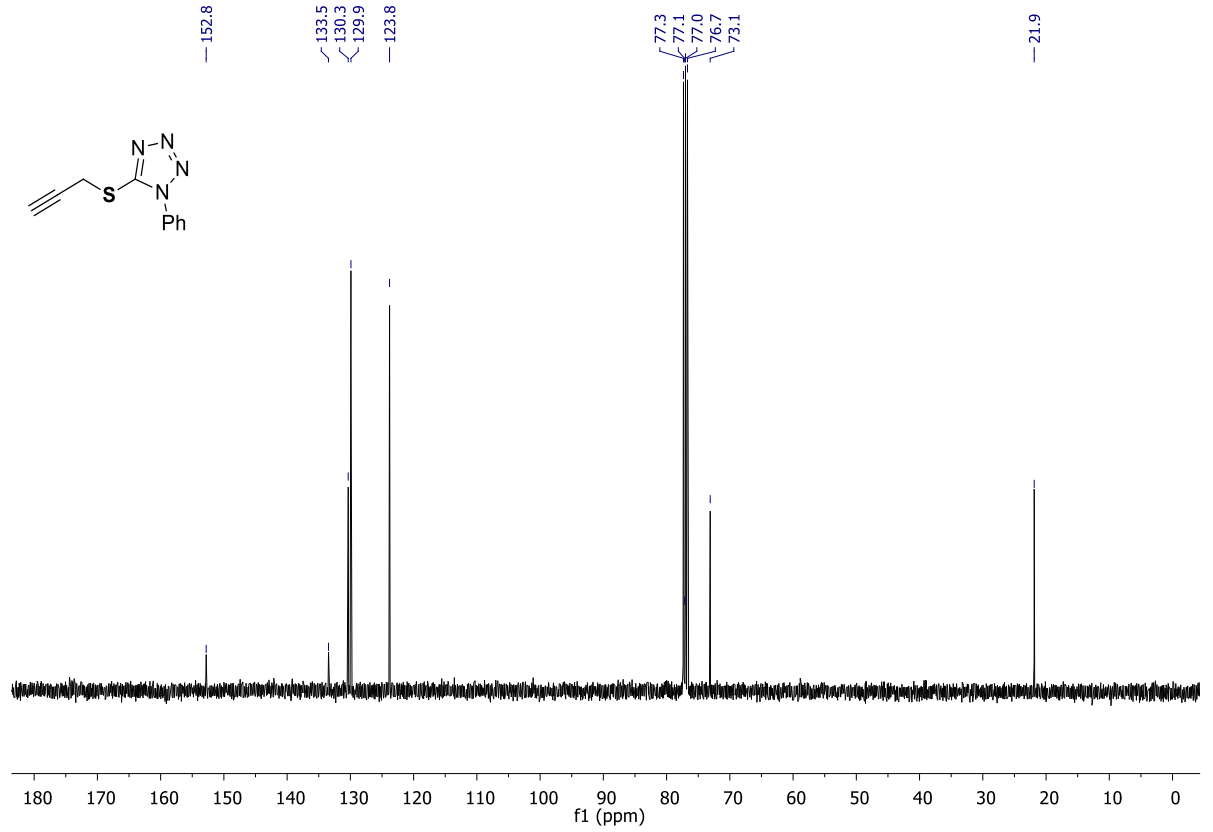

(3s,5s,7s)-Adamantan-1-yl(prop-2-yn-1-yl)sulfane (S2k)

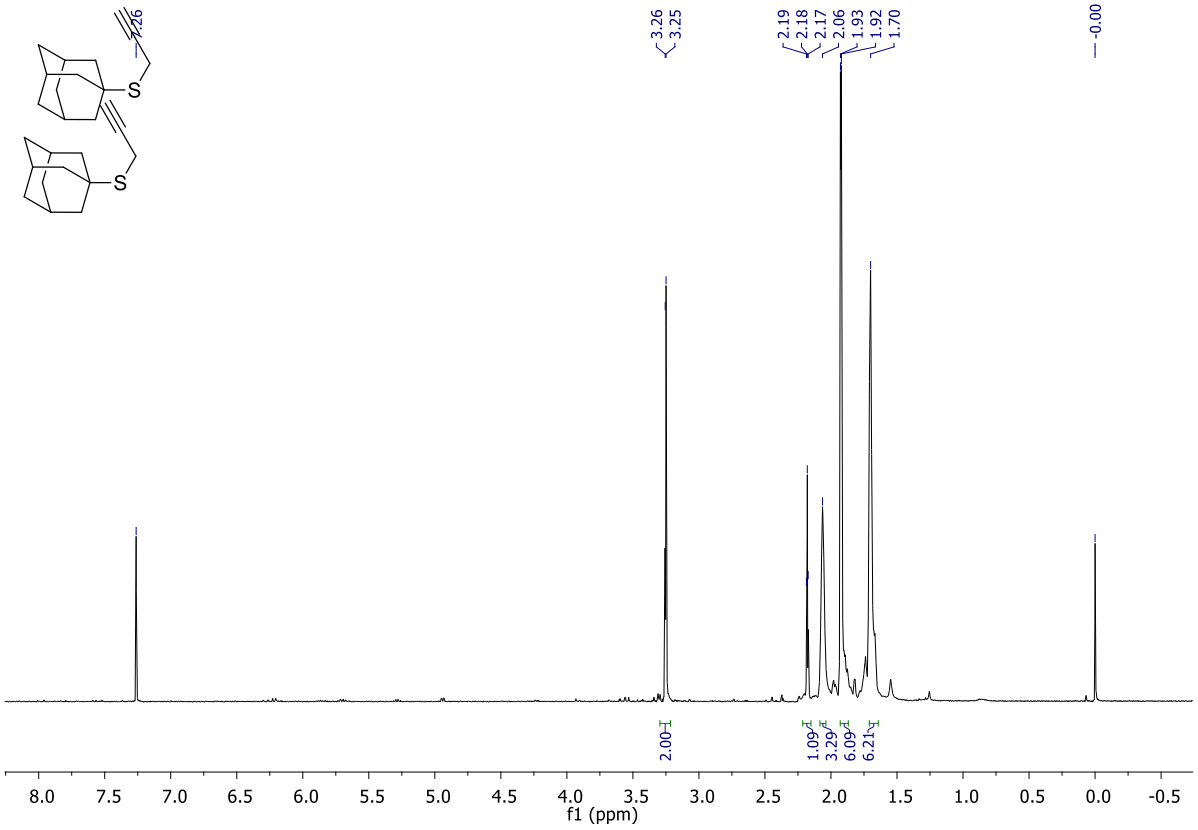

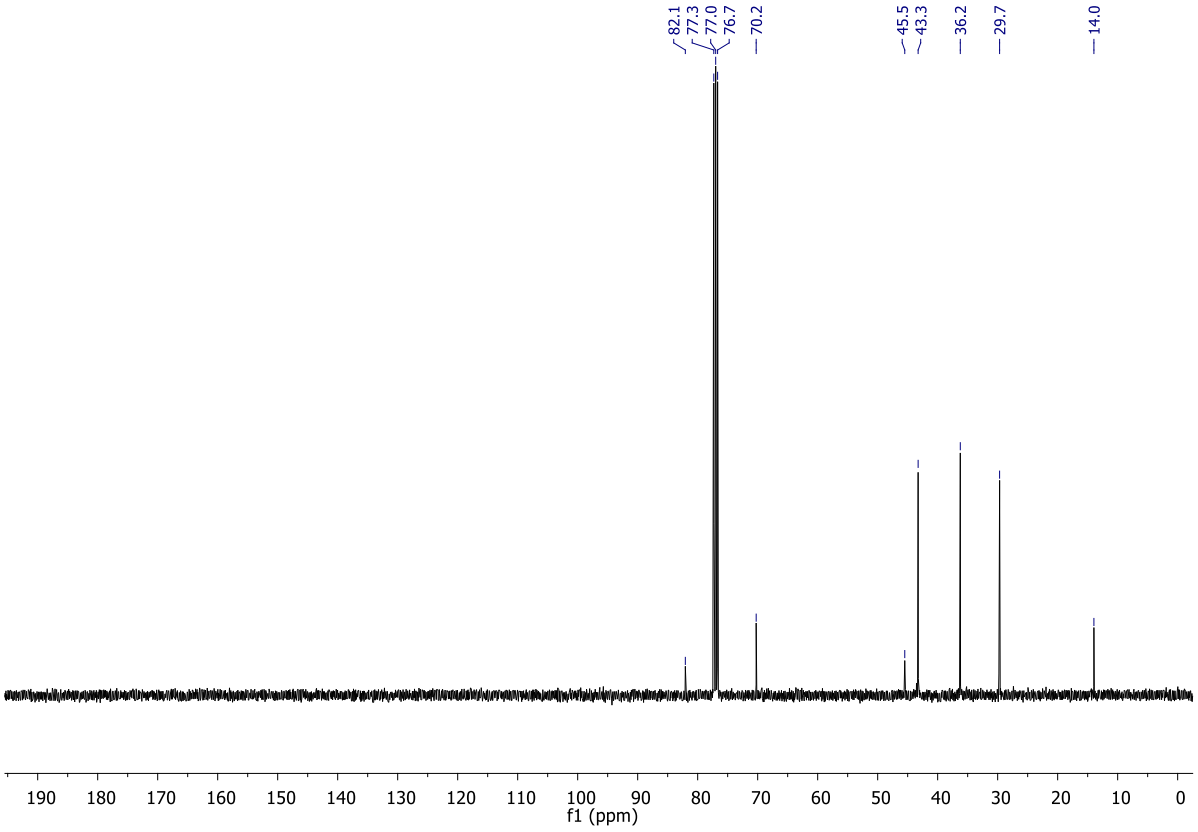

Methyl 2-(4-cyanophenyl)-2-(phenylthio)penta-3,4-dienoate (3)

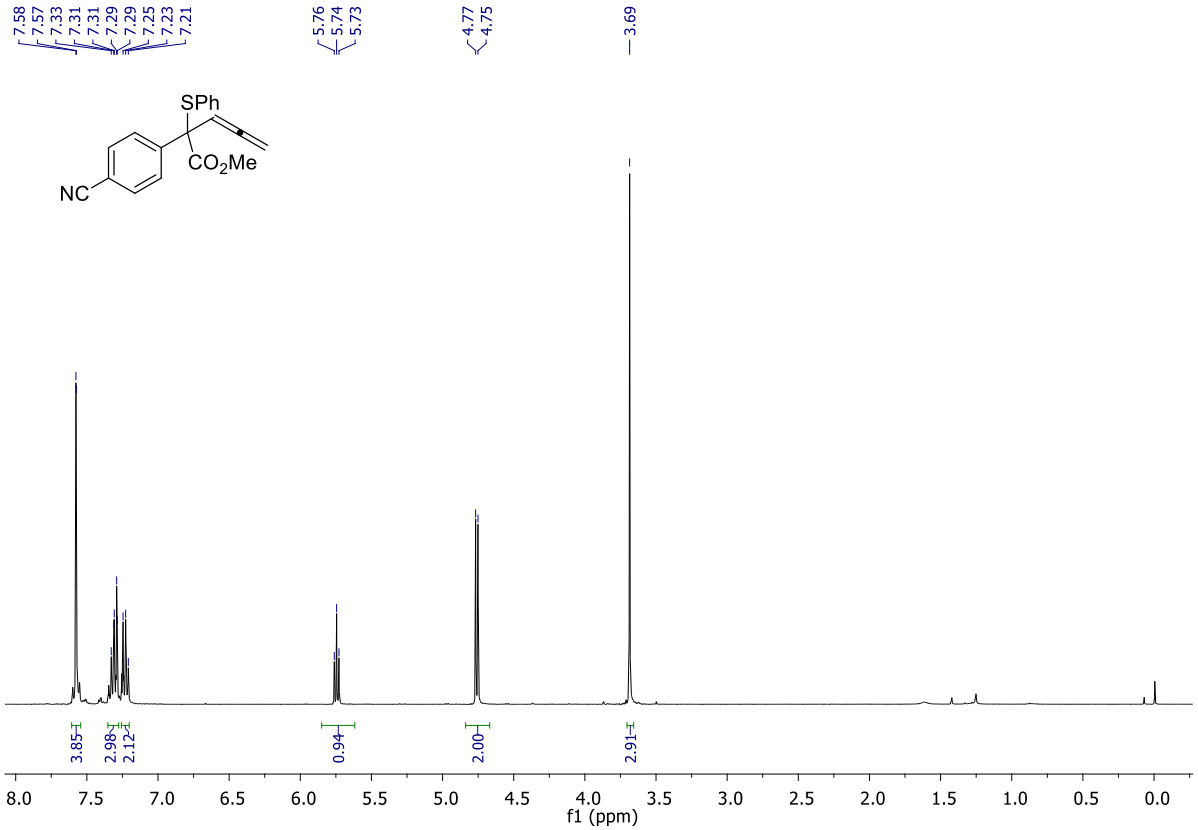

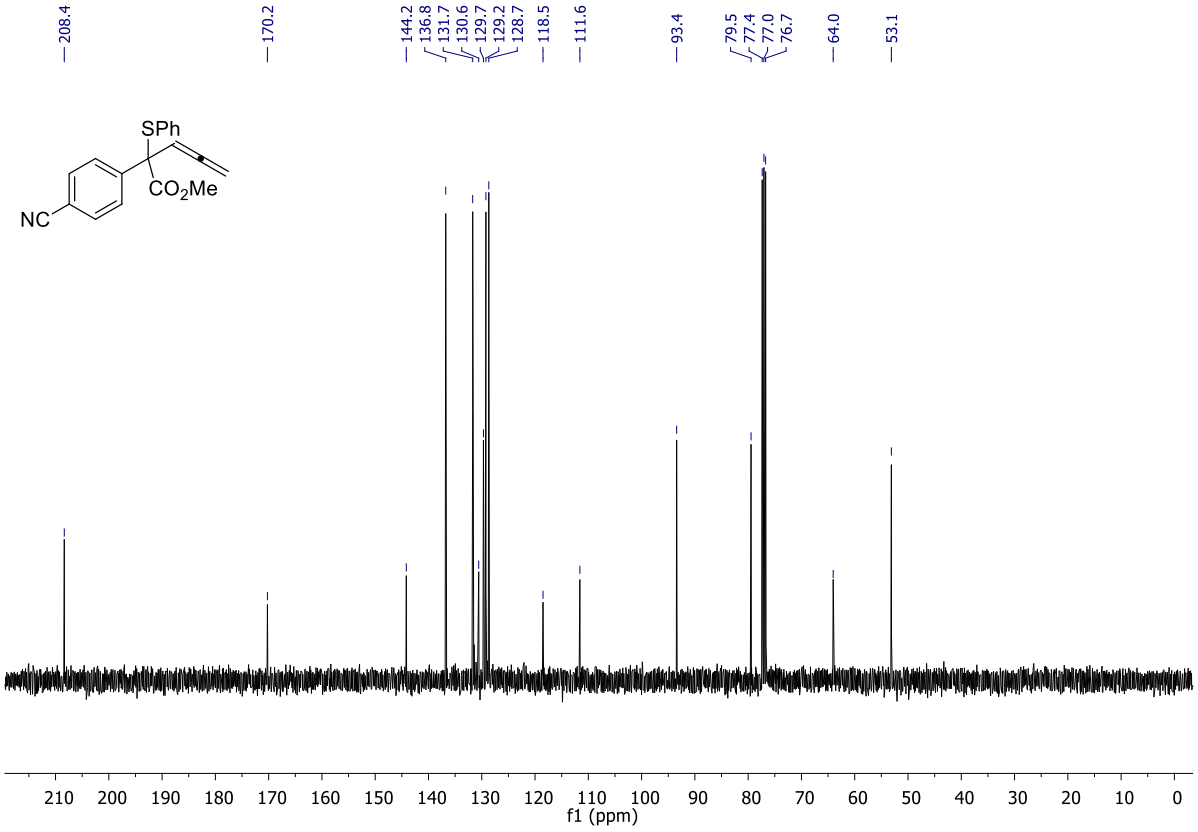

Methyl 4-(1-ethoxy-1-oxo-2-(phenylthio)penta-3,4-dien-2-yl)benzoate (4)

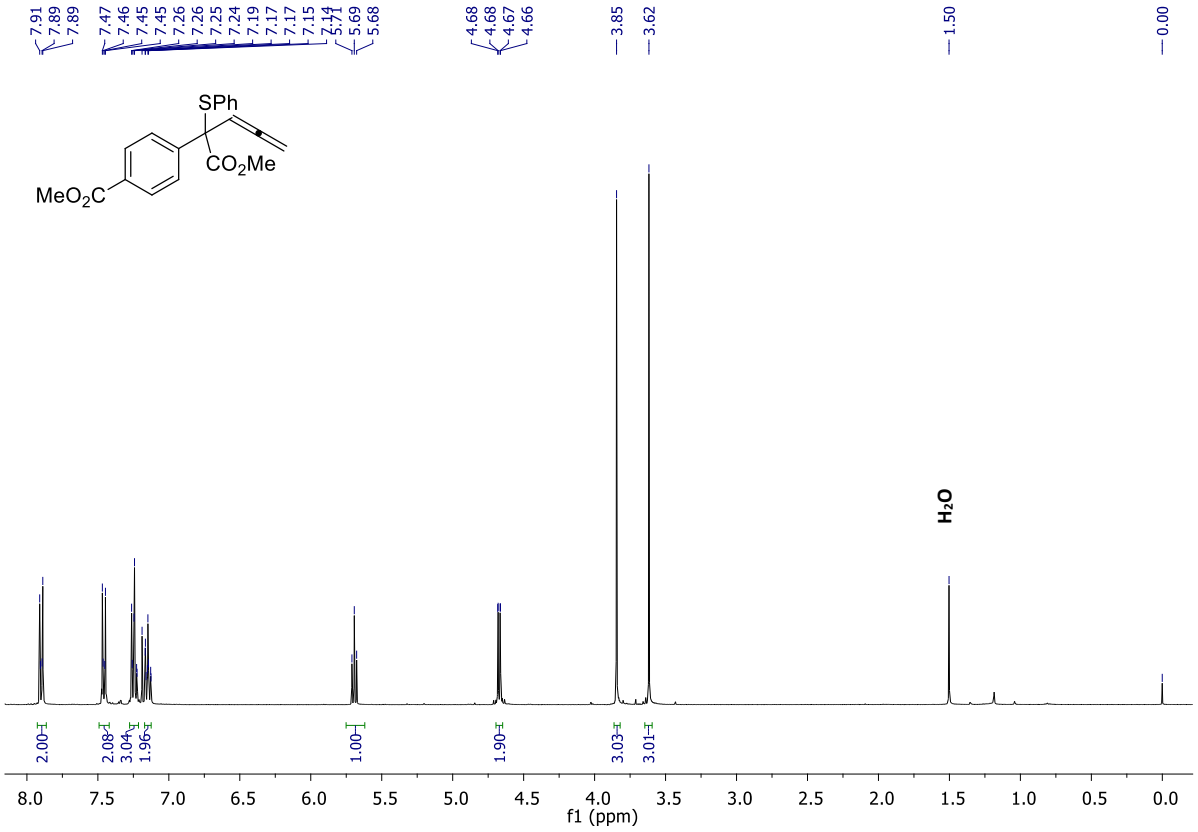

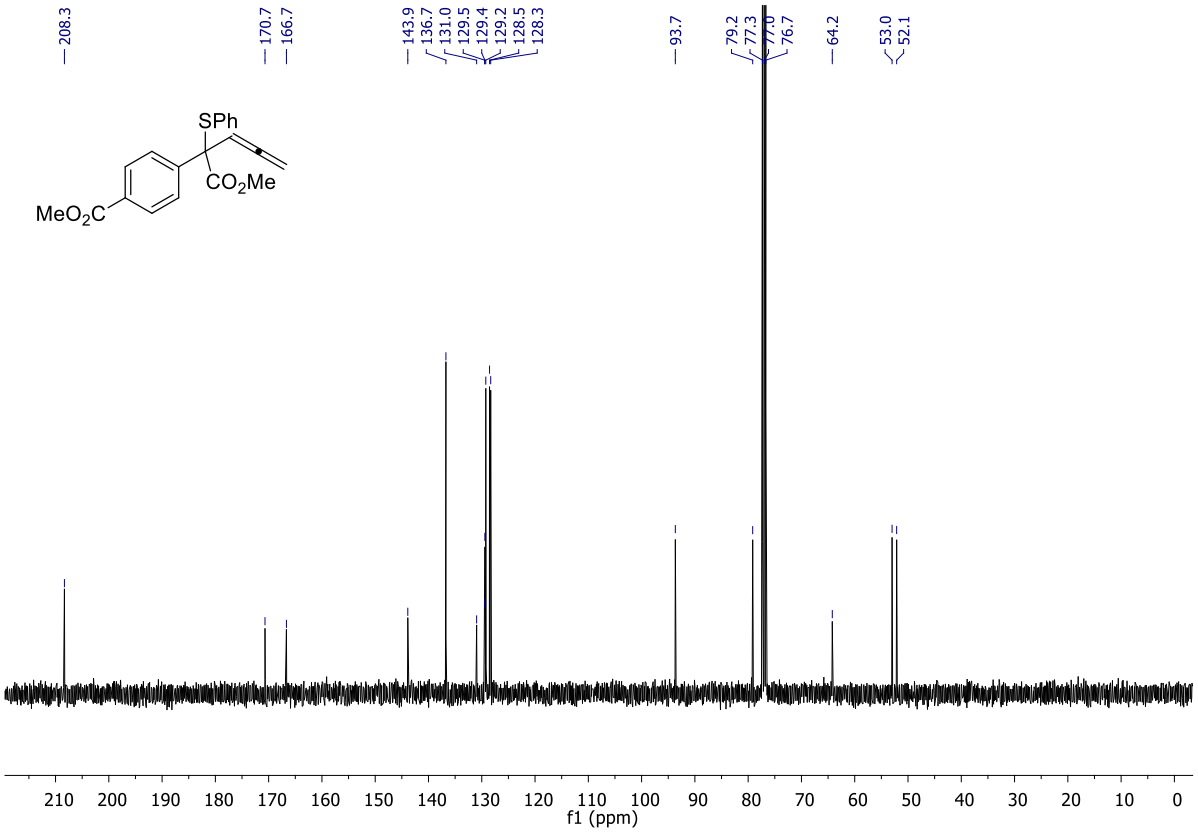

Methyl 2-(phenylthio)-2-(4-(trifluoromethyl)phenyl)penta-3,4-dienoate (5)

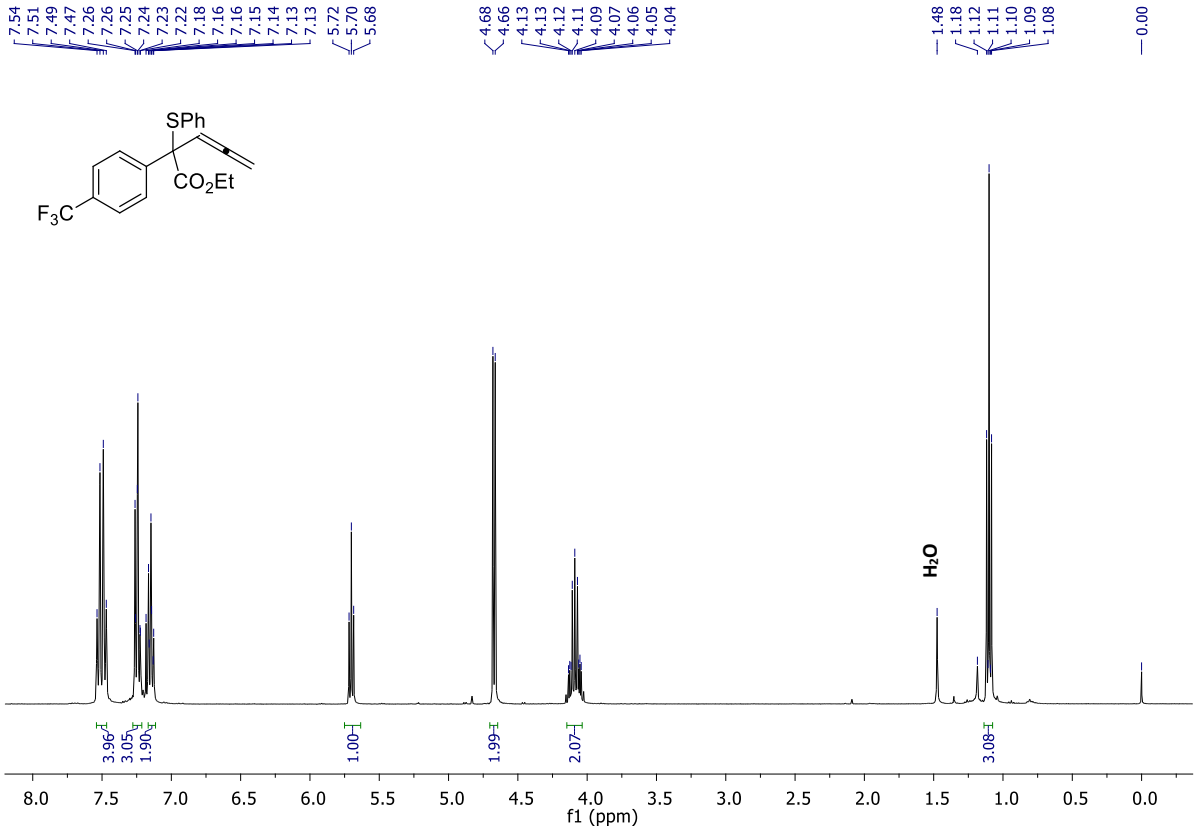

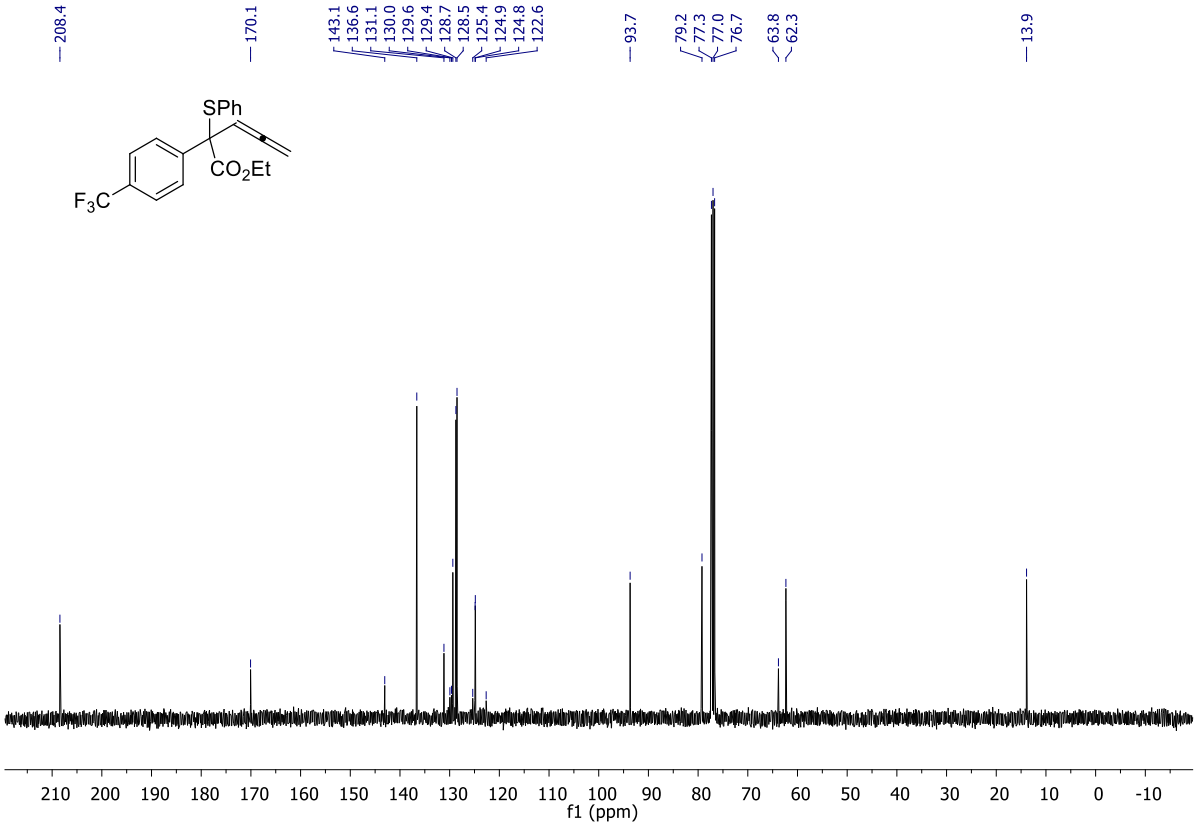

Methyl 2-(4-nitrophenyl)-2-(phenylthio)penta-3,4-dienoate (6)

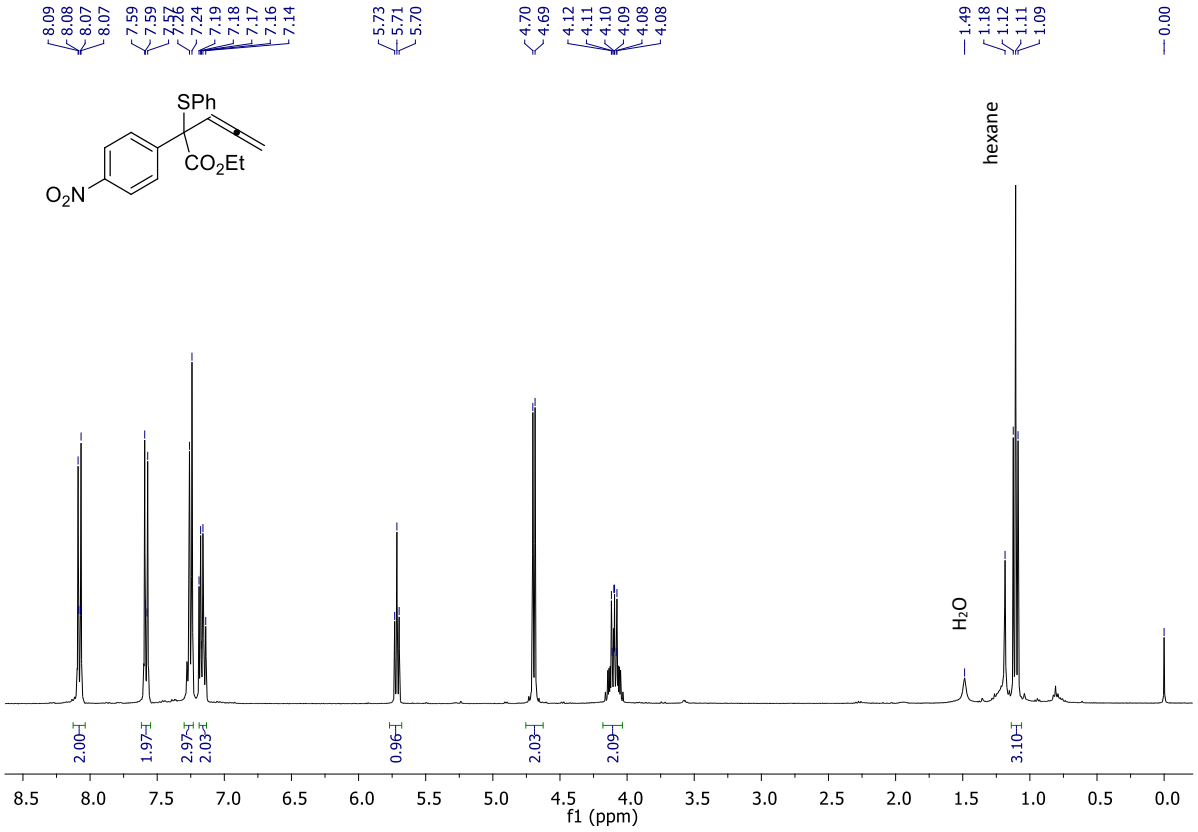

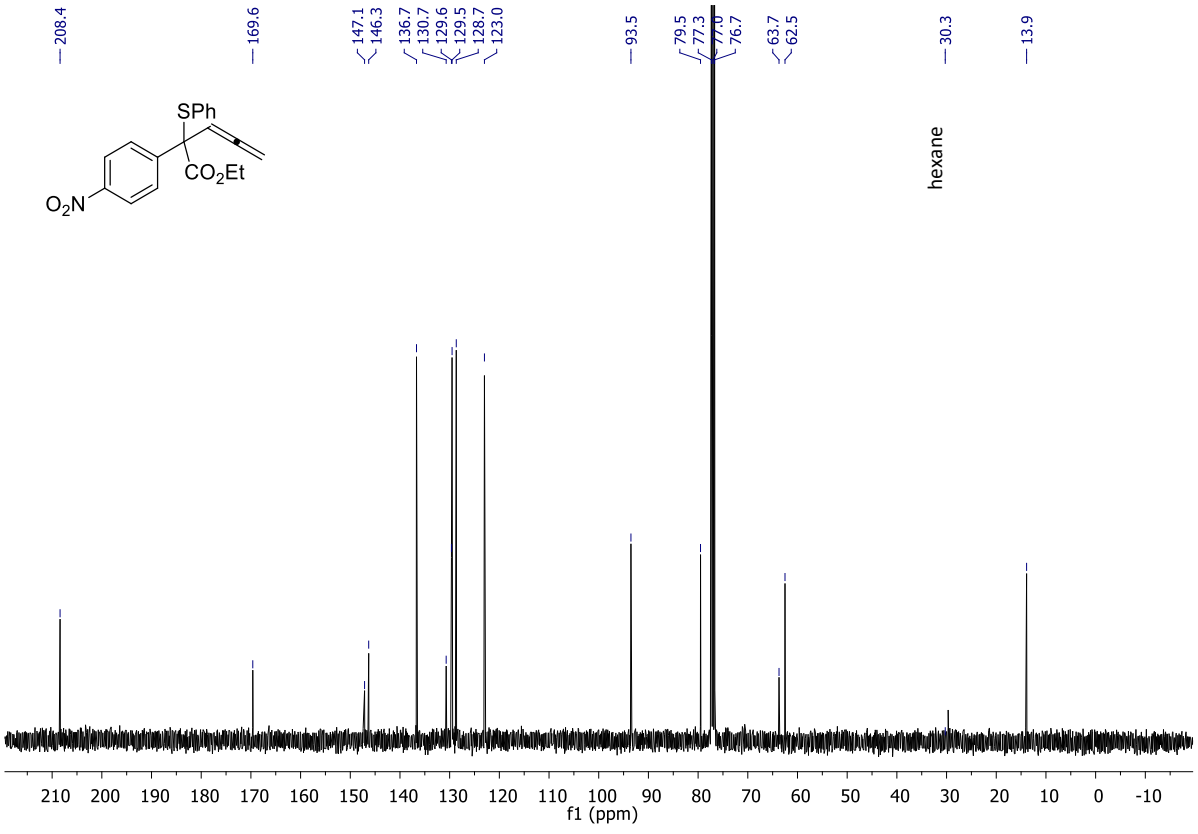

Ethyl 2-(4-bromophenyl)-2-(phenylthio)penta-3,4-dienoate (7)

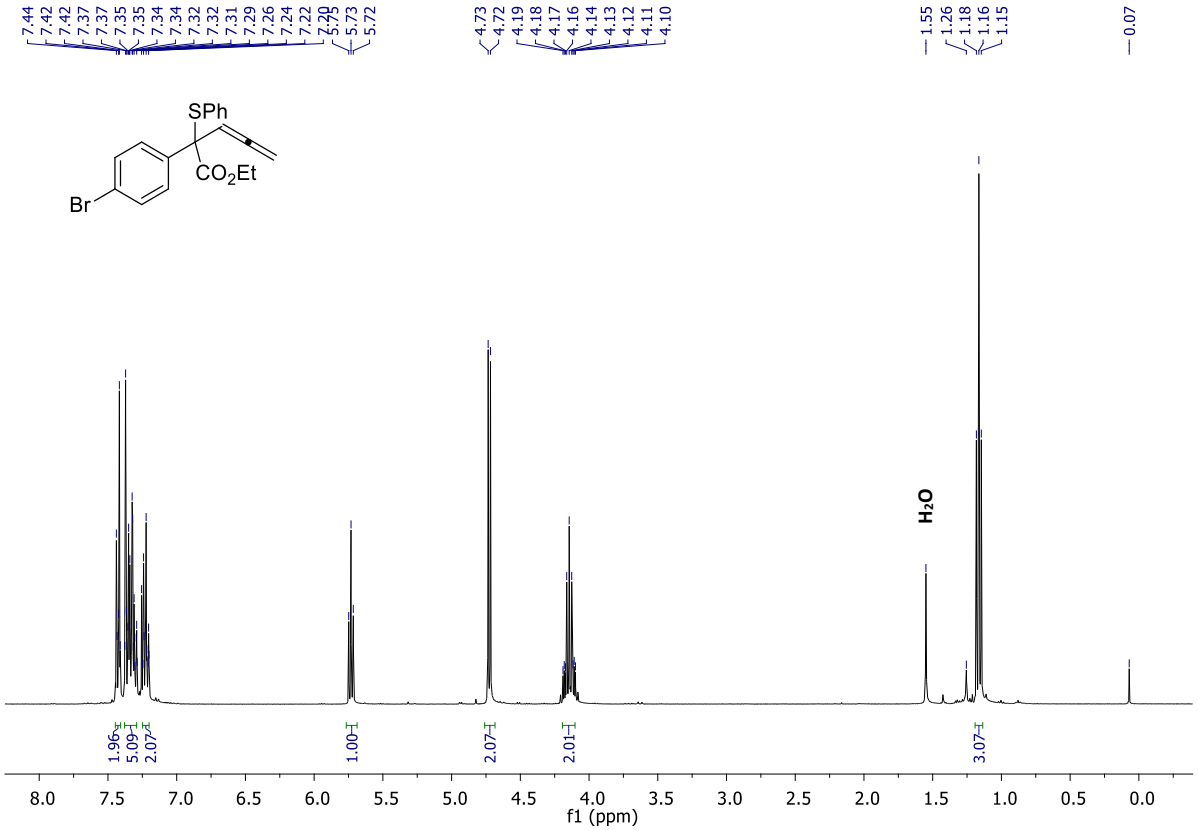

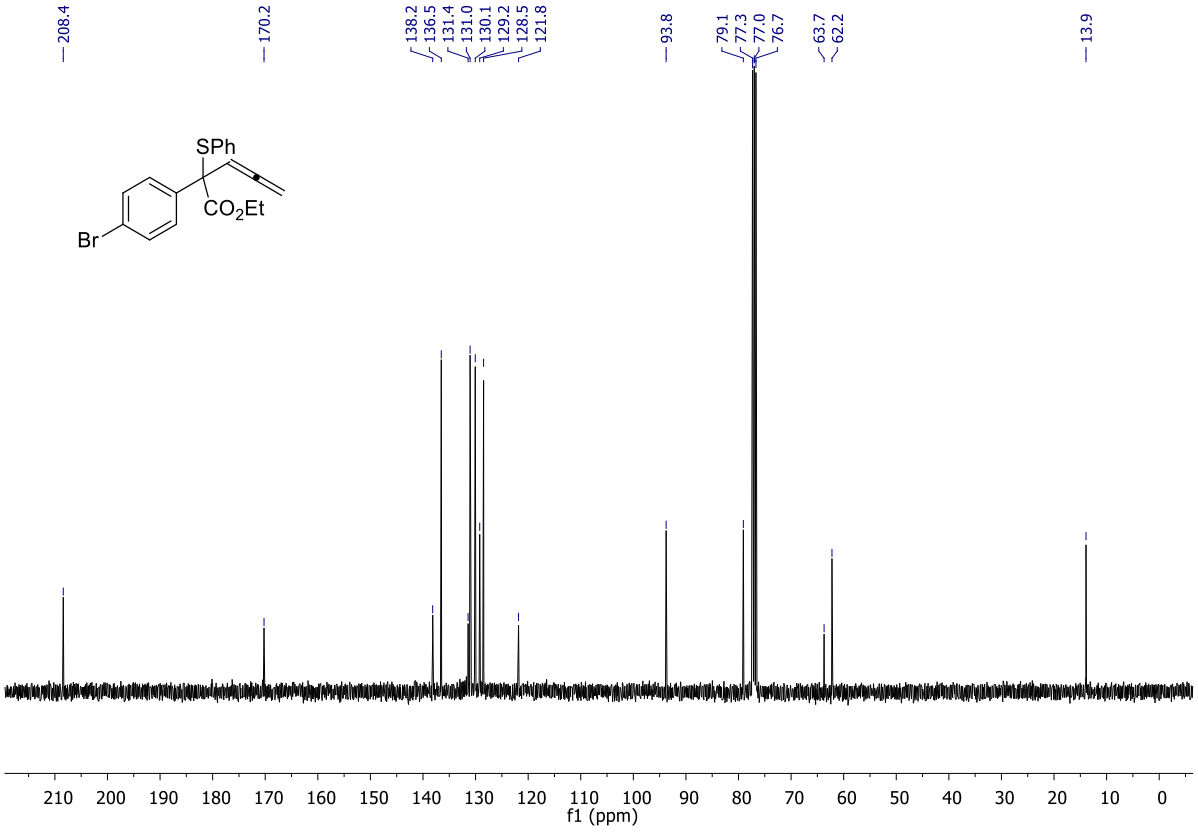

Methyl 2-(4-chlorophenyl)-2-(phenylthio)penta-3,4-dienoate (8)

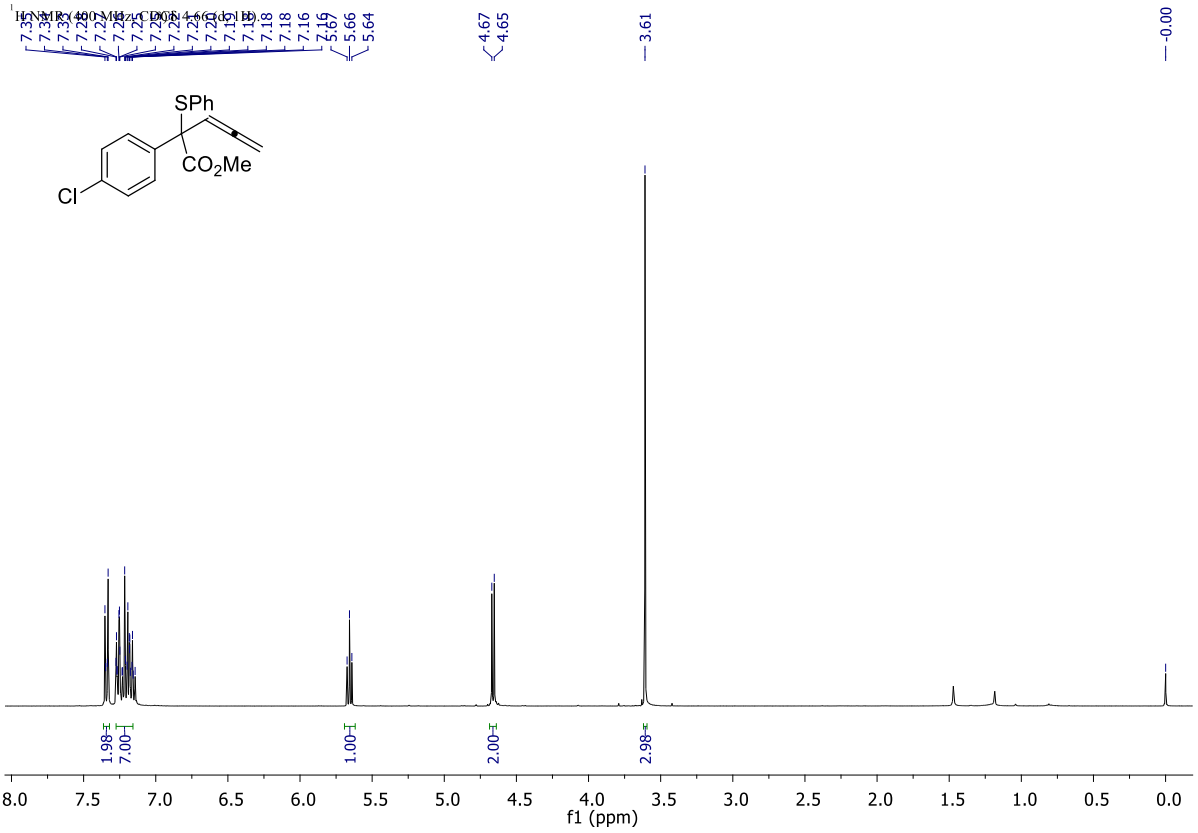

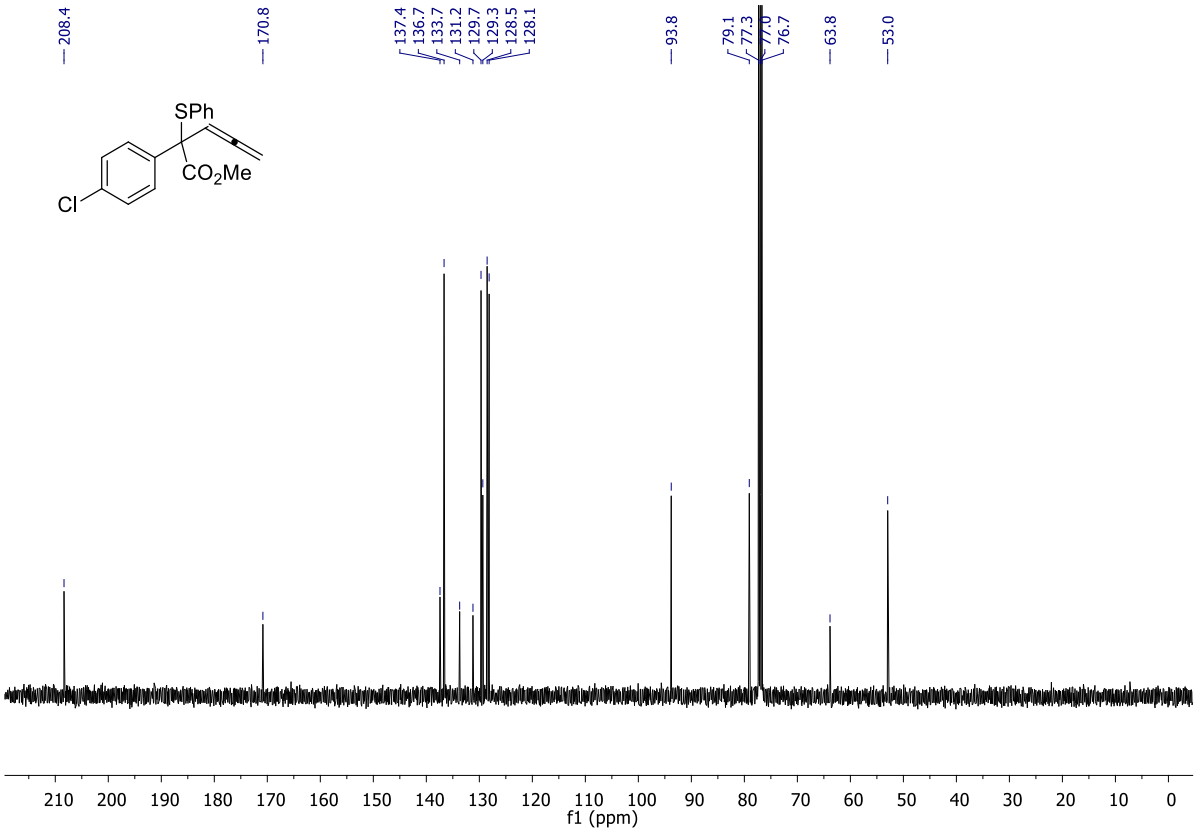

Ethyl 2-(4-fluorophenyl)-2-(phenylthio)penta-3,4-dienoate (9)

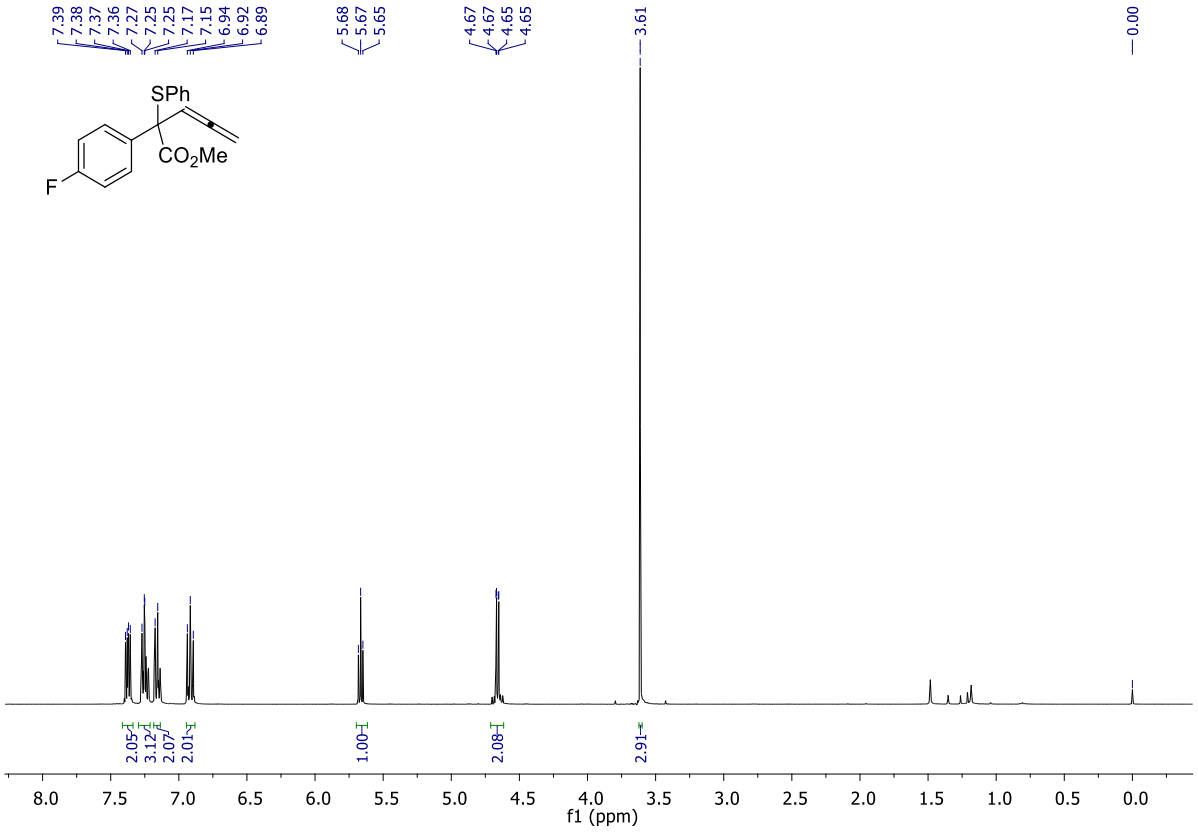

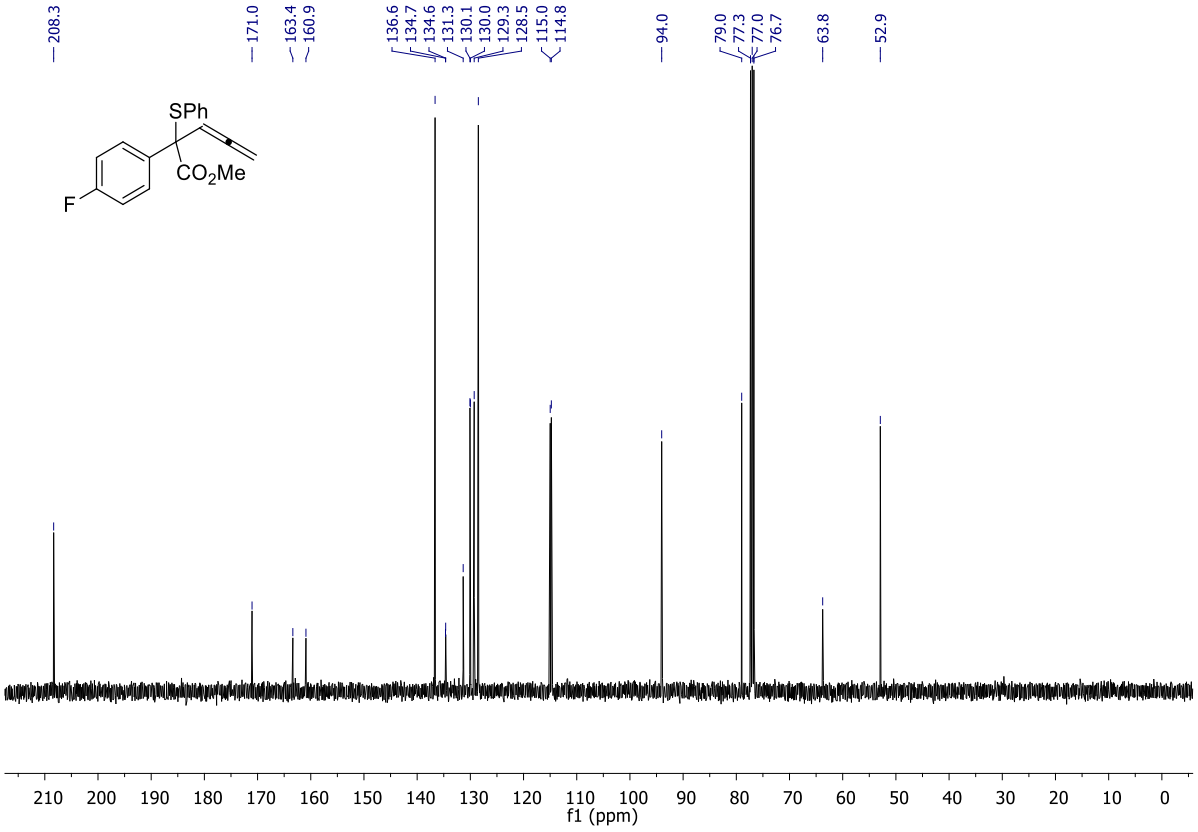

Methyl 2-(2-fluorophenyl)-2-(phenylthio)penta-3,4-dienoate (10)

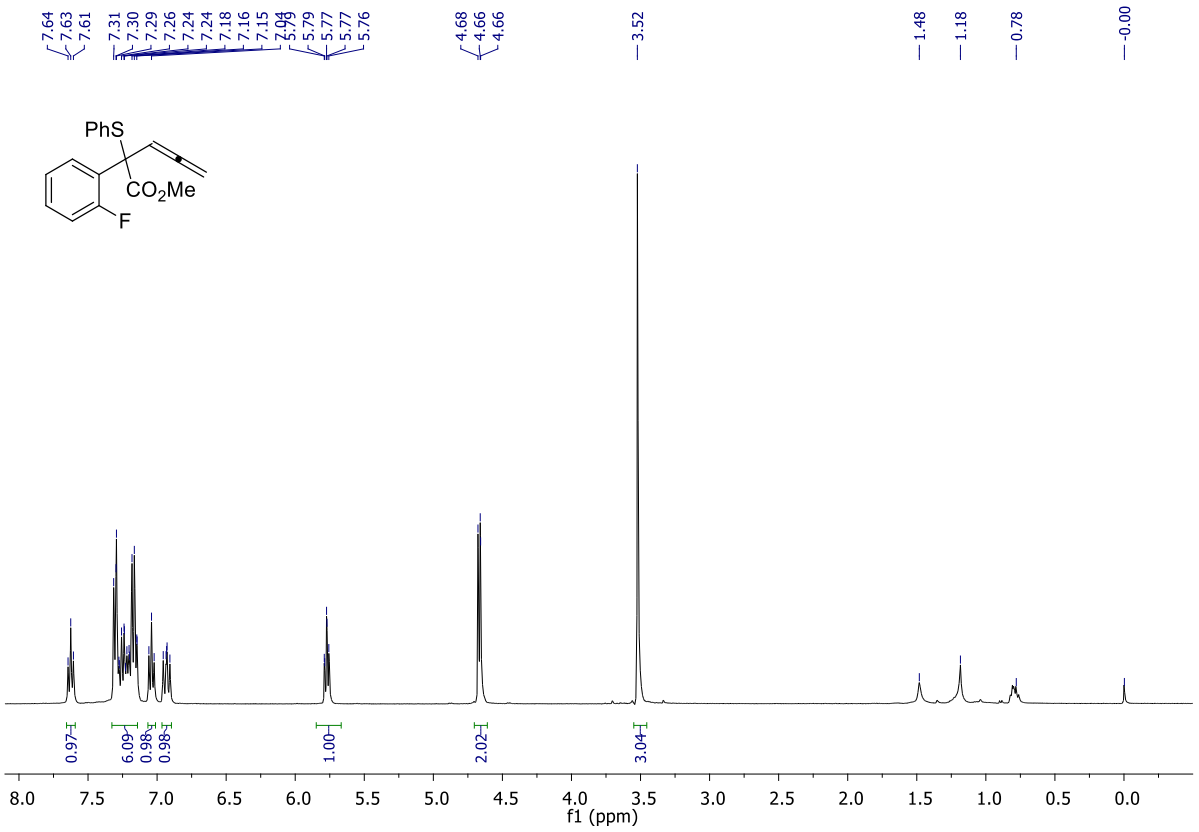

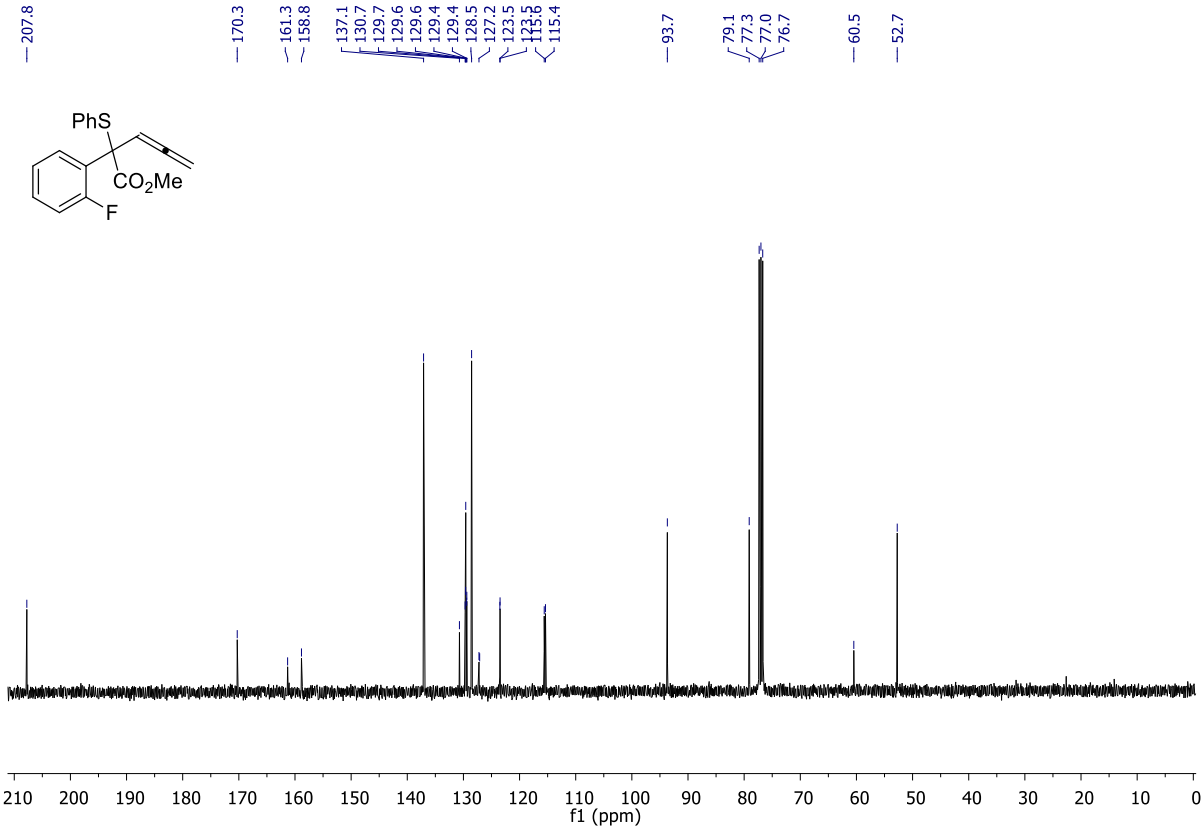

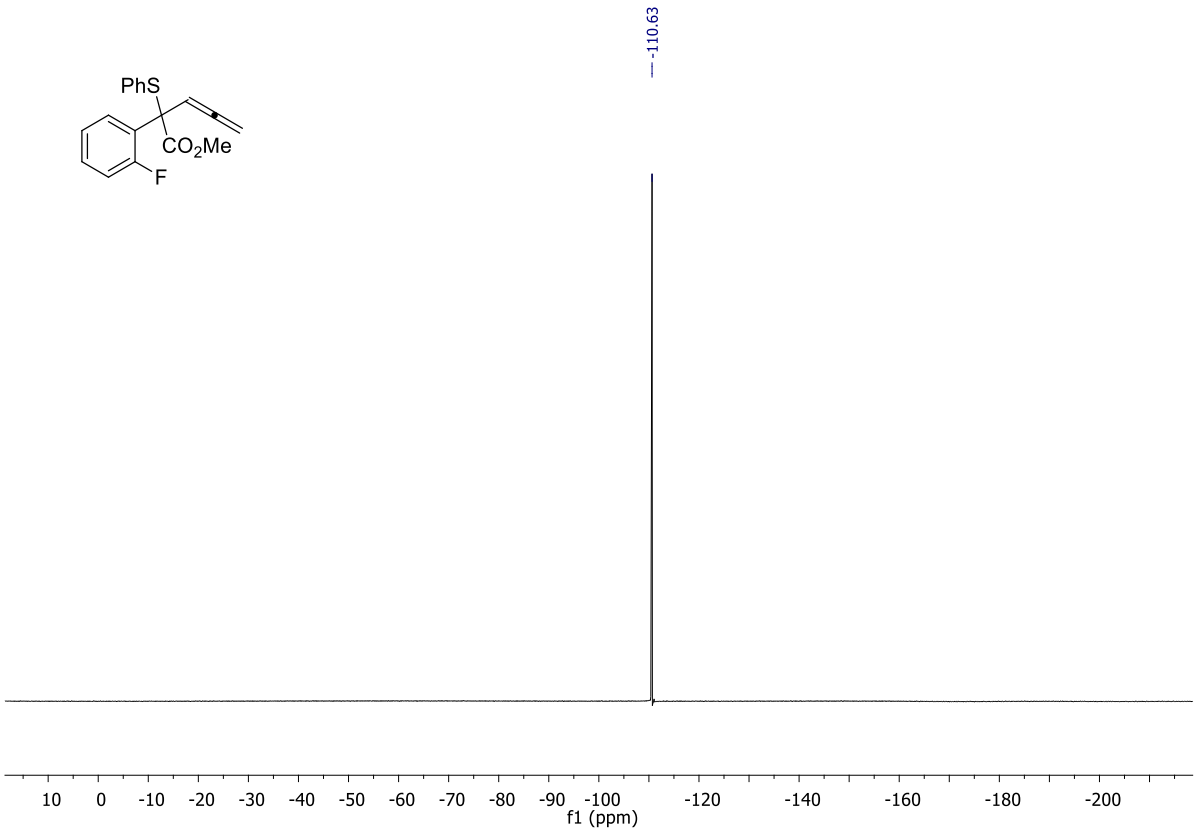

Methyl 2-(2-fluorophenyl)-2-(phenylthio)penta-3,4-dienoate (11)

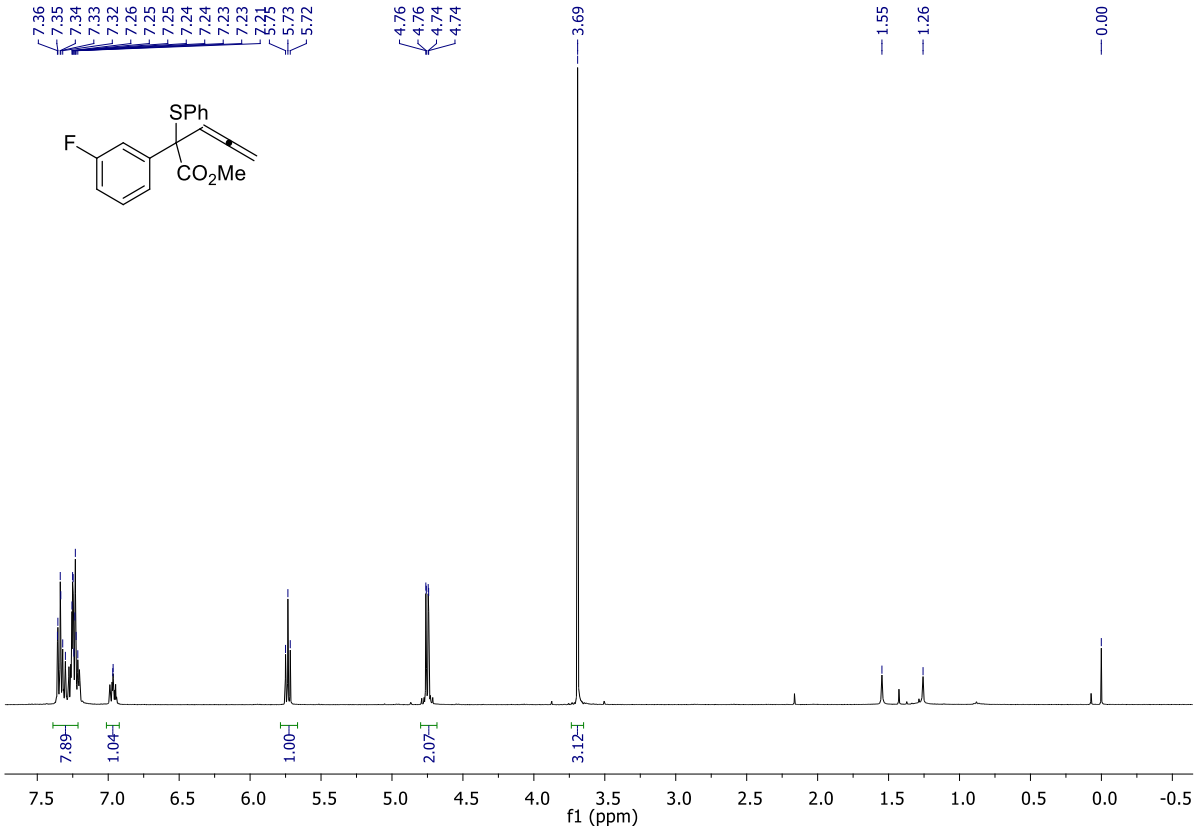

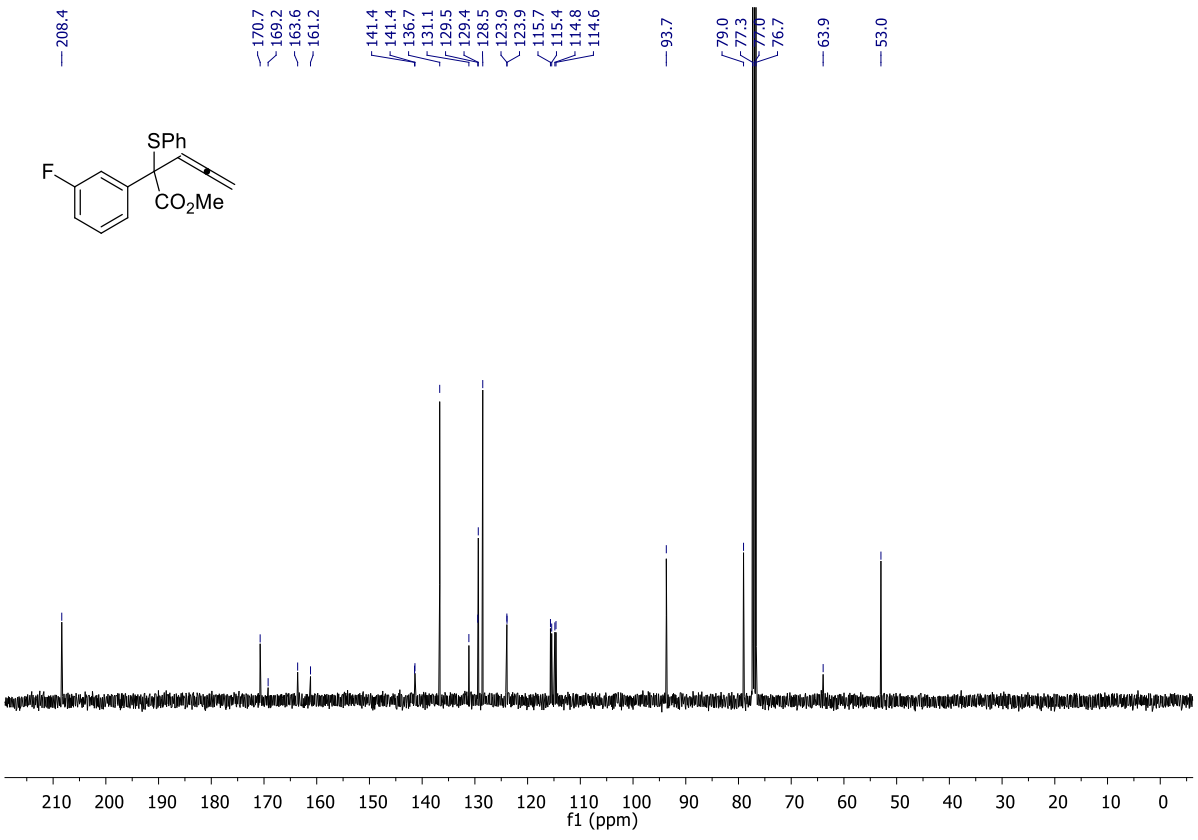

Methyl 2-phenyl-2-(phenylthio)penta-3,4-dienoate (12)

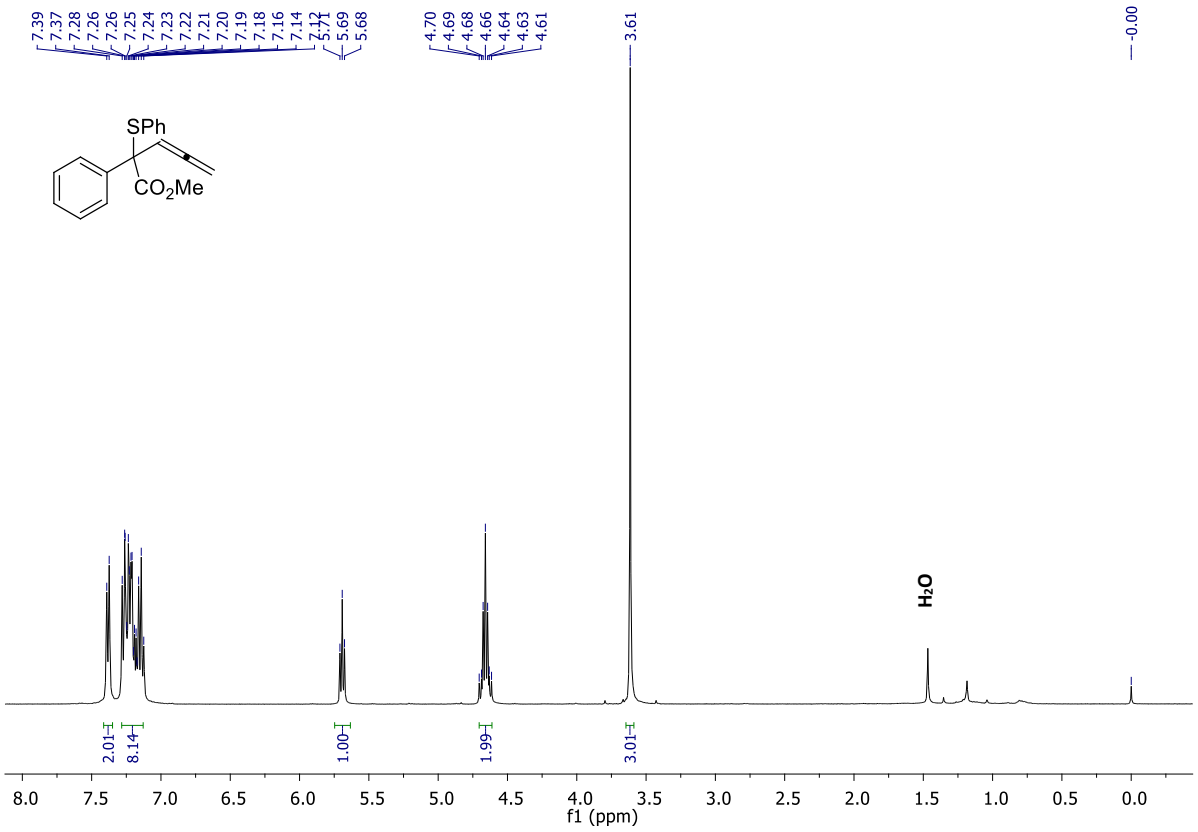

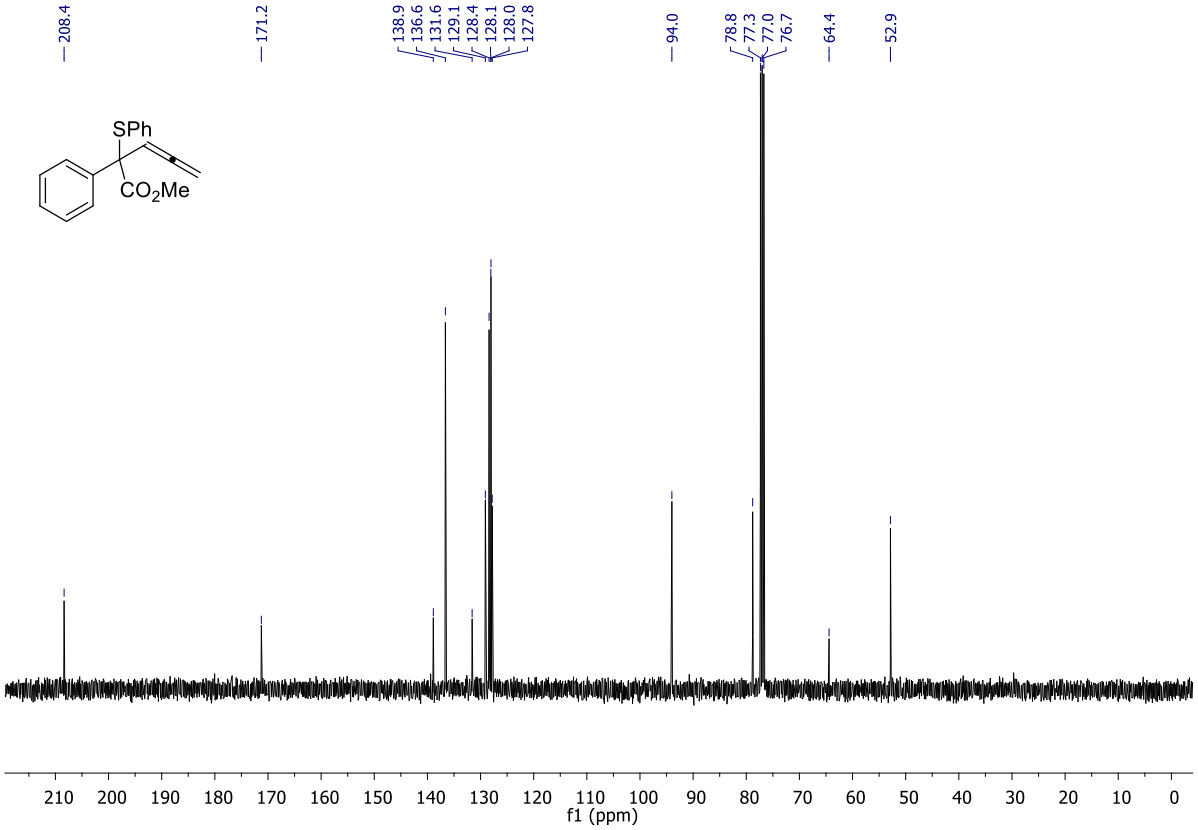

Methyl 2-(naphthalen-2-yl)-2-(phenylthio)penta-3,4-dienoate (13)

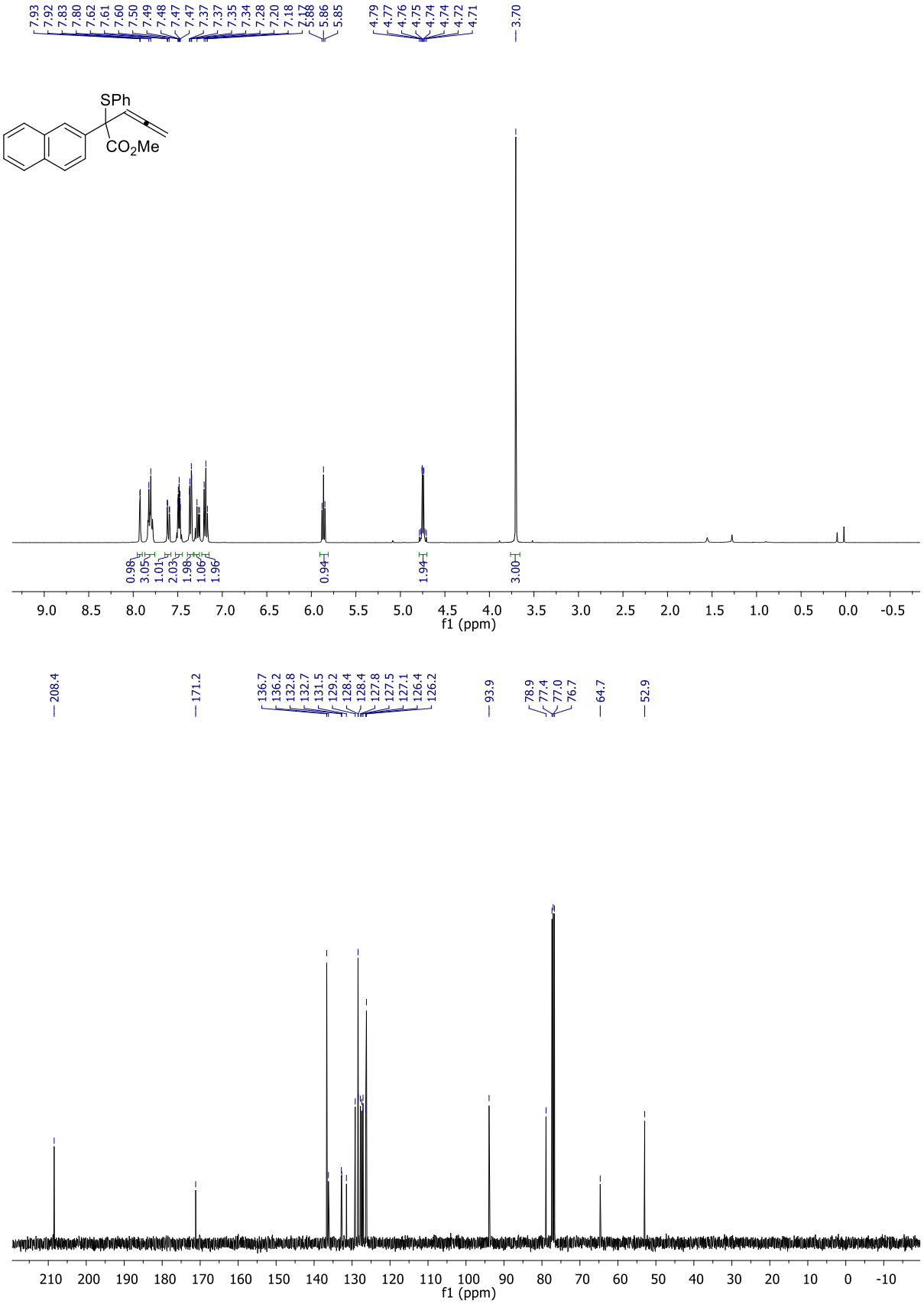

Methyl 2-(naphthalen-1-yl)-2-(phenylthio)penta-3,4-dienoate (14)

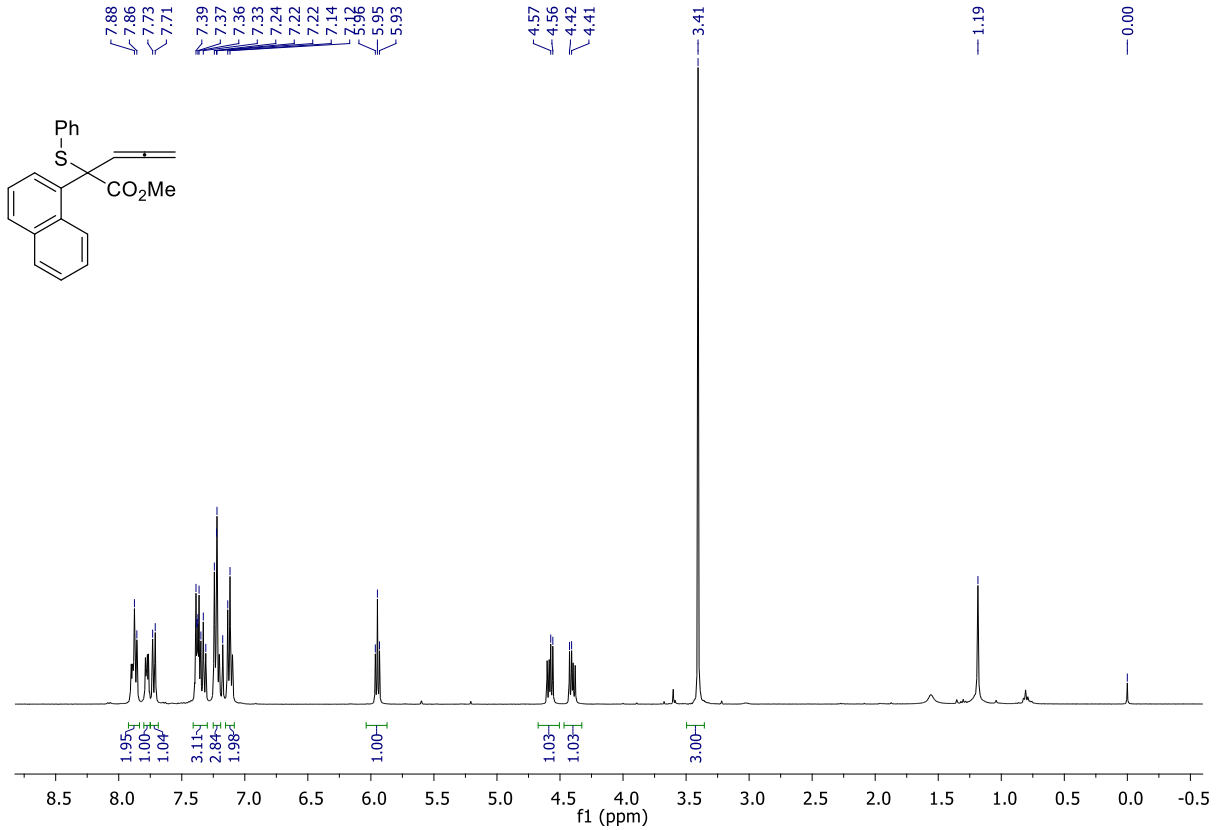

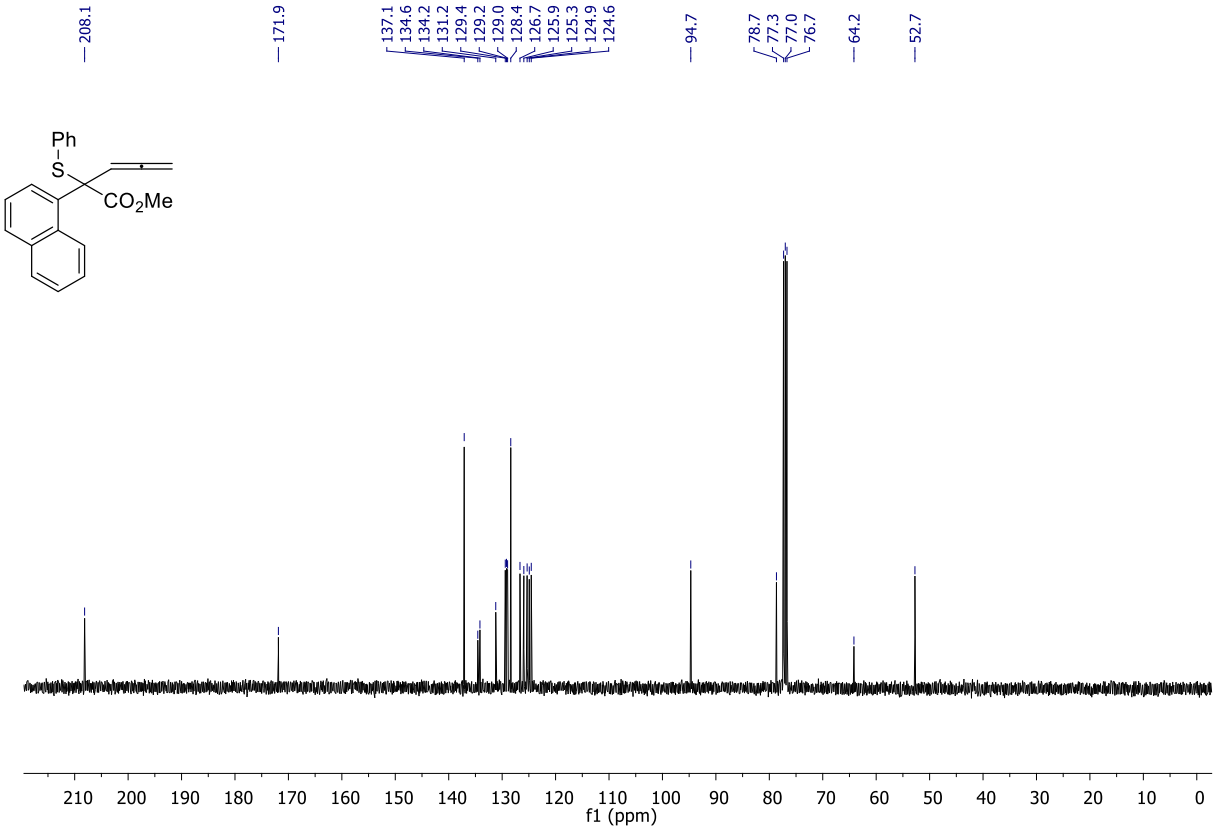

Methyl 2-[7-metoxy (naphthalen-2-yl)]-2-(phenylthio)penta-3,4-dienoate (15)

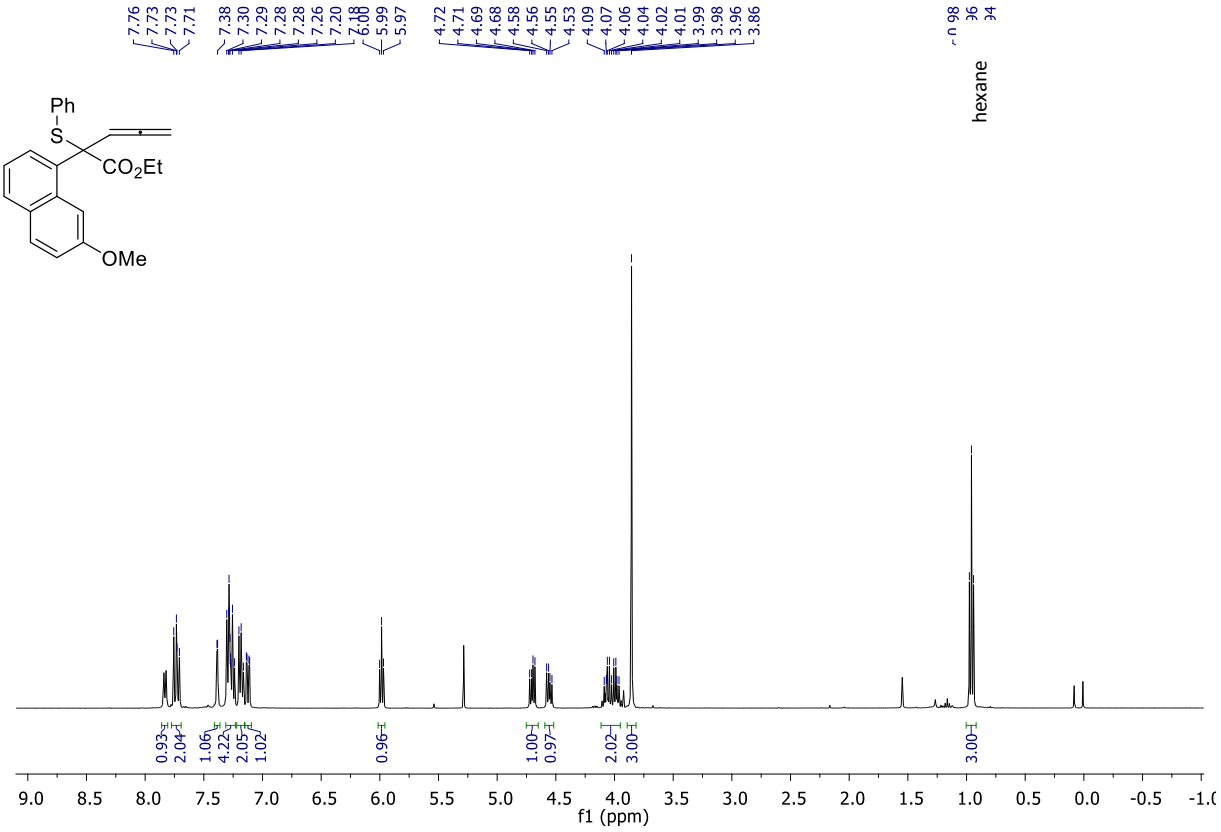

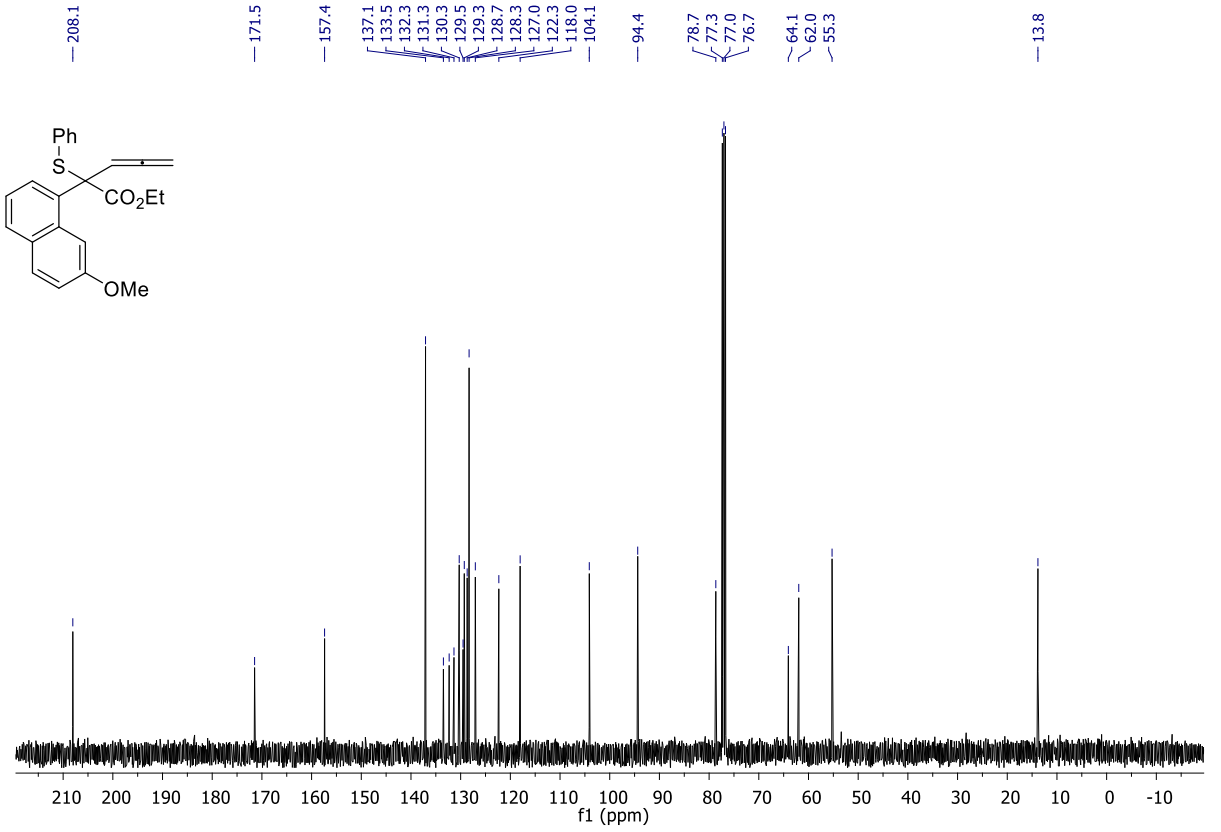

Methyl 2-(4-methoxyphenyl)-2-(phenylthio)penta-3,4-dienoate (16)

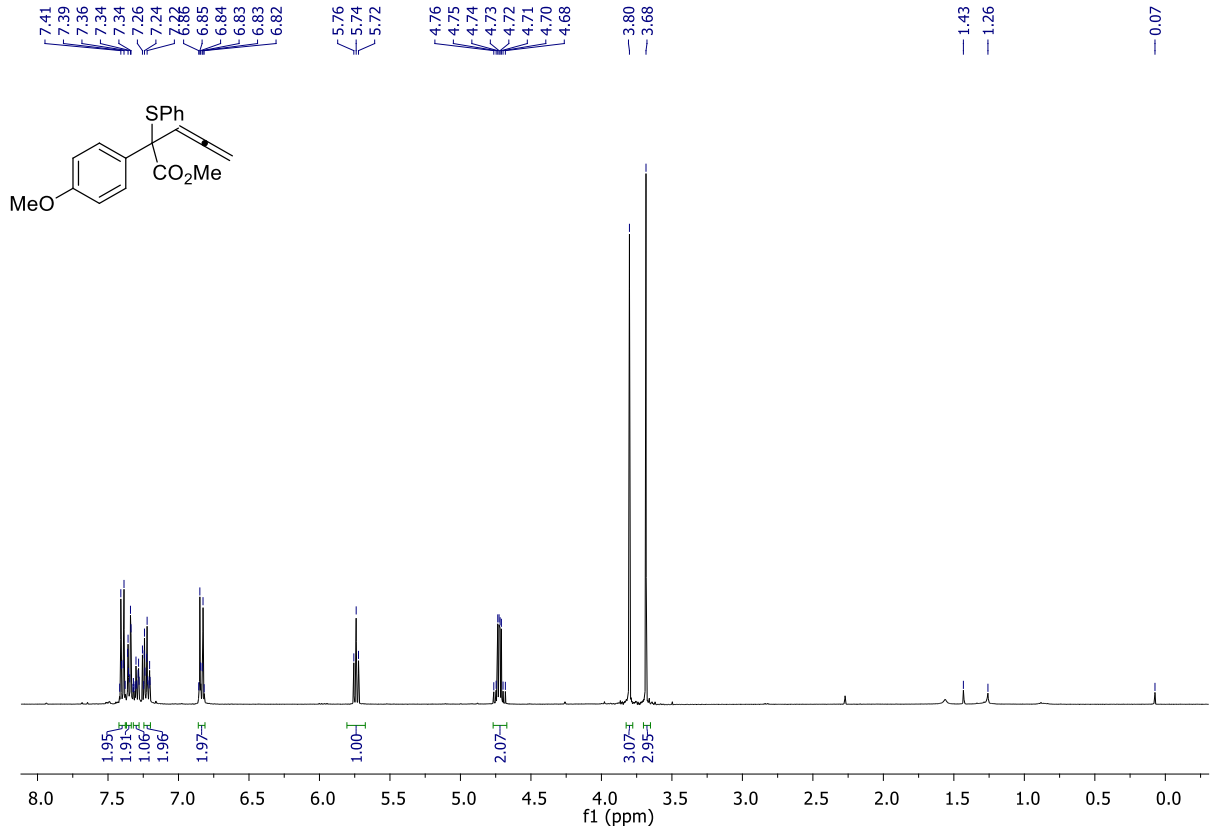

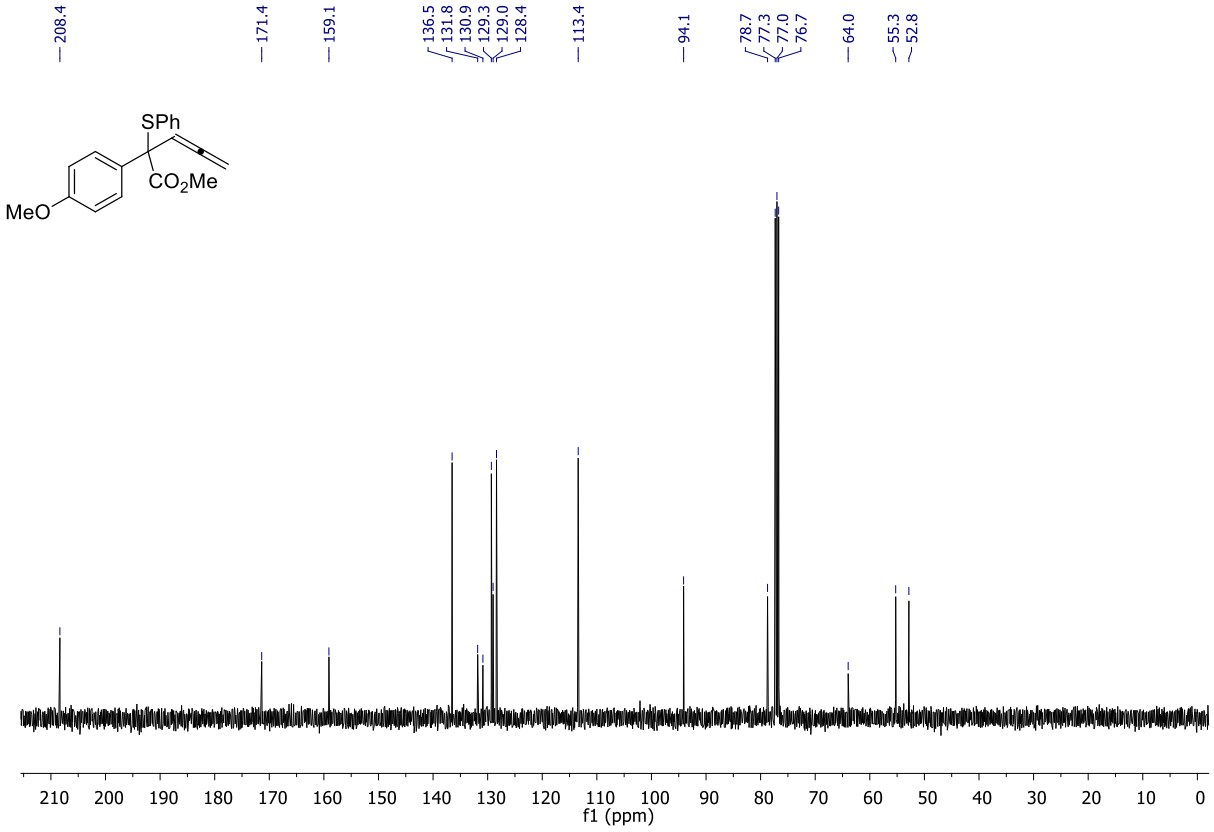

Methyl 2-(phenylthio)-2-(p-tolyl)penta-3,4-dienoate (17)

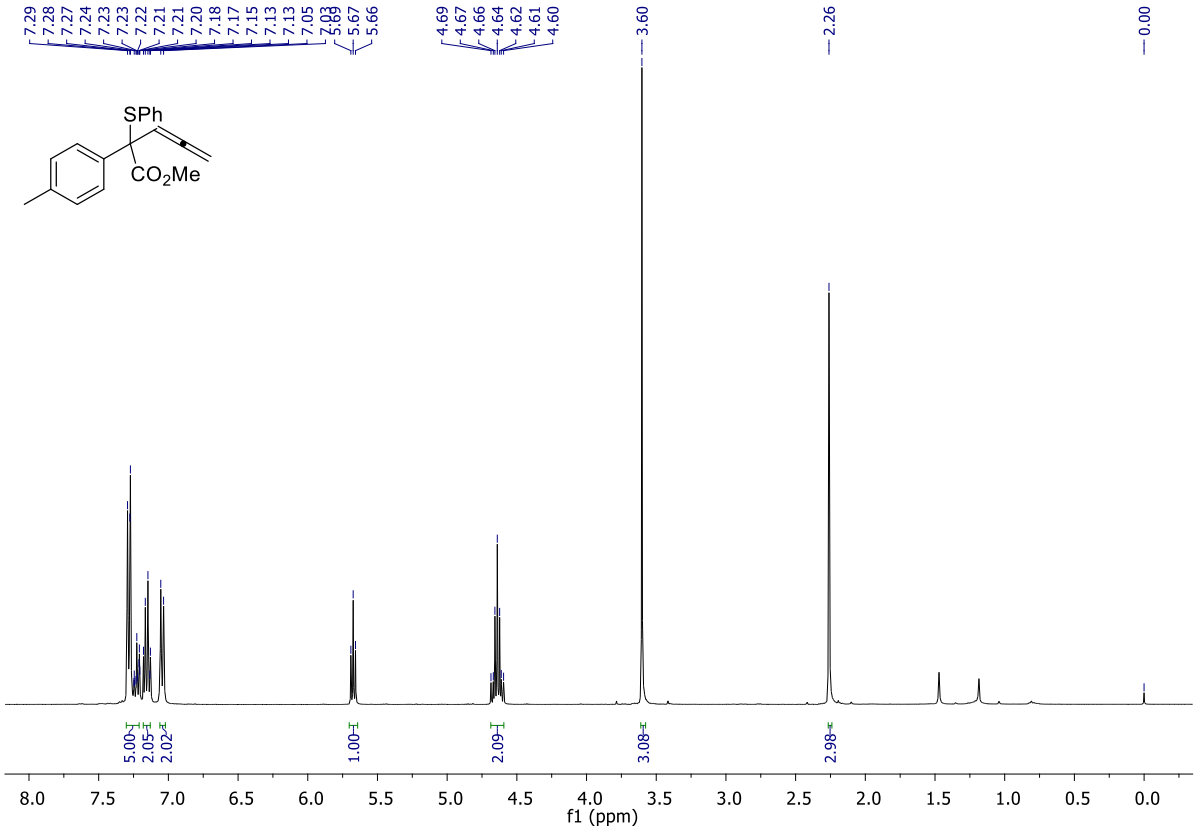

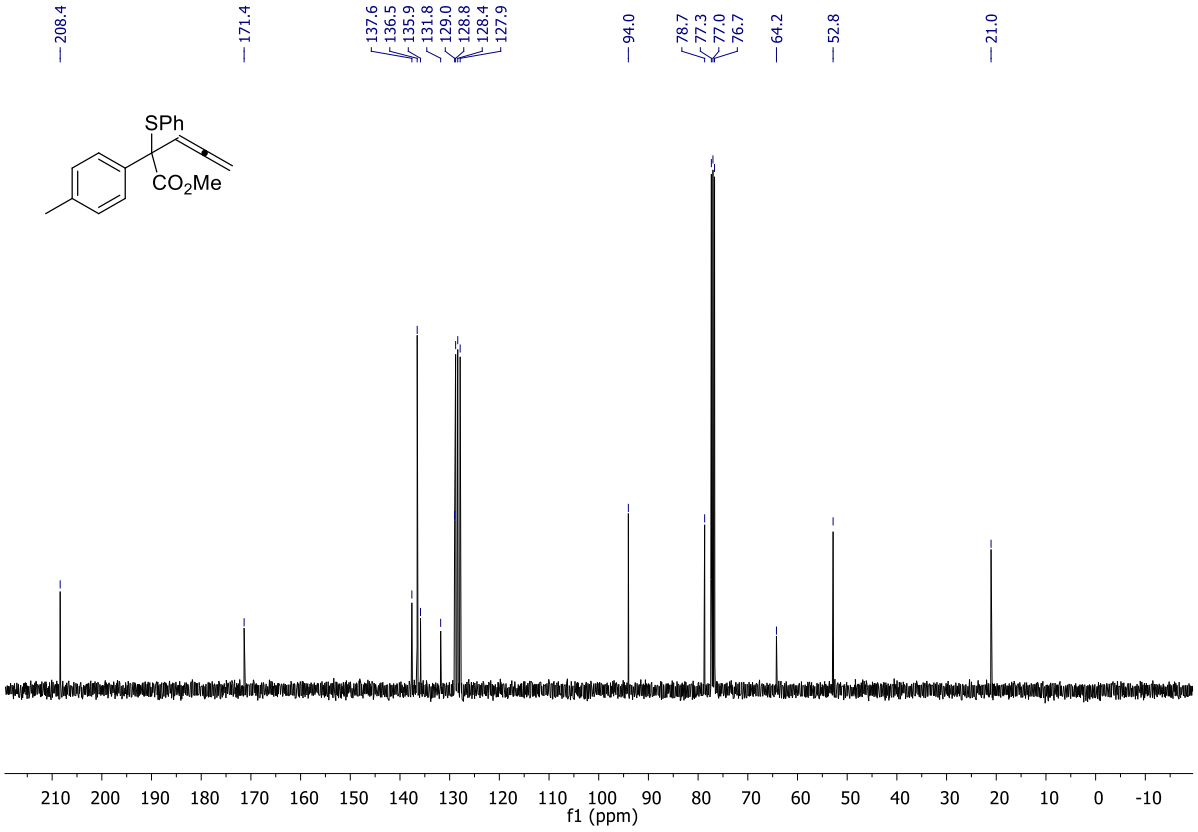

Methyl 2-(phenylthio)-2-(thiophen-3-yl)penta-3,4-dienoate (18)

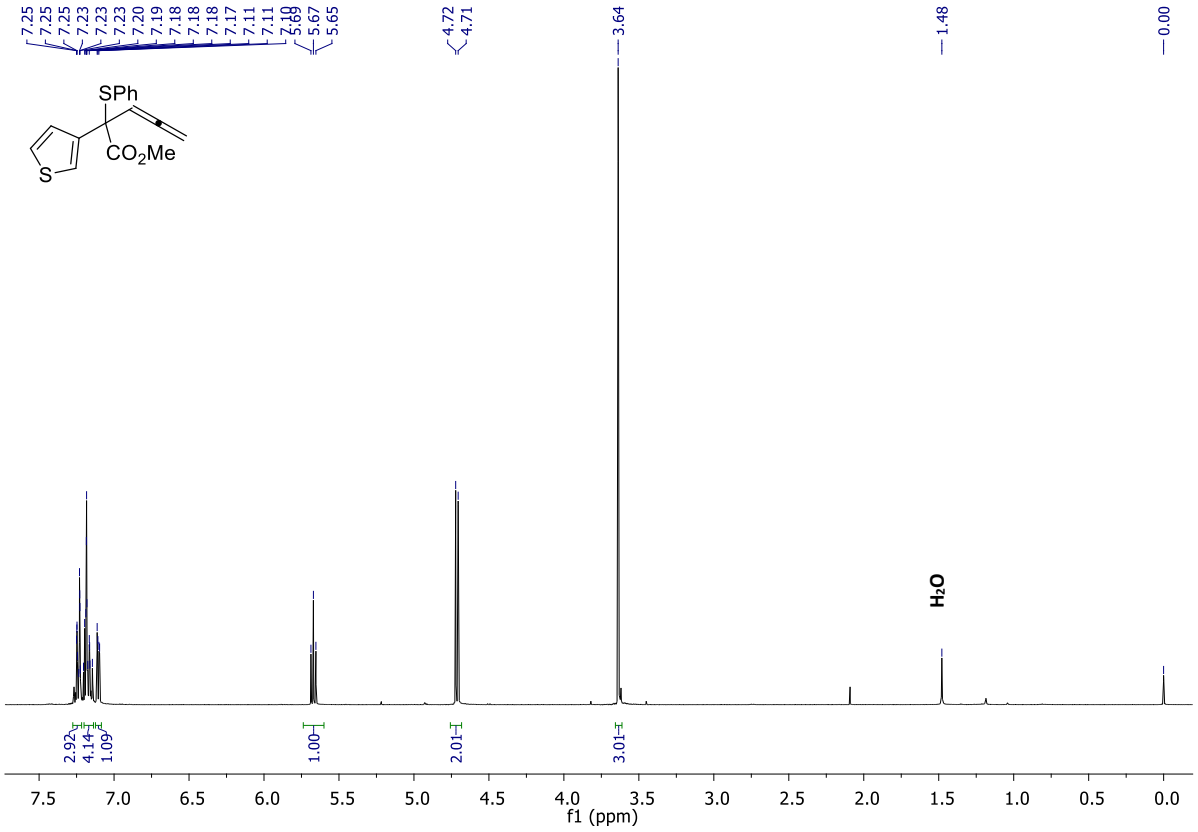

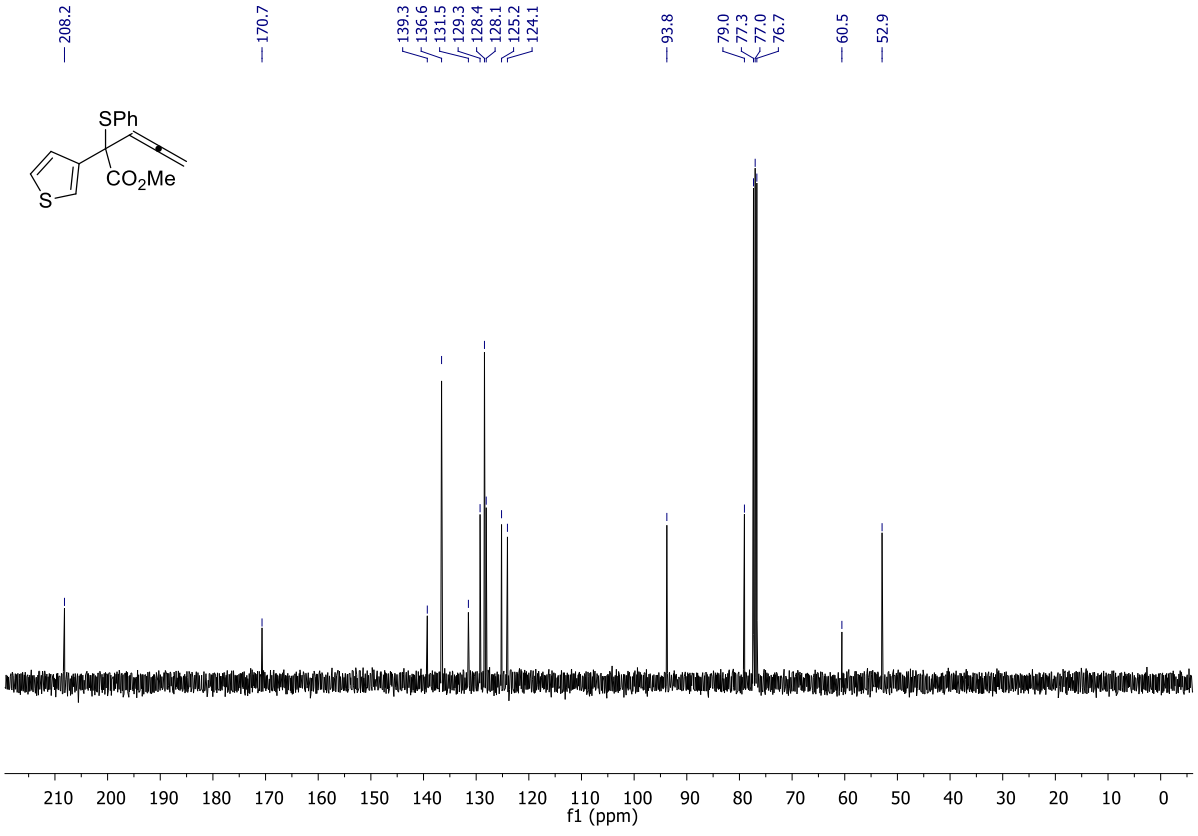

Allyl 2-phenyl-2-(phenylthio)penta-3,4-dienoate (19)

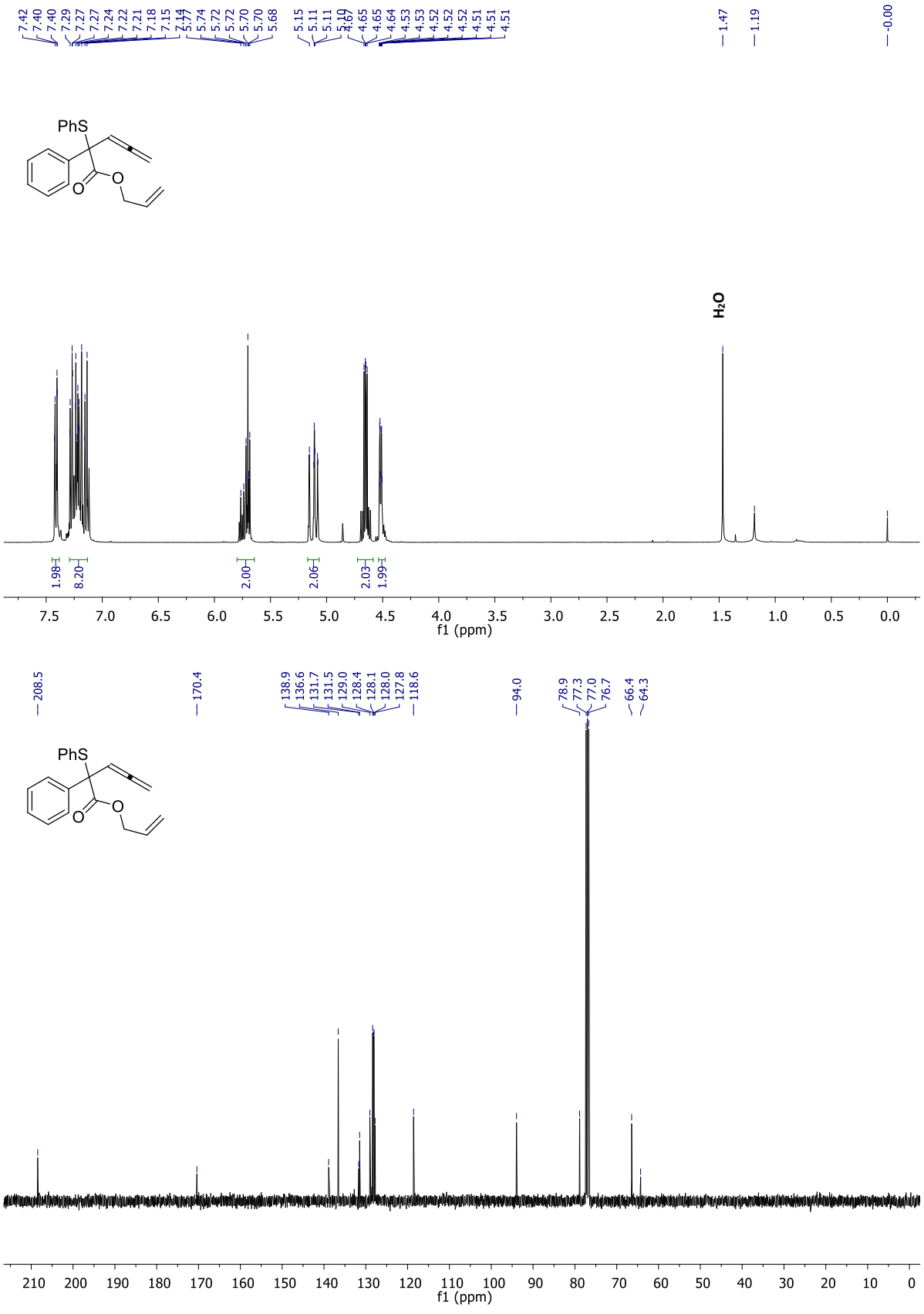

Benzyl 2-phenyl-2-(phenylthio)penta-3,4-dienoate (20)

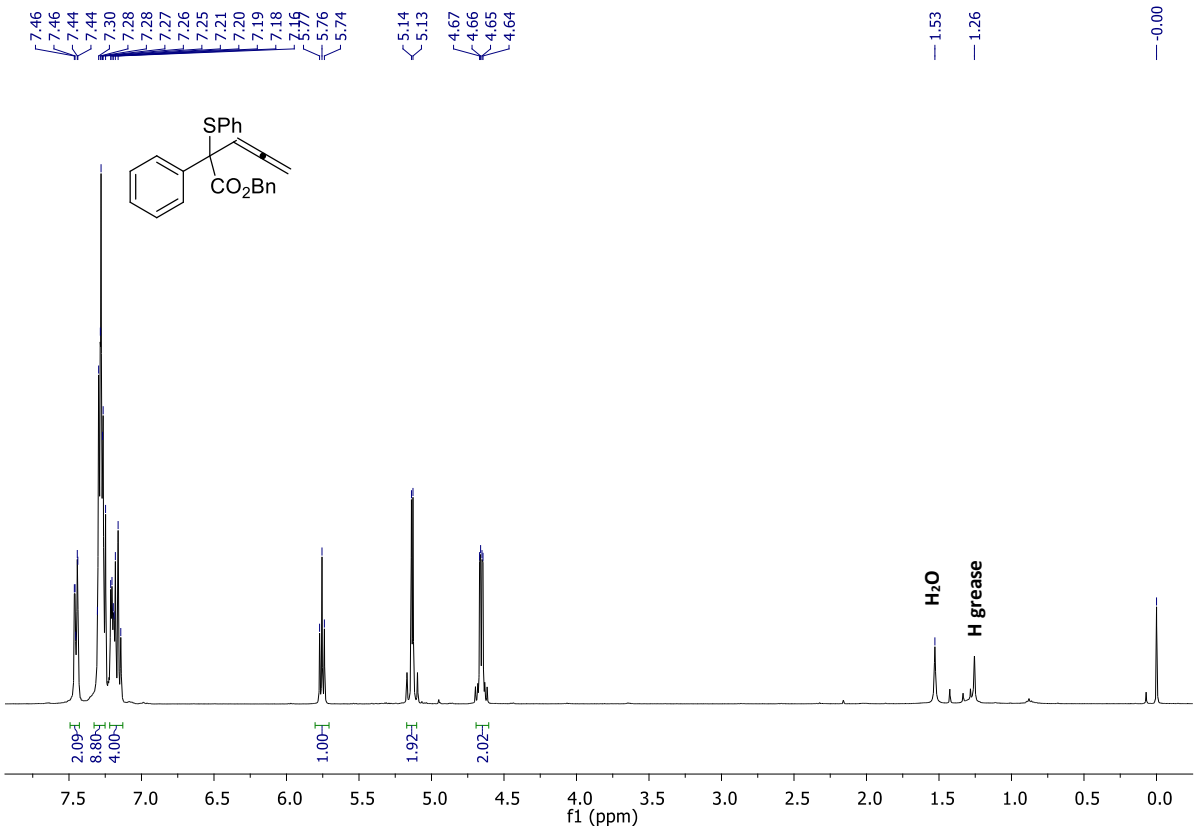

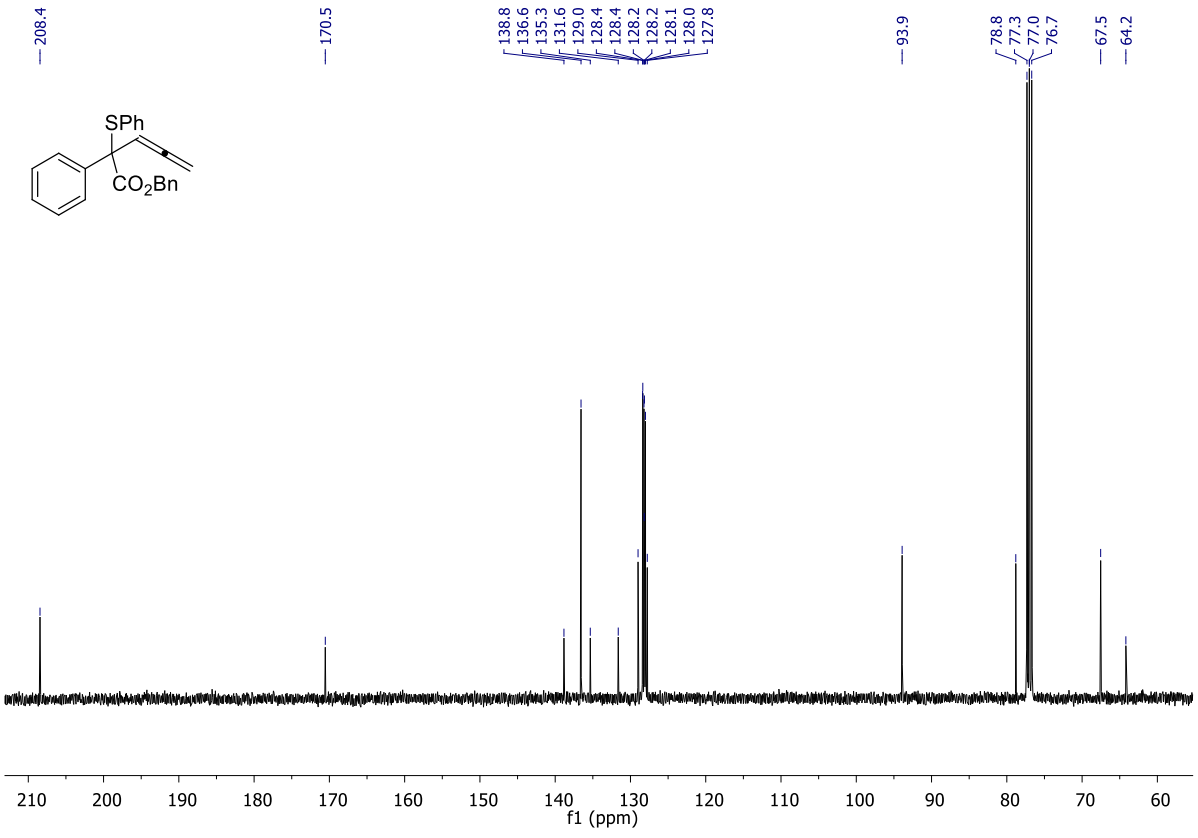

(1S,2S,5S)-2-Isopropyl-5-methylcyclohexyl 2-(4-fluorophenyl)-2-(phenylthio)penta-3,4-dienoate (21)

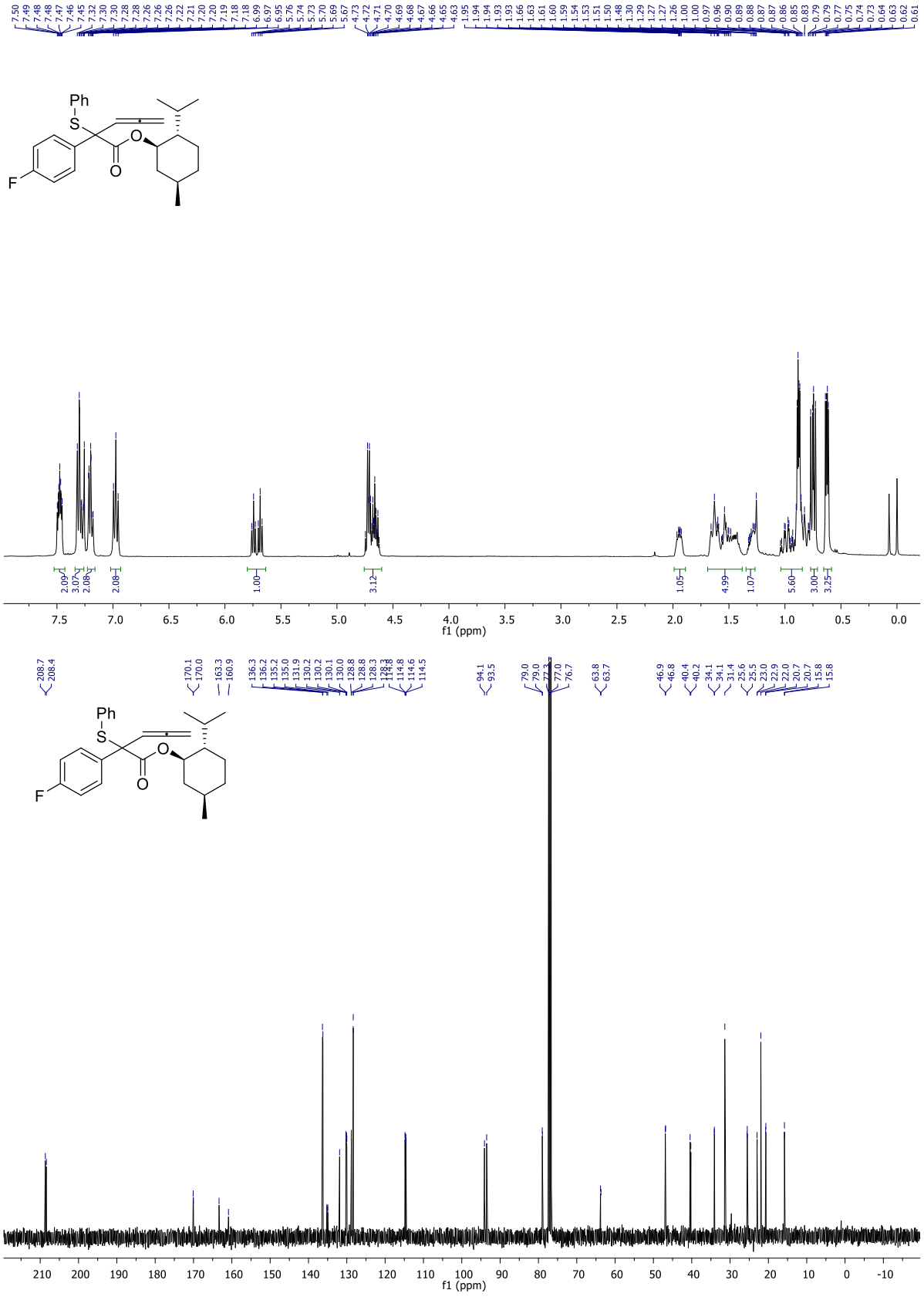

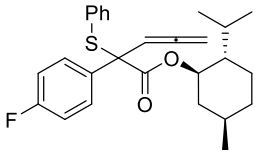

3-Phenyl-3-(phenylthio)hexa-4,5-dien-2-one (22)

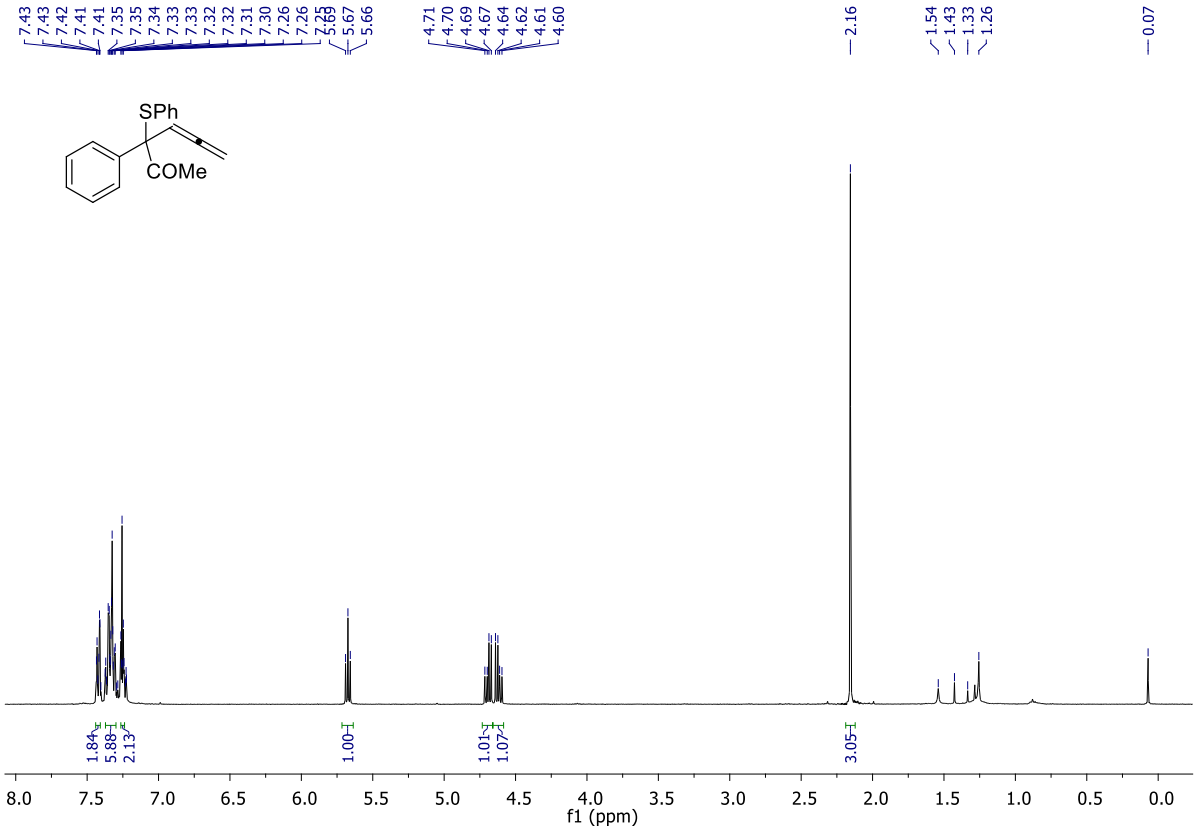

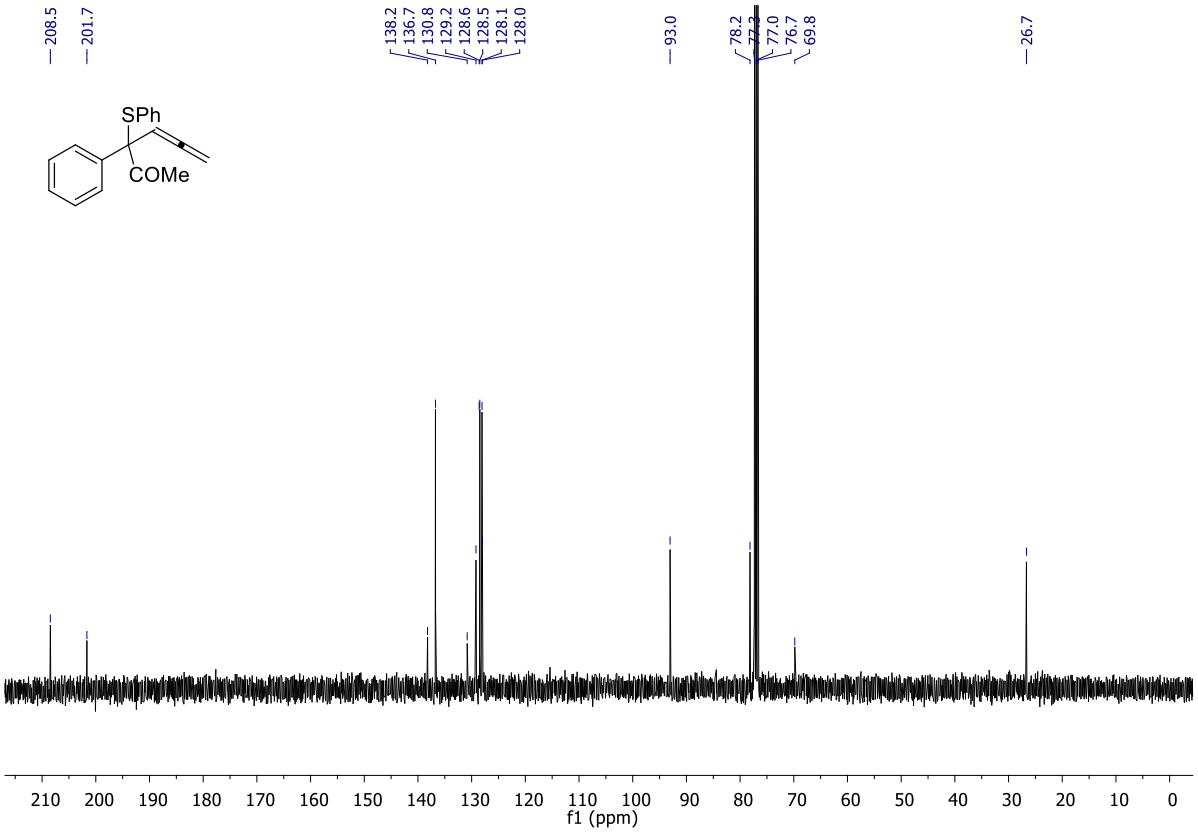

Methyl 2-(4-cyanophenyl)-2-((4-methoxyphenyl)thio)penta-3,4-dienoate (23)

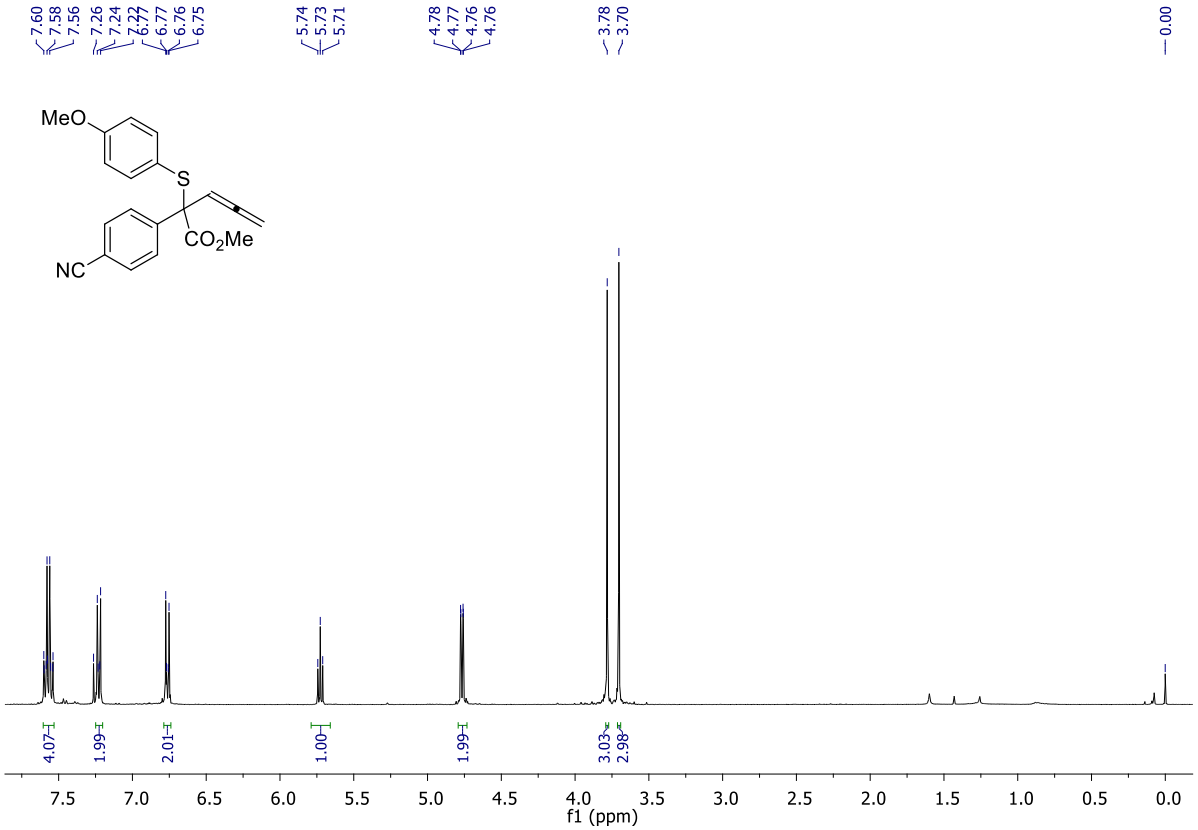

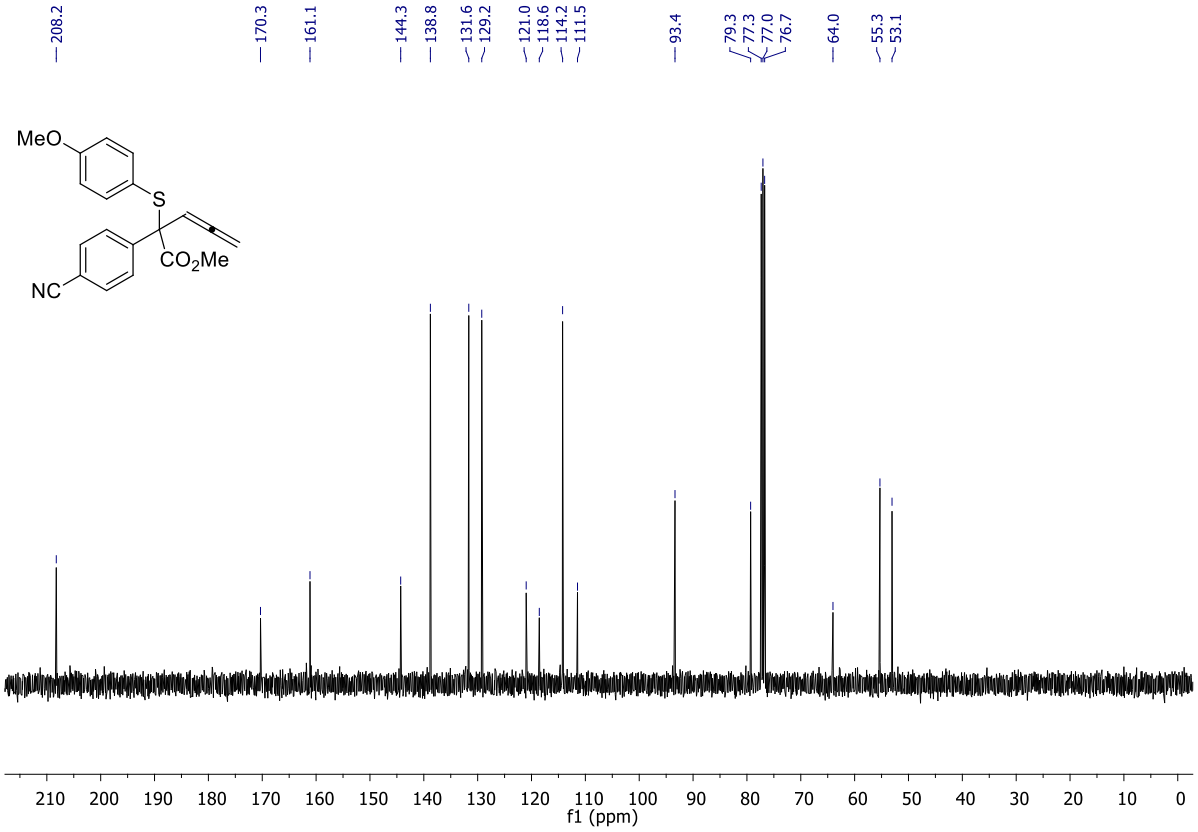

Methyl 2-((4-bromophenyl)thio)-2-(4-cyanophenyl)penta-3,4-dienoate (24)

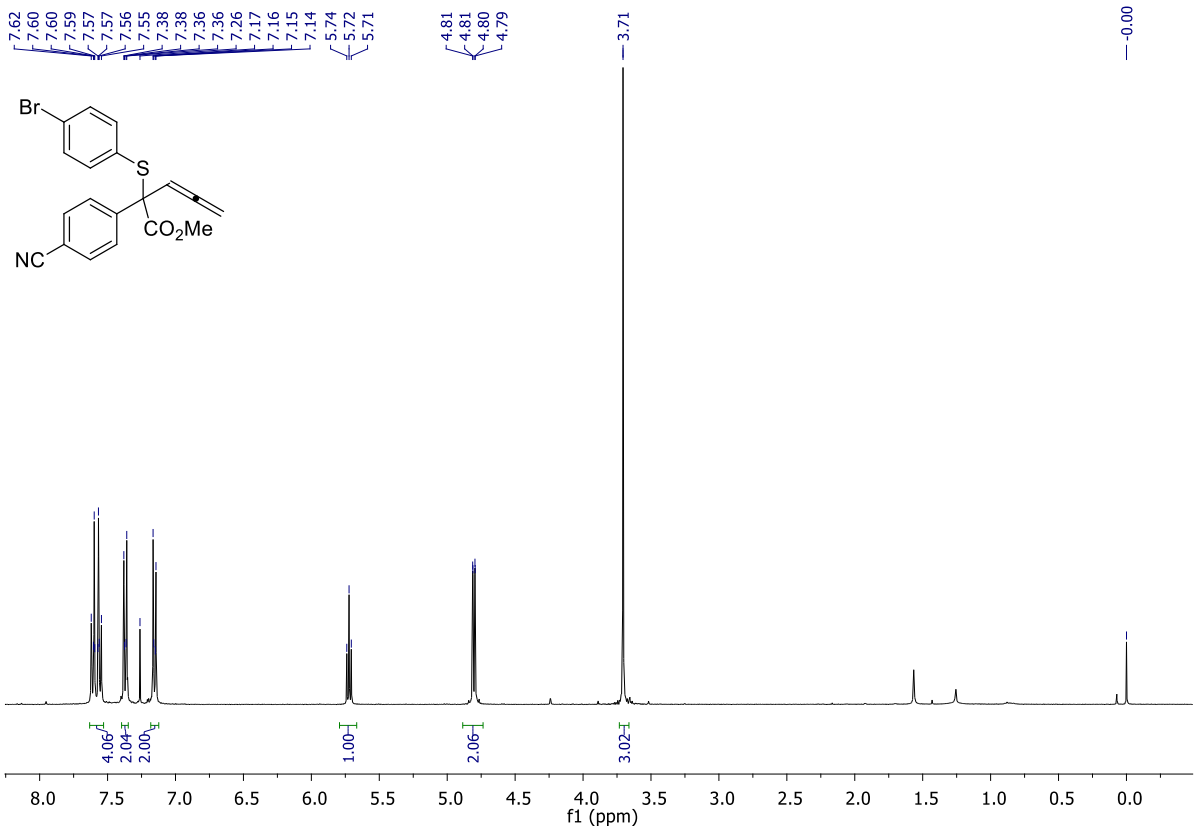

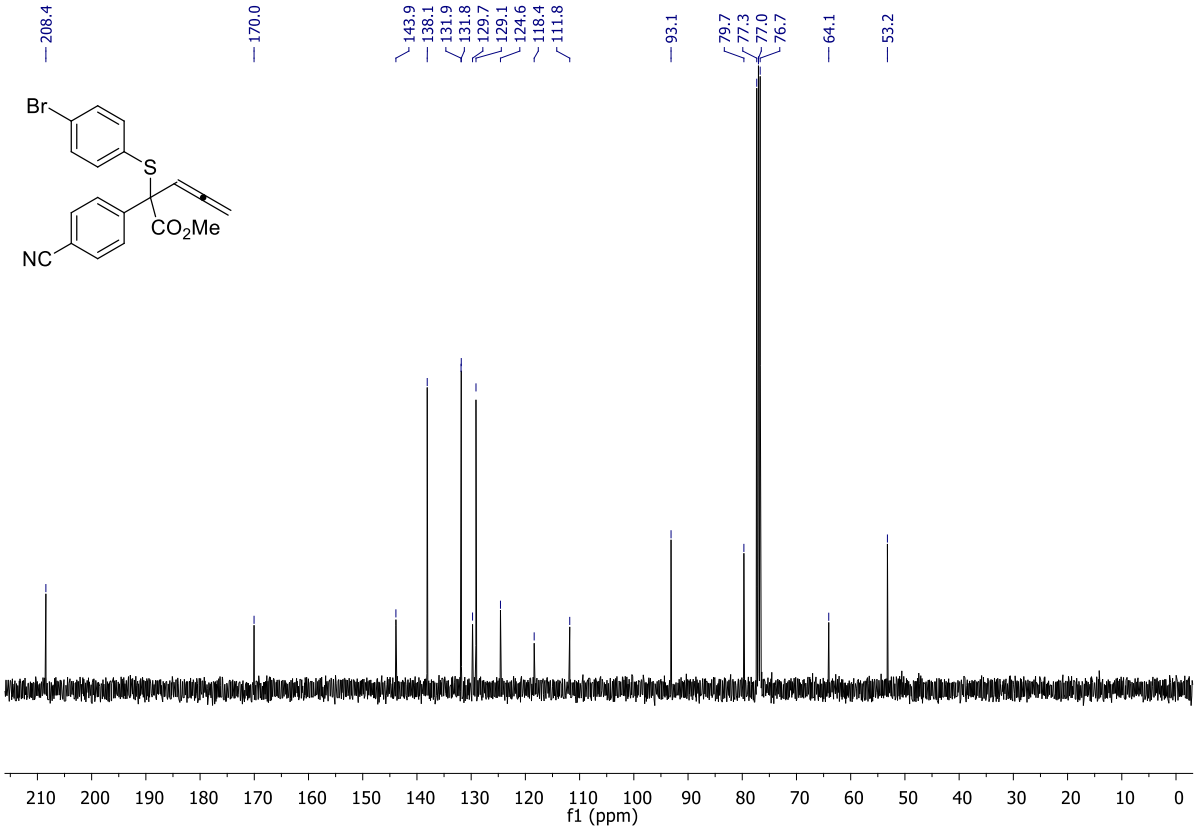

Methyl 2-((4-chlorophenyl)thio)-2-(4-cyanophenyl)penta-3,4-dienoate (25)

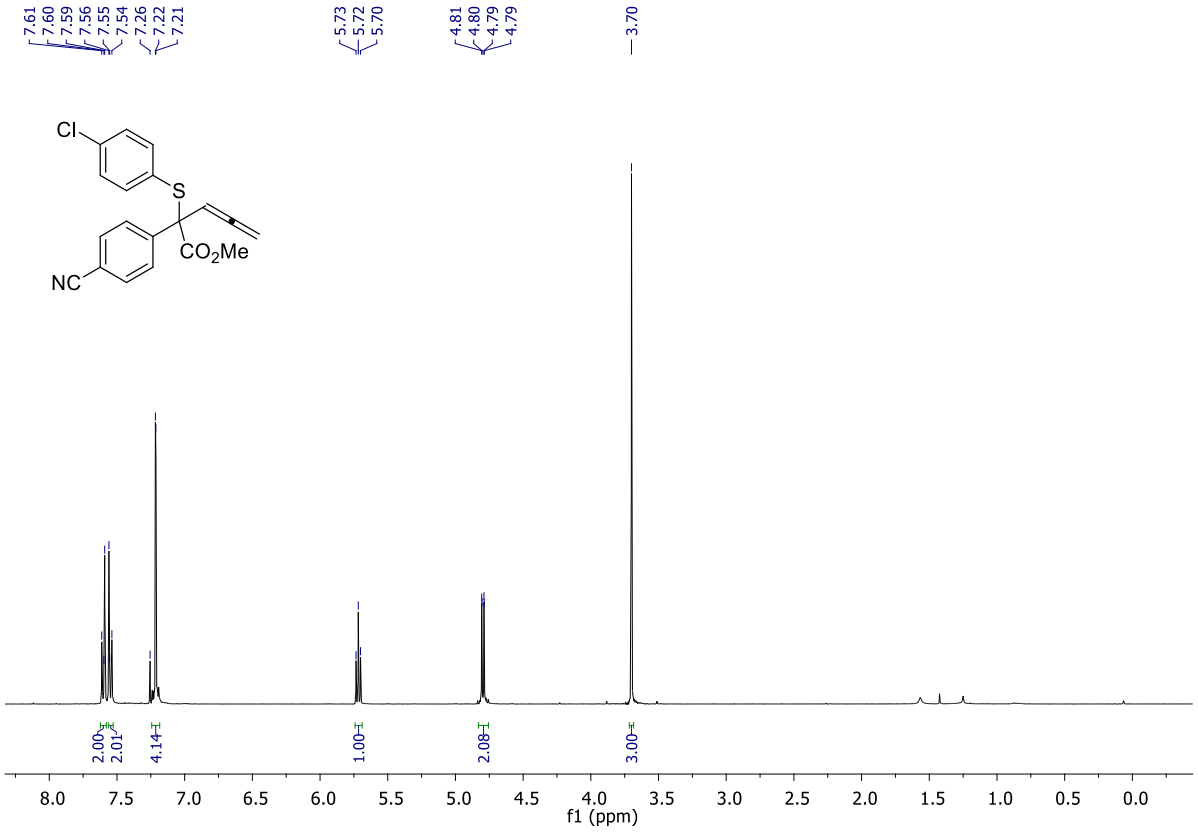

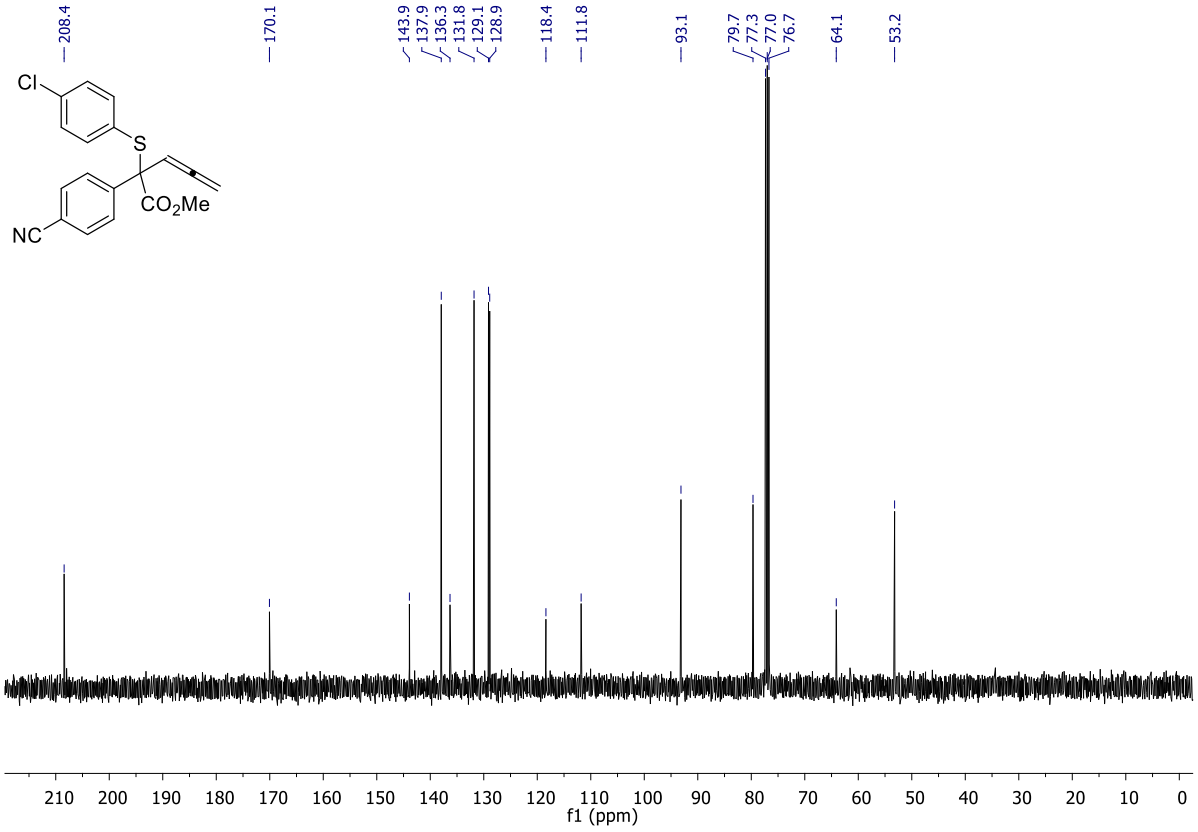

Methyl 2-(4-cyanophenyl)-2-(quinolin-2-ylthio)penta-3,4-dienoate (26)

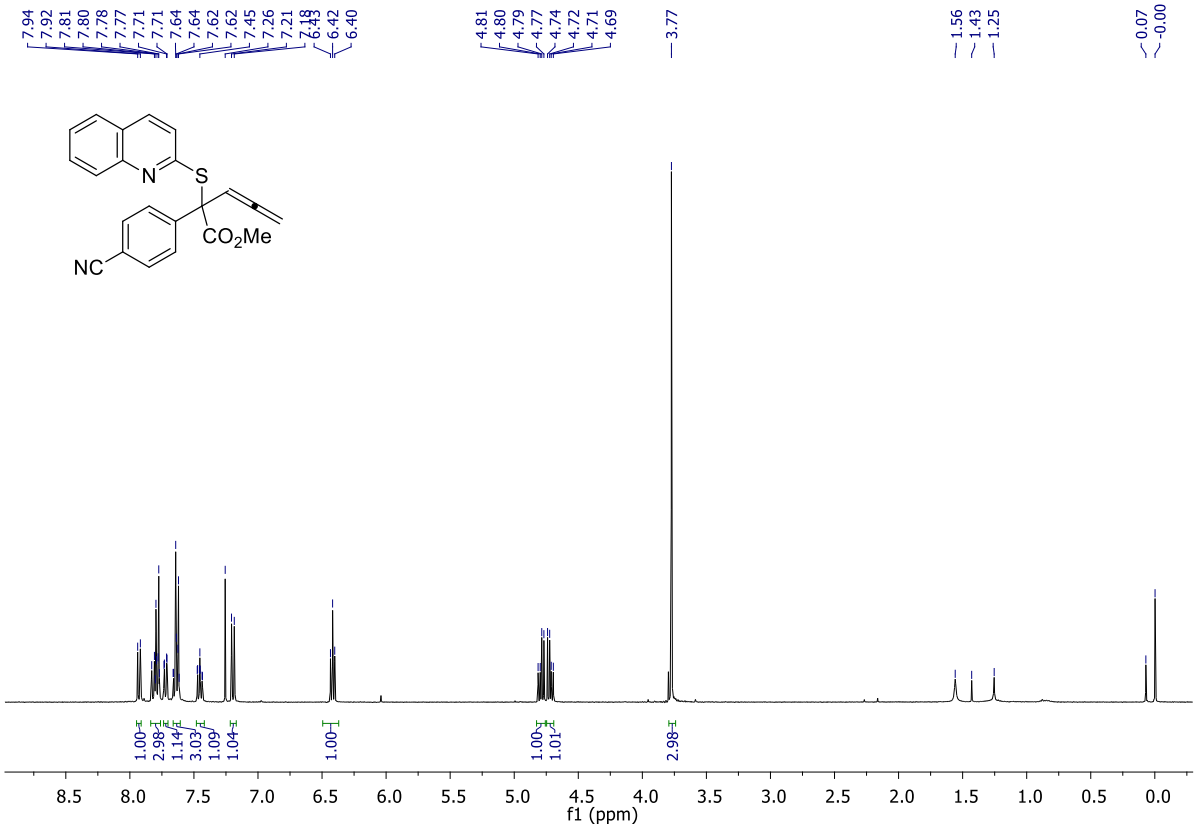

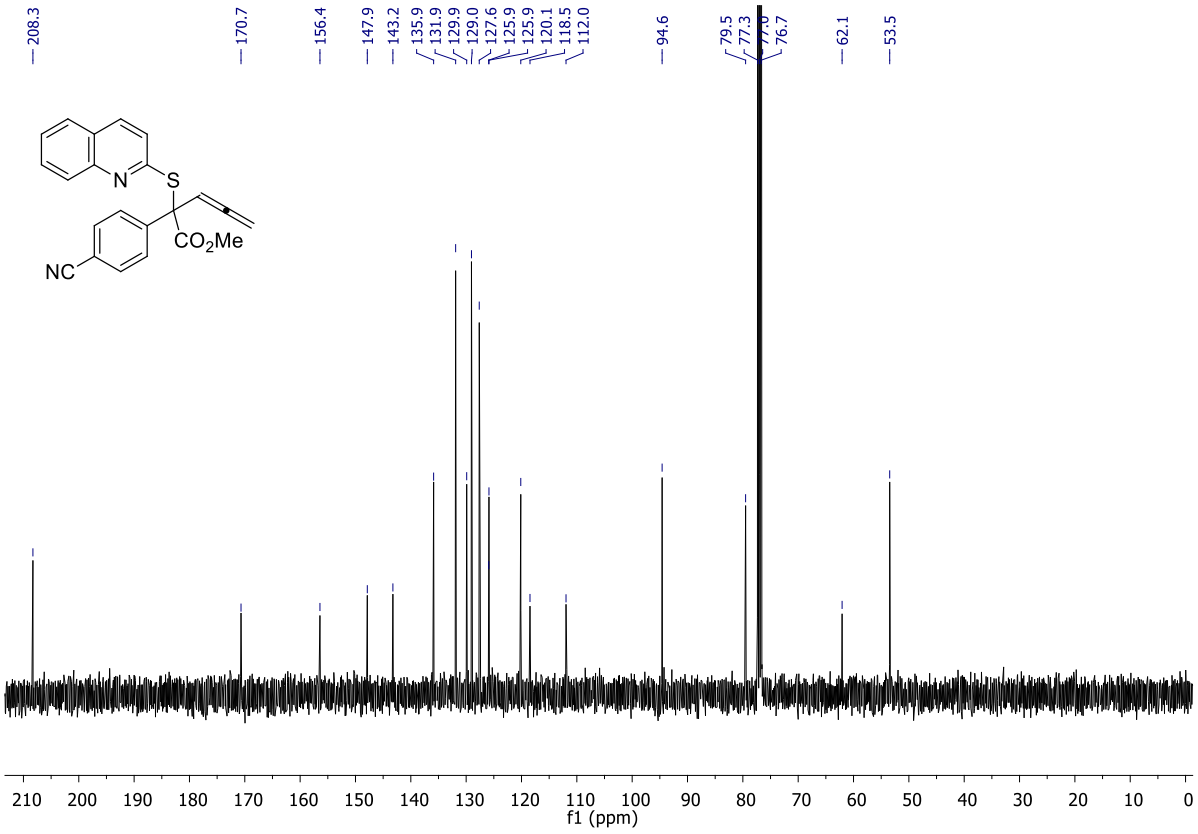

Methyl 2-(4-cyanophenyl)-2-(pyridin-2-ylthio)penta-3,4-dienoate (27) – unstable compound

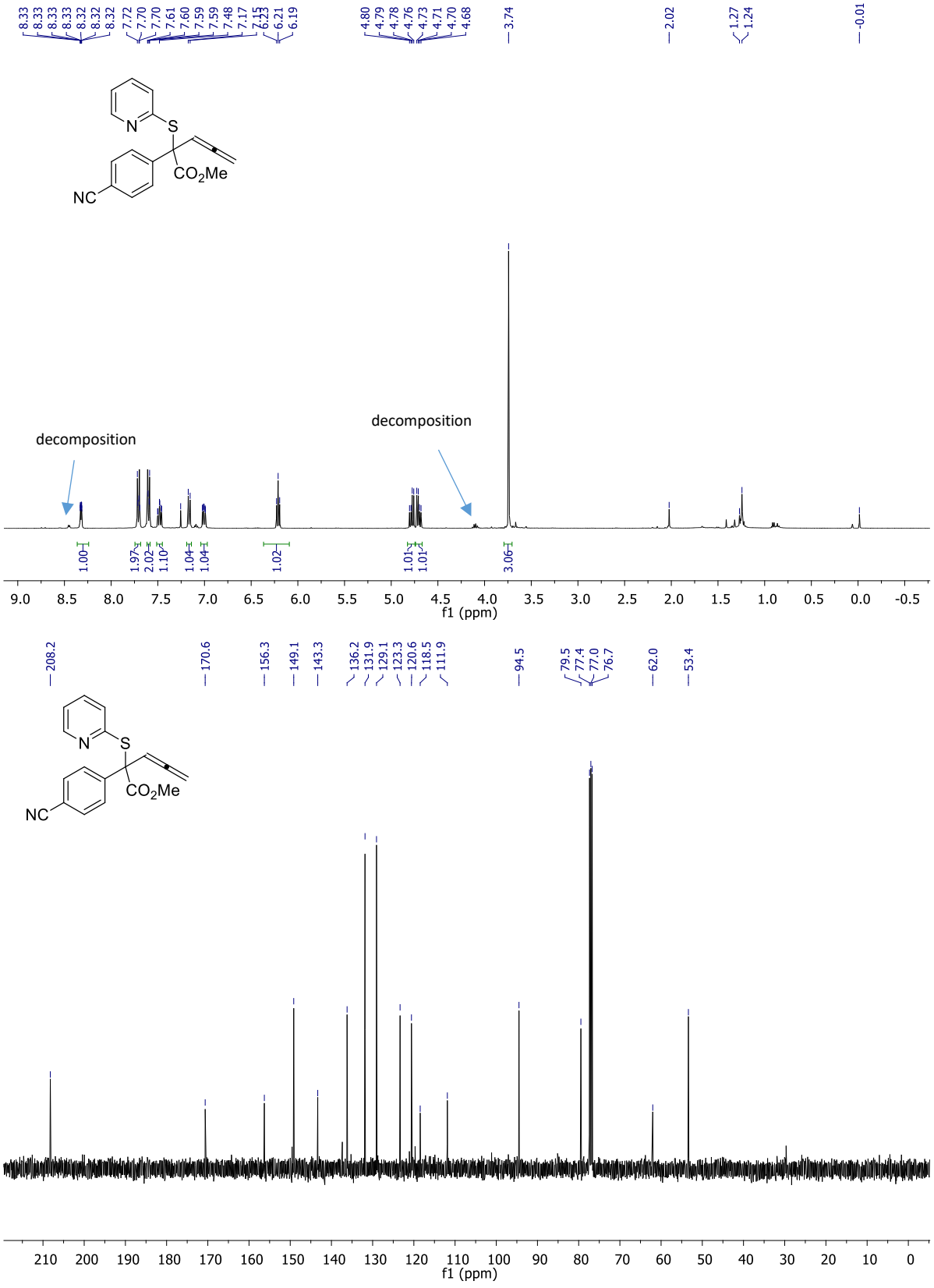

Methyl 2-(4-cyanophenyl)-2-((5-(trifluoromethyl)pyridin-2-yl)thio)penta-3,4-dienoate (28)

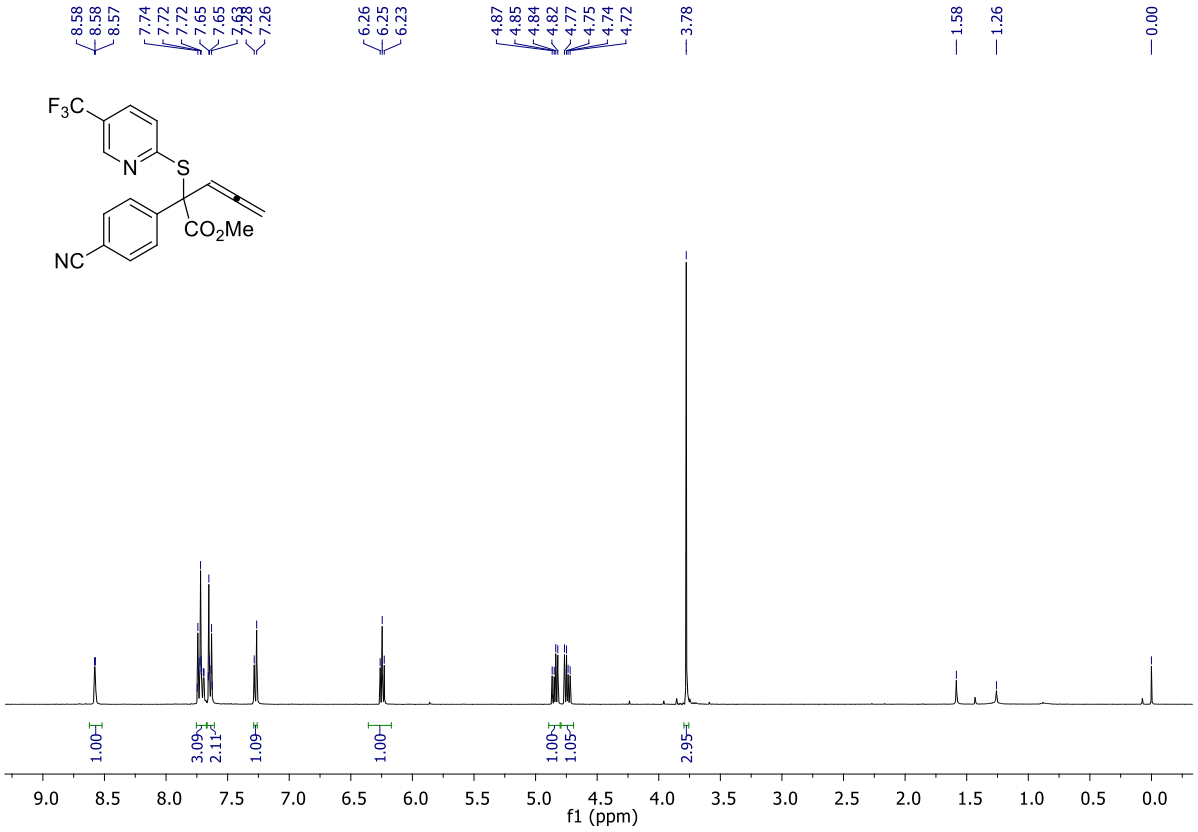

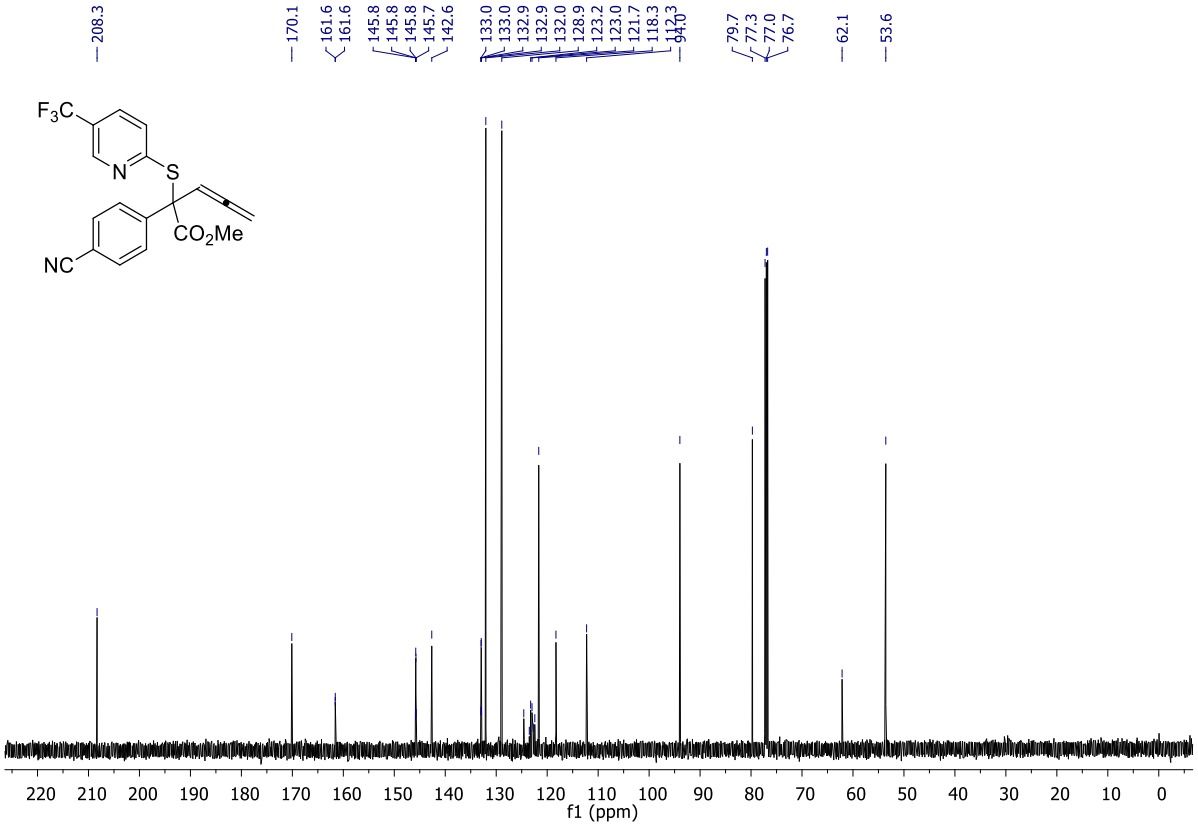

Methyl 2-(4-cyanophenyl)-2-((1-phenyl-1H-tetrazol-5-yl)thio)penta-3,4-dienoate (29) - unstable compound

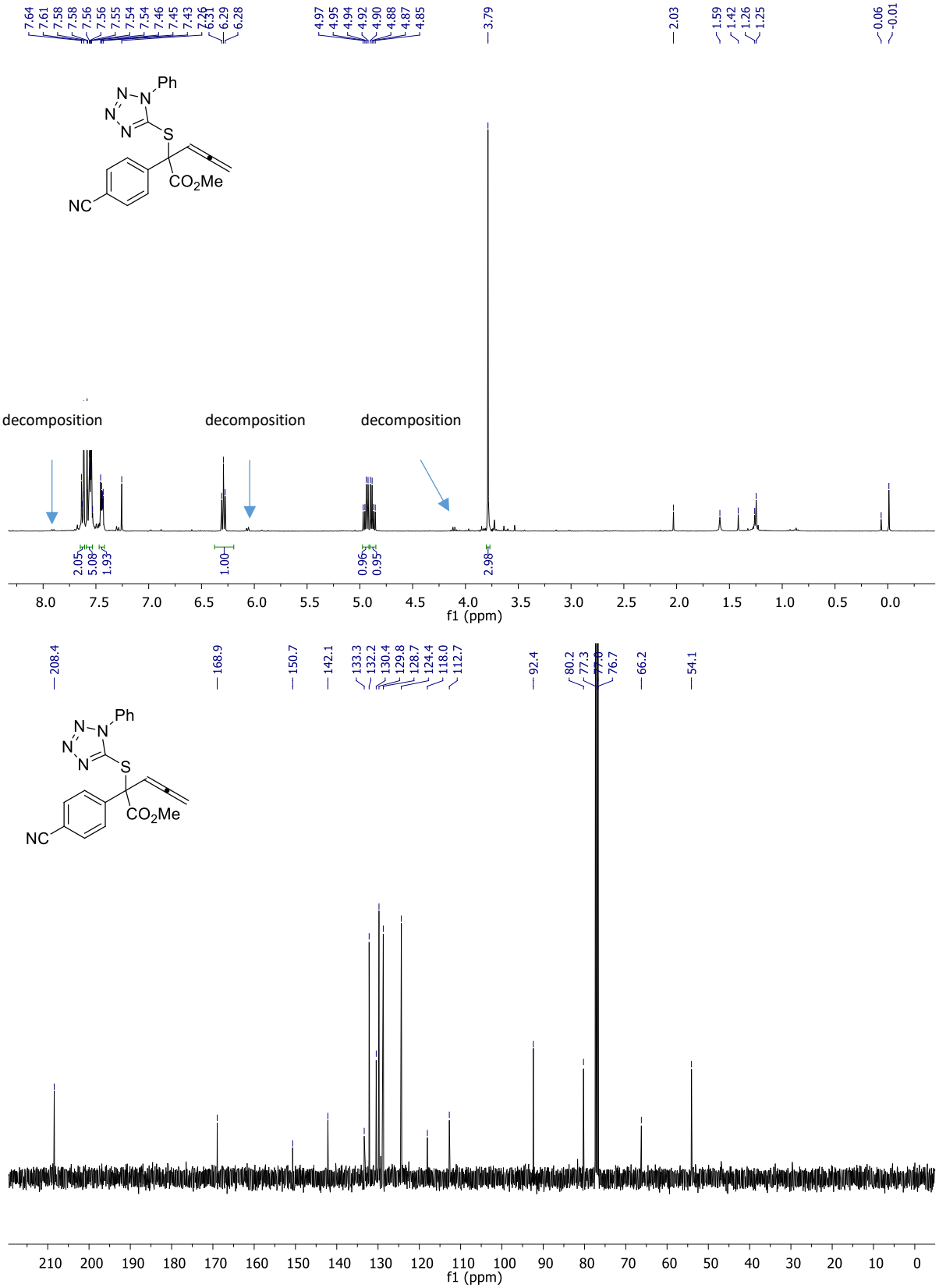

Methyl 2-(benzylthio)-2-(4-cyanophenyl)penta-3,4-dienoate (30)

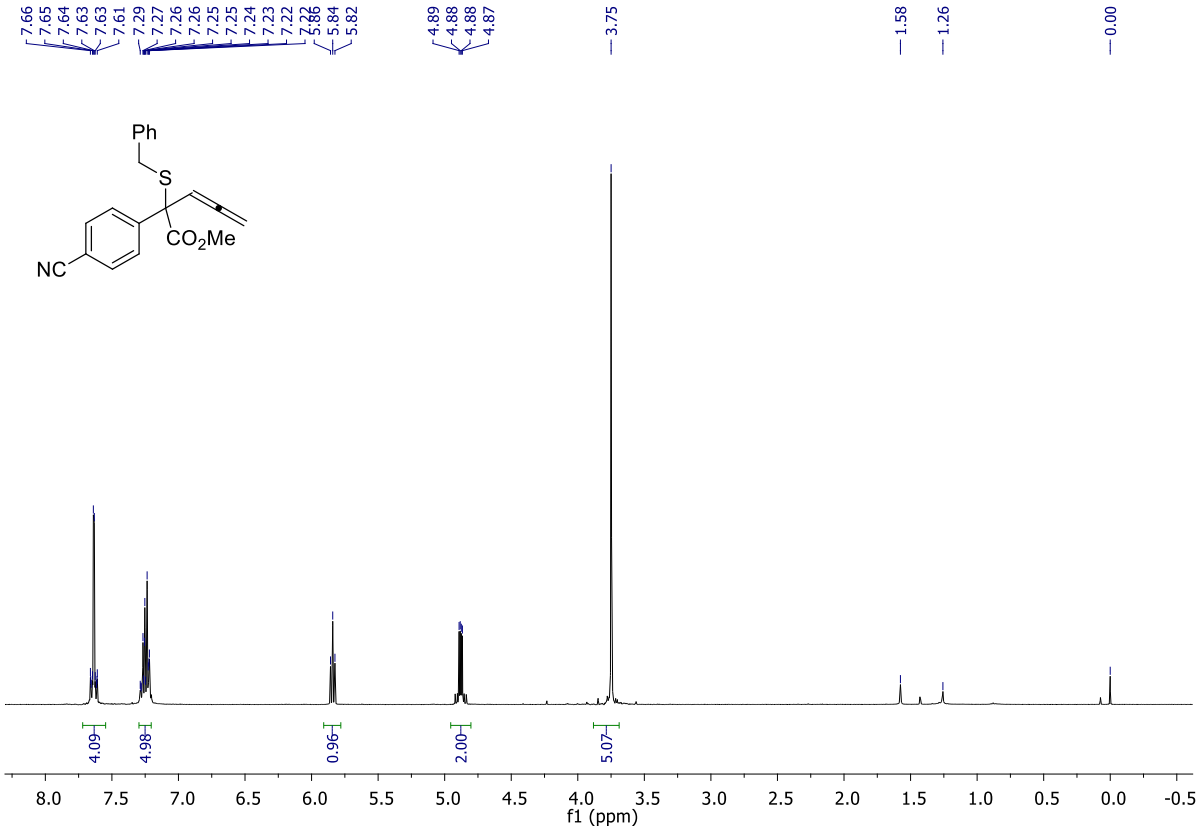

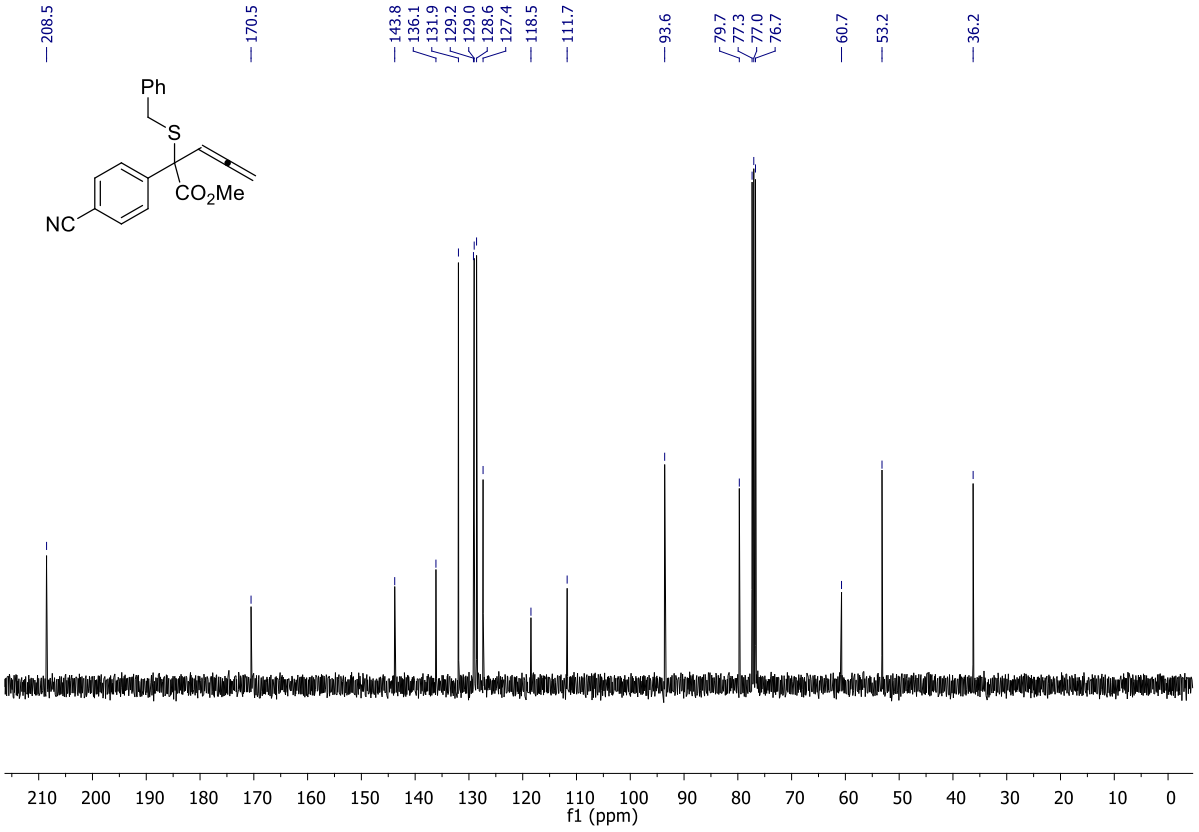

Methyl 2-(4-cyanophenyl)-2-(cyclohexylthio)penta-3,4-dienoate (31)

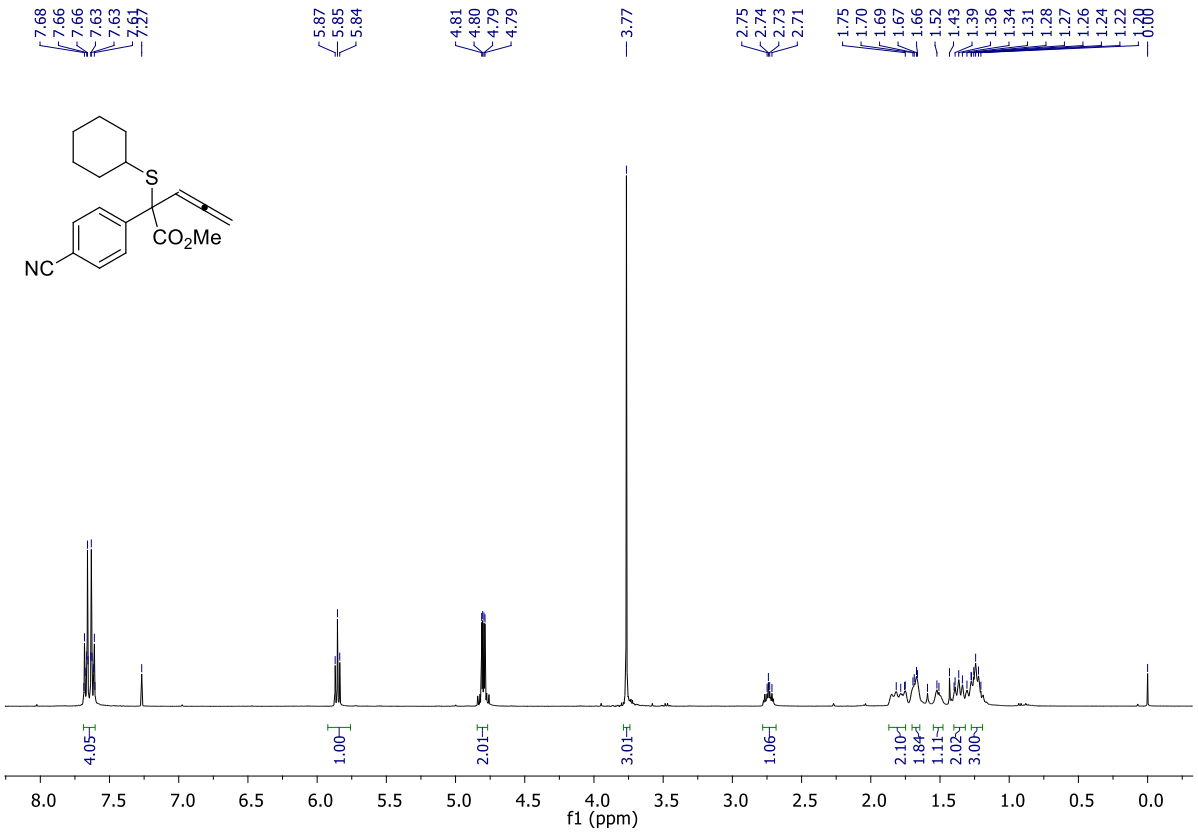

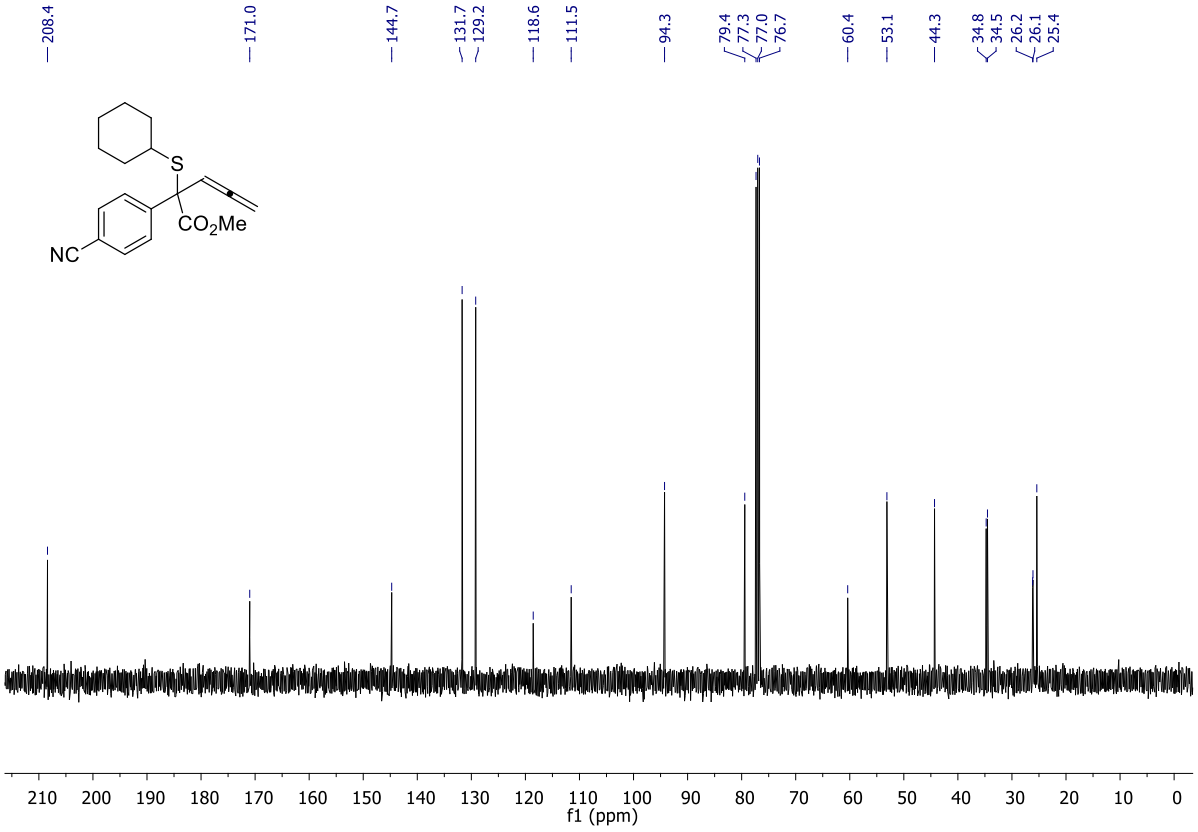

Methyl 2-((3s,5s,7s)-adamantan-1-ylthio)-2-(4-cyanophenyl)penta-3,4-dienoate (32)

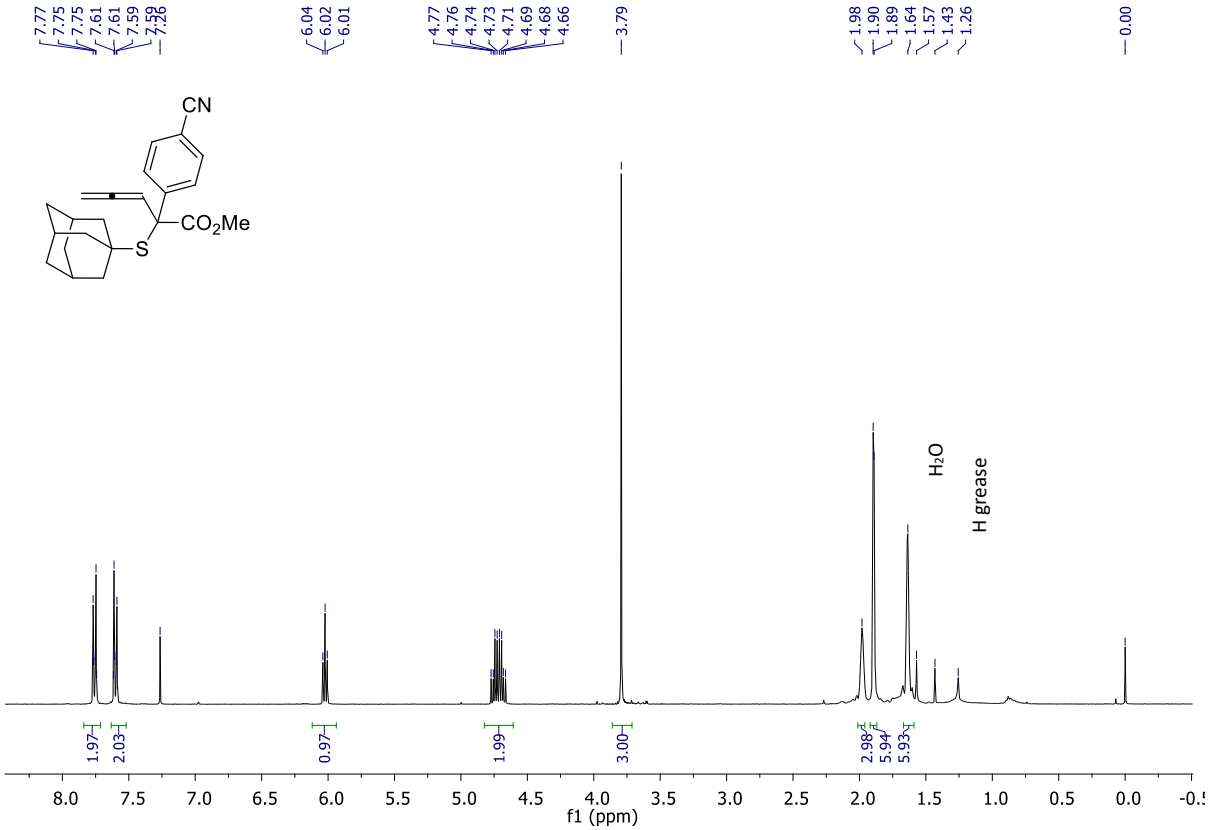

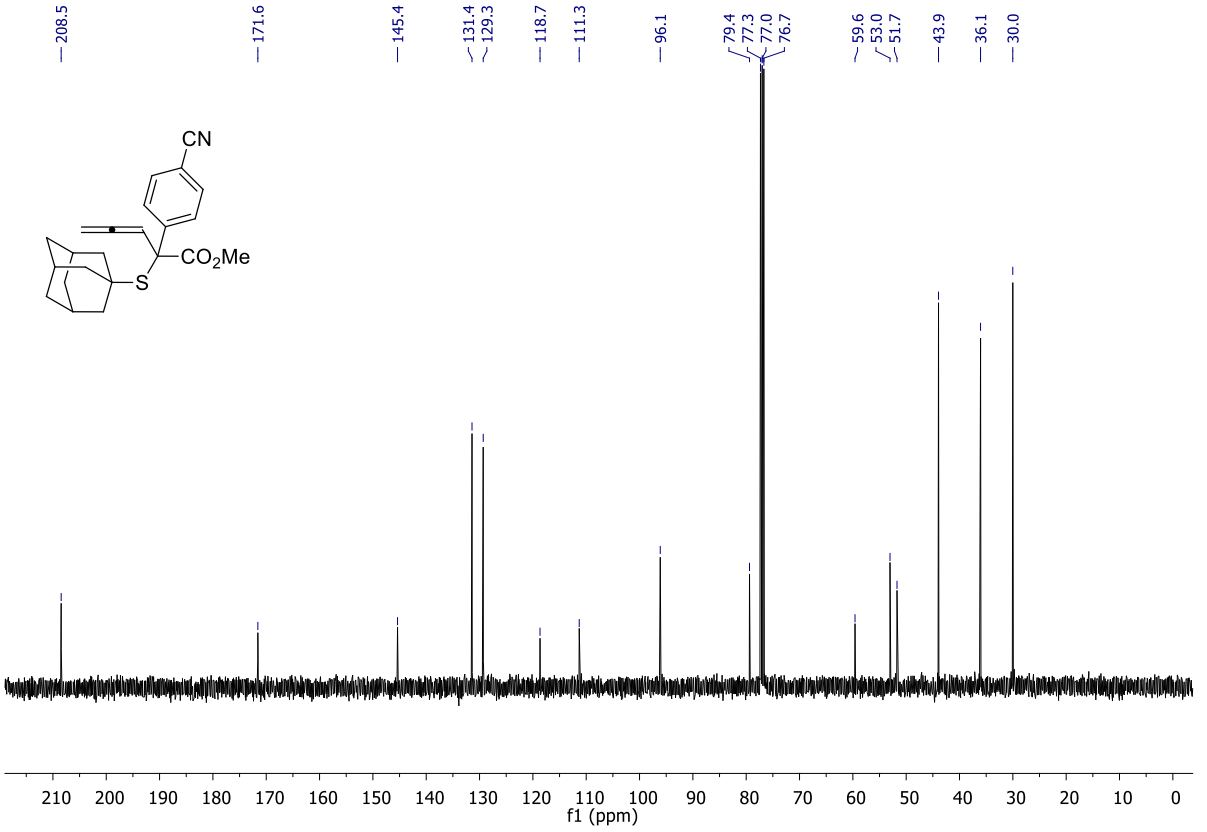

Methyl 2-((2-((tert-butoxycarbonyl)amino)-3-methoxy-3-oxopropyl)thio)-2-(4-cyanophenyl)penta-3,4-dienoate (33) (two diastereoisomers)

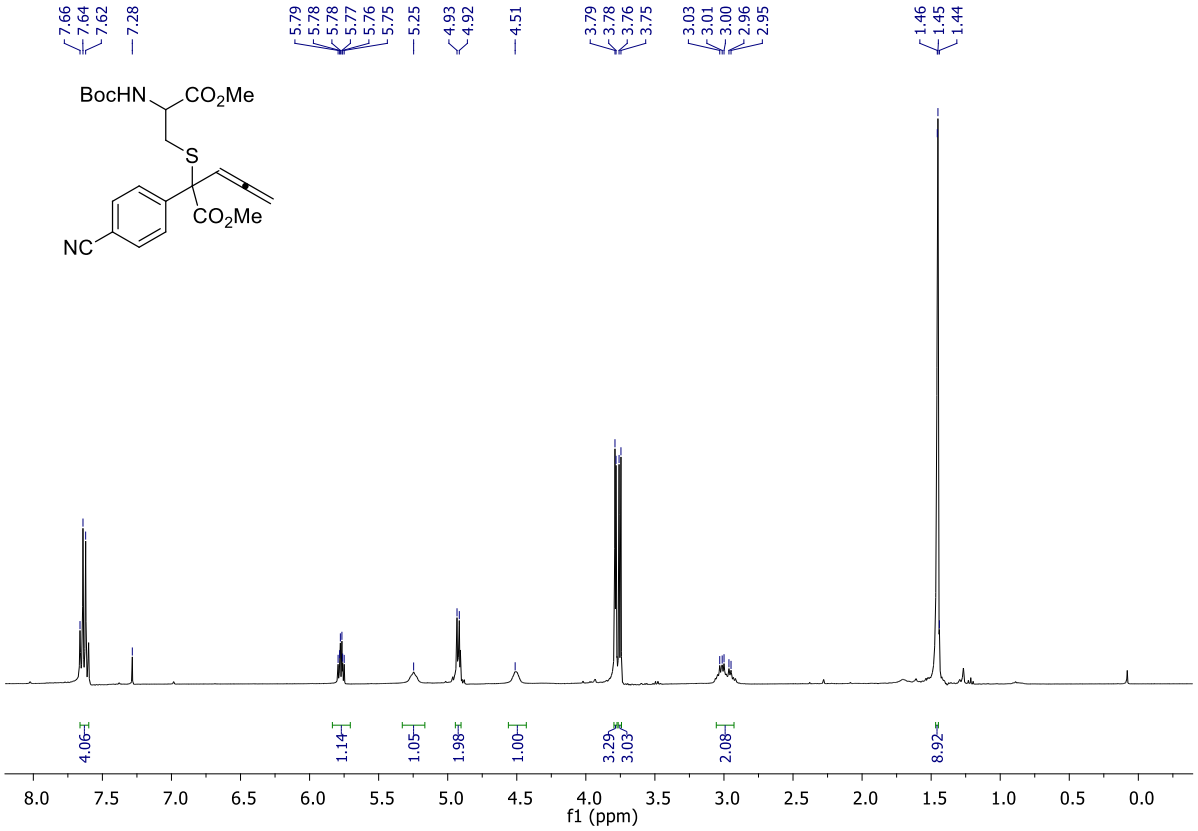

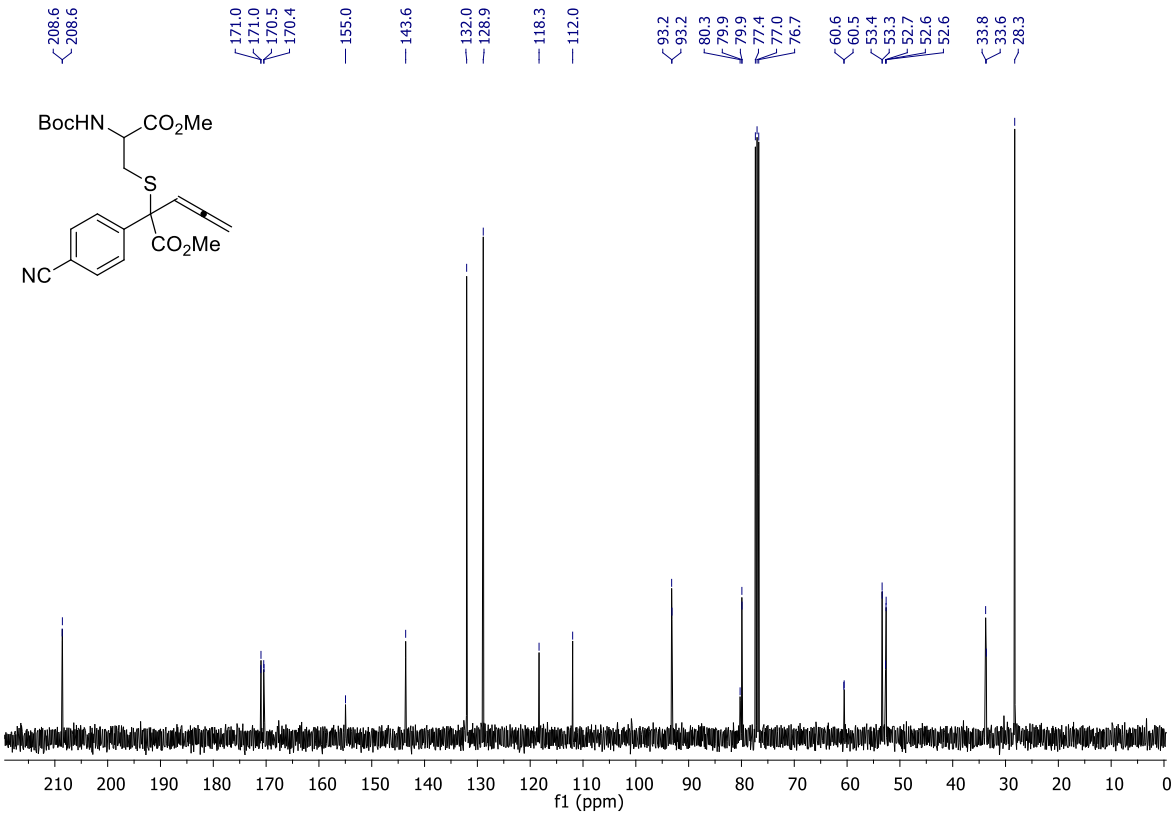

Methyl 2-(4-cyanophenyl)-2-(phenylthio)hexa-3,4-dienoate (34) (two diastereoisomers)

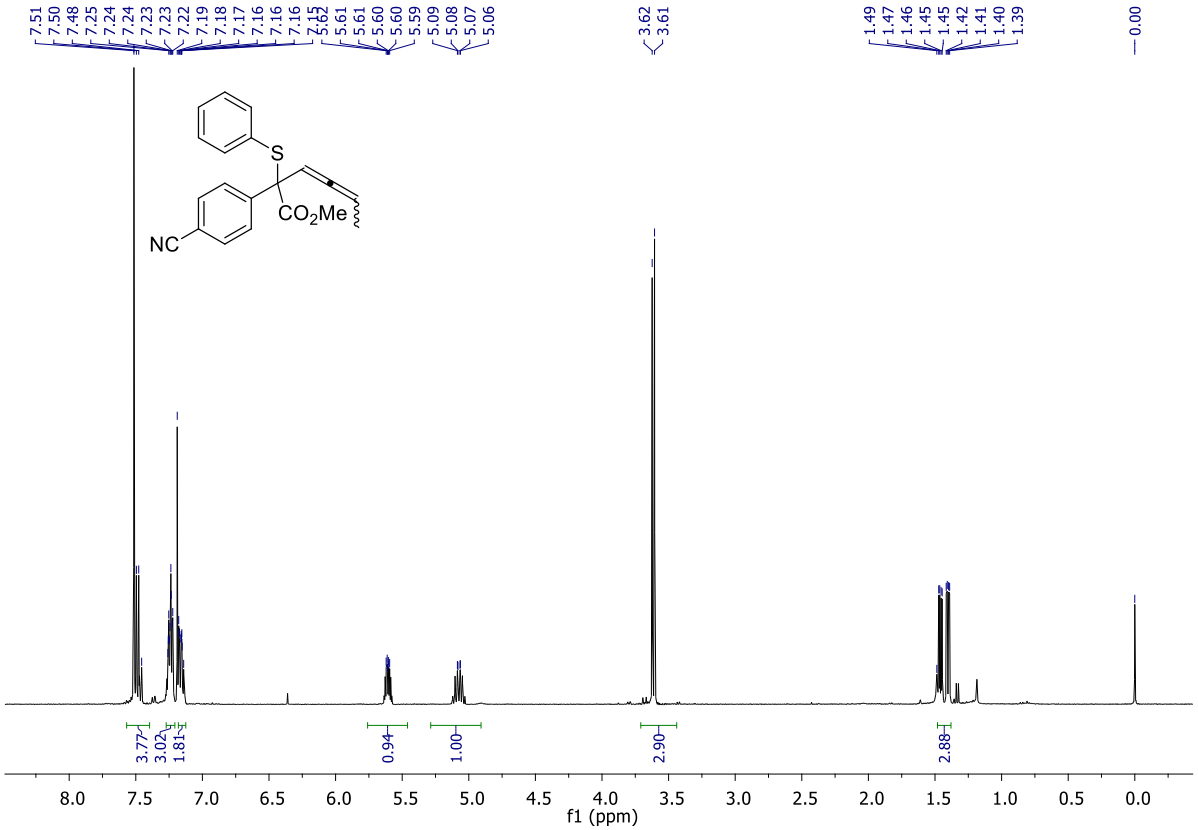

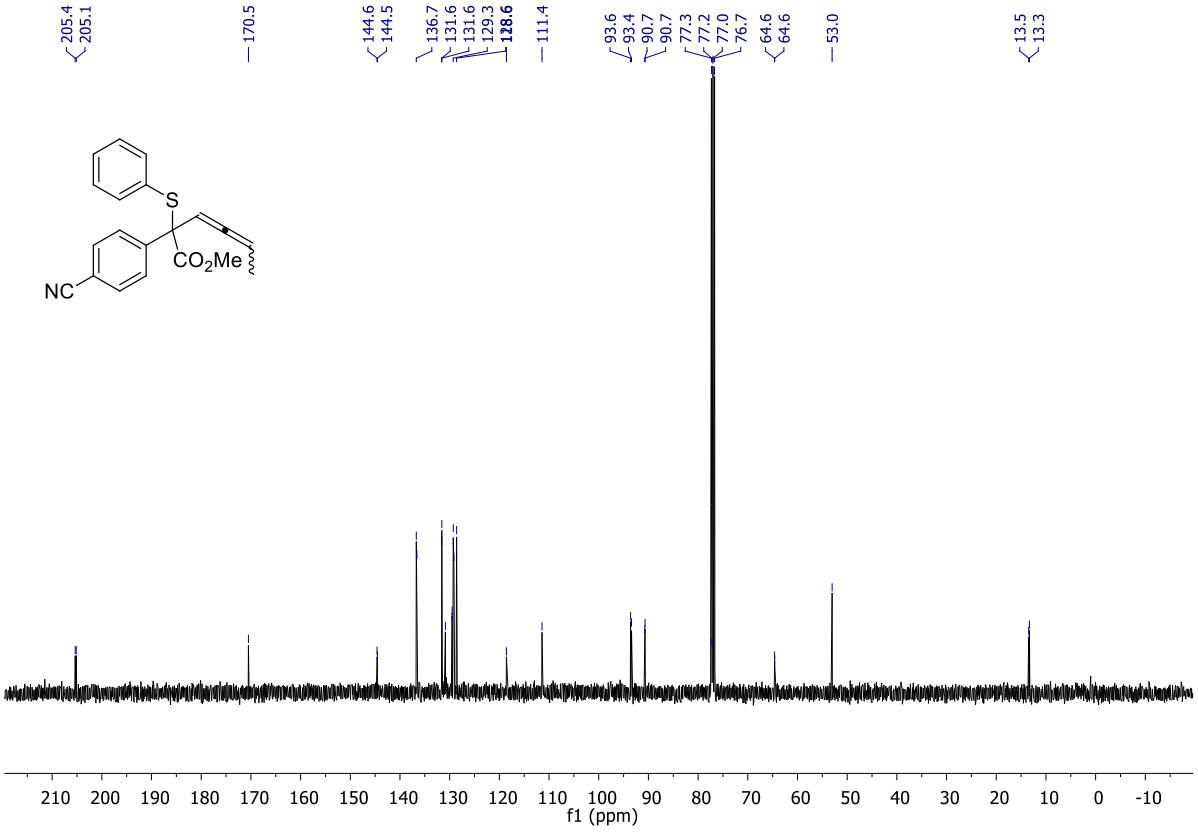

Methyl 2-(4-cyanophenyl)-3-methyl-2-(phenylthio)penta-3,4-dienoate (35)

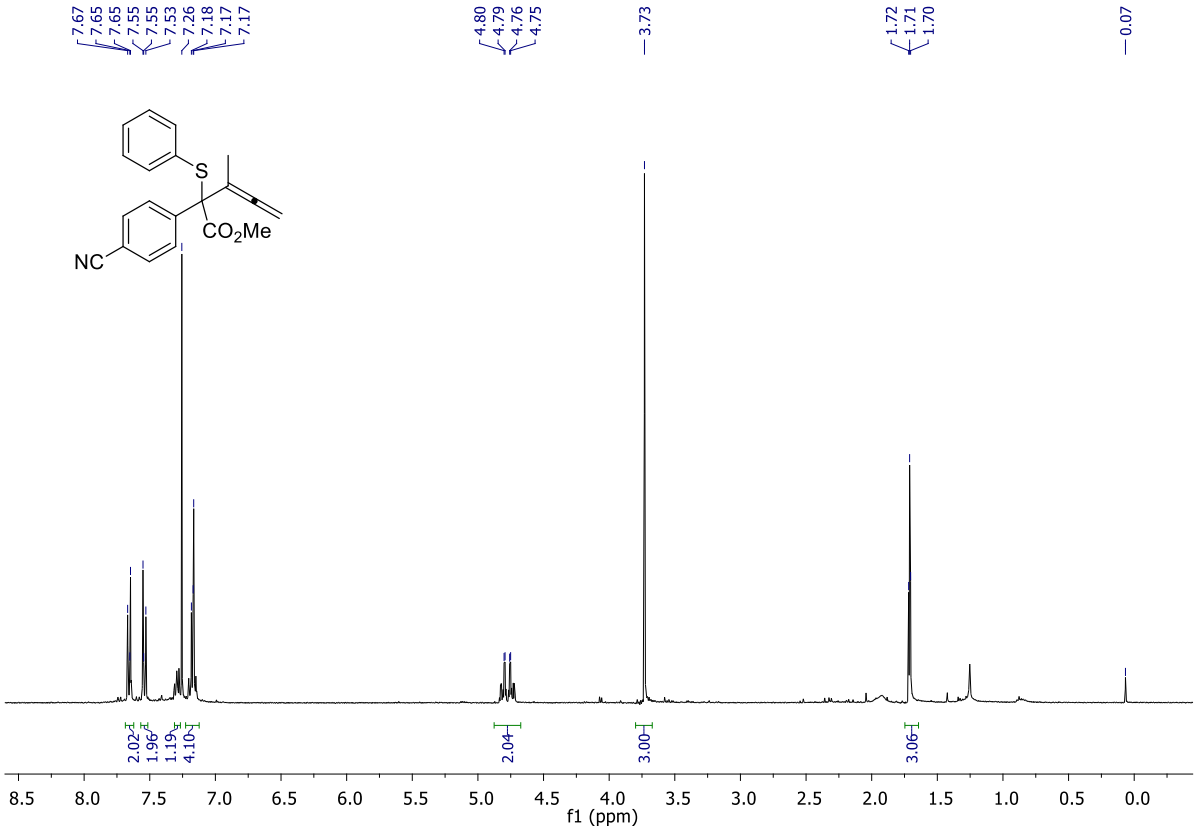

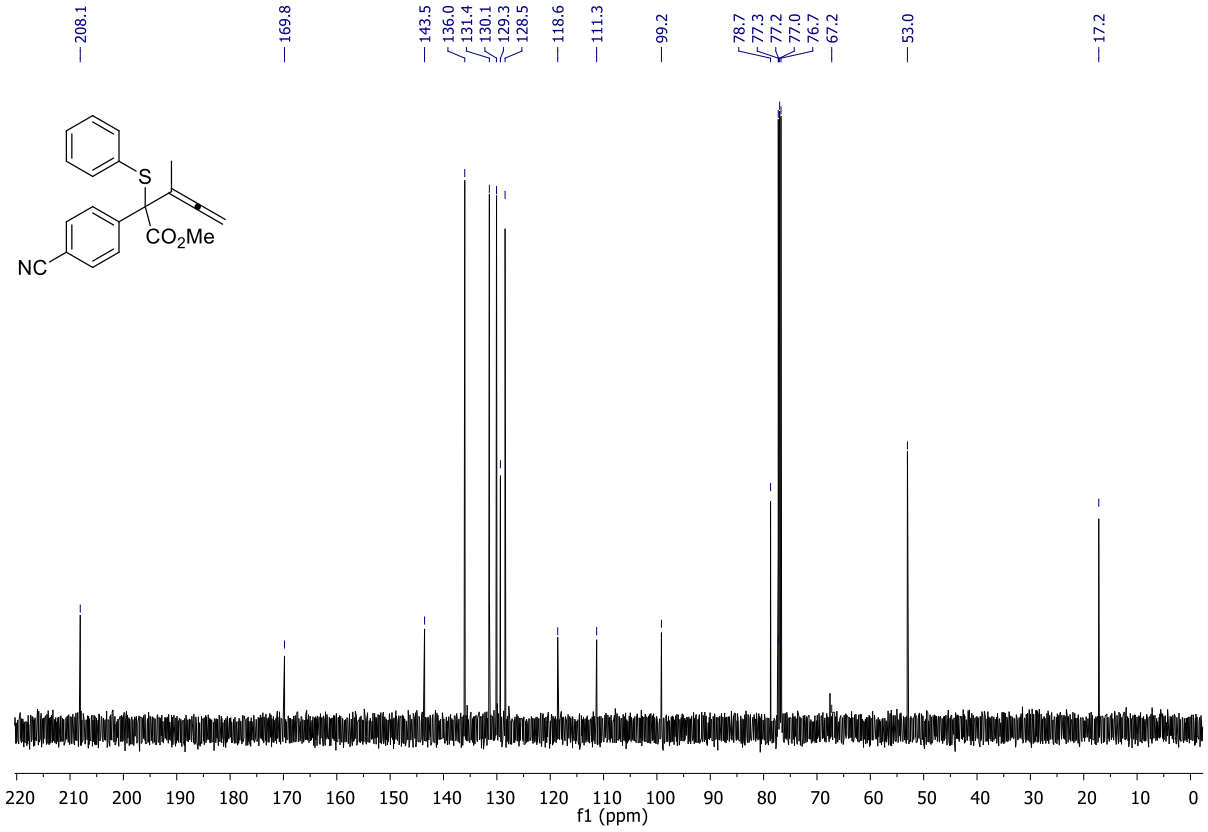

Methyl 4-(1-(methoxycarbonyl)-2,3-diphenylcyclopropyl)benzoate (S3a)

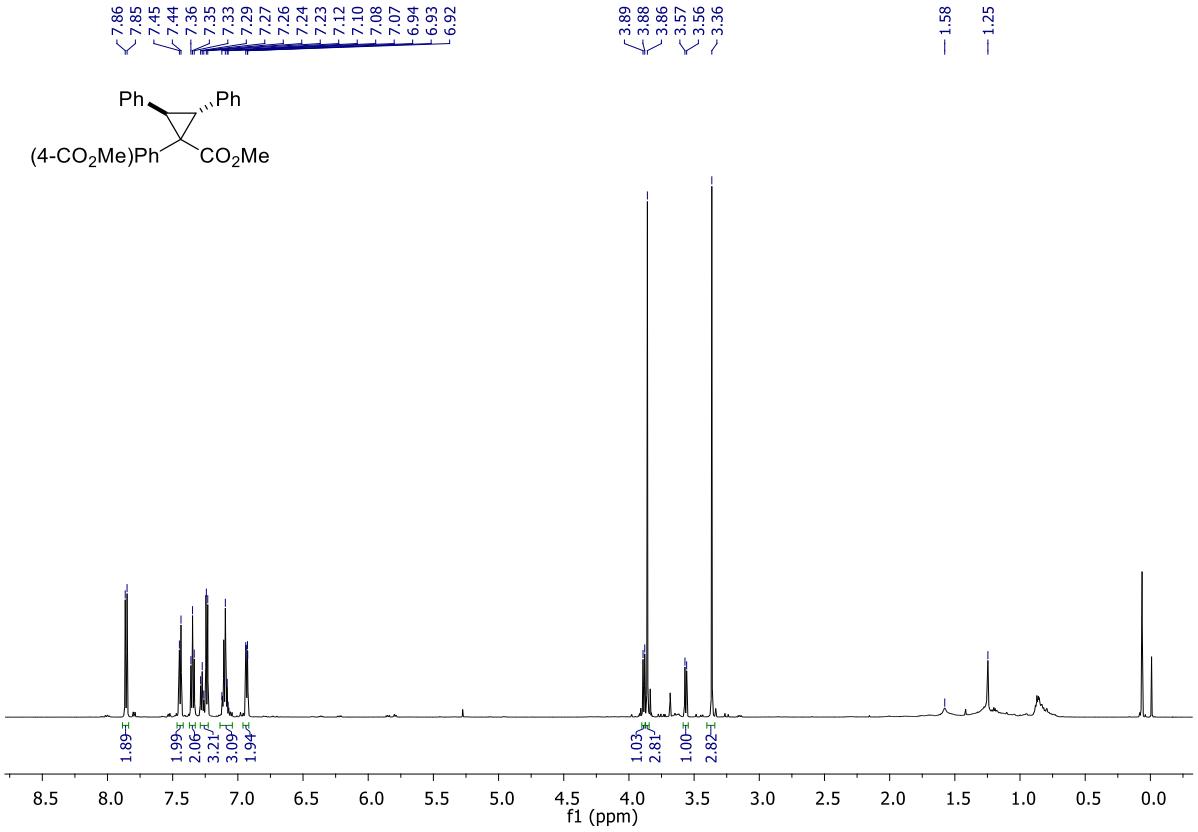

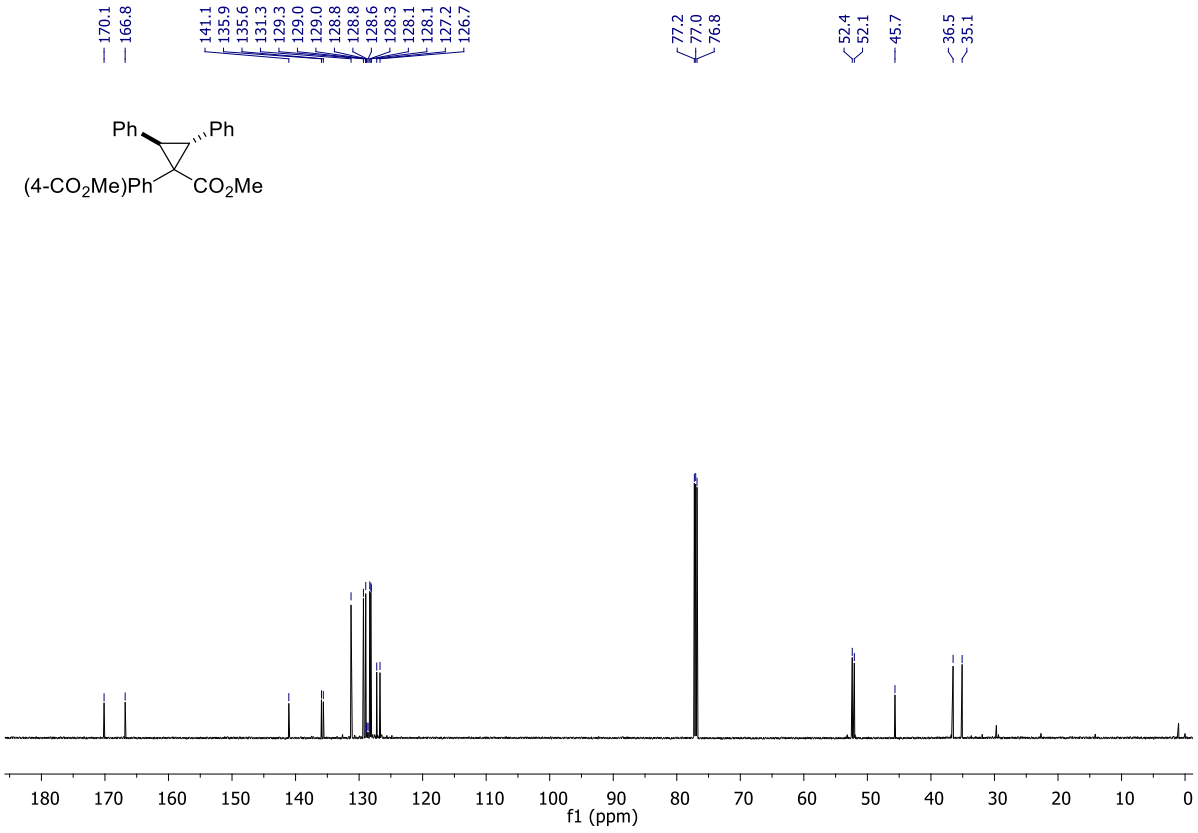

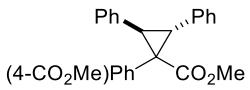

COSY

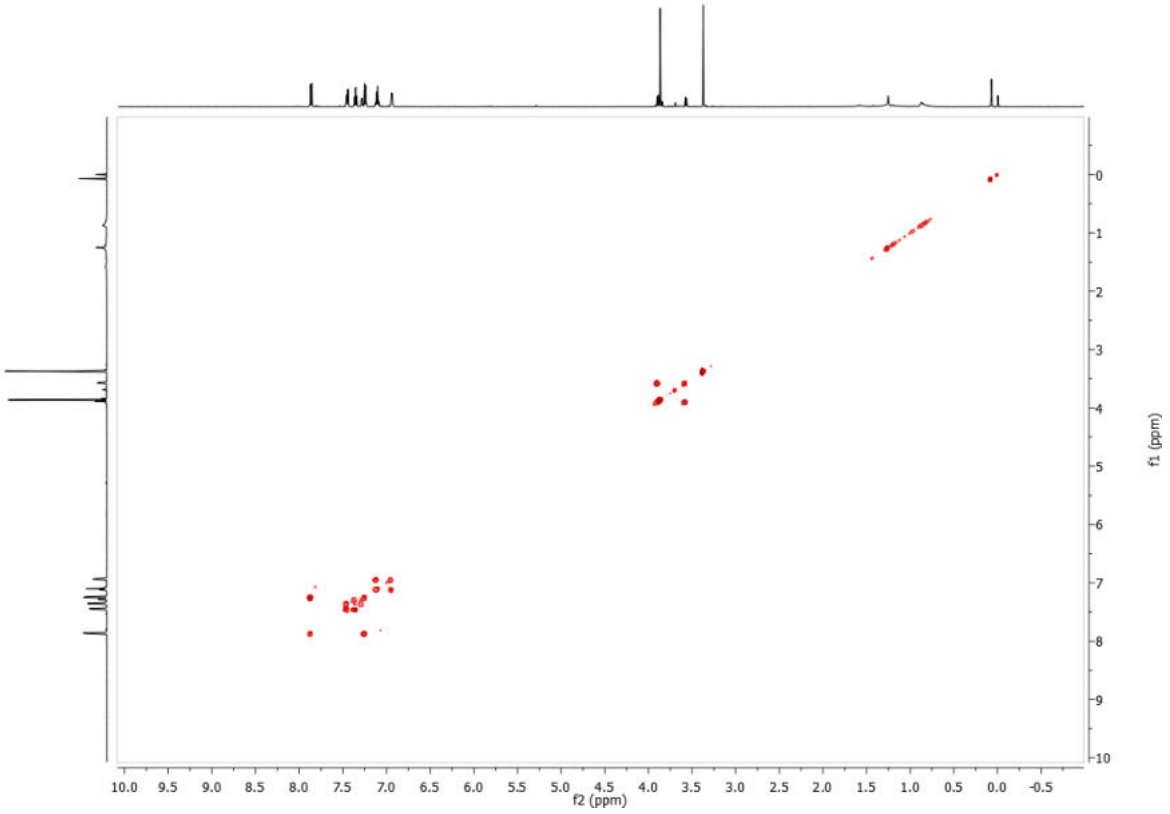

HSQC NMR

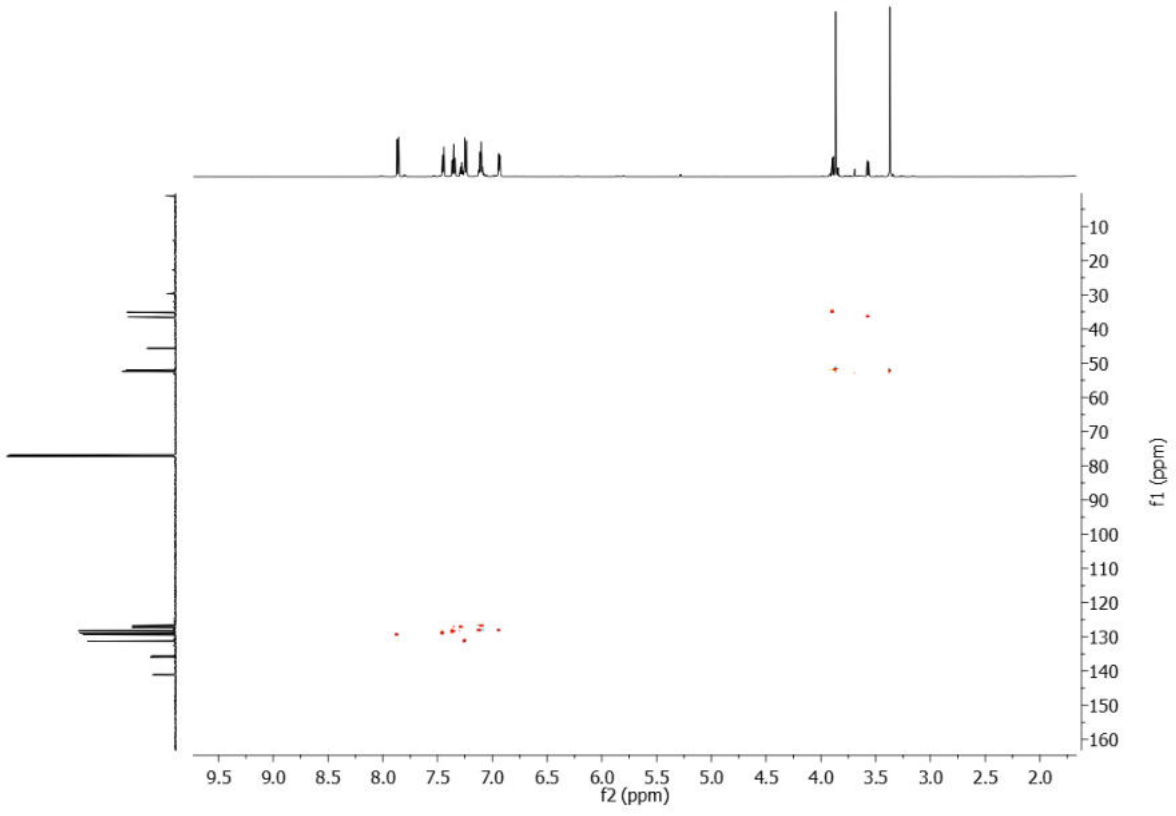

HMBC NMR

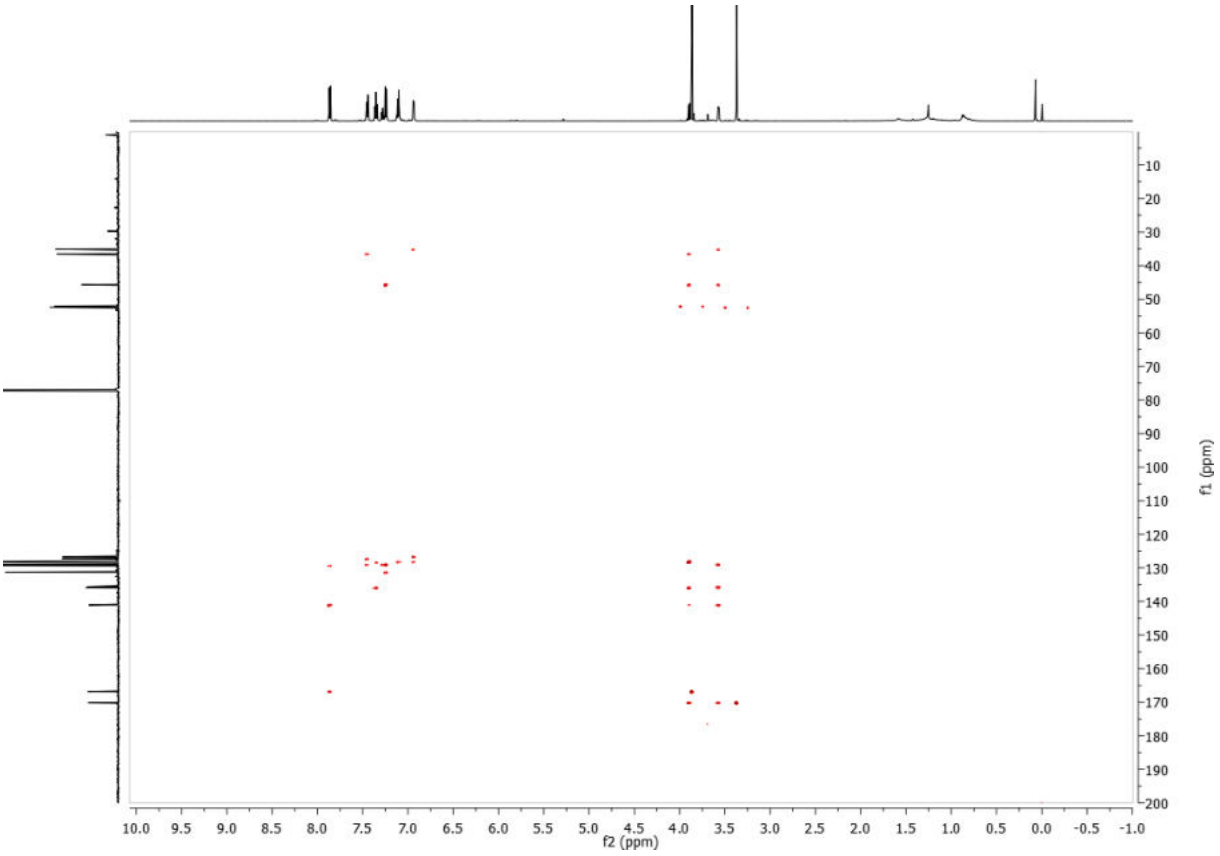

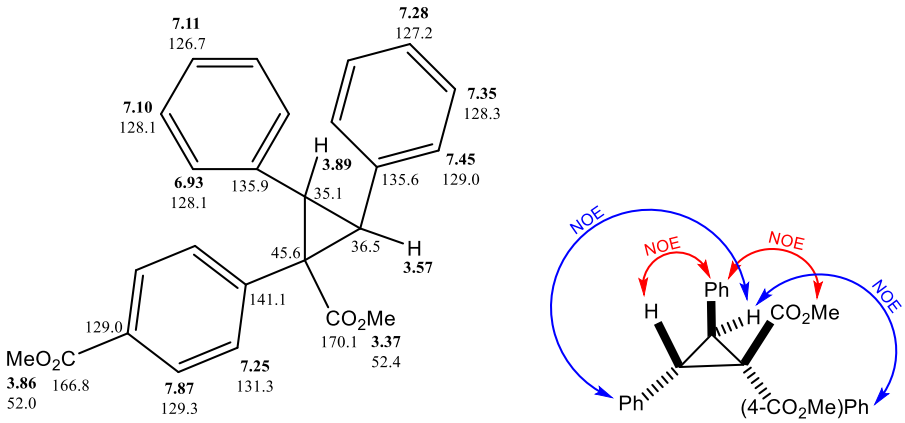

Figure S8. Cyclopropane **S3** stereochemistry (numbers indicate chemical shifts in ppm)

NOE effects - spectra

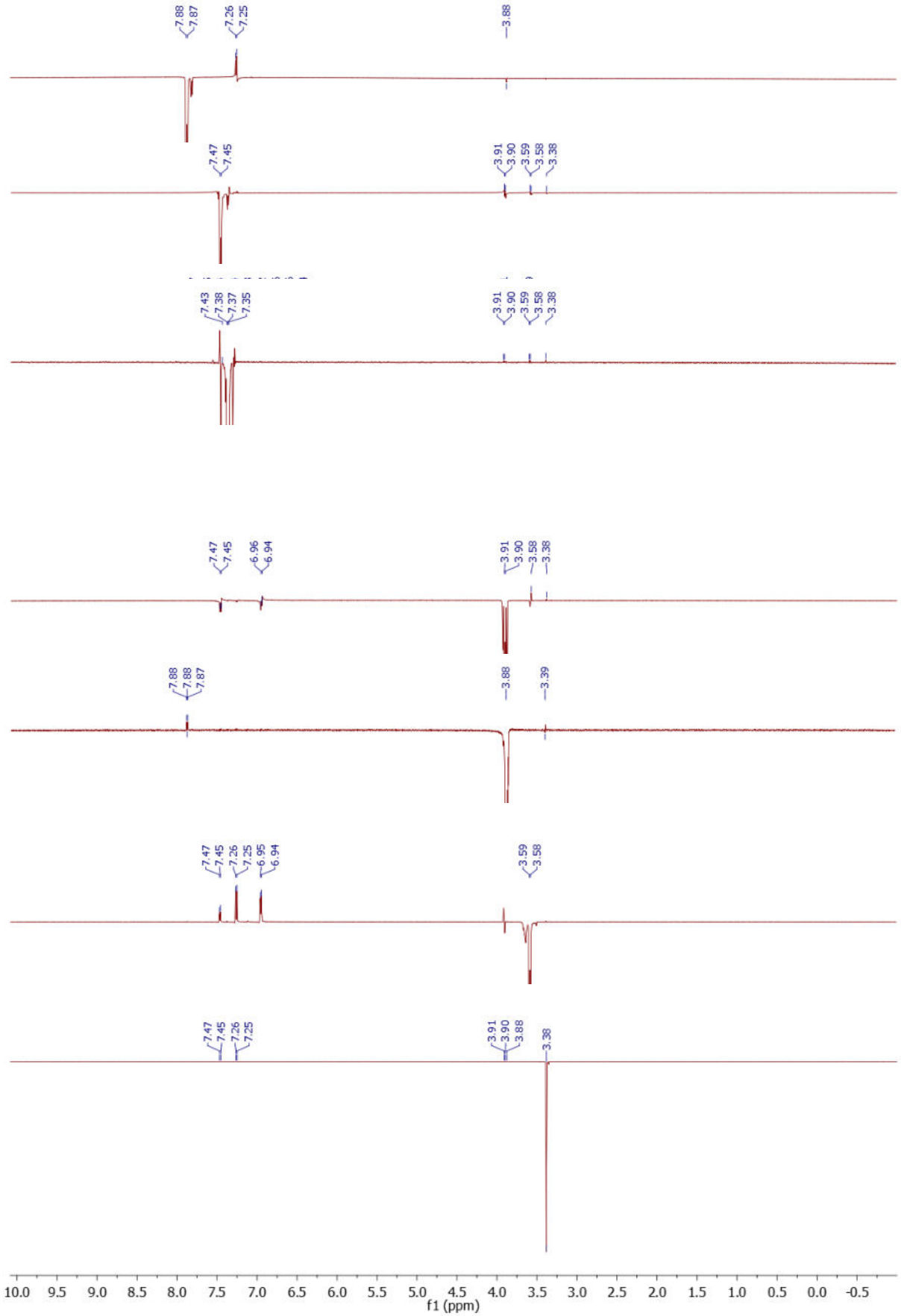

Methyl 4-(1-(methoxycarbonyl)-2,3-diphenylcyclopropyl)benzoate (S3b)

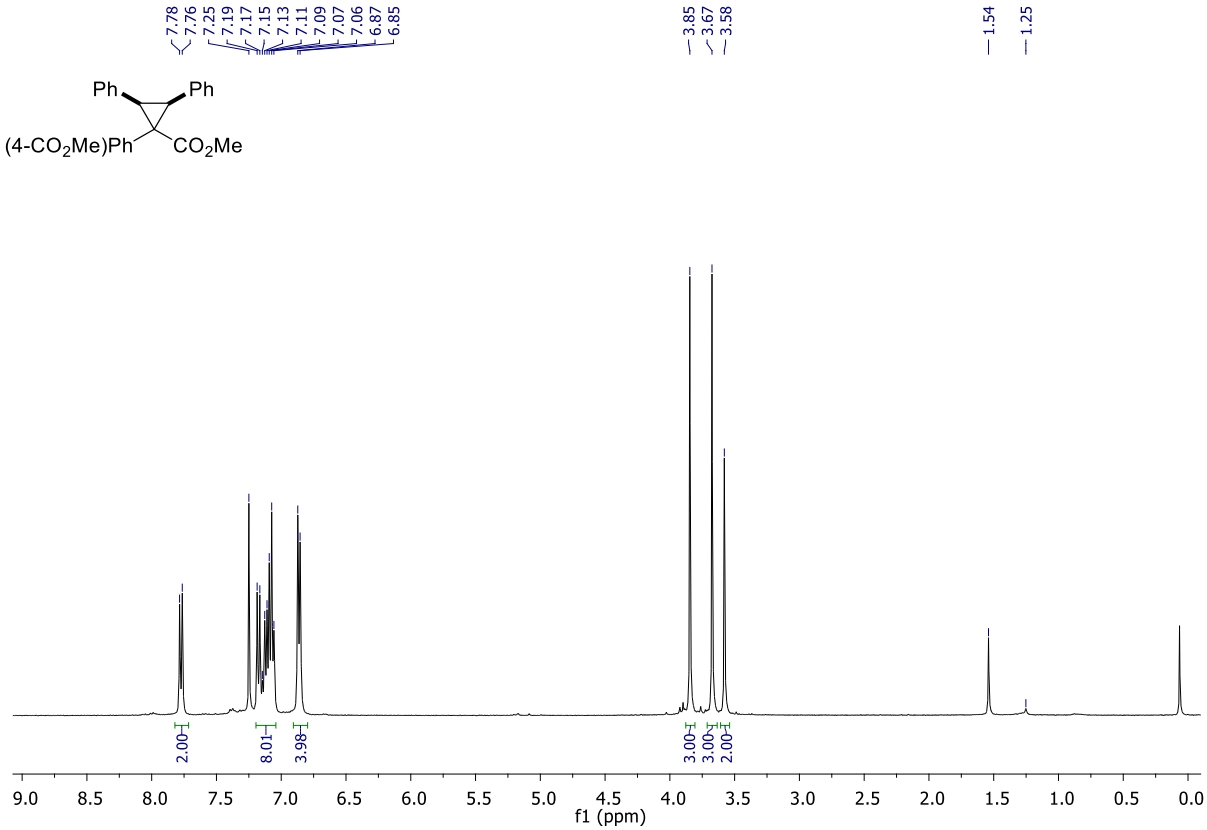

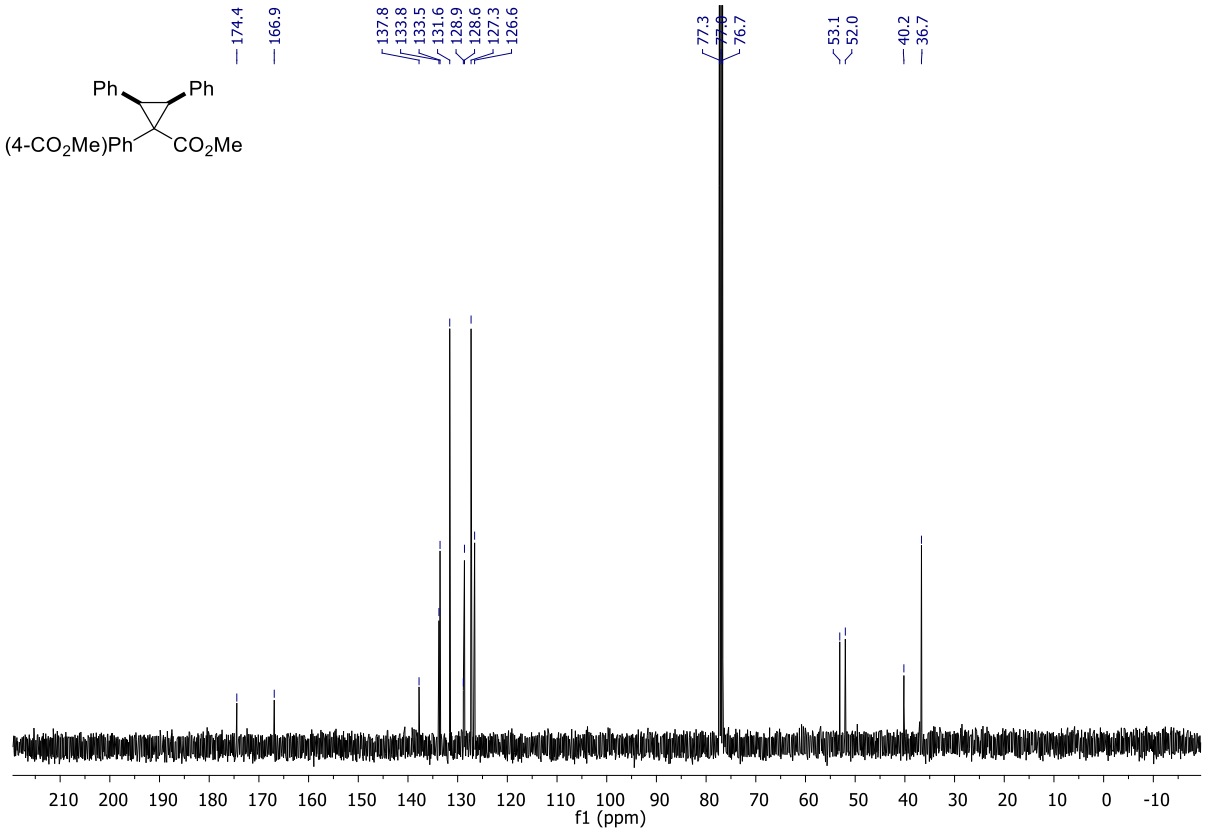

ACS Catalysis

pubs.acs.org/acscatalysis

Research Article

UV Light Is No Longer Required for the Photoactivation of 1,3,4-Oxadiazolines

Katarzyna Orłowska, João V. Santiago, Piotr Krajewski, Kacper Kisiel, Irena Deperasińska, Katarzyna Zawada, Wojciech Chaładaj,* and Dorota Gryko*

Cite This: *ACS Catal.* 2023, 13, 1964–1973

Read Online

ACCESS | Metrics & More | Article Recommendations | Supporting Information

ABSTRACT: Carbenes play a key role in a plethora of organic transformations. Although stabilized diazo carbonyl compounds predominate as a source of electrophilic carbenes, the hazardous nature of nonstabilized analogues calls for their in situ generation from stable precursors. Among these, 1,3,4-oxadiazolines serve as diazoalkane surrogates under UV light irradiation. In view of their high stability, diverse reactivities, and straightforward synthesis, milder methodologies for the activation of these compounds that permit the use of UV-light-sensitive substrates are highly valued. Herein, we report the visible-light-induced activation of oxadiazolines by triplet energy transfer catalysis that, in contrast to UV-induced processes, alters their reactivity and enables the generation of carbenes. The formed reactive species react with electron-poor olefins, thereby giving valuable spirocyclopropanes. Mechanistic investigations, both theoretical and experimental, uncover plausible pathways and highlight the importance of the triplet energy transfer steps.

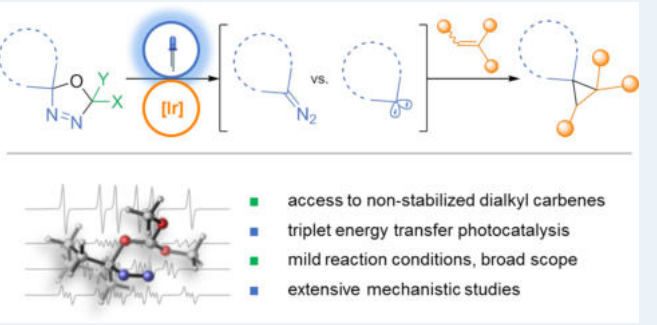

KEYWORDS: *triplet energy transfer photocatalysis, photosensitization, diazoalkanes and dialkyl carbenes, 1,3,4-oxadiazolines, visible-light induced transformations, spirocyclopropane synthesis*

INTRODUCTION

Carbene chemistry represents an extremely valuable branch of organic synthesis that has already proven to be a powerful tool for the construction of a wide range of C−C and C−X bonds,[1−3] including transformations of pharmaceutical interest.[4−6] Over the years, various precursors of carbene intermediates were developed, among which diazo carbonyl compounds stand at the forefront generating this reactive species under thermal[7] and photochemical[2,8−10] conditions or in metal-catalyzed reactions.[11−14] Most of their applications are, however, limited to stabilized reagents with at least one electron-withdrawing group adjacent to the diazo carbon atom.[7,15] In contrast, the safe synthetic use of nonstabilized counterparts requires in situ generation from, for example, hydrazones,[16−20] diazirines,[21,22] or 1,3,4-oxadiazolines.[23,24]

Compared with other diazo surrogates, 1,3,4-oxadiazolines exhibit high stability and the unique ability to provide distinct reactive intermediates depending on the conditions used (Scheme 1A). The well-known reactivity is based on thermolysis to ylides that spontaneously decompose into heteroatom-substituted carbenes.[24,25] Along this line, they have been widely studied by Warkentin and implemented as dimethoxycarbene surrogates in the synthesis of structurally diverse heterocycles.[26−30] Although effective in the formation of α-X (X = O, N, S) divalent carbon species, 1,3,4-oxadiazolines were only evidenced to give alkylidene carbenes trapped as pyridinium ylides under laser flash photolysis (LFP) at 308 nm.[31−33] When exposed to UV light, nonstabilized diazo compounds are, however, generated.[34−36] While the first photolysis report dates back to 1968,[34] it was only recently that the Ley group proposed their application as diazo precursors in UV-light-induced aryl−alkyl cross-coupling[37] and C−H functionalization reactions of aldehydes.[38−40]

The use of highly energetic UV light often, however, leads to undesired side reactions and precludes broader applications of these stabile and easily available precursors. To address these challenges, we propose a novel strategy for the activation of 1,3,4-oxadiazolines on the basis of the energy transfer event taking place under visible light irradiation. We illustrate the utility of the developed methodology in the photosensitized synthesis of the precious spirocyclopropane skeleton (Scheme 1B).

Received: October 28, 2022
Revised: December 16, 2022
Published: January 20, 2023

Scheme 1. Reactivity of oxadiazolines

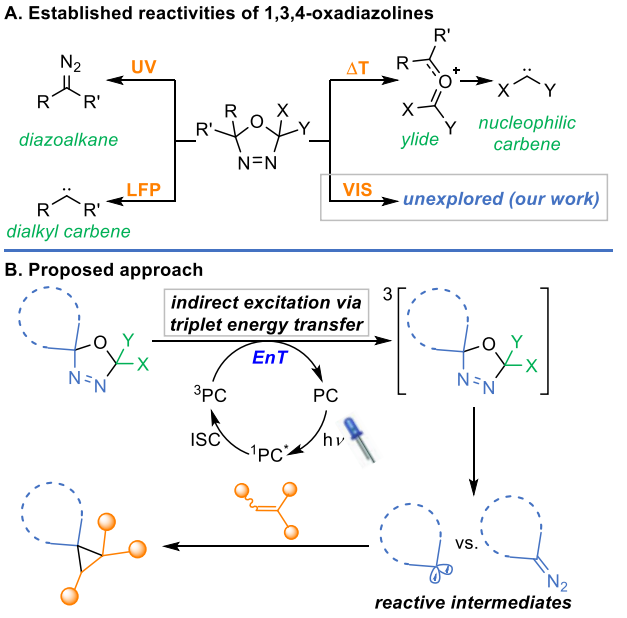

RESULTS AND DISCUSSION

Proposed Strategy. Visible-light-mediated energy transfer (*E*nT) catalysis has already emerged as a beneficial tool to give access to highly reactive species via indirect excitation (sensitization) of a substrate by a photocatalyst in its excited state.[41,42] Such processes occur productively if a sensitizer features a sufficient triplet energy level of lifetime long enough to transfer the energy to an intended molecule rather than to follow another relaxation pathway. The feasibility of the *E*nT process can therefore be estimated on the basis of the similarities between the triplet excited state energies of a photocatalyst and a substrate. Consequently, we began our investigations with density functional B3LYP/6-31G(d,p) calculations to assess $S_0 \rightarrow T_1$ excitation maxima corresponding to triplet energy values for a set of 5,5-cyclohexylidene oxadiazolines **1**–**5** with different substitution patterns at the position C_2 (Figure 1).

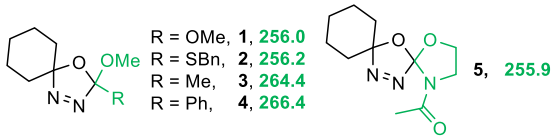

Figure 1. E_T values of oxadiazolines **1**–**5** (kJ/mol).

The calculated triplet energies are at a similar level with slightly lower values exhibited by compounds **1**, **2**, and **5**. In view of its stability and synthetic feasibility, the 5,5-cyclohexylidene-2,2-dimethoxy analogue **1** was selected for further theoretical investigations and initial experiments.

Considering the prospective rich chemistry of compound **1**, various decomposition pathways were computationally investigated at singlet (both ground and first excited) and triplet potential energy surfaces (PES) (Figure 2). Generally, concerted, one-step transformations were identified at singlet PESs, with considerably lower barrier heights for excited states. For example, cycloelimination of diazoalkane **7** from oxadiazoline **1** is associated with an activation energy of only 11.7 kJ/mol for the excited state S_1, which is significantly lower than the respective value for the ground state S_0 (121.0 kJ/mol). This is in line with the known facile UV-induced generation of diazoalkanes from 1,3,4-oxadiazolines.[23] On the contrary, a more complex reactivity pattern emerged for the system in the triplet spin state.

Typically, reaction trajectories involve consecutive bond cleavage and the presence of diradical intermediates. The most feasible pathway initiates with scission of the C_2–N_3 bond within oxadiazoline **1** leading to diazenyl intermediate **I** ($\Delta G‡$ = 14.1 kJ/mol), followed by a practically barrierless dissociation of N_2, and finally, the liberation of the triplet carbene **II** ($\Delta G‡$ = 52.3 kJ/mol). The elimination of diazoalkane **7** from intermediate **I** is also accessible ($\Delta G‡$ = 34.4 kJ/mol). Further analysis of the potential energy surface around **TS1** (Figure 2B) revealed a flat region and viability of the bifurcation of the reaction trajectory, thereby enabling direct decomposition of precursor **1** in the triplet state **T1** to compound **7**. Moreover, the subsequent carbene formation with the nitrogen extrusion from triplet diazoalkane **7** should proceed noticeably easier than for the molecule in the singlet ground state S_0 ($\Delta G‡$ = 63.8 kJ/mol from triplet **7** in comparison with $\Delta G‡$ = 125.1 kJ/mol calculated for the singlet ground state S_0). Given the relatively high barrier for this process, a prior relaxation of triplet diazoalkane **7** to a singlet ground state S_0 and further participation of the latter in reaction pathways seems also probable.

Taking into account the relatively high value of E_T = 256.0 kJ/mol [calculated with the B3LYP/6-31G(d,p)] for oxadiazoline **1**, among the typically used triplet sensitizers, iridium catalyst $\{Ir[dF(CF_3)ppy]_2(dtbpy)\}PF_6$ (**6**) with E_T = 258 kJ/mol should promote energy transfer from its exited state to compound **1**.[42] We supported our hypothesis by illuminating reagent **1** with blue light in the presence of catalyst **6**. Almost complete conversion of substrate **1** was observed, in contrast to the catalyst-free experiment (Scheme 2). Dimethyl carbonate (**8**), cyclohexanone (**9**), and cyclohexene (**10**) were identified as main products, with the latter one resulting from the 1,2-H migration, a transformation typical for alkylidene carbenes,[33] which suggests its formation in a triplet energy transfer process.

Cyclopropanation Optimization Studies. The known activation modes of oxadiazolines give access to ylides, diazo compounds, and carbenes — either dialkyl or heteroatom-substituted, both of nucleophilic type but differing in stability and reactivity.[43,44] Therefore, for the further studies, electron-poor olefins were selected as electrophilic reaction partners. The blue-light-induced model reaction of oxadiazoline **1** with phenyl–vinyl sulfone (**11**) in the presence of catalyst **6** furnished cyclopropane **12** in 41% yield (Table 1, entry 1) along with traces of (*E*)-olefin **13**. Control experiments proved light and the catalyst as factors required for the formation of product **12**, which is inaccessible via a thermal approach (entries 2–4). Optimization studies revealed that a simple modification, such as lowering an excess of oxadiazoline **1**, led to an almost 2-fold increase in the yield of cyclopropane **12** with traces of (*E*)-olefin **13** also formed (entry 5). It is noteworthy that the reaction is only slightly sensitive to the presence of air and moisture and proceeds effectively under blue light irradiation of both low and high intensity; however, a significant decrease of the yield was observed in the case of highly concentrated solutions [for details see Supporting Information (SI) Section 5]. Notably, we were able to reduce both the catalyst loading to only 0.25 mol % and the reaction time to 1 h while maintaining the high reaction efficacy (entry

https://doi.org/10.1021/acscatal.2c05319
ACS Catal. 2023, 13, 1964–1973

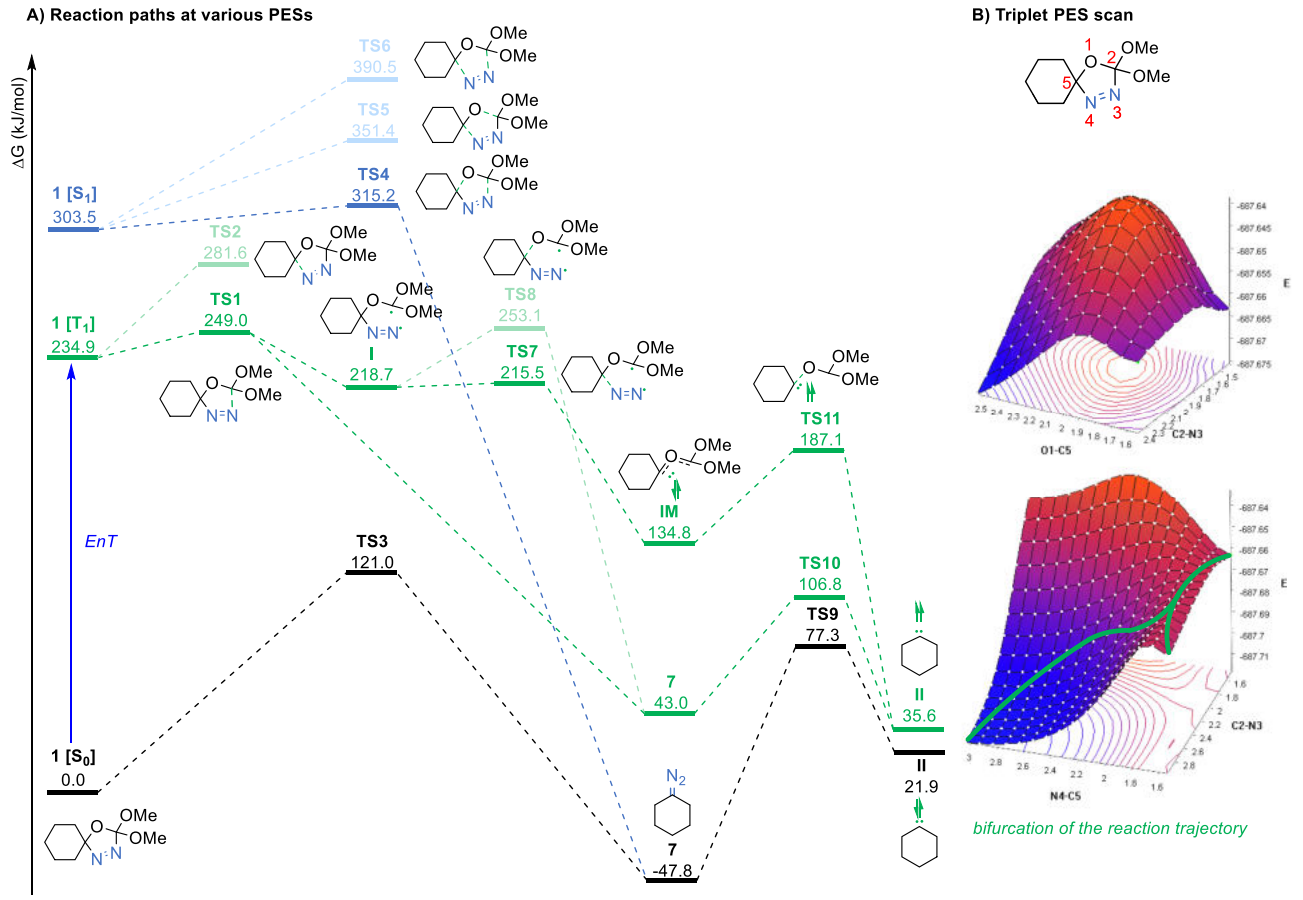

Figure 2. Various decomposition paths of oxadiazoline 1, calculated at the M06/6-311++G(d,p)/SMD(DCM)//B3LYP-D3/6-31G(d) level of theory (TD-DFT for S_1 PES).

Scheme 2. Initial Experiments—Proof of Concept[a]

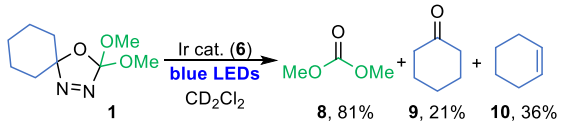

[a]Conditions: {Ir[dF(CF_3)ppy]$_2$(dtbpy)}PF_6 (**6**, 0.5 mol %), oxadiazoline (**1**, 0.1 mmol), CD_2Cl_2 (0.05 M), blue LEDs (450 nm, 25 W, for details see Supporting Information), Ar atmosphere, 17 h. NMR yields, CH_2Br_2 used as internal standard.

6). In contrast, the reaction exposed to UV irradiation without the catalyst added yielded compound **12** in only 10%, regardless of almost full conversion of the starting materials (entry 7), thus corroborating the significance of the triplet−triplet energy transfer process for the reaction selectivity.

We evaluated the influence of the substitution pattern at the position C_2 on the reaction yield by testing oxadiazolines **2**−**5** under the developed conditions (Scheme 3). Within all analogues tested, only reagent **1** proved to be an adequate substrate and efficiently furnished desired cyclopropane **12**. Thioalkoxy derivative **2** with a triplet state energy level almost equal to oxadiazoline **1** brought only 18% yield within a multitude of byproducts, along with dibenzyl sulfide. Although the calculated emission maxima for derivatives **3** and **4** are comparable, the reaction outcomes differ significantly. Oxadiazoline **3** yielded product **12** in 40% yield despite full conversion of olefin **11**. In this case, we cannot exclude the

Table 1. Background and Optimization Studies of Visible-Light-Induced Cyclopropanation

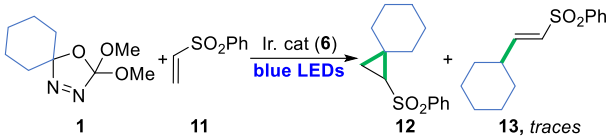

entry	deviation from standard conditions[a]	yield of **12** (%)[b]
1	none	41
2	no catalyst **6**	0
3	no light	0
4	no light, no catalyst **6**, in toluene, 110 °C	0
5	2.0 equiv of **1**	71
6[c]	0.25 mol % of catalyst **6**, 2.0 equiv of **1**, 1 h, 25 °C	81
7[cd]	UV light, no catalyst **6**, 2.0 equiv of **1**, 1 h, 25 °C	10

[a]Conditions: {Ir[dF(CF_3)ppy]$_2$(dtbpy)}PF_6 (**6**, 1 mol %), oxadiazoline (**1**, 0.5 mmol, 5.0 equiv), phenyl−vinyl sulfone (**11**, 0.1 mmol), DCM_{anh} (0.05 M), blue LEDs (450 nm, 25 W), 17 h, 18 °C. [b]Isolated yields. [c]DCM p.a. grade was used. [d]365 nm light was used.

formation of other reaction intermediates, since 2-methyl-2-methoxy derivatives are known to fragment unselectively upon thermolysis.[45,46] When oxadiazoline **4** was used, a complex mixture of products formed with only traces of the desired product and cyclohexyl benzoate, the latter presumably originating from a diradical species—an intermediate postulated for 2-phenyl derivatives.[47] Oxadiazoline **5**, which proved

https://doi.org/10.1021/acscatal.2c05319
ACS Catal. 2023, 13, 1964−1973

Scheme 3. Cyclopropanation with Various Oxadiazolines[b]

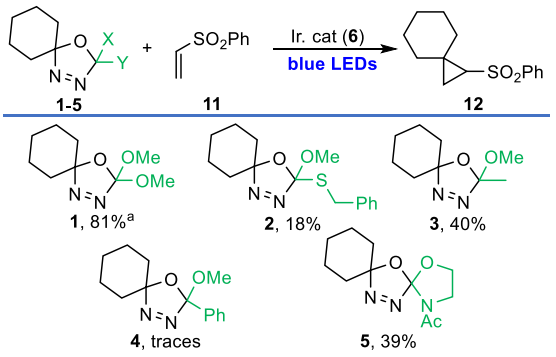

[a]Isolated yield. [b]Conditions: {Ir[dF(CF$_3$)ppy]$_2$(dtbpy)}PF$_6$ (**6**, 0.25 mol %), oxadiazoline (**1**−**5**, 0.4 mmol, 2.0 equiv), PVS (**11**, 0.2 mmol), DCM (0.05 M), blue LEDs (450 nm, 25 W), 1 h, 25 °C, GC yields.

unstable under electrochemical conditions (see SI Section 6.3), provided cyclopropane **12** with only a moderate yield.

These findings demonstrate that an appropriate E_T value is not the only prerequisite required for ensuring the reaction efficiency. Among crucial factors are also the stability, as well as reactivity, of generated intermediates, which we shall take into consideration.

Mechanistic Investigations. Various experiments were performed to investigate the reaction mechanism. The Stern−Volmer analysis confirmed the interaction between the excited state of photocatalyst **6** and oxadiazolines, revealing the correlation between the E_T value of the latter and their Ir fluorescence quenching ability (Figure 3). For oxadiazolines

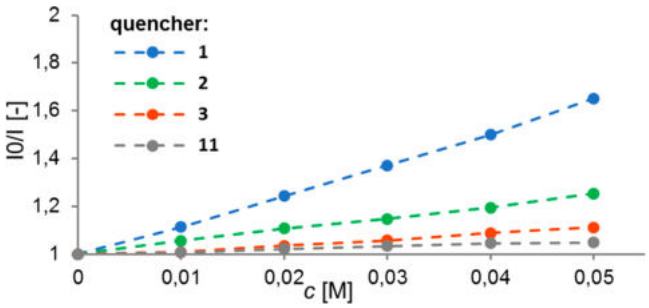

Figure 3. Stern−Volmer (SV) Analysis for Photocatalyt **6**.

1−**3**, the higher the E_T value is, the lower the quenching rate constant is [**1** (256.0 kJ/mol) < **2** (256.2 kJ/mol) < **3** (264.4 kJ/mol), and **1** (5.42×10^6 s^{-1} M^{-1}) > **2** (2.20×10^6 s^{-1} M^{-1}) > **3** (9.35×10^5 s^{-1} M^{-1})]. Thus, the lower the E_T is for oxadiazoline, the more intensive the quencher of the Ir catalyst luminescence is. In contrast, no significant influence of substrate **11** was observed on the fluorescence intensity of catalyst **6**.

Furthermore, the formation of product **12** via a competitive single electron transfer (SET) process was ruled out because oxadiazoline **1** exhibits oxidation and reduction potentials (for details see SI Section 6.3) significantly exceeding those of the examined photocatalysts (Table 2). Expectedly, sensitizers with low E_T values were not effective in catalyzing the cyclopropanation reaction (catalysts **14**−**16**). Although iridium catalysts **17** and **18** with triplet energy levels comparable with those of oxadiazoline **1** catalyzed the reaction, they were less efficient. Interestingly, the model reaction in the presence of a common organic triplet sensitizer, thioxanthone (**19**, λ_{max} = 360 nm),[50] which exhibits remarkably long-lived and highly energetic triplet species, provided cyclopropane **12** in diminished yield (63%), even upon increased catalyst loading and the use of violet light. The application of short-lived xanthone (**20**, λ_{max} = 340 nm)[50] also gave desired product **12** but in much lower yield (25%); pyrazoline **21** was isolated (70%) instead, similarly to the catalyst-free reaction performed under violet LEDs (Table 3, entries 1, 2).

The 1,3-dipolar cycloaddition of sulfone **11** to diazoalkane **7** leads to compound **22**, which isomerases to isolated heterocycle **21** (NMR analysis, see SI Section 6.7). The generation of the diazo compound from oxadiazoline **1** via direct photolysis exhibits slow kinetics because only traces of product **21** formed within 1 h in the catalyst-free conditions (entry 3). In contrast, the Ir-photosensitized cyclopropanation efficiently yields cyclopropane **12** after 1 h of irradiation (entry 4). The distinct distribution of products upon direct photolysis and in the Ir-catalyzed reaction unambiguously indicates that these processes operate via different mechanisms involving various reactive intermediates. While direct absorption of violet light by reagent **1** slowly leads to diazoalkane **7**, a triplet sensitization presumably gives fast access to dialkyl carbenes. If accessed in that way, as is typical for the triplet energy transfer process, they should possess triplet multiplicity and undergo stepwise addition to olefin **11**, thereby generating a diradical species. Overall, these studies reveal a high absorption coefficient and long excited state lifetime of a catalyst, together with its triplet energy level comparable with the E_T value of a substrate, as prerequisites for the reaction efficacy.

The radical nature of the mechanism was verified with experiments in the presence of TEMPO (Scheme 4A). The reaction was halted completely once the radical trap was added prior to exposure to light. When added just 2 min after the start of the reaction, cyclopropane **12** formed, though in a diminished yield along with pyrazoline **21**. ESI-MS analysis of the reaction mixture revealed the presence of a peak corresponding to TEMPO adduct **23**, formed from a radical generated upon the addition of triplet carbene to olefin **11**. The observation of pyrazoline **21** in the radical trapping experiment suggests the parallel diazoalkane **7** formation under the developed conditions. This was further supported by the isolation of heterocycle **21** when the reaction was stopped after 2 min (Scheme 4B). Because this compound is not observed under optimal conditions, one can conclude that 1-pyrazoline **22** converts to cyclopropane **12** during the reaction course. In fact, preprepared compound **22** efficiently transformed into cyclopropane **12** when exposed to blue LED irradiation in the presence of catalyst **6** (Scheme 4C). These results directly point to compound **22** and, therefore, diazoalkane **7** as intermediates involved along with carbene in the reaction mechanism.

Alkylidene carbenes, especially those with a cyclic structure, are extremely reactive species with short lifetimes (0.1−0.7 ns in C_6H_{12} for cyclohexylidene),[33] so for EPR measurements, DMPO (5,5-dimethyl-1-pyrroline *N*-oxide) and MNP (2-methyl-2-nitrosopropane) as spin traps were used, the latter being a typical carbene trapping agent.

Simulations performed with the EasySpin package in Matlab revealed EPR spectra of the reaction mixture as a superposition of multiple components when DMPO was applied, which predominantly arose from capturing the diazenyl radical **I**

https://doi.org/10.1021/acscatal.2c05319
ACS Catal. 2023, 13, 1964−1973

Table 2. Photophysical Properties of Commonly Used Photocatalysts

photocatalyst[a]	E_T [kJ/mol]		τ [ns]	yield of **12** [%][b,c]
$Ru(bpy)_3Cl_2$ (**14**)	205	increasing E_T	1100	0
$Ir[(dtbbpy)(ppy)_2]PF_6$ (**15**)	206		557	traces
fac-$Ir(ppy)_3$ (**16**)	231		1900	traces
$Ir[dF(Me)ppy)_2(dtbbpy)]PF_6$ (**17**)	252		1221	50
$[Ir(dFCF_3ppy)_2(bpy)]PF_6$ (**18**)	253		2280	49
$Ir[dF(CF_3)ppy)_2(dtbpy)]PF_6$ (**6**)	258		2300	(71)
thioxantone (**19**)	265		73000	63[d,e]
xanthone (**20**)	310		20	25[d,e]

[a]Photophysical properties of listed photocatalyst from reported data.[42,48,49] [b]Conditions: photocatalyst (1 mol %), oxadiazoline (**1**, 0.5 mmol, 5.0 equiv), phenyl−vinyl sulfone (**11**, 0.1 mmol), $DCM_{anh.}$ (0.05 M), blue LEDs (450 nm, 25 W), 17 h, 18 °C. [c]GC yields, isolated yields in parentheses. [d]Irradiation with violet LEDs (405 nm, 25 W). [e]2.5 mol % of catalyst loading.

Table 3. Oxadiazoline Reactivity under Violet Light Irradiation

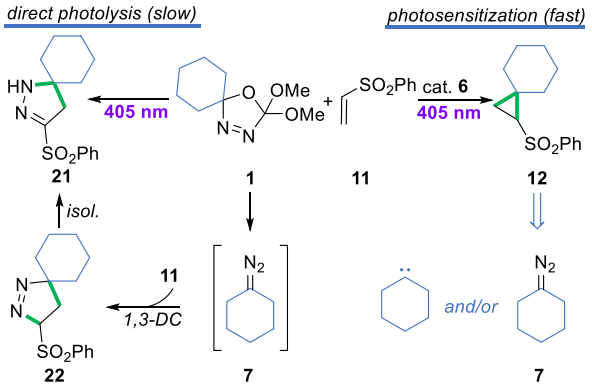

entry	conditions[a]	yield of **12** [%][b]	yield of **21** [%][b]
1	xanthone (**20**, 2.5 mol %), 17 h	25	70
2	catalyst-free, 17 h	15	62
3	catalyst-free, 1 h	0	traces
4	catalyst **6** (0.25 mol %), 1 h	84	0

[a]Conditions: oxadiazoline (**1**, 0.5 mmol, 5.0 equiv), phenyl−vinyl sulfone (**11**, 0.1 mmol), $DCM_{anh.}$ (0.05 M), violet LEDs (405 nm, 25 W), 18 °C. [b]Isolated yields.

Scheme 4. Mechanistic Experiments

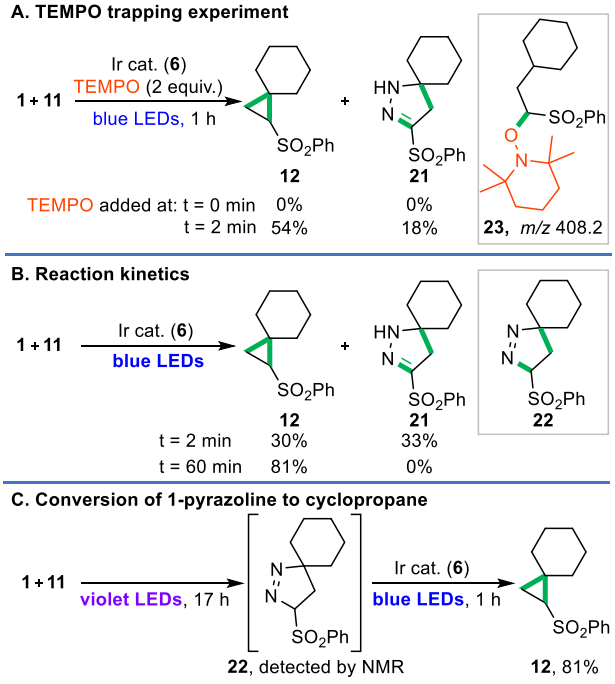

(Figure 4A, for details, see SI Section 6.9). However, one of the signals could be tentatively ascribed to a biradical species, which correlates well with carbene−DMPO adduct **c1** [Figure 4A, hyperfine couplings (HFCs): a_N = 1.22 mT, a_H = 2.27 mT for the nitroxide moiety and a_N = 0.31 mT, $a_{H(nitroxide)}$ = 1.87 mT, and $a_{H(CH_2)}$ = 1.45 mT for the cyclohexane moiety with rather fast spin exchange (J = 6.55 mT)]. The formation of carbene was further implied in an experiment with the MNP spin trap because a weak signal between the DTBN peaks (di-*tert*-butyl nitroxide) of parameters matching to a biradical adduct **c2** appeared (Figure 4B; for details see SI Section 6.9).

For better insight into the reaction mechanism, putative intermediates resulting from the reactivity of diazoalkane **7** toward olefin **11** were investigated computationally in both singlet (black) and triplet (green) spin states (Figure 5). At a singlet PES, the concerted cycloaddition of diazocyclohexane **7**, which provides product **22**, should proceed more feasibly (**TS12** with $\Delta G‡$ = 82.5 kJ/mol) than its prior denitrogenation through **TS9** that leads to singlet carbene **II** ($\Delta G‡$ = 125.1 kJ/mol).

In contrast, triplet **7** (calculated E_T = 195.8 kJ/mol, see SI Table T8), would preferentially lose the N_2 molecule rather than enter a stepwise addition to olefin **11** (**TS10** and **TS13**, $\Delta G‡$ = 63.8 and 77.9 kJ/mol). If a stepwise process occurs, the subsequent intermediate **IM1** is prone to dinitrogen elimination along a practically barrierless path leading to biradical **III**.

The alternative cyclization of **IM1** to heterocycle **22** through a **TS16** is hardly accessible ($\Delta G‡$ = 104.6 kJ/mol), while the

https://doi.org/10.1021/acscatal.2c05319
ACS Catal. 2023, 13, 1964−1973

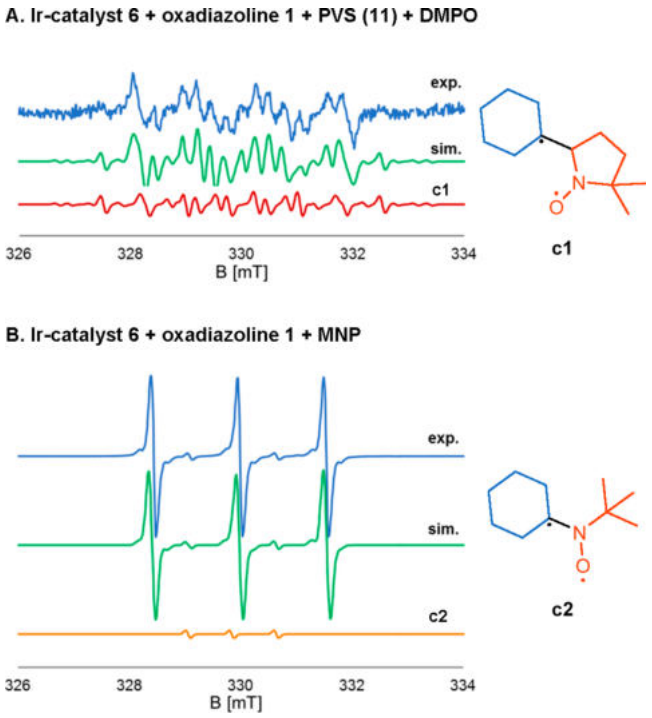

Figure 4. EPR spectra of selected reagents with (A) DMPO and (B) MNP used as the spin trap (spin traps added 15 s after irradiation); whole spectra (exp., experimental; sim., simulated) and selected components with plausible structures attached.

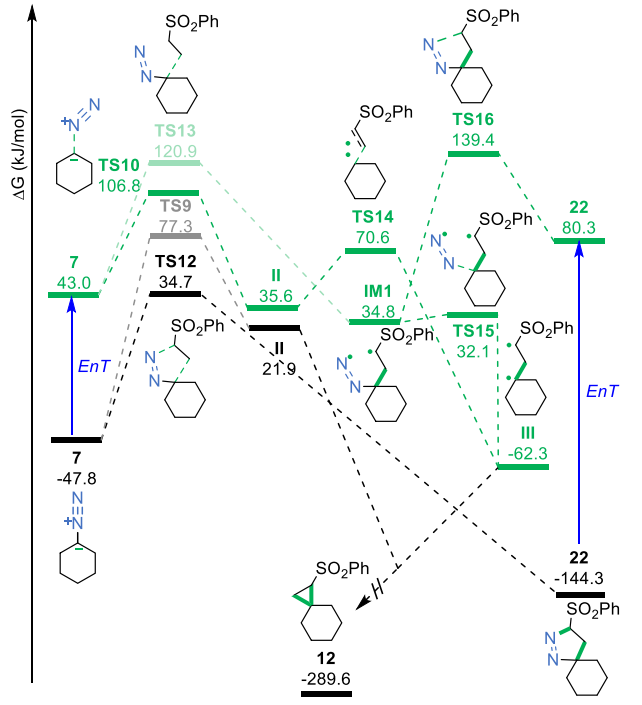

Figure 5. Plausible reaction paths calculated at the M06/6311+ +G(d,p) /SMD(DCM)//B3LYP-D3/6-31G(d) level of theory.

reverse decomposition process of triplet pyrazoline **22** (accessed via *E*nT from sensitizer **6**) ultimately leading to biradical **III** seems a viable reactivity channel (ΔG‡ = 59.1 kJ/mol). Conversely, the extrusion of nitrogen from compound **22** in a close-shell process is sluggish (ΔG‡ = 147.2 kJ/mol) but would lead to olefin **13**, which may also originate from the insertion of a singlet carbene **II** into the C−H bond of sulfone **11** (ΔG‡ = 81.5 kJ/mol).

On the basis of the above experimental and theoretical findings, a plausible mechanism is featured in Scheme 5. The

Scheme 5. Plausible mechanism

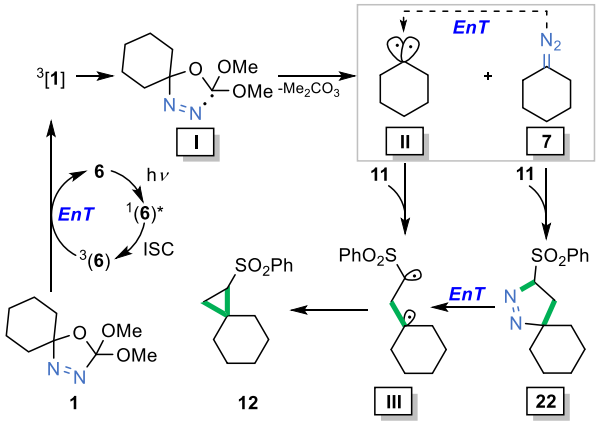

reaction is initiated with light absorption by catalyst **6** that, after intersystem crossing, transfers energy to oxadiazoline **1** in its triplet state. Consequently, the cleavage of the C_2-N_3 bond within oxadiazoline leads to the literature-known[36] diazenyl radical **I**, that decomposing to triplet carbene **II** and diazoalkane **7**. Regardless of the source of species **II**, in the presence of olefin **11**, it furnishes cyclopropane **12** in a stepwise manner with diradical intermediate **III**.

Concurrently, diazoalkane **7** undergoes 1,3-dipolar cycloaddition to olefin **11**, thereby giving pyrazoline **22**, which is an intermediate that upon photosensitization leads to spirocyclopropane **12** through intermediate **III**. Mechanistic experiments confirm both carbene and diazoalkane-mediated pathways; however, at this point, no evidence is known for if any pathway prevails.

Scope and Limitation Studies. The spirocyclopropane scaffold is found in numerous, naturally occurring, bioactive compounds and constitutes a useful building block in the synthesis of carbocycles and heterocycles, etc.[51−54] For this reason, efficient methods for their preparation are highly valued. Therefore, we resolved to evaluate the utility of the developed methodology in the synthesis of structurally diverse spirocyclopropanes (Scheme 6). To this end, reactions with a variety of oxadiazolines substituted variously at the C_5 position were performed. Starting materials bearing cycloalkylidenes of different size are well tolerated giving spirocyclic products **24**−**28** in decent yields (45−76%). Interestingly, the oxadiazoline containing the cyclopropyl moiety furnishes product **29** in 78% with the cyclopropyl group remaining intact. Although no rearrangement occurs, this cannot be recognized as evidence of a nonradical mechanism since diradical species thermally generated from the analogous 2-phenyl-2-methoxy derivative were postulated to undergo reactions that are faster than the cyclopropane ring opening.[47] A modest yield for oxetane **32** (36%) was observed, presumably because of the strain generated upon the formation of the spirocycle or because of the higher reactivity and, therefore, lower selectivity of the generated intermediates. Generally, for reactions leading to compounds **32**−**35**, a decrease in yield was observed; in contrast, *N*-tosyl derivative **36** formed productively (82%). Intrigued by the distinct reactivities displayed by oxadiazolines

https://doi.org/10.1021/acscatal.2c05319
ACS Catal. 2023, 13, 1964−1973

Scheme 6. Spirocyclopropane Synthesis under Visible Light Irradiation[c]

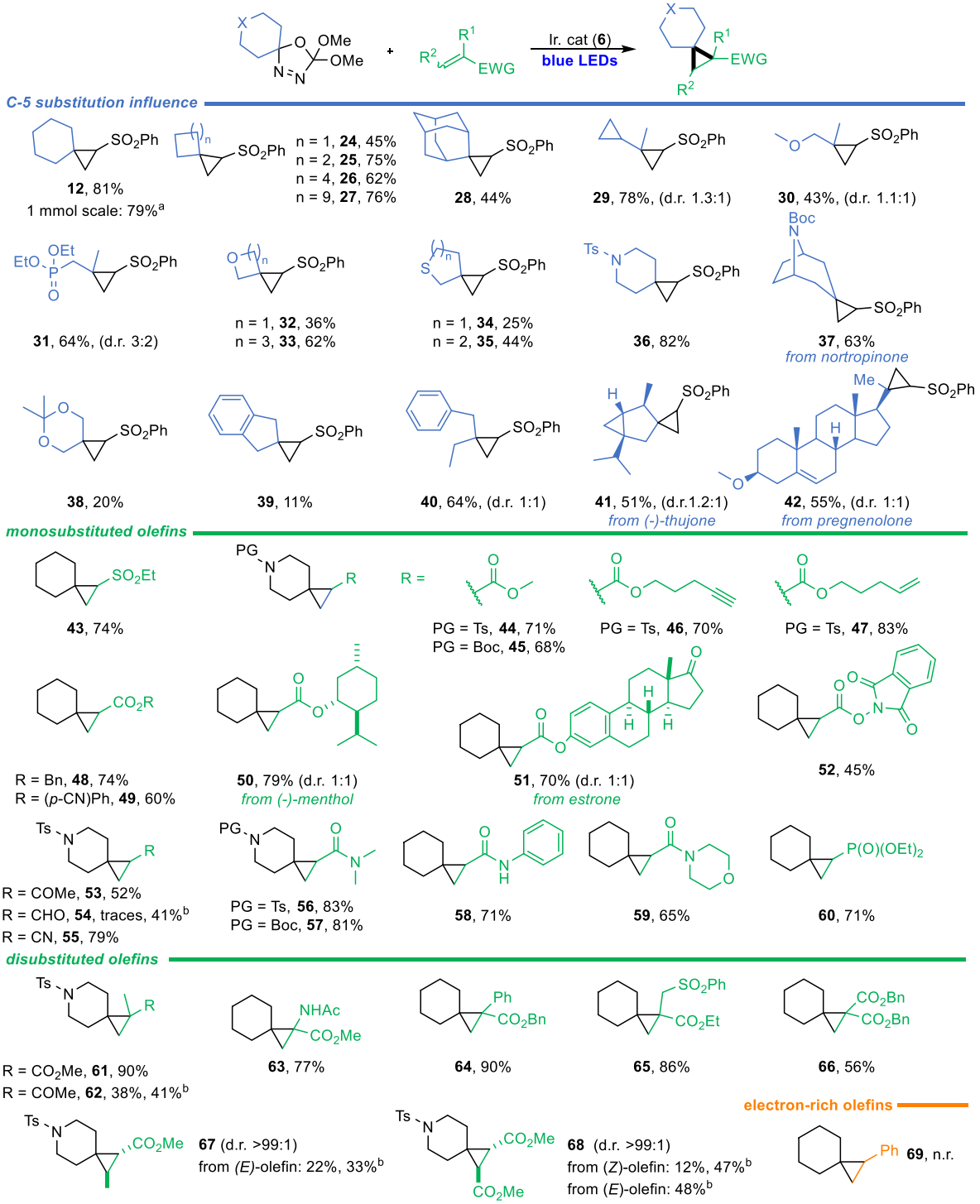

[a]Reaction performed on 10 W LEDs for 5 h. [b]Oxadiazoline used as the limiting substrate (5.0 equiv, 1.0 mmol); n.r. = no reaction. [c]Conditions: $\{Ir[dF(CF_3)ppy]_2(dtbpy)\}PF_6$ (**6**, 0.25 mol %), oxadiazoline (0.4 mmol, 2.0 equiv), olefin (0.2 mmol), DCM (0.05 M), blue LEDs (450 nm, 25 W), 1 h, 25 °C.

S10–**S12**, we estimated their E_T values (see SI Table T8). These are considerably lower than triplet energy levels predicted for 5,5-cyclohexylidene analogues **1**–**5**. The obtained values correspond well with the Stern–Volmer analysis (see SI Section 6.5), which revealed that reagent **S12** (E_T = 247.0 kJ/mol), which has a k_q remarkably higher than all other examined derivatives (1.18×10^7 s^{-1} M^{-1}), affords cyclopropane **36** in high yield (82%). Beneficially, oxadiazolines derived from naturally occurring nortropinone, (−)-α-thujone, and prognenolone efficiently furnished spirocycles **37**, **41**, and **42**, thereby emphasizing the utility of the developed method. Moreover, the reaction can be performed on a larger scale, but prolonged irradiation time is required

https://doi.org/10.1021/acscatal.2c05319
ACS Catal. 2023, 13, 1964−1973

Scheme 7. Preliminary Studies on Other Transformations

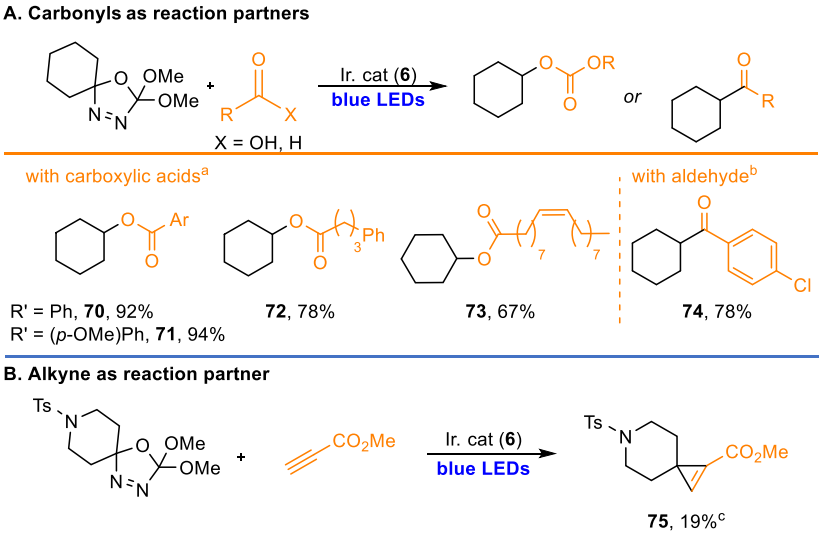

[a]Conditions: {Ir[dF(CF$_3$)ppy]$_2$(dtbpy)}PF$_6$ (**6**, 0.25 mol %), oxadiazoline (**1**, 0.2 mmol, 2.0 equiv), acid (0.1 mmol), DCM (0.1 M), blue LEDs (447 nm, 7 W), 1.5 h, 25 °C. [b]Conditions: {Ir[dF(CF$_3$)ppy]$_2$(dtbpy)}PF$_6$ (**6**, 0.25 mol %), oxadiazoline (**1**, 1.0 mmol, 5.0 equiv), aldehyde (0.2 mmol), DCM (0.05 M), blue LEDs (450 nm, 25 W), 2.5 h, 25 °C. [c]Conditions: {Ir[dF(CF$_3$)ppy]$_2$(dtbpy)}PF$_6$ (**6**, 0.25 mol %), oxadiazoline (**S12**, 0.4 mmol, 2.0 equiv), alkyne (0.2 mmol), DCM (0.05 M), blue LEDs (450 nm, 25 W), 1 h, 25 °C, NMR yield with 1,3,5-trimetoxybenzene used as internal standard.

(79% for cyclopropane **12** in the case of 5 h of irradiation with 5 W blue LEDs, Scheme 6).

Next, we explored the scope of olefins in conjunction with oxadiazolines **1** and **S12** (Scheme 6). Numerous olefins that carry various electron-withdrawing groups, including sulfone (**43**), ester (**44**–**52**), ketone (**53**), nitrile (**55**), amide (**56**–**59**), and phosphonate (**60**) moieties, are well tolerated. The reaction proceeds selectively in the presence of unactivated alkenes and alkynes to furnish **46** and **47** with high yields. It is noteworthy that our method is suitable for late-stage functionalizations, as evidenced by the cyclopropanation of olefins bearing menthol and estrone scaffolds (**50** and **51**, 79% and 70%, respectively). Although acrolein initially did not react productively, the modification of a substrate ratio enabled the synthesis of product **54** in decent yield (41%). Additionally, various *N*-protecting groups are well tolerated, thereby providing cyclopropanes **44** and **45**, as well as **56** and **57**, with comparable efficacies. Geminal olefins with either one EDG and one EWG or two EWG groups work similarly to monosubstituted alkenes with yields even up to 90% for **61** and **64**. Products **67** and **68** can be synthesized from vicinal alkenes, albeit in considerably lower yields that can be improved upon by increasing the amount of olefin used.

We could not observe any discrimination between the (*E*)- and (*Z*)-isomers of the starting material, with the more thermodynamically favorable *trans* diastereoisomer furnished solely from olefins of both configurations (products **67** and **68**), which further supports a stepwise, diradical-mediated mechanism. Expectedly, the reaction with styrene did not led to spirocycle **69**, indicating electron-rich olefins as a limitation of the method.

The developed strategy is not limited to the cyclopropanation reaction: preliminary studies also uncovered oxadiazolines as suitable starting materials for O–H insertion into carboxylic acids (Scheme 7A). Both aryl and alkyl carboxylic acids efficiently reacted with oxadiazoline **1**, which led to corresponding cyclohexyl esters **70**–**73** in yields up to 94%. When an aldehyde was applied as the reaction partner, ketone **74** was obtained similarly to the Ley et al. report.[38] Additionally, we were able to proceed a cyclopropenation reaction, albeit with low efficiency, possibly because of the low stability of cyclopropene **75** (Scheme 7B).

CONCLUSIONS

Herein, we have demonstrated that 1,3,4-oxadiazolines — known as extremely stable diazo precursors — give access to reactive dialkyl intermediates when activated by a photosensitizer under visible light irradiation, which we utilized for the efficient synthesis of spirocyclopropanes. The proposed approach not only eliminates the need for the use of highly energetic UV light, thus enabling broader applications, but also alters the reaction pathway. While the developed photosensitized method affords cyclopropanes, violet-light-mediated direct photolysis leads to 2-pyrazolines. The use of UV-light impedes the reaction selectivity. It is, therefore, the visible-light-induced energy transfer event from the excited state of the photocatalyst to 1,3,4-oxadiazolines that makes the reported method compatible with numerous electron-deficient olefins to furnish spirocyclopropanes productively.

Both experimental and theoretical investigations corroborate that alkylidene carbenes, as well as diazoalkanes, are intermediates in the reaction mechanism and reveal the appropriate triplet energy level of a sensitizer as crucial for the reaction efficacy. In addition, preliminary results, including the extension of the scope of the reaction partners to carbonyls and alkynes, are enclosed. Further studies on the reactivity of oxadiazolines under visible light irradiation are ongoing in our laboratories.

ASSOCIATED CONTENT

Supporting Information

The Supporting Information is available free of charge at https://pubs.acs.org/doi/10.1021/acscatal.2c05319.

https://doi.org/10.1021/acscatal.2c05319
ACS Catal. 2023, 13, 1964–1973

Supplemental experimental details and procedures, optimization studies, mechanistic experiments, DFT calculations, EPR measurements and simulations, and spectral data for all new compounds (PDF)

AUTHOR INFORMATION

Corresponding Authors

Wojciech Chaładaj − *Institute of Organic Chemistry, Polish Academy of Sciences, 01-224 Warsaw, Poland*; Email: wojciech.chaladaj@icho.edu.pl

Dorota Gryko − *Institute of Organic Chemistry, Polish Academy of Sciences, 01-224 Warsaw, Poland*; orcid.org/0000-0002-5197-4222; Email: dorota.gryko@icho.edu.pl

Authors

Katarzyna Orłowska − *Institute of Organic Chemistry, Polish Academy of Sciences, 01-224 Warsaw, Poland*

João V. Santiago − *Institute of Organic Chemistry, Polish Academy of Sciences, 01-224 Warsaw, Poland*; orcid.org/0000-0001-9315-3863

Piotr Krajewski − *Institute of Organic Chemistry, Polish Academy of Sciences, 01-224 Warsaw, Poland; Department of Chemistry, Warsaw University of Technology, 00-664 Warsaw, Poland*

Kacper Kisiel − *Institute of Organic Chemistry, Polish Academy of Sciences, 01-224 Warsaw, Poland*

Irena Deperasińska − *Institute of Physics, Polish Academy of Sciences, 02-668 Warsaw, Poland*

Katarzyna Zawada − *Faculty of Pharmacy with the Laboratory Medicine Division, Department of Physical Chemistry, Medical University of Warsaw, 02-097 Warsaw, Poland*

Complete contact information is available at: https://pubs.acs.org/10.1021/acscatal.2c05319

Author Contributions

K.O. and D.G.: methodology design. K.O., J.V.S., P.K., and K.K.: experimental investigations. K.Z.: EPR spectroscopy and simulations. I.D. and W.C.: calculations. K.O., D.G., and W.C.: manuscript writing, editing, reviewing. D.G.: supervision. All authors have given approval to the final version of the manuscript.

Notes

The authors declare no competing financial interest.

ACKNOWLEDGMENTS

The authors thank Prof. Grzegorz Mlostoń for providing an oxadiazoline sample for preliminary studies and helpful discussions. Financial support for this work was provided by the National Science Centre (OPUS no. 2019/35/B/ST4/03435; K.O., ETIUDA 2020/36/T/ST4/00208). Calculations have been carried out using resources provided by Wroclaw Centre for Networking and Supercomputing (grant no. 518) and by the Interdisciplinary Centre for Mathematical and Computational Modelling ICM, University of Warsaw under computational allocation no G87-1090.

REFERENCES

(1) Moss, R. A.; Doyle, M. P. *Contemporary Carbene Chemistry*; Wiley: New York, 2013; pp 325−551.

(2) Brinker, U. H. *Advances in Carbene Chemistry - Vol. 3*; JAI Press: Stamford, 2001; pp 287−316.

(3) Doyle, M. P.; Duffy, R.; Ratnikov, M.; Zhou, L. Catalytic Carbene Insertion into C-H Bonds. *Chem. Rev.* **2010**, *110*, 704−724.

(4) Davies, H. M. L.; Denton, J. R. Application of Donor/Acceptor-Carbenoids to the Synthesis of Natural Products. *Chem. Soc. Rev.* **2009**, *38*, 3061−3071.

(5) Harada, S. Development of Novel Methodology Using Diazo Compounds and Metal Catalysts. *Chem. Pharm. Bull.* **2021**, *69*, 1170−1178.

(6) Ge, S.-S.; Chen, B.; Wu, Y.- Y.; Long, Q.-S.; Zhao, Y.-L.; Wang, P.-Y.; Yang, S. Current Advances of Carbene-Mediated Photoaffinity Labeling in Medicinal Chemistry. *RSC Adv.* **2018**, *8*, 29428−29454.

(7) Regitz, M.; Maas, G. *Diazo Compounds: Properties and Synthesis*; Academic Press: Orlando, 1986; pp 65−195.

(8) Ciszewski, Ł. W.; Rybicka-Jasińska, K.; Gryko, D. Recent Developments in Photochemical Reactions of Diazo Compounds. *Org. Biomol. Chem.* **2019**, *17*, 432−448.

(9) Hua, T.-B.; Yang, Q.-Q.; Zou, Y.-Q. Recent Advances in Enantioselective Photochemical Reactions of Stabilized Diazo Compounds. *Molecules* **2019**, *24*, 3191−3212.

(10) Empel, C.; Pei, C.; Koenigs, R. M. Unlocking Novel Reaction Pathways of Diazoalkanes with Visible Light. *Chem. Commun.* **2022**, *58*, 2788−2798.

(11) Gillingham, D.; Fei, N. Catalytic X-H Insertion Reactions Based on Carbenoids. *Chem. Soc. Rev.* **2013**, *42*, 4918−4931.

(12) Doyle, M. P.; McKervey, M. A.; Ye, T. *Modern Catalytic Methods for Organic Synthesis with Diazo Compounds: From Cyclopropanes to Ylides*; Wiley: New York, 1998; pp 112−652.

(13) Dorwald, F. Z. *Metal Carbenes in Organic Synthesis*; Wiley: New York, 2008; pp 13−232.

(14) Doyle, M. P.; Forbes, D. C. Recent Advances in Asymmetric Catalytic Metal Carbene Transformations. *Chem. Rev.* **1998**, *98*, 911−936.

(15) Zhu, D.; Chen, L.; Fan, H.; Yao, Q.; Zhu, S. Recent Progress on Donor and Donor-Donor Carbenes. *Chem. Soc. Rev.* **2020**, *49*, 908−950.

(16) Shao, Z.; Zhang, H. N-Tosylhydrazones: Versatile Reagents for Metal-Catalyzed and Metal-Free Cross-Coupling Reactions. *Chem. Soc. Rev.* **2012**, *41*, 560−572.

(17) Xia, Y.; Wang, J. N-Tosylhydrazones: Versatile Synthons in the Construction of Cyclic Compounds. *Chem. Soc. Rev.* **2017**, *46*, 2306−2362.

(18) Wang, Y.; Wen, X.; Cui, X.; Wojtas, L.; Zhang, X. P. Asymmetric Radical Cyclopropanation of Alkenes with in Situ-Generated Donor-Substituted Diazo Reagents via Co(II)-Based Metalloradical Catalysis. *J. Am. Chem. Soc.* **2017**, *139*, 1049−1052.

(19) Ke, J.; Lee, W. -C. C.; Wang, X.; Wang, Y.; Wen, X.; Zhang, X. P. Metalloradical Activation of in Situ-Generated α-Alkynyldiazomethanes for Asymmetric Radical Cyclopropanation of Alkenes. *J. Am. Chem. Soc.* **2022**, *144*, 2368−2378.

(20) Wang, X.; Ke, J.; Zhu, Y.; Deb, A.; Xu, Y.; Zhang, X. P. Asymmetric Radical Process for General Synthesis of Chiral Heteroaryl Cyclopropanes. *J. Am. Chem. Soc.* **2021**, *143*, 11121−11129.

(21) Moss, R. A. Diazirines: Carbene Precursors Par Excellence. *Acc. Chem. Res.* **2006**, *39*, 267−272.

(22) Platz, M. S.; Huang, H.; Ford, F.; Toscano, J. Photochemical Rearrangements of Diazirines and Thermal Rearrangements of Carbenes. *Pure Appl. Chem.* **1997**, *69*, 803−807.

(23) Warkentin, J. Δ^3-1,3,4-Oxadiazolines. Versatile Sources of Reactive Intermediates. *J. Chem. Soc. Perkin Trans. 1* **2000**, *14*, 2161−2169.

(24) Warkentin, J. 2,5-Dihydro-1,3,4-Oxadiazoles and Bis-(Heteroatom-Substituted)Carbenes. *Acc. Chem. Res.* **2009**, *42*, 205−212.

(25) El-Saidi, M.; Kassam, K.; Pole, D. L.; Tadey, T.; Warkentin, J. 2,2-Dialkoxy-Δ^3-1,3,4-Oxadiazolines: Convenient Thermal Sources of Dialkoxycarbenes. *J. Am. Chem. Soc.* **1992**, *114*, 8751−8752.

(26) Aasmul, M.; Heimgartner, H.; Mloston, G. *2,2-Dimetoxy-5,5-Dimethyl-Δ^3-1,3,4-Oxadiazoline. Electronic Encyclopedia of Reagents for Organic Synthesis*; Paquette, L. A., Ed.; Wiley, 2012.
(27) Rigby, J. H.; Laurent, S.; Cavezza, A.; Heeg, M. J. Construction of the Azepinoindole Core Tricycle of the Stemona Alkaloids. *J. Org. Chem.* **1998**, *63*, 5587−5591.
(28) Rigby, J. H.; Cavezza, A.; Ahmed, G. Nucleophilic Carbenes in Organic Synthesis. Construction of Functionalized Hydroindolones via a Novel Reaction Pathway of Dimethoxycarbene. *J. Am. Chem. Soc.* **1996**, *118*, 12848−12849.
(29) Spino, C.; Rezaei, H.; Dupont-Gaudet, K.; Bélanger, F. Inter- and Intramolecular [4 + 1]-Cycloadditions between Electron-Poor Dienes and Electron-Rich Carbenes. *J. Am. Chem. Soc.* **2004**, *126*, 9926−9927.
(30) Rigby, J. H.; Sidique, S. Total Synthesis of (±)-Phenserine via [4 + 1] Cyclization of a Bis(Alkylthio)Carbene and an Indole Isocyanate. *Org. Lett.* **2007**, *9*, 1219−1221.
(31) Pezacki, J. P.; Pole, D. L.; Warkentin, J.; Chen, T.; Ford, F.; Toscano, J. P.; Fell, J.; Platz, M. S. Laser Flash and Dual Wavelength Photolysis of 3,4-Diaza-2,3-Dimetoxy-1-Oxa[4.5]spirooct-3-ene. Migration of Hydrogen and Carbon in Cyclobutylidene and in the Excited State of Its Precursor. *J. Am. Chem. Soc.* **1997**, *119*, 3191−3192.
(32) Pezacki, J. P.; Wood, P. D.; Gadosy, T. A.; Lusztyk, J.; Warkentin, J. Laser Flash Photolysis Studies of Oxygen and Sulfur Atom Transfer Reactions from Oxiranes and Thiiranes to Singlet Carbenes. *J. Am. Chem. Soc.* **1998**, *120*, 8681−8691.
(33) Pezacki, J. P.; Couture, P.; Dunn, J. A.; Warkentin, J.; Wood, P. D.; Lusztyk, J.; Ford, F.; Platz, M. S. Rate Constants for 1,2-Hydrogen Migration in Cyclohexylidene and in Substituted Cyclohexylidenes. *J. Org. Chem.* **1999**, *64*, 4456−4464.
(34) Hoffmann, R. W.; Luthardt, H. J. Thermolyse Und Photolyse von Δ^3-1.3.4-Oxdiazolinen. *Chem. Ber.* **1968**, *101*, 3861−3871.
(35) Pezacki, J. P.; Wagner, B. D.; Lew, C. S. Q.; Warkentin, J.; Lusztyk, J. Δ^3-1,3,4-Oxadiazolines: Photochemical Precursors to Diazoalkanes and Sec-Alkanediazonium Ions in Acidic Solution. *J. Am. Chem. Soc.* **1997**, *119*, 1789−1790.
(36) Majchrzak, M. W.; Bekhazi, M.; Tse-Sheepy, I.; Warkentin, J. Photolysis of 2-Alkoxy-Δ^3-1,3,4-Oxadiazolines: A New Route to Diazoalkanes. *J. Org. Chem.* **1989**, *54*, 1842−1845.
(37) Greb, A.; Poh, J. S.; Greed, S.; Battilocchio, C.; Pasau, P.; Blakemore, D. C.; Ley, S. V. A Versatile Route to Unstable Diazo Compounds via Oxadiazolines and Their Use in Aryl-Alkyl Cross-Coupling Reactions. *Angew. Chem., Int. Ed.* **2017**, *56*, 16602−16605.
(38) Dingwall, P.; Greb, A.; Crespin, L. N. S.; Labes, R.; Musio, B.; Poh, J.-S.; Pasau, P.; Blakemore, D. C.; Ley, S. V. C-H Functionalisation of Aldehydes Using Light Generated, Non-Stabilised Diazo Compounds in Flow. *Chem. Commun.* **2018**, *54*, 11685−11688.
(39) Chen, Y.; Leonardi, M.; Dingwall, P.; Labes, R.; Pasau, P.; Blakemore, D. C.; Ley, S. V. Photochemical Homologation for the Preparation of Aliphatic Aldehydes in Flow. *J. Org. Chem.* **2018**, *83*, 15558−15568.
(40) Chen, Y.; Blakemore, D. C.; Pasau, P.; Ley, S. V. Three-Component Assembly of Multiply Substituted Homoallylic Alcohols and Amines Using a Flow Chemistry Photoreactor. *Org. Lett.* **2018**, *20*, 6569−6572.
(41) Strieth-Kalthoff, F.; James, M. J.; Teders, M.; Pitzer, L.; Glorius, F. Energy Transfer Catalysis Mediated by Visible Light: Principles, Applications, Directions. *Chem. Soc. Rev.* **2018**, *47*, 7190−7202.
(42) Strieth-Kalthoff, F.; Glorius, F. Triplet Energy Transfer Photocatalysis: Unlocking the Next Level. *Chem.* **2020**, *6*, 1888−1903.
(43) Mieusset, J. L.; Brinker, U. H. The Carbene Reactivity Surface: A Classification. *J. Org. Chem.* **2008**, *73*, 1553−1558.
(44) Sander, W.; Kötting, C.; Hübert, R. Super-Electrophilic Carbenes and the Concept of Philicity. *J. Phys. Org. Chem.* **2000**, *13*, 561−568.
(45) Bekhazi, M.; Warkentin, J. Thermolysis of 2-Metoxy-2,5,5-Trimethyl-Δ^3-1,3,4-Oxadiazoline. Carbenes from Thermal Fragmentation of a Carbonyl Ylide Intermediate. *J. Am. Chem. Soc.* **1981**, *103*, 2473−2474.
(46) Békhazi, M.; Warkentin, J. Reactions of Carbenes with Acetone. Reversible Thermal Formation and Fragmentation of Carbonyl Ylides and Their Cycloaddition to Acetone. *J. Am. Chem. Soc.* **1983**, *105*, 1289−1292.
(47) Adam, W.; Finzel, R. UV-Laser Photochemistry: Retro-Cleavage in the Benzophenone-Sensitized Photolysis of Δ^3-1,3,4-Oxadiazolines into Diazoalkanes. *Tetrahedron Lett.* **1990**, *31*, 863−866.
(48) Teegardin, K.; Day, J. I.; Chan, J.; Weaver, J. Advances in Photocatalysis: A Microreview of Visible Light Mediated Ruthenium and Iridium Catalyzed Organic Transformations. *Org. Process Res. Dev.* **2016**, *20*, 1156−1163.
(49) Montalti, M.; Credi, A.; Prodi, L.; Gandolfi, M. T. *Handbook of Photochemistry*, 3rd ed.; CRC Press: Boca Raton, 2006; p 266.
(50) Romero, N. A.; Nicewicz, D. A. Organic Photoredox Catalysis. *Chem. Rev.* **2016**, *116*, 10075−10166.
(51) Wessjohann, L. A.; Brandt, W.; Thiemann, T. Biosynthesis and Metabolism of Cyclopropane Rings in Natural Compounds. *Chem. Rev.* **2003**, *103*, 1625−1648.
(52) Sarkar, T.; Das, B. K.; Talukdar, K.; Shah, T. A.; Punniyamurthy, T. Recent Advances in Stereoselective Ring Expansion of Spirocyclopropanes: Access to the Spirocyclic Compounds. *ACS Omega* **2020**, *5*, 26316−26328.
(53) Zheng, Y.; Tice, C. M.; Singh, S. B. The Use of Spirocyclic Scaffolds in Drug Discovery. *Bioorg. Med. Chem. Lett.* **2014**, *24*, 3673−3682.
(54) Zheng, Y.-J.; Tice, C. M. The Utilization of Spirocyclic Scaffolds in Novel Drug Discovery. *Expert Opin. Drug Discovery* **2016**, *11*, 831−834.

https://doi.org/10.1021/acscatal.2c05319
ACS Catal. 2023, 13, 1964−1973

Supporting Information

UV Light is no Longer Required for the Photoactivation of 1,3,4-Oxadiazolines

Katarzyna Orłowska,[a] João V. Santiago,[a] Piotr Krajewski,[a,b] Kacper Kisiel,[a] Irena Deperasińska,[c] Katarzyna Zawada,[d] Wojciech Chaładaj,[a,*] Dorota Gryko [a,*]

[a]Institute of Organic Chemistry Polish Academy of Sciences, Kasprzaka 44/52, 01-224 Warsaw, Poland

[b]Department of Chemistry, Warsaw University of Technology, Noakowskiego 3, 00-664 Warsaw, Poland

[c]Institute of Physics Polish Academy of Sciences, Al. Lotników 32/46, 02-668 Warsaw, Poland

[d]Faculty of Pharmacy with the Laboratory Medicine Division, Department of Physical Chemistry, Medical University of Warsaw, Banacha 1, 02-097 Warsaw, Poland

correspondence:

dorota.gryko@icho.edu.pl

wojciech.chaladaj@icho.edu.pl

Table of contents

1. General Information

Materials

All solvents and commercially available reagents were purchased from Sigma-Aldrich, TCI, Acros Organics as reagent grade and were used without further purification, unless otherwise stated. Photocatalysts **6**, **14-18** were purchased from Strem Chemicals. Thioxanthone (**19**) was purchased from Sigma Aldrich and xanthone (**20**) from TCI. Dry solvents were taken from Solvent Purification System (SPS) or purchased from Sigma Aldrich. All deuterated solvents used were purchased from Eurisotop.

General Procedures

Unless otherwise noted, reactions were performed without the exclusion of air or moisture. All the photochemical reactions were performed in 10 mL glassy vials sealed with aluminum caps containing a rubber septum. Reactions were monitored by thin layer chromatography (TLC), using 0.20 mm Merck silica plates (60F-254) and visualized using UV-light, potassium permanganate, cerium molybdate or anisaldehyde stain, with heat as a developing agent. Colum chromatography was performed on Merck silica gel 60 (230-400 mesh). GC yields were calibrated with dodecane as an internal standard. All yields determined by ^{1}H NMR analysis were obtained using dibromomethane as the internal standard. Isolated yields refer to spectroscopically (^{1}H NMR) homogeneous materials.

Instrumentation

NMR spectra were recorded at ambient temperature (unless otherwise stated) on Bruker 400 MHz or Varian 500, 600 MHz. Chemical shifts are reported in ppm relative to the tetramethyl silane signal or a residual undeuterated solvent peak (TMS 0 ppm for ^{1}H and ^{13}C, $CHCl_3$ – 7.26 ppm for ^{1}H and 77.16 ppm for ^{13}C, $(CD_3)_2CO$ – 2.05 ppm for ^{1}H and 29.8 ppm for ^{13}C, CD_2Cl_2 – 5.32 ppm for ^{1}H and 53.5 ppm for ^{13}C, $(CD_3)_2SO$ – 2.49 ppm for ^{1}H and 39.7 ppm for ^{13}C). Multiplicities are given as: singlet (s), doublet (d), triplet (t), quartet (q), multiplet (m) broad singlet (brs).
LR and HRMS. Low-resolution mass spectra (LRMS) were recorded on an Applied Biosystems API 365 mass spectrometer using electrospray ionization (ESI) technique. High-resolution mass spectra (HRMS) were recorded on Waters SYNAPT G2-S HDMS instrument using electrospray ionization (ESI) or atmospheric-pressure chemical ionization (APCI) with time-of-flight detector (TOF).
Elemental analysis (C, H, N) were performed using a PERKIN-ELMER 240 Elemental Analyzer.
Melting points were recorded on a Marienfeld MPM-H2 melting point apparatus and are uncorrected.
Cyclic voltammograms were recorded using Bio-Logic SP-50 potentiostate.
UV-Vis absorption spectra were recorded on UV-3600i Plus UV-Vis-NIR Spectrophotometer.
Fluorescence measurements were performed on Edinburgh Instruments FS5 Spectrofluorometer.
GC-MS analyses were performed using Shimadzu GCMS-QP2010 SE gas chromatograph with FID detector and Zebron ZB 5MSi column (length: 30.0 m; thickness: 0.25 um, diameter: 0.25 mm). **GC program:**

- time: 14.92 min;
- pressure: 90.8 kPa;
- total flow: 5.3mL/min;
- column flow: 1.11 mL/min;
- linear velocity: 27.5 cm/s;
- purge flow: 2.0 mL/min;
- split ratio: 2.0.

	Rate	Final Temperature	Hold Time
0	-	50.0	2.00
1	40.00	80.0	2.00
2	40.00	120.0	1.00
3	45.00	150.0	1.00
4	50.00	200.0	1.00
5	50.00	325.0	2.00

Preparative HPLC separations were performed using Knauer HPLC chromatograph with PDA detector and Preparative column chromatography Knauer EII 100-10 Si column (250 x 20 mm).
UV photoreactor Rayonet Model RPR-200 (wave length 254 nm) was employed to perform UV experiments.
Microwave assisted synthesis was performed using microwave oven CEM Discover-SP ActiVent in a sealed reaction vessel.

2. Photoreactor Setups

Light-mediated reactions studies (with an exception of photocatalyzed O-H insertion reactions) were carried out in UOSlab Miniphoto photoreactor (Figure F1). Blue (emission maximum at 450 nm) or violet (emission maximum at 405 nm) light was supplied to each reaction vial with the use of 7 LUMINUS LED units (of overall 25 W intensity when 100% power applied). The ambient temperature of LED block was maintained by cooling with Huber MiniChiller 300.

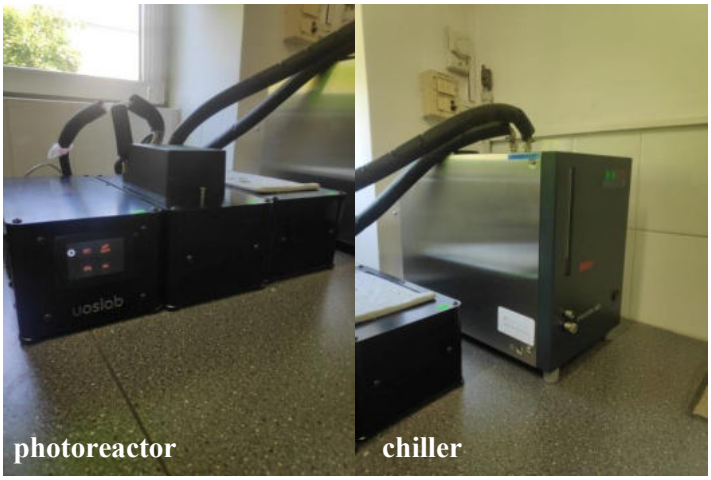

Figure F1. Standard photoreactor setup with chiller.

EPR experiments and 1 mmol scale synthesis of spirocyclopropane **1** were performed on a home-made photoreactor provided with 10 W blue light with emission maximum at 455 nm (Figure F2). The reaction mixture was cooled with a fan.

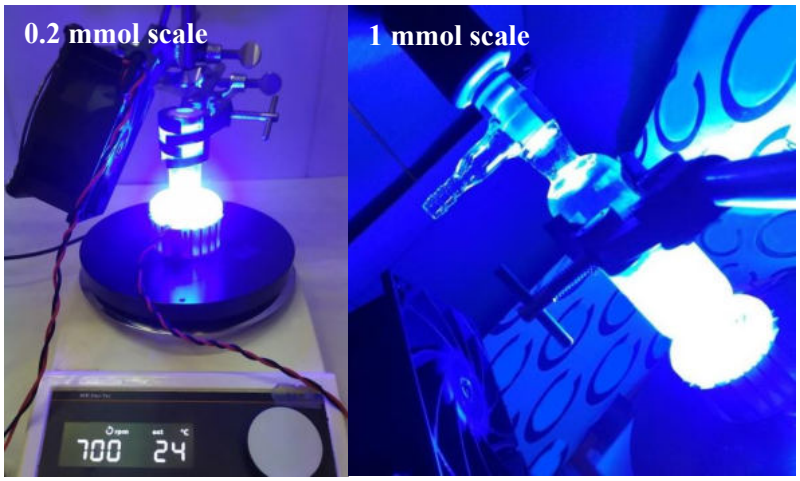

Figure F2. Home-made photoreactor cooled with a fan.

Experiment with irradiation on UV light (265 nm) was carried out with the use of Rayonet Model RPR-200 (wavelength 254 nm) photoreactor.

Preliminary studies on photosensitized O-H insertion reactions were carried out in a specially constructed photoreactor composed of cooling block (connected to Huber MiniChiller 300) and plate with blue LEDs of 7 W power with maximum emission at 446 nm (Figure F3).

Figure F3. Blue LEDs plate photoreactor.

3. General synthetic procedures

3.1. Preparation of 1,3,4-oxadiazolines

3.1.1. General procedure for the synthesis of 2,2-dimetoxy analogues

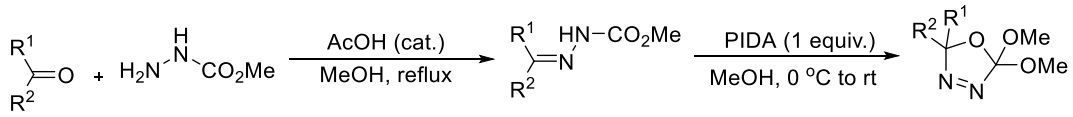

A solution of the corresponding ketone (1.0 equiv.), methyl hydrazinocarboxylate (1.1 equiv.) and acetic acid (0.03 equiv.) in methanol (c = 1.0 M for ketone) was refluxed for 1 h. After cooling the reaction mixture, water and DCM were added, layers were separated, and aqueous layer was washed with DCM. Combined organic layers were dried over sodium sulfate, filtrated, and evaporated *in vacuo*. Thus obtained hydrazone was dissolved in MeOH (c = 0.5 M) and (diacetoxyiodo)benzene (PIDA, 1.0 equiv.) was added portionwise over 10 minutes at 0 °C. The cooling bath was removed, and the reaction mixture was stirred for 1 h at ambient temperature. After that time, the crude reaction mixture was washed with saturated aqueous $NaHCO_3$ (3 x 25 mL). The organic layer was dried over sodium sulfate, filtrated, concentrated *in vacuo* and purified by column chromatography using hexanes/ethyl acetate to afford final product.

Note: The hydrazone synthesis may be performed under rt instead of 65 °C, however upon prolonged reaction times (reaction left overnight). In case the oxidation of hydrazone with PIDA is not completed after 1 hour, the addition of extra portion of PIDA (0.2 equiv.) is advised.

3.1.2. Synthesis of oxadiazolines 2-5

*Procedure for the synthesis of 3-(benzylthio)-3-methoxy-4-oxa-1,2-diazaspiro[4.5]dec-1-ene (**2**)*

Oxadiazoline obtained according to the slightly modified method reported by Warkentin.[1]

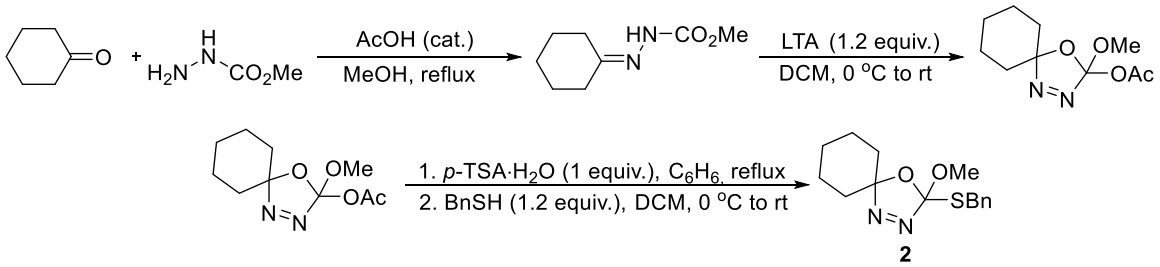

A solution of cyclohexanone (1.0 equiv., 20.0 mmol, 2.1 mL), methyl hydrazinocarboxylate (1.1 equiv., 22.0 mmol, 2.0 g) and acetic acid (0.03 equiv., 0.6 mmol, 34 µL) in methanol (8.0 mL, c = 2.5 M for cyclohexanone) was refluxed for 1 h. Then, water and DCM were added, layers were separated, and the aqueous layer was washed with DCM. Combined organic layers were dried over sodium sulfate, filtrated, and evaporated *in vacuo* to give cyclohexanone hydrazone. Thus obtained hydrazone was subsequently dissolved in DCM (8.0 mL, c = 2.5 M) and added dropwise over 1 h to the pre-cooled (0 °C) solution of lead tetraacetate (LTA, 1.2 equiv., 24.0 mmol, 10.6 g) and acetic acid (0.1 equiv., 2.0 mmol, 114 µL) in DCM (6.0 mL, c = 4.0 M for LTA). The cooling bath was removed, and the reaction mixture was stirred for additional 1 h at ambient temperature. After that time, the crude reaction mixture was filtered through celite and the filtrate was washed with saturated aqueous $NaHCO_3$ (2 x 25 mL). Aqueous layers were washed with DCM (2 x 25 mL) and combined organic layers were dried over

sodium sulfate, filtrated, and concentrated *in vacuo* to afford 2-acetoxy-2-methoxy-5,5-dimethyl-3-oxadiazoline (9.6 mmol, 2.18 g, 48% yield) contaminated with 17% of diazine by-product (as detected by NMR). Thus obtained mixture was used in the next step.

A solution of *p*-toluenesulfonic acid monohydrate (*p*-TSA·H_2O, 13.5 mol%, 1.3 mmol, 0.25 g) in benzene (10 mL, c = 0.13 M) was refluxed for 1 h in a Dean-Stark apparatus containing molecular sieves in the water trapping arm. After cooling to an ambient temperature, a solution of 2-acetoxy-2-methoxy-5,5-dimethyl-3-oxadiazoline (9.6 mmol, contaminated with 17% of diazine) and benzyl mercaptan (11.5 mmol, 1.2 equiv., 1.4 mL) in dichloromethane (7 mL, c = 1.4 M) was added and the mixture was further refluxed under argon overnight. After that time, the solution was cooled and KOH pellets (ca. 0.5 g) were added, and the mixture was stirred for additional 2 h. Subsequently, the reaction mixture was washed with water (3 x 25 mL) and the organic layer was dried over sodium sulfate, filtrated, concentrated *in vacuo* and purified by the column chromatography using hexanes/ethyl acetate to afford of final product as colorless oil (1.2 mmol, 340 mg, 13% yield).

*Procedure for the synthesis of 3-methoxy-3-methyl-4-oxa-1,2-diazaspiro[4.5]dec-1-ene (**3**)*

Oxadiazoline obtained according to the slightly modified method reported by Ley.[2]

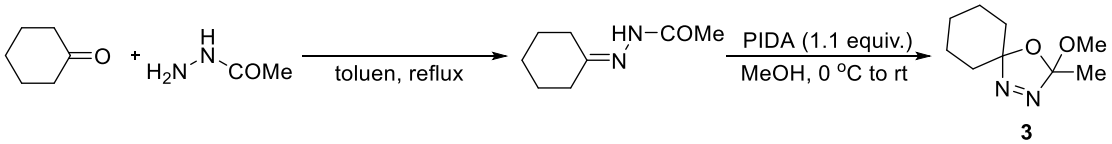

3

A solution of cyclohexanone (1.0 eq., 5.0 mmol, 0.52 mL) and acetic hydrazide (1.1 equiv., 5.5 mmol, 0.41 g) in toluene (15 mL, c = 0.33 M) was refluxed for 3 h. After that time, the mixture was cooled down, evaporated *in vacuo,* and subsequently dissolved in MeOH (7 mL, c = 0.7 M). The solution was cooled to 0 °C and (diacetoxyiodo)benzene (PIDA, 1.10 equiv., 5.50 mmol, 1.77 g) was added portionwise over 10 minutes. The cooling bath was removed, and the reaction mixture was stirred for 1 h at ambient temperature. Then, the crude reaction mixture was washed with saturated aqueous $NaHCO_3$ (3 x 25 mL). The organic layer was dried over sodium sulfate, filtrated, concentrated *in vacuo* and purified by column chromatography using hexanes/ethyl acetate to afford final product as colorless oil (4.50 mmol, 835 mg , 91%).

*Procedure for the synthesis of 3-methoxy-3-phenyl-4-oxa-1,2-diazaspiro[4.5]dec-1-ene (**4**)*

Hydrazone was obtained according to the procedure reported by Andrade.[3]

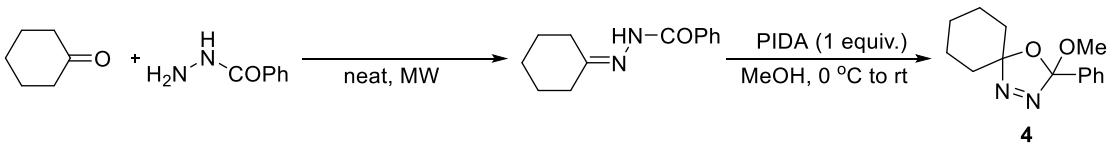

4

A neat mixture of cyclohexanone (1.0 eq., 5.0 mmol, 0.52 mL) and benzoyl hydrazide (1.0 equiv., 5.0 mmol, 0.68 g) was placed in a quartz tube and located in microwave reactor. The reaction was performed at 200 W for 5 min with the final temperature T = 152 °C. After that time, the solid formed was filtrated under reduced pressure and washed with dietyl ether. Thus obtained hydrazone was dissolved in MeOH (9 mL, c = 0.56 M) and the solution was cooled to 0 °C. Then, (diacetoxyiodo)benzene (PIDA, 1.0 equiv., 5.0 mmol, 1.61 g) was added portionwise over 10 minutes. The cooling bath was removed, and the reaction mixture was stirred for 1 h at ambient temperature. The

crude reaction mixture was washed with saturated aqueous $NaHCO_3$ (3 x 25 mL). The organic layer was dried over sodium sulfate, filtrated, concentrated *in vacuo* and purified by column chromatography using hexanes/ethyl acetate to afford final product as colorless oil (4.5 mmol, 1.11 g , 90%).

*Procedure for the synthesis of 1-(1,6-dioxa-4,13,14-triazadispiro[4.1.5^7.2^5]tetradec-13-en-4-yl) ethan-1-one (**5**)*

Oxadiazoline obtained according to the slightly modified method reported by Warkentin.[4]

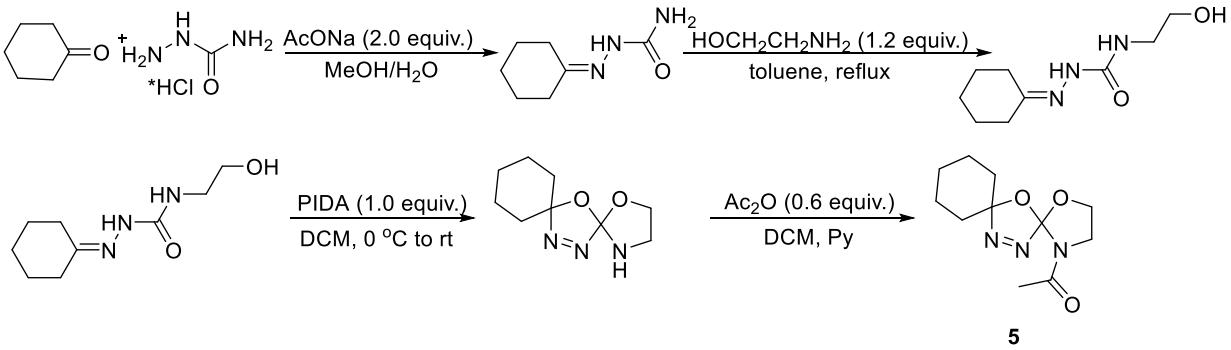

5

To a solution of semihydrazide hydrochloride (10.0 mmol, 1.12 g) and sodium acetate (20.0 mmol, 1.68 g) in water (10 mL, c = 1.0 M for semihydrazide hydrochloride), cyclohexanone was added (10 mmol, 1.0 mL) and the mixture was stirred vigorously for 10 minutes. After that time, precipitate formed was filtrated under reduced pressure, washed with cold water and dried to give semicarbazone as white solid (8.50 mmol, 1.32 g, 85% yield). Thus, obtained semicarbazone was dissolved in toluene (10 mL, c = 0.85 M) and etanoloamine was added (1.2 equiv., 10.2 mmol, 0.62 mL). The reaction mixture was refluxed under argon overnight (ca. 18 h). Then, the solution was cooled down and the precipitate formed was filtrated under reduced pressure and washed with diethyl ether to afford 2-hydroxyethyl semicarbazone as white solid (4.51 mmol, 0.90 g, 53% yield). The solid was further dissolved in DCM (5.0 mL, c = 0.90 M) and the solution was cooled down to 0 °C. (Diacetoxyiodo) benzene (PIDA, 1.0 equiv., 4.51 mmol, 1.45 g) was added over 1 h portionwise. The reaction temperature was kept 0 °C for additional 2 h and after that the cooling bath was removed and the mixture was stirred overnight at ambient temperature. Then, the crude reaction mixture was washed with saturated aqueous $NaHCO_3$ (3 x 25 mL). The organic layer was dried over sodium sulfate, filtrated, concentrated *in vacuo* and purified by column chromatography using hexanes/ethyl acetate to afford final product as colorless oil (2.89 mmol, 570 mg, 64%). Subsequently NH-oxadiazoline was dissolved in DCM (5.0 mL, c = 0.59 M) followed by the addition of pyridine (0.29 mmol, 23 μL). The mixture was stirred at ambient temperature for 5 min, then acetic anhydride (1.72 mmol, 0.163 mL) was added dropwise. After addition, the reaction was allowed to stir for 30 min, then the solution was diluted with DCM (5.0 mL) and washed with water (10 mL), aqueous $NaHCO_3$ (5%) (10 mL) and brine (10 mL). The organic layer was dried over sodium sulfate, filtrated, concentrated *in vacuo* and purified by column chromatography using hexanes/ethyl acetate to afford final product **5** as white solid (2.37 mmol, 567 mg, 82% yield).

3.2. Preparation of electron-deficient olefins

Electrophilic alkenes **S1**, **S2** and **S4-S9** were prepared according to literature procedures.

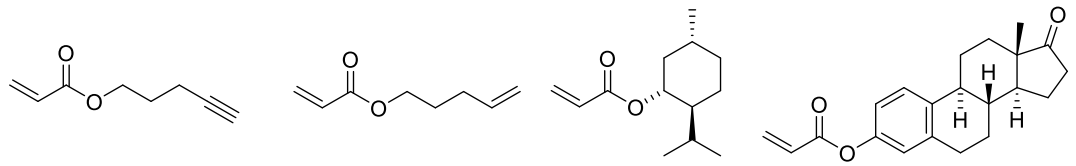

S1[5] **S2**[6] **S3**[7] **S4**[8]

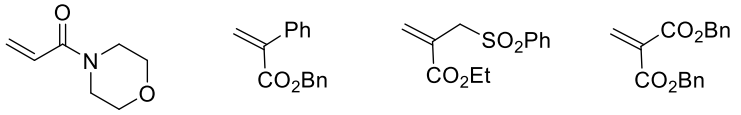

S5[9] **S6**[10] **S7**[11] **S8**[12]

*Procedure for the synthesis of 4-cyanophenyl acrylate (**S9**)*

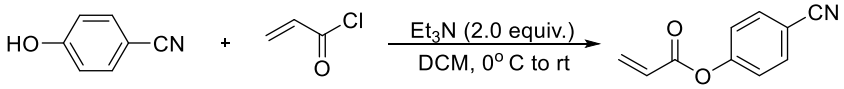

S9

To a stirred solution of 4-cyanophenol (1.5 equiv., 3.0 mmol, 0.36 g) and triethylamine (2.0 equiv., 4.0 mmol, 0.56 mL) in dry DCM (2.0 mL, c = 1.0 M for 4-cyanophenol), cooled to 0 °C, acryloyl chloride (1.0 equiv., 2.0 mmol, 0.16 mL) was added dropwise under argon atmosphere. The mixture was stirred at 0 °C for 30 min and subsequently warmed to room temperature and stirred for additional 6 h. After this time, the reaction mixture was diluted with DCM, and washed with 1 M HCl, 10% NaOH and brine. The organic layer was dried over Na_2SO_4, filtrated, and concentrated under reduced pressure. The crude product was purified by column chromatography (AcOEt/Hexanes) to afford compound **S9** as white solid (2.7 mmol, 0.31 g, 90% yield).

3.3 General procedure for the blue light-induced, photosensitized cyclopropanation of electron-poor olefins with 1,3,4-oxadiazolines

A glass vial equipped with a stirring bar and sealed with an aluminum cap with a rubber septum was charged with $Ir[dF(CF_3)ppy)_2(dtbpy)]PF_6$ (**6**, 0.25 mol%, 0.6 mg) dissolved in 4.0 mL of DCM (p.a. grade). The oxygen was removed from the solution by freeze-pump-thaw technique. Then oxadiazoline (0.4 mmol, 2 equiv.) and electron-deficient olefin (0.2 mmol) were added under argon atmosphere (if liquid, if solid – added prior DCM). The reaction mixture was placed in a photoreactor and irradiated with blue LED (450 nm, 25 W) for 1 h. After that time, the crude reaction mixture was concentrated *in vacuo* and purified by column chromatography using ethyl acetate/hexanes or acetone/hexanes to afford the final product.

*Note: The reaction proceeds in the presence of air atmosphere, however in a diminished yield (*Δ ~20%*).*

3.4. Representative procedure for the synthesis on 1 mmol scale

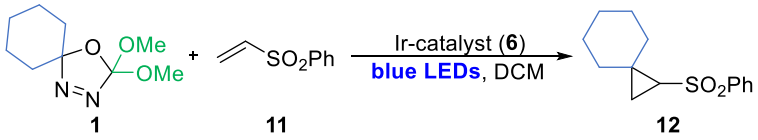

A Schlenk flask equipped with a stirring bar was charged with Ir[dF(CF$_3$)ppy)$_2$(dtbpy)]PF$_6$ (**6**, 0.25 mol%, 3.0 mg), phenyl-vinyl sulfone (**11**, 1.00 mmol, 168 mg) dissolved in 20.0 mL of DCM (p.a. grade). The oxygen was removed from the solution by freeze-pump-thaw technique. Then oxadiazoline **1** (2.0 mmol, 2 equiv., 360 µL, 400 mg) was added under argon atmosphere. The reaction mixture was placed ca. 1 cm above home-made photoreactor (Figure S2, 10 W) and irradiated with blue LED (455 nm, 10 W) for 5 h. After that time, the crude reaction mixture was concentrated *in vacuo* and purified by column chromatography (gradually from 5:95 to 1:9 v/v, ethyl acetate/hexanes) to afford 198 mg (0.8 mmol, **Yield = 79%**) of product **12** as white solid.

3.5 General procedure for the blue light-induced, photosensitized O–H insertion of carboxylic acids with 1,3,4-oxadiazolines

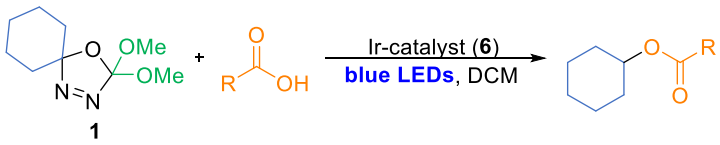

A glass vial equipped with a stirring bar and sealed with an aluminum cap with a rubber septum was charged with Ir[dF(CF$_3$)ppy)$_2$(dtbpy)]PF$_6$ (**6**, 0.25 mol%, 0.3 mg) dissolved in 1.0 mL of DCM (p.a. grade). The oxygen was removed from the solution by freeze-pump-thaw technique. Then oxadiazoline (0.2 mmol, 2 eq.) and carboxylic acid (0.1 mmol) were added under argon atmosphere (if liquid; if solid – added prior DCM). The reaction mixture was placed in a photoreactor and irradiated with blue LED (446 nm, 7 W) for 1.5 h. After that time, the crude reaction mixture was concentrated *in vacuo* and purified by column chromatography using ethyl acetate/hexanes to afford the final product.

3.6 General procedure for the blue light-induced, photosensitized functionalization of aldehyde

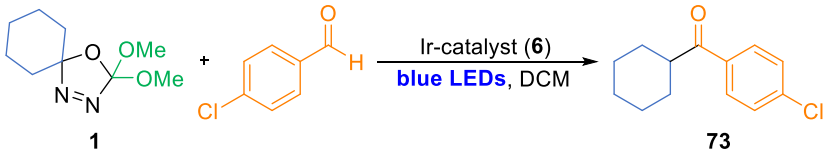

A glass vial equipped with a stirring bar and sealed with an aluminum cap with a rubber septum was charged with Ir[dF(CF$_3$)ppy)$_2$(dtbpy)]PF$_6$ (**6**, 0.25 mol%, 0.6 mg) and *p*-chlorobenzaldehyde (28 mg, 0.2 mmol) dissolved in 4.0 mL of DCM (p.a. grade). The solution was purged with argon. Then oxadiazoline **1** (1.0 mmol, 5 equiv., 180 µL) was added under argon atmosphere. The reaction mixture was placed in a photoreactor and irradiated with blue LED (450 nm, 25 W) for 2.5 h. After that time, the crude reaction mixture was concentrated *in vacuo* and purified by column chromatography using ethyl acetate/hexanes to afford 35 mg (0.16 mmol, **Yield = 78%**).of product **73** as colorless oil.

3.7 General procedure for the blue light-induced, photosensitized cyclopropenation

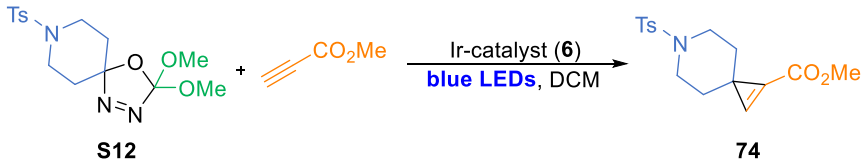

S12 **74**

A glass vial equipped with a stirring bar and sealed with an aluminum cap with a rubber septum was charged with Ir[dF(CF_3)ppy)$_2$(dtbpy)]PF_6 (**6**, 0.25 mol%, 0.6 mg) and oxadiazoline **S12** (143 mg, 0.4 mmol, 2 equiv.) dissolved in 4.0 mL of DCM (p.a. grade). The solution was purged with argon. Then alkyne (0.2 mmol, 18 µL) was added under argon atmosphere. The reaction mixture was placed in a photoreactor and irradiated with blue LED (450 nm, 25 W) for 1 h. After that time, the crude reaction mixture was concentrated *in vacuo* and purified by column chromatography using acetone/hexanes to afford product **74** as white solid (0.04 mmol, product of low stability, **Yield = 19%**, obtained from NMR spectra of crude reaction mixture using 1,3,5-trimetoxybenzene as internal standard).

4. Photosensitized decomposition of 5,5-cyclohexylidene- 2,2-dimetoxy-1,3,4-oxadiazoline (1)

Table T1. Blue-light induced decomposition of oxadiazoline **1**.

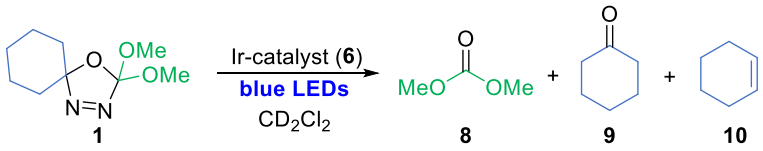

entry	deviation	Conversion of **1** [%][a]	Yield of **8** [%][a]	Yield of **9** [%][a]	Yield of **10** [%][a]
1	no catalyst **6**	<5	0	0	0
2	air atmosphere[b]	93	79	32	4
3	none	95	81	21	36

[a]based on NMR measurements with dibromomethane as internal standard; [b]reaction was not degassed.

*Photosensitized decomposition of oxadiazoline **1** - procedure:*

A glass vial equipped with a stirring bar and sealed with an aluminum cap with a rubber septum was charged with Ir[dF(CF_3)ppy)$_2$(dtbpy)]PF_6 (**6**, 0.5 mol%, 0.6 mg) dissolved in 0.5 mL of CD_2Cl_2. The oxygen was removed from the solution by freeze-pump-thaw technique and oxadiazoline **1** was added under argon atmosphere (0.1 mmol, 36 µL, 40 mg). The reaction mixture was placed in a photoreactor and irradiated with blue LEDs (450 nm, 25 W) overnight. Then, dibromometane as internal standard was added and the NMR measurements were performed.

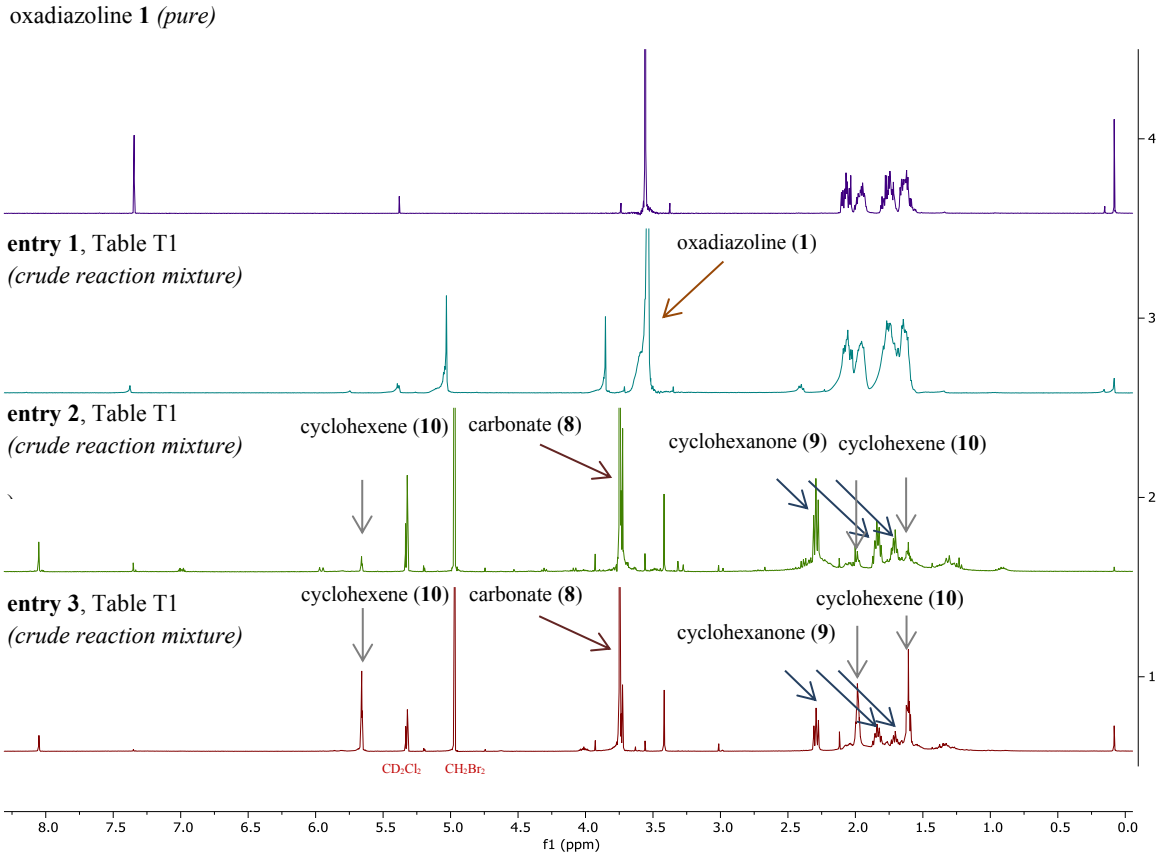

Figure F4. NMR spectra as evidence of the photocatalyzed decomposition of oxadiazoline **1**.

5. Optimization details

5.1. Model reaction

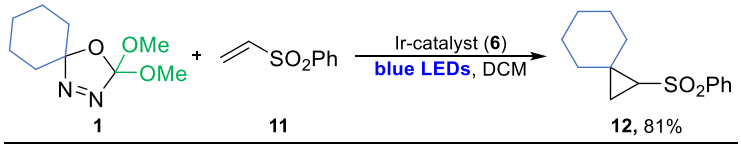

Optimal reaction conditions: Ir[dF(CF$_3$)ppy)$_2$(dtbpy)]PF$_6$ (**6**, 0.25 mol%), oxadiazoline **1** (0.2 mmol, 2 equiv.), phenyl vinyl sulfone (**11**, 0.1 mmol), DCM (c = 0.05 M), blue LEDs (450 nm, 25 W), Ar atmosphere, 25 °C, 1 h.

5.2. Background reactions

Entry	Deviations from tested conditions	Yield of **12** [%][a]
1	none	38 (41)[b]
2	no light	0
3	no Ir-catalyst (**6**)	0
4	no light, no Ir-catalyst (**6**)	0
5	air atmosphere (reaction was not degassed)	31
6	no light, no catalyst (**6**), dry toluene, 110 °C	0
7	UV light (265 nm) instead of blue LEDs	14

Reaction conditions: Ir[dF(CF$_3$)ppy)$_2$(dtbpy)]PF$_6$ (**6**, 1.0 mol%), oxadiazoline **1** (0.5 mmol, 5.0 equiv.), phenyl vinyl sulfone (**11**, 0.1 mmol), DCM dry (c = 0.05 M), blue LEDs (450 nm, 25 W), Ar atmosphere, 18 °C, 17 h; [a]GC yield; [b]isolated yield in parenthesis.

5.3. Influence of the substrates' ratio

Entry	**1** : **11** ratio	Yield of **12** [%][a]
1	10 : 1	18
2	5 : 1	38
3	4 : 1	36
4	3 : 1	57
5	2 : 1	67
6	1.75 : 1	49
7	1.5 : 1	47
8	1 : 1	27
9	1 : 2	51
10	1 : 5	52

Reaction conditions: Ir[dF(CF$_3$)ppy)$_2$(dtbpy)]PF$_6$ (**6**, 1.0 mol%), oxadiazoline **1** (*x* mmol) phenyl vinyl sulfone (**11**, *y* mmol), 0.1 mmol scale, DCM dry (c = 0.05 M), blue LEDs (450 mm, 25 W), Ar atmosphere, 18 °C, 17 h; [a]GC yield.

5.4. Influence of the photocatalyst

Entry	Photocatalyst	Yield of **12** [%][a]
1	$Ir[dF(CF_3)ppy)_2(dtbpy)]PF_6$	67
2[b]	$Ir[dF(CF_3)ppy)_2(dtbpy)]PF_6$	50
3	$Ir(ppy)_3$	traces
4	$Ir[(dtbbpy)(ppy)_2]PF_6$	traces
5	$Ir[(dF(Me)ppy)_2(dtbppy)]PF_6$	50
6[b]	$Ir[(dF(Me)ppy)_2(dtbppy)]PF_6$	26
7	$Ir[(dF(CF_3)ppy)_2(bpy)]PF_6$	49
8[b]	$Ir[(dF(CF_3)ppy)_2(bpy)]PF_6$	60
9	$Ru(bpy)_3Cl_2 \cdot 6H_2O$	0
10	*t*-BuMesAcr$^+BF_4^-$	0
11[c]	4-CzIPN	14
12	TPP	0
13	Methylene Blue	0
14	Thioxantone	37
15[b]	Thioxantone	57
16[b,d]	Xanthone	25

Reaction conditions: *catalyst* (1.0 mol%), oxadiazoline **1** (0.2 mmol, 2 equiv.), phenyl vinyl sulfone (**11**, 0.1 mmol), DCM dry (*c* = 0.05 M), blue LED (450 nm, 25 W), Ar atmosphere, 18 °C, 17 h; [a]GC yield; [b]violet LEDs instead of blue (405 nm, 25 W); [c]5 mol% of catalyst loading; [d]2.5 mol% of catalyst loading.

5.5. Influence of the solvent

Entry	Solvent	Yield of **12** [%][a]
1	DCM dry	67
2	DCM	65
3	DCE dry	46
4	DCE	47
5	dioxane	8
6	ethyl acetate	62
7	toluene	16
8	$CHCl_3$ dry	64
9	$CHCl_3$	62
10	THF	41
11	acetone	28
12	MeOH	9
13	DMSO	7
14	CH_3CN	53

Reaction conditions: $Ir[dF(CF_3)ppy)_2(dtbpy)]PF_6$ (**6**, 1.0 mol%), oxadiazoline **1** (0.2 mmol, 2 equiv.), phenyl vinyl sulfone (**11**, 0.1 mmol), *solvent* (c = 0.05 M), blue LED (450 nm, 25 W), Ar atmosphere, 18 °C, 17 h; [a]GC yield.

5.6. Influence of the olefin concentration

Entry	Concentration	Yield of **12** [%][a]
1	0.2 M	24
2	0.1 M	40
3	0.07 M	46
4	0.05 M	67
5	0.04 M	62
6	0.025 M	65

Reaction conditions: $Ir[dF(CF_3)ppy)_2(dtbpy)]PF_6$ (**6**, 1.0 mol%), oxadiazoline **1** (0.2 mmol, 2.0 equiv.), phenyl vinyl sulfone (**11**, 0.1 mmol), DCM dry (*c = x M*), blue LED (450 nm, 25 W), Ar atmosphere, 18 °C, 17 h; [a]GC yield.

5.7. Influence of the light intensity

Entry	Light power	Yield of **12** [%][a]
1	25 W	67
2	19 W	65
3	12 W	63

Reaction conditions: $Ir[dF(CF_3)ppy)_2(dtbpy)]PF_6$ (**6**, 1.0 mol%), oxadiazoline **1** (0.2 mmol, 2.0 equiv.), phenyl vinyl sulfone (**11**, 0.1 mmol), DCM dry (c = 0.05 M), blue LED (450 nm, *x W*), Ar atmosphere, 18 °C, 17 h; [a]GC yield.

5.8. Influence of the reaction time

Entry	Reaction time	Yield of **12** [%][a]
1	5 min	55
2	15 min	64
3	45 min	66
4	1 h	69
5	4 h	68
6	17 h	67

Reaction conditions: $Ir[dF(CF_3)ppy)_2(dtbpy)]PF_6$ (**6**, 1.0 mol%), oxadiazoline **1** (0.2 mmol, 2.0 equiv.), phenyl vinyl sulfone (**11**, 0.1 mmol), DCM dry (c = 0.05 M), blue LED (450 nm, 25 W), Ar atmosphere, 18 °C, *x h*; [a]GC yield.

5.9. Influence of temperature

Entry	Temperature[a]	Yield of **12** [%][b]
1	18 °C	69
2	25 °C	71

Reaction conditions: $Ir[dF(CF_3)ppy)_2(dtbpy)]PF_6$ (**6**, 1.0 mol%), oxadiazoline **1** (0.2 mmol, 2.0 equiv.), phenyl vinyl sulfone (**11**, 0.1 mmol), DCM dry (c = 0.05 M), blue LED (450 nm, 25 W), Ar atmosphere, *x °C*, 1 h; [a]temperature measured on LEDs block of photoreactor; [b]GC yield.

5.10. Influence of the catalyst loading

Entry	Catalyst loading	Yield of **12** [%][a]
1	1 mol%	71
2	0.5 mol%	79[b]
3	0.25 mol%	81[b]
4	0.1 mol%	65

Reaction conditions: $Ir[dF(CF_3)ppy)_2(dtbpy)]PF_6$ (**6**, *x mol%*), oxadiazoline **1** (0.2 mmol, 2.0 equiv.), phenyl vinyl sulfone (**11**, 0.1 mmol), DCM dry (c = 0.05 M), blue LED (450 nm, 25 W), Ar atmosphere, 25 ^oC, 1 h; [a]GC yield; [b]isolated yield.

6. Mechanistic studies

6.1. Proposed mechanism

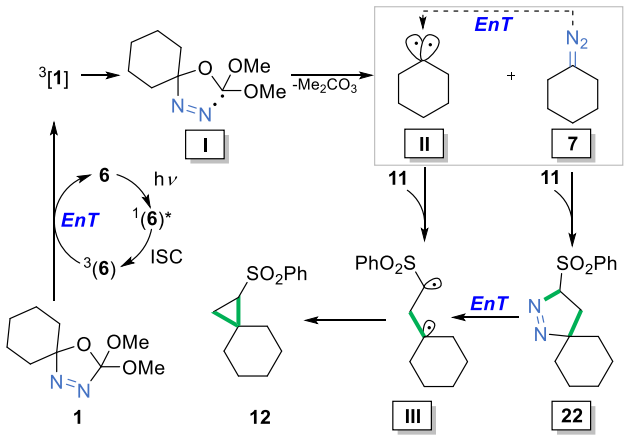

Scheme S1. Proposed mechanism of Ir-catalyzed spirocyclopropane synthesis.

6.2. UV-Vis spectra of starting materials

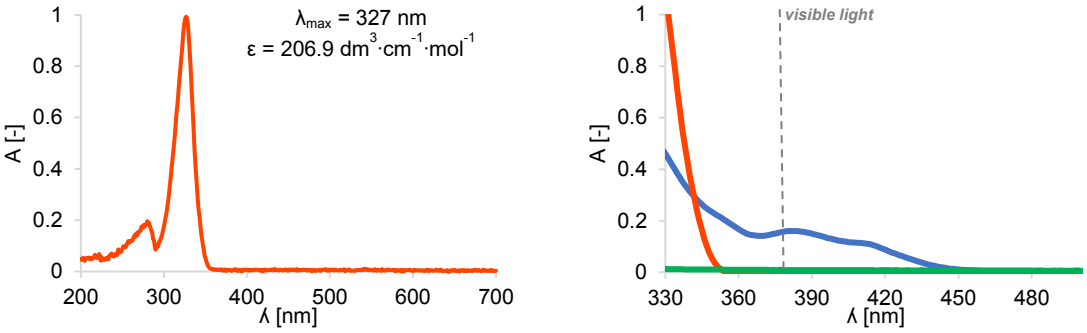

Figure F5. a) Oxadiazoline **1** UV-Vis spectrum (c = 4.8 mM in DCE). **b)** Absorbance of model starting materials in visible range, Ir[dF(CF$_3$)ppy)$_2$(dtbpy)]PF$_6$ (**6**, c = 25 μM in DCE), oxadiazoline **1** (c = 0.1 M in DCE), phenyl-vinyl sulfone **11** (c = 0.1 M in DCE).

Conclusion:

Starting materials **1** and **11** do not absorb light in the visible range, therefore direct photolysis of **1** on blue light is not possible (blue LEDs in UOSLAB photoreactor feature emission maximum at 450 nm). However, applied Ir-complex **6** absorbs light in violet range and though blue LEDs have maximum of emission at 450 nm (where absorption coefficient of catalyst **6** is negligible), they also emit radiation of lower intensity ca. +/- 50 nm to 450 nm and thus excitation of the catalyst **6** is likely to occur. Similarly, application of violet LEDs (maximum at 405 nm, emitting radiation in 405 nm +/- 50 nm range) may lead to direct photolysis of oxadiazoline **1** which absorbs in $\lambda \leq 360$ nm.

6.3. CV studies

Measurement conditions :

A cylindrical three-electrode cell was equipped with a glassy carbon working electrode, a 25 mm platinum wire as the counter electrode, and Ag/AgCl (3.0 M NaCl) electrode as the reference electrode. A typical scan rate used for measurements was 100 $mV \cdot s^{-1}$. The solutions of oxadiazolines **1-5** and **S10-S12** (c = 0.1 M) containing *n*-Bu_4NClO_4 as electrolyte (c = 0.1 M) in dry MeCN were deaerated by Ar gas bubbling before the measurements, and the cyclic voltammetry was carried out under an Ar gas atmosphere at room temperature.

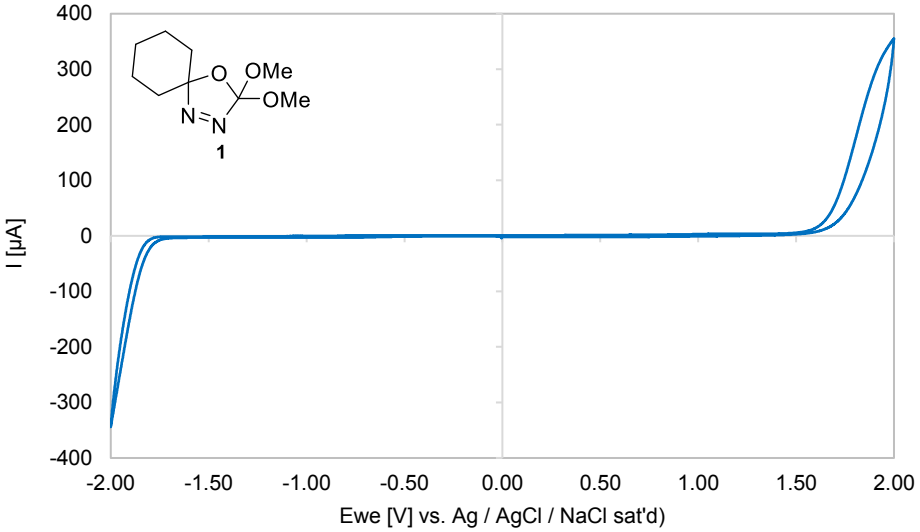

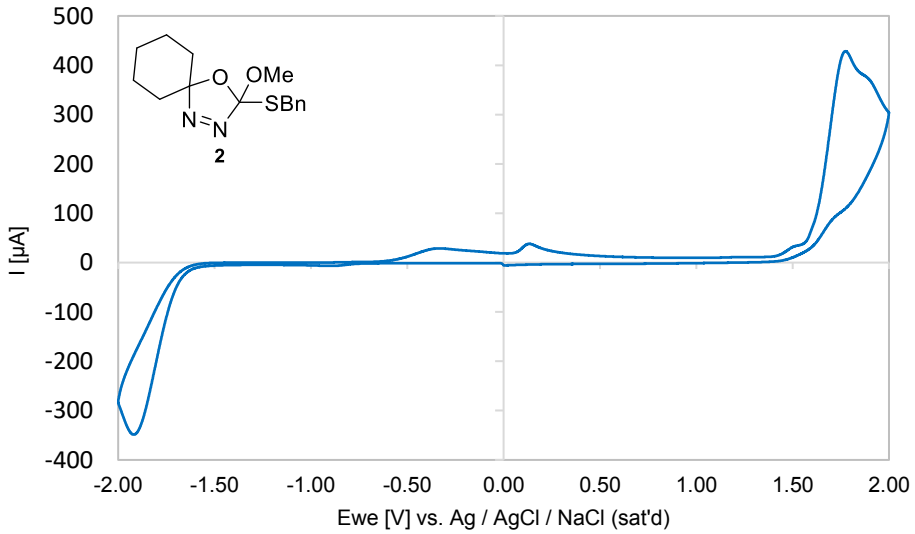

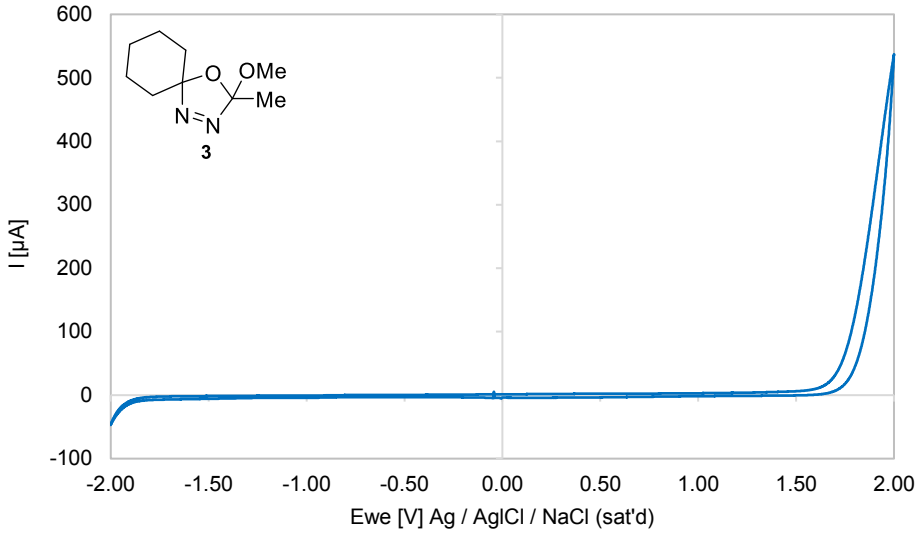

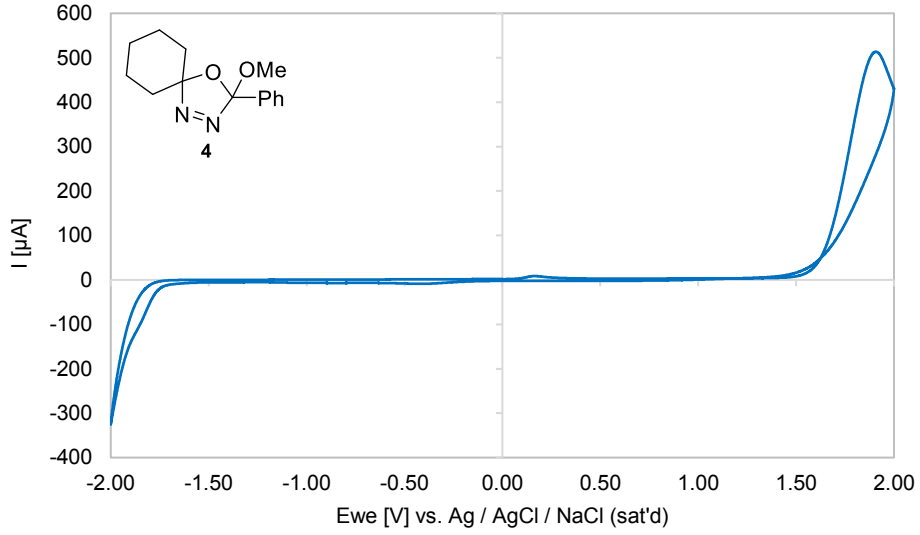

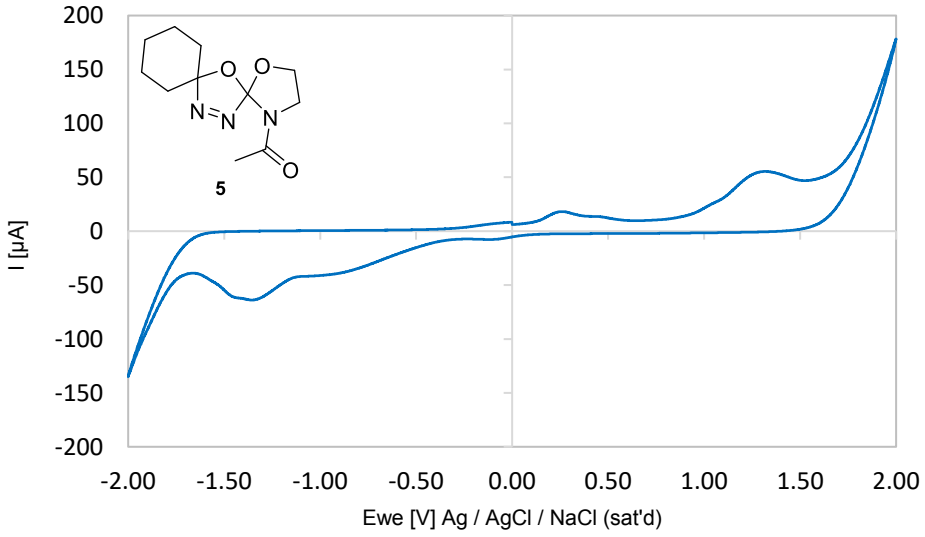

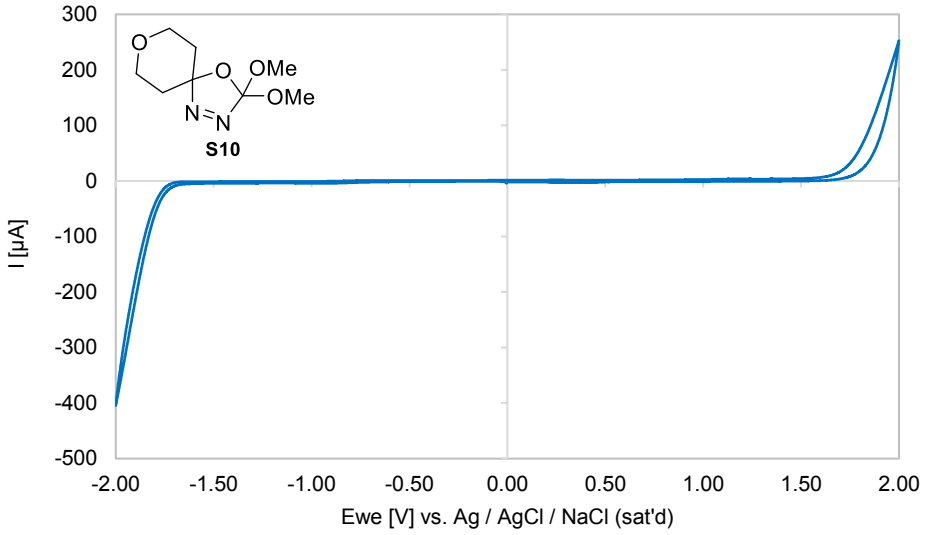

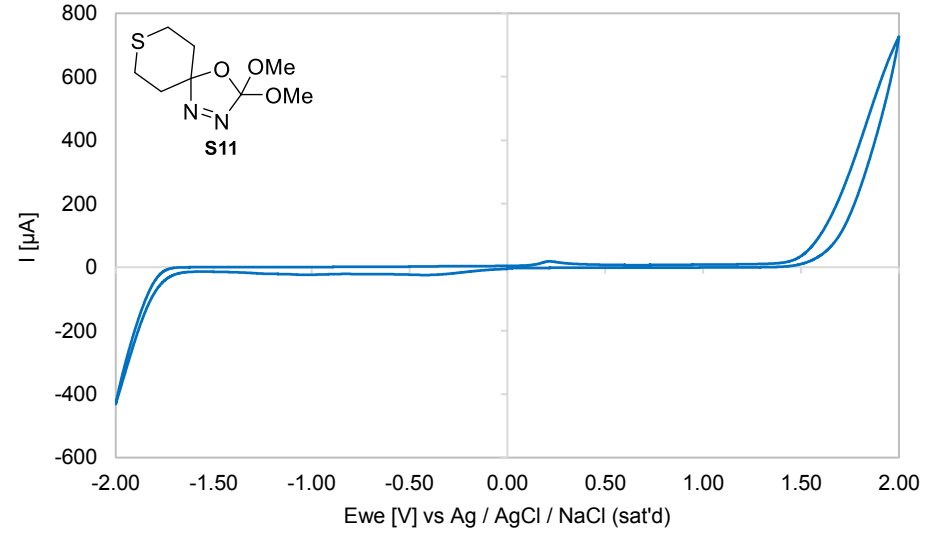

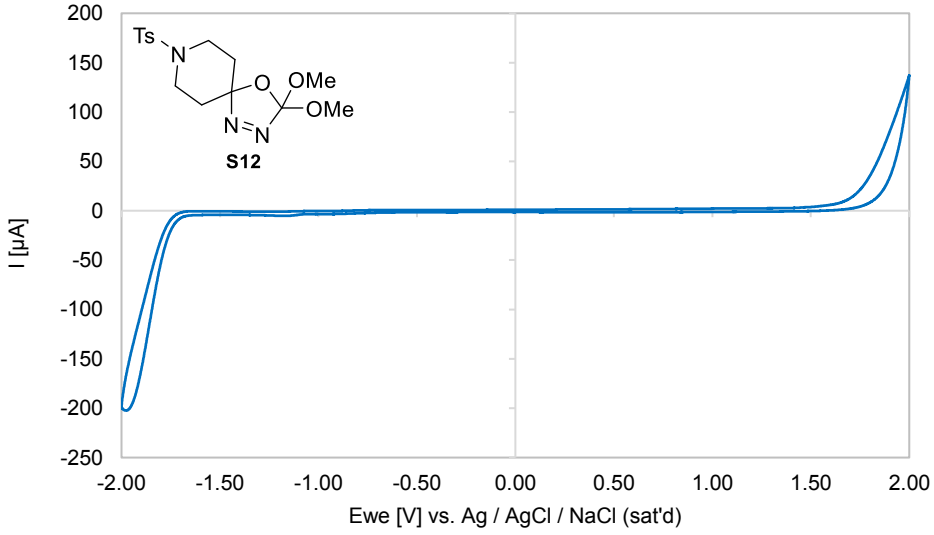

Conclusion:

Oxadiazolines **1-4** and **S10-S12** exhibit high oxidation and reduction potentials exceeding electrochemical properties of catalyst **6** (E_{ox}* = -0.89 V, E_{red}^{*} = +1.21 V),[13] thus the possibility of electron transfer events competing with triplet energy transfer from excited-state It-catalyst **6** can be excluded. On the other hand, oxadiazoline **5** appeared to be electrochemically unstable, which explains why although having E_T value comparable to that of oxadiazoline **1** is significantly less successful in developed cyclopropanation conditions.

6.4. Light ON/OFF experiment

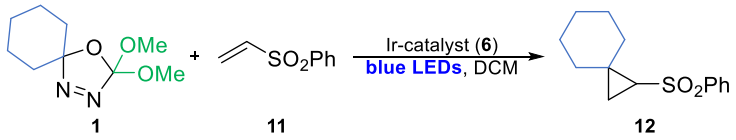

1 **11** **12**

The reaction was set up following the general cyclopropanation procedure (section 3.3) on 0.2 mmol scale with the addition of dodecane (40 µl) as an internal standard. The experiment was conducted for 60 min under alternating periods of irradiation (blue LEDs, blue intervals on Chart C1) and darkness (reaction vial coated with aluminum foil, grey intervals on Chart C1) and the yield was monitored by GC/FID.

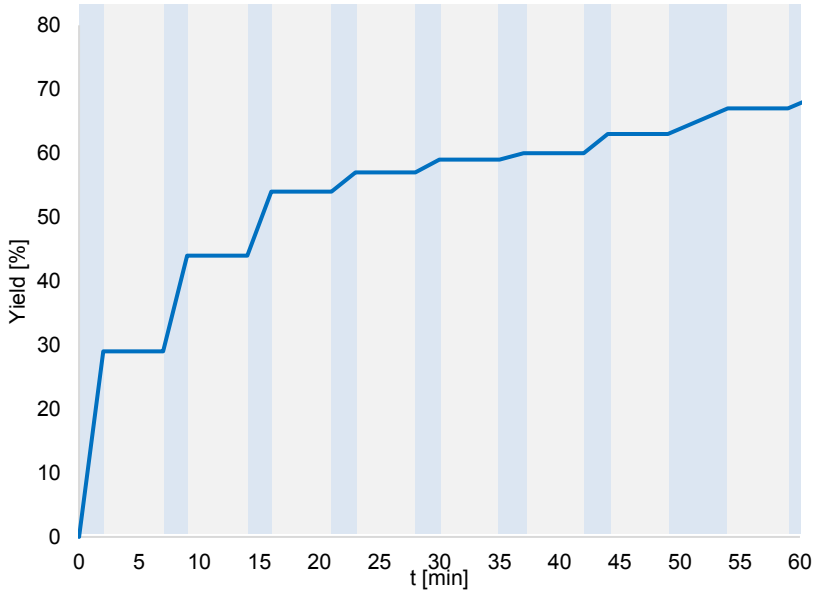

Chart C1. Light ON/OFF experiment performed on a model reaction.

Conclusion:

During light off phases no convertion of reagents occur as well as formation of cyclopropane **12** excluding the radical chain mechanism.

6.5. The Stern-Volmer analysis

The samples for Stern-Volmer analysis were prepared in a quartz screw-top cuvette equipped with a PTFE/silicone septum. The concentration of Ir[dF(CF$_3$)ppy)$_2$(dtbpy)]PF$_6$ (**6**) was experimentally selected as 25 μM so its absorbance at the excitation wavelength (382 nm) was kept between 0.1 and 0.2. Due to volatility of DCM, the experiments were conducted for DCE solutions.

The solvent was degassed by freeze-pump-thaw technique. DCE (2 mL for each sample) and the quencher were transferred to a cuvette under Ar atmosphere. The quenchers were added in 5 equal portions to ensure its concentrations ranging from 0.01 M to 0.05 M. After each addition of the quencher, both the optical absorption and emission spectra were recorded to ensure no significant increase of absorption at excitation wavelength (382 nm) occurs.

Stern-Volmer experiments were performed applying oxadiazolines **1-5**, **S10-S12** and phenyl-vinyl sulfone (**11**) as quenchers:

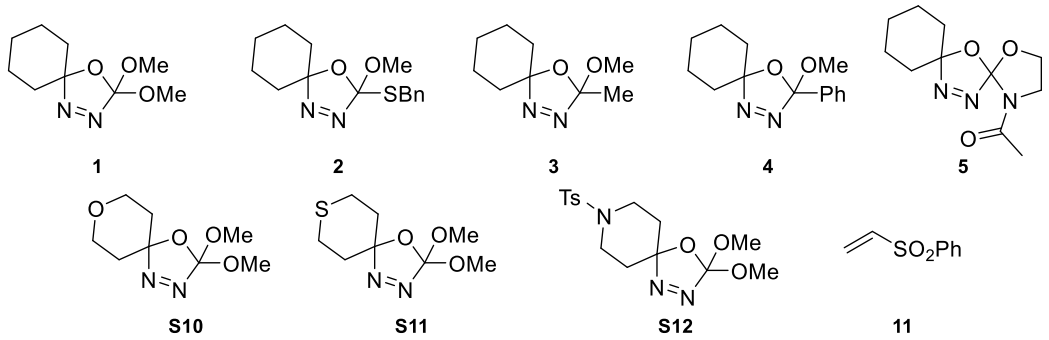

Rates of quenching for all tested quenchers k_q were determined using Stern–Volmer kinetics:

$$\frac{I_0}{I} = 1 + k_q \cdot \tau \cdot [Q]$$

where:
I_0 - the luminescence intensity without the quencher;
I - the luminescence intensity with the quencher added at [Q] concentration;
τ - the excited state lifetime of the PC, for Ir[dF(CF$_3$)ppy)$_2$(dtbpy)]PF$_6$ (**6**) τ = 2300 ns[13]
[Q] - concentration of the quencher for intensity I.

Stern-Volmer plots based on experimental data are depicted on Charts C2 and C3.

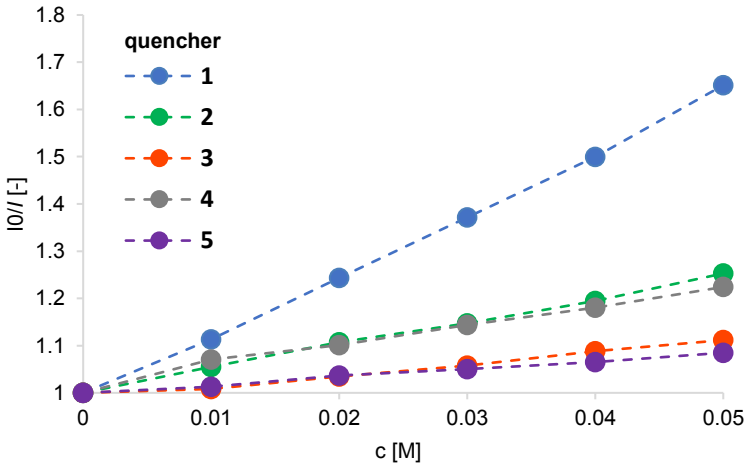

Chart C2. Stern-Volmer plot for oxadiazolines **1-5**.

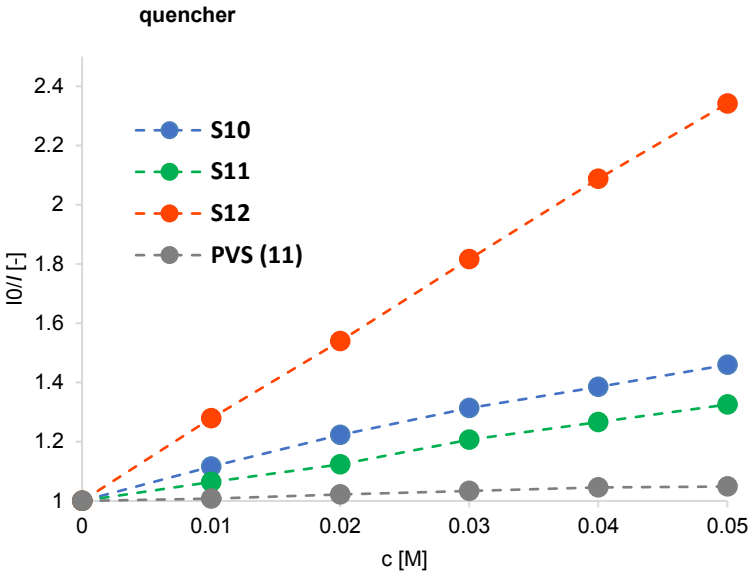

Chart S3. Stern-Volmer plot for oxadiazolines **S10-S12** and phenyl-vinyl sulfone (**11**).

Calculated quenching rates for each quencher are summarized in the Table T2.

Table T2. Luminescence quenching rate constants calculated for Ir[dF(CF_3)ppy)$_2$(dtbpy)]PF_6 (**6**) with quenchers **1-5**, **S10-S12** and **11** applied.

Quencher	Quenching rate constant k_q [$s^{-1} \cdot M^{-1}$]	Quencher	Quenching rate constant k_q [$s^{-1} \cdot M^{-1}$]
1	$5.42 \cdot 10^6$	**S10**	$4.01 \cdot 10^6$
2	$2.20 \cdot 10^6$	**S11**	$2.85 \cdot 10^6$
3	$9.35 \cdot 10^5$	**S12**	$1.18 \cdot 10^7$
4	$2.12 \cdot 10^6$	**11**	no quenching observed
5	$7.22 \cdot 10^5$		

Conclusion:

The Stern-Volmer analysis confirmed the interaction between excited-state Ir-catalyst **6** and oxadiazoline substrates. No quenching of the catalyst by phenyl-vinyl sulfone (**11**) was observed, therefore the initiation of the reaction by *EnT* process to olefin **11** is unlikely. The comparison of the calculated quenching rate constants for oxadiazolines **1-5** and **S10-S12** reveals that the higher k_q values observed correspond with the higher cyclopropanation yield (82% for **S12** > 81% for **1** > 62% for **S10**, 44% for **S11**). On the other hand, the lowest k_q was observed for oxadiazoline **5** which could be caused by its instability in the presence of catalyst **6**, affording only 39% of the cyclopropanation product (see electrochemical instability of reagent **5** in the range reachable by the redox abilities of catalyst **6,** Section 6.3.). Sufficient quenching rate is, however, not the only prerequisite for efficient reaction as oxadiazoline **4** with k_q value higher than **5** did not furnish cyclopropanation product.

6.6. Experiments with TEMPO radical trap

1 **11** **12** **21**

The reaction was set up following the general cyclopropanation procedure (section 3.3) on 0.1 mmol scale with the addition of TEMPO (0.2 mmol, 2.0 equiv., 31 mg) before irradiation (entry 1) or with TEMPO added after 2 min of irradiation as a degassed DCM solution (c = 0.4 M) to the reaction mixture (c = 0.067 M). The irradiation in both experiments was maintained for 60 min and after that time crude reaction mixtures were analyzed with the use of ESI MS, subsequently products were isolated by column chromatography.

Entry	TEMPO added	Yield of **12** [%][a]	Yield of **21** [%][a]
1	no	81	0
2	prior irradiation	0	0
3	after 2 min	54	18

Reaction conditions: Ir[dF(CF$_3$)ppy)$_2$(dtbpy)]PF$_6$ (**6**, 0.25 mol%), oxadiazoline **1** (0.2 mmol, 2 equiv.), phenyl vinyl sulfone (**11**, 0.1 mmol), TEMPO (0.2 mmol, 2.0 equiv.), DCM dry (c = 0.05 M), blue LED (450 nm, 25W), Ar atmosphere, 25 ^{o}C, 1 h; [a]isolated yields.

MS analysis of the crude reaction mixture when TEMPO was added after 2 min of irradiation revealed the presence of 408.2 m/z peak, corresponding to protonated TEMPO adduct **23**:

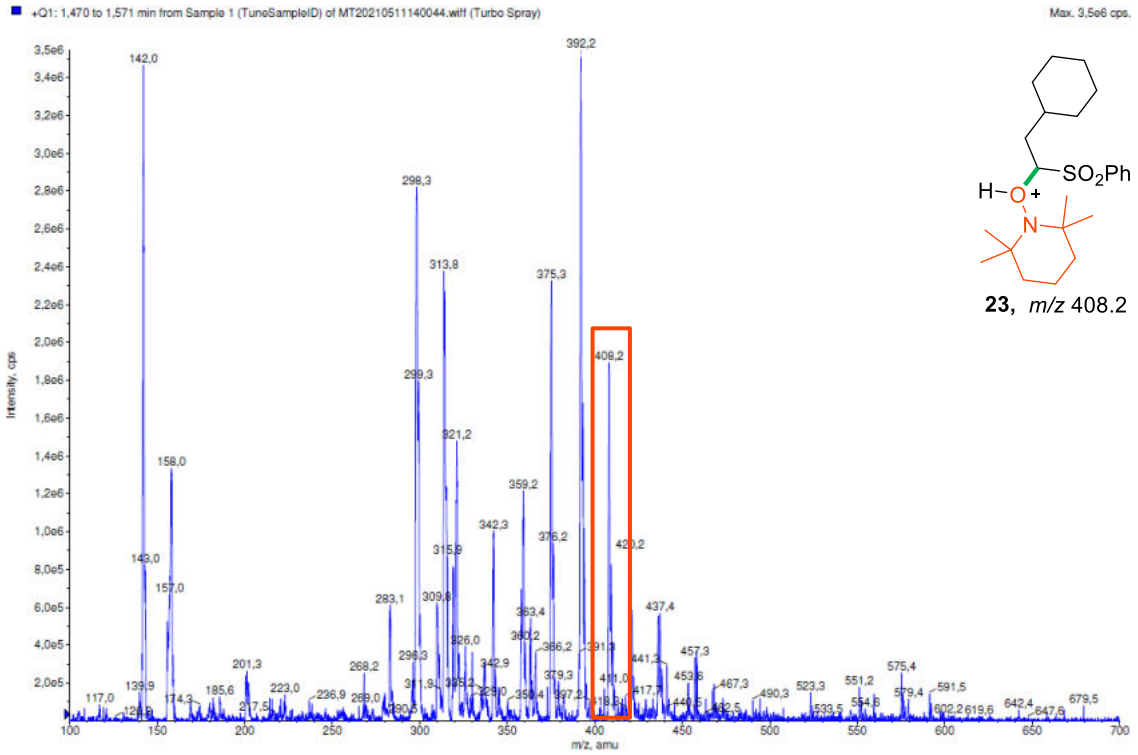

Figure F6. MS spectrum of crude reaction with the addition of TEMPO after 2 min.

Conclusion:

No product formation, when TEMPO is added prior irradiation, proves that the reaction is radical in nature. Observation of MS peak corresponding to adduct **23** suggests the formation of a radical species (intermediate **III**) generated upon addition of triplet carbene **II** to olefin **10**.

6.7. Identification of 1-pyrazoline 22 as a reaction intermediate

*Direct photolysis of oxadiazoline 1 in the presence of olefin **11***

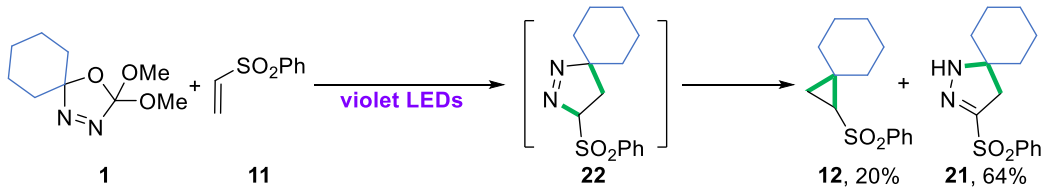

A glass vial equipped with a stirring bar and sealed with an aluminum cap with a rubber septum was charged with phenyl-vinyl sulfone (**11**, 0.20 mmol, 33.6 mg) dissolved in 4.0 mL DCM (p.a. grade). The oxygen was removed from the solution by freeze-pump-thaw technique. Then, oxadiazoline **1** (1.0 mmol, 5.0 equiv., 180 µL, 200 mg) was added under argon atmosphere. The reaction mixture was placed in a photoreactor and irradiated with violet LED (405 nm, 25 W) for 17 h. After that time, the crude reaction mixture was concentrated *in vacuo* and purified by column chromatography using ethyl acetate/hexanes to afford products **12** and **21**.

NMR of compound **21** (performed in $CDCl_3$) revealed its co-existance in solution with regioisomer **22** in ca. **21**:**22** = 8:1 ratio:

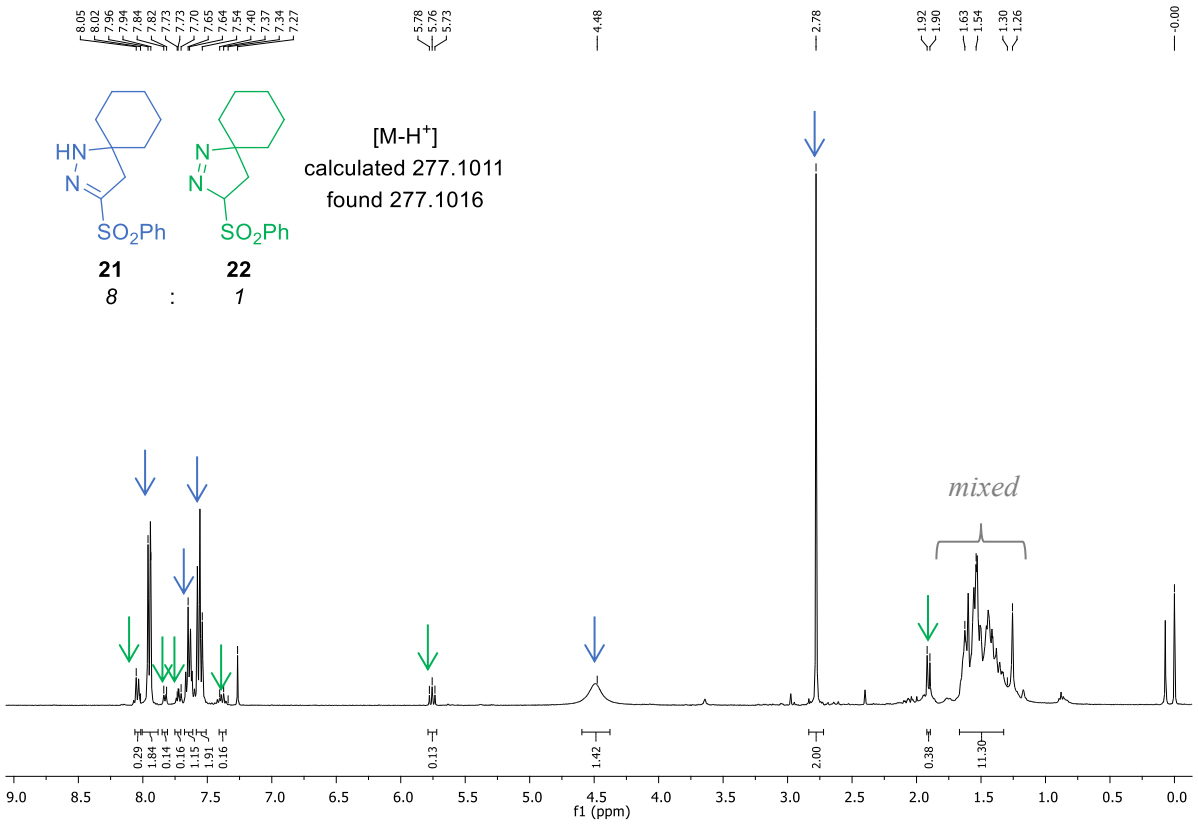

Figure F7. NMR spectrum of pyrazoline as a mixture of regioisomers.

Additionally, the violet light-induced photolysis of oxadiazoline **1** in the presence of olefin **11** was performed in CD_2Cl_2 instead of DCM and after 17 h, the crude reaction mixture was monitored with the NMR technique. This revealed 1-pyrazoline **22** as an intermediate while there are no signals corresponding to isomer **21** were present. Alongside, dimethyl carbonate (**8**), cyclohexanone (**9**), oxadiazoline **1** and traces of cyclopropane **12**, olefin **13** and phenyl-vinyl sulfone (**11**) can be observed.

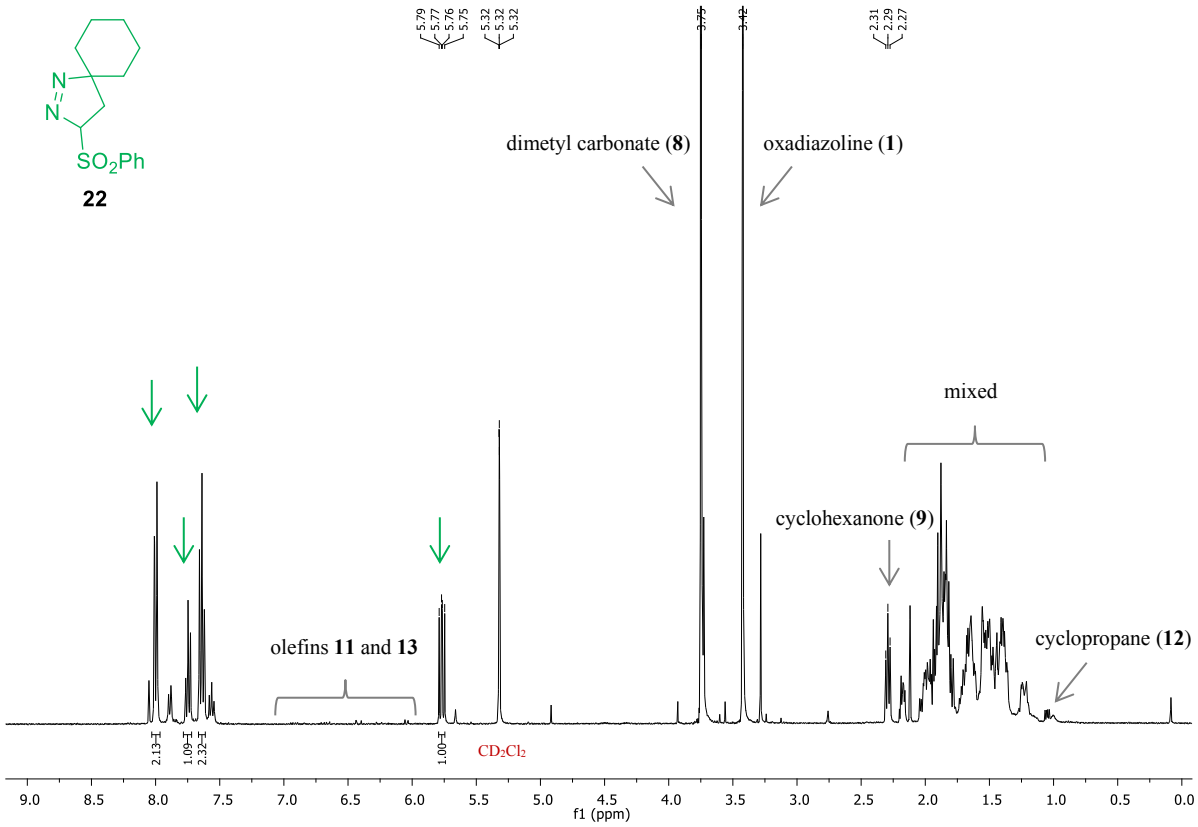

Figure F8. NMR spectrum of crude reaction mixture after violet light irradiation in the absence of Ir-catalyst **6**.

*1-Pyrazoline **22** convertion to cyclopropane **12** with the use of triplet energy catalysis*

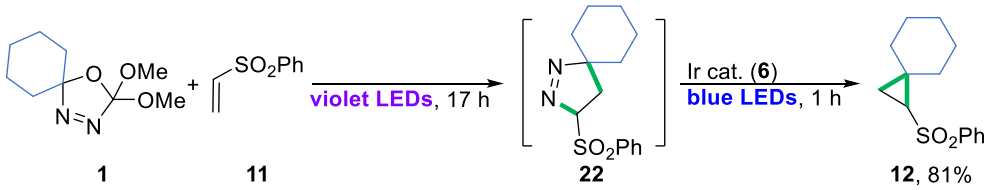

The violet light-induced photolysis of oxadiazoline **1** in the presence of phenyl-vinyl sulfone (**11**) was performed according to the abovementioned protocol. After **violet light** irradiation for 17 h, $Ir[dF(CF_3)ppy)_2(dtbpy)]PF_6$ (**6**, 0.25 mol%, 0.6 mg) in DCM solution (c = 1 mM) was added to the reaction mixture under argon atmosphere. The reaction vial was placed in a photoreactor and irradiated with **blue LEDs** (450 nm, 25 W) for 1 h. After that time, the crude reaction mixture was concentrated *in vacuo* and purified by column chromatography using ethyl acetate/hexanes to afford the final product **12**.

*Examination of 2-pyrazoline **21** as reaction intermediate*

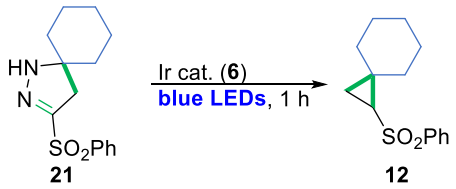

Entry	Catalyst **6**	Yield of **12** [%]
1	no	0
2	0.25 mol%	traces

A glass vial equipped with a stirring bar and sealed with an aluminum cap with a rubber septum was charged with Ir[dF(CF$_3$)ppy)$_2$(dtbpy)]PF$_6$ (**6**, 0.25 mol%, 0.3 mg, entry 1 only) and pyrazoline **21** (0.10 mmol, 27.8 mg) dissolved in 2.0 mL DCM (p.a. grade). The oxygen was removed from the solution by freeze-pump-thaw technique. The reaction mixture was placed in a photoreactor and irradiated with blue LEDs (405 nm, 25 W) for 1 h. After that time, the crude reaction mixture was concentrated *in vacuo*, CD_2Cl_2 was added, and the mixture was analyzed by NMR technique. No significant convertion of pyrazoline **21** to cyclopropane **12** at any conditions (entry 1 or 2) was observed.

*Identification of 2-pyrazoline **22** as an intermediate under blue light-photosensitized conditions*

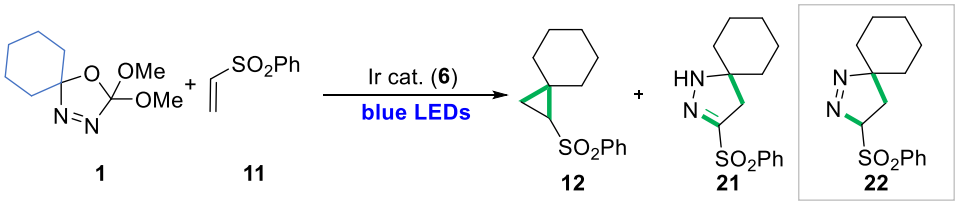

Entry	Reaction time	Yield of **12** [%][a]	Yield of **21** [%][a]
1	2 min	30	33
2	1 h (optimal conditions)	81	0

Reaction conditions: Ir[dF(CF$_3$)ppy)$_2$(dtbpy)]PF$_6$ (**6**, 0.25 mol%), oxadiazoline **1** (0.4 mmol, 2.0 equiv.), phenyl vinyl sulfone (**11**, 0.2 mmol), DCM (c = 0.05 M, p.a. grade), blue LEDs (450 nm, 25 W), Ar atmosphere, 25 °C; [a]isolated yields.

The reaction was set up following the general cyclopropanation procedure (section 3.3) on 0.2 mmol scale but the reaction mixture was irradiated with blue LEDs (21 W) for 2 min instead of 1 h. After that crude reaction mixture was concentrated *in vacuo* and products **12** and **21** were isolated by column chromatography.

Additional experiment in CD_2Cl_2 instead of DCM was performed. NMR analysis of the crude reaction mixture revealed compound **22** present as the reaction intermediate:

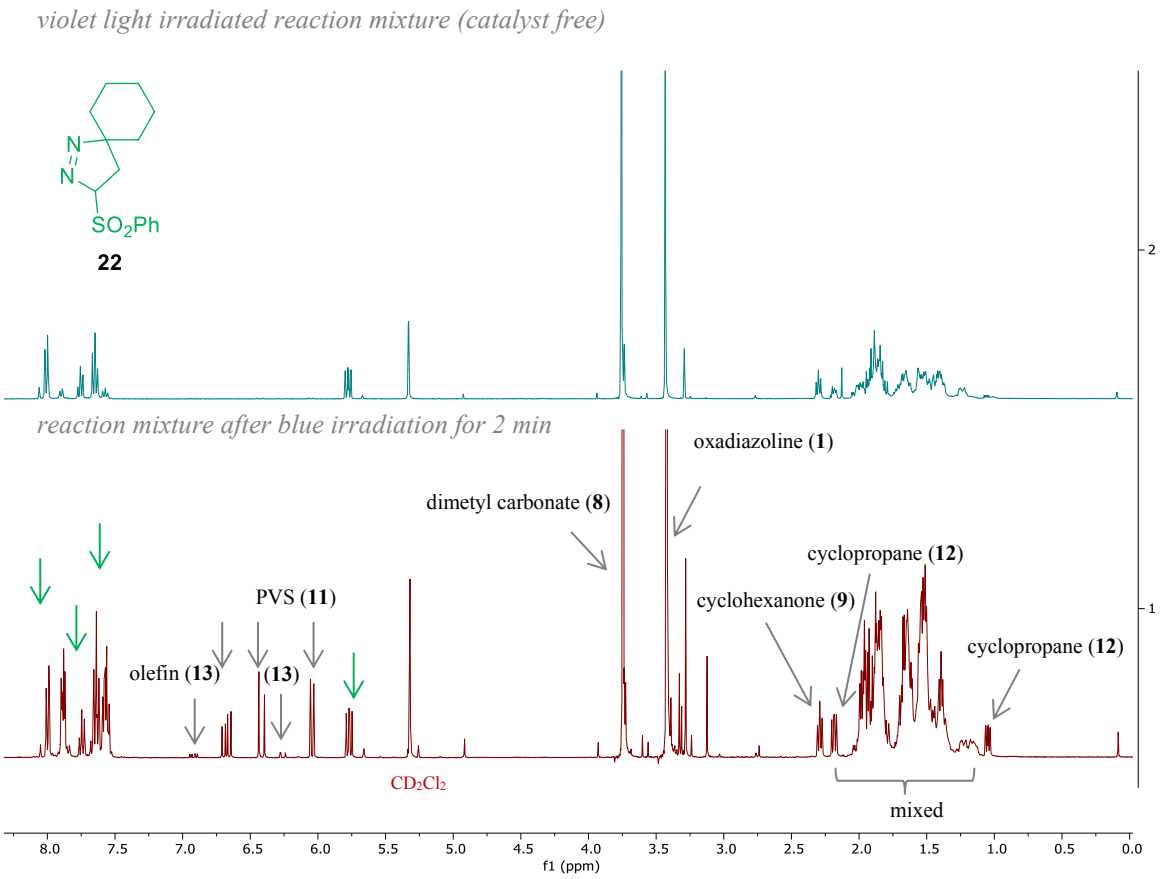

Figure F9. NMR spectrum of crude reaction mixture after blue light irradiation for 2 min in the presence of Ir-catalyst **6**.

Conclusion:

1-Pyrazoline **22**, formed as a product of 1,3-dipolar cycloaddition of generated diazoalkane **7** to phenyl-vinyl sulfone (**11**), was confirmed as a reaction intermediate that under triplet energy transfer catalysis undergoes convertion to cyclopropane **12**. This reaction pathway proceeds parallelly to the carbene-mediated mechanism under Ir-catalyzed blue light irradiation while under violet light catalyst-free conditions the diazoalkane generation and subsequent 1,3-cycloaddtion furnishing pyrazoline **22** is exclusive and no carbene formation occurs.

6.8. Kinetic studies

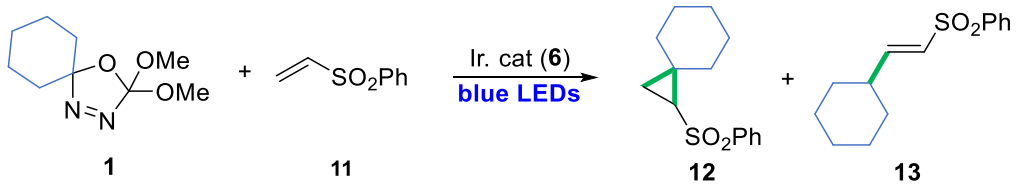

The reaction was set up following the general cyclopropanation procedure (section 3.3) on 0.1 mmol scale with the addition of dodecane (20 µl) as an internal standard. The experiment was conducted for 60 min and the reaction progress monitored was monitored with GC/FID (Charts C4 and C5).

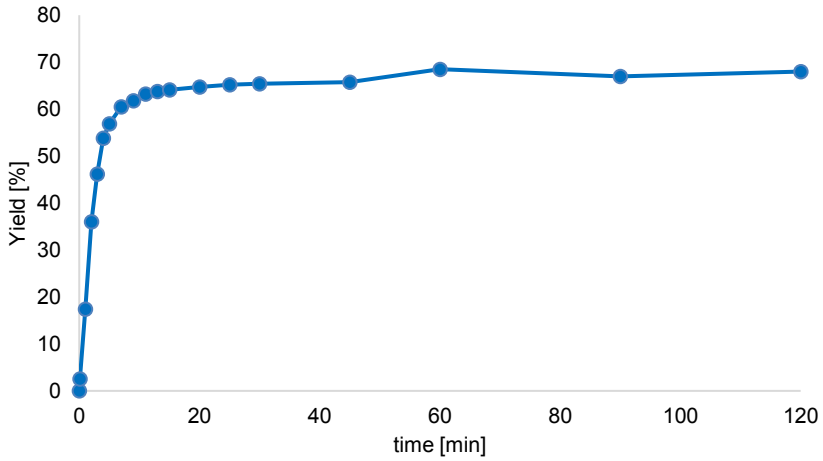

Chart C4. Kinetics of model reaction.

Additionally, the consumption of phenyl-vinyl sulfone (**11**) and the formation of cyclopropane **12** as well as olefin **13** as ratio of reagent to dodecane area (P/P_d) on GC chromatogram was monitored in time (Chart S5).

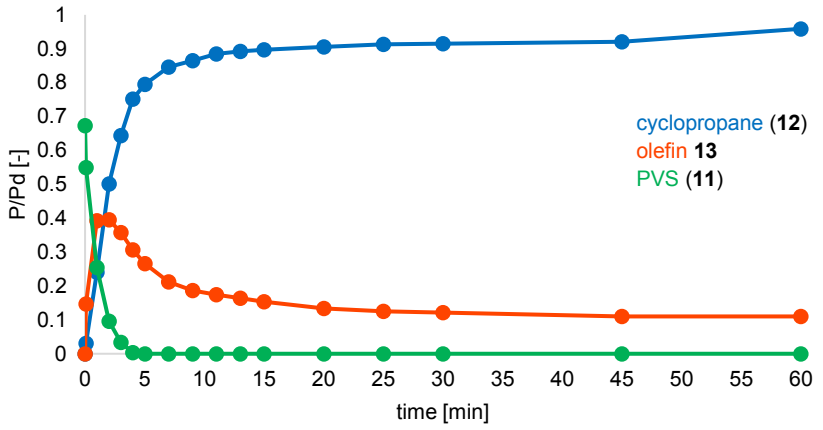

Chart C5. Convertion and of olefin and products formation.

Conclusions:

The studies revealed the fast formation of cyclopropane **12** accomplished within less than 1 hour and the fast consumption of olefin **11** completed within 5 min of irradiation. The rapid growth of olefin **13** to dodecane area ratio was observed within the first reaction minute with subsequent ratio decrease leading to the plateau after 20 min of irradiation. Further GC studies revealed pyrazolines unstable on GC conditions decomposing mostly to olefin **13**. Considering that, chart SX clearly supports parallel existence of carbene- and diazoalkane-mediated pathways.

6.9. EPR studies

Measurement conditions:

spin trap: 5,5- dimethyl-1-pyrroline N-oxide (DMPO) or 2-Methyl-2-nitrosopropane (MNP)

central magnetic field: 331 mT

sweep width: 16 mT

modulation amplitude: 0.08 mT

microwave power: 10 mW

sweep time: 45 s

number of scans: 4 to 16

simulation: EasySpin package in Matlab

Procedure for experiments with addition of the spin traps

Each experiment was set up in a vial equipped with a stirring bar and sealed with an aluminum cap with a rubber septum. The irradiation was performed in a handmade photoreactor (λ_{max} = 455 nm, 10 W, see Section 2). Due to short irradiation times (1 min), no fan for cooling was required. Dry DCM was used as solvent for all the measurements and the solutions were purged with argon before irradiation. The experiments were performed with two different spin traps - DMPO and MNP. DMPO was added as a solution in DCM under argon while MNP was added in as solid (after the addition, the argon purging was repeated). All the experiments were performed in two modes for each trap:

A- the spin trap was added prior to light exposure and the subsequent mixture was irradiated with blue light for 1 min, then the vial was opened and a sample for EPR measurement was collected with a capillary and placed in a spectrometer.

B- the solution was irradiated for 15 s, then a spin trap was added, and the subsequent mixture was irradiated for additional 45 s, then the vial was opened and a sample for EPR measurement was collected with a capillary and placed in a spectrometer.

*EPR spectrum of a mixture of oxadiazoline **1** and Ir-catalyst **6** with DMPO as spin trap:*

Conditions: Ir[dF(CF_3)ppy)$_2$(dtbpy)]PF_6 (**6**, 0.25 mol%), oxadiazoline **1** (0.2 mmol), dry DCM (c = 0.1 M), DMPO (0.1 mmol), blue LEDs (455 nm, 10 W), Ar atmosphere, 1 min.

The EPR spectrum of oxadiazoline **1** irradiated with blue light in the presence of photocatalyst **6** and DMPO is a superposition of four components (Figure F10A). While the first one is typical for an adduct of DMPO and carbon-centered radical, the second origins from a nitrogen-centered species. The spectral pattern of both is similar to that observed for carbene and azo radical adducts generated by the Pd-catalyzed thermal degradation of α-carbonyl diazomethanes.[14] These species (**c3** with HCFs: a_N = 1.47 mT, a_H = 2.09 mT and **c4** with HCFs: a_N = 1.51mT, a_H = 1.67, $a_{N\text{-}\beta}$ = 0.36 mT, Figure F11) possibly arise from capturing the diazenyl radical **I** (see Scheme S1) and we assume the additional components **c5** and **c6** (**c5** with HCFs: a_N = 1.25 mT, a_H = 0.86 mT, $a_{H\text{-}\gamma}$ = 0.21mT and **c6** with HCFs: a_N = 1.42 mT, a_H = 2.03, $a_{N\text{-}\gamma}$ = 0.15 mT) ascribed as O-centred and α-*N* C-centered radical adducts to result from either subsequent decomposition of species **I** or parallel initial C_5-O_1 bond breaking within oxadiazoline **1** (**c5** and **c6**). The relative signal intensities vary depending on the reaction time (Table T3). When DMPO was added prior irradiation, components of type **c3** and **c4** participated predominantly. The major contribution of **c5** and **c6** signals was observed in the case of trap addition after 15 s of irradiation. Besides, partial photodegradation of DMPO also occurred (DMPOX, a_N = 1.09 mT).

Table T3. Relative signal intensities of components **c3-c6** depending on the DMPO addition time.

	DMPO added in	
component	t = 0 s	t = 15 s
c3	42%	27%
c4	22%	12%
c5	12%	25%
c6	23%	33%

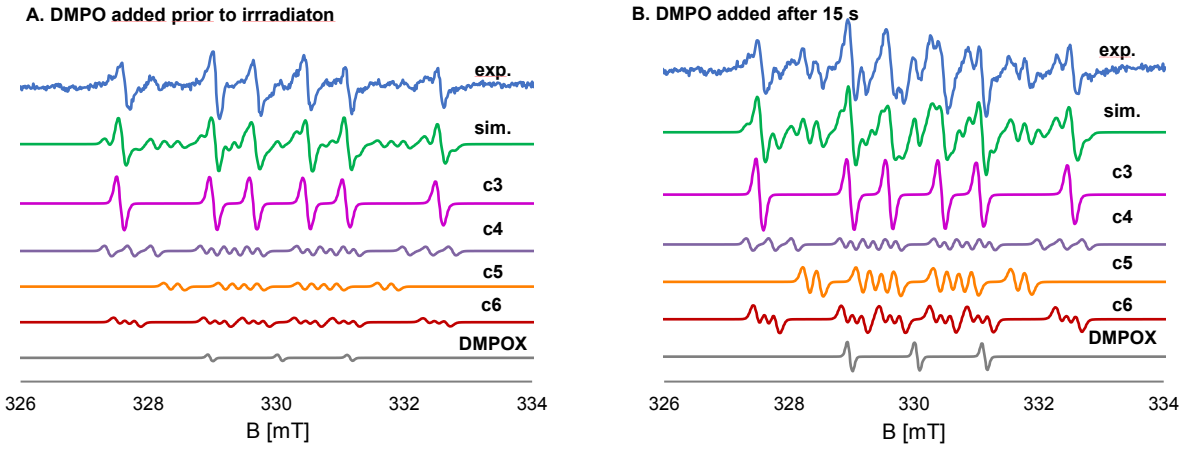

Figure F10. EPR spectra of oxadiazoline **1** and catalyst **6** in the presence of DMPO. **A –** DMPO was present in the system before irradiation, **B** – DMPO was added after 15 s of irradiation. exp.: experimental spectrum, sim.: simulation results – entire spectrum and single components.

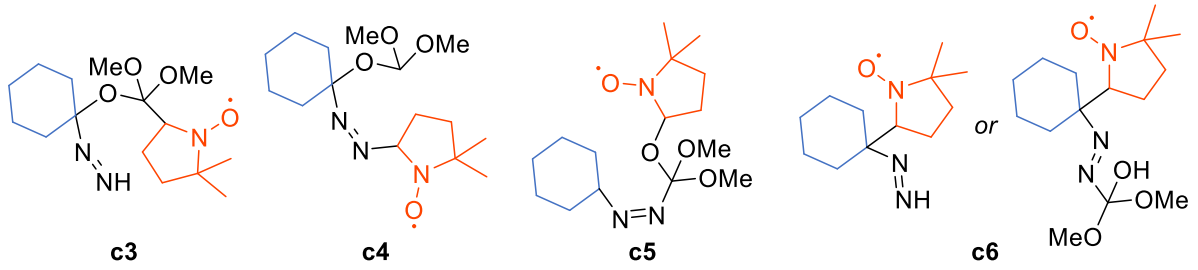

Figure F11. Postulated structures corresponding to components **c3-c6**.

*EPR spectrum of a mixture of olefin **11** and Ir-catalyst **6** with DMPO as spin trap:*

Conditions: Ir[dF(CF$_3$)ppy)$_2$(dtbpy)]PF$_6$ (**6**, 0.25 mol%), phenyl-vinyl sulfone (**11**, 0.1 mmol), dry DCM (c = 0.05 M), DMPO (0.1 mmol), blue LEDs (455 nm, 10 W), Ar atmosphere, 1 min.

When olefin **11** was irradiated in the presence of Ir-catalyst **6** and DMPO, the measured spectrum was dominated by the six-lines signal of parameters (a_N = 1.35 and a_H = 1.15, 88% of relative intensity when DMPO was added after 15 s) indicating the formation of oxygen-centered species **c7** (Figure F12B). The pattern of minor component (with HCFs: a_N = 1.24 mT, a_H = 1.41 mT) resembles spectra observed for DMPO/$SO_3^{\bullet-}$ adducts in both aqueous and organic solvents,[15,16] therefore suggesting parallel generation of sulfonyl radical $PhSO_2^{\bullet}$ (**c8**). While the spectra obtained from the experiment B gave spectra of relative high intensity (Figure F12B), the addition of the spin trap prior irradiation inhibited radical generation leading to spectrum of significantly lower total intensity (Figure F12A).

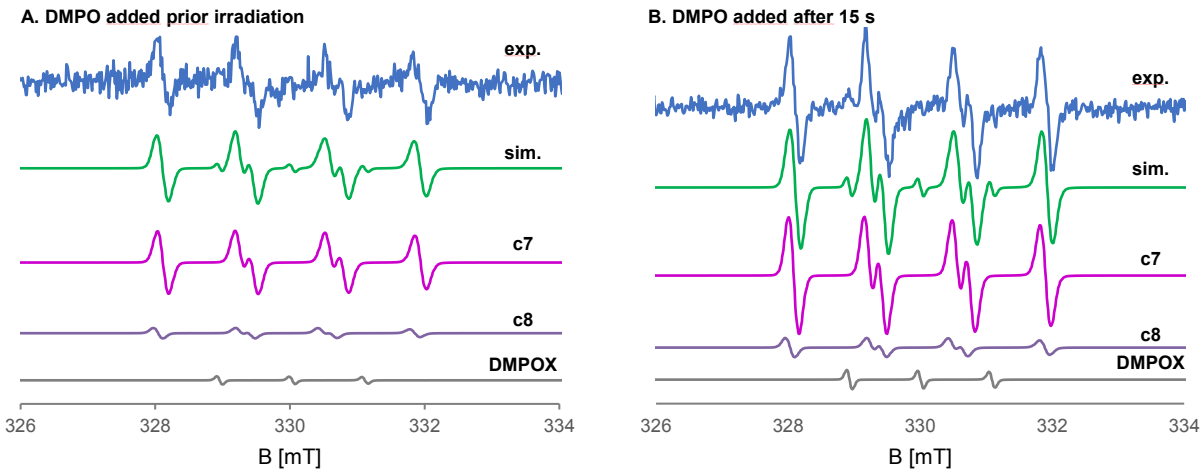

Figure F12. EPR spectra of olefin **11** and catalyst **6** in the presence of DMPO. **A –** DMPO was present in the system before irradiation, **B** – DMPO was added after 15 s of irradiation. exp.: experimental spectrum, sim.: simulation results – whole spectrum and single components.

*EPR spectrum of a mixture of oxadiazoline **1**, olefin **11** and Ir-catalyst **6** with DMPO as the spin trap:*

Conditions: Ir[dF(CF_3)ppy)$_2$(dtbpy)]PF_6 (**6**, 0.25 mol%), oxadiazoline **1** (0.2 mmol, 2.0 equiv.), phenyl-vinyl sulfone (**11**, 0.1 mmol), dry DCM (c = 0.05 M), DMPO (0.1 mmol), blue LEDs (455 nm, 10 W), Ar atmosphere, 1 min.

The analysis of the EPR spectrum of the entire reaction mixture in the presence of DMPO added before irradiation is a superposition of three components – **c7**, discussed above for the irradiated mixture of olefin **11**, and catalyst **6** with DMPO added, and two new signals **c9** and **c10** (Figure F13A). The component **c9**, constituting 4.5% of spectrum intensity, with a_N = 1.55 mT and a_H = 0.51 mT could be tentatively ascribed to a C-centered radical adduct with the oxygen atom in the vicinity of the carbon atom. The predominant signal **c10** (responsible for 66% of total intensity) corresponds to *O*-centered radical adduct (a_N = 1.32 mT, a_H = 0.72 mT, $a_{H\text{-}\gamma}$ = 0.16 mT). Both **c9** and **c10** arise from oxadiazoline radical species, as these were also observed in the EPR spectrum of the mixture of only oxadiazoline **1** and catalyst **6**, irradiated for 1 min with DMPO, but recorded 3.5 h after the first measurement and irradiation period. On the other hand, the EPR spectrum differs significantly, when the spin trap is added to the system after 15 s of irradiation, being predominantly the superposition of signals **c5** and **c7** discussed above (Figure F13B). These constitute 44 and 46% of total spectrum intensity, but a novel component (**c1**, of 7% intensity), undetected in partial systems was distinguished as well. This signal could be tentatively ascribed to a diradical species with spin density centered on the nitrogen atom of a nitroxide and a carbon atom of a carbon-centered radical (HFCs: a_N = 1.22 mT and a_H = 2.27 mT for nitroxide moiety and a_N = 0.31 mT, $a_{H(nitroxide)}$ = 1.87 mT and $a_{H(CH2)}$ = 1.45 mT for cyclohexane moiety with rather fast spin exchange (J = 6.55 mT)). These parameters correlate well with a carbene adduct and support its generation within the reaction mechanism.

It should be noted that although during abovementioned EPR experiments the radicals generated from olefin **11** were trapped, control experiments with PVS (**11**) exposed to blue light (25 W, 1 h) in the presence of Ir-catalyst **6** (0.25 mol%) revealed only residual convertion of olefin **11** (< 3%). This background experiment together with the Stern-Volmer analysis proves that phenyl-vinyl sulfone (**11**) is not activated via any photochemical process (single electron or triplet energy transfer events) at significant level. Considering high affinity of DMPO to *O*- and *S*-centered radicals, even though only traces of these are formed during EPR experiment, the corresponding signals (**c7** and **c8**) may be of relative high intensity.

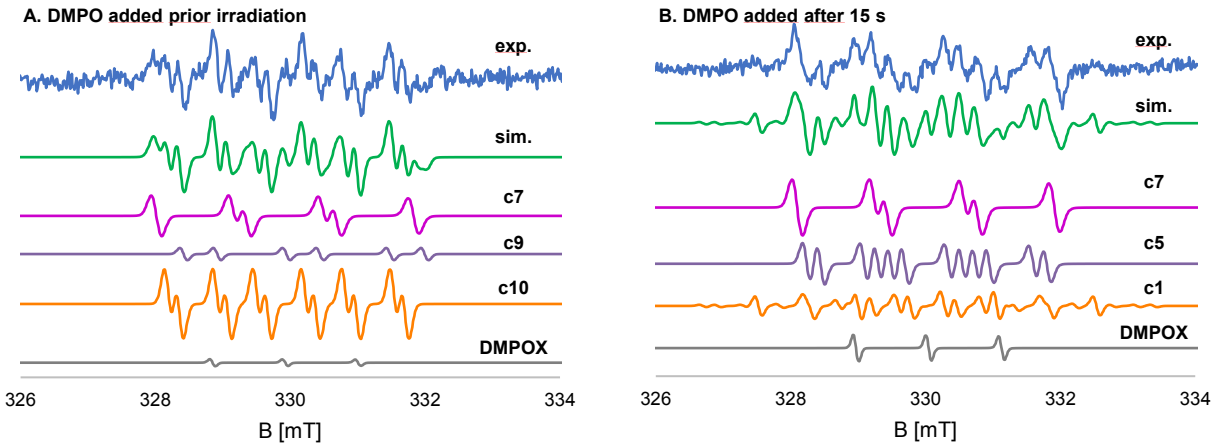

Figure F13. EPR spectra of oxadiazoline **1**, olefin **11** and catalyst **6** in the presence of DMPO. A – DMPO was present in the system before irradiation, B – DMPO was added after 15 s of irradiation. exp.: experimental spectrum, sim.: simulation results – whole spectrum and single components.

*EPR spectrum of a mixture of oxadiazoline **1**, olefin **11** and Ir-catalyst **6** with MNP as spin trap:*

Conditions: Ir[dF(CF_3)ppy)$_2$(dtbpy)]PF_6 (**6**, 0.25 mol%), oxadiazoline **1** (0.2 mmol, 2.0 equiv.), phenyl-vinyl sulfone (**11**, 0.1 mmol), dry DCM (c = 0.05 M), MNP (0.1 mmol), blue LEDs (455 nm, 10 W), Ar atmosphere, 1 min.

Although MNP undergoes degradation to DTBN radical (di-tert-butyl nitroxide) and the corresponding triplet signal vastly dominates the obtained spectra, when the entire reaction mixture was irradiated in the presence of MNP, the additional peaks **c2** could be seen between the DTBN peaks (Figure F14). Their position suggests the presence of a biradical *adduct, with unpaired electrons localized on NO group of a spin trap and a carbon atom,* with rapid spin exchange, i.e. with J>>A, when the apparent hyperfine splitting is half of the splitting in corresponding monoradical. The parameters obtained from simulation are: $a_{N(nitroxide)}$ = 1.25 mT, $a_{N(carbon)}$ = 0.33 mT.

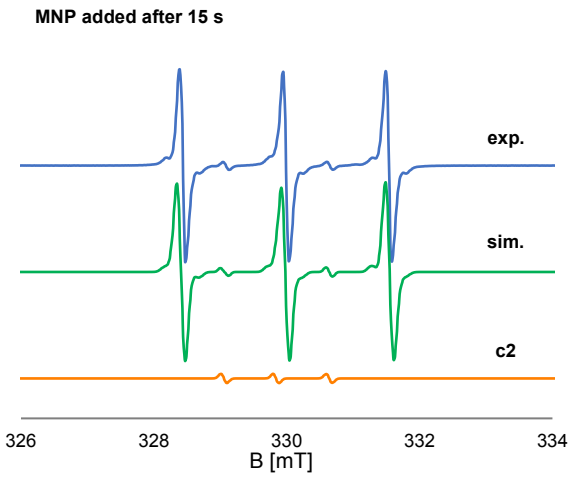

Figure F14. EPR spectra of the reaction mixture (oxadiazoline **1**, olefin **11** and catalyst **6**) in the presence of MNP. exp.: experimental spectrum, sim.: simulation results – whole spectrum and single biradical component.

The summarized properties of components **c1**-**c10** observed with the use EPR spectroscopy are summarized in Table T4.

Table T4. Summarized hyperfine splitting constants (HCFs) of components **c1**-**c10**.

DMPO used as spin trap				
component	a_N [mT]	a_H [mT]	other a [mT]	J [mT]
c1	1.22/0.31	2.27/1.87	/1.45 ($a_{H(CH2)}$)	6.55
c3	1.47	2.09		
c4	1.51	1.67	0.36 mT ($a_{N-\beta}$)	
c5	1.25	0.86	0.21 ($a_{H-\gamma}$)	
c6	1.42	2.03	0.15 ($a_{N-\gamma}$)	
c7	1.35	1.15		
c8	1.24	1.41		
c9	1.55	0.51		
c10	1.32	0.72	0.16 ($a_{H-\gamma}$)	
DMPOX	1.09			
MNP used as spin trap				
c2	1.25/0.33			7.21

Conclusion:

EPR experiments confirm the radical character of the reaction mechanism and reflect its complexity with the number of components simulated based on the experimental data. These studies essentially support the formation of diazenyl species **I** and carbene **II**, the latter supported with trapping with both DMPO and MNP spin traps. Although olefin **11** appeared to be a radical source within the measurements, the background experiments exclude its significant participation in radical generation during the reaction mechanism.

7. Computational methods

7.1. Estimation of triplet energy values for selected oxadiazolines

Performance of selected DFT methods

DFT calculations were performed with Gaussian 16 package.[17] TD-B3LYP, CAM-B6LYP and M06 functionals with the 6-31G(d,p) basis set were employed to calculate $S_0 \rightarrow S_1$, $S_0 \rightarrow T_1$, $T_1 \rightarrow S_0$ transitions for oxadiazolines **1**, **S10** and **S11** (Table T5). In general, computations performed at the TD-B3LYP/6-31G(d,p) level of theory gave approximately average absorption maxima of values obtained with CAM-B3LYP and M06 methods while $S_0 \rightarrow T_1$ and $T_1 \rightarrow S_0$ maxima comparable to those resulting from CAM-B3LYP calculations. *(All computations included in section 7.1. refer to oxadiazolines at vacuum conditions.)*

Table T5. Comparison of oxadiazoline transitions computed with commonly used DFT methods.

	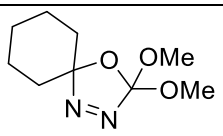 **1**			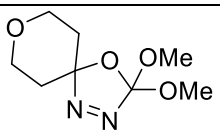 **S10**		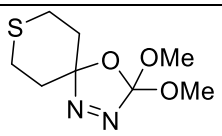 **S11**		
	TD-B3LYP	CAM-B3LYP	M06	TD-B3LYP	M06	TD-B3LYP	CAM-B3LYP	M06
Geometry optimized in ground singlet state								
$S_0 \rightarrow S_1$	334.0	326.7	346.9	350.9	361.6	351.5	339.1	361.7
$S_0 \rightarrow T_1$	467.3	466.0	439.3	484.9	454.3	485.5	480.1	454.7
Geometry optimized in triplet state								
$T_1 \rightarrow S_0$	506.1	503.5	495.9	515.7	505.1	515.8	509.1	504.5

Transitions characteristics for selected oxadiazolines and diazoalkane 7

For oxadiazolines **1-5** and **S10-S12** and diazoalkane **7** dipole moments (μ), absorption maxima, and intersystem crossing (ISC) transitions were calculated (Table T6), considering molecules of geometry optimized in singlet ground state S_0 (using density functional TD-B3LYP with the 6-31G(d,p) basis set) and in triplet state T_1 (using density functional UB3LYP with the 6-31G(d,p) basis set).

Table T6. Dipole moments and transition characteristics calculated for selected compounds.

	Geometry optimized in singlet ground state **S_0** *(TD-B3LYP/6-31G(d,p))*				Geometry optimized in triplet state **T_1** *(UB3LYP/6-31G(d,p))*	
Compound no.	μ [D]	$S_0 \rightarrow S_1$ [nm]	Absorption maxima	$S_0 \rightarrow T_1$ [nm]	μ [D]	$T_1 \rightarrow S_0$ [nm]
1	3.36	334.0	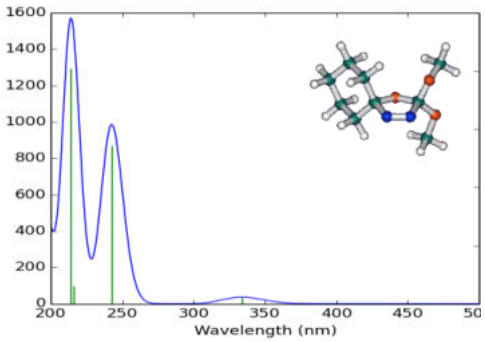	467.3	3.05	506.1
2	1.66	346.5	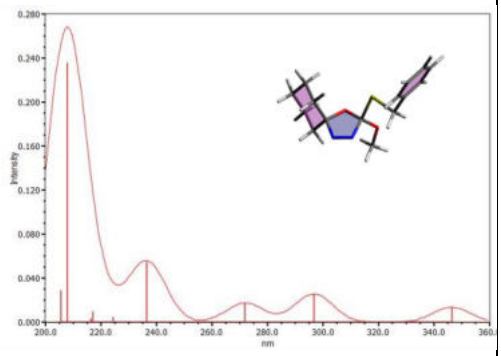	467.0	0.66	500.9
3	3.09	322.6	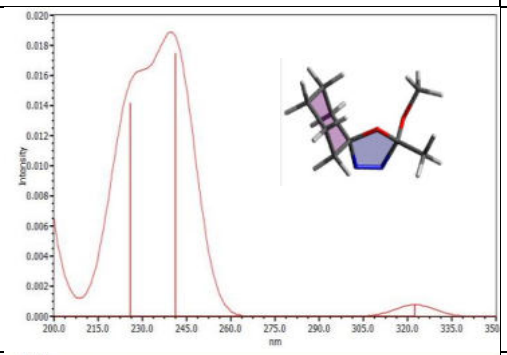	452.5	2.66	496.5
4	2.99	325.9	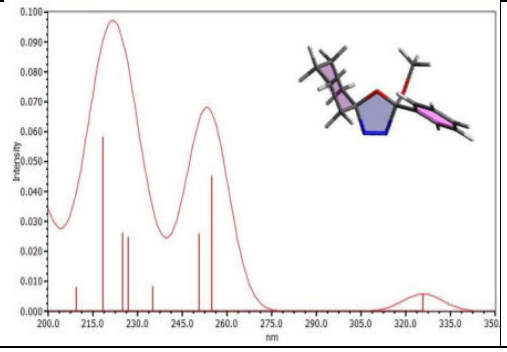	449.1	2.68	490.3

5	4.35	341.9	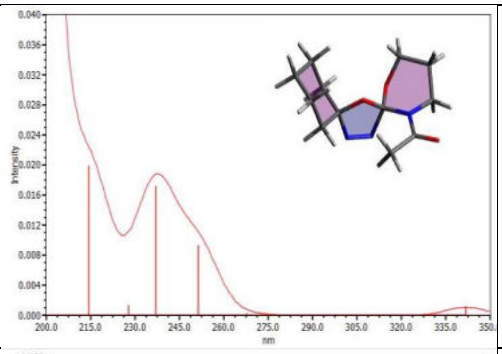	467.5	3.63	504.6
S10	1.32	350.9	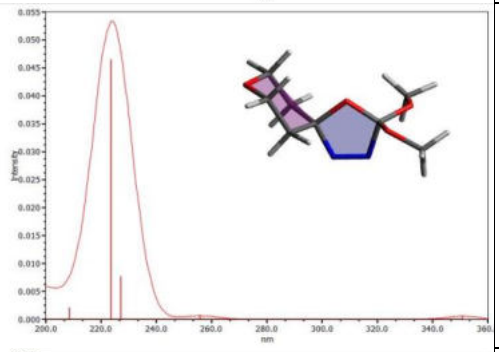	484.9	1.40	515.7
S11	1.65	351.5	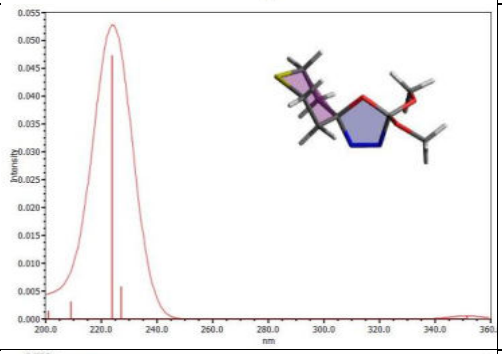	485.5	1.94	515.8
S12	5.05	349.5	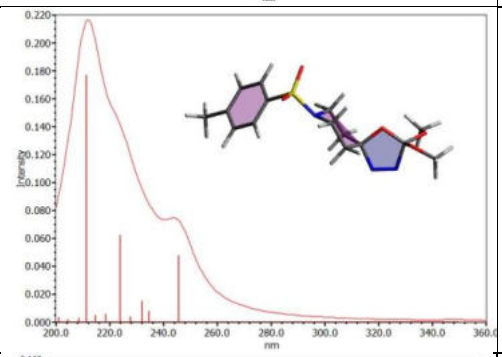	484.3	5.09	515.1
7	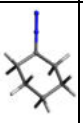 2. 60	$S_0 \rightarrow S_1$ 478.6 (f=0.000) $S_0 \rightarrow S_2$ 206.3 (f=0.135)	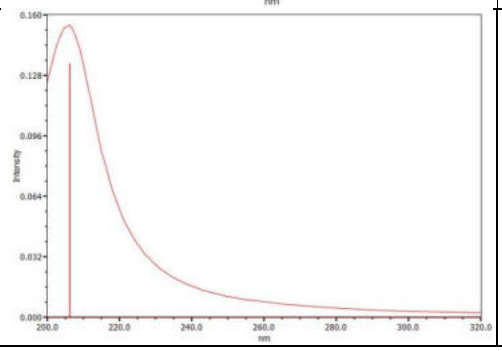	610.9	 3.87	1288.1

Molecule orientation and its influence on the absorption and emission

Characteristics summarized in Tables T3 and T4 were computed considering isomers possessing orientation of the lowest energies. To evaluate influence of molecule orientation, calculations for oxadiazolines **2**, **S10** and **S11** were performed for more energetic isomers (**a** and **b**) as well (Table T7). For most cases, more energetic isomers correspond to slightly blue-shifted absorption and emission.

Table T7. Influence of molecule orientation on the molecule characteristics.

	Isomer structure	Relative Energy [cm^{-1}]	μ [D][a]	$S_0 \rightarrow S_1$ [nm][a]	f[a]	$S_0 \rightarrow T_1$ [nm][a]	μ [D][b]	$T_u \rightarrow S_0$ [nm][b]
2		0	1.66	346.5	0.0137	467.0	0.66	500.9
2a	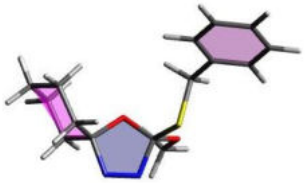	627	3.72	352.1	0.0046	474.9	3.38	494.4
S10	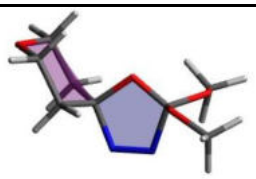	0	1.32	350.9	0.0006	484.9	1.4	515.7
S10a	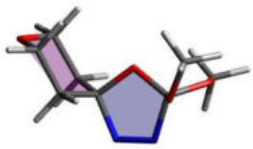	190	2.60	336.0	0.0005	468.9	2.28	502.2
S10b	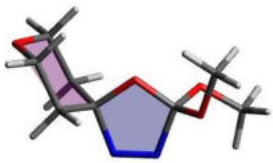	179	2.16	335.8	0.0005	467.0	2.02	503.3
S11	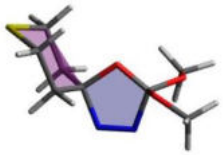	0	1.65	351.5	0.0006	485.5	1.94	515.8
S11a	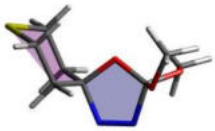	208	2.93	336.9	0.0006	469.3	2.08	502.6
S11b	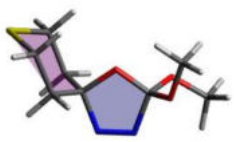	171	2.26	337.0	0.0006	467.7	2.29	504.0

[a] calculated with (B3LYP/6-31G(d,p)); [b] calculated with (UB3LYP/6-31G(d,p)).

Electronic states for singlet and triplet state-optimized molecules

Energy values corresponding to computed intersystem crossing transitions for molecules optimized both in the singlet ground and triplet states are summarized in Table T8. For all analyzed compounds, triplet energy values (E_T) referring to molecules of geometry optimized in S_0 state, calculated with the use of both TD-B3LYP/6-31G(d,p) and UB3LYP/6-31G(d,p) functionals are substantially higher than those observed for optimal triplet orientation. B3LYP/6-31G(d,p) method considering optimal singlet state S_o geometries gives the average E_T values which correlate well with the experimental data as highly energetic triplet sensitizers (of at least $E_T > 250$ but < 270 kJ mol^{-1}) are required for the reaction to proceed while application of $Ir(ppy)_3$ of slightly lower E_T = 243 kJ/mol^{-1} [13] gives only traces of cyclopropanation reaction (see Table 2, manuscript).

Table T8. Calculated triplet energy values depending on geometry optimization.

	Geometry optimized in S_0 state				Geometry optimized in T state *(UB3LYP/6-31G(d,p))*	
	(TD-B3LYP/6-31G(d,p))		*(UB3LYP/6-31G(d,p))*			
	$S_0 \rightarrow T_1$ [nm]	**E_T [kJ·mol^{-1}]**	$S_0 \rightarrow T_u$ [nm]	E_T [kJ·mol^{-1}]	$T_u \rightarrow S_0$ [nm]	E_T [kJ·mol^{-1}]
1	467.3	**256.0**	439.2	272.4	506.1	236.4
2	467.0	**256.2**	442.1	270.6	500.9	238.8
3	452.5	**264.4**	426.1	280.7	496.5	240.9
4	449.1	**266.4**	424.0	282.1	490.3	244.0
5	467.5	**255.9**	440.4	271.6	504.6	237.1
S10	484.9	**246.7**	456.5	262.1	515.7	232.0
S11	485.5	**246.4**	456.9	261.8	515.8	231.9
S12	484.3	**247.0**	455.7	262.5	515.1	232.2
7	610.9	**195.8**	459.6	260.3	1288.1	92.9

The diagram of the electronic states depicts relative orientation of singlet (ground and excited) and triplet state energies of oxadiazolines **1-5** and **S10-S12** (Chart C6). The energies corresponding to each oxadiazoline were calculated based on the geometry optimized in the ground state S_0 (opt. S_0) and considering geometries optimized in the triplet state (opt. T). S_1 and T_1 represent energy levels of lowest excited singlet and triplet state, calculated with R(restricted)B3LYP method. T_u denotes triplet energy levels calculated with U(unrestricted)B3LYP for geometries optimized in both ground singlet and in triplet state.

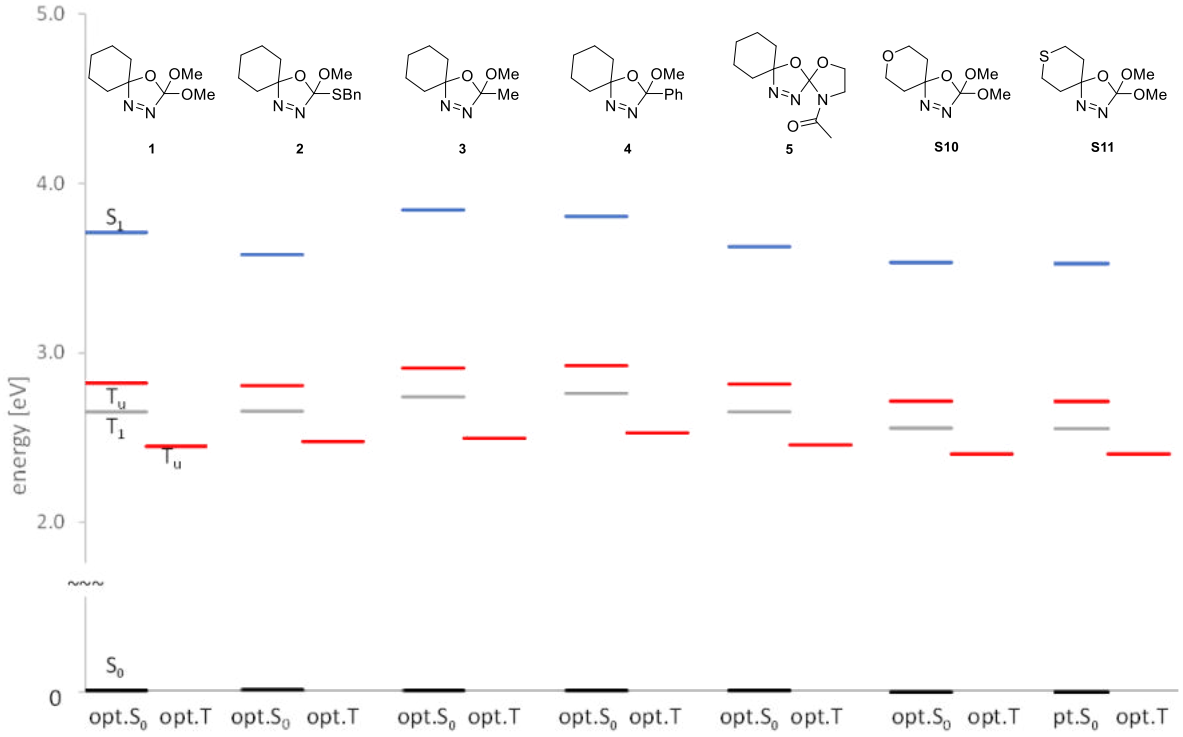

Chart C6. Singlet and triplet energy levels calculated for selected oxadiazolines.

7.2. Calculation of plausible reaction paths

7.2.1. Method

DFT calculations were performed with Gaussian 16 package.[17] Geometry optimizations were computed at the B3LYP/6-31G(d) level of theory with the D3 version of Grimme's empirical dispersion correction.[18] Frequency analysis was performed at the same level to provide correction to thermodynamic functions and confirm the nature of optimized structures (minima and transition states featured zero or one imaginary frequency, respectively). Single point energies were computed at the M06/6-311++G(d,p) level of theory involving solvation (dichloromethane) with SMD model.[19] Calculations for molecules in the first excited states (S1) were performed at the same levels of theory using TD-DFT methods. Molecular structures were visualized in CYLview.[20]

7.2.2. Potential energy surface scan for compound 22

Scans of potential energy surfaces for compound **22** (at singlet and triplet states) were performed at B3LYP/6-31G(d) level of theory.

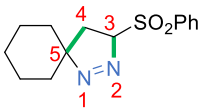

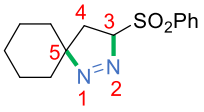

a) scan of PES for compound 22 in singlet state

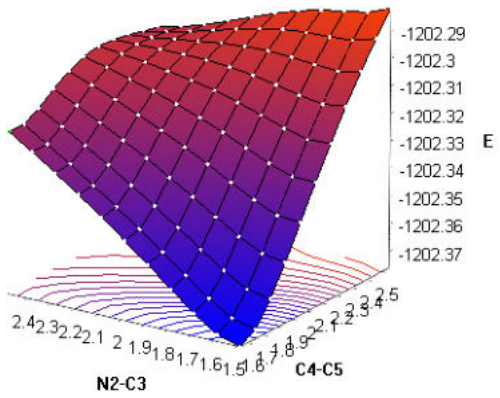

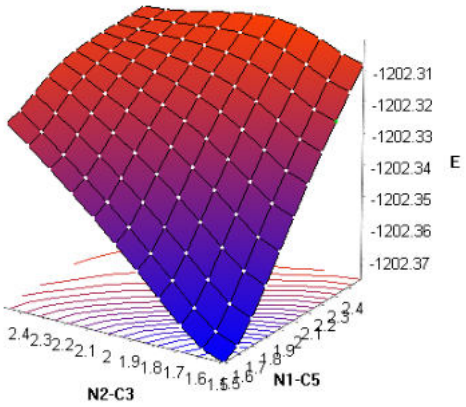

b) scan of PES for compound 22 in triplet state

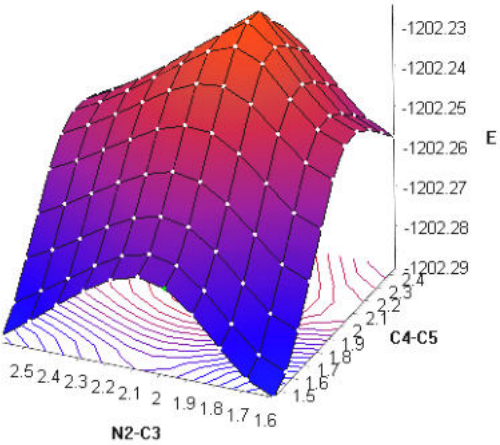

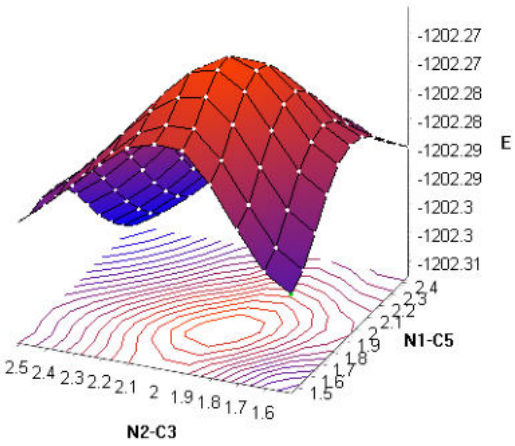

7.2.3. Optimized geometries, energies, and corrections to thermodynamic functions

S_0 PES

N_2

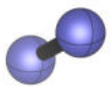

E (B3LYP-D3/6-31G(d)) = -109.524129
E (M06/6-311++G(d,p)/SMD(DCM)//B3LYP-D3/6-31G(d)) = -109.485126

Zero-point correction=	0.005598 (Hartree/Particle)
Thermal correction to Energy=	0.007959
Thermal correction to Enthalpy=	0.008903
Thermal correction to Gibbs Free Energy=	-0.012851

Charge = 0 Multiplicity = 1

N	0.00000000	0.00000000	0.55274900
N	0.00000000	0.00000000	-0.55274900

Dimethyl carbonate (8)

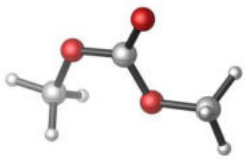

E (B3LYP-D3/6-31G(d)) = -343.609556
E (M06/6-311++G(d,p)/SMD(DCM)//B3LYP-D3/6-31G(d)) = -343.521788

Zero-point correction=	0.096038 (Hartree/Particle)
Thermal correction to Energy=	0.102829
Thermal correction to Enthalpy=	0.103773
Thermal correction to Gibbs Free Energy=	0.065417

Charge = 0 Multiplicity = 1

C	0.03890600	0.54028400	0.00003700
O	0.68860600	1.55636200	-0.00006700
O	-1.30261600	0.53792600	0.00009500
O	0.54989300	-0.71239700	0.00017800
C	-2.00842500	-0.71384000	-0.00009500
H	-3.06572900	-0.44479000	-0.00039100
H	-1.76865800	-1.29991500	-0.89200500
H	-1.76915400	-1.29987500	0.89198100
C	1.98671200	-0.76589600	-0.00009200
H	2.38743000	-0.27655600	0.89178100
H	2.23842400	-1.82711800	-0.00376600
H	2.38746400	-0.27015800	-0.88835700

Phenyl vinyl sulfone (11)

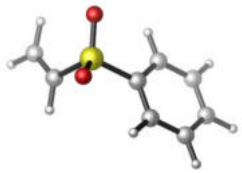

E (B3LYP-D3/6-31G(d)) = -858.226087
E (M06/6-311++G(d,p)/SMD(DCM)//B3LYP-D3/6-31G(d)) = -858.026697

Zero-point correction=	0.144002 (Hartree/Particle)
Thermal correction to Energy=	0.153959
Thermal correction to Enthalpy=	0.154904
Thermal correction to Gibbs Free Energy=	0.107710

Charge = 0 Multiplicity = 1

C	-2.72877900	-1.23733900	1.21772700

H	-2.95703100	-1.79648400	0.31461700
H	-3.19117300	-1.55538500	2.14809900
C	-1.91545600	-0.18693200	1.17897800
H	-1.64754100	0.43097900	2.03135200
S	-1.21760800	0.36770600	-0.37659800
C	0.54572400	0.10328100	-0.14258600
C	1.32633000	1.14274600	0.36586300
C	1.09580600	-1.13828200	-0.46804500
C	2.69083800	0.92578800	0.56109200
H	0.86916500	2.10314200	0.58073900
C	2.46064600	-1.34201600	-0.26892600
H	0.46237400	-1.91501100	-0.88390200
C	3.25437000	-0.31356700	0.24756000
H	3.31400100	1.72564600	0.95068700
H	2.90615200	-2.29971000	-0.52237800
H	4.31768800	-0.47713900	0.39971700
O	-1.67661400	-0.54766900	-1.43452100
O	-1.44448400	1.81999400	-0.45839600

1 [S_0]

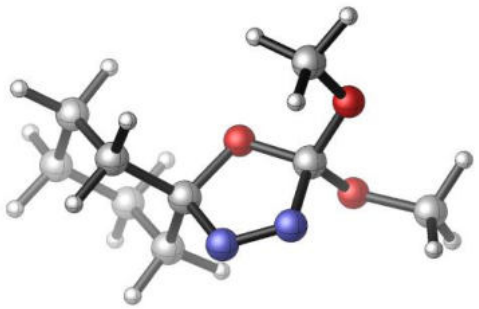

E (B3LYP-D3/6-31G(d)) = -687.751945
E (M06/6-311++G(d,p)/SMD(DCM)//B3LYP-D3/6-31G(d)) = -687.481081

Zero-point correction=	0.257698 (Hartree/Particle)
Thermal correction to Energy=	0.271191
Thermal correction to Enthalpy=	0.272136
Thermal correction to Gibbs Free Energy=	0.217709

Charge = 0 Multiplicity = 1

C	-1.45442400	-1.34008800	0.54881000
C	-2.45567000	-1.40236200	-0.61417400
C	-3.45719100	-0.23837000	-0.55639100
C	-2.73250400	1.11658900	-0.53023600
C	-1.73245800	1.18927700	0.63372600
C	-0.74520800	0.02294000	0.57400200
H	-4.14042100	-0.28414400	-1.41313400

H	-1.89738700	-1.35965300	-1.55775700
H	-2.98186700	-2.36421400	-0.59387900
H	-1.96869700	-1.47769200	1.50809900
H	-0.69168500	-2.12012700	0.45769100
H	-2.18893100	1.25909300	-1.47307400
H	-3.45380800	1.93842300	-0.44717100
H	-1.17011400	2.12976200	0.61855700
H	-2.25907500	1.13458100	1.59439100
H	-4.07652300	-0.33557700	0.34786400
C	1.41519700	-0.02838300	-0.15852000
N	0.18159600	0.06299600	1.73718300
N	1.35999200	0.05431400	1.36059400
O	0.10004300	0.16690300	-0.56898200
O	1.81781900	-1.29927800	-0.51890700
O	2.28288900	0.89768200	-0.69435200
C	3.19790400	-1.61190500	-0.28065700
H	3.29653600	-2.67664300	-0.50121100
H	3.84915700	-1.03258600	-0.94139600
H	3.47235500	-1.42470400	0.76287200
C	1.97590000	2.26297100	-0.40802300
H	1.98806600	2.45734800	0.67142700
H	2.75750200	2.85199300	-0.89100900
H	0.99848700	2.53650700	-0.82000800

TS1

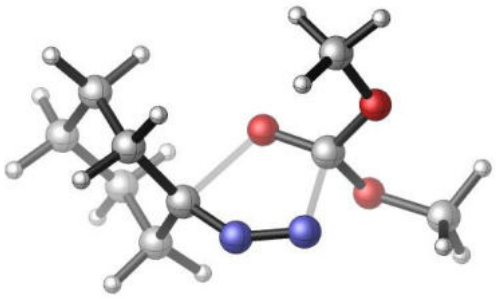

E (B3LYP-D3/6-31G(d)) = -687.701752
E (M06/6-311++G(d,p)/SMD(DCM)//B3LYP-D3/6-31G(d)) = -687.430996

Zero-point correction=	0.254330 (Hartree/Particle)
Thermal correction to Energy=	0.268445
Thermal correction to Enthalpy=	0.269389
Thermal correction to Gibbs Free Energy=	0.213728

Charge = 0 Multiplicity = 1

C	-1.64861200	-1.47150000	0.49389500
C	-2.44299400	-1.30861200	-0.81563400

C	-3.38277300	-0.09562700	-0.75864600
C	-2.60445200	1.19359600	-0.45777400
C	-1.82103600	1.08066600	0.86348500
C	-0.97822500	-0.16884700	0.85747200
H	-3.91984900	0.00606400	-1.70922500
H	-1.72734700	-1.18292200	-1.63363400
H	-3.00932800	-2.22828500	-1.00289100
H	-2.33318600	-1.75508100	1.30781200
H	-0.88828500	-2.25325500	0.40407800
H	-1.89183000	1.38925700	-1.26524200
H	-3.28408700	2.05144400	-0.39532300
H	-1.18203000	1.95440800	1.02791700
H	-2.52877000	1.02449900	1.70456700
H	-4.14494100	-0.25456900	0.01945300
C	1.43843400	-0.01764700	-0.37803400
N	0.06649800	-0.22767700	1.69137300
N	1.25415900	-0.19022900	1.54628100
O	0.24553500	0.12907700	-0.76814800
O	2.04198500	-1.21383900	-0.67419400
O	2.34325700	1.02689800	-0.45880500
C	3.40575500	-1.37154300	-0.27192500
H	3.64339900	-2.42372800	-0.44576300
H	4.06874500	-0.73784500	-0.86946700
H	3.53763100	-1.13248200	0.78817400
C	1.77342900	2.31883300	-0.30134700
H	1.32286000	2.43480600	0.69424800
H	2.59843200	3.02672900	-0.40552900
H	1.01061400	2.51330700	-1.06253000

7 [S_0]

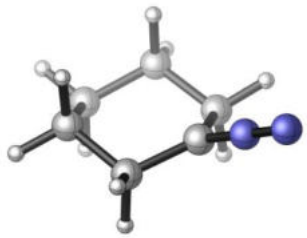

E (B3LYP-D3/6-31G(d)) = -344.125186
E (M06/6-311++G(d,p)/SMD(DCM)//B3LYP-D3/6-31G(d)) = -343.950574

Zero-point correction=	0.157245 (Hartree/Particle)
Thermal correction to Energy=	0.164615
Thermal correction to Enthalpy=	0.165560
Thermal correction to Gibbs Free Energy=	0.125350

Charge = 0 Multiplicity = 1

C	0.01205000	1.30066200	0.44579500
C	1.33636000	1.27222700	-0.34363700

C	2.14277700	0.00029800	-0.03428600
C	1.33683000	-1.27189800	-0.34377000
C	0.01252700	-1.30093000	0.44565900
C	-0.73327700	-0.00026800	0.25513400
H	3.07905600	0.00050100	-0.60570100
H	1.11271200	1.30725500	-1.41859900
H	1.92745100	2.16578700	-0.10606400
H	0.24234500	1.43984700	1.51527500
H	-0.60723800	2.15084000	0.14017600
H	1.11319900	-1.30690300	-1.41873600
H	1.92824700	-2.16526300	-0.10628200
H	-0.60644000	-2.15130800	0.13995000
H	0.24286000	-1.44012500	1.51513000
H	2.42371800	0.00029500	1.02994300
N	-1.97898300	-0.00050600	-0.07970100
N	-3.09237600	0.00029500	-0.38236500

TS9

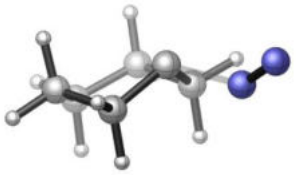

E (B3LYP-D3/6-31G(d)) = -344.066833
E (M06/6-311++G(d,p)/SMD(DCM)//B3LYP-D3/6-31G(d)) = -343.897342

Zero-point correction=	0.152639 (Hartree/Particle)
Thermal correction to Energy=	0.160606
Thermal correction to Enthalpy=	0.161550
Thermal correction to Gibbs Free Energy=	0.119769

Charge = 0 Multiplicity = 1

C	0.27894600	0.03598000	-1.23031000
C	0.27894600	-1.52745400	-1.26377300
C	0.93764400	-2.09783600	0.00000000
C	0.27894600	-1.52745400	1.26377300
C	0.27894600	0.03598000	1.23031000
C	-0.51443000	0.34935400	0.00000000
H	0.87504800	-3.19329900	0.00000000
H	-0.75478600	-1.88695500	-1.33815000
H	0.80266100	-1.85581900	-2.16892200
H	1.33330200	0.36528800	-1.21365900
H	-0.19197100	0.41867400	-2.14301700
H	-0.75478600	-1.88695500	1.33815000
H	0.80266100	-1.85581900	2.16892200

H	-0.19197100	0.41867400	2.14301700
H	1.33330200	0.36528800	1.21365900
H	2.00540300	-1.83813100	0.00000000
N	-0.66788900	2.39177300	0.00000000
N	-1.40251800	3.22788700	0.00000000

II [S_0]

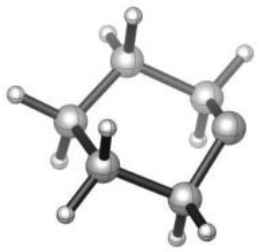

E (B3LYP-D3/6-31G(d)) = -234.541631
E (M06/6-311++G(d,p)/SMD(DCM)//B3LYP-D3/6-31G(d)) = -234.416976

Zero-point correction=	0.144911 (Hartree/Particle)
Thermal correction to Energy=	0.150544
Thermal correction to Enthalpy=	0.151488
Thermal correction to Gibbs Free Energy=	0.116290

Charge = 0 Multiplicity = 1

C	-0.03400000	-0.90463700	1.21346300
C	-0.03400000	0.67232500	1.26148900
C	0.62200300	1.24573500	0.00000000
C	-0.03400000	0.67232500	-1.26148900
C	-0.03400000	-0.90463700	-1.21346300
C	-0.84462600	-1.17149900	0.00000000
H	0.54837000	2.34087800	0.00000000
H	-1.06630900	1.03168400	1.34394500
H	0.49337200	0.98168400	2.17067400
H	1.02289900	-1.22915900	1.17710400
H	-0.49388400	-1.28092900	2.13479300
H	-1.06630900	1.03168400	-1.34394500
H	0.49337200	0.98168400	-2.17067400
H	-0.49388400	-1.28092900	-2.13479300
H	1.02289900	-1.22915900	-1.17710400
H	1.69120600	0.99488700	0.00000000

TS 12

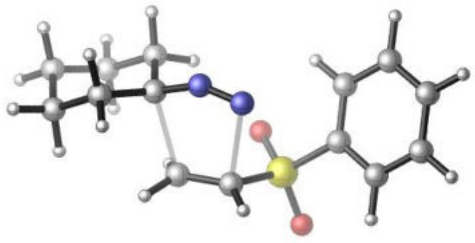

E (B3LYP-D3/6-31G(d)) = -1202.34951
E (M06/6-311++G(d,p)/SMD(DCM)//B3LYP-D3/6-31G(d)) = -1201.969746

Zero-point correction=	0.303331 (Hartree/Particle)
Thermal correction to Energy=	0.320687
Thermal correction to Enthalpy=	0.321631
Thermal correction to Gibbs Free Energy=	0.256992

Charge = 0 Multiplicity = 1

C	-3.32942200	-1.05222300	-1.22756700
C	-4.48595900	-0.10827500	-0.85662100
C	-4.80737200	-0.18523000	0.64281800
C	-3.57575300	0.16593600	1.48899600
C	-2.37646800	-0.74095800	1.16259000
C	-2.11909700	-0.77787400	-0.34370500
H	-5.63724400	0.48894200	0.88564500
H	-4.22032700	0.92385700	-1.11922000
H	-5.36590400	-0.37112500	-1.45509100
H	-3.66631100	-2.09031200	-1.08483900
H	-3.05408100	-0.94460800	-2.28330700
H	-3.30372300	1.21466100	1.31810400
H	-3.80281400	0.07530600	2.55734000
H	-1.47448400	-0.38719500	1.67175000
H	-2.59758700	-1.75802100	1.52015200
H	-5.14324700	-1.20343400	0.88938400
C	-1.29295600	1.19906700	-0.91708000
H	-1.63076400	1.63635500	0.01494700
H	-1.94374400	1.33488100	-1.77649700
C	0.05773200	1.04311300	-1.13193100
H	0.52439100	1.00951400	-2.10917600
N	-0.99235600	-1.43370100	-0.69011300
N	0.10761100	-1.37521400	-1.03971500
S	1.15588300	1.45034700	0.20461900
O	0.39678600	1.27400900	1.46402900
O	1.81403800	2.73702000	-0.09229000
C	2.44890600	0.19921800	0.17514600
C	2.36799000	-0.89258100	1.03962400
C	3.51532400	0.35013500	-0.71230800

C	3.37233500	-1.85980800	1.00352700
H	1.53657400	-0.96492900	1.73241800
C	4.50995300	-0.62708800	-0.74572800
H	3.56992600	1.22972500	-1.34564800
C	4.43711900	-1.73058300	0.10868100
H	3.32482600	-2.71243900	1.67516400
H	5.34663700	-0.52222800	-1.43076000
H	5.21637600	-2.48743800	0.08197400

12

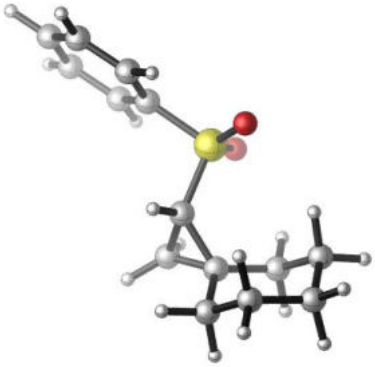

E (B3LYP-D3/6-31G(d)) = -1092.929251
E (M06/6-311++G(d,p)/SMD(DCM)//B3LYP-D3/6-31G(d)) = -1092.592624

Zero-point correction=	0.297442 (Hartree/Particle)
Thermal correction to Energy=	0.312497
Thermal correction to Enthalpy=	0.313441
Thermal correction to Gibbs Free Energy=	0.254306

Charge = 0 Multiplicity = 1

C	4.19422300	0.85132700	-0.36672300
C	3.30281700	-0.09385800	-1.18774800
C	2.66999200	-1.18005000	-0.30099600
C	1.91877800	-0.55304200	0.87010800
C	2.80676400	0.36838600	1.69966600
C	3.42435500	1.46333600	0.81453900
H	2.01039800	-1.82182400	-0.88944100
H	2.50077500	0.48053700	-1.66791600
H	3.88514200	-0.56475100	-1.98931600
H	5.05918900	0.29154200	0.02056100
H	4.59539100	1.64677000	-1.00688400
H	2.23843000	0.81108600	2.52830000
H	3.60653400	-0.23627100	2.15207800
H	2.61861600	2.10306500	0.42746300
H	4.08317900	2.10395000	1.41400900
H	3.45951800	-1.82023500	0.11982000

C	0.48163500	-0.07612700	0.72230400
C	0.79979100	-1.30297100	1.54256600
H	0.20582200	0.84551000	1.22984500
H	0.51706800	-2.25732100	1.10502000
H	0.67162000	-1.23017600	2.62005200
S	-0.43997400	-0.20678200	-0.80954500
C	-2.13465100	0.06134900	-0.26360500
C	-2.89545200	-1.03352200	0.15017200
C	-2.64795700	1.35925600	-0.25163300
C	-4.19910300	-0.81686500	0.59657200
H	-2.47256500	-2.03144100	0.10105600
C	-3.95317900	1.56287300	0.19716200
H	-2.03635700	2.18220800	-0.60730800
C	-4.72425600	0.47804700	0.62306200
H	-4.80677900	-1.65836200	0.91695200
H	-4.37013400	2.56590600	0.20737300
H	-5.74088800	0.64137600	0.97007300
O	-0.06139000	0.93414400	-1.66452800
O	-0.34460000	-1.59313000	-1.30693500

22 [S_0]

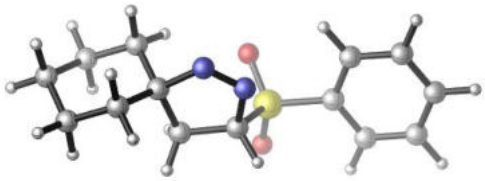

E (B3LYP-D3/6-31G(d)) = -1202.419528
E (M06/6-311++G(d,p)/SMD(DCM)//B3LYP-D3/6-31G(d)) = -1202.044127

Zero-point correction=	0.308370 (Hartree/Particle)
Thermal correction to Energy=	0.324801
Thermal correction to Enthalpy=	0.325745
Thermal correction to Gibbs Free Energy=	0.263159

Charge = 0 Multiplicity = 1

C	-3.39231000	-1.21029800	-0.97338100
C	-4.57750500	-0.23693600	-1.05754500
C	-5.04580600	0.18761400	0.34192400
C	-3.88723500	0.78843600	1.15057000
C	-2.69087400	-0.17206300	1.22694100
C	-2.21781800	-0.60818200	-0.17784500
H	-5.87184100	0.90529400	0.26567400
H	-4.28328700	0.65519000	-1.62951200
H	-5.39829200	-0.70623400	-1.61339700
H	-3.70791800	-2.13290900	-0.46981300

H	-3.04794500	-1.49552200	-1.97582600
H	-3.57313600	1.73461000	0.68697600
H	-4.21585300	1.03846500	2.16643300
H	-1.85133600	0.28521700	1.75966000
H	-2.97835100	-1.07512800	1.78097700
H	-5.43806600	-0.69285800	0.87165400
C	-1.45488300	0.50047200	-0.94629000
H	-1.55426000	1.48408100	-0.48159100
H	-1.79957000	0.59118800	-1.98001900
C	-0.01320900	-0.01546600	-0.92035200
H	0.50919300	-0.02444900	-1.88045400
N	-1.20534700	-1.69175300	0.01907100
N	-0.06556300	-1.39718100	-0.36999500
S	1.04640200	1.01384700	0.19146000
O	0.52075800	0.85917500	1.55887400
O	1.13290700	2.34168700	-0.44057000
C	2.65780000	0.23265300	0.10356600
C	2.89893400	-0.91289400	0.86541400
C	3.63103100	0.78803400	-0.72834300
C	4.15194700	-1.51778700	0.78126100
H	2.12029700	-1.31304300	1.50445800
C	4.88148400	0.17312000	-0.79903700
H	3.40848000	1.68910500	-1.29017700
C	5.13839200	-0.97681000	-0.04858800
H	4.35920100	-2.40955200	1.36540400
H	5.65423000	0.59401000	-1.43579300
H	6.11340000	-1.45271100	-0.10774800

TS for C-H insertion of II to 1

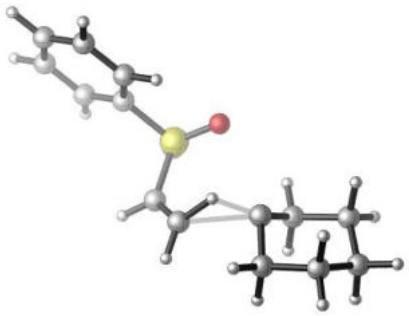

E (B3LYP-D3/6-31G(d)) = -1092.765578
E (M06/6-311++G(d,p)/SMD(DCM)//B3LYP-D3/6-31G(d)) = -1092.429393

Zero-point correction=	0.287365 (Hartree/Particle)
Thermal correction to Energy=	0.303741
Thermal correction to Enthalpy=	0.304685
Thermal correction to Gibbs Free Energy=	0.240775

Charge = 0 Multiplicity = 1

C	3.55308900	1.13033400	1.06473500
C	4.85123100	1.35320600	0.22797000
C	5.30681600	0.04485700	-0.43279200
C	4.17220600	-0.57929400	-1.25672500
C	2.89028500	-0.77039000	-0.38614900
C	2.55576100	0.61695400	0.06778600
H	6.18375300	0.22753700	-1.06680400
H	4.65407100	2.10855400	-0.54306400
H	5.62886900	1.75720000	0.88698100
H	3.80128500	0.42316500	1.87724900
H	3.24138700	2.07910200	1.51740500
H	3.93391100	0.06605600	-2.11143000
H	4.46633200	-1.55520600	-1.66027400
H	2.08747400	-1.20312700	-0.98597700
H	3.14848300	-1.47017800	0.42798900
H	5.61897600	-0.66380000	0.34732800
C	0.76375600	0.29264200	1.52013400
H	1.27000600	0.77084600	0.47246300
H	1.18823700	0.61536600	2.46751100
C	-0.34302200	-0.43672900	1.47309200
H	-0.91112500	-0.75928400	2.34525000
S	-1.07272200	-1.02237800	-0.06131100
O	-1.43056000	-2.43562700	0.14783300
O	-0.22327100	-0.59957100	-1.18616200
C	-2.59969700	-0.07475900	-0.14552200
C	-3.77118300	-0.62123200	0.38018400
C	-2.57566100	1.19361300	-0.72969500
C	-4.94682500	0.12857200	0.32408100
H	-3.75550700	-1.62048600	0.80309200
C	-3.75700400	1.93224400	-0.77928400
H	-1.64992900	1.57653200	-1.14729500
C	-4.93785000	1.40181500	-0.25082500
H	-5.86930600	-0.28349200	0.72309800
H	-3.75822300	2.91831400	-1.23490100
H	-5.85590000	1.98151700	-0.29295400

TS for C-H extrusion of N_2 from 22

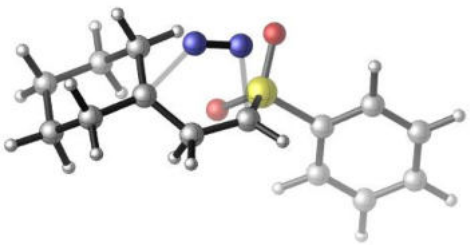

E (B3LYP-D3/6-31G(d)) = -1202.353595
E (M06/6-311++G(d,p)/SMD(DCM)//B3LYP-D3/6-31G(d)) = -1201.978659

Zero-point correction=	0.300682 (Hartree/Particle)
Thermal correction to Energy=	0.318637
Thermal correction to Enthalpy=	0.319581
Thermal correction to Gibbs Free Energy=	0.253757

Charge = 0 Multiplicity = 1

C	3.69135600	0.14107000	-1.26499400
C	4.14400400	-1.32123100	-0.98761800
C	4.23677800	-1.60123200	0.51851200
C	2.93155600	-1.24584100	1.24355600
C	2.52500000	0.22556600	0.95272700
C	2.42970300	0.45513300	-0.52185200
H	4.48523800	-2.65676800	0.68436700
H	3.41561000	-2.00379500	-1.44712900
H	5.10672100	-1.50046400	-1.48120000
H	4.47156400	0.82074300	-0.89462600
H	3.58163800	0.31457600	-2.34146900
H	2.11285000	-1.90029000	0.92817200
H	3.04172100	-1.37104100	2.32663400
H	1.60701500	0.49576900	1.47675600
H	3.32833200	0.87564300	1.32787000
H	5.06312000	-1.01224400	0.94256200
C	1.14970700	0.36707500	-1.28159900
H	1.14071200	-0.75111300	-1.32042400
H	1.30334400	0.71384900	-2.30842600
C	-0.15312100	0.78427500	-0.76986400
H	-0.87898000	1.21253100	-1.44913300
N	2.07389700	2.76030800	-0.26610600
N	0.97290100	2.95974600	-0.17437000
S	-0.85696000	-0.02474300	0.60818200
O	-0.84593600	0.82149600	1.82132200
O	-0.24759100	-1.37883700	0.70165700
C	-2.58360700	-0.22258300	0.13568800
C	-3.48521400	0.80751900	0.40825600
C	-2.98533400	-1.39681900	-0.50274100
C	-4.81576300	0.66136300	0.01338300
H	-3.14530200	1.69264000	0.93614600
C	-4.31951200	-1.53517600	-0.88498000
H	-2.26027500	-2.18551100	-0.67579300
C	-5.23107000	-0.50580400	-0.63280200
H	-5.52973500	1.45394100	0.21950000
H	-4.64923600	-2.44697400	-1.37536000
H	-6.26924500	-0.61714400	-0.93390300

T_1 PES

1 [T_1]

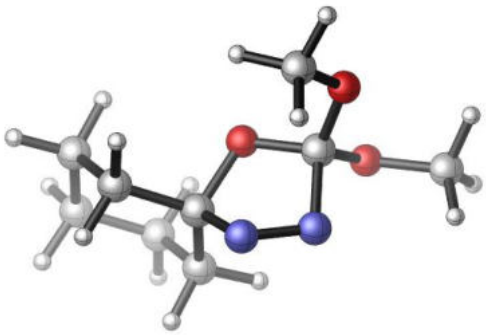

E (B3LYP-D3/6-31G(d)) = -687.663599
E (M06/6-311++G(d,p)/SMD(DCM)//B3LYP-D3/6-31G(d)) = -687.388668

Zero-point correction=	0.255374 (Hartree/Particle)
Thermal correction to Energy=	0.268941
Thermal correction to Enthalpy=	0.269886
Thermal correction to Gibbs Free Energy=	0.214781

Charge = 0 Multiplicity = 3

C	-1.39659100	-1.14259800	0.82785600
C	-2.35643200	-1.51203900	-0.31325300
C	-3.42102300	-0.42430700	-0.52428300
C	-2.77012500	0.94535400	-0.77266300
C	-1.80865800	1.32208200	0.36632900
C	-0.76790800	0.23297600	0.58033700
H	-4.07374700	-0.68974100	-1.36492900
H	-1.77084500	-1.63596200	-1.23266600
H	-2.82941300	-2.47789100	-0.09858700
H	-1.93604800	-1.09970400	1.78326100
H	-0.59499200	-1.88001500	0.92731000
H	-2.20727400	0.91736400	-1.71424900
H	-3.53511500	1.72403000	-0.87832100
H	-1.29524400	2.26717200	0.16219300
H	-2.36047700	1.44192700	1.30751400
H	-4.06243800	-0.36481000	0.36788900
C	1.41006300	-0.08000300	-0.18292500

N	0.23588000	0.63385100	1.60063900
N	1.28479800	-0.07466600	1.35572800
O	0.09662600	0.18291300	-0.60167800
O	1.74721600	-1.34541100	-0.57794100
O	2.31951700	0.81832800	-0.68633700
C	3.07584800	-1.75683100	-0.23888800
H	3.13435100	-2.81477500	-0.50005300
H	3.81867700	-1.18531100	-0.80271800
H	3.24759500	-1.62811300	0.83689700
C	2.09430100	2.19008600	-0.35920200
H	2.13752300	2.34657000	0.72455200
H	2.89634500	2.74617300	-0.84770100
H	1.12262900	2.52383200	-0.73715700

TS1

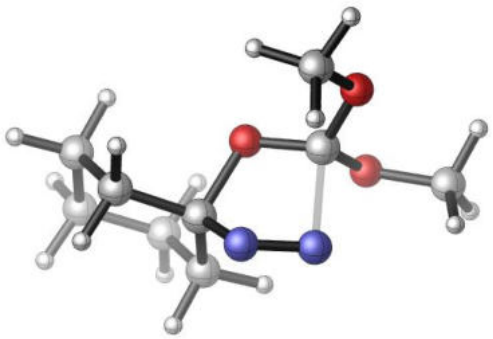

E (B3LYP-D3/6-31G(d)) = -687.657535
E (M06/6-311++G(d,p)/SMD(DCM)//B3LYP-D3/6-31G(d)) = -687.382094

Zero-point correction=	0.254228 (Hartree/Particle)
Thermal correction to Energy=	0.267890
Thermal correction to Enthalpy=	0.268834
Thermal correction to Gibbs Free Energy=	0.213553

Charge = 0 Multiplicity = 3

C	-1.33710000	-1.12050600	0.81896200
C	-2.24446200	-1.51077700	-0.35621400
C	-3.34970500	-0.46682700	-0.57954300
C	-2.75423000	0.93513000	-0.78329900
C	-1.84249700	1.33377100	0.38738000
C	-0.76843600	0.29011800	0.64575400
H	-3.96648300	-0.74412300	-1.44335500
H	-1.62953200	-1.59437900	-1.26086100
H	-2.68165700	-2.49966800	-0.17143900
H	-1.91024600	-1.12042400	1.75610500
H	-0.50894100	-1.82325100	0.93907200
H	-2.16741200	0.95006200	-1.71038400

H	-3.55128600	1.67993800	-0.89697400
H	-1.35913200	2.30031100	0.21190400
H	-2.42751500	1.42458200	1.31211900
H	-4.01785800	-0.45337200	0.29475300
C	1.37207500	-0.07727400	-0.35240900
N	0.17876200	0.71310200	1.66055600
N	1.22263100	0.02701200	1.62239800
O	0.11540700	0.29103600	-0.60910300
O	1.62024800	-1.38215200	-0.53593500
O	2.35898800	0.73113800	-0.77988400
C	2.93590600	-1.83283000	-0.16972900
H	2.89946100	-2.92086000	-0.23484400
H	3.68472900	-1.43530100	-0.85997400
H	3.15930800	-1.51737300	0.85349600
C	2.21191800	2.12552800	-0.47173800
H	2.23051800	2.26459200	0.61291500
H	3.06456400	2.61882800	-0.93953900
H	1.27377200	2.51146100	-0.87927700

TS2

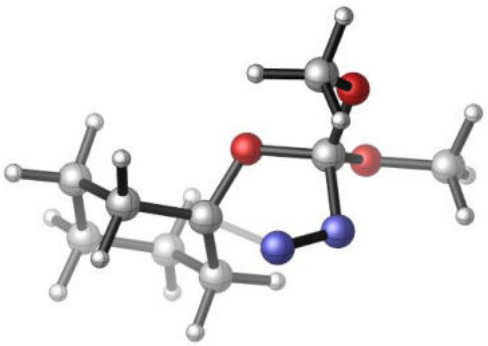

E (B3LYP-D3/6-31G(d)) = -687.643966
E (M06/6-311++G(d,p)/SMD(DCM)//B3LYP-D3/6-31G(d)) = -687.368075

Zero-point correction=	0.253094 (Hartree/Particle)
Thermal correction to Energy=	0.266850
Thermal correction to Enthalpy=	0.267794
Thermal correction to Gibbs Free Energy=	0.211944

Charge = 0 Multiplicity = 3

C	1.37071600	1.03704300	0.85148300
C	2.40504900	1.49975600	-0.20505800
C	3.50587300	0.44313700	-0.39917500
C	2.92034400	-0.92768000	-0.77811900
C	1.86605300	-1.38898900	0.26349300
C	0.84839300	-0.30782800	0.42928300
H	4.21304500	0.77286100	-1.17030000

H	1.88004900	1.66893700	-1.15391200
H	2.83938100	2.45915000	0.10157700
H	1.85686700	0.93778300	1.82954200
H	0.54960900	1.75210100	0.94315300
H	2.43512700	-0.86213500	-1.76042900
H	3.71349600	-1.68102400	-0.85711100
H	1.37999300	-2.31962400	-0.04438500
H	2.35619500	-1.55950200	1.22996400
H	4.08013900	0.34515000	0.53413100
C	-1.41751700	0.09579500	-0.16808500
N	-0.61729900	-0.83885700	1.74231700
N	-1.40838800	0.01639300	1.34386500
O	-0.10147800	-0.31534400	-0.57473900
O	-1.57993400	1.39723100	-0.56043000
O	-2.35223700	-0.69177700	-0.79334900
C	-2.85366200	1.96853400	-0.23882300
H	-2.78777300	3.01891800	-0.52766400
H	-3.65453900	1.47446500	-0.79701500
H	-3.04639400	1.88927900	0.83746100
C	-2.35511500	-2.08052400	-0.45381600
H	-2.63758100	-2.22946000	0.59358900
H	-3.09791700	-2.54011300	-1.10852200
H	-1.37150100	-2.52588300	-0.63232100

I

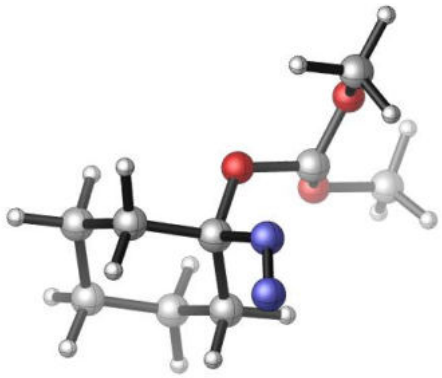

E (B3LYP-D3/6-31G(d)) = -687.669054
E (M06/6-311++G(d,p)/SMD(DCM)//B3LYP-D3/6-31G(d)) = -687.389906

Zero-point correction=	0.253620 (Hartree/Particle)
Thermal correction to Energy=	0.268835
Thermal correction to Enthalpy=	0.269779
Thermal correction to Gibbs Free Energy=	0.209846

Charge = 0 Multiplicity = 3

C	-1.13656100	-0.39606400	1.20456900
C	-1.77270000	-1.63088100	0.54610400

C	-2.94452000	-1.23763500	-0.36676200
C	-2.50733500	-0.20898900	-1.42088400
C	-1.88094900	1.02992300	-0.75931700
C	-0.71952300	0.62315300	0.14418700
H	-3.35637500	-2.12810900	-0.85720800
H	-1.00411000	-2.15116200	-0.03607300
H	-2.11041600	-2.32258400	1.32760300
H	-1.85391700	0.09991600	1.86959100
H	-0.26644700	-0.67403300	1.80632700
H	-1.76895300	-0.66174100	-2.09362000
H	-3.36036100	0.10068400	-2.03676200
H	-1.51545900	1.74020400	-1.50880600
H	-2.62270000	1.54702500	-0.13868800
H	-3.75414000	-0.80932500	0.24296000
C	1.48912100	-0.23568000	-0.10070700
N	-0.18086500	1.94006600	0.84170100
N	-0.75364100	2.45327700	1.72881400
O	0.31538300	0.17757700	-0.70676400
O	1.50265200	-1.59337500	0.04662900
O	2.61029900	0.22876200	-0.72535100
C	2.68228800	-2.12931100	0.65249000
H	2.47738100	-3.18796600	0.82238600
H	3.54819800	-2.01674100	-0.00679200
H	2.88815300	-1.63301500	1.60907400
C	2.71537500	1.65395000	-0.80335400
H	2.73514700	2.09699000	0.19831200
H	3.65329500	1.85614200	-1.32385400
H	1.87439400	2.07581600	-1.36212200

TS7

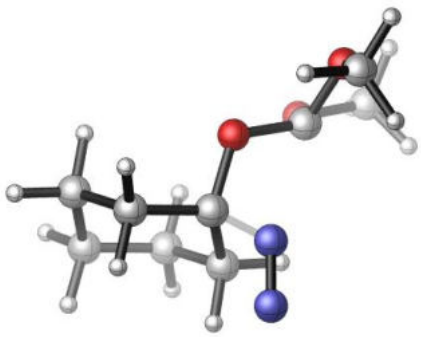

E (B3LYP-D3/6-31G(d)) = -687.66843
E (M06/6-311++G(d,p)/SMD(DCM)//B3LYP-D3/6-31G(d)) = -687.389709

Zero-point correction=	0.252353 (Hartree/Particle)
Thermal correction to Energy=	0.267406
Thermal correction to Enthalpy=	0.268350

Thermal correction to Gibbs Free Energy= 0.208399

Charge = 0 Multiplicity = 3

C	-1.11003400	-0.33475700	1.20519000
C	-1.77573500	-1.60586500	0.64317900
C	-2.95869000	-1.25856000	-0.27447200
C	-2.52941600	-0.30908900	-1.40413100
C	-1.87694800	0.96577500	-0.83475100
C	-0.71925500	0.59537900	0.07034900
H	-3.39036600	-2.17477500	-0.69574900
H	-1.02409100	-2.17419100	0.08375800
H	-2.10776100	-2.23871500	1.47551100
H	-1.81000600	0.21076600	1.84981900
H	-0.23100400	-0.58305800	1.80671300
H	-1.80587100	-0.81491500	-2.05558700
H	-3.38920400	-0.03339300	-2.02676300
H	-1.51553700	1.62026700	-1.63516700
H	-2.60620800	1.52946000	-0.24034100
H	-3.75169100	-0.77918400	0.31876100
C	1.49502600	-0.25817600	-0.09519700
N	-0.17363800	2.09375000	0.77544500
N	-0.80307600	2.60479000	1.60309500
O	0.33926700	0.17080700	-0.73307400
O	1.49043500	-1.61747700	0.02882400
O	2.63392700	0.20657800	-0.68356100
C	2.64844400	-2.17667000	0.65557800
H	2.42896900	-3.23627500	0.79873800
H	3.53270200	-2.05952600	0.02202200
H	2.83269000	-1.70123700	1.62701300
C	2.75511000	1.63242200	-0.73498300
H	2.75244500	2.05829500	0.27417600
H	3.70868500	1.83269900	-1.22688500
H	1.93320900	2.07198100	-1.30788400

TS8

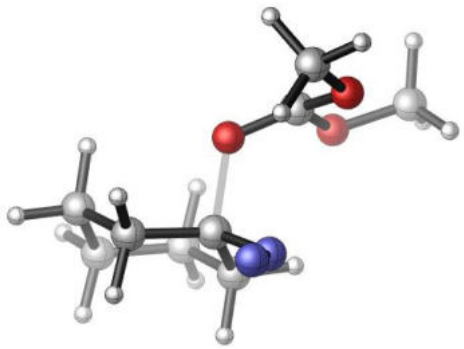

E (B3LYP-D3/6-31G(d)) = -687.657627

E (M06/6-311++G(d,p)/SMD(DCM)//B3LYP-D3/6-31G(d)) = -687.375617

Zero-point correction=	0.251913 (Hartree/Particle)
Thermal correction to Energy=	0.266788
Thermal correction to Enthalpy=	0.267732
Thermal correction to Gibbs Free Energy=	0.208642

Charge = 0 Multiplicity = 3

C	-1.19376200	-0.70760100	1.19290400
C	-1.95978300	-1.66973400	0.27417700
C	-3.12860200	-0.95561700	-0.42215200
C	-2.64353500	0.27559300	-1.20297000
C	-1.86398200	1.24859400	-0.30356100
C	-0.75625600	0.54079600	0.45230900
H	-3.64869600	-1.64736900	-1.09622500
H	-1.26501600	-2.06692800	-0.47429600
H	-2.32483700	-2.52045900	0.86218200
H	-1.85207700	-0.37960800	2.01276200
H	-0.32496000	-1.18848200	1.64733600
H	-1.98936200	-0.04732700	-2.02087000
H	-3.49252800	0.80204200	-1.65602800
H	-1.43344600	2.07127000	-0.88249400
H	-2.53447300	1.69737700	0.44351000
H	-3.86310400	-0.64066300	0.33460800
C	1.42522500	-0.41890600	-0.57475500
N	0.07358800	1.38777400	1.30949500
N	0.06940700	2.58256900	1.27476900
O	0.25029800	0.09772700	-0.78620500
O	1.46381300	-1.63631000	0.02191200
O	2.50059600	0.35850300	-0.28001200
C	2.75003300	-2.16429000	0.36420600
H	2.56499400	-3.18341600	0.70788600
H	3.41224100	-2.17830000	-0.50853400
H	3.21543600	-1.57574800	1.16003500
C	2.55011400	1.62894200	-0.94076300
H	1.81302400	2.31683500	-0.51812900
H	3.55747100	2.01133400	-0.76885600
H	2.36999700	1.51101100	-2.01466700

7 [T_1]

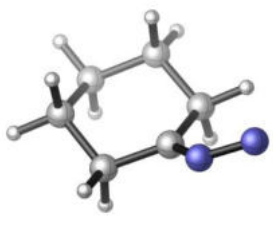

E (B3LYP-D3/6-31G(d)) = -344.089908
E (M06/6-311++G(d,p)/SMD(DCM)//B3LYP-D3/6-31G(d)) = -343.912847

Zero-point correction=	0.155101 (Hartree/Particle)
Thermal correction to Energy=	0.162540
Thermal correction to Enthalpy=	0.163485
Thermal correction to Gibbs Free Energy=	0.122206

Charge = 0 Multiplicity = 3

C	-0.23168200	1.14769900	0.48733900
C	1.09070600	1.39267000	-0.27636100
C	2.10854900	0.27344900	-0.01095400
C	1.53251200	-1.10181100	-0.37948800
C	0.21743200	-1.38022800	0.38637200
C	-0.74183300	-0.24235000	0.22991800
H	3.02908000	0.46039000	-0.57727000
H	0.87613000	1.44135700	-1.35246800
H	1.50192000	2.36751400	0.01117000
H	-0.03617200	1.25081000	1.56721200
H	-0.99291800	1.88692800	0.22182600
H	1.33073600	-1.13514700	-1.45872500
H	2.25618000	-1.89678400	-0.16442500
H	-0.25284600	-2.31222700	0.05840600
H	0.46044300	-1.49291800	1.45636000
H	2.38586600	0.27838900	1.05370800
N	-2.01168600	-0.51414800	-0.16199700
N	-2.90439000	0.31630700	-0.32896800

TS10

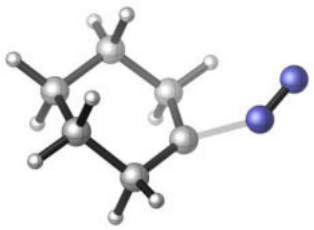

E (B3LYP-D3/6-31G(d)) = -344.061384
E (M06/6-311++G(d,p)/SMD(DCM)//B3LYP-D3/6-31G(d)) = -343.883963

Zero-point correction=	0.152014 (Hartree/Particle)
Thermal correction to Energy=	0.160058
Thermal correction to Enthalpy=	0.161003
Thermal correction to Gibbs Free Energy=	0.117631

Charge = 0 Multiplicity = 3

C	-0.13191200	1.15185000	0.71863000
C	1.00512100	1.40166300	-0.31228500
C	2.07345000	0.29873600	-0.24132500
C	1.46973800	-1.09090000	-0.50122200

C	0.34761700	-1.41442300	0.52562800
C	-0.56519200	-0.25942300	0.64531400
H	2.86912900	0.50240000	-0.96876200
H	0.56972900	1.41967900	-1.32010700
H	1.45064100	2.38839600	-0.13488000
H	0.24787200	1.37667800	1.73054700
H	-0.97526900	1.83133200	0.53902400
H	1.04241800	-1.11666300	-1.51240100
H	2.24397100	-1.86696500	-0.45676900
H	-0.20174500	-2.31747000	0.23319300
H	0.81553900	-1.62705100	1.50312700
H	2.54522200	0.31118800	0.75287800
N	-2.22650500	-0.54792600	-0.26423100
N	-2.88784400	0.34413400	-0.50352400

IM

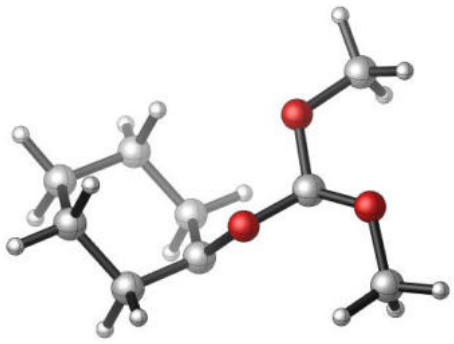

E (B3LYP-D3/6-31G(d)) = -578.158614
E (M06/6-311++G(d,p)/SMD(DCM)//B3LYP-D3/6-31G(d)) = -577.916481

Zero-point correction=	0.244306 (Hartree/Particle)
Thermal correction to Energy=	0.257493
Thermal correction to Enthalpy=	0.258437
Thermal correction to Gibbs Free Energy=	0.202418

Charge = 0 Multiplicity = 3

C	1.10890000	0.44336400	1.31543500
C	1.93743700	1.38063300	0.39824300
C	3.13092000	0.63224300	-0.21868800
C	2.68447600	-0.63149100	-0.97283800
C	1.86191100	-1.56565300	-0.04673600
C	0.72480200	-0.80275900	0.56515200
H	3.68380800	1.29762100	-0.89422700
H	1.27785800	1.74957900	-0.39656400
H	2.28375900	2.25307600	0.96792800
H	1.72285000	0.14730700	2.17738200
H	0.22738900	0.96194600	1.70440100

H	2.05263100	-0.34516100	-1.82389600
H	3.55285700	-1.16742700	-1.37737700
H	1.48639500	-2.43120400	-0.60432400
H	2.51303600	-1.94089400	0.75485300
H	3.83123400	0.34594800	0.58115900
C	-1.43721500	0.03041700	0.01837900
O	-0.34261900	-0.72814600	-0.34115200
O	-1.34835100	1.28353400	-0.51928400
O	-2.63126900	-0.57450700	-0.27153500
C	-2.43774900	2.15619900	-0.21264100
H	-2.15307400	3.13843300	-0.59480200
H	-3.36022400	1.82039300	-0.69652100
H	-2.59856600	2.21336300	0.87152900
C	-2.80115100	-1.86331000	0.31917800
H	-2.68419300	-1.81054600	1.40904900
H	-3.81569000	-2.18064700	0.07043000
H	-2.07615200	-2.57669300	-0.08616200

TS11

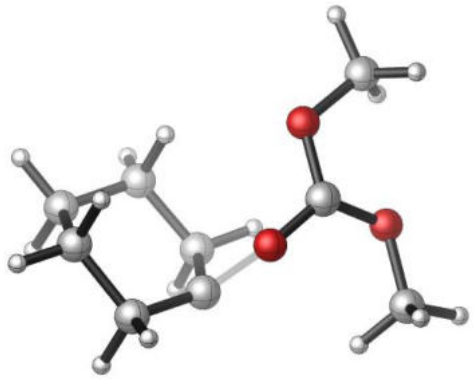

E (B3LYP-D3/6-31G(d)) = -578.132453
E (M06/6-311++G(d,p)/SMD(DCM)//B3LYP-D3/6-31G(d)) = -577.893457

Zero-point correction=	0.241203 (Hartree/Particle)
Thermal correction to Energy=	0.254537
Thermal correction to Enthalpy=	0.255481
Thermal correction to Gibbs Free Energy=	0.199322

Charge = 0 Multiplicity = 3

C	0.89860500	0.01719200	1.38153700
C	1.65640400	1.26425300	0.84659500
C	2.98133700	0.85974400	0.18046800
C	2.75969300	-0.14772300	-0.95936600
C	2.04417300	-1.42568700	-0.44017200
C	0.84861900	-1.03208500	0.33494300
H	3.49328700	1.75192900	-0.20245200
H	1.01344700	1.76564300	0.11461700

H	1.83503300	1.96811700	1.67006500
H	1.43412500	-0.37275300	2.26572700
H	-0.10681400	0.29397100	1.72143700
H	2.12865600	0.30876400	-1.73187800
H	3.71394600	-0.41970400	-1.42880000
H	1.76387800	-2.07648500	-1.27688400
H	2.74407100	-1.99405800	0.19744100
H	3.64894400	0.41448100	0.93434200
C	-1.47400900	-0.06805600	-0.57646200
O	-0.48166900	-0.77810100	-0.90515100
O	-1.37206900	1.28651600	-0.66420300
O	-2.40905700	-0.46953200	0.33957200
C	-2.48544800	2.07138400	-0.23049000
H	-2.23815100	3.10137200	-0.49459900
H	-3.40661000	1.76777700	-0.74059700
H	-2.63327600	1.98770800	0.85100800
C	-2.50611600	-1.88723300	0.50949000
H	-1.57472100	-2.29541700	0.91358800
H	-3.32683500	-2.04530500	1.21148300
H	-2.72616800	-2.37783600	-0.44549400

II [T_1]

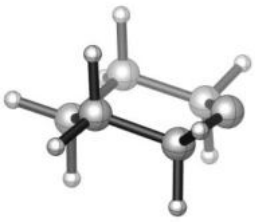

E (B3LYP-D3/6-31G(d)) = -234.546284
E (M06/6-311++G(d,p)/SMD(DCM)//B3LYP-D3/6-31G(d)) = -234.410608

Zero-point correction=	0.144912 (Hartree/Particle)
Thermal correction to Energy=	0.150551
Thermal correction to Enthalpy=	0.151495
Thermal correction to Gibbs Free Energy=	0.115151

Charge = 0 Multiplicity = 3

C	-0.08205400	-0.85041500	1.31428800
C	-0.08205400	0.70461300	1.27108800
C	0.61054800	1.22233700	0.00000000
C	-0.08205400	0.70461300	-1.27108800
C	-0.08205400	-0.85041500	-1.31428800
C	-0.49557000	-1.38610400	0.00000000
H	0.62127900	2.31965800	0.00000000
H	-1.12047100	1.06154700	1.28554000
H	0.40935200	1.09914500	2.16982400
H	0.94027800	-1.19392400	1.56716000

H	-0.73120000	-1.20918000	2.12429600
H	-1.12047100	1.06154700	-1.28554000
H	0.40935200	1.09914500	-2.16982400
H	-0.73120000	-1.20918000	-2.12429600
H	0.94027800	-1.19392400	-1.56716000
H	1.66223500	0.89739100	0.00000000

TS13

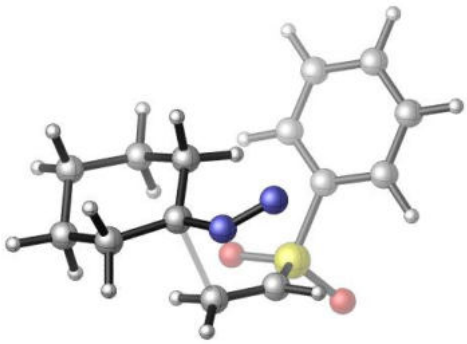

E (B3LYP-D3/6-31G(d)) = -1202.313409
E (M06/6-311++G(d,p)/SMD(DCM)//B3LYP-D3/6-31G(d)) = -1201.932056

Zero-point correction=	0.300660 (Hartree/Particle)
Thermal correction to Energy=	0.318641
Thermal correction to Enthalpy=	0.319585
Thermal correction to Gibbs Free Energy=	0.252113

Charge = 0 Multiplicity = 3

C	3.61742500	-0.13488200	0.57175900
C	3.85841200	-0.04777400	-0.94466300
C	3.13462400	-1.17620100	-1.69449800
C	1.62789600	-1.15683200	-1.39859700
C	1.34935000	-1.27537600	0.10728400
C	2.16140900	-0.30885700	0.93094600
H	3.30955000	-1.08196300	-2.77272200
H	3.50781500	0.92086000	-1.32339700
H	4.93661700	-0.08402300	-1.13900900
H	4.14899500	-1.01958800	0.96284100
H	4.04068600	0.72658100	1.10102900
H	1.18738300	-0.22798600	-1.77866400
H	1.12471100	-1.98030700	-1.91974300
H	0.28712900	-1.15785300	0.33442700
H	1.62152300	-2.28742100	0.45347300
H	3.55720300	-2.14467400	-1.38777300
C	1.35035500	1.68753800	0.56796800
H	1.67078600	1.77014600	-0.46547300

H	2.02786800	2.06990900	1.32513000
C	0.00496200	1.69419700	0.83265400
H	-0.41606400	1.75268000	1.83105000
N	1.92494200	-0.28846400	2.34636900
N	0.95936600	-0.75525300	2.87869300
S	-1.19685800	1.65719400	-0.47392700
O	-0.47607400	1.58083200	-1.75991800
O	-2.14761800	2.74605000	-0.19408000
C	-2.07434400	0.10441500	-0.24901900
C	-1.92800300	-0.90897300	-1.19762300
C	-2.89153700	-0.05568900	0.87337600
C	-2.60364900	-2.11442500	-1.00614100
H	-1.29586100	-0.74278300	-2.06271300
C	-3.55372400	-1.26798900	1.05824700
H	-3.01571600	0.75965600	1.57916500
C	-3.40767300	-2.29565700	0.12176200
H	-2.50221300	-2.91094200	-1.73773500
H	-4.18736500	-1.40904400	1.92888200
H	-3.92695800	-3.23835200	0.26988200

IM1

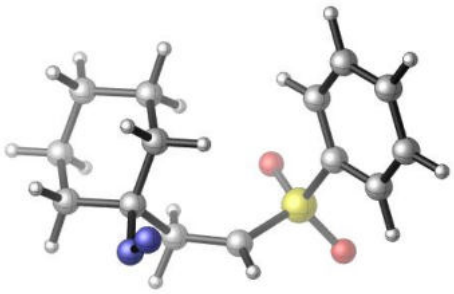

E (B3LYP-D3/6-31G(d)) = -1202.3467
E (M06/6-311++G(d,p)/SMD(DCM)//B3LYP-D3/6-31G(d)) = -1201.967563

Zero-point correction=	0.303071 (Hartree/Particle)
Thermal correction to Energy=	0.321134
Thermal correction to Enthalpy=	0.322078
Thermal correction to Gibbs Free Energy=	0.254841

Charge = 0 Multiplicity = 3

C	3.66096300	0.04071800	0.48183500
C	3.92229800	-0.08202000	-1.03023300
C	3.22378000	-1.31562300	-1.62232500
C	1.72083900	-1.31213400	-1.30398000
C	1.47670800	-1.20524300	0.21080800
C	2.15848900	0.03106800	0.80608200

H	3.38337100	-1.35552400	-2.70647100
H	3.57070200	0.82104200	-1.54655100
H	5.00391500	-0.13368700	-1.20330900
H	4.12165100	-0.81383300	0.99555100
H	4.12524600	0.94567800	0.89103600
H	1.23112300	-0.47746600	-1.82099900
H	1.25163300	-2.23112400	-1.67760900
H	0.40551400	-1.18938400	0.43760700
H	1.88696000	-2.09207300	0.71070500
H	3.67973900	-2.22340300	-1.20050700
C	1.48739000	1.37349600	0.40796000
H	1.62607100	1.54213400	-0.66276200
H	2.01533400	2.17473700	0.94476400
C	0.03911800	1.44394100	0.73088700
H	-0.33463800	1.42235600	1.75004800
N	2.07540500	0.02317200	2.37518400
N	1.49866300	-0.79693500	2.98656500
S	-1.19573800	1.56793900	-0.52406100
O	-0.52400300	1.40584900	-1.82843100
O	-2.01901900	2.75411900	-0.23169900
C	-2.21600400	0.11699400	-0.24307200
C	-1.97079300	-1.04549700	-0.97826000
C	-3.22291500	0.17519400	0.72401700
C	-2.74576800	-2.17708200	-0.72610500
H	-1.19658400	-1.04757700	-1.73769800
C	-3.98839900	-0.96439300	0.96801200
H	-3.40913700	1.10337800	1.25469100
C	-3.74729500	-2.13782100	0.24782900
H	-2.57087900	-3.08730300	-1.29239600
H	-4.77650100	-0.93500600	1.71477300
H	-4.34648600	-3.02296600	0.44215700

TS14

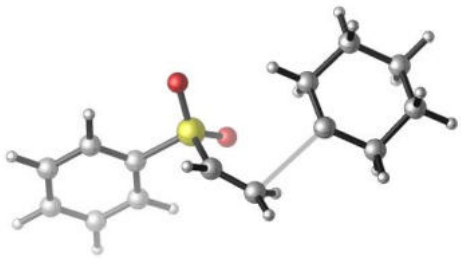

E (B3LYP-D3/6-31G(d)) = -1092.781833
E (M06/6-311++G(d,p)/SMD(DCM)//B3LYP-D3/6-31G(d)) = -1092.442574

Zero-point correction=	0.289809 (Hartree/Particle)
Thermal correction to Energy=	0.306493
Thermal correction to Enthalpy=	0.307437
Thermal correction to Gibbs Free Energy=	0.241467

Charge = 0 Multiplicity = 3

C	5.01812100	-0.46928400	0.91250000
C	4.04502200	-1.47841700	0.28074800
C	2.69800500	-0.79809400	-0.08496200
C	2.96447500	0.47004800	-0.79366700
C	4.00076200	1.45467200	-0.41842400
C	5.30972000	0.70586500	-0.03483100
H	2.06132700	-1.47212500	-0.67081100
H	4.49773400	-1.89628000	-0.62846600
H	3.85685600	-2.31584100	0.96402600
H	4.58428800	-0.08365400	1.84739600
H	5.95621400	-0.96980000	1.18395900
H	4.19549000	2.17682200	-1.22294000
H	3.66766900	2.04829800	0.45584500
H	5.78044000	0.32358700	-0.95028400
H	6.01533200	1.41105500	0.42312500
H	2.13239300	-0.59515000	0.84251100
C	-0.28242300	0.62302000	-1.17769100
C	0.60060500	1.58967300	-0.89413000
H	-0.59499800	0.33573500	-2.17681700
H	0.84680000	1.83106200	0.13441600
H	1.00225900	2.22516800	-1.67646200
S	-0.89616800	-0.43906200	0.11131800
C	-2.66731900	-0.12231900	0.11582000
C	-3.16912000	0.92303400	0.89398800
C	-3.50287300	-0.92147500	-0.66597900
C	-4.54005100	1.17618700	0.87811800
H	-2.49280700	1.50824500	1.50850000
C	-4.87309400	-0.65735200	-0.67404500
H	-3.08118400	-1.74291800	-1.23596300
C	-5.38882600	0.39009900	0.09309100
H	-4.94720900	1.98191200	1.48235000
H	-5.53762300	-1.27337200	-1.27319400
H	-6.45664500	0.59093600	0.08491100
O	-0.69946600	-1.83247200	-0.33103000
O	-0.35374300	0.03589300	1.39898000

III [T_1]

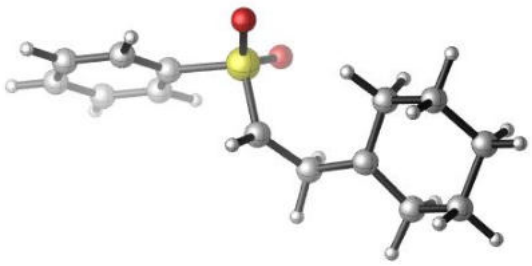

E (B3LYP-D3/6-31G(d)) = -1092.837521
E (M06/6-311++G(d,p)/SMD(DCM)//B3LYP-D3/6-31G(d)) = -1092.496022

Zero-point correction=	0.292142 (Hartree/Particle)
Thermal correction to Energy=	0.308587
Thermal correction to Enthalpy=	0.309532
Thermal correction to Gibbs Free Energy=	0.244286

Charge = 0 Multiplicity = 3

C	-5.19260000	0.41961600	0.11046900
C	-4.01392700	1.37704900	-0.10913500
C	-2.67632100	0.73610800	0.30625400
C	-2.48970000	-0.63859400	-0.27014900
C	-3.66524200	-1.57382400	-0.24786100
C	-4.97966300	-0.88736200	-0.66510300
H	-1.84395800	1.39614600	0.03378700
H	-3.96669600	1.64656300	-1.17366200
H	-4.16320500	2.30974700	0.44799500
H	-5.28619300	0.19524700	1.18379100
H	-6.13295000	0.89472200	-0.19638300
H	-3.47420600	-2.45112200	-0.88178700
H	-3.79317900	-1.97149700	0.77939800
H	-4.94258900	-0.66406100	-1.74053200
H	-5.82162000	-1.57353900	-0.51024800
H	-2.64188000	0.66735300	1.41145100
C	-0.00812500	-0.37518700	-0.69809500
C	-1.10892200	-1.27234300	-0.25257100
H	0.13534700	-0.09785300	-1.73886200
H	-0.87991200	-1.61898700	0.77061400
H	-1.11780100	-2.16446300	-0.89646100
S	0.92175900	0.59015600	0.45045400
C	2.62289100	0.13982100	0.08691600
C	3.19155300	-0.95077800	0.74977700
C	3.33745500	0.87769200	-0.85944900
C	4.50387900	-1.31211000	0.44800400
H	2.61476300	-1.48540800	1.49745100
C	4.64902300	0.50456000	-1.15328000
H	2.87348100	1.73659300	-1.33327200
C	5.22853800	-0.58875300	-0.50380600

H	4.96330900	-2.15323700	0.95925700
H	5.22063800	1.07135600	-1.88263500
H	6.25111100	-0.87415400	-0.73499500
O	0.75558300	2.01135700	0.08628500
O	0.60246400	0.10848400	1.80696500

TS15

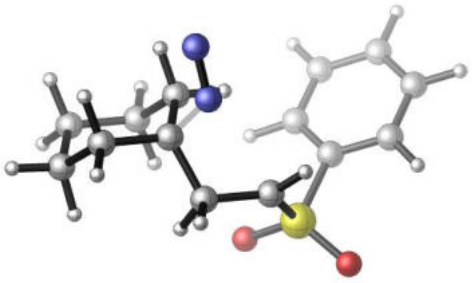

E (B3LYP-D3/6-31G(d)) = -1202.345651
E (M06/6-311++G(d,p)/SMD(DCM)//B3LYP-D3/6-31G(d)) = -1201.966614

Zero-point correction=	0.301446 (Hartree/Particle)
Thermal correction to Energy=	0.319468
Thermal correction to Enthalpy=	0.320413
Thermal correction to Gibbs Free Energy=	0.252856

Charge = 0 Multiplicity = 3

C	3.63019600	0.08553600	0.38405300
C	3.87824300	0.01568000	-1.13792600
C	3.18120800	-1.20365200	-1.76138800
C	1.68174100	-1.22518300	-1.42681100
C	1.45818900	-1.16508900	0.09806600
C	2.13829100	0.05871800	0.69278600
H	3.32799700	-1.20640000	-2.84818400
H	3.51102200	0.93285200	-1.61757200
H	4.95827000	-0.02144200	-1.32541300
H	4.09486400	-0.78601300	0.86389200
H	4.09701600	0.98016000	0.81386900
H	1.17738400	-0.37667600	-1.90646100
H	1.21514700	-2.13624300	-1.82269100

H	0.38869100	-1.16647500	0.33436900
H	1.89258200	-2.05898600	0.56462100
H	3.64948800	-2.12083600	-1.37520200
C	1.44163700	1.40297700	0.43626100
H	1.55067300	1.67172800	-0.61962300
H	1.96611600	2.16636500	1.02885400
C	0.00063400	1.41740300	0.79861200
H	-0.34104100	1.32563300	1.82487200
N	2.02231700	-0.10151700	2.43403400
N	2.38651100	-1.06866100	2.95057100
S	-1.26675100	1.58312400	-0.41775500
O	-0.62532400	1.49357300	-1.74438100
O	-2.10060700	2.74096600	-0.05035400
C	-2.26167700	0.10542600	-0.18567100
C	-2.02253600	-1.01380100	-0.98702200
C	-3.24491100	0.10031900	0.80714500
C	-2.77846400	-2.16665200	-0.77614600
H	-1.26780400	-0.96614200	-1.76449000
C	-3.99148100	-1.05991300	1.00941300
H	-3.42880700	0.99737000	1.38970000
C	-3.75569800	-2.19095200	0.22263700
H	-2.60815400	-3.04348200	-1.39418600
H	-4.76146800	-1.07918600	1.77520500
H	-4.34053300	-3.09217500	0.38412100

TS16

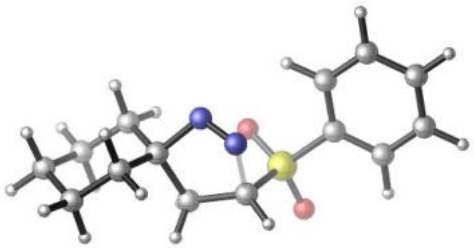

E (B3LYP-D3/6-31G(d)) = -1202.311456
E (M06/6-311++G(d,p)/SMD(DCM)//B3LYP-D3/6-31G(d)) = -1201.930136

Zero-point correction=	0.303564 (Hartree/Particle)
Thermal correction to Energy=	0.320275
Thermal correction to Enthalpy=	0.321219
Thermal correction to Gibbs Free Energy=	0.257256

Charge = 0 Multiplicity = 3

C	-3.11718600	-1.21765200	-1.01127800

C	-4.43605100	-0.42908400	-1.06383800
C	-4.98780900	-0.17562700	0.34727100
C	-3.94644400	0.53183000	1.22724900
C	-2.62770500	-0.25583600	1.28152700
C	-2.07405700	-0.52068400	-0.12344300
H	-5.90984700	0.41608500	0.29394600
H	-4.27521100	0.53470800	-1.56817300
H	-5.16548400	-0.97793200	-1.67179200
H	-3.31030900	-2.21356300	-0.59045100
H	-2.70042300	-1.36788600	-2.01407600
H	-3.76291900	1.54145700	0.83197500
H	-4.33016700	0.66767000	2.24542300
H	-1.87078500	0.26897900	1.87164000
H	-2.80249400	-1.22849300	1.76067900
H	-5.25476400	-1.13832300	0.80738200
C	-1.48100500	0.78234000	-0.81105400
H	-1.64118600	1.65176600	-0.16699300
H	-1.99203600	0.97718100	-1.75763300
C	0.00144500	0.58828800	-1.08597700
H	0.39437600	0.70044800	-2.09252100
N	-0.83885600	-1.40282600	0.02911100
N	-0.10784600	-1.33620700	-0.94595700
S	1.11156900	1.27387900	0.15081100
O	0.44437000	1.12385300	1.45609900
O	1.51927500	2.60466700	-0.34183200
C	2.54859800	0.20425700	0.12621900
C	2.52444400	-0.97713400	0.87167000
C	3.65994400	0.58079700	-0.62834500
C	3.64616600	-1.80312300	0.84845800
H	1.64393300	-1.23226200	1.45086200
C	4.77643100	-0.25656600	-0.64092500
H	3.64764400	1.51769000	-1.17532600
C	4.76716800	-1.44465700	0.09299900
H	3.64699600	-2.72600900	1.42108100
H	5.65291100	0.02197600	-1.21885600
H	5.63877100	-2.09337400	0.08044400

22 [T_1]

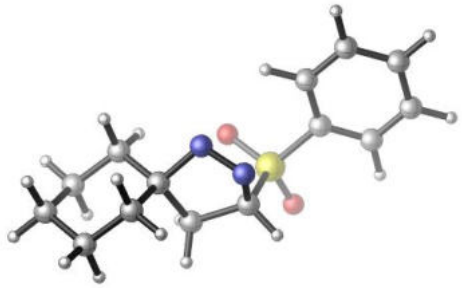

E (B3LYP-D3/6-31G(d)) = -1202.334472
E (M06/6-311++G(d,p)/SMD(DCM)//B3LYP-D3/6-31G(d)) = -1201.955226

Zero-point correction=	0.305981 (Hartree/Particle)
Thermal correction to Energy=	0.322598
Thermal correction to Enthalpy=	0.323542
Thermal correction to Gibbs Free Energy=	0.259834

Charge = 0 Multiplicity = 3

C	-3.11990300	-1.16438400	-1.06792800
C	-4.45452100	-0.40192500	-1.03734100
C	-4.97617000	-0.25026000	0.39934100
C	-3.92493500	0.41655800	1.29853400
C	-2.59344600	-0.35136200	1.27262100
C	-2.06737000	-0.50099600	-0.16091200
H	-5.90851600	0.32759000	0.40606800
H	-4.32301600	0.59542700	-1.48150300
H	-5.18855700	-0.92440300	-1.66269800
H	-3.27857600	-2.18974800	-0.70936900
H	-2.72671300	-1.23726000	-2.08873500
H	-3.76315600	1.45150500	0.96360200
H	-4.28581500	0.48153800	2.33203700
H	-1.83305400	0.14544400	1.88176400
H	-2.74259300	-1.35803500	1.68499600
H	-5.21635900	-1.24514900	0.80208500
C	-1.50822200	0.84566500	-0.77070900
H	-1.58718700	1.68210000	-0.07173300
H	-2.03701300	1.12310700	-1.68645500
C	-0.02904200	0.49504600	-1.10925000
H	0.35306200	0.87861300	-2.05608400
N	-0.80106700	-1.32204200	-0.10696200
N	-0.07295800	-0.95676300	-1.11629300
S	1.10268800	1.24582900	0.19184600
O	0.45136300	1.09138000	1.50607700
O	1.47814200	2.58003300	-0.31264900
C	2.54815000	0.18403800	0.15571200

C	2.50363800	-1.03955300	0.82879900
C	3.67479800	0.59962500	-0.55391000
C	3.62353800	-1.86800500	0.77891400
H	1.61063400	-1.32582400	1.37369700
C	4.79027000	-0.23815900	-0.58905400
H	3.67225700	1.56423300	-1.05071000
C	4.76192000	-1.46809000	0.07259100
H	3.60926000	-2.82400600	1.29417800
H	5.68005800	0.07064100	-1.13011300
H	5.63218500	-2.11791200	0.04035300

S_1 PES

1 [S_1]

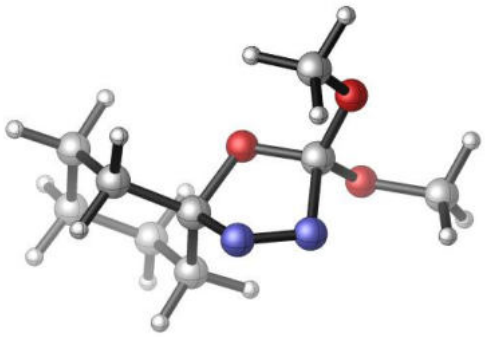

E (TD-B3LYP-D3/6-31G(d)) = -687.629918
E (TD-M06/6-311++G(d,p)/SMD(DCM)//TD-B3LYP-D3/6-31G(d)) = -687.362949

Zero-point correction=	0.254856 (Hartree/Particle)
Thermal correction to Energy=	0.268671
Thermal correction to Enthalpy=	0.269616
Thermal correction to Gibbs Free Energy=	0.215160

Charge = 0 Multiplicity = 1

C	-1.38244700	-1.14545800	0.80404500
C	-2.32772500	-1.49986700	-0.35392800

C	-3.40409900	-0.41927400	-0.54153000
C	-2.76944200	0.96499200	-0.74786900
C	-1.81900800	1.32648400	0.40611100
C	-0.76972600	0.24599200	0.60553200
H	-4.04906700	-0.66850400	-1.39323000
H	-1.73608300	-1.59297200	-1.27301600
H	-2.79073000	-2.47664800	-0.16703900
H	-1.93076800	-1.13120100	1.75486800
H	-0.56980600	-1.87185100	0.89694600
H	-2.20208500	0.96976500	-1.68715900
H	-3.54416400	1.73625100	-0.83712700
H	-1.31448700	2.28120300	0.22604900
H	-2.37665000	1.41929700	1.34666900
H	-4.05099700	-0.39273100	0.34821300
C	1.38411400	-0.07306700	-0.23043500
N	0.21687200	0.60287900	1.63818700
N	1.31661500	0.02887300	1.39433200
O	0.09108000	0.22100600	-0.60474000
O	1.68287000	-1.36746700	-0.52679300
O	2.31690500	0.76975900	-0.76183900
C	3.01283300	-1.78669400	-0.20040600
H	3.03719700	-2.86258400	-0.37779700
H	3.74639700	-1.27482900	-0.82915800
H	3.21182600	-1.57031200	0.85618300
C	2.18045900	2.14685900	-0.40419600
H	2.33160300	2.26944800	0.67371900
H	2.95624300	2.67549100	-0.96005300
H	1.19056600	2.52172400	-0.68267000

TS4

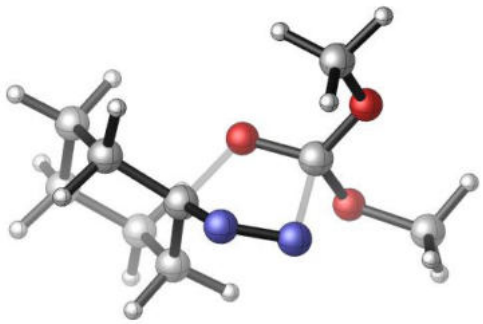

E (TD-B3LYP-D3/6-31G(d)) = -687.627198
E (TD-M06/6-311++G(d,p)/SMD(DCM)//TD-B3LYP-D3/6-31G(d)) = -687.357639

Zero-point correction=	0.253990 (Hartree/Particle)
Thermal correction to Energy=	0.267809
Thermal correction to Enthalpy=	0.268753

Thermal correction to Gibbs Free Energy= 0.214325

Charge = 0 Multiplicity = 1

C	1.33147600	1.12861400	0.80363100
C	2.21073800	1.50239600	-0.39749400
C	3.32930400	0.47004600	-0.60805900
C	2.75580700	-0.94750500	-0.76062600
C	1.87317400	-1.33480800	0.43646000
C	0.79373400	-0.30184800	0.69779200
H	3.92722200	0.73089000	-1.49007100
H	1.58057100	1.55183400	-1.29346300
H	2.63572900	2.50242300	-0.24507800
H	1.92429300	1.16566100	1.72823200
H	0.49043900	1.81493000	0.92471200
H	2.15265100	-0.99908700	-1.67543000
H	3.56459900	-1.68046000	-0.86810500
H	1.40037800	-2.31078800	0.28980100
H	2.47894800	-1.39856200	1.35057700
H	4.01187100	0.49420600	0.25482500
C	-1.34643000	0.07450700	-0.38478100
N	-0.14823200	-0.68318800	1.67990700
N	-1.27291800	-0.14241400	1.61238900
O	-0.12058900	-0.31756400	-0.63598100
O	-1.57360700	1.39438700	-0.47843300
O	-2.37351600	-0.68311700	-0.80668300
C	-2.89022500	1.84921800	-0.11665200
H	-2.82620200	2.93768400	-0.10291300
H	-3.62502100	1.51860500	-0.85509900
H	-3.14831700	1.46635800	0.87417900
C	-2.27286100	-2.08825000	-0.53121900
H	-2.30409500	-2.24057200	0.55172300
H	-3.13758900	-2.54360400	-1.01492300
H	-1.34403200	-2.49417600	-0.94057700

TS5

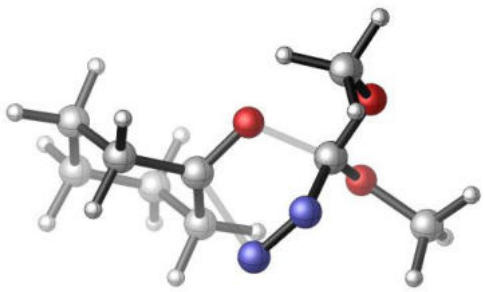

E (TD-B3LYP-D3/6-31G(d)) = -687.611338

E (TD-M06/6-311++G(d,p)/SMD(DCM)//TD-B3LYP-D3/6-31G(d)) = -687.340883

Zero-point correction=	0.252534 (Hartree/Particle)
Thermal correction to Energy=	0.266905
Thermal correction to Enthalpy=	0.267849
Thermal correction to Gibbs Free Energy=	0.211353

Charge = 0 Multiplicity = 1

C	1.37104200	1.20507000	0.31913200
C	2.59941200	1.31354300	-0.63068300
C	3.66448900	0.26078400	-0.29097400
C	3.08574200	-1.16188100	-0.33373900
C	1.84606400	-1.28169600	0.59183200
C	0.85869000	-0.21050900	0.22946600
H	4.51017000	0.34308400	-0.98532400
H	2.25819700	1.17755200	-1.66543300
H	3.01606000	2.32578600	-0.55781000
H	1.68897700	1.41532400	1.34604600
H	0.59461100	1.91480300	0.03735000
H	2.78386400	-1.40628600	-1.36096900
H	3.84094900	-1.89878500	-0.03472700
H	1.37444900	-2.26415700	0.50120500
H	2.16040700	-1.13992600	1.63324300
H	4.06082200	0.46027600	0.71544000
C	-1.60752500	-0.00406800	-0.12962000
N	-0.57591700	0.06063100	1.92684000
N	-1.54517100	-0.27269600	1.23662200
O	-0.09438200	-0.54110500	-0.59243200
O	-1.58279200	1.29810500	-0.56603300
O	-2.50059000	-0.71721500	-0.83809200
C	-2.68033100	2.08390400	-0.07785700
H	-2.55195300	3.07408900	-0.51826700
H	-3.63648200	1.65605400	-0.39834000
H	-2.64833800	2.15208600	1.01510500
C	-2.65213500	-2.09499600	-0.46595200
H	-3.11680900	-2.18125100	0.52111600
H	-3.29949200	-2.53154800	-1.22896200
H	-1.67839300	-2.59184600	-0.46107500

TS6

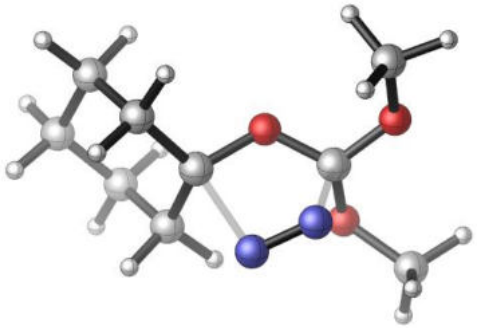

E (TD-B3LYP-D3/6-31G(d)) = -687.596478
E (TD-M06/6-311++G(d,p)/SMD(DCM)//TD-B3LYP-D3/6-31G(d)) = -687.325244

Zero-point correction=	0.251791 (Hartree/Particle)
Thermal correction to Energy=	0.266511
Thermal correction to Enthalpy=	0.267455
Thermal correction to Gibbs Free Energy=	0.210599

Charge = 0 Multiplicity = 1

C	-1.37398000	-1.28376200	0.34457200
C	-2.50312500	-1.31290900	-0.72445800
C	-3.55631400	-0.22753700	-0.44934900
C	-2.92617400	1.17173500	-0.36337100
C	-1.79450000	1.19800300	0.70313500
C	-0.82413800	0.09915500	0.44464800
H	-4.32694900	-0.24514200	-1.23037100
H	-2.05633900	-1.15152300	-1.71498500
H	-2.96690400	-2.30751900	-0.73850700
H	-1.79236600	-1.54298100	1.32499100
H	-0.59168000	-2.00815500	0.11692300
H	-2.50062200	1.44563700	-1.33835900
H	-3.68503100	1.92572300	-0.11814900
H	-1.28228100	2.16503400	0.71860100
H	-2.23398200	1.03320300	1.69491400
H	-4.06448000	-0.45213700	0.50013500
C	1.40902800	0.00217000	-0.40251700
N	0.59045900	-0.22989900	2.12147900
N	1.58374300	0.23893900	1.66176000
O	0.16578700	0.49516400	-0.45530600
O	1.54564400	-1.30037300	-0.60865600
O	2.36148300	0.77310500	-0.90956900
C	2.83517900	-1.85939300	-0.27509000
H	2.70382700	-2.93984900	-0.33160000
H	3.58895700	-1.52428600	-0.99204000
H	3.08965100	-1.53562800	0.73958800

C	2.30240700	2.18042500	-0.57823200
H	2.14793800	2.28011900	0.49808200
H	3.26656200	2.58630100	-0.88499700
H	1.49068700	2.65742300	-1.13468000

PES scan for 1 [T1] along O1-C5 and C2-N3

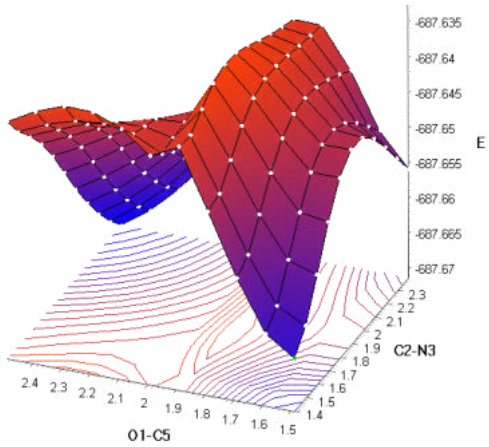

PES scan for compound **1** [T1] investigating O1-C5 and C2-N3 bond distances was performed at TD-B3LYP-D3/6-31G(d) level of theory. Analysis of the resulting PES surface revealed that scission of O1-C5 bond is less feasible than scission of C2-N3 (denoted at **TS2** in Figure 2) by 17.5 kJ/mol, and could lead to concomitant dissociation of C2-N3 bond (cycloelimination $N_2C(OMe)_2$). The decomposition pathways, which would ultimately produce dimetoxy carbene seem to be therefore inaccessible in the triplet state.

8. Characterization of synthesized compounds

8.1. 1,3,4-Oxadiazolines

3,3-dimethoxy-4-oxa-1,2-diazaspiro[4.5]dec-1-ene (1)[21]

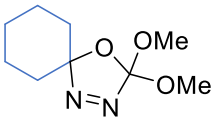

Synthesized according to the general procedure (20.0 mmol scale).
Yield: 3.04 g (76%), colorless oil from column chromatography (hexanes/AcOEt 99:1 to 95:5 (v/v)).
^{1}H NMR (400 MHz, $CDCl_3$): δ=3.47 (s, 6H), 2.03–1.93 (m, 2H), 1.94–1.81 (m, 2H), 1.74–1.60 (m, 3H), 1.60–1.46 ppm (m, 3H); **^{13}C NMR** (126 MHz, $CDCl_3$): δ=136.4, 121.2, 52.1, 33.8, 24.9, 22.9 ppm.

3-(benzylthio)-3-methoxy-4-oxa-1,2-diazaspiro[4.5]dec-1-ene (2)

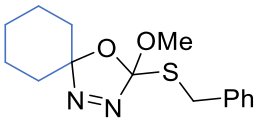

Synthesized according to the general procedure (10.0 mmol scale).
Yield: 340 mg (12%), colorless oil from column chromatography (hexanes/AcOEt 98:2 to 90:10 (v/v)).
^{1}H NMR (600 MHz, $CDCl_3$): δ=7.39–7.35 (m, 2H), 7.31 (t, *J* = 7.6 Hz, 2H), 7.27–7.21 (m, 1H), 4.19 (d, *J* = 12.8 Hz, 1H), 4.09 (d, *J* = 12.8 Hz, 1H), 3.40 (s, 3H), 2.04–1.91 (m, 2H), 1.91–1.78 (m, 2H), 1.70–1.56 (m, 5H), 1.55–1.47 ppm (m, 1H); **^{13}C NMR** (151 MHz, $CDCl_3$): δ=137.5, 135.9, 129.2, 128.7, 127.3, 124.8, 51.8, 35.1, 34.6, 32.8, 24.8, 23.0, 22.9 ppm; **HRMS** (ESI): *m/z* calcd for $C_{15}H_{20}N_2O_2S+Na^+$: 315.1143 [M+Na^+]; found: 315.1145.

3-methoxy-3-methyl-4-oxa-1,2-diazaspiro[4.5]dec-1-ene (3)[2]

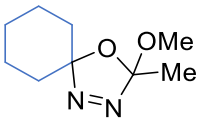

Synthesized according to the general procedure (5.0 mmol scale).
Yield: 838 mg (91%), colorless oil from column chromatography (hexanes/AcOEt 99:1 to 95:5 (v/v)).
^{1}H NMR (400 MHz, $CDCl_3$): δ=3.11 (s, 3H), 2.10–1.99 (m, 1H), 1.95–1.79 (m, 3H), 1.75–1.49 (m, 8H), 1.47–1.38 ppm (m, 1H); **^{13}C NMR** (101 MHz, $CDCl_3$): δ=132.6, 122.0, 50.6, 34.9, 33.7, 25.0, 24.1, 23.1, 23.0 ppm.

3-methoxy-3-phenyl-4-oxa-1,2-diazaspiro[4.5]dec-1-ene (4)[22]

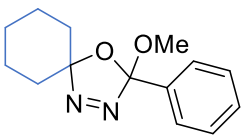

Synthesized according to the general procedure (5.0 mmol scale).

Yield: 985 mg (80%), colorless oil from column chromatography (hexanes/AcOEt 99:1 to 98:2 (v/v)). **^{1}H NMR** (600 MHz, $CDCl_3$): δ=7.72–7.67 (m, 2H), 7.45–7.36 (m, 3H), 3.24 (s, 3H), 2.18–2.11 (m, 1H), 1.99–1.85 (m, 3H), 1.84–1.66 (m, 4H), 1.62–1.50 ppm (m, 2H); **^{13}C NMR** (151 MHz, $CDCl_3$): δ=136.5, 132.5, 129.6, 128.6, 127.0, 124.0, 51.0, 34.2, 33.7, 25.0, 23.2, 23.1.ppm.

1-(1,6-dioxa-4,13,14-triazadispiro[4.1.57.25]tetradec-13-en-4-yl)ethan-1-one (5)[4]

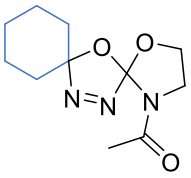

Synthesized according to the literature procedure[4] (10.0 mmol scale).
Yield: 567 mg (24% [overall yield for 4 steps]), white solid from column chromatography (hexanes/acetone 95:5 to 80:20 (v/v)).
^{1}H NMR (500 MHz, $CDCl_3$): [rotameric mixture] δ=4.42–4.15 (m, 2H), 4.05–3.87 (m, 2H), 2.21–2.09 (m, 3H), 2.03–1.93 (m, 1H), 1.93–1.73 (m, 4H), 1.72–1.39 ppm (m, 5H); **^{13}C NMR** (126 MHz, $CDCl_3$): [rotameric mixture] δ=168.0, 132.4, 122.7, 121.1, 65.2, 64.7, 46.3, 45.5, 35.1, 34.7, 31.8, 30.9, 25.0, 24.8, 24.1, 23.2, 23.0, 22.9, 22.7, 22.3 ppm; **HRMS** (ESI): *m/z* calcd for $C_{11}H_{17}N_3NaO_3$+Na^+: 262.1168 $[M+Na]^+$; found: 262.1174.

3,3-dimethoxy-4,8-dioxa-1,2-diazaspiro[4.5]dec-1-ene (S10)

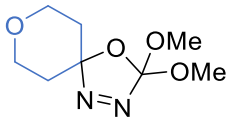

Synthesized according to the general procedure (5.0 mmol scale).
Yield: 455 mg (45%), colorless oil from column chromatography (hexanes/AcOEt 98:2 to 80:20 (v/v)).
^{1}H NMR (400 MHz, $CDCl_3$): δ=4.11–4.01 (m, 2H), 3.83 (ddd, *J* = 11.8, 8.7, 3.4 Hz, 2H), 3.49 (s, 6H), 2.24–2.13 (m, 2H), 1.67 (ddd, *J* = 5.3, 3.3, 1.4 Hz, 1H), 1.63 ppm (ddd, *J* = 5.0, 3.2, 1.4 Hz, 1H); **^{13}C NMR** (126 MHz, $CDCl_3$): δ=136.9, 117.9, 64.9, 52.2, 34.1 ppm; **HRMS** (APCI): *m/z* calcd for $C_8H_{15}N_2O_4$+H^+: 203.1032 $[M+H]^+$; found: 203.1033.

3,3-dimethoxy-4-oxa-8-thia-1,2-diazaspiro[4.5]dec-1-ene (S11)

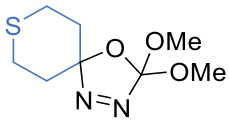

Synthesized according to the general procedure (7.50 mmol scale)
Yield: 802 mg (49%), colorless oil from column chromatography (hexanes/AcOEt 99:1 to 98:2 (v/v)).
^{1}H NMR (500 MHz, $CDCl_3$): δ=3.48 (s, 6H), 2.97–2.71 (m, 4H), 2.32 (ddd, *J* = 13.8, 10.2, 3.9 Hz, 2H), 1.81 ppm (ddd, *J* = 13.2, 5.4, 3.4 Hz, 2H); **^{13}C NMR** (126 MHz, $CDCl_3$): δ=137.1, 119.3, 52.2, 34.8, 25.3 ppm; **HRMS** (APCI): *m/z* calcd for $C_8H_{14}N_2O_3S$+H^+: 219.0803 $[M+H]^+$; found: 219.0810.

3,3-dimethoxy-8-tosyl-4-oxa-1,2,8-triazaspiro[4.5]dec-1-ene (S12)

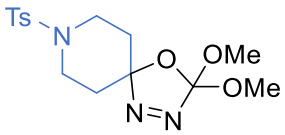

Synthesized according to the general procedure (20.0 mmol scale).
Yield: 1.43 g (20%), white solid from column chromatography (hexanes/acetone 95:5 to 80:20 (v/v)).
^{1}H NMR (500 MHz, $CDCl_3$): δ=7.66 (d, *J* = 8.3 Hz, 2H), 7.34 (d, *J* = 8.0 Hz, 2H), 3.67–3.59 (m, 2H), 3.43 (s, 6H), 2.99 (ddd, *J* = 12.5, 9.6, 3.1 Hz, 2H), 2.45 (s, 3H), 2.23 (ddd, *J* = 13.8, 9.6, 4.3 Hz, 2H), 1.74–1.65 (m, 2H) ppm; **^{13}C NMR** (126 MHz, $CDCl_3$): δ=144.1, 137.2, 133.4, 130.0, 127.8, 117.4, 52.3, 43.5, 33.0, 21.7 ppm; **HRMS** (ESI): *m/z* calcd for $C_{15}H_{21}N_3O_5S+Na^+$: 378.1100 [M+Na^+]; found: 378.1096.

7,7-dimethoxy-8-oxa-5,6-diazaspiro[3.4]oct-5-ene (S13)[23]

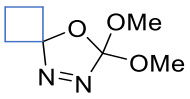

Synthesized according to the general procedure (5.0 mmol scale).
Yield: 233 mg (27%), colorless oil from column chromatography (toluene to toluene/MTBE 98:2 (v/v)).
^{1}H NMR (500 MHz, $CDCl_3$): δ=3.32 (s, 6H), 2.64–2.53 (m, 2H), 2.55–2.45 (m, 2H), 2.31–2.18 (m, 1H), 1.95 ppm (dtt, *J* = 11.2, 10.2, 3.2 Hz, 1H); **^{13}C NMR** (126 MHz, $CDCl_3$): δ=138.4, 118.0, 51.9, 32.9, 11.8 ppm.

3,3-dimethoxy-4-oxa-1,2-diazaspiro[4.4]non-1-ene (S14)

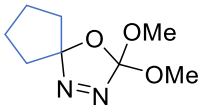

Synthesized according to the general procedure (21.1 mmol scale).
Yield: 3.18 g (81%), colorless oil from column chromatography (hexanes/AcOEt 99:1 to 95:5 (v/v)).
^{1}H NMR (500 MHz, $CDCl_3$): δ=3.42 (s, 6H), 2.23–2.16 (m, 2H), 2.01–1.87 (m, 4H), 1.85–1.77 (m, 2H); **^{13}C NMR** (126 MHz, $CDCl_3$): δ=137.1, 128.1, 52.0, 35.7, 25.3 ppm; **HRMS** (APCI): *m/z* calcd for $C_8H_{14}N_2O_3+H^+$: 187.1083: [M+H]$^+$; found: 187.1084.

3,3-dimethoxy-4-oxa-1,2-diazaspiro[4.6]undec-1-ene (S15)

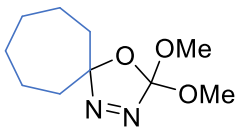

Synthesized according to the general procedure (24.0 mmol scale).
Yield: 4.37 g (85%), colorless oil from column chromatography (hexanes/AcOEt 99:1 to 95:5 (v/v)).
^{1}H NMR (500 MHz, $CDCl_3$): δ=3.45 (s, 6H), 2.12–2.03 (m, 2H), 1.84–1.74 (m, 2H), 1.76–1.62 ppm (m, 8H); **^{13}C NMR** (126 MHz, $CDCl_3$): δ=136.9, 124.9, 52.0, 36.5, 29.5, 23.2 ppm; **HRMS** (ESI): *m/z* calcd for $C_{10}H_{18}N_2O_3+Na^+$: 237.1215 [M+Na]$^+$; found: 237.1211.

3,3-dimethoxy-4-oxa-1,2-diazaspiro[4.11]hexadec-1-ene (S16)

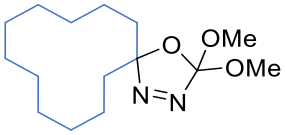

Synthesized according to the general procedure (10.0 mmol scale).
Yield: 1.72 g (60%), white solid from column chromatography (hexanes/AcOEt 99:1 to 95:5 (v/v)).
^{1}H NMR (600 MHz, $CDCl_3$): δ=3.47 (s, 6H), 1.88–1.80 (m, 2H), 1.71–1.60 (m, 6H), 1.44–1.36 ppm (m, 14H); **^{13}C NMR** (101 MHz, $CDCl_3$): δ=136.6, 124.8, 52.0, 40.5, 31.5, 26.2, 25.9, 24.9, 24.8, 24.4, 22.7, 22.5, 22.2, 20.0 ppm; **HRMS** (APCI): *m/z* calcd for $C_{15}H_{28}N_2O_3$+H^+: 285.2178 $[M+H]^+$; found: 285.2179.

(1R,3R,5R,7R)-5',5'-dimethoxy-5'H-spiro[adamantane-2,2'-[1,3,4]oxadiazole] (S17)[23]

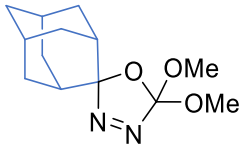

Synthesized according to the general procedure (10.0 mmol scale).
Yield: 2.27 g (90%), viscous colorless oil from column chromatography (hexanes/AcOEt 98:2 to 95:5 (v/v)).
^{1}H NMR (400 MHz, $CDCl_3$): δ=3.47 (s, 6H), 2.56 (d, *J* = 12.8 Hz, 2H), 2.12–2.03 (m, 3H), 1.95–1.84 (m, 3H), 1.83–1.76 (m, 3H), 1.77–1.69 ppm (m, 3H); **^{13}C NMR** (151 MHz, $CDCl_3$): δ=135.5, 124.6, 52.0, 37.3, 37.2, 35.0, 34.5, 27.4, 26.6 ppm.

2-cyclopropyl-5,5-dimethoxy-2-methyl-2,5-dihydro-1,3,4-oxadiazole (S18)

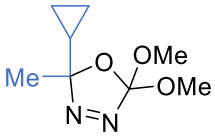

Synthesized according to the general procedure (5.0 mmol scale).
Yield: 490 mg (52%), colorless oil from column chromatography (hexanes to hexanes/AcOEt: 99:1 (v/v)).
^{1}H NMR (400 MHz, $CDCl_3$): δ=3.54 (s, 3H), 3.44 (s, 3H), 1.54 (s, 3H), 1.40–1.28 (m, 1H), 0.59–0.41 ppm (m, 4H); **^{13}C NMR** (101 MHz, $CDCl_3$): δ=137.2, 121.4, 52.2, 51.9, 22.7, 17.2, 1.8, 0.9 ppm; **HRMS** (APCI): *m/z* calcd for $C_8H_{14}N_2O_3$+H^+: 187.1083 $[M+H]^+$; found: 187.1084.

2,2-dimethoxy-5-(methoxymethyl)-5-methyl-2,5-dihydro-1,3,4-oxadiazole **(S19)**

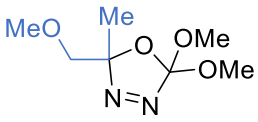

Synthesized according to the general procedure (20.0 mmol scale).
Yield: 1.21 g (32%), viscous colorless oil column chromatography (hexanes to hexanes/AcOEt 95:5 to 80:20 (v/v)).

^{1}H NMR (500 MHz, $CDCl_3$): δ=3.67 (d, *J* = 10.9 Hz, 1H), 3.63 (d, *J* = 10.9 Hz, 1H), 3.52 (s, 3H), 3.49 (s, 3H), 3.39 (s, 3H), 1.51 ppm (s, 3H); **^{13}C NMR** (126 MHz, $CDCl_3$): δ=137.7, 120.2, 74.7, 60.0, 52.4, 52.1, 19.8 ppm; **HRMS** (ESI): *m/z* calcd for $C_7H_{14}N_2O_4$+Na^+: 213.0851 $[M+Na]^+$; found: 213.0853.

***diethyl ((5,5-dimethoxy-2-methyl-2,5-dihydro-1,3,4-oxadiazol-2-yl)methyl)phosphonate* (S20)**

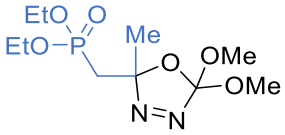

Synthesized according to the general procedure (5.0 mmol scale).
Yield: 756 mg (51%), colorless oil from column chromatography (hexanes/AcOEt 1:1 (v/v)).
^{1}H NMR (400 MHz, $CDCl_3$): δ=4.20–4.09 (m, 4H), 3.51 (s, 3H), 3.46 (s, 3H), 2.44 (dd, *J* = 19.7, 15.3 Hz, 1H), 2.05 (dd, *J* = 19.0, 15.4 Hz, 1H), 1.73 (s, 3H), 1.34 ppm (t, *J* = 7.1 Hz, 6H); **^{13}C NMR** (126 MHz, $CDCl_3$): δ=138.5, 117.6, 62.4 (d, $^3J_{(C\text{-}P)}$ = 6.5 Hz), 62.2 (d, $^3J_{(C\text{-}P)}$ = 6.4 Hz), 52.3, 52.2, 34.5 (d, $^1J_{(C\text{-}P)}$ = 142.6 Hz), 22.9, 16.5 ppm (d, $^3J_{(C\text{-}P)}$ = 6.2 Hz); **HRMS** (ESI): *m/z* calcd for $C_{10}H_{21}N_2O_6P$+Na^+: 319.1035 $[M+Na]^+$; found: 319.1038.

***7,7-dimethoxy-2,8-dioxa-5,6-diazaspiro[3.4]oct-5-ene* (S21)**

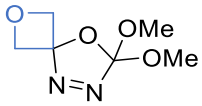

Synthesized according to the general procedure (5.00 mmol scale).
Yield: 113 mg (13%), viscous colorless oil from column chromatography (hexanes to hexanes/AcOEt 90:10 (v/v)).
^{1}H NMR (400 MHz, $CDCl_3$): δ=5.15–5.01 (m, 2H), 5.01–4.85 (m, 2H), 3.39 ppm (s, 6H); **^{13}C NMR** (101 MHz, $CDCl_3$): δ=138.9, 114.5, 78.0, 52.1 ppm; **HRMS** (APCI): *m/z* calcd for $C_6H_{10}N_2O_4$+H^+: 175.0719 $[M+H]^+$; found: 175.0722.

3,3-dimethoxy-4-oxa-7-thia-1,2-diazaspiro[4.4]non-1-ene (S22)

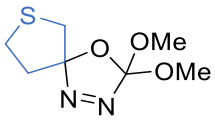

Synthesized according to the general procedure (20.0 mmol scale).
Yield: 817 mg (20%), colorless oil from column chromatography (hexanes/AcOEt 99:1 to 98:2 (v/v)).
^{1}H NMR (600 MHz, $CDCl_3$): δ=3.49 (s, 3H), 3.47 (s, 3H), 3.41 (d, *J* = 12.0 Hz, 1H), 3.16 (ddd, *J* = 10.6, 7.4, 4.6 Hz, 1H), 3.10 (ddd, *J* = 10.7, 9.0, 6.3 Hz, 1H), 2.84 (dd, *J* = 12.1, 1.0 Hz, 1H), 2.54 (ddd, *J* = 13.2, 8.9, 7.4 Hz, 1H), 2.15 ppm (ddd, *J* = 13.1, 6.1, 4.6 Hz, 1H); **^{13}C NMR** (151 MHz, $CDCl_3$): δ=137.8, 127.2, 52.4, 52.3, 39.3, 36.9, 29.7 ppm; **HRMS** (APCI): *m/z* calcd for $C_7H_{12}N_2O_3S$+H^+: 205.0647 $[M+H]^+$; found: 205.0651.

tert-butyl 3,3-dimethoxy-4-oxa-1,2,8-triazaspiro[4.5]dec-1-ene-8-carboxylate (S23)

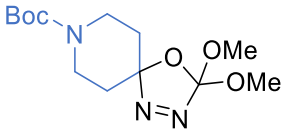

Synthesized according to the general procedure (5.0 mmol scale).
Yield: 1.22 g (81%), white solid from column chromatography (hexanes/AcOEt 95:5 to 80:20 (v/v)).
^{1}H NMR (500 MHz, $CDCl_3$): δ=3.95 (m, 2H), 3.48 (s, 6H), 3.39 (ddd, *J* = 13.4, 9.7, 3.5 Hz, 2H), 2.09 (ddd, *J* = 13.6, 9.9, 4.3 Hz, 2H), 1.62–1.54 (m, 2H), 1.48 ppm (s, 9H); **^{13}C NMR** (126 MHz, $CDCl_3$): δ= 154.7, 137.0, 118.8, 80.2, 52.2, 40.7, 33.3, 28.5 ppm; **HRMS** (ESI): *m/z* calcd for $C_{13}H_{24}N_3O_5$+Na^+: 324.1535 $[M+Na]^+$; found: 324.1528.

tert-butyl (1R,3S,5S)-5',5'-dimethoxy-5'H-8-azaspiro[bicyclo[3.2.1]octane-3,2'-[1,3,4]oxadiazole] -8-carboxylate (S24)

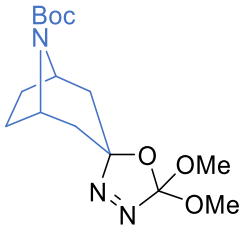

Synthesized according to the general procedure (3.1 mmol scale).
Yield: 619 mg (61%), white solid from column chromatography (hexanes to hexanes/AcOEt 80:20 (v/v)).
^{1}H NMR (500 MHz, $CDCl_3$): [rotameric mixture] δ=4.45–4.22 (m, 2H), 3.52–3.38 (m, 6H), 2.76–2.50 (m, 1H), 2.33–1.92 (m, 5H), 1.50 (s, 9H), 1.46–1.39 ppm (m, 2H); **^{13}C NMR** (126 MHz, $CDCl_3$): [rotameric mixture] δ=153.4, 138.8, 118.9, 80.0, 52.3, 51.8, 40.3, 37.8, 37.2, 28.6, 27.9, 27.2 ppm; **HRMS** (ESI): *m/z* calcd for $C_{15}H_{25}N_3O_5$+Na^+: 350.1692 $[M+Na]^+$; found: 350.1696.

3,3-dimethoxy-8,8-dimethyl-4,7,9-trioxa-1,2-diazaspiro[4.5]dec-1-ene (S25)

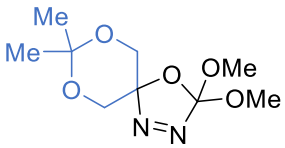

Synthesized according to the general procedure (3.9 mmol scale).
Yield: 216 mg (24%), yellowish oil from column chromatography (hexanes/AcOEt 99:1 to 90:10 (v/v)).
^{1}H NMR (400 MHz, $CDCl_3$): δ=4.12 (d, *J* = 12.5 Hz, 2H), 3.72 (d, *J* = 12.5 Hz, 2H), 3.48 (s, 6H), 1.55 (s, 3H), 1.49 ppm (s, 3H); **^{13}C NMR** (101 MHz, $CDCl_3$) δ 137.7, 115.9, 99.7, 62.9, 52.3, 24.0, 23.1 ppm; **HRMS** (ESI) *m/z* calcd for $C_9H_{16}N_2O_5$+Na^+: 255.0957 $[M+Na]^+$; found: 255.0950.

5',5'-dimethoxy-1,3-dihydro-5'H-spiro[indene-2,2'-[1,3,4]oxadiazole] (S26)

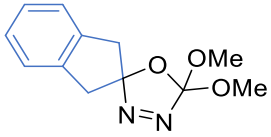

Synthesized according to the general procedure (4.10 mmol scale).
Yield: 431 mg (45%), viscous colorless oil from column chromatography (hexanes/AcOEt 99:1 to 95:5 (v/v)).
^{1}H NMR (400 MHz, $CDCl_3$): δ=7.25 (s, 4H), 3.53 (d, *J* = 16.9 Hz, 2H), 3.50 (s, 6H), 3.23 ppm (d, *J* = 16.9 Hz, 2H); **^{13}C NMR** (101 MHz, $CDCl_3$): δ=139.0, 138.1, 127.5, 126.5, 124.7, 52.2, 41.8 ppm; **HRMS** (ESI): *m/z* calcd for $C_{12}H_{14}N_2O_3$+Na^+: 257.0902 $[M+Na]^+$; found: 257.0901.

2-benzyl-2-ethyl-5,5-dimethoxy-2,5-dihydro-1,3,4-oxadiazole (S27)

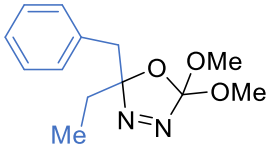

Synthesized according to the general procedure (5.0 mmol scale).
Yield: 939 mg (75%), colorless oil from column chromatography (toluene to toluene/MTBE 99:1 (v/v)).
^{1}H NMR (500 MHz, $CDCl_3$): δ=7.45–7.04 (m, 5H), 3.53 (s, 3H), 3.33 (s, 3H), 3.13 (q, *J* = 14.2 Hz, 2H), 1.88 (dq, *J* = 15.0, 7.5 Hz, 1H), 1.80 (dq, *J* = 14.8, 7.5 Hz, 1H), 0.89 ppm (t, *J* = 7.5 Hz, 3H); **^{13}C NMR** (126 MHz, $CDCl_3$): δ=137.0, 134.6, 130.8, 128.3, 127.2, 123.9, 52.2, 51.9, 42.1, 28.7, 7.6 ppm; **HRMS** (ESI): *m/z* calcd for $C_{13}H_{18}N_2O_3$+Na^+: 273.1215 $[M+Na]^+$; found: 273.1208.

(1S,4R,5R)-1-isopropyl-5',5'-dimethoxy-4-methyl-5'H-spiro[bicyclo[3.1.0]hexane-3,2' [1,3,4]oxadiazole] (S28)

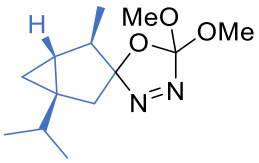

Synthesized according to the general procedure (3.00 mmol scale).
Yield: 389 mg (51%), colorless oil from column chromatography (hexanes to hexanes/AcOEt 98:2 (v/v)).
^{1}H NMR (600 MHz, $CDCl_3$): [mixture of diastereoisomers] (major diastereoisomer) δ=3.44 (s, 3H), 3.42 (s, 3H), 2.72 (dd, *J* = 14.0, 1.9 Hz, 1H), 2.10 (q, *J* = 7.3 Hz, 1H), 1.49 (d, *J* = 14.0 Hz, 1H), 1.42 (hept, *J* = 6.9 Hz, 1H), 1.25 (d, *J* = 7.3 Hz, 3H), 1.04 (d, *J* = 6.8 Hz, 3H), 1.03 – 0.98 (m, 1H), 0.92 (d, *J* = 6.9 Hz, 3H), 0.88 (dd, *J* = 5.2, 3.9 Hz, 1H), 0.48 ppm (ddd, *J* = 8.3, 5.2, 1.9 Hz, 1H); **^{13}C NMR** (151 MHz, $CDCl_3$): δ=137.5, 127.9, 52.1, 52.0, 47.4, 36.2, 33.8, 32.8, 29.7, 20.3, 20.0, 18.4, 15.5 ppm; **HRMS** (APCI): *m/z* calcd for $C_{13}H_{22}N_2O_3$+H^+: 255.1709 $[M+H]^+$; found: 255.1700.

(5S)-2,2-dimethoxy-5-((3S,8S,10R,13S,17S)-3-methoxy-10,13-dimethyl-2,3,4,7,8,9,10,11,12,13,14,15,16,17-tetradecahydro-1H-cyclopenta[a]phenanthren-17-yl)-5-methyl-2,5-dihydro-1,3,4-oxadiazole (S29)

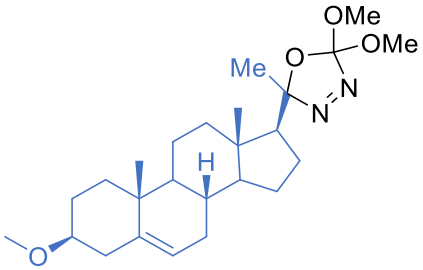

Synthesized according to the general procedure (3.30 mmol scale).
Yield: 652 mg (46%), white solid from column chromatography (hexanes/AcOEt 99:1 to 90:10 (v/v)). **^{1}H NMR** (500 MHz, $CDCl_3$): δ=5.37 – 5.32 (m, 1H), 4.00 (s, 3H), 3.48 (s, 3H), 3.35 (s, 3H), 3.04 (tt, *J* = 11.3, 4.5 Hz, 1H), 2.38 (ddd, *J* = 13.1, 4.8, 2.4 Hz, 1H), 2.21 – 2.10 (m, 2H), 2.01 (dtd, *J* = 17.6, 5.3, 2.8 Hz, 1H), 1.96–1.80 (m, 3H), 1.76–1.66 (m, 3H), 1.66–1.56 (m, 1H), 1.53–1.32 (m, 5H), 1.32–1.10 (m, 5H), 0.96 (s, 5H), 0.72 ppm (s, 3H); **^{13}C NMR** (126 MHz, $CDCl_3$): δ=163.0, 141.0, 121.7, 105.6, 80.6, 59.0, 55.7, 54.8, 53.0, 51.3, 49.8, 44.0, 38.9, 37.3, 37.0, 36.5, 32.5, 32.2, 28.2, 26.4, 25.2, 22.2, 21.7, 20.2, 19.5 ppm; **HRMS** (ESI): *m/z* calcd for $C_{25}H_{40}N_2O_4$+Na^+: 455.2890 $[M+Na]^+$; found: 455.2886.

8.2. Electron-deficient olefins

4-cyanophenyl acrylate (S9)

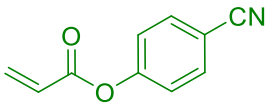

^{1}H NMR (500 MHz, $CDCl_3$): δ=7.74–7.66 (m, 2H), 7.31–7.26 (m, 2H), 6.64 (dd, *J* = 17.3, 1.1 Hz, 1H), 6.32 (dd, *J* = 17.3, 10.5 Hz, 1H), 6.08 ppm (dd, *J* = 10.5, 1.1 Hz, 1H); **^{13}C NMR** (126 MHz, $CDCl_3$): δ=163.7, 154.0, 133.9, 133.8, 127.3, 122.8, 118.3, 109.9 ppm; **HRMS** (APCI): *m/z* calcd for $C_{10}H_7NO_2$+H^+: 174.0555 $[M+H]^+$; found: 174.0558.

8.3. Scope of blue light-induced Ir-catalyzed cyclopropane synthesis

1-(phenylsulfonyl)spiro[2.5]octane (12)

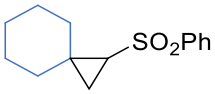

Synthesized according to the general procedure.
Yield: 41 mg (81%), white solid from column chromatography (hexanes/AcOEt 95:5 to 90:10 (v/v)). **m.p.** 123-124 ºC; **^{1}H NMR** (400 MHz, $CDCl_3$): δ=7.96–7.87 (m, 2H), 7.66–7.57 (m, 1H), 7.59–7.49 (m, 2H), 2.17 (dd, *J* = 8.3, 5.4 Hz, 1H), 1.97–1.81 (m, 2H), 1.70 – 1.58 (m, 1H), 1.57–1.33 (m, 7H), 1.19–1.09 (m, 1H), 1.04 ppm (dd, *J* = 8.3, 5.0 Hz, 1H); **^{13}C NMR** (151 MHz, $CDCl_3$): δ=142.3, 133.2, 129.2, 127.3, 45.2, 37.3, 31.4, 28.8, 25.9, 25.7, 25.6, 19.6 ppm; **HRMS** (ESI): *m/z* calcd for $C_{14}H_{18}O_2S$+Na^+: $[M+Na]^+$ 273.0925; found: 273.0921; **elemental analysis** calcd (%) for $C_{14}H_{18}O_2S$: C 67.17, H 7.25, S 12.81; found: C 67.16, H 7.25, S 12.67.

1-(phenylsulfonyl)spiro[2.3]hexane (24)

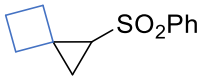

Synthesized according to the general procedure.
Yield: 20 mg (45%), viscous colorless oil from column chromatography (hexanes/AcOEt 95:5 to 80:20 (v/v)).
^{1}H NMR (500 MHz, $CDCl_3$): δ=7.91 (d, *J* = 7.0 Hz, 2H), 7.67–7.59 (m, 1H), 7.59–7.51 (m, 2H), 2.76 (dt, *J* = 12.3, 8.1 Hz, 1H), 2.38–2.22 (m, 3H), 2.19–2.07 (m, 1H), 2.06–1.94 (m, 2H), 1.53 (t, *J* = 5.5 Hz, 1H), 1.17 ppm (dd, *J* = 8.5, 5.5 Hz, 1H); **^{13}C NMR** (126 MHz, $CDCl_3$): δ=142.0, 133.2, 129.3, 127.3, 42.0, 30.7, 29.3, 27.7, 19.1, 18.0 ppm; **HRMS** (ESI): *m/z* calcd for $C_{12}H_{14}O_2S+H^+$: 223.0793 $[M+H]^+$; found: 223.0794.
GC Chromatogram*:* t_r = 7.451 min (> 99% purity).

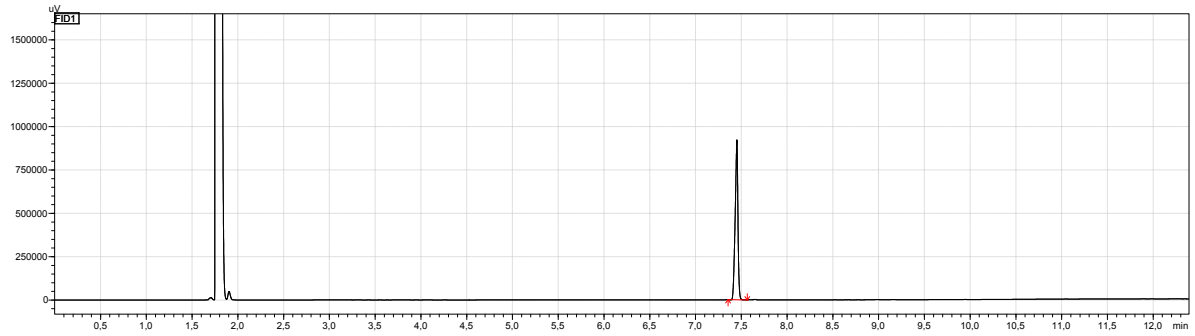

1-(phenylsulfonyl)spiro[2.4]heptane (25)

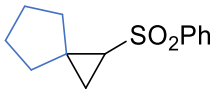

Synthesized according to the general procedure.
Yield: 36 mg (75%), white solid from column chromatography (hexanes/AcOEt 95:5 to 80:20 (v/v)).
m.p. 52-54ºC; **^{1}H NMR** (500 MHz,$CDCl_3$): δ=7.95–7.87 (m, 2H), 7.65–7.59 (m, 1H), 7.58–7.51 (m, 2H), 2.44 (dd, *J* = 8.5, 5.4 Hz, 1H), 2.25–2.15 (m, 1H), 1.89 (ddd, *J* = 13.3, 8.0, 5.1 Hz, 1H), 1.78–1.57 (m, 5H), 1.54 (t, *J* = 5.2 Hz, 1H), 1.52–1.42 (m, 1H), 1.16 ppm (dd, *J* = 8.5, 5.0 Hz, 1H); **^{13}C NMR** (126 MHz, $CDCl_3$): δ=142.1, 133.2, 129.3, 127.3, 44.0, 37.2, 33.2, 30.2, 26.4, 25.2, 20.6 ppm; **HRMS** (ESI): *m/z* calcd for $C_{13}H_{16}O_2S+Na^+$: 259.0769 $[M+Na]^+$; found: 259.0767; **elemental analysis** calcd (%) for $C_{13}H_{16}O_2S$: C 66.07, H 6.82; found: C 66.48, H 6.67.

1-(phenylsulfonyl)spiro[2.6]nonane (26)

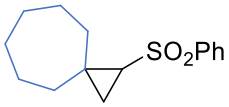

Synthesized according to the general procedure.
Yield: 33 mg (62%), viscous colorless oil from column chromatography (hexanes/AcOEt 95:5 to 85:15 (v/v)).
^{1}H NMR (600 MHz, $CDCl_3$): δ=7.93–7.90 (m, 2H), 7.64–7.60 (m, 1H), 7.58–7.52 (m, 2H), 2.21 (dd, *J* = 8.5, 5.6 Hz, 1H), 2.05–1.99 (m, 2H), 1.69–1.56 (m, 5H), 1.55–1.49 (m, 3H), 1.46

(t, J = 5.2 Hz, 2H), 1.41–1.34 (m, 1H), 1.09 ppm (dd, J = 8.4, 5.0 Hz, 1H); **^{13}C NMR** (151 MHz, $CDCl_3$): δ=142.4, 133.2, 129.2, 127.3, 46.2, 39.8, 33.2, 31.0, 28.0 (2 x C), 26.3, 25.9, 21.7 ppm; **HRMS** (ESI): *m/z* calcd for $C_{15}H_{20}O_2S+Na^+$: 287.1082 $[M+Na]^+$; found: 287.1089.
GC Chromatogram: t_r = 8.417 min (> 99% purity).

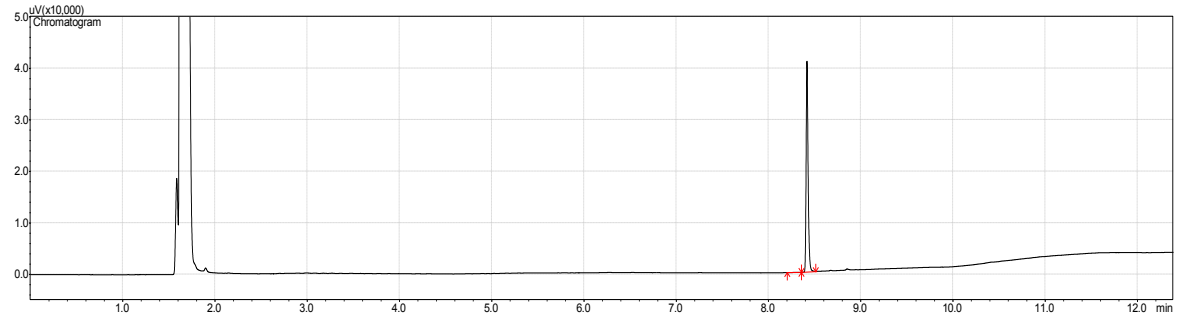

1-(phenylsulfonyl)spiro[2.11]tetradecane (27)

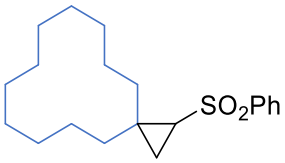

Synthesized according to the general procedure.
Yield: 51 mg (76%), white solid from column chromatography (hexanes/AcOEt 95:5 to 85:15 (v/v)).
m.p. 88-91 ºC; **^{1}H NMR** (500 MHz, $CDCl_3$): δ=7.64 – 7.59 (m, 2H), 7.64–7.59 (m, 1H), 7.57–7.51 (m, 2H), 2.15 (dd, J = 8.4, 5.6 Hz, 1H), 1.88 (ddd, J = 14.3, 11.0, 6.0 Hz, 1H), 1.75 (ddd, J = 14.5, 10.8, 4.2 Hz, 1H), 1.66–1.55 (m, 1H), 1.55–1.44 (m, 2H), 1.44–1.21 (m, 17H), 1.08–0.96 ppm (m, 2H); **^{13}C NMR** (126 MHz, $CDCl_3$): δ=142.4, 133.2, 129.2, 127.4, 45.2, 33.6, 32.1, 26.3 (2 x C), 26.1, 24.7, 22.4, 22.4 (2 x C), 22.3, 21.8, 21.2, 19.9 ppm; **HRMS** (ESI): *m/z* calcd for $C_{20}H_{30}O_2S+Na^+$: 357.1864 $[M+Na]^+$; found: 357.1861; **elemental analysis** calcd (%) for $C_{20}H_{30}O_2S$: C 71.81, H 9.04; found: C 71.62, H, 9.24.

(1R,3S,5R,7R)-2'-(phenylsulfonyl)spiro[adamantane-2,1'-cyclopropane] (28)

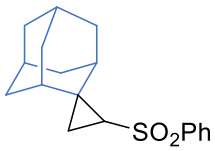

Synthesized according to the general procedure.
Yield: 27 mg (44%), viscous colorless oil from column chromatography (hexanes/AcOEt 95:5 to 85:15 (v/v)).
^{1}H NMR (500 MHz, $CDCl_3$): δ=7.97–7.90 (m, 2H), 7.65–7.57 (m, 1H), 7.58–7.50 (m, 2H), 2.43–2.35 (m, 1H), 2.13 (dd, J = 8.2, 5.5 Hz, 1H), 2.07–1.98 (m, 1H), 1.97–1.70 (m, 12H), 1.45 (t, J = 5.2 Hz, 1H), 1.02 ppm (dd, J = 8.2, 4.9 Hz, 1H); **^{13}C NMR** (126 MHz, $CDCl_3$): δ=142.5, 133.2, 129.2, 127.5, 46.0, 40.6, 39.2, 38.4, 37.5, 36.9, 36.7, 36.5, 36.4, 32.3, 30.7, 27.8, 27.4, 20.5 ppm; **HRMS** (ESI): *m/z* calcd for $C_{18}H_{22}O_2S+Na^+$: 325.1238 $[M+Na]^+$; found: 325.1236.
GC Chromatogram: t_r = 10.619 min (92% purity).

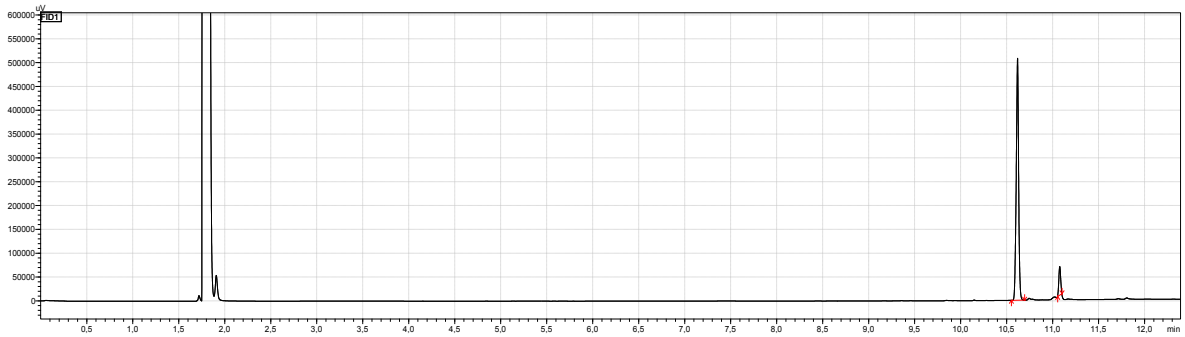

1-methyl-2-(phenylsulfonyl)-1,1'-bi(cyclopropane) (29)

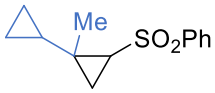

Synthesized according to the general procedure.
Yield: 37 mg (78%, *d.r.* 1.3:1), viscous colorless oil from column chromatography (hexanes/AcOEt 99:1 to 90:10 (v/v)).
^{1}H NMR (500 MHz, $CDCl_3$): δ=7.93–7.88 (m, 2H), 7.66–7.59 (m, 1H), 7.59–7.50 (m, 2H), 2.21 (dd, *J* = 8.7, 5.8 Hz, 1H), 1.52 (s, 3H), 1.30 (t, *J* = 5.6 Hz, 1H), 0.99 (tt, *J* = 8.3, 5.2 Hz, 1H), 0.91 (dd, *J* = 8.7, 5.5 Hz, 1H), 0.42 (ddd, *J* = 9.2, 8.2, 5.7, 4 1H), 0.28 (ddd, *J* = 9.2, 8.3, 5.9 Hz, 1H), 0.06 (ddt, *J* = 9.8, 6.0, 4.9 Hz, 1H), -0.12 ppm (ddt, *J* = 9.8, 5.3, 5.2 Hz, 1H); **^{13}C NMR** (126 MHz, $CDCl_3$): δ=142.3, 133.2, 129.3, 127.3, 43.3, 27.9, 18.2, 18.0, 16.3, 3.0, 1.9 ppm; **HRMS** (ESI): *m/z* calcd for $C_{13}H_{16}O_2S+Na^+$: 259.0769 $[M+Na]^+$; found: 259.0773.
GC Chromatogram: t_r = 7.661 min (91% purity).

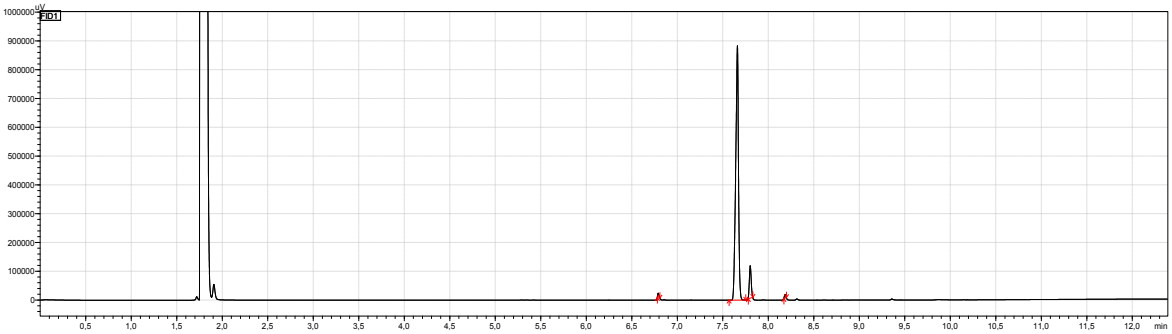

((2-(methoxymethyl)-2-methylcyclopropyl)sulfonyl)benzene (30)

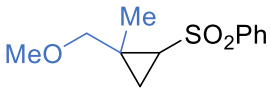

Synthesized according to the general procedure.
Yield: 21 mg (43%, *d.r.* 1.1:1), viscous colorless oil from column chromatography (hexanes/AcOEt 95:5 to 85:15 (v/v)).
^{1}H NMR (500 MHz, $CDCl_3$): [mixture of diastereoisomers] δ=7.97–7.86 (m, 4H), 7.65–7.58 (m, 2H), 7.59–7.50 (m, 4H), 3.75 (s, 2H), 3.38 (s, 3H), 3.23 (s, 3H), 3.14 (d, *J* = 9.8 Hz, 1H), 2.46 (dd, *J* = 8.6, 5.6 Hz, 1H), 2.29 (dd, *J* = 8.4, 5.8 Hz, 1H), 1.60 (t, *J* = 5.6 Hz, 1H), 1.48 (s, 3H), 1.44 (t, *J* = 5.4 Hz, 1H), 1.27 (dd, *J* = 8.7, 5.1 Hz, 1H), 1.20 (s, 3H), 1.15 (dd, *J* = 8.4, 5.4 Hz, 1H), 1.07 ppm (d, *J* = 6.9 Hz, 1H); **^{13}C NMR** (126 MHz, $CDCl_3$): δ=142.2, 141.9, 133.4, 133.3, 129.3, 129.2,

127.5, 127.4, 73.3, 58.9, 58.8, 44.7, 41.7, 36.5, 28.2, 26.6, 22.5, 19.1, 16.8, 14.7 ppm; **HRMS** (ESI): *m/z* calcd for $C_{12}H_{16}O_3S+Na^+$: 263.0718 $[M+Na]^+$; found: 263.0719; **elemental analysis** calcd (%) for $C_{12}H_{16}O_3S$: C 59.98, H 6.71; found: C 59.93, H 6.79.

diethyl ((1-methyl-2-(phenylsulfonyl)cyclopropyl)methyl)phosphonate (31)

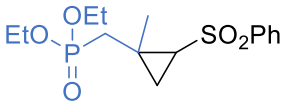

Synthesized according to the general procedure.
Yield: 44 mg (64%, *d.r.* 3:2), viscous colorless oil from column chromatography (hexanes/acetone 95:5 to 80:20 (v/v)).
^{1}H NMR (500 MHz, $CDCl_3$): δ=7.93 (dd, *J* = 7.8, 1.7 Hz, 2H), 7.66–7.59 (m, 1H), 7.55 (t, *J* = 7.7 Hz, 2H), 4.06–3.95 (m, 4H), 2.56 (dd, *J* = 8.7, 5.8 Hz, 1H), 1.85–1.67 (m, 3H), 1.56 (dd, *J* = 11.5, 1.7 Hz, 1H), 1.26 ppm (t, *J* = 7.0 Hz, 9H); **^{13}C NMR** (126 MHz, $CDCl_3$) δ 141.8, 133.4, 129.3, 127.6, 61.9 (d, *J* = 6.7 Hz), 61.8 (d, *J* = 6.6 Hz), 44.5 (d, *J* = 10.7 Hz), 36.5 (d, $^1J_{C-P}$ = 141.4 Hz), 22.4 (d, *J* = 4.7 Hz), 20.5 (d, *J* = 10.4 Hz), 17.8 (d, *J* = 2.1 Hz), 16.6 (d, *J* = 1.9 Hz), 16.6 (ppm d, *J* = 1.9 Hz); **HRMS** (ESI): *m/z* calcd for $C_{15}H_{23}O_5PS+Na^+$: 369.0902 $[M+Na]^+$; found: 369.0899; **elemental analysis** calcd (%) for $C_{15}H_{23}O_5PS$: C 52.01, H 6.69; found: C 52.18, H 7.02.

1-(phenylsulfonyl)-5-oxaspiro[2.3]hexane (32)

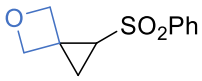

Synthesized according to the general procedure.
Yield: 16 mg (36%), colorless oil from column chromatography (hexanes/AcOEt 95:5 to 70:30 (v/v)).
^{1}H NMR (500 MHz, $CDCl_3$): δ=7.97–7.88 (m, 2H), 7.71–7.64 (m, 1H), 7.62–7.55 (m, 2H), 5.28 (d, *J* = 6.9 Hz, 1H), 4.92 (d, *J* = 7.0 Hz, 1H), 4.82 (d, *J* = 6.1 Hz, 1H), 4.64 (d, *J* = 6.0 Hz, 1H), 2.56 (dd, *J* = 8.8, 5.7 Hz, 1H), 1.68 (t, *J* = 6.0 Hz, 1H), 1.33 ppm (dd, *J* = 8.8, 6.4 Hz, 1H); **^{13}C NMR** (126 MHz, $CDCl_3$): δ=140.9, 133.8, 129.6, 127.5, 76.2, 39.6, 28.0, 15.7 ppm; **HRMS** (ESI): *m/z* calcd for $C_{11}H_{12}O_3S+Na^+$: 247.0405 $[M+Na]^+$; found: 247.0410.
GC Chromatogram: t_r = 7.834 min (98% purity).

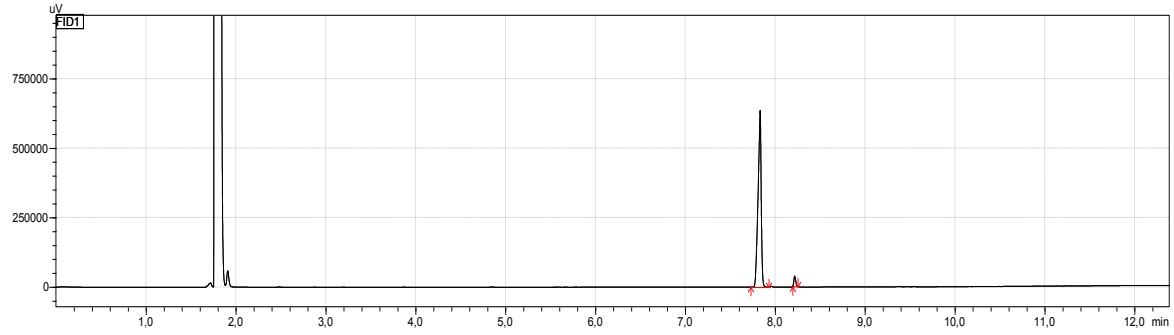

1-(phenylsulfonyl)-6-oxaspiro[2.5]octane (33)

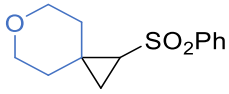

Synthesized according to the general procedure.
Yield: 31 mg (62%), white solid from column chromatography (hexanes/AcOEt 95:5 to 70:30 (v/v)).
m.p. 80-82 ºC; **^{1}H NMR** (500 MHz, $CDCl_3$): δ=7.94–7.89 (m, 2H), 7.68–7.61 (m, 1H), 7.60–7.53 (m, 2H), 3.80 (ddd, *J* = 11.5, 6.1, 3.8 Hz, 1H), 3.77–3.61 (m, 3H), 2.27 (dd, *J* = 8.4, 5.5 Hz, 1H), 2.18–2.07 (m, 1H), 2.05–1.96 (m, 1H), 1.60–1.51 (m, 2H), 1.28–1.21 (m, 1H), 1.16 ppm (dd, *J* = 8.4, 5.3 Hz, 1H); **^{13}C NMR** (126 MHz, $CDCl_3$): δ=141.9, 133.5, 129.4, 127.4, 67.6, 67.0, 44.5, 36.7, 29.4, 28.5, 18.9 ppm; **HRMS** (ESI): *m/z* calcd for $C_{13}H_{16}O_3S$+Na^+: 275.0718 $[M+Na]^+$; found: 275.0722; **elemental analysis** calcd (%) for $C_{13}H_{16}O_3S$ C 61.88, H 6.39, S 12.71; found: C 61.93, H 6.53, S 12.49.

1-(phenylsulfonyl)-5-thiaspiro[2.4]heptane (34)

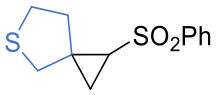

Synthesized according to the general procedure.
Yield: 13 mg (25%), viscous colorless oil from column chromatography (hexanes to hexanes/acetone 90:10 (v/v)).
^{1}H NMR (600 MHz, $CDCl_3$): δ=7.97–7.89 (m, 2H), 7.68–7.62 (m, 1H), 7.60–7.54 (m, 2H), 3.37 (d, *J* = 11.3 Hz, 1H), 3.12 (d, *J* = 11.3 Hz, 1H), 2.85 (ddd, *J* = 10.4, 8.6, 6.4 Hz, 1H), 2.76 (ddd, *J* = 10.4, 7.1, 4.4 Hz, 1H), 2.65 (dd, *J* = 8.6, 5.7 Hz, 1H), 2.08–2.02 (m, 1H), 1.73 (ddd, *J* = 12.6, 6.4, 4.4 Hz, 1H), 1.68 (t, *J* = 5.6 Hz, 1H), 1.28 ppm (dd, *J* = 8.6, 5.5 Hz, 1H); **^{13}C NMR** (151 MHz, $CDCl_3$): δ=141.2, 133.6, 129.4, 127.5, 43.0, 40.1, 35.3, 32.9, 29.1, 19.1 ppm; **HRMS** (ESI): *m/z* calcd for $C_{12}H_{14}O_2S_2$+Na^+: 277.0333 $[M+Na]^+$; found: 277.0338.
GC Chromatogram: t_r = 9.215 min (99% purity).

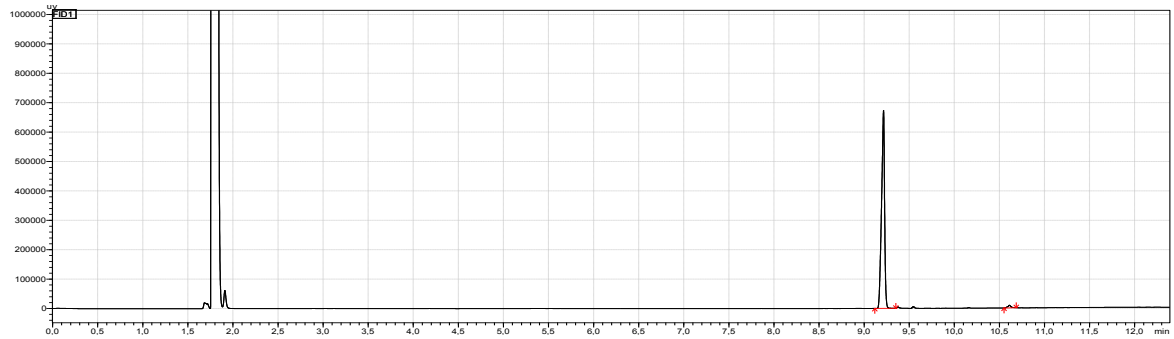

1-(phenylsulfonyl)-6-thiaspiro[2.5]octane (35)

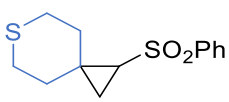

Synthesized according to the general procedure.
Yield: 24 mg (44%), white solid from column chromatography (hexanes/AcOEt 95:5 to 80:20 (v/v)).
m.p. 105-108 ºC; **^{1}H NMR** (500 MHz, $CDCl_3$): δ=7.95–7.87 (m, 2H), 7.68–7.61 (m, 1H), 7.60–7.53 (m, 2H), 2.81 (ddd, *J* = 13.6, 7.1, 3.9 Hz, 1H), 2.69 (ddd, *J* = 13.6, 7.5, 3.9 Hz, 1H), 2.63 (dd, *J* = 6.7,

4.5 Hz, 2H), 2.34–2.21 (m, 2H), 2.17 (dd, *J* = 8.4, 5.5 Hz, 1H), 1.70–1.60 (m, 1H), 1.59–1.50 (m, 1H), 1.48 (t, *J* = 5.4 Hz, 1H), 1.09 ppm (dd, *J* = 8.4, 5.3 Hz, 1H); **^{13}C NMR** (126 MHz, $CDCl_3$): δ=142.0, 133.5, 129.4, 127.4, 45.4, 38.5, 30.6, 30.5, 28.2, 27.8, 19.7 ppm; **HRMS** (ESI): *m/z* calcd for $C_{13}H_{16}O_2S_2$+Na^+: 291.0489 $[M+Na]^+$; found: 291.0494; **elemental analysis** calcd (%) for $C_{13}H_{16}O_2S_2$: C 58.18, H 6.01; found: C 58.15, H 5.84.

1-(phenylsulfonyl)-6-tosyl-6-azaspiro[2.5]octane (36)

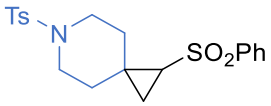

Synthesized according to the general procedure.
Yield: 67 mg (82%), white solid from column chromatography (hexanes/acetonet 95:5 to 80:20 (v/v)).
m.p. 187-189 ºC; **^{1}H NMR** (500 MHz, $CDCl_3$): δ=7.83 (d, *J* = 7.0 Hz, 2H), 7.63–7.58 (m, 3H), 7.55–7.48 (m, 2H), 7.32 (d, *J* = 7.9 Hz, 2H), 3.30–3.19 (m, 1H), 3.19–3.10 (m, 1H), 3.00–2.89 (m, 2H), 2.45 (s, 3H), 2.23 (dd, *J* = 8.5, 5.5 Hz, 1H), 2.18–2.04 (m, 2H), 1.59–1.50 (m, 1H), 1.44 (t, *J* = 5.5 Hz, 1H), 1.40–1.32 (m, 1H), 1.05 ppm (dd, *J* = 8.5, 5.4 Hz, 1H); **^{13}C NMR** (126 MHz, $CDCl_3$): δ=143.7, 141.5, 133.6, 133.5, 129.9, 129.4, 127.7, 127.3, 46.1, 45.6, 44.2, 35.5, 28.2, 27.9, 21.7, 18.3 ppm; **HRMS** (ESI): *m/z* calcd for $C_{20}H_{23}NO_4S_2$+Na^+: 428.0966 $[M+Na]^+$; found: 428.0972; **elemental analysis** calcd (%) for $C_{20}H_{23}NO_4S_2$: C 59.24, H 5.72, N 3.45; found: C 59.04, H 5.74, N 3.44.

tert-butyl (1R,3S,5S)-2'-(phenylsulfonyl)-8-azaspiro[bicyclo[3.2.1]octane-3,1'-cyclopropane]-8-carboxylate (37)

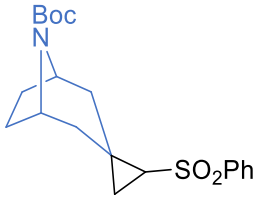

Synthesized according to the general procedure.
Yield: 48 mg (63%), white solid from column chromatography (hexanes/AcOEt 95:5 to 80:20 (v/v)).
m.p. 193-194 ºC; **^{1}H NMR** (600 MHz, DMSO-d_6, 70 ºC): δ=7.95–7.90 (m, 2H), 7.76–7.70 (m, 1H), 7.68–7.63 (m, 2H), 4.14–4.09 (m, 1H), 4.09–4.04 (m, 1H), 2.83 (dd, *J* = 8.6, 5.9 Hz, 1H), 2.28 (d, *J* = 14.2 Hz, 1H), 2.16 (ddd, *J* = 13.0, 8.5, 4.8 Hz, 1H), 2.04–1.93 (m, 2H), 1.93–1.81 (m, 2H), 1.82–1.73 (m, 1H), 1.43 (s, 9H), 1.10 (t, *J* = 5.5 Hz, 1H), 1.05 (d, *J* = 13.9 Hz, 1H), 0.92 ppm (dd, *J* = 8.6, 5.1 Hz, 1H); **^{13}C NMR** (151 MHz, DMSO-d_6, 70 ºC): δ=152.2, 141.6, 133.0, 129.0, 126.6, 78.1, 52.6, 45.2, 31.7, 27.9, 26.4, 26.1, 25.0, 15.9. ppm; **HRMS** (ESI): *m/z* calcd for $C_{20}H_{27}NO_4S$+Na^+: $[M+Na]^+$ 400.1558; found: 400.1551; **elemental analysis** calcd (%) for $C_{20}H_{27}NO_4S$: C 63.63, H 7.21, N 3.71, O; found: C 63.55, H 7.29, N 3.74.

6,6-dimethyl-1-(phenylsulfonyl)-5,7-dioxaspiro[2.5]octane (38)

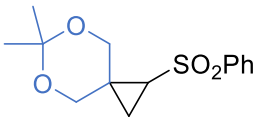

Synthesized according to the general procedure.

Yield: 11 mg (20%), viscous colorless oil from column chromatography (hexanes/AcOEt 90:10 to 70:30 (v/v)).
^{1}H NMR (500 MHz, $CDCl_3$): δ=8.03–7.98 (m, 2H), 7.67–7.62 (m, 1H), 7.59–7.53 (m, 2H), 4.40 (dd, *J* = 12.6, 1.3 Hz, 1H), 4.18 (d, *J* = 12.5 Hz, 1H), 3.66 (d, *J* = 12.0 Hz, 1H), 3.45 (dd, *J* = 12.0, 1.4 Hz, 1H), 2.42 (dd, *J* = 8.6, 5.6 Hz, 1H), 1.65 (t, *J* = 5.8 Hz, 1H), 1.43 (s, 3H), 1.26 (s, 3H), 1.22 (dd, *J* = 8.6, 5.9 Hz, 1H) ppm; **^{13}C NMR** (126 MHz, $CDCl_3$): δ=141.0, 133.6, 129.2, 127.9, 98.8, 66.8, 60.5, 43.0, 27.5, 24.6, 23.0, 15.0 ppm; **HRMS** (ESI): *m/z* calcd for $C_{14}H_{18}O_4S+Na^+$: 305.0823[M+Na]$^+$; found: 305.0819; **elemental analysis** calcd (%) for $C_{14}H_{18}O_4S$: C 59.55, H 6.43, S 11.35; found: C 59.31, H 6.41, S 11.35.

2-(phenylsulfonyl)-1',3'-dihydrospiro[cyclopropane-1,2'-indene](39)

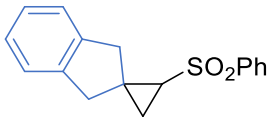

Synthesized according to the general procedure.
Yield: 6 mg (11%), viscous colorless oil from column chromatography (hexanes/AcOEt 95:5 to 80:20 (v/v)).
^{1}H NMR (500 MHz, $CDCl_3$): δ=7.96–7.90 (m, 2H), 7.65–7.58 (m, 1H), 7.57–7.50 (m, 2H), 7.25–7.23 (m, 1H), 7.21–7.12 (m, 3H), 3.65 (d, *J* = 16.9 Hz, 1H), 3.23 (dd, *J* = 16.4, 7.5 Hz, 2H), 2.70 (d, *J* = 15.9 Hz, 1H), 2.65 (dd, *J* = 8.6, 5.6 Hz, 1H), 1.71 (t, *J* = 5.5 Hz, 1H), 1.32 ppm (dd, *J* = 8.6, 5.3 Hz, 1H); **^{13}C NMR** (126 MHz, $CDCl_3$): δ=142.4, 141.7, 140.4, 133.4, 129.4, 127.4, 126.9, 126.6, 124.6, 124.1, 43.4, 43.1, 37.6, 31.5, 22.3 ppm; **HRMS** (ESI): *m/z* calcd for $C_{17}H_{16}O_2S+Na^+$: 307.0769 [M+Na]$^+$; found: 307.0770.
GC Chromatogram: t_r = 10.255min (98% purity).

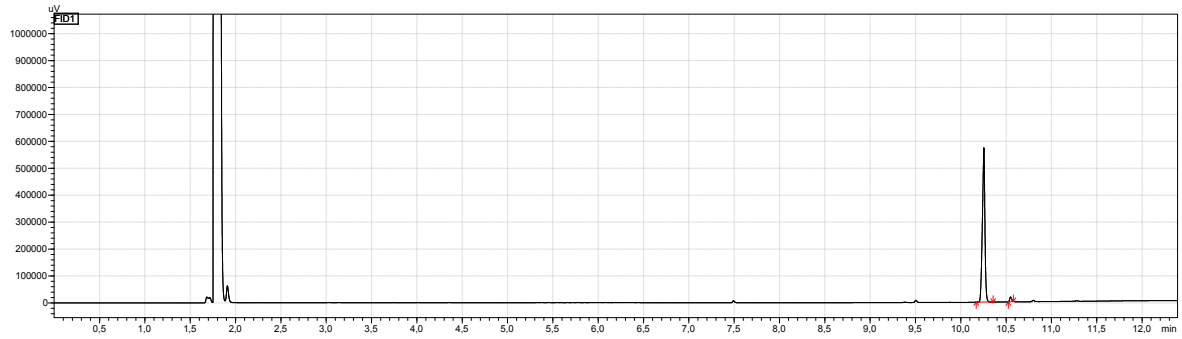

((2-benzyl-2-ethylcyclopropyl)sulfonyl)benzene (40)

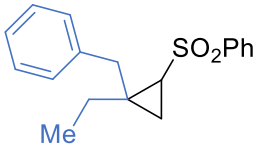

Synthesized according to the general procedure.
Yield: 39 mg (64%, *d.r.* 1:1), colorless oil from column chromatography (hexanes/AcOEt 95:5 to 85:15 (v/v)).
^{1}H NMR (600 MHz, $CDCl_3$): [mixture of diastereoisomers] δ=8.00–7.95 (m, 1H), 7.62–7.56 (m, 2H), 7.52–7.47 (m, 2H), 7.32–7.26 (m, 2H), 7.19–7.15 (m, 3H), 2.83 (d, *J* = 14.6 Hz, 1H), 2.45

(d, J = 14.5 Hz, 1H), 2.40 (dd, J = 8.6, 5.7 Hz, 1H), 1.89 (dq, J = 14.8, 7.5 Hz, 1H), 1.65 (dq, J = 14.1, 7.1 Hz, 1H), 1.49 (t, J = 5.4 Hz, 1H), 1.17 (ddd, J = 8.6, 5.2, 1.2 Hz, 1H), 1.07 ppm (t, J = 7.4 Hz, 3H); **^{13}C NMR** (151 MHz, $CDCl_3$): [mixture of diastereoisomers] δ=142.0 (2 x C), 139.3, 137.5, 133.4, 133.2, 129.3, 129.2, 128.5 (2 x C), 127.5, 127.3, 126.7, 126.5, 44.9, 44.0, 41.1, 33.5, 33.4, 33.1, 29.2, 21.8, 20.3, 17.9, 11.4, 10.5 ppm; **HRMS** (ESI): *m/ z* calcd for $C_{18}H_{20}O_2S+Na^+$: 323.1082 $[M+Na]^+$; found: 323.1089; **elemental analysis** calcd (%) for $C_{18}H_{20}O_2S$: C 71.97, H 6.71; found: C 71.84, H 6.62.

(1S,4R,5R)-1-isopropyl-4-methyl-2'-(phenylsulfonyl)spiro[bicyclo[3.1.0]hexane-3,1'-cyclopropane] (41)

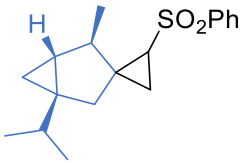

Synthesized according to the general procedure.
Yield: 31 mg (51%, *d.r.* 1:1.2) of white semisolid from column chromatography (hexanes to hexanes/acetone 95:5 (v/v)).
^{1}H NMR (500 MHz, $CDCl_3$): [mixture of diastereoisomers] δ=7.97–7.83 (m, 4H), 7.68–7.58 (m, 2H), 7.59–7.48 (m, 4H), 2.29 (dd, J = 8.7, 5.6 Hz, 1H), 2.29–2.20 (m, 2H), 2.15–2.01 (m, 2H), 1.76 (d, J = 13.0 Hz, 1H), 1.45–1.23 (m, 6H), 1.11 (dd, J = 8.7, 5.7 Hz, 1H), 1.04 (dd, J = 8.6, 4.9 Hz, 1H), 1.01–0.77 (m, 20H), 0.61 (dd, J = 4.9, 3.8 Hz, 1H), 0.36 (ddd, J = 8.0, 4.9, 1.4 Hz, 1H), 0.23 (dd, J = 5.3, 3.9 Hz, 1H), 0.08 ppm (ddd, J = 8.1, 5.2, 1.5 Hz, 1H); **^{13}C NMR** (126 MHz, $CDCl_3$): [mixture of diastereoisomers] δ=141.7 (2 x C), 133.4, 133.3, 129.3, 129.2, 127.8, 127.5, 46.7, 44.3, 44.2, 38.8, 35.7, 34.6, 34.2, 34.0, 32.7, 31.1, 30.4, 28.5, 28.3, 27.9, 24.1, 20.3 (2 x C), 19.9 (2 x C), 19.6, 19.2, 13.5, 13.0, 11.7 ppm; **HRMS** (ESI): *m/z* calcd for $C_{18}H_{24}O_2S+Na^+$: 327.1395 $[M+Na]^+$; found: 327.1394.
GC Chromatogram: [Diastereoisomers mixture] (97% purity): t_r = 9.410 min (minor); t_r = 10.559 min (major).

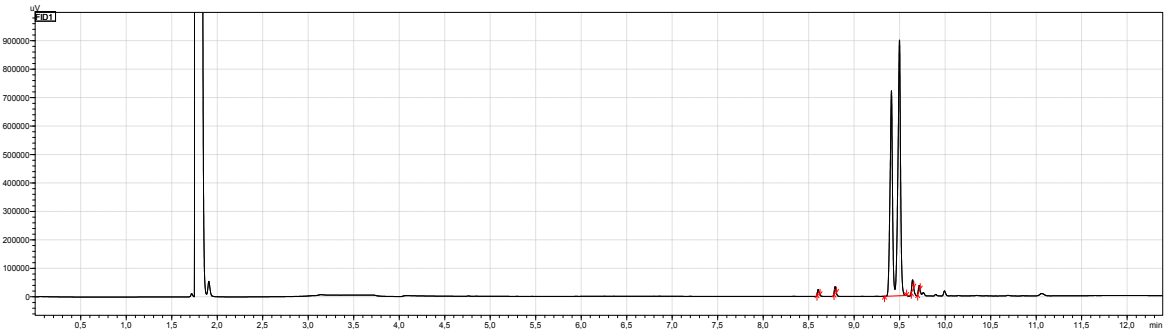

(3S,8S,10R,13S,17S)-3-methoxy-10,13-dimethyl-17-((1S)-1-methyl-2-(phenylsulfonyl)cyclopropyl)-2,3,4,7,8,9,10,11,12,13,14,15,16,17-tetradecahydro-1H-cyclopenta[a]phenanthrene (42)

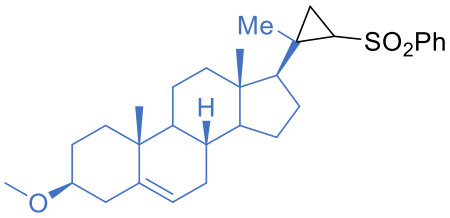

Synthesized according to the general procedure.
Yield: 53 mg (55%, *d.r.* 1:1), viscous colorless oil from column chromatography (hexanes/AcOEt 95:5 to 80:20 (v/v)).
^{1}H NMR (500 MHz, $CDCl_3$): [mixture of diastereoisomers] δ=7.99–7.79 (m, 2H), 7.66–7.58 (m, 1H), 7.58–7.51 (m, 2H), 5.38–5.29 (m, 1H), 3.39–3.30 (m, 3H), 3.12–2.99 (m, 1H), 2.45–2.33 (m, 1H), 2.30–1.59 (m, 8H), 1.56–0.78 (m, 21H), 0.62 (s, 1H), 0.57 ppm (s, 1H); **^{13}C NMR** (126 MHz, $CDCl_3$): δ=142.5, 142.4, 142.3, 141.2, 141.0, 133.3, 133.2, 129.2, 127.6, 127.4, 127.3, 121.7, 121.4, 80.5, 58.0, 57.1, 56.6, 56.3, 55.7, 55.6, 50.5, 50.3, 50.2, 49.5, 45.9, 44.5, 43.9, 43.6, 43.4, 42.9, 39.5, 39.3, 38.9, 38.8, 37.4, 37.3, 37.1, 37.0, 31.9, 31.7, 28.3, 28.2, 28.1, 26.8, 26.6, 24.4, 24.2, 23.9, 23.8, 23.4, 23.2, 23.1, 20.9, 20.8, 20.7, 19.5, 19.3, 19.0, 18.3, 16.6, 15.0, 13.4, 12.8 ppm; **HRMS** (ESI): *m/z* calcd for $C_{30}H_{42}O_3S+Na^+$: $[M+Na]^+$ 505.2752; found: 505.2754.
GC Chromatogram: t_r = 9.618 min (96% purity).

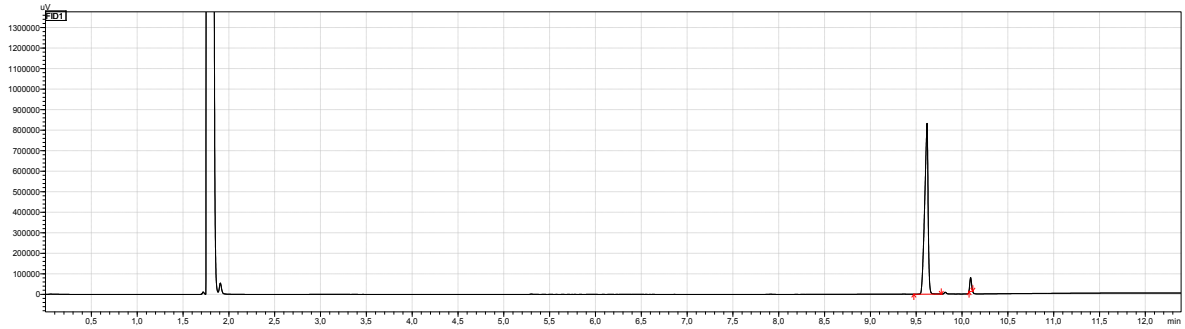

1-(ethylsulfonyl)spiro[2.5]octane (43)

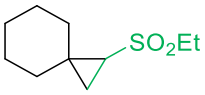

Synthesized according to the general procedure.
Yield: 30 mg (74%), colorless oil from column chromatography (hexanes/AcOEt 98:2 to 95:5 (v/v)).
^{1}H NMR (600 MHz, $CDCl_3$): δ=3.02 (m, 2H), 2.04 (dd, *J* = 8.4, 5.4 Hz, 1H), 1.89–1.84 (m, 1H), 1.84–1.77 (m, 1H), 1.74–1.68 (m, 1H), 1.67–1.57 (m, 2H), 1.57–1.44 (m, 4H), 1.42 (t, *J* = 7.5 Hz, 3H), 1.36 (t, *J* = 5.2 Hz, 1H), 1.18–1.11 (m, 1H), 1.07 ppm (dd, *J* = 8.4, 5.0 Hz, 1H); **^{13}C NMR** (151 MHz, $CDCl_3$): δ=49.8, 40.8, 37.3, 29.8, 28.8, 26.0, 25.7, 25.6, 18.5, 7.2 ppm; **HRMS** (ESI): *m/z* calcd for $C_{10}H_{18}O_2S+Na^+$: 225.0925 $[M+Na]^+$; found: 225.0932.
GC Chromatogram: t_r = 6.412 min (> 99% purity).

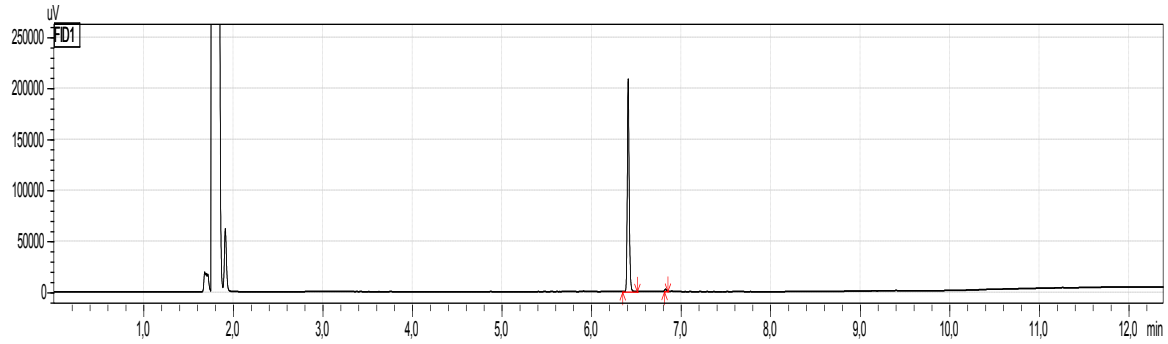

methyl 6-tosyl-6-azaspiro[2.5]octane-1-carboxylate (44)

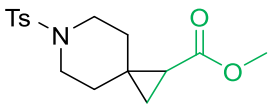

Synthesized according to the general procedure.
Yield: 46 mg (71%), white solid from column chromatography (hexanes/acetone 98:2 to 70:30 (v/v)). **m.p.** 90-93 ºC; **^{1}H NMR** (500 MHz, $CDCl_3$): δ=7.64 (d, *J* = 8.2 Hz, 2H), 7.32 (d, *J* = 8.0 Hz, 2H), 3.61 (s, 3H), 3.15 (ddd, *J* = 10.9, 7.0, 3.6 Hz, 1H), 3.05–2.92 (m, 3H), 2.44 (s, 3H), 1.87–1.76 (m, 2H), 1.64–1.55 (m, 1H), 1.52–1.41 (m, 2H), 1.06 (t, *J* = 5.0 Hz, 1H), 0.84 ppm (dd, *J* = 8.1, 4.7 Hz, 1H); **^{13}C NMR** (126 MHz, $CDCl_3$): δ=172.5, 143.6, 133.7, 129.8, 127.8, 51.8, 46.2, 45.9, 35.8, 28.0, 27.7, 25.0, 21.7, 19.9 ppm; **HRMS** (ESI): *m/z* calcd for $C_{16}H_{21}NO_4S+Na^+$: 346.1089[M+Na]$^+$; found: 346.1088; **elemental analysis** calcd (%) for $C_{16}H_{21}NO_4S$: C 59.42, H 6.55, N 4.33; found: C 59.31, H 6.51, N 4.34.

6-(tert-butyl) 1-methyl 6-azaspiro[2.5]octane-1,6-dicarboxylate (45)

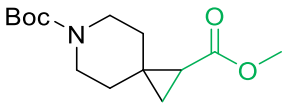

Synthesized according to the general procedure
Yield: 37 mg (68%), viscous oil from column chromatography (hexanes/AcOEt 95:5 to 80:20 (v/v)). **^{1}H NMR** (400 MHz, $CDCl_3$): δ=3.65 (s, 3H), 3.52–3.35 (m, 3H), 3.24 (ddd, *J* = 13.2, 7.4, 4.2 Hz, 1H), 1.75–1.59 (m, 2H), 1.54 (dd, *J* = 8.0, 5.4 Hz, 1H), 1.43 (s, 9H), 1.41–1.34 (m, 2H), 1.15 (t, *J* = 5.0 Hz, 1H), 0.92 ppm (dd, *J* = 8.0, 4.6 Hz, 1H); **^{13}C NMR** (101 MHz, $CDCl_3$): δ=172.8, 155.0, 79.6, 51.7, 43.5, 36.4, 28.7, 28.6, 25.1, 19.9 ppm; **HRMS** (ESI): *m/z* calcd for $C_{14}H_{23}NO_4+Na^+$: 292.1525 [M+Na]$^+$; found: 292.1522; **elemental analysis** calcd (%) for $C_{14}H_{23}NO_4$: C 62.43, H 8.61, N 5.20; found: C 62.40, H 8.77, N 5.24.

pent-4-yn-1-yl 6-tosyl-6-azaspiro[2.5]octane-1-carboxylate (46)

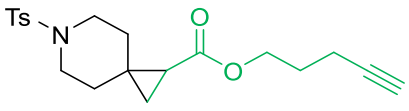

Synthesized according to the general procedure.
Yield: 53 mg (70%), colorless oil from column chromatography (hexanes/acetone 98:2 to 90:10 (v/v)). **^{1}H NMR** (500 MHz, $CDCl_3$): δ=7.64 (d, *J* = 8.2 Hz, 2H), 7.34 (d, *J* = 8.0 Hz, 2H), 4.11 (qt, *J* = 10.9, 6.3 Hz, 2H), 3.15–3.00 (m, 3H), 2.94–2.83 (m, 1H), 2.45 (s, 3H), 2.23–2.15 (m, 2H), 1.96

(t, *J* = 2.7 Hz, 1H), 1.86 (ddd, *J* = 13.6, 7.6, 3.7 Hz, 1H), 1.83–1.72 (m, 3H), 1.60–1.50 (m, 2H), 1.48 (dd, *J* = 8.0, 5.5 Hz, 1H), 1.08 (t, *J* = 5.1 Hz, 1H), 0.85 ppm (dd, *J* = 8.1, 4.7 Hz, 1H); **^{13}C NMR** (126 MHz, $CDCl_3$): δ=171.9, 143.6, 133.5, 129.8, 127.8, 83.0, 69.2, 63.1, 46.2, 45.9, 35.7, 28.0, 27.7, 27.6, 25.1, 21.6, 19.7, 15.2 ppm; **HRMS** (ESI): *m/z* calcd for $C_{20}H_{25}NO_4S+Na^+$: 398.1402 $[M+Na]^+$; found: 398.1404; **elemental analysis** calcd (%) for $C_{20}H_{25}NO_4S$: C 63.98, H 6.71, N 3.73; found: C 63.87, H 6.77, N 3.78.

pent-4-en-1-yl 6-tosyl-6-azaspiro[2.5]octane-1-carboxylate (47)

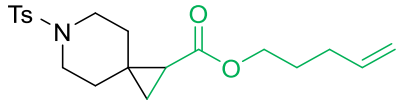

Synthesized according to the general procedure.
Yield: 63 mg (83%), colorless oil from column chromatography (hexanes/AcOEt 9:1 to 8:2 (v/v)).
^{1}H NMR (500 MHz, $CDCl_3$): δ=7.63 (d, *J* = 8.3 Hz, 2H), 7.31 (d, *J* = 8.0 Hz, 2H), 5.75 (ddt, *J* = 17.0, 10.2, 6.6 Hz, 1H), 5.03–4.94 (m, 2H), 4.05–3.96 (m, 2H), 3.12–2.98 (m, 3H), 2.95–2.87 (m, 1H), 2.42 (s, 3H), 2.07–2.01 (m, 2H), 1.89–1.74 (m, 2H), 1.68–1.59 (m, 2H), 1.55–1.50 (m, 2H), 1.47 (dd, *J* = 8.1, 5.5 Hz, 1H), 1.06 (t, *J* = 5.1 Hz, 1H), 0.83 ppm (dd, *J* = 8.1, 4.7 Hz, 1H); **^{13}C NMR** (126 MHz, $CDCl_3$): δ=172.0, 143.6, 137.4, 133.6, 129.8, 127.7, 115.5, 64.0, 46.2, 45.9, 35.8, 30.1, 28.0, 27.9, 27.6, 25.2, 21.6, 19.7 ppm; **HRMS** (ESI): *m/z* calcd for $C_{20}H_{27}NO_4S+Na^+$: 400.1558 $[M+Na]^+$; found: 400.1555; **elemental analysis** calcd (%) for $C_{20}H_{27}NO_4S$: C 63.63, H 7.21, N 3.71; found: C 63.65, H 7.41, N 3.75.

benzyl spiro[2.5]octane-1-carboxylate (48)

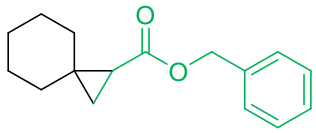

Synthesized according to the general procedure.
Yield: 36 mg (74%), colorless oil from column chromatography (hexanes to hexanes:Et_2O 99:1 (v/v)).
^{1}H NMR (400 MHz, $CDCl_3$): δ=7.45–7.20 (m, 5H), 5.21–4.98 (m, 2H), 1.66–1.21 (m, 11H), 1.11 (t, *J* = 4.8 Hz, 1H), 0.83 ppm (dd, *J* = 7.8, 4.3 Hz, 1H); **^{13}C NMR** (101 MHz, $CDCl_3$): δ=172.7, 136.6, 128.6, 128.3, 128.1, 66.2, 37.5, 31.1, 29.0, 26.2, 26.2, 25.8, 25.8, 21.0 ppm; **HRMS** (ESI): *m/z* calcd for $C_{16}H_{20}O_2+Na^+$: 267.1361 $[M+Na]^+$; found: 267.1359; **elemental analysis** calcd (%) for $C_{16}H_{20}O_2$: C 78.65, H 8.25; found: C 78.48, H 8.27.

4-cyanophenyl spiro[2.5]octane-1-carboxylate (49)

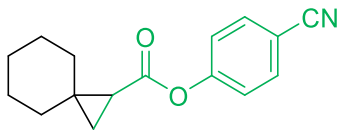

Synthesized according to the general procedure.
Yield: 31 mg (60%), white solid from column chromatography (hexanes/AcOEt 99:1 to 90:10 (v/v)).
m.p. 62-63 ºC; **^{1}H NMR** (600 MHz, $CDCl_3$): δ=7.68 (d, *J* = 8.7 Hz, 2H), 7.22 (d, *J* = 8.6 Hz, 2H), 1.70 (dd, *J* = 7.7, 5.4 Hz, 1H), 1.69–1.57 (m, 6H), 1.55–1.44 (m, 2H), 1.44–1.32 (m, 2H), 1.24

(t, J = 4.9 Hz, 1H), 1.04 ppm (dd, J = 7.7, 4.5 Hz, 1H); **^{13}C NMR** (151 MHz, $CDCl_3$): δ=170.6, 154.4, 133.7, 123.0, 118.5, 109.5, 37.4, 33.1, 28.9, 26.2, 26.0, 26.0, 25.8, 22.1 ppm; **HRMS** (APCI): *m/z* calcd for $C_{16}H_{17}NO_2$+H^+: 256.1338 $[M+H]^+$; found: 256.1337; **elemental analysis** calcd (%) for $C_{16}H_{17}NO_2$: C 75.27, H 6.71; N 5.49; found: C 75.02, H 6.77, N 5.42.

(1R,2S,5R)-2-isopropyl-5-methylcyclohexyl spiro[2.5]octane-1-carboxylate (50)

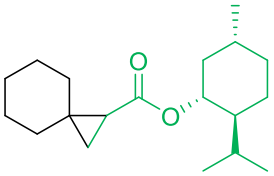

Synthesized according to the general procedure.
Yield: 46 mg (79%), white solid from column chromatography (hexanes to hexanes/AcOEt 97:3 (v/v)).
m.p. 87-89 ºC; **^{1}H NMR** (600 MHz, $CDCl_3$): [mixture of diastereoisomers] δ=4.67 (tt, J = 10.7, 4.8 Hz, 1H), 2.05–1.97 (m, 1H), 1.97–1.88 (m, 2H), 1.72–1.63 (m, 2H), 1.63–1.29 (m, 11H), 1.29–1.20 (m, 1H), 1.11–1.00 (m, 2H), 1.00–0.94 (m, 1H), 0.92–0.82 (m, 7H), 0.79 (dd, J = 7.9, 4.0 Hz, 1H), 0.78–0.73 ppm (m, 3H); **^{13}C NMR** (151 MHz, $CDCl_3$): [mixture of diastereoisomers] δ=172.5, 172.4, 74.1, 74.0, 47.3, 47.2, 41.3, 41.3, 37.7, 37.6, 34.5 (2C), 31.6, 30.8, 30.6, 29.0, 26.6, 26.5 (2 x C), 26.4, 26.3 (2 x C), 25.9 (3 x C), 25.7, 23.7, 23.6, 22.2 (2 x C), 21.0, 20.9, 20.7, 20.5, 16.6, 16.5 ppm; **HRMS** (ESI): *m/z* calcd for $C_{19}H_{32}O_2$+Na^+: 315.2300 $[M+Na]^+$; found: 315.2304; **elemental analysis** calcd (%) for $C_{19}H_{32}O_2$: C 78.03, H 11.03; found: C 78.13, H 11.01.

(8R,9S,13S,14S)-13-methyl-17-oxo-7,8,9,11,12,13,14,15,16,17-decahydro-6H cyclopenta[a] phenanthren-3-y spiro[2.5]octane-1-carboxylate (51)

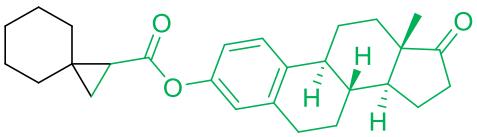

Synthesized according to the general procedure.
Yield: 57 mg (70%), white solid from column chromatography (hexanes/AcOEt 98:2 to 90:10 (v/v)).
m.p. 159-162 ºC; **^{1}H NMR** (600 MHz, $CDCl_3$): [mixture of diastereoisomers] δ=7.27 (d, J = 8.7 Hz, 1H), 6.85 (d, J = 8.5 Hz, 1H), 6.81 (s, 1H), 2.94–2.87 (m, 2H), 2.50 (dd, J = 19.0, 8.7 Hz, 1H), 2.43–2.37 (m, 1H), 2.28 (td, J = 10.9, 4.2 Hz, 1H), 2.14 (dt, J = 18.8, 8.9 Hz, 1H), 2.09–1.98 (m, 2H), 1.99–1.93 (m, 1H), 1.75–1.56 (m, 9H), 1.54–1.37 (m, 7H), 1.37–1.29 (m, 1H), 1.20 (t, J = 4.9 Hz, 1H), 0.97 (dd, J = 7.7, 4.4 Hz, 1H), 0.90 ppm (s, 3H); **^{13}C NMR** (151 MHz, $CDCl_3$): [mixture of diastereoisomers] δ=220.9, 171.7 (2 x C), 149.0, 138.0, 137.2, 126.4, 121.8 (2 x C), 119.0 (2 x C), 50.6, 48.1, 44.3, 38.2, 37.5, 36.0, 32.1, 32.0, 31.7, 29.5, 29.0, 26.5, 26.2, 26.1 (2 x C), 26.0, 25.9 (2 x C), 25.8, 21.7, 21.5 (2 x C), 14.0 ppm; **HRMS** (ESI): *m/z* calcd for $C_{27}H_{34}O_3$+Na^+: 429.2406 $[M+Na]^+$; found: 429.2414; **elemental analysis** calcd (%) for $C_{27}H_{34}O_3$: C 79.76, H 8.43; found: C 79.52, H 8.45.

1,3-dioxoisoindolin-2-yl spiro[2.5]octane-1-carboxylate (52)[24]

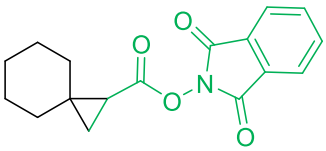

Synthesized according to the general procedure.
Yield: 27 mg (45%), viscous colorless oil from column chromatography (hexanes/AcOEt 98:2 to 90:10 (v/v)).
^{1}H NMR (500 MHz, $CDCl_3$): δ=7.88 (dd, *J* = 5.5, 3.1 Hz, 2H), 7.77 (dd, *J* = 5.5, 3.1 Hz, 2H), 1.79 (dd, *J* = 7.8, 5.4 Hz, 1H), 1.71–1.54 (m, 7H), 1.51–1.42 (m, 1H), 1.41–1.31 (m, 1H), 1.27 (dd, *J* = 10.2, 5.1 Hz, 2H), 1.15 ppm (dd, *J* = 7.9, 4.6 Hz, 1H); **^{13}C NMR** (126 MHz, $CDCl_3$): δ=169.0, 162.4, 134.8, 129.2, 124.0, 37.3, 34.1, 28.9, 26.1, 25.8, 25.4, 23.1, 22.8 ppm.

1-(6-tosyl-6-azaspiro[2.5]octan-1-yl)ethan-1-one (53)

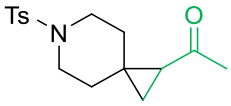

Synthesized according to the general procedure.
Yield: 32 mg (52%), colorless viscous oil from column chromatography (hexanes/AcOEt 95:5 to 80:20 (v/v)).
^{1}H NMR (600 MHz, $CDCl_3$): δ=7.65–7.61 (m, 2H), 7.32 (d, *J* = 8.0 Hz, 2H), 3.12 (ddd, *J* = 11.1, 7.0, 3.7 Hz, 1H), 3.00 (ddd, *J* = 11.5, 7.8, 3.5 Hz, 1H), 2.95–2.88 (m, 2H), 2.43 (s, 3H), 2.16 (s, 3H), 1.83 (dd, *J* = 7.7, 5.5 Hz, 1H), 1.77–1.60 (m, 3H), 1.50 (ddd, *J* = 13.4, 7.0, 3.5 Hz, 1H), 1.21 (t, *J* = 4.9 Hz, 1H), 0.81 ppm (dd, *J* = 7.7, 4.4 Hz, 1H); **^{13}C NMR** (151 MHz, $CDCl_3$): δ=193.1, 142.4, 133.2, 129.2, 127.3, 46.2, 39.8, 33.2, 31.0, 28.0, 27.9, 26.3, 25.9, 21.7 ppm; **HRMS** (ESI): *m/z* calcd for $C_{16}H_{21}NO_3S+Na^+$: 330.1140 $[M+Na]^+$; found: 330.1145.
GC Chromatogram: t_r = 8.417 min (99% purity).

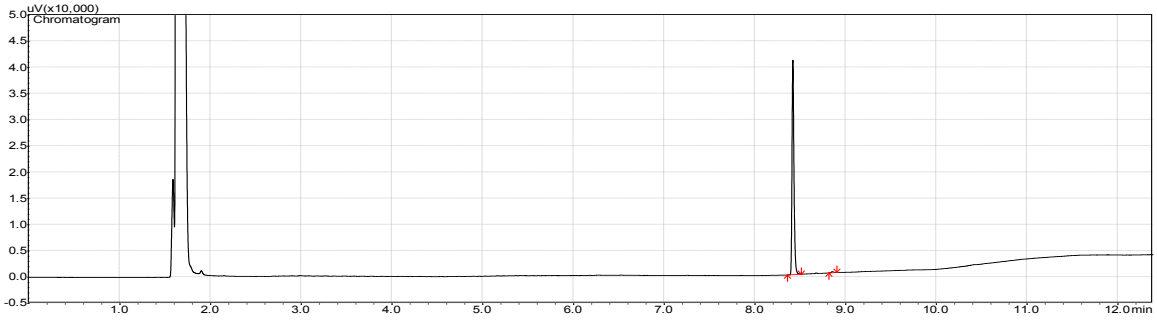

(6-tosyl-6-azaspiro[2.5]octan-1-yl)methanol (54')

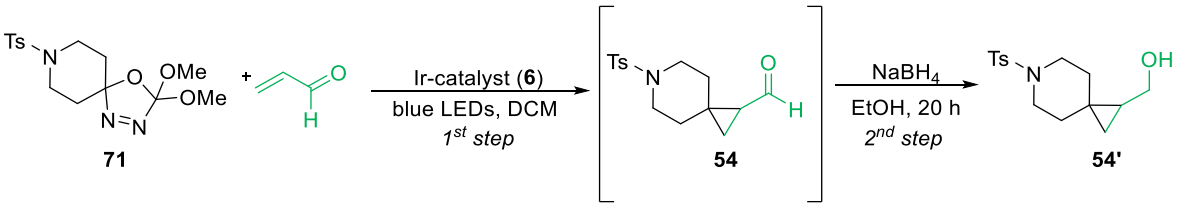

Synthesized in 2 steps according to the general procedure (1st step) followed by aldehyde reduction[25] (2nd step) reported on the literature.

Yield: 55 mg (46% [2 steps]), colorless oil from column chromatography (hexanes to hexanes/AcOEt 70:30 (v/v)).
^{1}H NMR (500 MHz, $CDCl_3$): δ=7.65 (d, *J* = 8.3 Hz, 2H), 7.32 (d, *J* = 8.0 Hz, 2H), 3.65 (dd, *J* = 11.4, 6.7 Hz, 1H), 3.47 (dd, *J* = 11.4, 8.2 Hz, 1H), 3.28 (ddd, *J* = 11.0, 6.8, 3.8 Hz, 1H), 3.21 (ddd, *J* = 11.4, 6.6, 4.5 Hz, 1H), 2.95 – 2.84 (m, 2H), 2.44 (s, 3H), 1.75 (ddd, *J* = 12.8, 8.4, 3.7 Hz, 1H), 1.61 (ddd, *J* = 12.8, 8.5, 3.7 Hz, 1H), 1.55–1.47 (m, 1H), 1.38–1.29 (m, 1H), 1.21 (bs, 1H), 1.00–0.85 (m, 1H), 0.48 (dd, *J* = 8.6, 4.8 Hz, 1H), 0.15 ppm (t, *J* = 5.2 Hz, 1H); **^{13}C NMR** (126 MHz, $CDCl_3$): δ=143.5, 133.8, 129.8, 127.8, 62.9, 46.2, 46.0, 36.1, 29.7, 25.7, 21.7, 21.6, 15.8 ppm; **HRMS** (ESI): *m/z* calcd for $C_{15}H_{21}NO_3S+Na^+$: 318.1140 $[M+Na]^+$; found: 318.1144.
GC Chromatogram: t_r = 10.559 min (> 99% purity).

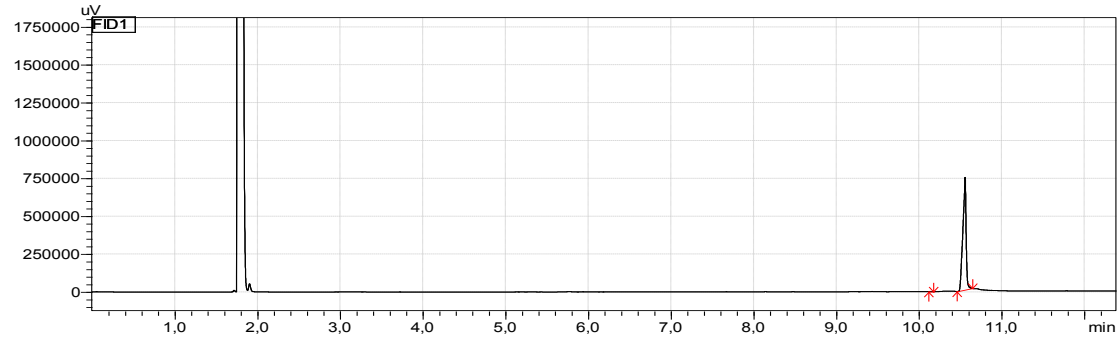

6-tosyl-6-azaspiro[2.5]octane-1-carbonitrile (55)

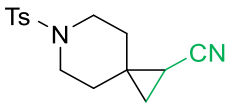

Synthesized according to the general procedure.
Yield: 46 mg (79%), white solid from column chromatography (hexanes/acetone 97:3 to 70:30 (v/v)).
m.p. 123-125 ºC; **^{1}H NMR** (600 MHz, $CDCl_3$): δ=7.64 (d, *J* = 8.2 Hz, 2H), 7.34 (d, *J* = 7.9 Hz, 2H), 3.41–3.27 (m, 2H), 2.92 (ddd, *J* = 12.0, 9.1, 3.3 Hz, 1H), 2.82 (ddd, *J* = 12.0, 9.0, 3.3 Hz, 1H), 2.45 (s, 3H), 1.90 (ddd, *J* = 13.4, 9.1, 3.9 Hz, 1H), 1.80–1.67 (m, 2H), 1.37–1.29 (m, 1H), 1.19 (dd, *J* = 8.6, 5.3 Hz, 1H), 1.04–0.98 ppm (m, 2H); **^{13}C NMR** (151 MHz, $CDCl_3$): δ=143.9, 133.3, 129.9, 127.7, 119.8, 45.5, 33.9, 31.1, 25.3, 21.7 (2 x C), 19.9, 8.7 ppm; **HRMS** (ESI): *m/z* calcd for $C_{15}H_{18}N_2O_2S+Na^+$: 313.0987 $[M+Na]^+$; found: 313.0994; **elemental analysis** calcd (%) for $C_{15}H_{18}N_2O_2S$: C 62.04, H 6.25, N 9.65; found: C 62.05, H 6.21, N 9.62.

N,N-dimethyl-6-tosyl-6-azaspiro[2.5]octane-1-carboxamide (56)

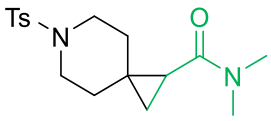

Synthesized according to the general procedure.
Yield: 56 mg (83%), yellowish solid from column chromatography (hexanes/acetone 95:5 to 60:40 (v/v)).
m.p. 137-140 ºC; **^{1}H NMR** (500 MHz, $CDCl_3$): δ=7.63 (d, *J* = 8.3 Hz, 2H), 7.32 (d, *J* = 8.0 Hz, 2H), 3.33
(dt, *J* = 10.0, 4.5 Hz, 1H), 3.19 (dt, *J* = 10.6, 4.9 Hz, 1H), 2.96 (s, 3H), 2.90 (s, 3H), 2.81 (ddd, *J* = 11.9, 9.2, 3.3 Hz, 1H), 2.73 (ddd, *J* = 12.0, 9.2, 3.4 Hz, 1H), 2.43 (s, 3H), 1.81

(ddd, J = 13.2, 9.1, 3.9 Hz, 1H), 1.75–1.66 (m, 1H), 1.57 (dd, J = 8.0, 5.3 Hz, 1H), 1.56–1.48 (m, 1H), 1.40–1.31 (m, 1H), 1.15 (t, J = 4.9 Hz, 1H), 0.65 ppm (dd, J = 8.1, 4.6 Hz, 1H); **^{13}C NMR** (126 MHz, $CDCl_3$): δ=170.1, 143.6, 133.4, 129.7, 127.8, 46.3, 46.1, 37.4, 35.7, 35.6, 28.5, 25.8, 25.3, 21.6, 17.6 ppm; **HRMS** (ESI): *m/z* calcd for $C_{17}H_{24}N_2O_3S+Na^+$: 359.1405 $[M+Na]^+$; found: 359.1413.
GC Chromatogram: t_r = 11.057 min (99% purity).

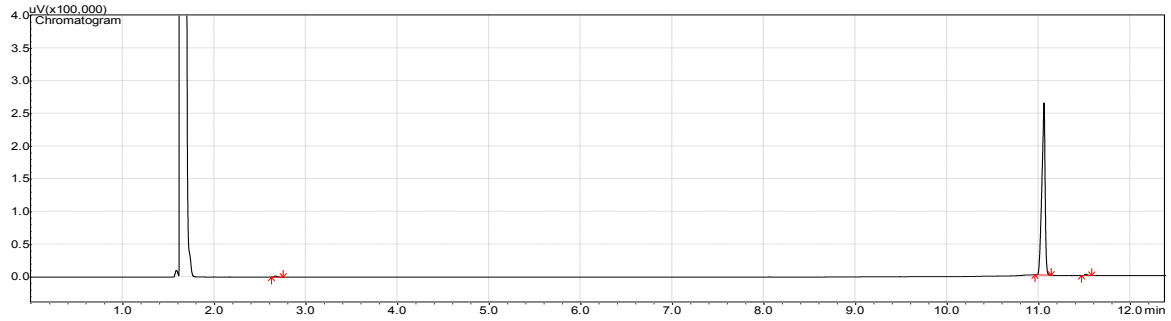

tert-butyl 1-(dimethylcarbamoyl)-6-azaspiro[2.5]octane-6-carboxylate (57)

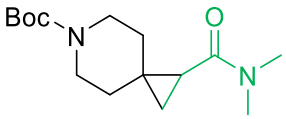

Synthesized according to the general procedure.
Yield: 46 mg (81%), yellowish solid from column chromatography (hexanes/acetone 95:5 to 70:30 (v/v)).
m.p. 104-106 ºC; **^{1}H NMR** (500 MHz, $CDCl_3$): δ=3.66–3.53 (m, 1H), 3.47–3.39 (m, 1H), 3.34 (ddd, J = 12.6, 8.5, 3.4 Hz, 1H), 3.26 (ddd, J = 12.8, 8.5, 3.5 Hz, 1H), 3.13 (s, 3H), 2.95 (s, 3H), 1.63 (dd, J = 7.7, 5.5 Hz, 1H), 1.60–1.51 (m, 2H), 1.45 (s, 9H), 1.44–1.39 (m, 1H), 1.38–1.30 (m, 1H), 1.27 (t, J = 4.8 Hz, 1H), 0.76 ppm (dd, J = 7.8, 4.4 Hz, 1H); **^{13}C NMR** (126 MHz, $CDCl_3$): δ=170.5, 155.0, 79.6, 43.9, 37.6, 36.2, 35.8, 29.8, 29.0, 28.6, 26.8, 25.6, 17.6 ppm; **HRMS** (ESI): *m/z* calcd for $C_{15}H_{26}N_2O_3+Na^+$: 305.1841 $[M+Na]^+$; found: 305.1852.
GC Chromatogram: t_r = 7.605 min (98% purity).

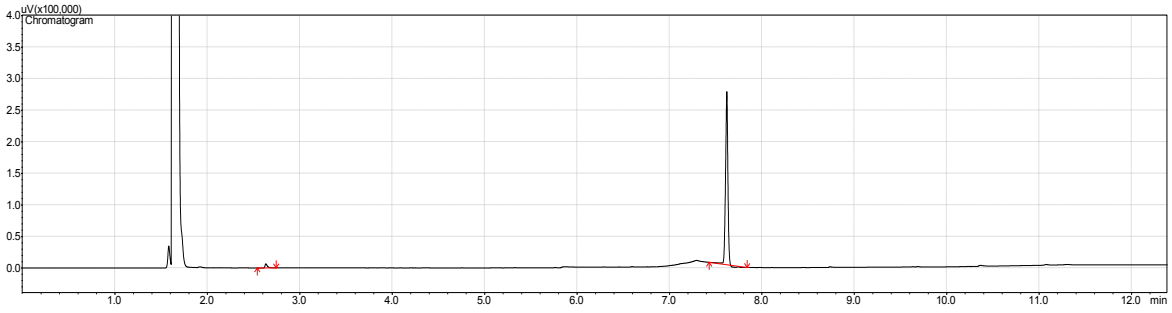

N-phenylspiro[2.5]octane-1-carboxamide (58)[26]

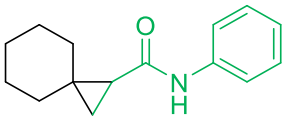

Synthesized according to the general procedure.

Yield: 33 mg (71%), white solid from column chromatography (hexanes/AcOEt 98:2 to 95:5 (v/v)).
^{1}H NMR (400 MHz, $CDCl_3$): δ=7.50 (d, *J* = 6.8 Hz, 2H), 7.38 (s, 1H), 7.30 (t, *J* = 7.7 Hz, 2H), 7.13–7.03 (m, 1H), 1.69–1.48 (m, 7H), 1.46–1.29 (m, 4H), 1.22 (t, *J* = 4.7 Hz, 1H), 0.80 ppm (dd, *J* = 7.2, 4.3 Hz, 1H); **^{13}C NMR** (126 MHz, $CDCl_3$): δ=169.9, 138.5, 129.1, 123.9, 119.8, 37.7, 30.6, 29.4, 28.8, 26.3, 26.1, 25.9, 19.6 ppm.

morpholino(spiro[2.5]octan-1-yl)methanone (59)

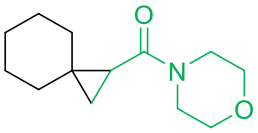

Synthesized according to the general procedure.
Yield: 29 mg (65%), pale oil from column chromatography (hexanes/AcOEt 90:10 to 60:40 (v/v)).
^{1}H NMR (500 MHz, $CDCl_3$): δ=3.80–3.57 (m, 7H), 3.56–3.47 (m, 1H), 1.63–1.27 (m, 11H), 1.20 (t, *J* = 4.6 Hz, 1H), 0.68 ppm (dd, *J* = 7.7, 4.3 Hz, 1H); **^{13}C NMR** (101 MHz, $CDCl_3$): δ=169.8, 67.2, 67.0, 46.3, 42.4, 37.2, 29.7, 28.8, 26.4, 26.2, 26.0, 25.8, 18.0 ppm; **HRMS** (ESI): *m/z* calcd for $C_{13}H_{21}NO_2$+Na^+: 246.1470 $[M+Na]^+$; found: 246.1477.
GC Chromatogram: t_r = 7.313 min (> 99% purity).

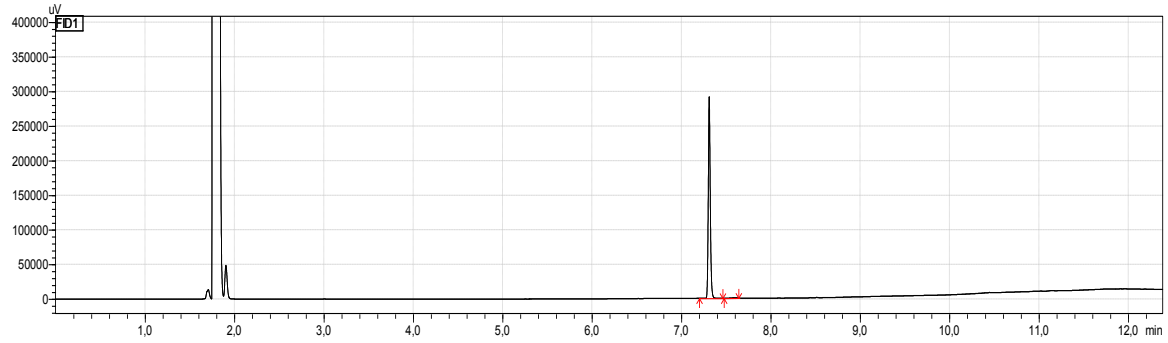

dimethyl spiro[2.5]octan-1-ylphosphonate (60)

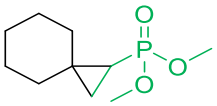

Synthesized according to the general procedure.
Yield: 31 mg (71%), white solid from column chromatography (hexanes/AcOEt 9:1 to 7:3 (v/v)).
^{1}H NMR (500 MHz, $CDCl_3$): δ=3.73 (d, *J* = 2.4 Hz, 3H), 3.71 (d, *J* = 2.2 Hz, 3H), 1.76–1.61 (m, 3H), 1.60–1.38 (m, 6H), 1.20–1.11 (m, 1H), 1.00 (ddd, *J* = 18.3, 6.2, 4.1 Hz, 1H), 0.84 (td, *J* = 9.2, 4.1 Hz, 1H), 0.59 ppm (ddd, *J* = 9.1, 6.2, 2.7 Hz, 1H); **^{13}C NMR** (126 MHz, $CDCl_3$): δ=52.3 (d, $J_{(C-P)}$ = 6.0 Hz), 52.3 (d, $J_{(C-P)}$ = 6.3 Hz), 37.85(d, *J* = 4.1 Hz), 30.8 (d, $J_{(C-P)}$ = 4.8 Hz), 26.5 (d, $J_{(C-P)}$ = 4.1 Hz), 26.1, 25.9 (d, $J_{(C-P)}$ = 2.0 Hz), 25.6, 18.0 (d, $J_{(C-P)}$ = 5.1 Hz), 16.4 (d, $^1J_{(C-P)}$ = 192.4 Hz) ppm; **HRMS** (ESI): *m/z* calcd for $C_{10}H_{19}O_3P$+Na^+: 241.0970 $[M+Na]^+$; found: 241.0958.
GC Chromatogram: t_r = 11.057 min (> 99% purity).

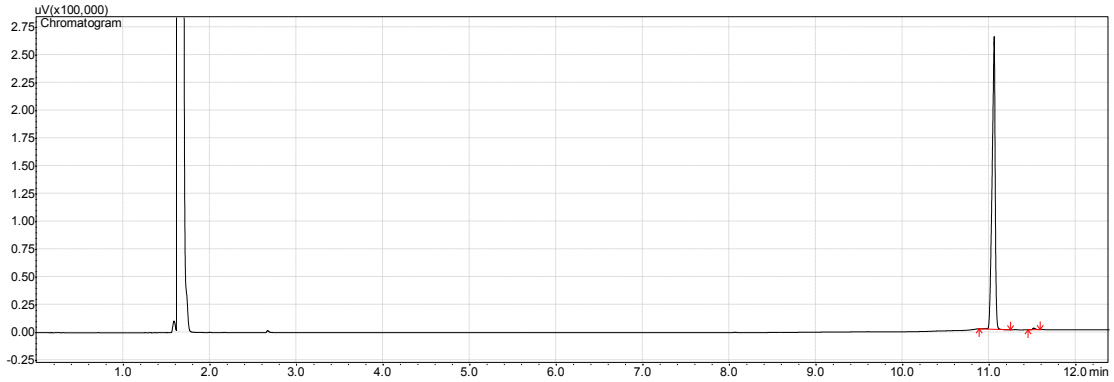

methyl 1-methyl-6-tosyl-6-azaspiro[2.5]octane-1-carboxylate (61)

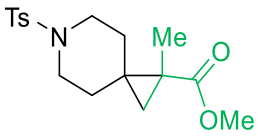

Synthesized according to the general procedure.
Yield: 61 mg (90%), white solid from column chromatography (hexanes/acetone 98:2 to 80:20 (v/v)).
m.p. 136-139 ºC; **^{1}H NMR** (500 MHz, $CDCl_3$): δ=7.63 (d, *J* = 7.5 Hz, 2H), 7.32 (d, *J* = 7.9 Hz, 2H), 3.62 (s, 3H), 3.40–3.32 (m, 1H), 3.29–3.21 (m, 1H), 2.80–2.68 (m, 2H), 2.44 (s, 3H), 1.89–1.77 (m, 1H), 1.74–1.56 (m, 2H), 1.53–1.43 (m, 1H), 1.30–1.22 (m, 4H), 0.40 ppm (d, *J* = 4.7 Hz, 1H); **^{13}C NMR** (126 MHz, $CDCl_3$): δ=174.2, 143.6, 133.7, 129.8, 127.8, 52.0, 46.0, 46.0, 30.9, 29.8, 29.1, 28.5, 24.7, 21.7, 16.1 ppm; **HRMS** (ESI): *m/z* calcd for $C_{17}H_{23}NO_4S$+Na^+: 360.1245 $[M+Na]^+$; found: 360.1233; **elemental analysis** calcd (%) for $C_{17}H_{23}NO_4S$: C 60.51, H 6.87, N 4.15; found: C 60.31, H 6.66, N 4.16.

1-(1-methyl-6-tosyl-6-azaspiro[2.5]octan-1-yl)ethan-1-one (62)

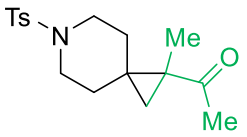

Synthesized according to the general procedure.
Yield: 26 mg (41%), white solid from column chromatography (hexanes/AcOEt 95:5 to 80:20 (v/v)).
m.p. 144-145 ºC; **^{1}H NMR** (500 MHz, $CDCl_3$): δ=7.62 (d, *J* = 8.1 Hz, 2H), 7.31 (d, *J* = 8.0 Hz, 2H), 3.40-3.49 (m, 1H), 3.33–3.25 (m, 1H), 2.64 (*J* =11.7, 10.3, 3.0 Hz,1H), 2.56 (ddd, *J* = 11.4, 10.0, 3.2 Hz, 1H), 2.43 (s, 3H), 2.13 (s, 3H), 1.89 (ddd, *J* = 13.8, 10.0, 3.8 Hz, 1H), 1.55 (ddd, *J* = 13.7, 9.9, 3.8 Hz, 1H), 1.46 (1.50–1.42 (m, 1H), 1.36 (1.41–1.33 (m, 5H), 0.28 ppm (d, *J* = 4.3 Hz, 1H); **^{13}C NMR** (126 MHz, $CDCl_3$): δ=207.9, 143.6, 133.4, 129.8, 127.8, 46.4, 46.1, 36.0, 30.9, 30.7, 29.0, 28.8, 24.0, 21.6, 16.6 ppm; **HRMS** (APCI): *m/z* calcd for $C_{17}H_{23}NO_3S$+H^+: 322.1477 $[M+H]^+$; found: 322.1479; **elemental analysis** calcd (%) for $C_{17}H_{23}NO_3S$: C 63.52, H 7.21, N 4.36, S 9.97; found: C 63.51, H 7.17, N 4.37, S 9.93.

methyl 1-acetamidospiro[2.5]octane-1-carboxylate (63)

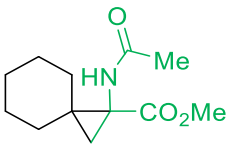

Synthesized according to the general procedure.
Yield: 35 mg (77%), white solid from column chromatography (hexanes/acetone 95:5 to 70:30 (v/v)).
m.p. 171-173 ºC; **^{1}H NMR** (500 MHz, DMSO-d_6, 70 ºC): δ=7.97 (bs, 1H), 3.59 (s, 3H), 1.84 (s, 3H), 1.74–1.64 (m, 1H), 1.64–1.31 (m, 10H), 0.77 ppm (d, J = 5.0 Hz, 1H); **^{13}C NMR** (126 MHz, DMSO-d_6, 70 ºC): δ=171.0, 170.2, 51.2, 42.1, 33.3, 31.3, 28.9, 26.4, 25.4, 24.7, 24.6, 22.0 ppm; **HRMS** (ESI): *m/z* calcd for $C_{12}H_{19}NO_3$+Na^+: 248.1263 $[M+Na]^+$; found: 242.1269; **elemental analysis** calcd (%) for $C_{12}H_{19}NO_3$: C 63.98, H 8.50, N 6.22; found: C 63.97, H 8.44, N 6.21.

benzyl 1-phenylspiro[2.5]octane-1-carboxylate (64)

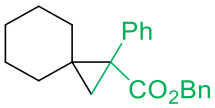

Synthesized according to the general procedure.
Yield: 58 mg (90%), white off oil from column chromatography (hexanes to hexanes/AcOEt 98:2 (v/v)).
^{1}H NMR (500 MHz, $CDCl_3$): δ=7.42 (d, J = 7.1 Hz, 2H), 7.32–7.16 (m, 8H), 5.12 (d, J = 12.8 Hz, 1H), 5.01 (d, J = 12.8 Hz, 1H), 1.68–1.53 (m, 5H), 1.53–1.37 (m, 2H), 1.36–1.22 (m, 3H), 1.11 (d, J = 4.6 Hz, 1H), 0.72–0.60 ppm (m, 1H); **^{13}C NMR** (126 MHz, $CDCl_3$): δ=171.9, 137.6, 136.5, 131.6, 128.5, 127.9, 127.8, 127.7, 127.0, 66.6, 40.8, 34.1, 33.5, 31.3, 26.3, 25.8, 25.5, 23.8 ppm; **HRMS** (ESI): *m/z* calcd for $C_{22}H_{24}O_2$+Na^+: 343.1674 $[M+Na]^+$; found: 343.1673; **elemental analysis** calcd (%) for $C_{22}H_{24}O_2$: C 82.46, H 7.55; found: C 82.26, H 7.50.

ethyl 1-((phenylsulfonyl)methyl)spiro[2.5]octane-1-carboxylate (65)

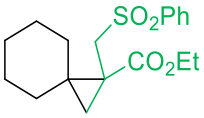

Synthesized according to the general procedure.
Yield: 58 mg (86%), white off oil from column chromatography (hexanes/acetone 98:2 to 93:7 (v/v)).
^{1}H NMR (400 MHz, $CDCl_3$): δ=7.96–7.85 (m, 2H), 7.68–7.59 (m, 1H), 7.54 (dd, J = 8.4, 6.9 Hz, 2H), 4.34 (d, J = 14.9 Hz, 1H), 3.94 (dq, J = 10.8, 7.1 Hz, 1H), 3.82 (dq, J = 10.7, 7.1 Hz, 1H), 2.99 (d, J = 14.9 Hz, 1H), 1.52–1.32 (m, 11H), 1.17 (t, J = 7.1 Hz, 3H), 0.81 ppm (d, J = 5.6 Hz, 1H); **^{13}C NMR** (151 MHz, $CDCl_3$): δ=170.9, 139.5, 133.8, 129.2, 128.8, 61.2, 57.2, 33.1, 32.8, 30.5, 29.5, 26.0, 25.7, 25.3, 22.2, 14.2 ppm; **HRMS** (ESI): *m/z* calcd for $C_{18}H_{24}O_4S$+Na^+: 359.1293 $[M+Na]^+$; found: 359.1295; **elemental analysis** calcd (%) for $C_{18}H_{24}O_4S$: C 64.26, H 7.19; found: C 64.15, H 7.23.

dibenzyl spiro[2.5]octane-1,1-dicarboxylate (66)

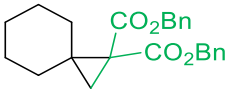

Synthesized according to the general procedure.
Yield: 42 mg (56%), viscous colorless oil from column chromatography (hexanes/AcOEt 95:5 to 80:20 (v/v)).
^{1}H NMR (500 MHz, $CDCl_3$): δ=7.38–7.25 (m, 10H), 5.13 (s, 4H), 1.65–1.54 (m, 5H), 1.51–1.35 ppm (m, 7H); **^{13}C NMR** (126 MHz, $CDCl_3$): δ=168.7, 135.9, 128.6, 128.3, 128.3, 67.2, 39.9, 36.9, 31.7, 26.1, 26.0, 25.6 ppm; **HRMS** (ESI): *m/z* calcd for $C_{24}H_{26}O_4$+Na^+: 401.1729 $[M+Na]^+$; found: 401.1728.
GC Chromatogram: t_r = 7.962 min (> 99% purity).

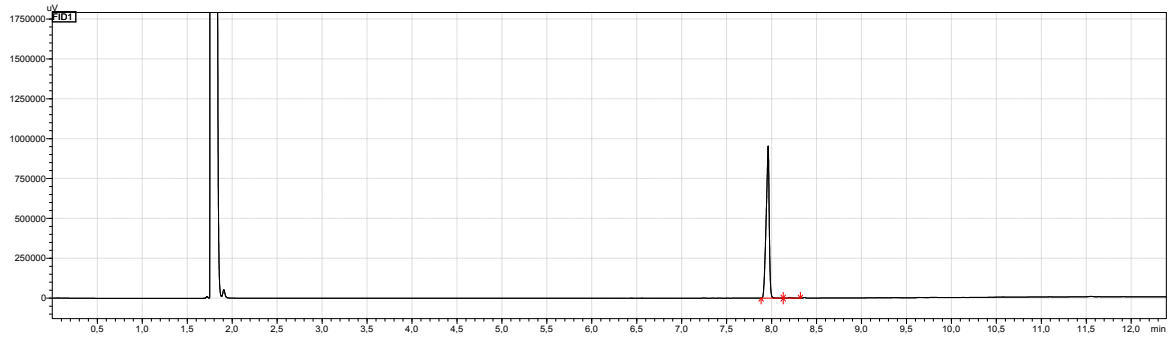

methyl 2-methyl-6-tosyl-6-azaspiro[2.5]octane-1-carboxylate (67)

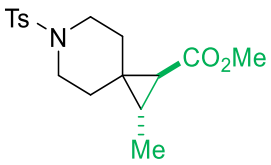

Synthesized according to the general procedure.
Yield: 22 mg (33%), viscous yellowish oil from column chromatography (hexanes/acetone 98:2 to 90:10 (v/v)).
^{1}H NMR (500 MHz, $CDCl_3$): δ=7.64 (d, *J* = 8.2 Hz, 2H), 7.32 (d, *J* = 8.0 Hz, 2H), 3.58 (s, 3H), 3.17 (ddd, *J* = 11.1, 6.9, 3.6 Hz, 1H), 3.14–3.08 (m, 1H), 2.97 (ddd, *J* = 11.6, 8.3, 3.4 Hz, 1H), 2.77 (ddd, *J* = 11.6, 8.0, 3.8 Hz, 1H), 2.44 (s, 3H), 1.90–1.76 (m, 2H), 1.70 (ddd, *J* = 13.6, 8.3, 3.7 Hz, 1H), 1.59–1.50 (m, 1H), 1.40 (quint, *J* = 6.0 Hz, 1H), 1.13 (d, *J* = 5.4 Hz, 1H), 1.06 ppm (d, *J* = 6.4 Hz, 3H); **^{13}C NMR** (126 MHz, $CDCl_3$): δ=172.7, 143.6, 133.8, 129.8, 127.8, 51.7, 46.2, 46.0, 32.1, 32.0, 30.6, 29.5, 26.7, 21.7, 12.4 ppm; **HRMS** (ESI): *m/z* calcd for $C_{17}H_{23}NO_4S$+Na^+: 360.1245 $[M+Na]^+$; found: 360.1250.
GC Chromatogram: t_r = 10.659 min (98% purity).

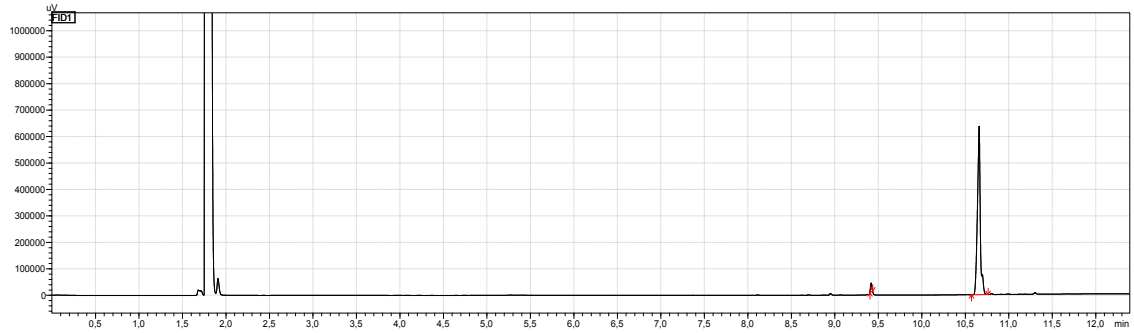

dimethyl 6-tosyl-6-azaspiro[2.5]octane-1,2-dicarboxylate (68)

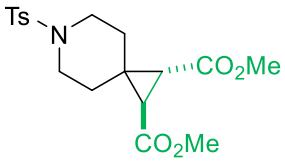

Synthesized according to the general procedure.
Yield: 36 mg (47%), viscous colorless oil from column chromatography (hexanes/acetone 98:2 to 80:20 (v/v)).
^{1}H NMR (500 MHz, $CDCl_3$): δ=7.63 (d, *J* = 8.3 Hz, 2H), 7.32 (d, *J* = 8.2 Hz, 2H), 3.63 (s, 6H), 3.12–3.02 (m, 2H), 3.02–2.90 (m, 2H), 2.43 (s, 3H), 2.20 (s, 2H), 1.94–1.85 (m, 2H), 1.86–1.78 ppm (m, 2H); **^{13}C NMR** (126 MHz, $CDCl_3$): δ=170.2, 143.7, 133.7, 129.8, 127.7, 52.2, 45.8, 34.7, 32.0, 29.3, 21.6 ppm; **HRMS** (ESI): *m/z* calcd for $C_{18}H_{23}NO_6S+Na^+$: 404.1144 $[M+Na]^+$; found: 404.1147.
GC Chromatogram: t_r = 10.832 min (> 99% purity).

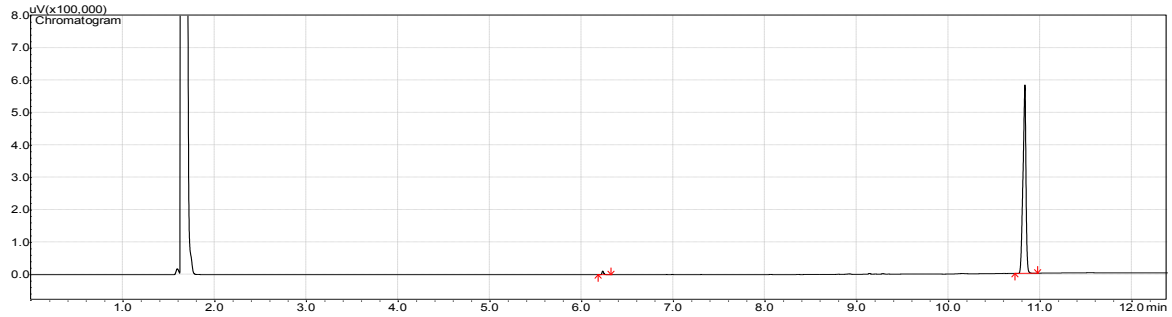

8.4. Scope of preliminary studies on blue light-induced Ir-catalyzed reactions with carboxylic acids, aldehydes and alkynes

Cyclohexyl benzoate (70)[27]

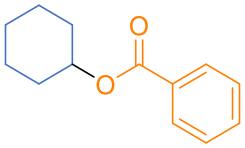

Synthesized according to the general procedure.
Yield: 20 mg (92%), colorless oil from column chromatography (hexanes to hexanes/AcOEt 9:1 (v/v)).

^{1}H NMR (400 MHz, $CDCl_3$): δ=8.07–8.03 (m, 2H), 7.57–7.51 (m, 1H), 7.46–7.41 (m, 2H), 5.08–5.00 (m, 1H), 1.99–1.91 (m, 2H), 1.85–1.75 (m, 2H), 1.66–1.53 (m, 3H), 1.51–1.30 (m, 3H) ppm; **^{13}C NMR** (101 MHz, $CDCl_3$) δ 166.0, 132.6, 131.2, 129.7, 128.5, 73.1, 31.8, 25.6, 23.8 ppm.

Cyclohexyl p-methoxybenzoate (71)[28]

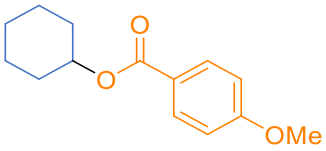

Synthesized according to the general procedure.
Yield: 22 mg (94%), colorless oil from column (hexanes to hexanes/AcOEt 9:1 (v/v)).
^{1}H NMR (500 MHz, $CDCl_3$): δ=8.00 (d, *J* = Hz, 2H), 6.91 (d, *J* = 8.9 Hz, 2H), 5.04–4.97 (m, 1H), 3.86 (s, 3H), 1.97–1.91 (m, 2H), 1.83–1.75 (m, 2H), 1.62–1.53 (m, 3H), 1.49–1.40 (m, 2H), 1.39–1.30 ppm (m, 1H); **^{13}C NMR** (126 MHz, $CDCl_3$): δ=165.9, 163.3, 131.7, 123.7, 113.6, 72.8, 55.6, 31.9, 25.7, 23.4.

Cyclohexyl 4-phenylbutanoate (72)[29]

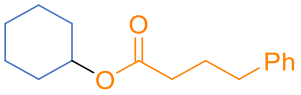

Synthesized according to the general procedure.
Yield: 19 mg (78%), colorless oil from column chromatography (hexanes to hexanes/AcOEt 9:1 (v/v)).
^{1}H NMR (400 MHz, $CDCl_3$): δ=7.31–7.26 (m, 2H), 7.21–7.15 (m, 3H), 4.81–4.72, 2.65 (t, *J* = 7.7 Hz, 2H), 2.30 (t, *J* = 7.4 Hz, 2H), 1.99–1.91 (m, 2H), 1.87–1.81 (m, 2H), 1.75–1.68 (m, 2H), 1.46–1.20 ppm (m, 6H); **^{13}C NMR** (101 MHz, $CDCl_3$): δ=173.1, 141.7, 128.6, 128.5, 126.1, 72.6, 35.3, 34.2, 31.8, 26.9, 25.6, 23.9 ppm.

Cyclohexyl oleate (73)

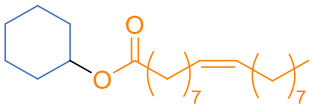

Synthesized according to the general procedure.
Yield: 28 mg (67%), colorless oil from column chromatography (hexanes to hexanes/AcOEt 9:1 (v/v)).
^{1}H NMR (400 MHz, $CDCl_3$): δ=5.39–5.30 (m, 2H), 4.79–4.71 (m, 1H), 2.27 (t, *J* = 7.5 Hz, 2H), 2.05–1.97 (m, 4H), 1.87–1.80 (m, 2H), 1.75–1.67 (m, 2H), 1.65–1.58 (m, 2H), 1.46–1.20 (m, 26H), 0.88 ppm (t, *J* = 6.9 Hz, 3H); **^{13}C NMR** (101 MHz, $CDCl_3$): δ=173.5, 130.1, 129.9, 72.4, 34.9, 32.1, 31.8, 29.9, 29.8, 29.7, 29.5, 29.5, 29.3, 29.3, 27.4, 27.3, 25.6, 25.3, 23.9, 22.8, 14.2 ppm; **HRMS** (ESI): *m/z* calcd for $C_{24}H_{44}O_2$+Na^+: 387.3239 $[M+Na]^+$; found: 387.3240; **elemental analysis** calcd (%) for $C_{24}H_{44}O_2$: C 79.06, H 12.16; found: C 78.85, H 12.18.

(4-chlorophenyl)(cyclohexyl)methanone (74)[30]

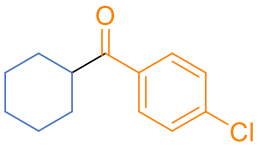

Synthesized according to the general procedure.
Yield: 35 mg (78%), colorless oil from column chromatography (hexnes to hexanes/AcOEt 95:5 (v/v)).
^{1}H NMR (400 MHz, $CDCl_3$): δ=7.94–7.82 (m, 2H), 7.46–7.38 (m, 2H), 3.20 (tt, *J* = 11.3, 3.2 Hz, 1H), 1.94–1.80 (m, 4H), 179–1.70 (m, 1H), 1.54–1.24 ppm (m, 5H); **^{13}C NMR** (101 MHz, $CDCl_3$): δ=202.5, 139.1, 134.7, 129.7, 128.9, 45.6, 29.4, 25.9, 25.8. ppm.

methyl 6-tosyl-6-azaspiro[2.5]oct-1-ene-1-carboxylate (75)

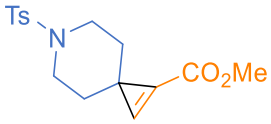

74

Synthesized according to the general procedure.
Yield: (19%, NMR yield with the use of 1,3,5-trimetoxybenzene as internal standard, product unstable), white solid from column chromatography (hexane/acetone from 98:2 to 7:3 (v/v)), repurified with the use of HPLC.
^{1}H NMR (400 MHz, $CDCl_3$): δ=7.68-7.58 (m, 2H), 7.52 (s, 1H), 7.32–7.24 (m, 2H), 3.90 (s, 3H), 3.59–3.52 (m, 2H), 3.37–3.30 (m, 2H), 2.40 (s, 3H), 2.06–1.96 (m, 2H), 1.60-1.52 ppm (m, 2H); **^{13}C NMR** (101 MHz, $CDCl_3$): δ=161.0, 151.5, 148.3, 144.1, 133.1, 129.9, 129.7, 95.6, 52.6, 44.1, 29.6, 21.5. ppm.

9. References

[1] Er, H.-T; Pole, D. L.; Warkentin, J. (Alkylthio)- and (phenylthio)methoxycarbenes from oxadiazolines. *Can. J. Chem.* **1996**, *74*, 1480-1489.

[2] Greb, A.; Poh, J.-S.; Greed, S.; Battilocchio, C.; Pasau, P.; Blakemore, D. C.; Ley, S. V. A Versatile Route to Unstable Diazo Compounds via Oxadiazolines and their Use in Aryl–Alkyl Cross-Coupling Reactions. *Angew. Chem. Int. Ed.* **2017**, *56*, 16602-16605.

[3] Andrade, M. M.; Barros, M. T. Fast Synthesis of *N*-Acylhydrazones Employing a Microwave Assisted Neat Protocol. *J. Comb. Chem.* **2010**, *12*, 245-247.

[4] Couture, P.; Warkentin, J. Spiro-fused 2-alkoxy-2-amino-Δ^3-1,3,4-oxadiazolines. Synthesis and thermolysis to corresponding aminooxycarbenes. *Can. J. Chem.* **1997**, *75*, 1264-1280.

[5] Ociepa, M.; Wierzba, A. J.; Turkowska, J.; Gryko D. Polarity-Reversal Strategy for the Functionalization of Electrophilic Strained Molecules via Light-Driven Cobalt Catalysis. *J. Am. Chem. Soc.* **2020**, *142*, 5355-5361.

[6] Qi, X.; Yu, F.; Chen, P.; Liu, G. Intermolecular Palladium-Catalyzed Oxidative Fluorocarbonylation of Unactivated Alkenes: Efficient Access to β-Fluorocarboxylic Esters. *Angew. Chem. Int. Ed.* **2017**, *56*, 12692-12696.

[7] Oikawa, M.; Sugeno, Y.; Tukada, H.; Takasaki, Y.; Takamizawa, S.; Irie, R. Four Stereoisomers of 2-Aminomethyl-1-cyclopropanecarboxylic Acid: Synthesis and Biological Evaluation. *Bull. Chem. Soc. Jpn.* **2019**, *92*, 1816-1823.

[8] Hell, S. M.; Meyer, C. F.; Laudadio, G.; Misale, A.; Willis, M. C.; Nöel, T.; Trabanco, A. A.; Gouverneur, V. Silyl Radical-Mediated Activation of Sulfamoyl Chlorides Enables Direct Access to Aliphatic Sulfonamides from Alkenes. *J. Am. Chem. Soc.* **2020**, *142*, 720-725.

[9] Palkowitz, M. D.; Tan, B.; Hu, H.; Roth, K.; Bauer, R. A. Synthesis of Diverse N-Acryloyl Azetidines and Evaluation of Their Enhanced Thiol Reactivities. *Org. Lett.* **2017**, *19*, 2270-2273.

[10] Dai, Z.-Y.; Nong, Z.-S.; Song, S.; Wang P.-S. Asymmetric Photocatalytic C(sp3)–H Bond Addition to α-Substituted Acrylates. *Org. Lett.* **2021**, *23*, 3157-3161.

[11] Wu, Z.; Xu, Y.; Zhang, H.; Wu, X.; Zhu, C. Radical-mediated sulfonyl alkynylation, allylation, and cyanation of propellane. *Chem. Commun.* **2021**, *57*, 6066-6069.

[12] Van, K. N.; Romo, D. Multicomponent, Enantioselective Michael–Michael-Aldol-β-Lactonizations Delivering Complex β-Lactones. *J. Org. Chem.* **2018**, *83*, 632-643.

[13] Prier, C. K.; Rankic, D. A.; MacMillan, D. W. C. Visible Light Photoredox Catalysis with Transition Metal Complexes: Applications in Organic Synthesis. *Chem. Rev.* **2013**, *113*, 5322-5363.

[14] Li, F.; Xiao, L.; Liu, L. Metal-Diazo Radicals of α-Carbonyl Diazomethanes. *Sci. Rep.* **2016**, *6*, 22876, 1-8.

[15] Liu, K. J.; Miyake, M.; Panz, T.; Swartz, H. Evaluation of DEPMPO as a spin trapping agent in biological systems. *Free Rad. Biol. Med.* **1999**, *26*, 714-721.

[16] Huang, X.; Luo, S.; Burghaus, O.; Webster, R. D.; Harms, K.; Meggers, E. Combining the catalytic enantioselective reaction of visible-light-generated radicals with a by-product utilization system. *Chem. Sci.* **2017**, *8*, 7126-7131.

[17] Gaussian 16, Revision B.01, Frisch, M. J.; Trucks, G. W.; Schlegel, H. B.; Scuseria, G. E.; Robb, M. A.; Cheeseman, J. R.; Scalmani, G.; Barone, V.; Petersson, G. A.; Nakatsuji, H.; Li, X.; Caricato, M.; Marenich, A. V.; Bloino, J.; Janesko, B. G.; Gomperts, R.; Mennucci, B.; Hratchian, H. P.; Ortiz, J. V.; Izmaylov, A. F.; Sonnenberg, J. L.; Williams-Young, D.; Ding, F.; Lipparini, F.; Egidi, F.; Goings, J.; Peng, B.; Petrone, A.; Henderson, T.; Ranasinghe, D.; Zakrzewski, V. G.; Gao, J.; Rega, N.; Zheng, G.; Liang, W.; Hada, M.; Ehara, M.; Toyota, K.; Fukuda, R.; Hasegawa, J.; Ishida, M.; Nakajima, T.; Honda, Y.; Kitao, O.; Nakai, H.; Vreven, T.; Throssell, K.; Montgomery, Jr., J. A.; Peralta, J. E.; Ogliaro, F.; Bearpark, M. J.; Heyd, J. J.; Brothers, E. N.; Kudin, K. N.; Staroverov, V. N.; Keith, T. A.; Kobayashi, R.; Normand, J.; Raghavachari, K.; Rendell, A. P.; Burant, J. C.; Iyengar, S. S.; Tomasi, J.; Cossi, M.; Millam, J. M.; Klene, M.; Adamo, C.; Cammi, R.; Ochterski, J. W.; Martin, R. L.; Morokuma, K.; Farkas, O.; Foresman, J. B.; and Fox, D. J. Gaussian, Inc., Wallingford CT, 2016.

[18] Grimme, S.; Antony, J.; Ehrlich, S.; Krieg, H. A consistent and accurate ab initio parametrization of density functional dispersion correction (DFT-D) for the 94 elements H-Pu. *J. Chem. Phys.* **2010**, *132*, 154104, 1-14.

[19] Marenich, A. V.; Cramer, C. J.; Truhlar, D. G. Universal Solvation Model Based on Solute Electron Density and on a Continuum Model of the Solvent Defined by the Bulk Dielectric Constant and Atomic Surface Tensions. *J. Phys. Chem. B* **2009**, *113*, 6378-6396.

[20] Legault, C. Y. CYLview, 1.0b; Université de Sherbrooke, **2009**, http://www.cylview.org.

[21] Pezacki, J. P.; Couture, P.; Dunn, J. A.; Warkentin, J.; Wood, P. D.; Lusztyk, J.; Ford, F.; Platz, M. S. *J. Org. Chem.* **1999**, *64*, 4456.

[22] Yang, R.-Y.; Dai, L.-X. Hypervalent Iodine Oxidation of *N*-Acylhydrazones and *N*-Phenylsemicarbazone: An Efficient Method for the Synthesis of Derivatives of 1,3,4-Oxadiazoles and Δ^3-1,3,4-Oxadiazolines. *J. Org. Chem.* **1993**, *58*, 3381-3383.

[23] Pezacki, J. P.; Wood, P. D.; Gadosy, T. A.; Lusztyk, J.; Warkentin, J. Laser Flash Photolysis Studies of Oxygen and Sulfur Atom Transfer Reactions from Oxiranes and Thiiranes to Singlet Carbenes[1]. *J. Am. Chem. Soc.* **1998**, *120*, 8681-8691.

[24] Montesinos-Magraner, M.; Costantini, M.; Ramírez-Contreras, R.; Muratore, M. E.; Johansson, M. J.; Mendoza, A. General Cyclopropane Assembly by Enantioselective Transfer of a Redox-Active Carbene to Aliphatic Olefins. *Angew. Chem. Int. Ed.* **2019**, *58*, 5930-5935.

[25] Koul, A.; Klebl, B.; Mueller, G. Heterobicyclic Compounds As Pharmaceutically Active Agents (WO2005023818/A2) (2005). Dievini Hopp Biotech Holding Gmbh & Co. Kg.

[26] Jeganathan, A.; Richardson, S. K.; Mani, R. S.; Haley, B. E.; Watt, D. S. Selective reactions of azide-substituted α-diazo amides with olefins and alcohols using rhodium(II) catalysts. *J. Org. Chem.* **1986**, *51*, 5362-5367.

[27] Gaspa, S.; Porcheddu, A.; De Luca, L. Metal-Free Direct Oxidation of Aldehydes to Esters Using TCCA. *Org. Lett.* **2015**, *17*, 3666-3669.

[28] He, X.; Li, Y.; Fu, H.; Zheng, X.; Chen, H.; Li, R.; Yu, X. Synthesis of Unsymmetrical *N*-Heterocyclic Carbene–Nitrogen–Phosphine Chelated Ruthenium(II) Complexes and Their Reactivity in Acceptorless Dehydrogenative Coupling of Alcohols to Esters. *Organometallics* **2019**, *38*, 1750-1760.

[29] Xu, J.-X.; Kuai, C.-S.; Wu, X.-F. Cobalt-Catalyzed Four-Component Carbonylation of Methylarenes with Ethylene and Alcohols. *J. Org. Chem.* **2022**, *87*, 6371-6377.

[30] Zhang, X.; Wang, Z.; Fan, X.; Wang, J. Synthesis of Ketones through Microwave Irradiation Promoted Metal-Free Alkylation of Aldehydes by Activation of C(sp^3)–H Bond. *J. Org. Chem.* **2015**, *80*, 10660-10667.

10. NMR spectra

3,3-dimethoxy-4-oxa-1,2-diazaspiro[4.5]dec-1-ene (1)

^{1}H NMR ($CDCl_3$, 400 MHz)

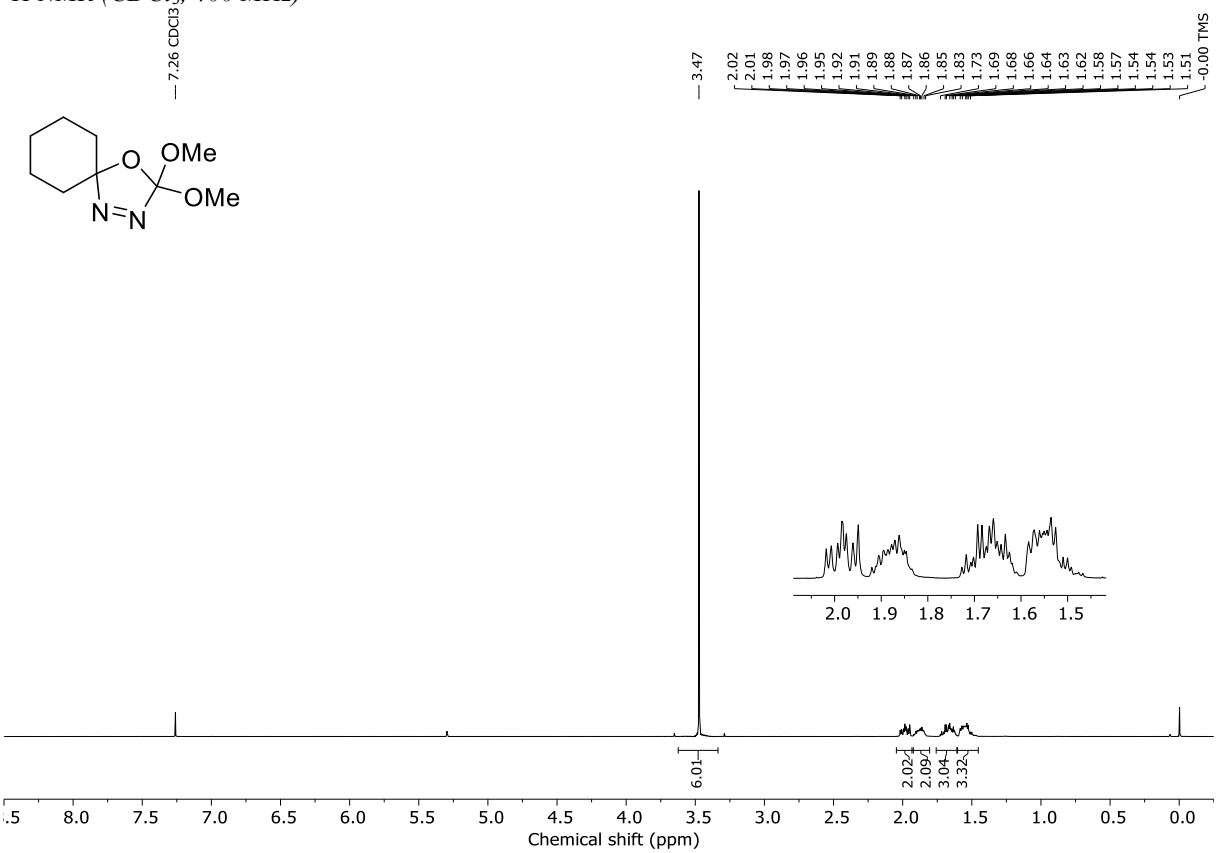

^{13}C NMR ($CDCl_3$, 126 MHz)

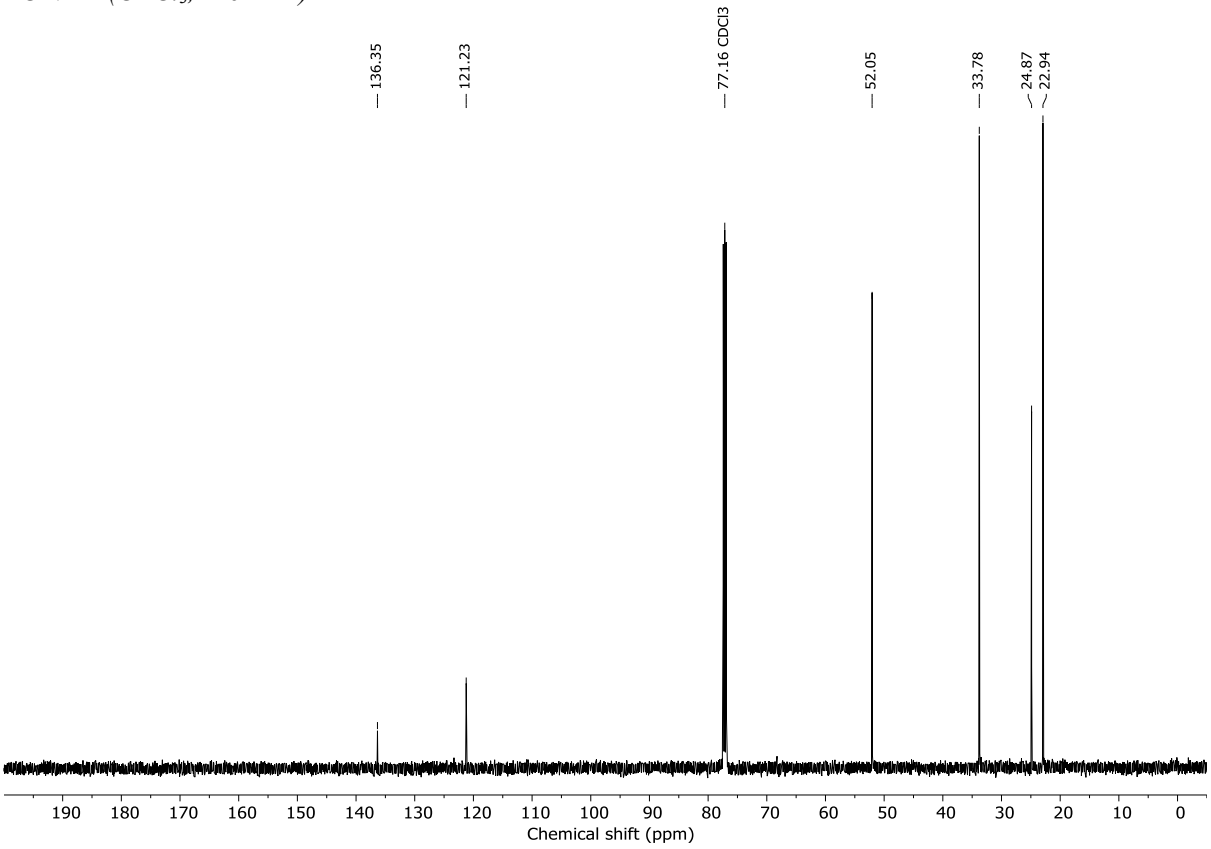

3-(benzylthio)-3-methoxy-4-oxa-1,2-diazaspiro[4.5]dec-1-ene (2)

^{1}H NMR ($CDCl_3$, 600 MHz)

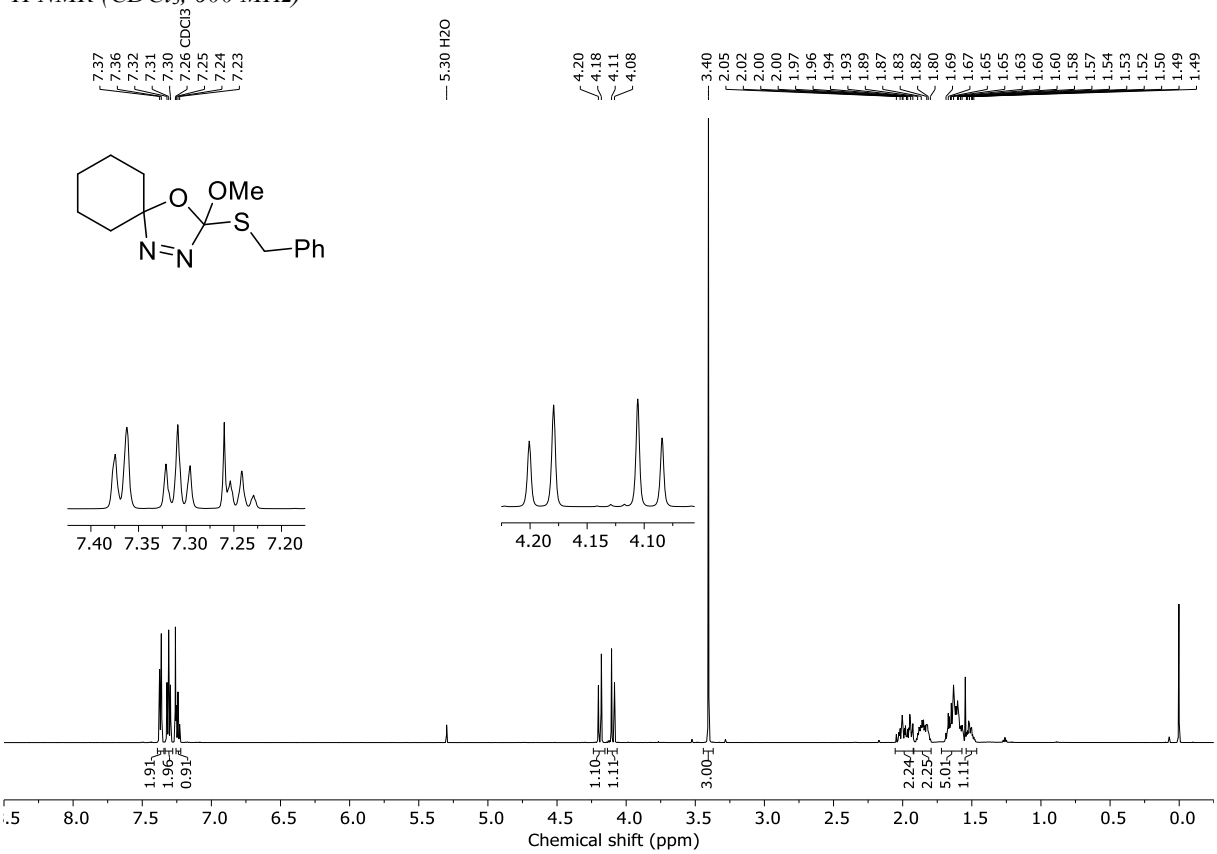

^{13}C NMR ($CDCl_3$, 126 MHz)

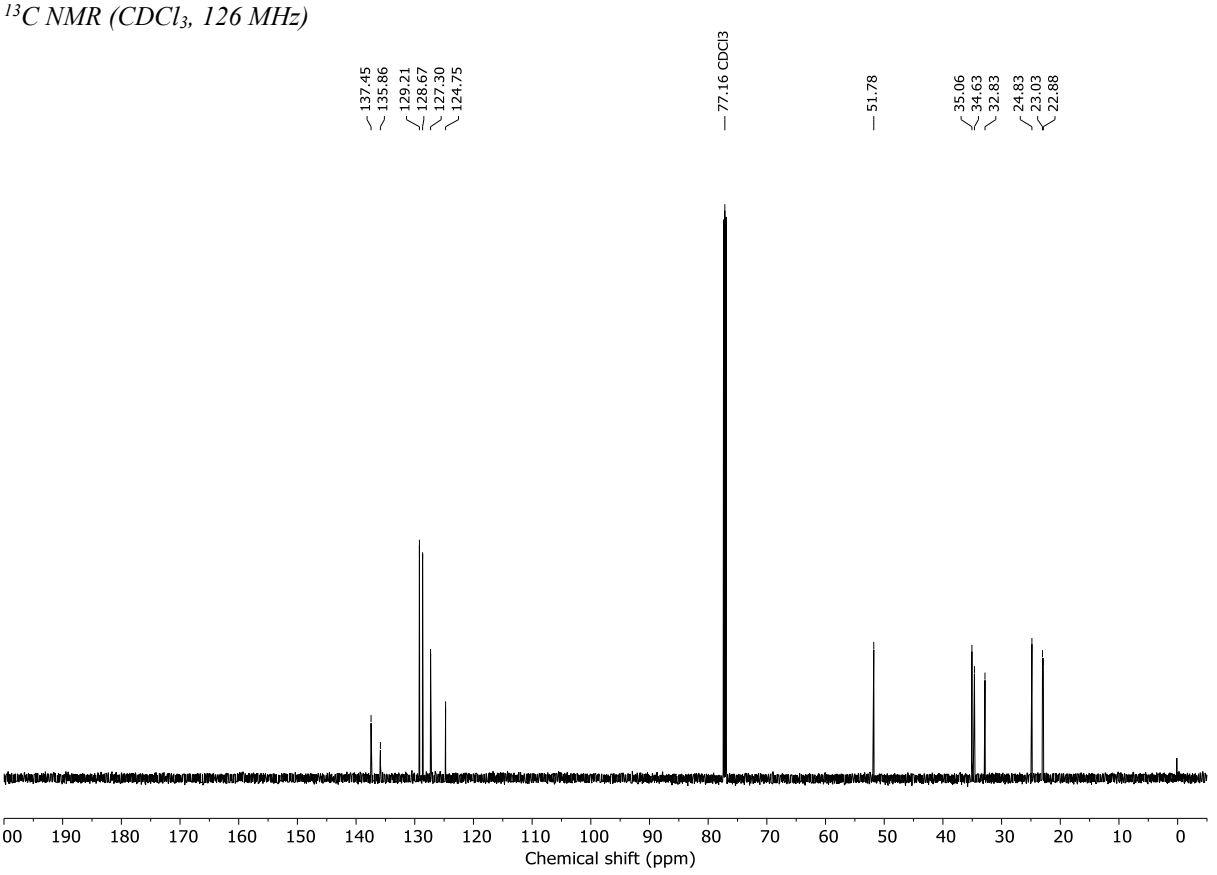

3-methoxy-3-methyl-4-oxa-1,2-diazaspiro[4.5]dec-1-ene (3)

^{1}H NMR ($CDCl_3$, 400 MHz)

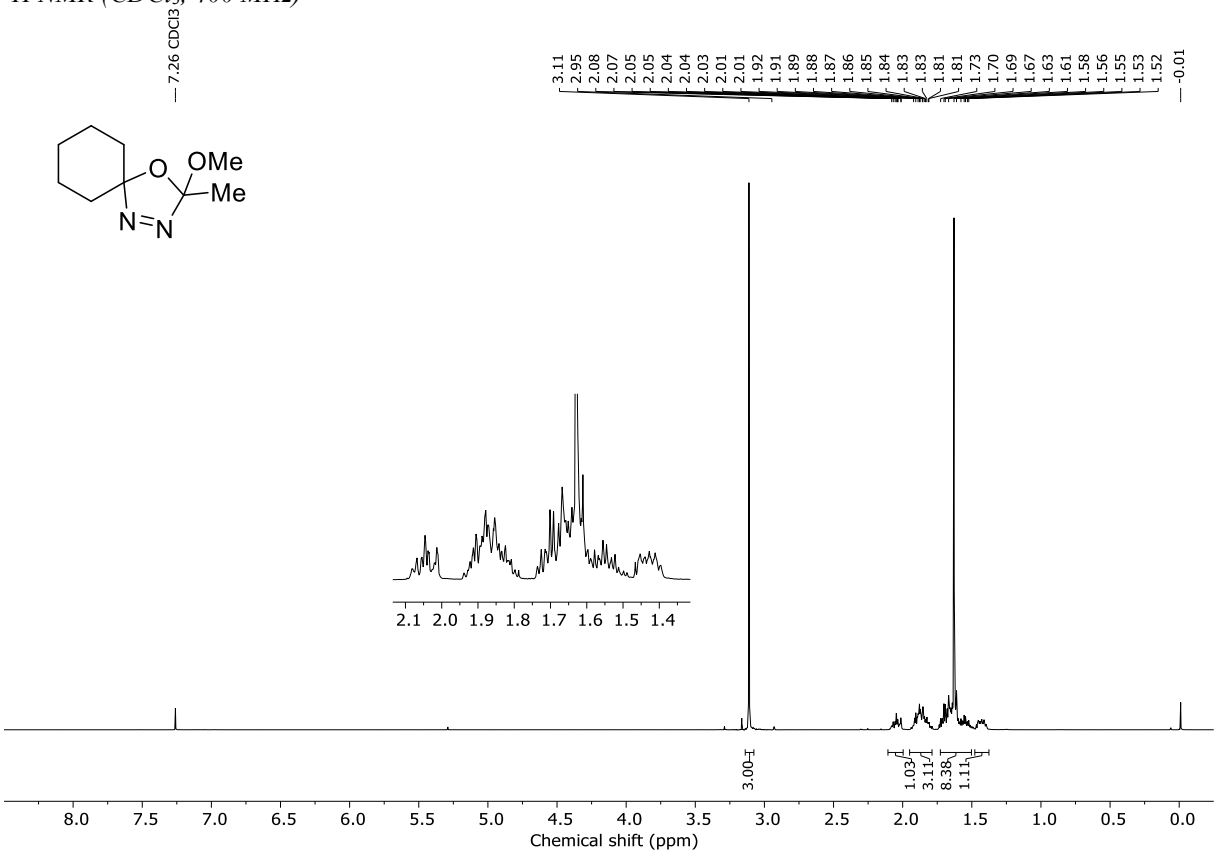

^{13}C NMR ($CDCl_3$, 101 MHz)

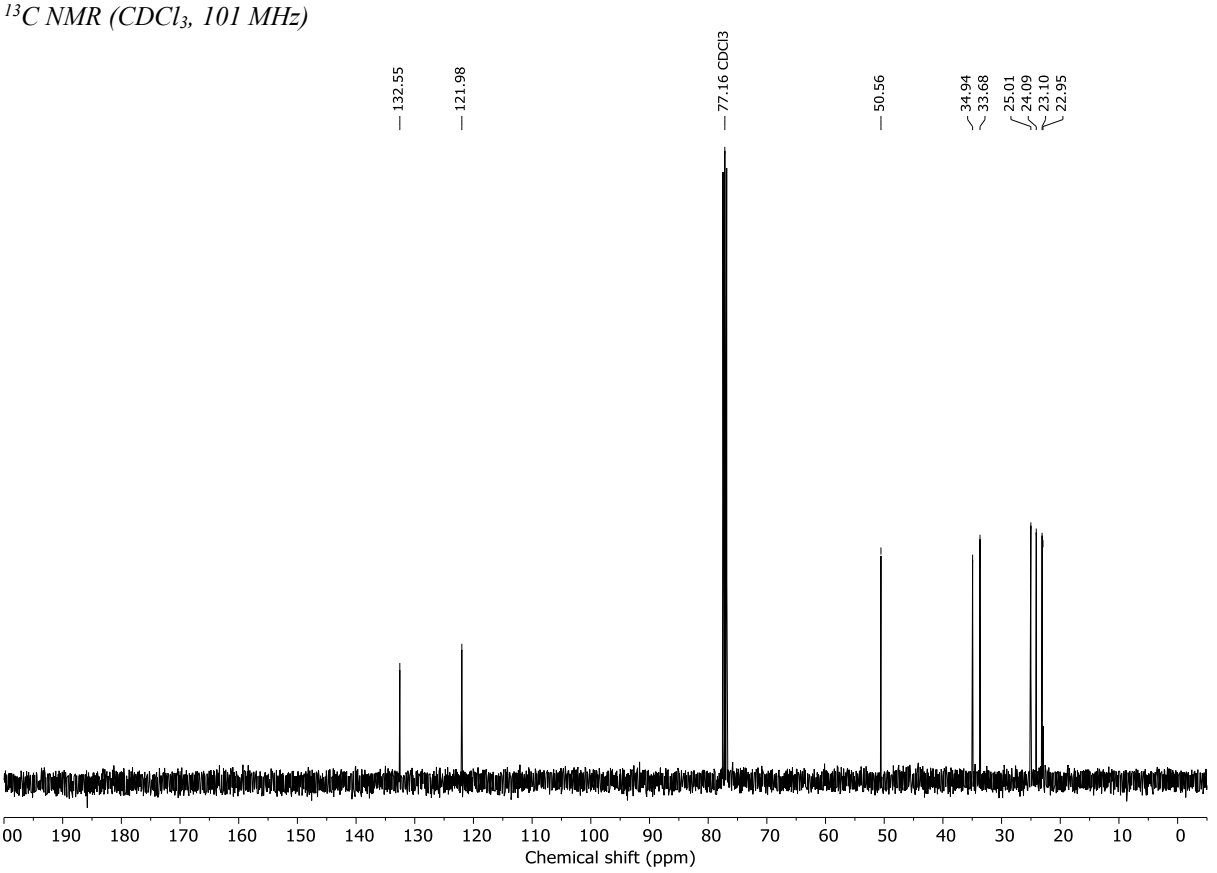

3-methoxy-3-phenyl-4-oxa-1,2-diazaspiro[4.5]dec-1-ene (4)

^{1}H NMR ($CDCl_3$, 600 MHz)

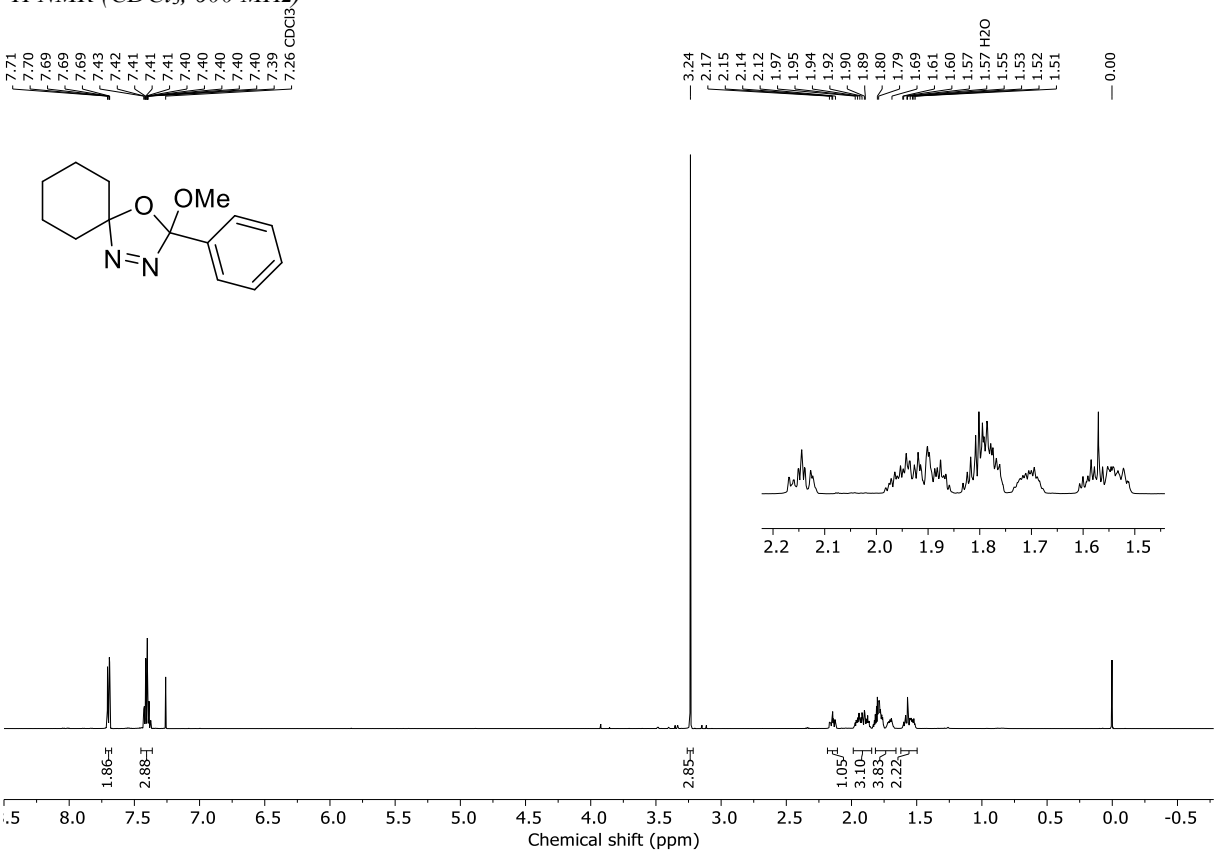

^{13}C NMR ($CDCl_3$, 151 MHz)

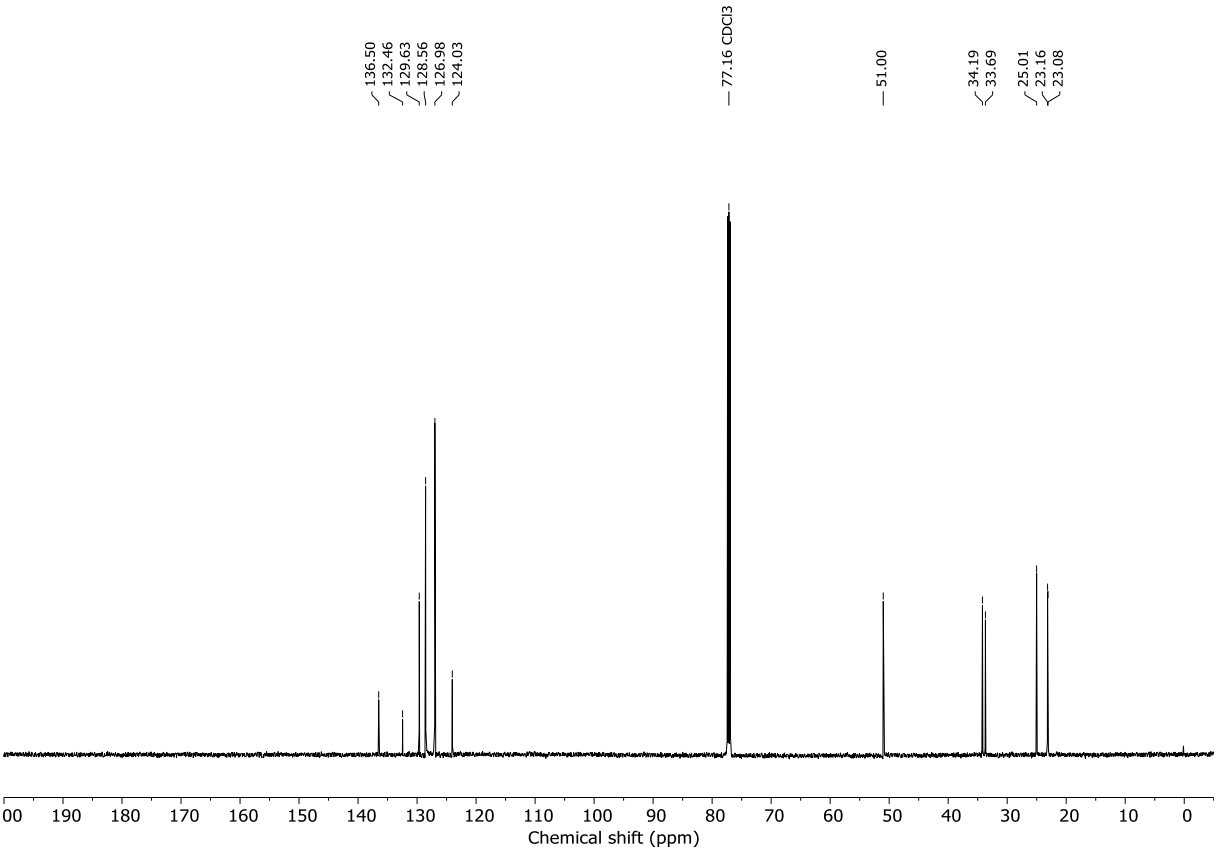

1-(1,6-dioxa-4,13,14-triazadispiro[4.1.57.25]tetradec-13-en-4-yl)ethan-1-one (5)

^{1}H NMR ($CDCl_3$, 500 MHz)

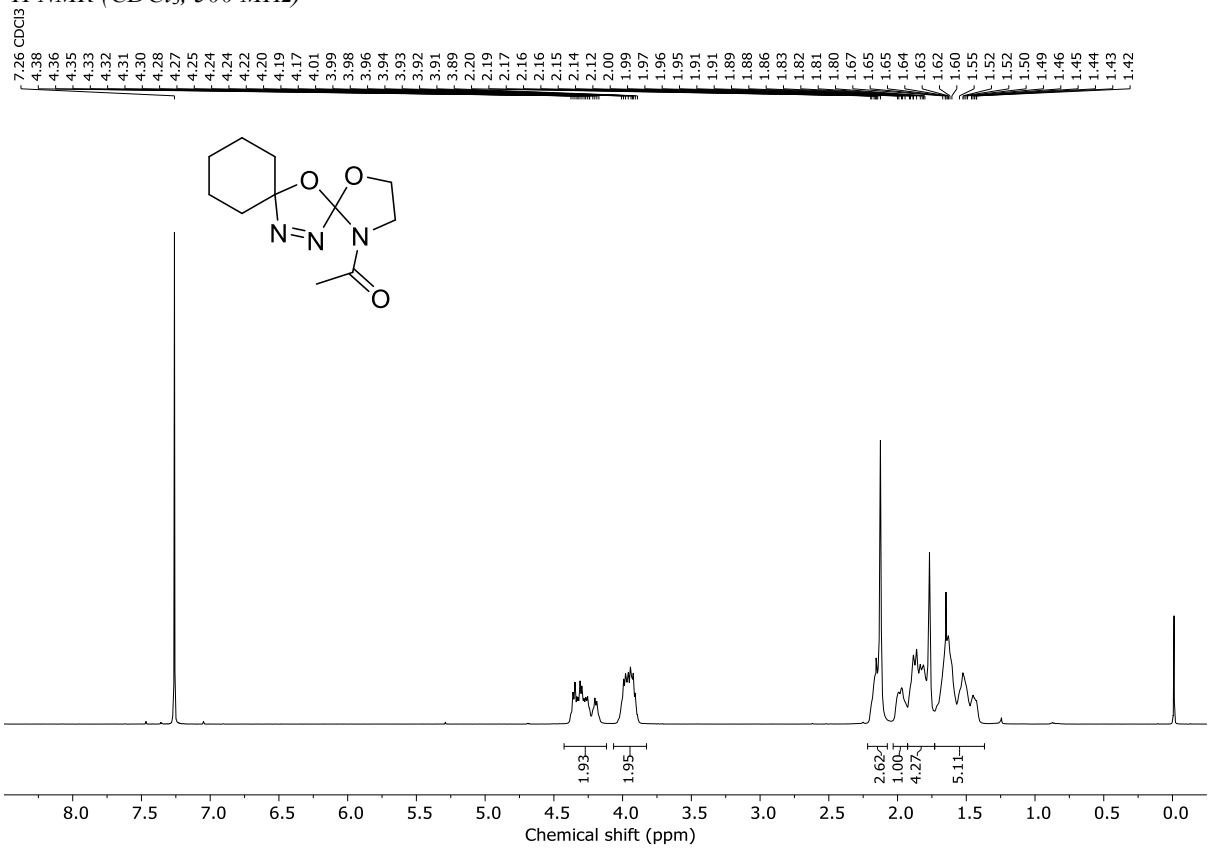

^{13}C NMR ($CDCl_3$, 126 MHz)

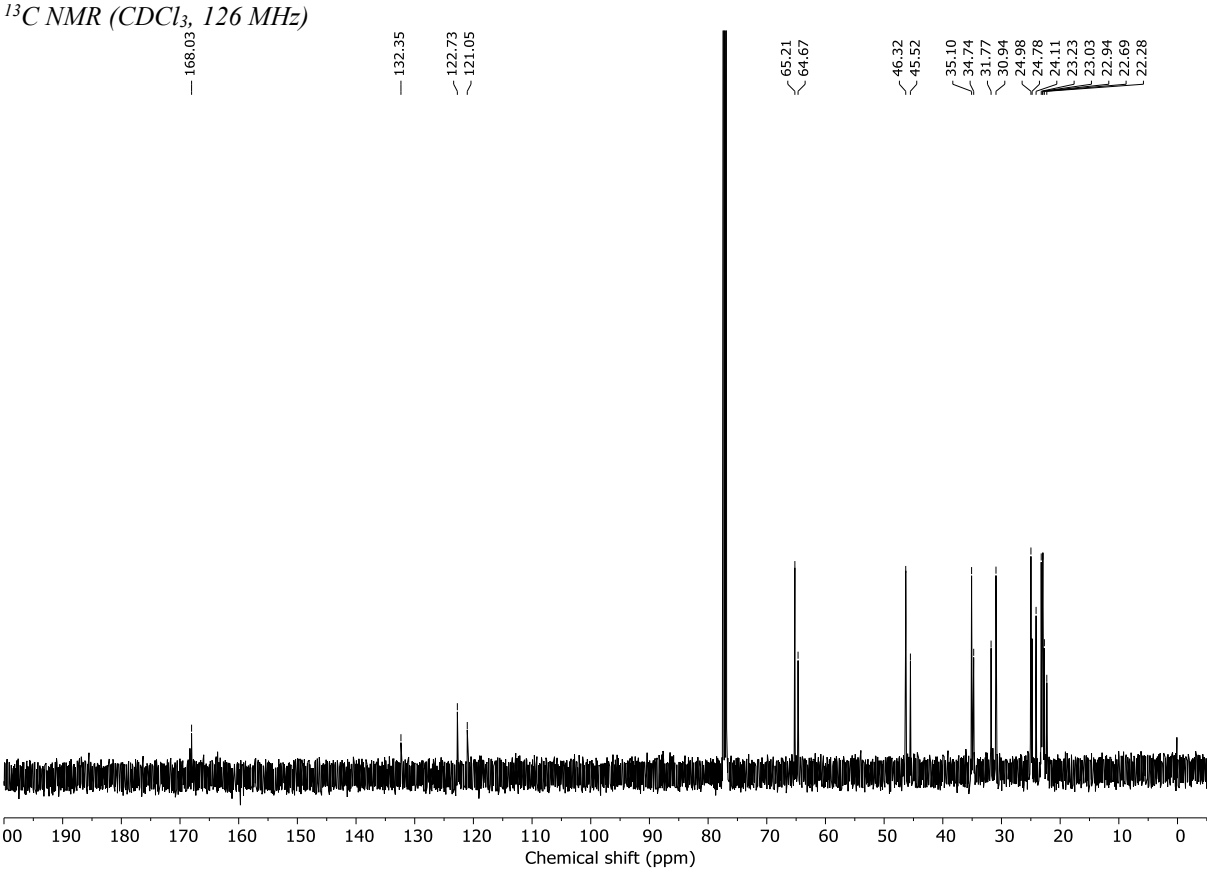

3,3-dimethoxy-4,8-dioxa-1,2-diazaspiro[4.5]dec-1-ene (S10)

^{1}H NMR ($CDCl_3$, 400 MHz)

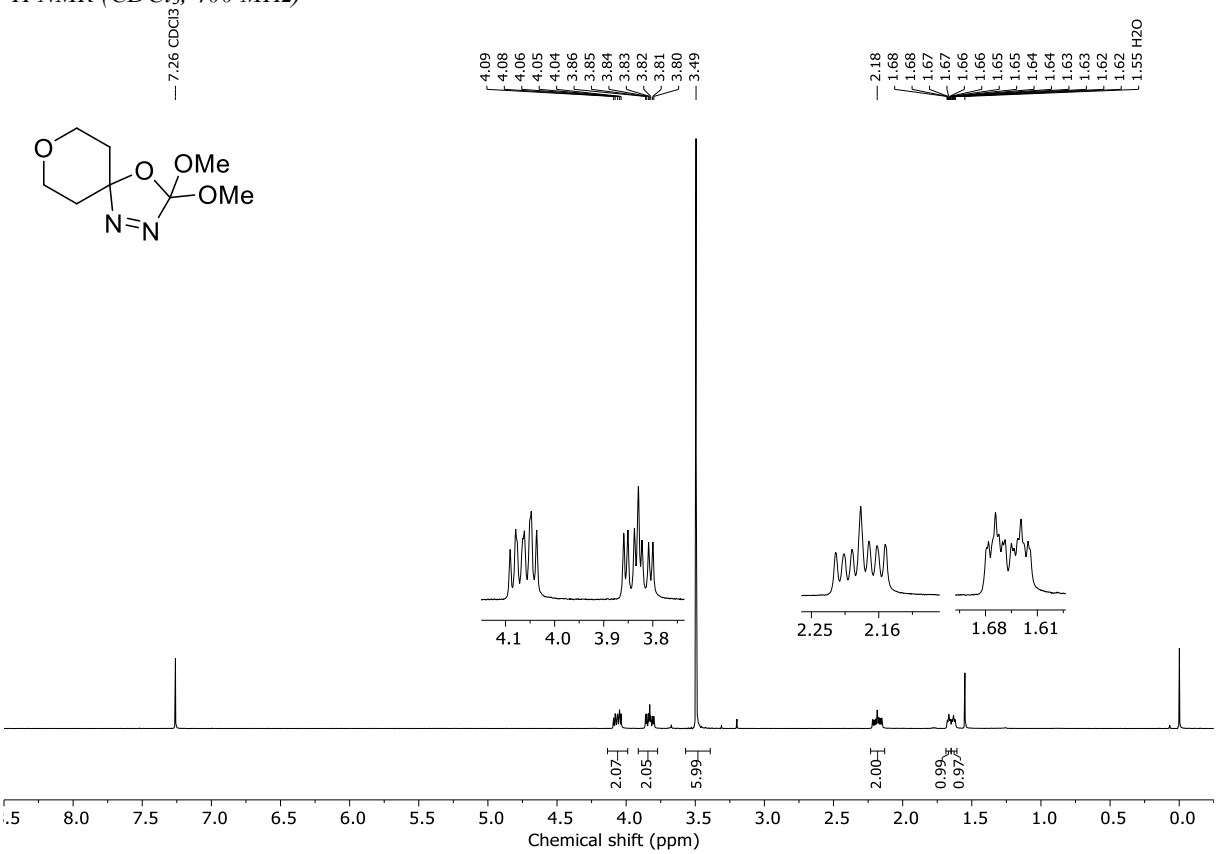

^{13}C NMR ($CDCl_3$, 126 MHz)

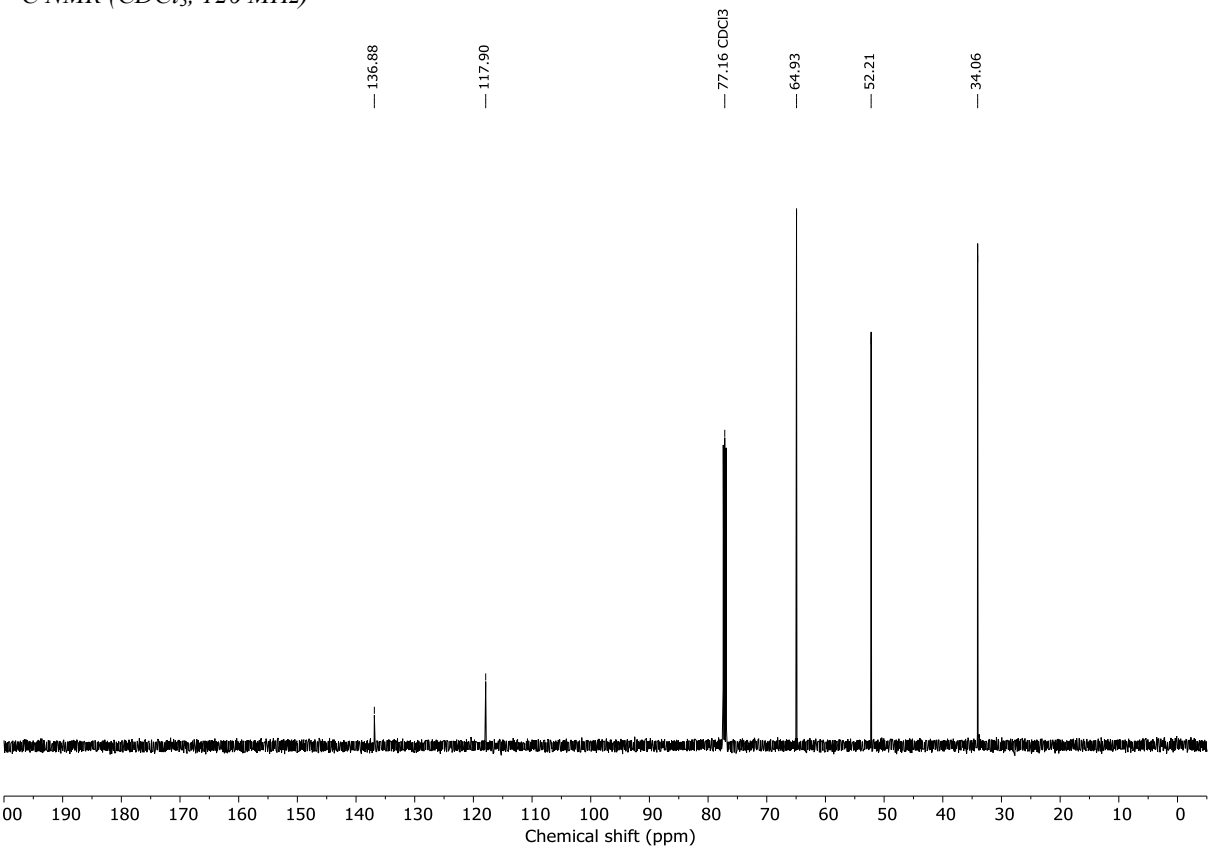

3,3-dimethoxy-4-oxa-8-thia-1,2-diazaspiro[4.5]dec-1-ene (S11)

^{1}H NMR ($CDCl_3$, 600 MHz)

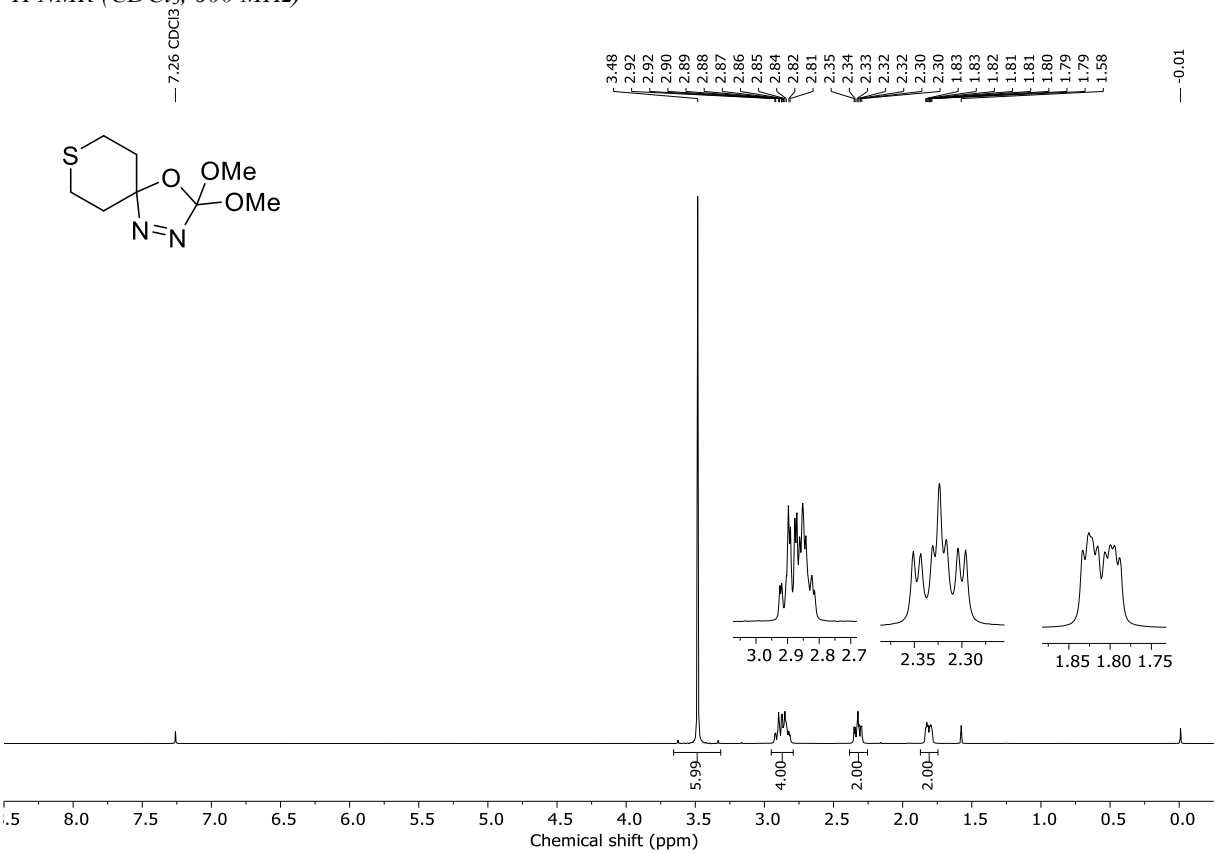

^{13}C NMR ($CDCl_3$, 151 MHz)

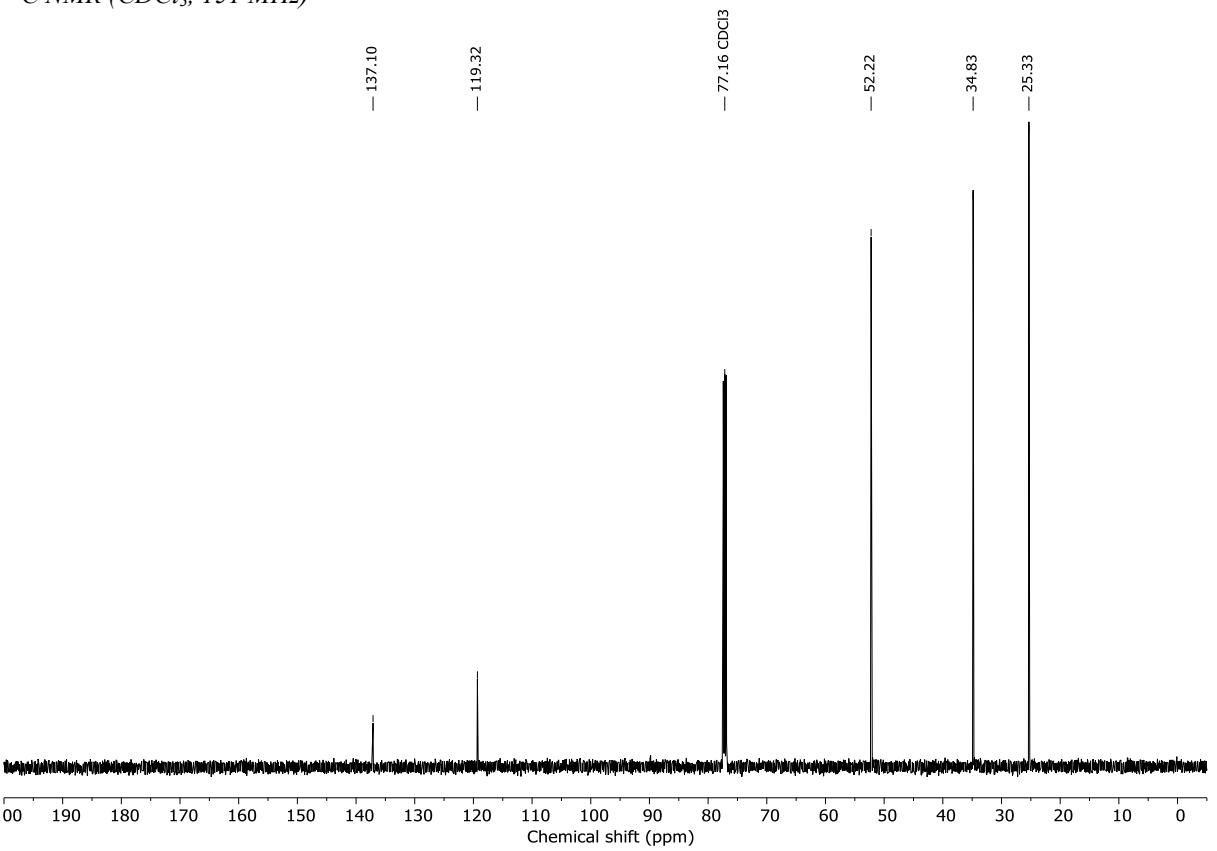

3,3-dimethoxy-8-tosyl-4-oxa-1,2,8-triazaspiro[4.5]dec-1-ene (S12)

^{1}H NMR ($CDCl_3$, 500 MHz)

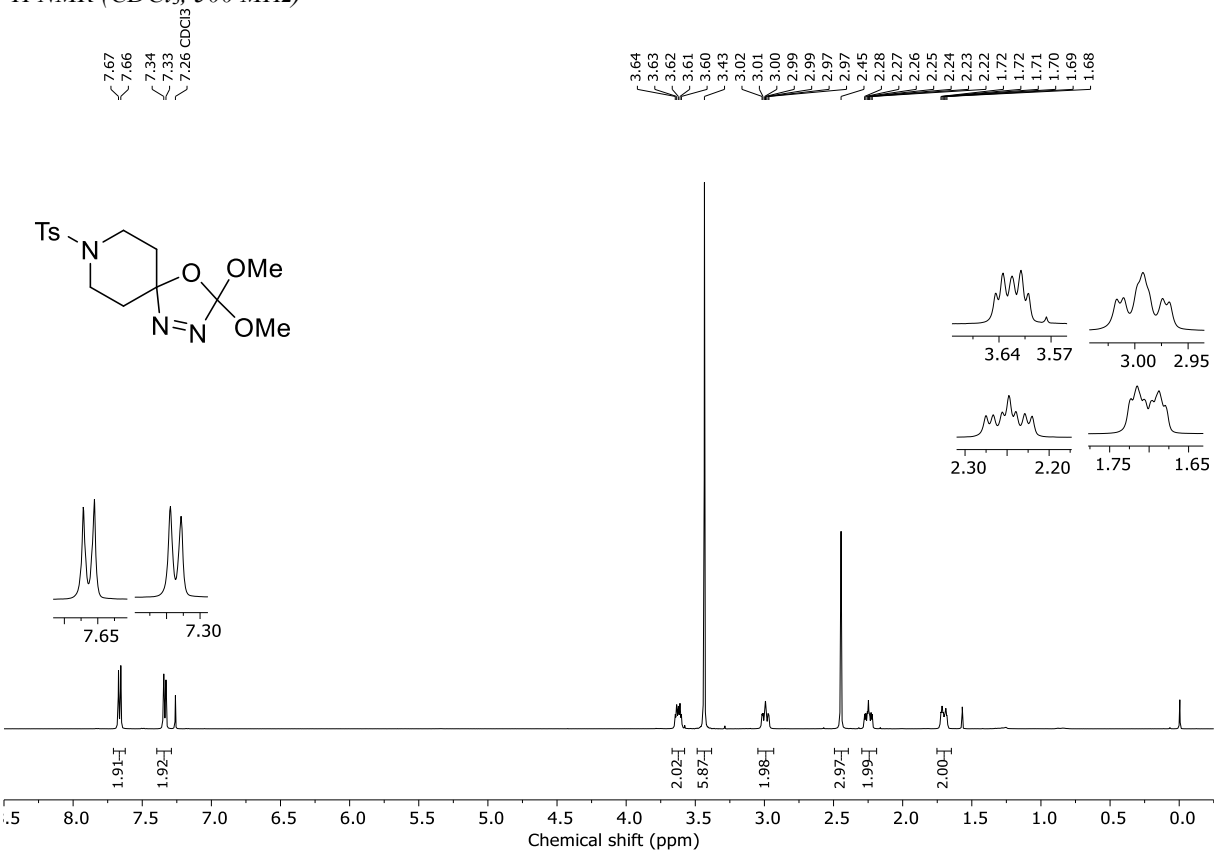

^{13}C NMR ($CDCl_3$, 126 MHz)

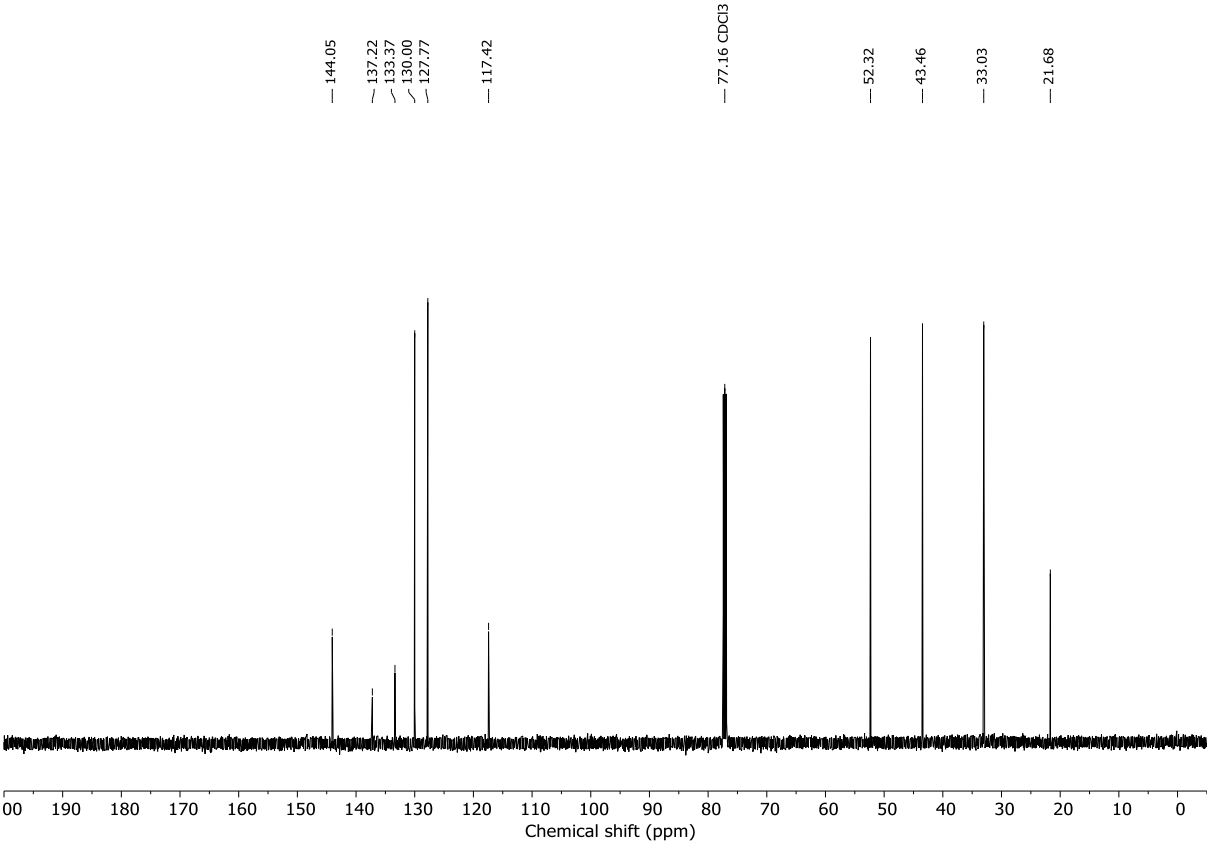

7,7-dimethoxy-8-oxa-5,6-diazaspiro[3.4]oct-5-ene (S13)

^{1}H NMR ($CDCl_3$, 500 MHz)

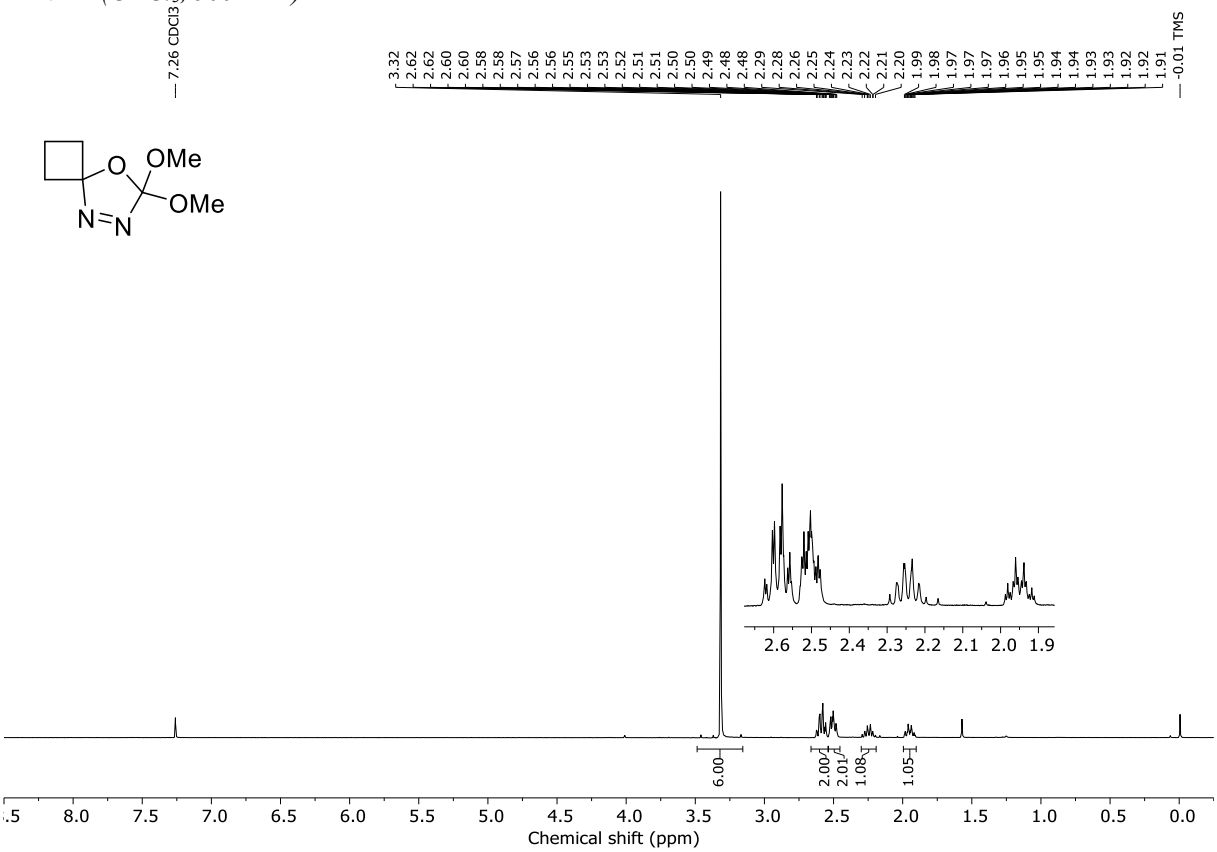

^{13}C NMR ($CDCl_3$, 126 MHz)

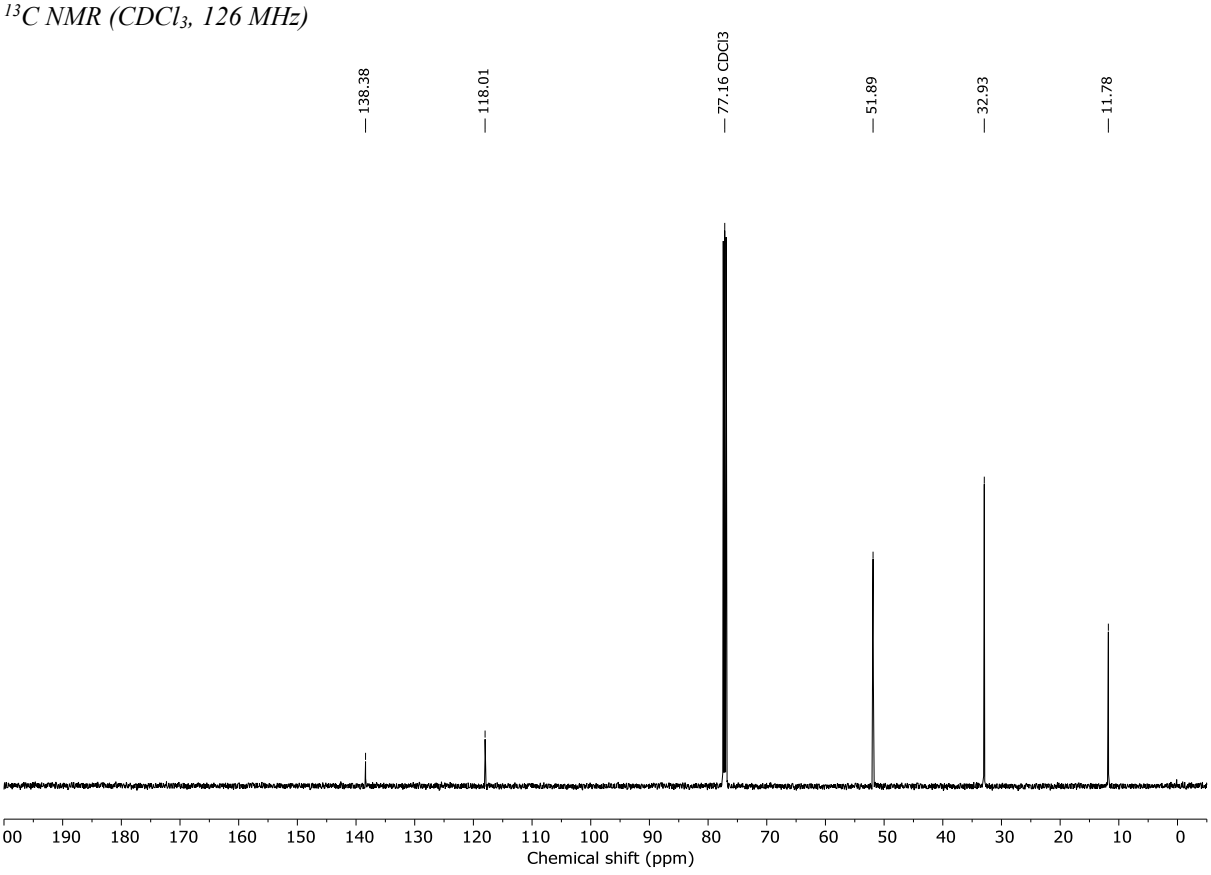

3,3-dimethoxy-4-oxa-1,2-diazaspiro[4.4]non-1-ene (S14)

^{1}H NMR ($CDCl_3$, 500 MHz)

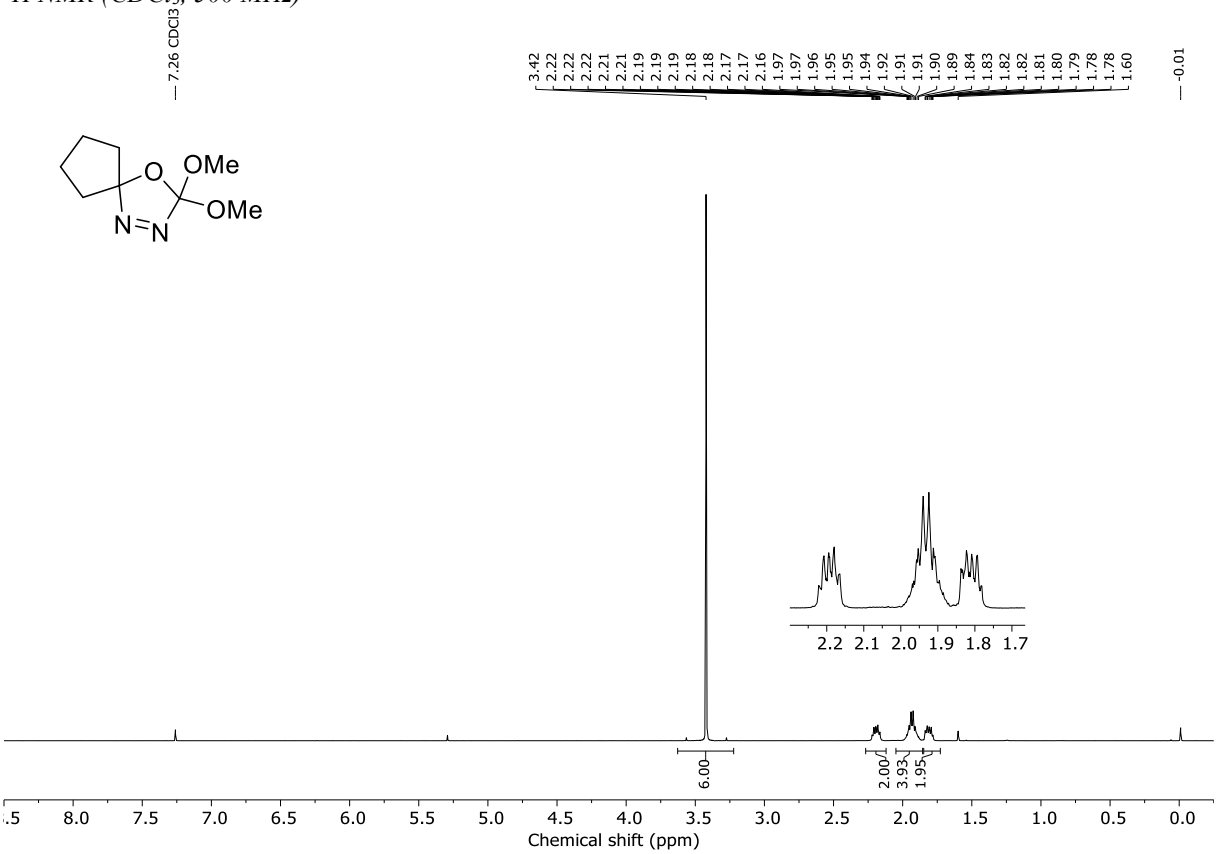

^{13}C NMR ($CDCl_3$, 126 MHz)

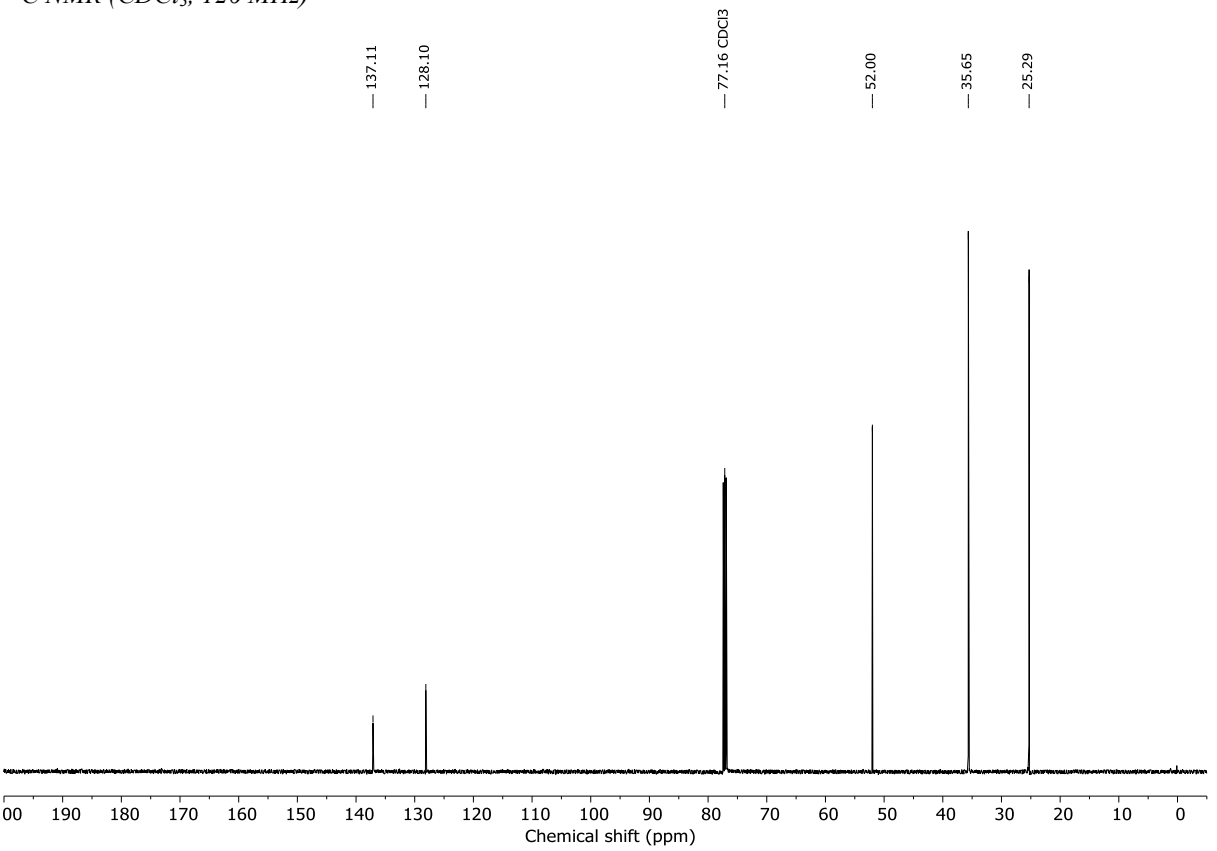

3,3-dimethoxy-4-oxa-1,2-diazaspiro[4.6]undec-1-ene (S15)

^{1}H NMR ($CDCl_3$, 500 MHz)

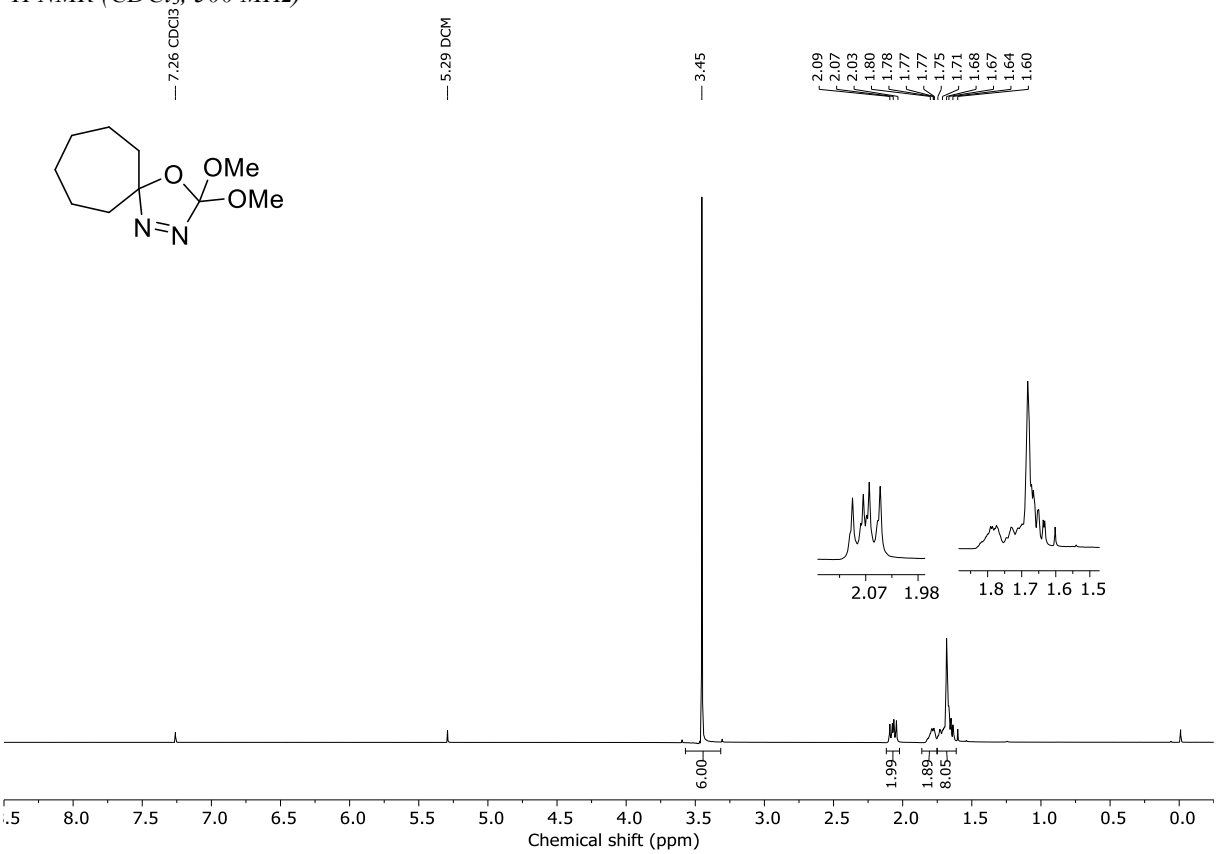

^{13}C NMR ($CDCl_3$, 126 MHz)

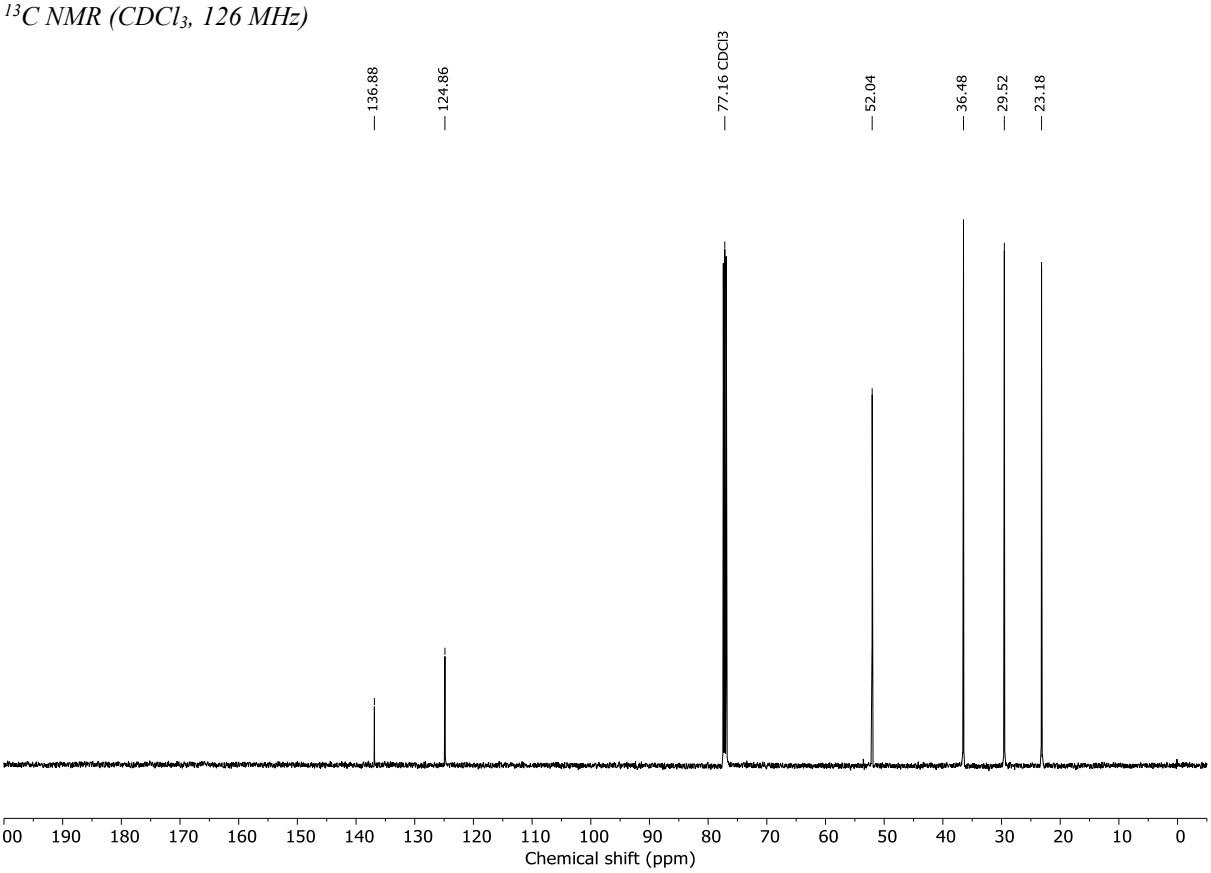

3,3-dimethoxy-4-oxa-1,2-diazaspiro[4.11]hexadec-1-ene (S16)

^{1}H NMR ($CDCl_3$, 600 MHz)

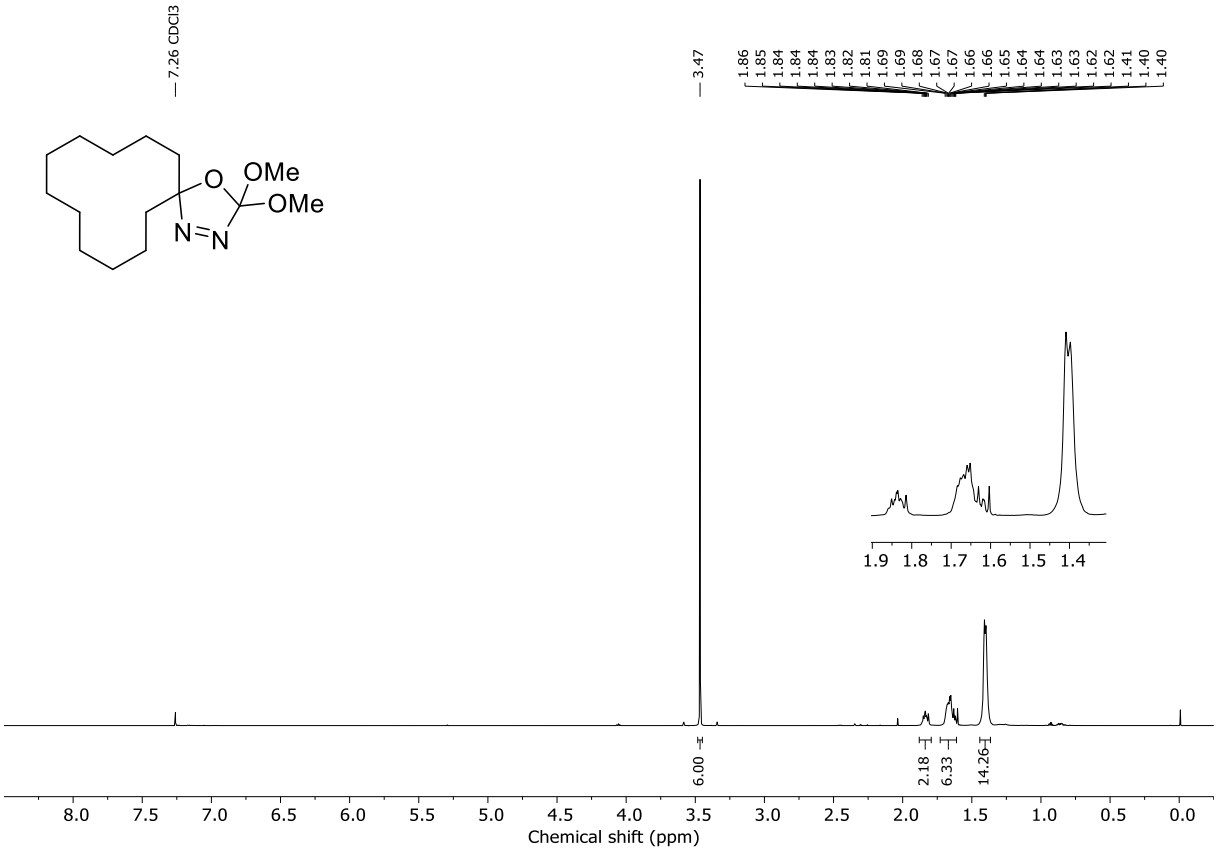

^{13}C NMR ($CDCl_3$, 151 MHz)

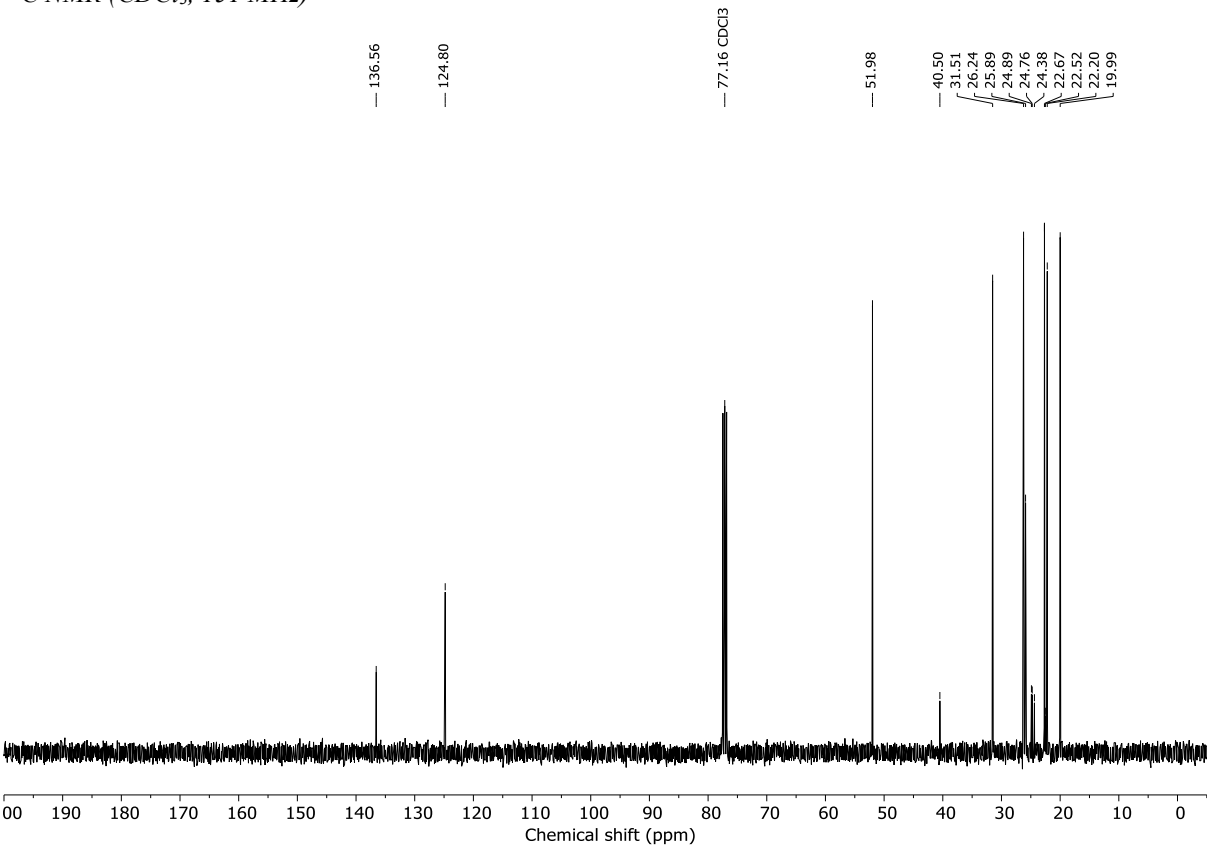

(1R,3R,5R,7R)-5',5'-dimethoxy-5'H-spiro[adamantane-2,2'-[1,3,4]oxadiazole] (S17)

^{1}H NMR ($CDCl_3$, 500 MHz)

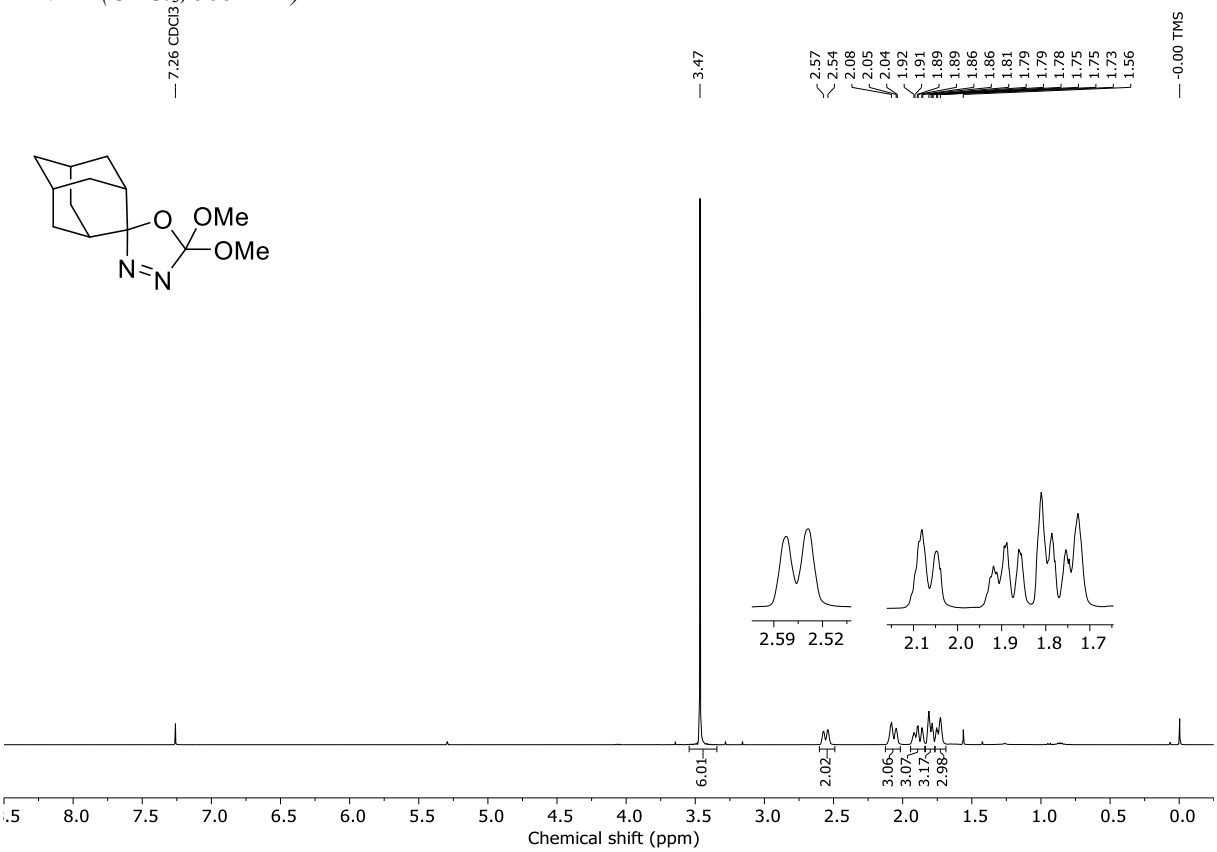

^{13}C NMR ($CDCl_3$, 151 MHz)

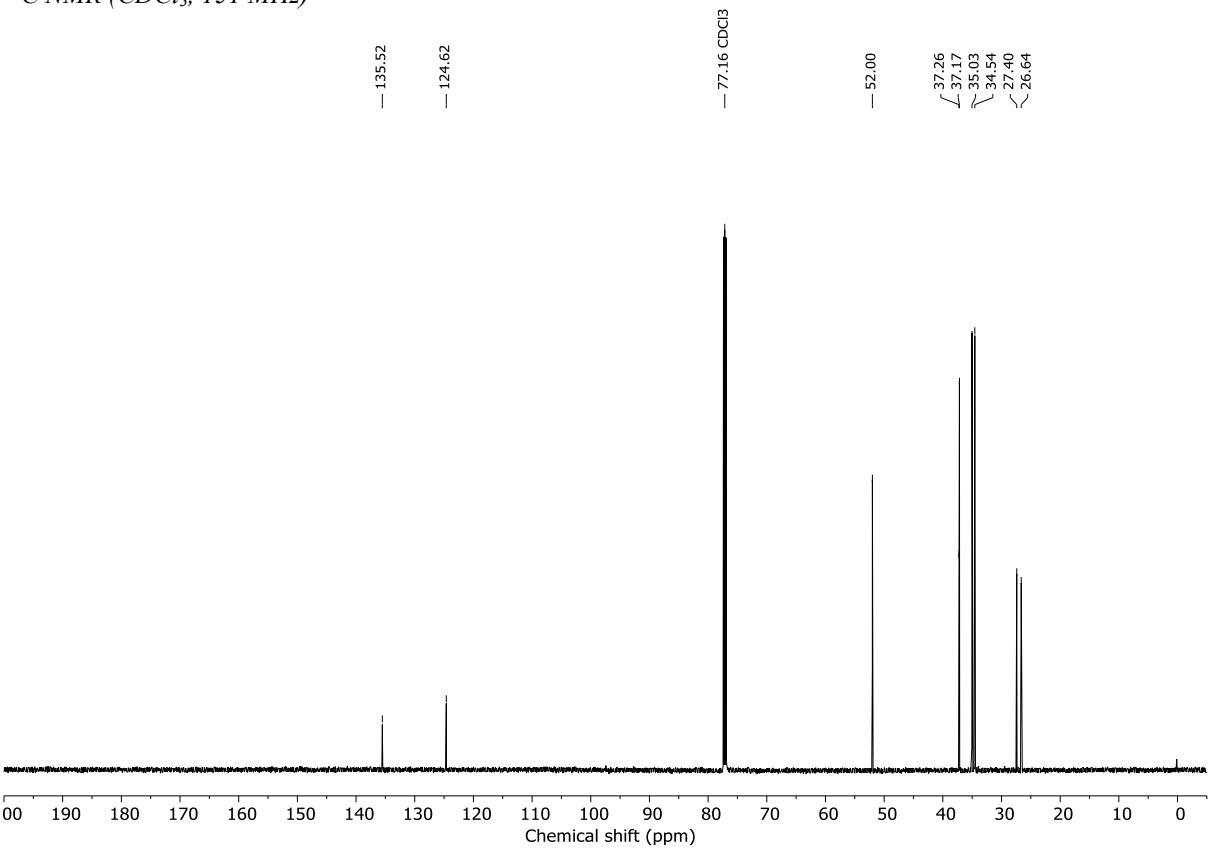

2-cyclopropyl-5,5-dimethoxy-2-methyl-2,5-dihydro-1,3,4-oxadiazole (S18)

^{1}H NMR ($CDCl_3$, 400 MHz)

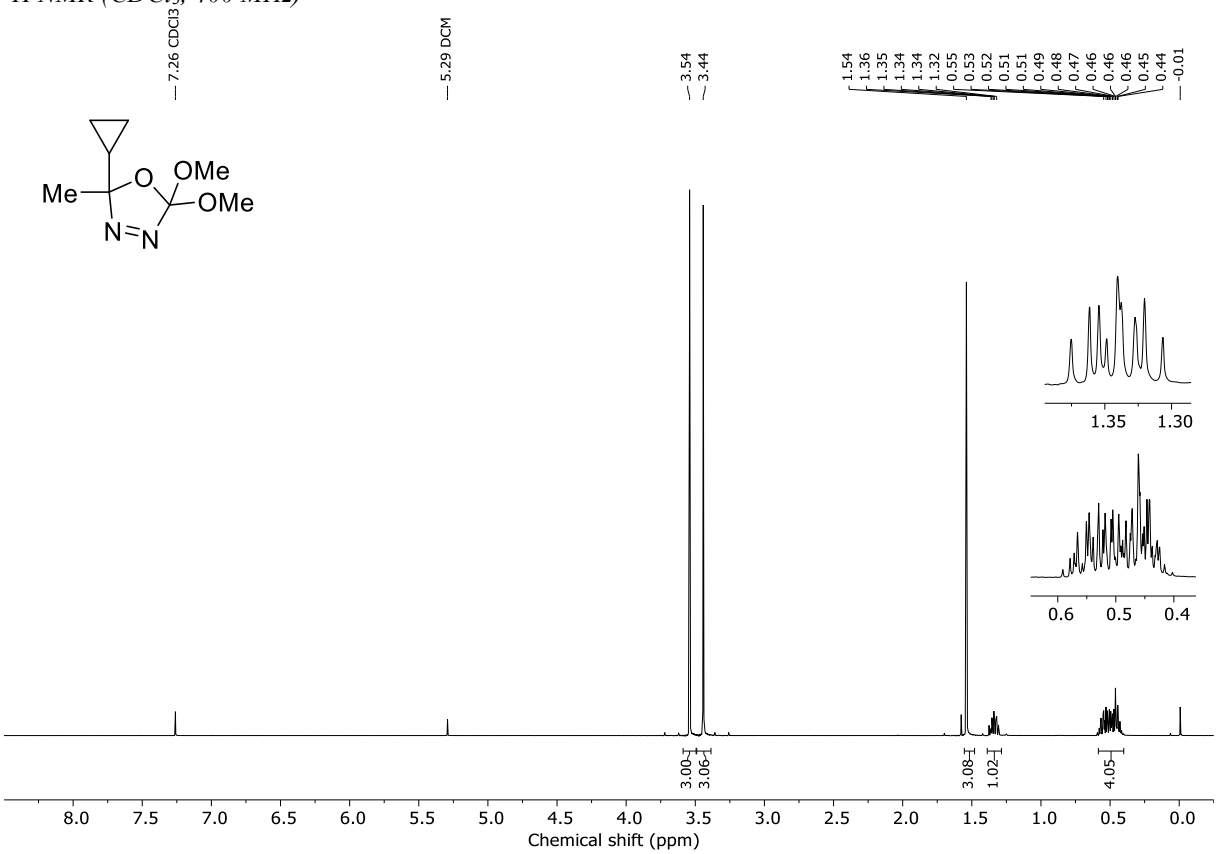

^{13}C NMR ($CDCl_3$, 101 MHz)

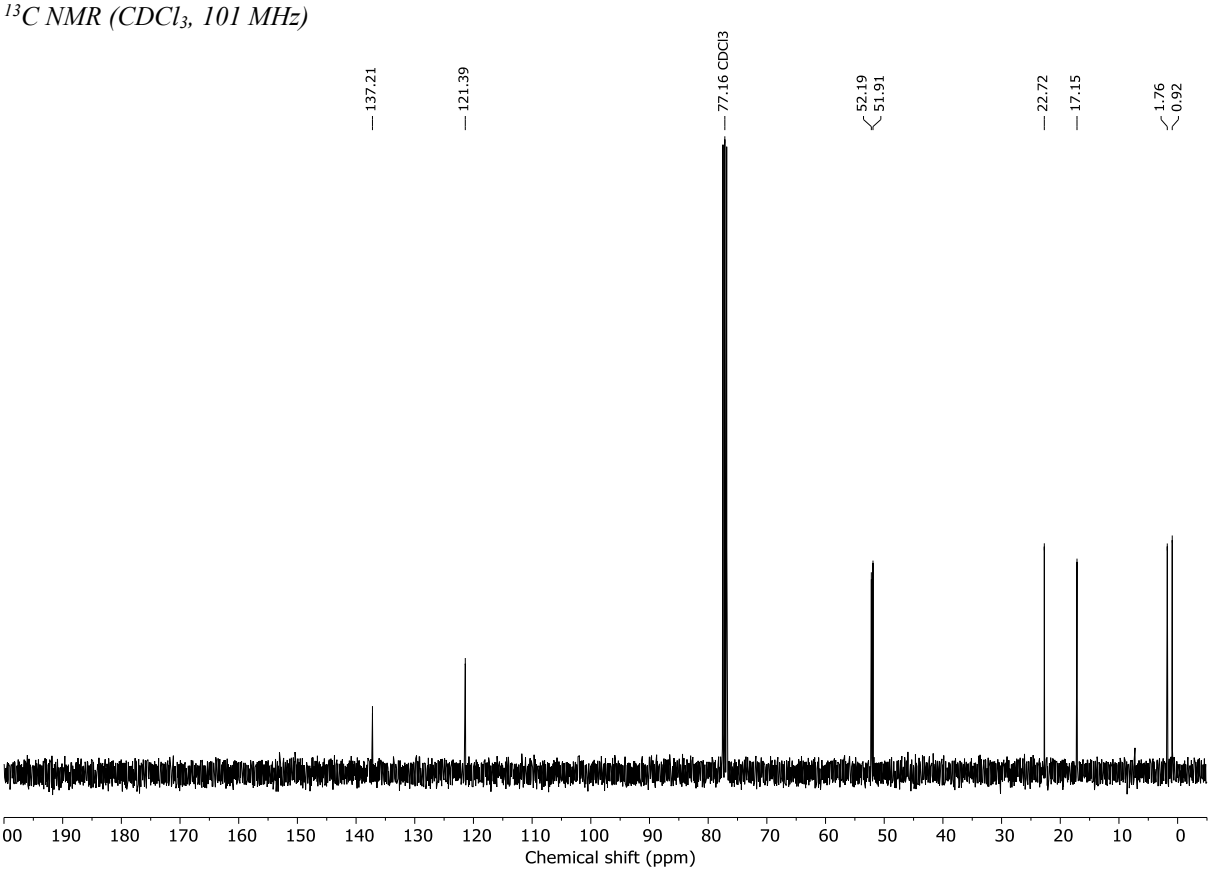

2,2-dimethoxy-5-(methoxymethyl)-5-methyl-2,5-dihydro-1,3,4-oxadiazole (S19)

^{1}H NMR ($CDCl_3$, 500 MHz)

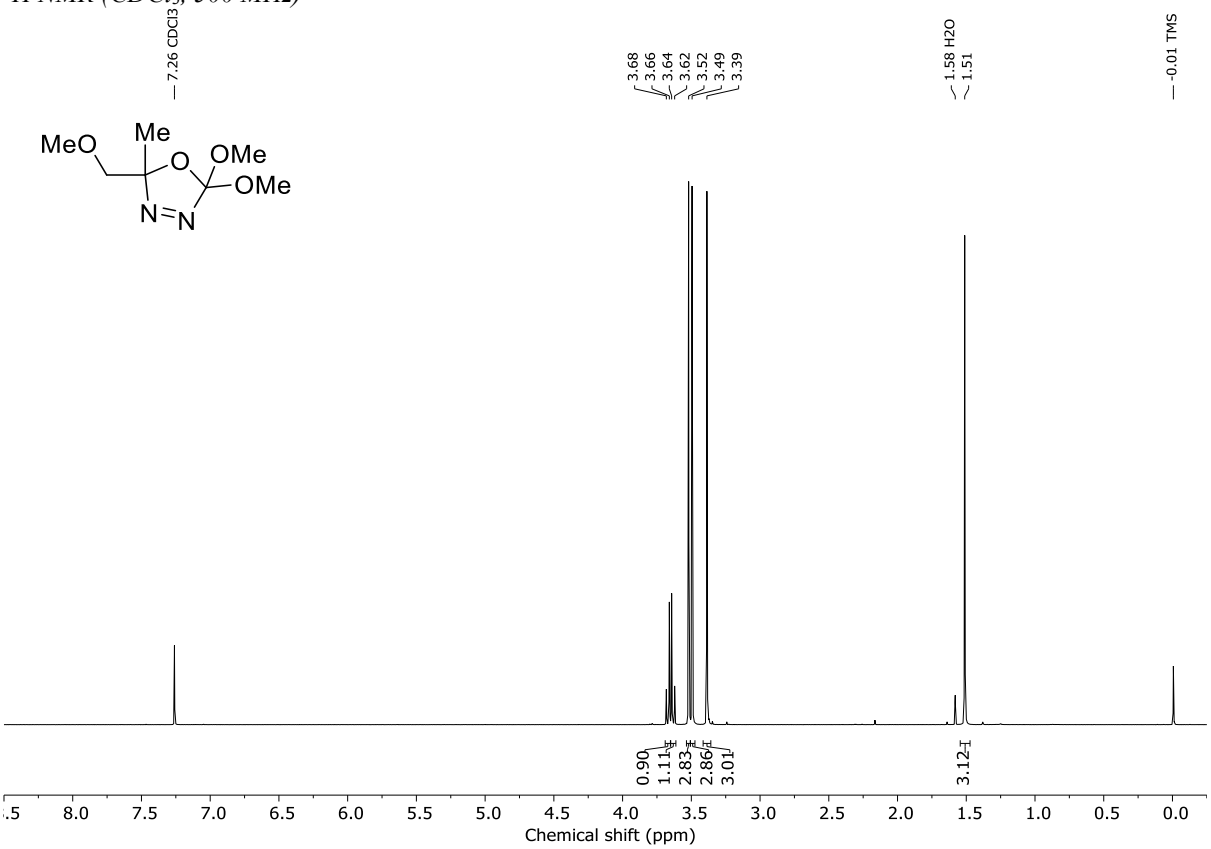

^{13}C NMR ($CDCl_3$, 126 MHz)

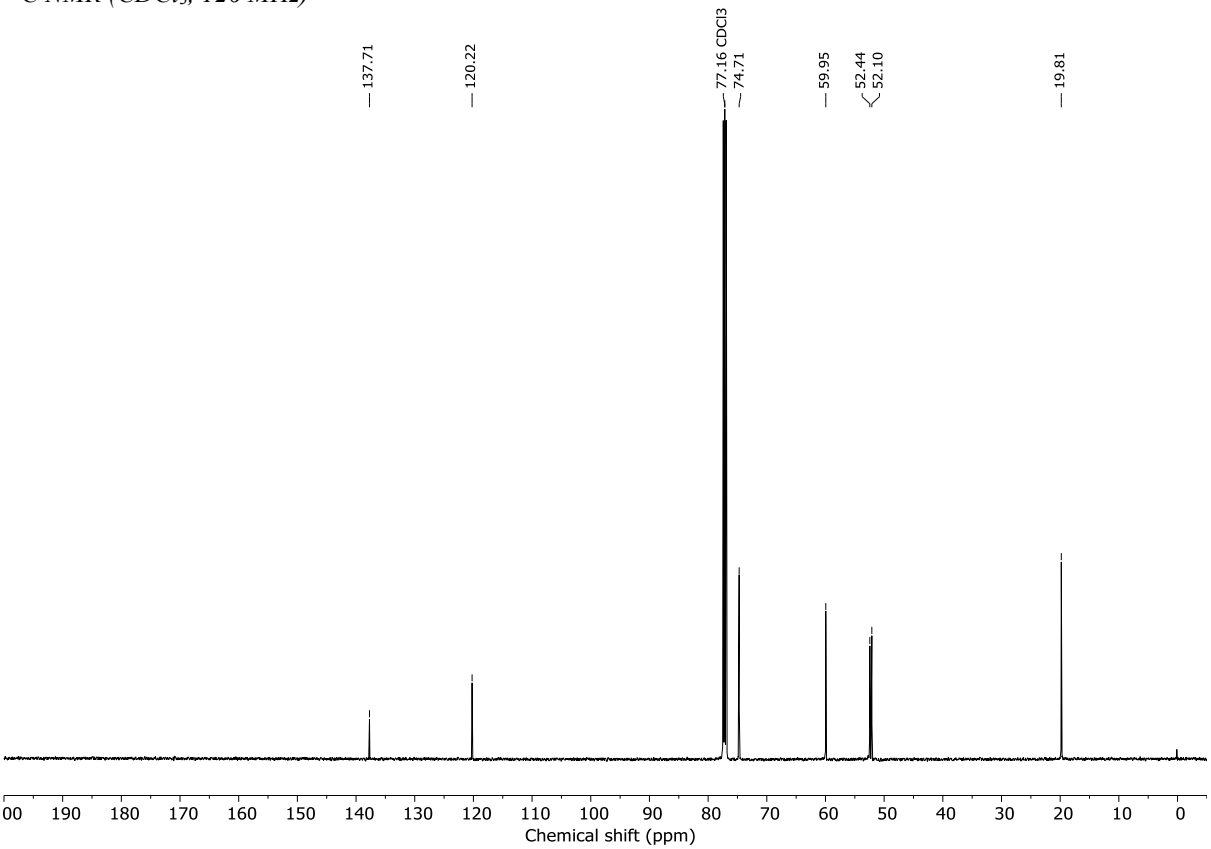

diethyl ((5,5-dimethoxy-2-methyl-2,5-dihydro-1,3,4-oxadiazol-2-yl)methyl)phosphonate (S20)

^{1}H NMR ($CDCl_3$, 400 MHz)

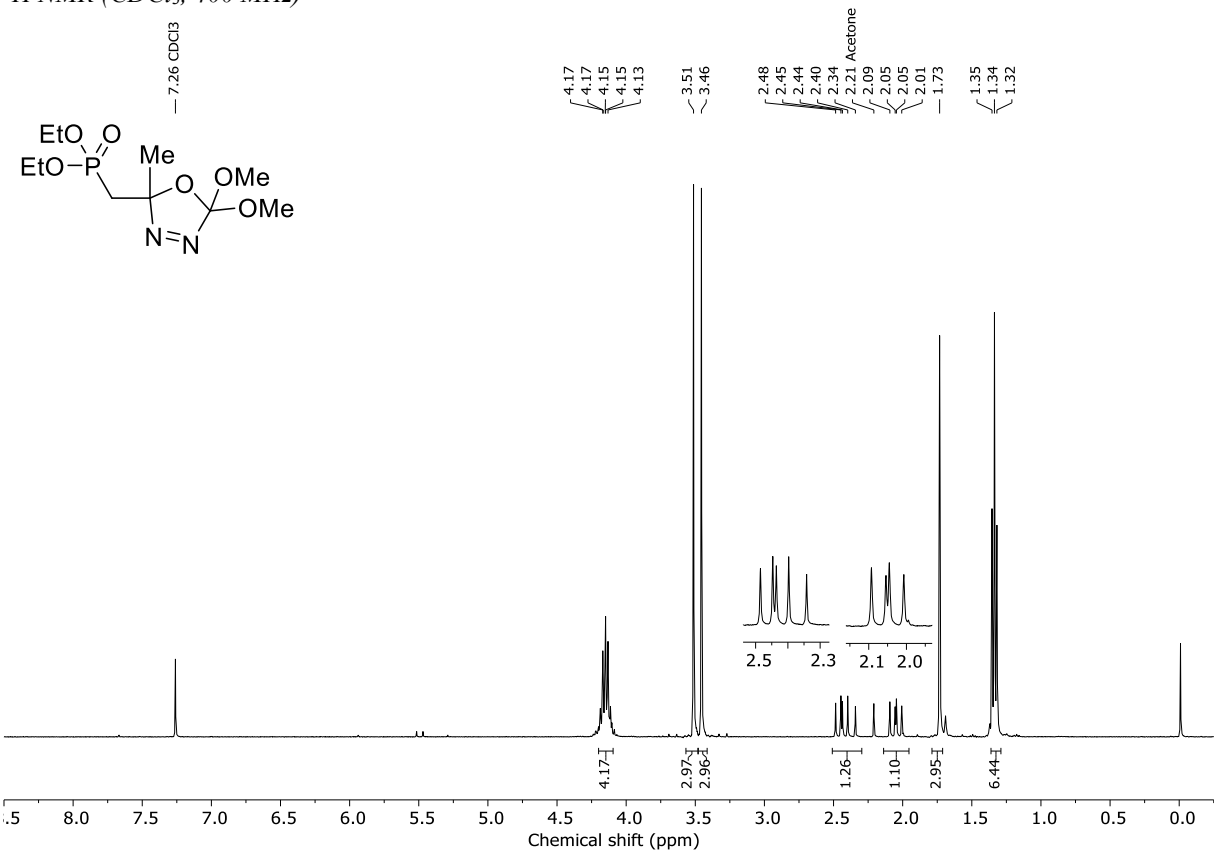

^{13}C NMR ($CDCl_3$, 126 MHz)

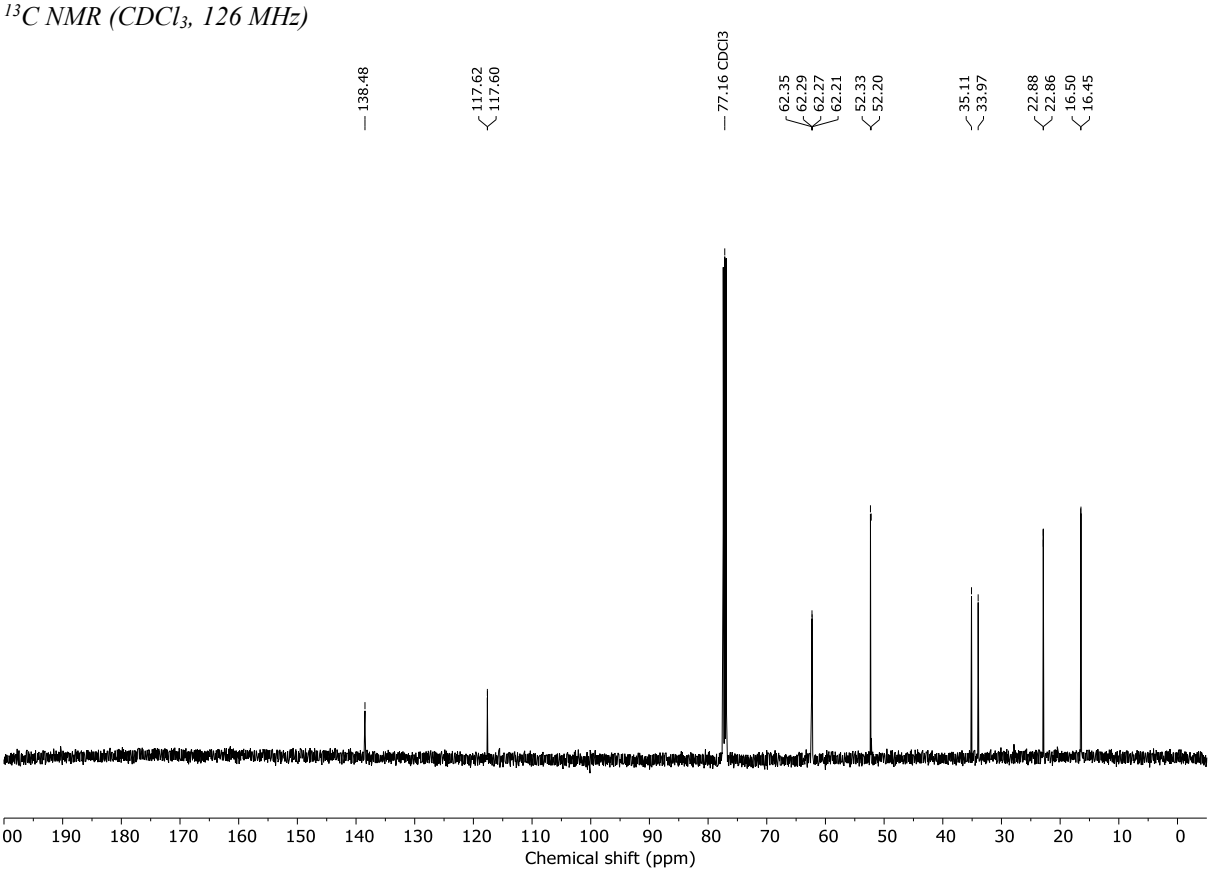

7,7-dimethoxy-2,8-dioxa-5,6-diazaspiro[3.4]oct-5-ene (S21)

^{1}H NMR ($CDCl_3$, 400 MHz)

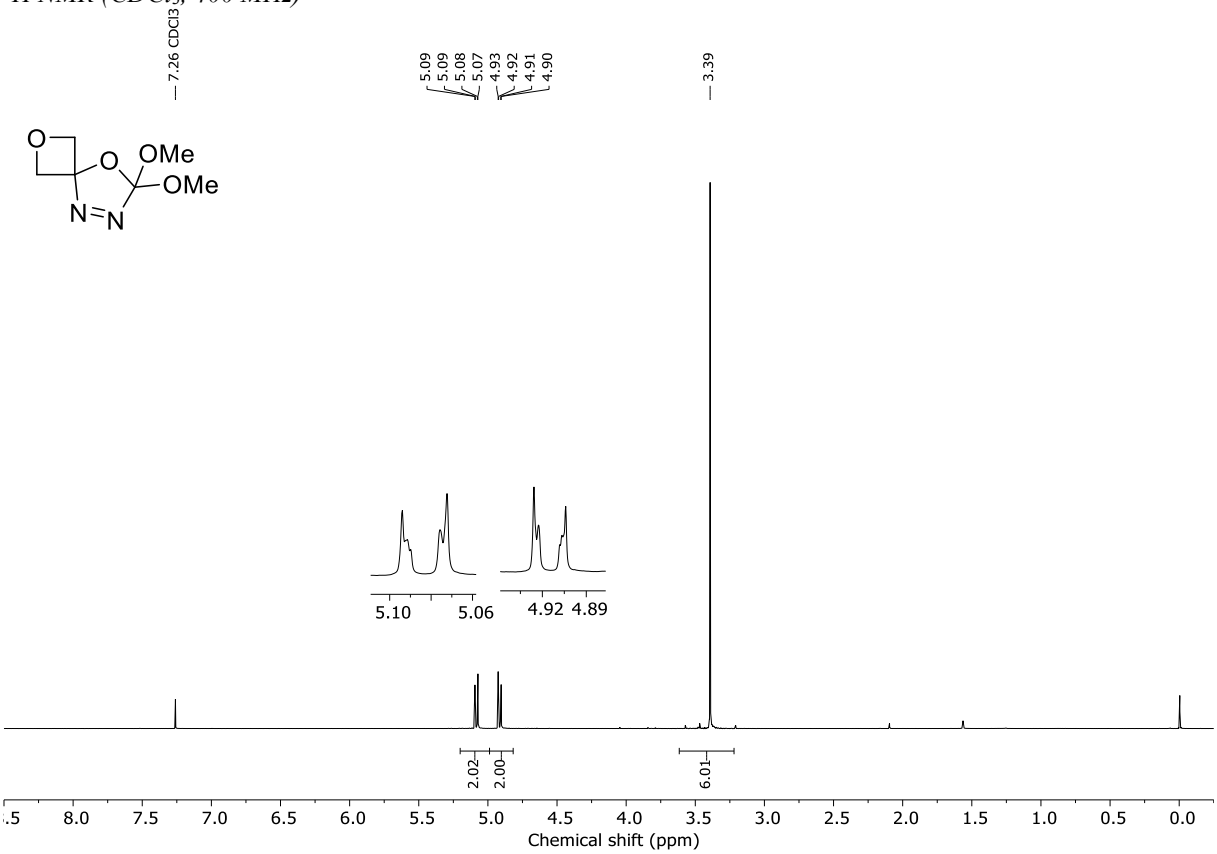

^{13}C NMR ($CDCl_3$, 101 MHz)

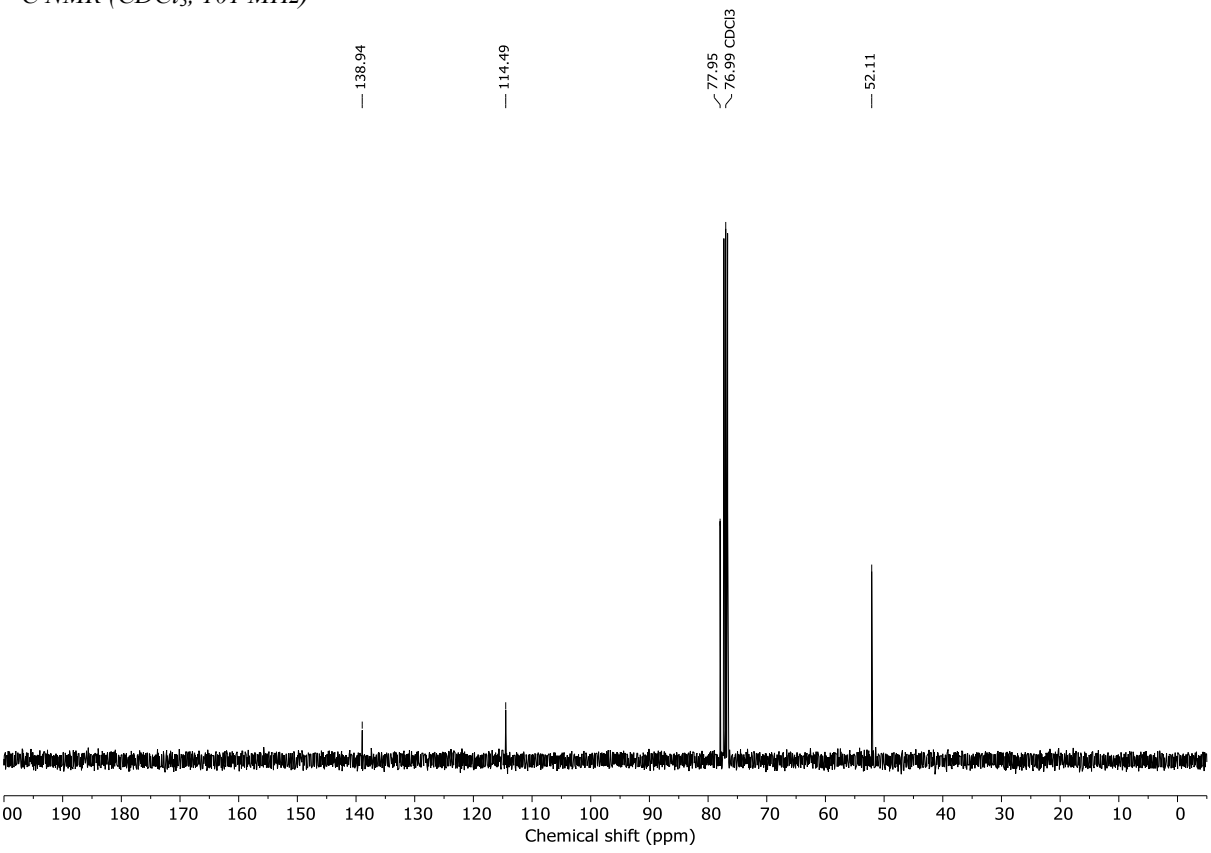

3,3-dimethoxy-4-oxa-7-thia-1,2-diazaspiro[4.4]non-1-ene (S22)

^{1}H NMR ($CDCl_3$, 600 MHz)

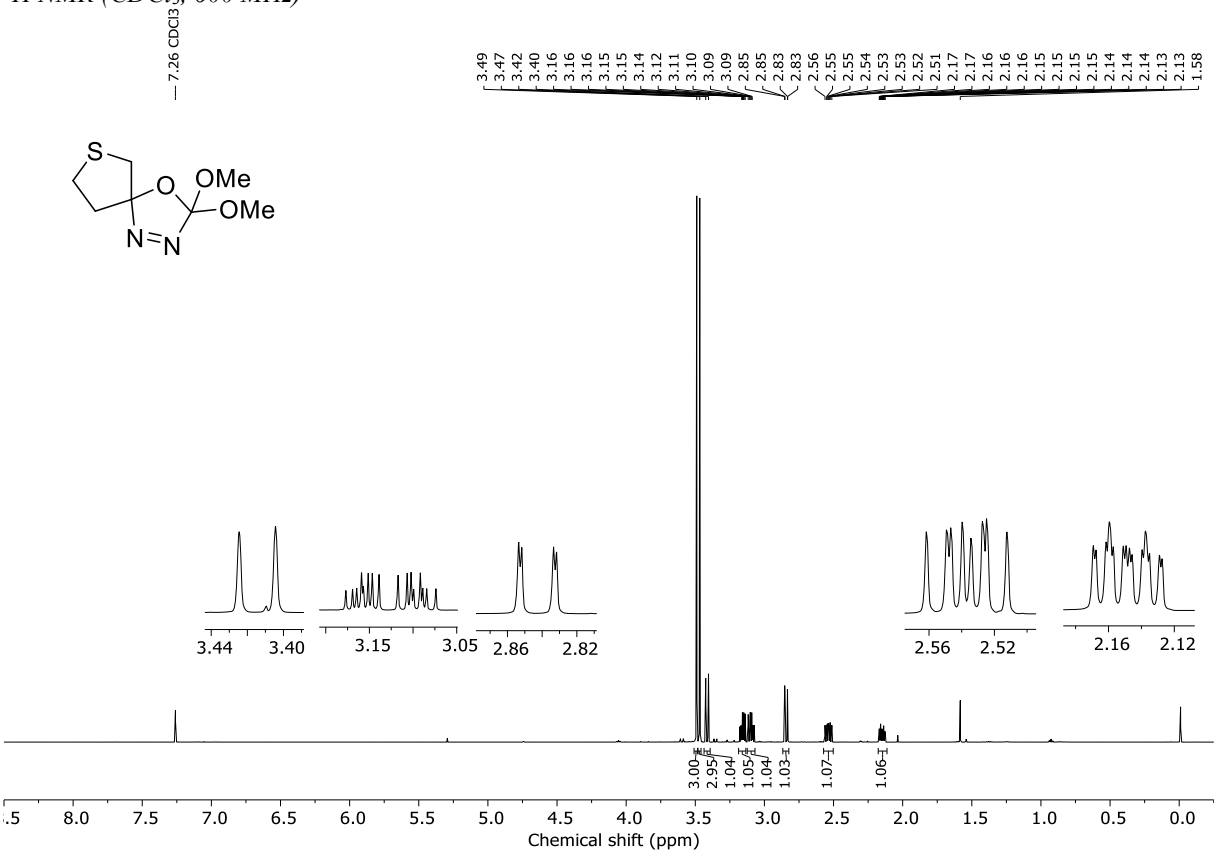

^{13}C NMR ($CDCl_3$, 151 MHz)

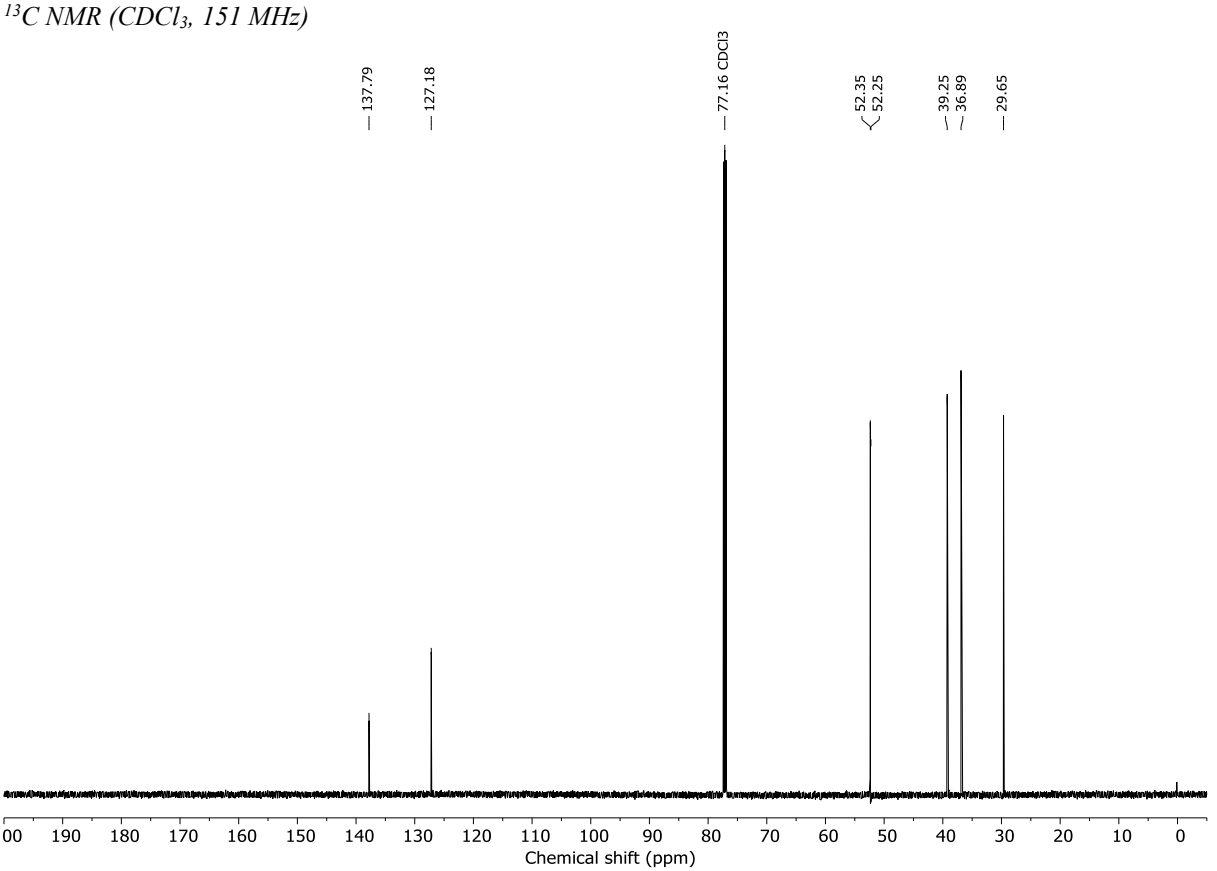

tert-butyl 3,3-dimethoxy-4-oxa-1,2,8-triazaspiro[4.5]dec-1-ene-8-carboxylate (S23)

^{1}H NMR ($CDCl_3$, 500 MHz)

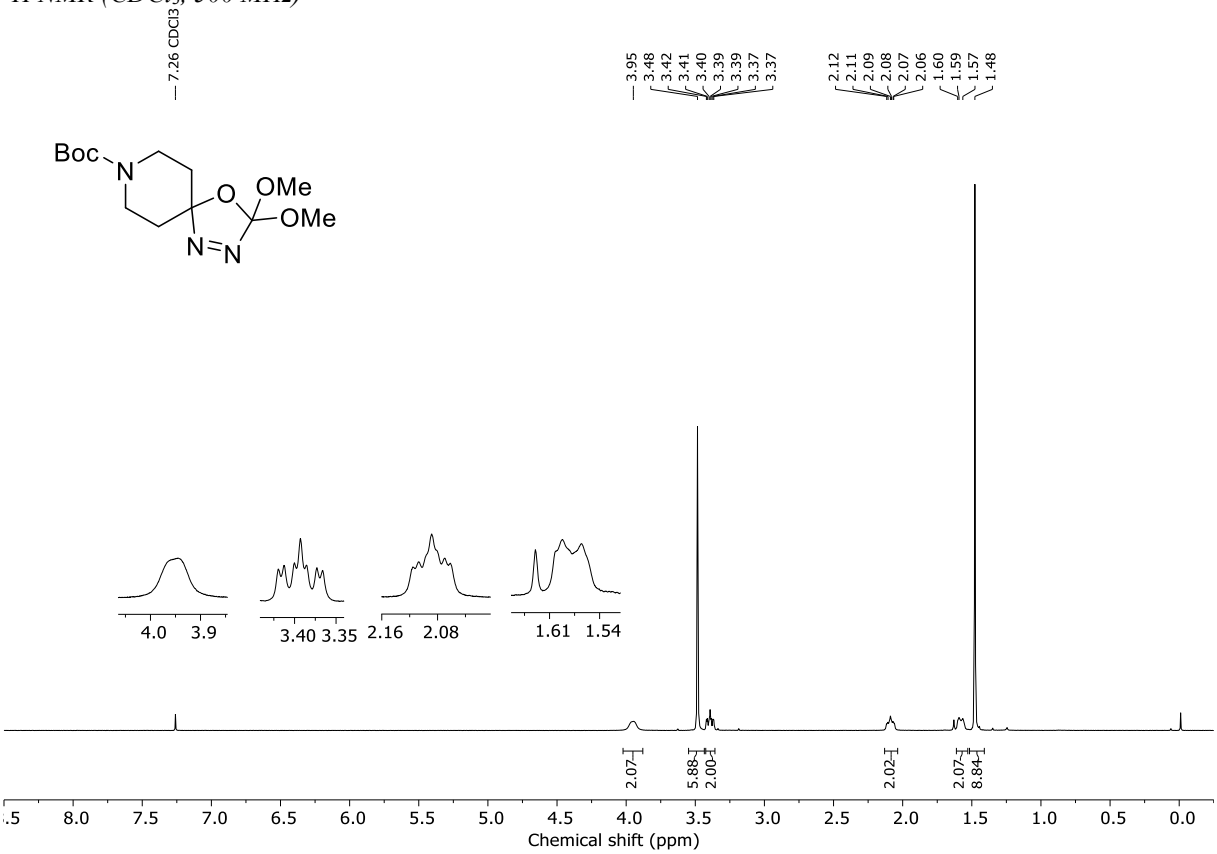

^{13}C NMR ($CDCl_3$, 126 MHz)

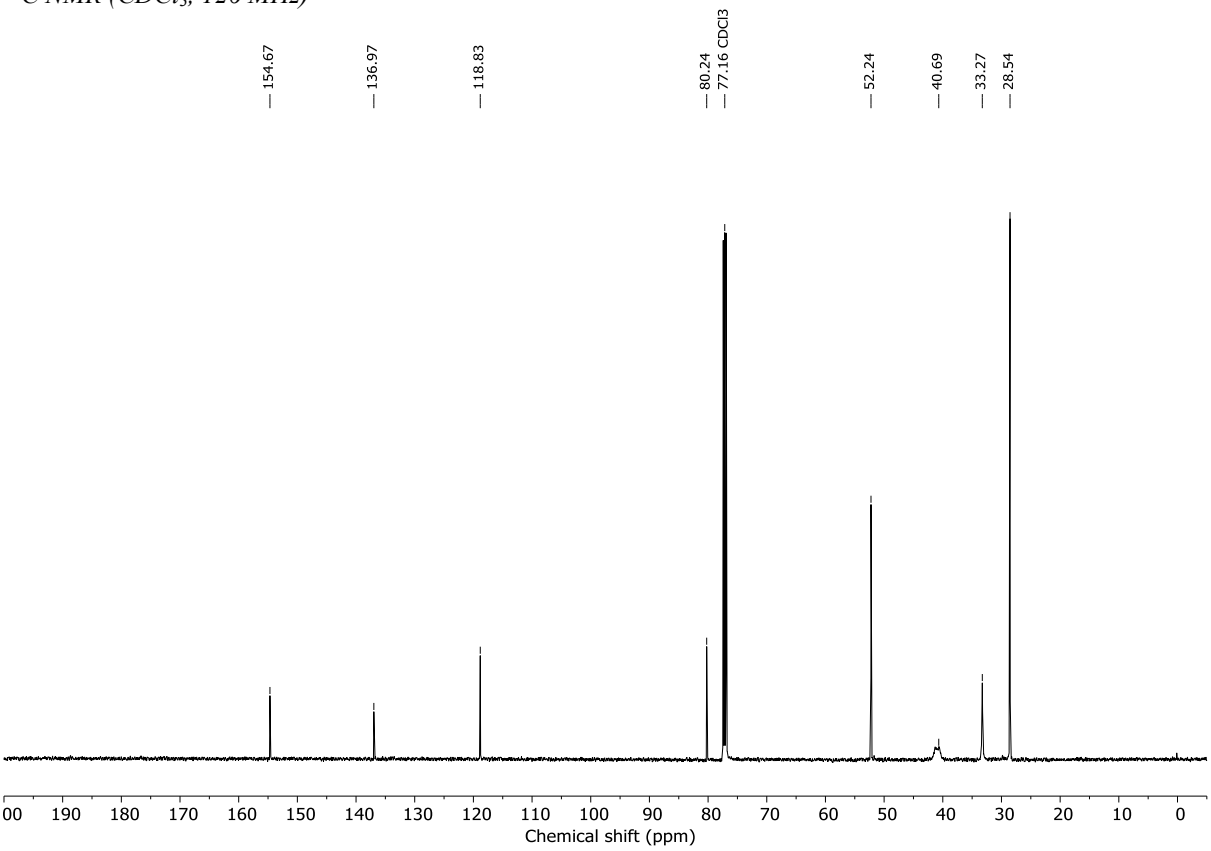

tert-butyl (1R,3S,5S)-5',5'-dimethoxy-5'H-8-azaspiro[bicyclo[3.2.1]octane-3,2'-[1,3,4]oxadiazole]-8-carboxylate (S24)

^{1}H NMR ($CDCl_3$, 500 MHz)

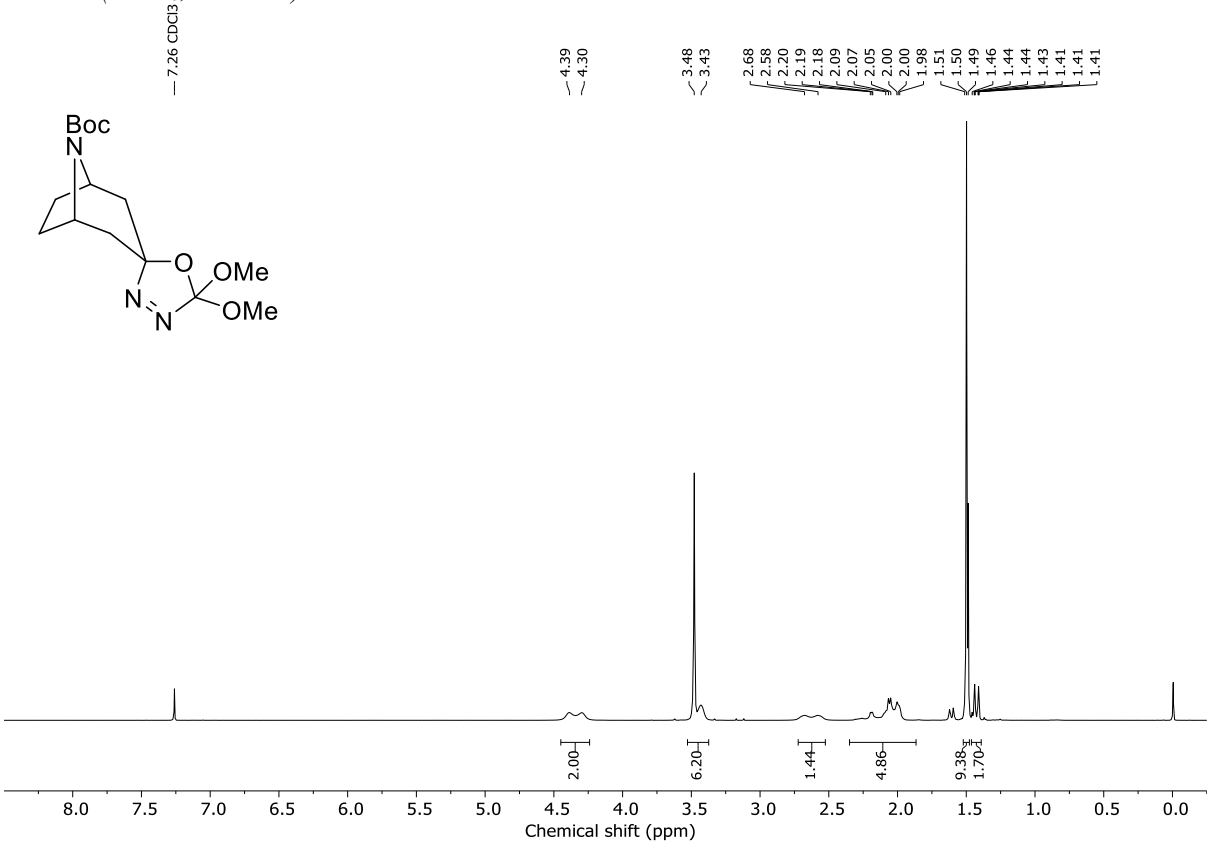

^{13}C NMR ($CDCl_3$, 126 MHz)

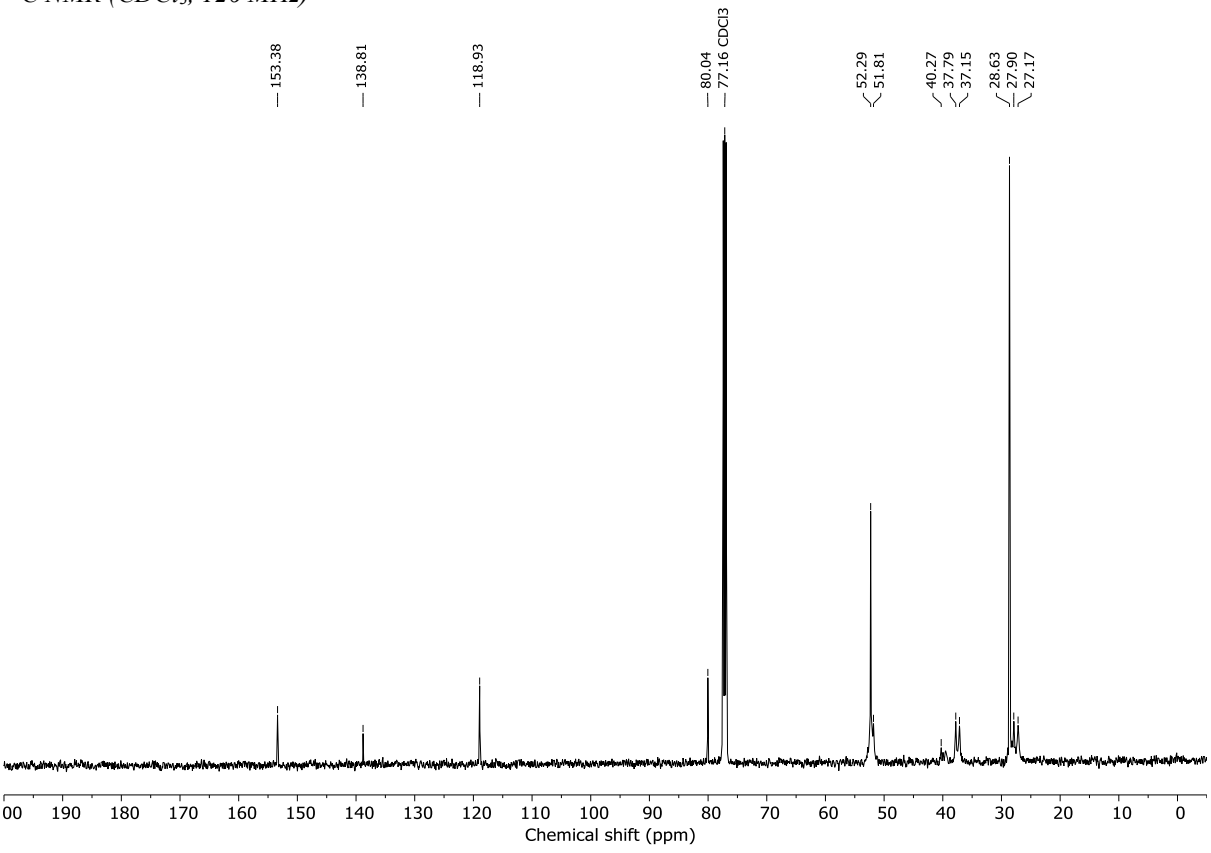

3,3-dimethoxy-8,8-dimethyl-4,7,9-trioxa-1,2-diazaspiro[4.5]dec-1-ene (S25)

^{1}H NMR ($CDCl_3$, 500 MHz)

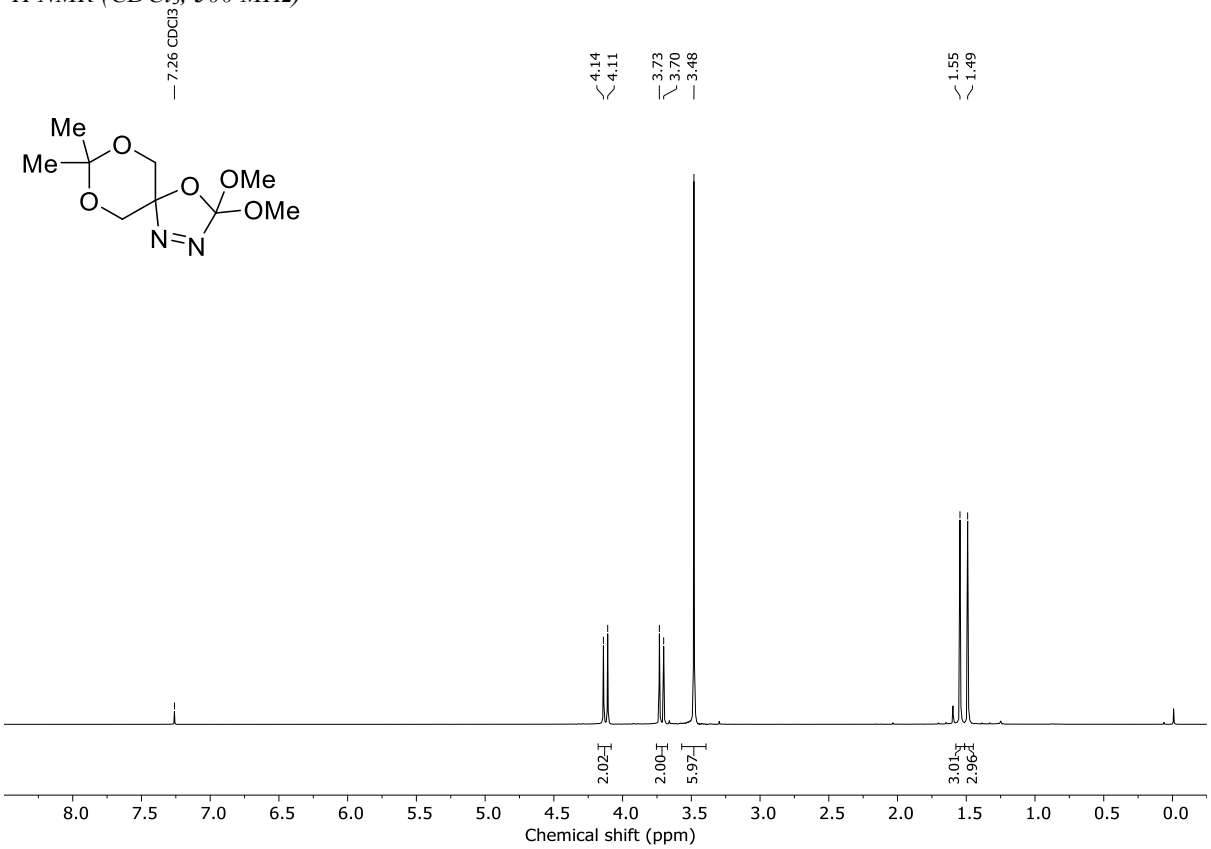

^{13}C NMR ($CDCl_3$, 126 MHz)

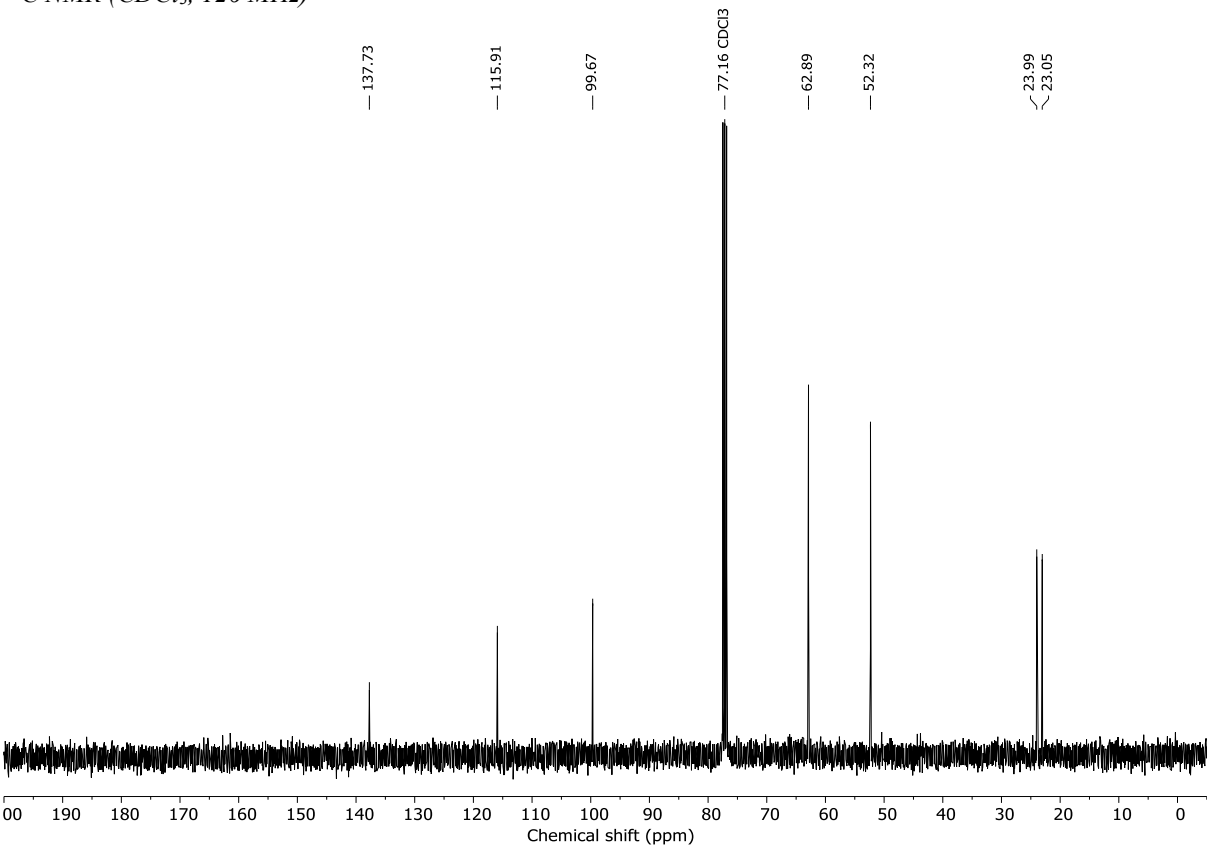

5',5'-dimethoxy-1,3-dihydro-5'H-spiro[indene-2,2'-[1,3,4]oxadiazole] (S26)

^{1}H NMR ($CDCl_3$, 400 MHz)

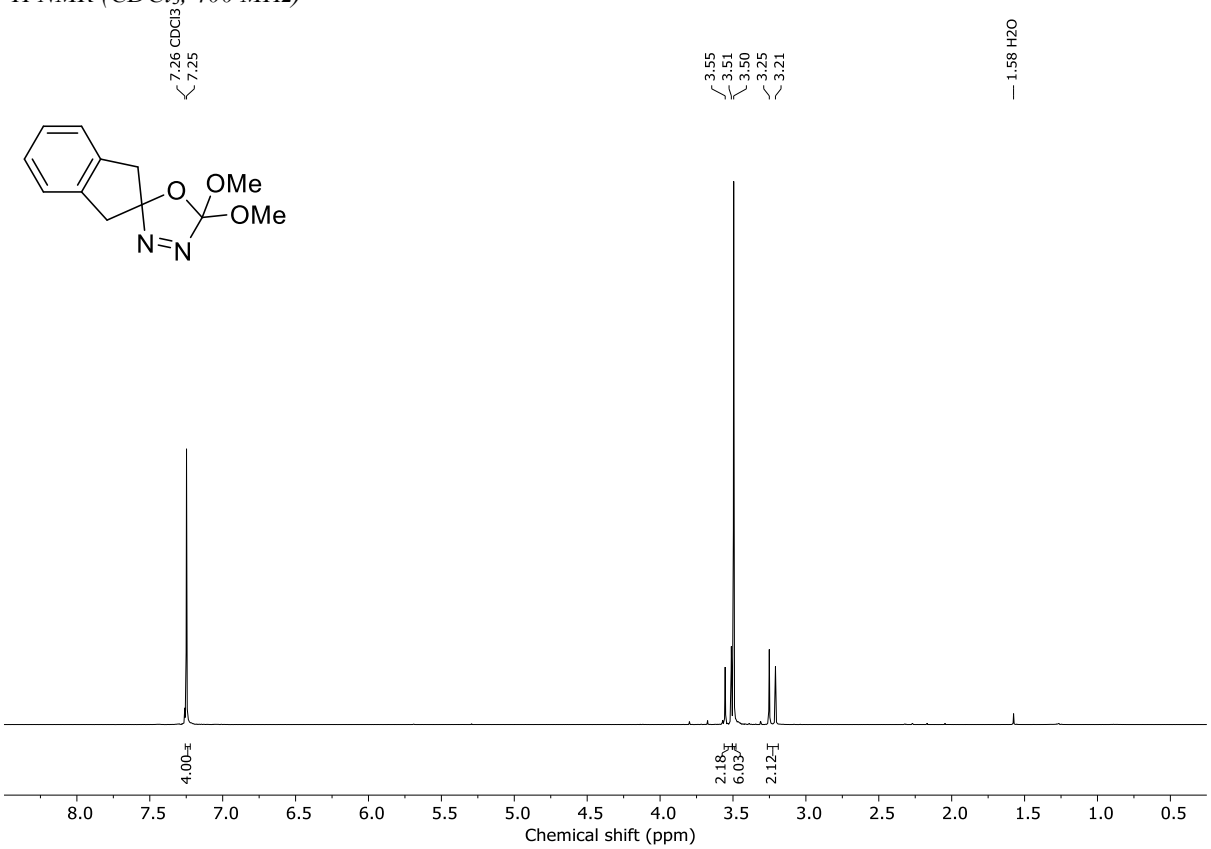

^{13}C NMR ($CDCl_3$, 101 MHz)

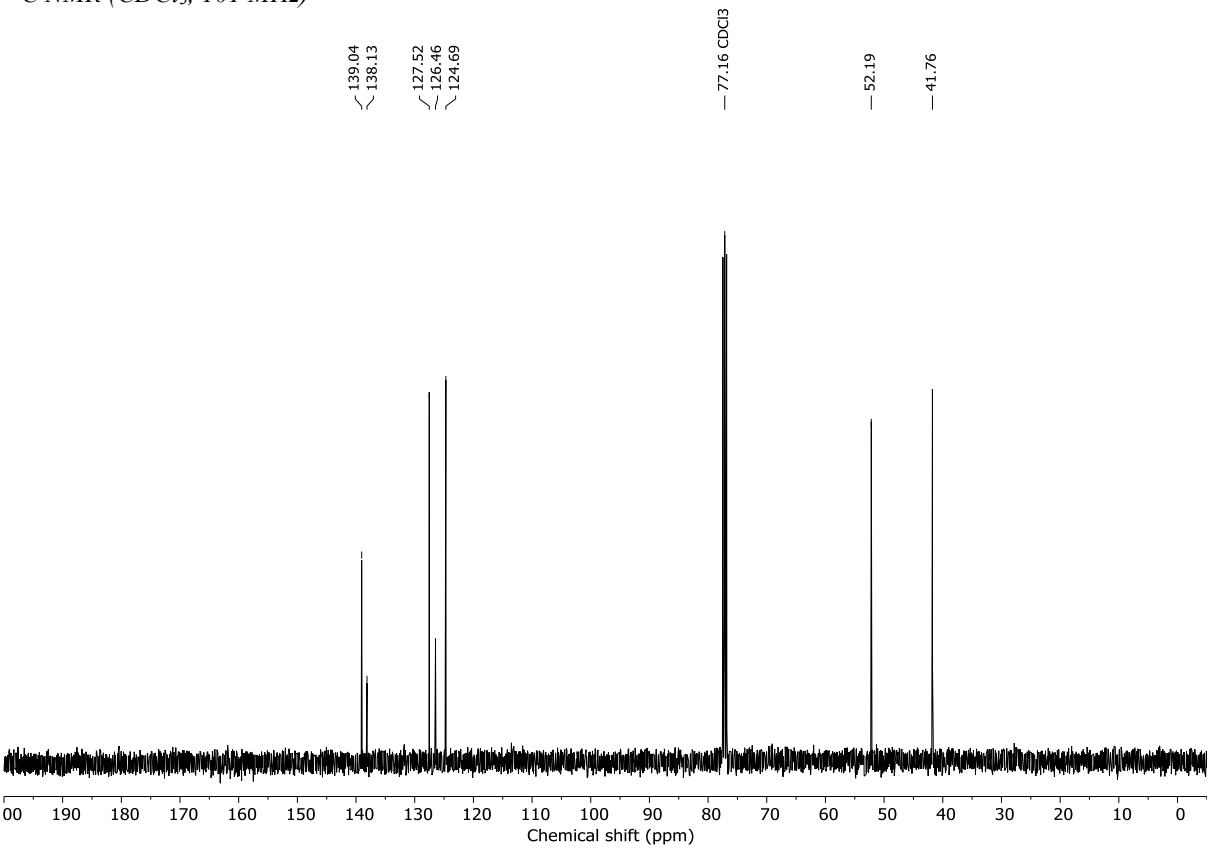

2-benzyl-2-ethyl-5,5-dimethoxy-2,5-dihydro-1,3,4-oxadiazole (S27)

^{1}H NMR ($CDCl_3$, 500 MHz)

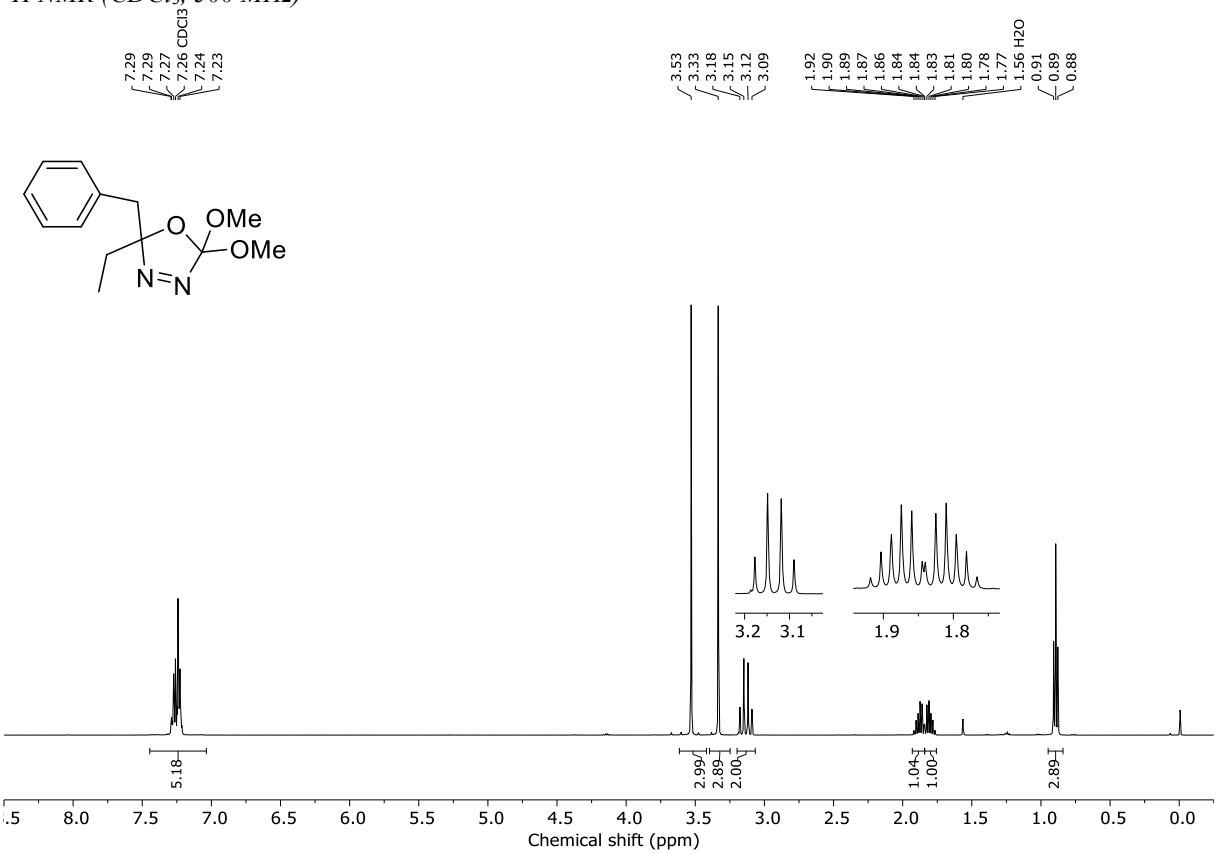

^{13}C NMR ($CDCl_3$, 126 MHz)

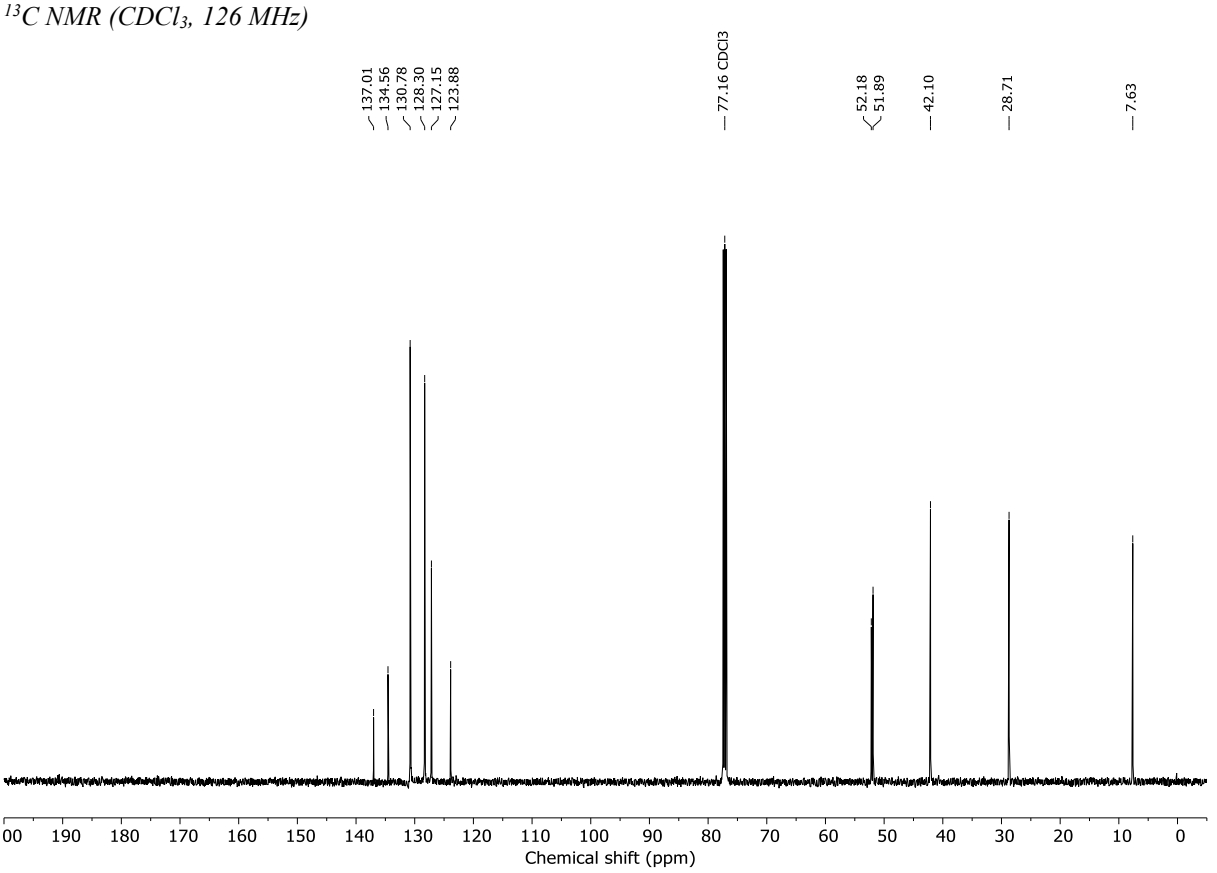

(1S,4R,5R)-1-isopropyl-5',5'-dimethoxy-4-methyl-5'H-spiro[bicyclo[3.1.0]hexane-3,2'-[1,3,4]oxadiazole] (S28)

^{1}H NMR ($CDCl_3$, 600 MHz)

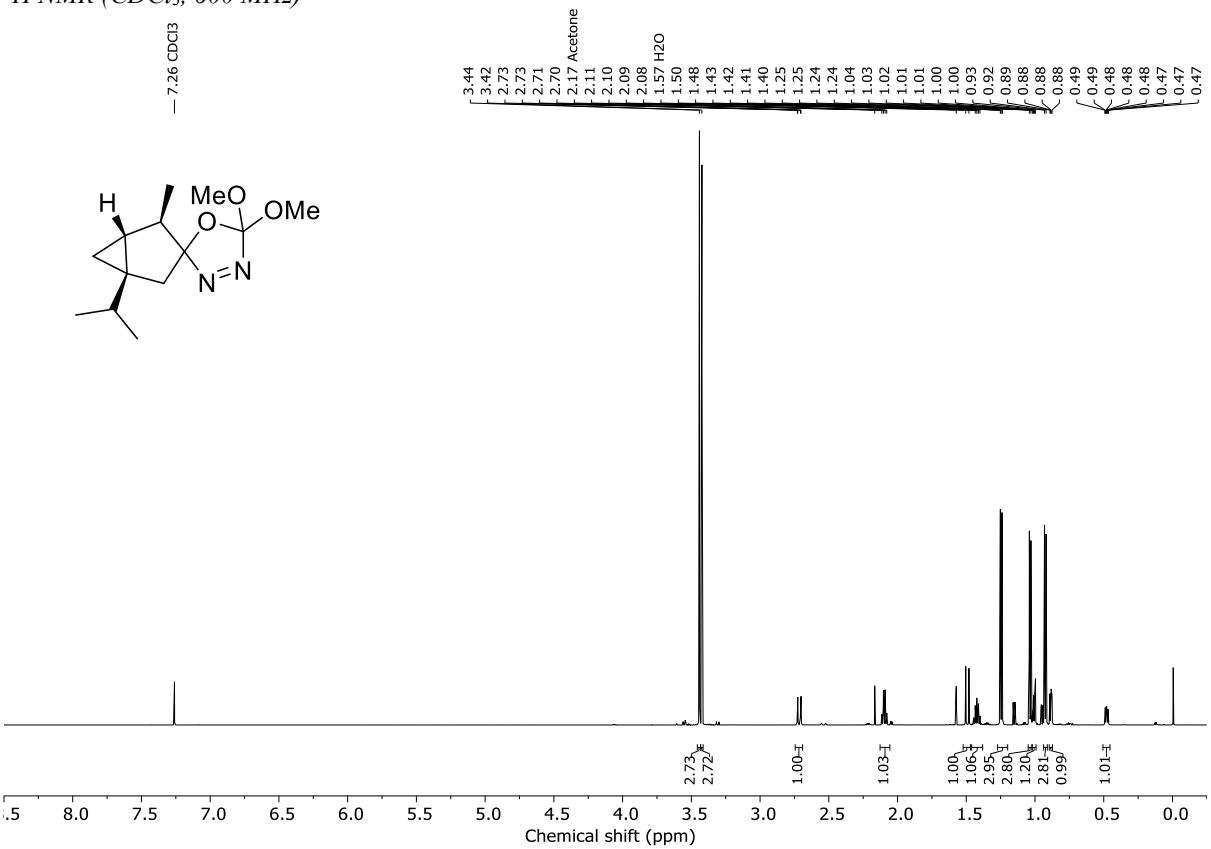

^{13}C NMR ($CDCl_3$, 151 MHz)

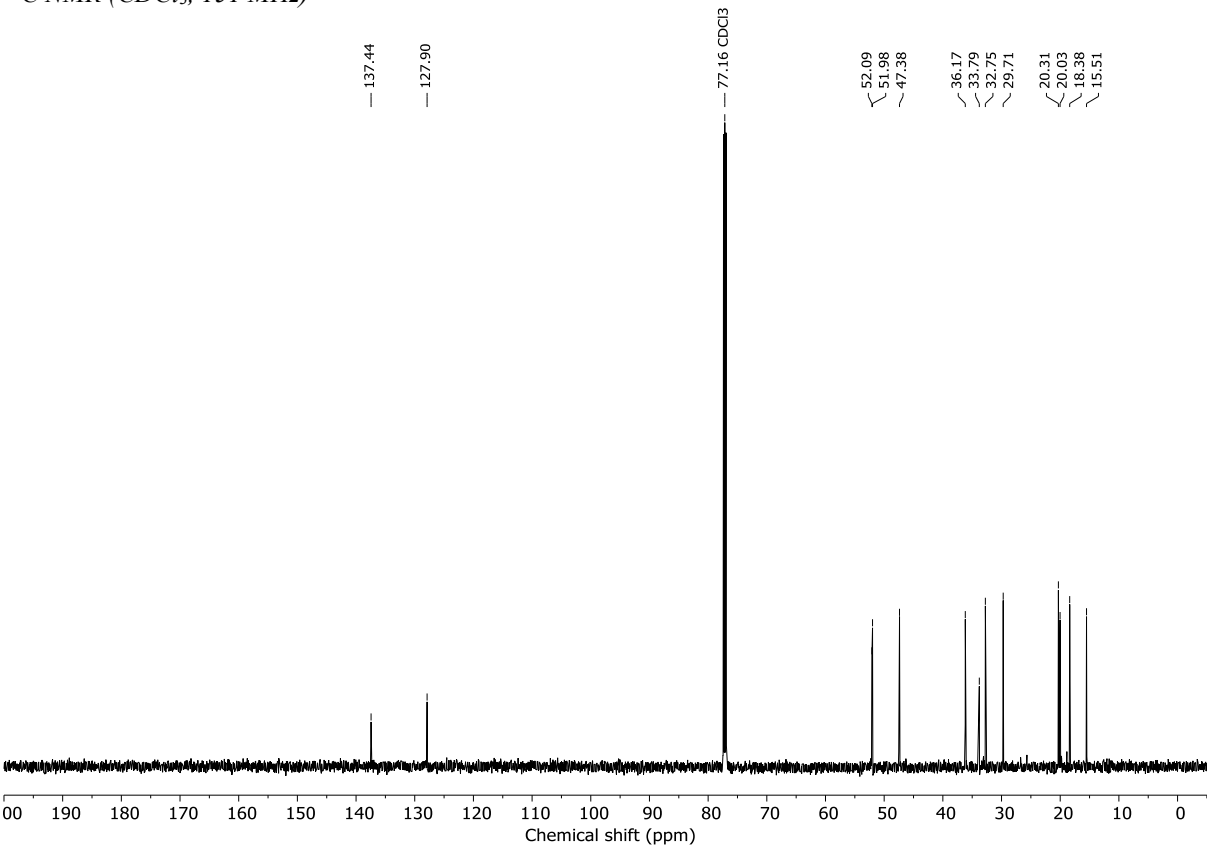

(5S)-2,2-dimethoxy-5-((8S,10R,13S,17S)-3-methoxy-10,13-dimethyl-2,3,4,7,8,9,10,11,12,13,14,15,16,17-tetradecahydro-1H-cyclopenta[a]phenanthren-17-yl)-5-methyl-2,5-dihydro-1,3,4-oxadiazole (S29)

^{1}H NMR ($CDCl_3$, 500 MHz)

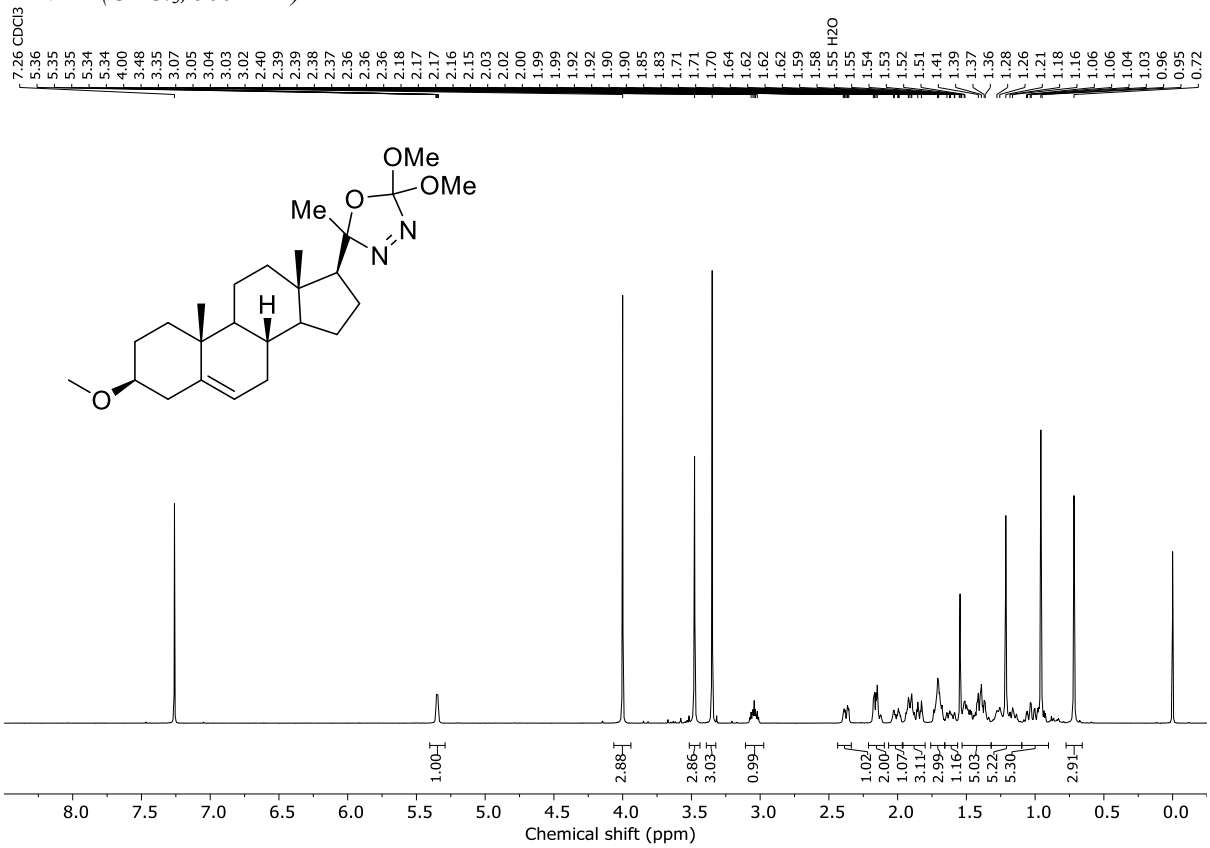

^{13}C NMR ($CDCl_3$, 126 MHz)

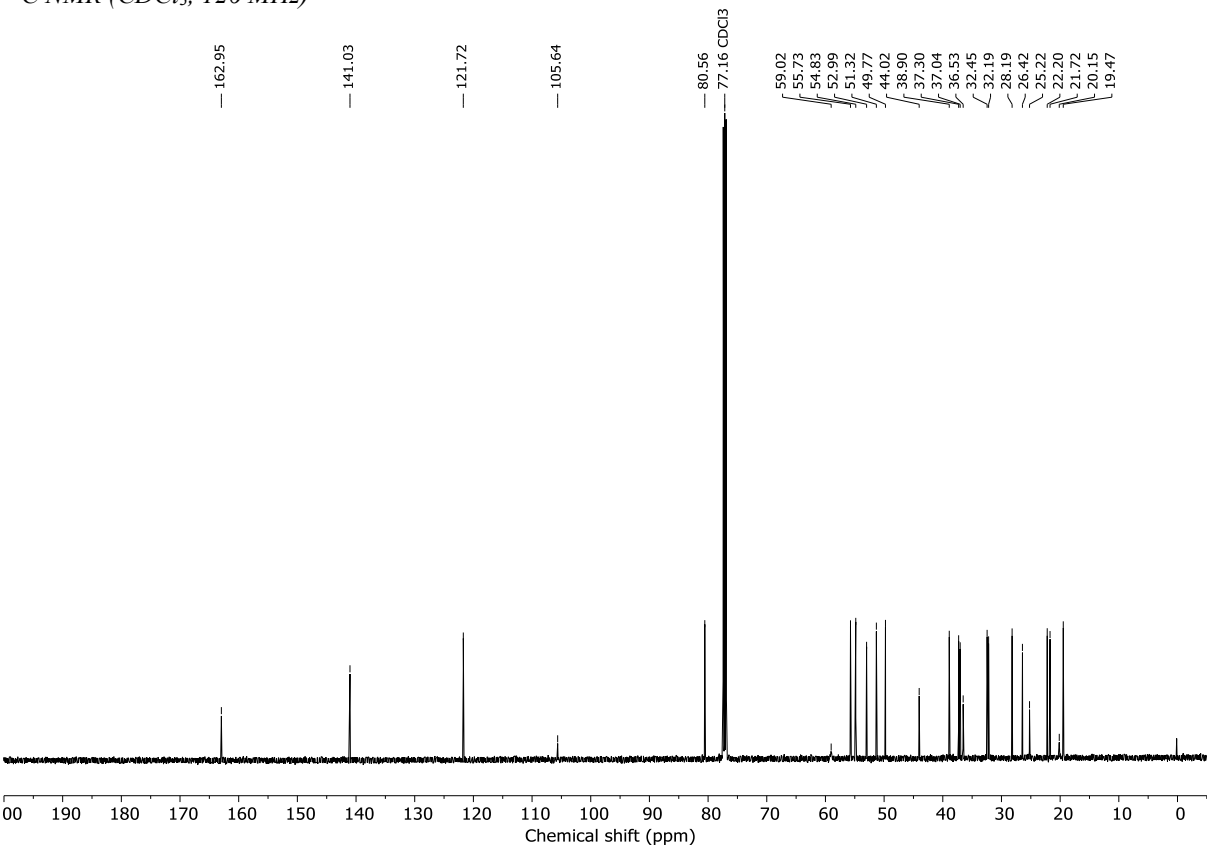

4-acryloylbenzonitrile (S9)

^{1}H NMR ($CDCl_3$, 600 MHz)

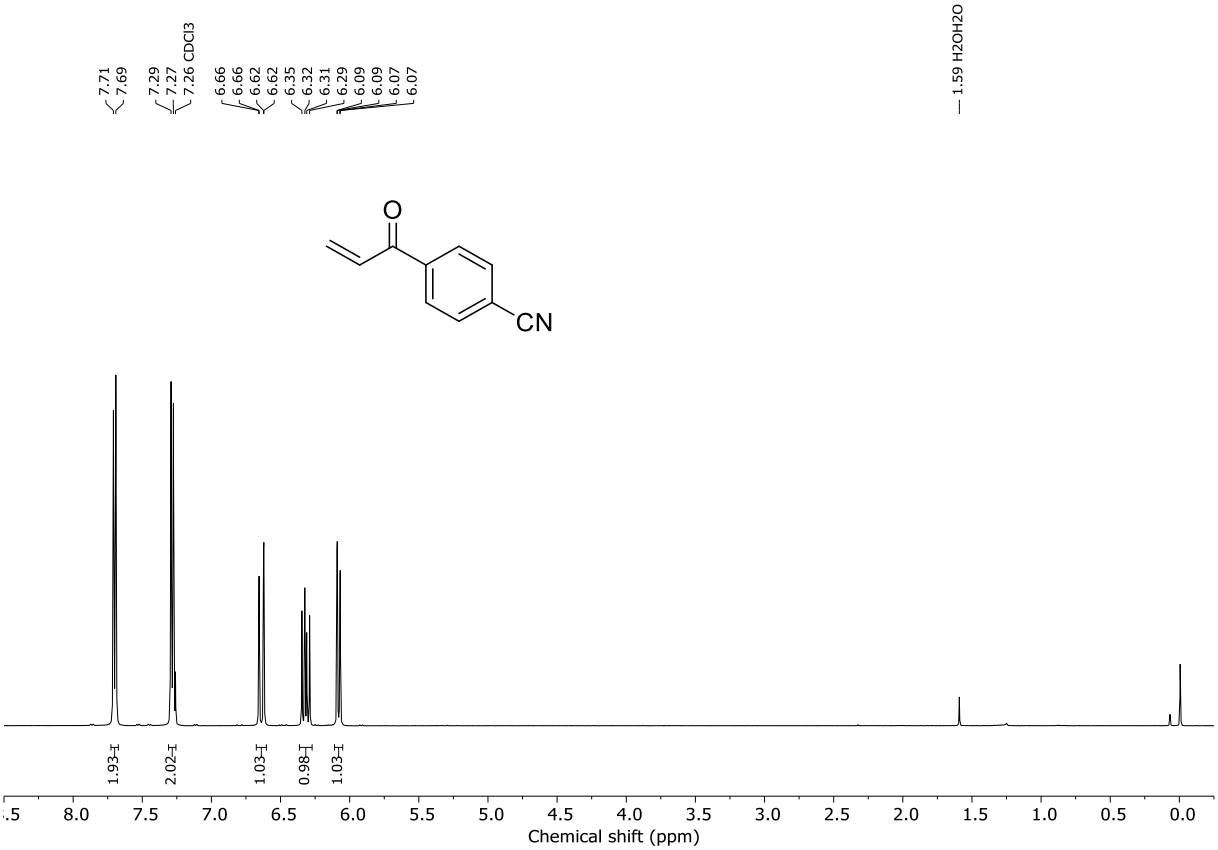

^{13}C NMR ($CDCl_3$, 151 MHz)

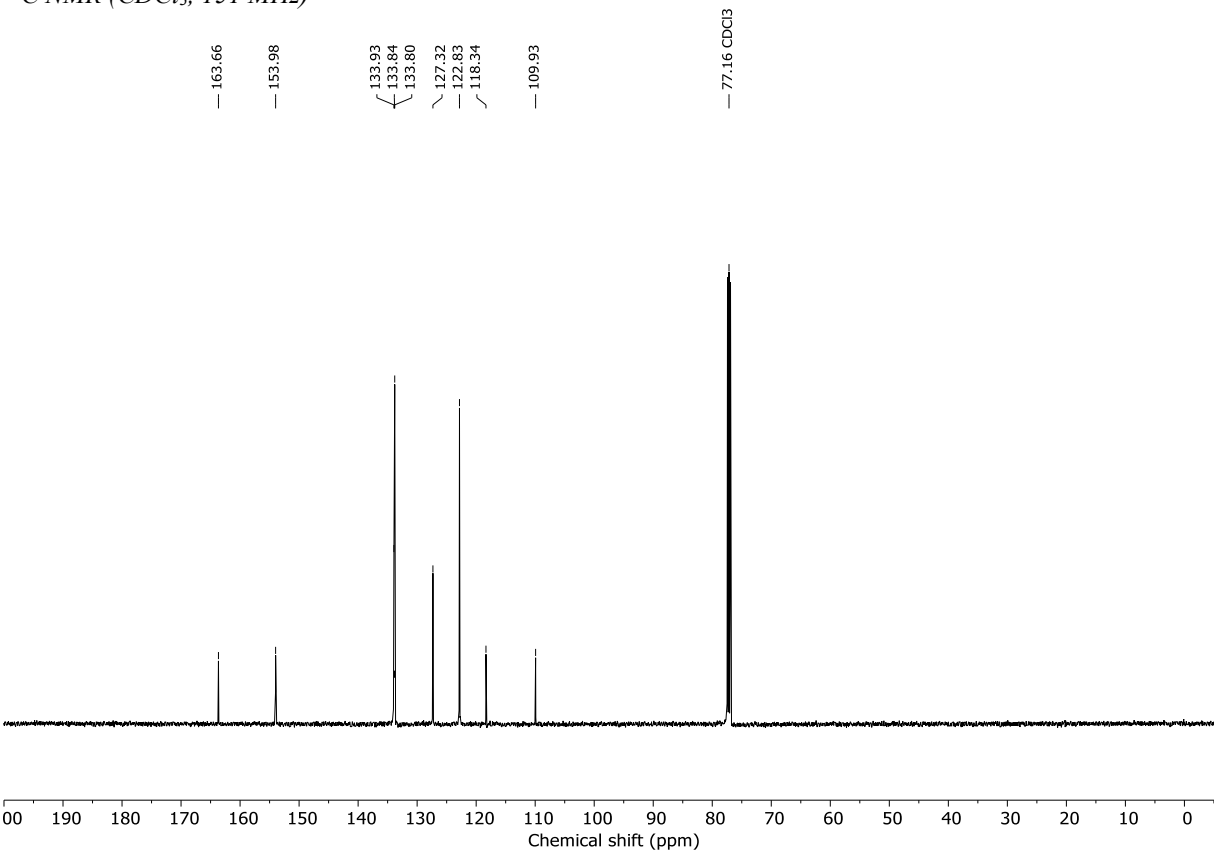

1-(phenylsulfonyl)spiro[2.5]octane (12)

^{1}H NMR ($CDCl_3$, 400 MHz)

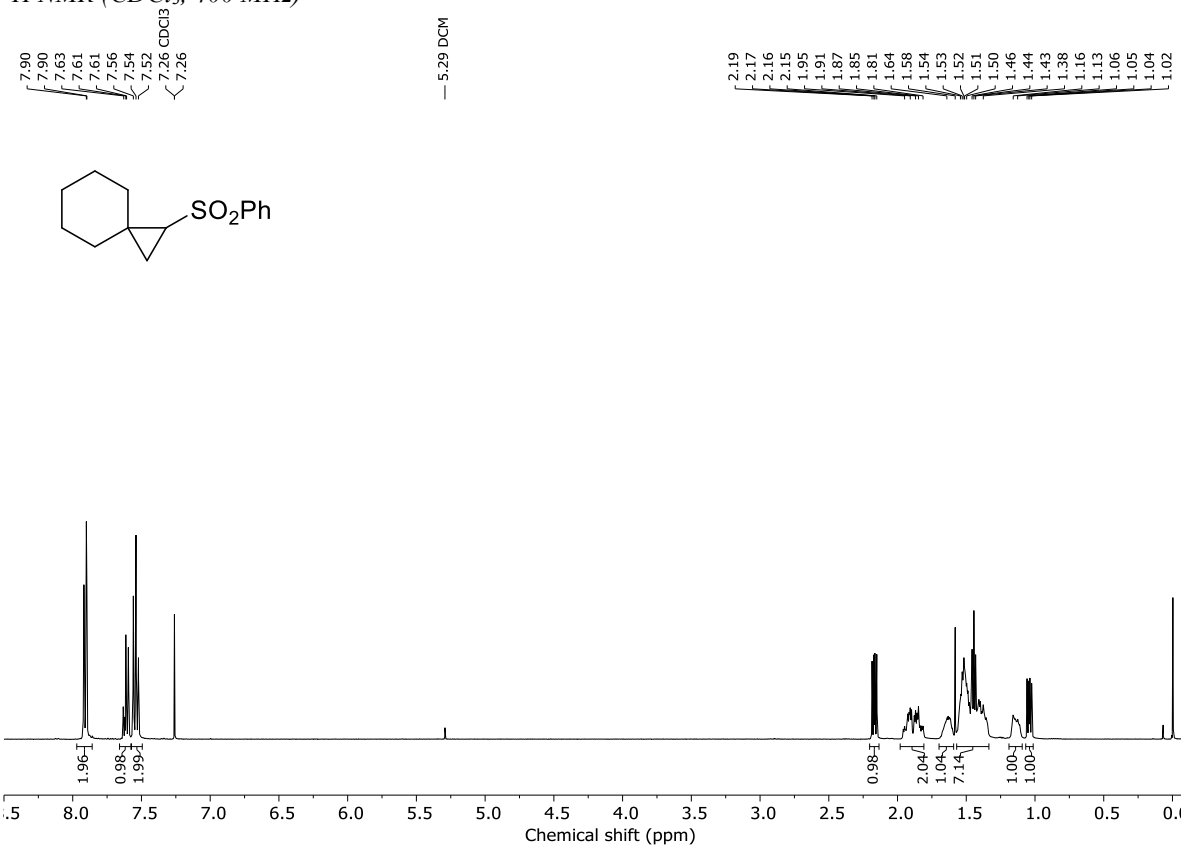

^{13}C NMR ($CDCl_3$, 126 MHz)

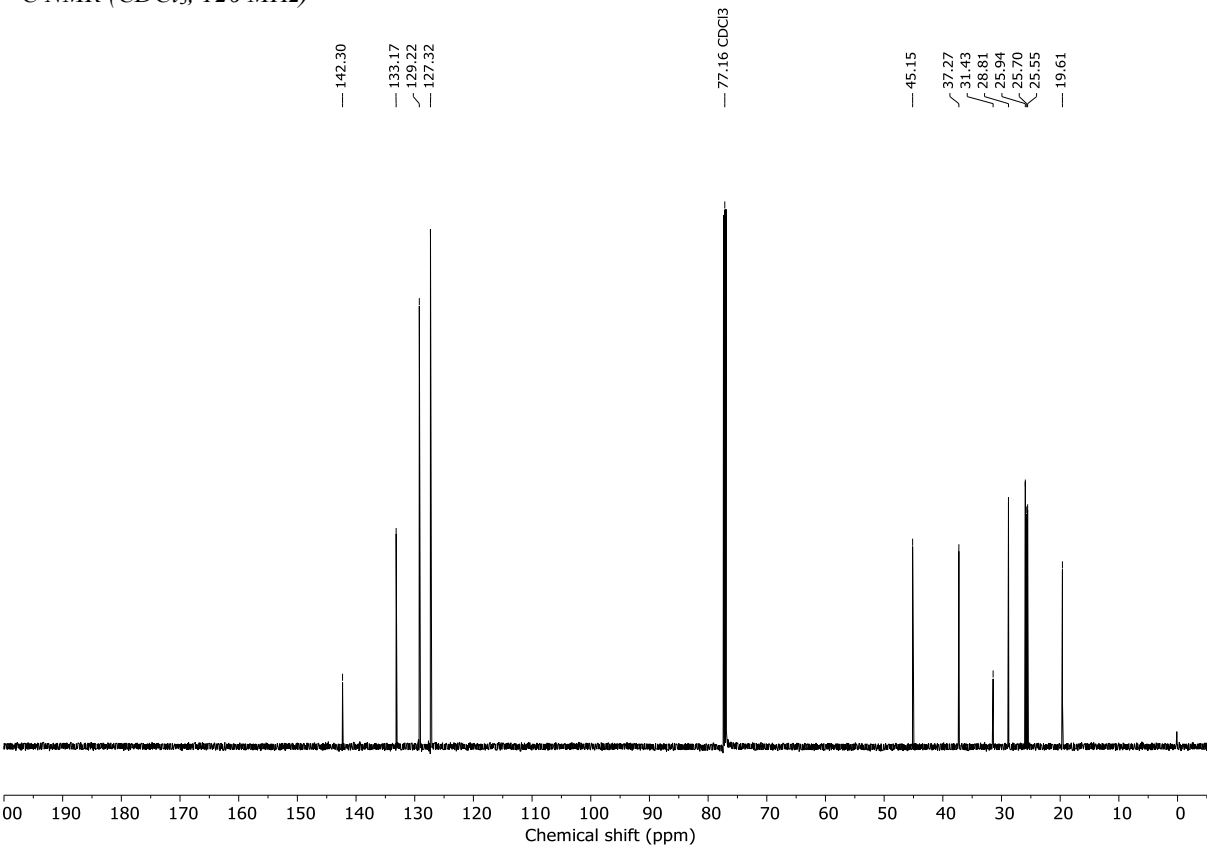

1-(phenylsulfonyl)spiro[2.3]hexane (24)

^{1}H NMR ($CDCl_3$, 500 MHz)

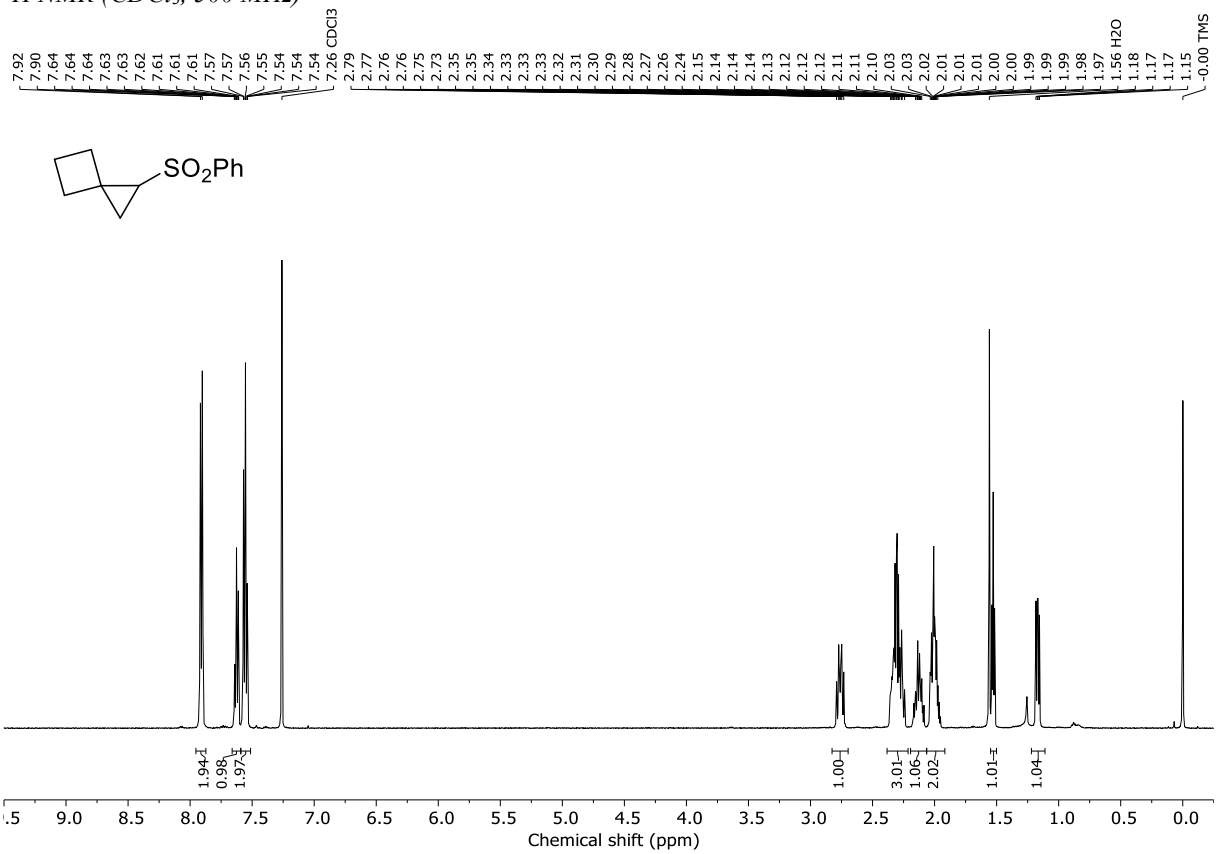

^{13}C NMR ($CDCl_3$, 126 MHz)

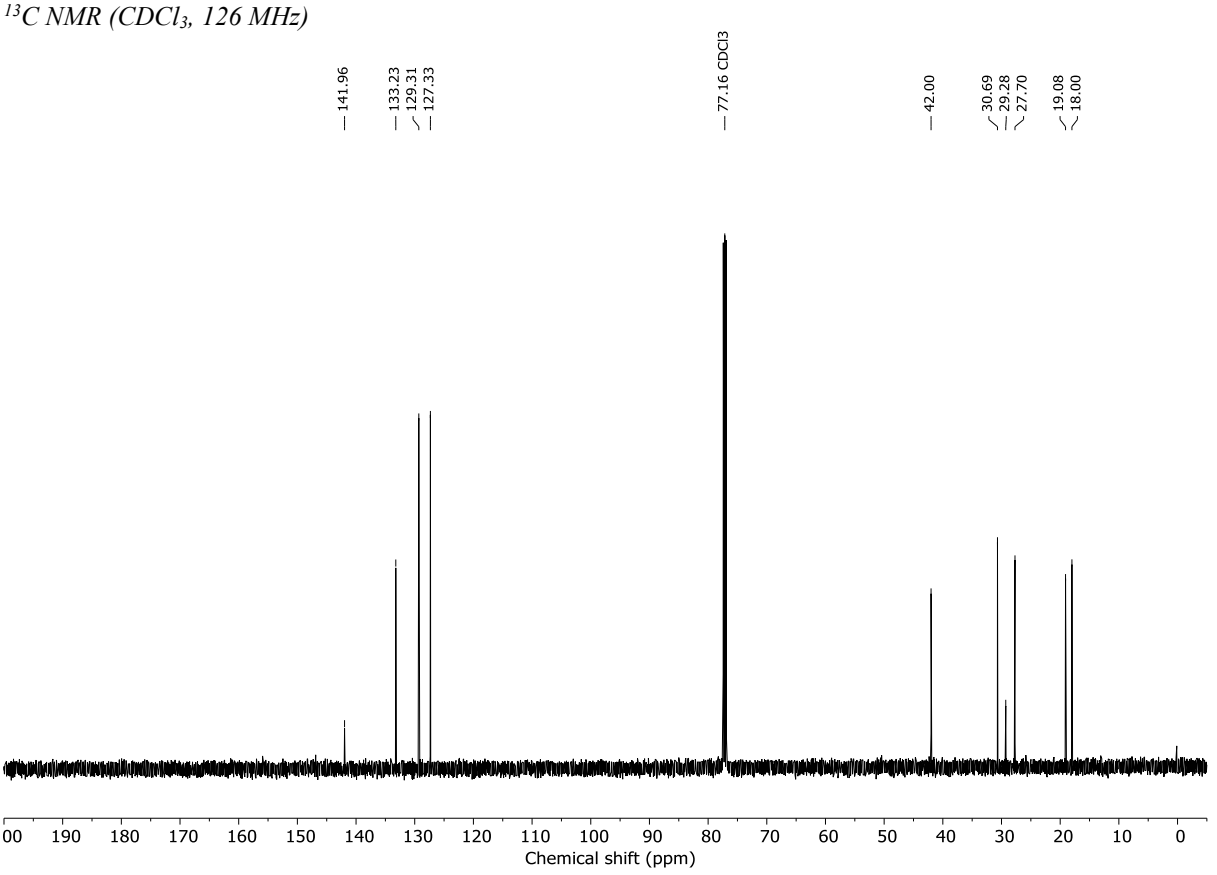

1-(phenylsulfonyl)spiro[2.4]heptane (25)

^{1}H NMR ($CDCl_3$, 500 MHz)

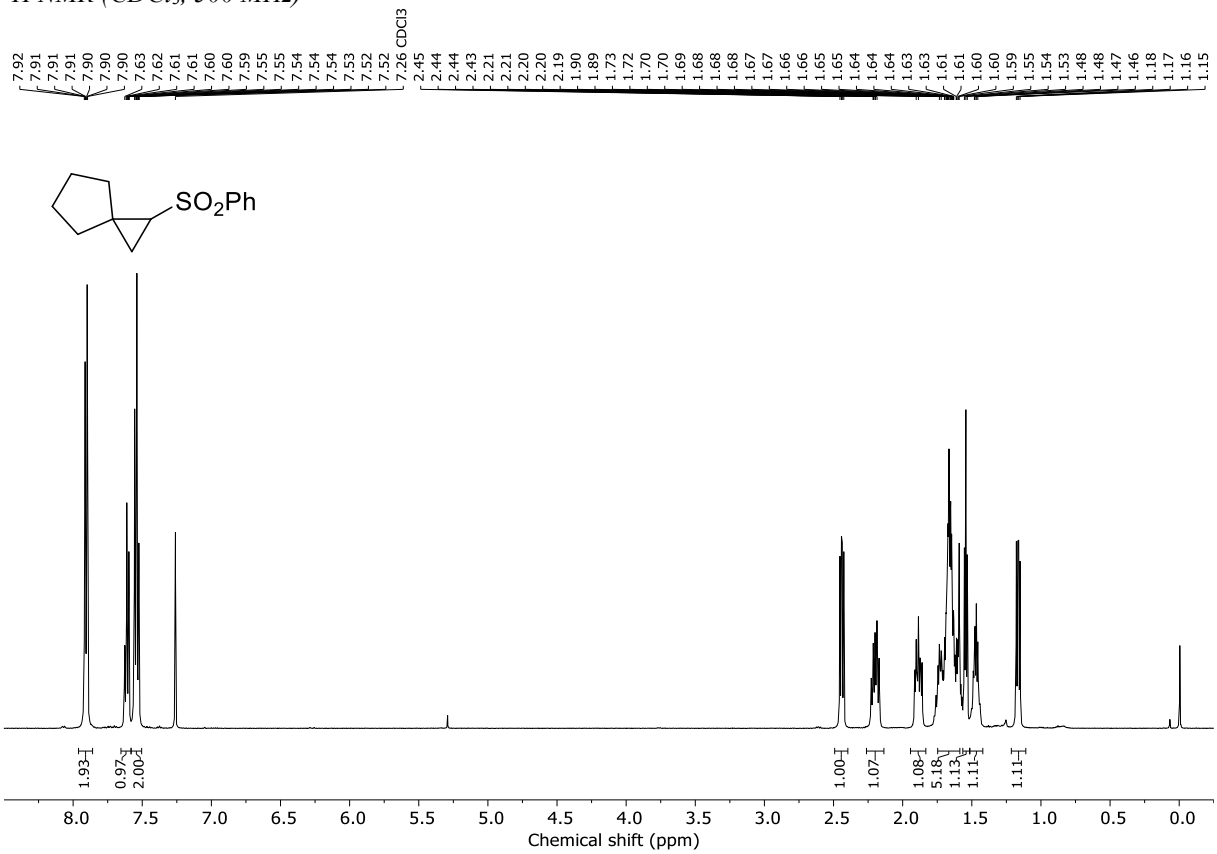

^{13}C NMR ($CDCl_3$, 126 MHz)

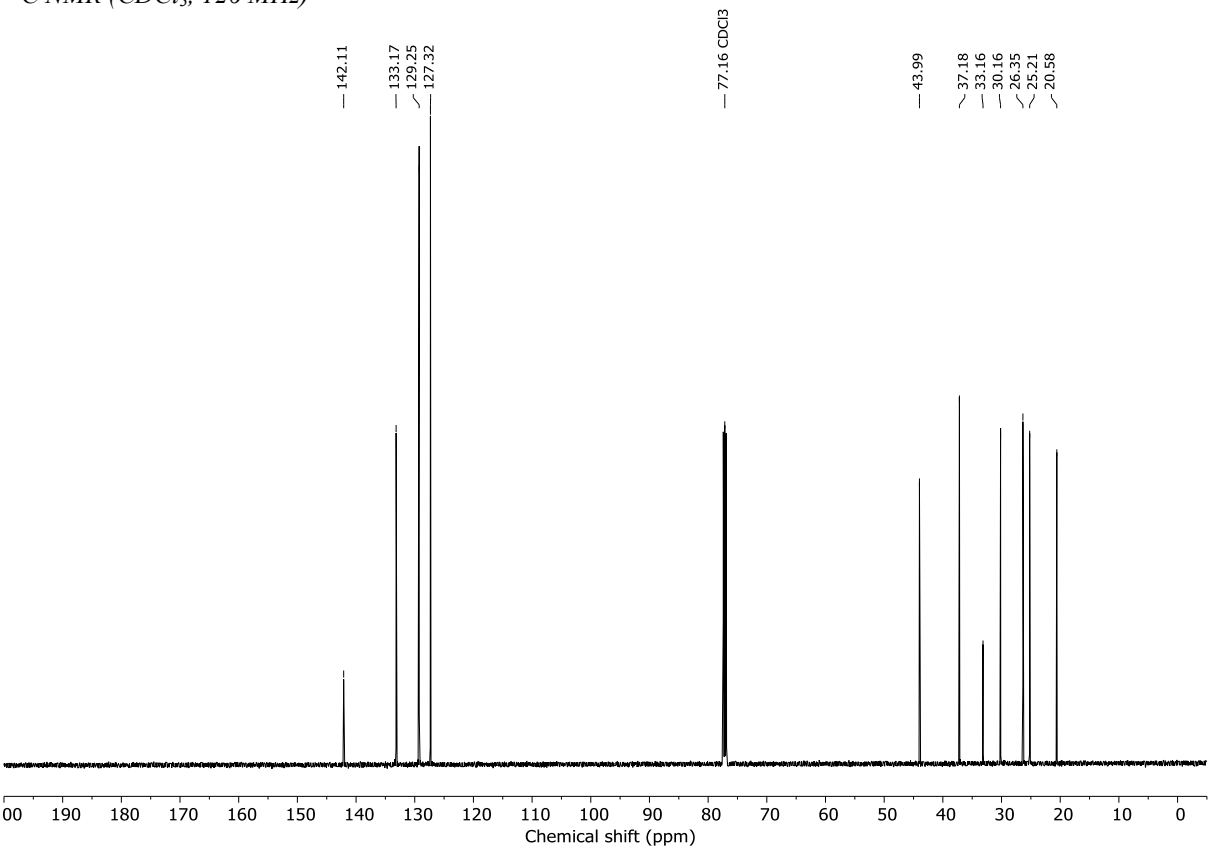

1-(phenylsulfonyl)spiro[2.6]nonane (26)

^{1}H NMR ($CDCl_3$, 600 MHz)

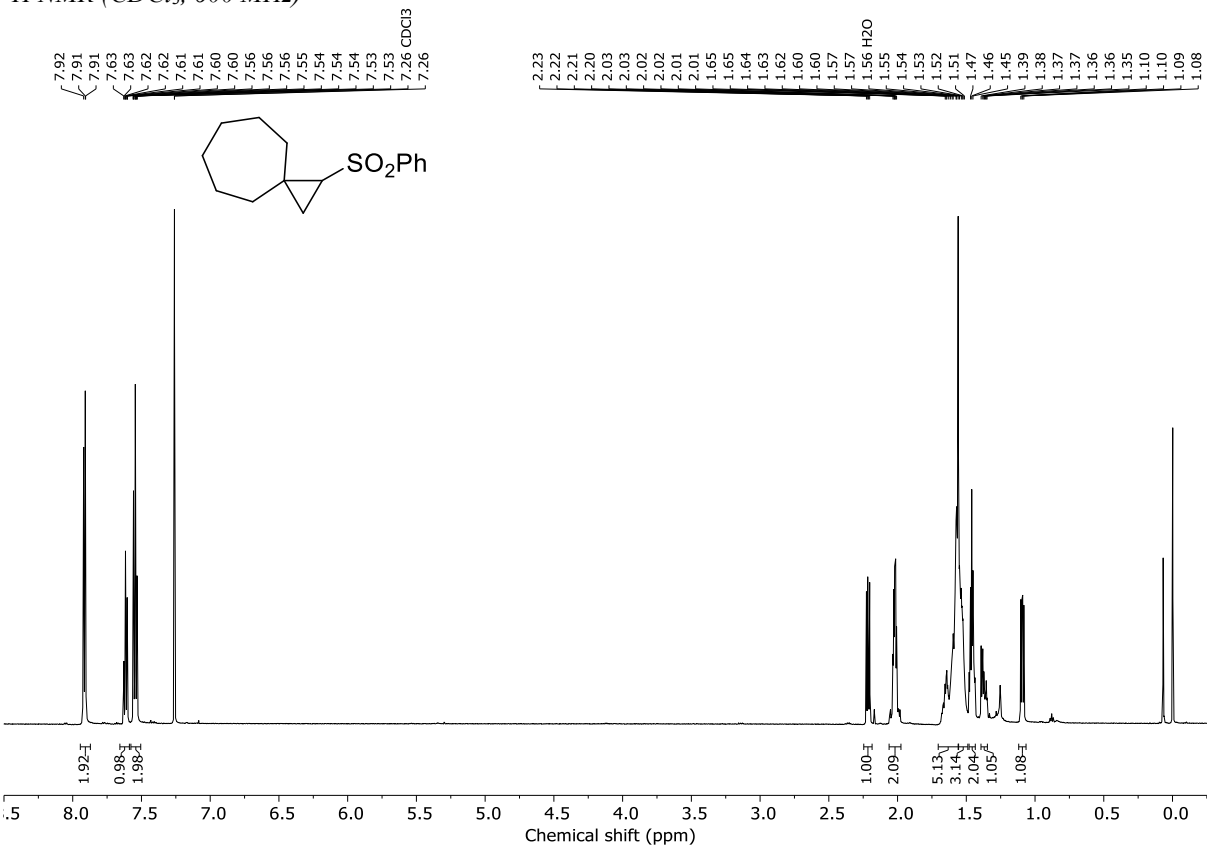

^{13}C NMR ($CDCl_3$, 151 MHz)

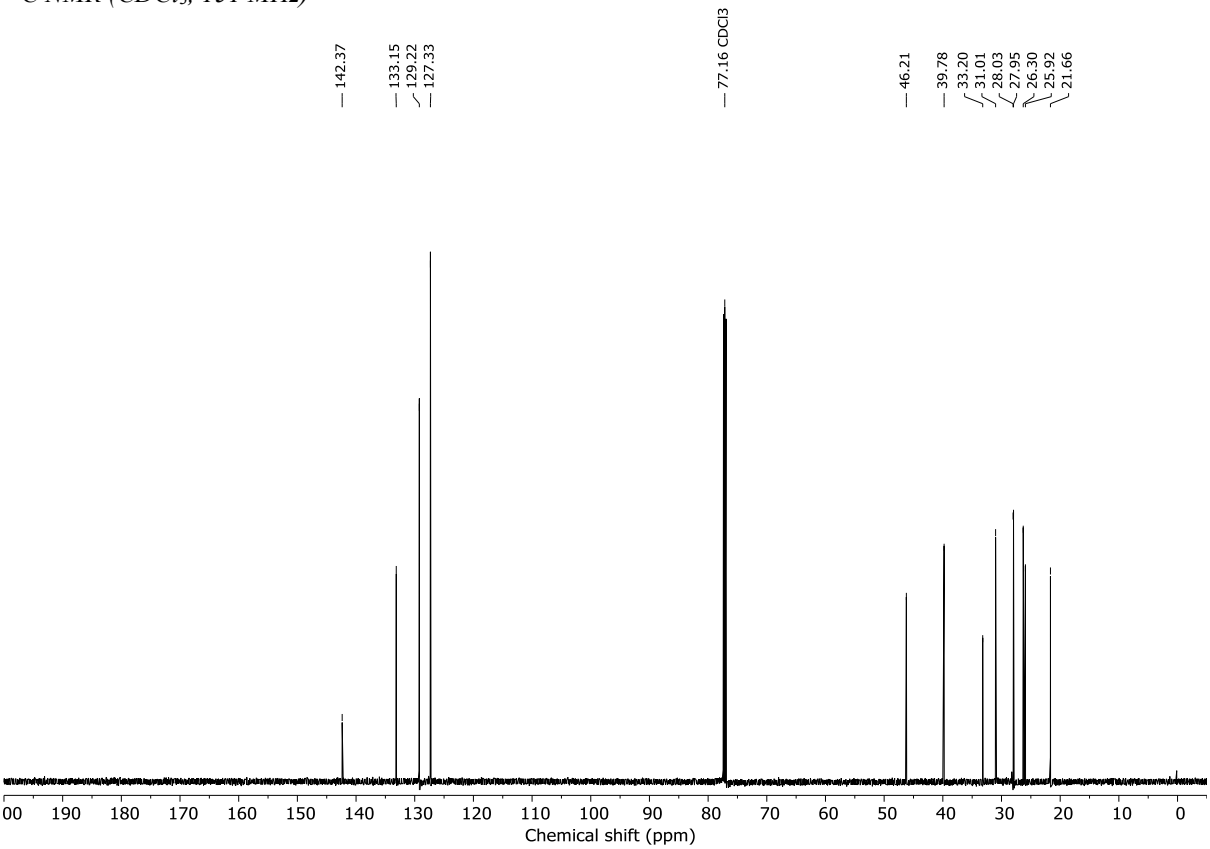

1-(phenylsulfonyl)spiro[2.11]tetradecane (27)

^{1}H NMR ($CDCl_3$, 500 MHz)

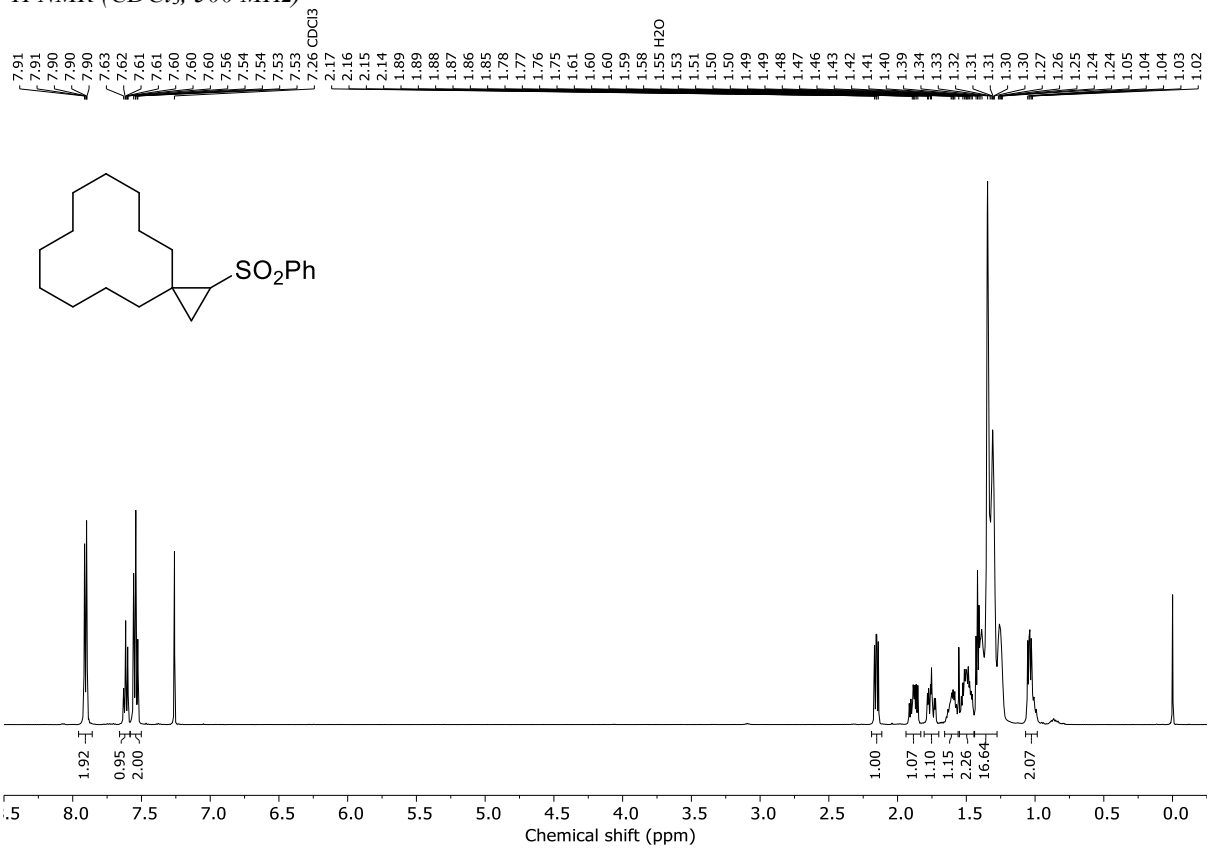

^{13}C NMR ($CDCl_3$, 126 MHz)

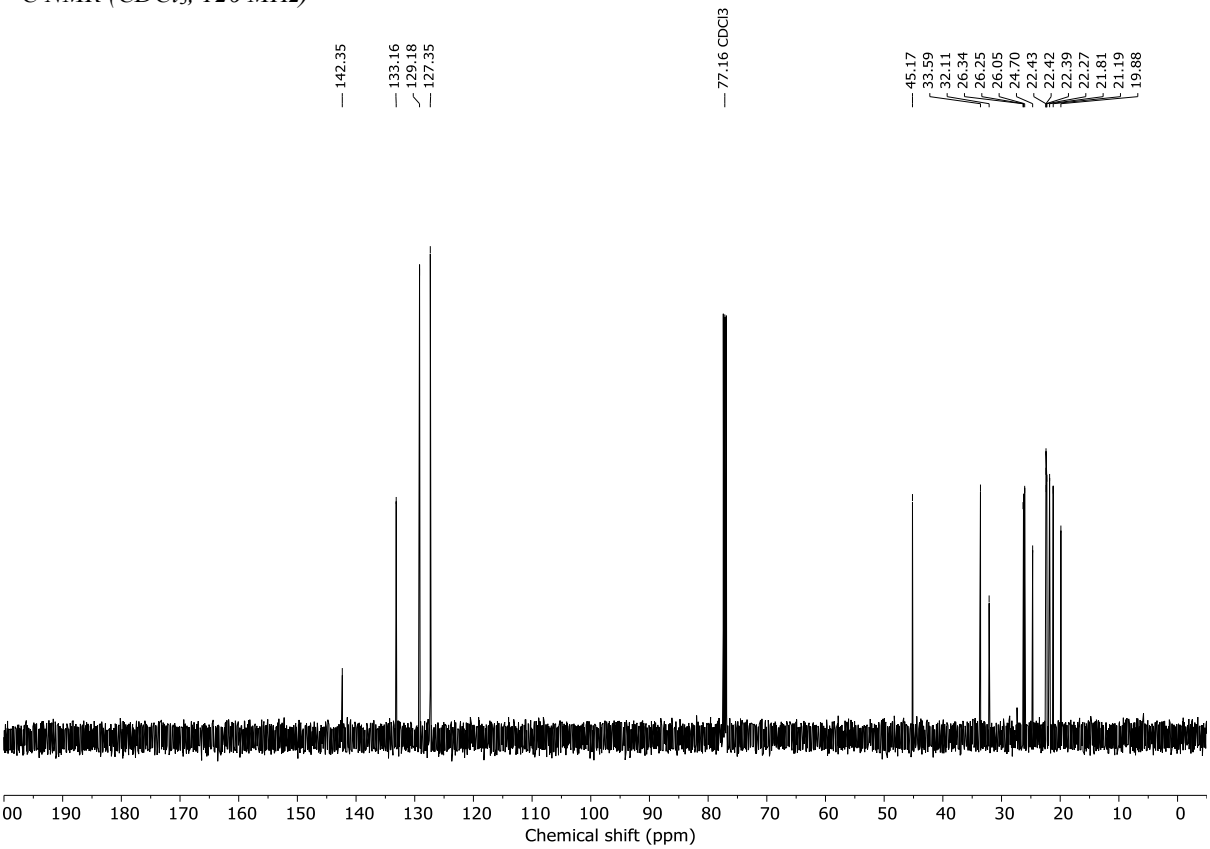

(1R,3S,5R,7R)-2'-(phenylsulfonyl)spiro[adamantane-2,1'-cyclopropane] (28)

^{1}H NMR ($CDCl_3$, 500 MHz)

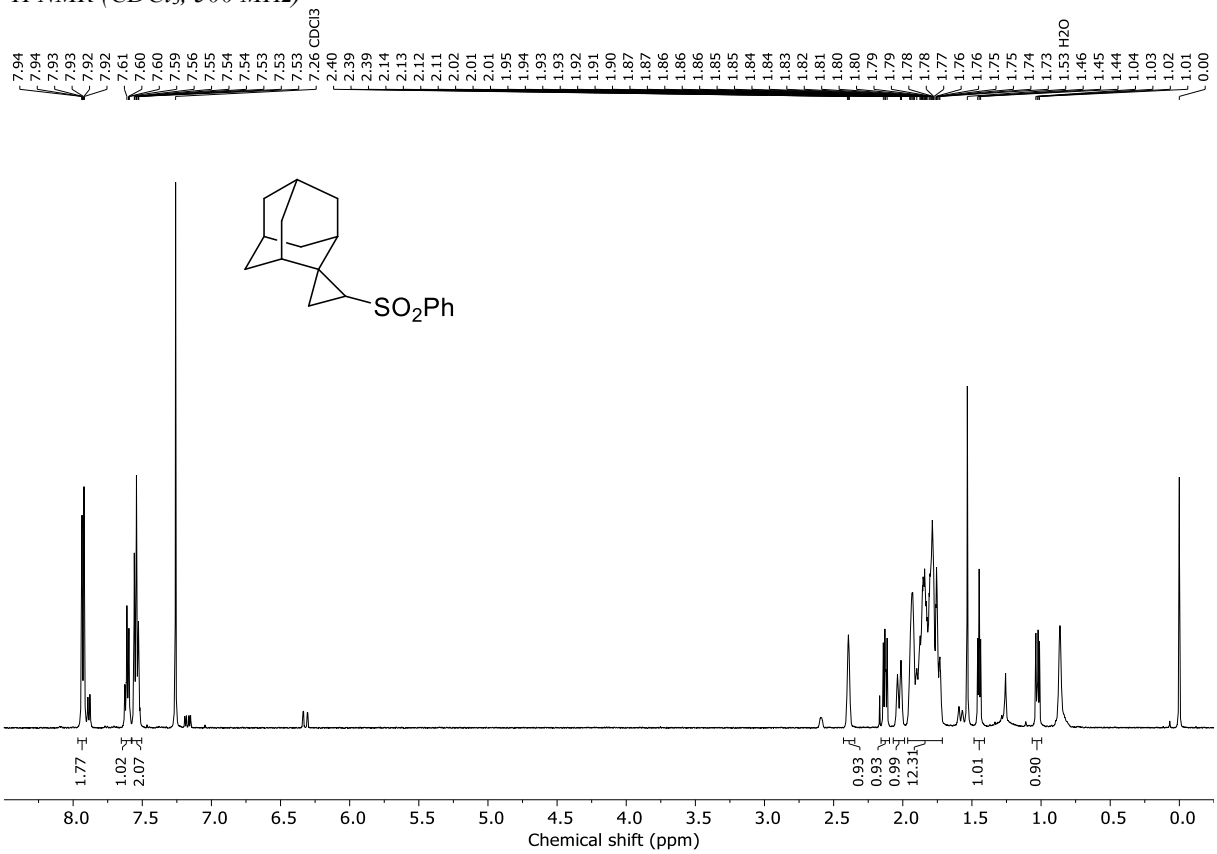

^{13}C NMR ($CDCl_3$, 126 MHz)

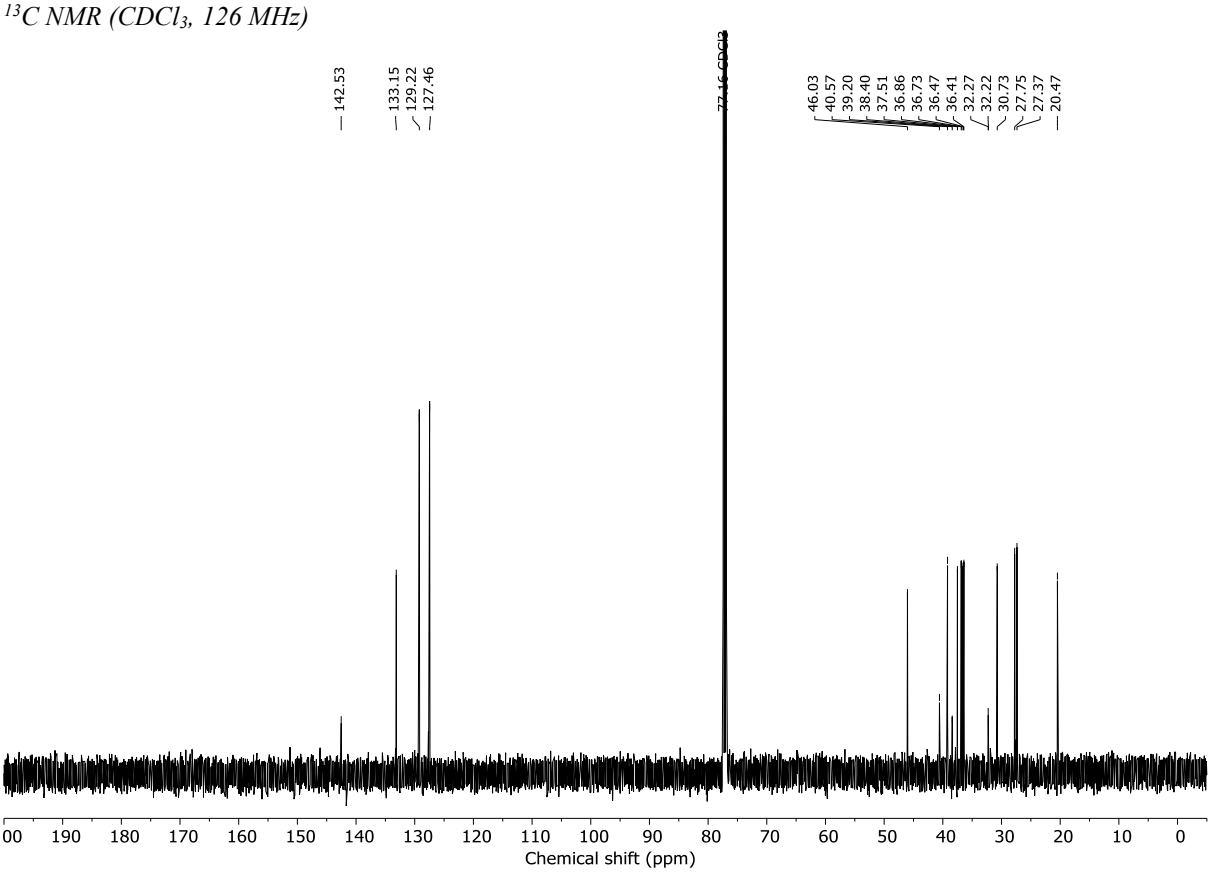

1-methyl-2-(phenylsulfonyl)-1,1'-bi(cyclopropane) (29)

^{1}H NMR ($CDCl_3$, 500 MHz)

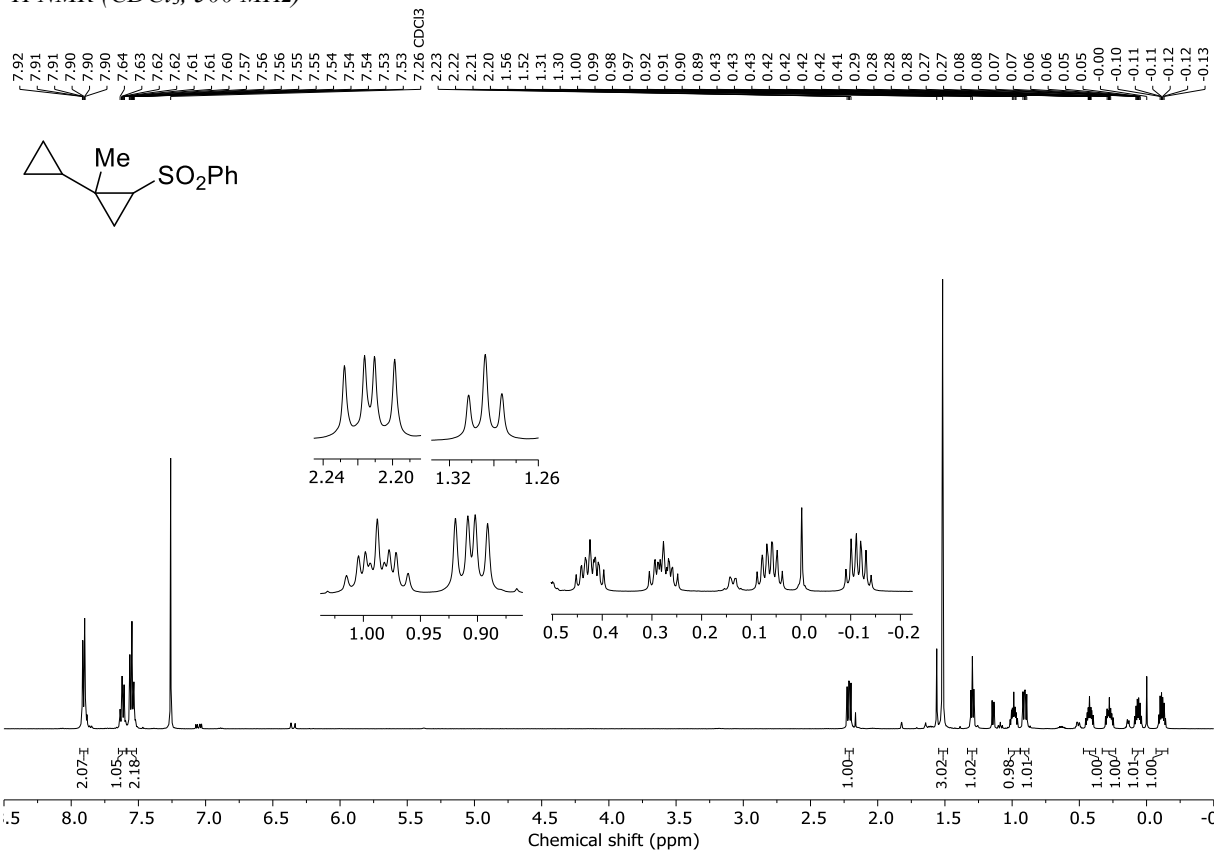

^{13}C NMR ($CDCl_3$, 126 MHz)

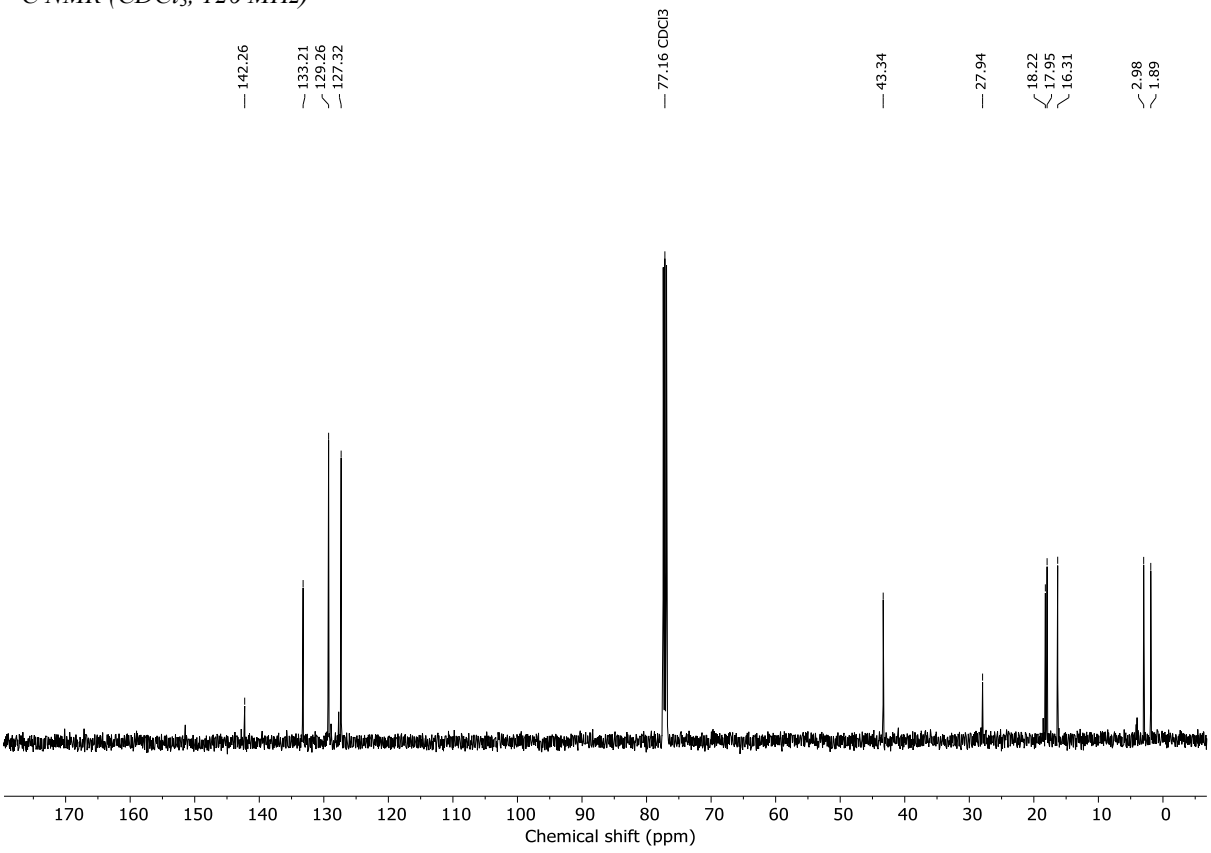

((2-(methoxymethyl)-2-methylcyclopropyl)sulfonyl)benzene (30)

^{1}H NMR ($CDCl_3$, 500 MHz)

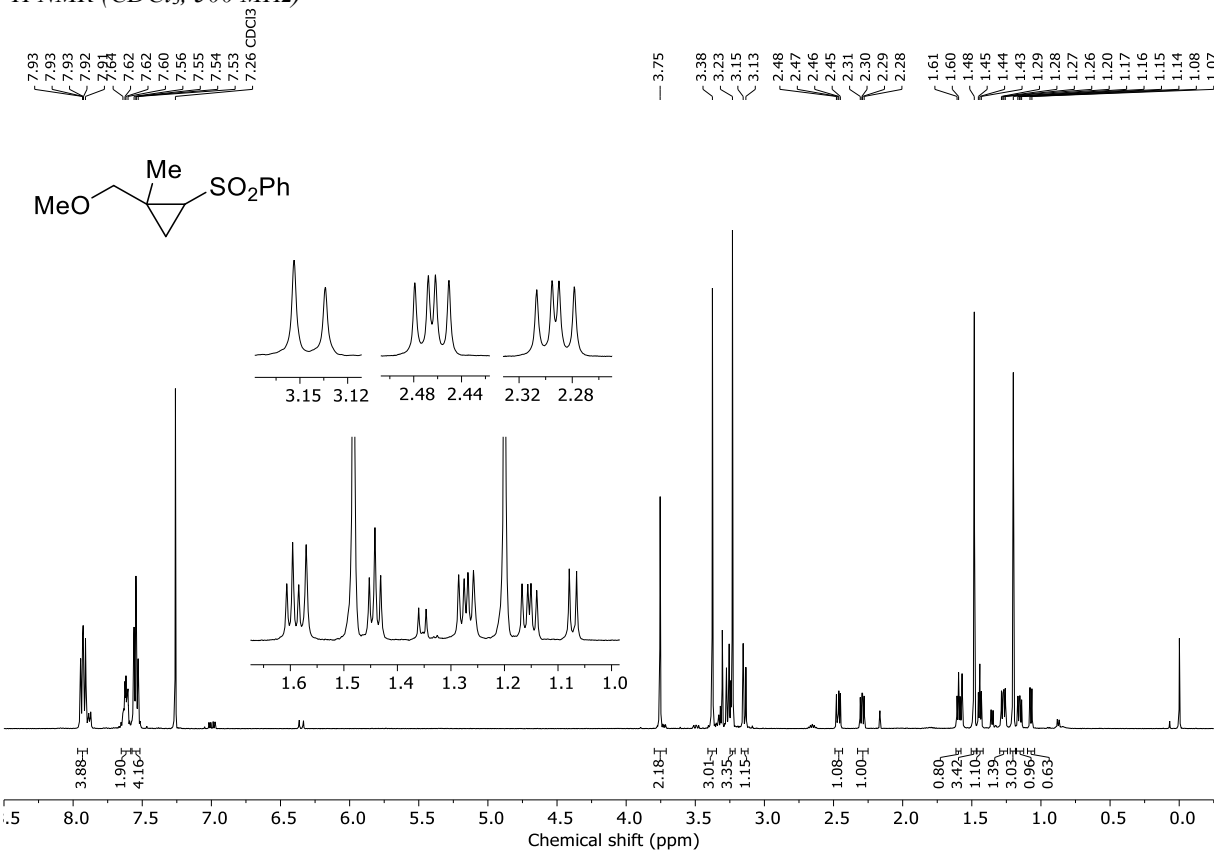

^{13}C NMR ($CDCl_3$, 126 MHz)

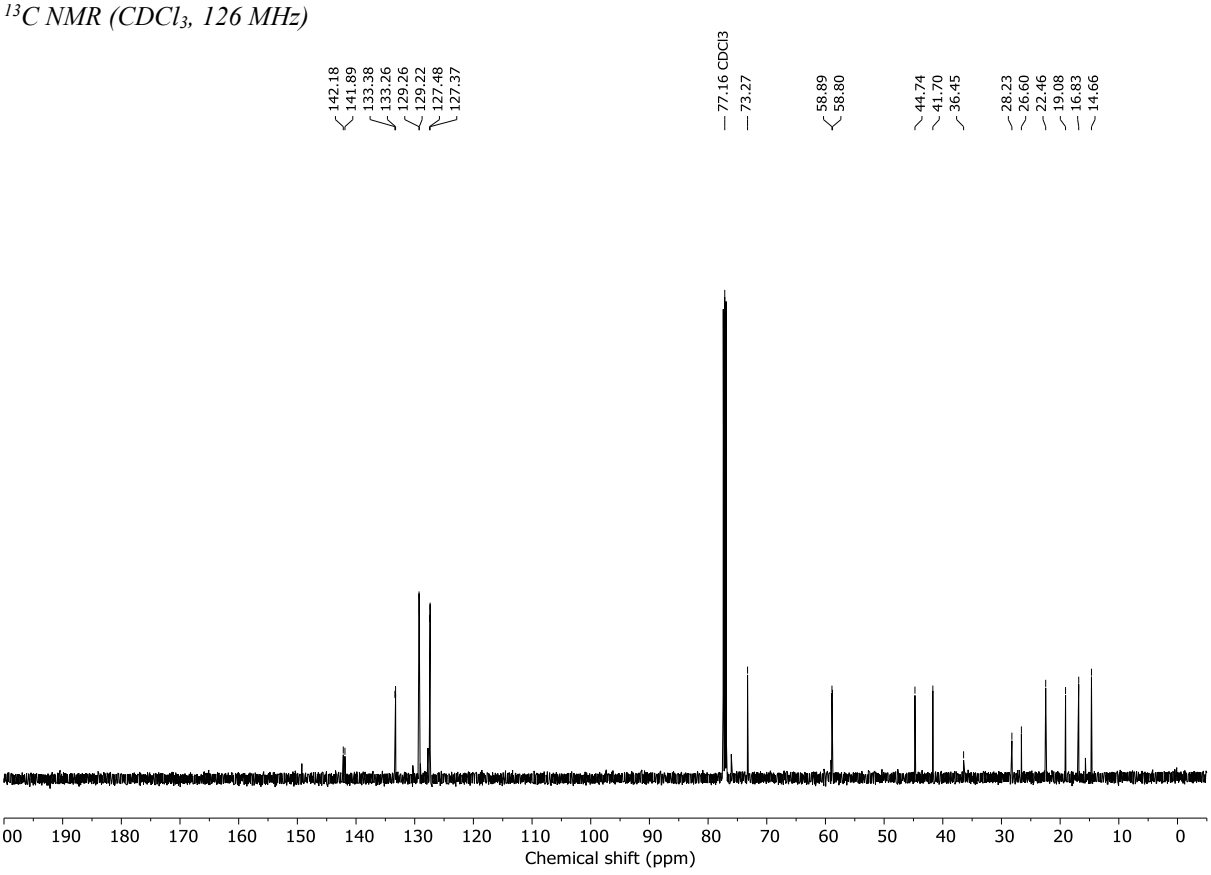

diethyl ((1-methyl-2-(phenylsulfonyl)cyclopropyl)methyl)phosphonate (31)

^{1}H NMR ($CDCl_3$, 500 MHz)

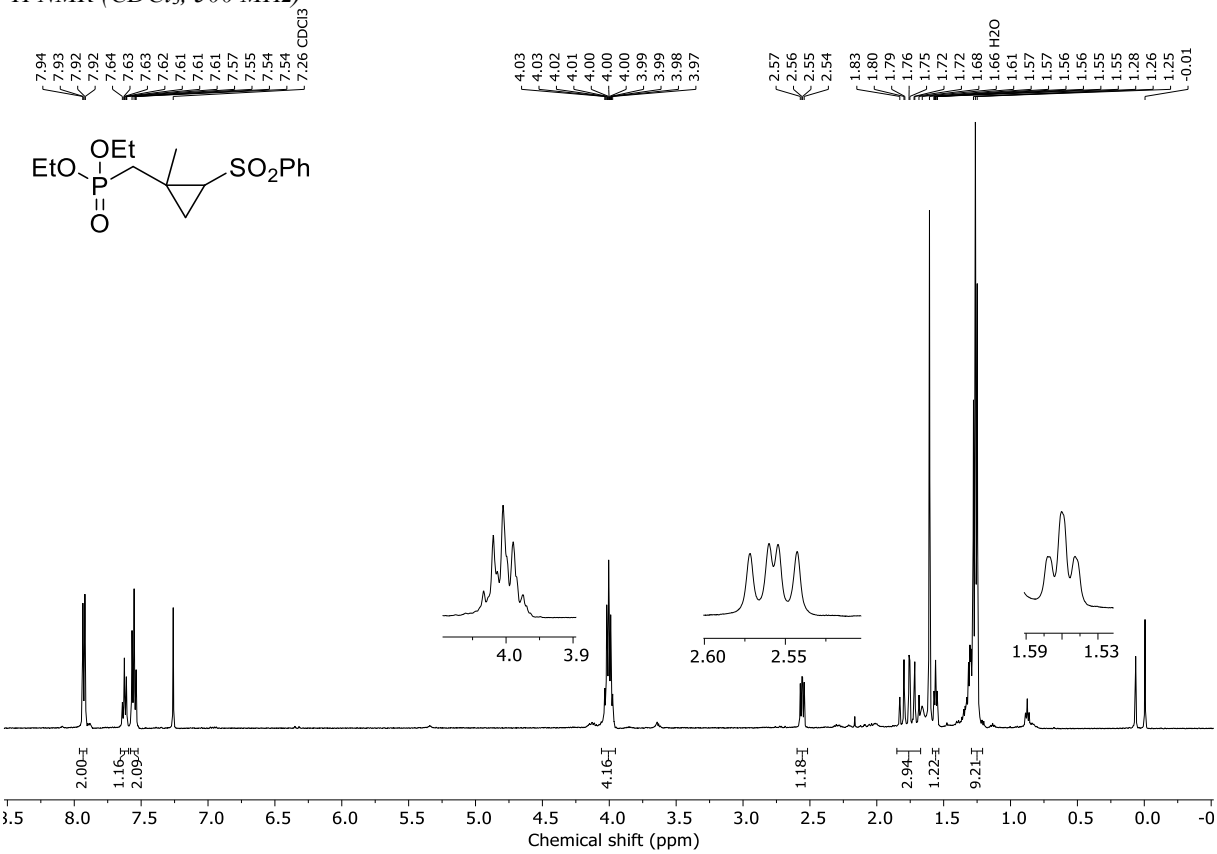

^{13}C NMR ($CDCl_3$, 126 MHz)

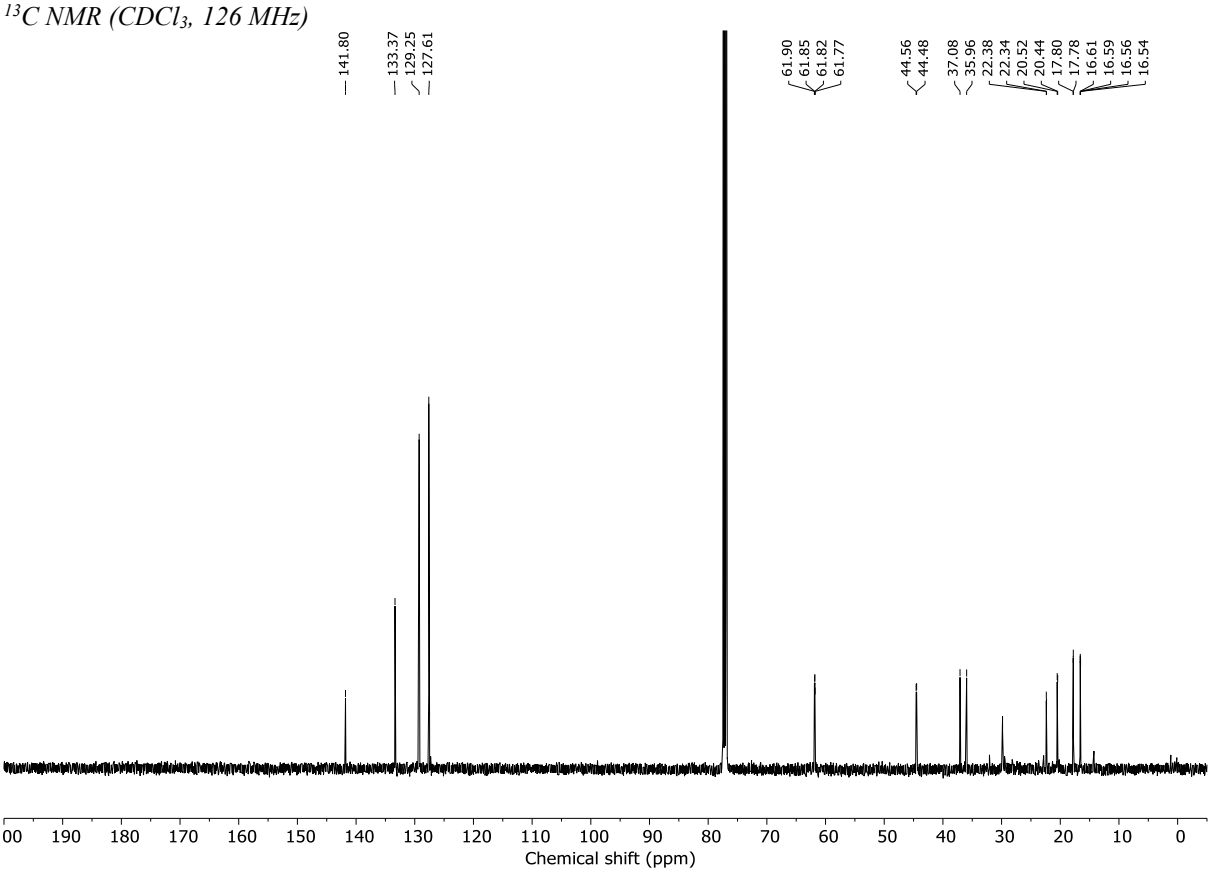

1-(phenylsulfonyl)-5-oxaspiro[2.3]hexane (32)

^{1}H NMR ($CDCl_3$, 500 MHz)

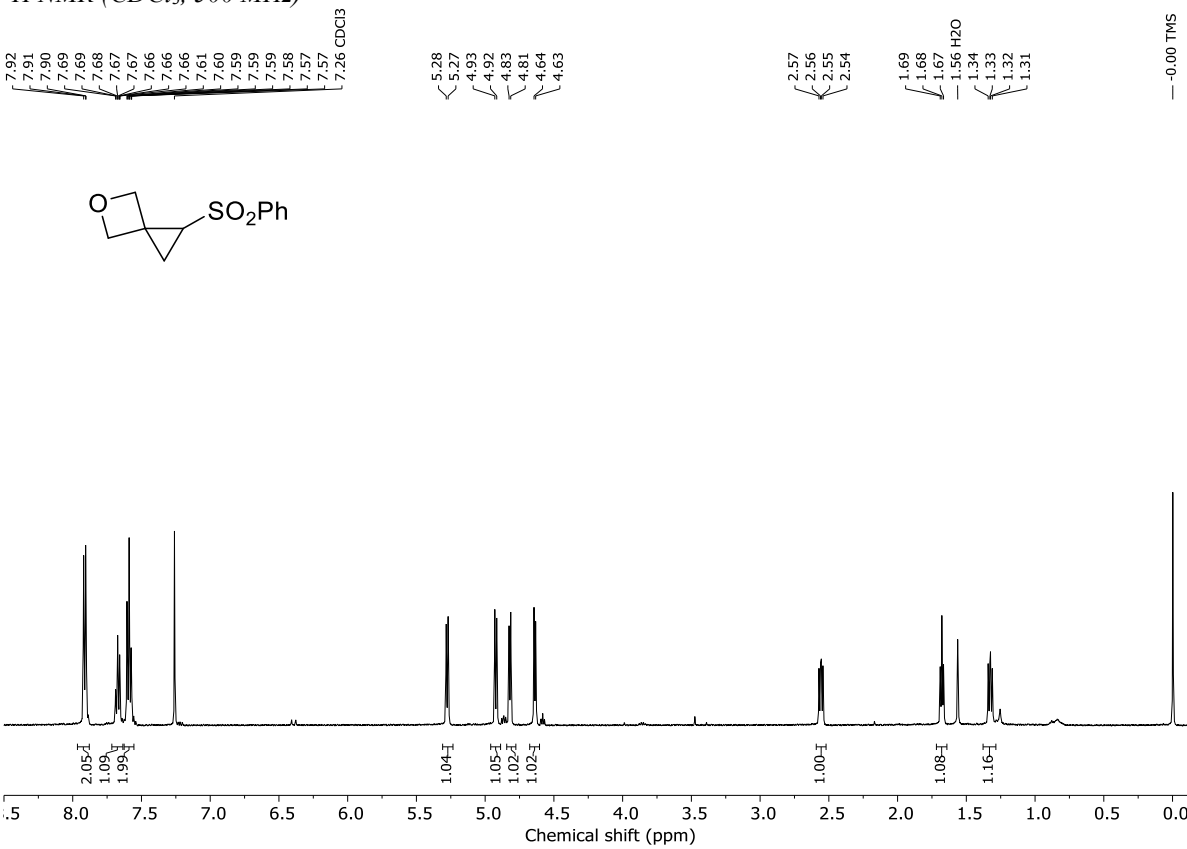

^{13}C NMR ($CDCl_3$, 126 MHz)

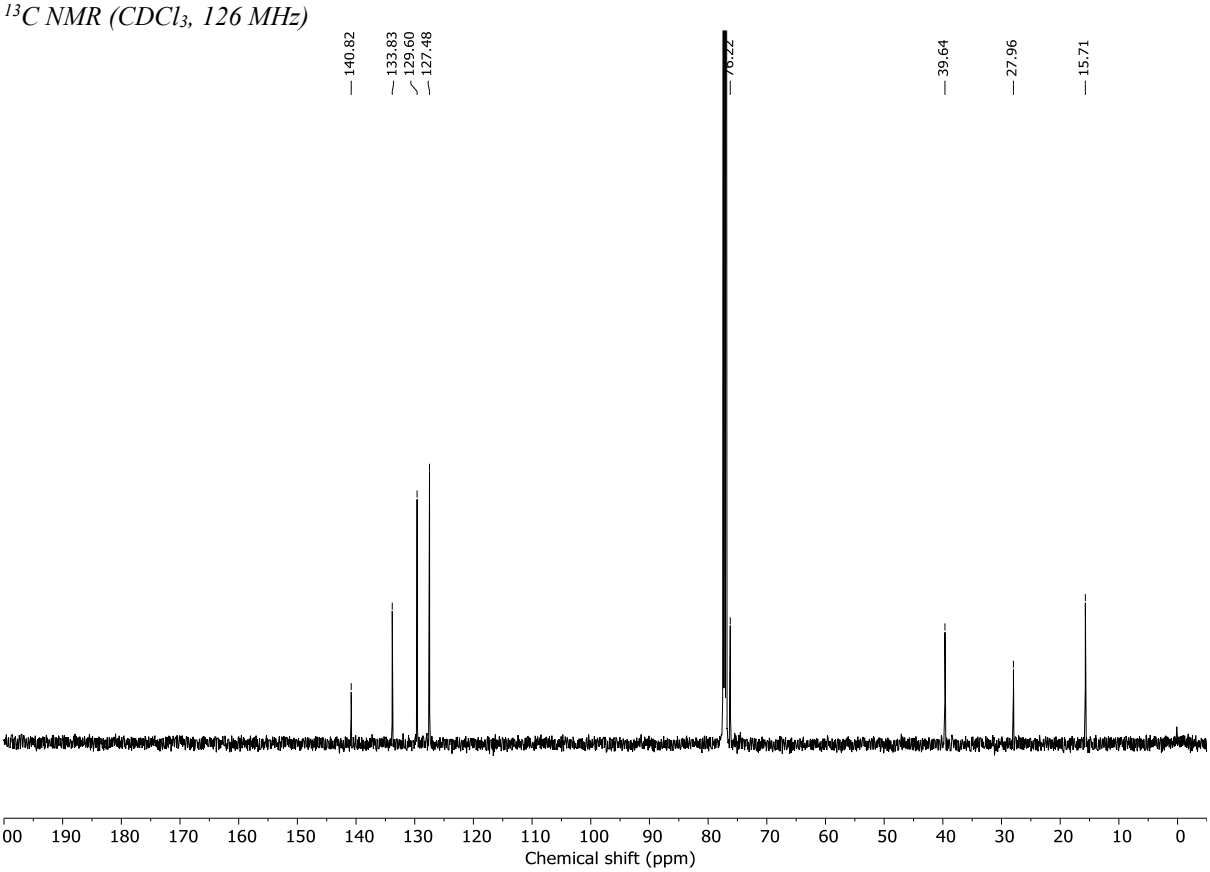

1-(phenylsulfonyl)-6-oxaspiro[2.5]octane (33)

^{1}H NMR ($CDCl_3$, 500 MHz)

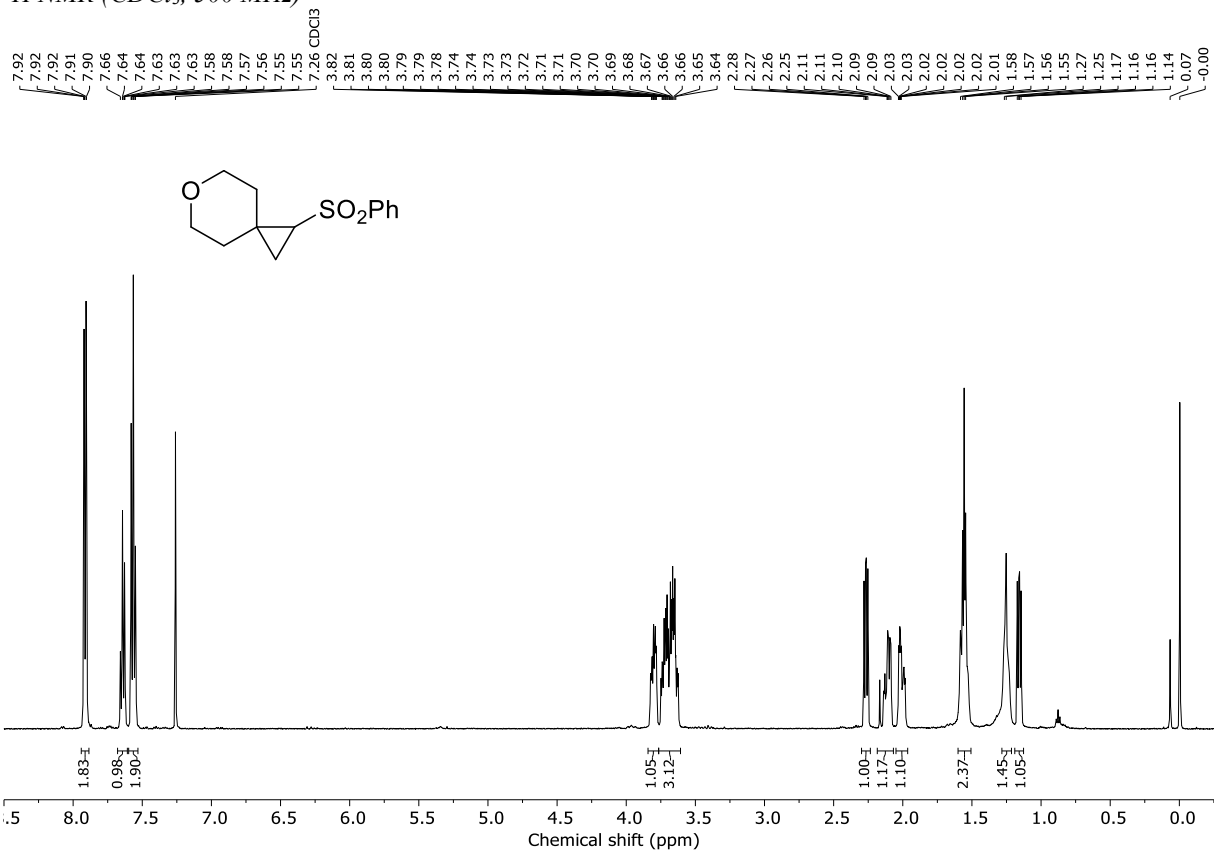

^{13}C NMR ($CDCl_3$, 126 MHz)

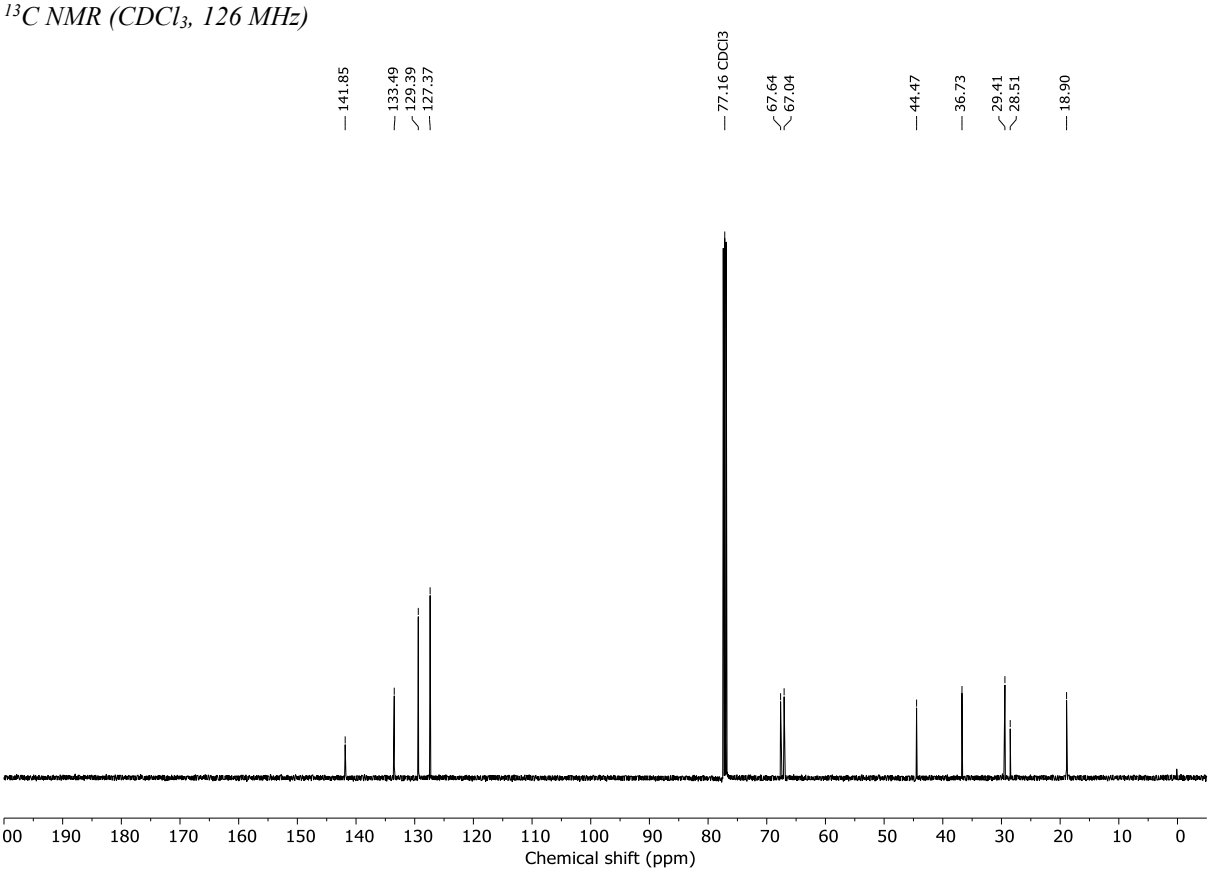

1-(phenylsulfonyl)-5-thiaspiro[2.4]heptane (34)

^{1}H NMR ($CDCl_3$, 600 MHz)

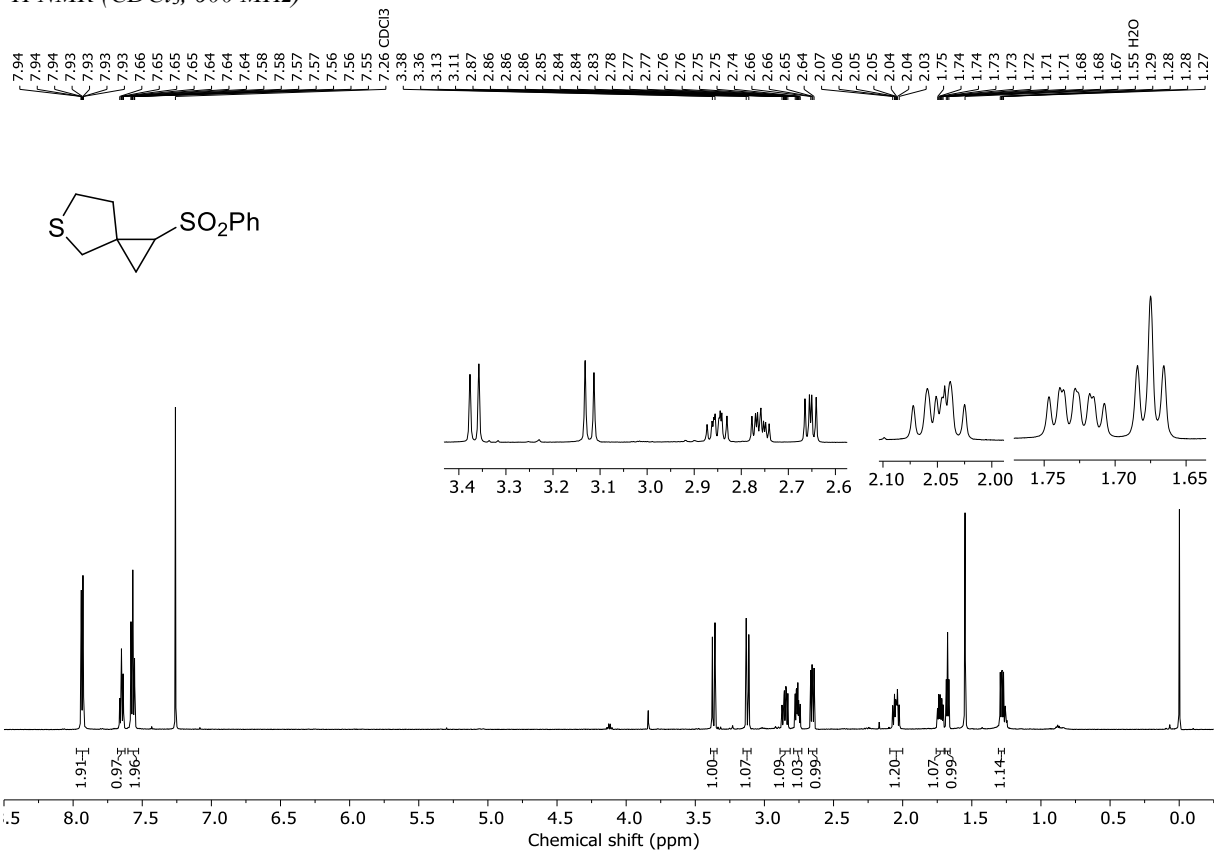

^{13}C NMR ($CDCl_3$, 151 MHz)

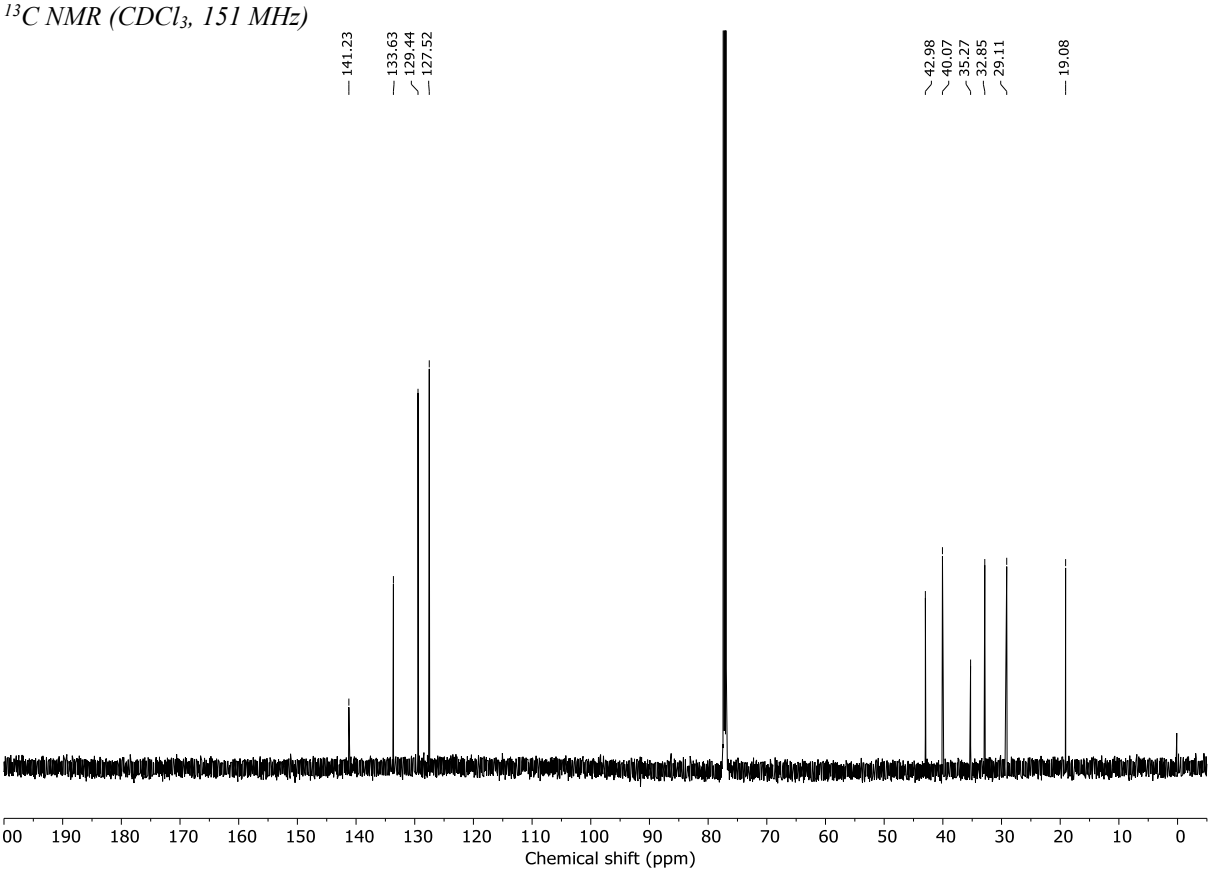

1-(phenylsulfonyl)-6-thiaspiro[2.5]octane (35)

^{1}H NMR ($CDCl_3$, 500 MHz)

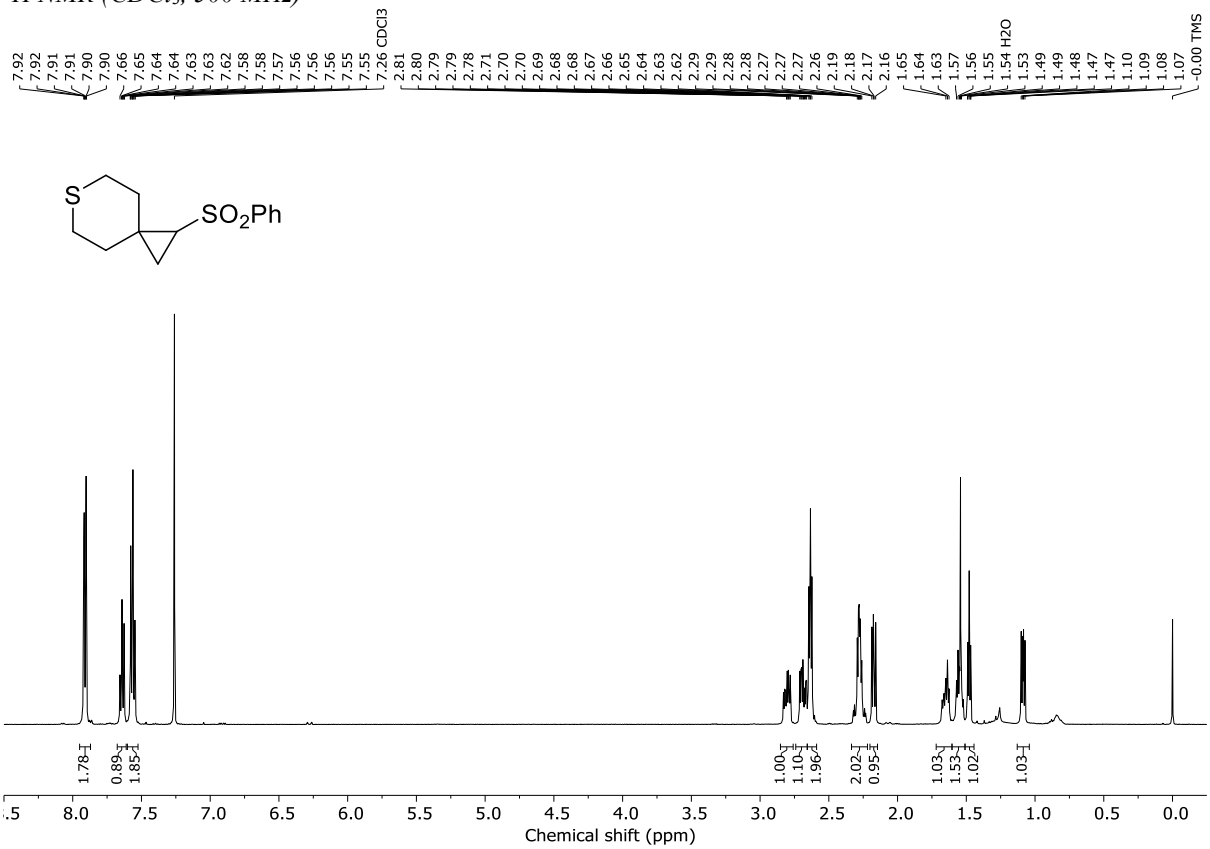

^{13}C NMR ($CDCl_3$, 126 MHz)

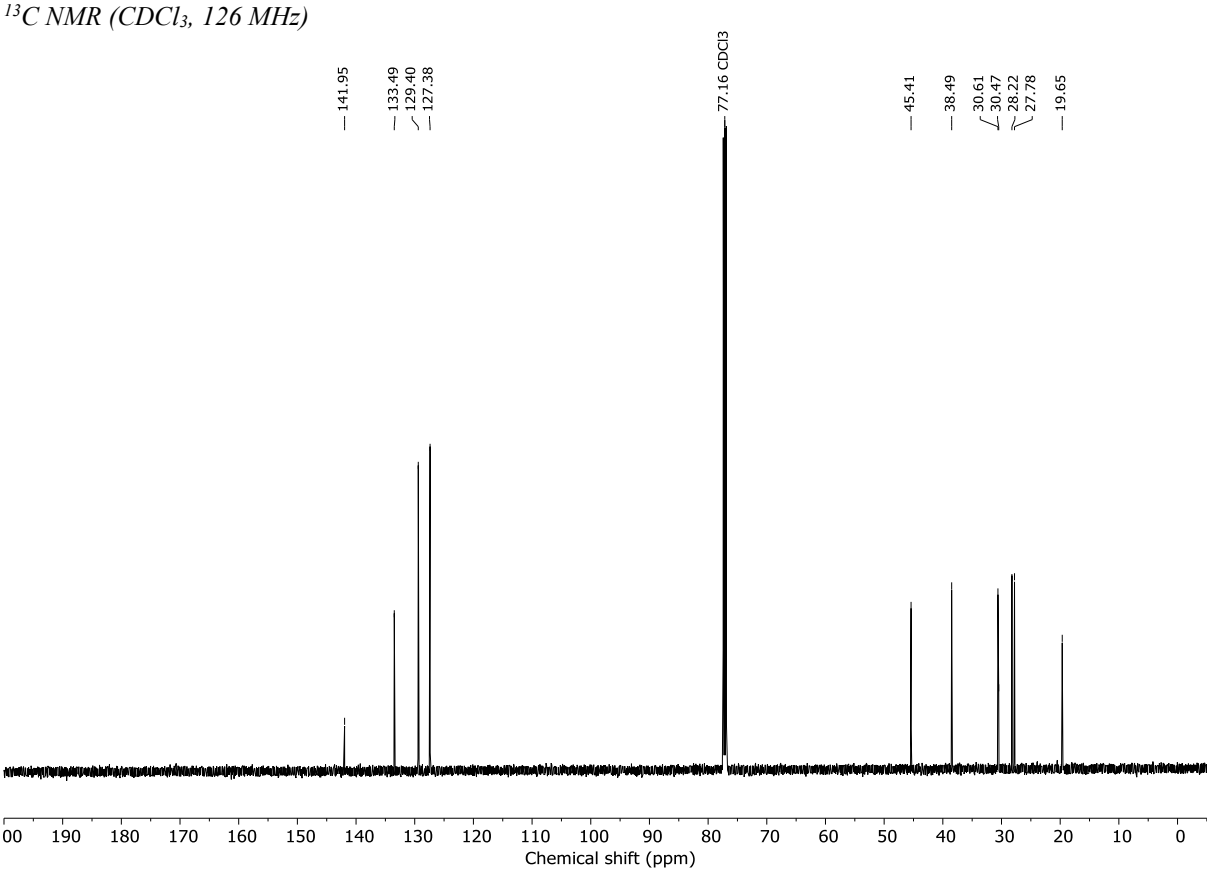

1-(phenylsulfonyl)-6-tosyl-6-azaspiro[2.5]octane (36)

^{1}H NMR ($CDCl_3$, 500 MHz)

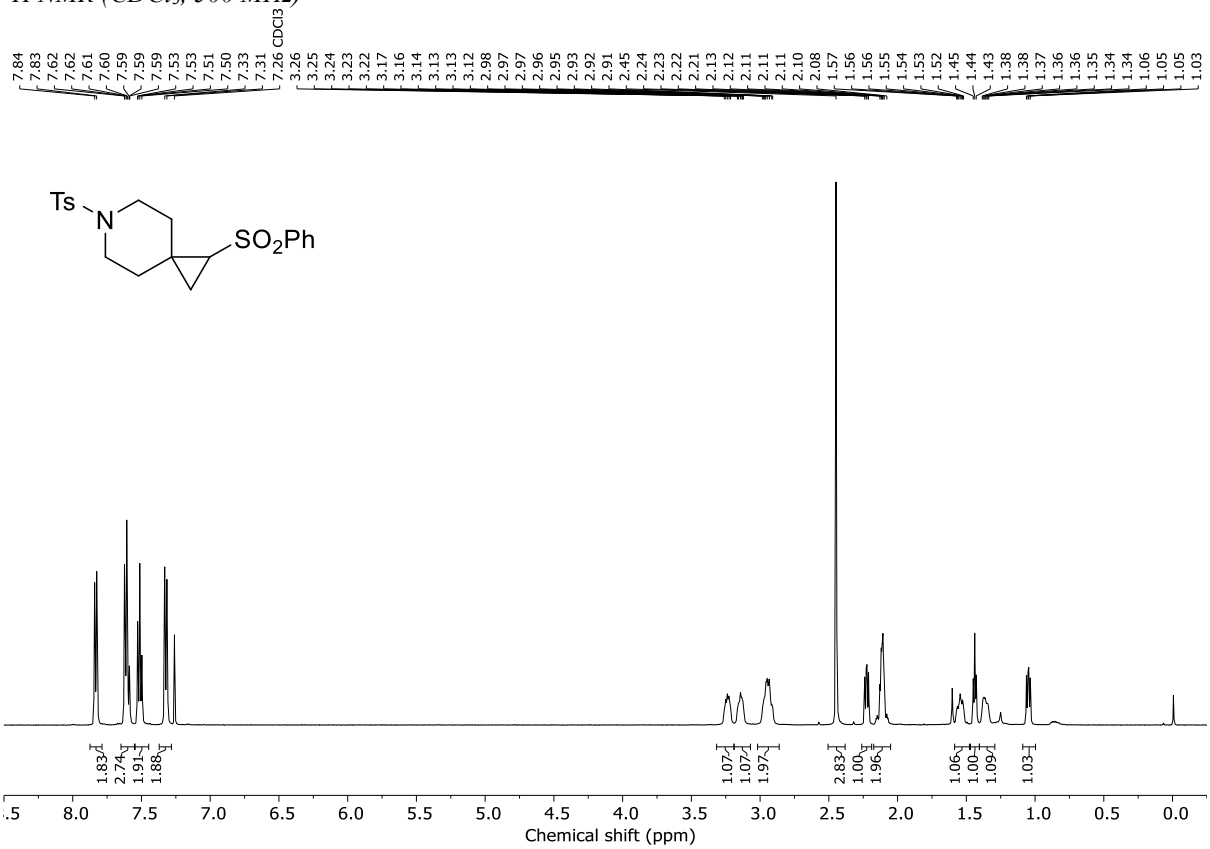

^{13}C NMR ($CDCl_3$, 126 MHz)

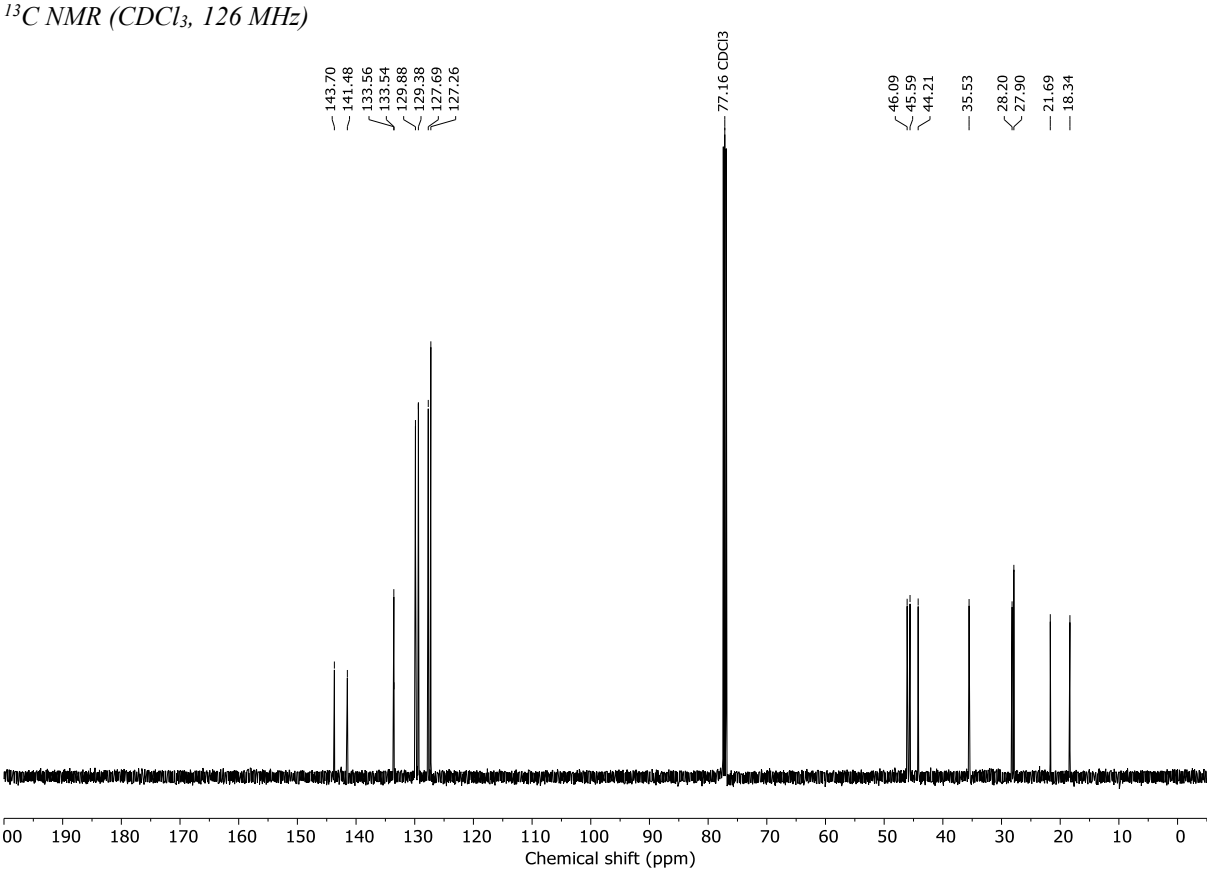

tert-butyl (1R,3S,5S)-2'-(phenylsulfonyl)-8-azaspiro[bicyclo[3.2.1]octane-3,1'-cyclopropane]-8-carboxylate (37)

^{1}H NMR (DMSO-d6, 70 ºC) 600 MHz

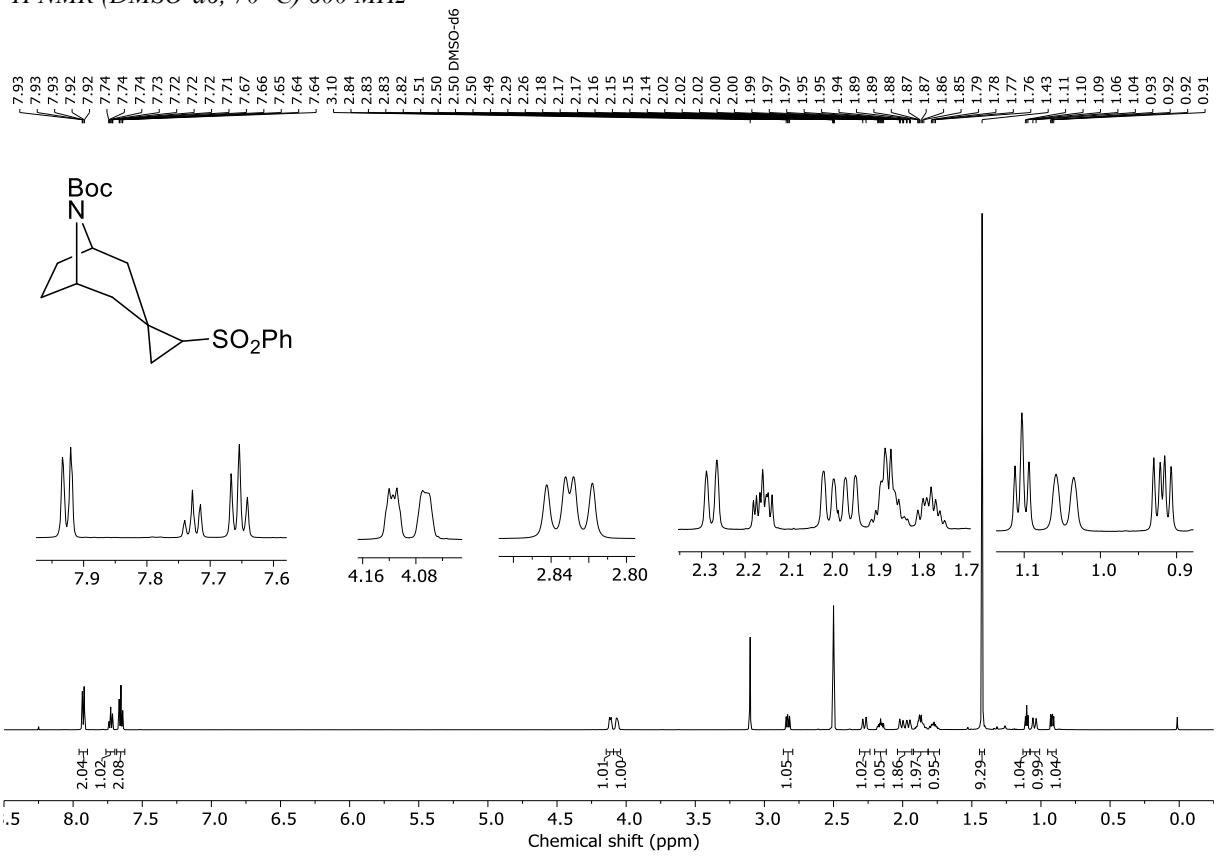

^{13}C NMR (DMSO-d6, 70 ºC) 151 MHz

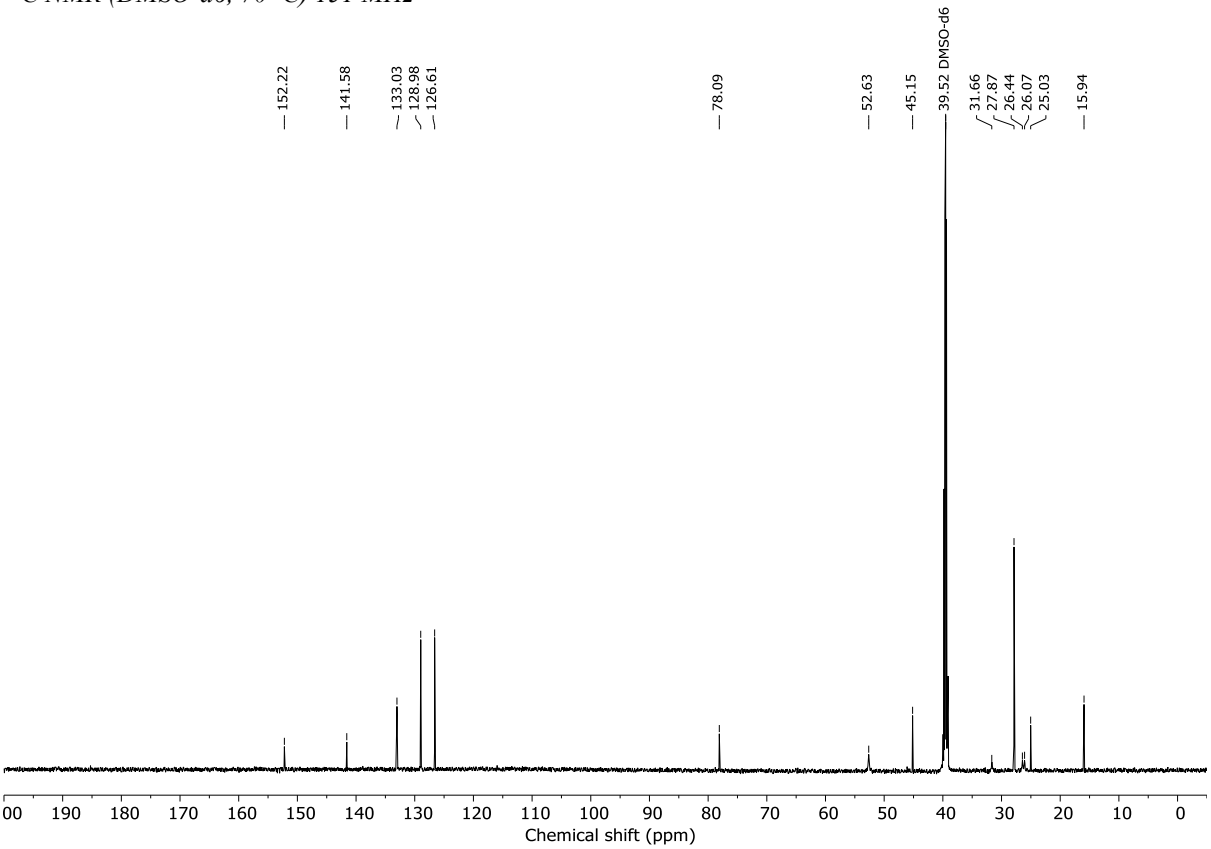

6,6-dimethyl-1-(phenylsulfonyl)-5,7-dioxaspiro[2.5]octane (38)

^{1}H NMR ($CDCl_3$, 500 MHz)

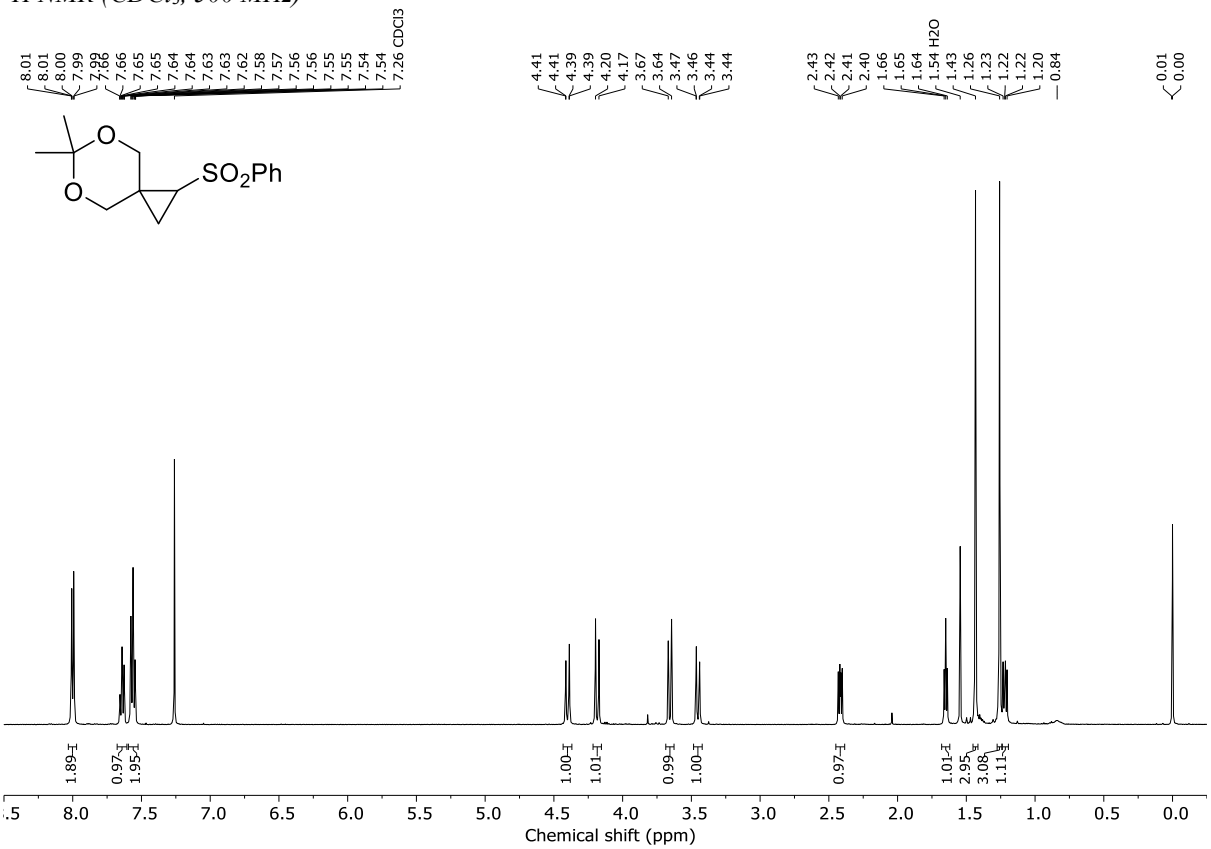

^{13}C NMR ($CDCl_3$, 126 MHz)

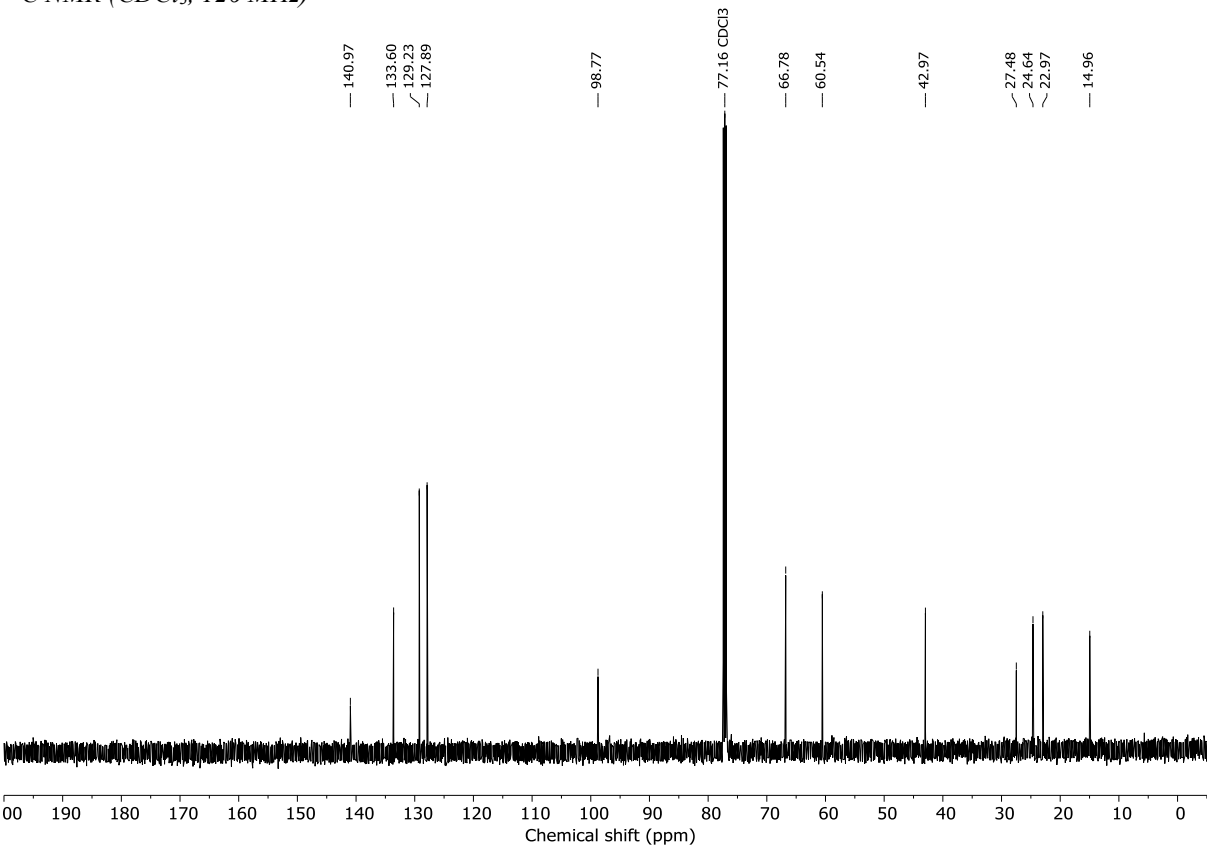

(phenylsulfonyl)-1',3'-dihydrospiro[cyclopropane-1,2'-indene](39)

^{1}H NMR ($CDCl_3$, 500 MHz)

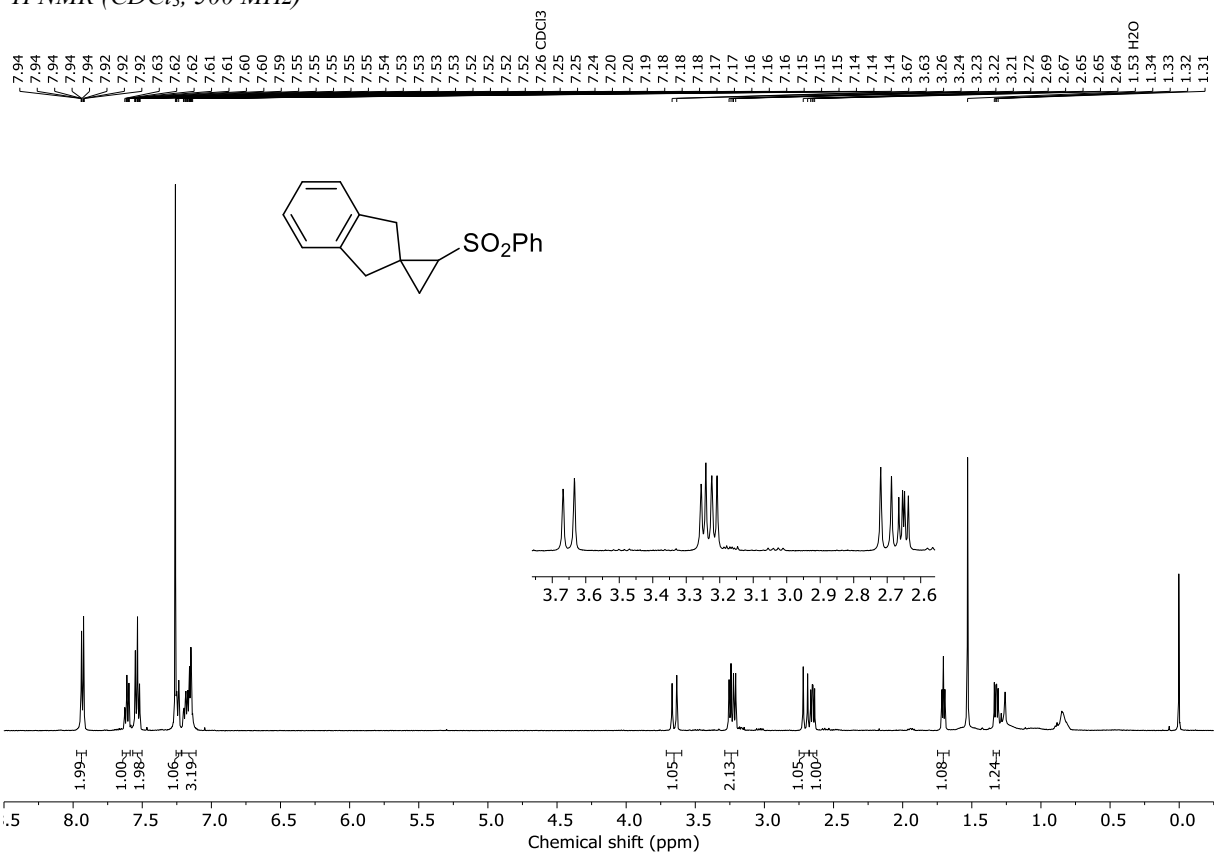

^{13}C NMR ($CDCl_3$, 126 MHz)

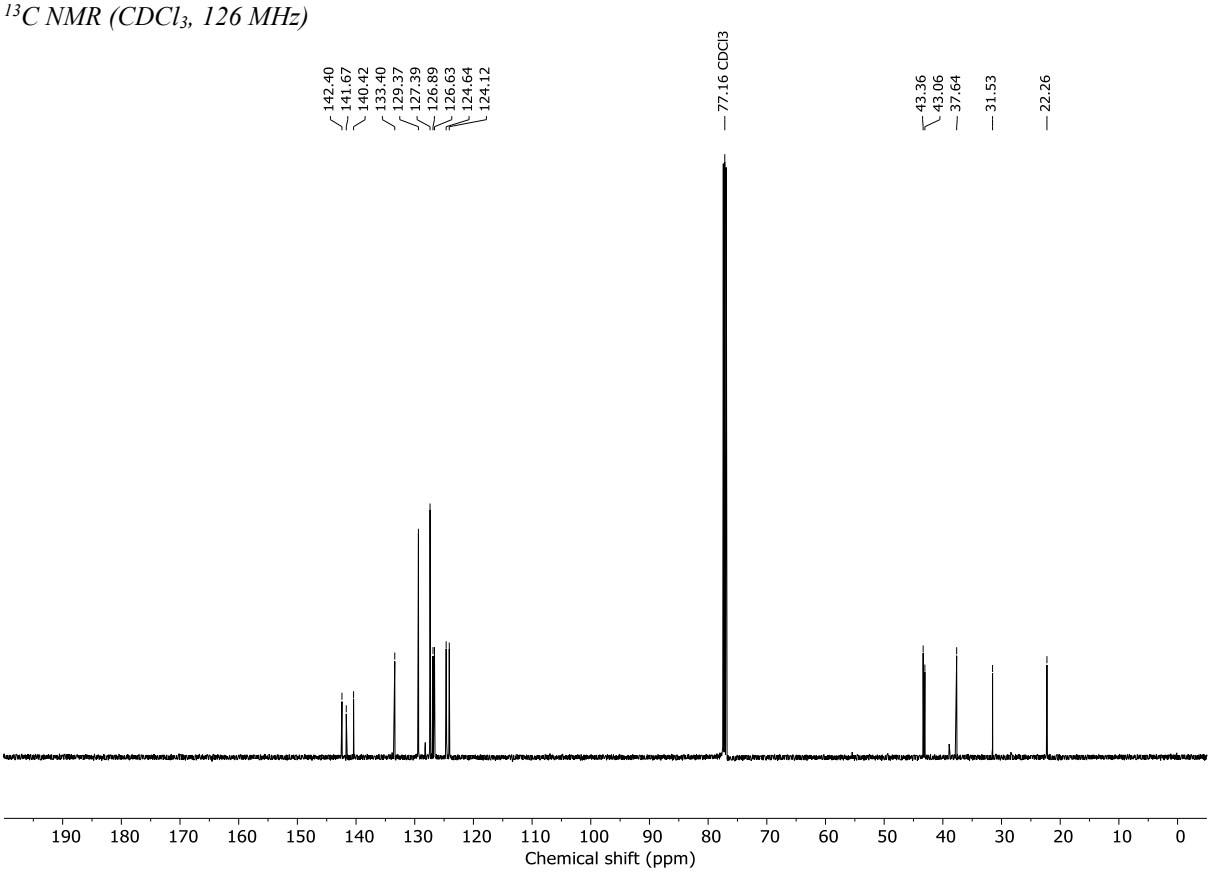

((2-benzyl-2-ethylcyclopropyl)sulfonyl)benzene (40)

^{1}H NMR ($CDCl_3$, 600 MHz)

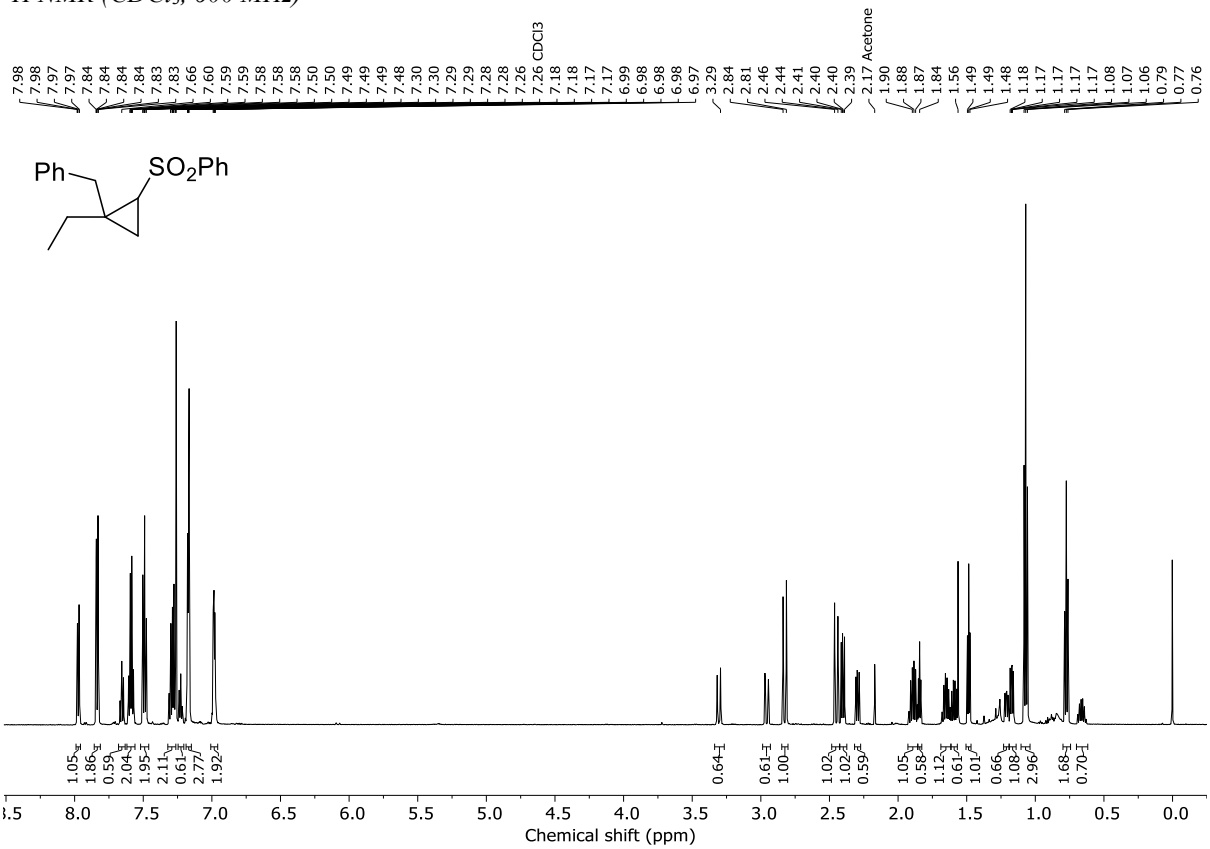

^{13}C NMR ($CDCl_3$, 151 MHz)

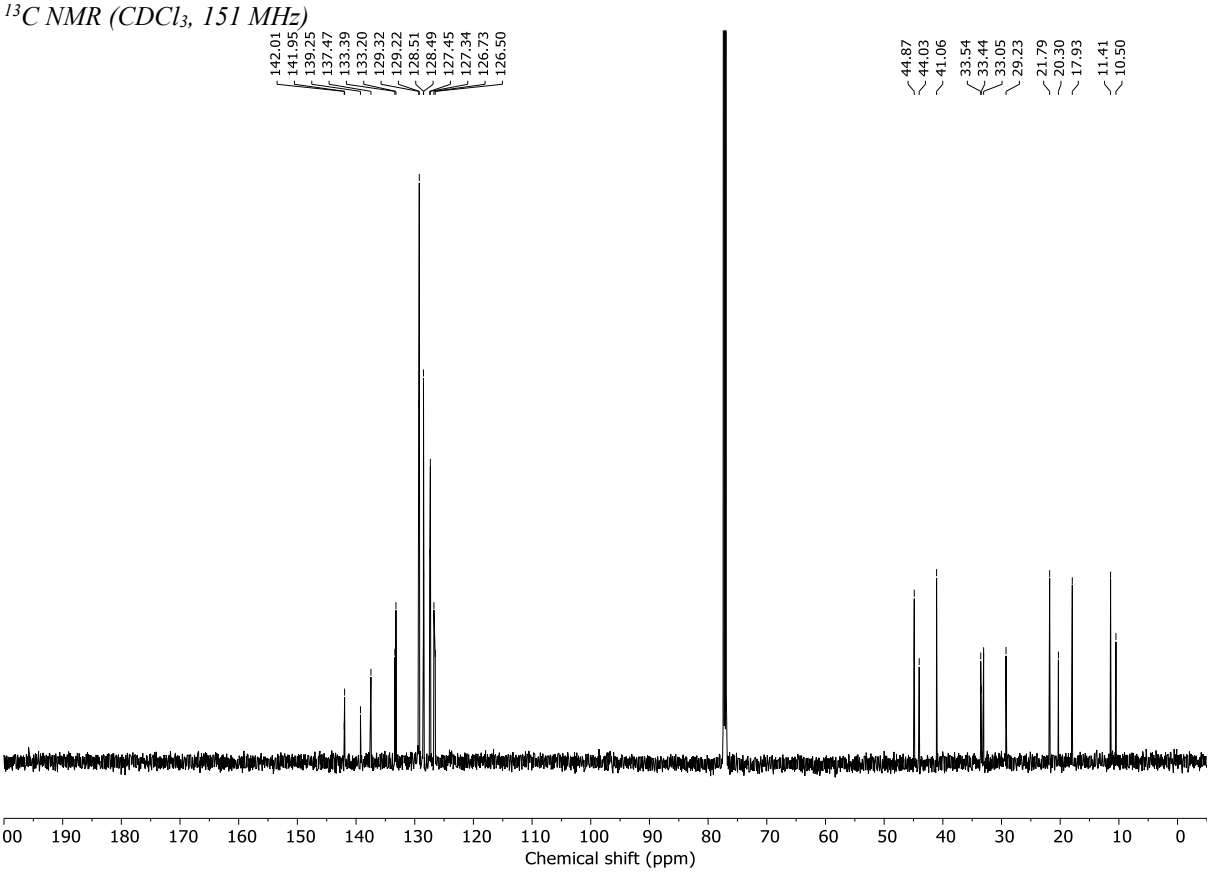

(1S,4R,5R)-1-isopropyl-4-methyl-2'-(phenylsulfonyl)spiro[bicyclo[3.1.0]hexane-3,1'-cyclopropane] (41)

^{1}H NMR ($CDCl_3$, 500 MHz)

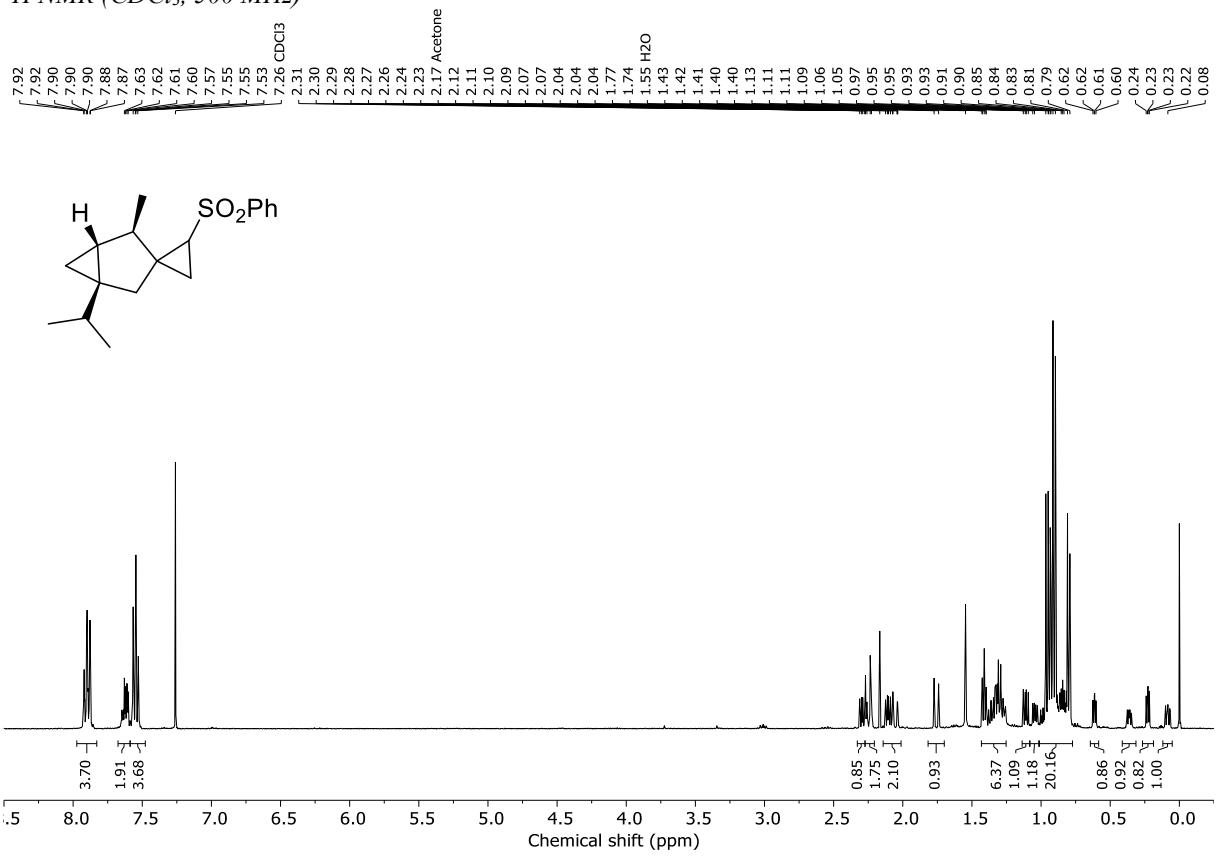

^{13}C NMR ($CDCl_3$, 126 MHz)

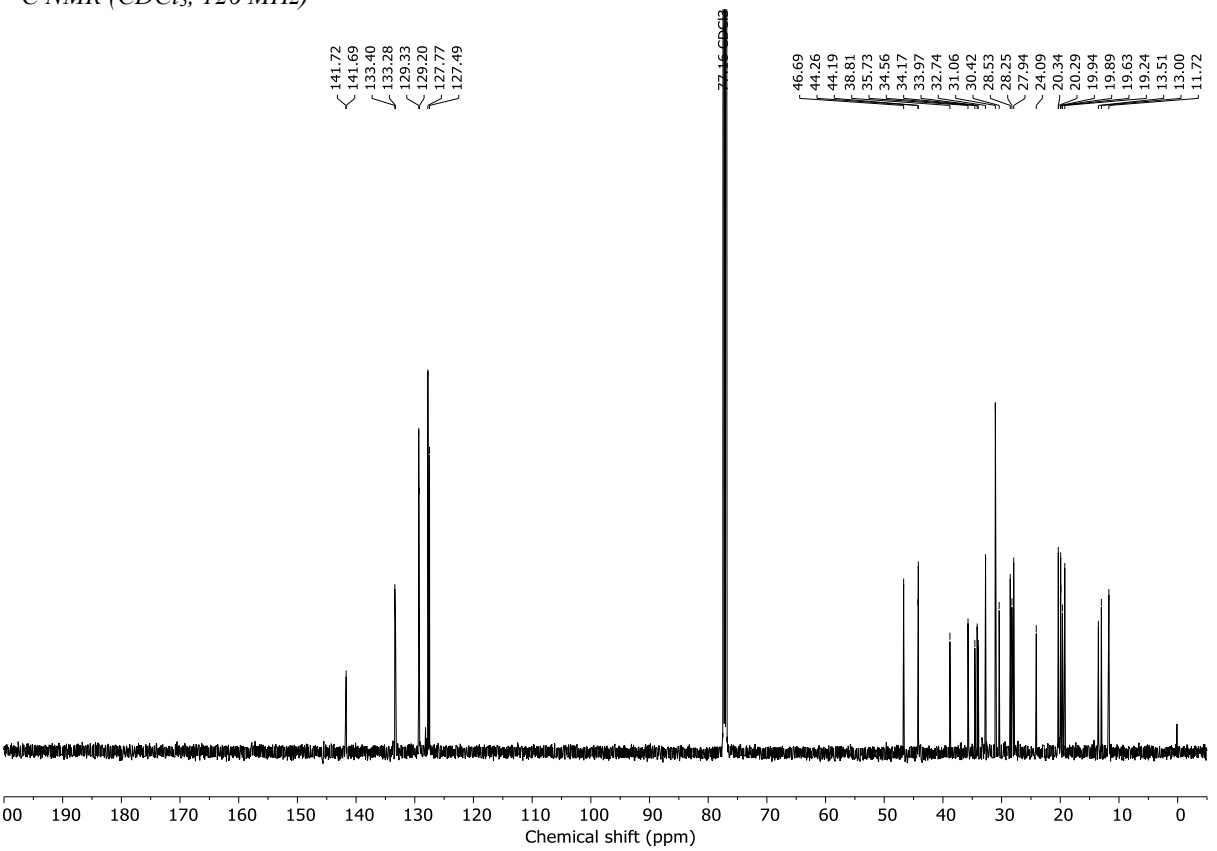

(8S,10R,13S)-3-methoxy-10,13-dimethyl-17-(1-methyl-2-(phenylsulfonyl)cyclopropyl)-2,3,4,7,8,9, 10,11,12,13,14,15,16,17-tetradecahydro-1H-cyclopenta[a]phenanthrene (42)

^{1}H NMR ($CDCl_3$, 500 MHz)

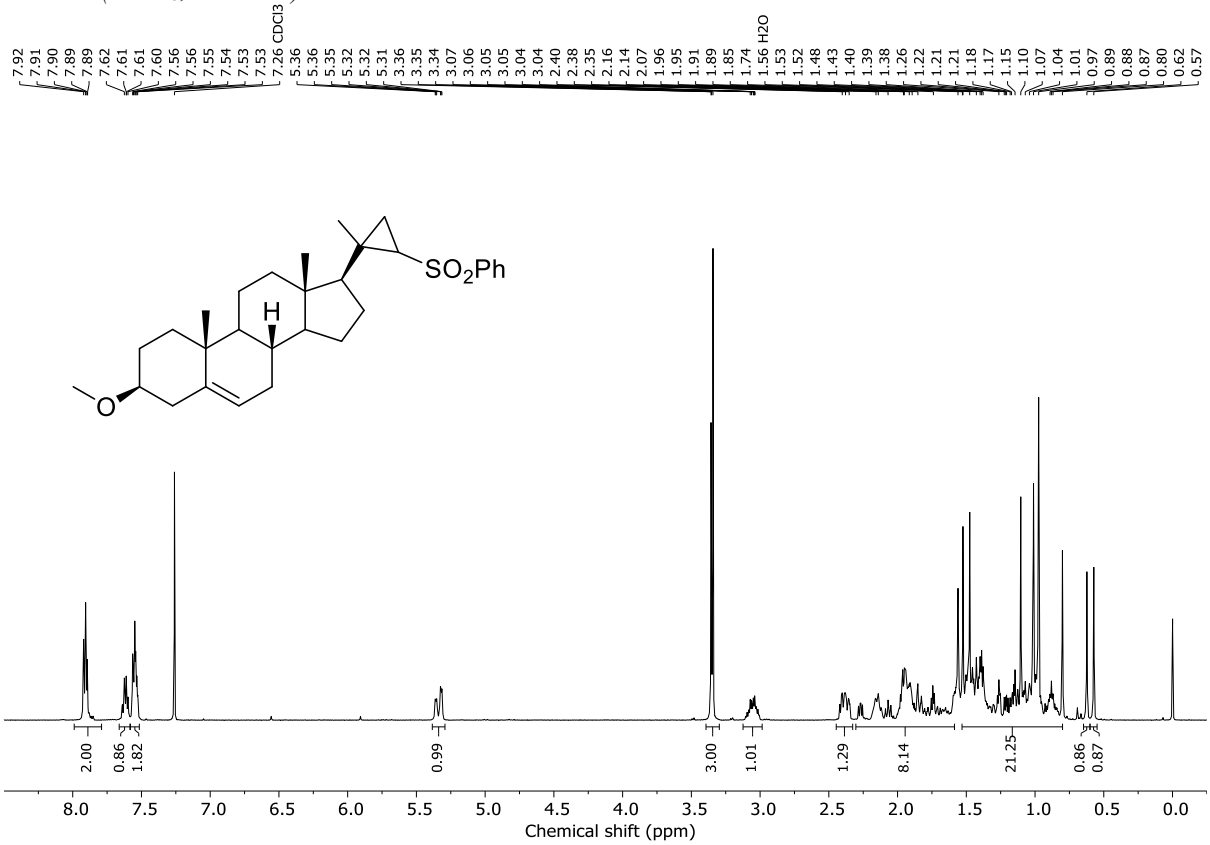

^{13}C NMR ($CDCl_3$, 126 MHz)

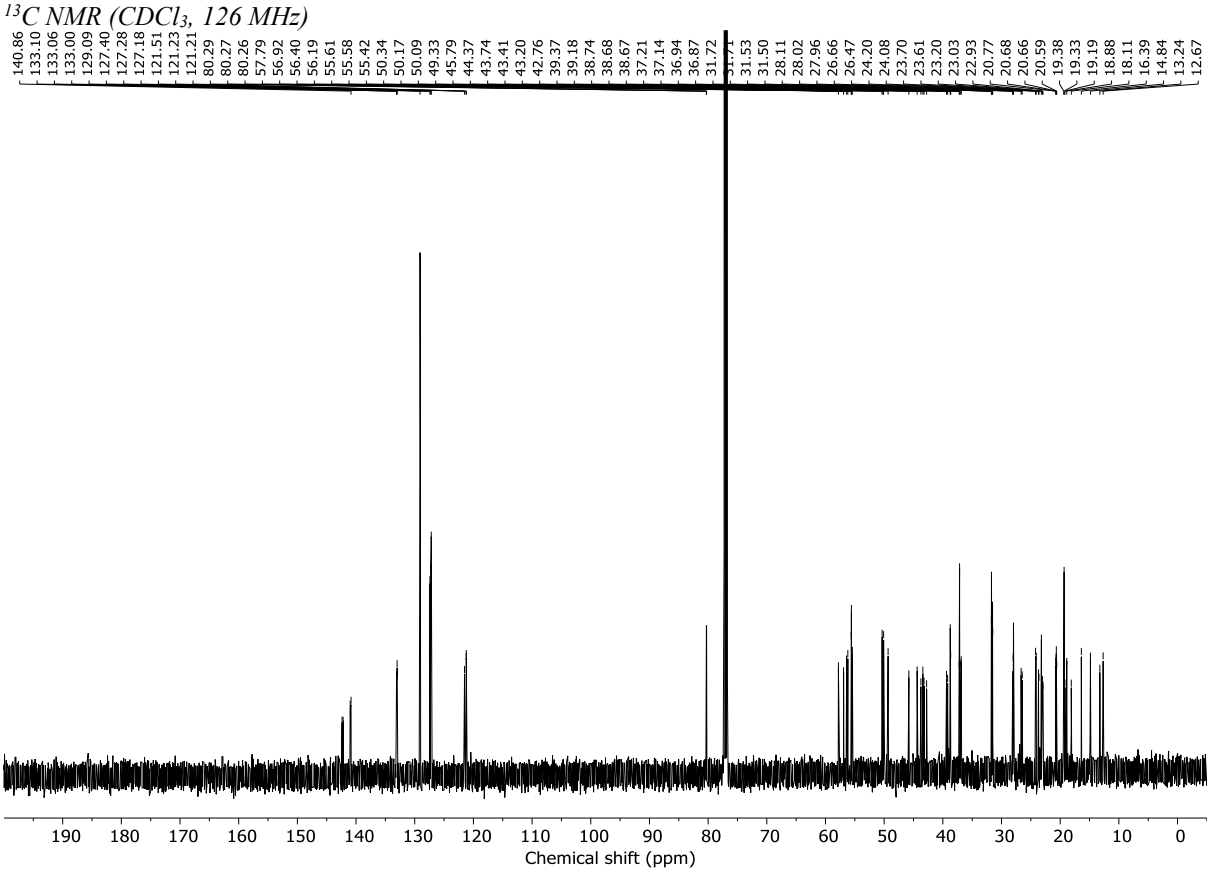

1-(ethylsulfonyl)spiro[2.5]octane (43)

^{1}H NMR ($CDCl_3$, 600 MHz)

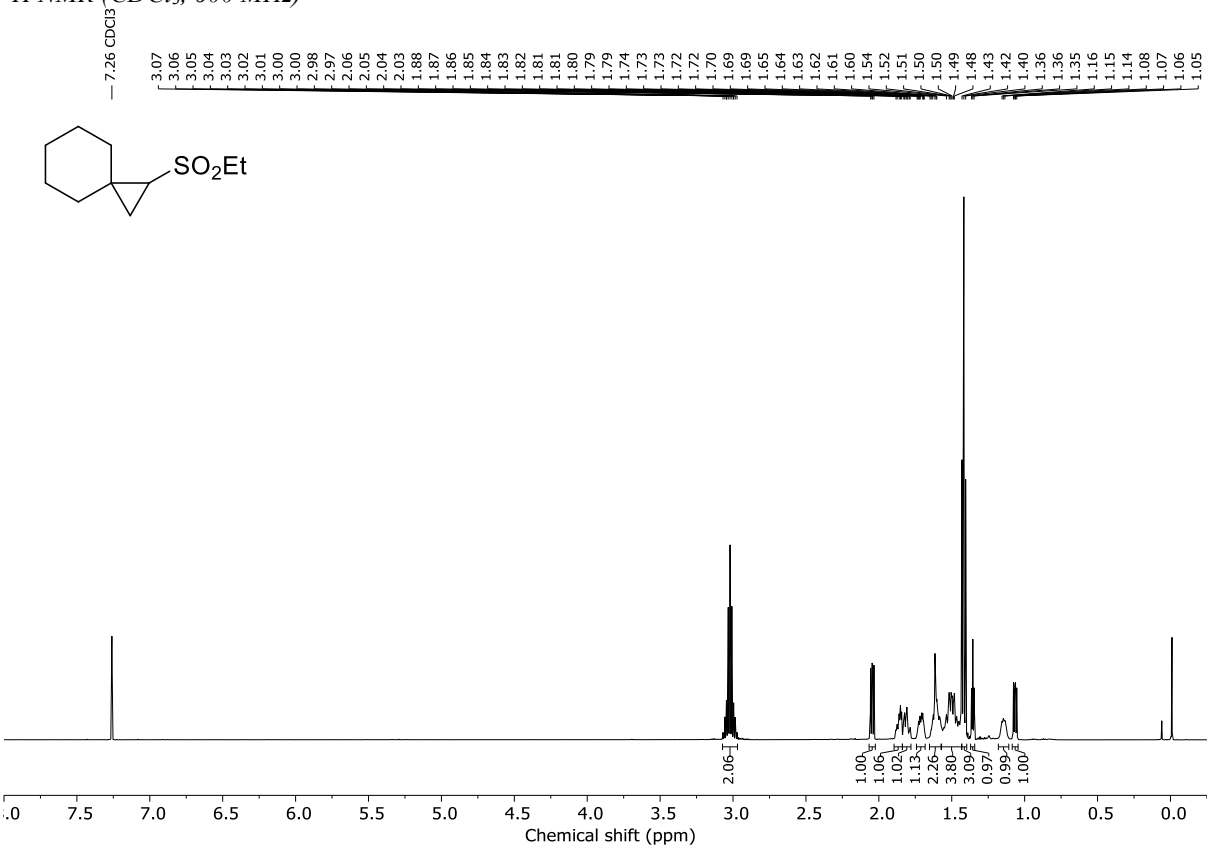

^{13}C NMR ($CDCl_3$, 151 MHz)

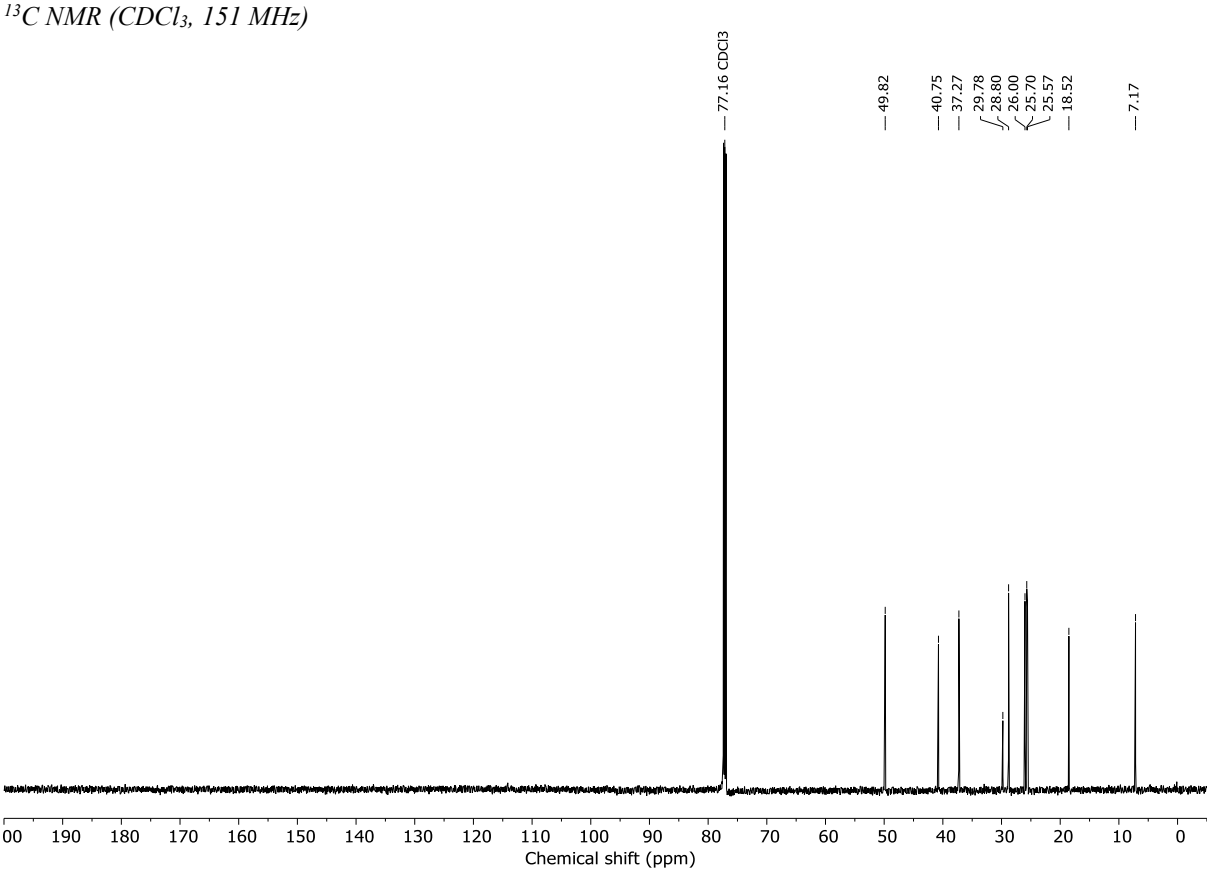

methyl 6-tosyl-6-azaspiro[2.5]octane-1-carboxylate (44)

^{1}H NMR ($CDCl_3$, 500 MHz)

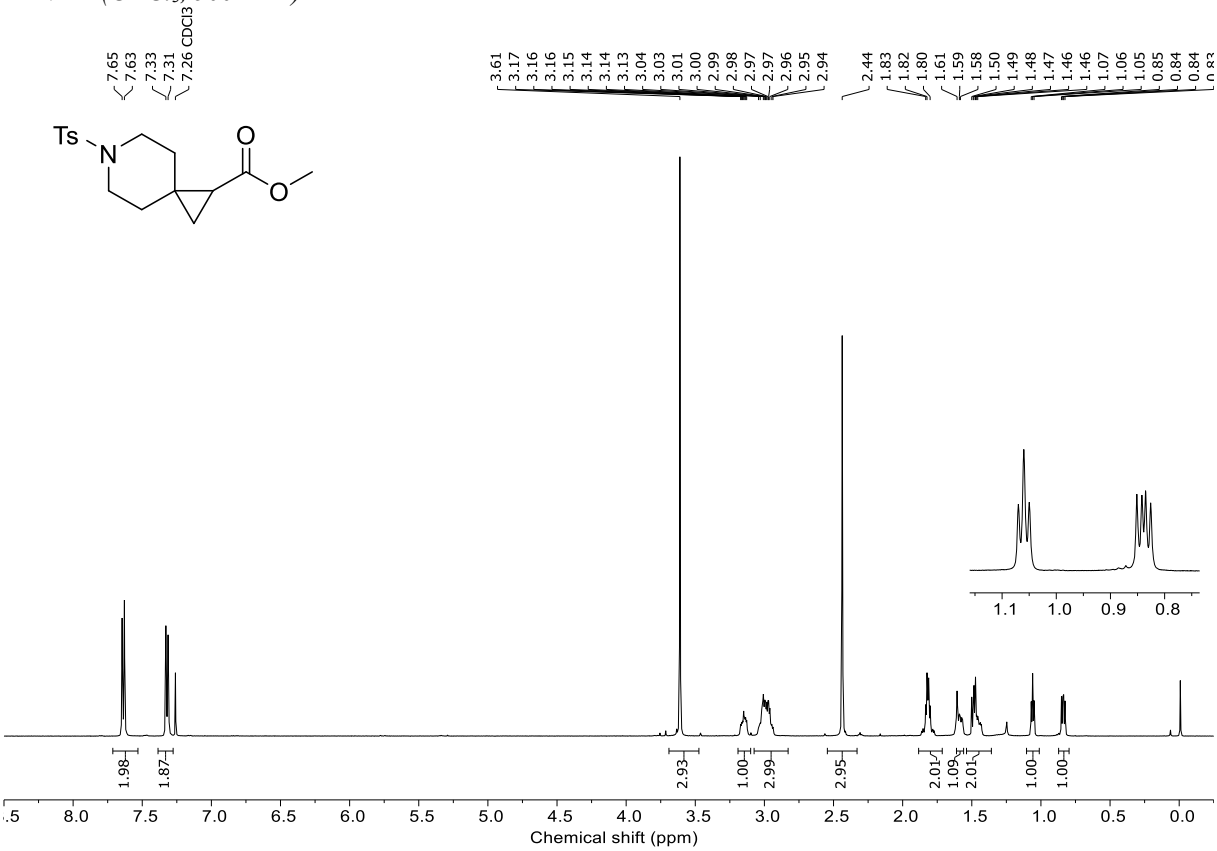

^{13}C NMR ($CDCl_3$, 126 MHz)

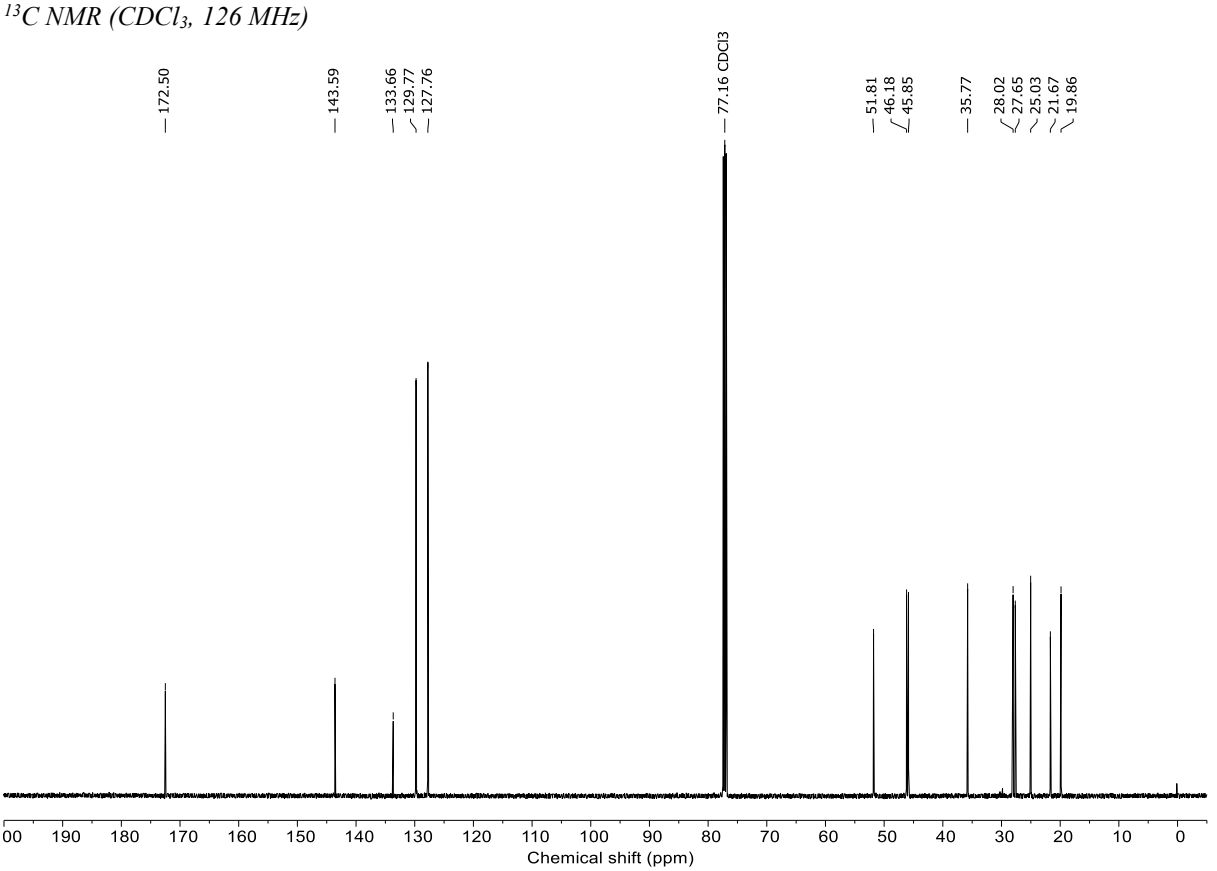

6-(tert-butyl) 1-methyl 6-azaspiro[2.5]octane-1,6-dicarboxylate (45)

^{1}H NMR ($CDCl_3$, 400 MHz)

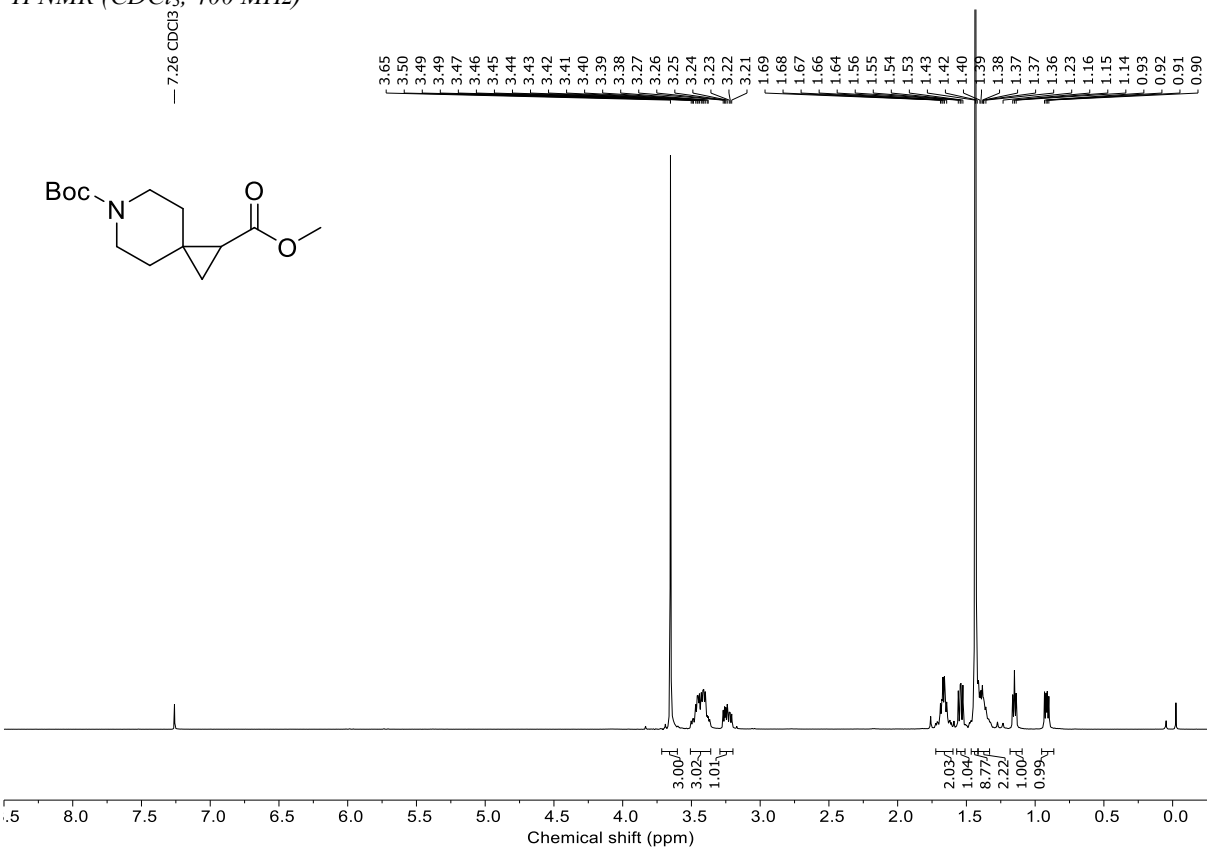

^{13}C NMR ($CDCl_3$, 101 MHz)

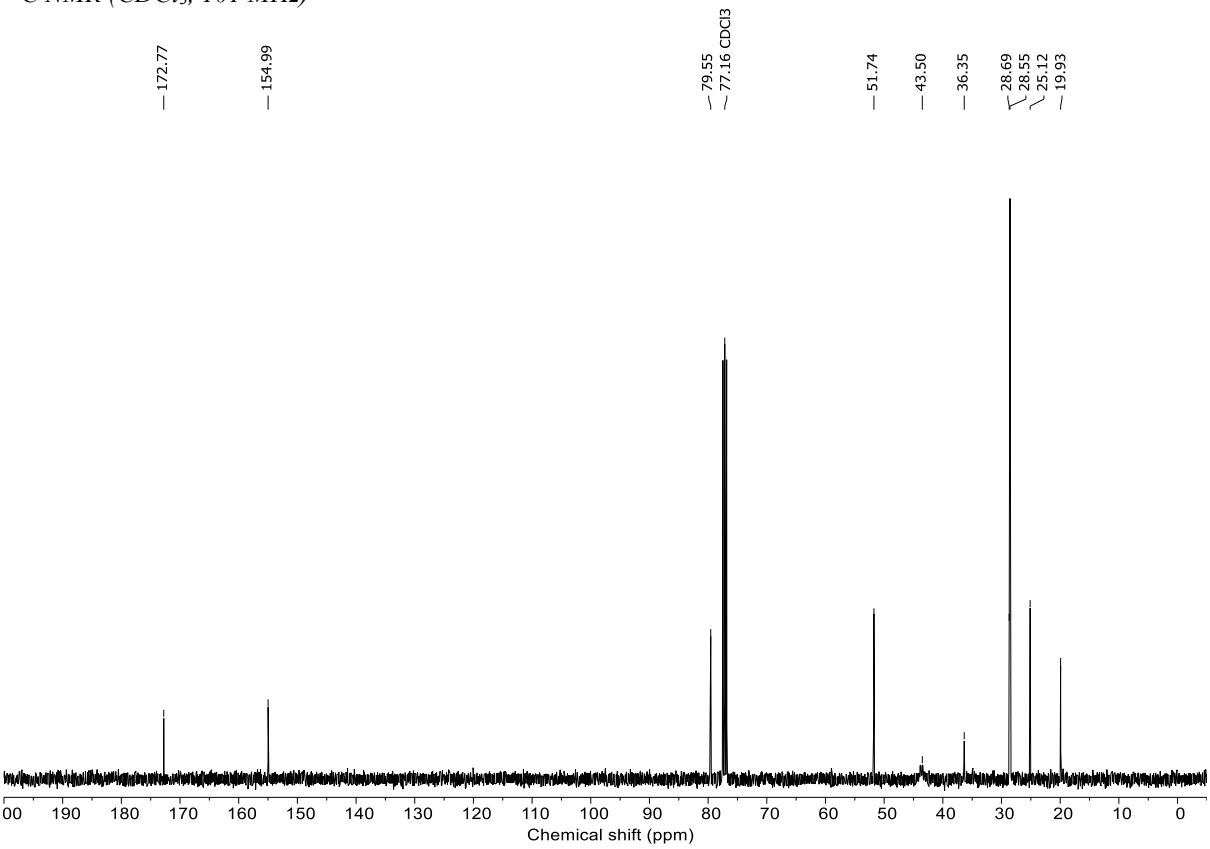

pent-4-yn-1-yl 6-tosyl-6-azaspiro[2.5]octane-1-carboxylate (46)

^{1}H NMR ($CDCl_3$, 500 MHz)

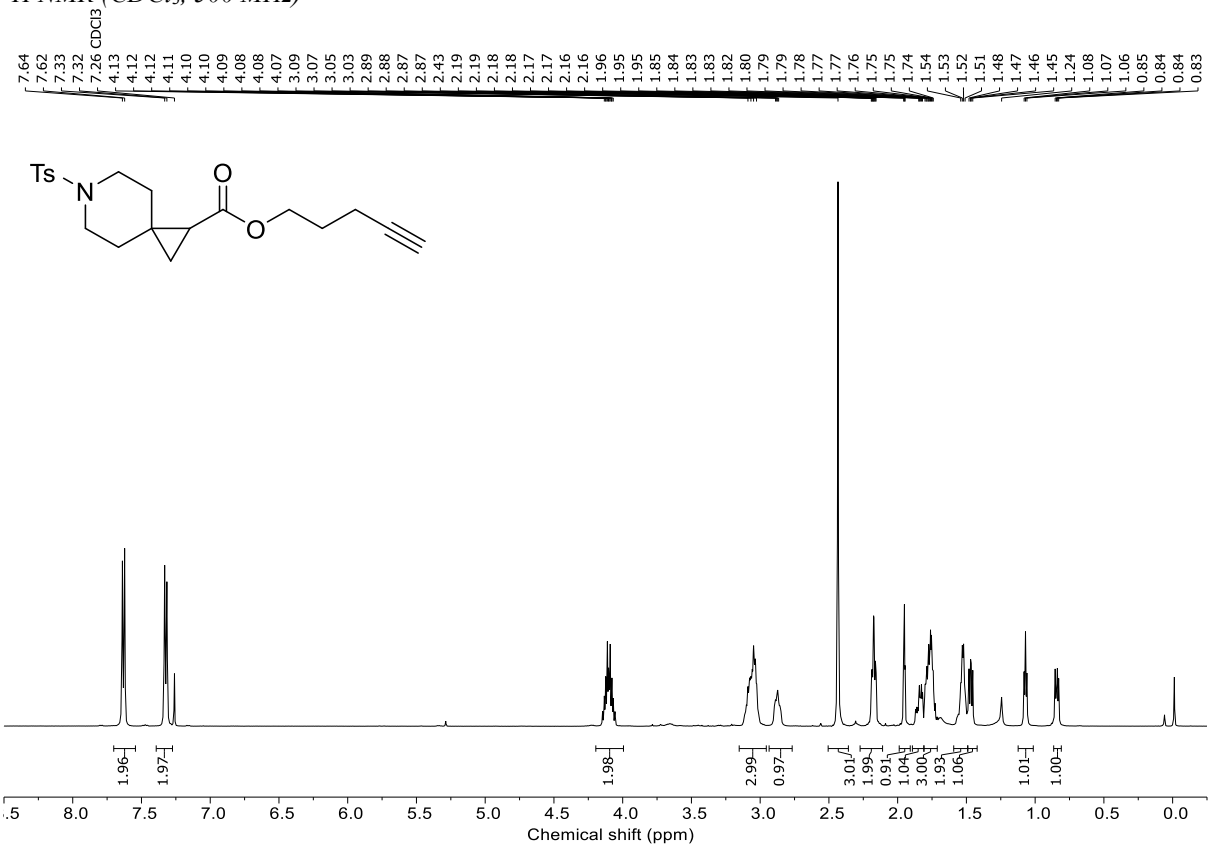

^{13}C NMR ($CDCl_3$, 126 MHz)

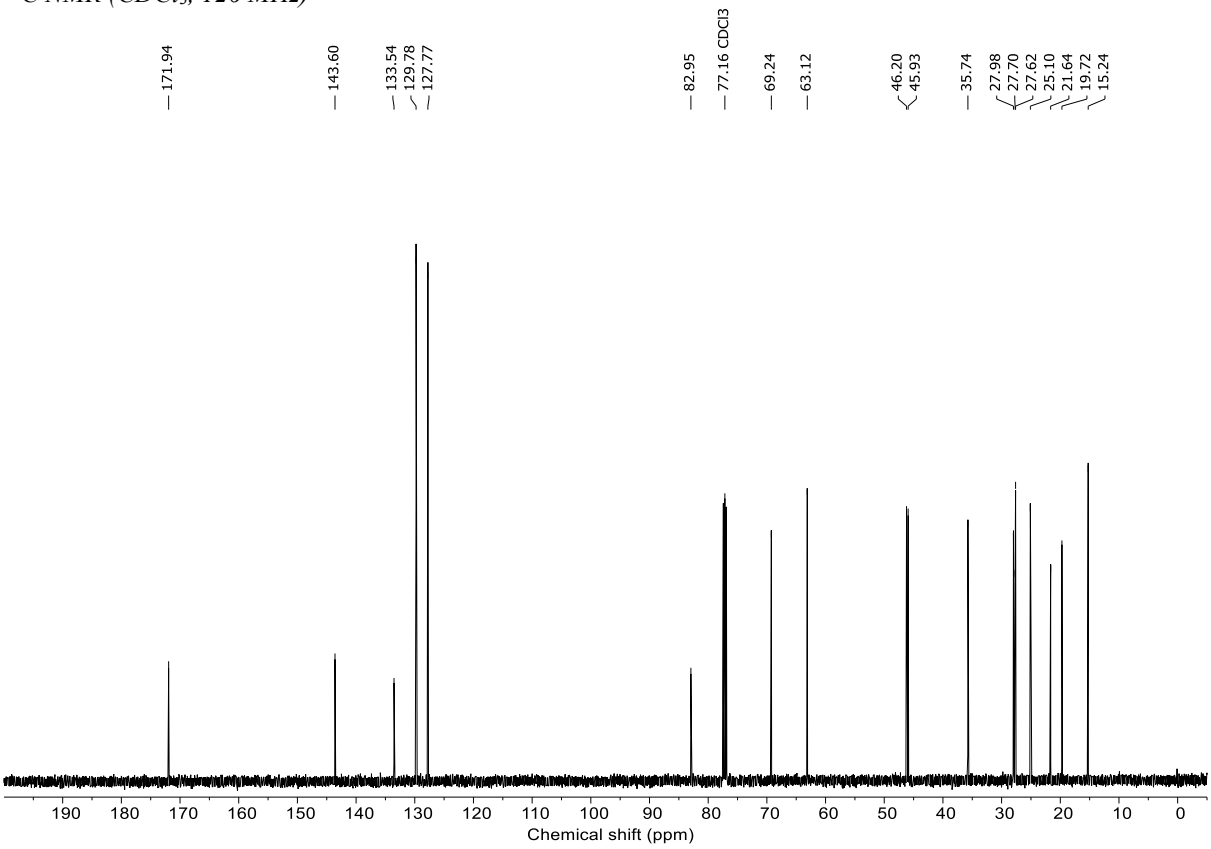

pent-4-en-1-yl 6-tosyl-6-azaspiro[2.5]octane-1-carboxylate (47)

^{1}H NMR ($CDCl_3$, 500 MHz)

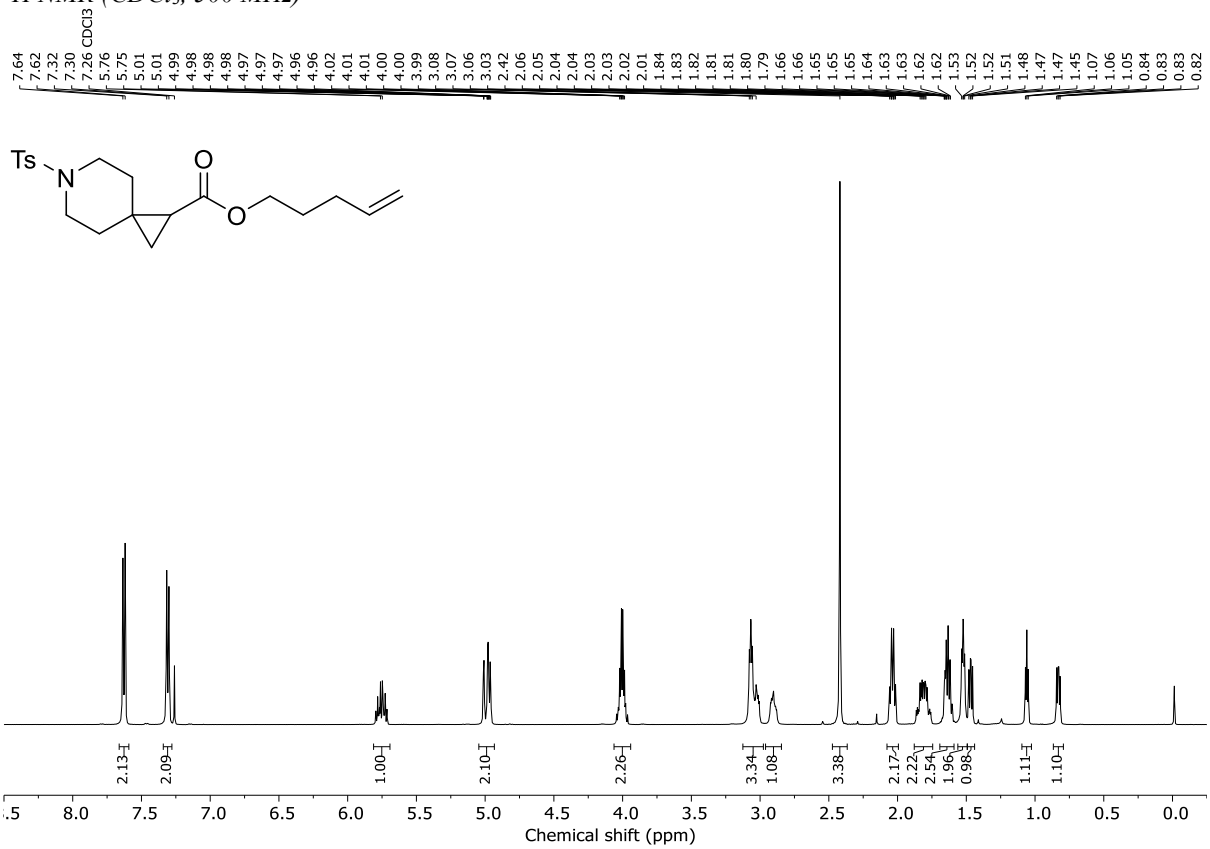

^{13}C NMR ($CDCl_3$, 126 MHz)

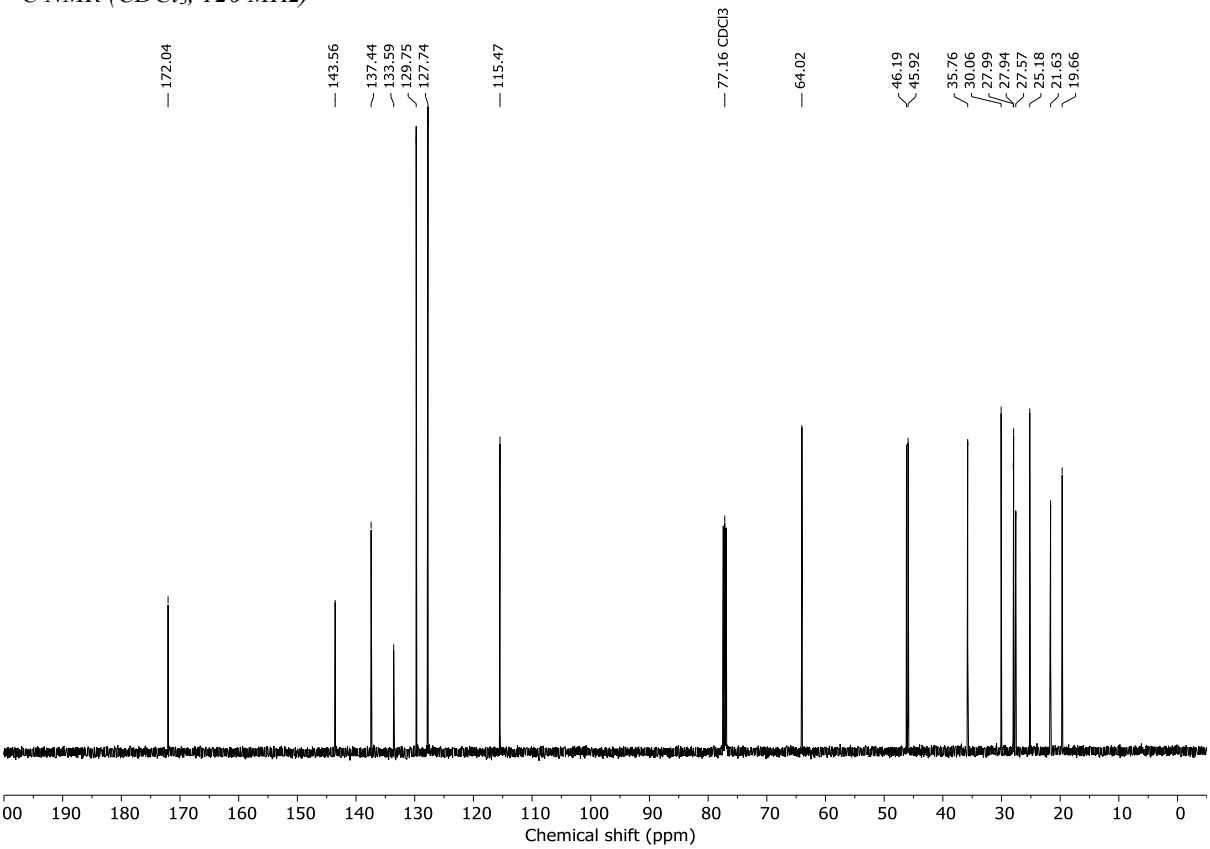

benzyl spiro[2.5]octane-1-carboxylate (48)

^{1}H NMR ($CDCl_3$, 400 MHz)

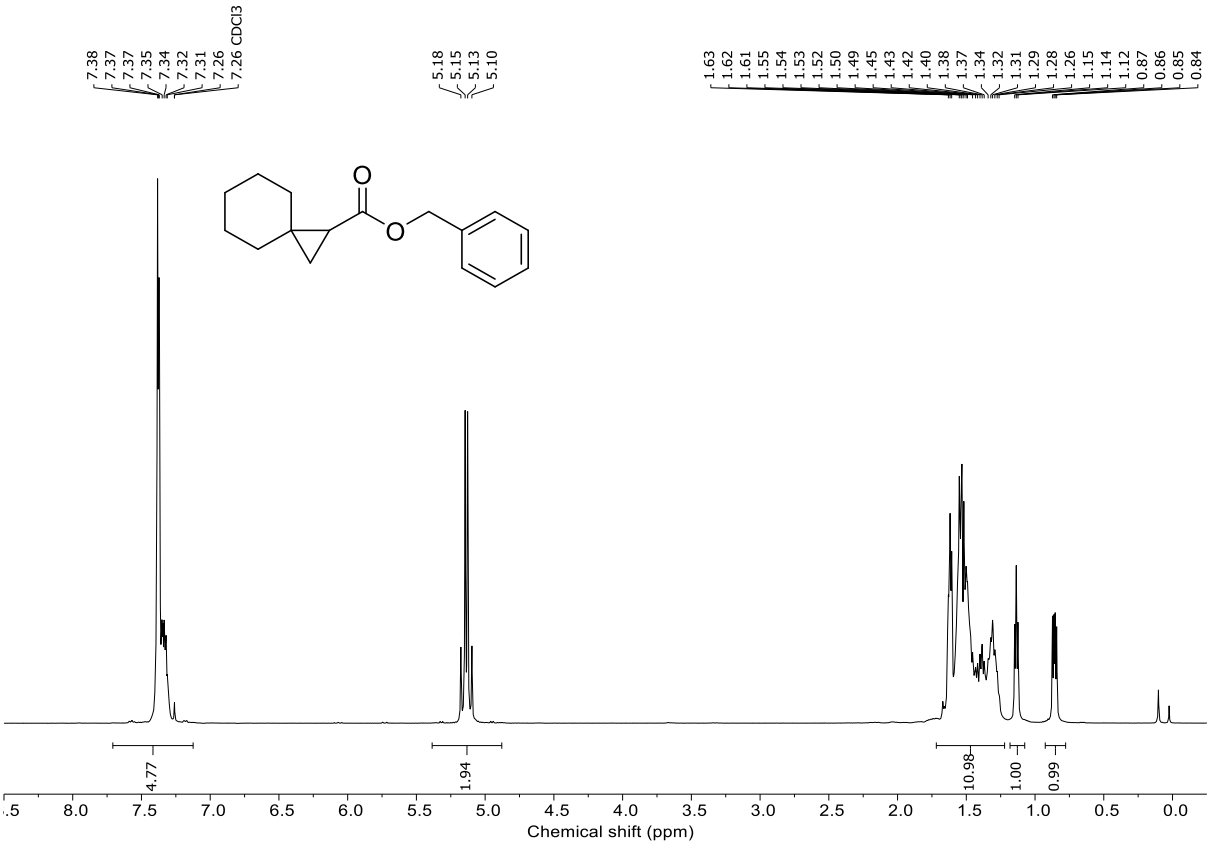

^{13}C NMR ($CDCl_3$, 101 MHz)

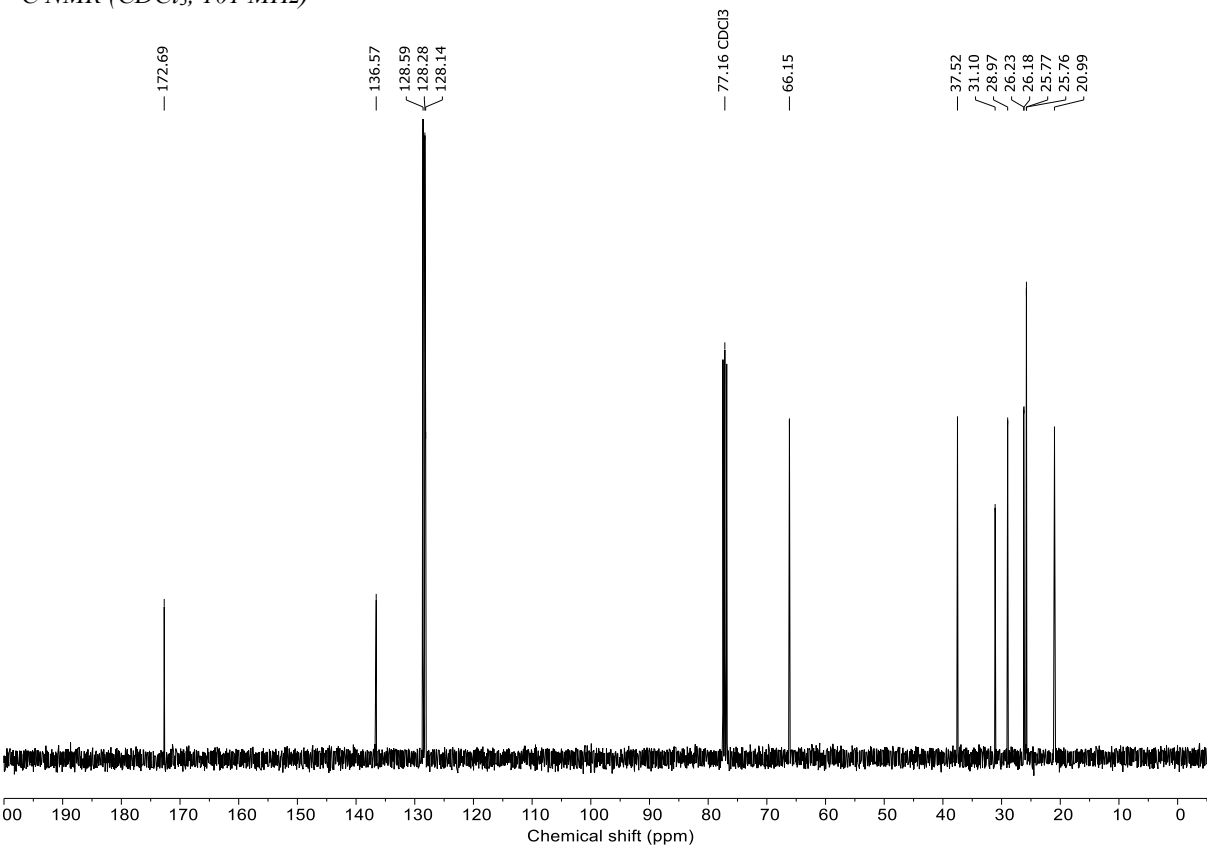

4-cyanophenyl spiro[2.5]octane-1-carboxylate (49)

^{1}H NMR ($CDCl_3$, 600 MHz)

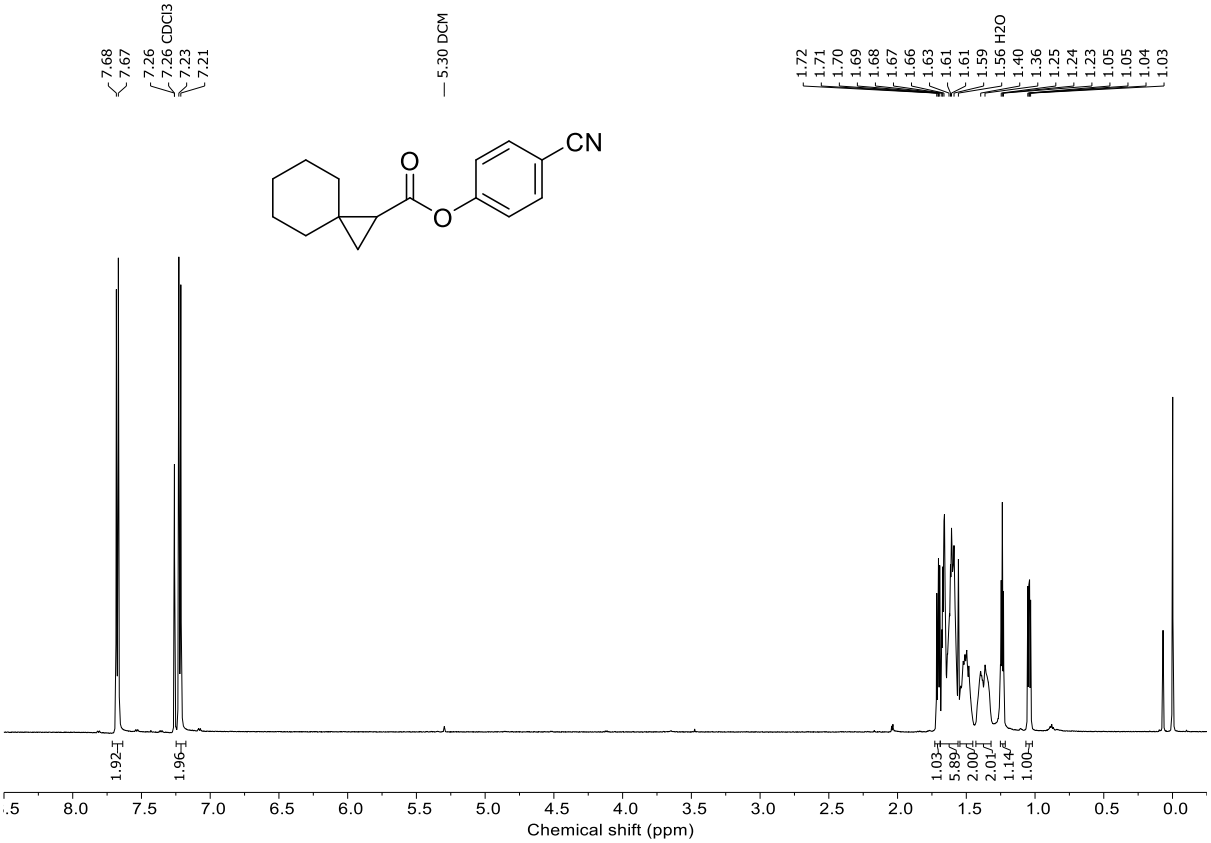

^{13}C NMR ($CDCl_3$, 151 MHz)

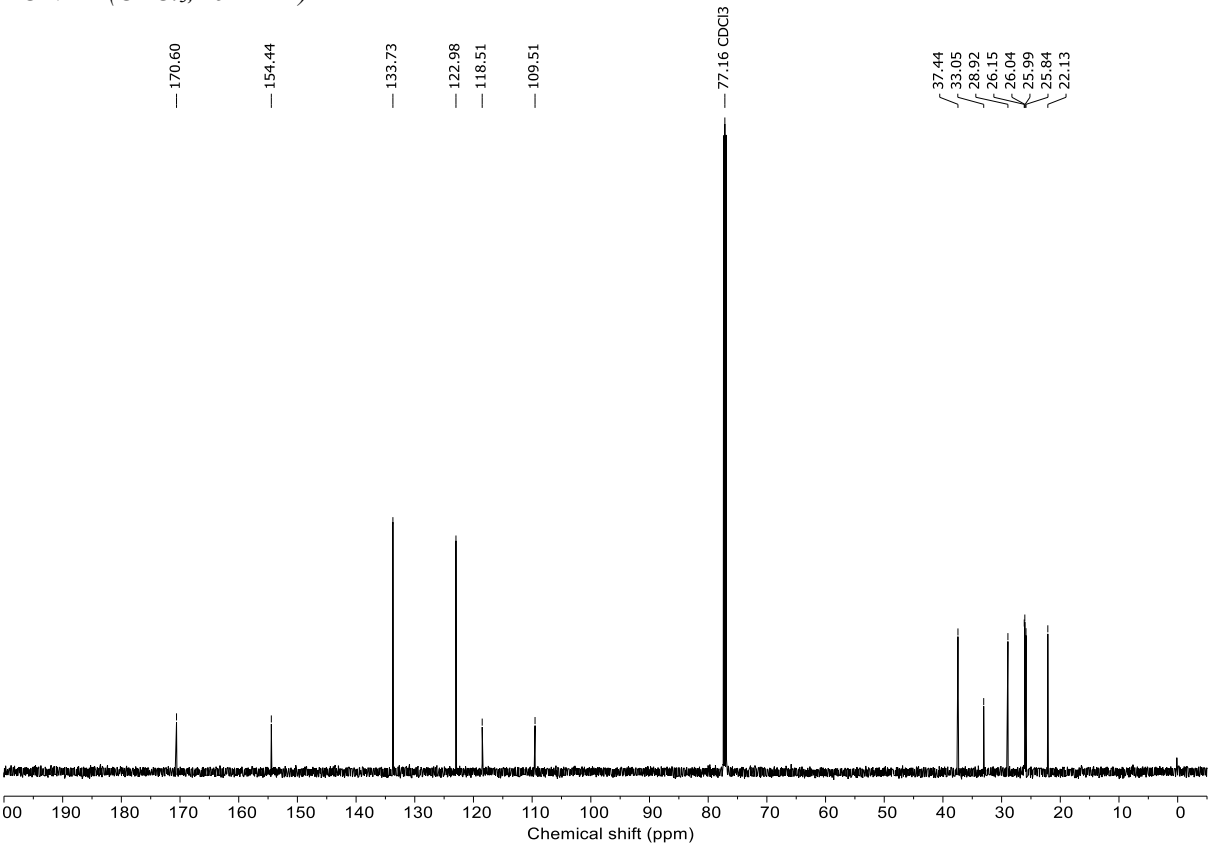

(1R,2S,5R)-2-isopropyl-5-methylcyclohexyl spiro[2.5]octane-1-carboxylate (50)

^{1}H NMR ($CDCl_3$, 600 MHz)

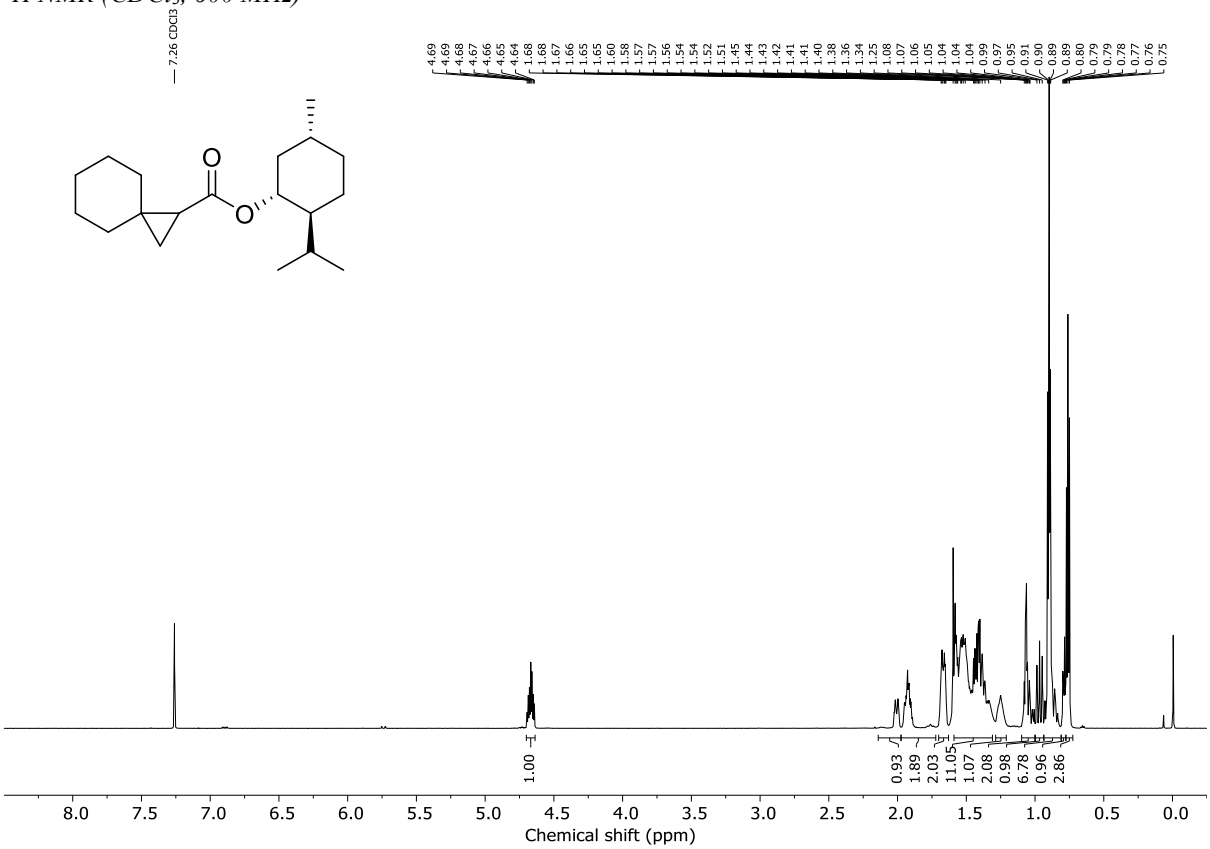

^{13}C NMR ($CDCl_3$, 151 MHz)

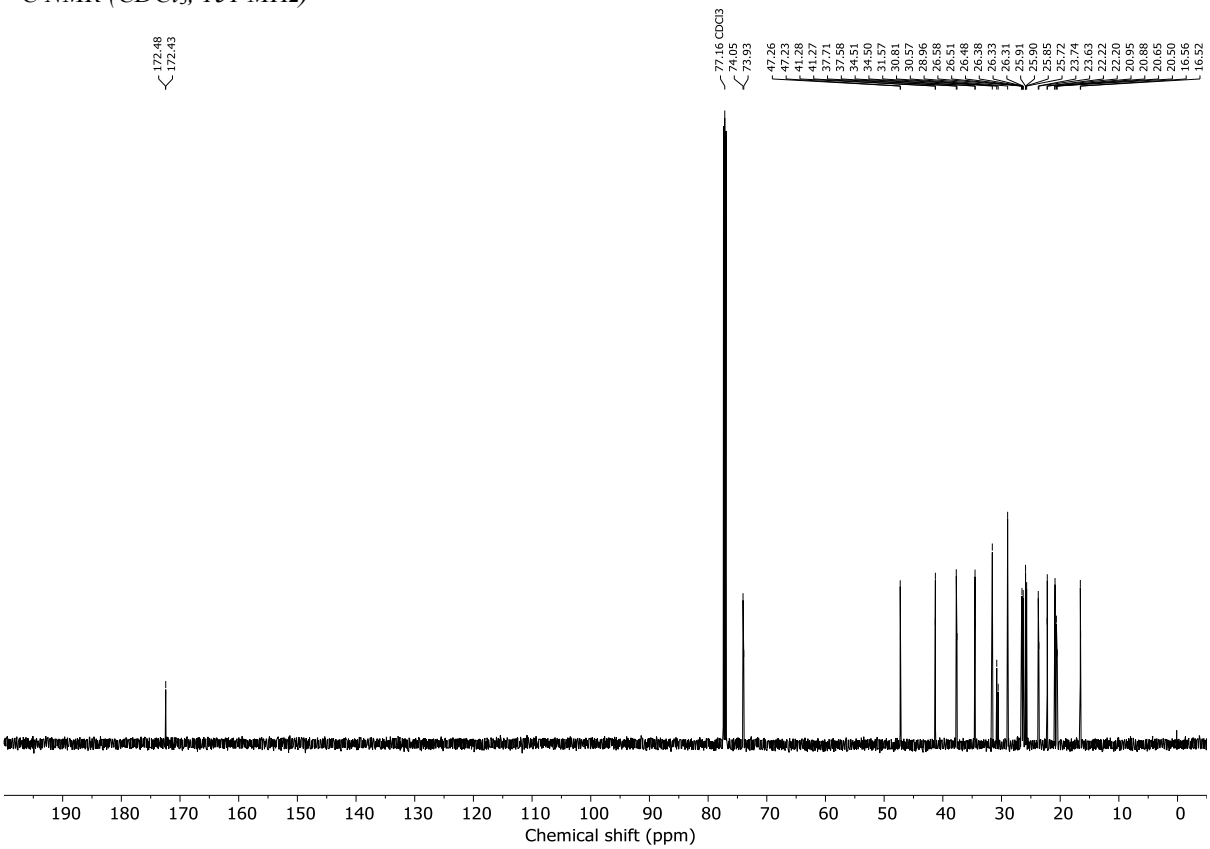

(8R,9S,13S,14S)-13-methyl-17-oxo-7,8,9,11,12,13,14,15,16,17-decahydro-6H cyclopenta[a] phenanthren-3-y spiro[2.5]octane-1-carboxylate (51)

^{1}H NMR ($CDCl_3$, 600 MHz)

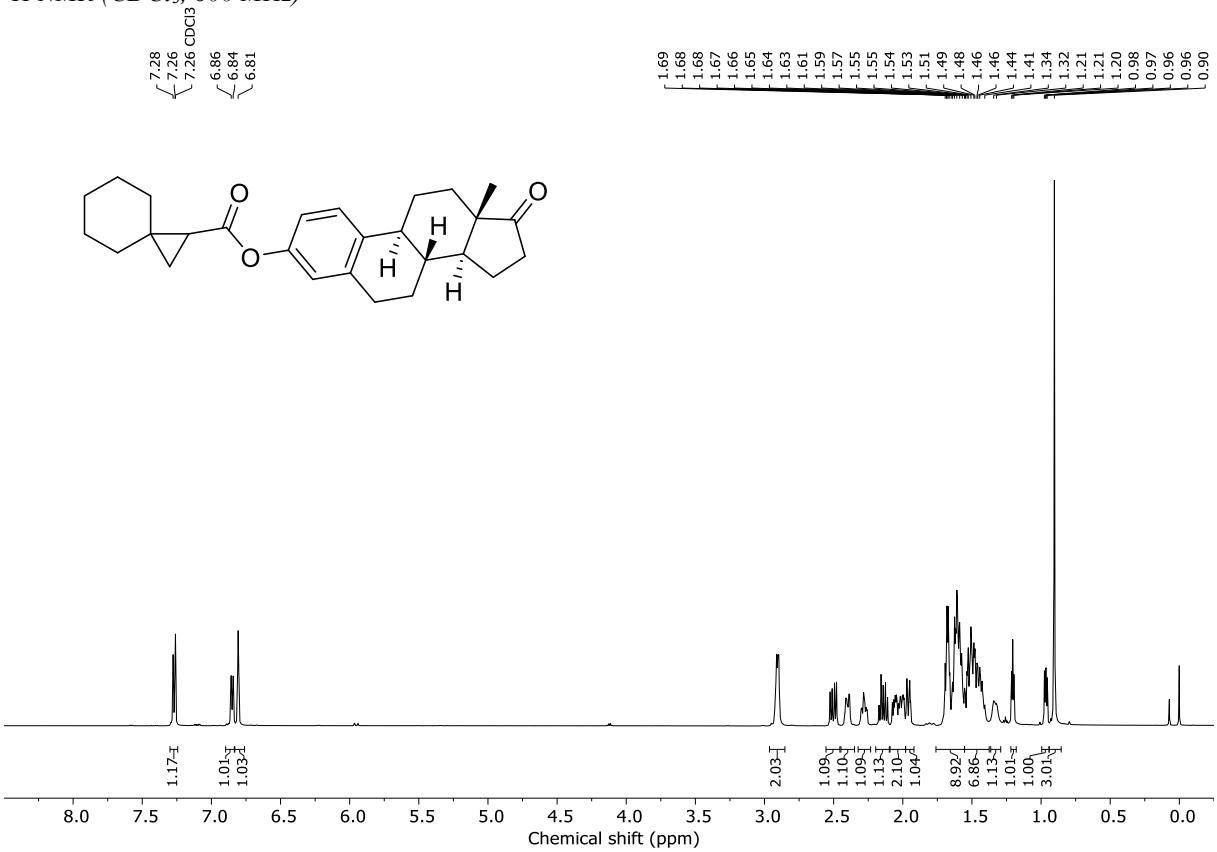

^{13}C NMR ($CDCl_3$, 151 MHz)

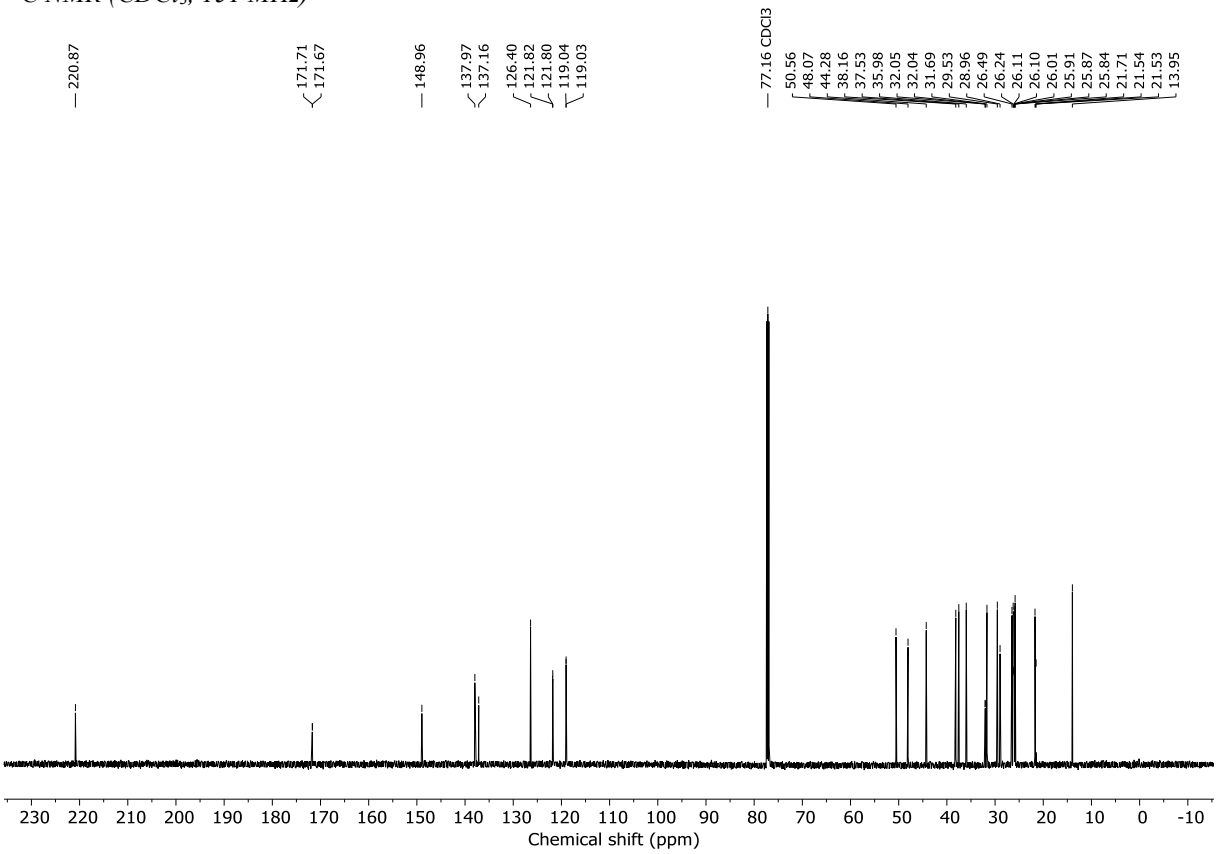

1,3-dioxoisoindolin-2-yl spiro[2.5]octane-1-carboxylate (52)

^{1}H NMR ($CDCl_3$, 500 MHz)

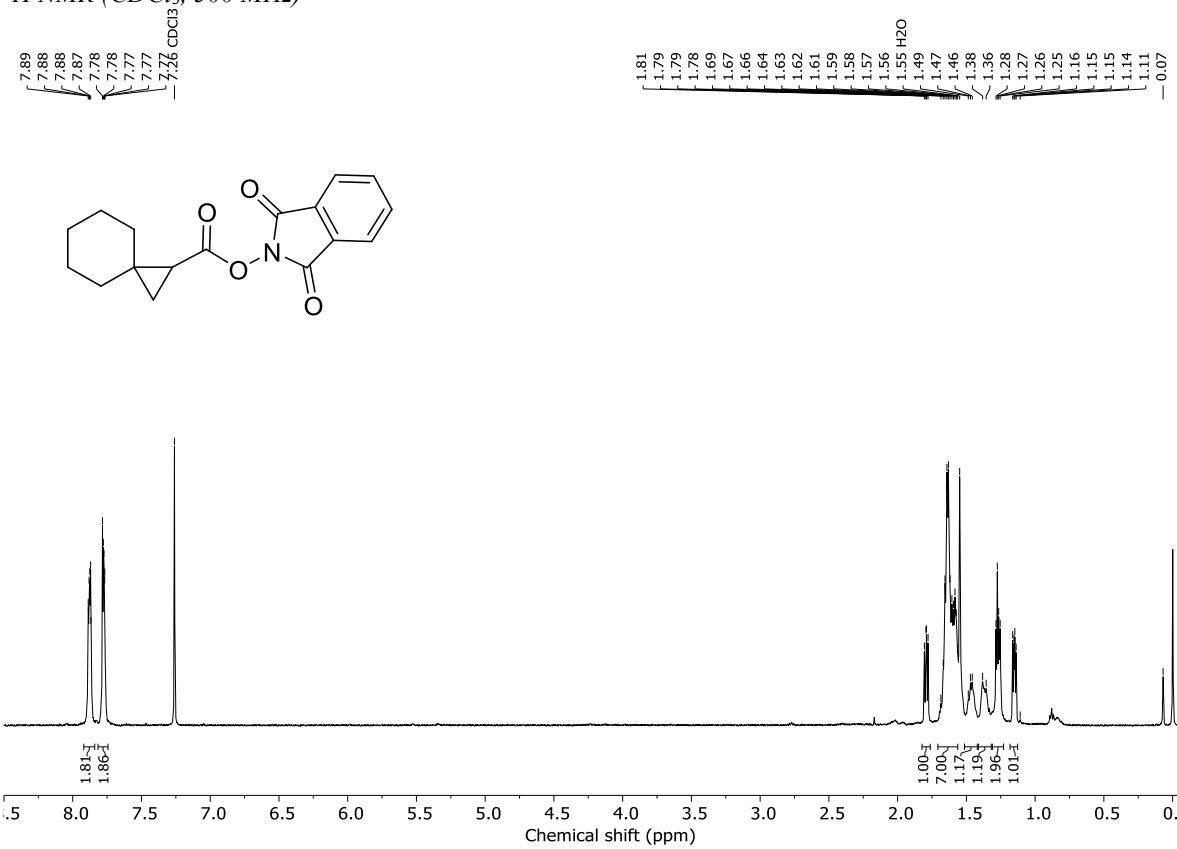

^{13}C NMR ($CDCl_3$, 126 MHz)

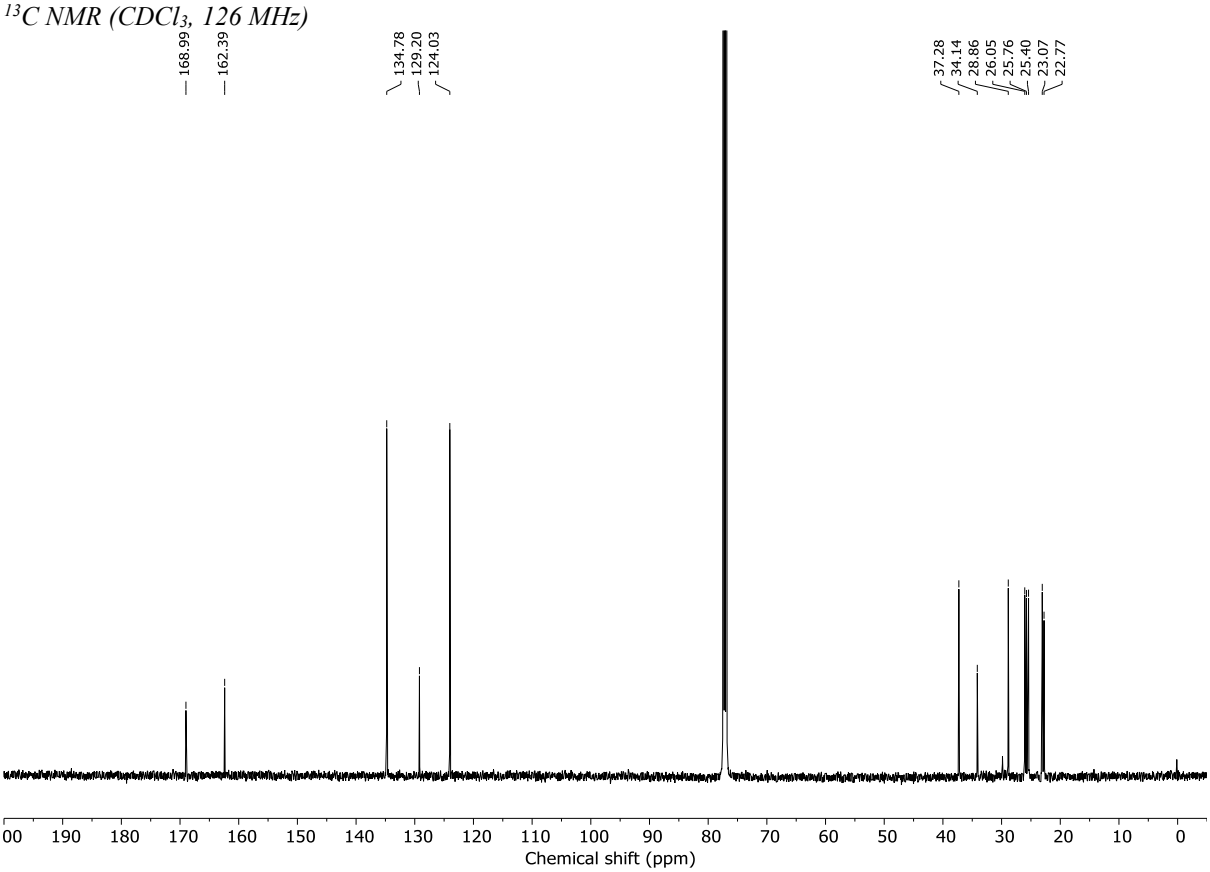

1-(6-tosyl-6-azaspiro[2.5]octan-1-yl)ethan-1-one (53)

^{1}H NMR ($CDCl_3$, 600 MHz)

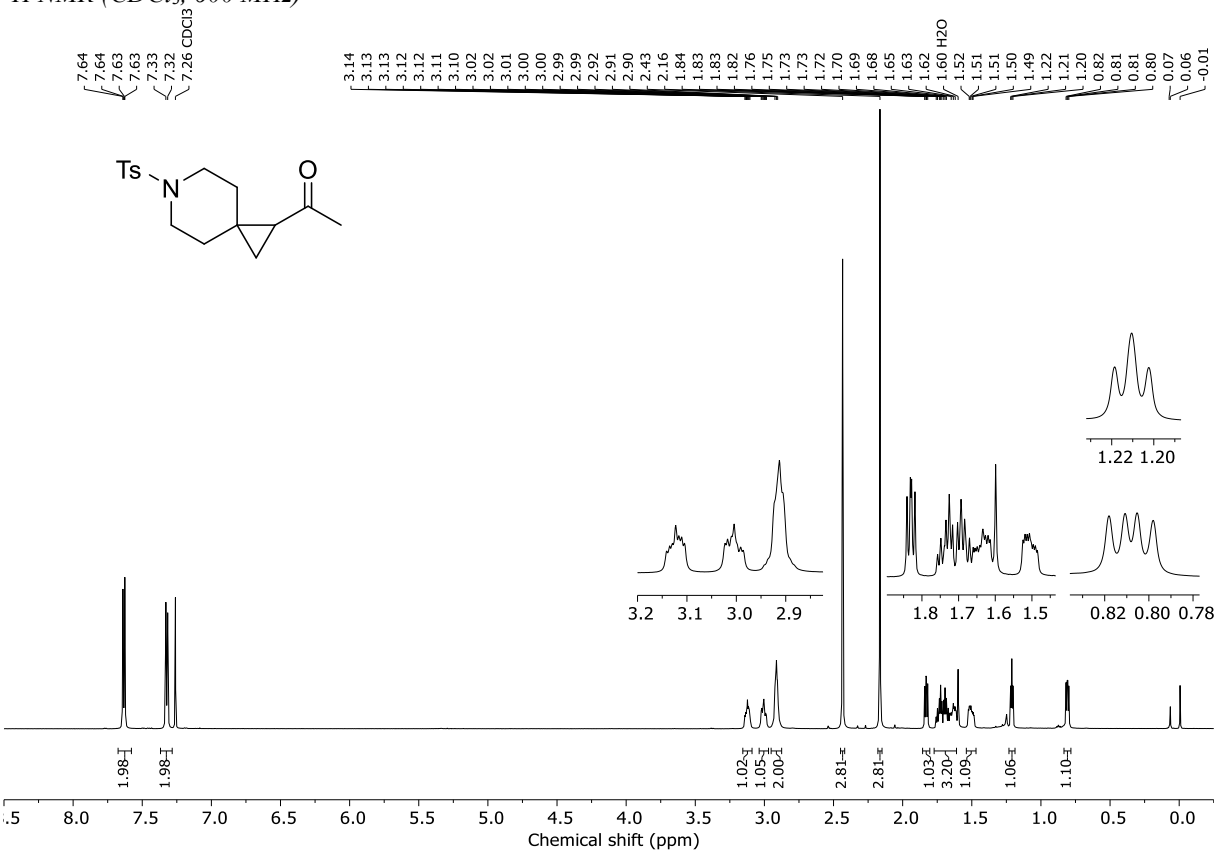

^{13}C NMR ($CDCl_3$, 151 MHz)

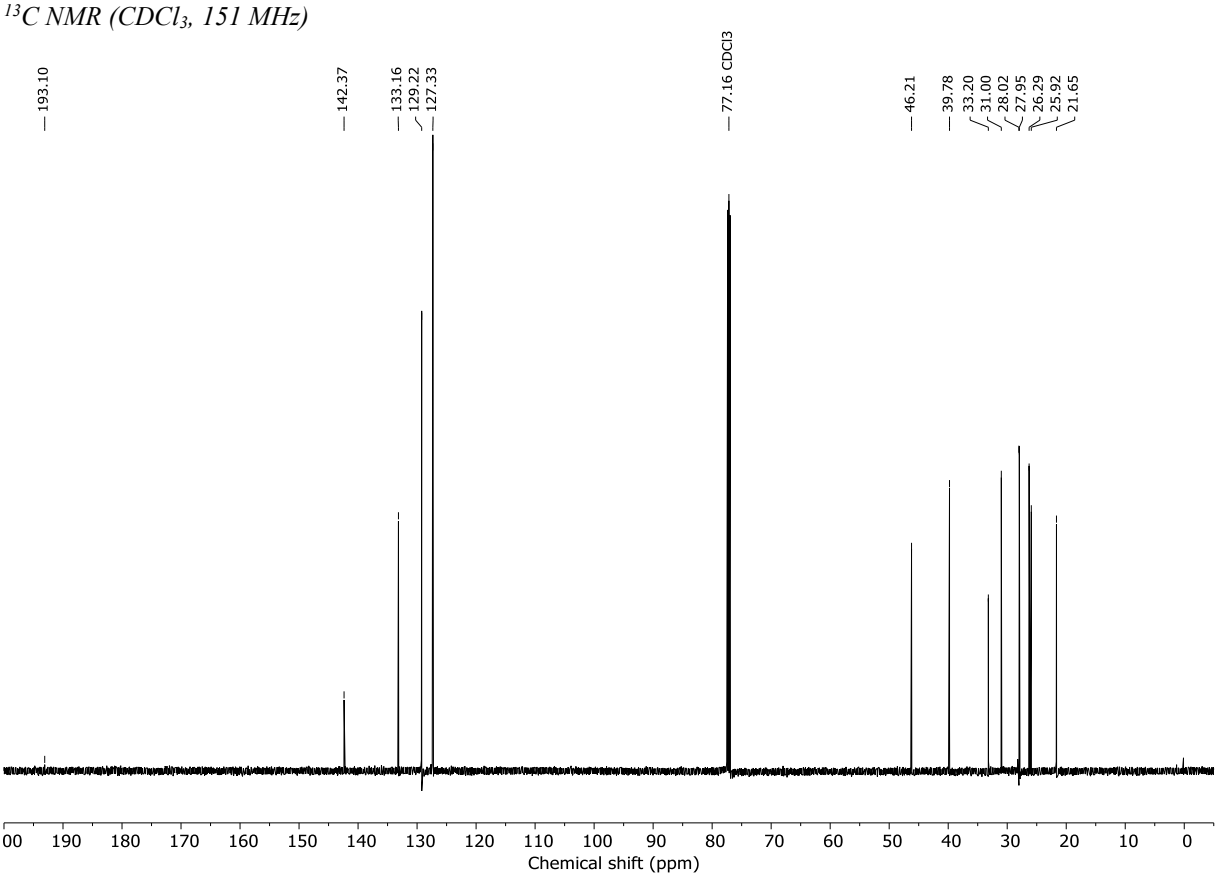

(6-tosyl-6-azaspiro[2.5]octan-1-yl)methanol (54)

^{1}H NMR ($CDCl_3$, 500 MHz)

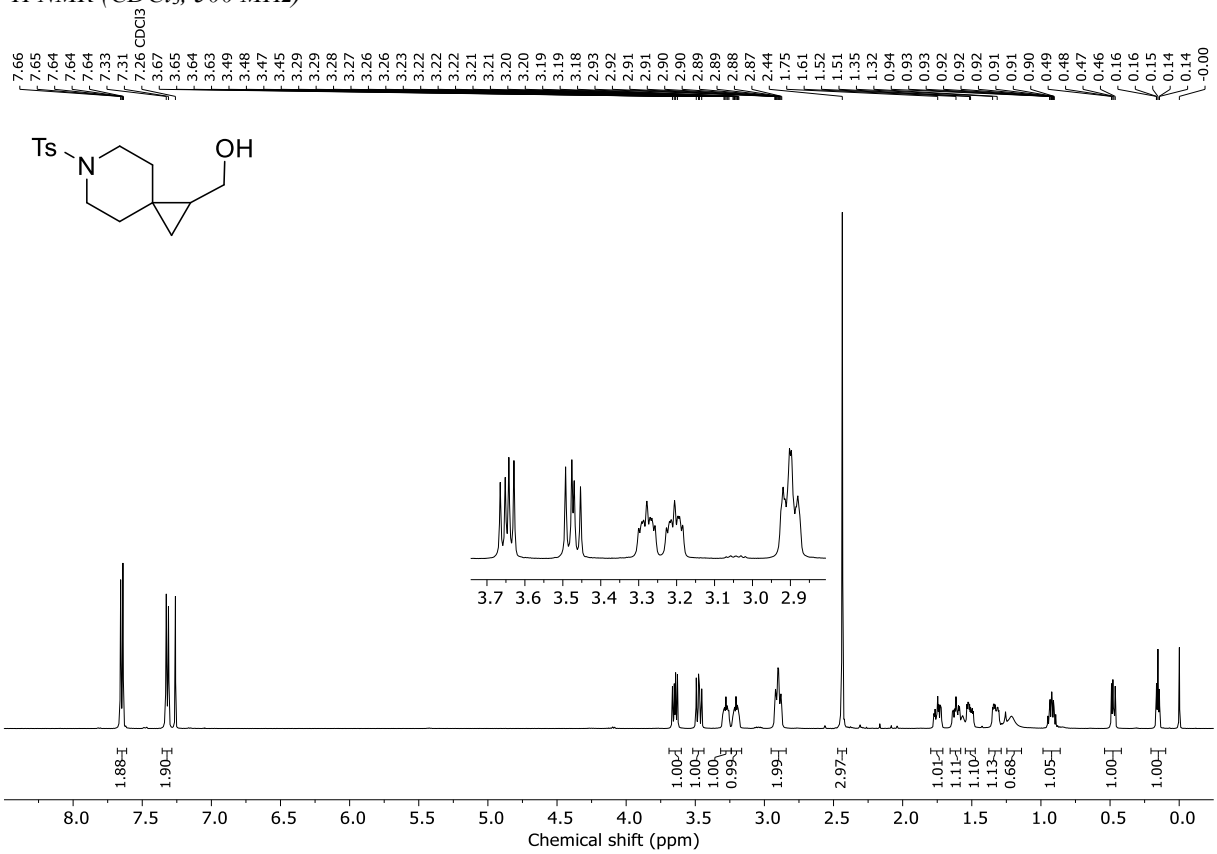

^{13}C NMR ($CDCl_3$, 126 MHz)

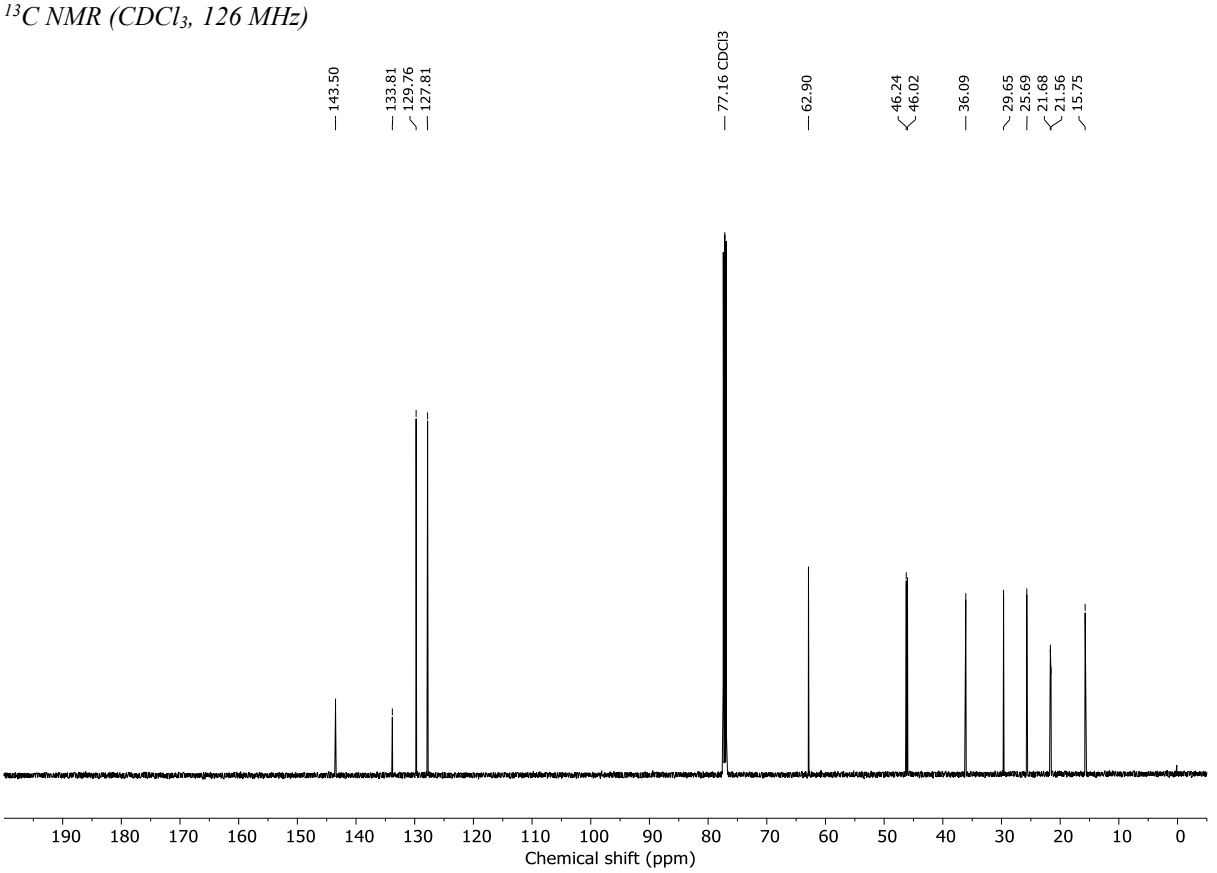

6-tosyl-6-azaspiro[2.5]octane-1-carbonitrile (55)

^{1}H NMR ($CDCl_3$, 600 MHz)

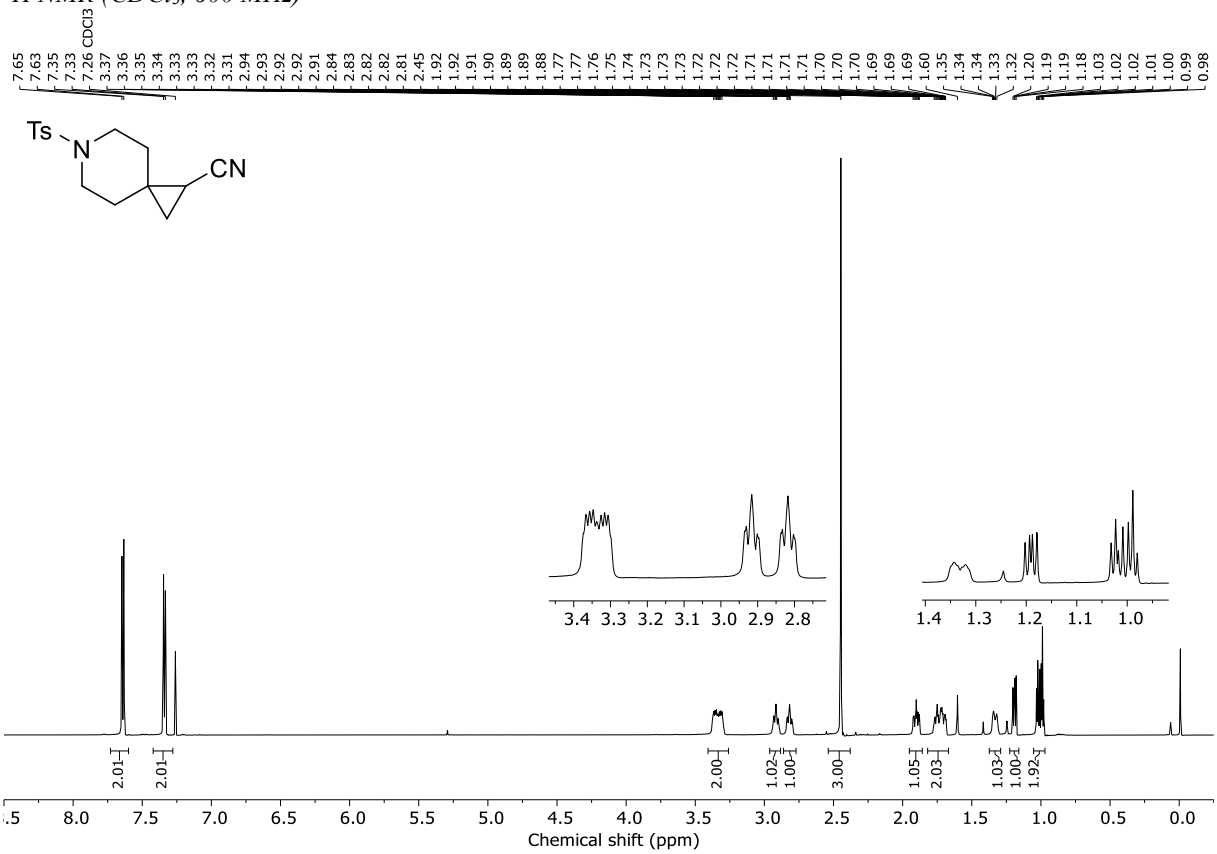

^{13}C NMR ($CDCl_3$, 151 MHz)

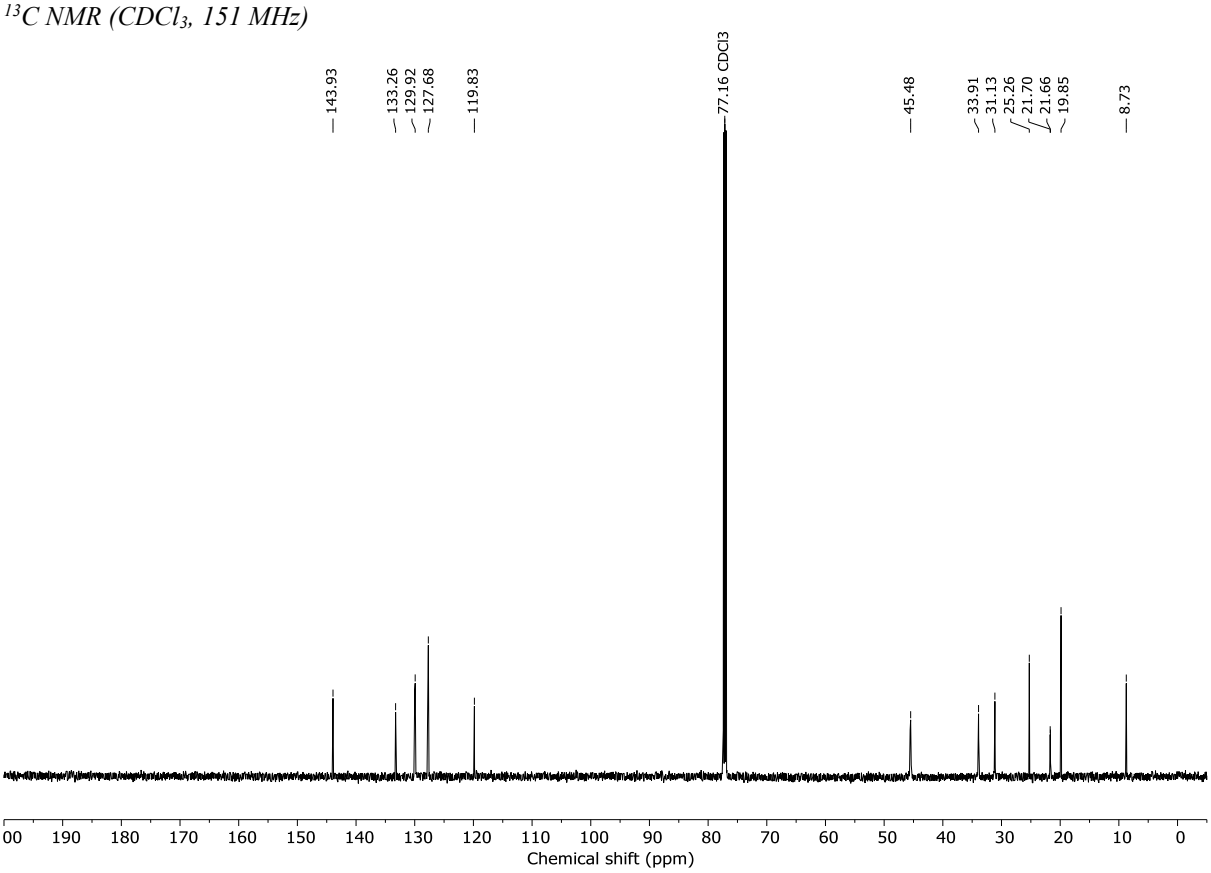

N,N-dimethyl-6-tosyl-6-azaspiro[2.5]octane-1-carboxamide (56)

^{1}H NMR ($CDCl_3$, 500 MHz)

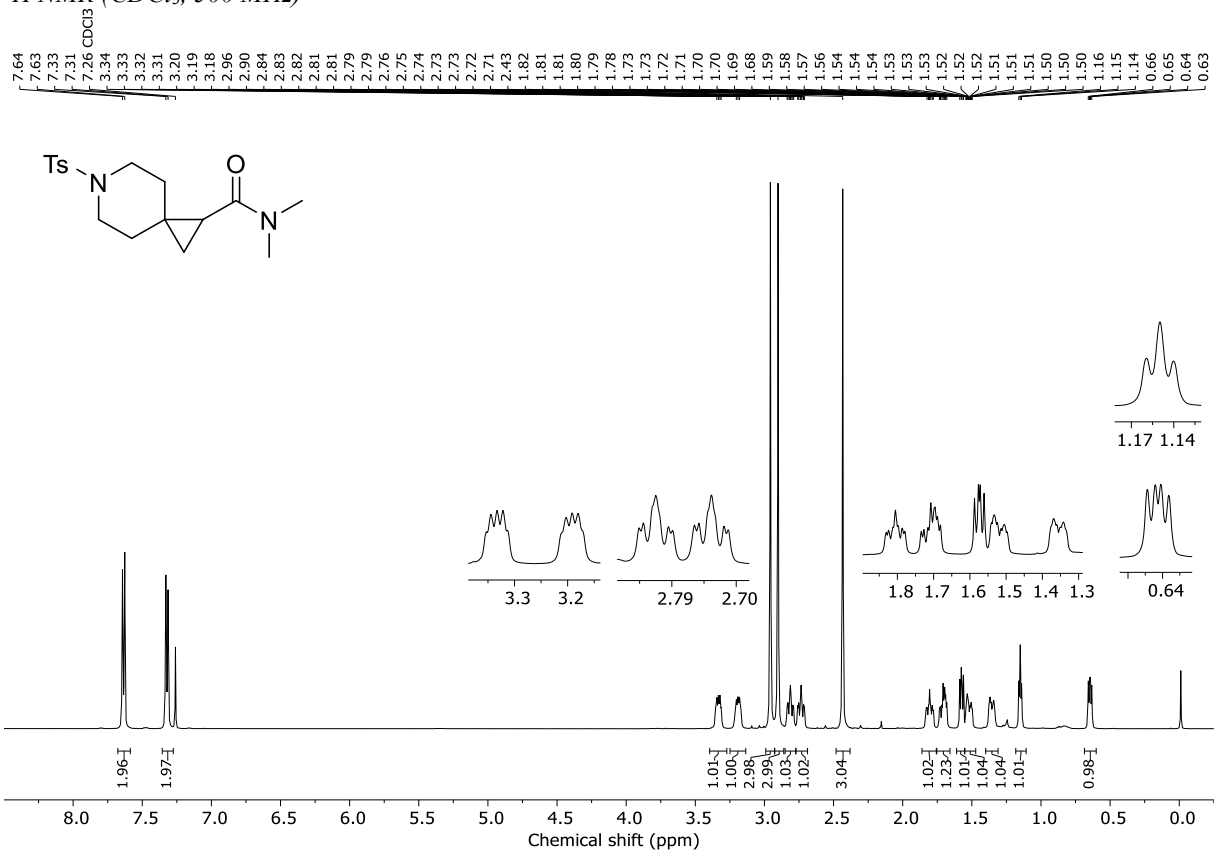

^{13}C NMR ($CDCl_3$, 126 MHz)

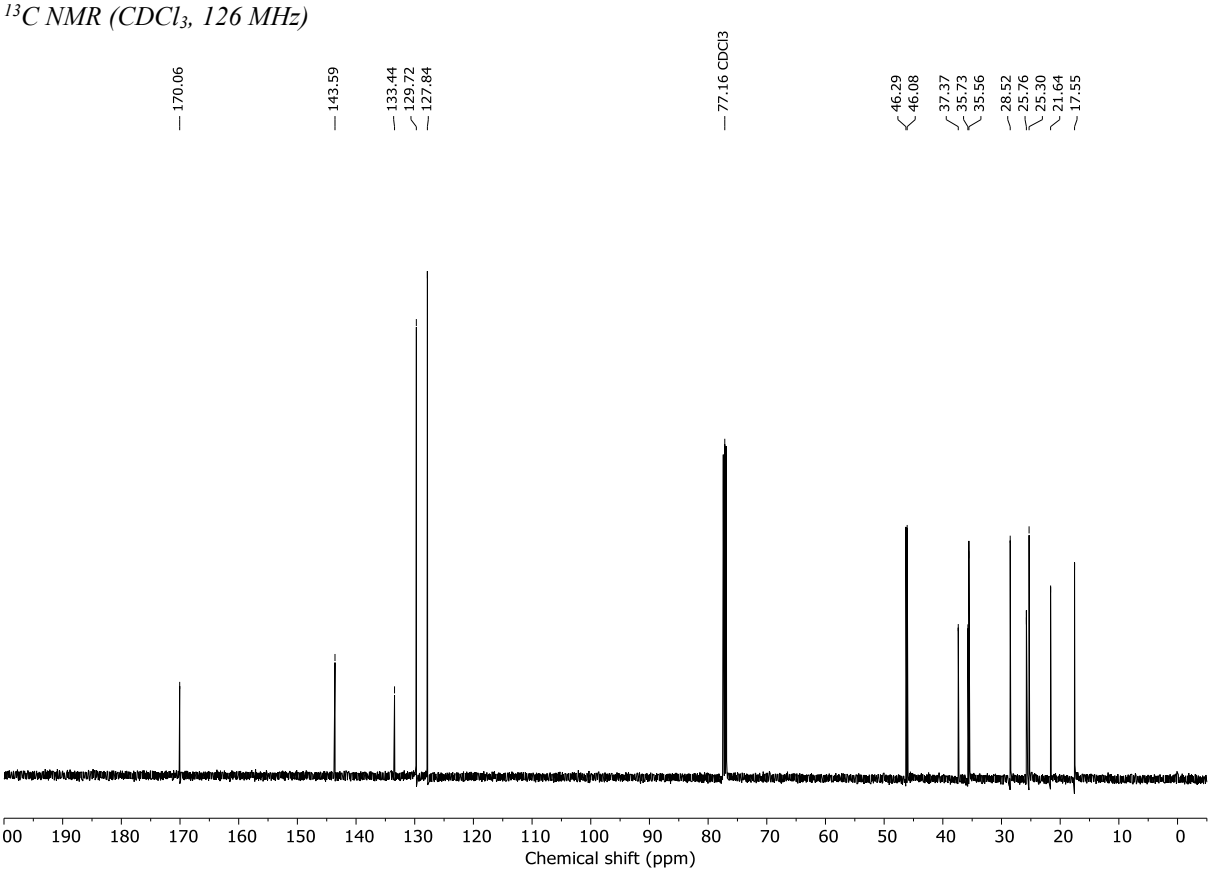

tert-butyl 1-(dimethylcarbamoyl)-6-azaspiro[2.5]octane-6-carboxylate (57)

^{1}H NMR ($CDCl_3$, 500 MHz)

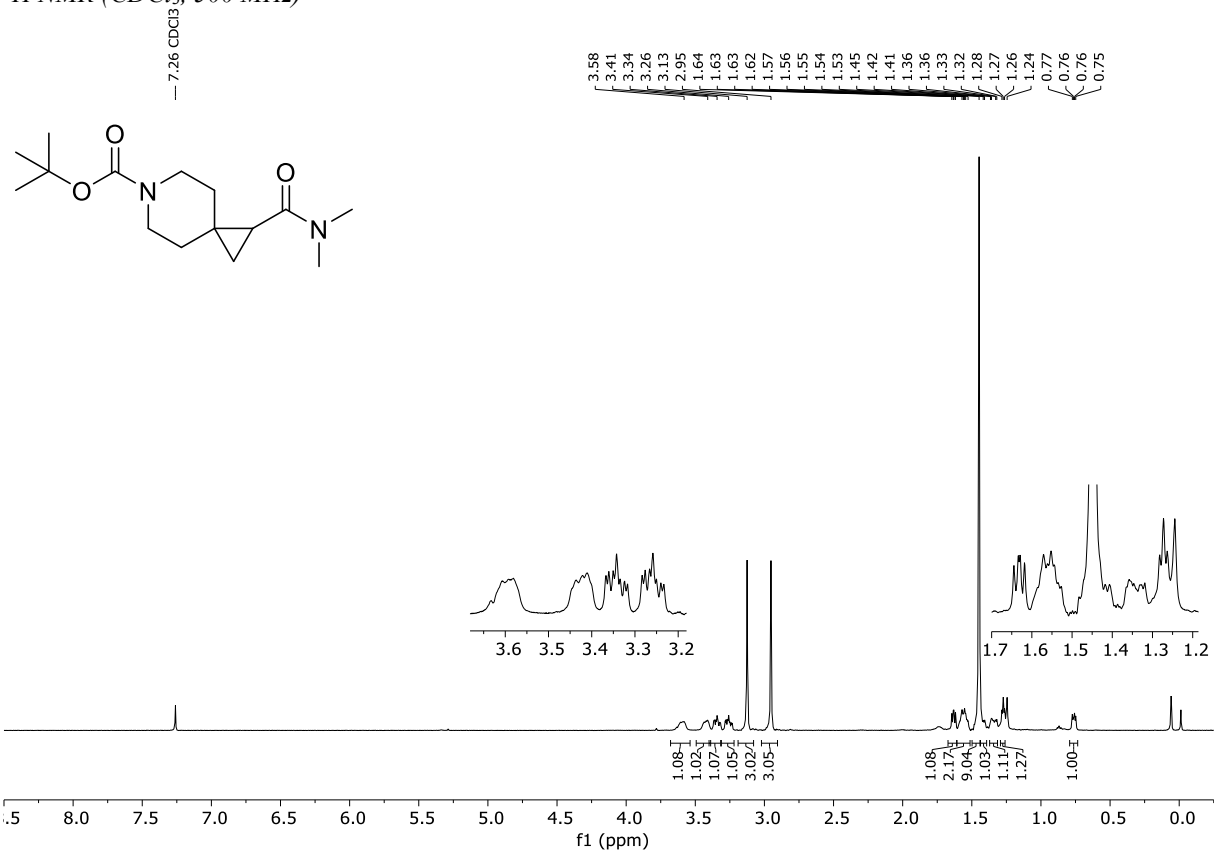

^{13}C NMR ($CDCl_3$, 126 MHz)

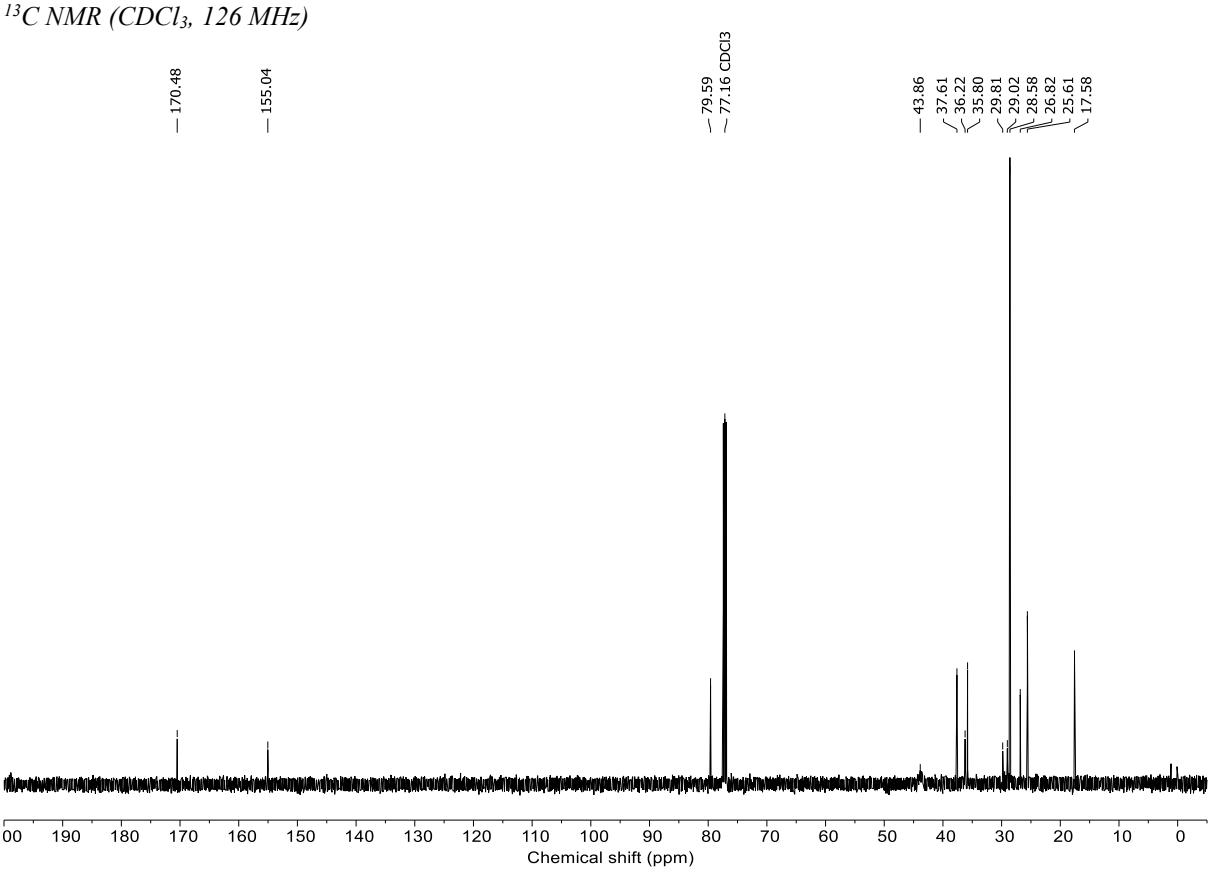

N-phenylspiro[2.5]octane-1-carboxamide (58)

^{1}H NMR ($CDCl_3$, 500 MHz)

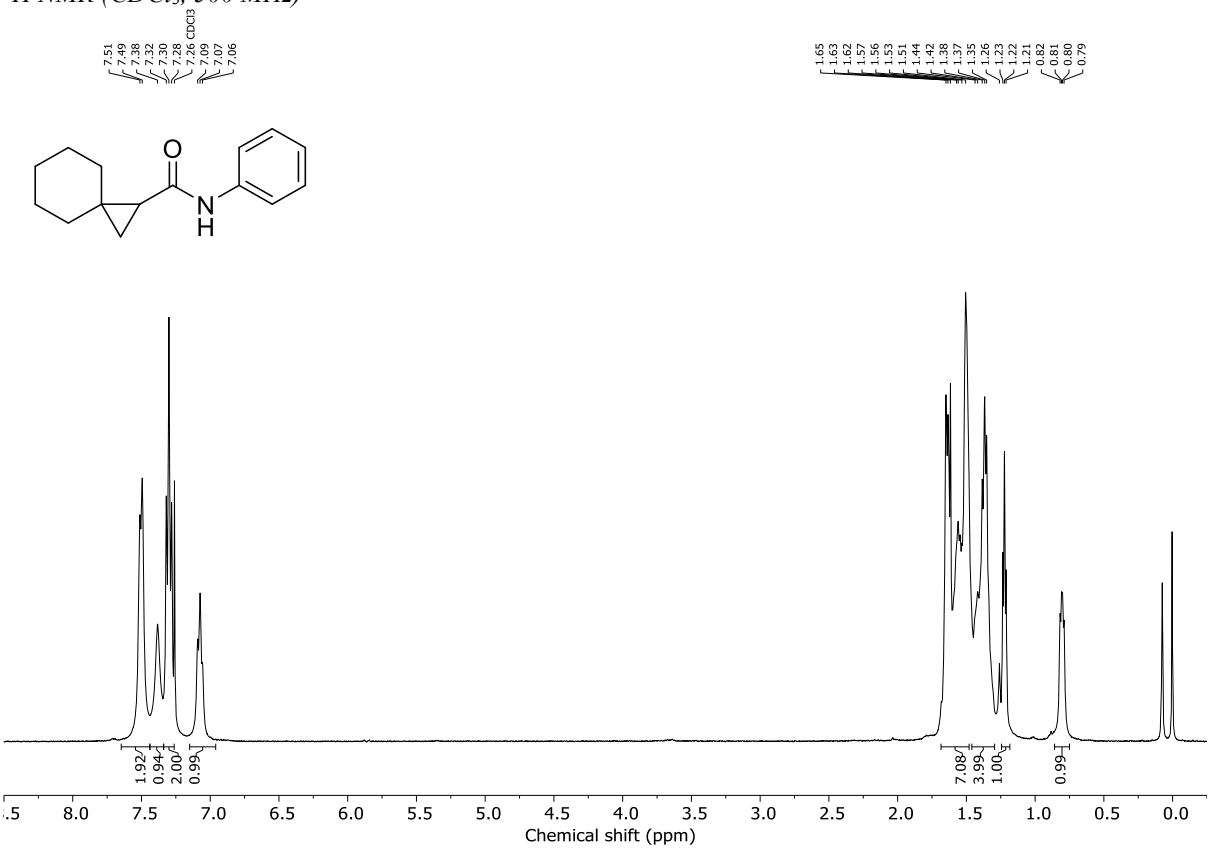

^{13}C NMR ($CDCl_3$, 126 MHz)

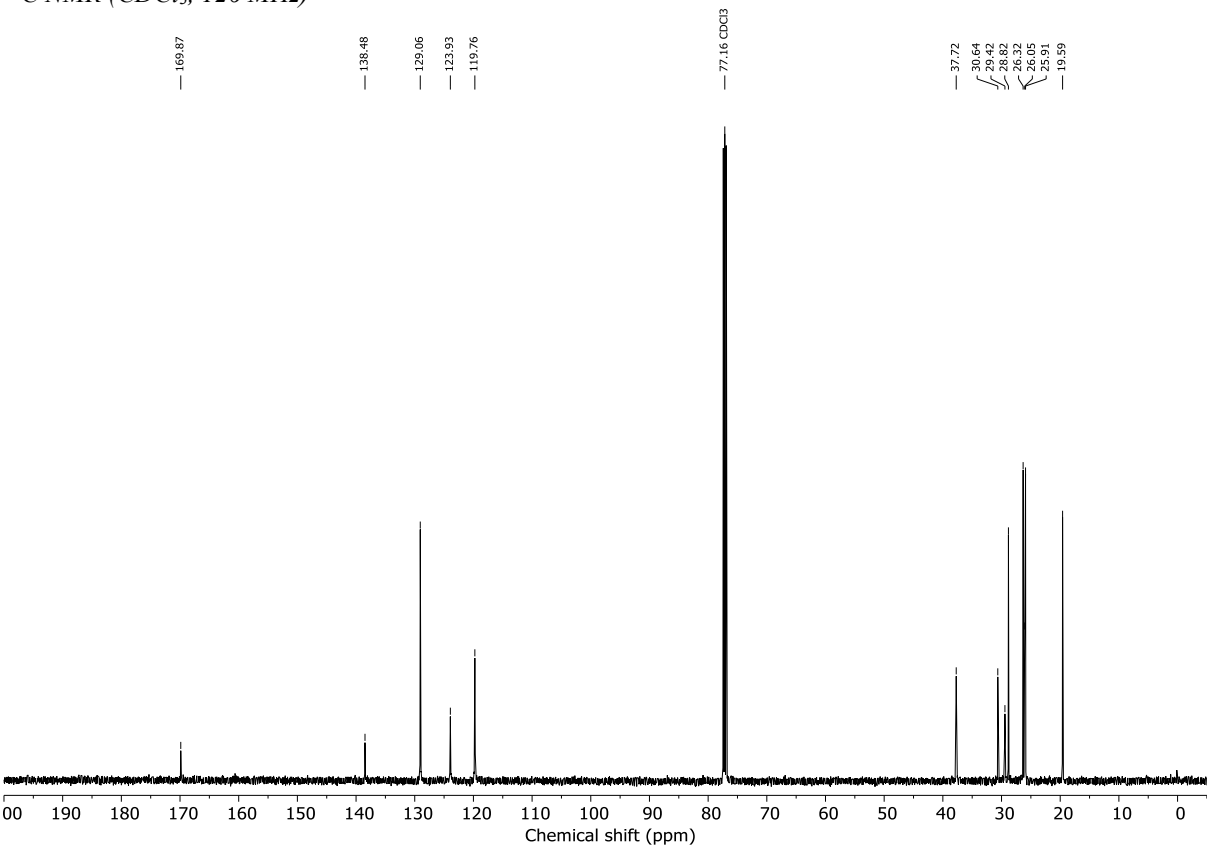

morpholino(spiro[2.5]octan-1-yl)methanone (59)

^{1}H NMR ($CDCl_3$, 400 MHz)

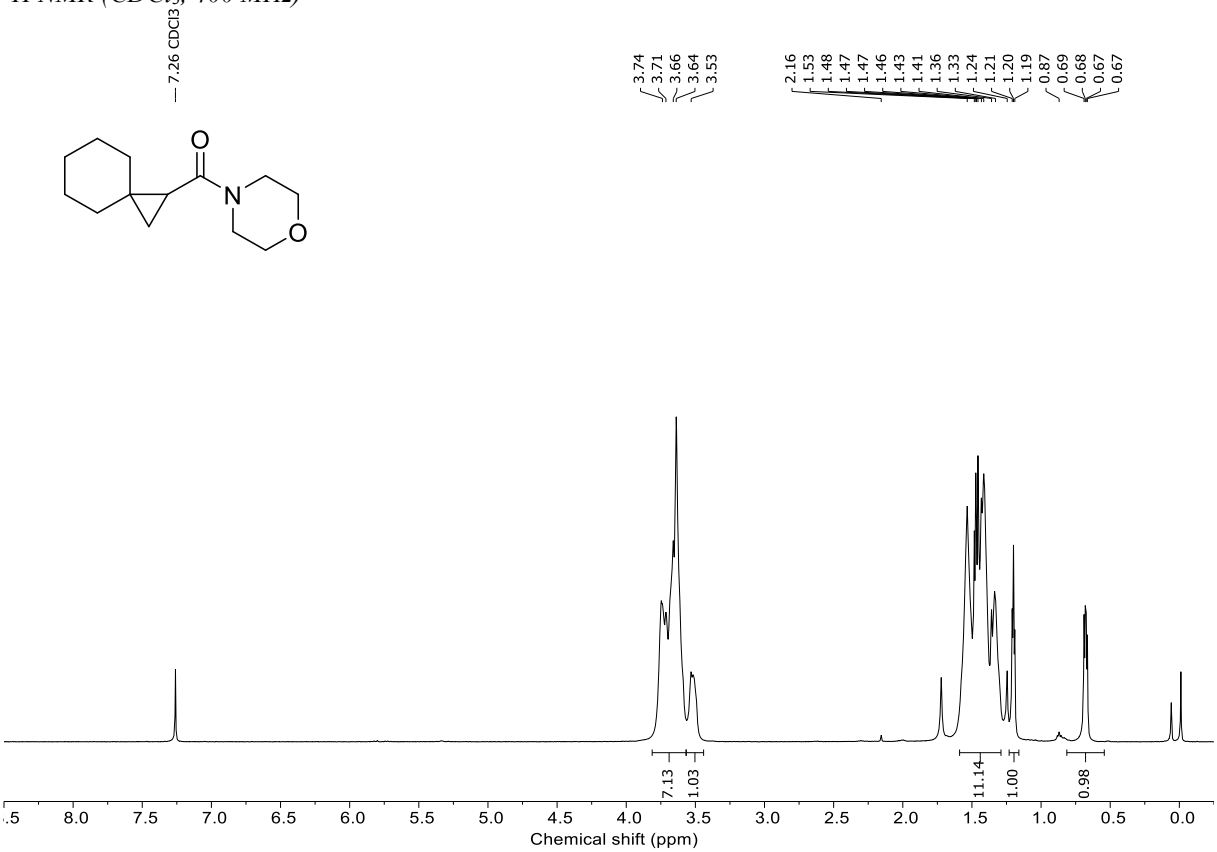

^{13}C NMR ($CDCl_3$, 126 MHz)

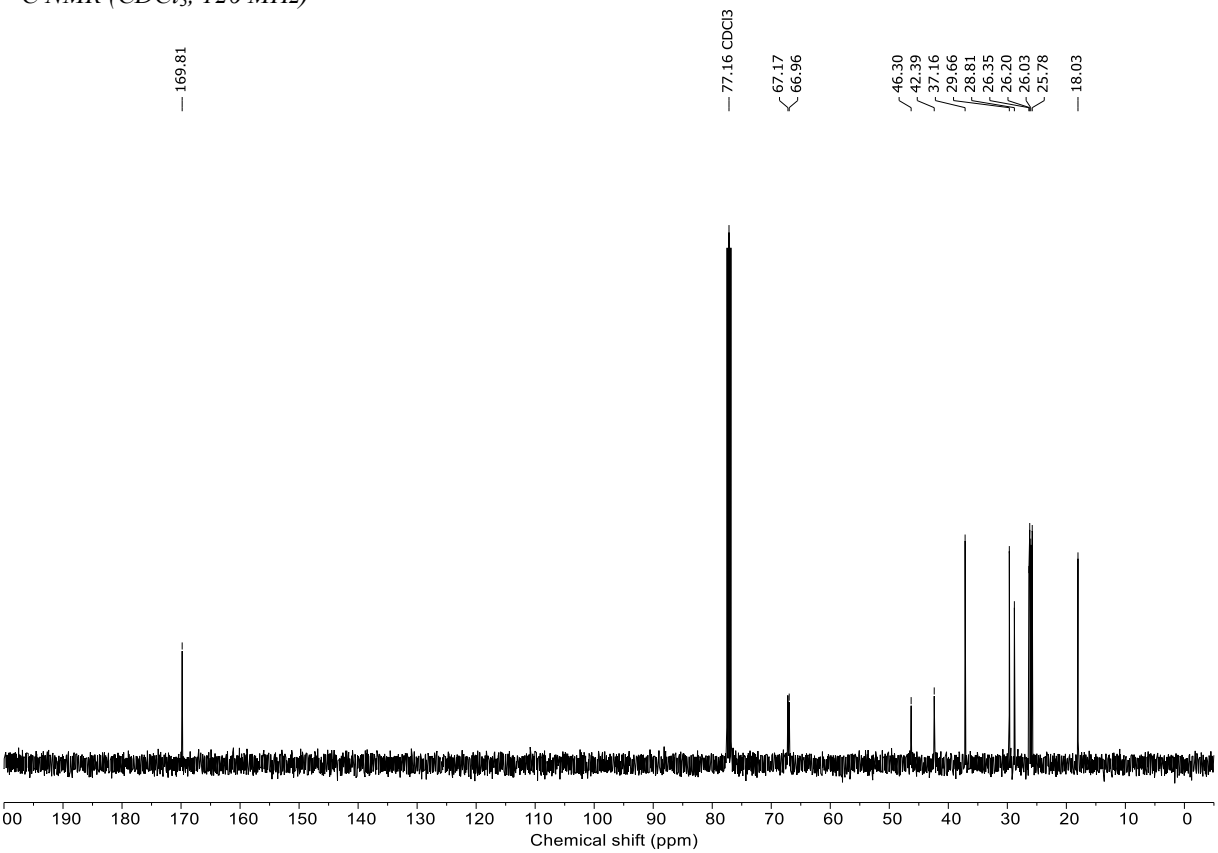

dimethyl spiro[2.5]octan-1-ylphosphonate (60)

^{1}H NMR ($CDCl_3$, 500 MHz)

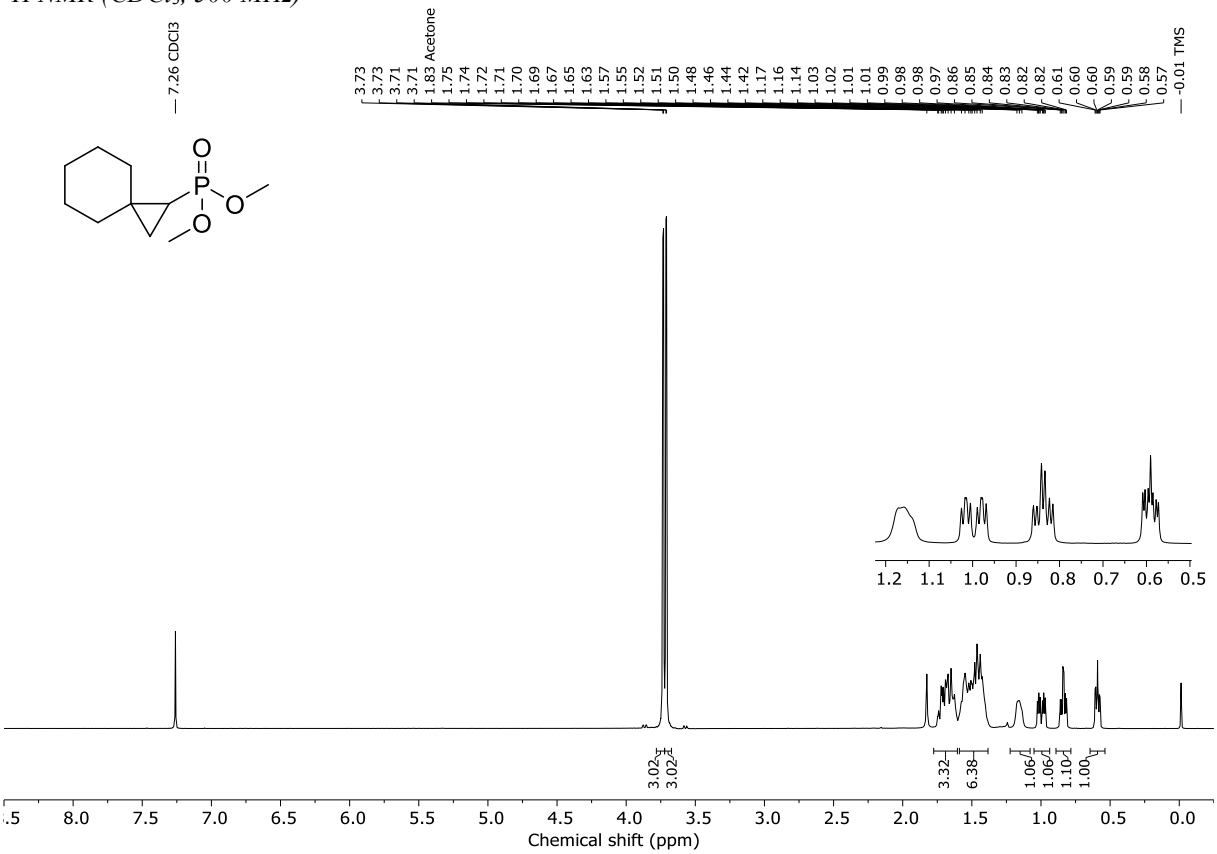

^{13}C NMR ($CDCl_3$, 126 MHz)

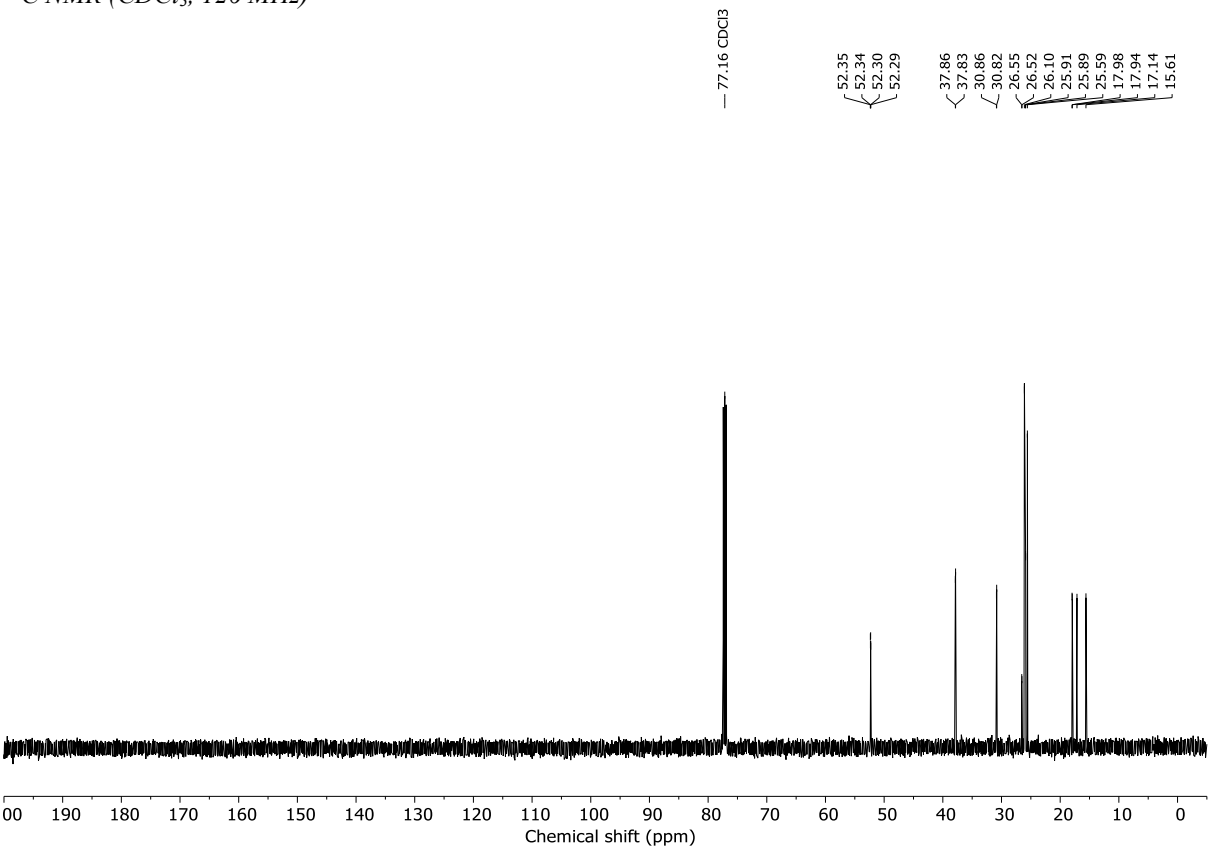

methyl 1-methyl-6-tosyl-6-azaspiro[2.5]octane-1-carboxylate (61)

^{1}H NMR ($CDCl_3$, 500 MHz)

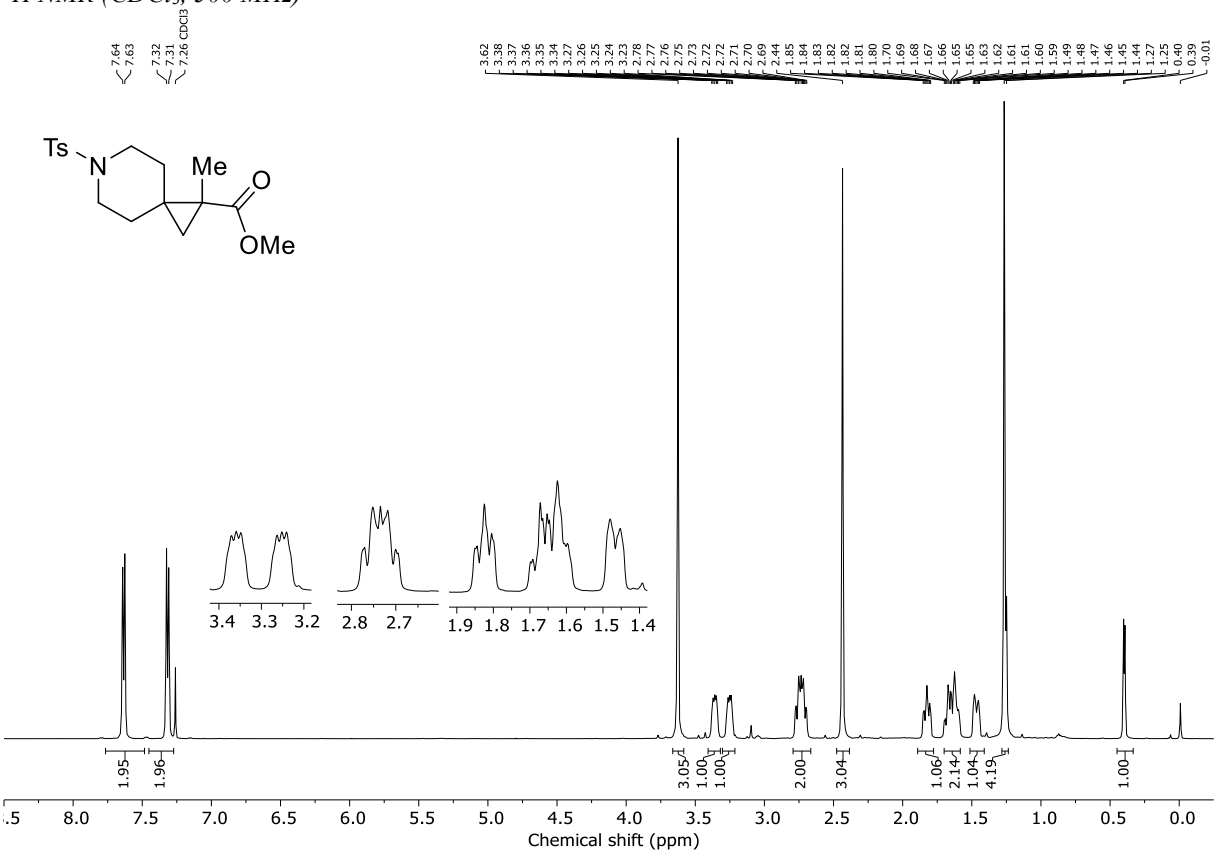

^{13}C NMR ($CDCl_3$, 126 MHz)

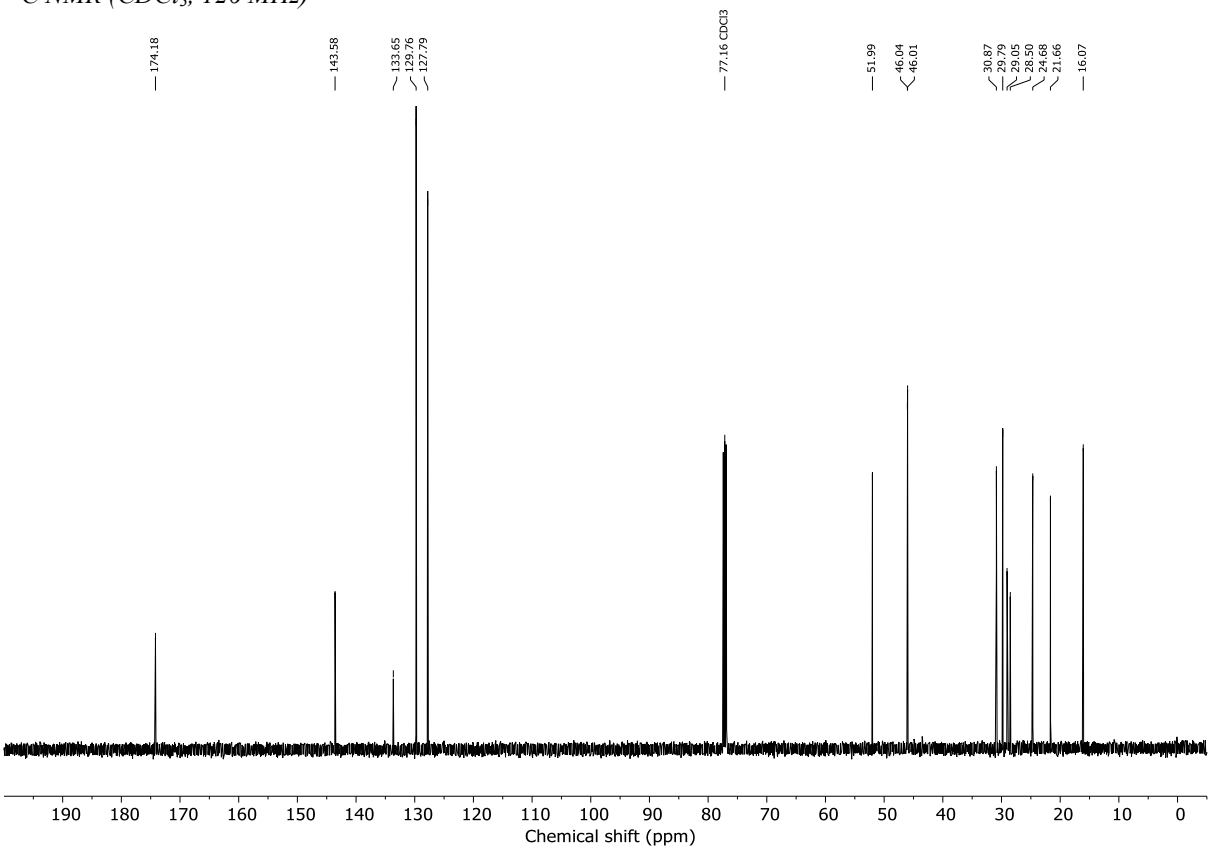

1-(1-methyl-6-tosyl-6-azaspiro[2.5]octan-1-yl)ethan-1-one (62)

^{1}H NMR ($CDCl_3$, 500 MHz)

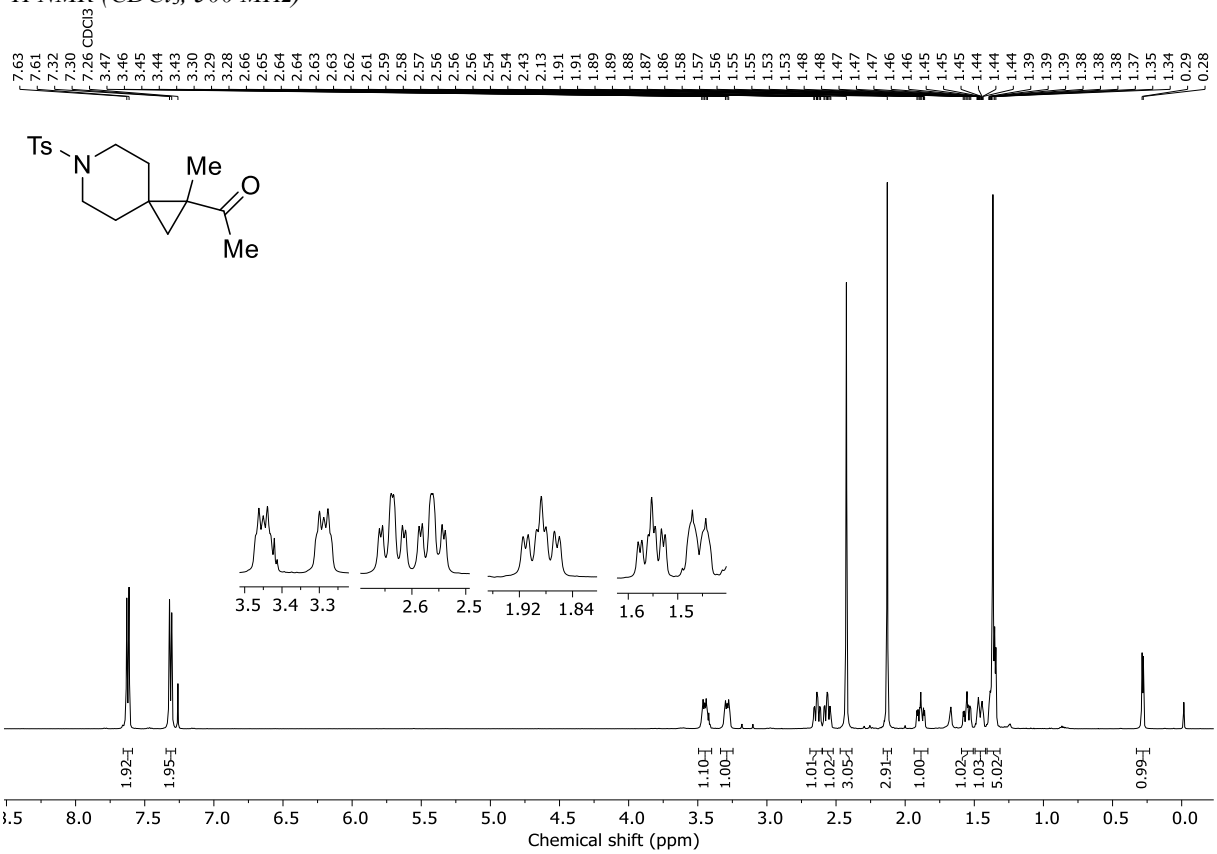

^{13}C NMR ($CDCl_3$, 126 MHz)

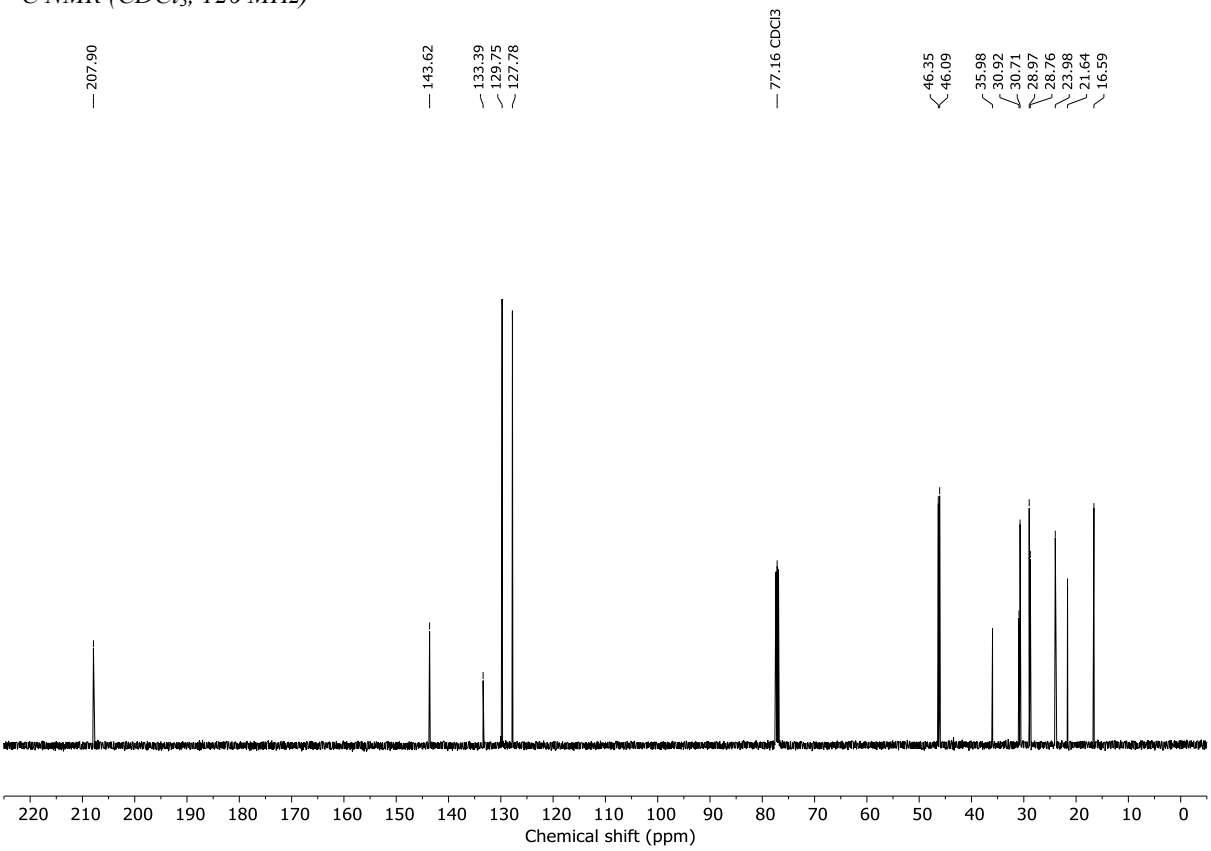

methyl 1-acetamidospiro[2.5]octane-1-carboxylate (63)

^{1}H NMR (DMSO-d6, 70 ºC) 500 MHz

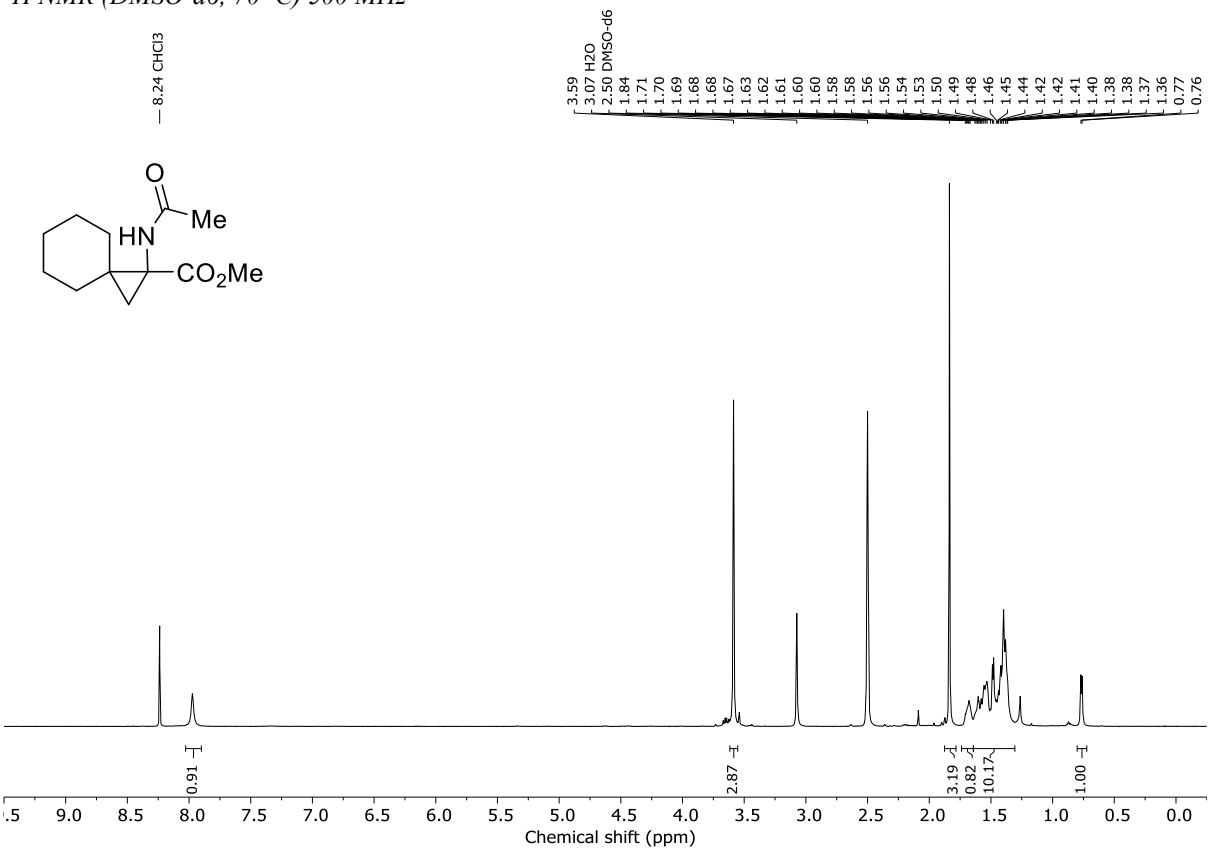

^{13}C NMR (DMSO-d6, 70 ºC) 126 MHz

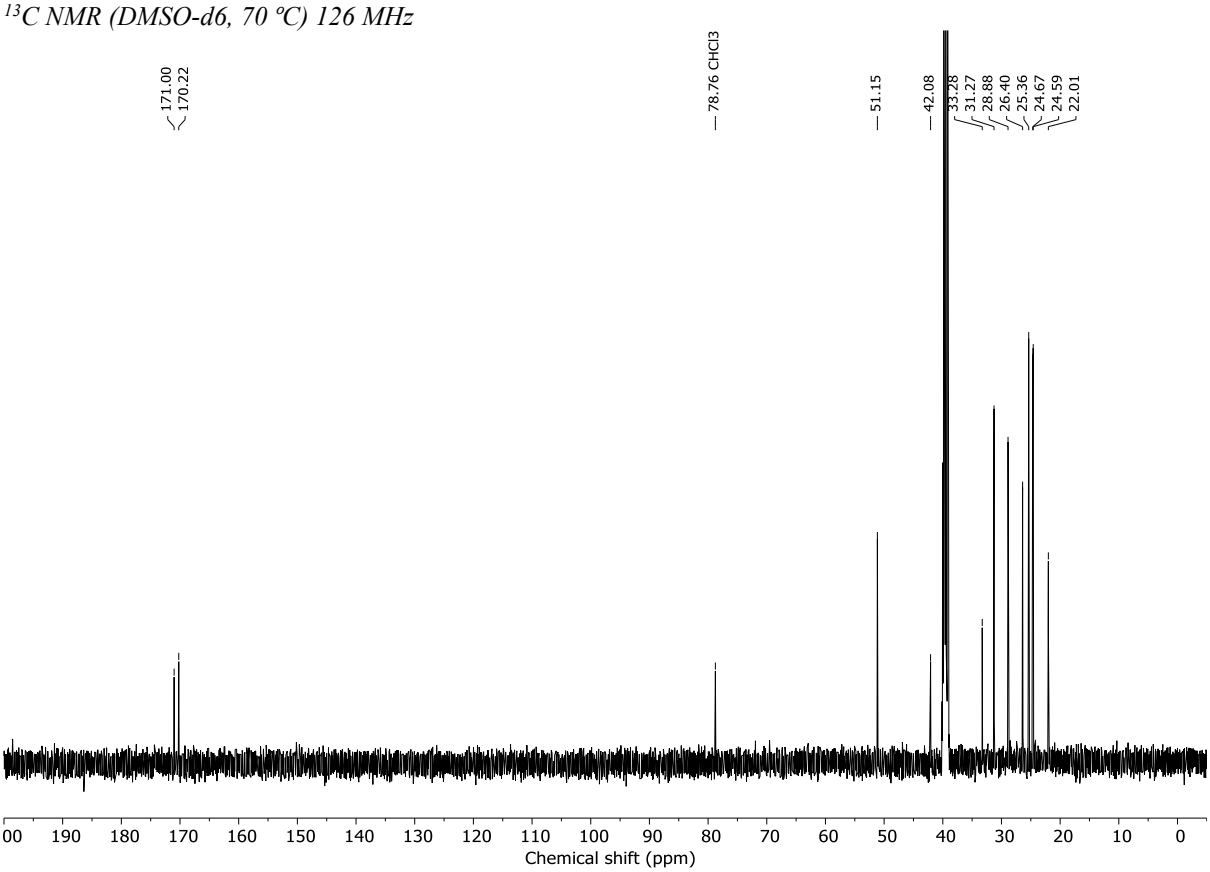

benzyl 1-phenylspiro[2.5]octane-1-carboxylate (64)

^{1}H NMR ($CDCl_3$, 500 MHz)

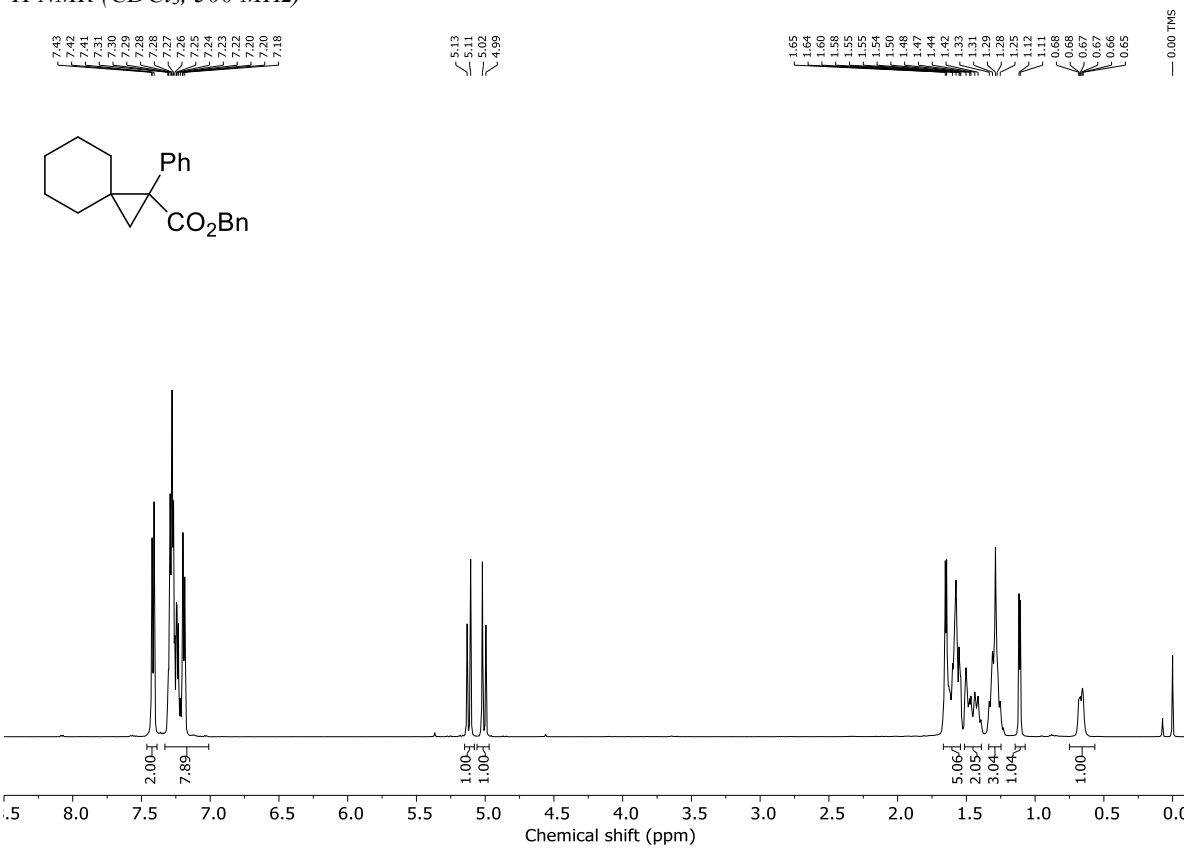

^{13}C NMR ($CDCl_3$, 126 MHz)

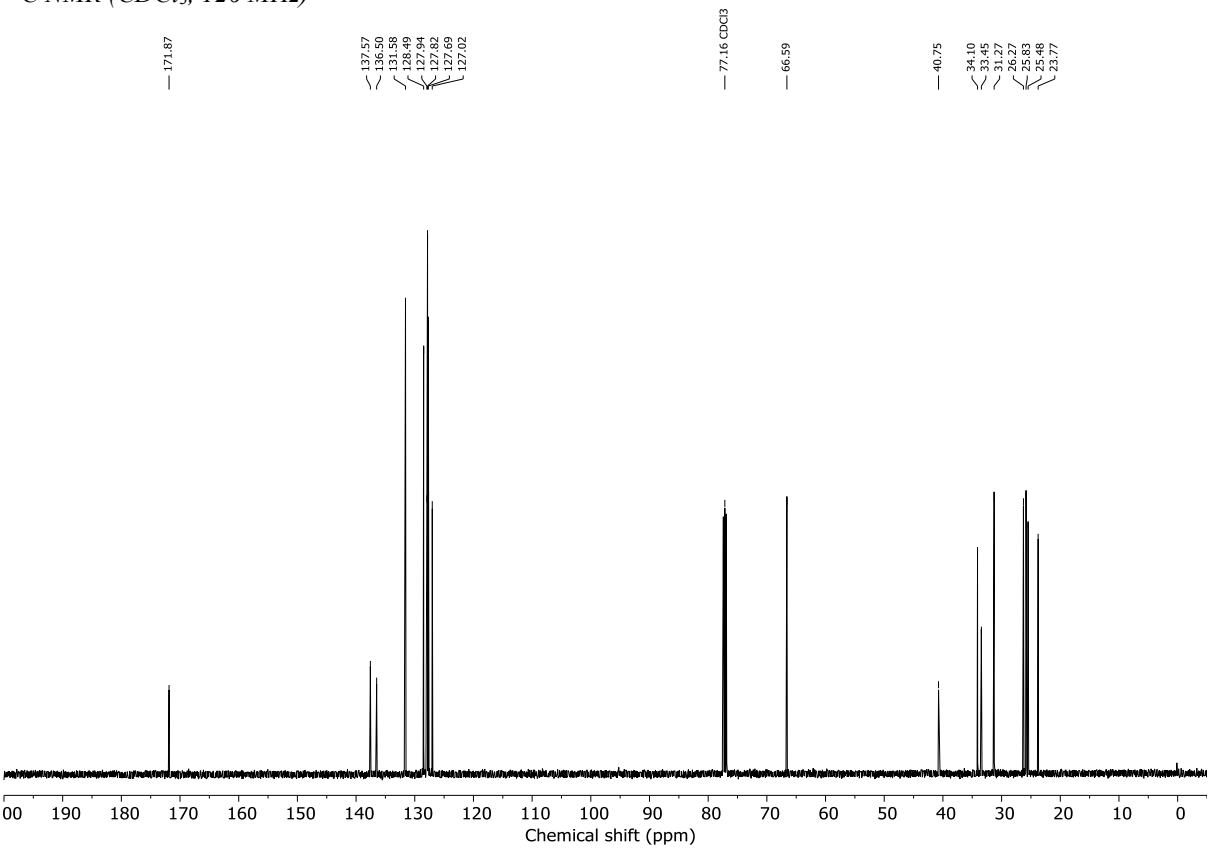

ethyl 1-((phenylsulfonyl)methyl)spiro[2.5]octane-1-carboxylate (65)

^{1}H NMR ($CDCl_3$, 400 MHz)

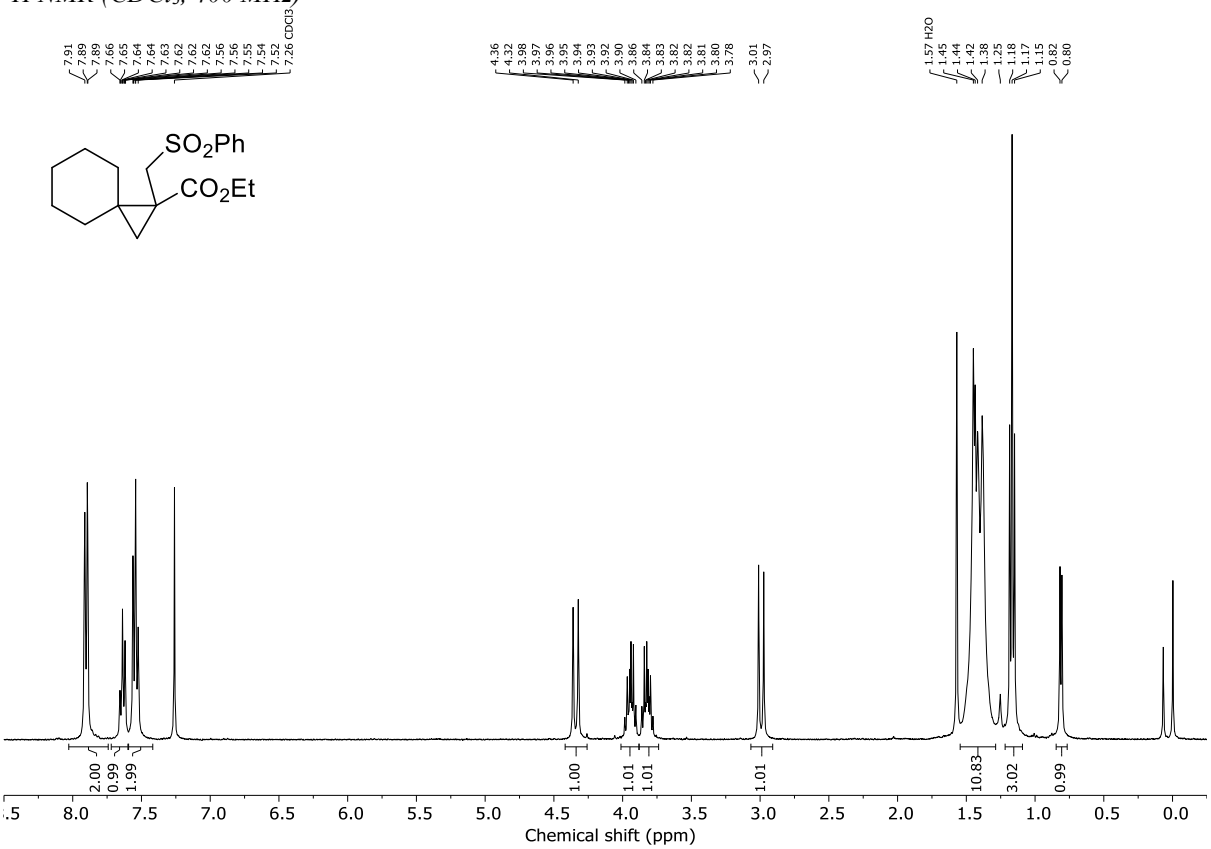

^{13}C NMR ($CDCl_3$, 151 MHz)

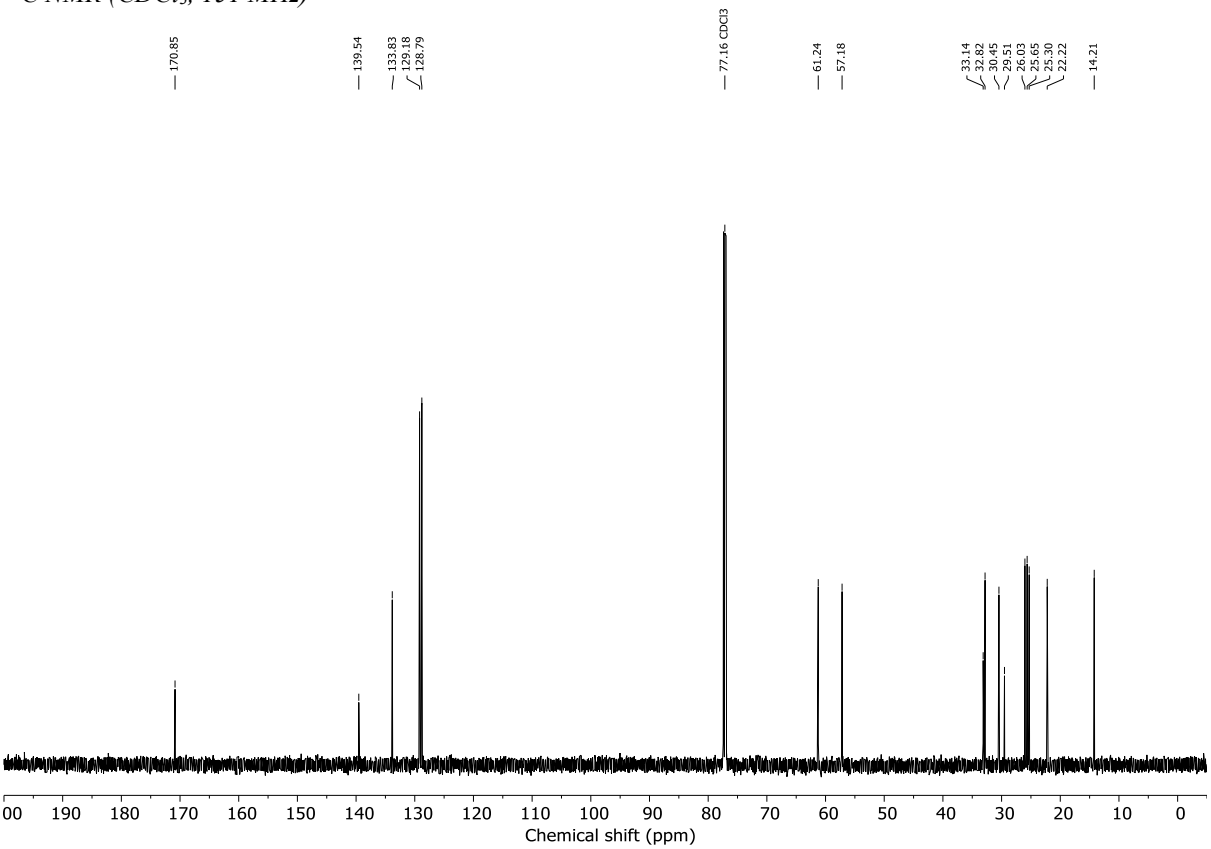

dibenzyl spiro[2.5]octane-1,1-dicarboxylate (66)

^{1}H NMR ($CDCl_3$, 500 MHz)

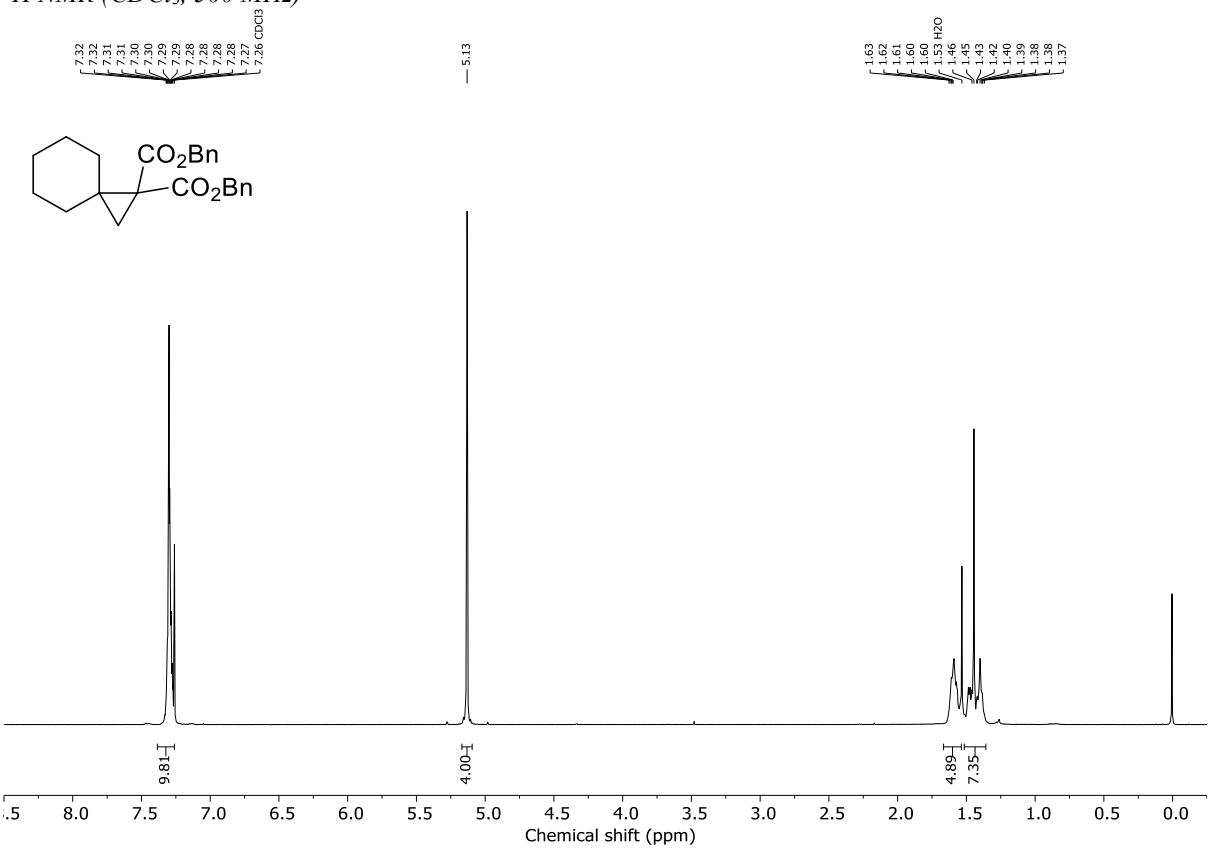

^{13}C NMR ($CDCl_3$, 126 MHz)

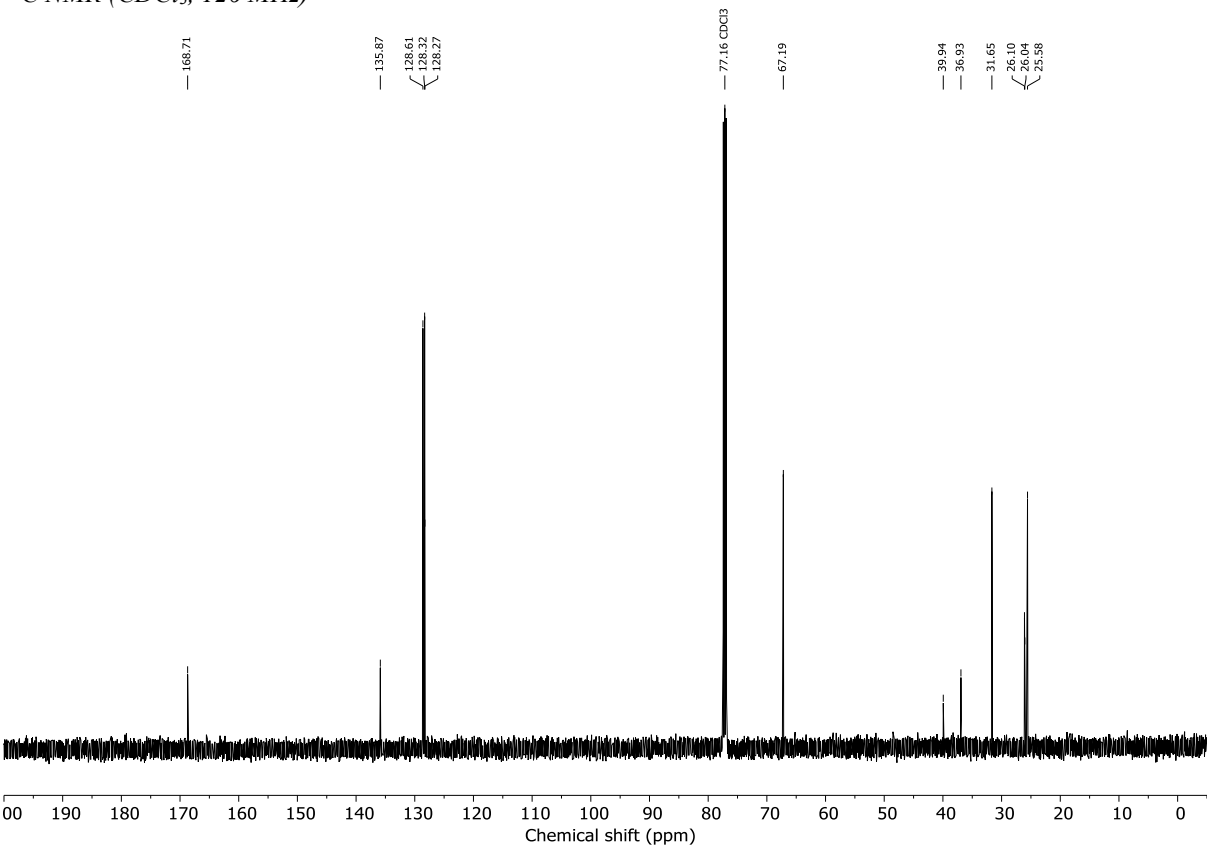

methyl 2-methyl-6-tosyl-6-azaspiro[2.5]octane-1-carboxylate (67)

^{1}H NMR ($CDCl_3$, 500 MHz)

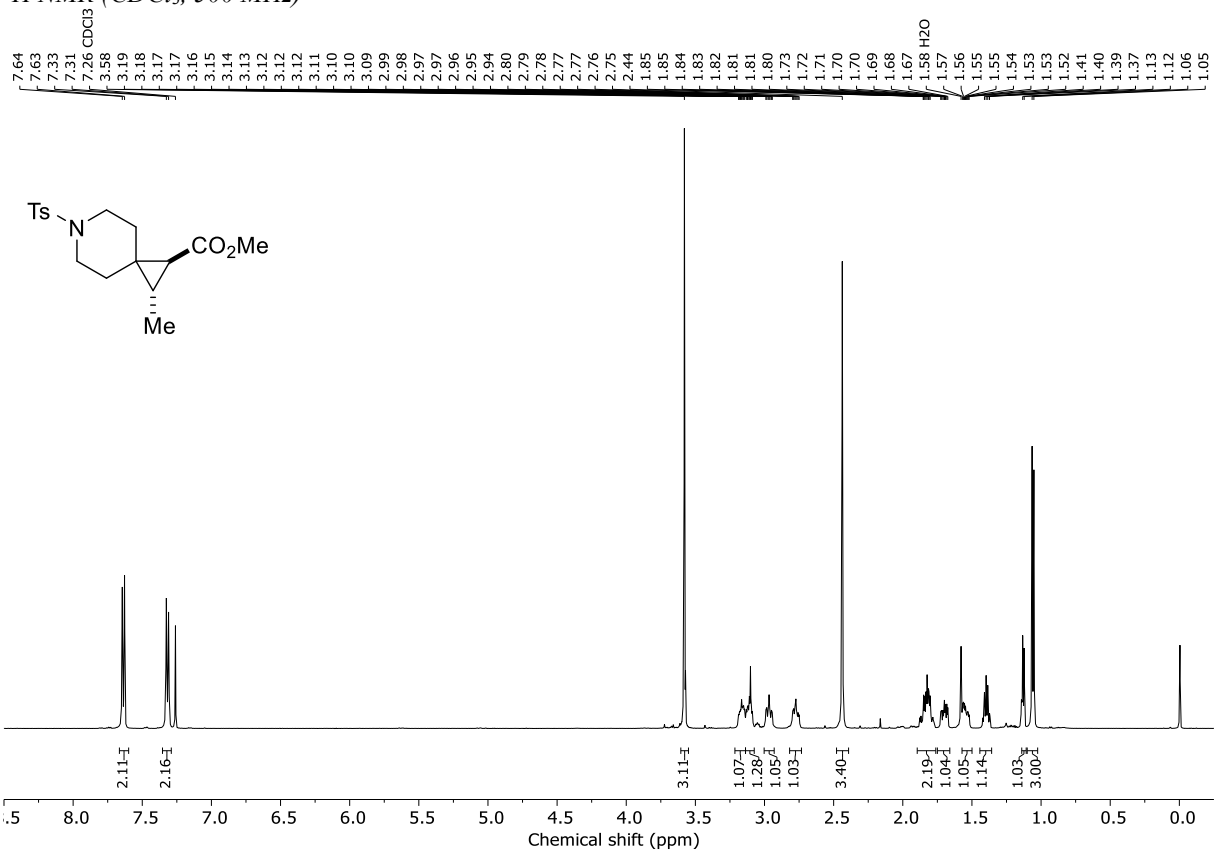

^{13}C NMR ($CDCl_3$, 126 MHz)

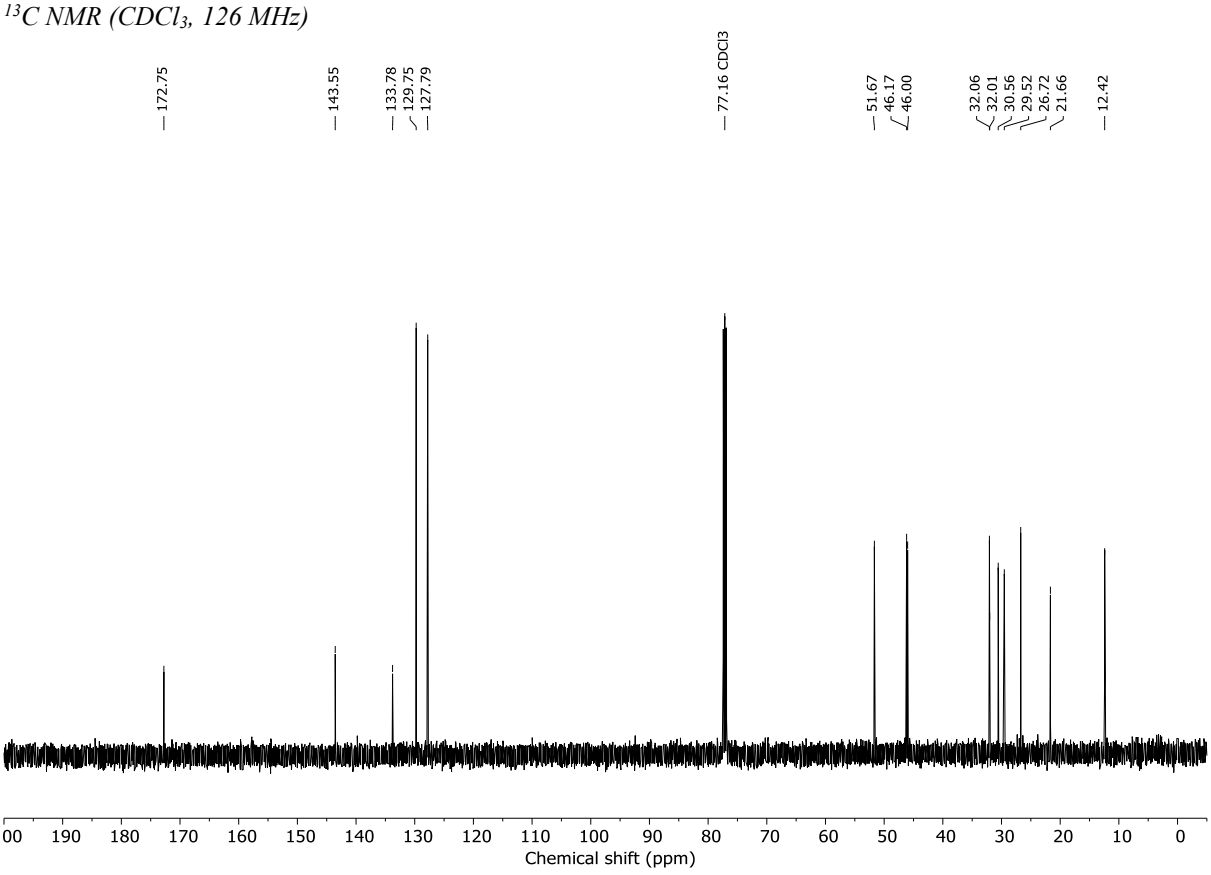

NOESY:

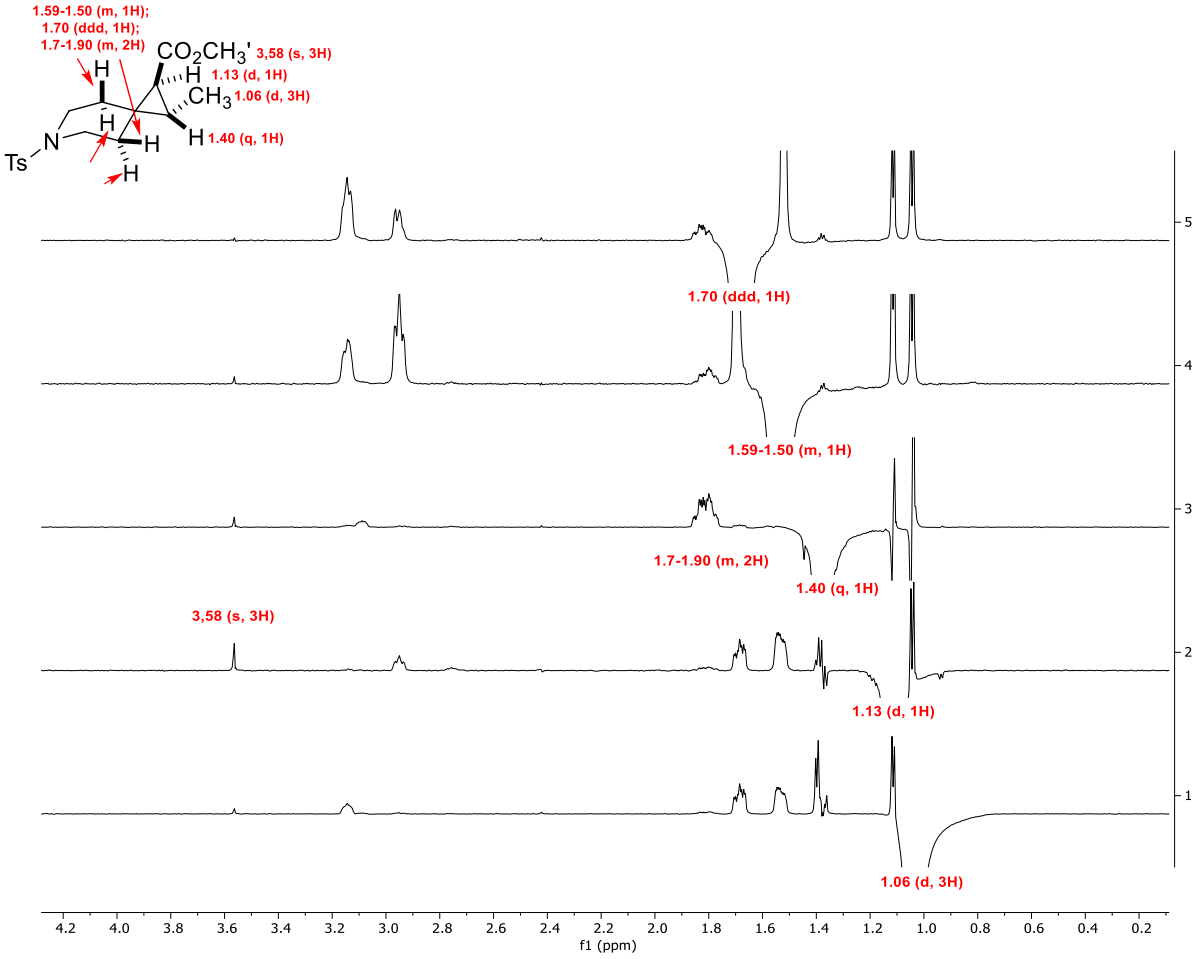

dimethyl 6-tosyl-6-azaspiro[2.5]octane-1,2-dicarboxylate (68)

^{1}H NMR ($CDCl_3$, 500 MHz)

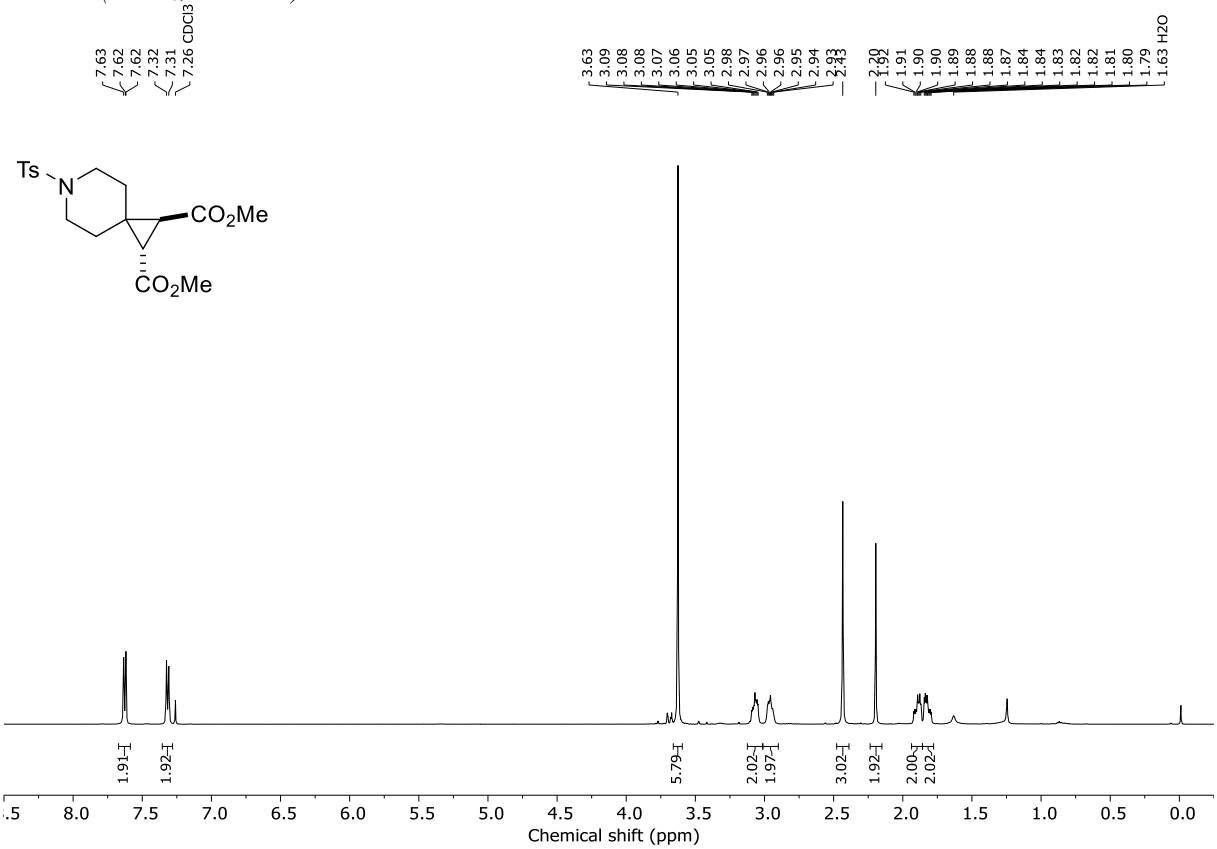

^{13}C NMR ($CDCl_3$, 126 MHz)

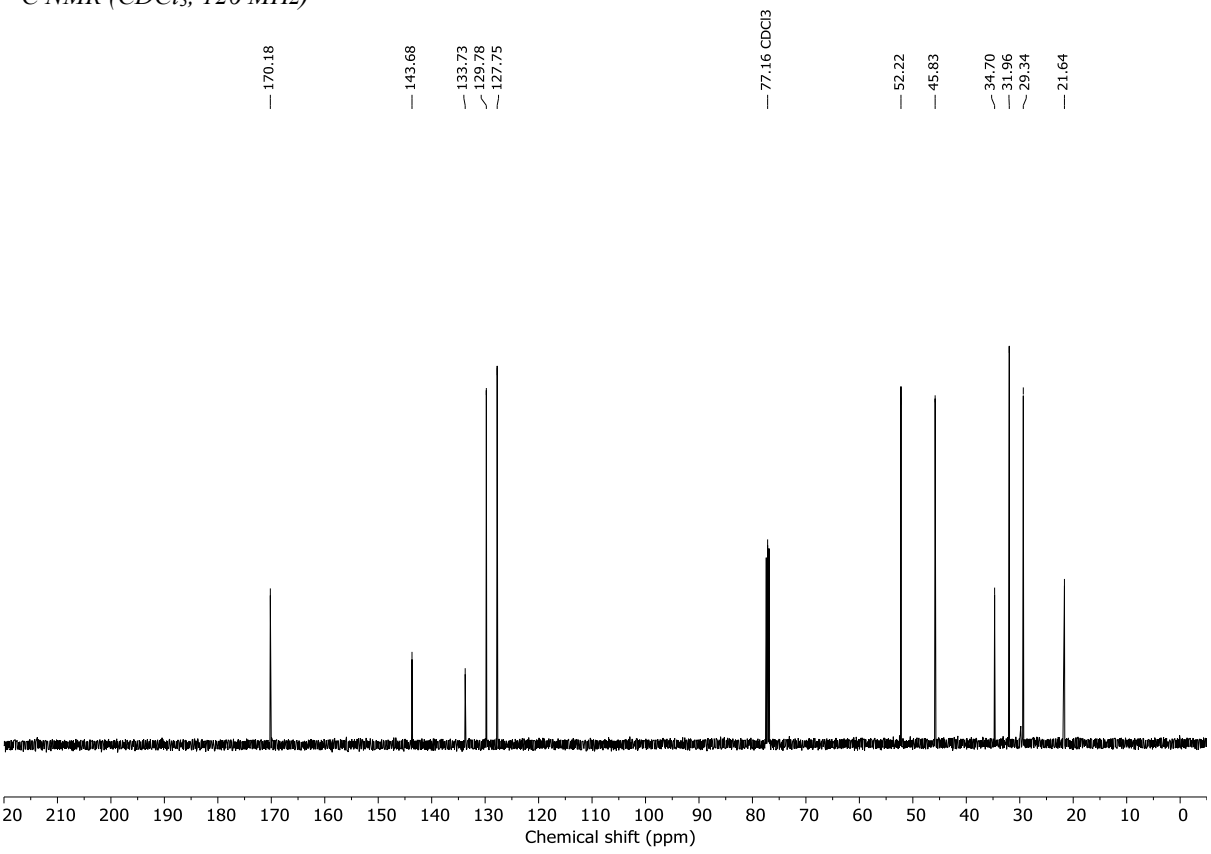

Cyclohexyl benzoate (70)

^{1}H NMR ($CDCl_3$, 400 MHz)

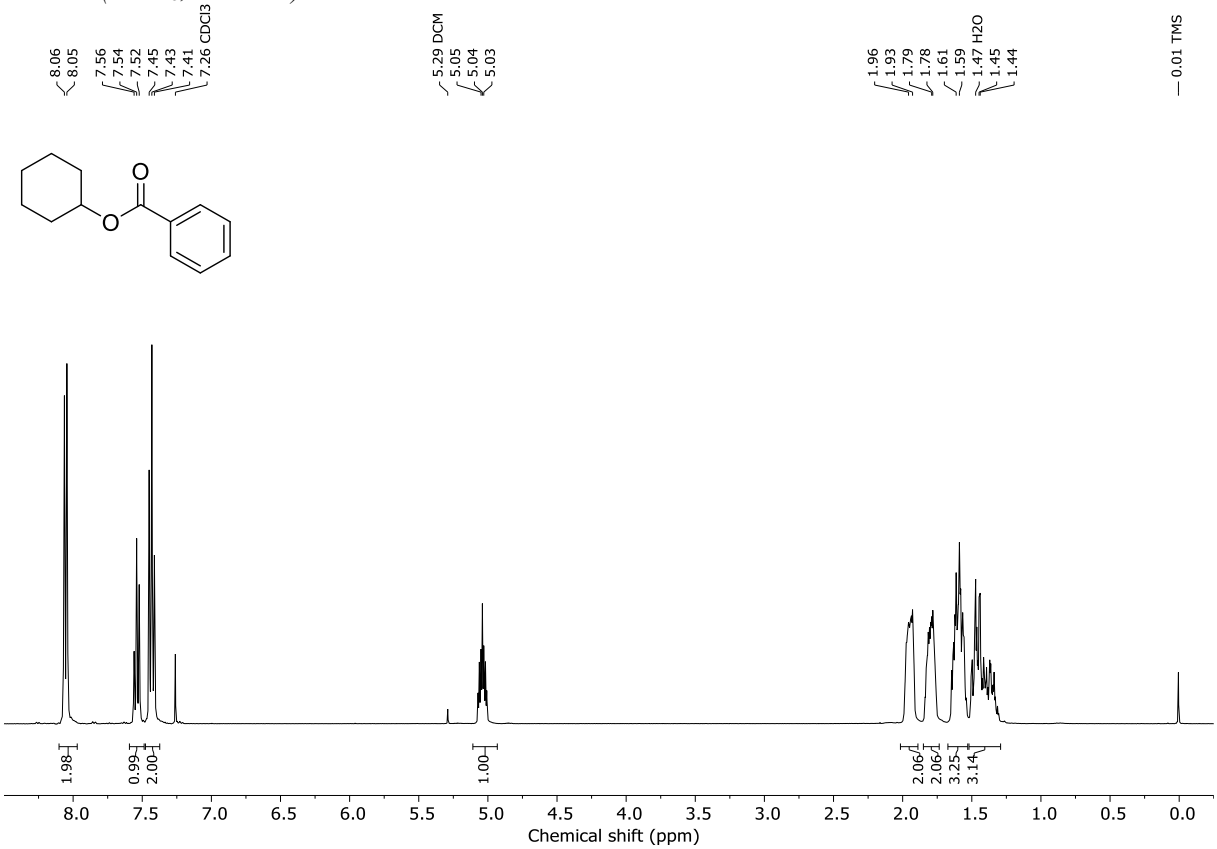

^{13}C NMR ($CDCl_3$, 101 MHz)

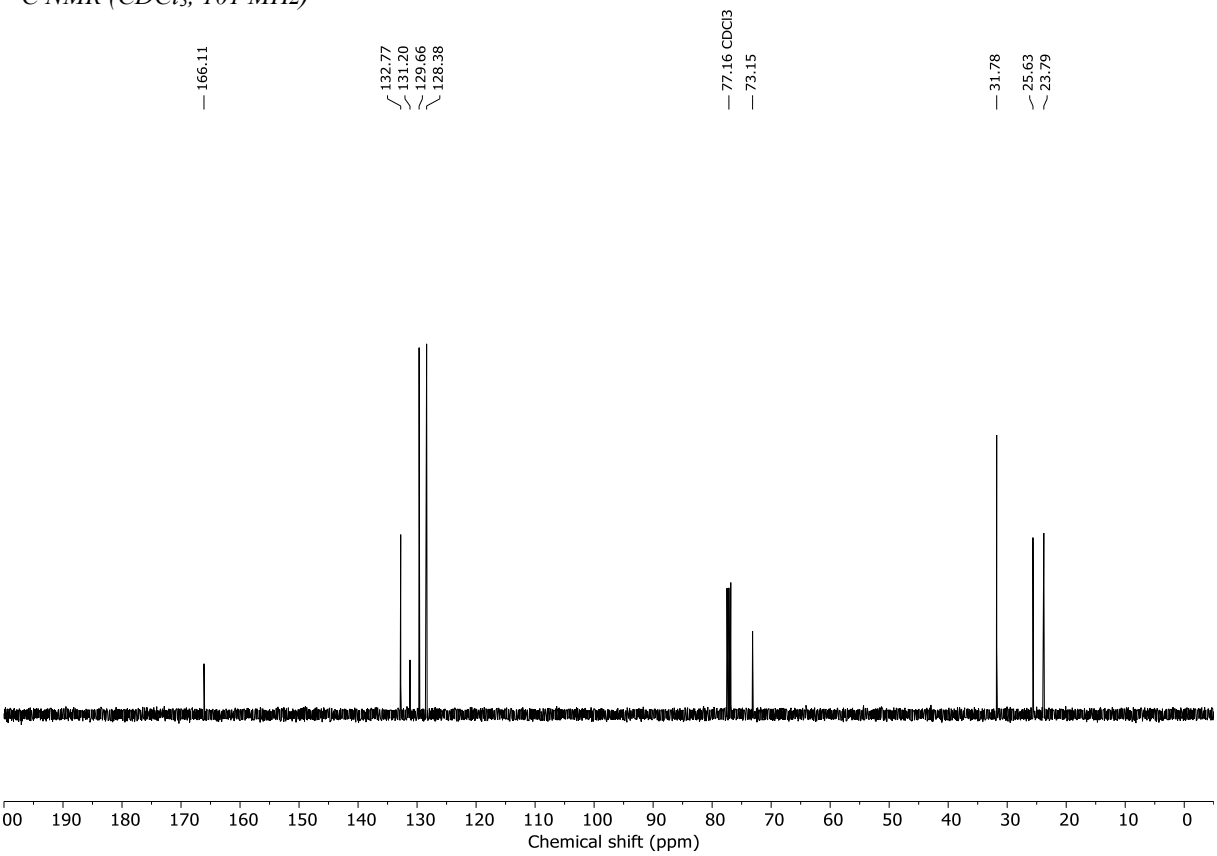

Cyclohexyl p-methoxybenzoate (71)

^{1}H NMR ($CDCl_3$, 500 MHz)

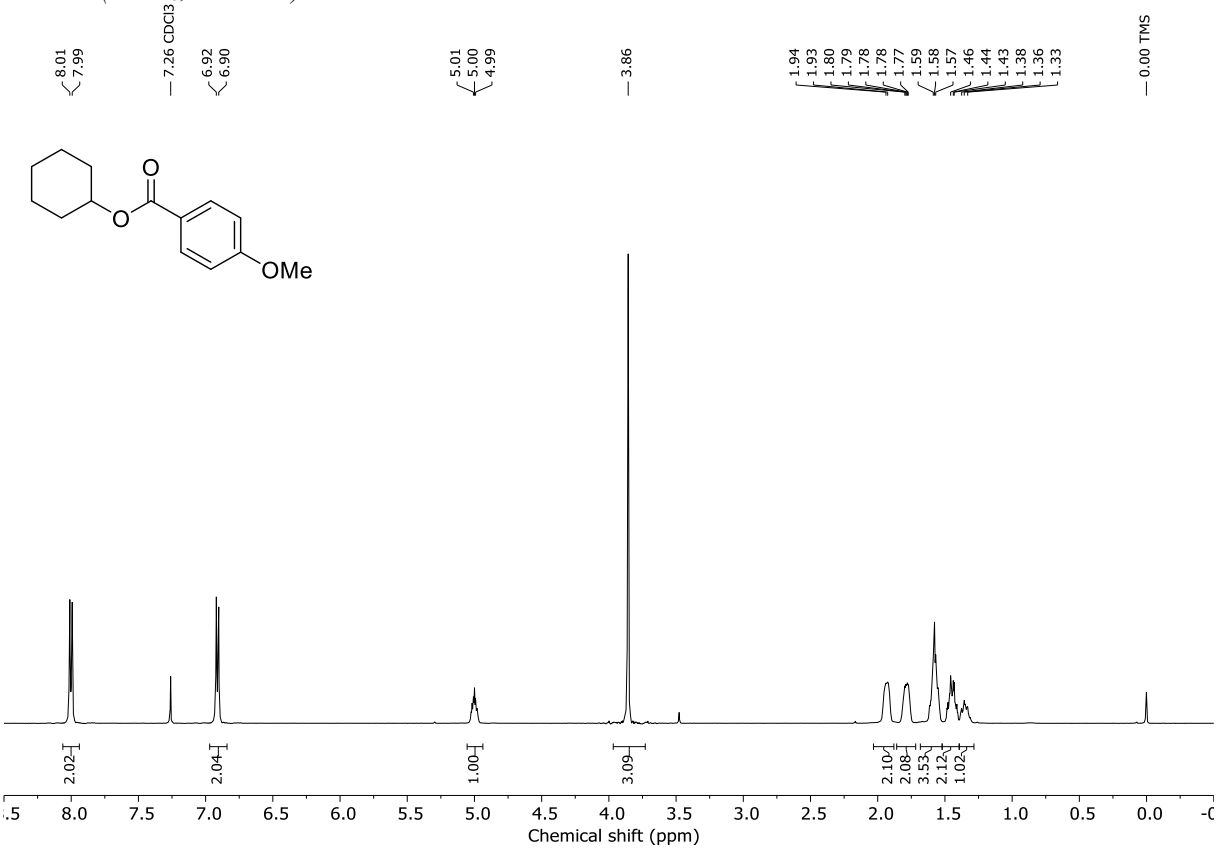

^{13}C NMR ($CDCl_3$, 101 MHz)

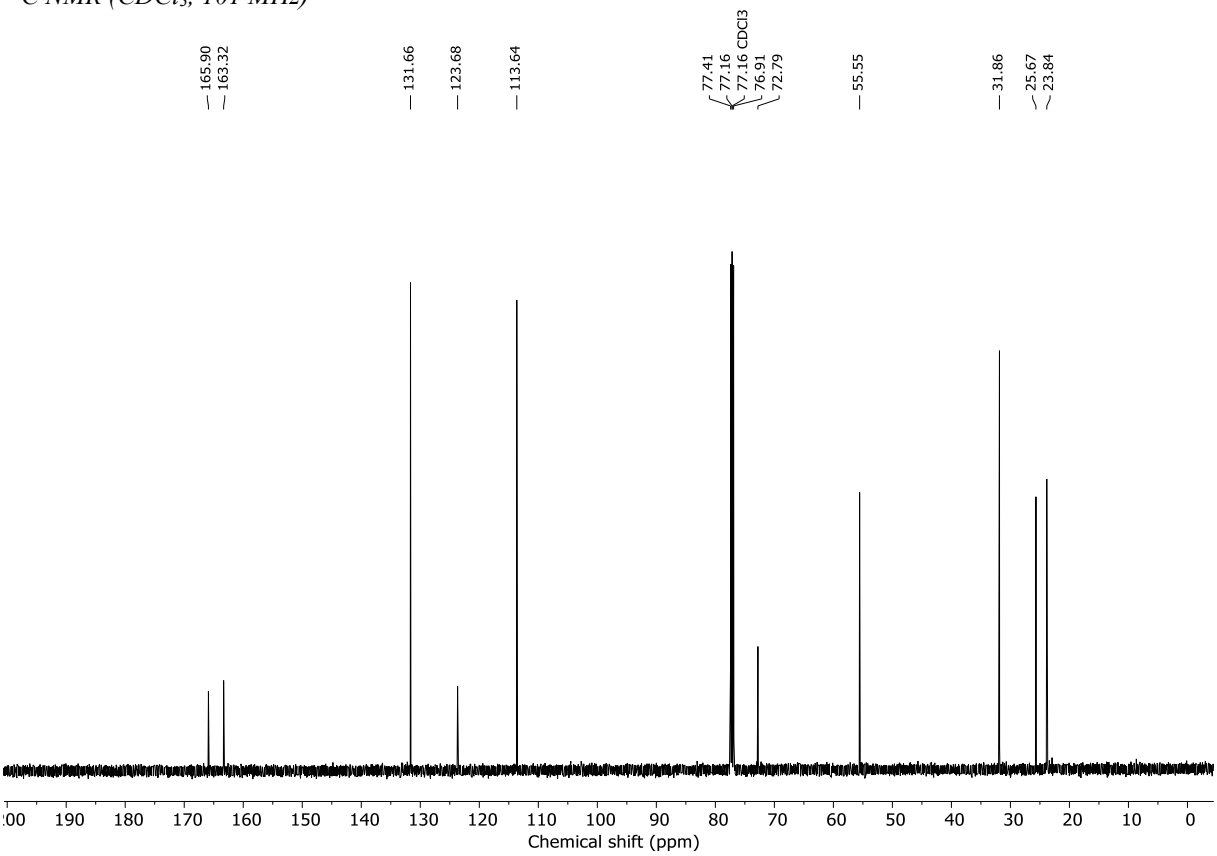

Cyclohexyl 4-phenylbutanoate (72)

^{1}H NMR ($CDCl_3$, 400 MHz)

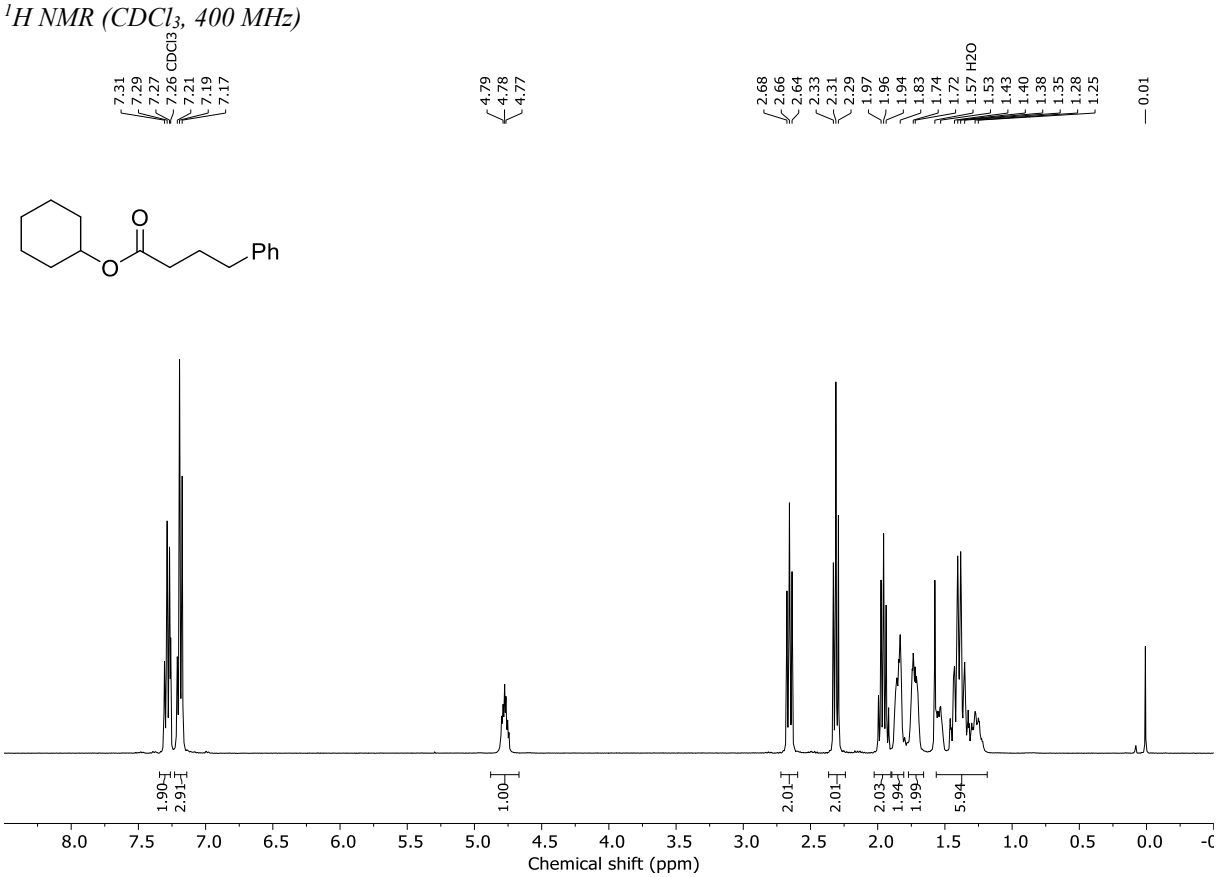

^{13}C NMR ($CDCl_3$, 101 MHz)

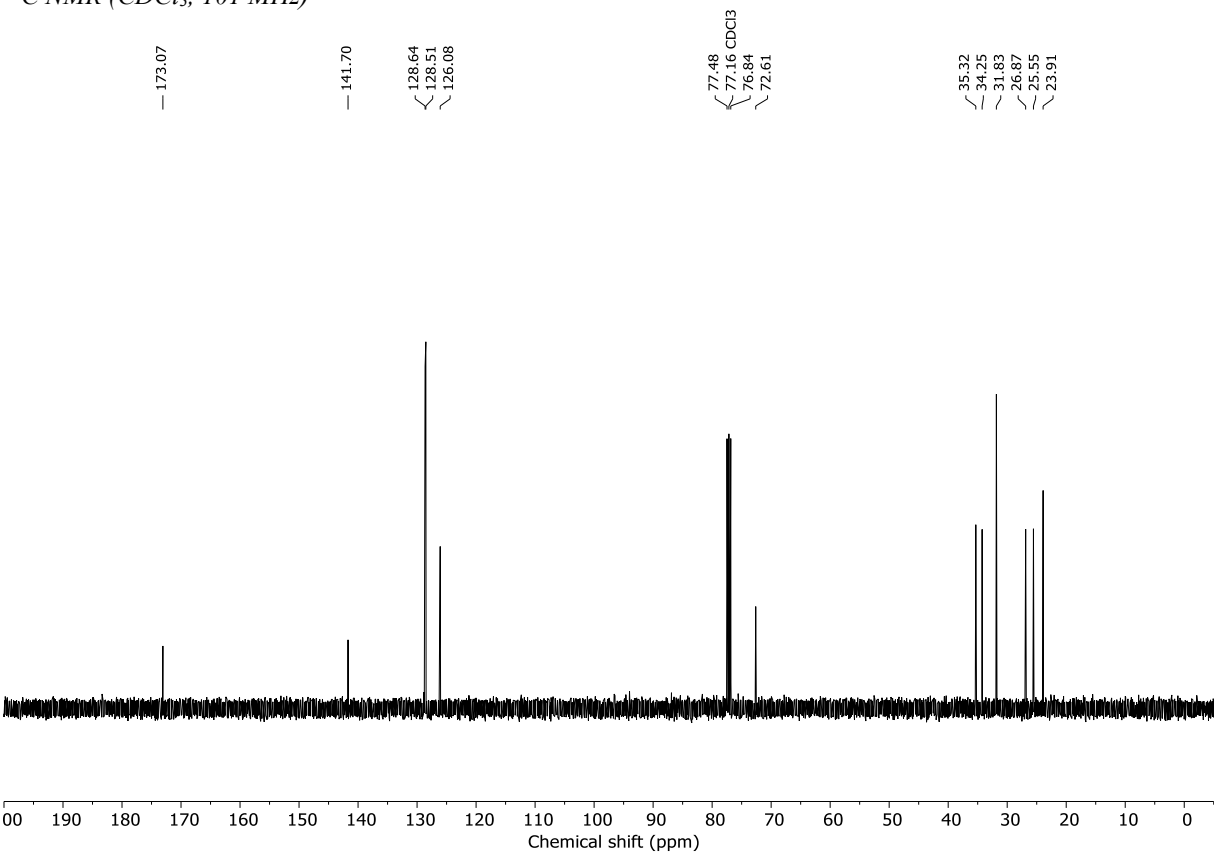

Cyclohexyl oleate (73)

^{1}H NMR ($CDCl_3$, 400 MHz)

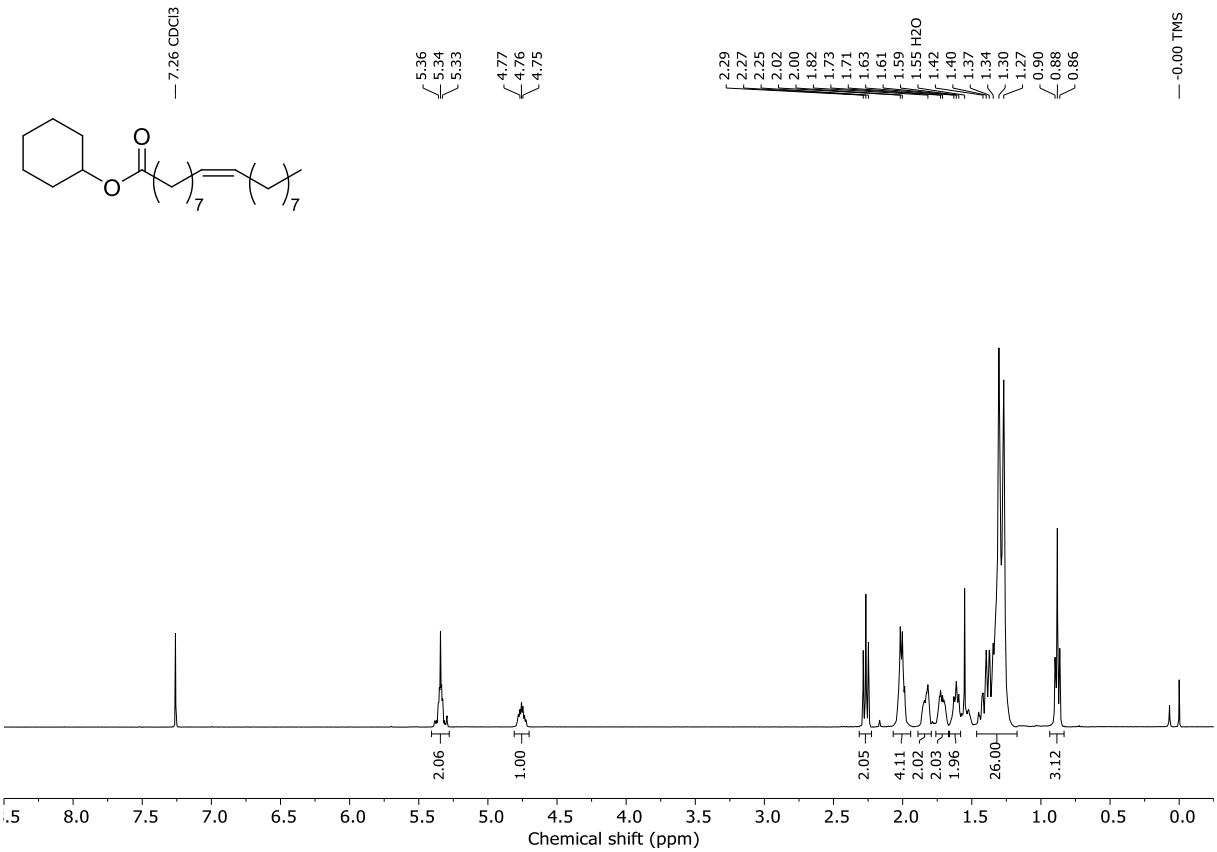

^{13}C NMR ($CDCl_3$, 101 MHz)

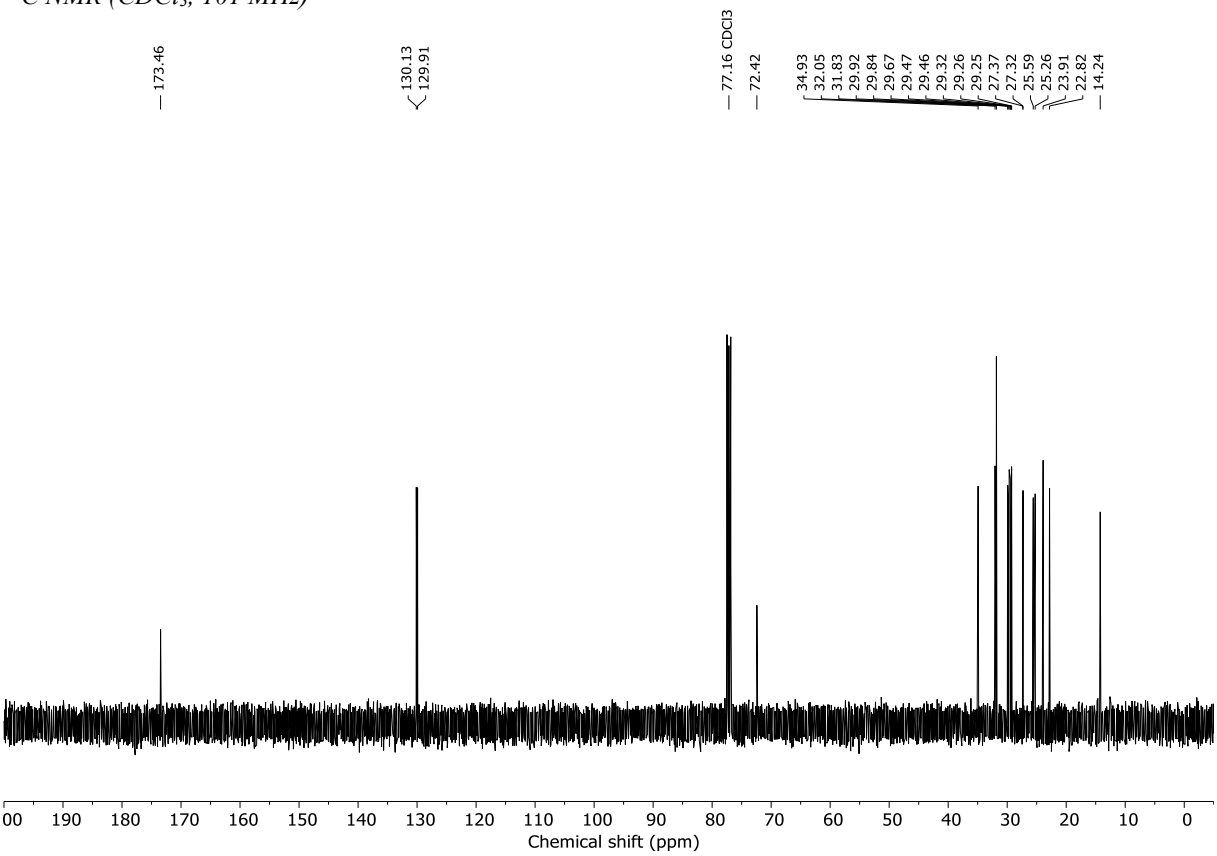

(4-chlorophenyl)(cyclohexyl)methanone (74)

^{1}H NMR ($CDCl_3$, 400 MHz)

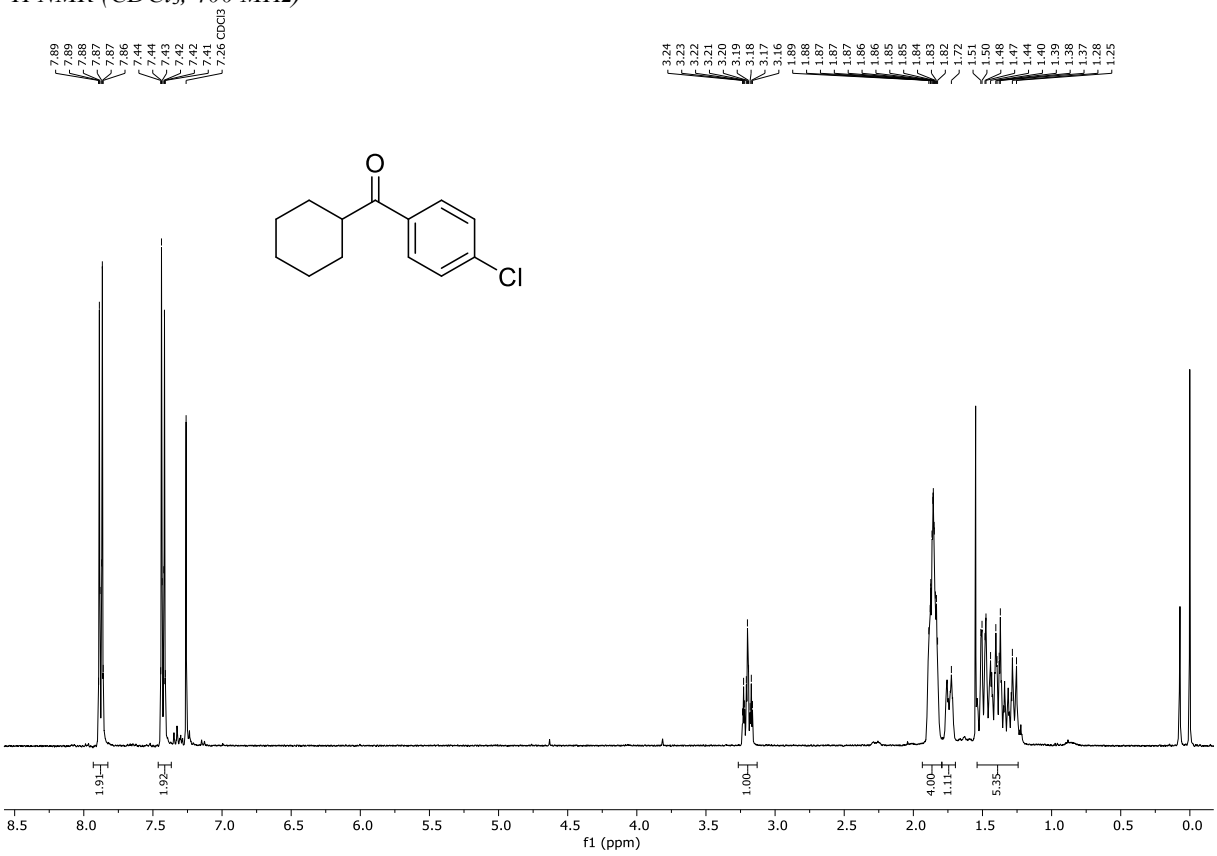

^{13}C NMR ($CDCl_3$, 101 MHz)

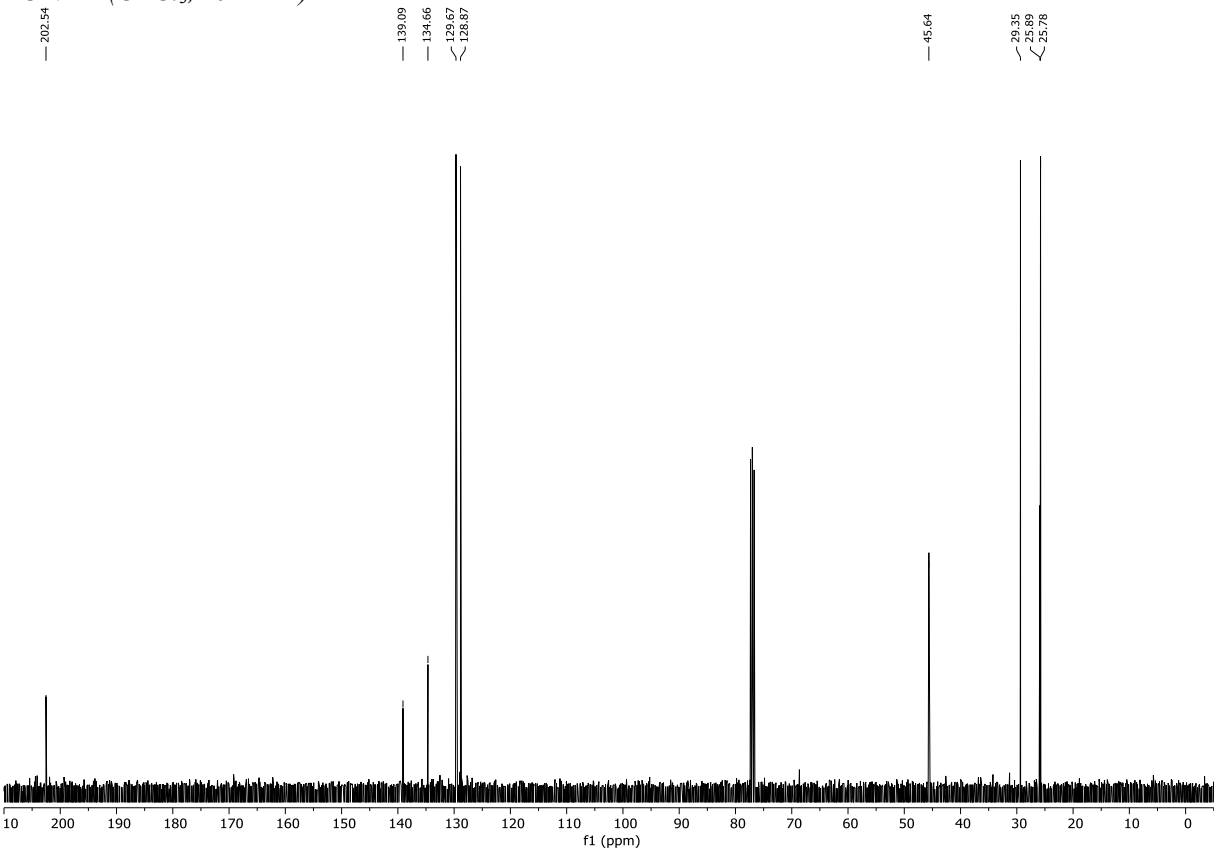

methyl 6-tosyl-6-azaspiro[2.5]oct-1-ene-1-carboxylate (75)

^{1}H NMR ($CDCl_3$, 400 MHz)

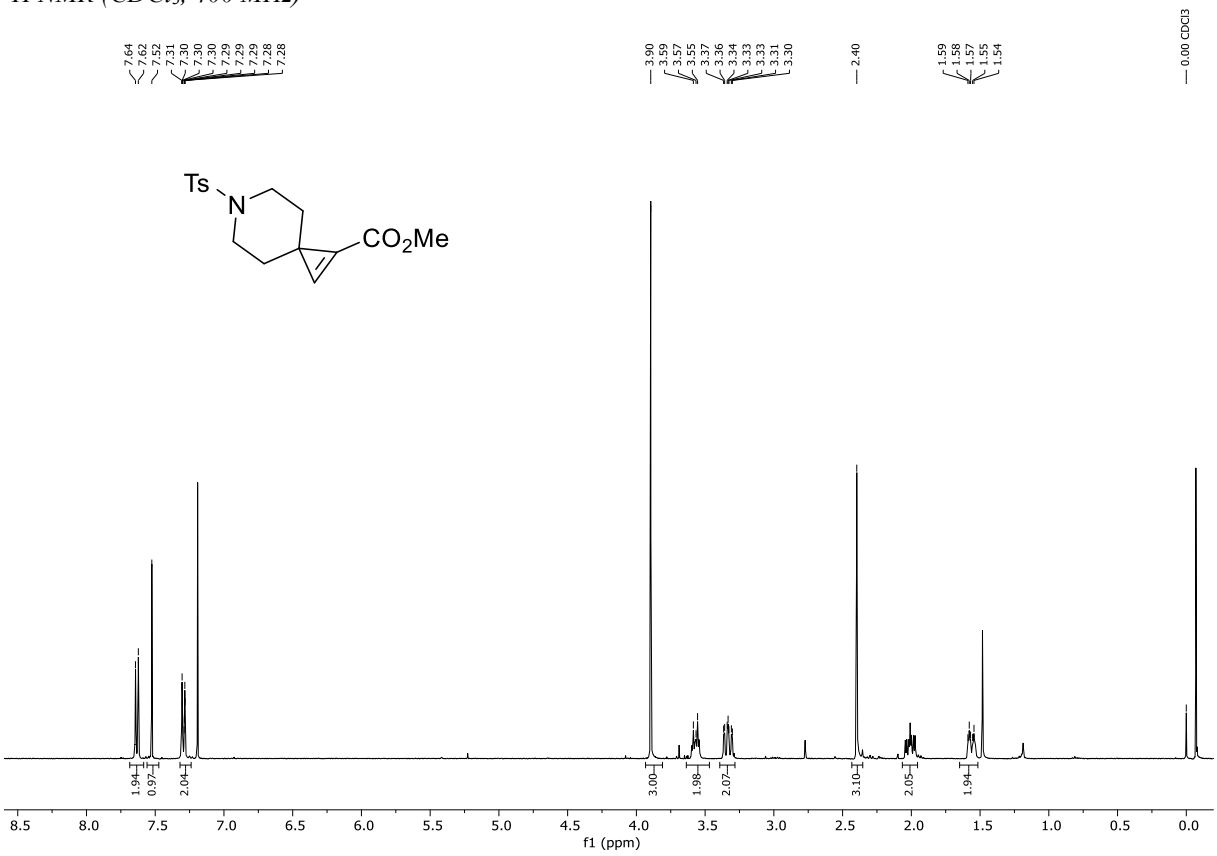

^{13}C NMR ($CDCl_3$, 101 MHz)

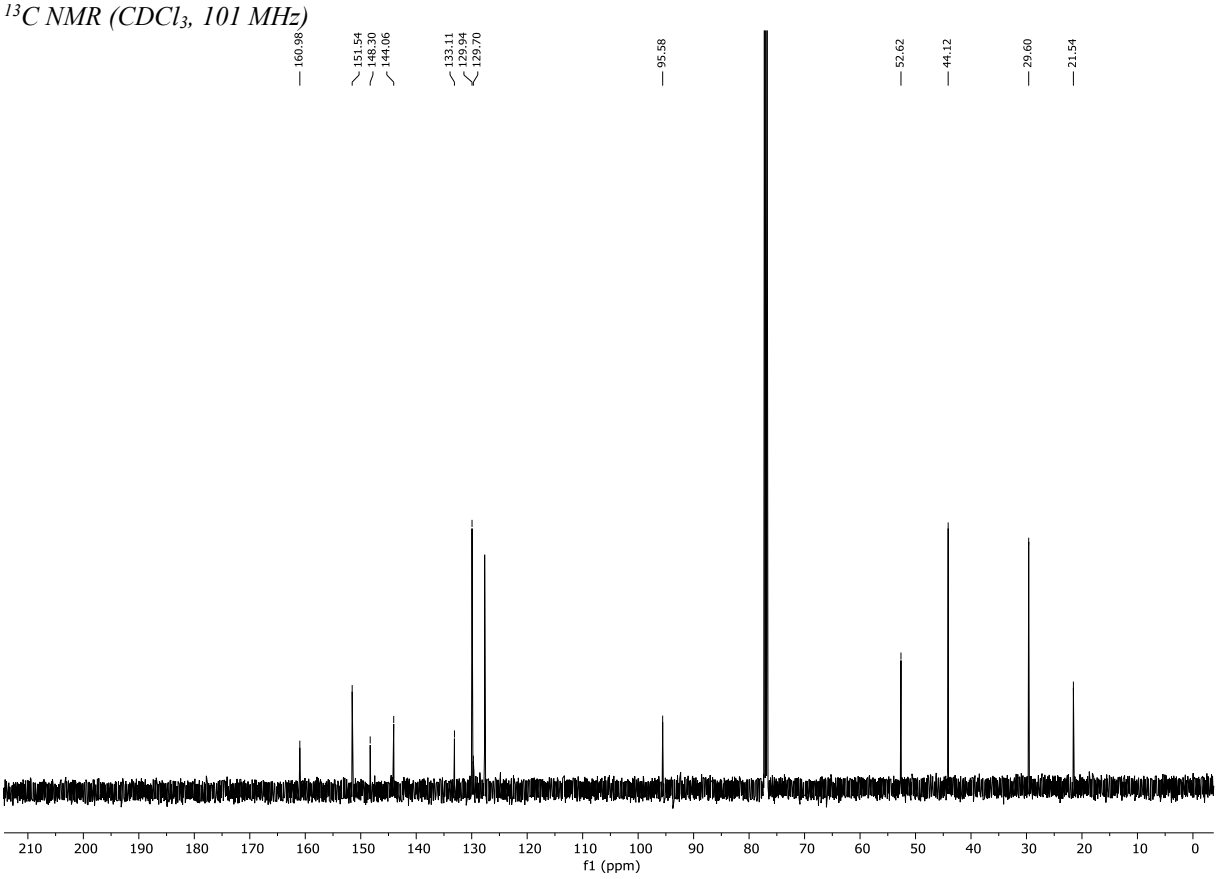

DEPT-135

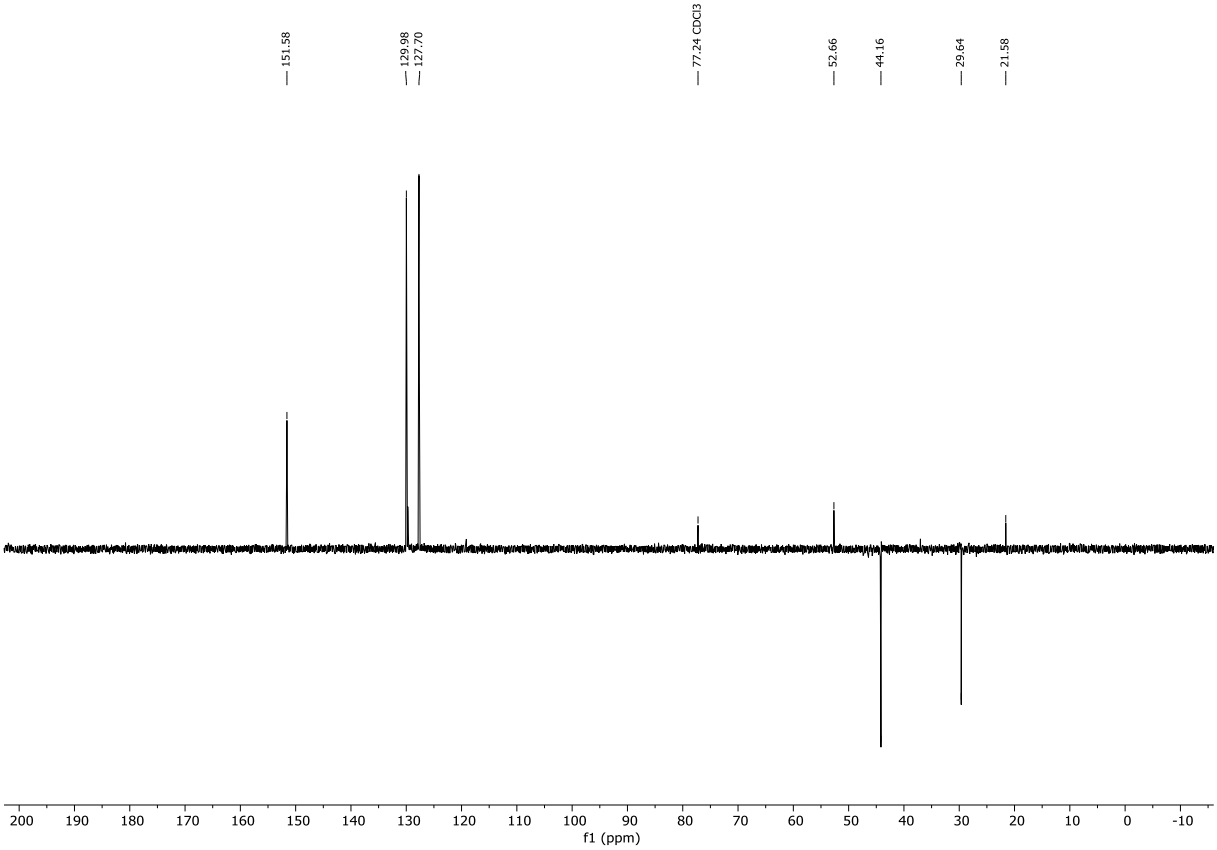

ChemComm

COMMUNICATION

View Article Online
View Journal

Cite this: DOI: 10.1039/d3cc05174a

Received 20th October 2023,
Accepted 15th November 2023

DOI: 10.1039/d3cc05174a

rsc.li/chemcomm

Unlocking the reactivity of diazo compounds in red light with the use of photochemical tools†

Katarzyna Orłowska, Klaudia Łuczak, Piotr Krajewski, João V. Santiago, Katarzyna Rybicka-Jasińska* and Dorota Gryko *

Structurally diversified diazoalkanes can be activated under red light irradiation relying on direct photolysis, photosensitization or photoredox catalysis.

Bioorthogonal chemistry represents chemical transformations that proceed selectively in biological environments without perturbing the structure of biomolecules or interfering with biochemical pathways.[1–6] Several photoactivated methods have been designed, yet most of them employ short-wavelength light emitting sources.[7–10] The phototoxicity of high energetic photons makes them inappropriate for biological applications. Therefore, switching to less energetic light is desirable. Along this line, tetrazole bioorthogonal chemistry was performed under NIR radiation *via* two-photon excitation or upconversion processes.[11,12] Dihydrotetrazine oxidation *in vivo* can also be achieved with less energetic photons.[13] Yet, red light-induced reactions even in synthetic chemistry call for in depth studies.[14]

Diazoalkanes are versatile reactants for photochemical synthesis of small/complex structures[15–17] and functionalization of bioactive compounds.[18–21] They have been utilized in enzymatic cyclopropanation, ring expansion, cyclopropenation, or insertion reactions.[22–27] So far, however, generation of carbenes in biological systems is mostly limited to diazirines that are activated in UV/violet light.[28–30] In view of benefits arising from the application of low energetic photons, red light-induced diazo chemistry is highly desirable. Given the structural diversity of diazoalkanes, they can be directly photolyzed or activated *via* photocatalytic processes under visible light (even red, Fig. 1A). We wondered whether it is possible to unlock the potential of red light toward the generation of reactive species from structurally diversified diazo compounds utilizing various photochemical modes. While studying the photocatalytic activity of porphyrins under red-light irradiation, we found that they catalyze photoalkylation of aldehydes with ethyl diazoacetate.[31] Herein, we present our comprehensive study on the red light-induced photolysis, photosensitization, and photoredox-driven generation of reactive intermediates from diazo reagents (Fig. 1B).

Photolysis – Direct photolysis of diazoalkanes enables carbene generation with no catalyst required. Although acceptor-only and acceptor/acceptor diazo compounds exhibit light absorption beyond the visible range, replacing H/one of the acceptor groups with an aryl substituent bathochromically shifts the λ_{max} toward the visible spectrum.[16,32] By increasing the donating character of the phenyl ring, λ_{max} is shifted even further (for –OMe, λ_{max} = 543 nm),[33] and has an impact on the carbene spin state. Given the ubiquity of free hydroxy-, amino-, and thio-groups in natural compounds, we focused on red light-induced photolysis of diaryldiazoalkanes in the presence of alcohols, amines, and thiols (Scheme 1). The light-induced method works well for primary alcohols efficiently affording ethers **1–5**. Incorporation into the phenolic O–H bond, a

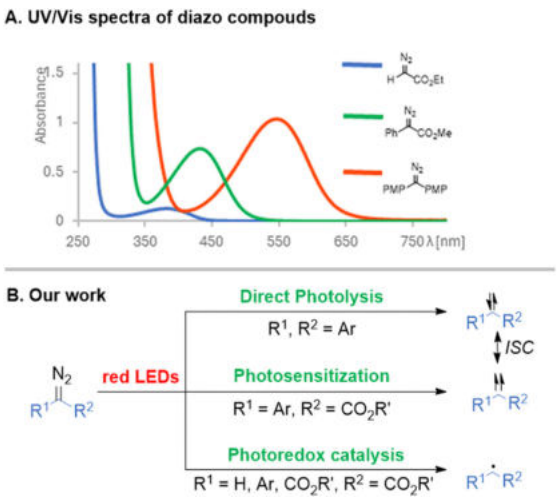

Fig. 1 Red light-induced reactions of diazoalkanes.

Institute of Organic Chemistry, Polish Academy of Sciences, Kasprzaka 44/52 01-224, Warsaw, Poland. E-mail: dorota.gryko@icho.edu.pl

† Electronic supplementary information (ESI) available. See DOI: https://doi.org/10.1039/d3cc05174a

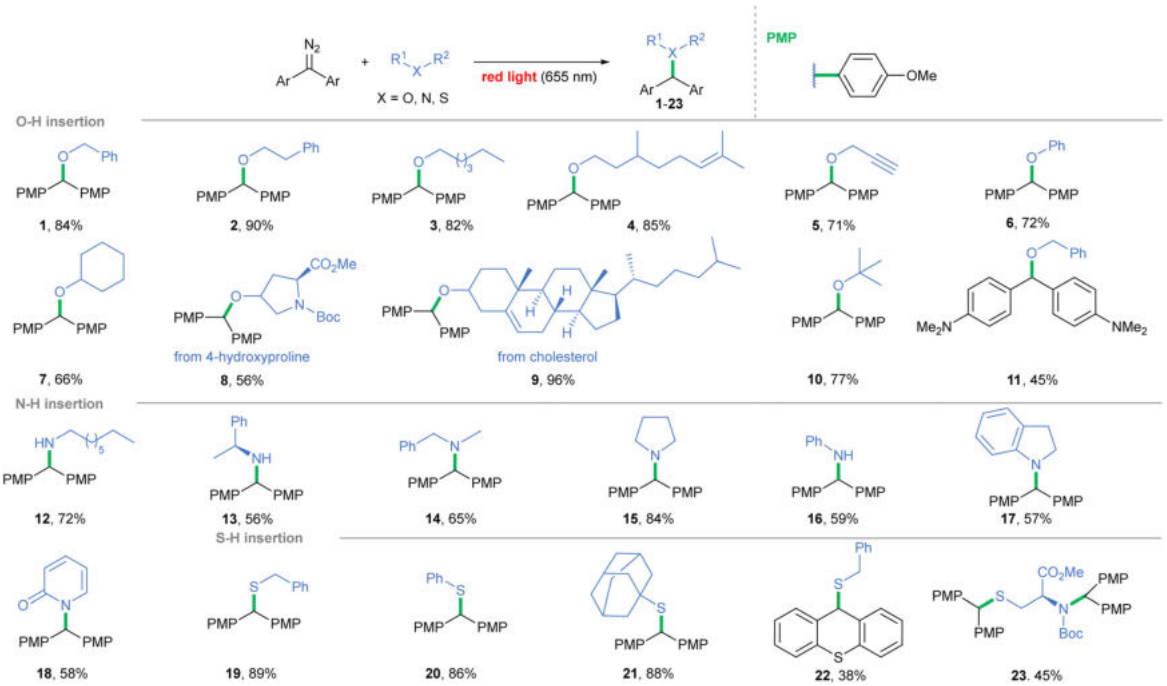

Scheme 1 Scope of red light-induced carbene insertion into the X–H bond.

tyrosine model, also proved successful (**6**, 72%). Secondary and tertiary alcohols were slightly less effective (**7**, **8** and **10**), but cholesterol derivative **9** formed almost quantitatively. On the other hand, irradiation of diaryl diazoalkane bearing amino groups at *p*-positions (λ_{max} = 566 nm)[34] in the presence of benzyl alcohol led to product **11** in a diminished yield (45%). Noteworthily, when beneficial, the substrate ratio could be reversed and diazoalkane excess could be used instead. Benzyl and aromatic amines formed in a slightly diminished yield, in contrast with productive amine **15** formation (84%). 2-Hydroxypyridine gave a mixture of O–H and N–H insertion products but, upon isolation, full conversion to amide **18** occurred. The scope of tolerated thiols is broad, and even thiophenol and bulky adamantanethiol efficiently furnished products **20** and **21**. Furthermore, the feasibility of the method was examined with *N*-Boc protected cysteine ester, and insertion occurred on both the N–H and S–H bonds (**23**, 74%).

Photosensitization - Most carbene precursors, including diazo compounds, do not, however, absorb red light (Fig. 1A), and for their activation photocatalytic approaches are required. Among these, photosensitization with the use of a dye of proper E_T level gives access to triplet excited states *via* triplet–triplet energy transfer (EnT).[35,36] Only recently, mild Ir-sensitized strategies to access triplet carbenes from diazirines and 1,3,4-oksadiazolines under blue light irradiation were proposed by MacMillan and our group,[30,37] but approaches relying on red light remain challenging. Porphyrins are sensitizers widely applied in photooxidation, photodynamic therapy and artificial photosynthesis.[38–41] We tested these red-light-absorbing organic dyes for photosensitization of diazoalkanes. When aryldiazoesters ($E_T \approx 133$ kJ mol^{-1}, calculated using SMD(DCM)/M06/6-311++g(d,p)//B3LYP-D3/6-31g(d)), were irradiated with red light in the presence of H_2TPP (E_T = 138 kJ mol^{-1})[42] and oxygen, β-ketoesters **24–26** formed (Scheme 2A).

For more electrophilic aryl diazoalkane, a loss of selectivity was observed (**26**, 40%). Since porphyrins are well-known $^1O_2$ sensitizers,[38,39] maintaining oxygen-free conditions was crucial to prevent competitive oxidation pathways in consecutive O–H insertion (Scheme 2A) and cyclopropanation (Scheme 2B, see ESI†). The insertion into O–H carboxylic bonds works for

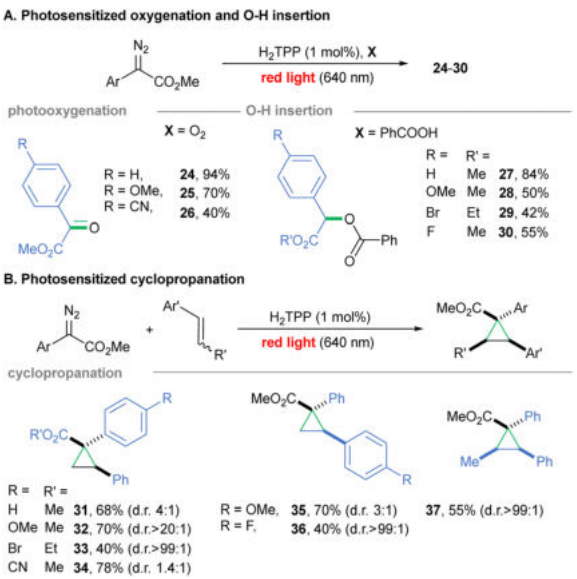

Scheme 2 Red light-induced photosensitized transformations of diazo compounds.

various aryldiazoesters leading to products **27–30**. Electron-poor aryldiazo ester reached the highest cyclopropanation productivity (**34**, 90%). The method is suitable for both electron-rich and -poor styrenes, with a better outcome for *p*-methoxy-styrene-derived product **35** (70%). A modest yield was observed when the internal olefin was subjected to the reaction conditions giving cyclopropane **37** (55%). α-Diazo esters, diazomalonates, and aryldiazoketones possessing higher E_T values than porphyrin (calculated E_T = 158 kJ mol^{-1} for EDA) cannot, in principle, be activated under the developed conditions. Intuitively, the reaction rate for diazoalkane transformation depends on the carbene rate formation, which for the red light-mediated EnT-approach occurs slower than *via* direct photolysis under blue light (see ESI†).

Photoredox catalysis – To unlock the red-light mediated reactivity of yet unconquered α-diazo esters, we screened the possibilities offered by photoredox catalysis. These acceptor-only types of diazoalkanes are reduced to alkyl radicals *via* proton coupled electron transfer (PCET, E_{RED} = −1.28 V *vs.* SCE for EDA).[43] In this view, numerous blue light-induced methodologies utilizing diazoesters as surrogates of alkyl radicals have been reported.[43–48] Recently, we have proved that porphyrins are suitable photo-oxidants and photo-reductants for red light-mediated organic transformations.[31] Therefore, we harnessed their photoredox abilities to tune already reported blue light-induced, radical-based transformations of α-diazoesters and applied them on red illumination instead. Our studies were initiated with the redesign of the photocatalyzed synthesis of γ-oximino esters, originally performed by Li under blue light with the use of α-diazoester, styrene and TBN as starting materials.[43] Optimization studies substantially shortened the reaction time (reported on blue: 60 h) to 37 h by thermally accelerating the isomerization of the nitroso compound to the final product **38** (see ESI†). Our method works well for various α-diazoesters giving esters **38**, **40** and **41** in yields comparable to those reported by Li (Scheme 3A). A slight yield decrease was observed for *trans*-anethole, though with a similar *E*/*Z* ratio (product **39**). Due to solubility problems, the synthesis of pregnenolone-derived ester **42** was less efficient. For the Ru-catalyzed reaction a key step relies on the reduction of diazo ester by the photocatalyst in the excited state. In our case, as the reduction potential of the porphyrin in the excited state (−0.91 *vs.* SCE)[31] is higher than that of EDA (−1.28 V *vs.* SCE), we assume that the excited porphyrin oxidizes DIPEA, thus generating a strongly reducing porphyrin radical anion, similar to the mechanism reported for the generation of radicals from aminopyridinium salts.[49]

Next, we examined an analogous PCET-based approach toward phenanthridines utilizing isocyanobiphenyls and diazoalkanes.[50] Scheme 3B shows the optimization of the red light-mediated protocol-enabled synthesis of heterocycles **43–47** with better productivity or comparable to the Xuan methodology. Finally, there are methodologies involving diazo reagents in which the diazo moiety remains intact or does not generate reactive intermediates. To fill the picture of the photochemistry of diazo compounds under red-light

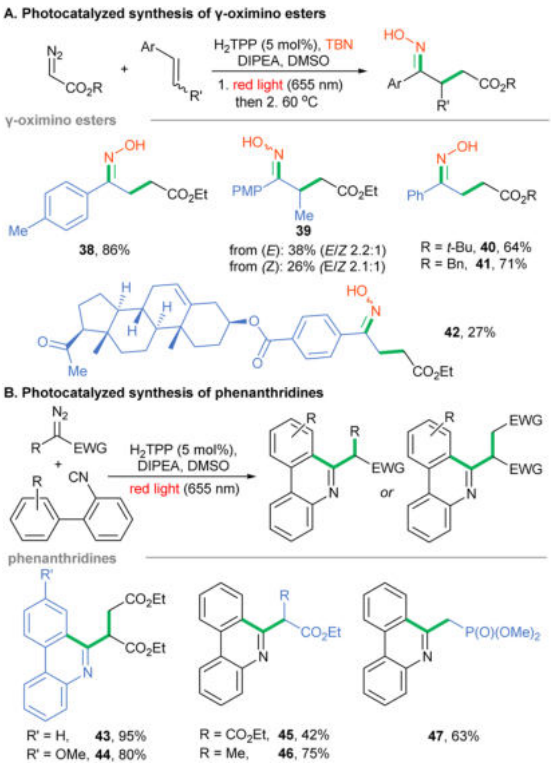

Scheme 3 Diazo compounds as radical precursors in red light-mediated photocatalyzed transformations.

irradiation, such transformations were studied. Given that sole H_2TPP is unable to photoreduce EDA, we tested H_2TPP as a photo-oxidant of diversely substituted tetrahydroisoquinolines in the presence of EDA and red light, similar to Zhou's report.[51] In fact, products **48–51** were obtained in decent yields (Scheme 4A). Furthermore, diazo compounds have been shown to react with radicals generated under photochemical conditions, including alkyl radicals generated from NHPI esters in the presence of Rose Bengal on yellow LEDs.[52] We performed this transformation with the H_2TPP catalyst instead, under red light irradiation. A wide range of donor/acceptor diazoalkanes reacted under the developed conditions to give hydrazones **52–56** (Scheme 4B).

In summary, this study demonstrates that photochemistry provides tools for red light-driven activation of various diazo compounds. A proper structural modification of diazoalkane results in a bathochromic shift of the absorption maxima allowing for direct photolysis under low-energetic, red-light irradiation. If this pathway is not possible, we induce transformations of diazo compounds taking advantage of nature-inspired dyes, established as safe and effective for photodynamic therapy and artificial photosynthesis. The triplet energy level of the porphyrin excited state is sufficient for productive EnT to aryl-diazo esters giving access to triplet carbenes. Other diazoalkanes may be activated through porphyrin-mediated photoredox processes by undergoing reduction to alkyl radicals or by serving as radical acceptors. Therefore, three-modes of

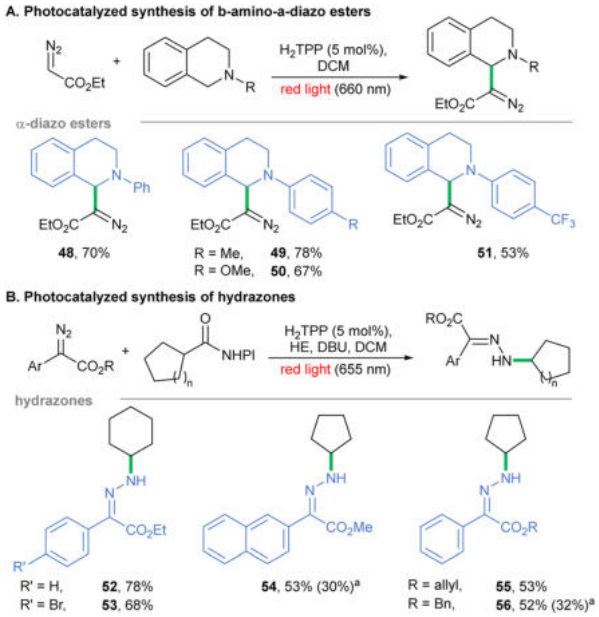

Scheme 4 Diazo compounds as radical acceptors in red light-mediated photocatalyzed transformations. [a]Reaction set under blue light irradiation (25 W, 455 nm).

activation of diazo compounds under red-light irradiation have been unlocked.

Financial support for this work was provided by National Science Center, Poland, grant number Maestro UMO-2020/38/A/ST4/00185.

Conflicts of interest

There are no conflicts to declare.

Notes and references

1 E. M. Sletten and C. R. Bertozzi, *Angew. Chem., Int. Ed.*, 2009, **48**, 6974.
2 C. R. Bertozzi, *Acc. Chem. Res.*, 2011, **44**, 651.
3 N. K. Devaraj, *ACS Cent. Sci.*, 2018, **4**, 952.
4 S. Jia and E. M. Sletten, *ACS Chem. Biol.*, 2022, **17**, 3255.
5 J. Li, H. Kong, C. Zhu and Y. Zhang, *Chem. Sci.*, 2020, **11**, 3390.
6 B. D. Fairbanks, L. J. Macdougall, S. Mavila, J. Sinha, B. J. Kirkpatrick, K. S. Anseth and C. N. Bowman, *Chem. Rev.*, 2021, **121**, 6915.
7 G. S. Kumar and Q. Lin, *Chem. Rev.*, 2021, **121**, 6991.
8 W. Song, Y. Wang, J. Qu, M. M. Madden and Q. Lin, *Angew. Chem., Int. Ed.*, 2008, **47**, 2832.
9 W. Song, Y. Wang, J. Qu and Q. Lin, *J. Am. Chem. Soc.*, 2008, **130**, 9654.
10 P. An, T. M. Lewandowski, T. G. Erbay, P. Liu and Q. Lin, *J. Am. Chem. Soc.*, 2018, **140**, 4860.
11 Z. Yu, T. Y. Ohulchanskyy, P. An, P. N. Prasad and Q. Lin, *J. Am. Chem. Soc.*, 2013, **135**, 16766.
12 P. Lederhose, Z. Chen, R. Muller, J. P. Blinco, S. Wu and C. Barner-Kowollik, *Angew. Chem., Int. Ed.*, 2016, **55**, 12195.
13 C. Wang, H. Zhang, T. Zhang, X. Zou, H. Wang, J. E. Rosenberger, R. Vannam, W. S. Trout, J. B. Grimm, L. D. Lavis, C. Thorpe, X. Jia, Z. Li and J. M. Fox, *J. Am. Chem. Soc.*, 2021, **143**, 10793.
14 N. Sellet, M. Cormier and J. P. Goddard, *Org. Chem. Front.*, 2021, **8**, 6783.
15 Z. Yang, M. L. Stivanin, I. D. Jurberg and R. M. Koenigs, *Chem. Soc. Rev.*, 2020, **49**, 6833.
16 J. Durka, J. Turkowska and D. Gryko, *ACS Sustainable Chem. Eng.*, 2021, **9**, 8895.
17 Ł. W. Ciszewski, K. Rybicka-Jasińska and D. Gryko, *Org. Biomol. Chem.*, 2019, **17**, 432.
18 H. M. L. Davies and J. R. Denton, *Chem. Soc. Rev.*, 2009, **38**, 3061.
19 S.-S. Ge, B. Chen, Y.-Y. Wu, Q.-S. Long, Y.-L. Zhao, P.-Y. Wanga and S. Yang, *RSC Adv.*, 2018, **8**, 29428.
20 S. Harada, *Chem. Pharm. Bull.*, 2021, **69**, 1170.
21 K. A. Mix, M. R. Aronoff and R. T. Raines, *ACS Chem. Biol.*, 2016, **11**, 3233.
22 Z. Liu and F. H. Arnold, *Curr. Opin. Biotechnol*, 2021, **69**, 43.
23 B. J. Wittmann, A. M. Knight, J. L. Hofstra, S. E. Reisman, S. B. J. Kan and F. H. Arnold, *ACS Catal.*, 2020, **10**, 7112.
24 R. Mao, D. J. Wackelin, C. S. Jamieson, T. Rogge, S. Gao, A. Das, D. M. Taylor, K. N. Houk and F. H. Arnold, *J. Am. Chem. Soc.*, 2023, **145**, 16176.
25 D. C. Miller, R. G. Lal, L. A. Marchetti and F. H. Arnold, *J. Am. Chem. Soc.*, 2022, **144**, 4739.
26 K. Chen, X. Huang, S. B. Jennifer Kan, R. K. Zhang and F. H. Arnold, *Science*, 2018, **360**, 71.
27 R. K. Zhang, K. Chen, X. Huang, L. Wohlschlager, H. Renata and F. H. Arnold, *Nature*, 2019, **565**, 67.
28 A. Blencowe and W. Hayes, *Soft Matter*, 2005, **1**, 178.
29 S. W. Huth, J. V. Oakley, C. P. Seath, J. B. Geri, A. D. Trowbridge, D. L. Parker Jr., F. P. Rodriguez-Rivera, A. G. Schwaid, C. Ramil, K. A. Ryu, C. H. White, O. O. Fadeyi, R. C. Oslund and D. W. C. MacMillan, *J. Am. Chem. Soc.*, 2023, **145**, 16289.
30 J. B. Geri, J. V. Oakley, T. Reyes-Robles, T. Wang, S. J. McCarver, C. H. White, F. P. Rodriguez-Rivera, D. L. Parker Jr., E. C. Hett, O. O. Fadeyi, R. C. Oslund and D. W. C. MacMillan, *Science*, 2020, **367**, 1091.
31 K. Rybicka-Jasińska, T. Wdowik, K. Łuczak, A. J. Wierzba, O. Drapała and D. Gryko, *ACS Org. Inorg. Au*, 2022, **2**, 422.
32 I. D. Jurberg and H. M. L. Davies, *Chem. Sci.*, 2018, **9**, 5112.
33 S. Jana, C. Pei, C. Empel and R. M. Koenigs, *Angew. Chem., Int. Ed.*, 2021, **60**, 13271.
34 R. W. R. Humphreys and D. R. Arnold, *Can. J. Chem.*, 1979, **57**, 2652.
35 F. Strieth-Kalthoff and F. Glorius, *Chem*, 2020, **6**, 1888.
36 F. Strieth-Kalthoff, M. J. James, M. Teders, L. Pitzer and F. Glorius, *Chem. Soc. Rev.*, 2018, **47**, 7190.
37 K. Orłowska, J. V. Santiago, P. Krajewski, K. Kisiel, I. Deperasińska, K. Zawada, W. Chaładaj and D. Gryko, *ACS Catal.*, 2023, **13**, 1964.
38 R. Costa e Silva, L. O. da Silva, A. de Andrade Bartolomeu, T. J. Brocksom and K. T. de Oliveira, *Beilstein J. Org. Chem.*, 2020, **16**, 917.
39 J. Kou, D. Dou and L. Yang, *Oncotarget*, 2017, **8**, 81591.
40 D. Gust, T. A. Moore and A. L. Moore, *Acc. Chem. Res.*, 2009, **42**, 1890.
41 R. Seely, *Photochem. Photobiol.*, 1978, **27**, 639.
42 L. G. Arnaut, Design of porphyrin-based photosensitizers for photodynamic therapy, in *Advances in Inorganic Chemistry*, ed. R. van Eldik and G. Stochel, Academic Press, 2011, ch. 5, vol. 63, pp. 187–233.
43 Y. Liu, K. Zhu, J. Zhao and P. Li, *Org. Lett.*, 2022, **24**, 6834.
44 F. Li, S. Zhu and R. M. Koenigs, *Chem. Commun.*, 2022, **58**, 7526.
45 Ł. W. Ciszewski, J. Durka and D. Gryko, *Org. Lett.*, 2019, **21**, 7028.
46 X. Huang, R. D. Webster, K. Harms and E. Meggers, *J. Am. Chem. Soc.*, 2016, **138**, 12636.
47 Y.-L. Su, G. X. Liu, L. De Angelis, R. He, A. Al-Sayyed, K. S. Schanze, W.-H. Hu, H. Qiu and M. P. Doyle, *ACS Catal.*, 2022, **12**, 1357.
48 Y. L. Su, G. X. Liu, J. W. Liu, L. Tram, H. Qiu and M. P. Doyle, *J. Am. Chem. Soc.*, 2020, **142**, 13846.
49 K. Goliszewska, K. Rybicka-Jasińska, J. A. Clark, V. I. Vullev and D. Gryko, *ACS Catal.*, 2020, **10**, 5920.
50 H. B. Ye, X. Y. Zhou, L. Li, X. K. He and J. Xuan, *Org. Lett.*, 2022, **24**, 6018.
51 T. Xiao, L. Li, G. Lin, Z. W. Mao and L. Zhou, *Org. Lett.*, 2014, **16**, 4232.
52 C. M. Chan, Q. Xing, Y. C. Chow, S. F. Hung and W. Y. Yu, *Org. Lett.*, 2019, **21**, 8037.

Supporting Information

Unlocking the Reactivity of Diazo Compounds on Red Light with the Use of Photochemical Tools

Katarzyna Orłowska, ‡ Klaudia Łuczak,‡ Piotr Krajewski,‡ João V. Santiago, Katarzyna Rybicka-Jasińska,* Dorota Gryko*

Institute of Organic Chemistry, Polish Academy of Sciences,
Kasprzaka 44/52, 01-224 Warsaw, Poland

correspondence:

dorota.gryko@icho.edu.pl

katarzyna.rybicka-jasinska@icho.edu.pl

Table of contents

1. General Information

Materials

All solvents and commercially available reagents were purchased from Sigma-Aldrich, TCI, Acros Organics and Alfa Aesar as reagent grade and were used without further purification, unless otherwise stated. Porphyrin catalysts were purchased from PorphyChem. Dry solvents were taken from Solvent Purification System (SPS) or purchased from Sigma Aldrich. All deuterated solvents used were purchased from Eurisotop.

General Procedures

Unless otherwise noted, reactions were performed without the exclusion of air or moisture. All the photochemical reactions were performed in 10 mL glassy vials sealed with aluminum caps containing a rubber septum. Reactions were monitored by thin layer chromatography (TLC), using 0.20 mm Merck silica plates (60F-254) and visualized using UV-light, potassium permanganate, cerium molybdate or anisaldehyde stain, with heat as a developing agent. Colum chromatography was performed on Merck silica gel 60 (230-400 mesh). GC yields were calibrated with dodecane as an internal standard. All yields determined by ^{1}H NMR analysis were obtained using dibromomethane or 1,3,5-trimethoxybenzene as the internal standard. Isolated yields refer to spectroscopically (^{1}H NMR) homogeneous materials. Structural assignments were made with additional information from gCOSY, gHSQC, and NOESY experiments.

Instrumentation

NMR spectra were recorded at ambient temperature (unless otherwise stated) on Bruker 400 MHz or Varian 500, 600 MHz. Chemical shifts are reported in ppm relative to the tetramethyl silane signal or a residual undeuterated solvent peak (TMS 0 ppm for ^{1}H and ^{13}C, $CHCl_3$ – 7.26 ppm for ^{1}H and 77.16 ppm for ^{13}C, $(CD_3)_2CO$ – 2.05 ppm for ^{1}H and 29.8 ppm for ^{13}C, CD_2Cl_2 – 5.32 ppm for ^{1}H and 53.5 ppm for ^{13}C, $(CD_3)_2SO$ – 2.49 ppm for ^{1}H and 39.7 ppm for ^{13}C). Multiplicities are given as: singlet (s), doublet (d), triplet (t), quartet (q), multiplet (m) broad singlet (brs).

LR and HRMS. Low-resolution mass spectra (LRMS) were recorded on an Applied Biosystems API 365 mass spectrometer using electrospray ionization (ESI) technique. High-resolution mass spectra (HRMS) were recorded on Waters SYNAPT G2-S HDMS instrument using electrospray ionization (ESI) or atmospheric-pressure chemical ionization (APCI) with time-of-flight detector (TOF).

Elemental analysis (C, H, N) were performed using a PERKIN-ELMER 240 Elemental Analyzer.

GC-MS analyses were performed using Shimadzu GCMS-QP2010 SE gas chromatograph with FID detector and Zebron ZB 5MSi column (length: 30.0 m; thickness: 0.25 um, diameter: 0.25 mm). **GC program:**

- time: 14.92 min;
- pressure: 90.8 kPa;
- total flow: 5.3mL/min;
- column flow: 1.11 mL/min;
- linear velocity: 27.5 cm/s;

- purge flow: 2.0 mL/min;
- split ratio: 2.0.

	Rate	Final Temperature	Hold Time
0	-	50.0	2.00
1	40.00	80.0	2.00
2	40.00	120.0	1.00
3	45.00	150.0	1.00
4	50.00	200.0	1.00
5	50.00	325.0	2.00

Flash column chromatography was performed on CombiFlash NextGen 300 Flash Chromatography System.

2. Photoreactor Setups

Red-light induced transformations were performed with the use of one of the following setups:

- **Studies on direct photolysis of diaryldiazoalkanes, photocatalyzed synthesis of γ-oximinoesters, phenantridines and hydrazones:**

The experiments were carried out in UOSlab Miniphoto photoreactor (Figure F1). Red (emission maximum at 655 nm) light was supplied to each reaction vial with the use of 7 LUMINUS LED units (of overall 25 W intensity when 100% power applied). The ambient temperature of LED block was maintained by cooling with Huber MiniChiller 300 ($T_{reaction}$ ~30°C).

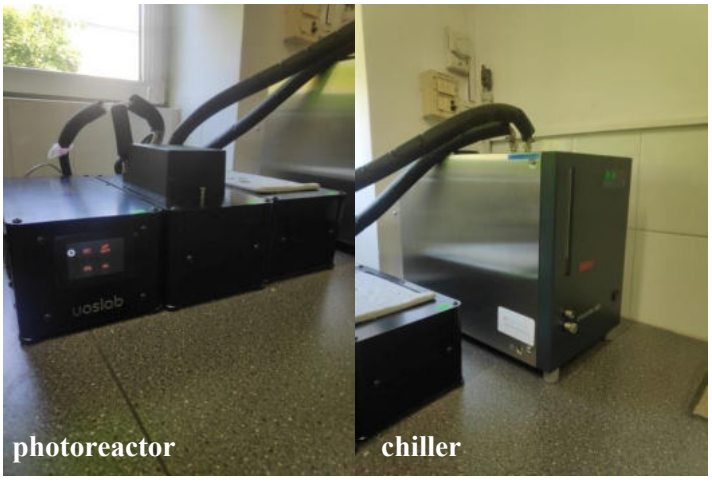

Figure F1. Standard photoreactor setup (655 nm, 25 W) with chiller.

- **Studies on photosensitized oxygenation of aryldiazoesters, photocatalyzed synthesis of β-amino-α-diazoesters:**

The experiments were carried out in a specially constructed photoreactor composed of cooling block (connected to Huber MiniChiller 300) and plate with red LEDs of 3 W power with maximum emission at 660 nm (Figure F2) ($T_{reaction}$ ~30°C).

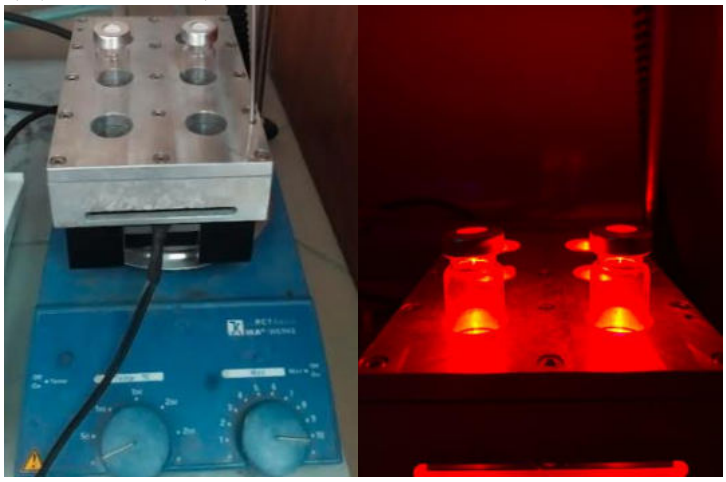

Figure F2. Standard photoreactor setup (660 nm, 3 W).

- **Studies on photosensitized O-H insertion of aryldiazoesters with benzoic acid and photosensitized cyclopropanation with aryldiazoesters:**

The experiments were carried out with the use of commercially available Kessil lamps. Red (emission maximum at 640 nm) light was supplied to each reaction vial with the use of two Kessil lamps, each of overall 40 W intensity (when 100% power applied), placed at opposite sites (Figure F3). The ambient temperature of LED block was maintained by cooling with the use of fans ($T_{reaction}$ ~30°C)

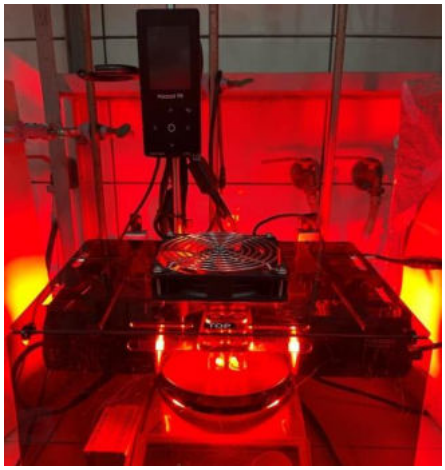

Figure F3. Standard photoreactor setup (640 nm, 2 x 40 W).

3. General synthetic procedures

3.1. Preparation of diazo compounds

Ethyl diazoacetate, *t*-butyl diazoacetate and benzyl diazoacetate are commercially available reagents (stab. with DCM) and were purchased from Sigma-Aldrich. All other diazo compounds were synthesized according to literature procedures. The observed characterization data (^{1}H and ^{13}C NMR) are consistent with those previously reported.[1-11]

3.1.1. Synthesis of 4,4'-(diazomethylene)bis(methoxybenzene) (S1)

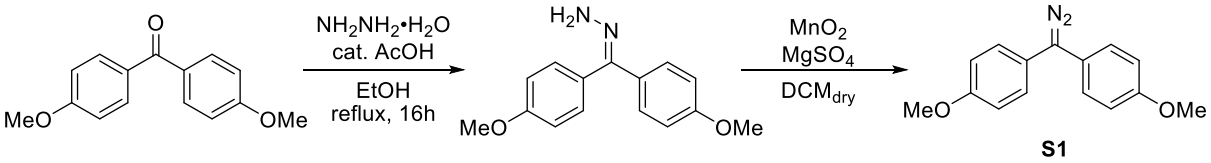

S1

Step 1: Following the reported literature.[1] Hydrazine monohydrate (100 mmol, 4.9 mL) was added to benzophenone derivative (10 mmol, 2.4 g) in EtOH (20 mL). Then AcOH (0.17 mL) was added and the mixture was heated at reflux for 16 h. After cooling to room temperature, benzophenone hydrazone precipitated. The crude mixture was filtrated and solid was washed with small amount of cold EtOH. Crystals were dried on vacuum pump to obtain pure benzophenone hydrazone derivative (2.3 g, 89% yield).

Step 2: Following the reported literature.[1] The suspension of benzophenone hydrazone derivative (5 mmol, 1.3 g) and anhydrous $MgSO_4$ (6.5 mmol, 0.8 g) in DCM (13 mL) was cooled to 0 °C. To this rapidly stirring mixture activated MnO_2 (25 mmol, 2.2 g) was added in one portion. The reaction mixture was warmed to room temperature and stirred for 3 h. The mixture was filtrated through Celite® and washed until the filtrate became colorless. After removal of the solvent under reduced pressure, the residue was purified by column chromatography using silica gel (neutralized by washing with Et_3N/PE = 1:10) with Et_3N/hexane = 1:20 as eluent to afford diaryldiazomethane **S1** (1.3 g, 99% yield) as a purple solid which was stored at -20 °C under argon. The characterization data (^{1}H and ^{13}C NMR) are consistent with those reported in literature.[1]

3.1.2. Synthesis of 4,4'-(diazomethylene)bis(N,N-dimethylaniline) (S2)

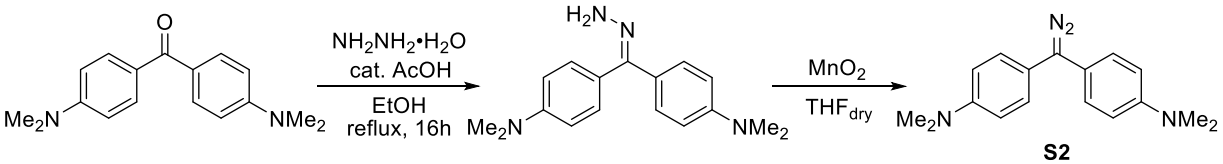

S2

Step 1: Following the reported literature,[1] analogously to Step 1 in 3.1.1. The product was obtained as a yellow needle-shaped crystals (2.4 g, yield 84%).

Step 2: Following the reported literature.[2] Activated MnO_2 (4.0 mmol, 350 mg) was added to rapidly stirred solution of the Michler's ketone hydrazone in THF (2 mL) cooled to -78 °C (0.4 mmol, 113 mg). The resulting mixture was stirred for 5 min -78 °C and then warmed to 0 °C and stirred an additional 20 min in in the absence of light (aluminum foil coated). Obtained solution of diazo compound **S2**

derivative was then transferred through a hydrophobic PTFE syringe filter into a glass vial equipped with a stirring bar (0.5 mL of THF was used for washing flask) and used to perform O-H insertion without further purification.

3.1.3. Synthesis of 9-diazo-9H-thioxanthene (S3)

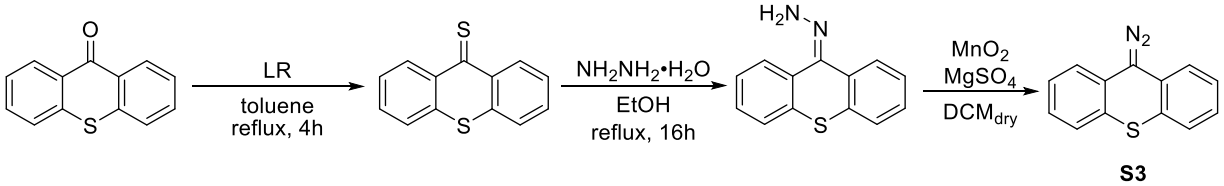

S3

Step 1: Following the modified procedure described in the literature.[12] In a round-bottomed flask equipped with reflux condenser with balloon and a magnetic stirrer ketone (6 mmol, 1.3 g) was dissolved in toluene (25 mL). Lawesson's reagent (LR, 3 mmol, 1.2 g) was added to the mixture. The reaction mixture was stirred in reflux for 4 h. After cooling to room temperature, the mixture was filtrated by silica plug using DCM/toluene = 1:10 as an eluent. After removal of the solvent under reduced pressure brown solid was obtained, used in the second step without further purification.

Step 2: Following the reported literature.[13] Crude thioxanthene-9-thione synthesized in *step 1* was dissolved in EtOH (22 mL) and hydrazine monohydrate (36 mmol, 1.7 mL) was added dropwise. Solution was heated under reflux for 2 h and filtered while hot. The filtrate was then cooled to room temperature and stored at -78 ºC overnight. The resulting gray-yellow solid precipitated. After filtration and drying on vacuum pump pure thioxanthene-9-thione hydrazone was obtained (281 mg, 23% yield after 2 steps).

Step 3: Following the reported literature,[1] analogously to Step 2 in 3.1.1. Crude product was purified using alumina gel column chromatography and pentane as eluent to afford diaryldiazomethane **S3** as a green solid (131 mg, 47% yield) which was stored at -20 °C under argon. The observed characterization data (^{1}H and ^{13}C NMR) are consistent with those reported in the literature.[3]

3.1.4. Synthesis of aryldiazoesters S4-S11

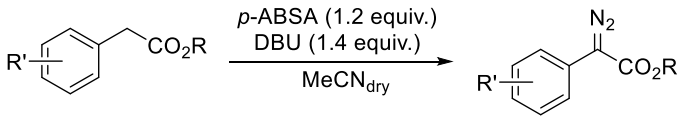

S4-S11

Following the reported literature.[4] A solution of a carbanion precursor (2 mmol) and *p*-acetamidobenzenesulfonyl azide (*p*-ABSA, 2.4 mmol, 0.6 g) in anhydrous MeCN (2.0 mL) was stirred under argon atmosphere at 0 °C. DBU (3.2 mmol, 0.5 mL) was added dropwise, then cooling bath was removed. The mixture was stirred until full conversion of the starting material was observed by the TLC. The reaction was quenched with sat. NH_4Cl and extracted with DCM (3 times), combined organic layers were washed with brine and dried over magnesium sulfate. The mixture was then filtered and evaporated *in vacuo*, crude product was purified by column chromatography (hexane:AcOEt as eluent**).**

3.1.5. Synthesis of ethyl 2-diazopropanoate (S12)

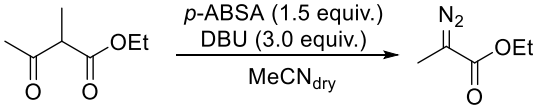

S12

Following the reported procedure.[9] A solution of a ethyl 2-methyl-3-oxobutanoate (10 mmol, 1.2 mL) and *p*-acetamidobenzenesulfonyl azide (*p*-ABSA, 15 mmol, 3.6 g) in anhydrous MeCN (20 mL) was stirred under argon atmosphere at 0 °C. DBU (30 mmol, 4.5 mL) was added dropwise. The reaction mixture was then allowed to warm to room temperature and stirred overnight. Then, the reaction mixture was quenched with 1 M HCl (20 mL), and extracted with hexane (3 x 50 mL). The organic layers were combined and washed with saturated solution of $NaHCO_3$ (50 mL), brine (50 mL), and dried over anhydrous $MgSO_4$. The solvent was removed under reduced pressure and the mixture was purified by flash column chromatography using Et_2O/pentane = 1:50 to give diazo compound **S12** as yellow oil (0.9 g, 70%). The observed characterization data (^{1}H and ^{13}C NMR) are consistent with those reported in the literature.[9]

3.1.6. Synthesis of diethyl 2-diazomalonate (S13)

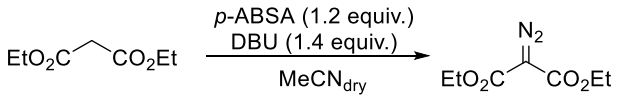

S13

Following the reported literature,[1] analogously to aryldiazoester synthesis (3.1.4). The observed characterization data (^{1}H and ^{13}C NMR) are consistent with those reported in the literature.[10]

3.1.7. Synthesis of dimethyl (diazomethyl)phosphonate (S14)

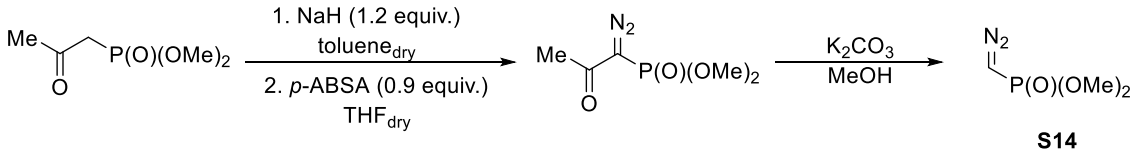

S14

Step 1: Following the reported literature.[11] To a solution of dimethyl (2-oxopropyl)phosphonate (20 mmol, 2.7 mL) in dry toluene (40 mL) cooled to 0 °C, NaH (24 mmol, 1.0 g of NaH 60% disp. in mineral oil) was added portionwise. The mixture was stirred at 0 °C for 1 hour and then a solution of *p*-acetamidobenzenesulfonyl azide (*p*-ABSA, 18 mmol, 4.3 g) in anhydrous THF (15 mL) was added dropwise. The mixture was stirred at room temperature for 24 h. Hexane (20 mL) was added and the precipitate was filtered off, washed with ether (3 x 20 mL). The filtrate was evaporated and the residue was purified by flash column chromatography on silica gel (hexane:ethyl acetate) to dimethyl (1-diazo-2-oxopropyl)phosphonate as a yellow liquid (3.4 g, 90 %).

Step 2: Following the modified procedure described in the literature.[11] A solution of dimethyl (1-diazo-2-oxopropyl)phosphonate (18 mmol, 3.4 g) in methanol (20 mL) was stirred with potassium carbonate (9 mmol, 1.2 g) for 25 min. The precipitate was filtered off and the filtrate was evaporated under reduced pressure. The residue was purified by flash column chromatography on silica gel (hexane:ethyl acetate) to give diazo compound **S14** as yellow liquid (2.2 g, 80 %).

3.2. Preparation of other starting materials

Along with diazo compounds, starting materials **S15-S23** were synthesized according to literature procedures. The observed characterization data (^{1}H and ^{13}C NMR) are consistent with those previously reported.[14-17]

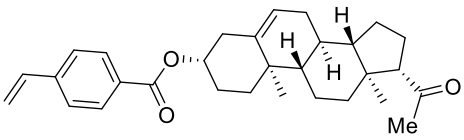

S15[14]

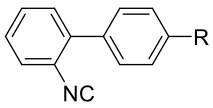

R = H, **S16**[15]
R = OMe, **S17**[15]

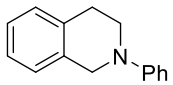

S18[16]

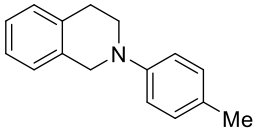

S19[16]

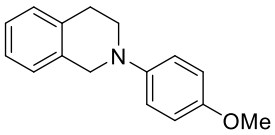

S20[16]

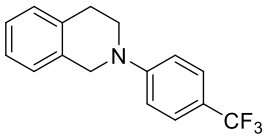

S21[16]

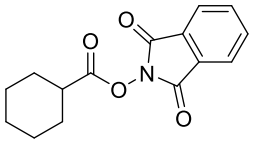

S22[17]

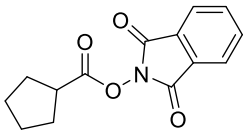

S23[17]

3.3. General procedure for the red light-induced O-H insertion of diaryldiazoalkanes with alcohols

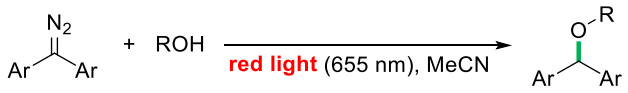

Mechanism:

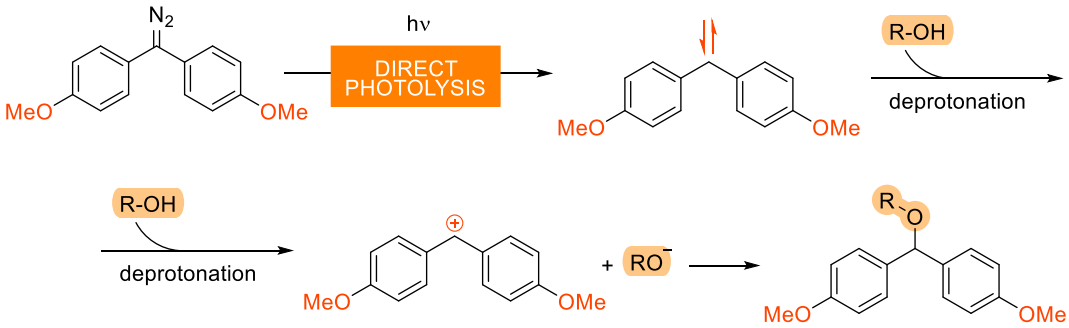

To a glass vial equipped with a stirring bar diazoalkane (0.2 mmol) was added. A vial was sealed with an aluminum cap with a rubber septum and charged with 2.0 mL of MeCN and alcohol (2 mmol, 10 equiv.). The reaction mixture was placed in a photoreactor and irradiated with red LEDs (25 W, 655 nm) until full discoloring of the purple solution was achieved (ca. 135 min). After that time, the crude reaction mixture was concentrated *in vacuo* and the residue was purified by flash column chromatography on silica gel using hexane:AcOEt as eluent to afford final product.

*Note: In the case of products **8**, **9**, **11** other substrates ratio was used. Additionally, for product **11** THF was used instead of MeCN at altered concentration.*

3.4. General procedure for the red light-induced N-H insertion of diaryldiazoalkanes with amines

To a glass vial equipped with a stirring bar 4,4'-(diazomethylene)bis(methoxybenzene) (**S1**, 0.4 mmol, 2 equiv.) was added. The vial was sealed with an aluminum cap with a rubber septum, purged with argon and charged with 2.0 mL of dry DCM and amine (0.2 mmol). The reaction mixture was placed in a photoreactor and irradiated with red LEDs (25 W, 655 nm) until full discoloring of the purple solution was achieved (ca. 135 min). After that time, the crude reaction mixture was concentrated *in vacuo* and the residue was purified by flash column chromatography on silica gel using Et_3N:hexane as eluent to afford the final product.

*Note: In the case of product **13** other substrates ratio was used.*

3.5. General procedure for the red light-induced S-H insertion of diaryldiazoalkanes with thiols

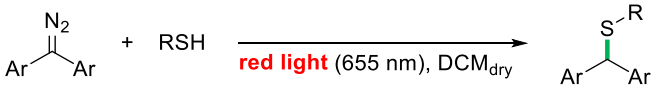

To a glass vial equipped with a stirring bar model diazo compound (0.4 mmol, 2 equiv.) was added. The vial was sealed with an aluminum cap with a rubber septum, purged with argon and charged with 2.0 mL of dry DCM and thiol (0.2 mmol). The reaction mixture was placed in a photoreactor and irradiated with red LEDs (25 W, 655 nm) until full discoloring of the purple solution was achieved (ca. 135 min). After that time, the crude reaction mixture was concentrated *in vacuo* and the residue was purified by flash column chromatography on silica gel using hexane:AcOEt as an eluent to afford the final product.

*Note: In the case of product **22** and **23** other substrates ratio was used.*

3.6. General procedure for the red light-induced, photosensitized oxygenation of aryldiazoesters

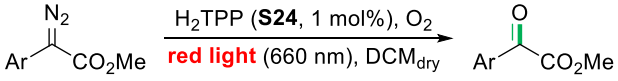

A glass vial equipped with a stirring bar was charged with tetraphenylporphyrin (H_2TPP, **S24**, 0.001 mmol, 0.6 mg), α-diazoester (0.1 mmol) and dry DCM (1.0 mL). A vial was sealed with an aluminum cap with a rubber septum and air was removed from the solution by freeze-pump-thaw technique, followed by refilling the vial with oxygen with O_2 balloon. The reaction mixture was placed in a photoreactor and irradiated with red LEDs (3 W, 660 nm) for 1 h. After that time, the reaction mixture was concentrated *in vacuo* and the residue was purified by flash column chromatography on silica gel using hexane:AcOEt as eluent to afford the final product.

Mechanism:

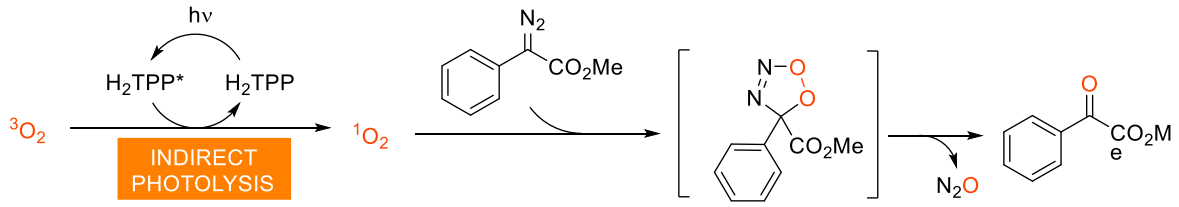

Failed substrates:

diazo compounds

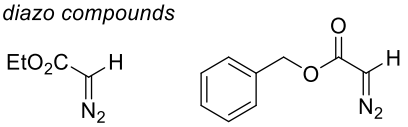

3.7. General procedure for the red light-induced, photosensitized O-H insertion of aryldiazoesters with benzoic acid

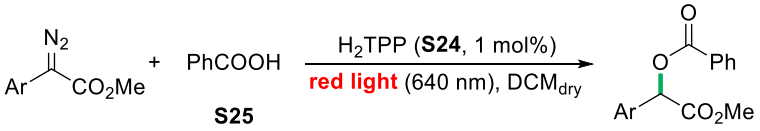

A glass vial equipped with a stirring bar was charged with tetraphenylporphyrin (H_2TPP, **S24**, 0.001 mmol, 0.6 mg), α-diazoester (0.1 mmol) and benzoic acid (**S25**, 0.2 mmol, 24.4 mg, 2 equiv.). A vial was sealed with an aluminum cap with a rubber septum impaled with a needle and placed in glovebox to remove air and maintain oxygen-free conditions. Dry DCM was added (1.0 mL) followed up by a needle removal. The vial was removed from glovebox and irradiated with two Kessil lamps (2 x 40 W, 640 nm) while stirring for 16 h. After that time, the crude mixture was concentrated *in vacuo* and the residue was purified by flash column chromatography on silica gel using hexane:AcOEt as eluent to afford final product.

Mechanism:

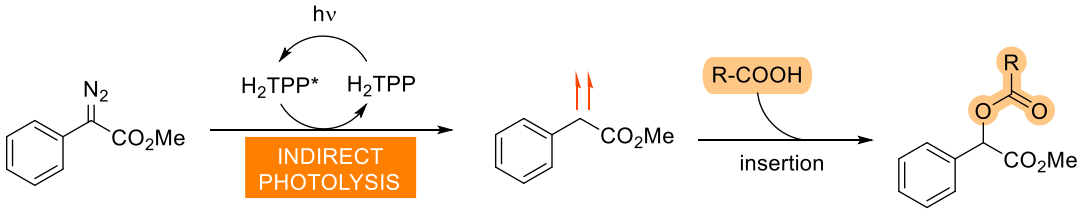

Failed substrates:

acids

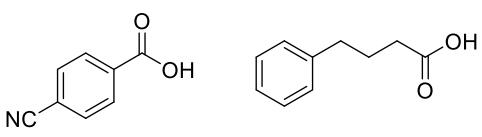

arylodiazoester

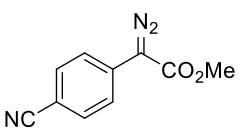

3.8. General procedure for the red light-induced, photosensitized cyclopropanation with aryldiazoesters

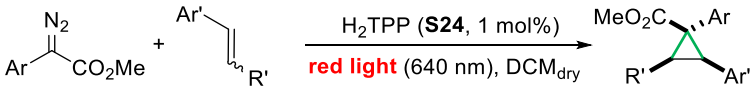

A glass vial equipped with a stirring bar was charged with tetraphenylporphyrin (H_2TPP, **S24**, 0.001 mmol, 0.6 mg) and α-diazoester (0.1 mmol). The vial was sealed with an aluminum cap with a rubber septum impaled with a needle and placed in glovebox to remove air and maintain oxygen-free conditions. Dry DCM (1.0 mL) and olefin (1.0 mmol, 10 equiv.) were added followed up by a needle removal. The vial was removed from glovebox and irradiated with two Kessil lamps (2 x 40 W, 640 nm) while stirring for 16 h. After that time, the crude mixture was concentrated *in vacuo* and the residue was purified by flash column chromatography on silica gel using hexane:AcOEt as eluent to afford final product.

Mechanism:

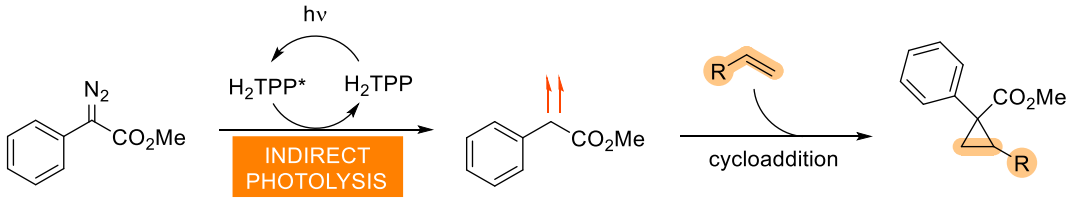

3.9. General procedure for the red light-induced, photocatalyzed synthesis of γ-oximinoesters

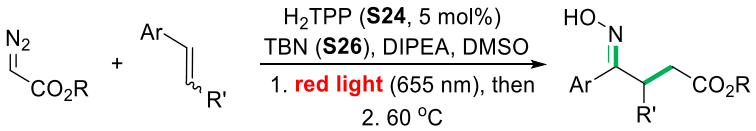

A glass vial equipped with a stirring bar was charged with tetraphenylporphyrin (H_2TPP, **S24**, 0.01 mmol, 6.2 mg) and DMSO (p.a. grade, 4.0 mL). The vial was sealed with an aluminum cap with a rubber septum and oxygen was removed from the solution by freeze-pump-thaw technique. Then, olefin (0.2 mmol - if liquid, solid is added prior the solvent), *N*,*N*-diisopropylethylamine (DIPEA, 0.6 mmol, 105 µL, 3 equiv.) and α-diazoester (0.4 mmol, 2 equiv.) were added under Ar atmosphere. The reaction mixture was stirred for 10 min. After that time, *t*-butyl nitrite (TBN, **S26**, 0.4 mmol, 48 µL, 2 equiv.) was added under Ar atmosphere and the vial was placed in a photoreactor and irradiated with red LEDs (25 W, 655 nm). After 17 h, the vial was placed in an oil bath and stirred at 60 °C for an additional 20 h. The reaction mixture washed with water (2 x 25 mL) and aqueous layers were washed with DCM (3 x 25 mL). Combined organic layers were dried over sodium sulfate, filtrated, and concentrated *in vacuo.* The residue was purified by flash column chromatography on silica gel using hexane:AcOEt as eluent to afford the final product.

*Note: The synthesis of product **42** required prolonged irradiation time (66 h) and using MeCN as co-solvent for better olefin solubility, concentration was altered as well.*

Failed substrates:

diazoesters

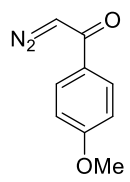

low conversion of diazo

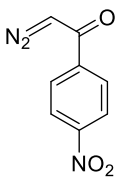

diazo fully converted, traces of product, low selectivity, messy

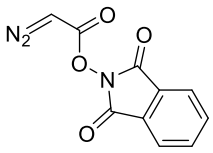

diazo fully converted, NHPI and Phtalimide present in high amount

Mechanism:

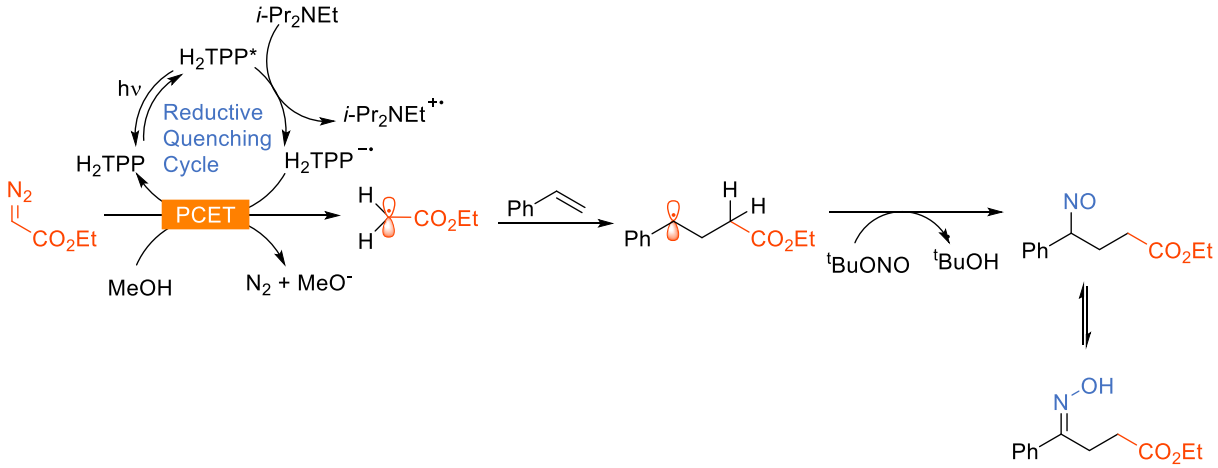

3.10. General procedure for the red light-induced, photocatalyzed synthesis of phenantridines

To a glass vial equipped with a stirring bar tetraphenylporphyrin (H_2TPP, **S24**, 0.01 mmol, 6.2 mg) was added. The vial was purged with argon, charged with dry DMSO (1.0 mL) and sealed with an aluminum cap with a rubber septum. Oxygen was removed from the solution by freeze-pump-thaw technique and isocyanate (0.2 mmol, if liquid – solid isocyanate is added prior the solvent), diazoalkane (1.0 mmol, 5 equiv.) and DIPEA (0.2 mmol, 35 µL, 1 equiv.) were added under Ar atmosphere. Then, the vial was placed in a photoreactor and irradiated with red LEDs (25 W, 655 nm) for 18 h. After that time, the crude reaction mixture was washed with water (2 x 25 mL) and aqueous layers were washed with DCM (3 x 25 mL). Combined organic layers were dried over sodium sulfate, filtrated, and concentrated *in vacuo*. The residue was purified by flash column chromatography on silica gel using hexane:acetone as eluent to afford the final product.

Failed substrates:

arylodiazoester

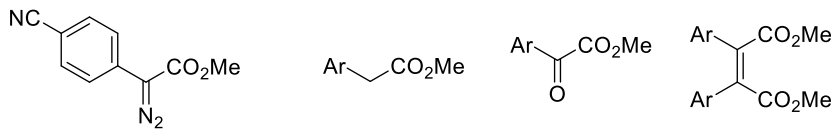

80% diazo conversion
75% isocyanobiphenyl conversion

unselective decomposition,
diazo-derived products observed

Mechanism:

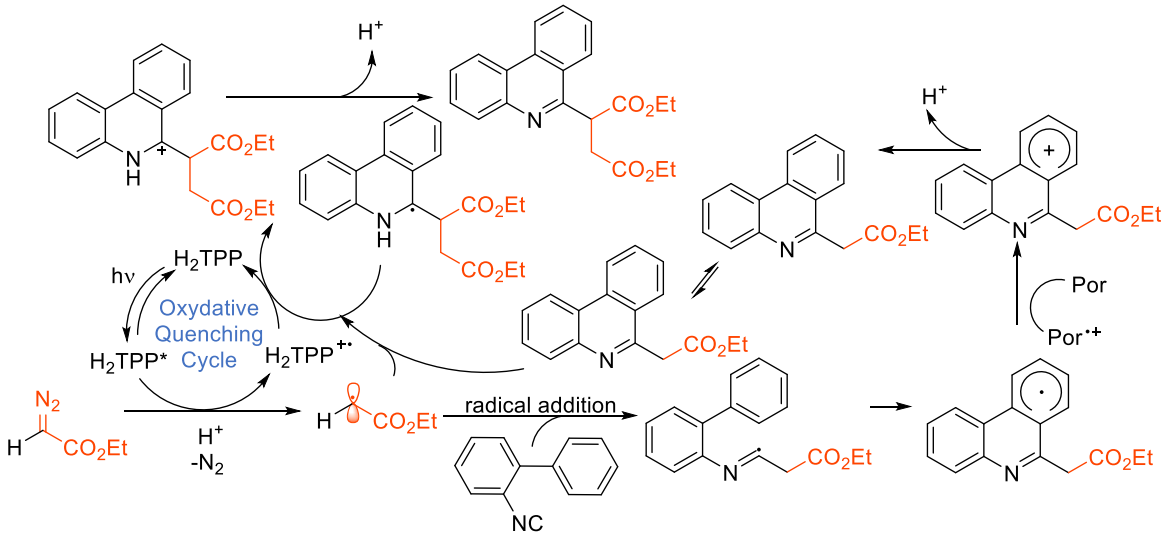

3.11. General procedure for the red light-induced, photocatalyzed synthesis of β-amino-α-diazo esters

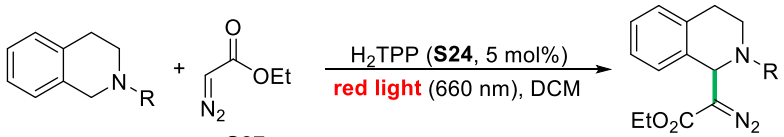

A glass vial equipped with a stirring bar was charged with tetrahydroisoquinoline (0.1 mmol) and 1/3 portion of tetraphenylporphyrin (H_2TPP, **S24**, 0.002 mmol, 1.0 mg). The vial was sealed with an aluminum cap with a rubber septum followed by the addition of DCM p.a. (0.5 mL) and ethyl diazoacetate solution (**S27**, 13% wt.in DCM, 0.3 mmol, 36 µL, 3 equiv.). The reaction mixture was placed in a photoreactor and irradiated with red LEDs (3 W, 660 nm) for 48 h at 30 °C. During that time, two additional portions of tetraphenylporphyrin were added in 12 h intervals.* After 48 h, the crude reaction mixture was concentrated *in vacuo* and purified by flash column chromatography on silica gel using hexane/AcOEt 99:1 to afford the final product.

*Note: *Tetraphenylporphyrin (H_2TPP) was added in 3 equal portions every 12 h (at 0, 12 and 24 h irradiation time). In total, 5 mol% of H_2TPP (0.05 mmol, 3.0 mg) was added into the vial.*

Failed substrates:

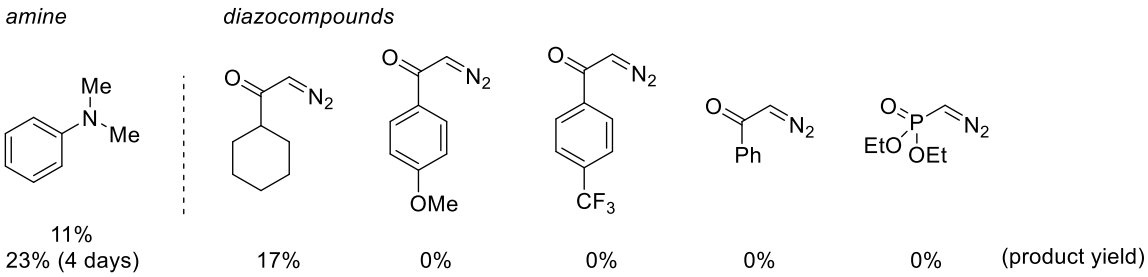

Mechanism:

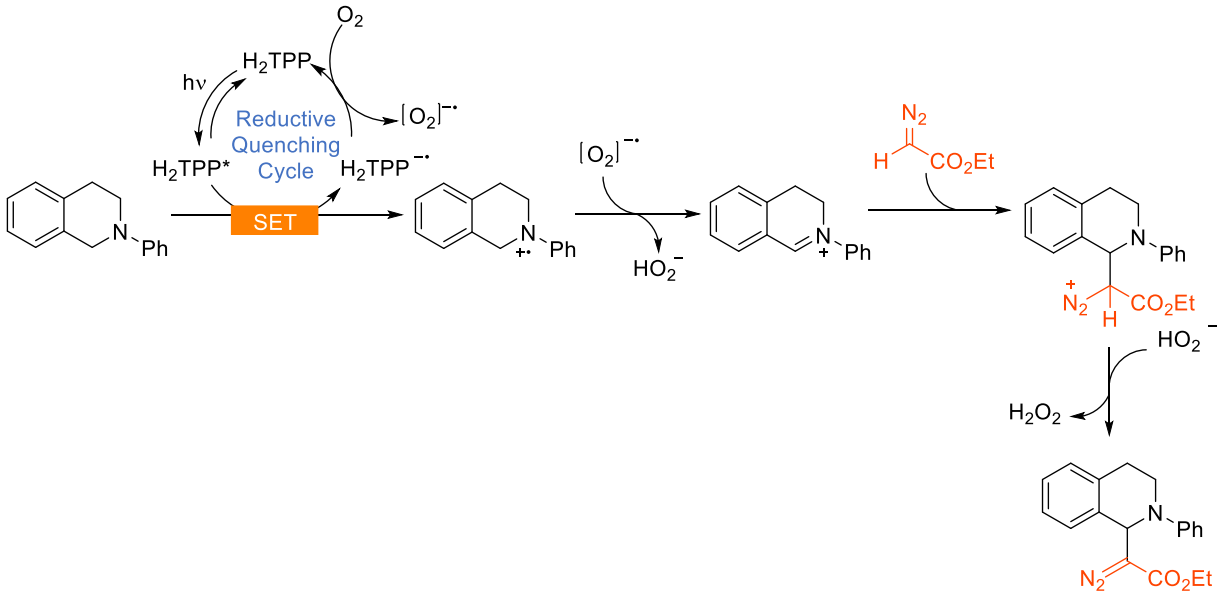

3.12. General procedure for the red light-induced, photocatalyzed synthesis of hydrazones

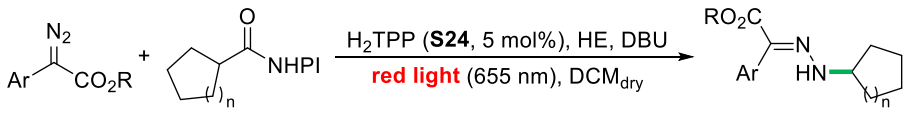

A glass vial equipped with a stirring bar was charged with tetraphenylporphyrin (H_2TPP, **S24**, 0.01 mmol, 6.2 mg), α-diazoester (0.2 mmol), NHPI ester (0.3 mmol, 1.5 equiv.) and Hantzsch ester (HE, 0.24 mmol mmol, 1.2 equiv.). A vial was sealed with an aluminum cap with a rubber septum impaled with a needle and placed in glovebox to remove air and maintain oxygen-free conditions. Dry DCM (2.0 mL) and DBU (0.46 mmol, 69 µL, 2.3 equiv.) were added followed up by a needle removal. The vial was removed from glovebox and was placed in a photoreactor for irradiation with red LEDs (25 W, 655 nm) for 18 h. After that time, the crude reaction mixture was concentrated *in vacuo* and the residue was purified by flash column chromatography on silica gel using hexane:DCM:AcOEt as eluent to afford the final product.

Failed substrates:

arylodiazoesters

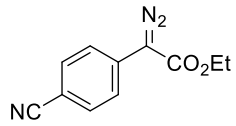

<20% of product (NMR)

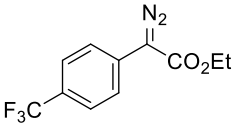

product not obtained

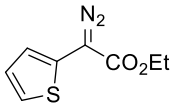

8% of product (NMR)

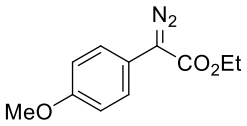

<30% of product (NMR)

Mechanism:

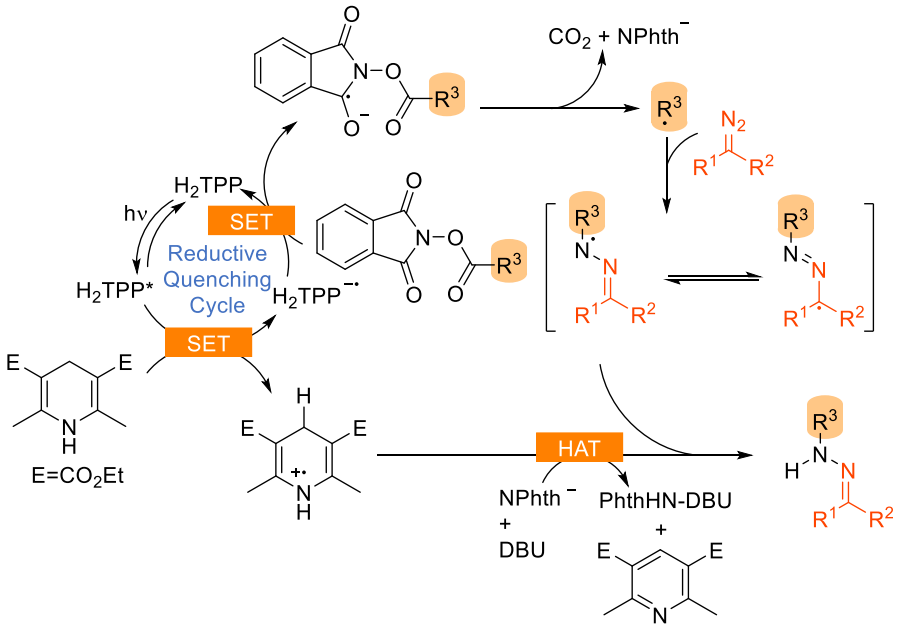

4. Optimization details

4.1. Optimization of the red light-induced O-H insertion of diaryldiazoalkanes with alcohols

Model reaction

Optimal reaction conditions: 4,4'-(diazomethylene)bis(methoxybenzene) (**S1**, 0.2 mmol), benzyl alcohol (**S28**, 2 mmol, 10 equiv.), MeCN (c = 0.1 M), red LEDs (655 nm, 25 W), air atmosphere, 25 °C, 135 min.

Background reactions

entry	deviation from reaction conditions	yield of **1** [%][a]
1	no light	0
2	none	64
3	dry DCM was used	67
4	air atmosphere	63

Reaction conditions: diazoalkane **S1** (0.2 mmol), benzyl alcohol (**S28**, 2.0 mmol, 10 equiv.), DCM (p.a. grade, c = 0.1 M), red LEDs (655 nm, 25 W), Ar atmosphere, T = 25 °C, 1 h; [a]isolated yield.

Solvent screening

entry	solvent	yield of **1** [%][a]
1	DCM	64
2	DCE	21
3*	benzene	47
4	$CHCl_3$	70
5	MeCN	67
6[c,d]	MeCN	79[b]
7[d,e]	MeCN	84

Reaction conditions: diazoalkane **S1** (0.2 mmol), benzyl alcohol (**S28**, 2.0 mmol, 10 equiv.), *solvent* (c = 0.1 M), red LEDs (655 nm, 25 W), Ar atmosphere, T = 25 °C, 1 h; [a]isolated yield. [b]GC yield. [c]0.1 mmol scale. [d]air atmosphere. [e] reaction time was prolonged to 135 min (to ensure full conversion of diazoalkane **S1**). *In $CHCl_3$ decomposition of diazo compound **S1** was observed over few hours without irradiation.

Concentration effects

entry	concentration [M]	yield of **1** [%][a]
1	0.05	75
2	0.1	79
3*	0.2	79

Reaction conditions: diazoalkane **S1** (0.1 mmol), benzyl alcohol (**S28**, 1.0 mmol, 10 equiv.), MeCN (c = *x* M), red LEDs (655 nm, 25 W), air atmosphere, T = 25 °C, 1 h; [a]GC yield. *not homogenous mixture.

Light intensity

entry	light intensity [W]	irradiation time* [min]	yield of **1** [%][a]
1	25	60	79
2	13	135	74
3	6	240	72

Reaction conditions: diazoalkane **S1** (0.1 mmol), benzyl alcohol (**S28**, 1.0 mmol, 10 equiv.), MeCN (c = 0.1 M), red LEDs (655 nm, *x* W), air atmosphere, T = 25 °C; [a]GC yield. *the reaction mixture was irradiated until full discoloring of violet solution.

Temperature

entry	temperature [°C]	irradiation time* [min]	yield of **1** [%][a]
1	25	60	79
2	16	145	74

Reaction conditions: diazoalkane **S1** (0.1 mmol), benzyl alcohol (**S28**, 1.0 mmol, 10 equiv.), MeCN (c = 0.1 M), red LEDs (655 nm, 25 W), air atmosphere, T = *x* °C; [a]GC yield. *the reaction mixture was irradiated until full discoloring of violet solution.

Substrates ratio

entry	**S1**:**S28** ratio [mol/mol]	yield of **1** [%][a]
1	5:1	81
2	2:1	81
3	1:1	56
4	1:2	64
5	1:5	74
6	1:10	79
7	1:15	75

Reaction conditions: diazoalkane **S1** (*x* mmol), benzyl alcohol (**S28**, *y* mmol), MeCN (c = 0.1 M), red LEDs (655 nm, 25 W), air atmosphere, T = 25 °C, 1 h; [a]GC yield.

Addition of diazo compound

entry	diazo portions	irradiation time* [min]	yield of **1** [%][a]
1	one, before irradiation	60	79
2	two, second added after 30 min	130	78

Reaction conditions: diazoalkane **S1** (0.1 mmol), benzyl alcohol (**S28**, 1.0 mmol, 10 equiv.), MeCN (c = 0.1 M), red LEDs (655 nm, 25 W), air atmosphere, T = 25 °C; [a]GC yield. *the reaction mixture was irradiated until full discoloring of violet solution.

4.2. Optimization of the red light-induced N-H insertion of diaryldiazoalkanes with amines

Model reaction

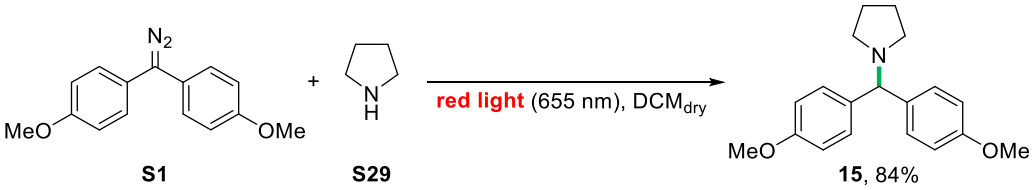

Optimal reaction conditions: 4,4'-(diazomethylene)bis(methoxybenzene) (**S1**, 0.4 mmol, 2 equiv.), pyrrolidine (**S29**, 0.2 mmol), dry DCM (c = 0.1 M), red LEDs (655 nm, 25 W), Ar atmosphere, 25 °C, 135 min.

Background reactions

entry	deviation from reaction conditions	yield of **15** [%][a]
1	no light	0
2	none	44
3[b]	dry MeCN was used	45

Reaction conditions: diazoalkane **S1** (0.2 mmol), pyrrolidine (**S29**, 2.0 mmol, 10 equiv.), MeCN (c = 0.1 M), red LEDs (655 nm, 25 W), air atmosphere, T = 25 °C, 135 min; [a]isolated yield. [b]Ar atmosphere.

Solvent screening

entry	solvent	yield of **15** [%][a]
1	dry MeCN	46
2	dry DMF	54
3	dry DCM	70

Reaction conditions: diazoalkane **S1** (0.2 mmol), pyrrolidine (**S29**, 2.0 mmol, 10 equiv.), *solvent* (c = 0.1 M), red LEDs (655 nm, 25 W), Ar atmosphere, T = 25 °C, 135 min; [a]isolated yield.

Substrates ratio

entry	**S1**:**S29** ratio [mol/mol]	yield of **15** [%][a]
1	2:1	84
2	1:2	74
4	1:4	77
4	1:5	74
5	1:10	70

Reaction conditions: diazoalkane **S1** (*x* mmol), pyrrolidine (**S29**, *y* mmol), dry DCM (c = 0.1 M), red LEDs (655 nm, 25 W), Ar atmosphere, T = 25 °C, 120 min; [a]isolated yield.

For primary amines, additional optimization of substrates ratio was undertaken, due to unsatisfactory yields observed when conditions optimal for secondary amines were used (entry 2, 44%, product **13**):

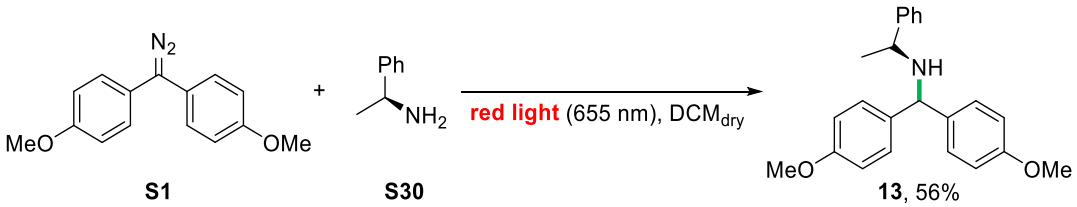

Substrates ratio – primary amine

entry	**S1**:**S30** ratio [mol/mol]	yield of **13** [%][a]
1	3:1	64 (56)
2	2:1	44
4	1:2	26
4	1:3	22
5	1:4	24

Reaction conditions: diazoalkane **S1** (*x* mmol), *(S)*-1-phenylethan-1-amine (**S30**, *y* mmol), dry DCM (c = 0.1 M), red LEDs (655 nm, 25 W), Ar atmosphere, T = 25 °C, 135 min; [a] yields determined by the ^{1}H NMR using 1,3,5-trimetoxybenzene as internal standard, isolated yields in parenthesis.

4.3. Optimization of the red light-induced S-H insertion of diaryldiazoalkanes with thiols

Model reaction

Optimal reaction conditions: 4,4'-(diazomethylene)bis(methoxybenzene) (**S1**, 0.4 mmol, 2 equiv.), benzyl mercaptan (**S31**, 0.2 mmol), dry DCM (c = 0.1 M), red LEDs (655 nm, 25 W), Ar atmosphere, 25 °C, 135 min.

Background reactions

entry	deviation from reaction conditions	yield of **19** [%][a]
1	no light	0
2	none	65
3	dry MeCN used as solvent	49

Reaction conditions: diazoalkane **S1** (0.2 mmol), benzyl mercaptan (**S31**, 2.0 mmol, 10 equiv.), dry DCM (c = 0.1 M), red LEDs (655 nm, 25 W), Ar atmosphere, T = 25 °C, 1 h; [a]isolated yield.

Substrates ratio

entry	**S1**:**S31** ratio [mol/mol]	yield of **19** [%][a]
1	2:1	>99 (89)
2	1:4	82
3	1:10	77

Reaction conditions: diazoalkane **S1** (*x* mmol), benzyl mercaptan (**S31**, *y* mmol), dry DCM (c = 0.1 M), red LEDs (655 nm, 25 W), Ar atmosphere, T = 25 °C, 135 min; [a] yields determined by the ^{1}H NMR using 1,3,5-trimetoxybenzene as internal standard, isolated yields in parenthesis.

4.4. Optimization of the red light-induced, photosensitized oxygenation of aryldiazoesters

Model reaction

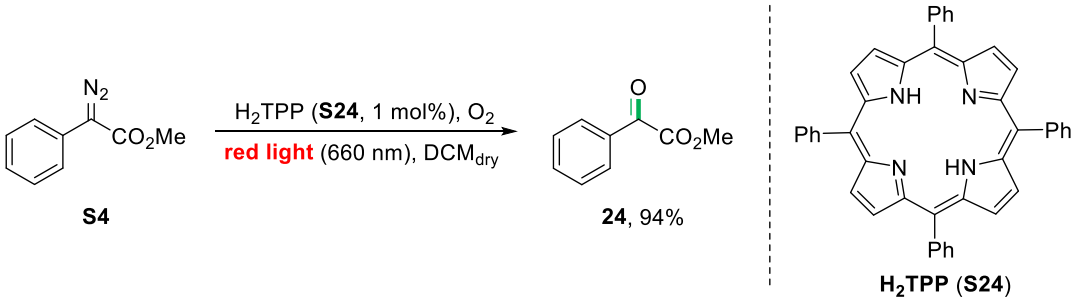

Optimal reaction conditions: H_2TPP (**S24**, 1 mol%), methyl 2-diazo-2-phenylacetate (**S4**, 0.1 mmol), dry DCM (c = 0.1 M), red LEDs (660 nm, 3 W), O_2 atmosphere, 25 °C, 1 h.

Background reactions

entry	deviation from reaction conditions	yield of **24** [%]
1	none	60 (58)[a]
2	no light	0
3	no H_2TPP (**S24**)	0
4	no light, no H_2TPP (**S24**)	0
5	no light, heated to 35 °C, no H_2TPP (**S24**)	0

Reaction conditions: H_2TPP (**S24**, 1 mol%), diazoalkane **S4** (0.1 mmol), dry DCM (c = 0.1 M), red LEDs (660 nm, 3 W), Ar atmosphere, T = 25 °C, 18 h; [a]GC yield, isolated yield in parenthesis.

Solvent screening

entry	solvent	yield of **24** [%][a]
1	dry DCM	60
2	dry 1,4-dioxane	53
3	dry THF	49
4	dry acetone	45
5	dry MeCN	44
6	dry C_6F_6	47

Reaction conditions: H_2TPP (**S24**, 1 mol%), diazoalkane **S4** (0.1 mmol), *solvent* (c = 0.1 M), red LEDs (660 nm, 3 W), Ar atmosphere, T = 25 °C, 1 h; [a]GC yield.

Concentration effects

entry	concentration [M]	yield of **24** [%][a]
1	0.2	50
2	0.1	60
3	0.05	54
4	0.03	45
5	0.02	38

Reaction conditions: H_2TPP (**S24**, 1 mol%), diazoalkane **S4** (0.1 mmol), dry DCM (c = *x* M), red LEDs (660 nm, 3 W), Ar atmosphere, T = 25 °C, 1 h; [a]GC yield.

Photocatalyst screening

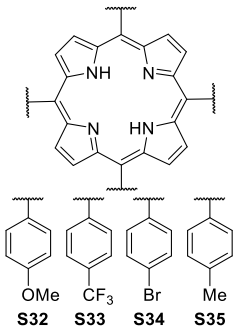

S32 **S33** **S34** **S35**

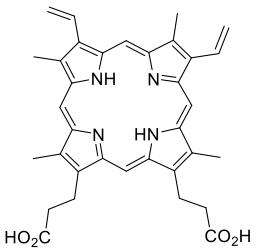

S36

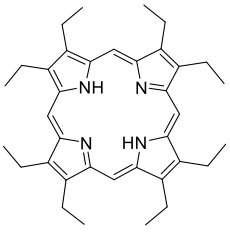

S37

entry	photocatalyst	yield of **24** [%][a]
1	H_2TPP (**S24**)	60
2	H_2T(*p*-OMe)PP (**S32**)	62
3	H_2T(*p*-CF_3)PP (**S33**)	60
4	H_2T(*p*-Br)PP (**S34**)	59
5	H_2T(*p*-Me)PP (**S35**)	48
6	PPIX (**S36**)	37
7	octaethylporphyrin (**S37**)	60

Reaction conditions: photocatalyst (***x***, 1 mol%), diazoalkane **S4** (0.1 mmol), dry DCM (c = 0.1 M), red LEDs (660 nm, 3 W), Ar atmosphere, T = 25 °C, 1 h; [a]GC yield.

Photocatalyst loading

entry	catalyst **S24** loading [mol%]	yield of **24** [%][a]
1	0.2	28
2	0.5	55
3	1.0	60
4	1.5	61
5	2.0	60
6	5.0	22
7	10.0	17

Reaction conditions: H_2TPP (**S24**, *x* mol%), diazoalkane **S4** (0.1 mmol), dry DCM (c = 0.1 M), red LEDs (660 nm, 3 W), Ar atmosphere, T = 25 °C, 1 h; [a]GC yield.

Oxygen access

entry	oxygen access via:	yield of **24** [%][a]
1	closed vial (air atmosphere)	60
2	closed vial with a needle (air atmosphere)	61
3	closed vial with O_2 balloon (O_2 atmosphere)	53
4[b]	closed vial with O_2 balloon (O_2 atmosphere)	79
5*	freeze-pump-thaw with O_2	94

Reaction conditions: H_2TPP (**S24**, 1 mol%), diazoalkane **S4** (0.1 mmol), dry DCM (c = 0.1 M), red LEDs (660 nm, 3 W), *x* atmosphere, T = 25 °C, 1 h; [a]GC yield. [b]catalyst **S24** added in 2 equal portions (0.5 mol% each, 2nd after 3 h). *air was removed from the vial by freeze-pump-thaw technique and the vial was purged with O_2.

4.5. Optimization of the red light-induced, photocatalyzed synthesis of γ-oximinoesters

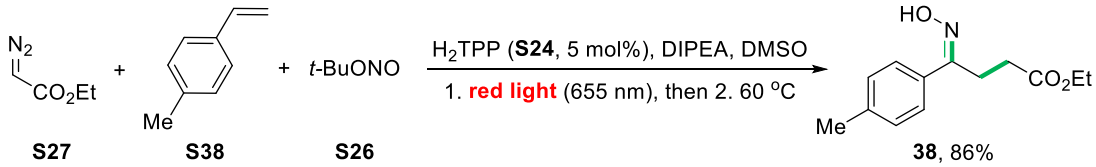

S27 **S38** **S26** **38**, 86%

Optimal reaction conditions: H_2TPP (**S24**, 5 mol%), ethyl diazoacetate (**S27**, 0.4 mmol, 2 equiv.), 4-methyl-styrene (**S38**, 0.2 mmol), TBN (**S26**, 0.4 mmol, 2 equiv.), DIPEA (0.6 mmol, 3 equiv.), DMSO (c = 0.05 M), Ar atmosphere, irradiation with red LEDs (655 nm, 25 W) at 25 °C for 20 h, then heating (60 °C, 18 h).

Background reactions

entry	deviation from reaction conditions	yield of **38** [%][a]
1	none	42
2	no light	0
3	no H_2TPP (**S24**)	0
4	no light, no H_2TPP (**S24**)	0
5	dry solvents were used	36

Reaction conditions: H_2TPP (**S24**, 5 mol%), olefin **S38** (0.2 mmol), diazoalkane **S27** (0.4 mmol, 2 equiv.), TBN (**S26**, 0.4 mmol, 2 equiv.), DIPEA (0.6 mmol, 3 equiv.), MeOH/ DCM (1:1 v/v, c = 0.1 M), red LEDs (655 nm, 25 W), Ar atmosphere, T = 25 °C, 60 h; [a]isolated yield.

Solvent & catalyst screening

entry	photocatalyst	solvent system	yield of **38** [%][a]
1	H_2TPP (**S24**)	MeOH/DCM = 1/1 (v/v)	42
2		dry toluene	<5
3		dry DMSO	63
4		MeOH/dry DMSO = 1/1 (v/v)	64
5		dry MeOH/dry DMSO = 1/1 (v/v)	60
6		MeOH/dry DMF= 1/1 (v/v)	61
7	H_2T(*p*-OMe)PP (**S32**)	dry MeCN	40
8	Rose Bengal	MeOH	21

Reaction conditions: *catalyst* (5 mol%), olefin **S38** (0.2 mmol), diazoalkane **S27** (0.4 mmol, 2 equiv.), TBN (**S26**, 0.4 mmol, 2 equiv.), DIPEA (0.6 mmol, 3 equiv.), *solvent* (c = 0.1 M), red LEDs (655 nm, 25 W), Ar atmosphere, T = 25 °C, 60 h; [a]isolated yield.

Concentration effects

entry	concentration [M]	yield of **38** [%][a]
1	0.05	69
2	0.1	64
3	0.2	45

Reaction conditions: H_2TPP (**S24**, 5 mol%), olefin **S38** (0.2 mmol), diazoalkane **S27** (0.4 mmol, 2 equiv.), TBN (**S26**, 0.4 mmol, 2 equiv.), DIPEA (0.6 mmol, 3 equiv.), MeOH/dry DMSO (1:1 v/v, c = *x* M), red LEDs (655 nm, 25 W), Ar atmosphere, T = 25 °C, 60 h; [a]isolated yield.

Irradiation time & heating time

entry	irradiation time [h]	then heating time (at 60°C) [h]	yield of **38** [%][a]
1	20	no	53
2	60	no	64
3	115	no	55
4	20	2	56
5	20	6	60
6	20	18	76
7[b]	20	18	78
8[b,c]	20	18	67
9[b,d]	20	18	86

Reaction conditions: H_2TPP (**S24**, 5 mol%), olefin **S38** (0.2 mmol), diazoalkane **S27** (0.4 mmol, 2 equiv.), TBN (**S26**, 0.4 mmol, 2 equiv.), DIPEA (0.6 mmol, 3 equiv.), MeOH/dry DMSO (1:1, v/v, c = 0.1 M), Ar atmosphere, red LEDs (655 nm, 25 W), T = 25 °C, *x* h; then then the reaction vial (if noted) was placed in oil bath and stirred for *y* time at 60 °C. [a]isolated yield. [b]c = 0.05 M. [c]3.0 equiv. of EDA (**S27**) was used. [d]DMSO as solvent.

4.6. Optimization of the red light-induced, photocatalyzed synthesis of phenantridines

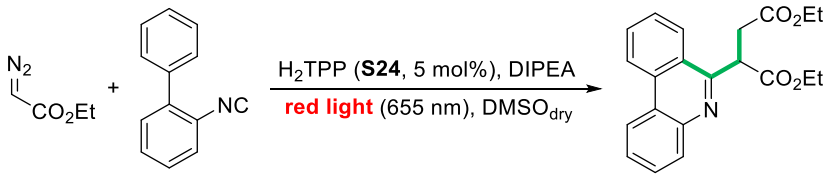

S27 **S16** **43**, 95%

Optimal reaction conditions: H_2TPP (**S24**, 5 mol%), ethyl diazoacetate (**S27**, 1.0 mmol, 5 equiv.), 2-isocyano-1,1'-biphenyl (**S16**, 0.2 mmol), DIPEA (0.2 mmol, 1 equiv.), dry DMSO (c = 0.2 M), Ar atmosphere, red LEDs (655 nm, 25 W), 25 °C, 18 h.

Background & Optimization

entry	deviation from reaction conditions	yield of **38** [%][a]
1	none	59
2	no light	0
3	no H_2TPP (**S24**)	0
4	no light, no H_2TPP (**S24**)	0
5	DMSO as solvent	64
6	DMSO as solvent, 0.05 M	56
7	DMSO as solvent, 2 equiv. of DIPEA	67
8	dry DMSO as solvent	>99 (95)

Reaction conditions: H_2TPP (**S24**, 5 mol%), ethyl diazoacetate (**S27**, 1.0 mmol, 5 equiv.), 2-isocyano-1,1'-biphenyl (**S16**, 0.2 mmol), DIPEA (0.2 mmol, 1 equiv.), dry MeOH/dry DCM (1:1, v/v, c = 0.2 M), Ar atmosphere, red LEDs (655 nm, 25 W), 25 °C, 18 h. [a]yields determined by the ^1H NMR using dibromomethane as internal standard, isolated yield in parenthesis.

4.7. Optimization of the red light-induced, photocatalyzed synthesis of β-amino-α-diazo esters

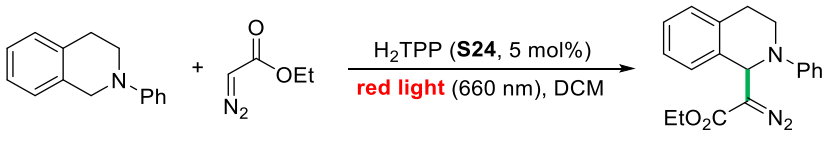

S18 **S27** **48**, 70%

Optimal reaction conditions: H_2TPP (**S24**, 5 mol%), 2-phenyl-1,2,3,4-tetrahydroisoquinoline (**S18**, 0.1 mmol), ethyl diazoacetate (**S27**, 0.3 mmol, 3 equiv.), DCM (c = 0.2 M), air atmosphere, red LEDs (660 nm, 3 W), 25 °C, 48 h.

Background reactions

entry	deviation from reaction conditions	yield of **48** [%][a]
1	O_2 balloon	22
2	no light	0
3	no H_2TPP (**S24**)	traces
4	no light, no H_2TPP (**S24**)	0

Reaction conditions: H_2TPP (**S24**, 1 mol%), tetrahydroisoquinoline **S18** (0.1 mmol), diazoalkane **S27** (0.3 mmol, 3 equiv.), DCM (c = 0.1 M), air atmosphere, red LEDs (660 nm, 3 W), 25 °C, 20 h. [a]yields determined by the ^1H NMR using 1,3,5-trimetoxybenzene as internal standard.

Catalyst screening

entry	catalyst	yield of **48** [%][a]
1	H_2TPP (**S24**)	22
2	H_2T(*p*-OMe)PP (**S32**)	38
3	H_2T(*p*-CF_3)PP (**S33**)	34
4	PPIX (**S36**)	23

Reaction conditions: *catalyst* (1 mol%), tetrahydroisoquinoline **S18** (0.1 mmol), diazoalkane **S27** (0.3 mmol, 3 equiv.), DCM (c = 0.1 M), air atmosphere, red LEDs (660 nm, 3 W), 25 °C, 20 h. [a]yields determined by the ^{1}H NMR using 1,3,5-trimetoxybenzene as internal standard.

Solvent screening

entry	solvent	yield of **48** [%][a]
1	DCM	22
2[b]	DCM	42
3	MeCN	37
4	DMF	17

Reaction conditions: H_2TPP (**S24**, 1 mol%), tetrahydroisoquinoline **S18** (0.1 mmol), diazoalkane **S27** (0.3 mmol, 3 equiv.), *solvent* (c = 0.1 M), air atmosphere, red LEDs (660 nm, 3 W), 25 °C, 20 h. [a]yields determined by the ^{1}H NMR using 1,3,5-trimetoxybenzene as internal standard. [b]c = 0.2 M.

Light intensity

entry	light intensity [W]	yield of **48** [%][a]
1	3 W	42
2[b]	3 W	63
3[b,c]	3 W	51
4[b,d]	3 W	77 (70)
5	25 W	38
6	40 W	40

Reaction conditions: H_2TPP (**S24**, 1 mol%), tetrahydroisoquinoline **S18** (0.1 mmol), diazoalkane **S27** (0.3 mmol, 3 equiv.), DCM (c = 0.2 M), air atmosphere, red LEDs (660 nm, 3 W), 25 °C, 20 h. [a]yields determined by the ^{1}H NMR using 1,3,5-trimetoxybenzene as internal standard, isolated yield in parenthesis. [b]48 h. [c]1.5 equiv. of **S27**. [d]5 mol% of catalyst **S24** added in 3 portions.

4.8. Optimization of the red light-induced, photocatalyzed synthesis of hydrazones

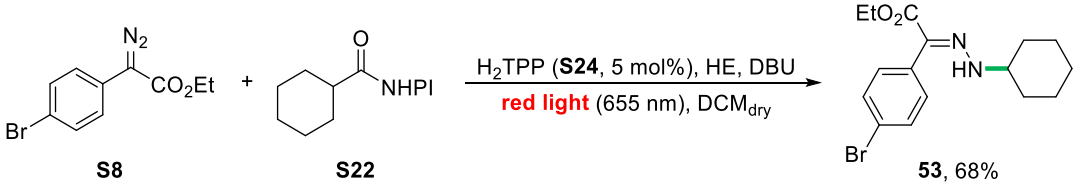

S8 **S22** **53**, 68%

Optimal reaction conditions: H_2TPP (**S24**, 5 mol%), ethyl 2-(4-bromophenyl)-2-diazoacetate (**S8**, 0.2 mmol), NHPI ester **S22** (0.3 mmol, 1.5 equiv.), Hantzsch ester (0.24 mmol, 1.2 equiv.), DBU (0.46 mmol, 2.3 equiv.), dry DCM (c = 0.1 M), Ar atmosphere, red LEDs (655 nm, 25 W), 25 °C, 18 h.

Background & Optimization

entry	deviation from reaction conditions	yield of **53** [%][a]
1	none	28
2	no light	0
3	no H_2TPP (**S24**)	0
4	no light, no H_2TPP (**S24**)	0
5	Rose Bengal instead of **S24**	24
6	reaction set in glove box*	66 (68)

Reaction conditions: H_2TPP (**S24**, 5 mol%), diazo compound **S8** (0.2 mmol), NHPI ester **S22** (0.3 mmol, 1.5 equiv.), Hantzsch ester (0.24 mmol, 1.2 equiv.), DBU (0.46 mmol, 2.3 equiv.), dry DCM (c = 0.1 M), Ar atmosphere, red LEDs (655 nm, 25 W), 25 ^{o}C, 18 h. [a] yields determined by the ^{1}H NMR using dibromomethane as internal standard, isolated yield in parenthesis. *entry 1-5: degassed with freeze-pump-thaw technique.

5. Mechanistic studies

5.1. Detection of $^1O_2$ - oxygen photosensitization by porphyrin catalyst

Porphyrins are known as efficient $^1O_2$ photosensitizers,[18-20] therefore when oxygen atmosphere is maintained in the reaction vial, $^1O_2$ is most likely generated by porphyrin catalyst in the excited state. Red light-induced, TPP-sensitized aryldiazoester indirect photolysis to carbenes is rather a slow process (see kinetics studies, section 5.2.), while the photooxygenation of arylodiazoesters is completed within 1 hour. Thus, the plausible mechanism assumes the aryldiazoester is attacked by generated $^1O_2$ and β-ketoester is formed upon the extrusion of N_2O, analogously to Wei's report.[21]

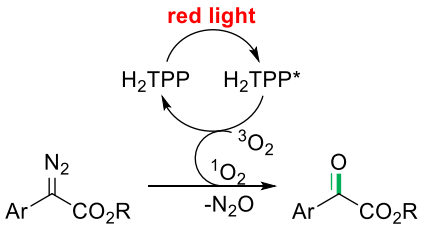

To confirm $^1O_2$ generation by H_2TPP sensitizer under red light irradiation, we performed an experiment with the addition of established $^1O_2$ probe, 1,3-diphenyl-1,3-dihydroisobenzofuran (**S39**).[22] The reaction was set up following the general oxygenation procedure (section 3.6.) on 0.1 mmol scale with the addition of probe **S39** (0.05 mmol, 14 mg). When diazo compound **S4** was irradiated with red light in the presence of H_2TPP (**S24**) and reagent **S39**, diminished yield of β-ketoester **24** was observed (33%). 56% of diazo ester **S4** remained unreacted and instead, 1,2-dibenzoylbenzene (**S41**) formed as a result of oxidation of probe **S39** followed by subsequent dehydratation of endoperoxide **S40** (detected by GC-MS analysis, Figure F4).

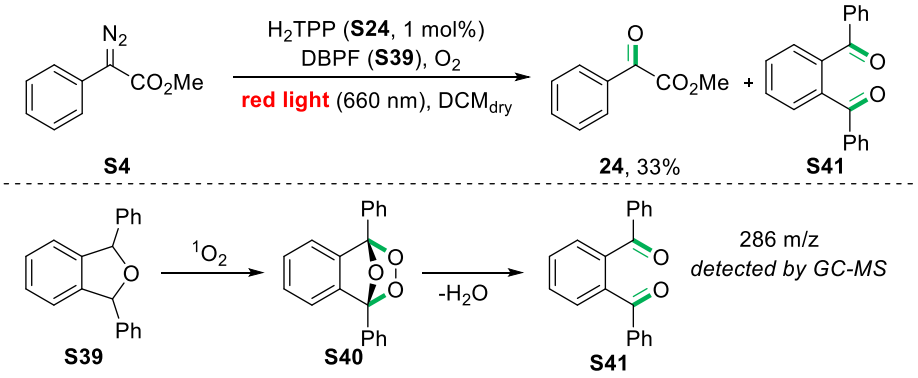

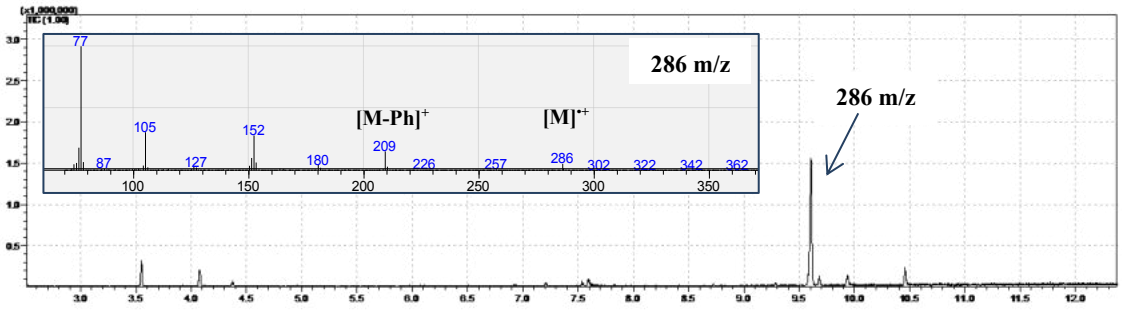

Figure F4. GC-MS chromatogram for the detection of product **S41** and the fragmentation of the 286 m/z peak.

5.2. Kinetic studies

Red light-induced, photosensitized oxygenation of aryldiazoesters

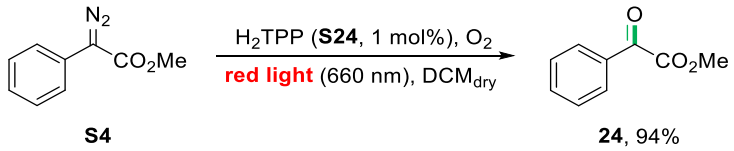

S4 **24**, 94%

The reaction was set up following the general photooxygenation procedure (section 3.3.) on 0.1 mmol scale with the addition of dodecane as an internal standard. The experiment was conducted for 1 h and the reaction progress over time was monitored with GC/FID. The kinetics studies reveal fast product **24** formation within ca. 30 min of irradiation (Charts C1).

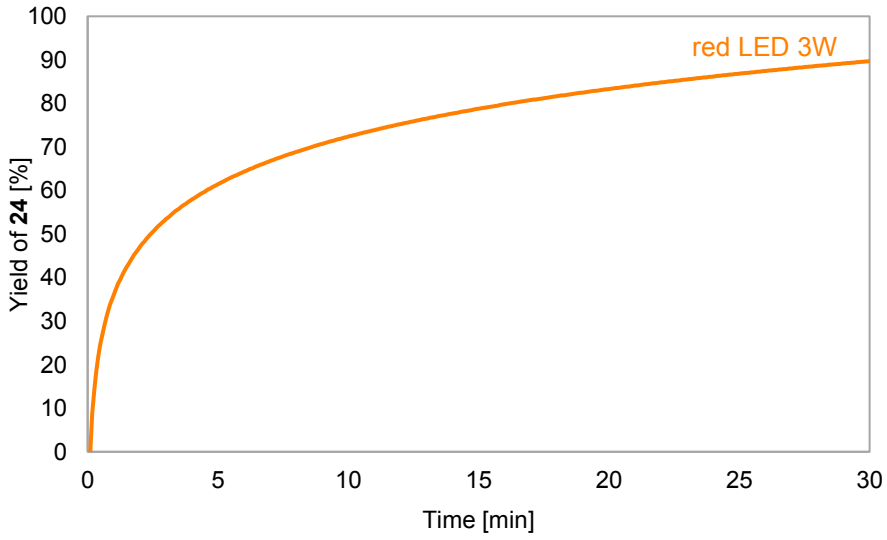

Chart C1. Kinetics of β-ketoester **24** formation.

Red light-induced, photosensitized cyclopropanation with aryldiazoesters

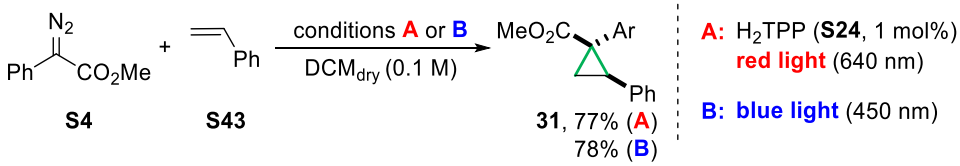

S4 **S43** **31**, 77% (**A**) 78% (**B**)

Two parallel experiments were performed to compare kinetics of TPP-sensitized red, light-mediated (conditions **A**) and catalyst-free, blue light-induced (conditions **B**) cyclopropanation reactions. Reaction A was set up following the general photosensitized cyclopropanation procedure (section 3.4.) on 0.1 mmol scale with the addition of dodecane as an internal standard. Reaction B was set up on 0.1 mmol scale without degassing reaction mixture with the addition of dodecane as an internal standard. The experiments were conducted for 18 h and the reaction progress over time was monitored with GC/FID. The kinetics studies reveal fast blue light-induced product **31** formation (78%) completed within 0.5 h of irradiation and slow photosensitized protocol yielding 77% of cyclopropane **31** within 18 h (Chart C2).

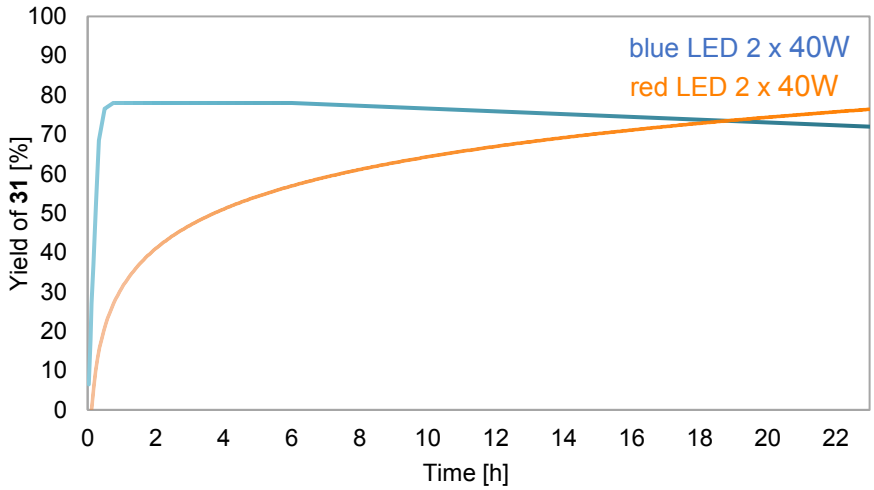

Chart C2. Kinetics of blue light and TPP-catalyzed, red light-induced cyclopropane **31** formation.

5.3. Competition between photooxygenation and cyclopropanation

Experiments on red light-induced, TPP-sensitized cyclopropanation revealed that depending on the oxygen concentration, photooxygenation of diazoalkane **S4** via $^1O_2$ to β-ketoester **24** competes with the cyclopropanation and results in decrease of yield of the desired product **31**. When oxygen-free conditions were maintained (entry 1), cyclopropane **31** formed exclusively in high yield (81%). On the other hand, even traces of oxygen diminished the cyclopropanation yield and side product **24** was observed. Reaction performed on air resulted in low reaction selectivity giving almost equal amounts of products **24** and **31**.

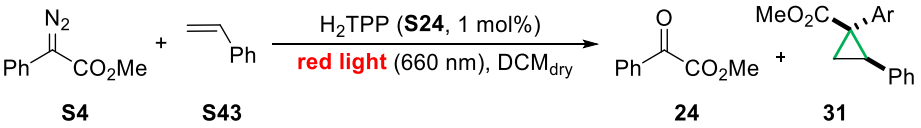

S4 **S43** **24** **31**

entry	oxygen access	yield of **24** [%][a]	yield of **31** [%][a]
1	set in glove box (<0.5 ppm O_2)	0	81
2	freeze-pump-thaw (Ar atmosphere)	14	58
3	air atmosphere	28	30

Reaction conditions: H_2TPP (**S24**, 5 mol%), diazoalkane **S4** (0.1 mmol), olefin **S43** (1.0 mmol, 10 equiv.), dry DCM (c = 0.1 M), red LEDs (660 nm, 3 W), T = 25 °C, 18 h. [a]GC yield.

6. Characterization of synthesized compounds

6.1. Photochemical O-H Insertion of diaryldiazoalkanes with alcohols

1-[bis(methoxyphenyl)methyl] benzyl ether (1)[23]

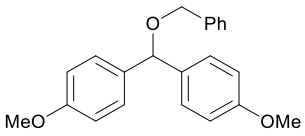

Synthesized according to the general procedure (section 3.3.).
Yield: 56 mg (84%), obtained as colorless oil from flash column chromatography using hexanes/AcOEt eluent system.
^{1}H NMR (500 MHz, $CDCl_3$): δ = 7.37 – 7.32 (m, 4H), 7.29 – 7.24 (m, 5H), 6.87 – 6.84 (m, 4H), 5.36 (s, 1H), 4.51 (s, 2H), 3.78 (s, 6H) ppm. **^{13}C NMR** (126 MHz, $CDCl_3$): δ = 158.9, 138.6, 134.6, 128.3, 127.7, 127.4, 113.7, 81.5, 70.2, 55.3 ppm.

4,4'-(phenethoxymethylene)bis(methoxybenzene) (2)

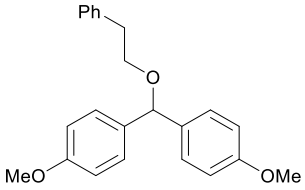

Synthesized according to the general procedure (section 3.3.).
Yield: 63 mg (90%), obtained as colorless oil from flash column chromatography using hexanes/AcOEt eluent system.
^{1}H NMR (600 MHz, $CDCl_3$): δ = 7.28 – 7.23 (m, 2H), 7.21 – 7.16 (m, 7H), 6.83 – 6.80 (m, 4H), 5.26 (s, 1H), 3.76 (s, 6H), 3.63 (t, J = 7.1 Hz, 2H), 2,94 (t, J = 7.1 Hz, 2H) ppm. **^{13}C NMR** (151 MHz, $CDCl_3$): δ = 158.8, 139.2, 134.8, 129.0, 128.2, 128.1, 126.1, 113.7, 82.8, 69.8, 55.2, 36.5 ppm; **HRMS** (EI): m/z calcd for $C_{23}H_{24}O_3^{\bullet+}$: 348.1725 $[M]^{\bullet+}$; found: 348.1738; **elemental analysis** calcd (%) for $C_{23}H_{24}O_3$: C 79.28, H 6.94; found: C 79.24, H 6.98.

4,4'-((hexyloxy)methylene)bis(methoxybenzene) (3)

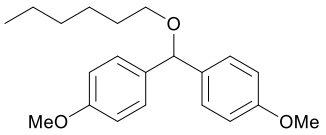

Synthesized according to the general procedure (section 3.3.).
Yield: 54 mg (82%), obtained as colorless oil from flash column chromatography using hexanes/AcOEt eluent system.
^{1}H NMR (600 MHz, $CDCl_3$): δ = 7.24 (m, 4H), 6.85 (m, 4H), 5,25 (s, 1H), 3.78 (s, 6H), 3.41 (t, J = 6.6 Hz, 2H), 1.65 – 1.60 (m, 2H), 1.40 – 1.35 (m, 2H), 1.34 – 1.24 (m, 4H), 0.88 (t, J = 7.1 Hz, 3H) ppm. **^{13}C NMR** (151 MHz, $CDCl_3$): δ = 158.7, 135.1, 128.1, 113.6, 82.6, 69.0, 55.2, 31.7, 29.9, 25.9, 22.6, 14.1 ppm; **HRMS** (EI): m/z calcd for $C_{21}H_{28}O_3^{\bullet+}$: 328.2038 $[M]^{\bullet+}$; found: 328.2029; **elemental analysis** calcd (%) for $C_{21}H_{28}O_3$: C 76.79, H 8.59; found: C 76.56, H 8.63.

4,4'-(((3,7-dimethyloct-6-en-1-yl)oxy)methylene)bis(methoxybenzene) (4)

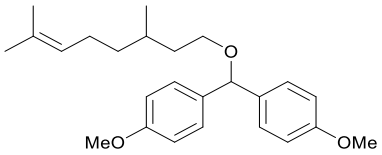

Synthesized according to the general procedure (section 3.3.).
Yield: 65 mg (85%), obtained as white solid from flash column chromatography using hexanes/AcOEt eluent system.
^{1}H NMR (600 MHz, $CDCl_3$): δ = 7.24 – 7.22 (m, 4H), 6.85 – 6.83 (m, 4H), 5.24 (s, 1H), 5.10 – 5.07 (m, 1H), 3.78 (m, 6H), 3.47 – 3.40 (m, 2H), 2.03 – 1.90 (m, 2H), 1.70 – 1.65 (m, 4H), 1.64 – 1.59 (m, 4H), 1.47 – 1.41 (m, 1H), 1.35 – 1.29 (m, 1H), 1.16 – 1.10 (m, 1H), 0.86 (d, *J* = 6.6 Hz, 3H) ppm. **^{13}C NMR** (151 MHz, $CDCl_3$): δ = 158.7, 135.1, 131.0, 128.1, 124.9, 113.6, 82.7, 67.2, 55.2, 37.1, 36.9, 29.6, 25.7, 25.5, 19.6, 17.6 ppm; **HRMS** (ESI): m/z calcd for $C_{25}H_{34}O_3$+Na^+: 405.2406 $[M+Na]^+$; found: 405.2412; **elemental analysis** calcd (%) for $C_{25}H_{34}O_3$: C 78.49, H 8.96; found: C 78.23, H 8.97.

4,4'-((prop-2-yn-1-yloxy)methylene)bis(methoxybenzene) (5)

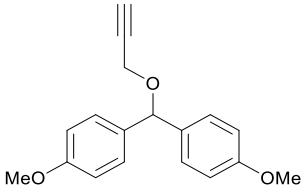

Synthesized according to the general procedure (section 3.3.).
Yield: 40 mg (71%), obtained as colorless oil from flash column chromatography using hexanes/AcOEt eluent system.
^{1}H NMR (600 MHz, $CDCl_3$): δ = 7.26 – 7.24 (m, 4H), 6.87 – 6.84 (m, 4H), 5.58 (s, 1H), 4.11 (d, *J* = 2.4 Hz, 2H), 3.78 (s, 6H), 2.44 (t, *J* = 2.4 Hz, 1H) ppm. **^{13}C NMR** (151 MHz, $CDCl_3$): δ = 159.0, 133.5, 128.5, 113.8, 80.8, 79.9, 74.4, 55.5, 55.2 ppm; **HRMS** (ESI): m/z calcd for $C_{18}H_{18}O_3$+Na^+: 305.1154 $[M+Na]^+$; found: 305.1154; **elemental analysis** calcd (%) for $C_{18}H_{18}O_3$: C 76,57, H 6,43; found: C 76,56, H 6,54.

4,4'-(phenoxymethylene)bis(methoxybenzene) (6)

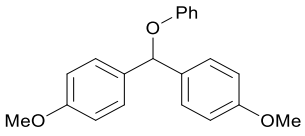

Synthesized according to the general procedure (section 3.3.).
Yield: 46 mg (72%), obtained as white solid from flash column chromatography using hexanes/AcOEt eluent system.
^{1}H NMR (600 MHz, $CDCl_3$): δ = 7.31 – 7.28 (m, 4H), 7.22 – 7.18 (m, 2H), 6.94 – 6.92 (m, 2H), 6.90 – 6.85 (m, 5H), 6.14 (s, 1H), 3.77 (s, 6H) ppm. **^{13}C NMR** (151 MHz, $CDCl_3$): δ = 159.0, 158.2, 133.7, 129.3, 128.2, 120.8, 116.1, 113.9, 80.9, 55.2 ppm; **HRMS** (APCI): m/z calcd for $C_{21}H_{19}O_3^{\bullet-}$: 319.1334 $[M]^{\bullet-}$; found: 319.1335; **elemental analysis** calcd (%) for $C_{21}H_{20}O_3$: C 78,73, H 6,29; found: C 78,49, H 6,35.

4,4'-((cyclohexyloxy)methylene)bis(methoxybenzene) (7)

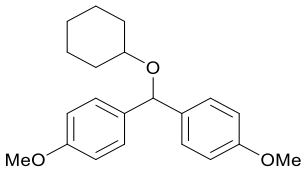

Synthesized according to the general procedure (section 3.3.).
Yield: 43 mg (66%), obtained as colorless oil from flash column chromatography using hexanes/AcOEt eluent system.
^{1}H NMR (600 MHz, $CDCl_3$): δ = 7.25 (d, *J* = 8.7 Hz, 4H), 6.86 (d, *J* = 8.7 Hz, 4H), 5.48 (s, 1H), 3.79 (s, 6H), 3.37 – 3.31 (m, 1H), 1.93 – 1.90 (m, 2H), 1.76 – 1.74 (m, 2H), 1.54 – 1.49 (m, 1H), 1.46 – 1.40 (m, 2H), 1.28 – 1.18 (m, 3H) ppm. **^{13}C NMR** (151 MHz, $CDCl_3$): δ = 158.7, 135.6, 128.3, 113.6, 79.0, 74.7, 55.2, 32.4, 25.9, 24.2 ppm; **HRMS** (EI): m/z calcd for $C_{21}H_{26}O_3^{\bullet+}$: 326.1882 $[M]^{\bullet+}$; found: 326.1891; **elemental analysis** calcd (%) for $C_{21}H_{26}O_3$: C 77,27, H 8,03; found: C 77,36, H 8,02.

1-(tert-butyl) 2-methyl 4-(bis(4-methoxyphenyl)methoxy)pyrrolidine-1,2-dicarboxylate (8)

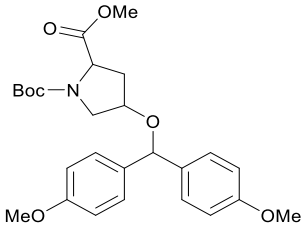

Synthesized according to the general procedure using 2.0 eq. of diazo compound and 2 mL of MeCN (section 3.3.). Product isolated as a mixture of diastereoisomers by silica gel column chromatography.
Yield: 53 mg (56%, d.r. 3:2), obtained as colorless oil from flash column chromatography using hexanes/AcOEt eluent system.
^{1}H NMR (600 MHz, $CDCl_3$): δ = 7.22 – 7.16 (m, 4H), 6.87 – 6.82 (m, 4H), 5.33 – 5,31 (m, 1H), 4.48 – 4.37 (m, 1H), 4.18 – 4.13 (m, 1H), 3.79 – 3.77 (m, 6H), 3.72 – 3.70 (m, 4H), 3.56 – 3.53 (m, 1H), 2.42 – 2.34 (m, 1H), 2.03 – 1.98 (m, 1H), 1.44 – 1.41 (m, 9H) ppm. **^{13}C NMR** (151 MHz, $CDCl_3$): δ = 173.6, 173.4, 159.1, 159.0, 154.4, 153.8, 134.2, 134.1, 133.9, 128.4, 128.3, 128.2, 113.8, 113.8, 113.77, 81.0, 80.9, 80.1, 80.1, 75.1, 74.1, 58.1, 57.7, 55.2, 52.1, 52.0, 51.6, 36.9, 35.9, 28.4, 28.2 ppm; **HRMS** (ESI): m/z calcd for $C_{23}H_{33}NO_7$+Na^+: 494.2155 $[M+Na]^+$; found: 494.2159; **elemental analysis** calcd (%) for $C_{26}H_{33}NO_7$: C 66.23, H 7.05, N 2.97; found: C 66.38, H 7.07, N 3.09.

(8S,9S,10R,13R,14S,17R)-3-(bis(4-methoxyphenyl)methoxy)-10,13-dimethyl-17-((R)-6-methyl heptan-2-yl)-2,3,4,7,8,9,10,11,12,13,14,15,16,17-tetradecahydro-1H-cyclopenta[a]phenanthrene (9)

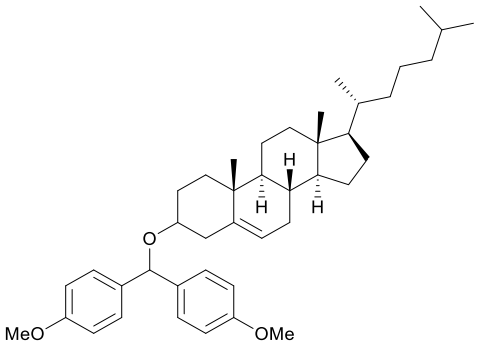

Synthesized according to the general procedure on 0.1 mmol scale using 5.0 eq. of diazo compound and 3 mL of MeCN (section 3.3.).
Yield: 59 mg (96%), obtained as white solid from flash column chromatography using hexanes/MTBE eluent system.
^{1}H NMR (600 MHz, $CDCl_3$): δ = 7.24 – 7.22 (m, 4H), 6.84 – 6.83 (m, 4H), 5.48 (s, 1H), 5.29 (d, *J* = 5.3 Hz, 1H), 3.77 (s, 6H), 3.27 – 3.22 (m, 1H), 2.39 – 2.31 (m, 2H), 2.00 – 1.90 (m, 3H), 1.84 – 1.78 (m, 2H), 1.61 – 1.31 (m, 11H), 1.27 – 1.21 (m, 1H), 1.17 – 1.01 (m, 6H), 1.01 – 0.92 (m, 6H), 0.90 (d, *J* = 6.5 Hz, 3H), 0.86 (dd, *J* = 6.6, 2.7 Hz, 6H), 0.66 (s, 3H) ppm. **^{13}C NMR** (151 MHz, $CDCl_3$): δ = 158,7, 141,1, 135,4, 128,2, 121,4, 113,7, 79,4, 76,6, 56,8, 56,1, 55,2, 50,2, 42,3, 39,8, 39,5, 39,4, 37,2, 36,9, 36,2, 35,8, 31,9, 31,9, 28,6, 28,2, 28,0, 24,3, 23,8, 22,8, 22,6, 21,0, 19,4, 18,7, 11,8 ppm; **HRMS** (ESI): m/z calcd for $C_{42}H_{60}O_3$+Na^+: 635.4440 $[M+Na]^+$; found: 635.4448; **elemental analysis** calcd (%) for $C_{42}H_{60}O_3$: C 82.30, H 9.87; found: C 82.24, H 9.89.

4,4'-(tert-butoxymethylene)bis(methoxybenzene) (10)

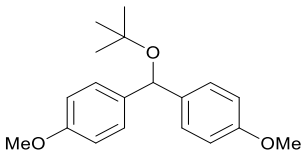

Synthesized according to the general procedure (section 3.3.).
Yield: 46 mg (77%), obtained as colorless oil from flash column chromatography using hexanes/AcOEt eluent system.
^{1}H NMR (600 MHz, $CDCl_3$): δ = 7.22 (d, *J* = 8.7 Hz, 4H), 6.81 (d, *J* = 8.7 Hz, 4H), 5.51 (s, 1H), 3.76 (s, 6H), 1.21 (s, 9H) ppm. **^{13}C NMR** (151 MHz, $CDCl_3$): δ = 158.3, 137.6, 128.0, 113.5, 74.8, 74.7, 55.2, 28.8 ppm; **HRMS** (EI): m/z calcd for $C_{42}H_{60}O_3^{\bullet+}$: 300.1725 $[M]^{\bullet+}$; found: 300.1722; **elemental analysis** calcd (%) for $C_{19}H_{24}O_3$: C 75.97, H 8.05; found: C 76.00, H 8.09.

4,4'-((benzyloxy)methylene)bis(N,N-dimethylaniline) (11)

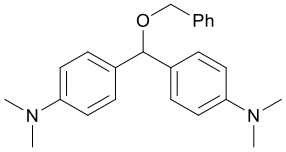

Synthesized according to the general procedure (section 3.3.).
Yield: 32 mg (45%), obtained as blue solid from flash column chromatography using hexanes/acetone eluent system.
^{1}H NMR (600 MHz, $CDCl_3$): δ = 7.38 – 7.36 (m, 2H), 7.34 – 7.31 (m, 2H), 7.27 – 7.21 (m, 5H), 6.70 – 6.68 (m, 4H), 5.31 (s, 1H), 4.51 (s, 2H), 2.91 (s, 12H) ppm. **^{13}C NMR** (151 MHz, $CDCl_3$): δ = 149.9, 139.1, 130.7, 128.2, 128.1, 127.7, 127.2, 112.4, 81.9, 70.0, 40.7 ppm; **HRMS** (ESI): m/z calcd for $C_{24}H_{29}N_2O^+$: 361.2280 $[M+H]^+$; found: 362.2286; **elemental analysis** calcd (%) for $C_{24}H_{28}N_2O$: C 79.96, H 7.83, N 7.77; found: C 79.74, H 7.87, N 7.98.

6.2. Photochemical N-H Insertion of diaryldiazoalkanes with alcohols

N-(bis(4-methoxyphenyl)methyl)octan-1-amine (12)

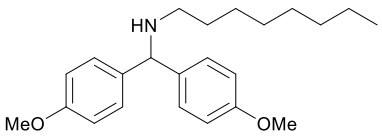

Synthesized according to the general procedure (section 3.4.).
Yield: 51 mg (72%), obtained as colorless oil from flash column chromatography using hexanes/Et_3N eluent system.
^{1}H NMR (600 MHz, $CDCl_3$): δ = 7.28 (d, *J* = 8.2 Hz, 4H), 6.82 (d, *J* = 8.2 Hz, 4H), 4.72 (s, 1H), 3.76 (s, 6H), 2.53 (t, *J* = 7.0 Hz, 2H), 1.52 – 1.46 (m, 2H), 1.40 (bs, 1H), 1.31 – 1 .25 (m, 10H), 0.87 (t, *J* = 7.0 Hz, 3H) ppm. **^{13}C NMR** (151 MHz, $CDCl_3$): δ = 158.4, 137.0, 128.2, 113.8, 66.3, 55.2, 48.3, 31.8, 30.3, 29.5, 29.3, 27.4, 22.6, 14.1 ppm; **HRMS** (EI): m/z calcd for $C_{23}H_{33}NO_2^{\bullet+}$: 355.2511 $[M]^{\bullet+}$; found: 355.2508; **elemental analysis** calcd (%) for $C_{23}H_{33}NO_2$: C 77.70, H 9.36, N 3.94; found: C 77.65, H 9.17, N 4.11.

(S)-N-(bis(4-methoxyphenyl)methyl)-1-phenylethan-1-amine (13)

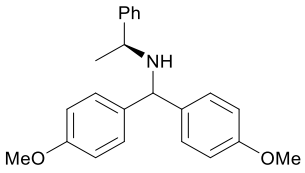

Synthesized according to the general procedure (section 3.4.) using 3 eq. of diazo compound.
Yield: 39 mg (56%), obtained as yellow oil from flash column chromatography using hexanes/Et_3N eluent system.
^{1}H NMR (600 MHz, $CDCl_3$): δ = 7.34 – 7.31 (m, 2H), 7.25 – 7.21 (m, 5H), 7.18 – 7.16 (m, 2H), 6.86 – 6.84 (m, 2H), 6.78 – 6.77 (m, 2H), 4.53 (s, 1H), 3.79 (s, 3H), 3.74 (s, 3H), 3.65 (q, *J* = 6.7 Hz, 1H), 1.75 (bs, 1H), 1.35 (d, *J* = 6.7 Hz, 3H) ppm. **^{13}C NMR** (151 MHz, $CDCl_3$): δ = 158.5, 158.4, 145.7, 137.3, 136.0, 128.5, 128.4, 128.3, 126.8, 126.7, 113.8, 113.7, 62.4, 55.2, 55.1, 24.4 ppm; **HRMS** (EI): m/z calcd for $C_{23}H_{25}NO_2^{\bullet+}$: 347.1885 $[M]^{\bullet+}$; found: 347.1886; **elemental analysis** calcd (%) for $C_{23}H_{25}NO_2$: C 79.51, H 7.25, N 4.03; found: C 79.54, H 7.20, N 3.91.

N-benzyl-1,1-bis(4-methoxyphenyl)-N-methylmethanamine (14)[24]

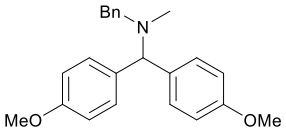

Synthesized according to the general procedure (section 3.4.).
Yield: 39 mg (65%), obtained as colorless oil from flash column chromatography using hexanes/acetone eluent system.
^{1}H NMR (600 MHz, $CDCl_3$): δ = 7.42 – 7.39 (m, 6H), 7.35 – 7.31 (m, 2H), 7.26 – 7.23 (m, 1H), 6.87 – 6.85 (m, 4H), 4.42 (s, 1H), 3.78 (s, 6H), 3.49 (s, 2H), 2.06 (s, 3H) ppm. **^{13}C NMR** (151 MHz, $CDCl_3$): δ = 158.4, 140.1, 135.4, 129.0, 128.6, 128.2, 126.7, 113.8, 73.8, 59.6, 55.2, 40.1 ppm.

1-[bis(methoxyphenyl)methyl]pyrrolidine (15)[25]

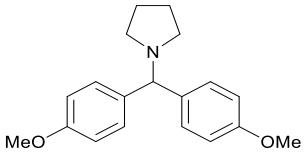

Synthesized according to the general procedure (section 3.4.).
Yield: 50 mg (84%), obtained as colorless oil from flash column chromatography using hexanes/acetone eluent system.
^{1}H NMR (600 MHz, $CDCl_3$): δ = 7.35 – 7.32 (m, 4H), 6.81 – 6.78 (m, 4H), 4.07(s, 1H), 3.75 (s, 6H), 2.40 (bs, 4H), 1.76 (bs, 4H) ppm. **^{13}C NMR** (151 MHz, $CDCl_3$): δ = 158.3, 137.0, 128.3, 113.7, 75.0, 55.2, 53.7, 23.5 ppm.

N-(bis(4-methoxyphenyl)methyl)aniline (16)[24]

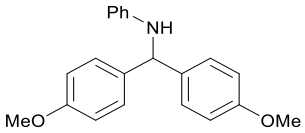

Synthesized according to the general procedure (section 3.4.).
Yield: 38 mg (59%), obtained as colorless oil from flash column chromatography using hexanes/THF eluent system.
^{1}H NMR (600 MHz, $CDCl_3$): δ = 7.25 – 7.23 (m, 5H), 7.12 – 7.09 (m, 2H), 6.86 – 6.84 (m, 4H), 6.69 – 6.66 (m, 1H), 6.54 – 6.52 (m, 2H), 5.41 (s, 1H), 4.15 (bs, 1H), 3.78 (s, 6H) ppm. **^{13}C NMR** (151 MHz, $CDCl_3$): δ = 158.7, 147.4, 135.4, 129.1, 128.5, 117.5, 114.0, 113.4, 61.7, 55.3 ppm.

1-(bis(4-methoxyphenyl)methyl)indoline (17)

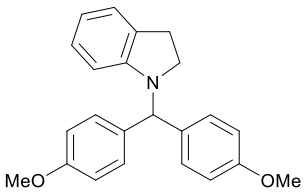

Synthesized according to the general procedure (section 3.4.).
Yield: 39 mg (57%), obtained as off-white solid from flash column chromatography using hexanes/THF eluent system.
^{1}H NMR (600 MHz, $CDCl_3$): δ = 7.24 – 7.22 (m, 4H), 7.06 – 7.04 (m, 1H), 6.93 – 6.89 (m, 1H), 6.85 – 6.83 (m, 4H), 6.62 – 6.59 (m, 1H), 6.19 – 6.18 (m, 1H), 5.45 (s, 1H), 3.78 (s, 6H), 3.17 (t, J = 8.3 Hz, 2H), 2.91 (t, J = 8.3 Hz, 2H) ppm. **^{13}C NMR** (151 MHz, $CDCl_3$): δ = 158.6, 152.0, 133.7, 130.4, 129.5, 127.1, 124.2, 117.3, 113.7, 108.1, 65.3, 55.2, 51.3, 28.3 ppm; **HRMS** (EI): m/z calcd for $C_{23}H_{23}NO_2^{\bullet+}$: 345.1729 $[M]^{\bullet+}$; found: 345.1730; **elemental analysis** calcd (%) for $C_{23}H_{23}NO_2$: C 79.97, H 6.71, N 4.05; found: C 79.97, H 6.73, N 3.93.

1-(bis(4-methoxyphenyl)methyl)pyridin-2(1H)-one (18)

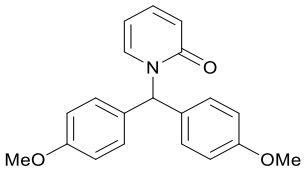

Synthesized according to the general procedure for O-H insertion (section 3.3.). Crude NMR of reaction mixture reveals formation of both N-H and O-H insertion products (1:1.6 ratio) but the ether product converts to amine **18** on silica gel at the purification step.
Yield: 37 mg (58%), obtained as white solid from flash column chromatography using hexanes/acetone eluent system.
^{1}H NMR (600 MHz, $CDCl_3$): δ = 7.39 (s, 1H), 7.30 (ddd, *J* = 8.9, 6.5, 2.0 Hz, 1H), 7.15 (ddd, *J* = 7.0, 2.1, 0.7 Hz, 1H), 7.07 – 7.04 (m, 4H), 6.88 – 6.86 (m, 4H), 6.60 (ddd, *J* = 9.1, 1.5, 0.7 Hz, 1H), 6.10 (td, *J* = 6.8, 1.4 Hz, 1H), 3.79 (s, 6H) ppm. **^{13}C NMR** (151 MHz, $CDCl_3$): δ = 162.5, 159.2, 138.9, 135.8, 131.1, 129.9, 120.8, 114.1, 105.6, 61.0, 55.3; **HRMS** (ESI): m/z calcd for $C_{20}H_{19}NO_3Na^+$: 344.1263 $[M+Na]^+$; found: 344.1264; **elemental analysis** calcd (%) for $C_{20}H_{19}NO_3$: C 74.75, H 5.96, N 4.36; found: C 74.76, H 5.87, N 4.49.

6.3. Photochemical S-H Insertion of diaryldiazoalkanes with alcohols

benzyl(bis(4-methoxyphenyl)methyl)sulfane (19)[26]

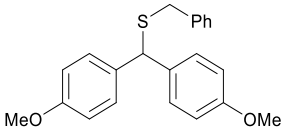

Synthesized according to the general procedure (section 3.5.).
Yield: 62 mg (89%), obtained as white solid from flash column chromatography using hexanes/acetone eluent system.
^{1}H NMR (600 MHz, $CDCl_3$): δ = 7.30 – 7.26 (m, 6H), 7.24 – 7.20 (m, 3H), 6.84 – 6.82 (m, 4H), 4.87 (s, 1H), 3.77 (s, 6H), 3.52 (s, 2H) ppm. **^{13}C NMR** (151 MHz, $CDCl_3$): δ = 158.6, 138.1, 133.4, 129.4, 129.0, 128.4, 126.9, 113.9, 55.2, 51.9, 36.6 ppm.

(bis(4-methoxyphenyl)methyl)(phenyl)sulfane (20)[24]

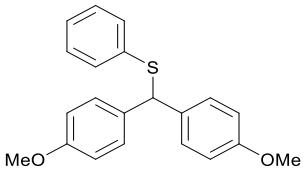

Synthesized according to the general procedure (section 3.5.).
Yield: 58 mg (86%), obtained as yellow solid from flash column chromatography using hexanes/Et_2O eluent system.
^{1}H NMR (600 MHz, $CDCl_3$): δ = 7.31 (d, *J* = 8.7 Hz, 4H), 7.22 – 7.20 (m, 2H), 7.18 – 7.15 (m, 2H), 7.13 – 7.10 (m, 1H), 6.82 (d, *J* = 8.7 Hz, 4H), 5.48 (s, 1H), 3.77 (s, 6H) ppm. **^{13}C NMR** (151 MHz, $CDCl_3$): δ = 158.7, 136.5, 133.4, 130.3, 129.4, 128.7, 126.3, 113.9, 56.1, 55.2 ppm.

adamantan-1-yl(bis(4-methoxyphenyl)methyl)sulfane (21)

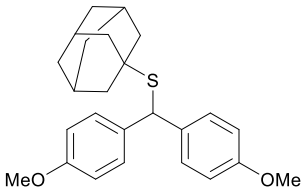

Synthesized according to the general procedure (section 3.5.).
Yield: 69 mg (88%), obtained as white solid from flash column chromatography using hexanes/AcOEt eluent system.
^{1}H NMR (600 MHz, $CDCl_3$): δ = 7.33 – 7.30 (m, 4H), 6.82 – 6.79 (m, 4H), 5.23 (s, 1H), 3.76 (s, 6H), 1.96 (bs, 3H), 1.81 (m, 6H), 1.65 – 1.58 (m, 6H) ppm. **^{13}C NMR** (151 MHz, $CDCl_3$): δ = 158.2, 136.0, 129.3, 113.7, 55.2, 48.2, 46.8, 43.9, 36.3, 29.8 ppm; **HRMS** (ESI): m/z calcd for $C_{25}H_{30}O_2SNa^+$: 417.1864 $[M+Na]^+$; found: 417.1861; **elemental analysis** calcd (%) for $C_{25}H_{30}O_2S$: 76.10, H 7.66, S 8.13; found: C 75.99 H 7.63, S 7.96.

9-(benzylthio)-9H-thioxanthene (22)

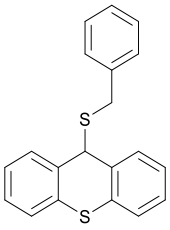

Synthesized according to the general procedure (section 3.5.) on 0.2 mmol scale using 4.0 eq. of benzyl mercaptan.
Yield: 24 mg (38%), obtained as white solid from flash column chromatography using hexanes/toluene eluent system.
^{1}H NMR (600 MHz, $CDCl_3$): δ = 7.45 – 7.43 (m, 2H), 7.38 – 7.32 (m, 4H), 7.27 – 7.19 (m, 7H), 5.12 (s, 1H), 3.54 (s, 2H) ppm. **^{13}C NMR** (151 MHz, $CDCl_3$): δ = 137.7, 133.7, 133.4, 129.0, 128.8, 128.5, 127.4, 127.2, 127.0, 126.3, 50.1, 36.2 ppm; **HRMS** (ESI): m/z calcd for $C_{20}H_{16}S_2Na^+$: 343.0591 $[M+Na]^+$; found: 343.0594.

methyl N,S-bis(bis(4-methoxyphenyl)methyl)-N-(tert-butoxycarbonyl)-L-cysteinate (23)

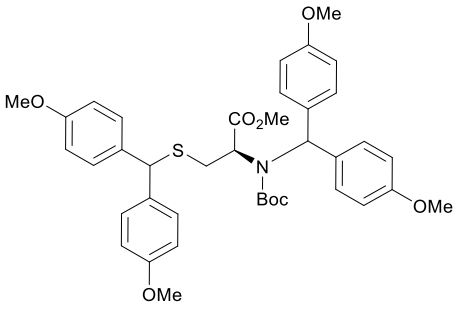

Synthesized according to the general procedure (section 3.5.) on 0.2 mmol scale using 2.0 eq. of diazo compound and 2 mL of dry DCM.
Yield: 66 mg (45%), obtained as white solid from flash column chromatography using hexanes/AcOEt eluent system.

^{1}H NMR (600 MHz, $CDCl_3$): δ = 7.27 – 7.24 (m, 4H), 7.20 – 7.16 (m, 4H), 6.85 – 6.78 (m, 8H), 6.01 (bs, 1H), 4.83 (s, 1H), 4.05 (bs, 1H), 3.81 (s, 3H), 3.79 (s, 3H), 3.78 (s, 3H), 3.75 (s, 3H), 3.64 (bs, 3H), 3.14 (dd, J = 13.6, 8.1 Hz, 1H), 2.40 (bs, 1H), 1.26 (bs, 9H) ppm. **^{13}C NMR** (151 MHz, $CDCl_3$): δ = 171.4, 158.7, 158.7, 158.5, 133.9, 133.6, 130.1, 129.4, 129.3, 113.8, 113.8, 113.7, 113.5, 81.0, 64.5, 59.5, 55.2, 55.2, 55.2, 53.6, 52.1, 28.11 ppm; **HRMS** (ESI): m/z calcd for $C_{39}H_{45}NO_8SNa^+$: 710.2764 $[M+Na]^+$; found: 710.2756; **elemental analysis** calcd (%) for $C_{39}H_{45}NO_8S$: C 68.10, H 6.59, N 2.04, S, 4.66; found: C 67.98, H 6.62, N 2.16, S 4.90.

6.4. Photosensitized oxygenation of aryldiazoesters

methyl 2-oxo-2-phenylacetate (24)[21]

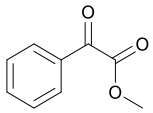

Synthesized according to the general procedure (section 3.6.).
Yield: 15 mg (94%), obtained as white solid from flash column chromatography using hexanes/AcOEt eluent system.
^{1}H NMR (600 MHz, $CDCl_3$): δ = 8.02 (d, *J* = 8.0 Hz, 2H), 7.67 (t, *J* = 7.4 Hz, 1H), 7.52 (t, *J* = 7.7 Hz, 2H), 3.99 (s, 3H) ppm. **^{13}C NMR** (151 MHz, $CDCl_3$): δ = 186.0, 135.0, 132.5, 130.1, 128.9, 52.8 ppm.

methyl 4-methoxybenzoate (25)[21]

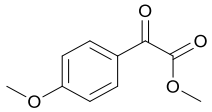

Synthesized according to the general procedure (section 3.6.).
Yield: 14 mg (70%), obtained as white solid from flash column chromatography using hexanes/AcOEt eluent system.
^{1}H NMR (600 MHz, $CDCl_3$): δ = 8.05 – 7.96 (m, 2H), 7.01 – 6.93 (m, 2H), 3.96 (s, 3H), 3.90 (s, 3H) ppm. **^{13}C NMR** (151 MHz, $CDCl_3$): δ = 184.4, 165.1, 164.3, 132.7, 125.5, 114.2, 55.6, 52.6 ppm.

methyl 2-(4-cyanophenyl)-2-oxoacetate (26)[21]

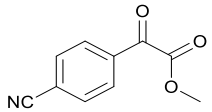

Synthesized according to the general procedure (section 3.6.).
Yield: 8 mg (40%), obtained as white solid from flash column chromatography using hexanes/AcOEt eluent system.
^{1}H NMR (600 MHz, $CDCl_3$): δ = 8.17 (d, *J* = 8.6 Hz, 2H), 7.81 (d, *J* = 8.6 Hz, 2H), 4.00 (s, 3H) ppm.
^{13}C NMR (151 MHz, $CDCl_3$): δ = 184.0, 162.6, 135.5, 132.6, 130.5, 118.0, 117.5, 53.2 ppm.

6.5. Photosensitized O-H insertion of aryldiazoesters with carboxylic acids

2-methoxy-2-oxo-1-phenylethyl benzoate (27)[27]

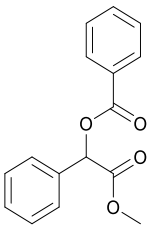

Synthesized according to the general procedure (section 3.7.).
Yield: 23 mg (84%), obtained as off-white solid from flash column chromatography using hexanes/AcOEt eluent system.
^{1}H NMR (600 MHz, $CDCl_3$): δ = 8.16 – 8.10 (m, 2H), 7.59 (d, *J* = 7.0 Hz, 3H), 7.44 (dt, *J* = 17.9, 6.9 Hz, 5H), 6.18 (s, 1H), 3.76 (s, 3H) ppm. **^{13}C NMR** (151 MHz, $CDCl_3$): δ = 169.3, 165.9, 134.0, 133.5, 130, 129.3, 129.3, 128.9, 128.4, 127.6, 74.9, 52.6 ppm.

2-methoxy-1-(4-methoxyphenyl)-2-oxoethyl benzoate (28)[28]

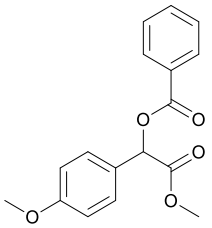

Synthesized according to the general procedure (section 3.7.).
Yield: 15 mg (50%), obtained as off-white solid from flash column chromatography using hexanes/AcOEt eluent system.
^{1}H NMR (600 MHz, $CDCl_3$): δ = 8.12 (d, *J* = 7.5 Hz, 2H), 7.58 (t, *J* = 7.2 Hz, 1H), 7.50 (d, *J* = 8.6 Hz, 2H), 7.45 (t, *J* = 7.7 Hz, 2H), 6.95 (d, *J* = 8.5 Hz, 2H), 6.12 (s, 1H), 3.83 (s, 3H), 3.75 (s, 3H) ppm. **^{13}C NMR** (151 MHz, $CDCl_3$): δ = 169.5, 165.9, 160.4, 133.4, 129.9, 129.3, 129.1, 128.4, 126.1, 114.3, 74.5, 55.3, 52.6. ppm.

1-(4-bromophenyl)-2-ethoxy-2-oxoethyl benzoate (29)[27]

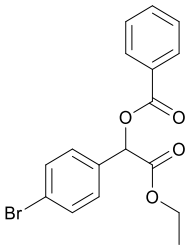

Synthesized according to the general procedure (section 3.7.).
Yield: 15 mg (42%), obtained as colorless oil from flash column chromatography using hexanes/AcOEt eluent system.

^{1}H NMR (600 MHz, $CDCl_3$): δ = 8.11 (d, *J* = 7.1 Hz, 2H), 7.64 – 7.52 (m, 3H), 7.47 (dt, *J* = 7.4, 3.5 Hz, 4H), 6.11 (s, 1H), 4.30 – 4.15 (m, 2H), 1.24 (t, *J* = 7.1 Hz, 3H) ppm. **^{13}C NMR** (151 MHz, $CDCl_3$): δ = 168.3, 165.7, 133.5, 133.2, 132.0, 129.9, 129.2, 129.1, 128.5, 123.4, 74.3, 61.5, 14.0 ppm.

1-(4-fluorophenyl)-2-methoxy-2-oxoethyl benzoate (30)[27]

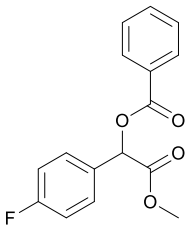

Synthesized according to the general procedure (section 3.7.).
Yield: 17 mg (55%), obtained as off-white solid from flash column chromatography using hexanes/AcOEt eluent system.
^{1}H NMR (600 MHz, $CDCl_3$): δ = 8.12 (d, *J* = 8.4 Hz, 2H), 7.65 – 7.53 (m, 3H), 7.47 (t, *J* = 7.8 Hz, 2H), 7.12 (t, *J* = 8.6 Hz, 2H), 6.16 (s, 1H), 3.76 (s, 3H) ppm. **^{13}C NMR** (151 MHz, $CDCl_3$): δ = 169.1, 165.7, 164.2, 133.6, 130.0, 129.6, 129.5, 129.1, 128.5, 116.0, 115.8, 74.1, 52.7ppm.

6.6. Photosensitized cyclopropanation of aryldiazoesters with olefins

methyl 1,2-diphenylcyclopropane-1-carboxylate (31)[7]

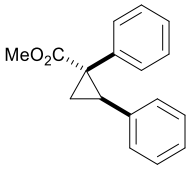

Synthesized according to the general procedure (section 3.8.).
Yield: 15 mg (68%), white solid obtained as mixture of diastereoisomers (d.r. 77:23) from flash column chromatography using hexanes/AcOEt eluent system.
^{1}H NMR (600 MHz, $CDCl_3$): δ 7.52 (minor, d, *J* = 7.8 Hz, 2H), 7.35 (minor, dt, *J* = 27.2, 7.4 Hz, 8H), 7.16 – 7.09 (m, 3H), 7.05 (ddd, *J* = 13.0, 5.4, 2.0 Hz, 5H), 6.81 – 6.73 (m, 2H), 3.67 (s, 3H), 3.31 (minor, s, 3H), 3.19 – 3.08 (m, 1H), 2.88 (minor, t, *J* = 8.2 Hz, 1H), 2.35 (minor, dd, *J* = 7.2, 5.2 Hz, 1H), 2.14 (dd, *J* = 9.3, 4.9 Hz, 1H), 1.89 (dd, *J* = 7.1, 5.1 Hz, 1H), 1.62 (minor, dd, *J* = 9.0, 5.0 Hz, 1H) ppm.

^{13}C NMR (151 MHz, $CDCl_3$) δ 174.3, 140.3, 136.5, 136.4, 134.7, 131.9, 130.2, 129.0, 128.3, 128.0, 127.7, 127.6, 127.3, 127.0, 126.8, 126.3, 52.6, 51.9, 37.4, 33.2, 33.1, 29.7, 20.4, 18.3 ppm.

methyl 1-(4-methoxyphenyl)-2-phenylcyclopropane-1-carboxylate (32)[29]

Synthesized according to the general procedure (section 3.8.).
Yield: 15 mg (70%), white solid, obtained as mixture of diastereoisomers (d.r. 98:2) from flash column chromatography using hexanes/AcOEt eluent system.
^{1}H NMR (500 MHz, $CDCl_3$): δ = 7.44 (minor, d, 2H), 7.34 (minor, m, 5H), 7.22 (m, 2H), 7.07 (m, 3H), 6.94 (minor, d, *J* = 8.6 Hz, 2H), 6.82 – 6.72 (m, 2H), 6.67 (d, *J* = 8.6 Hz, 2H), 3.83 (minor, s, 3H), 3.73 (s, 3H), 3.67 (s, 3H), 3.30 (minor, s, 3H), 3.08 (dd, *J* = 9.1, 7.5 Hz, 1H), 2.82 (minor, m, 1H), 2.30 (minor,

m, 1H), 2.13 (dd, *J* = 9.3, 4.8 Hz, 1H), 1.83 (dd, *J* = 7.2, 4.9 Hz, 1H), 1.60 (minor, m, 1H) ppm. **^{13}C NMR** (151 MHz, $CDCl_3$): (minor+major) δ = 158.4, 136.5, 132.9, 128.1, 127.7, 126.8, 126.2, 113.1, 55.0, 52.6, 36.6, 33.2, 20.2. ppm.

ethyl 1-(4-bromophenyl)-2-phenylcyclopropane-1-carboxylate (33)[7]

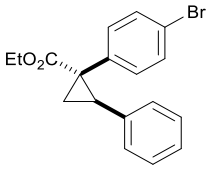

Synthesized according to the general procedure (section 3.8.).
Yield: 14 mg (40%), off-white solid obtained as single diastereoisomer (d.r. >99:1) from flash column chromatography using hexanes/AcOEt eluent system.
^{1}H NMR (600 MHz, $CDCl_3$): δ = 7.24 – 7.22 (m, 2H), 7.10 – 7.05 (m, 3H), 6.89 – 6.86 (m, 2H), 6.78 – 6.75 (m, 2H), 4.18 – 4.06 (m, 2H), 3.08 (dd, *J* = 9.3, 7.3 Hz, 1H), 2.12 (dd, *J* = 9.3, 5.0 Hz, 1H), 1.82 (dd, *J* = 7.3, 5.0 Hz, 1H), 1.17 (t, *J* = 7.1 Hz, 3H) ppm. **^{13}C NMR** (151 MHz, $CDCl_3$): δ = 173.2, 136.0, 134.1, 133.5, 130.8, 128.0, 127.9, 126.5, 121.1, 61.4, 37.0, 32.9, 20.0, 14.1 ppm.

methyl 1-(4-cyanophenyl)-2-phenylcyclopropane-1-carboxylate (34)

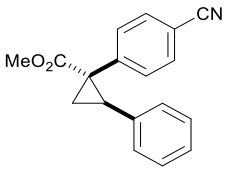

Synthesized according to the general procedure (section 3.8.).
Yield: 25 mg (78%), off-white solid obtained as mixture of diastereoisomers (d.r. 61:39) from flash column chromatography using hexanes/AcOEt eluent system.
^{1}H NMR (600 MHz, $CDCl_3$) both diastereoisomers: δ 7.67 (d, *J* = 8.3 Hz, 2H), 7.61 (d, *J* = 8.3 Hz, 2H), 7.41 (d, *J* = 8.3 Hz, 2H), 7.36 – 7.31 (m, 4H), 7.27 (m, 2H), 7.13 (d, *J* = 8.3 Hz, 2H), 7.11 – 7.05 (m, 2H), 6.76 (dd, *J* = 6.5, 3.0 Hz, 2H), 3.68 (s, 3H), 3.31 (s, 3H), 3.18 (dd, *J* = 9.2, 7.5 Hz, 1H), 2.89 – 2.82 (m, 1H), 2.41 (dd, *J* = 7.6, 5.3 Hz, 1H), 2.23 – 2.17 (m, 1H), 1.91 (dd, *J* = 7.3, 5.2 Hz, 1H), 1.65 (dd, *J* = 9.2, 5.3 Hz, 1H) ppm. ppm.
^{13}C NMR (151 MHz, $CDCl_3$) both diastereoisomers: δ = 173.0, 169.9, 145.4, 140.5, 135.6, 135.2, 132.6, 132.2, 131.5, 130.9, 128.9, 128.2, 128.0, 127.9, 127.1, 126.9, 118.7, 118.7, 111.2, 110.9, 52.8, 52.1, 37.9, 37.2, 33.5, 33.4, 19.9, 18.4 ppm; **HRMS** (ESI): m/z calcd for $C_{18}H_{15}NO_2^+$: 278,1176 $[M+H]^+$; found: 278,1185. **GC chromatogram:** t_r = 8,717 min, (86% purity, 78% yield)

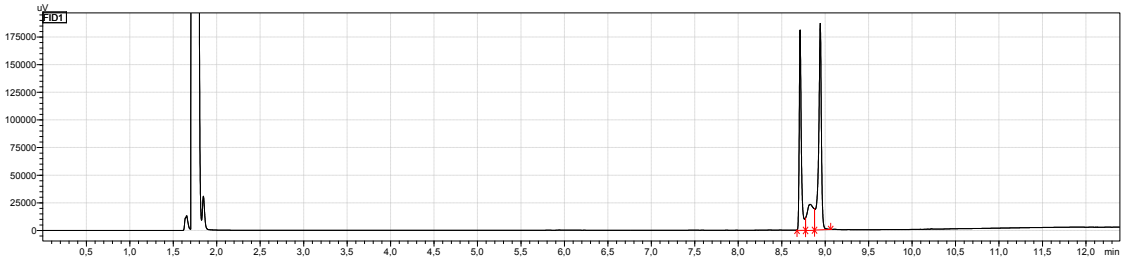

methyl 2-(4-methoxyphenyl)-1-phenylcyclopropane-1-carboxylate (35)[30]

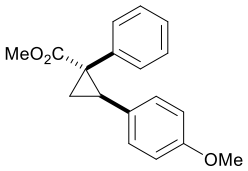

Synthesized according to the general procedure (section 3.8.).
Yield: 20 mg (70%), white solid obtained as mixture of diastereoisomers (d.r. 78:22) from flash column chromatography using hexanes/AcOEt eluent system.
^{1}H NMR (500 MHz,$CDCl_3$) δ 7.49 (minor, d, *J* = 7.3 Hz, 2H), 7.36 (minor, t, *J* = 7.5 Hz, 2H), 7.27 (minor, m, 3H), 7.14-7.12 (m, 3H), 7.02 (m, 2H), 6.85 (minor, d, *J* = 8.6 Hz, 2H), 6.68 (d, *J* = 8.7 Hz, 2H), 6.60 (d, *J* = 8.7 Hz, 2H), 3.80 (minor, s, 3H), 3.69 (s, 3H), 3.65 (s, 3H), 3.32 (minor, s, 3H), 3.06 (dd, *J* = 9.2, 7.6 Hz, 1H), 2.81 (minor, m, 1H), 2.29 (minor, dd, *J* = 7.4, 5.1 Hz, 1H), 2.11 (dd, *J* = 9.4, 4.9 Hz, 1H), 1.80 (dd, *J* = 7.2, 4.9 Hz, 1H), 1.59 (minor, m, 1H) ppm.

^{13}C NMR (151 MHz, $CDCl_3$) δ 174.4 (minor + major), 158.5 (minor), 158.1, 134.9 (minor + major), 132.0 (minor + major), 130.2, 130.0, 129.0 (minor + major), 128.5, 128.3, 128.3, 127.7, 127.3, 126.9, 113.5, 113.2, 55.2, 55.1, 52.5, 52.0, 37.04 (minor + major), 32.7, 32.6, 20.5, 18.4 ppm.

methyl 2-(4-fluorophenyl)-1-phenylcyclopropane-1-carboxylate (36)[31]

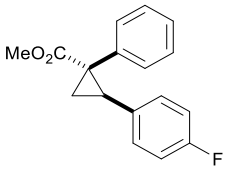

Synthesized according to the general procedure (section 3.8.).
Yield: 11 mg (40%), yellowish oil obtained as single diastereoisomer (d.r. >99:1) from flash column chromatography using hexanes/AcOEt eluent system.
^{1}H NMR (600 MHz, $CDCl_3$): δ = 7.17 – 7.11 (m, 3H), 7.05 – 6.97 (m, 2H), 6.78 – 6.66 (m, 4H), 3.66 (s, 3H), 3.10 (dd, *J* = 9.3, 7.3 Hz, 1H), 2.14 (dd, *J* = 9.4, 5.0 Hz, 1H), 1.83 (dd, *J* = 7.2, 5.0 Hz, 1H) ppm.
^{13}C NMR (151 MHz, $CDCl_3$): δ = 174.2, 162.4, 134.5, 132.1, 132.1, 131.9, 129.4, 129.4, 127.8, 127.1, 114.7, 114.5, 52.6, 37.2, 32.3, 20.5 ppm. **^{19}F NMR** (470 MHz, $CDCl_3$): δ = -116.48 (m, 1F).

methyl 2-methyl-1,3-diphenylcyclopropane-1-carboxylate (37)[34]

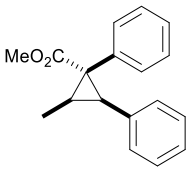

Synthesized according to the general procedure (section 3.8.).
Yield: 15 mg (55%), white solid obtained as single diastereoisomer (d.r. >99:1) from flash column chromatography using hexanes/AcOEt eluent system. (Structure confirmed by NOE, see NMR section). **^{1}H NMR** (500 MHz, $CDCl_3$): δ = 7.34 – 7.26 (m, 3H), 7.13 (dt, *J* = 5.2, 2.9 Hz, 3H), 7.08 – 7.01 (m, 2H), 6.82 – 6.69 (m, 2H), 3.62 (s, 3H), 3.10 (d, *J* = 10.3 Hz, 1H), 2.38 (dq, *J* = 10.2, 6.8 Hz, 1H), 1.26 (d, *J* = 6.7 Hz, 4H) ppm. **^{13}C NMR** (151 MHz, $CDCl_3$): δ = 13C NMR (150 MHz, $CDCl_3$) δ 175.5, 136.2, 133.2, 132.3, 130.6, 127.8, 127.5, 127.2, 52.7, 38.0, 36.5, 27.8, 10.8 ppm.

6.7. Photocatalyzed synthesis of γ-oximinoesters

ethyl (E)-4-(hydroxyimino)-4-(p-tolyl)butanoate (38)[32]

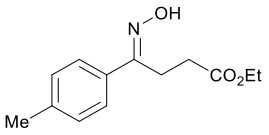

Synthesized according to the general procedure (section 3.9.).
Yield: 41 mg (86%), obtained as white solid from flash column chromatography using hexanes/AcOEt eluent system.

^{1}H NMR (600 MHz, DMSO-d_6): δ = 11.21 (s, 1 H), 7.50 (d, *J* = 8.1 Hz, 2 H), 7.17 (d, *J* = 8.1 Hz, 2 H), 4.01 (q, *J* = 7.1 Hz, 2 H), 2.91 (t, *J* = 7.9 Hz, 2 H), 2.44 (t, *J* = 7.9 Hz, 2 H), 2.31 (s, 3 H), 1.13 (t, *J* = 7.1 Hz, 3 H) ppm. **^{13}C NMR** (151 MHz, DMSO-d_6): δ = 172.0, 155.2, 138.2, 132.9, 129.0,125.7, 60.0, 30.4, 21.0, 20.8, 14.0 ppm.

ethyl 4-(hydroxyimino)-5-(4-methoxyphenyl)-3-methylpentanoate (39)[32]

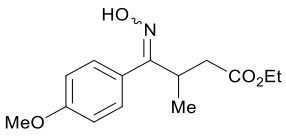

Synthesized according to the general procedure (section 3.9.).
Yield: from *trans*-anethole: 21 mg (38%, E/Z ratio: 2.2:1), from *cis*-anethole: 15 mg (26%, E/Z ratio: 2.1:1), yellowish oil obtained from flash column chromatography using hexanes/AcOEt eluent system. **^{1}H NMR** (600 MHz, $CDCl_3$): major isomer: δ = 8.81 (s, 1H), 7.46 – 7.40 (m, 2H), 6.91 – 6.86 (m, 2H), 4.09 (q, *J* = 7.1 Hz, 2H), 3.82 (s, 3H), 3.78 – 3.71 (m, 1H), 2.88 (dd, *J* = 16.1, 7.2 Hz, 1H), 2.63 (dd, *J* = 16.1, 7.9 Hz, 1H), 1.33 (d, *J* = 7.1 Hz 3H), 1.20 (t, *J* = 7.1 Hz, 3H) ppm; minor isomer: δ = 8.34 (s, 1H), 7.38 – 7.33 (m, 2H), 6.96 – 6.92 (m, 2H), 4.17 – 4.14 (m, 2H), 3.83 (s, 3H), 3.28 – 3.19 (m, 1H), 2.72 (dd, *J* = 15.8, 7.3 Hz, 1H), 2.36 (dd, *J* = 15.8, 7.3 Hz, 1H), 1.25 (t, *J* = 7.2 Hz 3H), 1.14 (d, *J* = 7.0 Hz, 3H) ppm. The mixture of **^{13}C NMR** (151 MHz, $CDCl_3$): δ = 172.4, 172.4, 161.5, 160.6, 160.1,

159.8, 129.4, 128.7, 128.5, 125.2, 113.8, 113.6, 60.4, 60.4, 55.3, 55.2, 38.8, 38.1, 36.4, 31.4, 18.4, 16.8, 14.2, 14.1.

tert-butyl (E)-4-(hydroxyimino)-4-phenylbutanoate (40)[32]

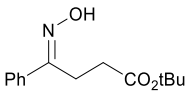

Synthesized according to the general procedure (section 3.9.).
Yield: 32 mg (64%), obtained as yellowish oil from flash column chromatography using hexanes/AcOEt eluent system.
^{1}H NMR (600 MHz, DMSO-d_6): δ = 7 11.31 (s, 1H), 7.63 – 7.59 (m, 2 H), 7.40 – 7.34 (m, 3 H), 2.91 (t, *J* = 7.8 Hz, 2 H), 2.38 (t, *J* = 7.8 Hz, 2 H), 1.33 (s, 9 H). 1ppm. **^{13}C NMR** (151 MHz, DMSO-d_6): δ = 171.2, 155.5, 135.8, 128.6, 128.4, 125.9, 79.8, 31.5, 27.6, 21.2.

benzyl (E)-4-(hydroxyimino)-4-phenylbutanoate (41)[32]

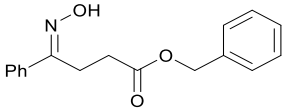

Synthesized according to the general procedure (section 3.9.).
Yield: 40 mg (71%), obtained as yellowish oil from flash column chromatography using hexanes/AcOEt eluent system.
^{1}H NMR (500 MHz, DMSO-d_6): δ = 11.35 (s, 1H), 7.67 – 7.58 (m, 2 H), 7.41 – 7.28 (m, 8 H), 5.05 (s, 2 H), 2.98 (t, *J* = 7.5 Hz, 2 H), 2.56 (t, *J* = 7.8 Hz, 2H) ppm. **^{13}C NMR** (151 MHz, DMSO-d_6): δ = 171.9, 155.3, 136.1, 135.7, 128.7, 128.4, 128.4, 128.0, 127.9, 125.8, 65.6, 30.3, 21.1 ppm.

(3S,8S,9S,10R,13S,14S,17S)-17-acetyl-10,13-dimethyl-2,3,4,7,8,9,10,11,12,13,14,15,16,17-tetradeca hydro-1H-cyclopenta[a]phenanthren-3-yl 4-(4-ethoxy-1-(hydroxyimino)-4-oxobutyl) benzoate (42)[32]

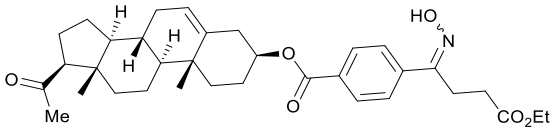

Synthesized according to the general procedure (section 3.9.).
Yield: 30 mg (27%), obtained as white solid from flash column chromatography using hexanes/AcOEt eluent system.
^{1}H NMR (500 MHz, DMSO-d_6): δ = δ 11.64 (s, 1 H), 7.95 (d, *J* = 8.3 Hz, 2 H), 7.77 (d, *J* = 8.3 Hz, 2 H), 5.44 – 5.35 (m, 1 H), 4.77 – 4.68 (m, 1 H), 4.00 (q, *J* = 7.1 Hz, 2 H), 2.97 (t, *J* = 7.8 Hz, 2 H), 2.57 (t, *J* = 9.0 Hz, 1 H), 2.49 – 2.46 (m, 2 H), 2.45 – 2.40 (m, 2 H), 2.06 (s, 3 H), 2.05 – 1.85 (m, 5 H), 1.76 – 1.67 (m, 1 H), 1.66 – 1.50 (m, 4 H), 1.49 – 1.36 (m, 3 H), 1.19 – 1.09 (m, 6 H), 1.05 – 0.96 (m, 4 H), 0.54 (s, 3 H) ppm. **^{13}C NMR** (126 MHz, $CDCl_3$): δ = 208.6, 172.0, 164.9, 154.8, 140.2, 139.5, 130.0, 129.4, 126.1, 122.3, 74.2, 62.6, 60.1, 56.1, 49.4, 43.3, 38.0, 37.7, 36.6, 36.2, 31.4, 31.3, 31.3, 30.2, 27.4, 24.1, 22.3, 21.0, 20.6, 19.1, 14.1, 13.0 ppm.

6.8. Photocatalyzed synthesis of phenantridines

diethyl 2-(phenanthridin-6-yl)succinate (43)[15]

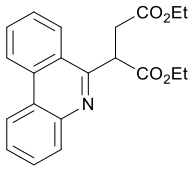

Synthesized according to the general procedure (section 3.10.).
Yield: 67 mg (95%), obtained as yellow oil from flash column chromatography using hexanes/acetone eluent system.
^{1}H NMR (500 MHz, $CDCl_3$): δ = 8.65 (d, *J* = 8.3 Hz, 1H), 8.54 (d, *J* = 7.8 Hz, 1H), 8.36 (d, *J* = 8.2 Hz, 1H), 8.11 (d, *J* = 7.4 Hz, 1H), 7.84 (t, *J* = 7.6 Hz, 1H), 7.75 – 7.66 (m, 2H), 7.66 – 7.60 (m, 1H), 5.23 (dd, *J* = 8.1, 6.3 Hz, 1H), 4.22 – 4.07(m, 4H), 3.44 (dd, *J* = 17.0, 8.1 Hz, 1H), 3.25 (dd, J = 17.0, 6.3 Hz, 1H), 1.21 (t, *J* = 7.1 Hz, 3H), 1.14 (t, *J* = 7.1 Hz, 3H) ppm. **^{13}C NMR** (126 MHz, $CDCl_3$): δ = 172.0, 171.7, 156.8, 143.3, 133.2, 130.4, 130.2, 128.5, 127.5, 127.0, 125.8, 124.9, 123.8, 122.5, 121.8, 61.3, 60.7, 46.0, 35.6, 14.1, 14.0 ppm.

diethyl 2-(8-methoxyphenanthridin-6-yl)succinate (44)[15]

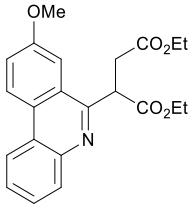

Synthesized according to the general procedure (section 3.10.).
Yield: 61 mg (80%), obtained as yellow oil from flash column chromatography using hexanes/acetone eluent system.
^{1}H NMR (500 MHz, $CDCl_3$): δ = 8.56 (d, *J* = 9.1 Hz, 1H), 8.46 (dd, *J* = 7.9, 1.6 Hz, 1H), 8.12 – 8.06 (m 1H), 7.71 (d, *J* = 2.5 Hz, 1H), 7.68 – 7.58 (m, 2H), 7.48 (dd, *J* = 9.0, 2.6 Hz, 1H), 5.15 (dd, *J* = 8.1, 6,2 Hz, 1H), 4.24 – 4.09 (m, 4H), 4.00 (s, 3H), 3.47 (dd, *J* = 17.1, 8.1 Hz, 1H), 3.25 (dd, *J* = 17.1, 6.3 Hz, 1H), 1.23 (t, *J* = 7.2 Hz, 3H), 1.16 (t, *J* = 7.1 Hz, 3H) ppm. **^{13}C NMR** (126 MHz, $CDCl_3$): δ = 172.2, 171.8, 158.8, 155.8, 142.6, 130.2, 127.6, 127.6, 127.1, 126.3, 124.2, 123.9, 121.4, 121.2, 105.9, 61.3, 60.7, 55.6, 46.4, 35.5, 14.2, 14.1 ppm.

diethyl 2-(phenanthridin-6-yl)malonate (45)[15]

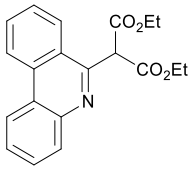

Synthesized according to the general procedure (section 3.10.).
Yield: 28 mg (42%), obtained as yellow solid from flash column chromatography using hexanes/acetone eluent system.

^{1}H NMR (600 MHz, $CDCl_3$): δ = 8.67 (d, *J* = 8.4 Hz, 1H), 8.57 (d, *J* = 8.4 Hz, 1H), 8.14 (d, *J* = 7.9 Hz, 1H), 8.01 (d, *J* = 8.2 Hz, 1H), 7.85 (t, *J* = 7.3 Hz, 1H), 7.75 – 7.64 (m, 3H), 5.63 (s, 1H), 4.38 – 4.26 (m, 4H), 1.28 (t, *J* = 7.1 Hz, 6H) ppm. **^{13}C NMR** (151 MHz, $CDCl_3$): δ = 167.5, 153.6, 143.3, 133.2, 130.6, 130.5, 128.6, 127.6, 127.4, 125.2, 125.0, 124.0, 122.7, 121.9, 62.0, 59.5, 14.1. ppm.

ethyl 2-(phenanthridin-6-yl)propanoate (46)[15]

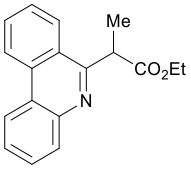

Synthesized according to the general procedure (section 3.10.).
Yield: 42 mg (75%), obtained as yellow oil from flash column chromatography using hexanes/acetone eluent system.
^{1}H NMR (600 MHz, $CDCl_3$): δ = 8.67 (d, J = 8.3 Hzm 1H), 8.56 (d, *J* = 8.1, 1H), 8.22 (d, *J* = 8.2, 1H), 8.15 (dd, *J* = 8.1, 1.2 Hz, 1H), 7.87 – 7.81 (m, 1H), 7.74 – 7.67 (m, 2H), 7.67 – 7.63 (m, 1H), 4.74 (q, *J* = 7.1 Hz, 1H), 4.26 – 4.13 (m, 2H), 1.78 (d, *J* = 7.1 Hz, 3H), 1.16 (t, *J* = 7.1 Hz, 3H) ppm. **^{13}C NMR** (151 MHz, $CDCl_3$): δ = 173.7, 159.5, 143.6, 133.3, 130.3, 130.2, 128.6, 127.4, 126.8, 125.6, 124.7, 123.7, 122.7, 121.8, 60.9, 45.6, 16.4, 14.1 ppm.

dimethyl (phenanthridin-6-ylmethyl)phosphonate (47)[15]

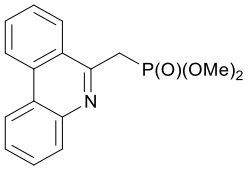

Synthesized according to the general procedure (section 3.10.).
Yield: 38 mg (63%), obtained as yellow oil from flash column chromatography using hexanes/acetone eluent system.
^{1}H NMR (500 MHz, $CDCl_3$): δ = 8.65 (d, *J* = 8.3 Hz, 1H), 8.56 (d, *J* = 7.8 Hz, 1H), 8.34 (d, *J* = 8.3 Hz, 1H), 8.14 (d, *J* = 8.5 Hz, 1H), 7.89 – 7.83 (m, 1H), 7.77 – 7.70 (m, 2H), 7.68 – 7.63 (m, 1H), 4.07 (s, 1H), 4.03 (s, 1H), 3.76 (s, 3H), 3.74 (s, 3H) ppm. **^{13}C NMR** (126 MHz, $CDCl_3$): δ = 153.3 (d, *J* = 8.9 Hz), 143.6 (d, *J* = 2.7 Hz), 133.1, 130.8, 129.7, 128.7, 127.5, 127.1, 127.0, 125.4 (d, *J* = 3.4 Hz), 123.9, 122.3, 122.0, 53.0 (d, *J* = 6.5 Hz), 35.0, 33.9 ppm.

6.9. Photocatalyzed synthesis of β-amino-α-diazo esters

ethyl 2-diazo-2-(2-phenyl-1,2,3,4-tetrahydroisoquinolin-1-yl)acetate (48)[33]

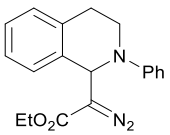

Synthesized according to the general procedure (section 3.11.).
Yield: 22 mg (70%), obtained as yellowish oil from flash column chromatography using hexanes/AcOEt eluent system.

^{1}H NMR (600 MHz, $CDCl_3$): δ = 7.33–7.13 (m, 6H), 7.07 (d, *J* = 7.8 Hz, 2H), 6.90–6.82 (m, 1H), 5.79 (s, 1H), 4.26–4.14 (m, 2H), 3.66–3.53 (m, 2H), 3.03 (dt, *J* = 16.2, 6.5 Hz, 1H), 2.89 (dt, *J* = 16.1, 5.3 Hz, 1H), 1.24 (t, *J* = 7.2 Hz, 3H) ppm. **^{13}C NMR** (151 MHz, $CDCl_3$): δ = 166.5, 149.1, 135.4, 134.7, 129.4, 128.8, 127.7, 127.6, 126.8, 119.8, 116.4, 61.1, 56.5, 43.9, 28.1, 14.6 ppm.

***ethyl 2-diazo-2-(2-(p-tolyl)-1,2,3,4-tetrahydroisoquinolin-1-yl)acetate (49)*[33]**

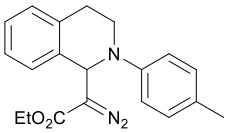

Synthesized according to the general procedure (section 3.11.).
Yield: 25 mg (78%), obtained as yellowish oil from flash column chromatography using hexanes/AcOEt eluent system.
^{1}H NMR (500 MHz, $CDCl_3$): δ = 7.33–7.27 (m, 1H), 7.24–7.18 (m, 2H), 7.19–7.14 (m, 1H), 7.10 (d, *J* = 8.5 Hz, 2H), 6.99 (d, *J* = 8.5 Hz, 2H), 5.74 (s, 1H), 4.25–4.15 (m, 2H), 3.60–3.50 (m, 2H), 3.06–2.97 (m, 1H), 2.90 (dt, *J* = 16.1, 5.3 Hz, 1H), 2.28 (s, 3H), 1.23 (t, *J* = 7.1 Hz, 3H) ppm. **^{13}C NMR** (126 MHz, $CDCl_3$): δ = 166.6, 147.0, 135.4, 134.8, 129.8, 129.6, 128.8, 127.7, 127.5, 126.7, 117.2, 61.0, 56.8, 44.6, 28.3, 20.6, 14.5 ppm.

***ethyl 2-diazo-2-(2-(4-methoxyphenyl)-1,2,3,4-tetrahydroisoquinolin-1-yl)acetate (50)*[33]**

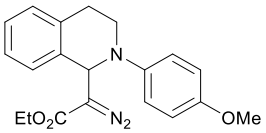

Synthesized according to the general procedure (section 3.11.).
Yield: 24 mg (67%), obtained as yellowish oil from flash column chromatography using hexanes/AcOEt eluent system.
^{1}H NMR (500 MHz, $CDCl_3$): δ = 7.30–7.23 (m, 1H), 7.24–7.17 (m, 2H), 7.19–7.12 (m, 1H), 7.06 (d, *J* = 9.0 Hz, 2H), 6.85 (d, *J* = 9.0 Hz, 2H), 5.61 (s, 1H), 4.21–4.08 (m, 2H), 3.77 (s, 3H), 3.54–3.36 (m, 2H), 3.05–2.84 (m, 2H), 1.19 (t, *J* = 7.1 Hz, 3H) ppm. **^{13}C NMR** (126 MHz, $CDCl_3$): δ = 166.7, 154.7, 143.8, 135.4, 134.7, 128.9, 127.7, 127.5, 126.7, 120.6, 114.6, 61.0, 57.9, 55.7, 46.2, 28.7, 14.5 ppm.

***ethyl 2-diazo-2-(2-(4-(trifluoromethyl)phenyl)-1,2,3,4-tetrahydroisoquinolin-1-yl)acetate (51)*[33]**

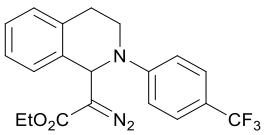

Yield: 23 mg (53%), obtained as yellowish oil from flash column chromatography using hexanes/AcOEt eluent system.
^{1}H NMR (500 MHz, $CDCl_3$): δ = (d, *J* = 8.6 Hz, 2H), 7.33–7.27 (m, 1H), 7.27–7.21 (m, 2H), 7.21–7.15 (m, 1H), 7.08 (d, *J* = 8.6 Hz, 2H), 5.86 (s, 1H), 4.26 (q, *J* = 7.1 Hz, 2H), 3.73 (dt, *J* = 12.8, 5.6 Hz, 1H), 3.63 (ddd, *J* = 12.8, 8.5, 4.5 Hz, 1H), 3.06 (ddd, *J* = 16.1, 8.5, 5.0 Hz, 1H), 2.88 (ddd, *J* = 16.1, 6.0, 4.4 Hz, 1H), 1.27 (t, *J* = 7.1 Hz, 3H) ppm. **^{13}C NMR** (126 MHz, $CDCl_3$): δ = 166.3, 150.9, 135.0, 134.1, 128.0, 127.6, 127.1, 126.7 (q, *J* = 3.8 Hz), 124.9 (q, *J* = 270.4 Hz), 120.4 (q, *J* = 32.7 Hz), 114.1, 61.4, 55.8, 43.0, 27.6, 14.6 ppm.

6.10. Photocatalyzed synthesis of hydrazones

ethyl (Z)-2-(2-cyclohexylhydrazineylidene)-2-phenylacetate (52)[17]

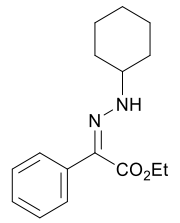

Exact Mass: 274,1681

Synthesized according to the general procedure (section 3.12.).
Yield: 43 mg (78%), obtained as colorless oil from flash column chromatography using hexanes/DCM/AcOEt eluent system.
^{1}H NMR (500 MHz, $CDCl_3$): δ = 10.62 (s, 1H), 7.57– 6.49 (m, 2H), 7.35 – 7.27 (m, 2H), 7.27 – 7.19 (m, 1H), 4.27 (q, *J* = 7.1 Hz, 2H), 3.54 – 3.37 (m, 1H), 2.11 – 1.95 (m, 2H), 1.85 – 1.70 (m, 2H), 1.67 – 1.57 (m, 1H), 1.46 – 1.34 (m, 3H), 1.31 (t, *J* = 7.1 Hz, 3H), 1.29 – 1.15 (m, 2H) ppm. **^{13}C NMR** (126 MHz, $CDCl_3$): δ = 163.9, 137.7, 128.4, 127.9, 126.7, 124.6, 60.3, 59.3, 32.7, 25.8, 24.7, 14.4 ppm; **HRMS** (ESI): m/z calcd for $C_{16}H_{23}N_2O_2^+$: 275.1760 $[M+H]^+$; found: 275.1759; **GC chromatogram:** t_r = 9.251 min, (98% purity).

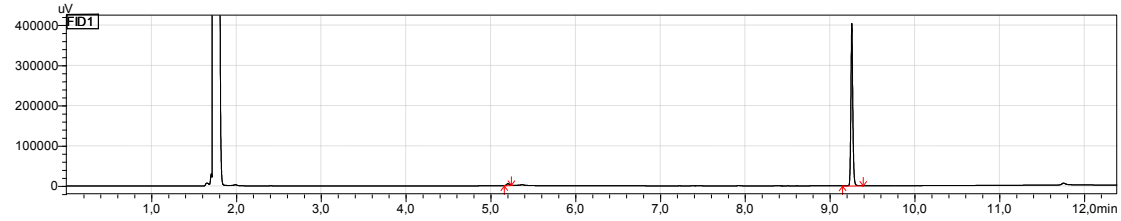

ethyl (Z)-2-(4-bromophenyl)-2-(2-cyclohexylhydrazineylidene)acetate (53)[17]

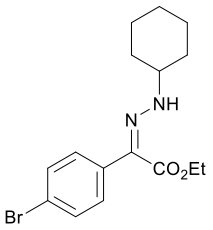

Synthesized according to the general procedure (section 3.12.).
Yield: 48 mg (68%), obtained as colorless oil from flash column chromatography using hexanes/DCM/AcOEt eluent system.
^{1}H NMR (500 MHz, $CDCl_3$): δ = 10.70 (d, *J* = 5.1 Hz, 1H), 7.45 – 7.49 (m, 4H), 4.27 (q, *J* = 7.1 Hz, 2H), 3.51 – 3.39 (m, 1H), 2.09 – 1.95 (m, 2H), 1.83 – 1.71 (m, 2H), 1.68 – 1.59 (m, 1H), 1.47 – 1.35 (m, 4H), 1.32 (t, *J* = 7.1 Hz, 3H), 1.30 – 1.17 (m, 2H) ppm. **^{13}C NMR** (126 MHz, $CDCl_3$): δ = 163.5, 136.5, 130.8, 129.8, 123.2, 120.5, 60.3, 59.3, 32.5, 25.6, 24.5, 14.3.ppm.

methyl (Z)-2-(2-cyclopentylhydrazineylidene)-2-(naphthalen-2-yl)acetate (54)[17]

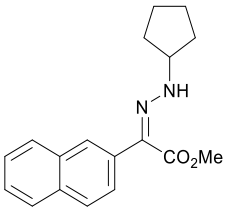

Synthesized according to the general procedure (section 3.12.).
Yield: 31 mg (53%), obtained as colorless oil from flash column chromatography using hexanes/DCM/AcOEt eluent system.
^{1}H NMR (600 MHz, $CDCl_3$): δ = 10.67 (d, *J* = 4.0 Hz, 1H), 7.98 – 7.96 (m, 1H), 7.84 – 7.77 (m, 3H), 7.68 (dd, *J* = 8.6, 1.7 Hz, 1H), 7.46 – 7.39 (m, 2H), 4.14 – 4.06 (m, 1H), 3.82 (s, 3H), 2.03 – 1.95 (m, 2H), 1.83 – 1.70 (m, 4H), 1.69 – 1.59 (m, 2H) ppm. **^{13}C NMR** (151 MHz, $CDCl_3$): δ = 164.3, 134.7, 133.2, 132.4, 128.2, 127.5, 127.1, 126.8, 126.6, 125.8, 125.6, 124.3, 62.2, 51.2, 32.5, 23.9. ppm.

allyl (Z)-2-(2-cyclopentylhydrazineylidene)-2-phenylacetate (55)[17]

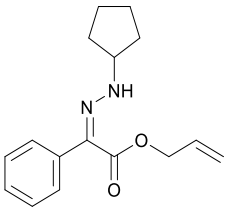

Synthesized according to the general procedure (section 3.12.).
Yield: 29 mg (53%), obtained as colorless oil from flash column chromatography using hexanes/DCM/AcOEt eluent system.
^{1}H NMR (600 MHz, $CDCl_3$): δ = 10.61 (s, 1H), 7.56 – 7.51 (m, 2H), 7.32 (t, *J* = 7.7 Hz, 2H), 7.27 – 7.21 (m, 1H), 6.00 – 5.91 (m, 1H), 5.32 (dd, *J* = 17.2, 1.4 Hz, 1H), 5.24 (d, *J* = 10.4, 1.4 Hz, 1H), 4.70 (d, *J* = 5.5 Hz, 2H), 4.10 – 4.03 (m, 1H), 1.99 – 1.93 (m, 2H), 1.79 – 1.71 (m, 4H), 1.65 – 1.59 (m, 2H) ppm. **^{13}C NMR** (151 MHz, $CDCl_3$): δ = 163.3, 137.3, 132.0, 128.3, 127.7, 126.7, 124.3, 118.2, 64.7, 62.2, 32.5, 23.9 ppm.

benzyl (Z)-2-(2-cyclopentylhydrazineylidene)-2-phenylacetate (56)[17]

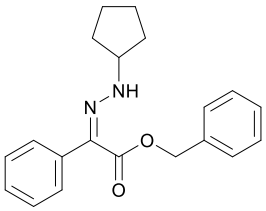

Synthesized according to the general procedure (section 3.12.).
Yield: 34 mg (52%), obtained as colorless oil from flash column chromatography using hexanes/DCM/AcOEt eluent system.
^{1}H NMR (500 MHz, $CDCl_3$): δ = 10.61 (d, *J* = 2.7 Hz, 1H), 7.56 – 7.50 (m, 2H), 7.35 (d, *J* = 4.3 Hz, 4H), 7.30 (t, *J* = 7.4 Hz 2H), 5.25 (s, 2H), 4.05 (d, J = 4.7 Hz, 1H), 2.00 – 1.89 (m, 2H), 1.80 – 1.69 (m, 4H), 1.66 – 1.57 (m, 2H) ppm. **^{13}C NMR** (126 MHz, $CDCl_3$): δ = 163.4, 137.3, 135.9, 128.5, 128.3, 128.1, 127.9, 127.7, 126.7, 124.3, 65.7, 62.2, 32.5, 23.9. ppm.

7. References

[1] Q. Wang, Y. Qu, H. Tian, Y. Liu, H. Song, Q. Wang, *Chem. Eur. J.* 2019, **25**, 8686-8690.

[2] A. G. Tskhovrebov, R. Goddard, A. Fürstner, *Angew. Chem. Int. Ed.* 2018, **57**, 8089-8094.

[3] A. Levy, S. Cohen, S. Pogodin, I. Agranat, *Struct. Chem.* 2015, **26**, 1565-1584.

[4] W.-W. Chan, S.-H.Yeung, Z. Zhou, A. S. C. Chan, A.W.-Y.Yu, *Org. Lett*. 2010, **12**, 604–607.

[5] Y. Zhang, Y. Yao, L. He, Y. Liu, L. Shi, *Adv. Synth. Catal.* 2017, **359**, 2754-2761.

[6] K. Orłowska, K. Rybicka-Jasińska, P. Krajewski, D. Gryko, *Org. Lett.* 2020, **22**, 1018-1021.

[7] I.D**.** Jurberg, H. M. L.Davies, *Chem. Sci.* 2018, **9**, 5112-5118.

[8] S. T. R. Müller, A. Murat, P. Hellier, T. Wirth, *Org. Process Res. Dev.* 2016, **20**, 495–502.

[9] D.P. Hari, J. Waser, *J. Am. Chem. Soc.* 2016, **138**, 2190–2193.

[10] N.T. Koduri, H. Scott, B. Hileman, J. Cox, M. Coffin, L. Glicksberg, S.R. Hussaini, *Org. Lett.* 2012, **14**, 440-443.

[11] T. Du, F. Du, Y. Ning, Y. Peng, *Org. Lett.* 2015, **17**, 1308–1311.

[12] N. Assadi, S. Pogodin, S.Cohen, I. Agranat *Struct. Chem.* 2012, **23**, 771-790.

[13] A. C. Coleman, J. Areephong, J. Vicario, W. R. Meetsma, W. R. Browne, B. L. Feringa, *Angew. Chem. Int. Ed.* 2010, **49**, 6580-6584.

[14] S.-Q. Quo, H.-Q. Yang, A.-L. Wang, Y.-Z. Jiang, G.-Q. Xu, Y.-C. Luo, Z.-X. Chen, P.-F. Xu, *Green. Chem.* 2021, **23**, 9571-9576.

[15] H. -B. Ye, X. -Y. Zhou, L. Li, X. -K. He, J. Xuan, *Org. Lett.* 2022, **24**, 6018-6023.

[16] W. Xie, N. Liu, B. Gong, S. Ning, X. Che, L. Cui, J. Xiang, *Eur. J. Org. Chem.* ***2019***, *14*, 2498-2501.

[17] C.-M. Chan, Q. Xing, Y.-C. Chow, S.-F. Hung, W.-Y. Yu, *Org. Lett.* 2019, **21**, 8037-8043.

[18] K. Rybicka-Jasińska, D. Gryko, *Photochemistry RSC* 2021, **49**, 411-456.

[19] R. Costa e Silva, L. O. da Silva, A. de Andrade Bartolomeu, T. J. Brocksom, K. T. de Oliveira *Beilstein J. Org. Chem.* 2020, **16**, 917–955.

[20] A.A. Buglak, M. A. Filatov, M. A. Hussain, M. Sugimoto, M. *J. Photochem. Photobiol. A* 2020, **403**, 112833.

[21] R. Liu, Q. Liu, H. Meng, H. Ding, J. Hao, Z.; Ji, H. Yue, W. Wei, *Org. Chem. Front.* 2021, **8**, 1970-1975.

[22] T. Entardas, S. Waldron, M. Volk, M. *J. Photochem. Photobiol. B*. 2020, **204**, 111787.

[23] T. Thiemann, *Lett. Org. Chem.* 2009, **6**, 515–525.

[24] K. N. Babu, F. Massarwe, I. Shioukhi, A. Masarwa, *Angew. Chem., Int. Ed.* 2021, **60**, 26199–26209.

[25] O. Tomashenko, V. Sokolov, A. Tomashevskiy, H. A. Buchholz, U. Welz-Biermann, V. Chaplinski, A. de Meijere, A. *Eur. J. Org. Chem.* 2008, **30**, 5107–5111.

[26] M. Lanzi, J. Merad, D. V. Boyarskaya, G. Maestri, C. Allain, G. Masson, *Org. Lett.* 2018, **20**, 5247–5250.

[27] C. Empel, T. V. Nguyen, R. M. Koenigs, *Org. Lett.* 2021, **23**, 548–553.

[28] E.D. Couch, T. J. Auvil, A. E. Mattson, *Chem. Eur. J.* 2014, **20**, 8283-8287.

[29] D. Sakuma, K. Yamada, K. Sasazawa, Y. Nishii, *Chem. Lett.* 2015, **44**, 818-820.

[30] Q. Zhao, Q.-Y. Yao, Y. Zhang, T. Xu, J. Zhang, X. Chen,. *Eur. J. Org. Chem.* 2022, **35**, 5112-5118.

[31] L. Chen, M. O. Bovee, B. E. Lemma, K. S. M. Keithley, S. L. Pilson, M. G. Coleman, J. Mack *Angew. Chem., Int. Ed.* 2015, **54**, 11084-11087.

[32] Y. Liu, K. Zhu, J. Zhao, P. Li, *Org. Lett.* 2022*,* **24**, 6834-6838.

[33] T. Xiao, L. Li, G. Lin, Z. Mao, L. Zhou, *Org. Lett.* 2014*,* **16**, 4232-4235.

[34] J.L.Thompson, H. M. L. Davies, *J. Am. Chem. Soc.*, 2007, **19**, 6090-6091.

8. NMR spectra

1-[bis(methoxyphenyl)methyl] benzyl ether (1)

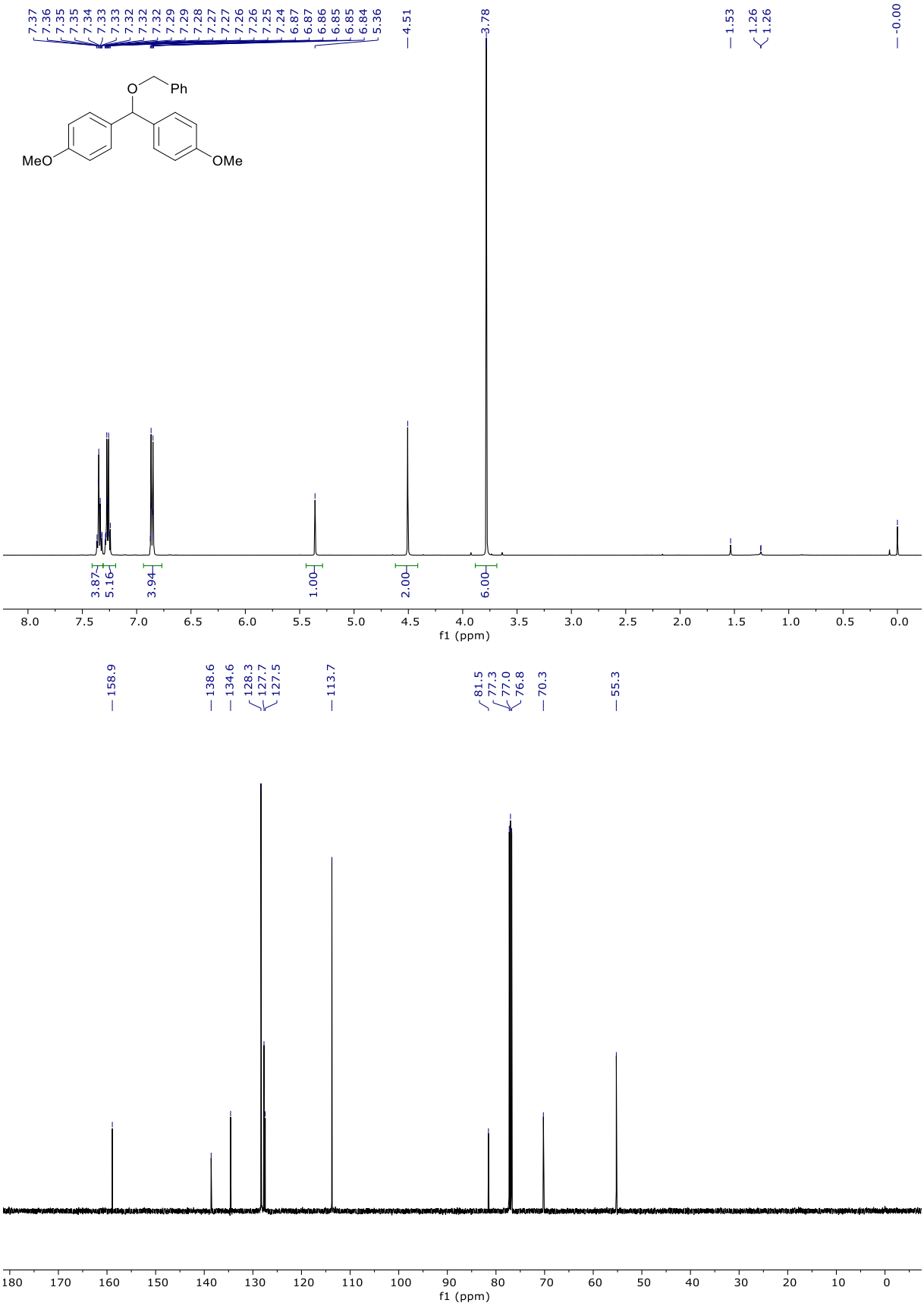

4,4'-(phenethoxymethylene)bis(methoxybenzene) (2)

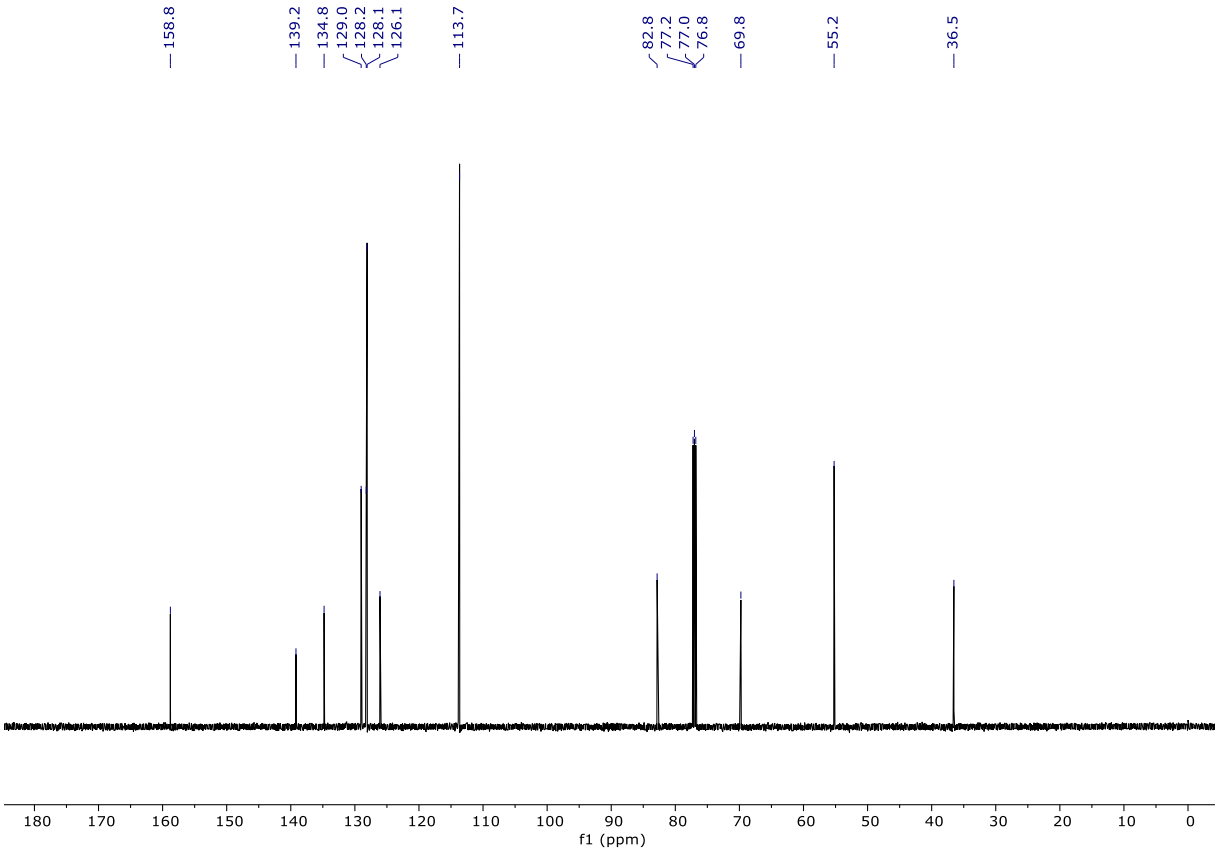

4,4'-((hexyloxy)methylene)bis(methoxybenzene) (3)

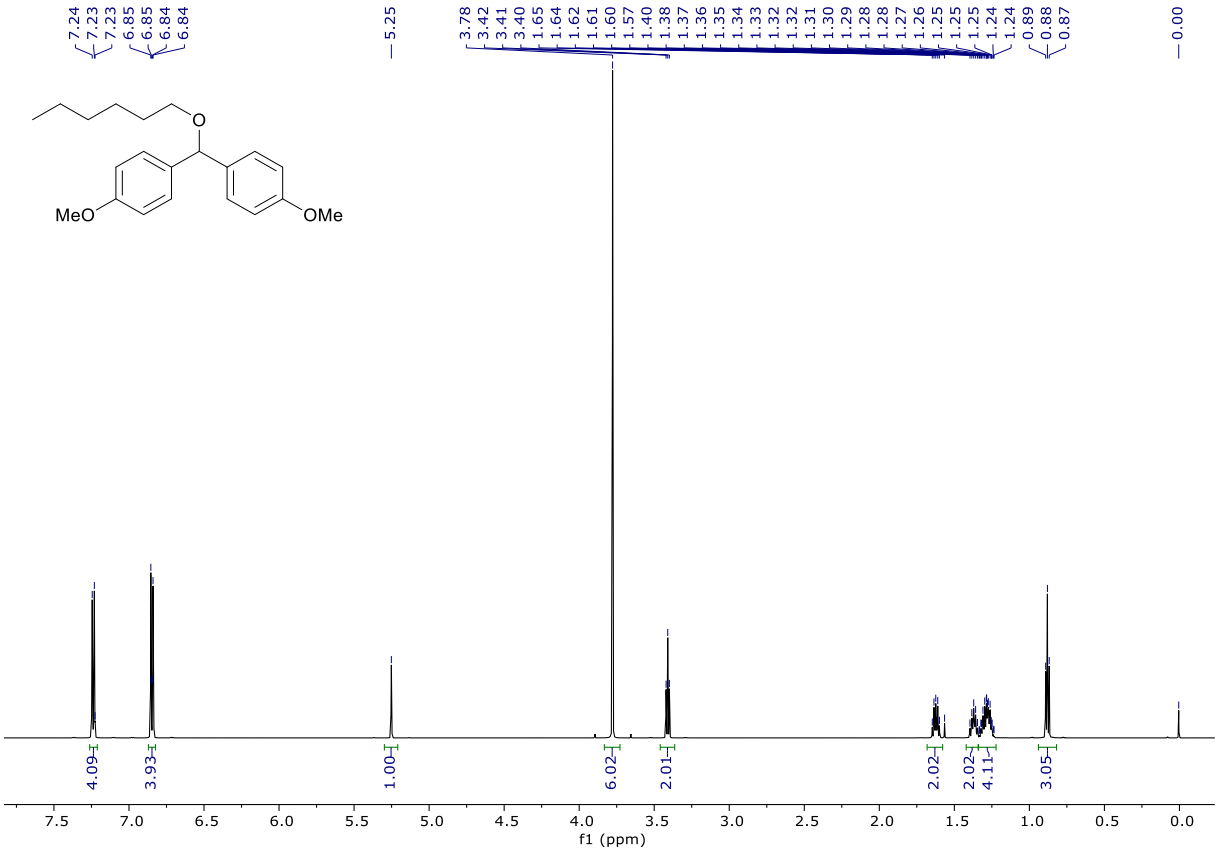

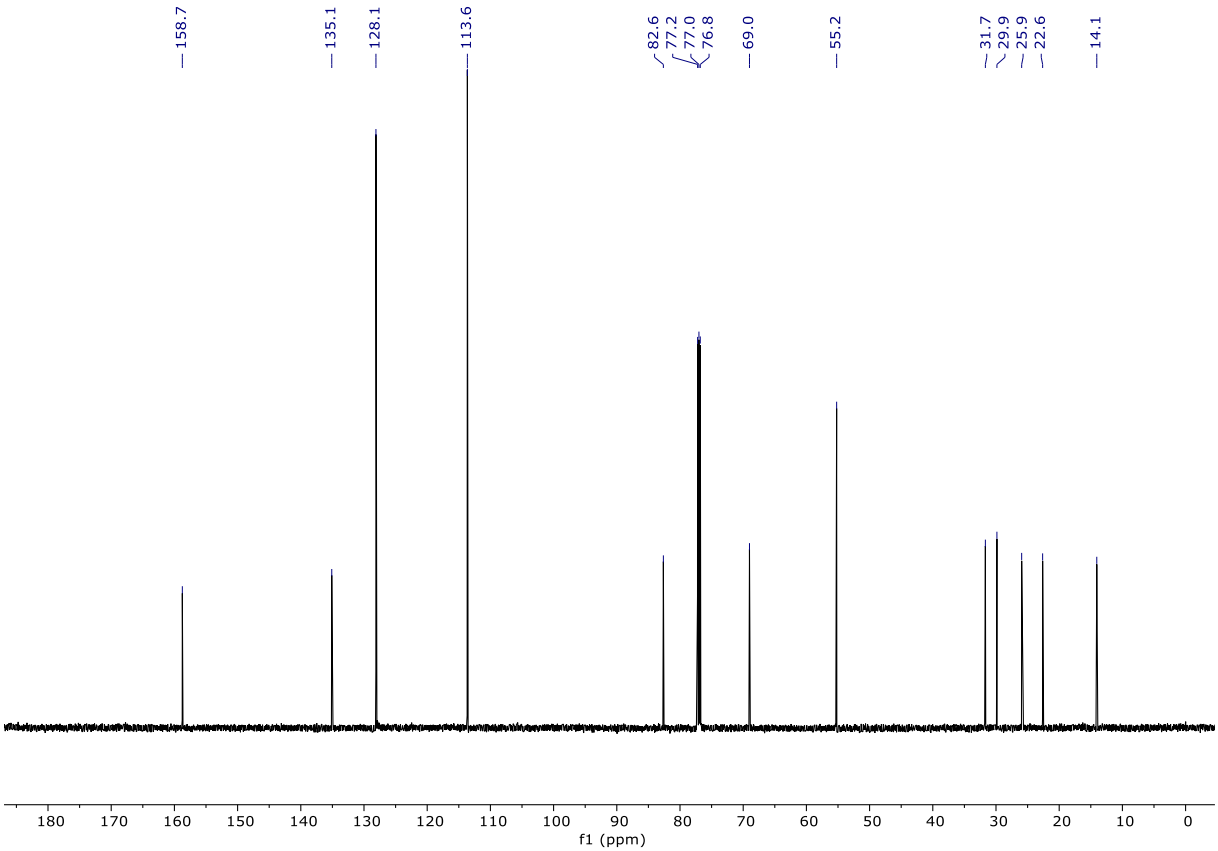

4,4'-(((3,7-dimethyloct-6-en-1-yl)oxy)methylene)bis(methoxybenzene) (4)

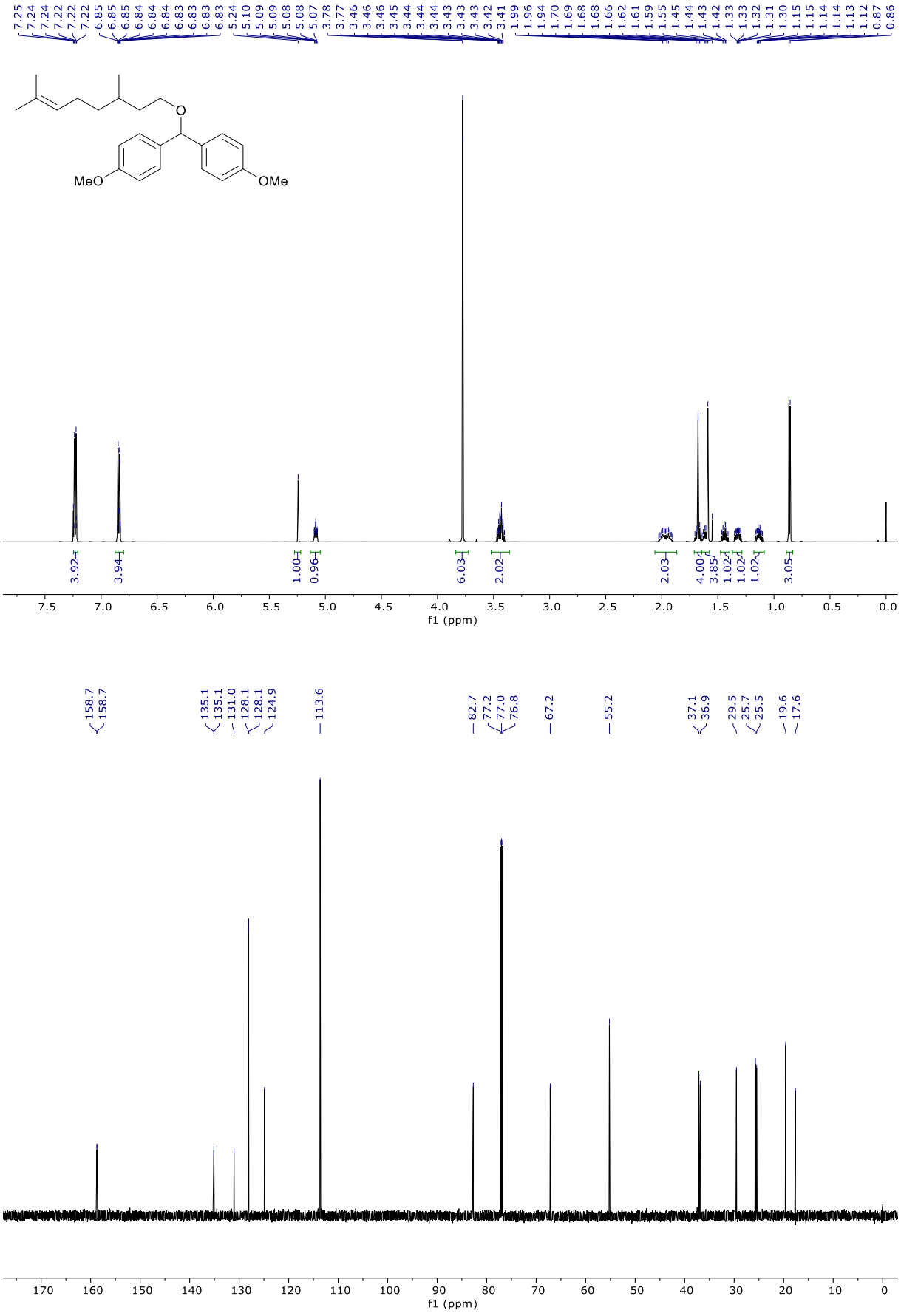

4,4'-((prop-2-yn-1-yloxy)methylene)bis(methoxybenzene) (5)

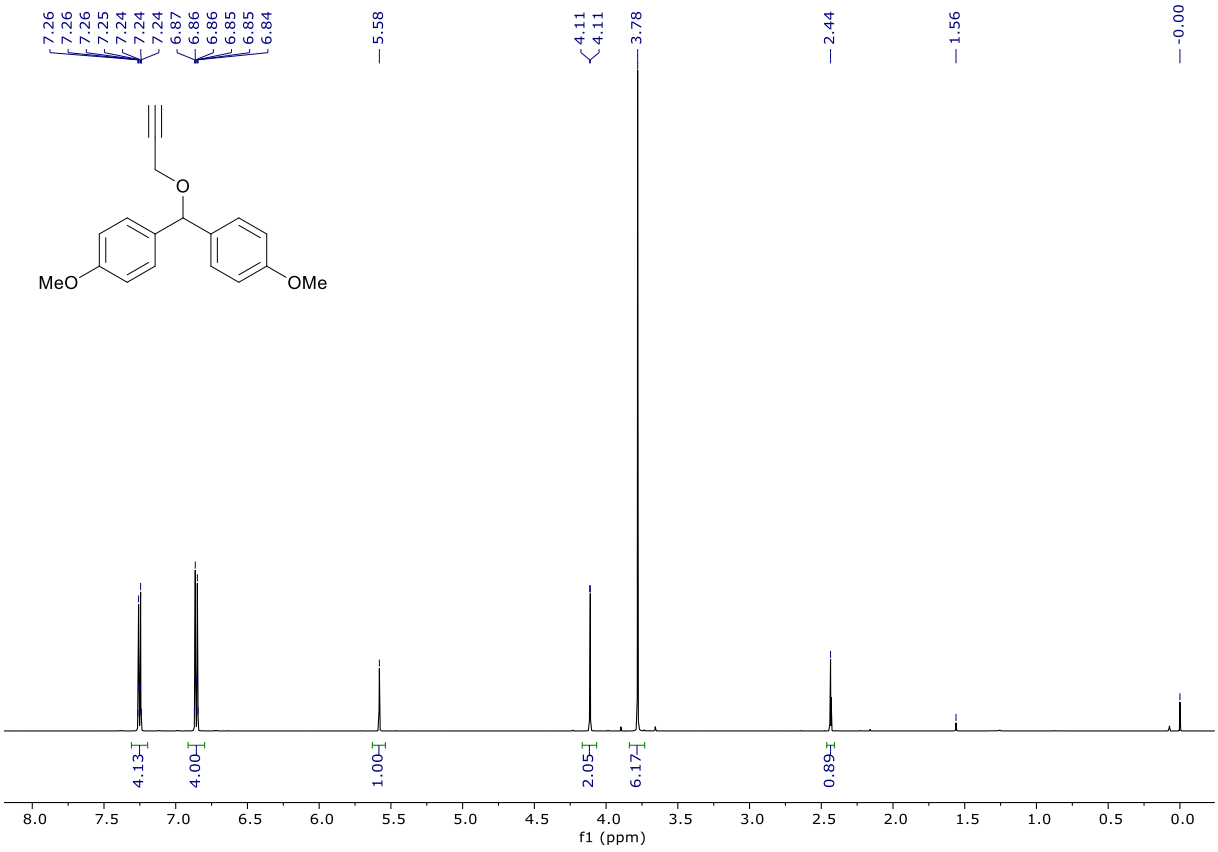

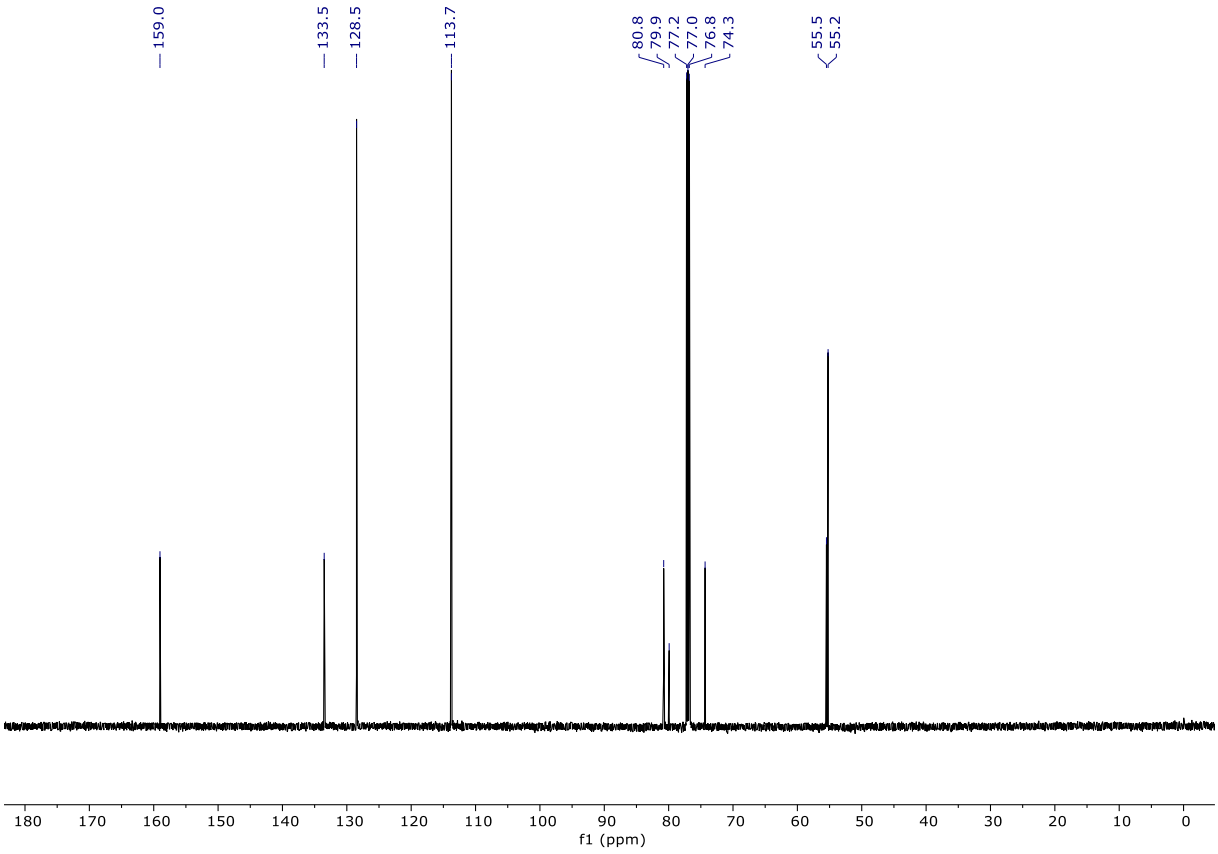

4,4'-(phenoxymethylene)bis(methoxybenzene) (6)

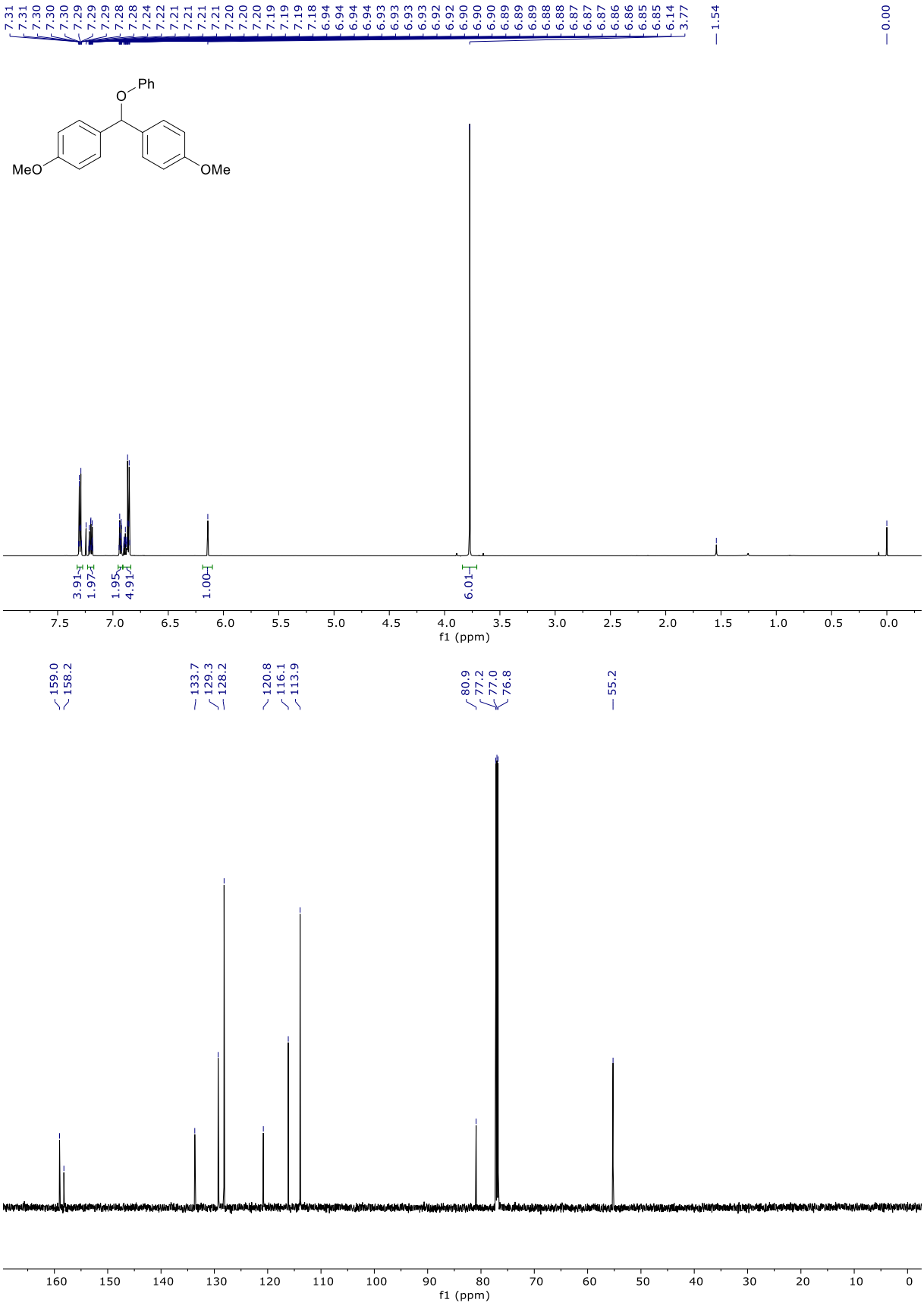

4,4'-((cyclohexyloxy)methylene)bis(methoxybenzene) (7)

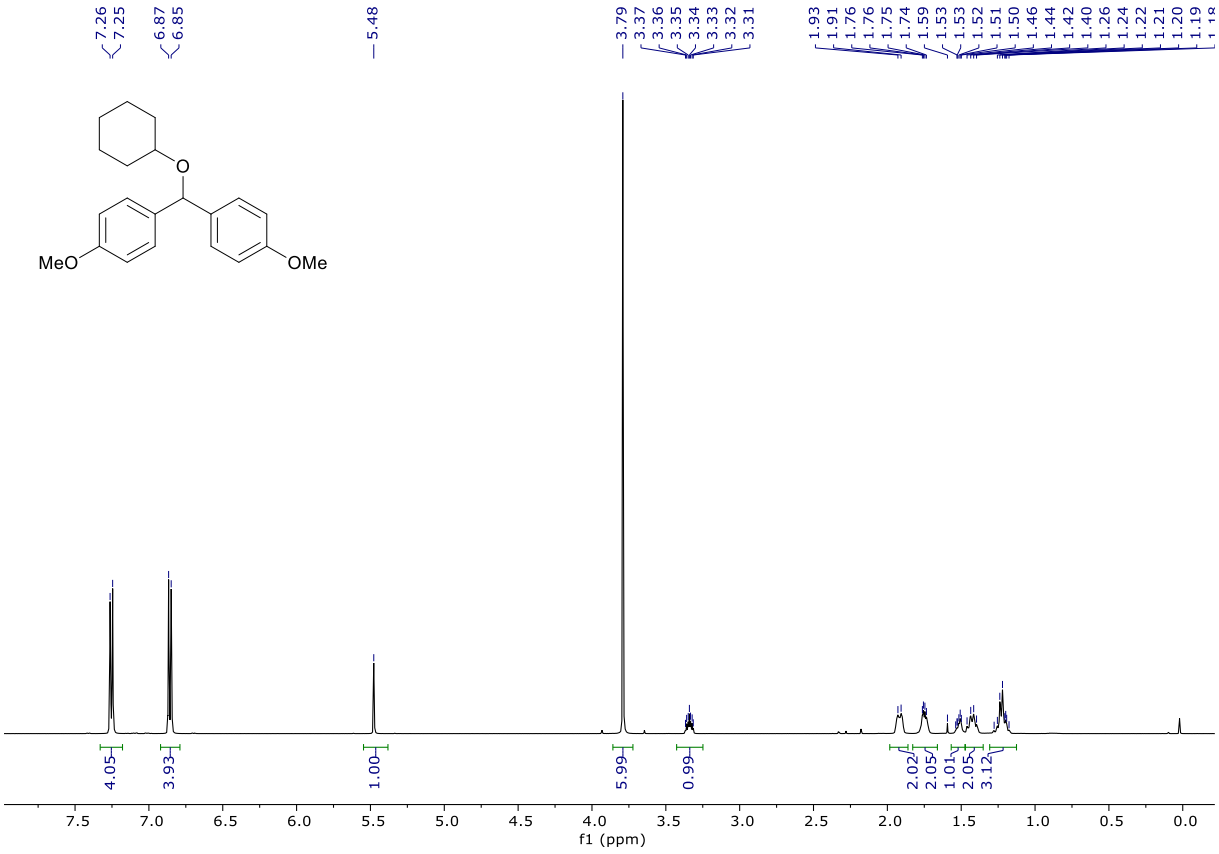

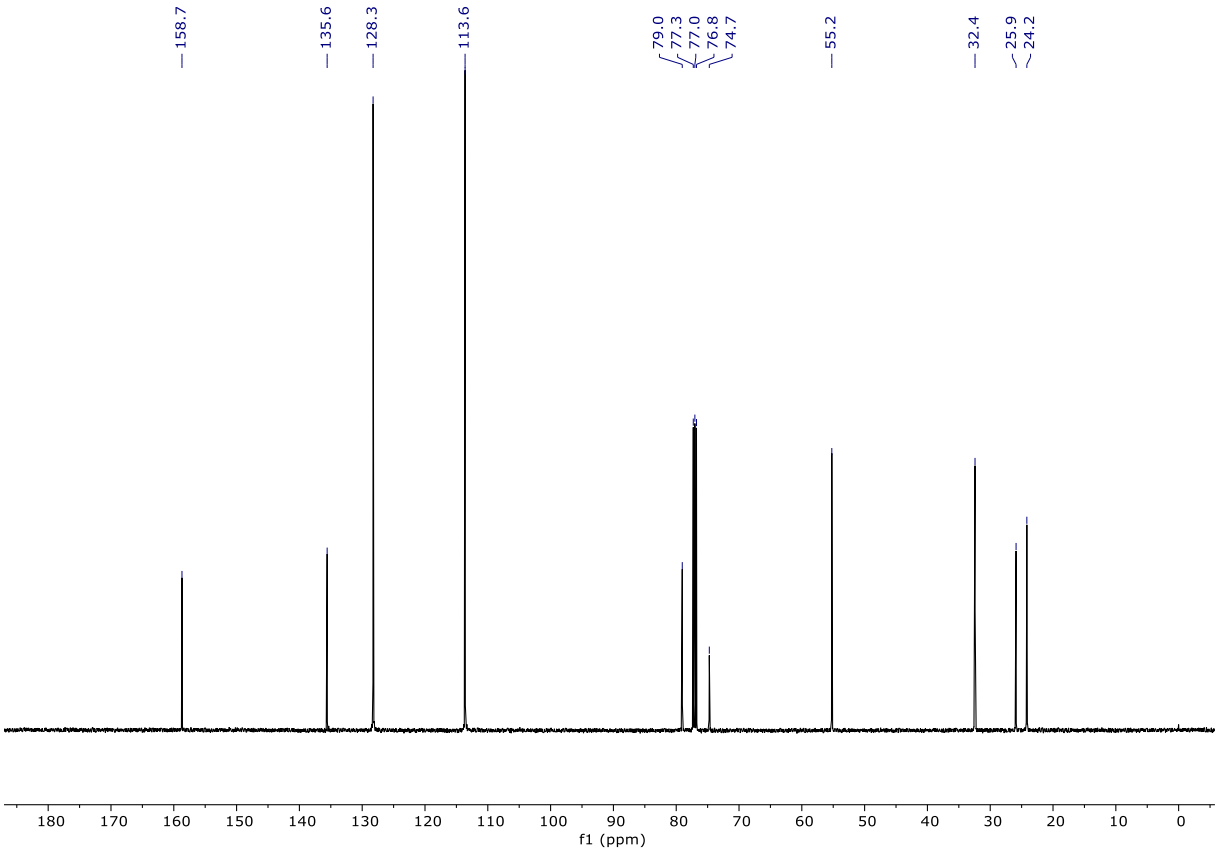

1-(tert-butyl) 2-methyl 4-(bis(4-methoxyphenyl)methoxy)pyrrolidine-1,2-dicarboxylate (8)

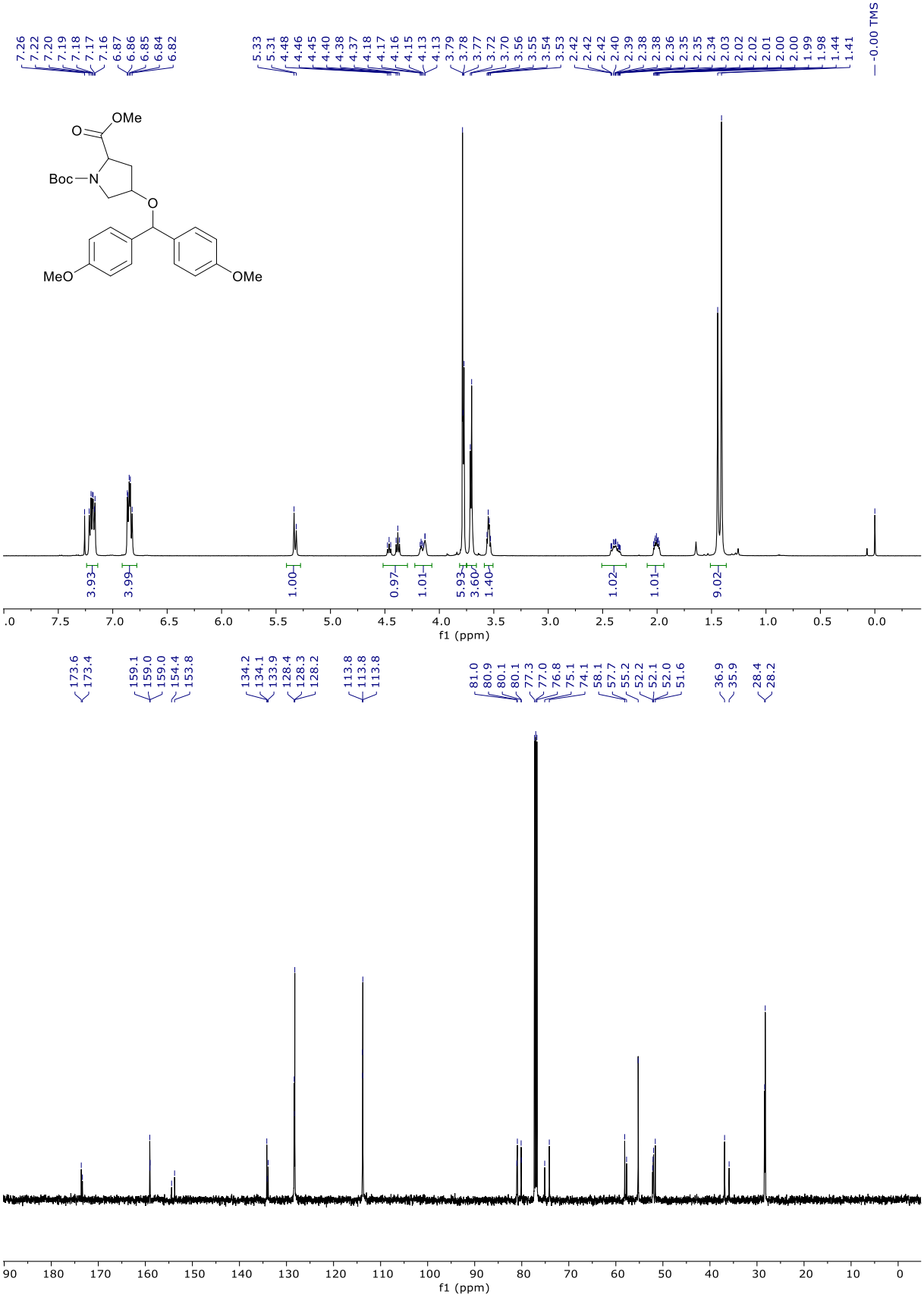

(8S,9S,10R,13R,14S,17R)-3-(bis(4-methoxyphenyl)methoxy)-10,13-dimethyl-17-((R)-6-methy lheptan-2-yl)-2,3,4,7,8,9,10,11,12,13,14,15,16,17-tetradecahydro-1H-cyclopenta[a]phenanthrene (9)

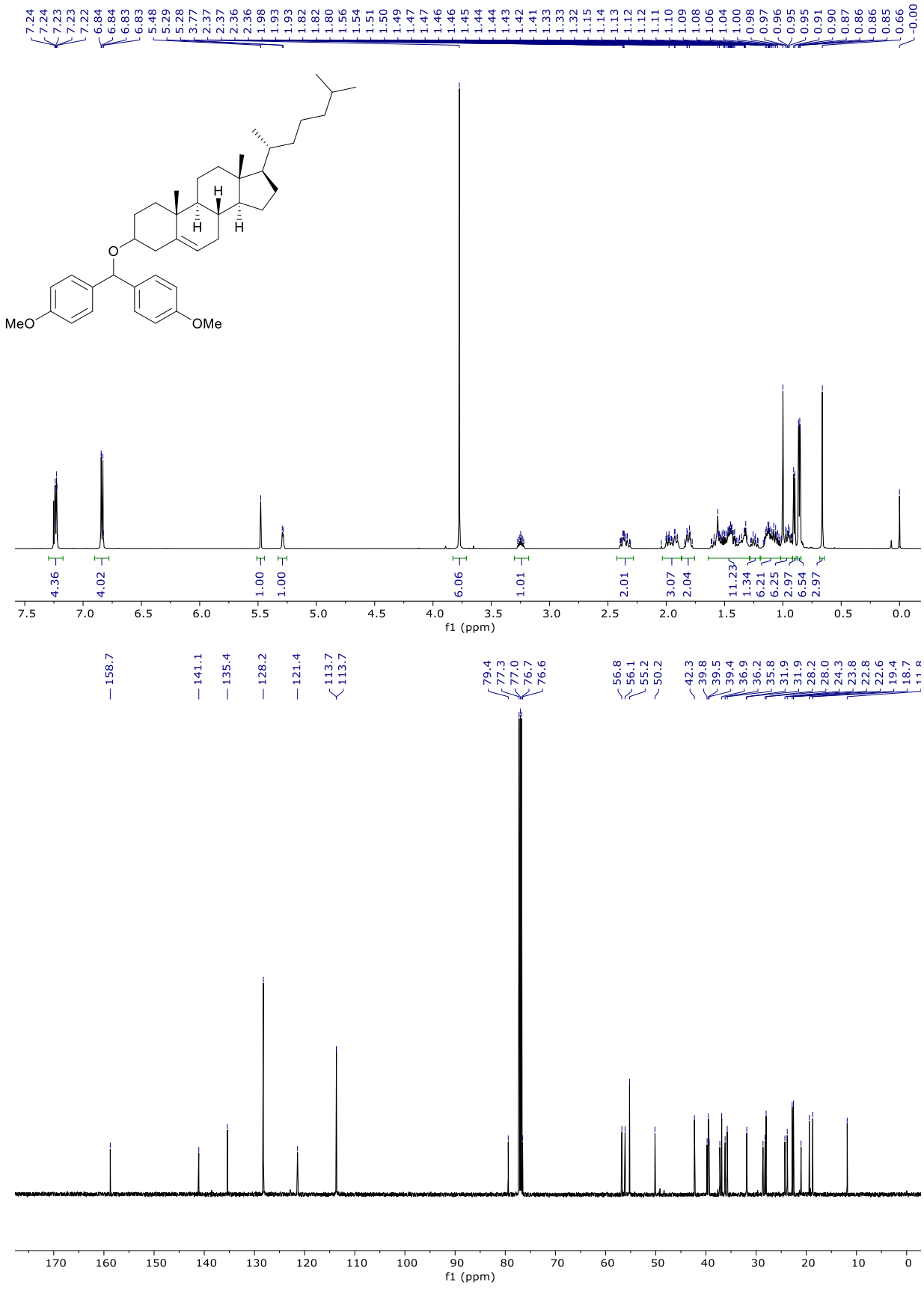

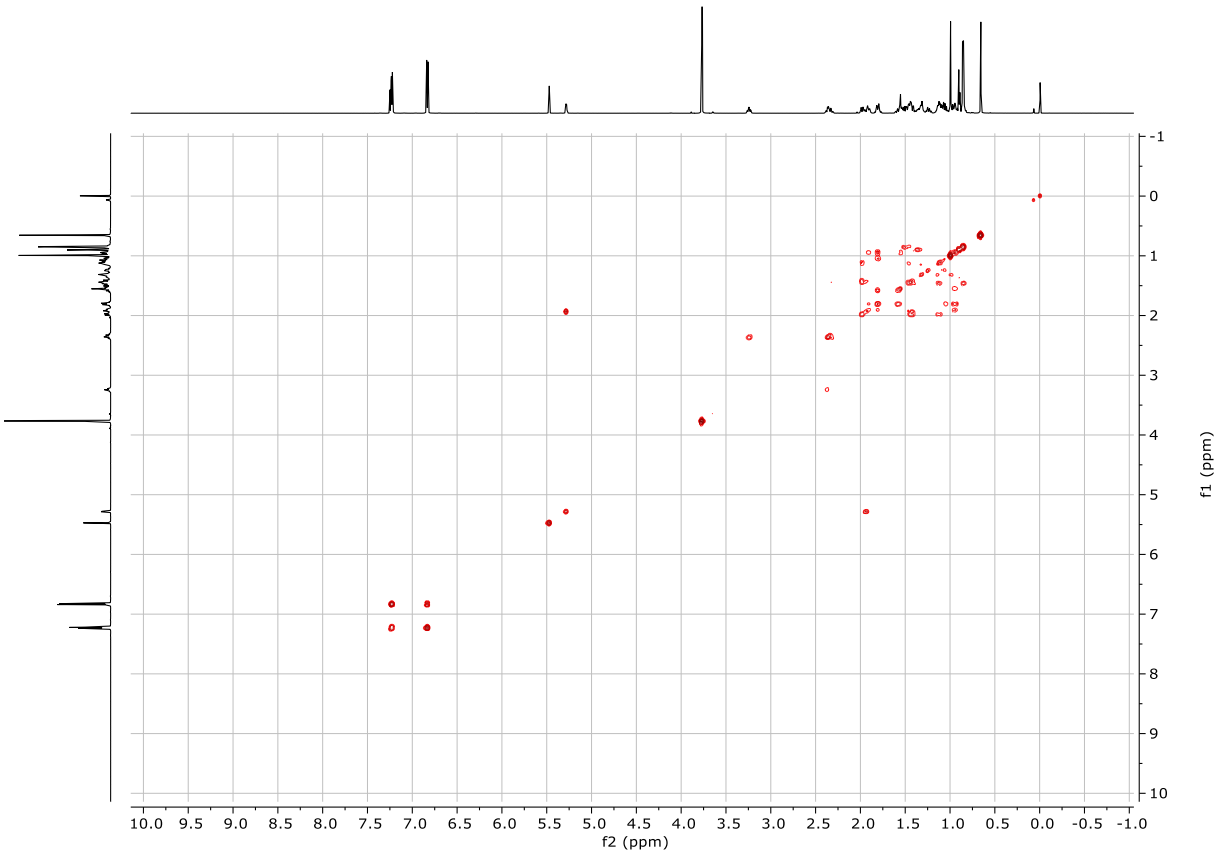

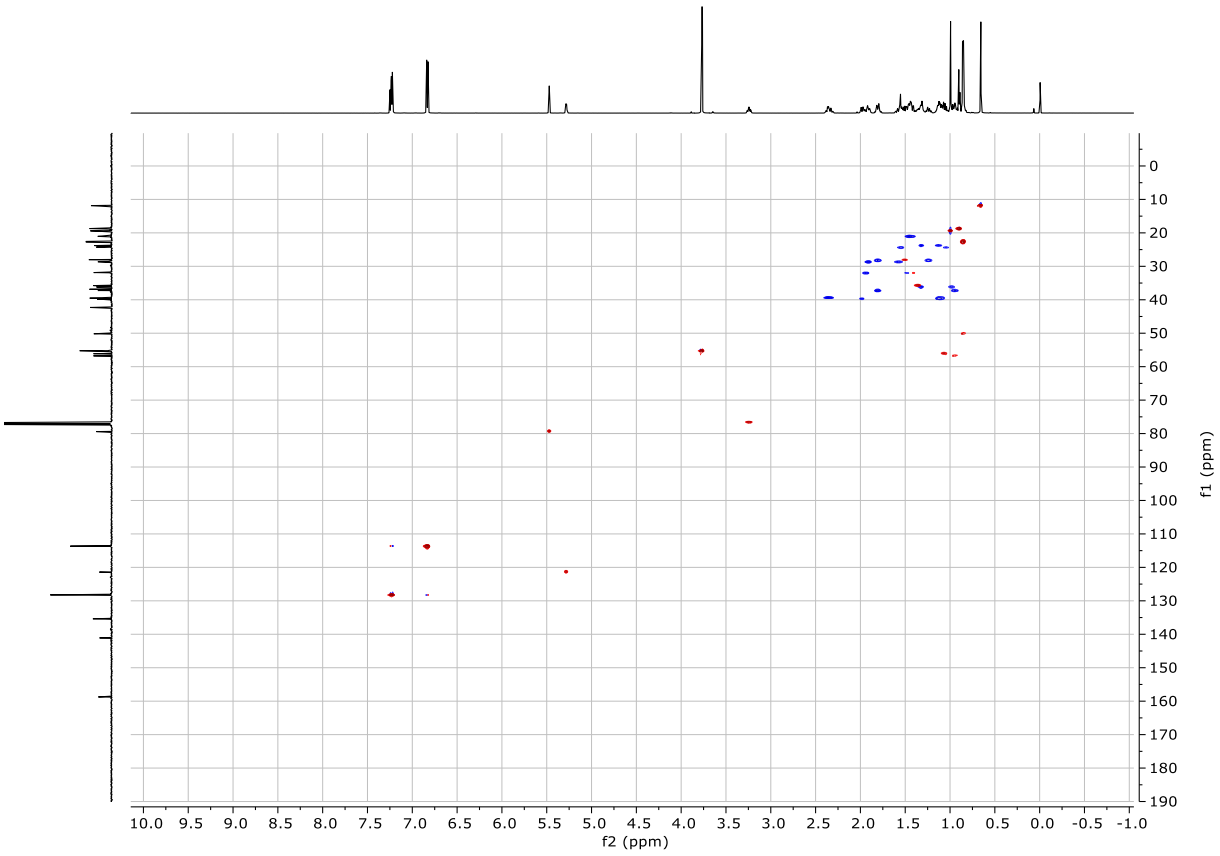

4,4'-(tert-butoxymethylene)bis(methoxybenzene) (10)

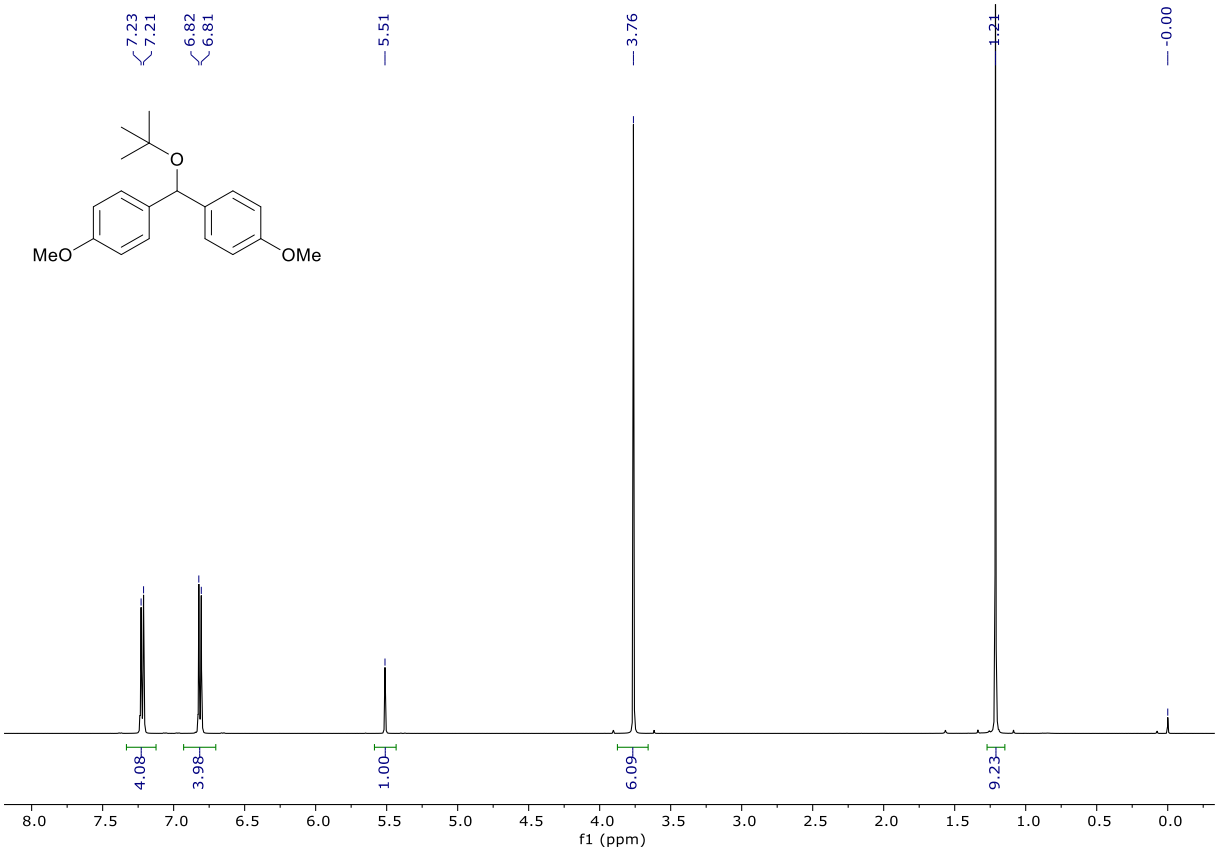

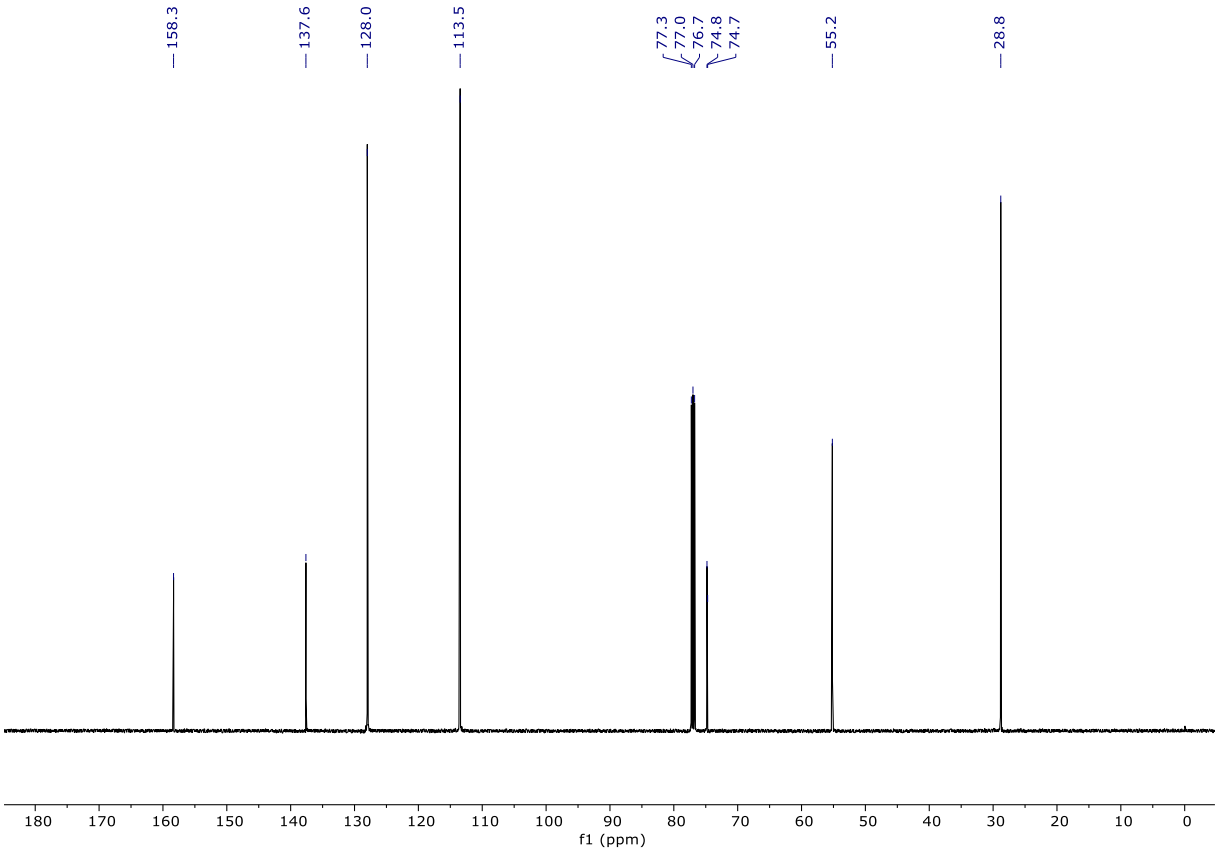

4,4'-((benzyloxy)methylene)bis(N,N-dimethylaniline) (11)

N-(bis(4-methoxyphenyl)methyl)octan-1-amine (12)

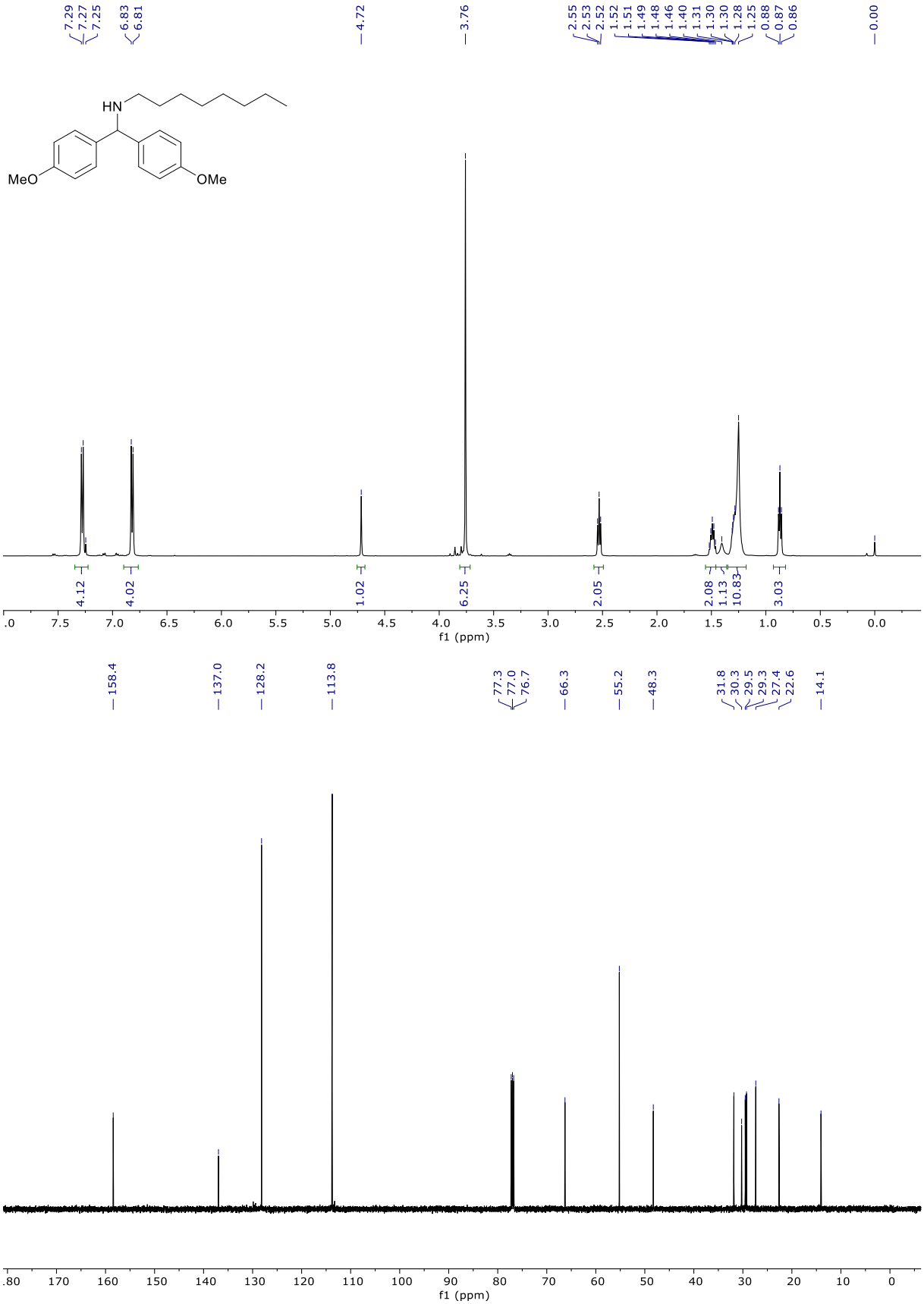

(S)-N-(bis(4-methoxyphenyl)methyl)-1-phenylethan-1-amine (13)

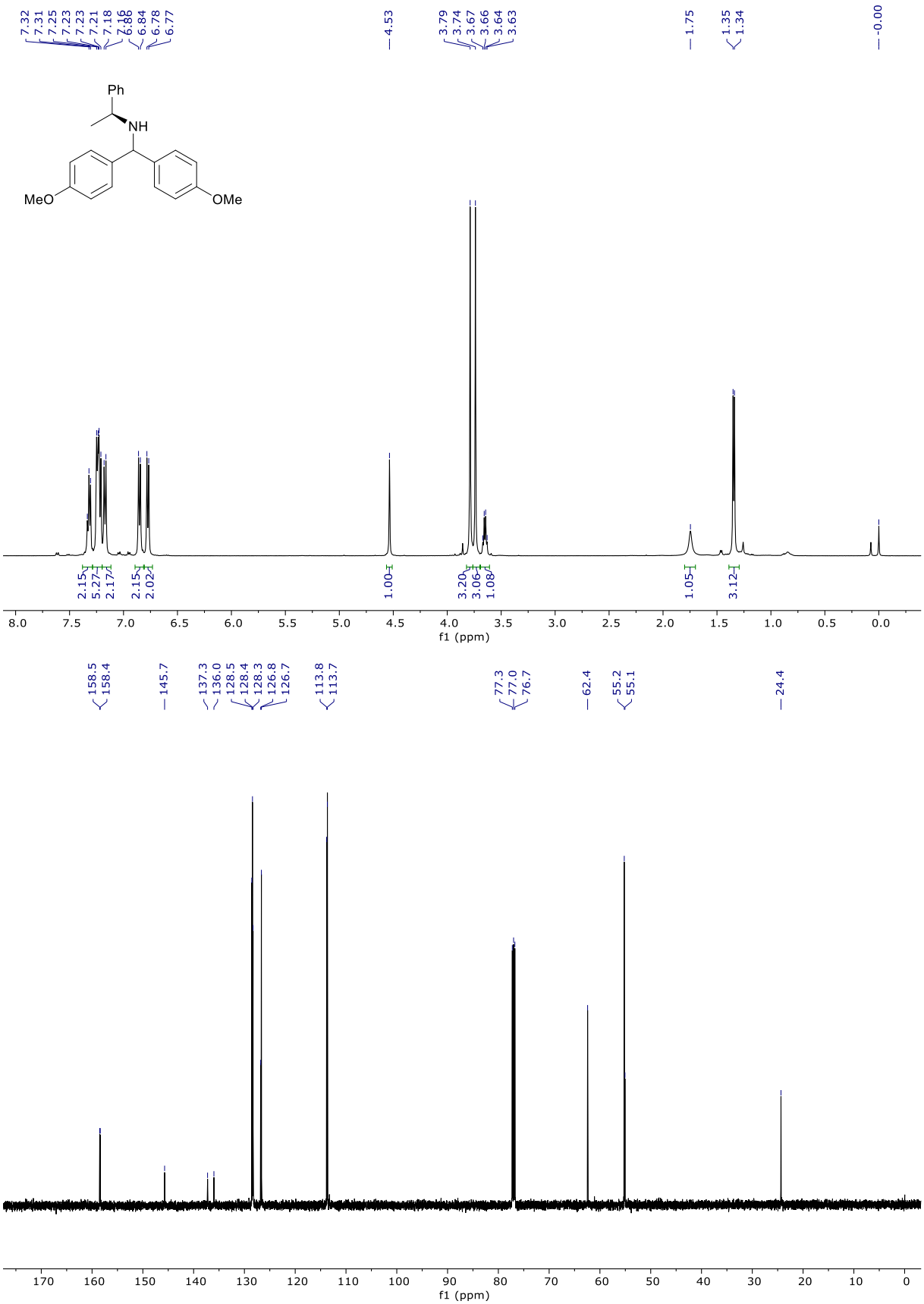

N-benzyl-1,1-bis(4-methoxyphenyl)-N-methylmethanamine (14)

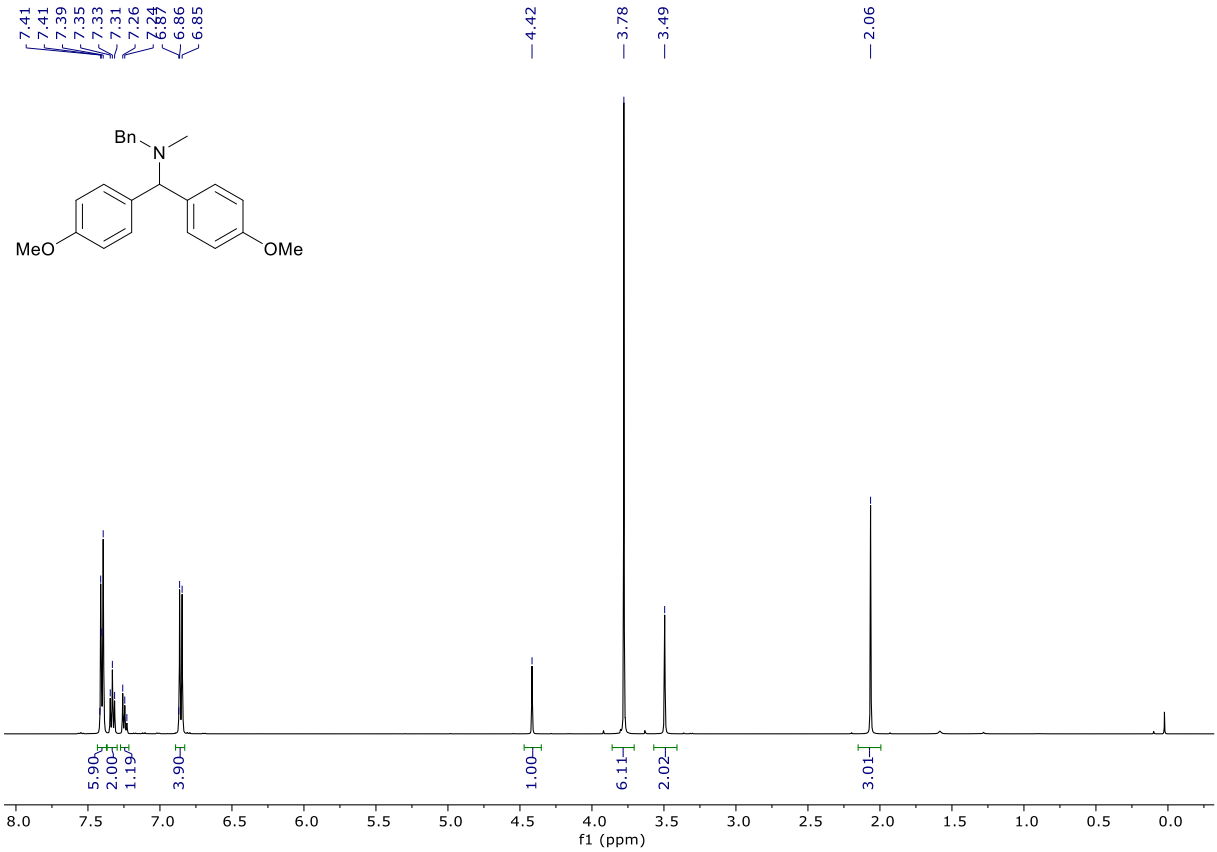

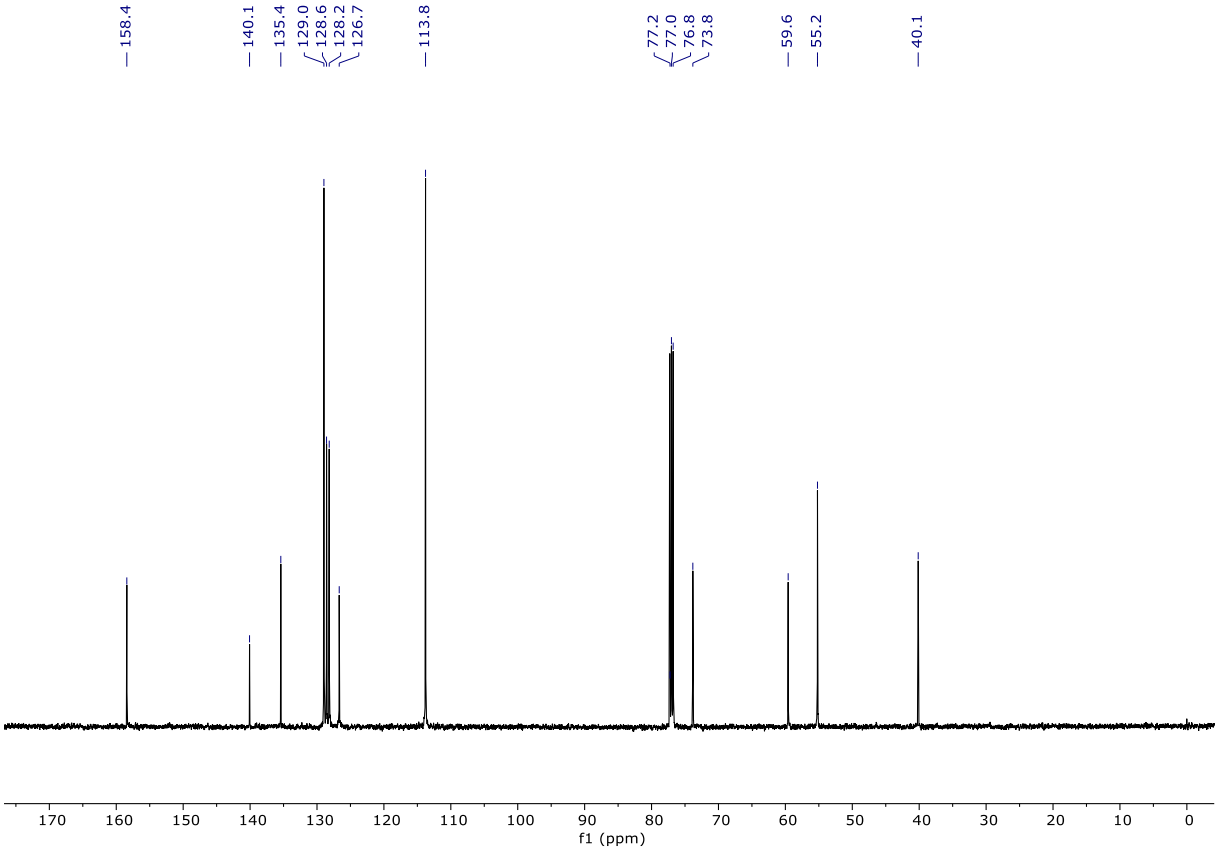

1-[bis(methoxyphenyl)methyl]pyrrolidine (15)

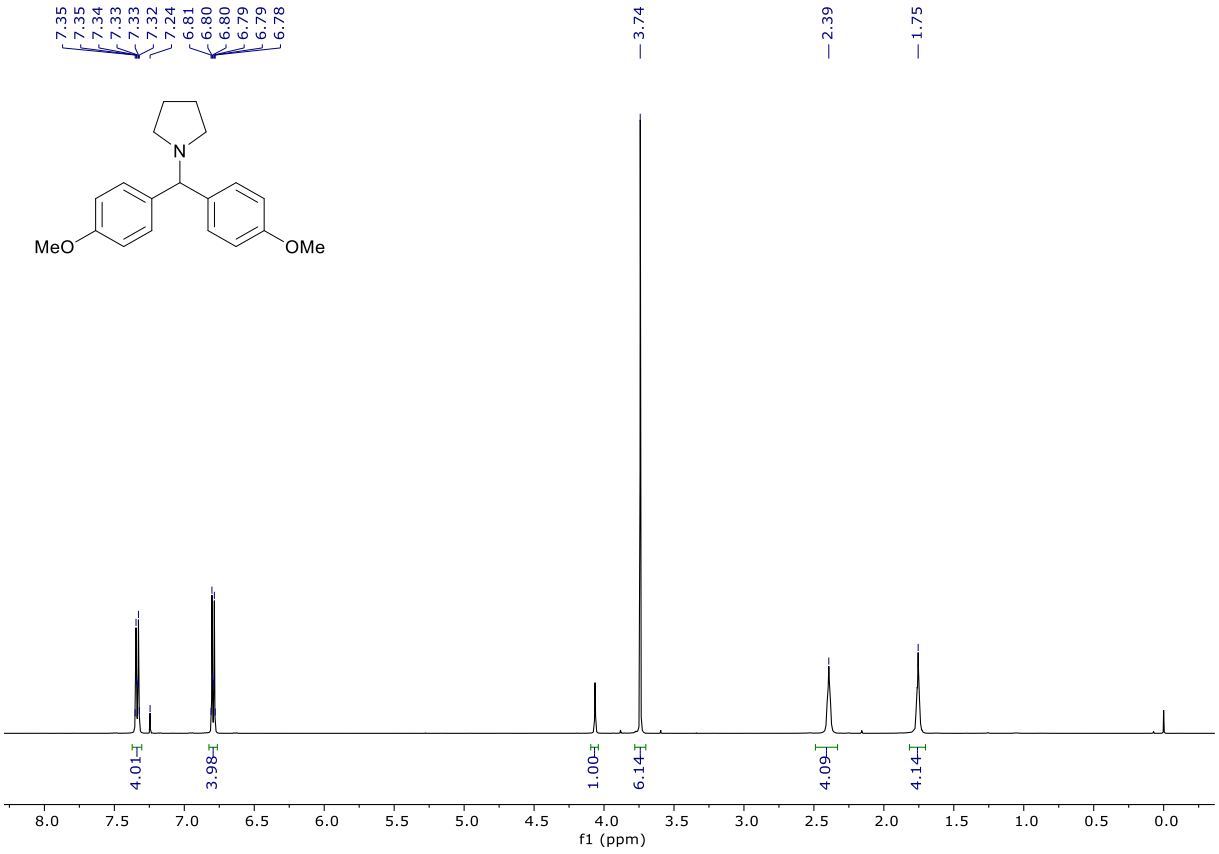

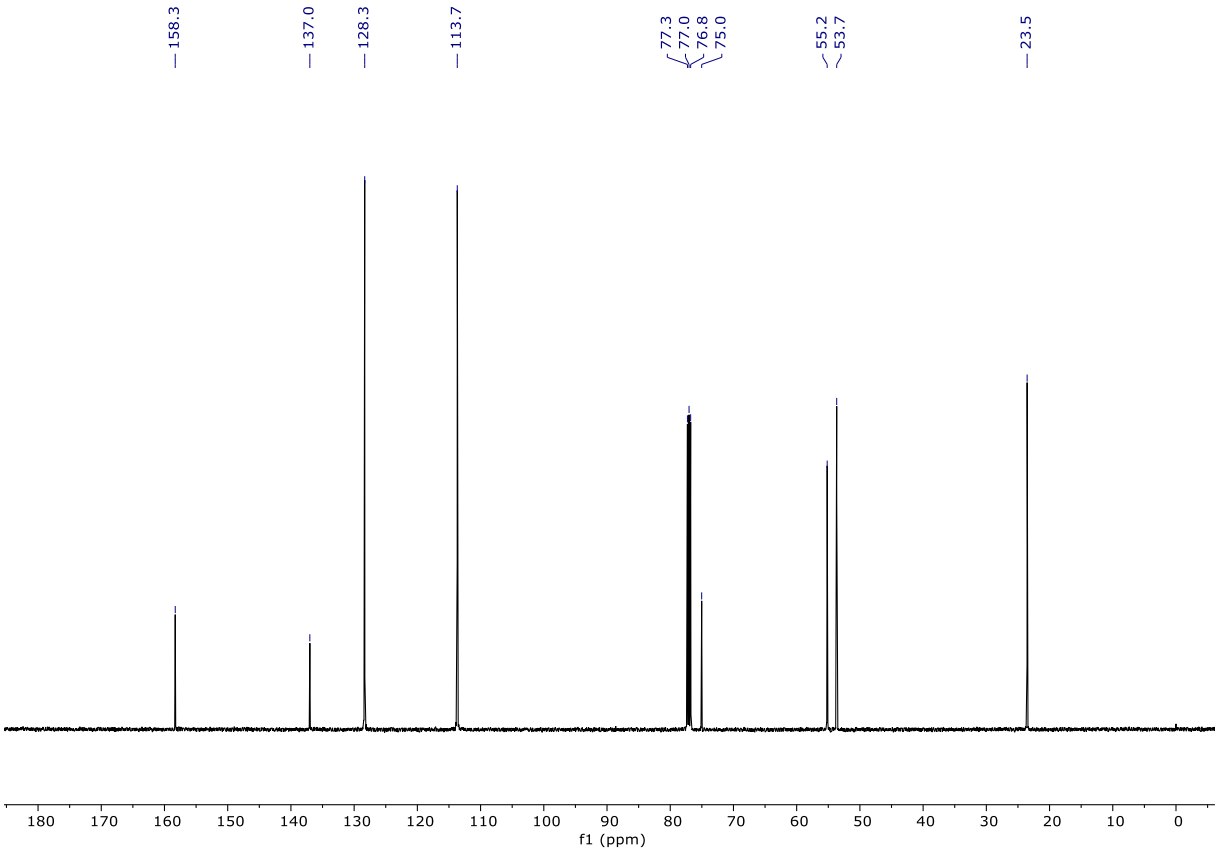

N-(bis(4-methoxyphenyl)methyl)aniline (16)

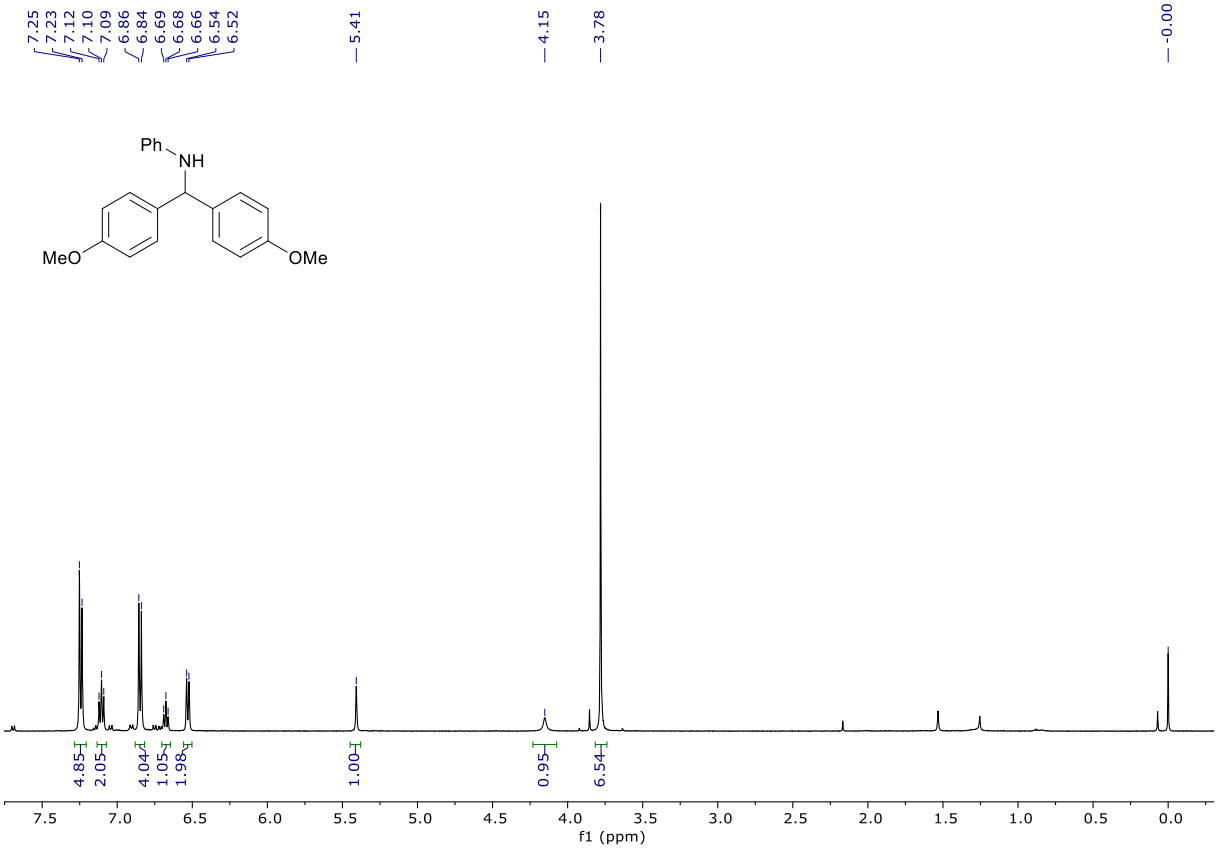

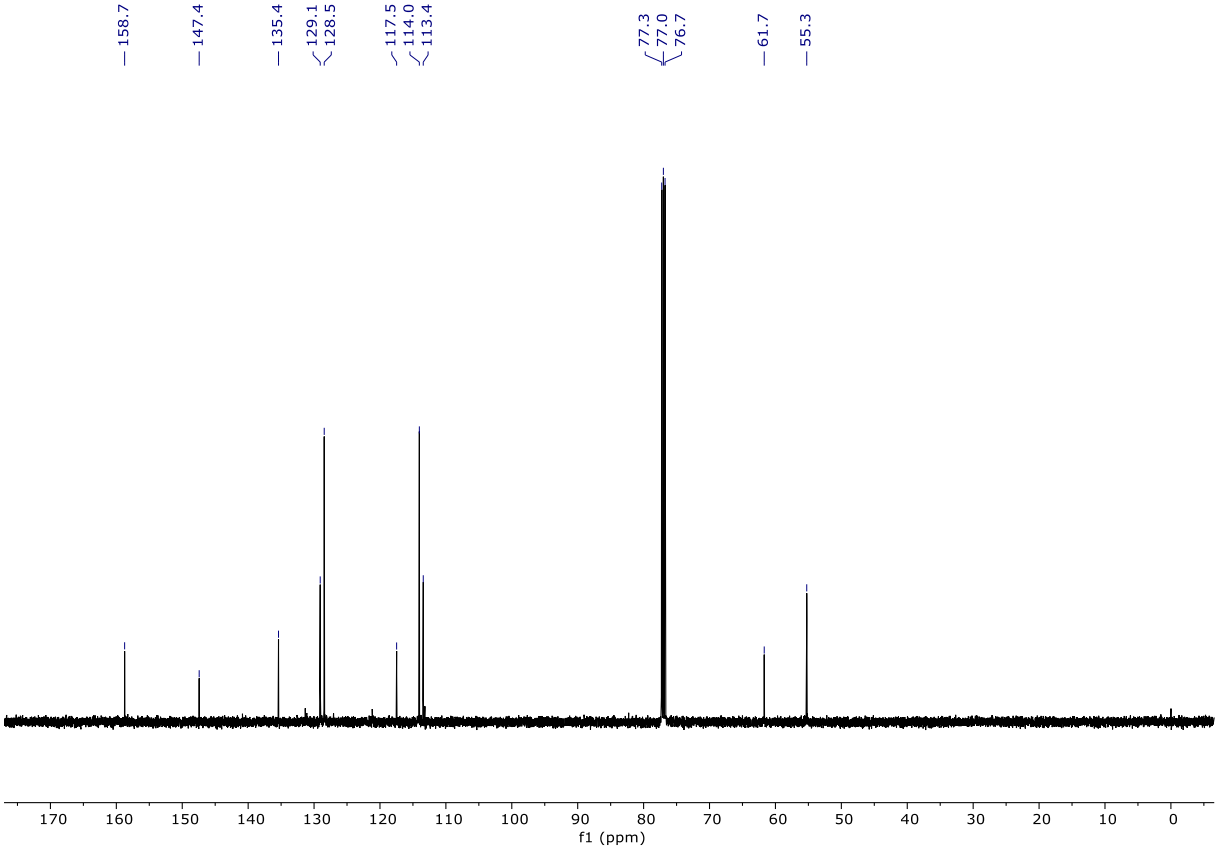

1-(bis(4-methoxyphenyl)methyl)indoline (17)

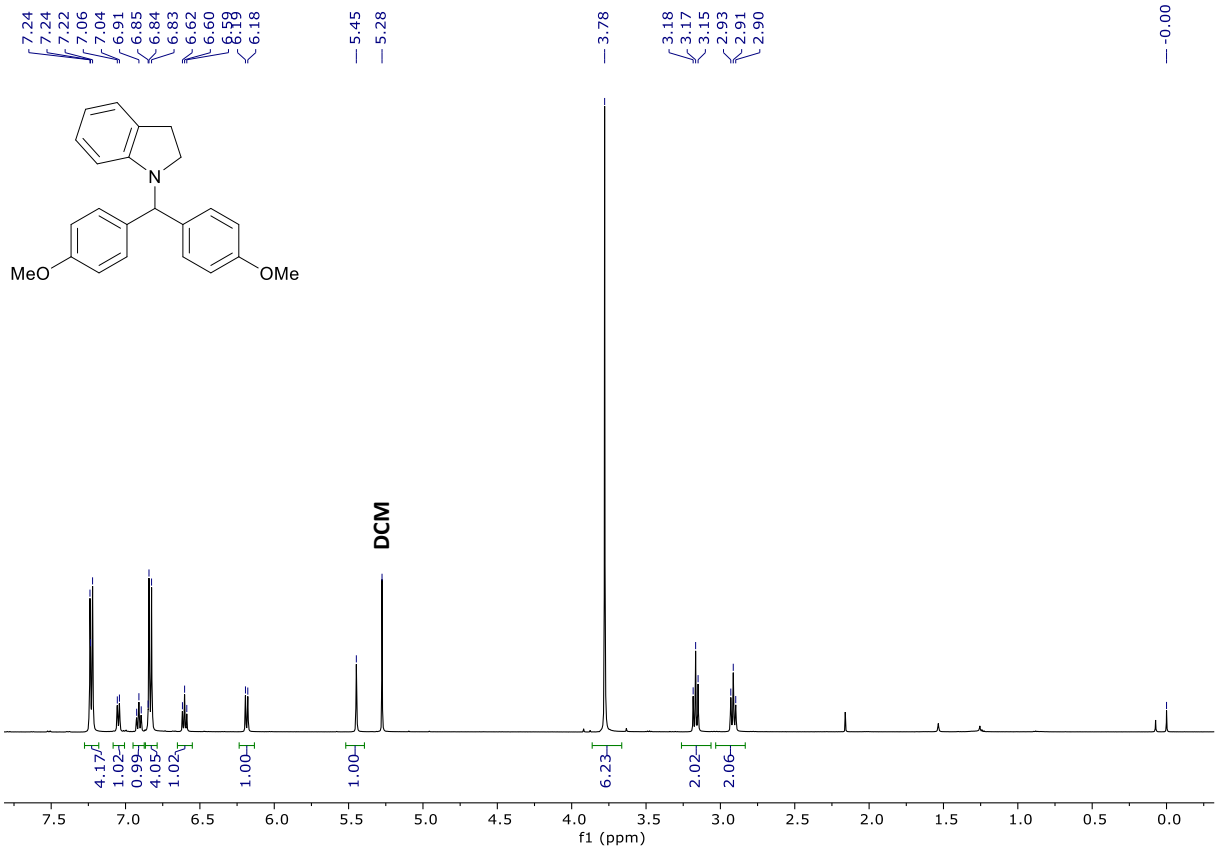

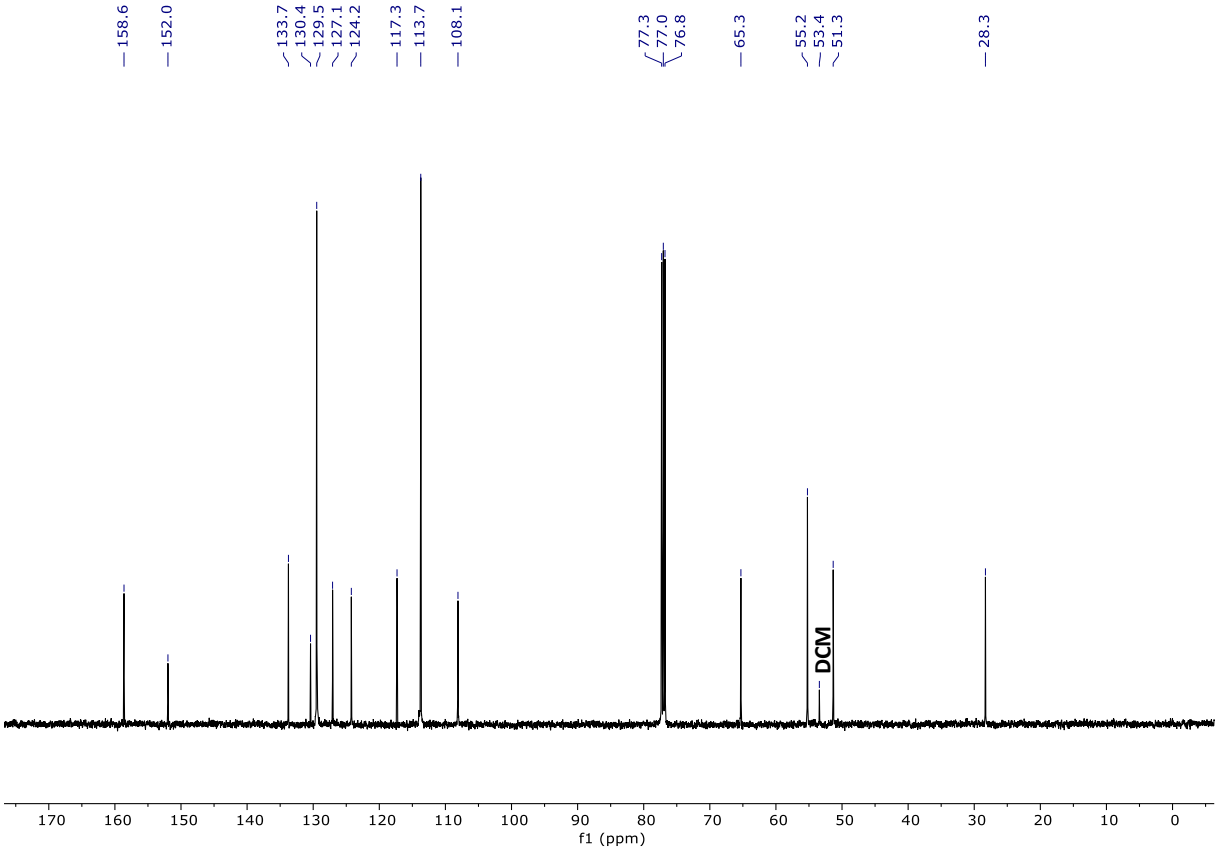

1-(bis(4-methoxyphenyl)methyl)pyridin-2(1H)-one (18)

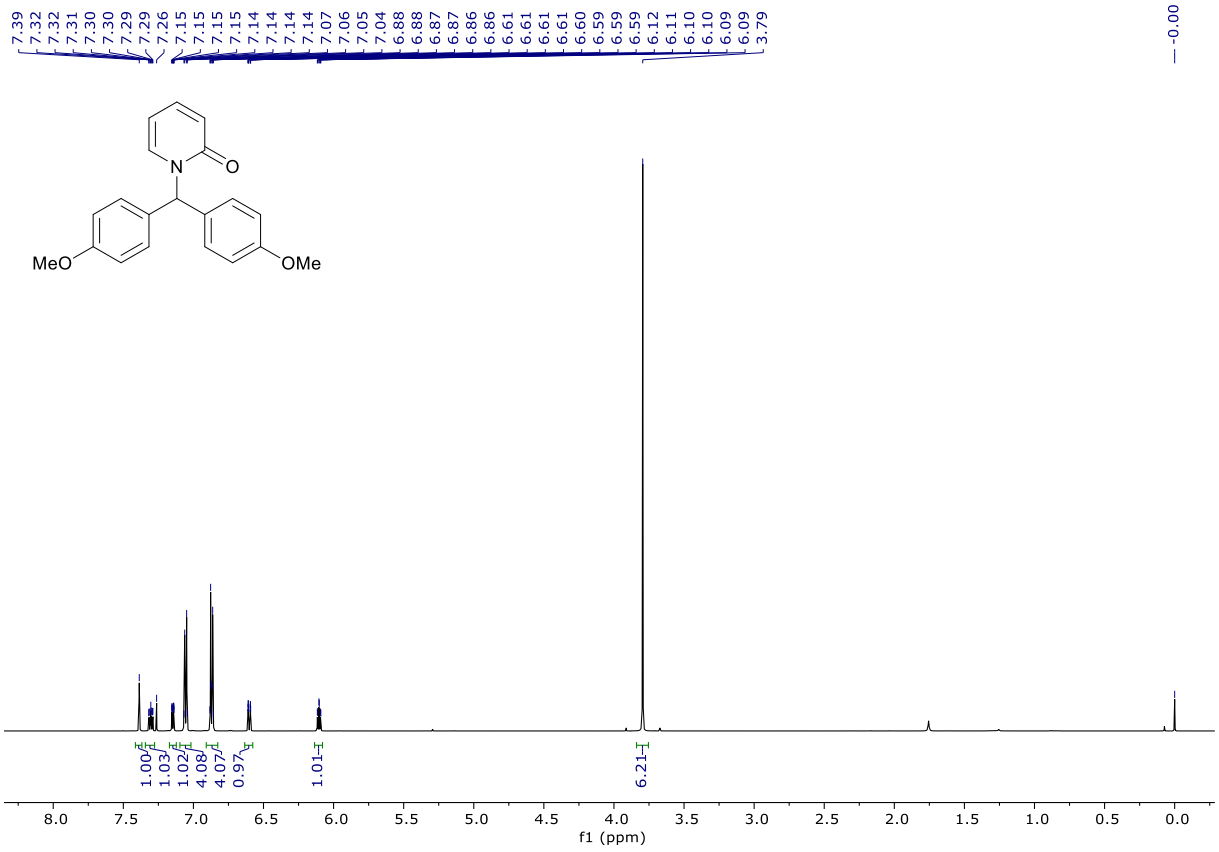

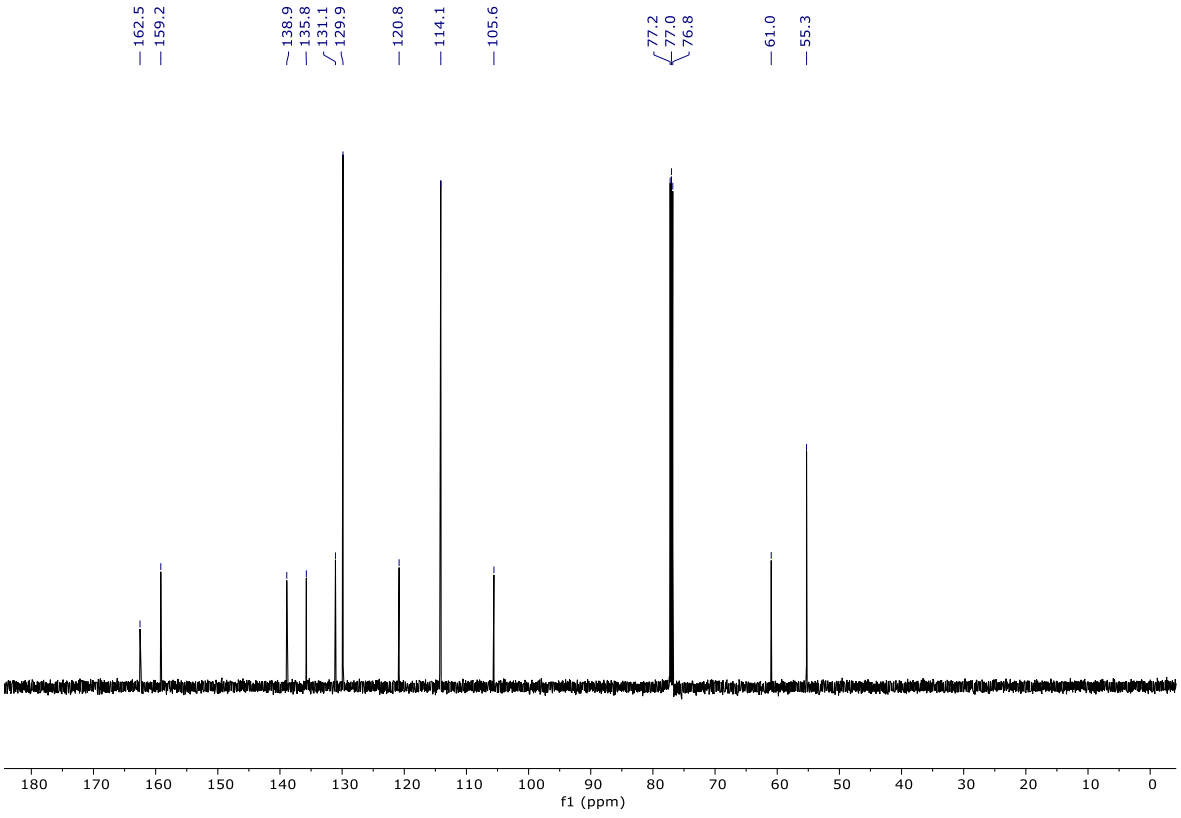

benzyl(bis(4-methoxyphenyl)methyl)sulfane (19)

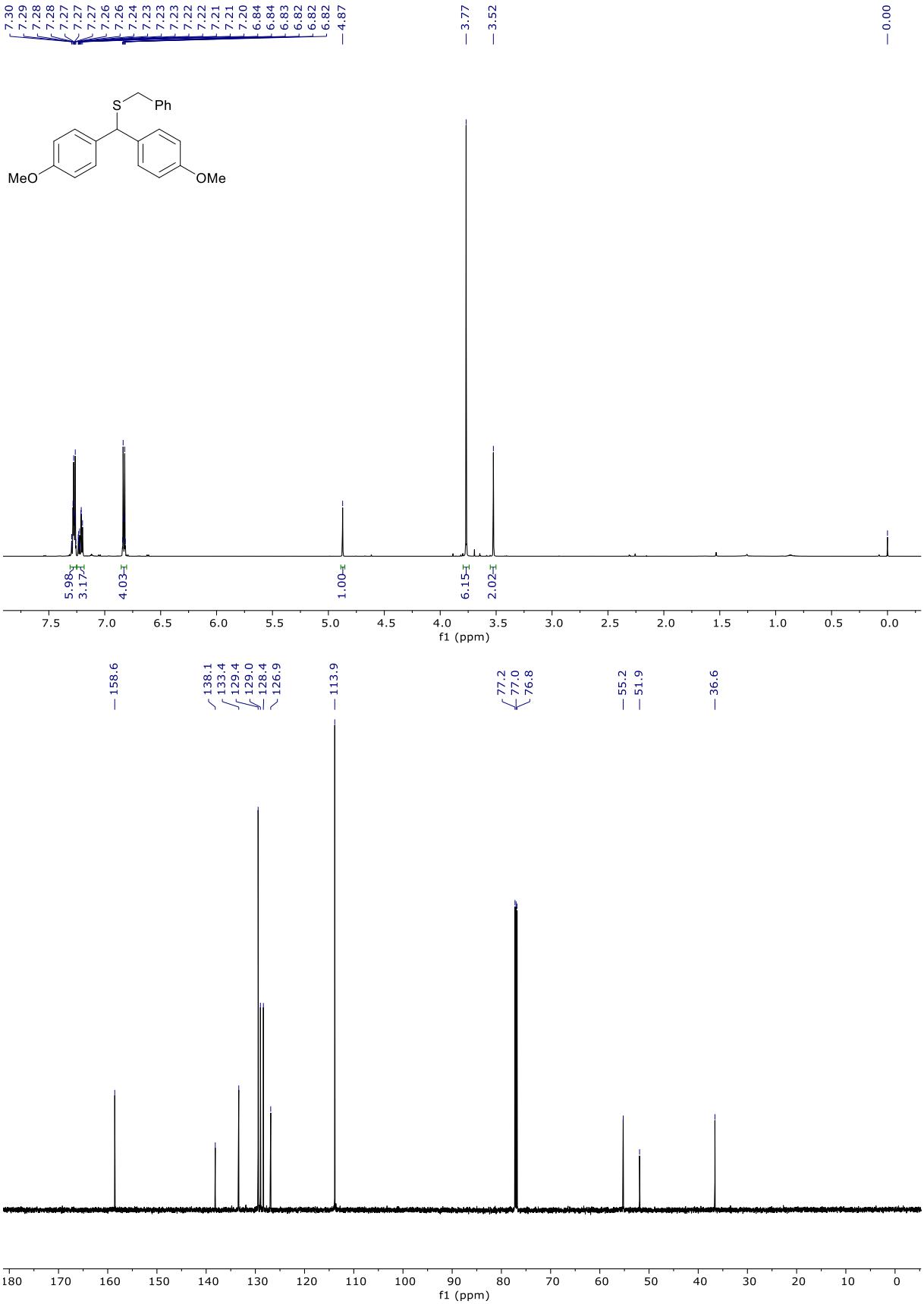

(bis(4-methoxyphenyl)methyl)(phenyl)sulfane (20)

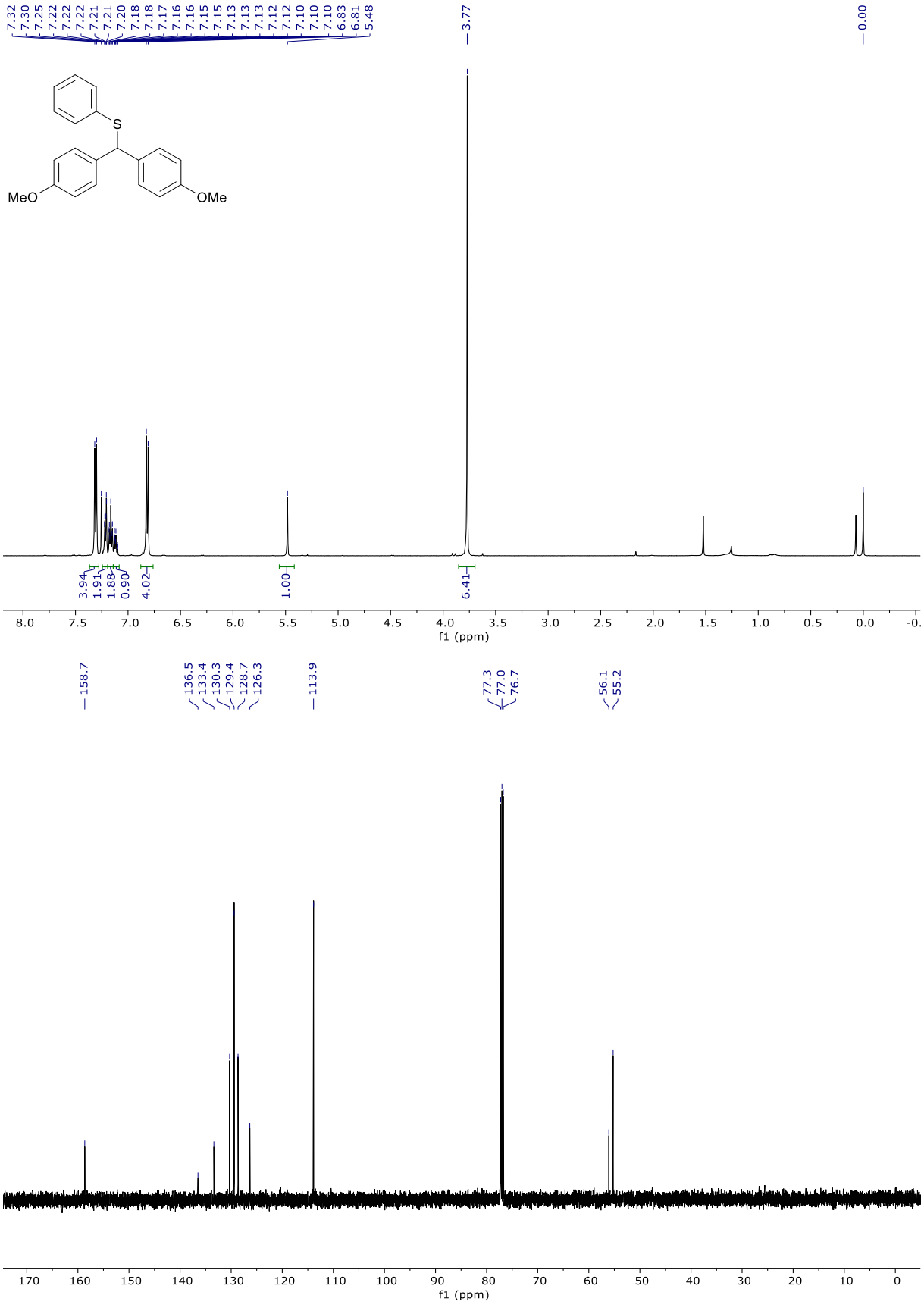

adamantan-1-yl(bis(4-methoxyphenyl)methyl)sulfane (21)

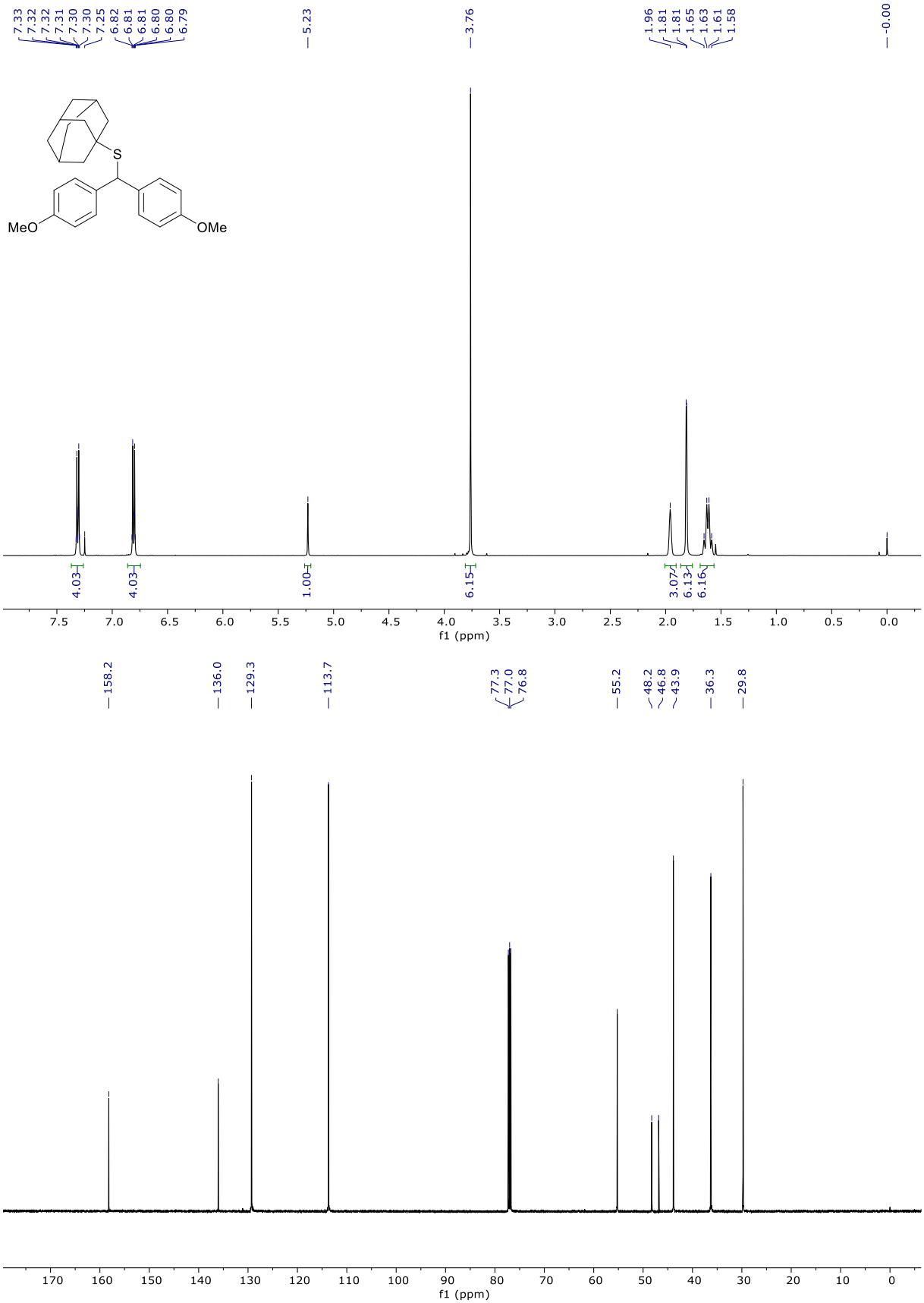

9-(benzylthio)-9H-thioxanthene (22)

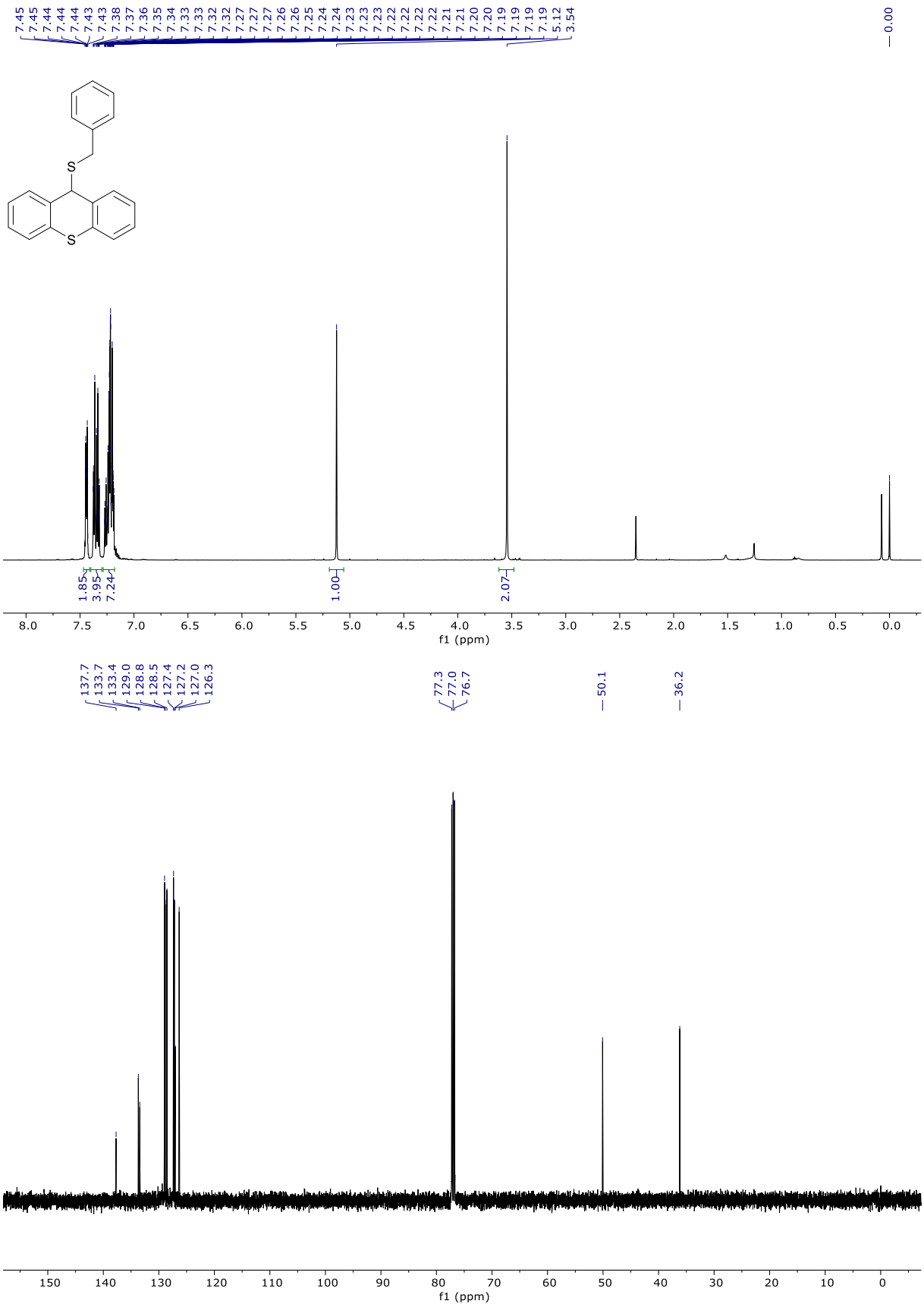

methyl N,S-bis(bis(4-methoxyphenyl)methyl)-N-(tert-butoxycarbonyl)-L-cysteinate (23)

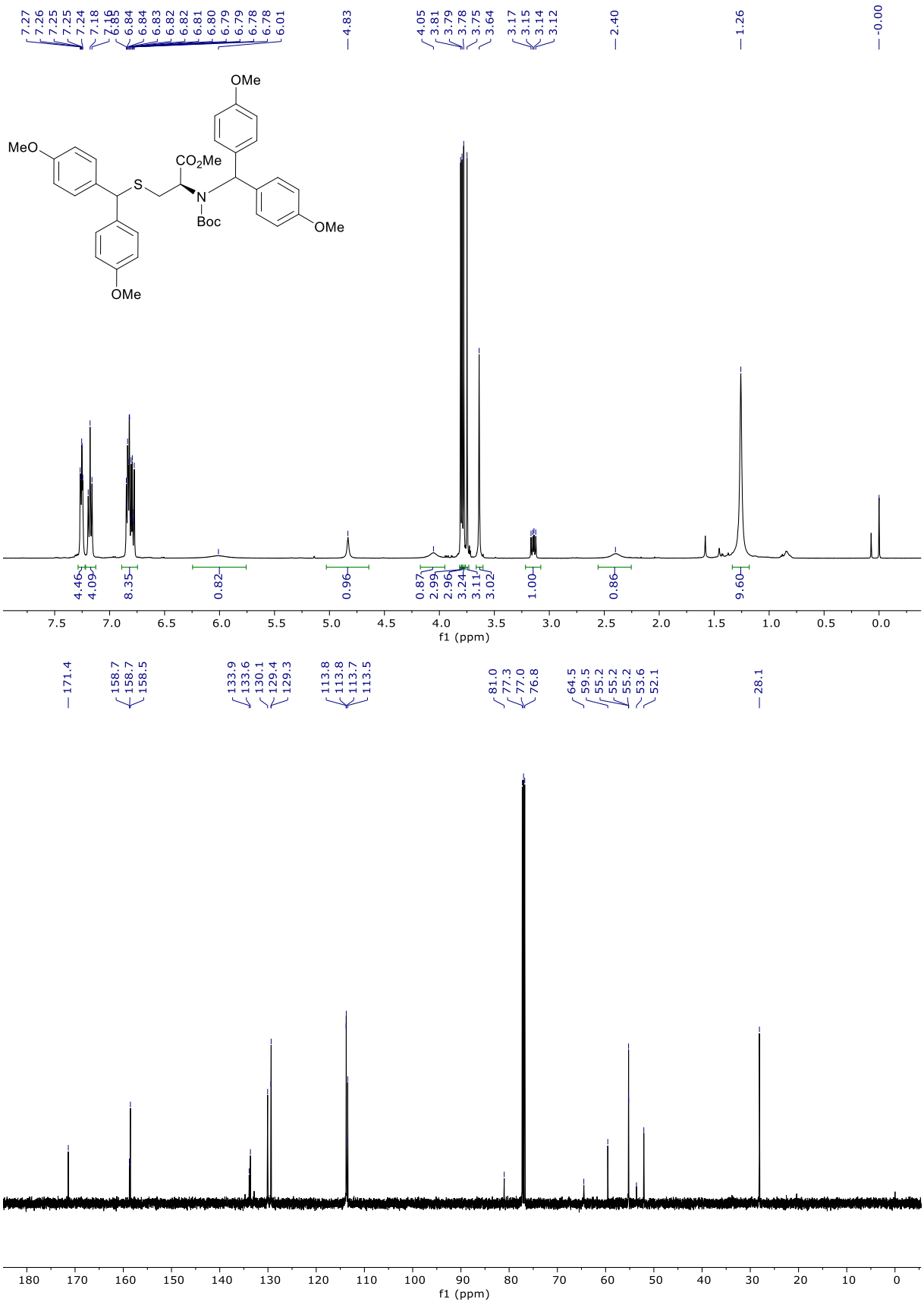

methyl 2-oxo-2-phenylacetate (24)

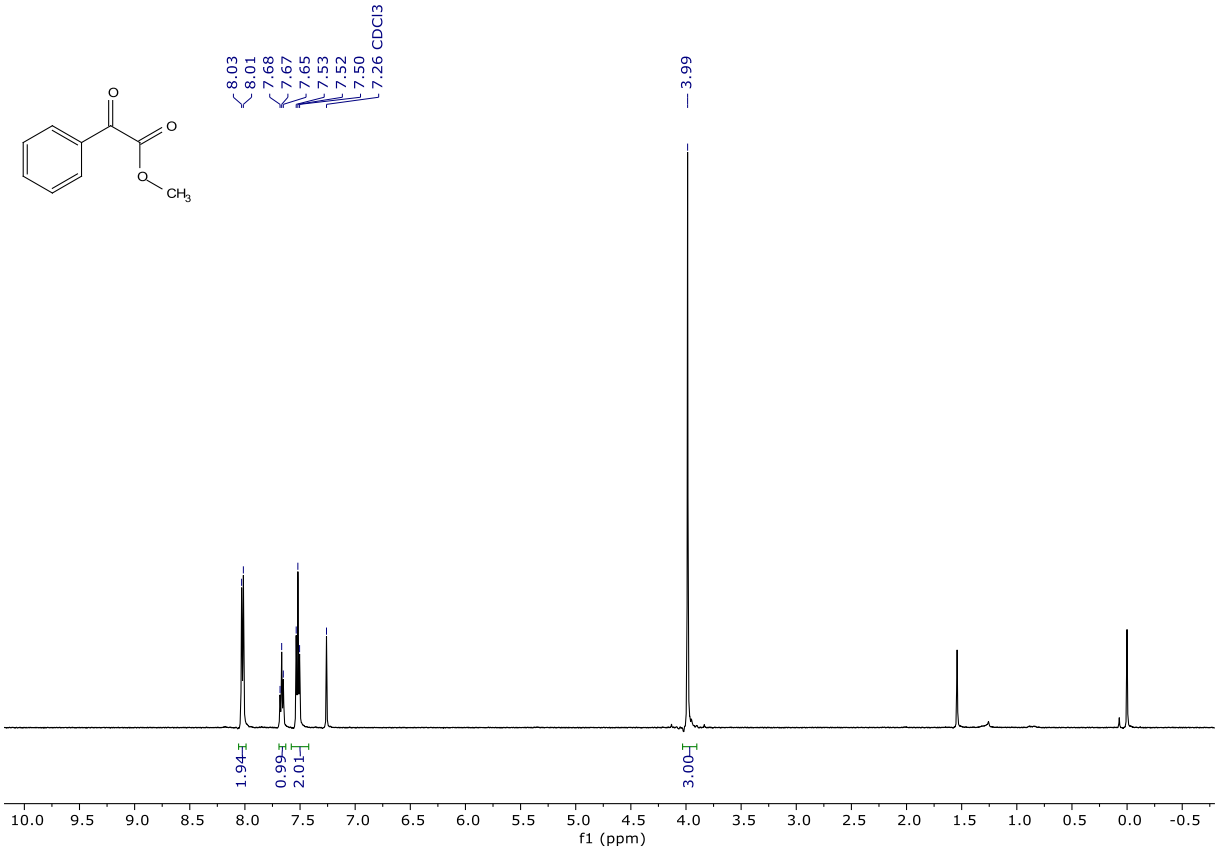

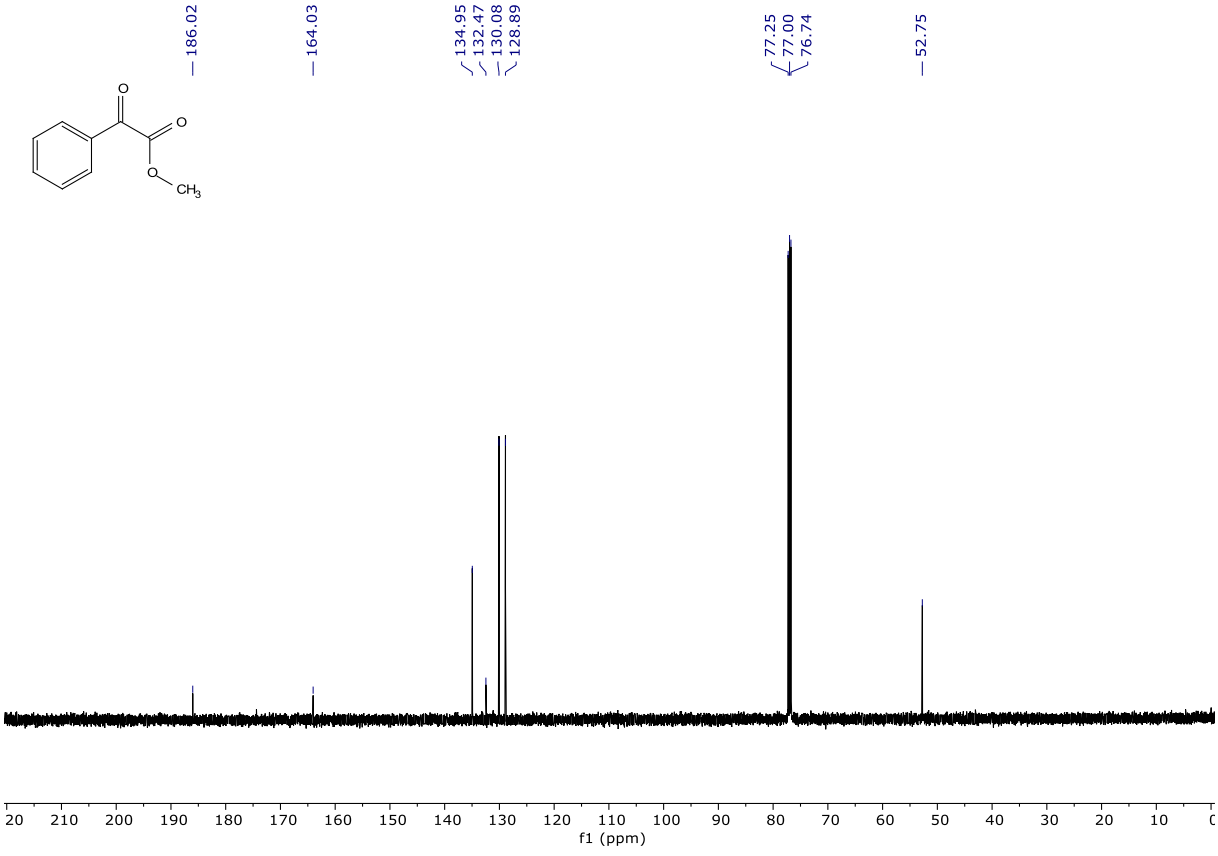

methyl 4-methoxybenzoate (25)

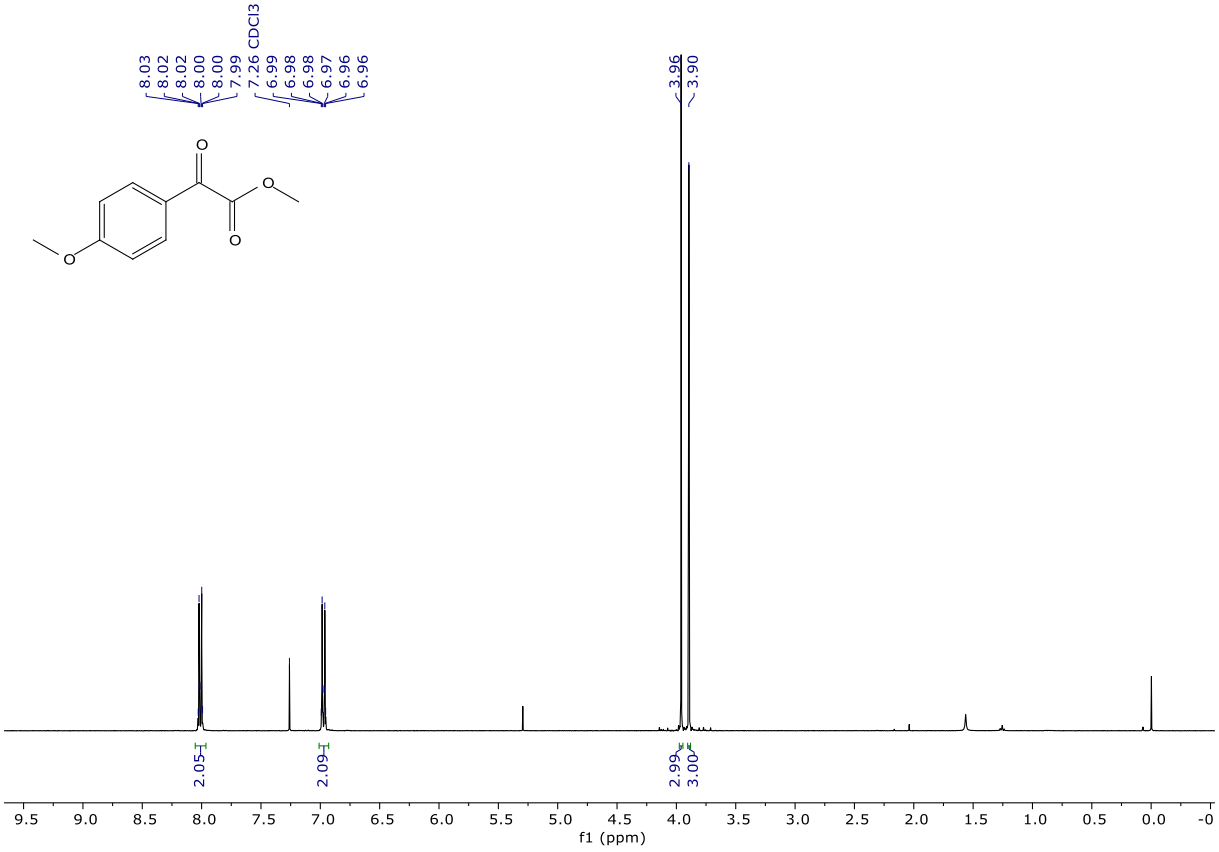

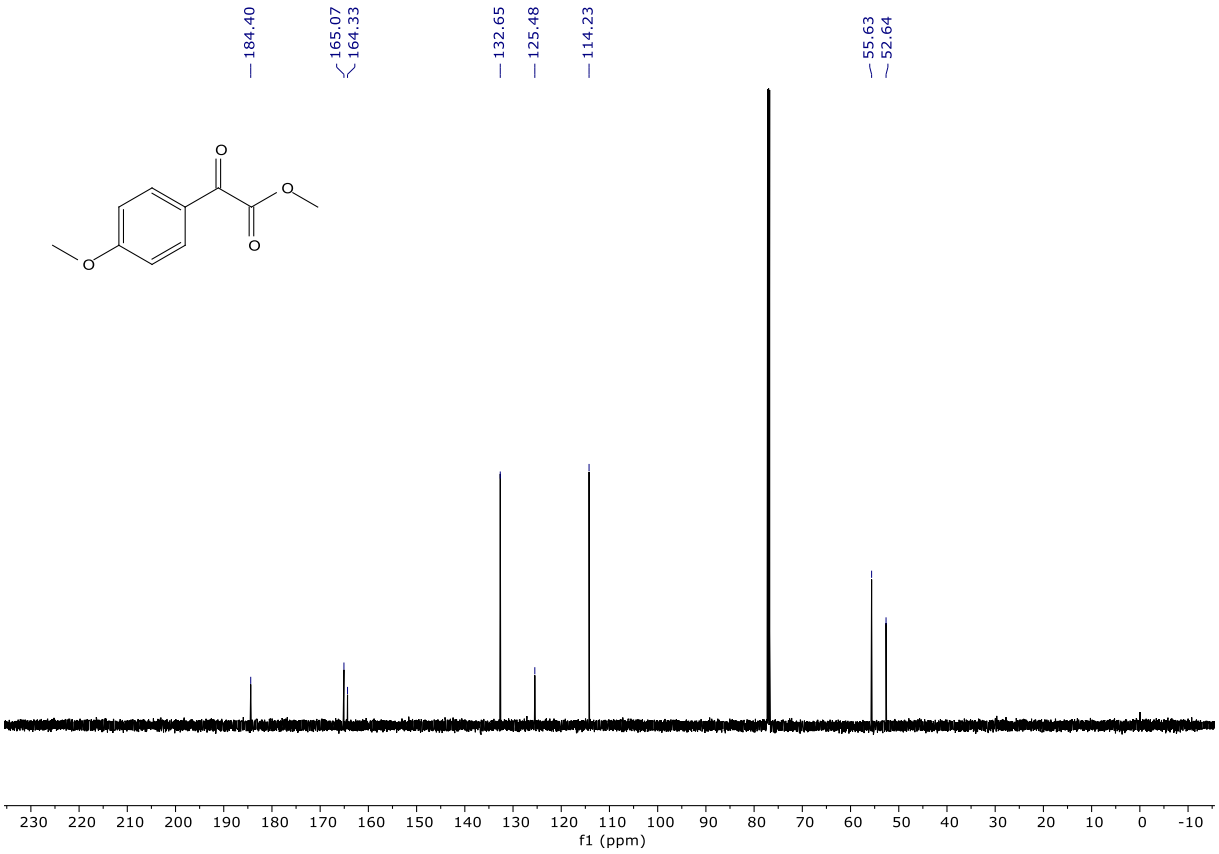

methyl 2-(4-cyanophenyl)-2-oxoacetate (26)

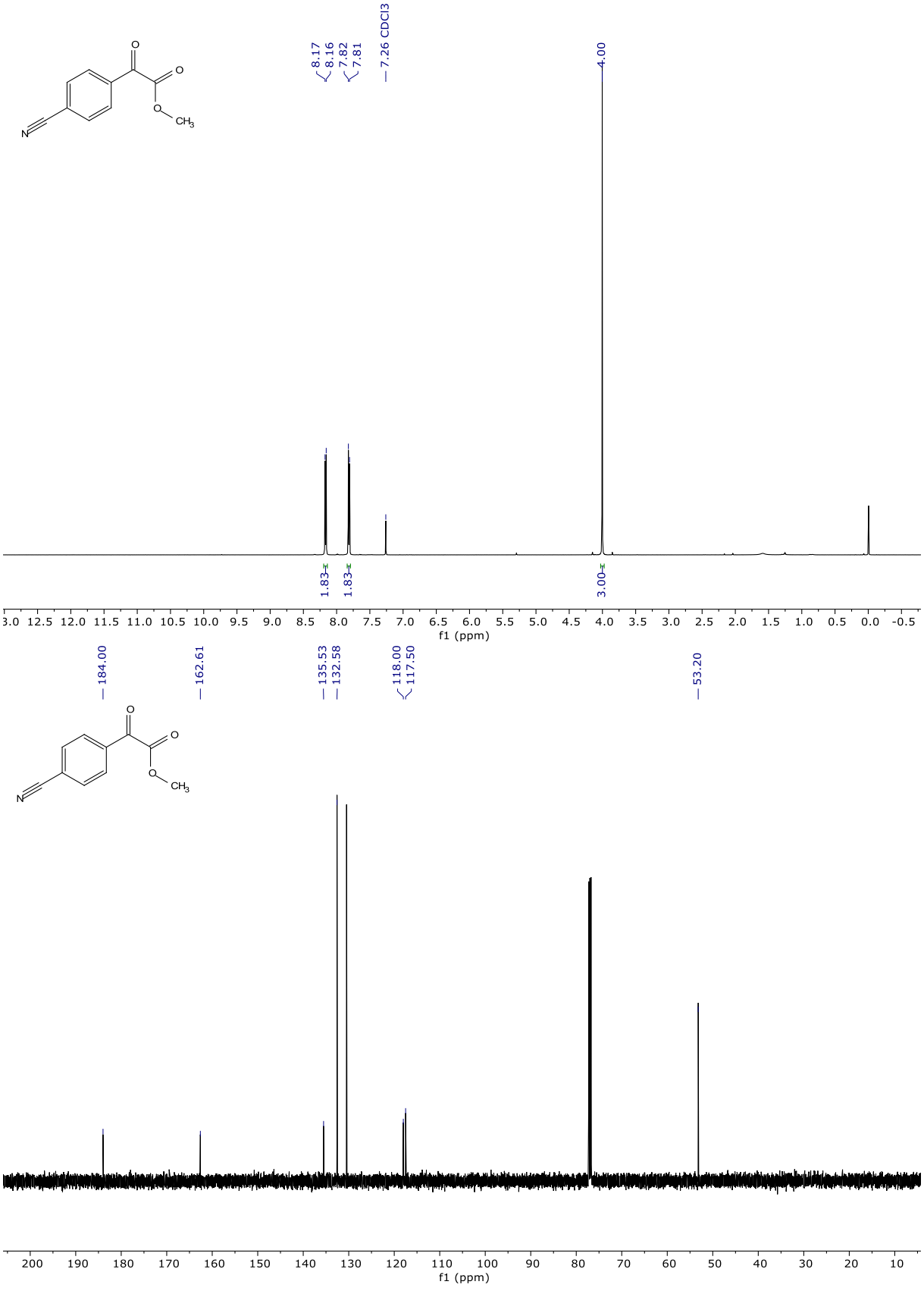

2-methoxy-2-oxo-1-phenylethyl benzoate (27)

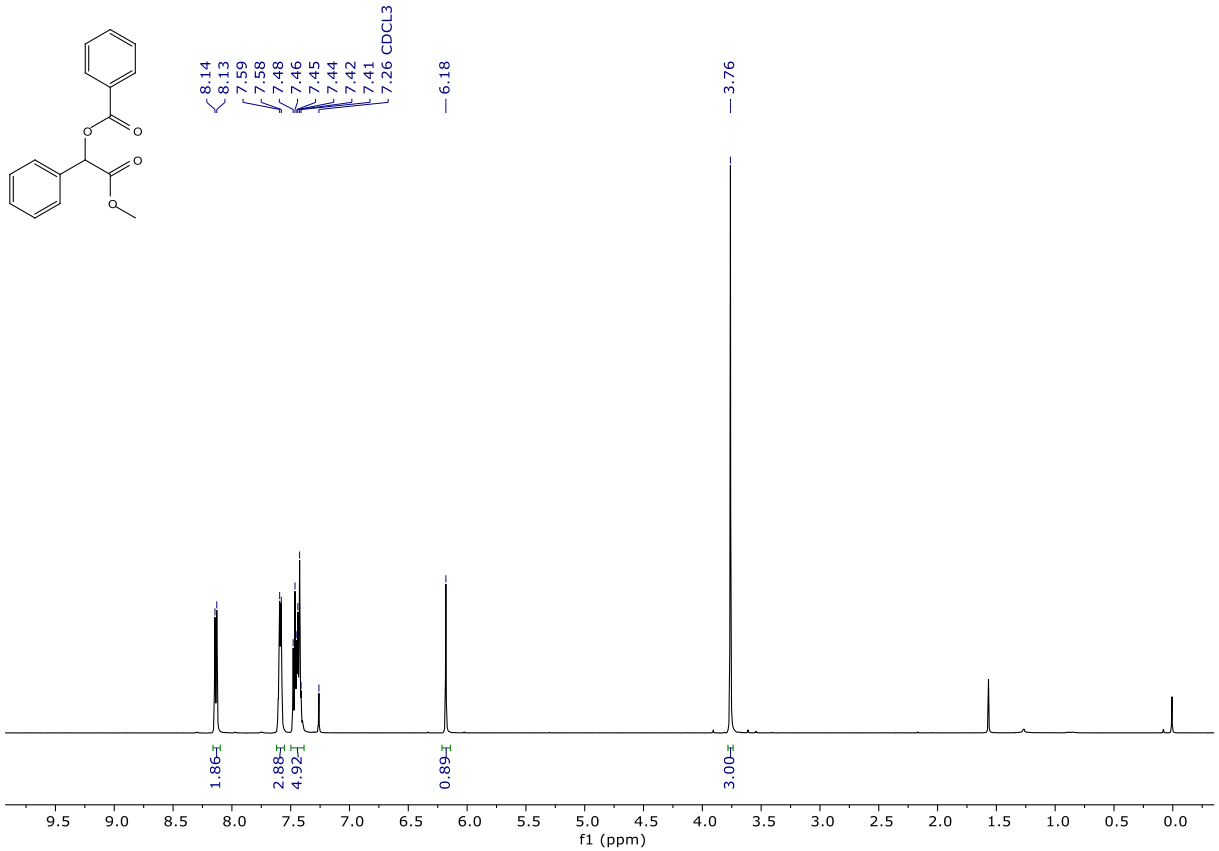

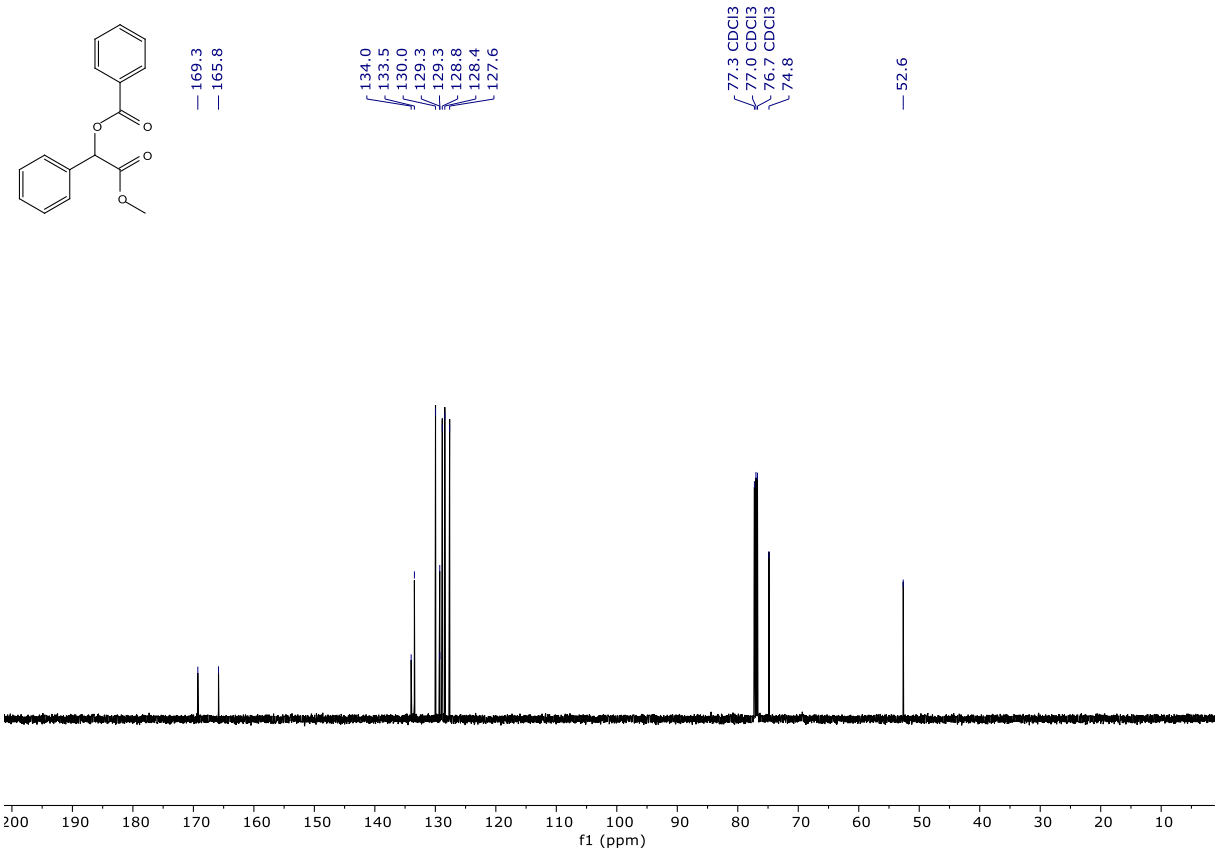

2-methoxy-1-(4-methoxyphenyl)-2-oxoethyl benzoate (28)

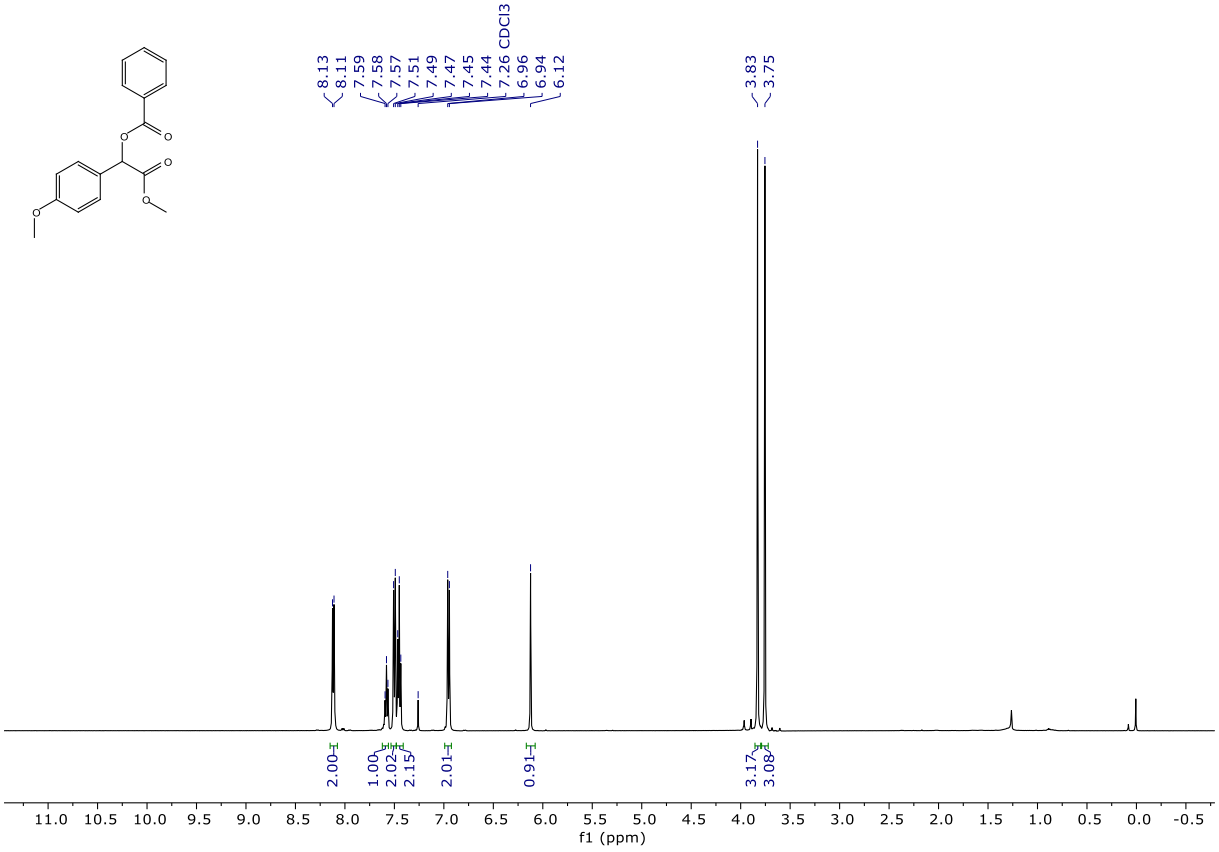

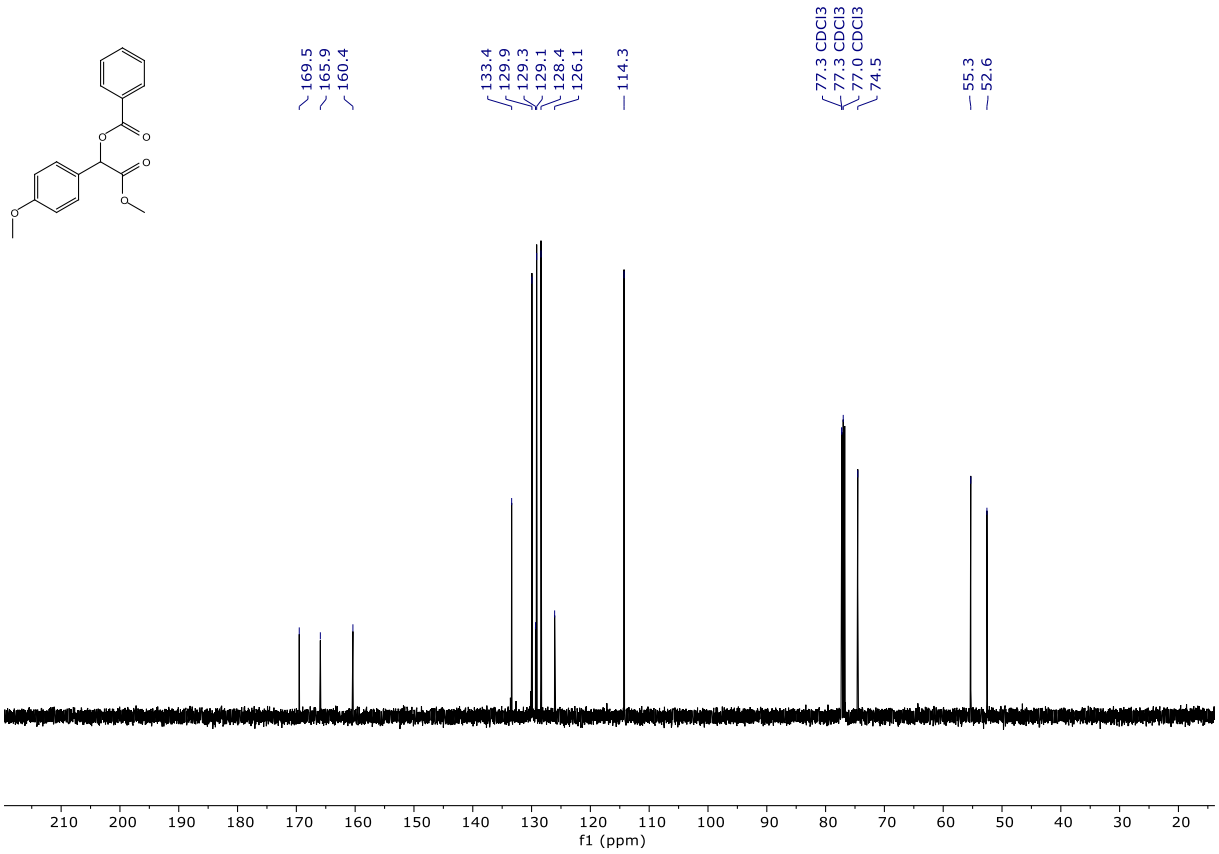

1-(4-bromophenyl)-2-ethoxy-2-oxoethyl benzoate (29)

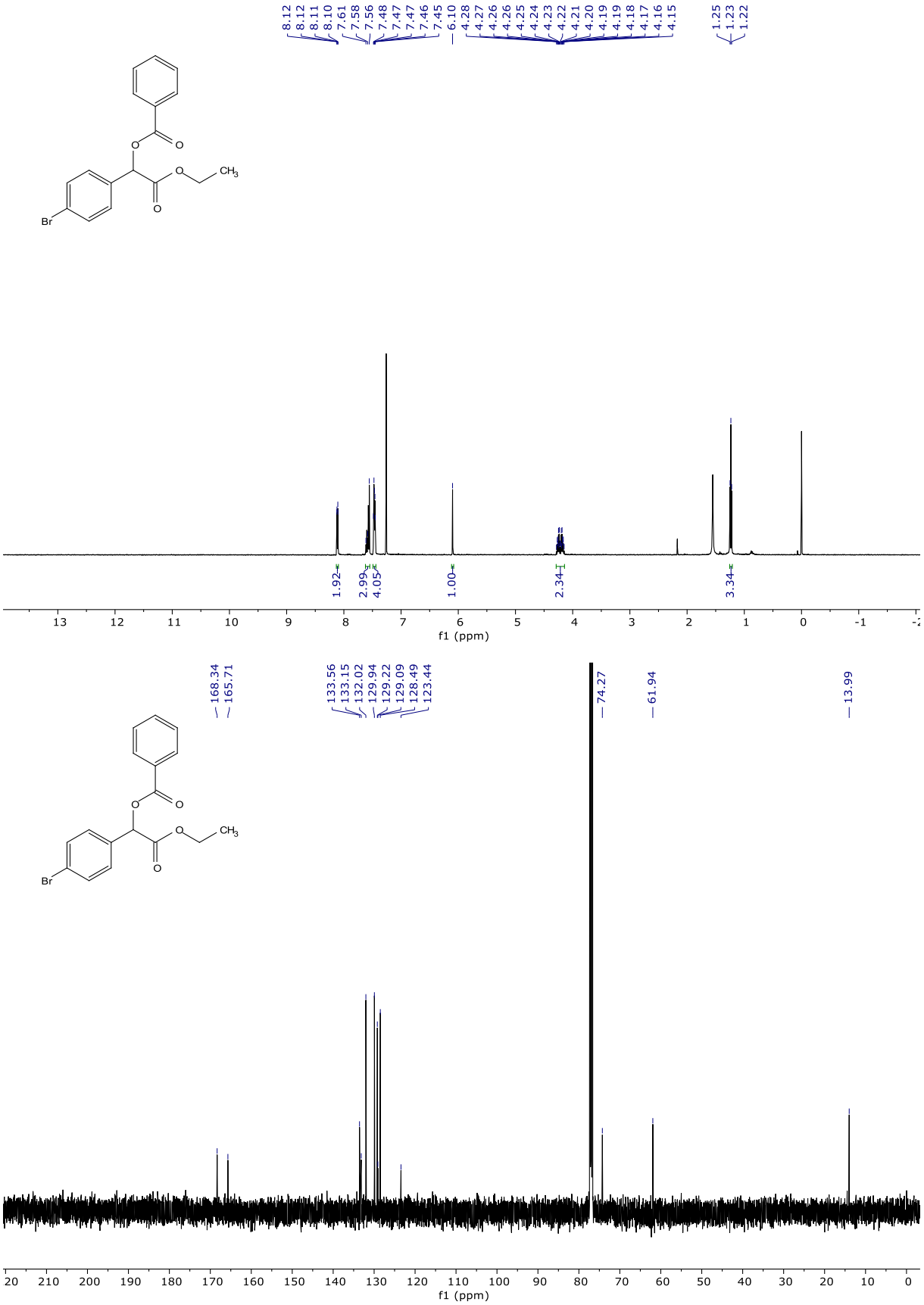

1-(4-fluorophenyl)-2-methoxy-2-oxoethyl benzoate (30)

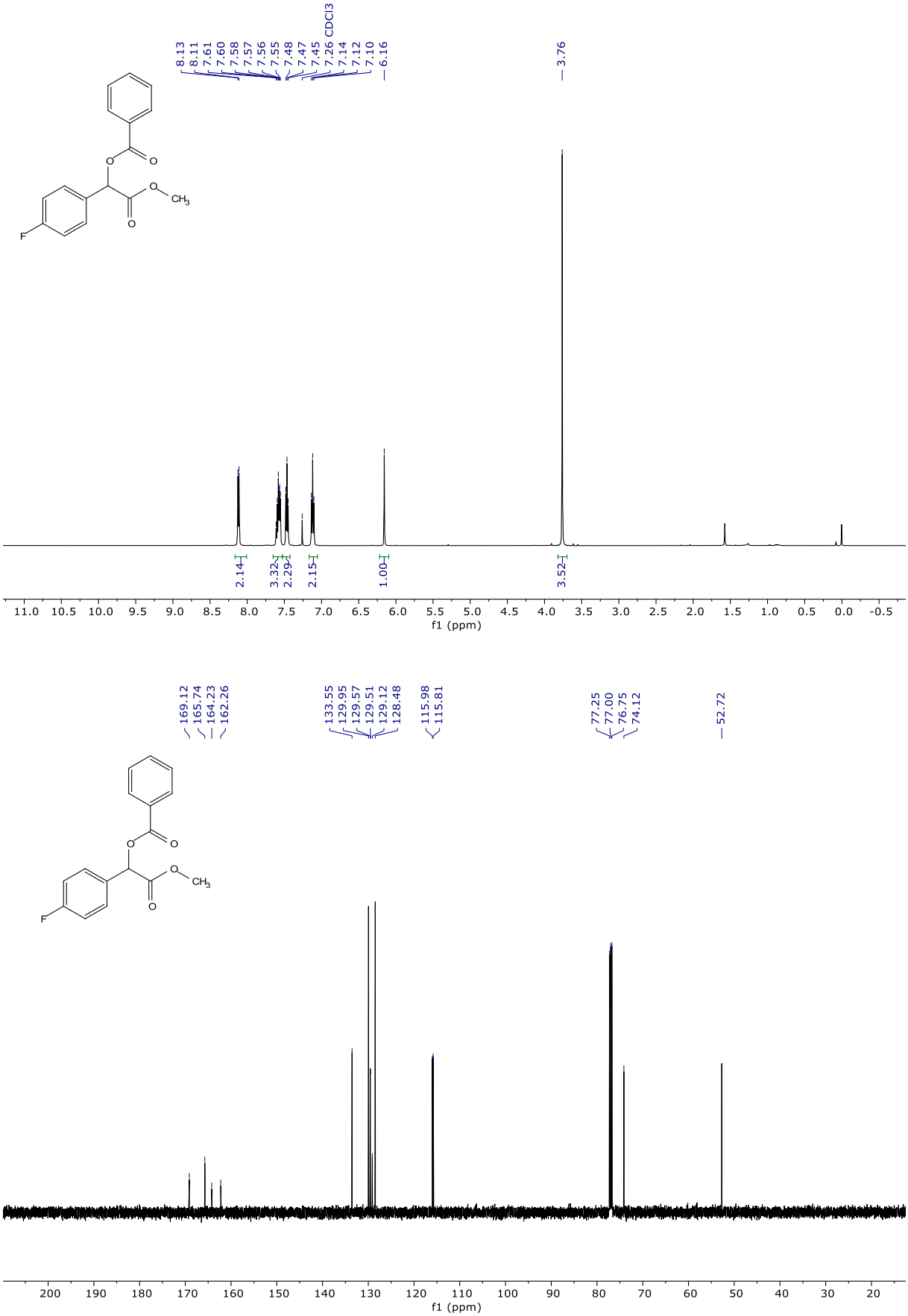

methyl 1,2-diphenylcyclopropane-1-carboxylate (31)

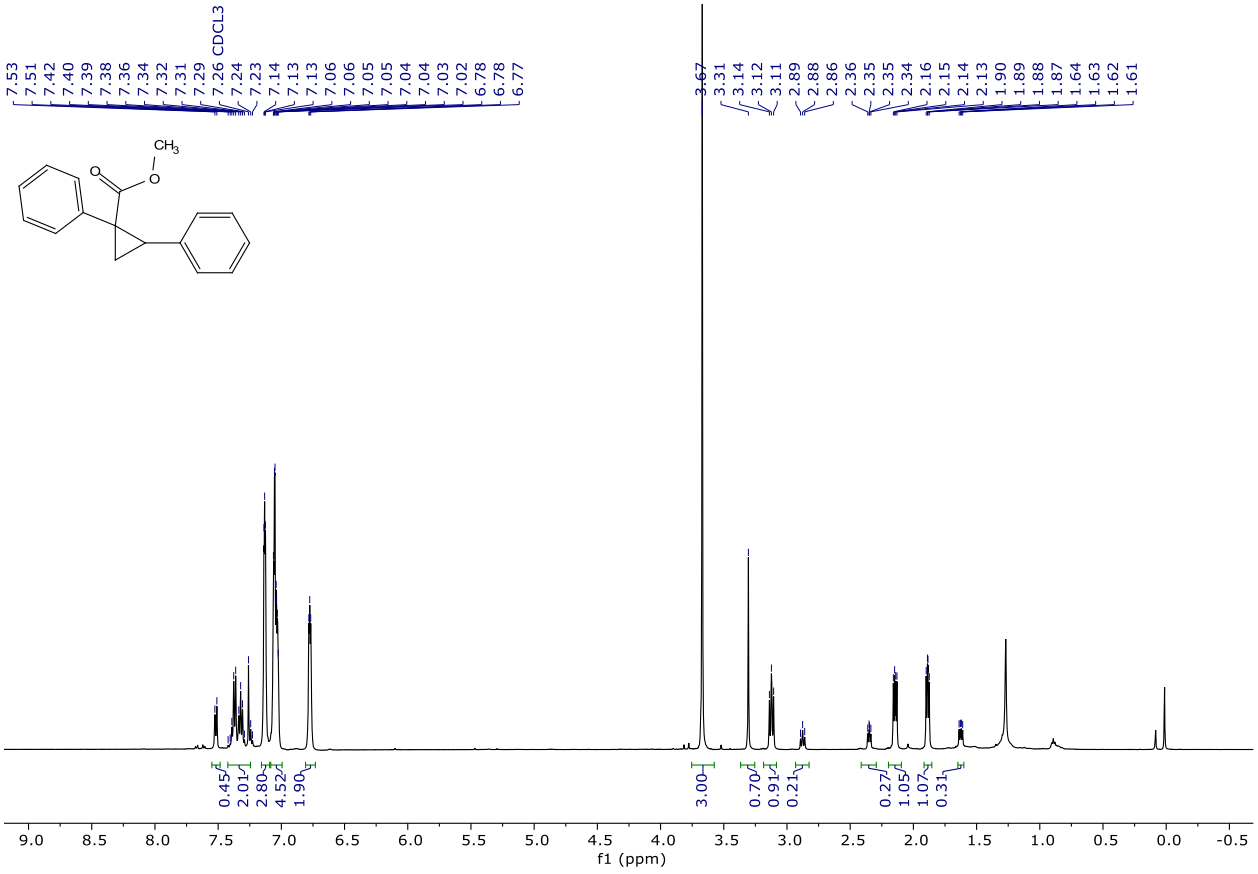

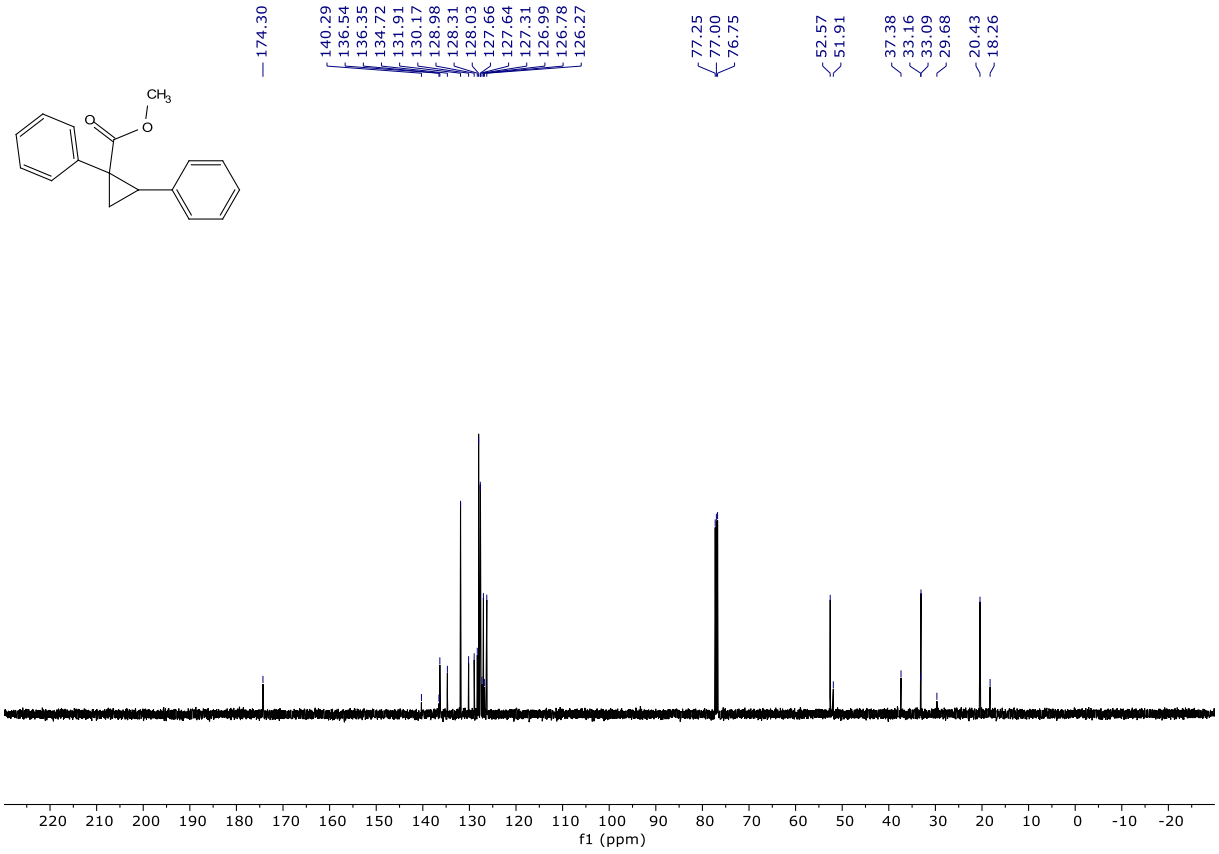

methyl 1-(4-methoxyphenyl)-2-phenylcyclopropane-1-carboxylate (32)

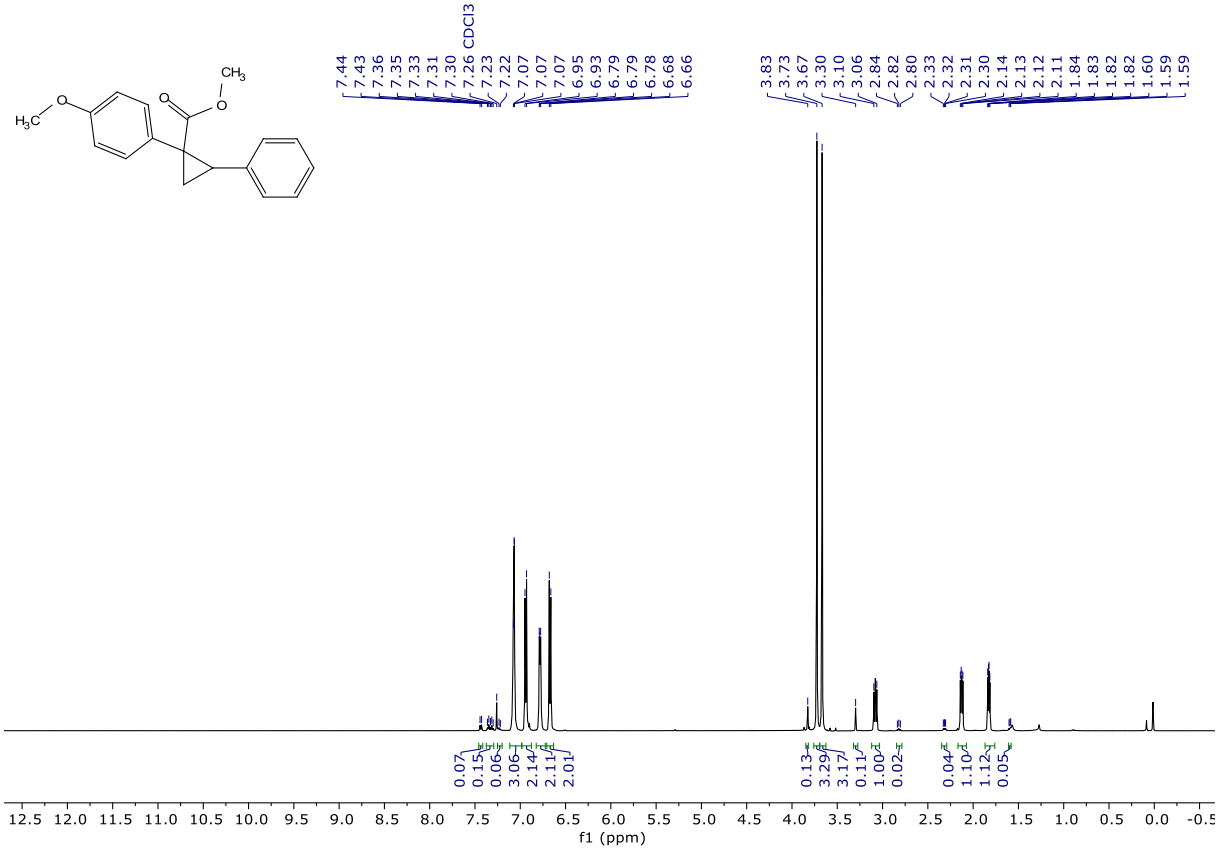

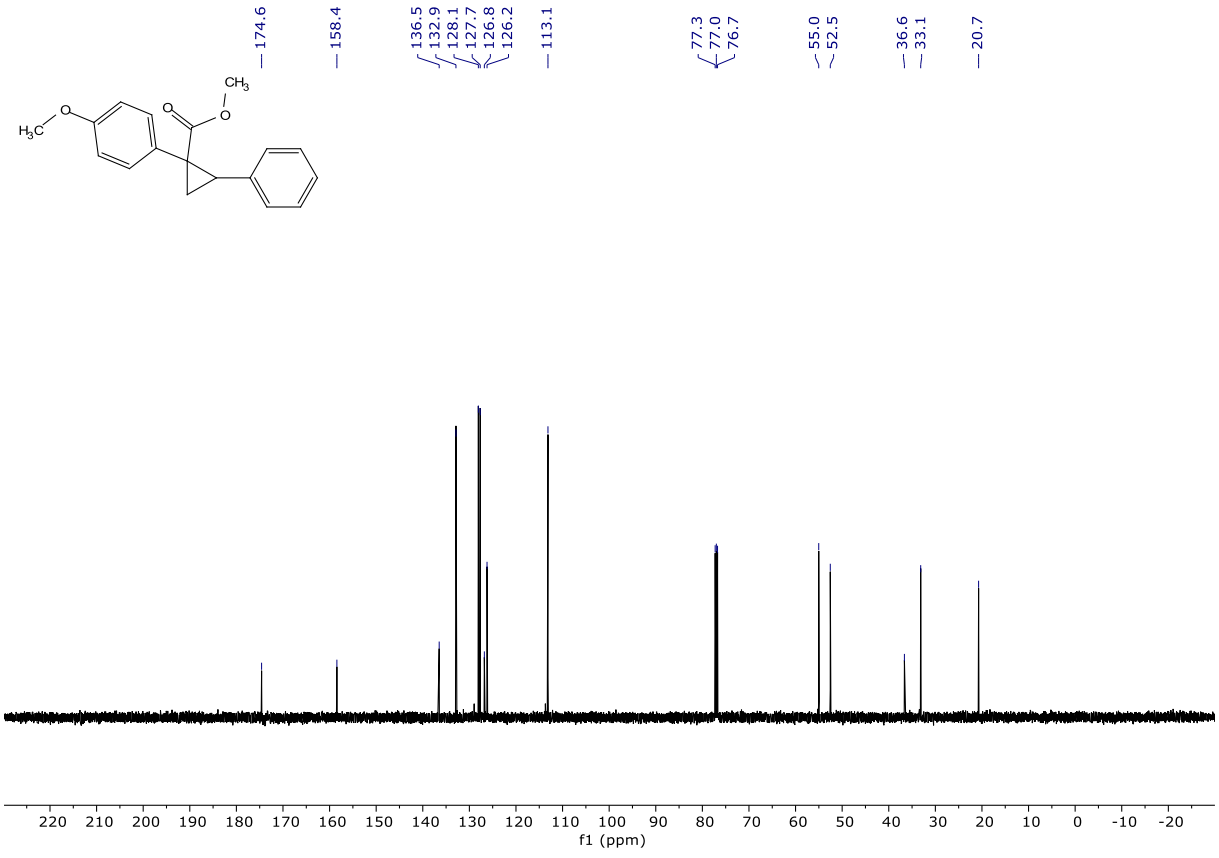

ethyl 1-(4-bromophenyl)-2-phenylcyclopropane-1-carboxylate (33)

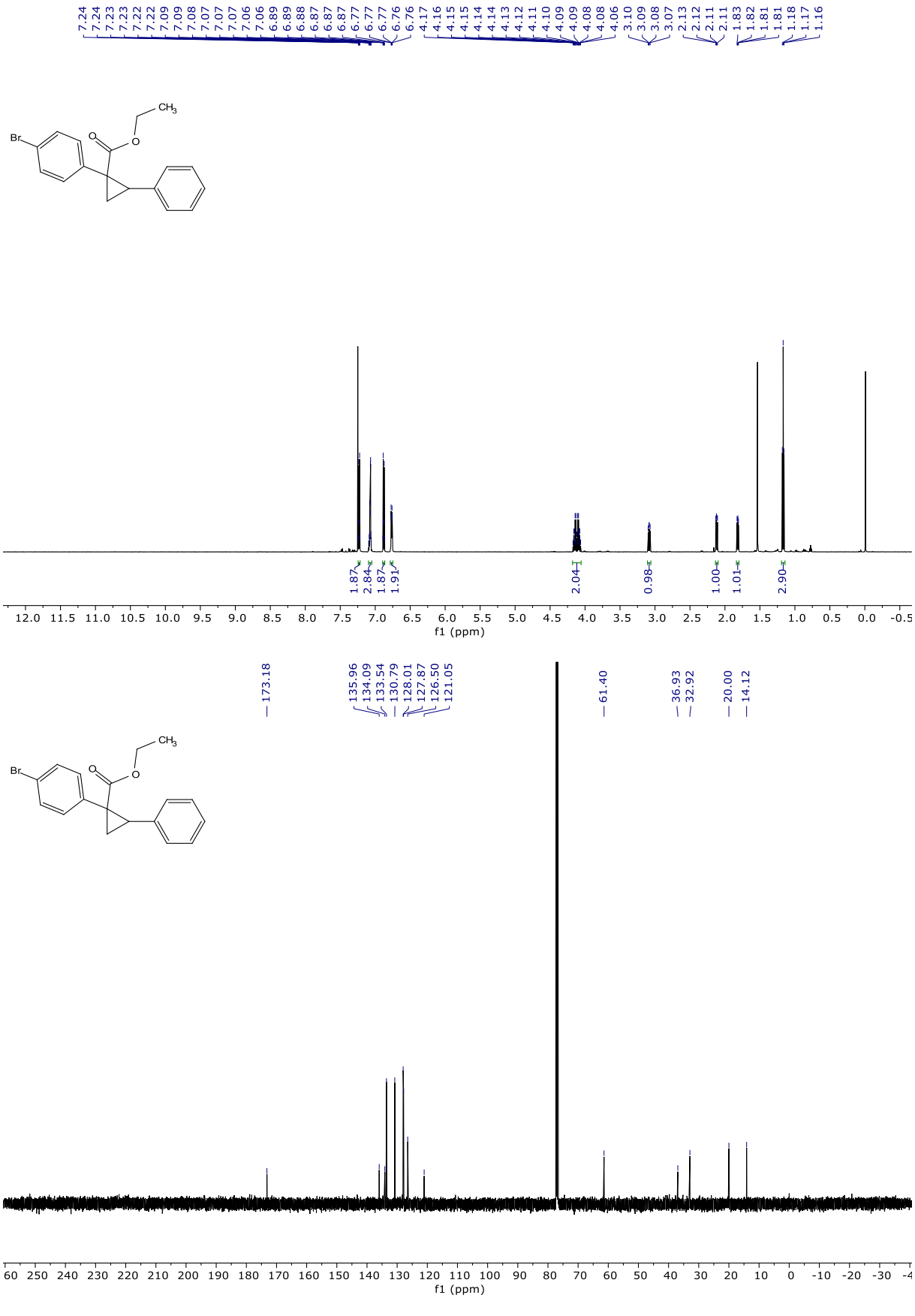

methyl 1-(4-cyanophenyl)-2-phenylcyclopropane-1-carboxylate (34) [86% purity]

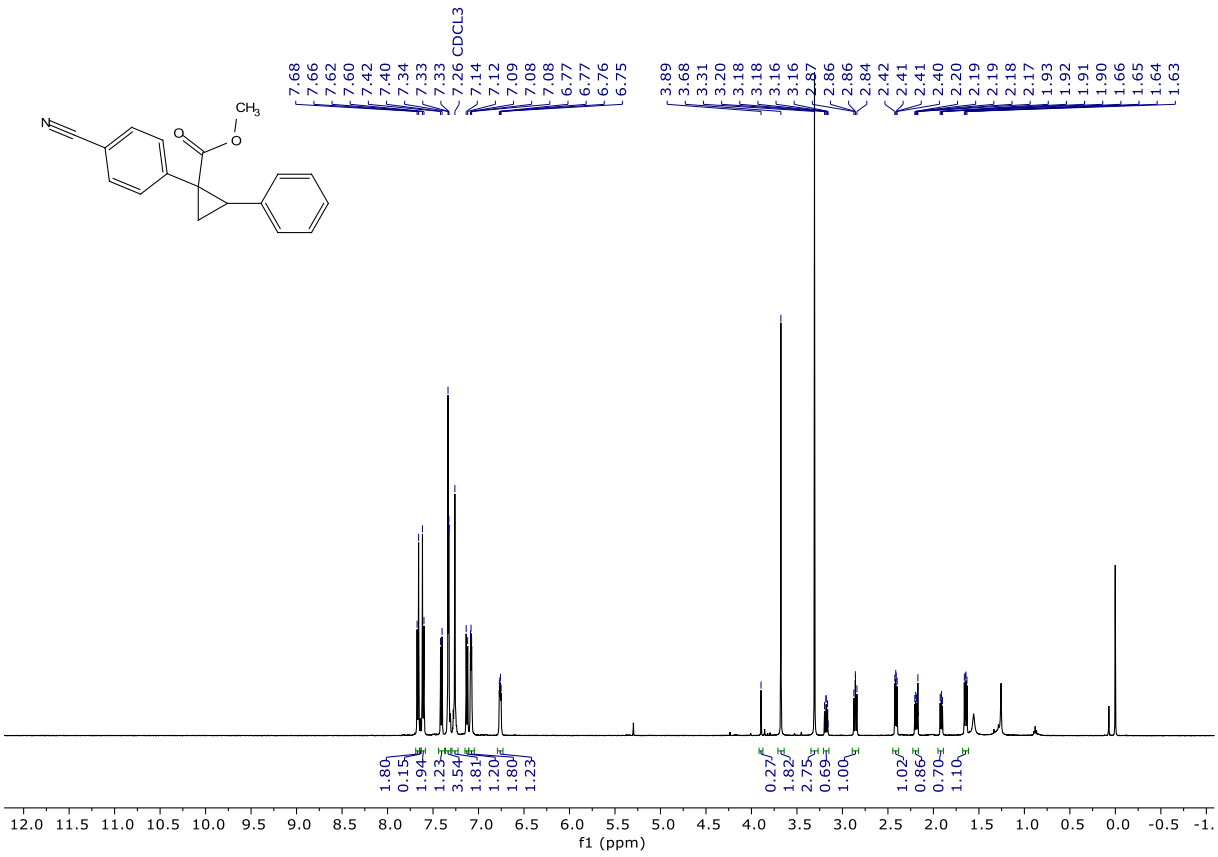

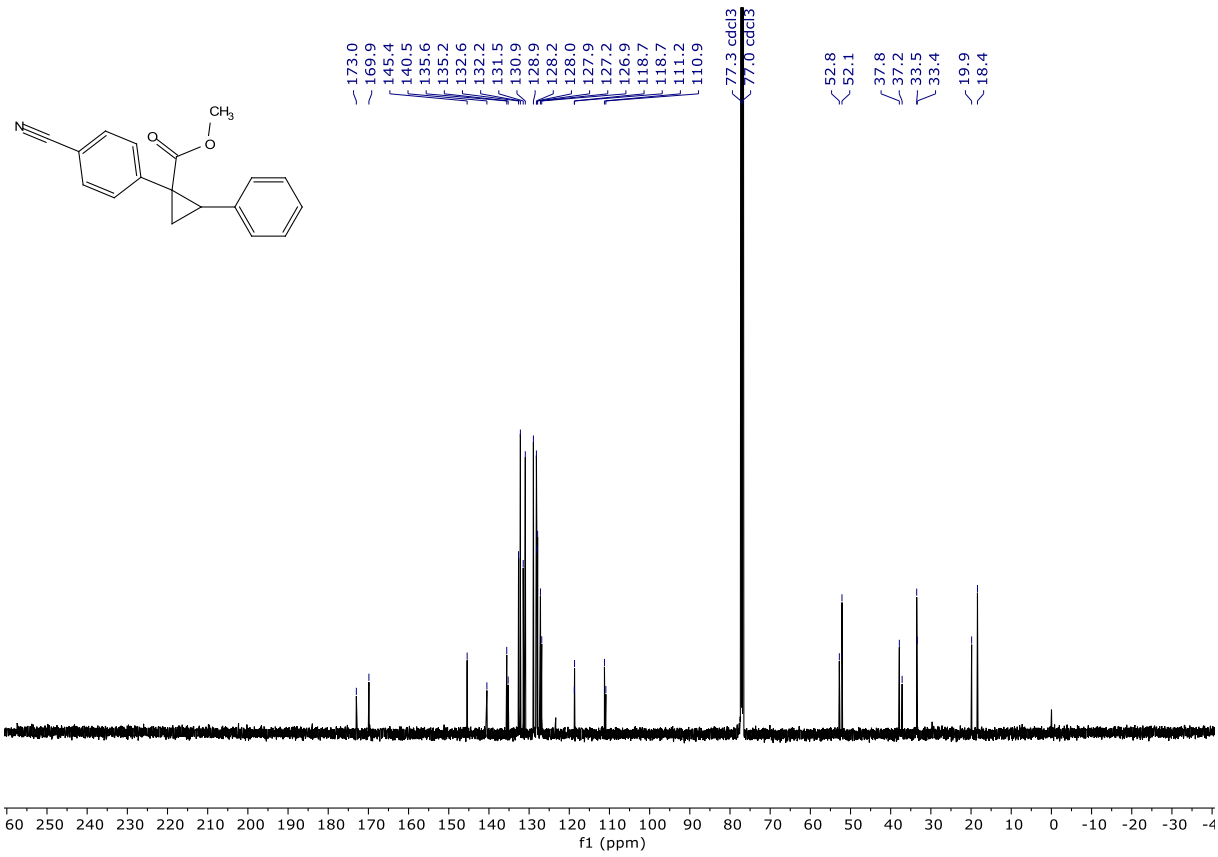

methyl 2-(4-methoxyphenyl)-1-phenylcyclopropane-1-carboxylate (35)

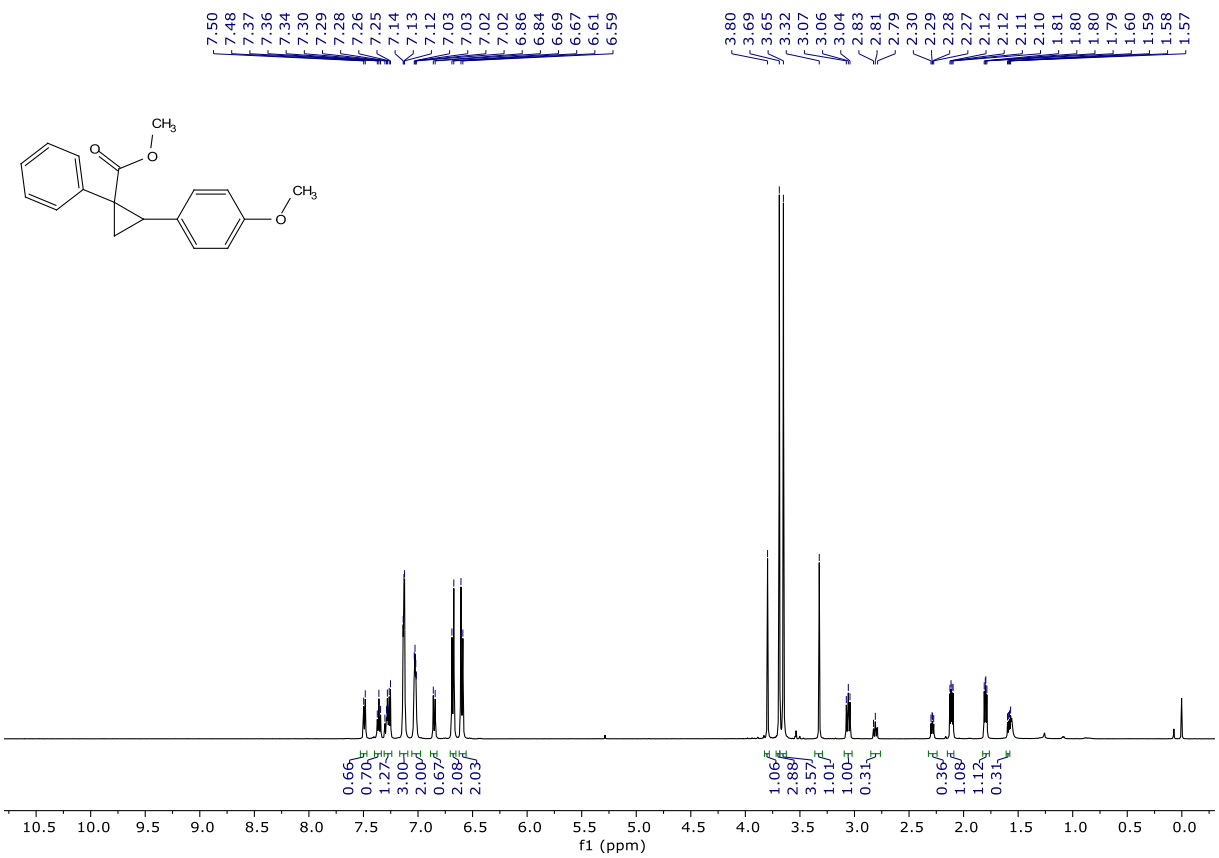

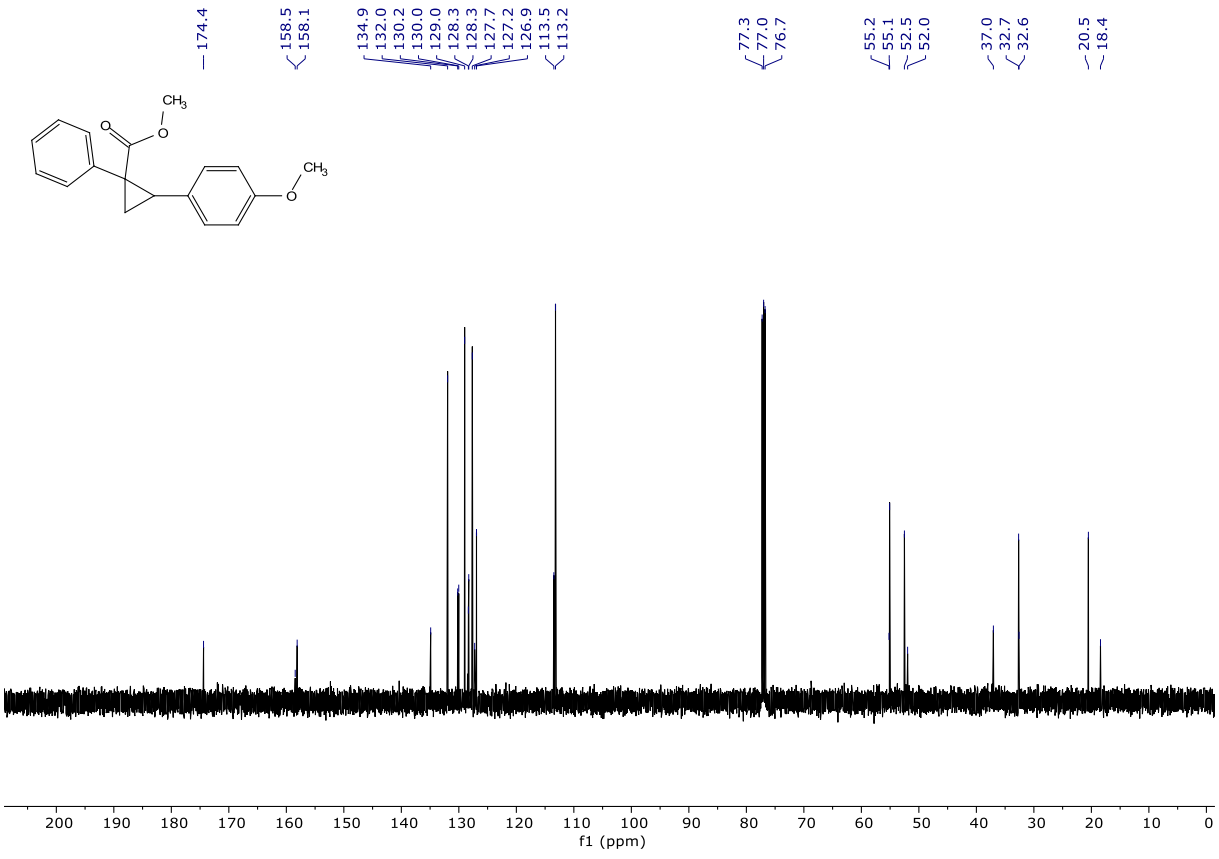

methyl 2-(4-fluorophenyl)-1-phenylcyclopropane-1-carboxylate (36)

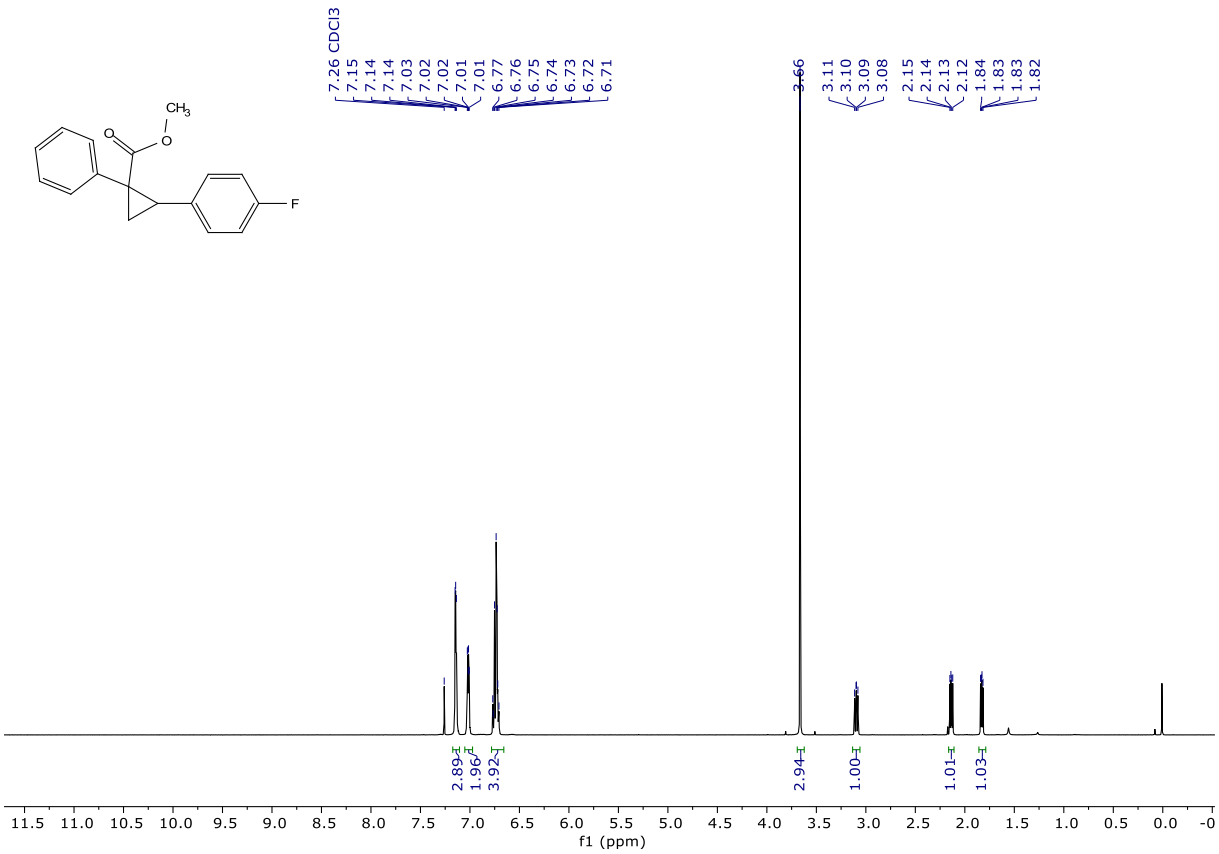

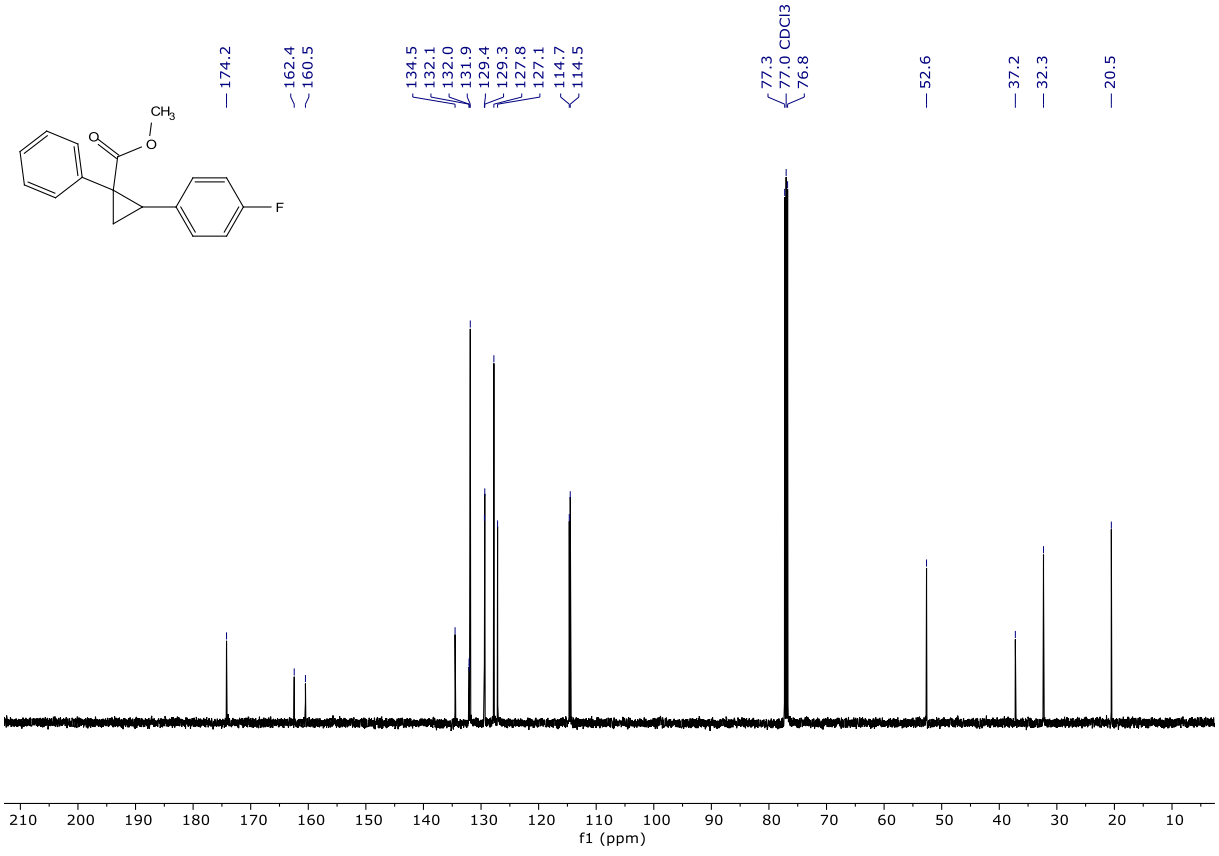

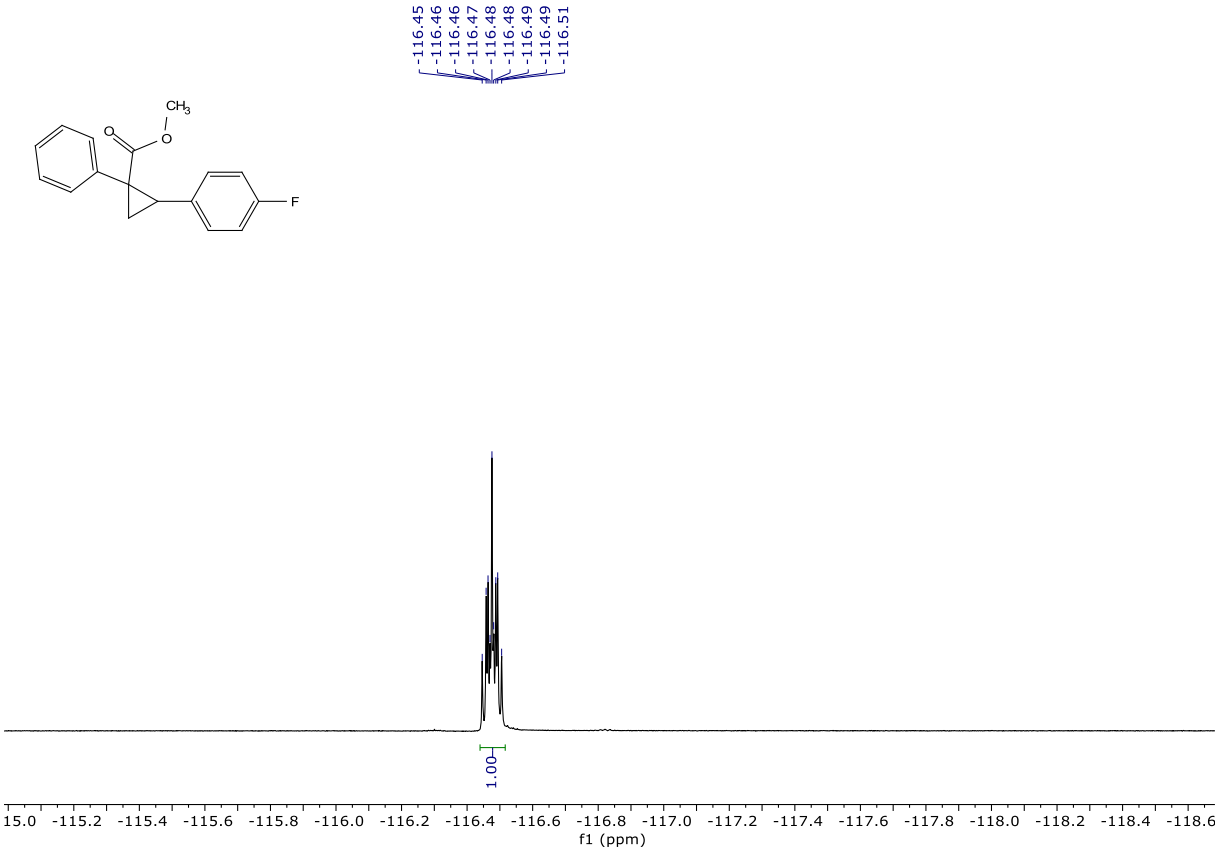

methyl 2-methyl-1,3-diphenylcyclopropane-1-carboxylate (37)

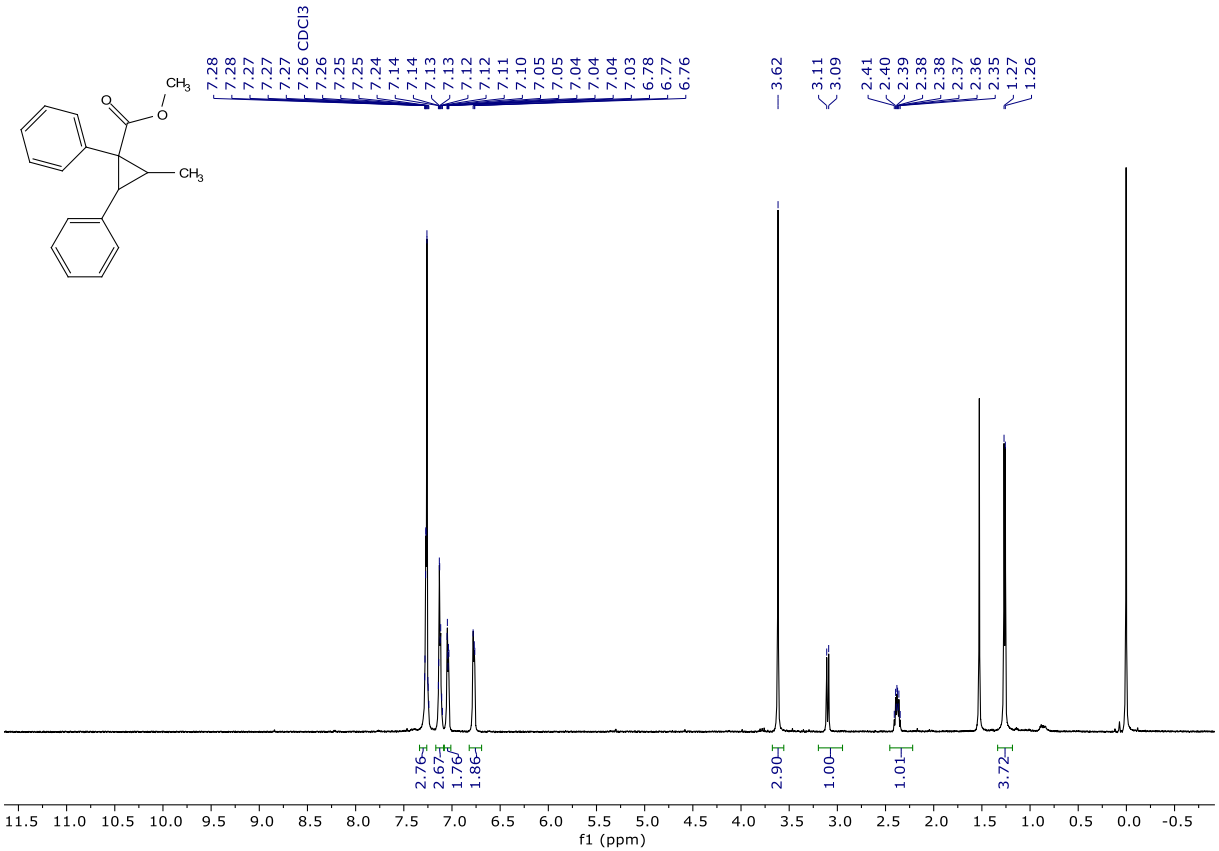

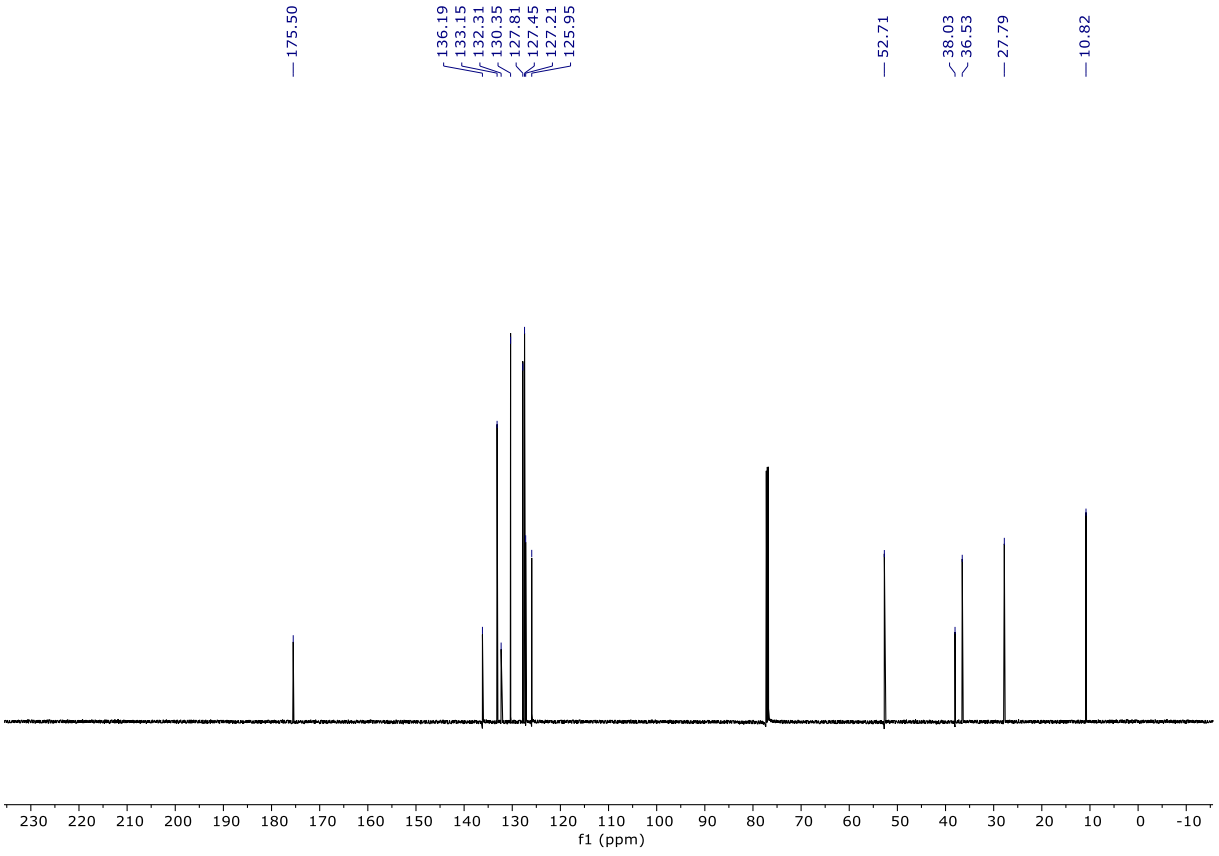

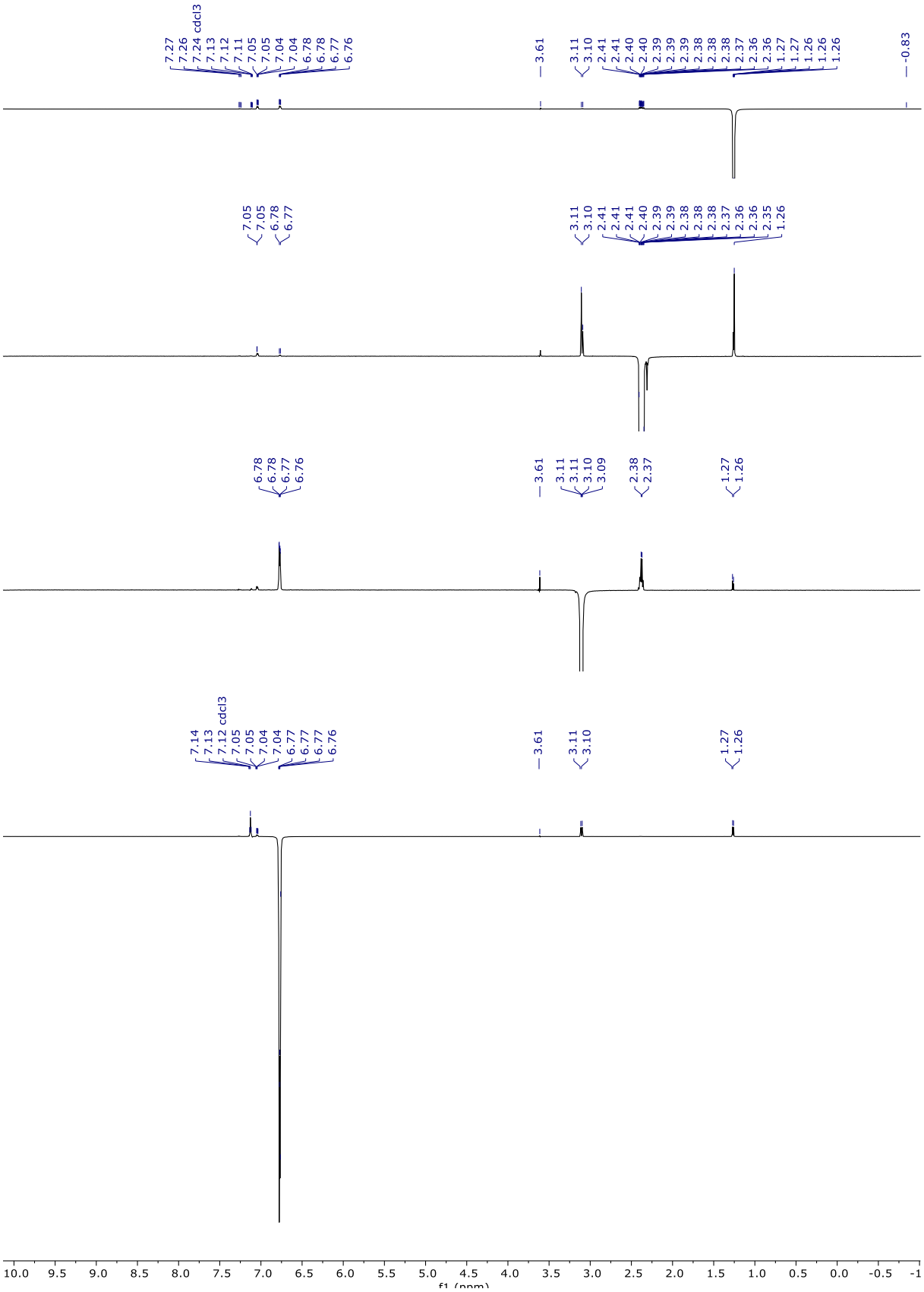

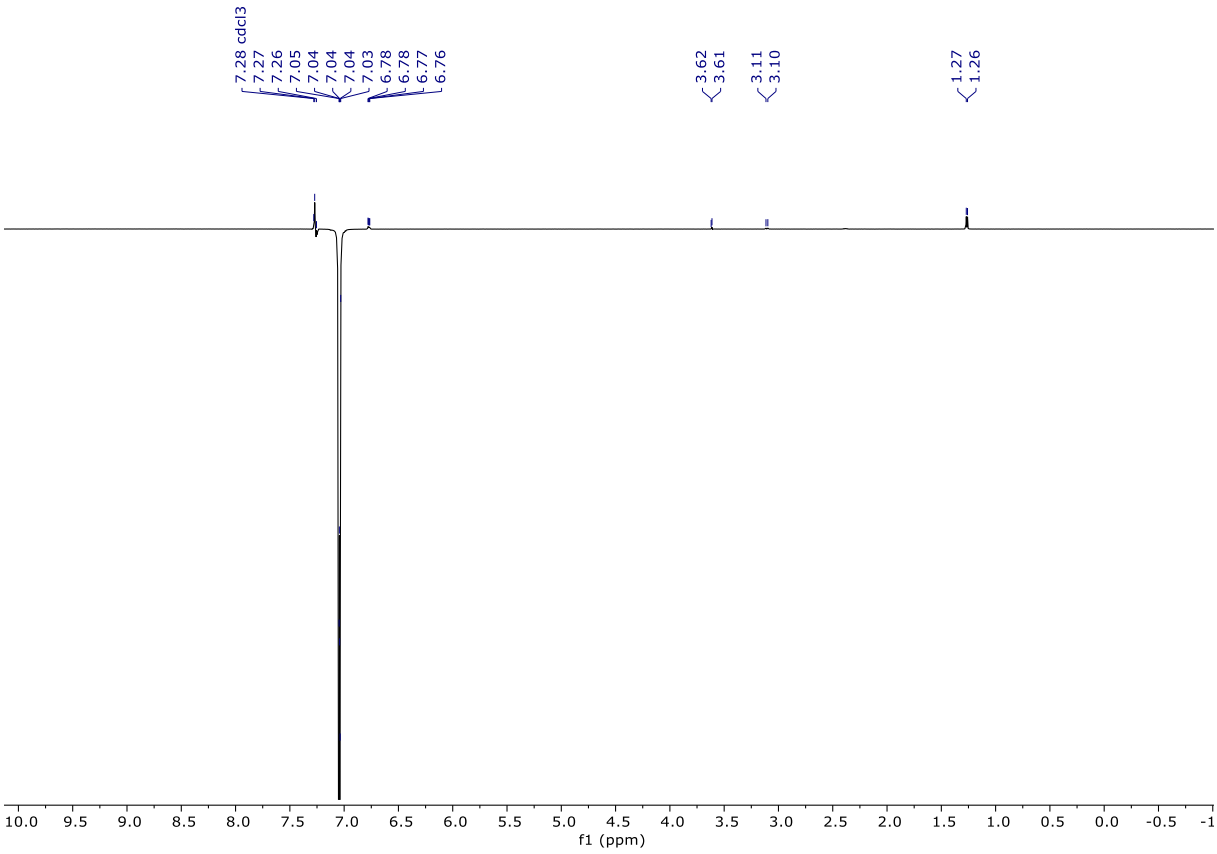

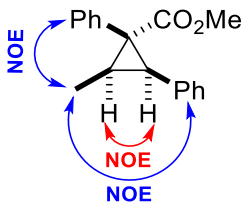

ethyl (E)-4-(hydroxyimino)-4-(p-tolyl)butanoate (38)

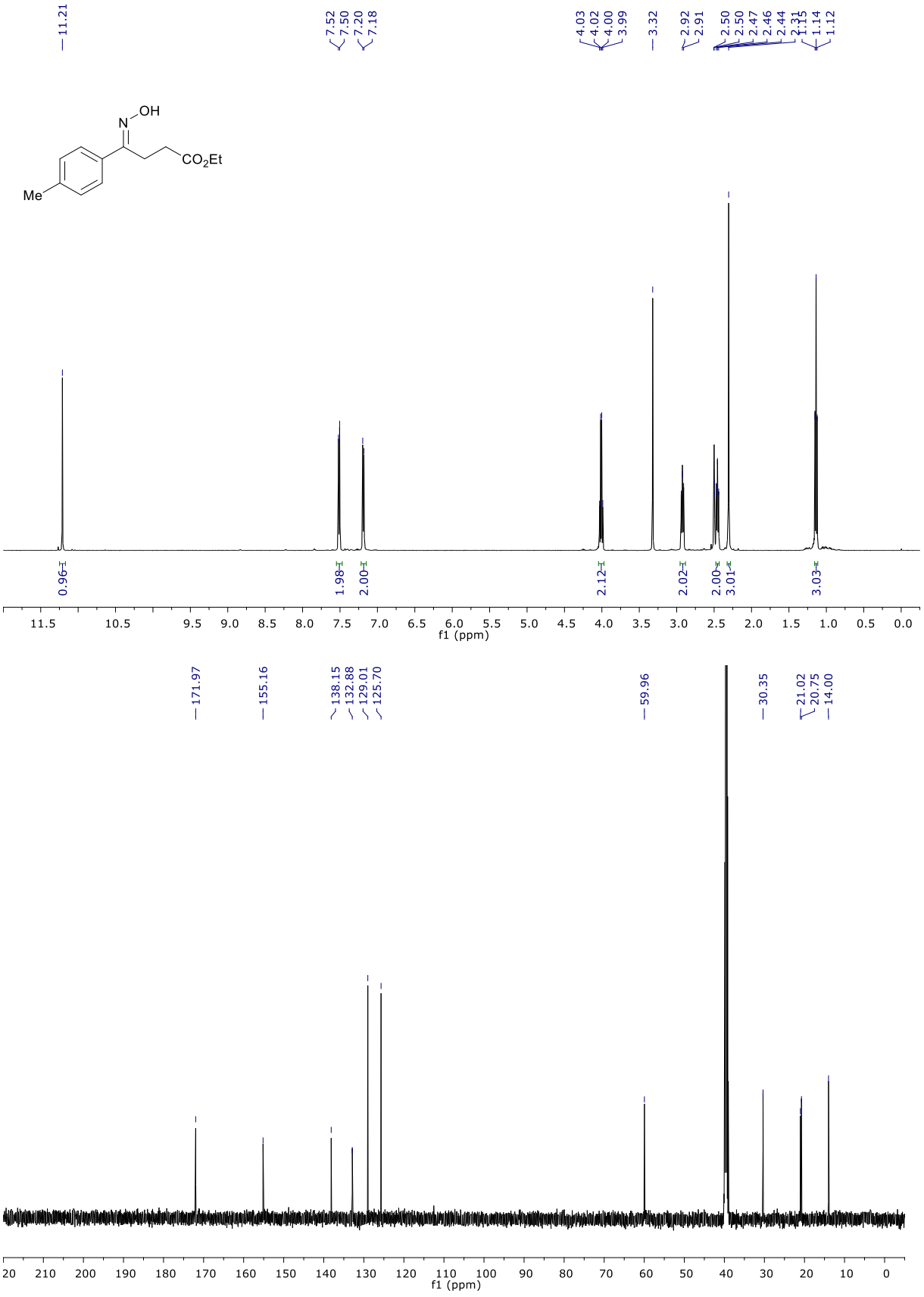

ethyl 4-(hydroxyimino)-5-(4-methoxyphenyl)-3-methylpentanoate (39)

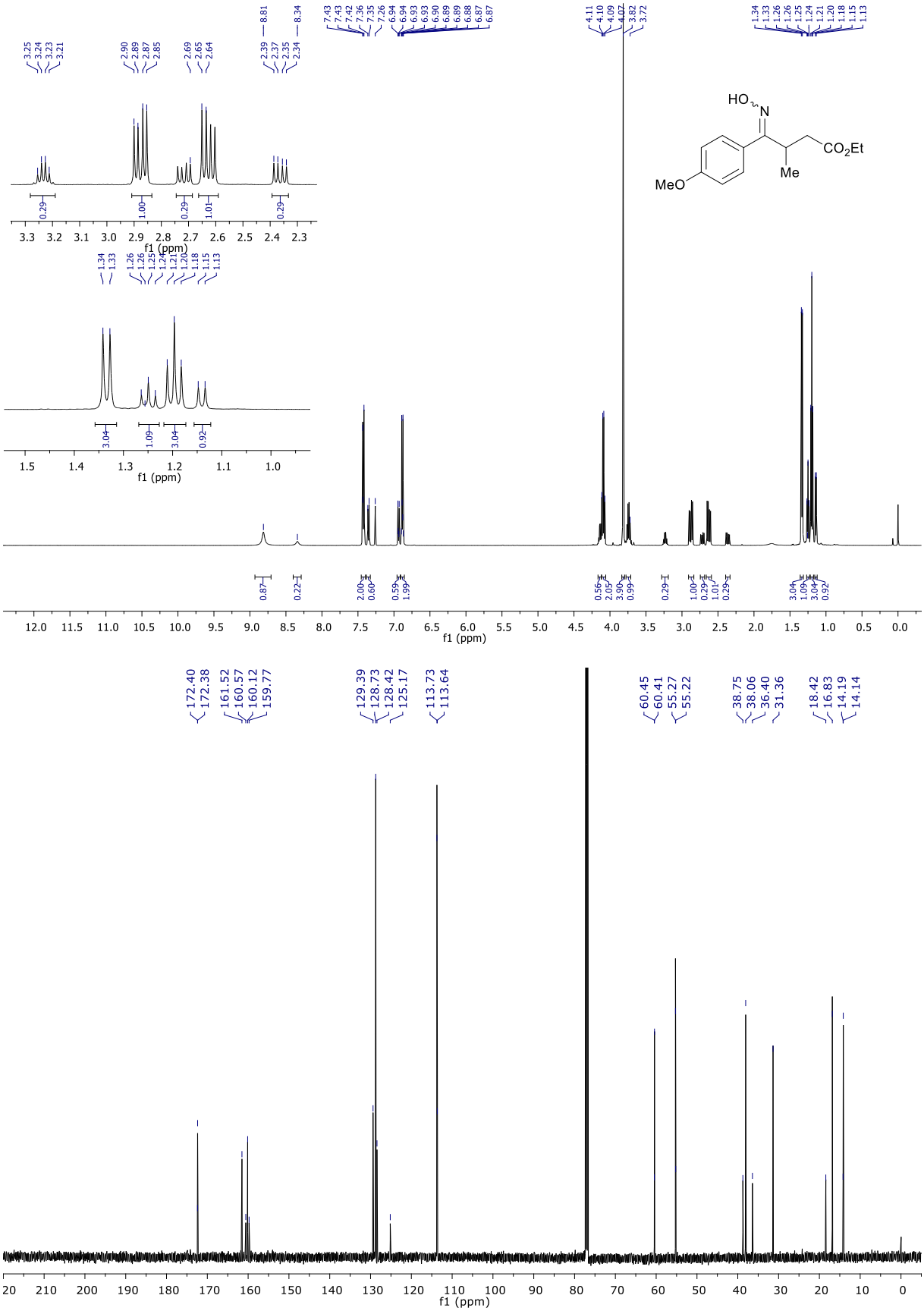

tert-butyl (E)-4-(hydroxyimino)-4-phenylbutanoate (40)

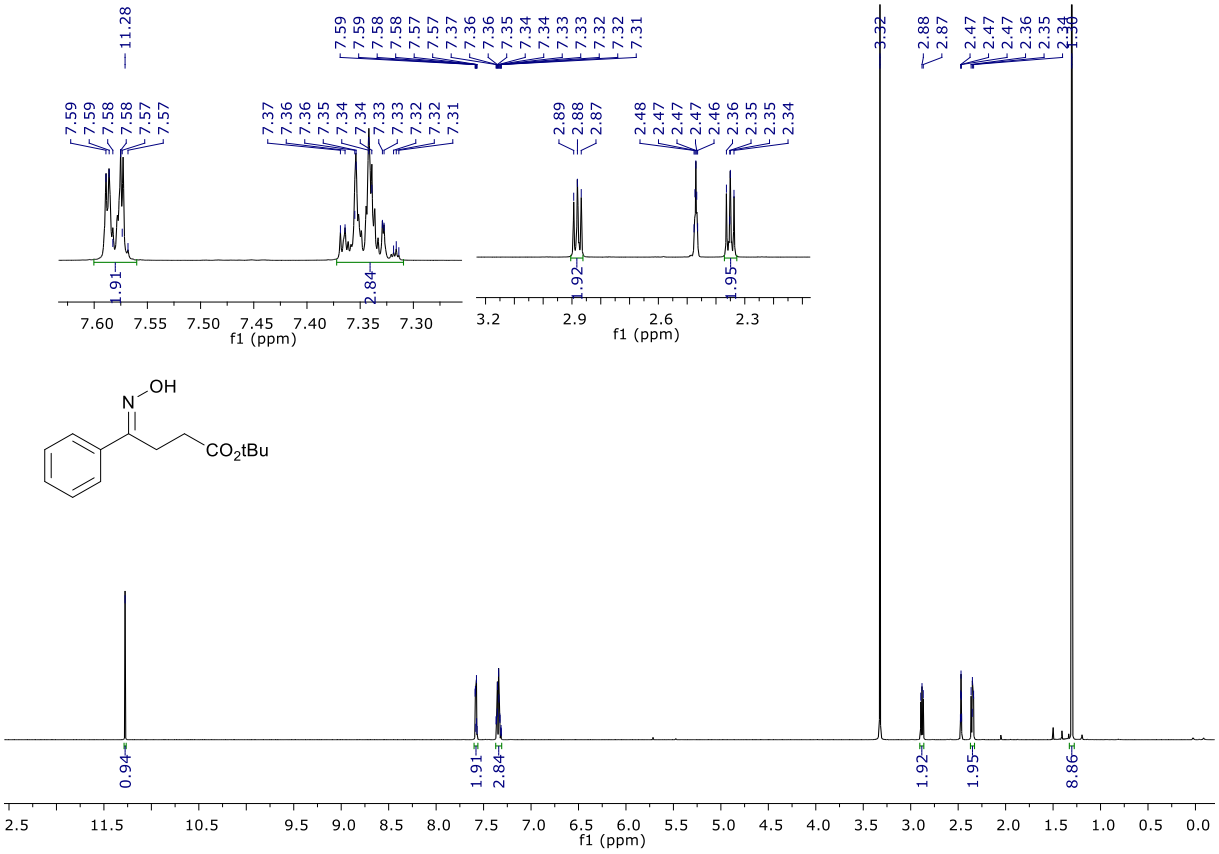

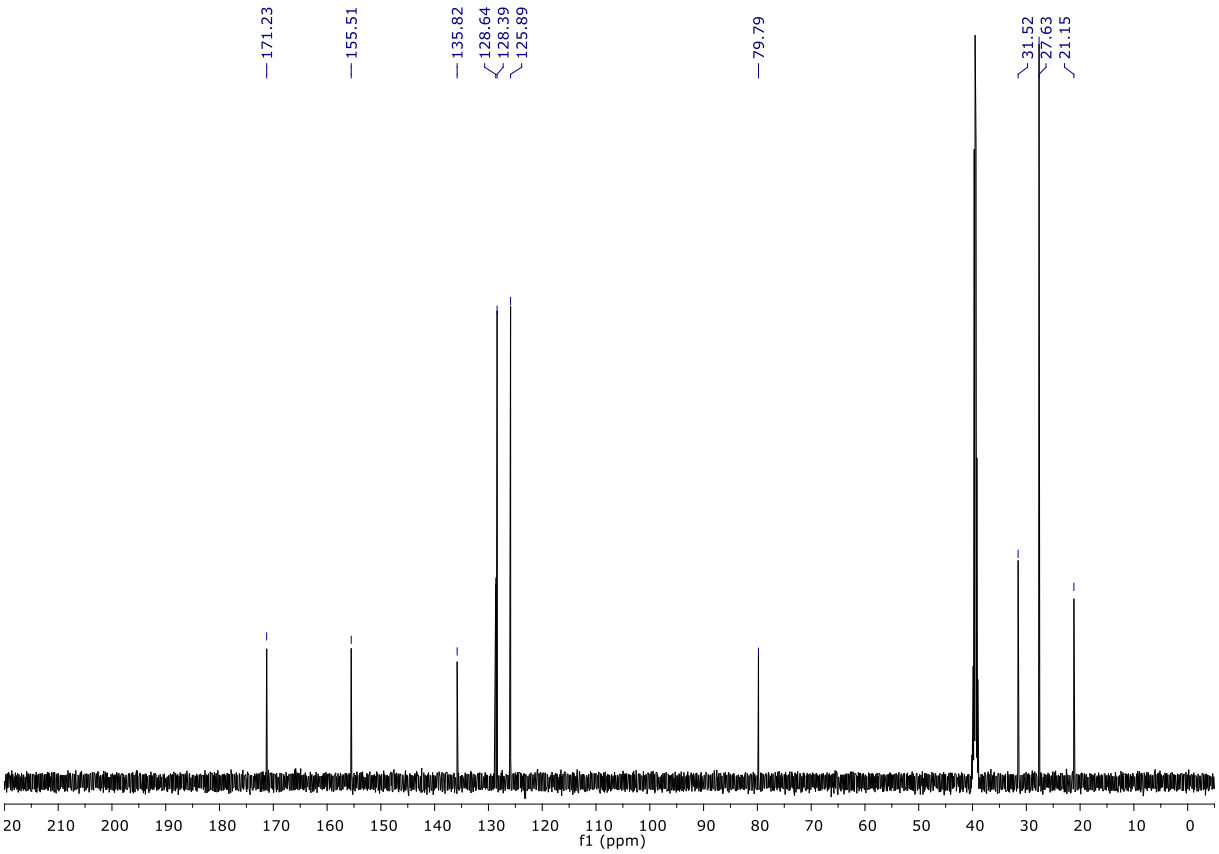

benzyl (E)-4-(hydroxyimino)-4-phenylbutanoate (41)

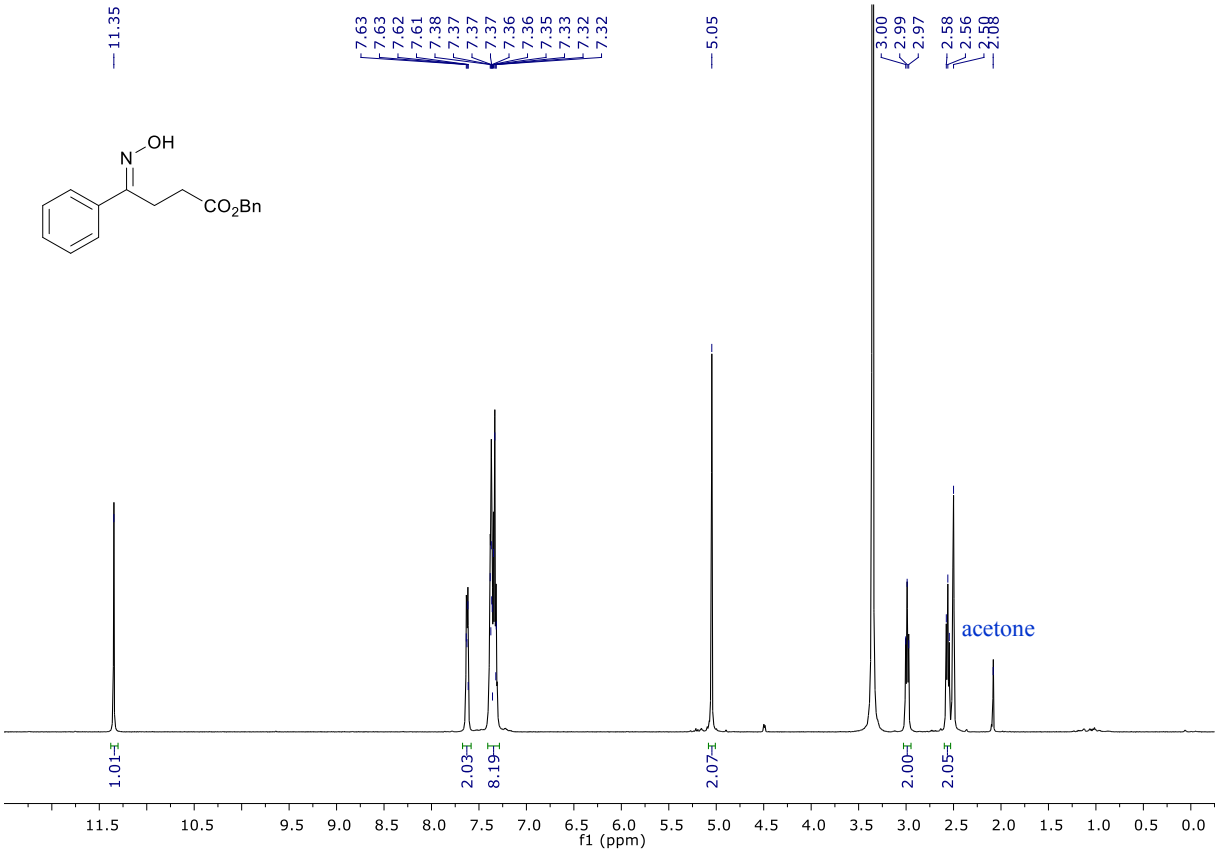

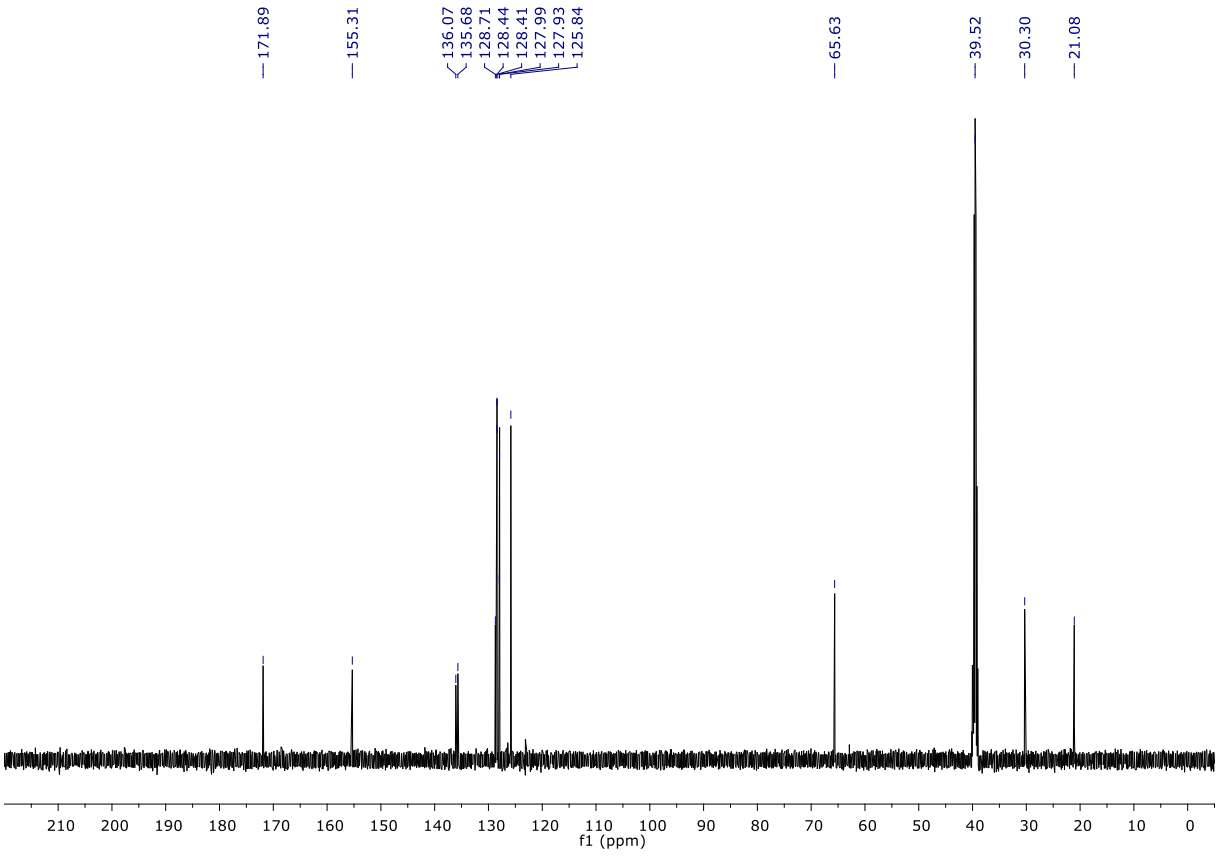

(3S,8S,9S,10R,13S,14S,17S)-17-acetyl-10,13-dimethyl-2,3,4,7,8,9,10,11,12,13,14,15,16,17-tetradeca hydro-1H-cyclopenta[a]phenanthren-3-yl 4-(4-ethoxy-1-(hydroxyimino)-4-oxobutyl) benzoate (42)

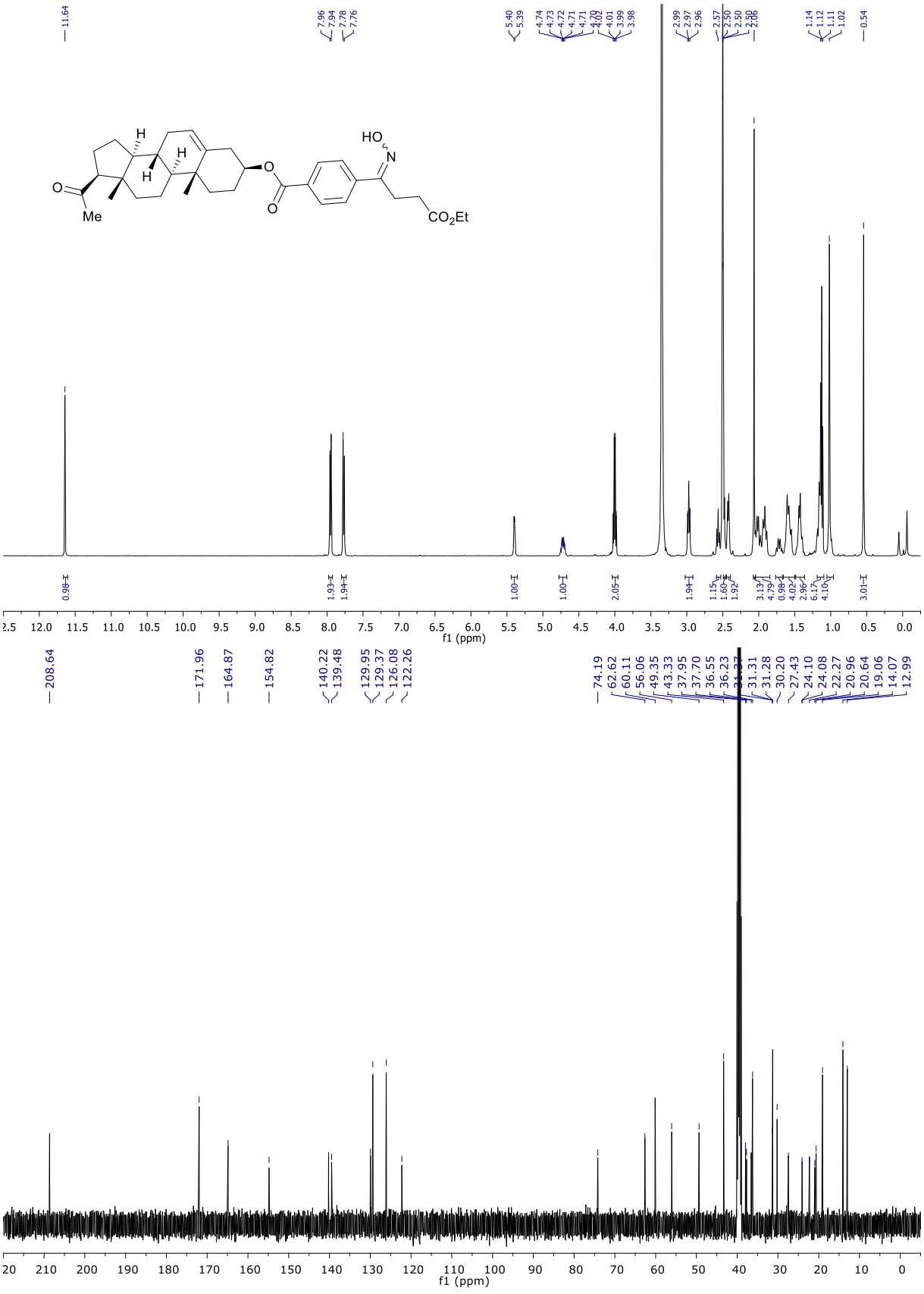

diethyl 2-(phenanthridin-6-yl)succinate (43)

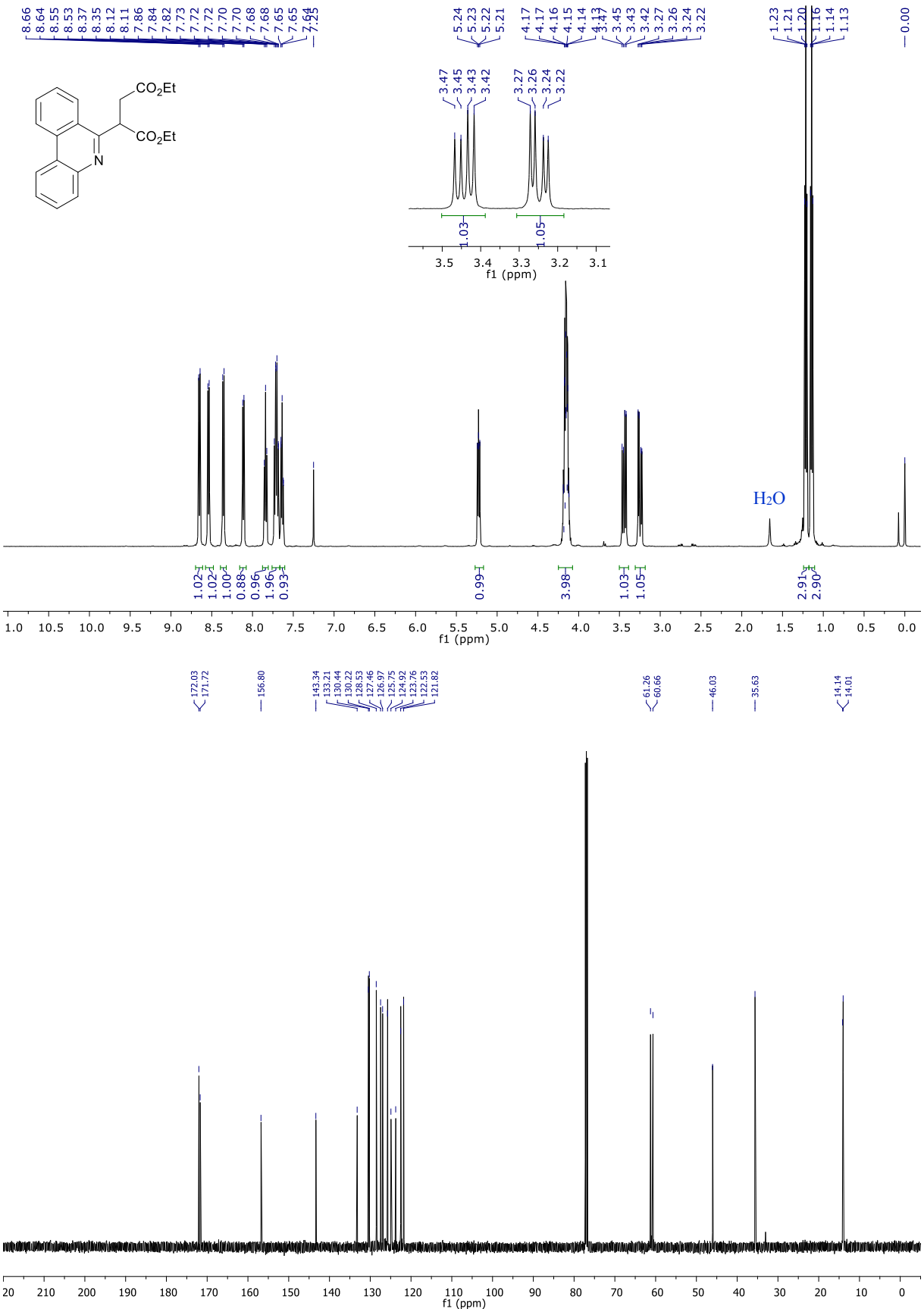

diethyl 2-(8-methoxyphenanthridin-6-yl)succinate (44)

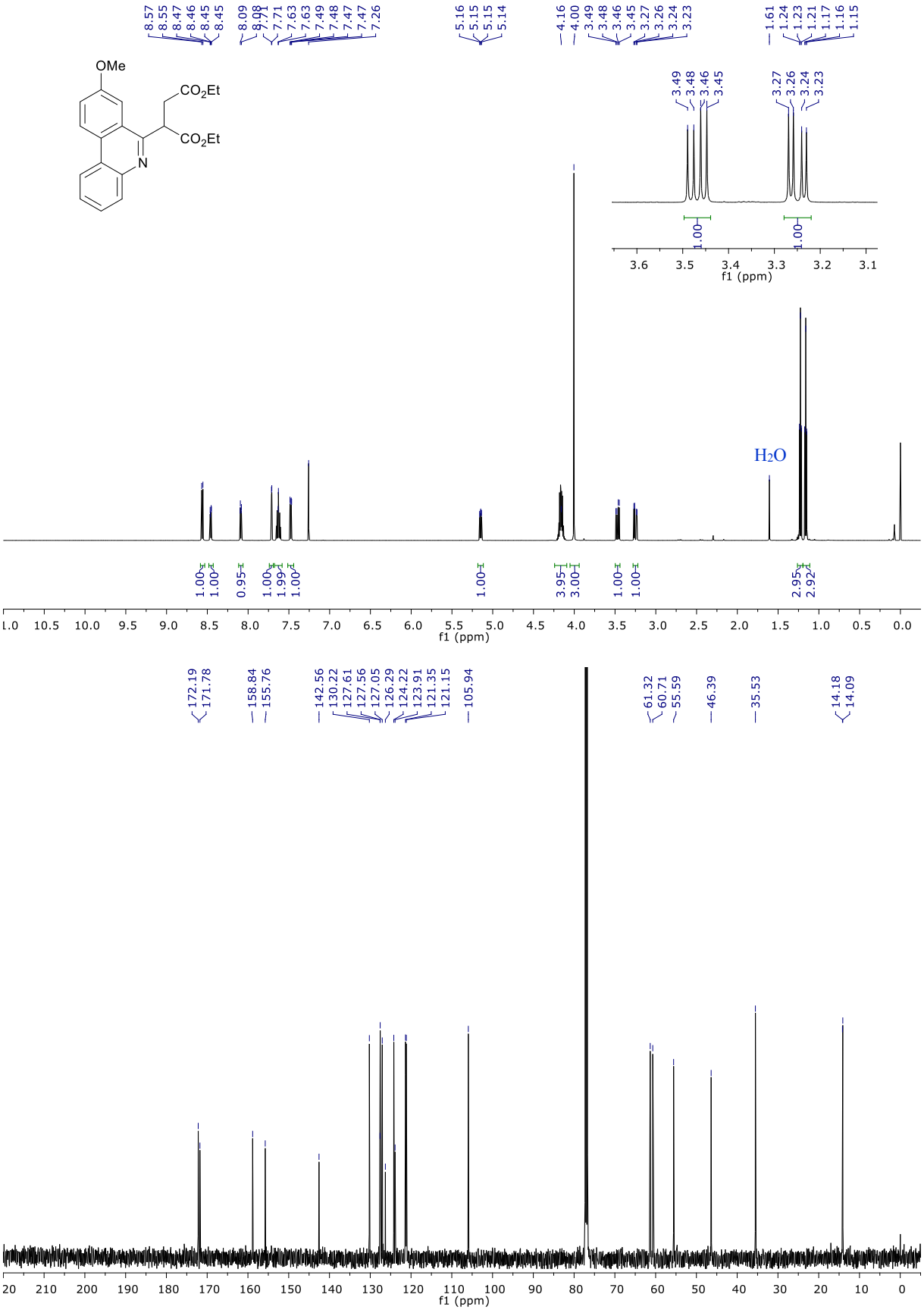

diethyl 2-(phenanthridin-6-yl)malonate (45)

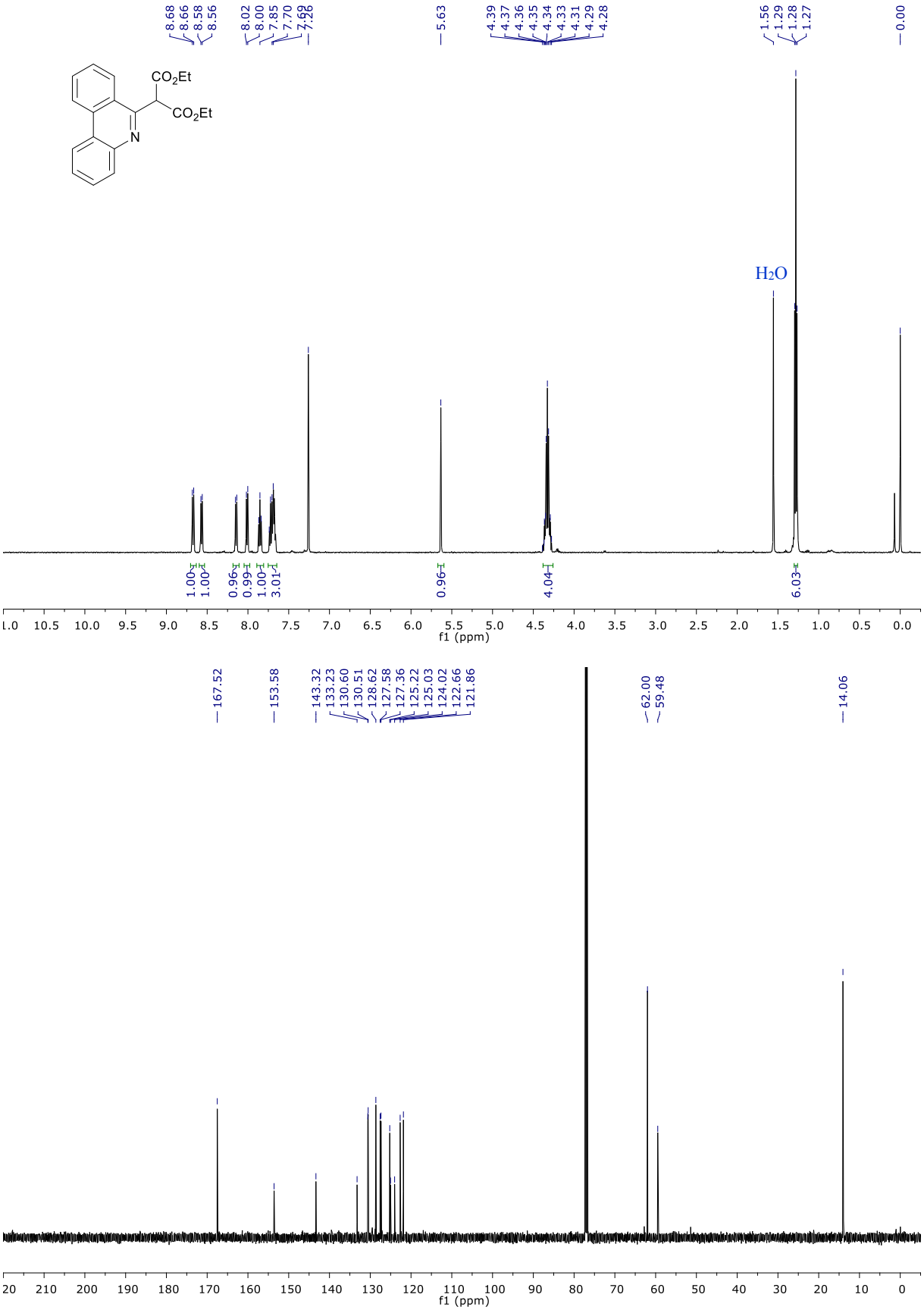

ethyl 2-(phenanthridin-6-yl)propanoate (46)

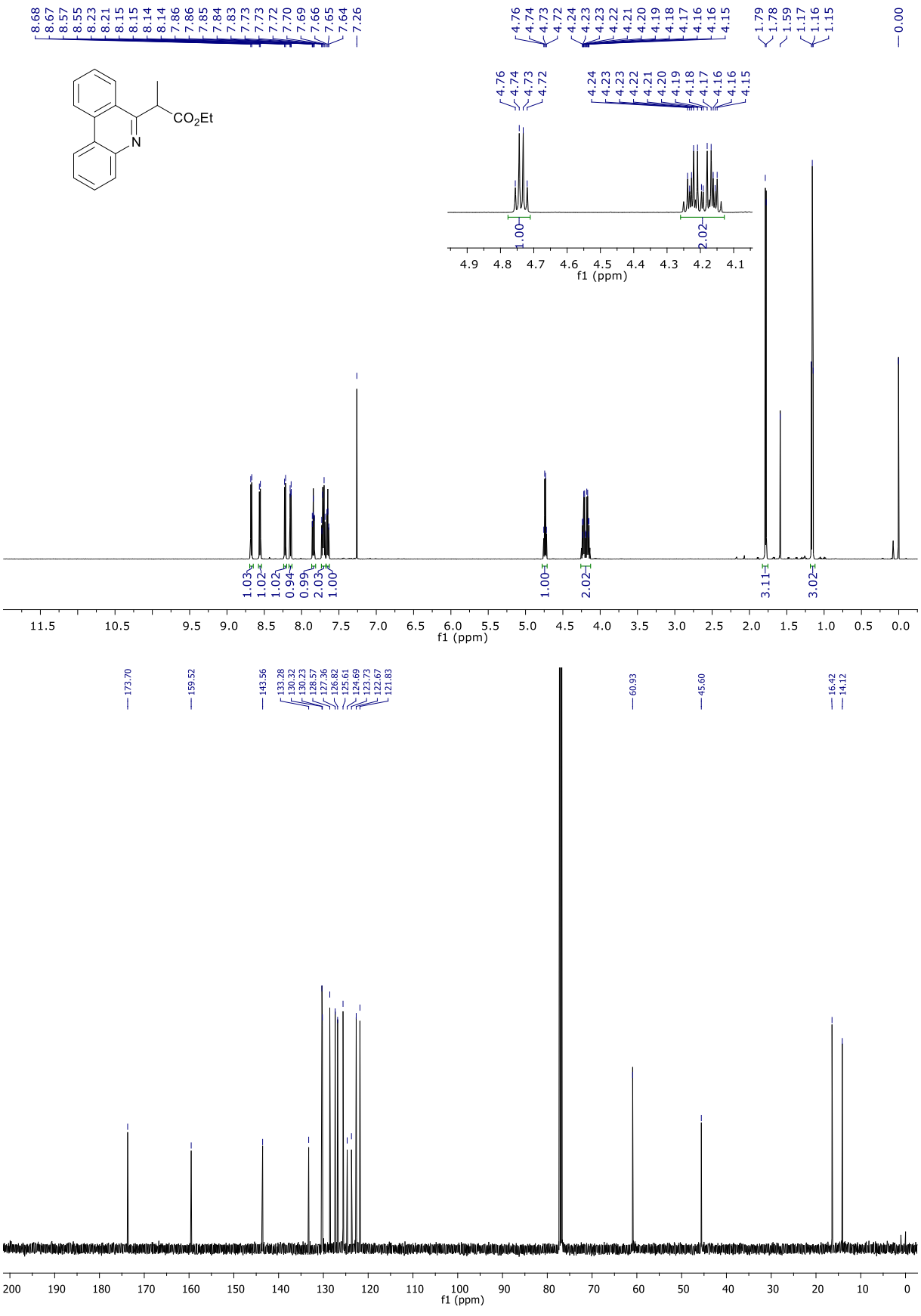

dimethyl (phenanthridin-6-ylmethyl)phosphonate (47)

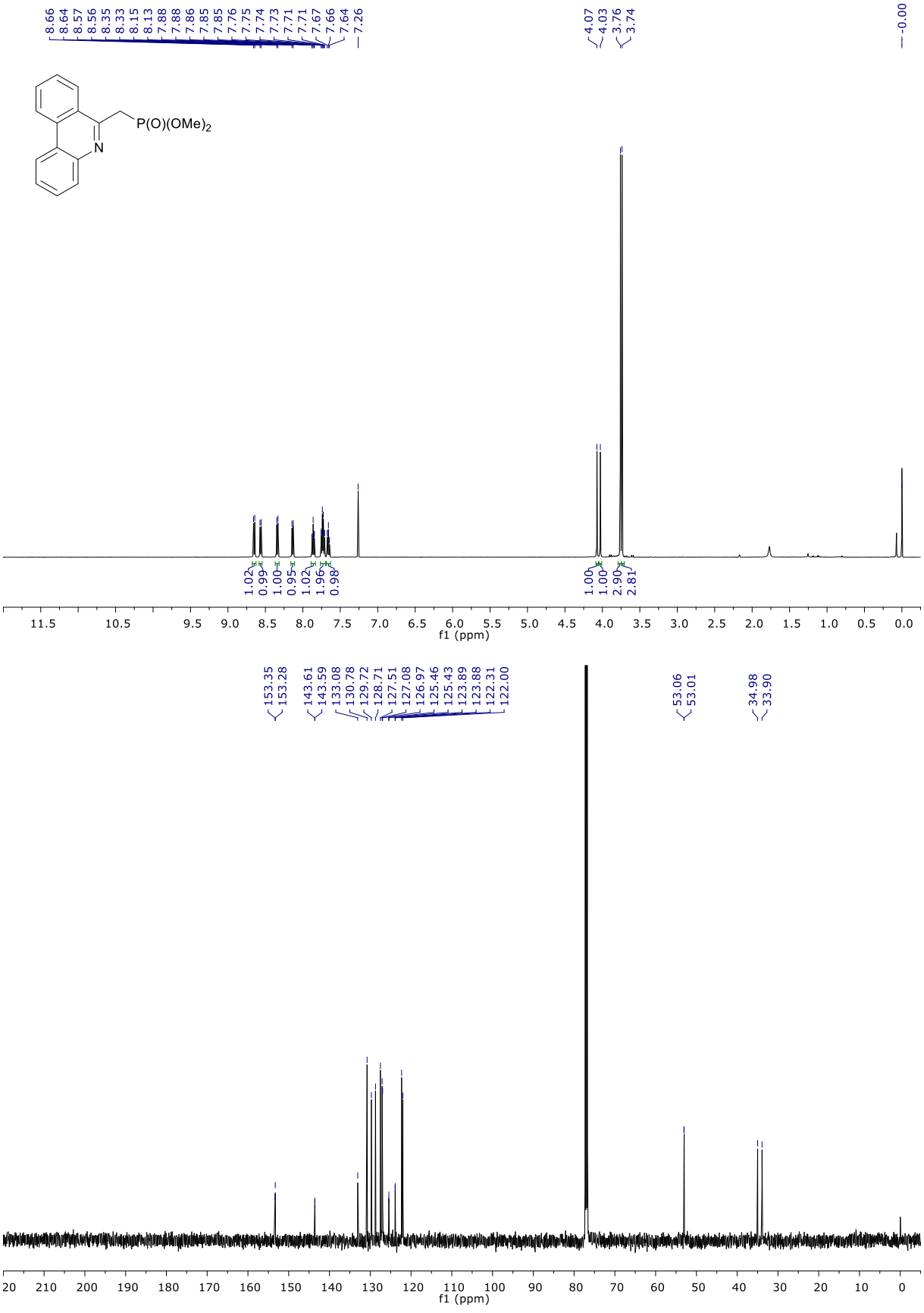

ethyl 2-diazo-2-(2-phenyl-1,2,3,4-tetrahydroisoquinolin-1-yl)acetate (48)

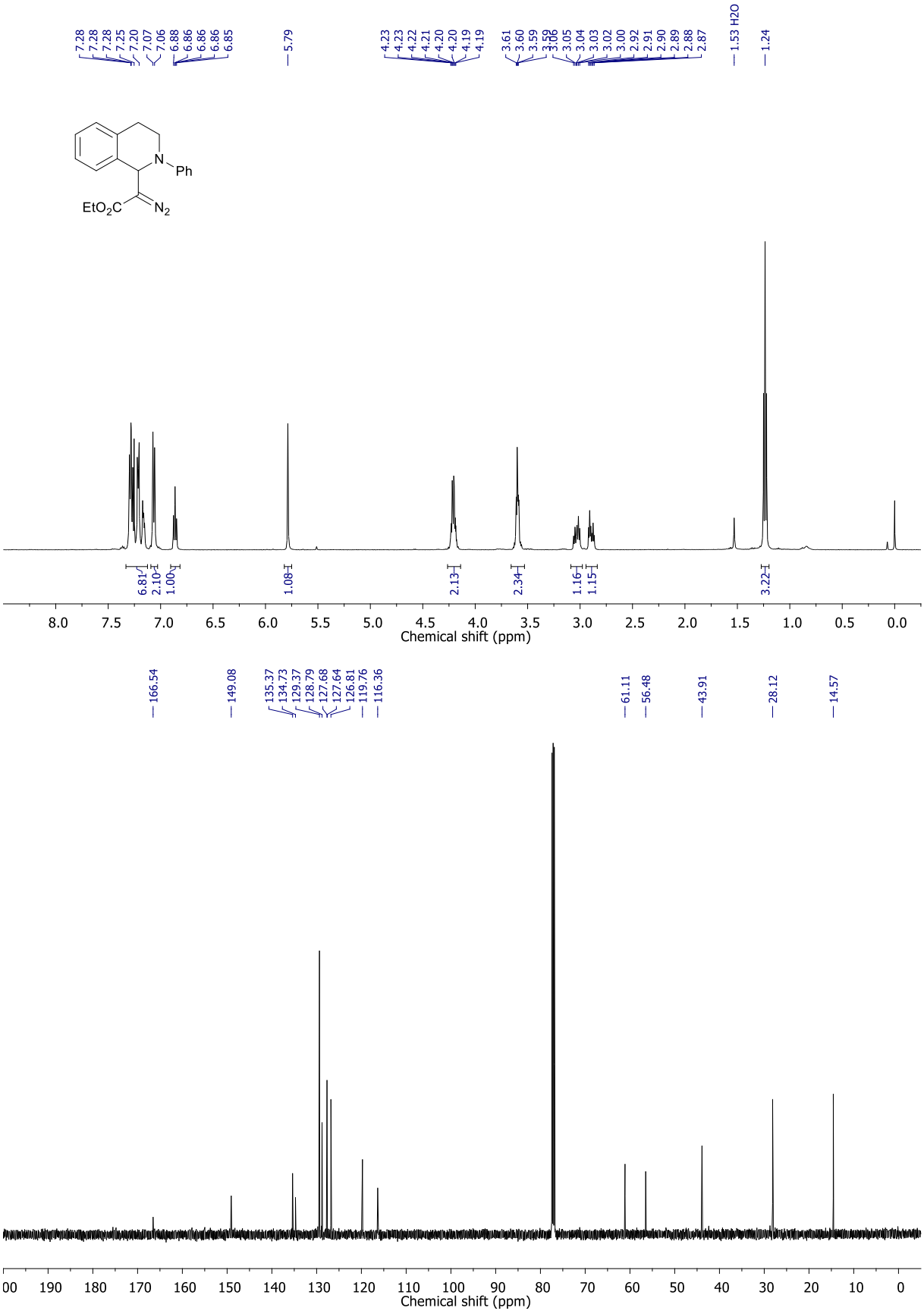

ethyl 2-diazo-2-(2-(p-tolyl)-1,2,3,4-tetrahydroisoquinolin-1-yl)acetate (49)

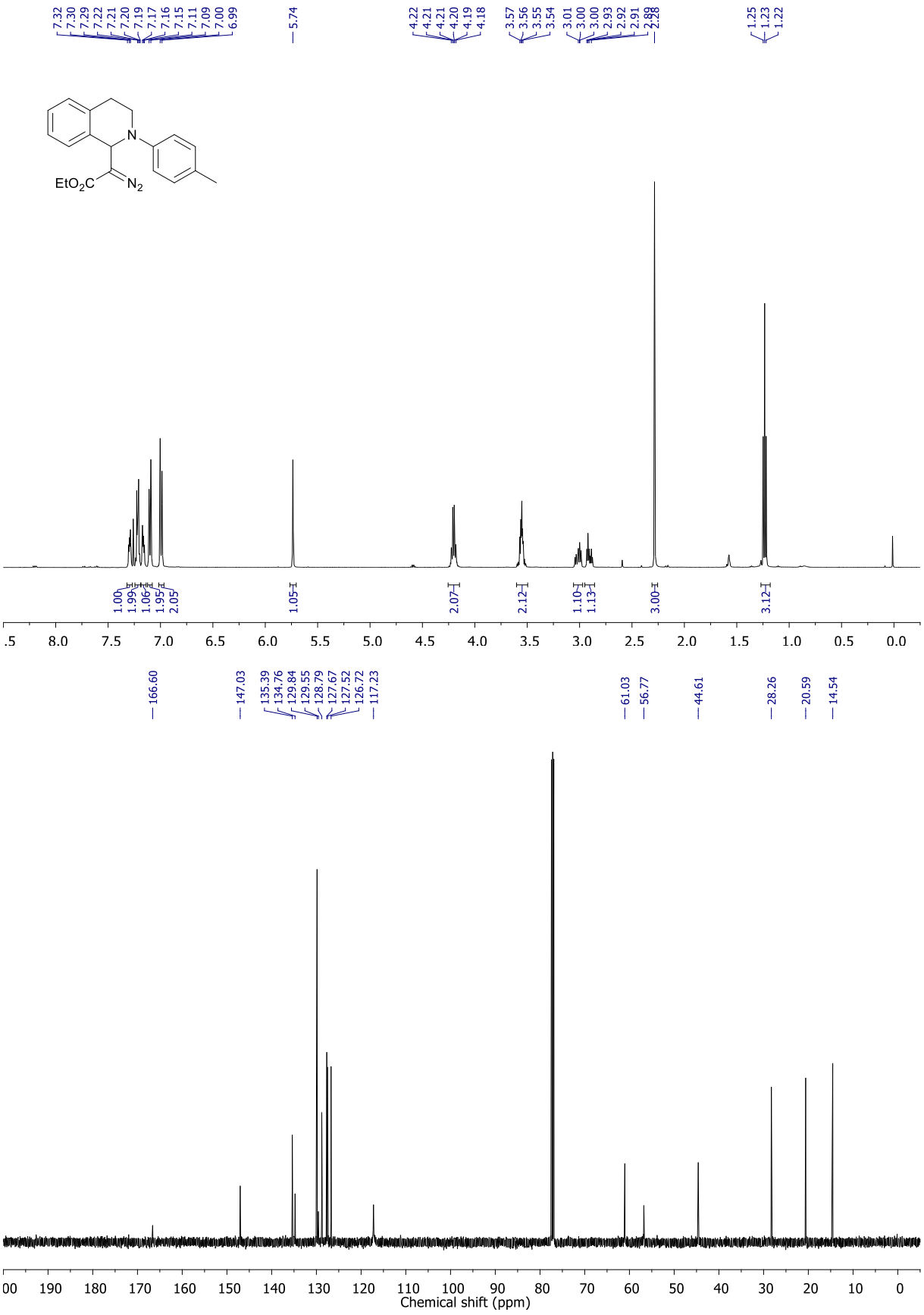

ethyl 2-diazo-2-(2-(4-methoxyphenyl)-1,2,3,4-tetrahydroisoquinolin-1-yl)acetate (50)

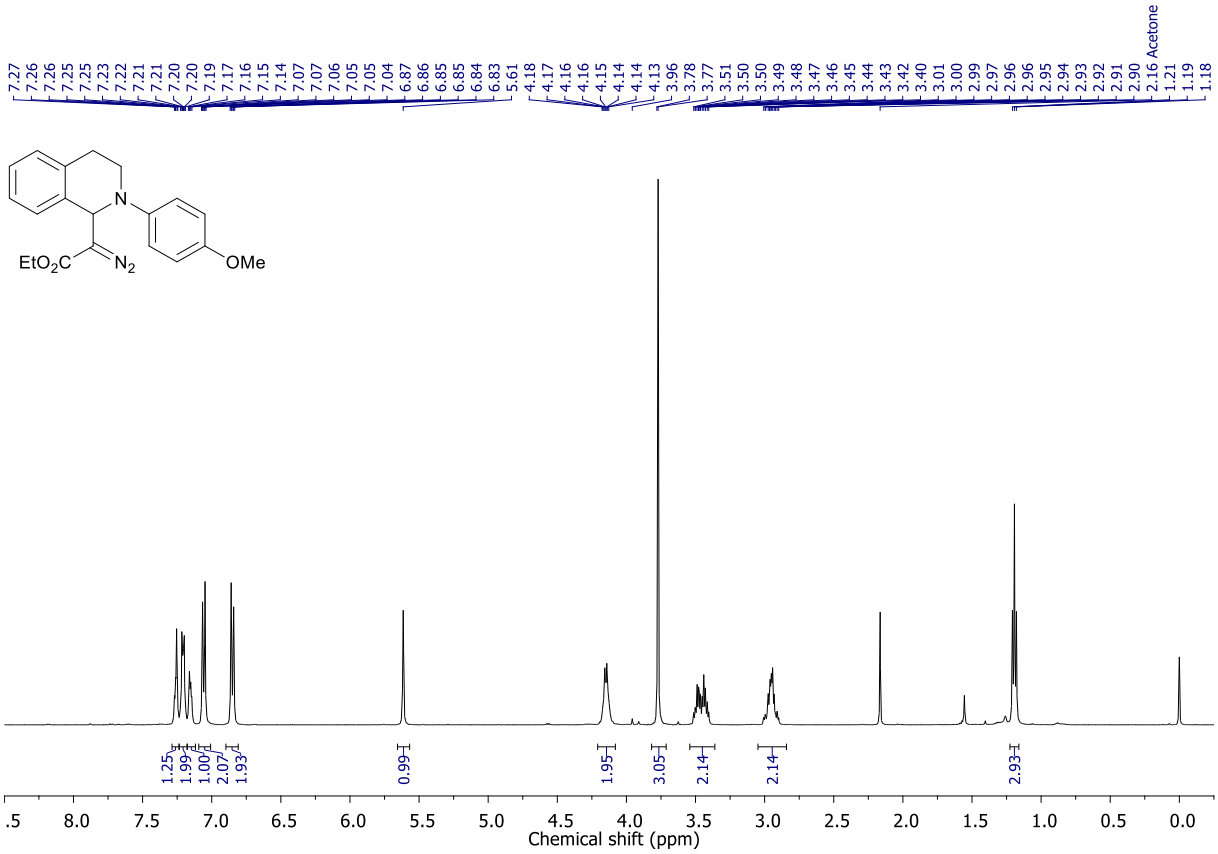

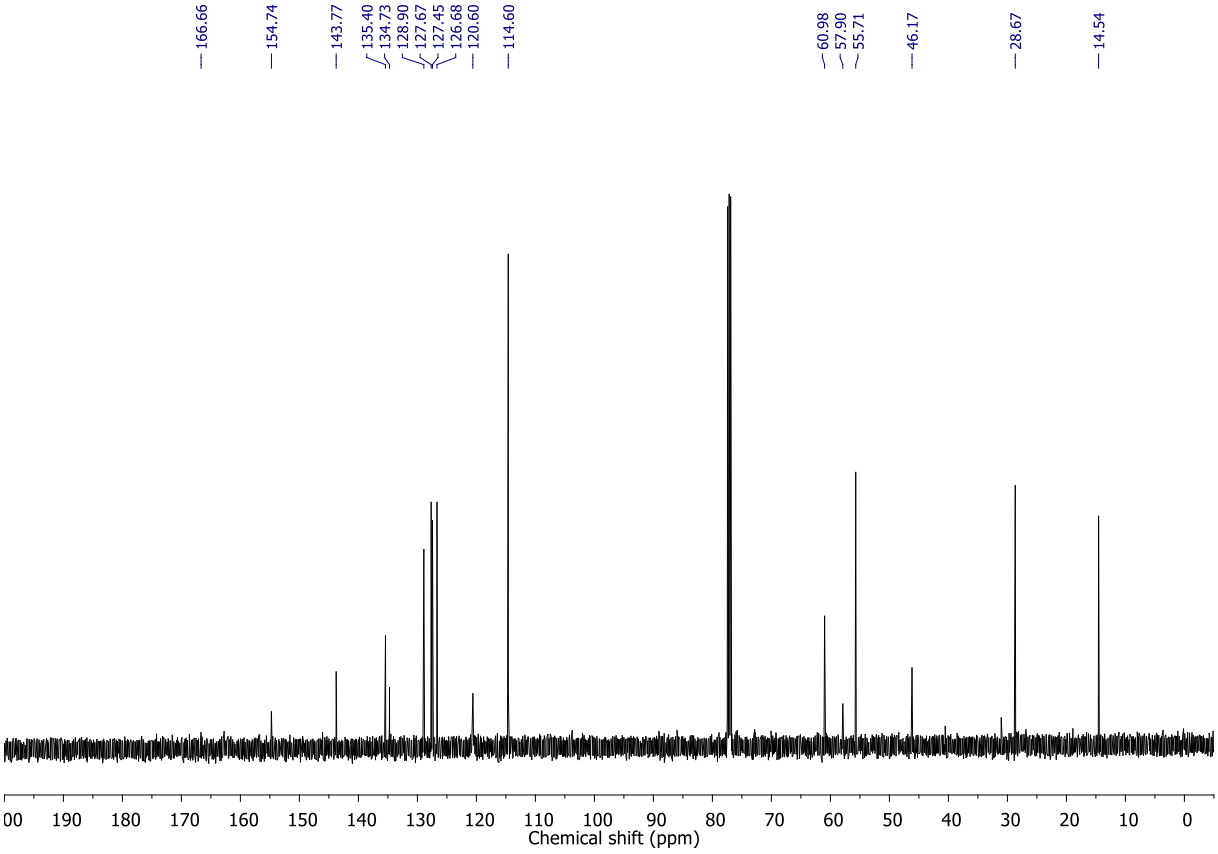

ethyl 2-diazo-2-(2-(4-(trifluoromethyl)phenyl)-1,2,3,4-tetrahydroisoquinolin-1-yl)acetate (51)

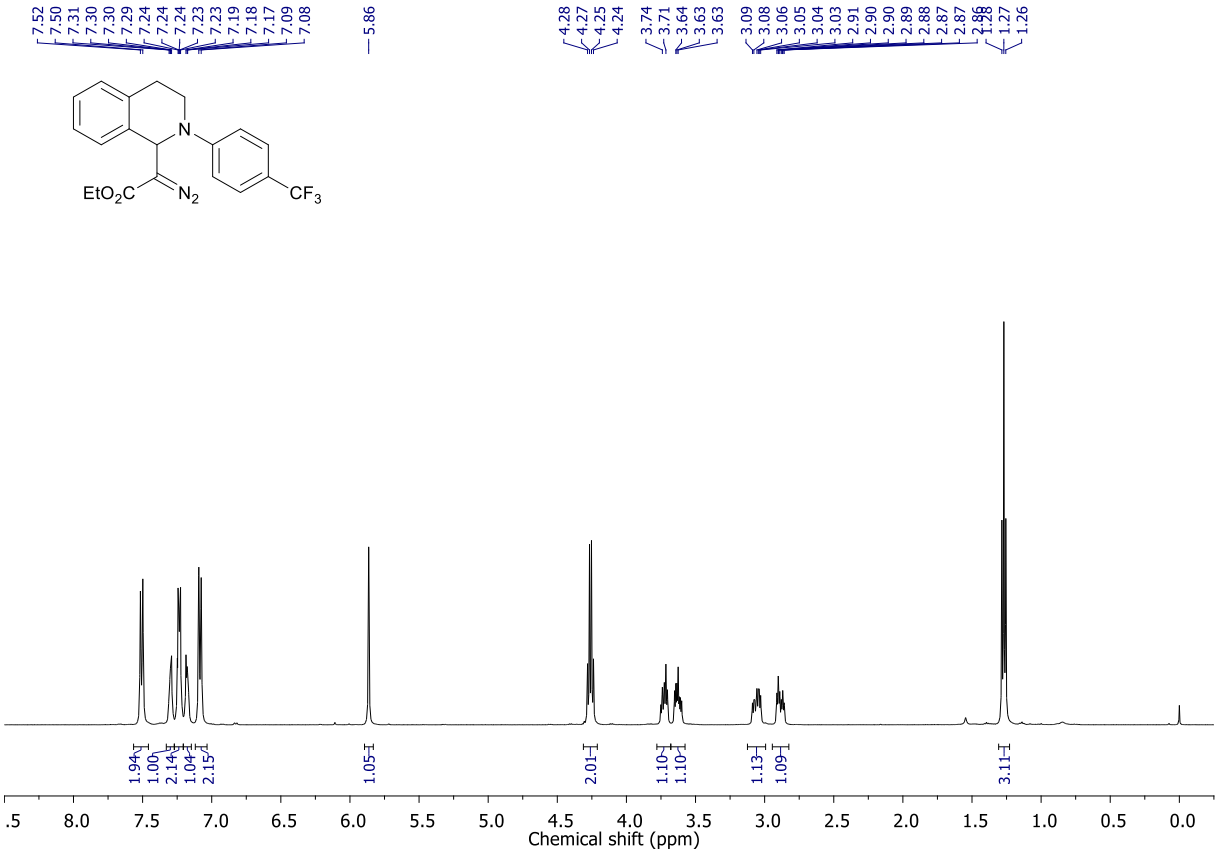

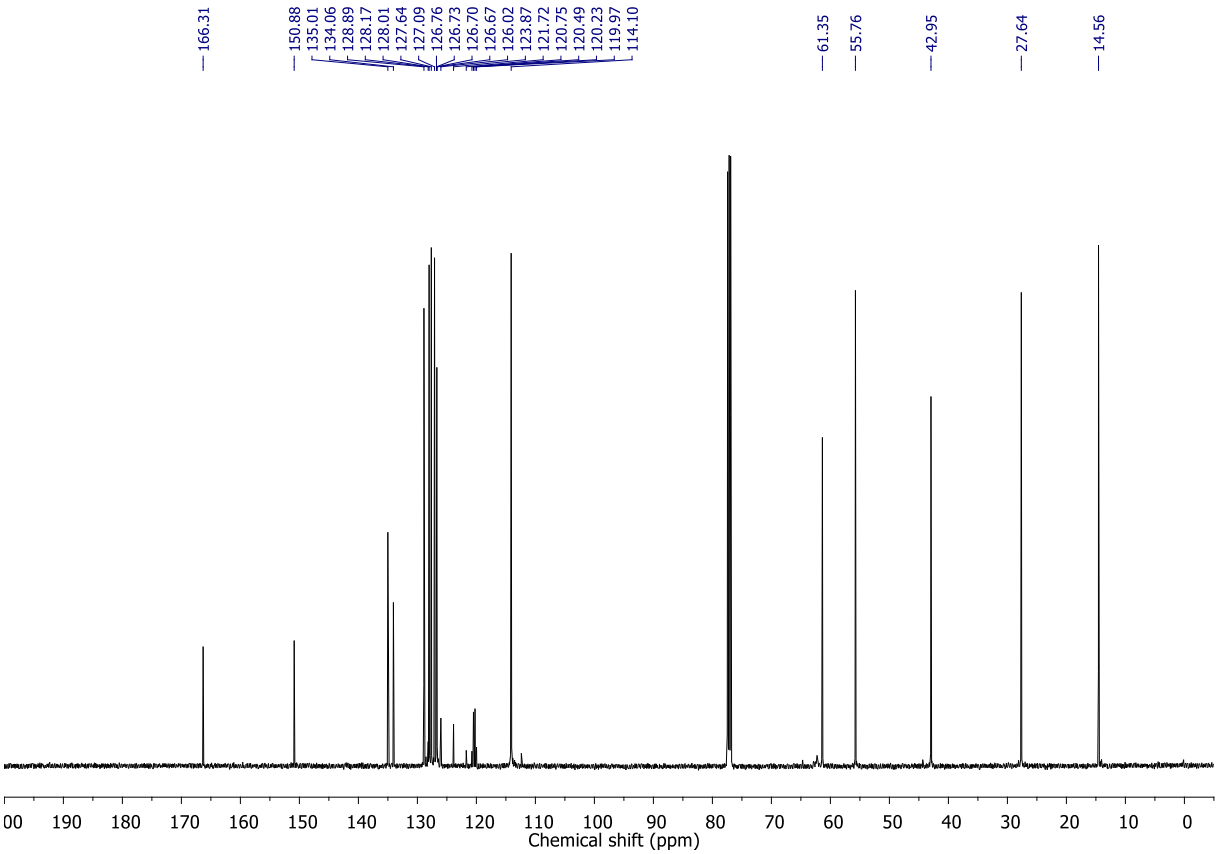

ethyl (Z)-2-(2-cyclohexylhydrazineylidene)-2-phenylacetate (52)

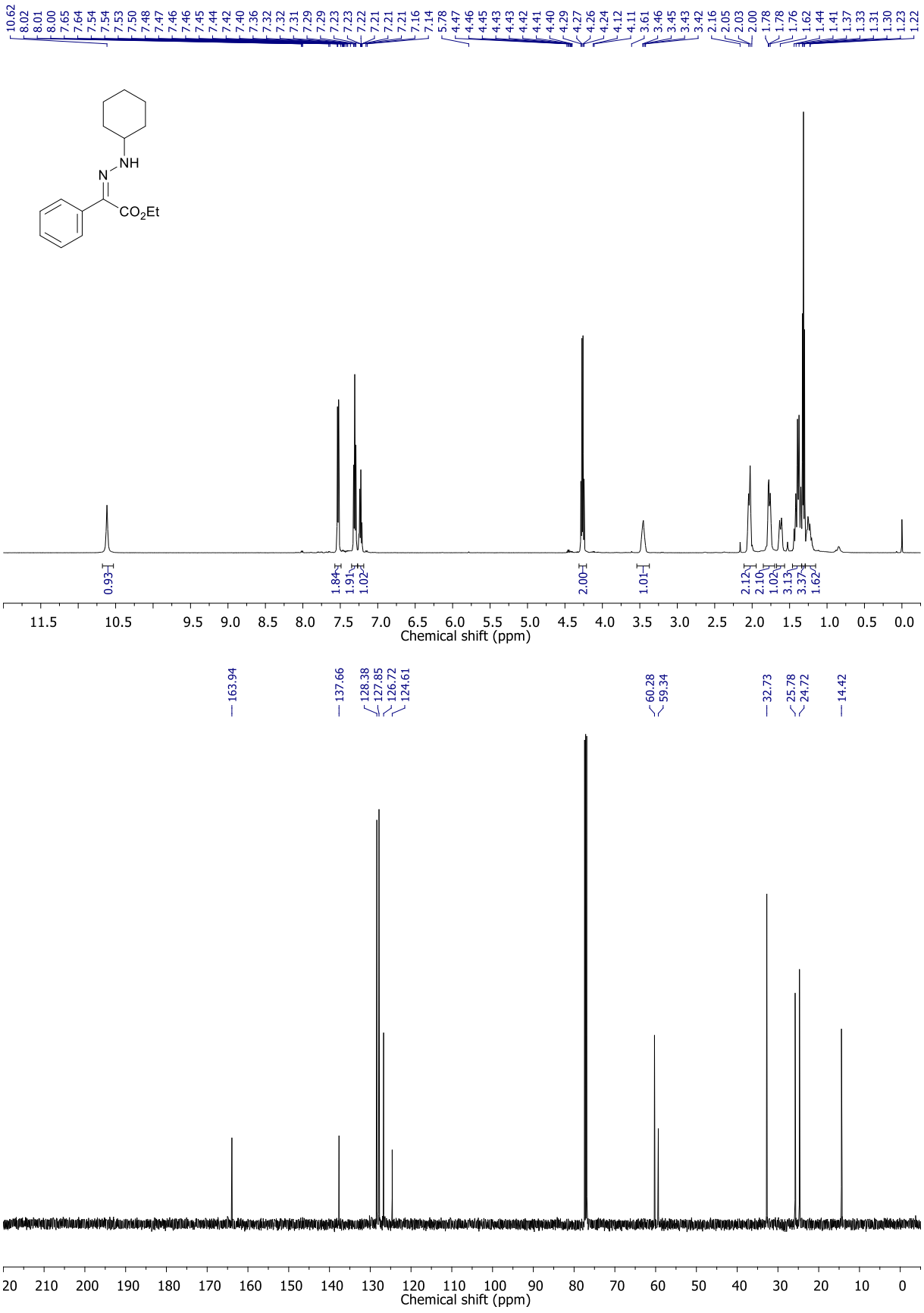

ethyl (Z)-2-(4-bromophenyl)-2-(2-cyclohexylhydrazineylidene)acetate (53)

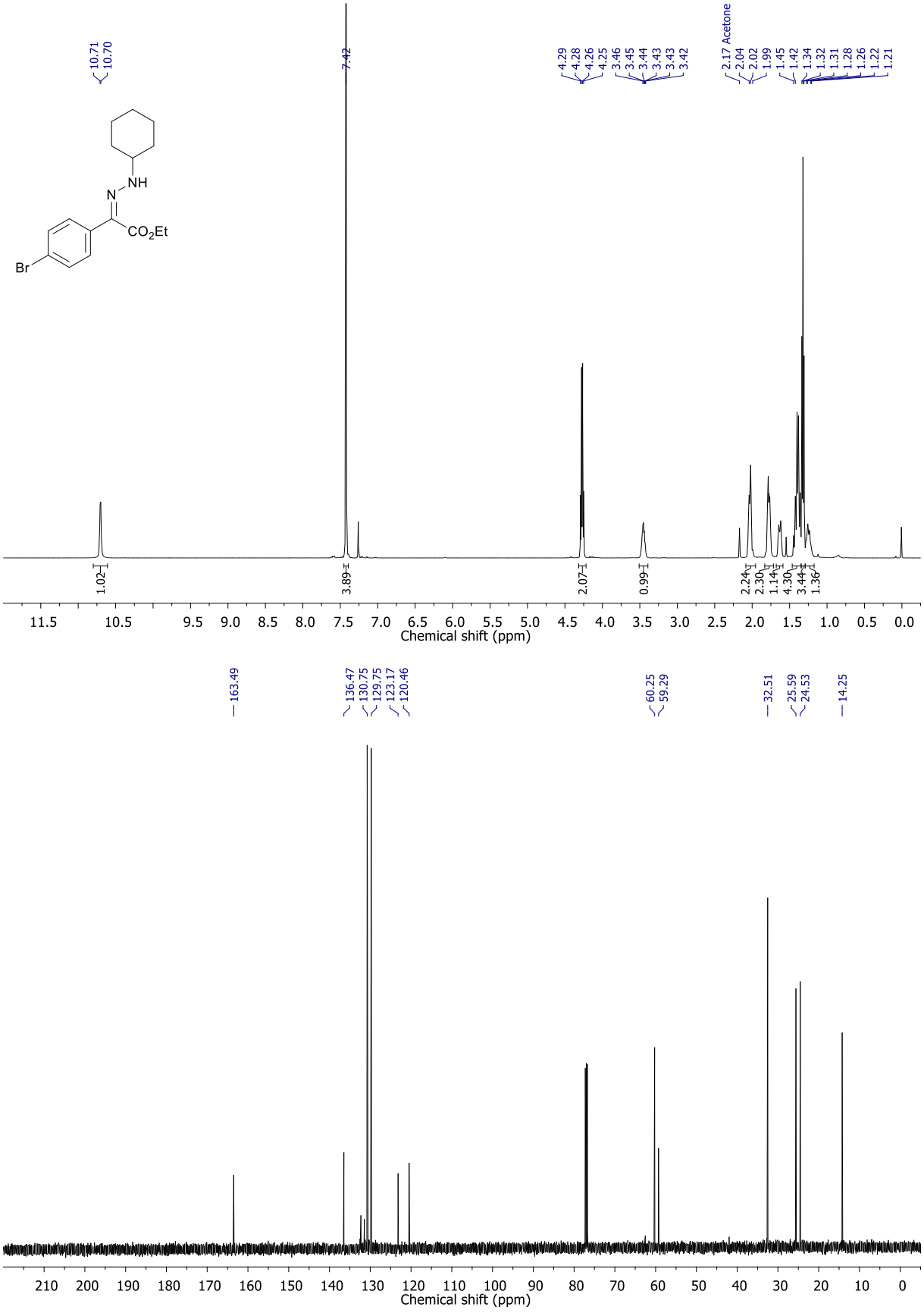

methyl (Z)-2-(2-cyclopentylhydrazineylidene)-2-(naphthalen-2-yl)acetate (54)

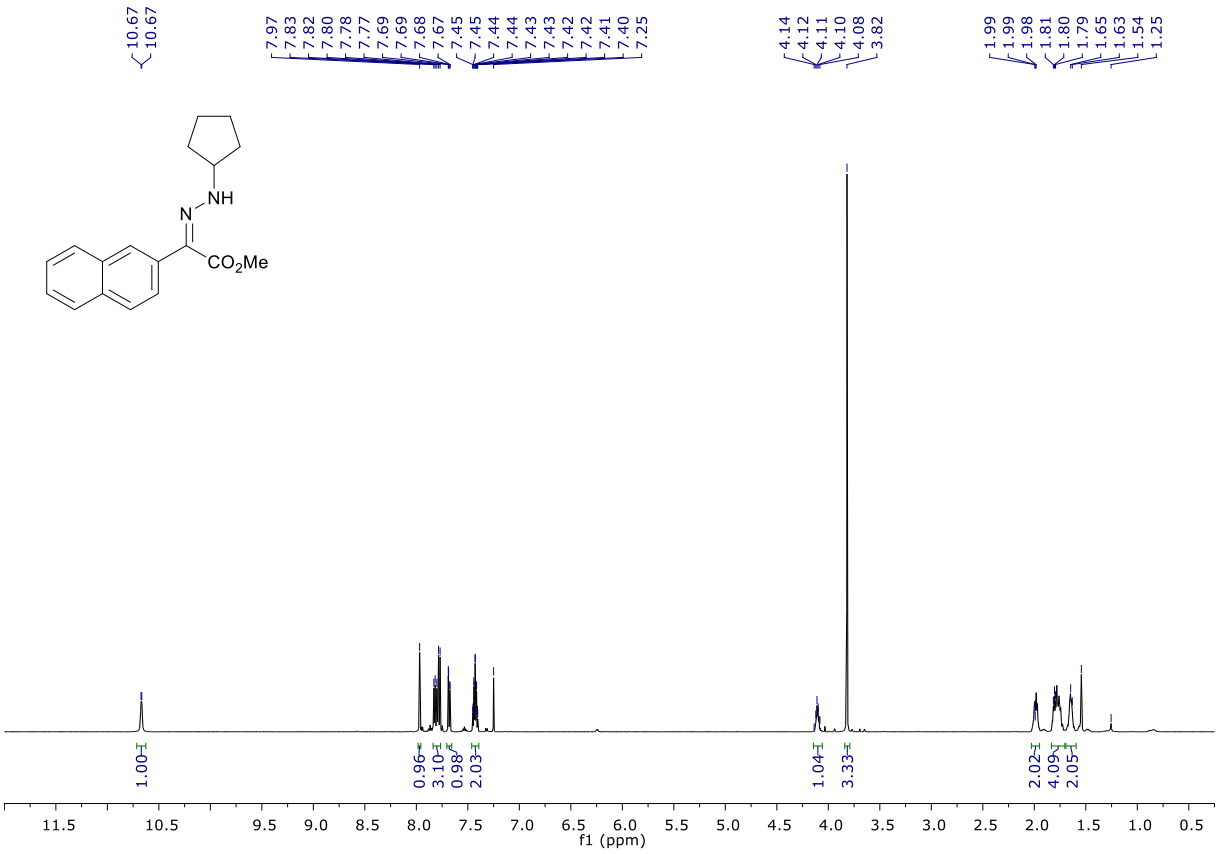

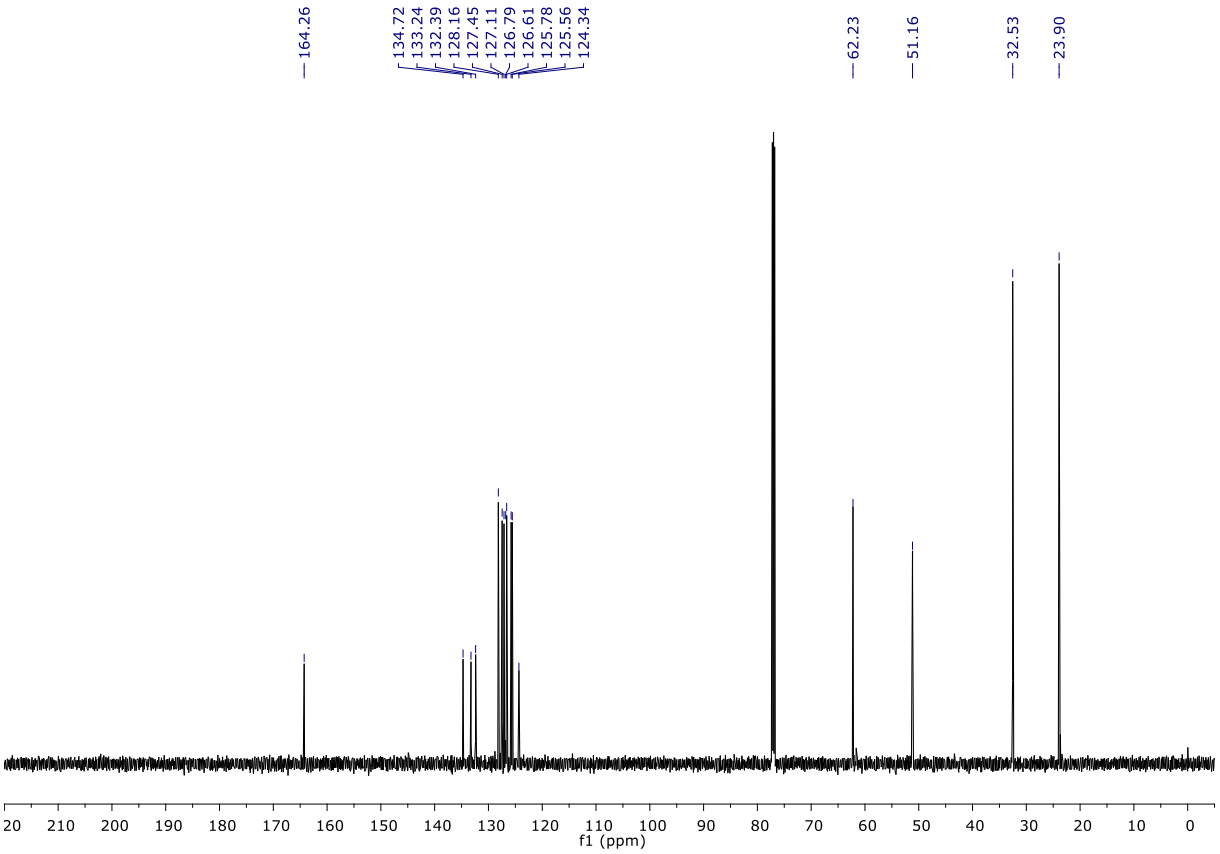

allyl (Z)-2-(2-cyclopentylhydrazineylidene)-2-phenylacetate (55)

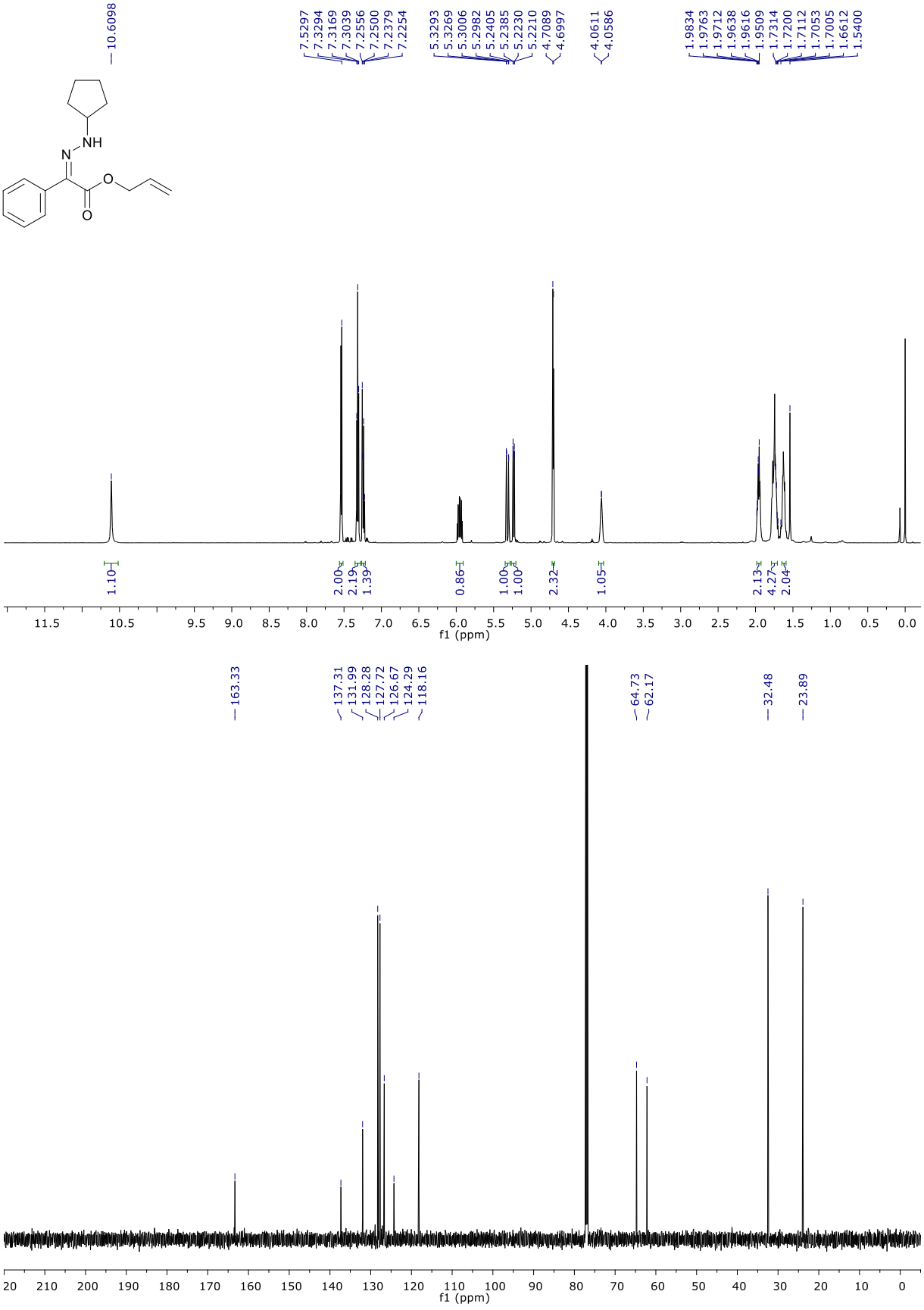

benzyl (Z)-2-(2-cyclopentylhydrazineylidene)-2-phenylacetate (56)

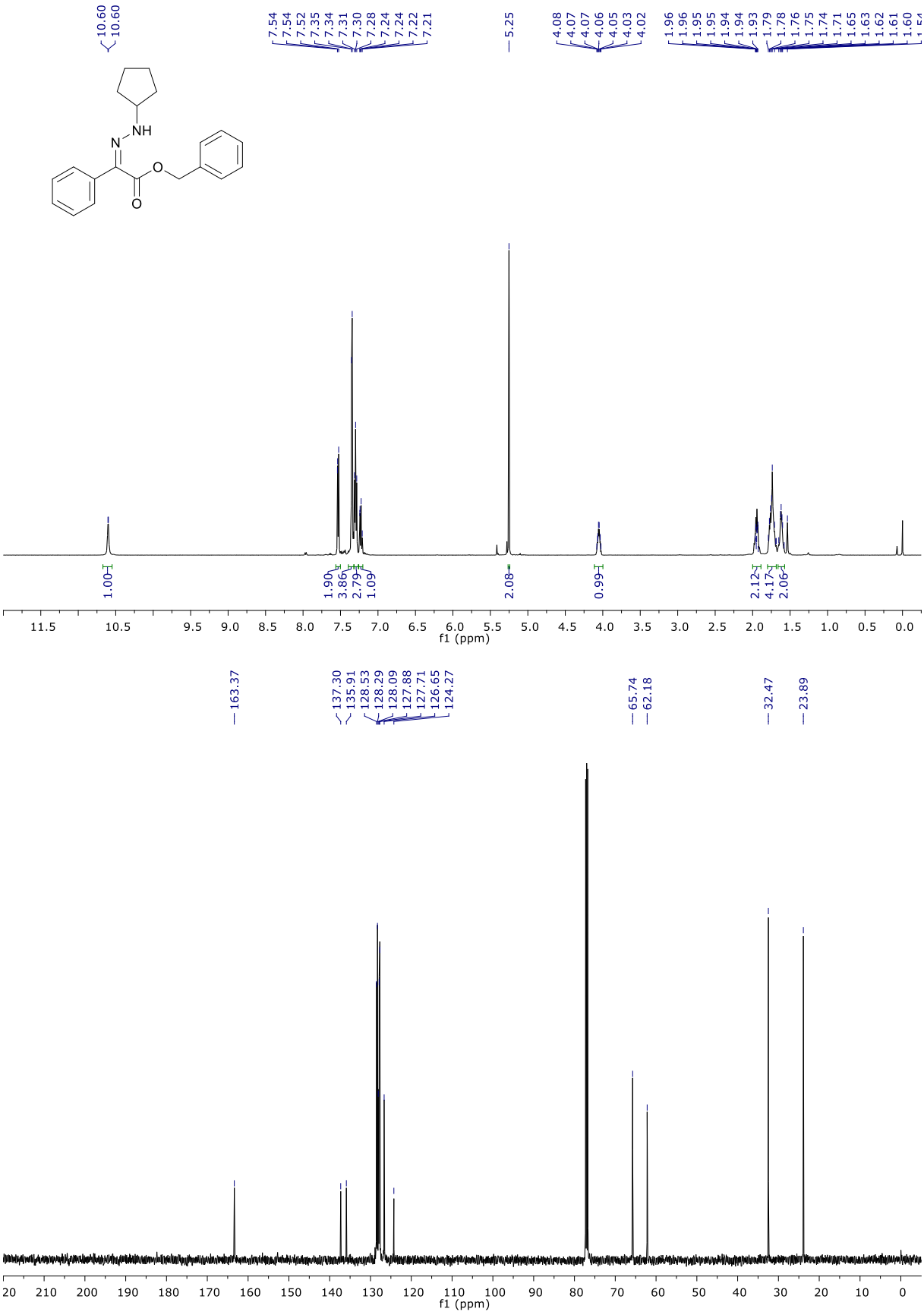

9. Oświadczenia autorów publikacji

Instytut Chemii Organicznej
Polskiej Akademii Nauk

mgr inż. Katarzyna Orłowska
doktorant, Zespół XV
+48 22 343 21 18
katarzyna.orlowska@icho.edu.pl

Instytut Chemii Organicznej PAN
ul. Kasprzaka 44/52
01-224 Warszawa, Polska

Warszawa, 04.12.2023r.

Oświadczam, że mój wkład w powstanie poniższych publikacji polegał na:

› K. Goliszewska, **K. Orłowska**, D. Gryko Photoorganocatalysis in Organic Synthesis, Chapter 4: Sulfur Heterocycles. World Scientific Publishing Company, 2019.

dokonaniu przeglądu literaturowego i przygotowaniu części rozdziału dotyczących zastosowania barwników heterocyklicznych tj. tiazyny, sole tiapyryliowe, struktury polimeryczne (sekcje 4.3, 4.4, 4.5), rejestracji widm absorpcji i emisji oraz przygotowaniu wszystkich wykresów absorpcji i emisji zamieszczonych w rozdziale (Figure 4.1., Chart 4.2., Chart 4.3).

› **K. Orłowska**, K. Rybicka-Jasińska, P. Krajewski, D. Gryko *Org. Lett.* **2020**, *22*, 1018–1021.
Photochemical Doyle–Kirmse Reaction: A Route to Allenes

współopracowaniu koncepcji badań, współuczestnictwie w badaniach optymalizacyjnych i syntezie diazo związków, dokonaniu pomiarów absorpcji diazo związków **S1a-S1u**, zbadaniu zakresu i ograniczeń stosowalności metody w odniesieniu do diazo związków (synteza związków **3-22**), przeprowadzeniu wszystkich badań mechanistycznych, interpretacji otrzymanych wyników i przygotowaniu manuskryptu.

› **K. Orłowska**, J.V. Santiago, P. Krajewski, K. Kisiel, I. Deperasińska, K. Zawada, W. Chaładaj, D. Gryko *ACS Catal.* **2023**, *13*, 1964-1973.
UV Light Is No Longer Required for the Photoactivation of 1,3,4-Oxadiazolines

współopracowaniu koncepcji badań, przeprowadzeniu eksperymentów wstępnych oraz całych badań optymalizacyjnych, współuczestnictwie w badaniu zakresu i ograniczeń stosowalności metody w odniesieniu do 1,3,4-oksadiazolin oraz olefin (synteza związków **12-27**, **29**, **31**, **33**, **35**, **36**, **39**, **40**, **42- 53**, **55-65**, **67**, **68**), przeprowadzeniu wszystkich eksperymentów mechanistycznych (w tym współuczestnictwo w przeprowadzeniu pomiarów EPR), uczestnictwie w interpretacji otrzymanych wyników i przygotowaniu manuskryptu.

› **K. Orłowska**, K. Łuczak, P. Krajewski, J.V. Santiago, K. Rybicka-Jasińska, D. Gryko *Chem. Commun.* **2023**, *DOI: 10.1039/d3cc05174a*
Unlocking the Reactivity of Diazo Compounds on Red Light with the Use of Photochemical Tools

współopracowaniu koncepcji badań, optymalizacji warunków fotokatalitycznych reakcji syntezy oksymów, fenantrydyn i hydrazonów oraz wstępnym zbadaniu zakresu stosowalności zoptymalizowanych metod (synteza związków **38-47**, **52-56**), interpretacji wyników i przygotowaniu manuskryptu

Potwierdzam zgodność z prawdą: Dorota Gryko Digitally signed by Dorota Gryko Date: 2023.12.05 14:26:32 +01'00'

(podpis Promotora)

Katarzyna Chrzeszko

Instytut Chemii Organicznej
Polskiej Akademii Nauk

Prof. dr hab. Dorota Gryko
Kierownik zespołu XV
+48 22 343 20 51
dorota.gryko@icho.edu.pl

Instytut Chemii Organicznej PAN
ul. Kasprzaka 44/52
01-224 Warszawa, Polska

Warszawa, 04.12.2023r.

Oświadczam, że mój wkład w powstanie poniższych publikacji polegał na:

- K. Goliszewska, K. Orłowska, D. Gryko Photoorganocatalysis in Organic Synthesis, Chapter 4: Sulfur Heterocycles. World Scientific Publishing Company, 2019.

  współopracowaniu koncepcji przeglądu i uczestnictwie w jego pisaniu.

- K. Orłowska, K. Rybicka-Jasińska, P. Krajewski, D. Gryko *Org. Lett.* **2020**, *22*, 1018–1021.
  Photochemical Doyle–Kirmse Reaction: A Route to Allenes

  współopracowaniu koncepcji badań, interpretacji wyników i przygotowaniu manuskryptu

- K. Orłowska, J.V. Santiago, P. Krajewski, K. Kisiel, I. Deperasińska, K. Zawada, W. Chaładaj, D. Gryko *ACS Catal.* **2023**, *13*, 1964-1973.
  UV Light Is No Longer Required for the Photoactivation of 1,3,4-Oxadiazolines

  współopracowaniu koncepcji badań, interpretacji wyników i przygotowaniu manuskryptu

- K. Orłowska, K. Łuczak, P. Krajewski, J.V. Santiago, K. Rybicka-Jasińska, D. Gryko *Chem. Commun.* **2023**, *DOI: 10.1039/d3cc05174a*
  Unlocking the Reactivity of Diazo Compounds on Red Light with the Use of Photochemical Tools

  współopracowaniu koncepcji badań, interpretacji wyników i przygotowaniu manuskryptu

Dorota Gryko

Digitally signed by Dorota Gryko
Date: 2023.12.04 14:08:59 +01'00'

Instytut Chemii Organicznej
Polskiej Akademii Nauk

dr Katarzyna Goliszewska
Dział Grantów
+48 22 343 23 32
katarzyna.goliszewska@icho.edu.pl

Instytut Chemii Organicznej PAN
ul. Kasprzaka 44/52
01-224 Warszawa, Polska

Warszawa, 24.11.2023r.

Oświadczam, że mój wkład w powstanie poniższego rozdziału w monografii naukowej polegał na:

- K. Goliszewska, K. Orłowska, D. Gryko Photoorganocatalysis in Organic Synthesis, Chapter 4: Sulfur Heterocycles. World Scientific Publishing Company, 2019.
  dokonaniu przeglądu literaturowego i zgromadzeniu literatury dotyczącej opisywanych zagadnień, przygotowaniu części rozdziału dotyczącej wstępu oraz zastosowania błękitu metylenowego jako fotouczulacza oraz katalizatora fotoredoks (sekcje 4.1 i 4.2).

Katarzyna Goliszewska

Instytut Chemii Organicznej
Polskiej Akademii Nauk

dr Katarzyna Rybicka-Jasińska
Kierownik zespołu XVb
+48 22 343 21 09
katarzyna.rybicka-jasinska@icho.edu.pl

Instytut Chemii Organicznej PAN
ul. Kasprzaka 44/52
01-224 Warszawa, Polska

Warszawa, 22.11.2023r.

Oświadczam, że mój wkład w powstanie poniższych publikacji polegał na:

- K. Orłowska, K. Rybicka-Jasińska, P. Krajewski, D. Gryko *Org. Lett.* **2020**, *22*, 1018–1021. Photochemical Doyle–Kirmse Reaction: A Route to Allenes

  współopracowaniu koncepcji badań, współuczestnictwie w badaniach optymalizacyjnych, zbadaniu zakresu stosowalności i ograniczeń metody w odniesieniu do sulfidów, uczestnictwie w interpretacji wyników i przygotowaniu manuskryptu

- K. Orłowska, K. Łuczak, P. Krajewski, J.V. Santiago, K. Rybicka-Jasińska, D. Gryko *Chem. Commun.* **2023**, *DOI: 10.1039/d3cc05174a* Unlocking the Reactivity of Diazo Compounds on Red Light with the Use of Photochemical Tools
  współopracowaniu koncepcji badań, interpretacji wyników i przygotowaniu manuskryptu

Katarzyna Rybicka-Jasińska

Elektronicznie podpisany przez Katarzyna Rybicka-Jasińska
Data: 2023.11.23 16:10:15 +01'00'

Instytut Chemii Organicznej
Polskiej Akademii Nauk

mgr inż. Piotr Krajewski
doktorant, Zespół XV
+48 22 343 21 18
piotr.krajewski@icho.edu.pl

Instytut Chemii Organicznej PAN
ul. Kasprzaka 44/52
01-224 Warszawa, Polska

Warszawa, 22.11.2023r.

Oświadczam, że mój wkład w powstanie poniższych publikacji polegał na:

- K. Orłowska, K. Rybicka-Jasińska, P. Krajewski, D. Gryko *Org. Lett.* **2020**, *22*, 1018–1021.
  Photochemical Doyle–Kirmse Reaction: A Route to Allenes

  uczestnictwie w procesie optymalizacji reakcji oraz syntezie substratów

- K. Orłowska, J.V. Santiago, P. Krajewski, K. Kisiel, I. Deperasińska, K. Zawada, W. Chaładaj, D. Gryko *ACS Catal.* **2023**, *13*, 1964-1973.
  UV Light Is No Longer Required for the Photoactivation of 1,3,4-Oxadiazolines

  syntezie substratów oraz uczestnictwie w oczyszczaniu otrzymanych produktów

- K. Orłowska, K. Łuczak, P. Krajewski, J.V. Santiago, K. Rybicka-Jasińska, D. Gryko *Chem. Commun.* **2023**, *DOI: 10.1039/d3cc05174a*
  Unlocking the Reactivity of Diazo Compounds on Red Light with the Use of Photochemical Tools

  optymalizacji warunków reakcji O-H, N-H i S-H insercji z udziałem diarylodiazoalkanów oraz zbadaniu zakresu stosowalności metod, interpretacji otrzymanych wyników i uczestnictwie w przygotowaniu manuskryptu

Krajewski

Instytut Chemii Organicznej
Polskiej Akademii Nauk

João Victor Santiago
Postdoc position, Team XV
+48 22 343 21 12
santiago.jv@icho.edu.pl

Instytut Chemii Organicznej PAN
ul. Kasprzaka 44/52
01-224 Warszawa, Polska

Warszawa, 01.09.2023r.

To whom it may concern, I declare that my contribution to the following publications included:

- K. Orłowska, J.V. Santiago, P. Krajewski, K. Kisiel, I. Deperasińska, K. Zawada, W. Chaładaj, D. Gryko *ACS Catal.* **2023**, *13*, 1964-1973.
  UV Light Is No Longer Required for the Photoactivation of 1,3,4-Oxadiazolines

  substrates' synthesis, synthesis of compounds **28**, **30**, **32**, **34**, **37**, **38**, **41**, **54**, **66**, participation in purification of obtained products and manuscript preparation

- K. Orłowska, K. Łuczak, P. Krajewski, J.V. Santiago, K. Rybicka-Jasińska, D. Gryko *Chem. Commun.* **2023**, *DOI: 10.1039/d3cc05174a*
  Unlocking the Reactivity of Diazo Compounds on Red Light with the Use of Photochemical Tools

  optimization of reaction conditions for photocatalyzed synthesis of β-amino-α-diazoesters and synthesis of products **48**-**51**.

João Victor Santiago da Silva

Instytut Chemii Organicznej
Polskiej Akademii Nauk

mgr inż. Kacper Kisiel
doktorant, Zespół XV
+48 22 343 21 12
kacper.kisiel@icho.edu.pl

Instytut Chemii Organicznej PAN
ul. Kasprzaka 44/52
01-224 Warszawa, Polska

Warszawa, 22.11.2023r.

Oświadczam, że mój wkład w powstanie poniższej publikacji polegał na:

- **K. Orłowska**, J.V. Santiago, P. Krajewski, K. Kisiel, I. Deperasińska, K. Zawada, W. Chaładaj,
  D. Gryko *ACS Catal.* **2023**, *13*, 1964-1973.
  UV Light Is No Longer Required for the Photoactivation of 1,3,4-Oxadiazolines
  syntezie i oczyszczeniu produktów **70-73**

Kacper Kisiel

INSTYTUT FIZYKI POLSKIEJ AKADEMII NAUK

INSTITUTE OF PHYSICS, POLISH ACADEMY OF SCIENCES

02-668 WARSZAWA, Al. LOTNIKÓW 32/46
fax: (48-22) 843-0926; http://info.ifpan.edu.pl

dr hab. Irena Deperasińska

e-mail: deper@ifpan.edu.pl

Warszawa, 28 listopada 2023

Oświadczenie

Oświadczam, że mój wkład w powstanie poniższej publikacji:

K. Orłowska, J.V. Santiago, P. Krajewski, K. Kisiel, I. Deperasińska, K. Zawada, W. Chaładaj, D. Gryko *ACS Catal.* **2023**, *13*, 1964-1973.

UV Light Is No Longer Required for the Photoactivation of 1,3,4-Oxadiazolines

polegał na przeprowadzeniu obliczeń DFT dotyczących wartości energii trypletowych oksadiazolin **1**, **2**, **3**, **4**, **5**, **S10**, **S11**, **S12** oraz diazoalkanu **7**.

Irena Deperasińska

WARSZAWSKI
UNIWERSYTET
MEDYCZNY

ZAKŁAD CHEMII ORGANICZNEJ I FIZYCZNEJ

Warszawa, 22.11.2023

OŚWIADCZENIE

Oświadczam, że mój wkład w powstanie poniższej publikacji:

K. Orłowska, J.V. Santiago, P. Krajewski, K. Kisiel, I. Deperasińska, K. Zawada, W. Chaładaj, D. Gryko, *UV Light Is No Longer Required for the Photoactivation of 1,3,4-Oxadiazolines.* ACS Catal. 2023, *13*, 1964-1973

polegał na przeprowadzeniu pomiarów EPR oraz obliczeń potrzebnych do interpretacji wyników EPR (symulacja widm), analizie i interpretacji otrzymanych wyników, a także przygotowaniu części manuskryptu dotyczącej badań EPR.

K Zawada
Katarzyna Zawada

ul. Banacha 1
02-097 Warszawa
www.wum.ed.pl

tel.: +48 22 57 20 950
malgorzata.lisowska@wum.edu.pl

Instytut Chemii Organicznej
Polskiej Akademii Nauk

mgr inż. Klaudia Łuczak
doktorant, Zespół XV
+48 22 343 21 18
klaudia.luczak@icho.edu.pl

Instytut Chemii Organicznej PAN
ul. Kasprzaka 44/52
01-224 Warszawa, Polska

Warszawa, 22.11.2023r.

Oświadczam, że mój wkład w powstanie poniższej publikacji polegał na:

› K. Orłowska, K. Łuczak, P. Krajewski, J.V. Santiago, K. Rybicka-Jasińska, D. Gryko *Chem. Commun.* **2023**, *DOI: 10.1039/d3cc05174a*
Unlocking the Reactivity of Diazo Compounds on Red Light with the Use of Photochemical Tools

optymalizacji warunków reakcji i zbadaniu zakresu stosowalności rekcji fotosensybilizacji α-arylo-α-diazoestrów z udziałem tlenu, kwasu benzoesowego i styrenów, analizie otrzymanych wyników oraz współuczestnictwie w przygotowaniu manuskryptu

Łuczak Klaudia

Instytut Chemii Organicznej
Polskiej Akademii Nauk

dr hab. Wojciech Chaładaj, prof. IChO PAN
Kierownik zespołu VI
+48 22 343 30 65
wojciech.chaladaj@icho.edu.pl

Instytut Chemii Organicznej PAN
ul. Kasprzaka 44/52
01-224 Warszawa, Polska

Warszawa, 22.11.2023r.

Oświadczam, że mój wkład w powstanie poniższej publikacji polegał na:

› K. Orłowska, J.V. Santiago, P. Krajewski, K. Kisiel, I. Deperasińska, K. Zawada, W. Chaładaj, D. Gryko *ACS Catal.* **2023**, *13*, 1964-1973.
UV Light Is No Longer Required for the Photoactivation of 1,3,4-Oxadiazolines

przeprowadzeniu obliczeń DFT mechanizmu reakcji, analizy i interpretacji otrzymanych danych oraz przygotowaniu części manuskryptu dotyczącej tych danych.

Wojciech Jan Chaładaj
Digitally signed by Wojciech Jan Chaładaj
Date: 2023.11.22 08:56:07 +01'00'